LKT Laboratories, Inc.
545 Phalen Blvd.
St. Paul, MN 55130-5303

2016-2018 Catalog

LKT Laboratories, Inc.

Biochemicals for Life Science Research

2016-2018

Immunomodulators
Cardiovascular agents
Chemopreventive agents
Chemotherapeutics
Antimicrobials
Neurotransmitter modulators
Signaling pathway inhibitors
Anti-inflammatory agents
Natural products

Tel: 651-644-8424
Toll Free Tel: 888-558-5227
Fax: 651-644-8357
Toll Free Fax: 888-558-7329
Web: lktlabs.com

LKT Laboratories Inc. is focused on the production and distribution of high purity biochemicals for all types of life science research, including cancer biology, immunology, cardiovascular studies, microbiology, and neuroscience. Our product library includes a wide variety of compounds that can be used for a broad spectrum of in vitro and in vivo research applications.

PRICING, TERMS, AND SPECIFICATIONS

Prices and specifications shown are current at the time of printing. Prices and specifications are subject to change without notice. For the most up to date pricing, please visit lktlabs.com. All prices are in US dollars. LKT ships orders F.O.B, St. Paul, MN, USA. Payment terms for all domestic orders are net 30 days from the date of invoice. We request that all international orders be prepaid. LKT accepts Visa, Mastercard, Discover, and American Express. Sales, use, excise, and other applicable taxes will be charged.

SHIPPING INFORMATION

Products from stock will be shipped within 24 hours by the most efficient method available (generally 2 day air unless otherwise requested) upon receipt of the purchase order. Freight charges are prepaid and added to the invoice. They will be shipped using the customers own courier account (FedEx, DHL, or UPS) for express delivery.

SPECIAL HANDLING

Certain items may require special handling, packaging, or shipping (e.g. hazardous materials, dry ice shipping, etc.). In such cases extra charges must be levied to cover the costs of the specialized requirements. Items that require long-term cold storage may not necessarily be shipped on ice. Please include the name, telephone number, or fax number of the person who will be knowledgeable in handling special shipments to avoid delay in customs clearance or proper storage of the materials.

SAFE HANDLING

Many of the products offered in this catalog may still be investigational in nature or may never have been manufactured or used on a commercial scale. Therefore, many of the items may not yet have been tested for toxicological or other hazardous properties. The burden of providing adequate precautions to safeguard workers and the general public from either known or undemonstrated potential hazards of such materials rests with the user. Since most of our products are sold for research and development purposes, LKT makes the assumption that the user will take safety precautions which are appropriate to the type and quantity of material in question and which are consistent with the requirements of any regulatory agency.

USE OF PRODUCTS

LKT's products are intended solely for laboratory research purposes and are not to be used for any other purposes. Buyer acknowledges that the products have not been tested by LKT for safety or efficacy. Buyer expressly represents and warrants to LKT that Buyer will properly test, use, manufacture and market any products purchased from LKT and/or materials produced with products purchased from LKT in accordance with the

practices of a reasonable person who is an expert in the field and in strict compliance with all applicable laws and regulations, now and hereinafter enacted. Buyer has responsibility to verify the hazards and to conduct any further research necessary to learn the hazards involved in using products purchased from LKT. Buyer also has the duty to warn Buyer's customers and any auxiliary personnel (such as freight handlers, etc.) of any risks involved in using or handling the products. Buyer agrees to comply with instructions, if any, furnished by LKT relating to the use of the products and to not misuse the products in any manner. If the products purchased from LKT are to be repackaged, relabeled, or used as starting material or components of other products, Buyer will verify LKT's assay of the products. No products purchased from LKT shall be considered to be foods, drugs, medical devices, or cosmetics.

WARRANTIES AND DISCLAIMERS

LKT warrants that its products shall conform to the description of such products as provided by LKT through LKT's catalog, analytical data, or other literature. **This warranty is exclusive and LKT makes no other warranty, express or implied, including any implied warranty of merchantability or fitness for any particular purpose.**

LKT's sole and exclusive liability and Buyer's exclusive remedy with respect to products proved to LKT's satisfaction to be defective or nonconforming shall be replacement of such products without charge or refund of the purchase price, at LKT's sole discretion, upon the return of such products in accordance with LKT's instructions. LKT shall not in any event be liable for incidental, consequential, or special damages of any kind resulting from any use or failure of the products. This limitation expressly includes but is not limited to damages to a third party occasioned by such product. All claims must be brought within 60 days after receipt of the material by the Buyer, regardless of their nature.

RETURN POLICY

Contact our customer service department for a return authorization within 30 days for replacement of any product sold by LKT Labs that does not meet the standards indicated by the product specification.

ORDERING INFORMATION

Phone:	(651) 644-8424 (888) 558-5227
Fax:	(651) 644-8357 (888) 558-7329
Location:	LKT Laboratories, Inc. 545 Phalen Blvd. St. Paul, Minnesota 55130
Email:	getinfo@lktlabs.com
Web:	lktlabs.com

Table of Contents

Pim Kinase Inhibitors

Pim kinases are serine/threonine kinases that play a significant role in cell cycle progression and apoptosis. There are two isoforms of Pim kinase: Pim-1 and Pim-2. Both kinases are expressed in lymphoid cells and are necessary for cytokine-dependent proliferation[1].

Most research has examined the structure and function of Pim-1, although both are potentially involved in tumorigenesis. Pim-1 activates cell cycle regulator Cdc25, stimulating cell cycle progression. As a result, it may induce unchecked cell growth. Because of this role, inhibition of Pim-1 shows benefit in the treatment of various cancers.

AZD-1208 (A9708) is a Pim-1 inhibitor that induces cell cycle arrest and apoptosis in acute myelogenous leukemia cells and inhibits phosphorylation of downstream targets such as Bcl-2, 4EBP1, p70S6K, and S6[2].

SMI-4a (S4932) is another Pim-1 inhibitor. This compound prevents phosphorylation of eIF4B, suppresses tumor growth, and induces cell cycle arrest and apoptosis in myeloid and lymphoid cells[3].

Proteasome inhibitor **MLN-2238 (M4455)** modulates expression of tumor suppressor miR33b and down-regulates Pim-1 activity in multiple myeloma cells[4].

1. Bachmann M, Möröy T. Int J Biochem Cell Biol. 2005 Apr;37(4):726-30.
2. Keeton EK, McEachern K, Dillman KS, et al. Blood. 2014 Feb 6;123(6):905-13.
3. Yang J, Wang J, Chen K, et al. Cancer Res. 2013 Aug 1;73(15):4898-908.
4. Tian Z, Zhao JJ, Tai YT, et al. Blood. 2012 Nov 8;120(19):3958-67.

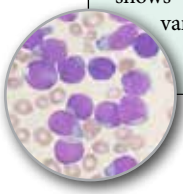

Some Pim-1 kinase inhibitors induce apoptosis in leukemia cells

ALK Inhibitors

Tyrosine kinases such as anaplastic lymphoma kinase (ALK) are becoming major targets in the development of new chemotherapeutics. ALK plays an important role in the development of the brain; it also drives the progression of several cancers, including anaplastic large-cell lymphoma, neuroblastoma, and non-small cell lung cancer.

When the ALK gene is mutated or fused with other genes, it often produces extra or abberent proteins. Overactive ALK stimulates JAK/STAT, PI3K/Akt, and ERK, promoting unregulated cell cycle progression, survival, and proliferation[1]. Inhibition of ALK prevents these downstream effects, minimizing cancer cell signaling and tumor growth.

Crizotinib (C6935) is an inhibitor of ALK that also suppresses activity of ROS1 and c-MET. In cancer cells, this compound upregulates expression of pro-apoptotic BIM and downregulates expression of anti-apoptotic survivin to induce apoptosis[2].

CH5424802 (C2900) targets both wild-type and mutant L1196M ALK, inducing regression of non-small cell lung cancer metastasis in the brain[3].

Several new ALK inhibitors also inhibit IGF-1R, an additional target in preventing growth of non-small cell lung cancer and large-cell lymphoma cells[4-6]. Representative products that target both of these kinases include **LDK378 (L1340)**, **AZD3463 (A9600)**, and **GSK-1838705A (G7540)**.

1. Grande E, Bolós MV, Arriola E. Mol Cancer Ther. 2011 Apr;10(4):569-79.
2. Okamoto W, Okamoto I, Arao T, et al. Mol Cancer Ther. 2012 Jul;11(7):1557-64.
3. Kodama T, Hasegawa M, Takanashi K, et al. Cancer Chemother Pharmacol. 2014 Nov;74(5):1023-8.
4. www.clinicaltrials.gov/show/NCT01685060
5. Yang B. Protein Kinases in Drug Discovery Conference. 2013.
6. Sabbatini P, Korenchuk S, Rowand JL, et al. Mol Cancer Ther. 2009 Oct;8(10):2811-20.

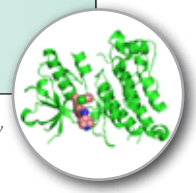

Crizotinib binds ALK with high potency

Fluorouracil

5-Fluorouracil (F4480) is a pyrimidine nucleoside analog used to treat a wide variety of cancers. This compound inhibits thymidylate synthase, preventing the formation of dTMP from dUMP and suppressing thymidine synthesis. Without thymidine, DNA can not replicate and cells undergo a thymineless death[1-2].

Capecitabine (C0162) and **Ftorafur (F7657)** are prodrugs of 5-fluorouracil that feature improved pharmacokinetic parameters. Other 5-fluorouracil analogs include **Carmofur (C0174)** and **Floxuridine (F4557)**.

1. Longley DB, Harkin DP, and Johnston PG. Nat Rev Cancer. 2003 May;3(5):330-8.
2. Tanaka F, Fukuse T, Wada H, et al. Curr Pharm Biotechnol. 2000 Sep;1(2):137-64.

Cytarabine

Cytarabine (C9778) is a nucleoside analog of cytosine. Cytarabine is incorporated into DNA and RNA, inhibiting DNA polymerase and RNA polymerase; this also causes chain termination, preventing DNA repair and synthesis[1].

Cytarabine is clinically used to treat chronic lymphocytic leukemia, acute lymphocytic leukemia, and non-Hodgkin lymphoma[2]. This compound is too toxic to use as an antiviral agent, but in some models it inhibits growth and replication of herpesviruses such as cytomegalovirus and varicella-zoster [3].

1. Inagaki A, Nakamura T, Wakisaka G. Cancer Res. 1969 Dec;29(12):2169-76.
2. Zhang W, Ding Y, Wu H, et al. Medicine (Baltimore). 2014 Dec;93(27):e134.
3. Lauter CB, Bailey EJ, Lerner AM. Antimicrob Agents Chemother. 1974 Nov;6(5):598-602.

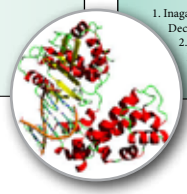

Cytarabine inhibits DNA polymerase activity

Carmustine

Carmustine (C0173) is used to treat brain cancers, lymphomas, and multiple myeloma[1-2]. This compound is a nitrosourea DNA alkylator that forms interstrand crosslinks in DNA, preventing DNA replication and transcription and inducing cell death. This compound is often administered with MGMT inhibitors such as **Lomeguatrib (L5750)** or **O^6-Benzylguanine (B1855)**; these compounds prevent the repair of DNA, enhancing the efficacy of DNA alkylators such as carmustine.

1. Drabløs F, Feyzi E, Aas PA, et al. DNA Repair (Amst). 2004 Nov 2;3(11):1389-407.
2. Khan O and Middleton MR. Expert Opin Investig Drugs. 2007 Oct;16(10):1573-84.

Cyclophosphamide

Cyclophosphamide (C9609) is a commonly used nitrogen mustard DNA alkylating agent with broad application in cancer chemotherapy. Like other nitrogen mustards, this compound alkylates the N7 nitrogen of guanine bases on DNA; this causes DNA crosslinks and inhibits DNA replication and transcription[1-2].

Cyclophosphamide is also used in clinical settings to treat autoimmune diseases such as multiple sclerosis, rheumatoid arthritis, and systemic lupus erythematosus[3].

1. Hall AG and Tilby MJ. Blood Rev. 1992 Sep;6(3):163-73.
2. Pratt WB, Ruddon RW, et al. The Anticancer Drugs. Oxford University Press. 1994.
3. Makhani N, Gorman MP, Branson HM, et al. Neurology. 2009 Jun 16;72(24):2076-82.

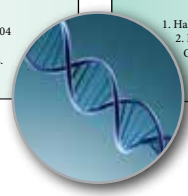

Carmustine and Cyclophosphamide induce DNA strand cross links

Gemcitabine Hydrochloride

Gemcitabine Hydrochloride (G1745) is a chemotherapeutic antimetabolite that demonstrates benefit in the treatment of various solid tumors such as non-small cell lung cancer (NSCLC), pancreatic cancer, ovarian cancer, bladder cancer, breast cancer, and others[1-5]. Gemcitabine also treats lymphomas and esophageal cancer. This compound is often used in combination with other chemotherapeutics such as **Carboplatin (C0171)** and **Cisplatin (C3374)**.

Gemcitabine is a 2'-deoxycytidine analog that terminates DNA chain elongation and prevents replication and transcription when incorporated into DNA. Gemcitabine also inhibits the activity of ribonucleoside reductase, preventing the production of deoxyribonucleotides and eventually inducing cellular apoptosis and death[2]. The overall actions that gemcitabine metabolites exert on cellular regulatory processes serve to enhance the overall inhibitory activities on cell growth, a relatively rare interaction observed from other anticancer compounds known as "self-potentiation". Gemcitabine also induces telomere shortening by stabilizing TRF2 and displays antiviral activity against strains of HIV and feline leukemia virus[6-7].

1. Matsui K and Fukuoka M. Gan To Kagaku Ryoho. 1992;19: 2127-32.
2. Hui YF, Reitz. J. Am. J. Health Syst. Pharm. 1997;54:162-70.
3. Lilenbaum RC and Green MR. J. Clin. Oncol. 1993;11:1391-402.
4. Ruiz van Haperen VW and Peters GJ. Pharm. World Sci. 16: 1994;104-12.
5. Christgen M, Schniewind B, Jueschke A, et al. Cancer Lett. 2005;227(2):193-200.
6. Su CH, Chu WC, Lan KH, et al.. Eur J Cancer. 2012 Dec;48(18):3465-74.
7. Greggs WM 3rd, Clouser CL, Patterson SE, et al. J Gen Virol. 2012 Apr;93(Pt 4):900-5.

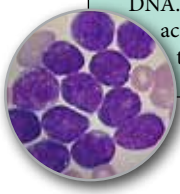

Gemcitabine is an effective chemotherapy drug used to treat various cancers

Bleomycins

Bleomycins are glycopeptides initially produced by *Streptomyces verticillus* that exhibit potent anticancer and antibiotic activities.

Bleomycin Sulfate (B4518), a mixture of bleomycins, contains the predominant components of commercially available bleomycin. Bleomycin is used to treat several cancers, including squamous cell carcinoma, testicular cancer, and Hodgkin lymphoma; it is also a component of the ABVD chemotherapy regimen. Bleomycin causes strand breaks in DNA and prevents incorporation of thymidine into DNA[1-3].

Bleomycin has two primary structural domains: the bithiazole DNA interaction site and a metal binding site[1]. Bleomycin can chelate iron at the second site, generating reactive oxygen species that cause DNA degradation[4].

Bleomycin A5 HCl (A4517) can induce two separate modes of cell death: necrosis and apoptosis. Bleomycin A5 may also potentially treat hemangioma, as it has shown benefit in cellular and animal models[5].

1. Benitz-Bribiesca L and Sanchez-Suarez P. Ann. N.Y. Acad. Sci. 1999;887:133-49.
2. Vorobjev PE, Smith JB, Pyshnaya IA, et al. Bioconjug Chem. 2003 Nov-Dec;14(6):1307-13.
3. Liu Y, Wu F, and Zou G. Anal Chim Acta. 2007 Sep 19;599(2):310-4.
4. Sugiura Y, Suzuki T, Otsuka M, et al. J. Biol. Chem. 1983;258(2):1328-36.
5. Li P, Li DF, Guo ZT, et al. Zhonghua Kou Qiang Yi Xue Za Zhi. 2013 Jan;48(1):18-22.

Bleomycin was first produced by the bacterium Streptomyces verticillus

Curcuminoids

Curcumin (C8069) is a key component of turmeric, a member of the ginger family. Curcuminoids are responsible for the yellow color of turmeric.

Like many other plant-based phenols, curcuminoids display a range of biological activities in research models. These compounds display antioxidative, antimicrobial, and anticancer properties.

In cellular models of glioma, curcumin downregulates expression of Shh, Smo, GLI1, cyclin D1, and Bcl-2, inhibiting proliferation and migration and inducing apoptosis. Curcumin also decreases tumor volume and prolongs survival in animal models[1].

Curcumin decreases levels of NADPH-oxidase mRNA and hydrogen peroxide, decreasing oxidative stress in animal models of exercise[2].

Other curcuminoids such as **Dimethoxycurcumin (D3449)** display similar biological activities with a stronger pharmacokinetic profile. This compound induces DNA damage and apoptosis in breast cancer cells[3]. Also, **Bisdemethoxycurcumin (B3573)** inhibits activity of DNMT1 and α-amylase and may induce phase II enzyme activation[4-6].

Also available: **Curcumin, high purity (C8070), 3,4-Difluorobenzocurcumin (D3420),** and **Demethoxycurcumin (D1850)**.

1. Du WZ, Feng Y, Wang XF, et al. 2013 Dec;19(12):926-36.
2. Kawanishi N, Kato K, Takahashi M, et al. 2013 Nov 22;441(3):573-8.
3. Kunwar A, Jayakumar S, Srivastava AK, et al. Arch Toxicol. 2012 Apr;86(4):603-14.
4. Ponnusamy S, Zinjarde S, Bhargava S, et al. Food Chem. 2012 Dec 15;135(4):2638-42.
5. Liu YL, Yang HP, Zhou XD, et al. Curr Cancer Drug Targets. 2011 Nov;11(9):1098-110.
6. Kou MC, Chiou SY, Weng CY, et al. Mol Nutr Food Res. 2013 Sep;57(9):1598-610.

Curcumin is a caffeic acid derivative found in turmeric

Carotenoids

Carotenoids are pigments that can be found in the chloroplasts and chromoplasts of plants, fungi, and bacteria. Structurally, carotenoids are terpenes consisting of eight isoprene units. Carotenoids typically absorb wavelengths ranging from 400-550 nanometers (violet to green light), causing them to appear red, orange, or yellow[1].

Most carotenoids are antioxidants, protecting against oxidative damage. These compounds are highly effective free radical scavengers.

Capsanthin (C0260) is a carotenoid first isolated from *Capsicum* that exhibits anticancer activity. Capsanthin inhibits TPA-induced tumor development in vitro and in vivo[2].

Canthaxanthin (C0168) scavenges radicals and inhibits lipid peroxidation in vitro[3]. In other models, this compound inhibits MCA-induced carcinogenesis[4].

β-Carotene (C0269) is a red-orange terpene pigment that can be found in many plants and fruits; this compound is a prodrug for vitamin A. β-Carotene is used in research studies to quantify antioxidative activity. In various models, this compound also protects against DNA damage and inflammation[5-6].

1. Armstrong GA and Hearst JE. FASEB J. 1996 Feb;10(2):228-37.
2. Maoka T, Mochida K, Kozuka M, et al. Cancer Lett. 2001 Oct 30;172(2):103-9.
3. Palozza P, Luberto C, Ricci P, et al. Arch Biochem Biophys. 1996 Jan 15;325(2):145-51.
4. Pung A, Rundhaug JE, Yoshizawa CN, et al. Carcinogenesis. 1988 Sep;9(9):1533-9.
5. Berti AP, Düsman E, Mariucci RG, et al. Genet Mol Res. 2014 Mar 31;13(1):2248-58.
6. Di Tomo P, Canali R, Ciavardelli D, et al. Mol Nutr Food Res. 2012 Feb;56(2):217-27.

β-Carotene is a red-orange pigment that can be found in carrots, sweet potatoes, and pumpkins

Isothiocyanates

Isothiocyanates are organosulfur compounds that contain an N=C=S chemical group. Some isothiocyanates are isolated from natural sources and may be metabolites of glucosinolates. In humans, intake of cruciferous vegetables such as broccoli, watercress Brussels sprouts, radishes, and mustard is the primary dietary source of isothiocyanates[1].

Isothiocyanates are well known for their inhibition of phase I enzymes such as cytochrome P450s, which oxidize compounds and potentially produce mutagenic intermediates. Isothiocyanates also induce expression of phase II enzymes such as quinone reductase, glutathione-S-transferase, and heme oxygenase; these enzymes detoxify mutagenic intermediates, minimizing oxidative damage and inflammation.

Benzyl Isothiocyanate (BITC, B1653) and **Phenethyl Isothiocyanate (PEITC, P2508)** inhibit chemically-induced carcinogenesis in several models[2]. BITC inhibits squamous cell carcinoma cell invasion and migration and induces apoptosis and autophagy in prostate cancer cells[3]. In animal models, BITC also suppresses the development of mammary gland tumors[4].

3-Phenylpropyl Isothiocyanate (PPITC, P2515) and **4-Phenylbutyl Isothiocyanate (PBITC, P2510)** are also isothiocyanates that display anticancer benefit[4]. In animal models, PPITC decreases lung tumor formation induced by benzopyrene and NNK[5]. In similar models, PBITC exhibits chemopreventive activity, limiting the development of pancreatic dysplasia and adenocarcinoma[6]. Studies investigating the effect of alkyl chain length of phenylalkyl isothiocyanates on tobacco specific nitrosamine-induced lung tumorigenesis revealed that PPITC and PBITC may be some of the most effective isothiocyanates[7].

Some isothiocyanates, such as **Phenylhexyl Isothiocyanate (PHITC, P2922)** have been shown to inhibit the activity of histone deacetylases (HDACs), likely strengthening their anticancer activity.

Other isothiocyanates include **Alyssin (A4496), Erucin (E6880), Iberin (I0416),** and **Iberverin (I0418)**. Like other isothiocyanates, these also induce phase II enzyme activity. Erucin inhibits telomerase, preventing growth of hepatocellular carcinoma cells; it also decreases tumor weight in models of bladder cancer[9-10]. In cancer cells, iberin decreases expression of cyclin-dependent kinases and induces expression of p21, inducing cell cycle arrest and apoptosis[11]. Iberverin, a homolog of erucin, decreases expression of androgen receptors in prostate cancer cells, showing potential efficacy in the treatment of prostate cancer[12].

Also available: **R-Sulforaphane (S8046)**, **S-Sulforaphane (S8045), R,S-Sulforaphane (S8044)**, **Phenyl-isothiocyanate (PITC, P2513)**, and many other cysteine-isothiocyanate and glutathione-isothiocyanate conjugates.

1. Fenwick GR, Heaney RK, Mullin WJ. CRC Crit. Rev. Food Sci. Nutr. 1983;18, 123-201.
2. Wattenberg LW. Carcinogenesis. 1987;8,1971-73.
3. Kim M, Cho HJ, Kwon GT, et al. Mol Carcinog. 2014 Apr 11.
4. Wolf MA, Claudio PP. . Nutr Cancer. 2014;66(2):285-94.
5. Hecht SS, Upadhyaya P, Wang M, et al. Carcinogenesis. 2002 Sep;23(9):1455-61.
6. Son HY, Nishikawa A, Furukawa F, et al. Cancer Lett. 2000 Nov 28;160(2):141-7.
7. Morse MA, Eklind KI, Amin SG, Hecht SS, Chung F-L. Carcinogenesis. 1989;10, 1757-1759.
8. Lu Q, Lin X, Feng J, et al. J Hematol Oncol. 2008 Jun 9;1:6.
9. Herz C, Hertrampf A, Zimmermann S, et al. J Cell Mol Med. 2014 Sep 25.
10. Abbaoui B, Riedl KM, Ralston RA, et al. Mol Nutr Food Res. 2012 Nov;56(11):1675-87.
11. Jadhav U, Ezhilarasan R, Vaughn SF, et al. Int J Mol Med. 2007 Mar;19(3):353-61.
12. Kim SH, Singh SV. Mol Cancer Ther. 2009 Jul;8(7):1946-54.

Some isothiocyanates are found in cruciferous vegetables

Sulforaphane

R-Sulforaphane (S8046) is an organosulfur compound derived from metabolism of glucoraphanin, a glucosinolate. This compound is a natural product that contains an isothiocyanate (N=C=S) moiety. Isothiocyanates can be found in cruciferous vegetables such as kale, broccoli, cauliflower, radish, and cabbage[1-3].

Sulforaphane, also known as 4-methylsulfinylbutyl isothiocyanate or (-)-1-isothiocyanato-4-(*R*)-(methylsulfinyl) butane, displays a variety of biological properties including anticancer, antimicrobial, antioxidative, anti-inflammatory, and neuroprotective activities. In cellular models, sulforaphane inhibits growth and survival of bacteria such as *Escherichia coli* and *Helicobacter pylori*[4-5].

Synthetic **R,S-Sulforaphane (S8044)** is a racemic mixture that exhibits chemopreventive benefit, inhibiting cell proliferation and preventing tumor growth in animal models of melanoma[6]. Like other isothiocyanates, sulforaphane also induces expression and activity of phase II detoxifying enzymes such as glutathione peroxidase, quinone reductase, and glutathione-S-transferase. Phase II enzymes convert electrophiles into less toxic and more easily excretable products[7-12]. The induction of phase II enzymes is mediated by MAPK signaling pathways[12]. In human prostate cell lines, sulforaphane induces phase II enzyme activity and to increase the synthesis of glutathione[13]. Sulforaphane is also a strong phase I enzyme inhibitor; it inhibits cytochromes P450 2E1 and P450 1A2, two metabolizing enzymes associated with activation of carcinogens[14-15].

Additionally, this compound also induces expression of Nrf2, a transcription factor involved in the regulation of endogenous antioxidants. Increased expression of Nrf2 protects against oxidative damage triggered by inflammation or other injury[6].

Sulforaphane may also indirectly inhibit histone deacetylases (HDACs) and STAT5 in vitro by downregulating their expression[16-17]. Additionally, sulforaphane also inhibits the aryl hydrocarbon receptor, a transcription factor that regulates cytochrome P450 enzymes[18].

R-Sulforaphane is the naturally isolated isomer of synthetic **S-Sulforaphane (S8045)**, which exhibits similar but less potent chemopreventive and antioxidative properties[19-20].

1. Misiewicz I, et al. Acta Biochimica Polonica. 2004;51(3):711-21.
2. Verhoeven DT, Goldbohm RA, et al. Chem. Biol. Interact. 1997;103:79-129.
3. Talalay P, Zhang Y. Biochem. Soc. Trans. 1996;24:806-10.
4. Fahey JW, Haristoy X, et al. Proc. Natl. Acad. Sci. U. S. A. 2002;99(11):7610-15.
5. Wu HZ, Fei HJ, Zhao YL, et al. Sichuan Da Xue Xue Bao Yi Xue Ban. 2012 May;43(3):386-90.
6. Kleszczyński K, Ernst IM, Wagner AE, et al. Pharmacol Res. 2013 Dec;78:28-40..
7. Gamet-Payrastre L, Li P, et al. Cancer Res. 2000;60:1426-1433.
8. Wattenberg LW, Shafer HW, et al. Proc Am. Assoc. ncer Res. 1989;30:181.
9. Lori R, Bernadi R, et al. Bioorg Med Chem Lett. 1999;9:1047-48.
10. Zhang Y, Talalay P, Cho C, Posner GH. Proc. Natl. Acad. Aci. USA 89:2399-2403 (1992).
11. Yu R, Lei W, et al. J. Biol. Chem. 1999.274:27545-52.
12. Maheo K, Morel F, et al. Cancer Res. 1997;57:3649-52.
13. Brooks JD, Paton VG, Vidanes G. Cancer Epidemiol. Biomark. Prev. 2001;10:949-954.
14. Singletary K, MacDonald C. Cancer Lett.2000; 155:47-54.
15. Fimognari C, Nusse M, et al. Biochem. Pharmacol. 2004;68(6):1133-38.
16. Myzak MC, Karplus PA, et al. Cancer Res. 2004;64(16):5767-74.
17. Pinz S, Unser S, Rascle A. PLoS One. 2014 Jun 9;9(6):e99391.
18. Abdull Razis AF, Hanlon N, Soltys E, et al. Arch Toxicol. 2012 Oct;86(10):1505-14.
19. Abdull Razis AF, Hanlon N, Soltys E, et al. Arch Toxicol. 2012 Oct;86(10):1505-14.
20. Abdull Razis AF, Bagatta M, De Nicola GR, et al. Arch Toxicol. 2011 Aug;85(8):919-27.

R-Sulforaphane is isolated from broccoli

Ginsenosides

Ginseng displays many biological activities, including antioxidative, neuroprotective, and anticancer properties[1]. The most commonly studied species of ginseng are *Panax ginseng* (Korean or Chinese ginseng), *Panax quinquefolius* (American ginseng,) and *Panax japonicus* (Japanese ginseng).

The active ingredients in ginseng are ginsenosides, which belong to the chemical class of compounds known as triterpene saponins. Many of these ginsenosides have been isolated and identified. Most ginsenosides can be separated into two groups: **Panaxadiols** and **Panaxatriols**. In addition to the triterpene saponins, many other active ingredients have also been identified.

Many ginsenosides display anticancer activity in cellular and animal models of cancer. **Ginsenoside Rg3** inhibits cell growth in osteosarcoma cells by inducing strand breaks in double-stranded DNA[2]. **Ginsenoside Rh2** induces proliferation of β-cells by indirectly activating PDX-1 and Akt; it also improves glucose tolerance in animal models[3]. Ginsenoside Rh2 decreases levels of amyloid-β protein in animal models of Alzheimer's disease, improving deficits in learning and memory[4].

In adipocytes, **Ginsenoside Rb2** increases expression of SREBP and decreases levels of cholesterol and triglycerides[5]. In animal models of melanoma, this compound also suppresses neovascularization and tumor growth[6].

Ginsenosides Rb1 and Rg1 are two triterpene saponins that are responsible for the centrally-mediated effects of ginseng. In animal models, ginsenoside Rb1 improves energy metabolism by increasing food intake, skeletal muscle ATP content, and motor activity[7]. In animal models of aging, ginsenoside Rg1 ameliorates decreases in cognitive capacity and neurogenesis and suppresses astrocyte activation and inflammatory cytokine production. This compound also increases activity of glutathione peroxidase, superoxide dismutase, and telomerase, decreasing oxidative damage[8].

1. Attele AS, Wu JA, et al. Biochem. Pharm. 1999;58:1685-93.
2. Zhang YH, Li HD, Li B, et al. Oncol Rep. 2014 Feb;31(2):919-25.
3. Wang Y, Wang H, Liu Y, et al. Horm Metab Res. 2012 Jan;44(1):33-40.
4. Qiu J, Li W, Feng SH, et al. Genet Mol Res. 2014 May 9;13(2):3586-98.
5. Kim EJ, Lee HI, Chung KJ, et al. BMB Rep. 2009 Apr 30;42(4):194-9.
6. Sato K, Mochizuki M, Saiki I, et al. Biol Pharm Bull. 1994;17(5):635-9.
7. Tan SJ, Li N, Zhou F, et al. J Surg Res. 2014 May 2.
8. Zhu J, Mu X, Zeng J, et al. PLoS One. 2014 Jun 30;9(6):e101291.

Ginsenosides are found in Ginseng

LKT Products:

G3460 Ginsenoside F_1	G3456 Ginsenoside Rd	G3552 20(S)-Ginsenoside Rg_3
G3461 Ginsenoside F_2	G3457 Ginsenoside Re	G3558 20(R)-Ginsenoside Rh_2
G3462 Ginsenoside F_3	G3458 Ginsenoside Rg_1	N5778 Notoginsenoside R_1
G3454 Ginsenoside Rb_1	G3459 Ginsenoside Rg_2	P0253 Panaxadiol
G3453 Ginsenoside Rb_2	G3556 Ginsenoside Rg_3	P0254 Panaxatriol
G3554 Ginsenoside Rb_3	G3557 Ginsenoside Rh_1	P6957 Protopanaxadiol
G3455 Ginsenoside Rc	G3453 Ginsenoside Rh_2	P6958 Protopanaxatriol
		P7318 Pseudoginsenoside F11

Auraptene

Auraptene (A8070) is a monoterpene coumarin that can be found in many species of citrus fruits. Auraptene displays a broad variety of biological activities, including chemopreventive, anti-inflammatory, neuroprotective, anti-parasitic, antihypertensive, and anti-diabetic properties.

In animal models of carcinogenesis, auraptene prevents the development of oral cancer. Dietary administration of auraptene reduces the frequency of tongue carcinoma induced by 4-nitroquinoline 1-oxide. This effect is likely related to the ability of auraptene to increase activity of glutathione-S-transferase and quinone reductase[1].

In a model of N-methylnitrosourea-induced mammary carcinogenesis, auraptene delays tumor formation; it also arrests IGF-1-stimulated cell cycle progression at the S phase in breast cancer cells[2].

Auraptene limits LPS-induced neuro-inflammation in vivo as well. In these models, auraptene decreases activation of microglia and expression of COX-2[3].

In high fat diet-fed animals, auraptene suppresses hyperlipidemia and decreases triglyceride accumulation, potentially through activation of PPARα receptors. Administration of auraptene also improves diet-induced hyperglycemia and abnormal glucose tolerance[4].

1. Tanaka T, Kawabata K, Kakumoto M, et al. Carcinogenesis. 1998 Mar;19(3):425-31.
2. Krishnan P, Kleiner-Hancock H. Int J Breast Cancer. 2012;2012:502092.
3. Okuyama S, Yamamoto K, Mori H, et al. Evid Based Complement Alternat Med. 2014;2014:408503.
4. Takahashi N, Senda M, Lin S, et al. Mol Nutr Food Res. 2011 Dec;55(12):1791-7.

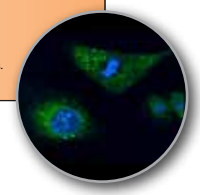

Auraptene decreases activation of microglia

Erucin

Erucin (E6880) is an isothiocyanate that can be found in arugula and other cruciferous vegetables. Erucin is a reduced analog of sulforaphane. Like other isothiocyanates, erucin exhibits a wide variety of biological activities in research models, including anticancer, antioxidative, chemopreventive, anti-inflammatory, and neuroprotective properties.

In cellular models, erucin suppresses benzo(a)pyrene-induced genotoxicity by inducing activity of detoxifying enzymes such as quinone reductase and glutathione-S-transferase[1-3]. Erucin also induces apoptosis in hepatocellular carcinoma cells and decreases telomerase activity in animal models of liver cancer[4]. In breast cancer cells, erucin induces cell cycle arrest and apoptosis by impairing microtubule dynamics[5].

The ability of erucin to increase levels of antioxidative enzymes is also neuroprotective. Erucin suppresses 6-OHDA-induced neurotoxicity and neuronal apoptosis in cellular models of Parkinson's disease[6].

Erucin also inhibits LPS-induced production of nitric oxide and PGE2 and expression of COX-2, IL-6, IL-1β, and TNF-α in macrophages. In animal models, erucin suppresses formation of phorbol ester-induced ear edema[7].

1. Hanlon N, Coldham N, Sauer MJ, et al. Chem Biol Interact. 2009 Jan 27;177(2):115-20.
2. Lamy E, Schröder J, Paulus S, et al. Food Chem Toxicol. 2008 Jul;46(7):2415-21.
3. Zhang Y, Talalay P, Cho CG, et al. Proc Natl Acad Sci U S A. 1992 Mar 15;89(6):2399-403.
4. Herz C, Hertrampf A, Zimmermann S, et al. J Cell Mol Med. 2014 Dec;18(12):2393-403.
5. Azarenko O, Jordan MA, Wilson L. PLoS One. 2014 Jun 20;9(6):e100599.
6. Tarozzi A, Morroni F, Bolondi C, et al. Int J Mol Sci. 2012;13(9):10899-910.
7. Cho HJ, Lee KW, Park JH. Int J Mol Sci. 2013 Oct 15;14(10):20564-77.

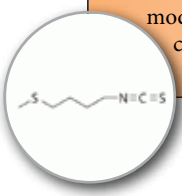

Erucin contains an N=C=S group, a feature of isothiocyanates

Indoles

Several indole-based compounds can be found in cruciferous vegetables such as cabbage, broccoli, and Brussels sprouts[1-2]. They are derived from a common parent compound, glucobrassicin. Consumption of cruciferous vegetables is linked to lower rates of cancer. Several indole compounds display anticancer properties[3-4].

In models of nasopharyngeal carcinoma, **Indole-3-carbinol (I5213)** inhibits cell proliferation and decreases tumor growth[5]. Indole-3-carbinol also displays anti-metastatic activity, suppressing cell migration and invasion and decreasing ERK signaling in breast cancer cells[6].

3,3'-Diindolylmethane (D3232) is a dimer of indole-3-carbinol. In cellular and animal models of nasopharyngeal carcinoma, 3,3'-diindolylmethane inhibits cellular invasion as well as metastasis and tumor growth; it also suppresses activity of HDAC2[7-8]. Additionally, this compound exhibits anti-inflammatory and immunomodulatory activities. 3,3'-Diindolylmethane limits the development of experimental autoimmune encephalitis (EAE) by suppressing T cell signaling in animal models[9].

Brassinin (B6801) inhibits DMBA-induced skin tumor formation and induces regression of mammary gland tumors[10-11].

1. Goetz JK, Schravdolf HR. Phytochemistry 1983;22:905-8.
2. Takasugi M, Katsui M, et al. J. Chem. Soc. Chem. Commun. 1986;1077-8.
3. Wattenberg LW, Loub WD. Cancer Res. 1978;38:1410-3.
4. Chung FL, Morse MA, Eklind KI. Cancer Res. 1992;52:2719s-22s.
5. Mao CG, Tao ZZ, Chen Z, et al. Exp Ther Med. 2014 Jul;8(1):207-12.
6. Hung WC, Chang HC. J Agric Food Chem. 2009 Jan 14;57(1):76-82.
7. Chen C, Chen SM, Xu B, et al. Carcinogenesis. 2013 Aug;34(8):1815-21.
8. Beaver LM, Yu TW, Sokolowski EI, et al. Toxicol Appl Pharmacol. 2012 Sep 15;263(3):345-51.
9. Rouse M, Rao R, Nagarkatti M, et al. J Pharmacol Exp Ther. 2014 Aug;350(2):341-52.
10. Mehta RG, Liu J, Constantinou A, et al. Carcinogenesis. 1995 Feb;16(2):399-404.
11. Banerjee T, Duhadaway JB, Gaspari P, et al. Oncogene. 2008 May 1;27(20):2851-7.

Indoles can be isolated from many cruciferous vegetables, including cabbage

Organosulfur Compounds

Many anticancer compounds that can be found in onion and garlic are organosulfurs; these are released when the bulbs are cut and exposed to oxygen. The relationship of organosufur compounds to cancer prevention has been the subject of several reviews[1-3]. These compounds display efficacy in the prevention of lung, esophagus, forestomach, colon, and mammary tumors[1].

Diallyl Sulfide (D3201) decreases diethylstilbestrol-induced DNA damage and carcinogenesis in vitro and in vivo; it also inhibits the development of colon polyps in other carcinogenesis models[4-5].

Allyl Disulfide (A4544) induces G2/M phase cell cycle arrest and apoptosis in leukemia cells[6]. Allyl disulfide also induces phase II enzyme activity[7].

Diallyl Trisulfide (D3202) induces phase II enzyme activity as well, increasing levels of catalase, superoxide dismutase, and glutathione peroxidase[8]. Diallyl trisulfide also suppresses histone deacetylase activity and prevents tumor growth in models of glioblastoma[9].

Like other organosulfurs, **Dipropyl Sulfide (D3262)** induces activity of phase II enzymes[10]. Additionally, this compound decreases N-nitrosamine-induced DNA damage in vitro and prevents the development of benzopyrene-induced carcinogenesis in vivo[11].

1. Wargovich MJ, Uda N, Woods C, et al. Biochem. Soc. Trans. 1996;24:811-4.
2. Lea MA. Adv. Exp. Med. Biol. 1996;401:147-54.
3. Wargovich MJ, Uda N. Adv. Exp. Med. Biol. 1996;401:171-7.
4. McCaskill ML, Rogan E, D Thomas R. Steroids. 2014 Sep 30.
5. Kang JS, Kim TM, Shim TJ, et al. Asian Pac J Cancer Prev. 2012;13(4):1115-8.
6. Dasgupta P, Bandyopadhyay SS. Nutr Cancer. 2013;65(4):611-22.
7. Chung LY. J Med Food. 2006 Summer;9(2):205-13.
8. Sumedha N, Miltonprabu S. Hum Exp Toxicol. 2014 Jul 25.
9. Wallace GC 4th, Haar CP, Vandergrift WA 3rd, et al. J Neurooncol. 2013 Aug;114(1):43-50.
10. Tsai CW, Liu KL, Lin CY, et al. . J Agric Food Chem. 2011 Apr 13;59(7):3398-405.
11. Srivastava SK, Hu X, Xia H, et al. Cancer Lett. 1997 Sep 16;118(1):61-7.

Organosulfur compounds can be found in onions and garlic

Antiretrovirals

Antiretrovirals are antiviral compounds that are active against HIV. Antiretrovirals can be grouped into several classes, including protease inhibitors, reverse transcriptase inhibitors, and integrase inhibitors[1].

Many reverse transcriptase inhibitors are nucleoside analogs that can be incorporated into viral DNA to prevent DNA replication. **Zalcitabine (D3212)** is a pyrimidine nucleoside analog used to treat HIV[2]. **Azidothymidine (A3212)** is a thymidine nucleoside analog; in addition to inhibiting reverse transcriptase, it also inhibits DNA polymerase[3].

Lopinavir (L5682) is an inhibitor of HIV protease with anticancer activity. In meningioma cells, this compound induces cell cycle arrest and inhibits cell growth[4]. **Indinavir Sulfate (I5313)** also shows anticancer activity, inhibiting adenocarcinoma tumor growth in vivo[5].

Elvitegravir (E4785) is an inhibitor of HIV integrase[6]. **HCKFWW (H3275)** is a peptide inhibitor of integrase-mediated 3' processing and integration that displays activity against HIV as well as other retroviruses[7].

1. Moore RD, Chaisson RE. AIDS. 1999 Oct 1;13(14):1933-42.
2. Balzarini J. Verh K Acad Geneeskd Belg. 1991;53(1):61-98.
3. Parker WB, White EL, Shaddix SC, et al. J Biol Chem. 1991 Jan 25;266(3):1754-62.
4. Johnson MD, O'Connell M, Pilcher W. J Neurooncol. 2011 Feb;101(3):441-8.
5. Toschi E, Sgadari C, Malavasi L, et al. Int J Cancer. 2011 Jan 1;128(1):82-93.
6. Shimura K, Kodama E, Sakagami Y, et al. J Virol. 2008 Jan;82(2):764-74.
7. Puras Lutzke RA, Eppens NA, Weber PA, et al. Proc Natl Acad Sci U S A. 1995 Dec 5;92(25):11456-60.

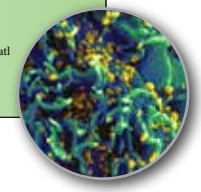

HIV attacks T cells

Azole Antifungals

Azole compounds are most often used as fungicides in agriculture and as human or veterinary anti-fungal agents. These compounds display a broad range of antifungal activity, suppressing infection of plants and animals by *Aspergillus*, *Botrytis*, *Malassezia*, *Candida*, and *Alternaria*. Azole antifungals act by inhibiting the enzyme sterol 14α-demethylase, preventing conversion of lanosterol to ergosterol. Suppressing levels of ergosterol prevents cell wall synthesis in fungi, as ergosterol is an essential component of the fungal cell wall[1].

Azoles include triazoles, thiazoles, and imidazoles.

1. Venkatakrishan K, von Moltke LL, Greenblatt D. J. Clin. Pharmacokinet. 2000;38:111-80.

Triazoles:
Fluconazole (F4682)
Itraconazole (I7870)
Cyproconazole (C9863)
Difenoconazole (D3320)
Epoxiconazole (E6259)
Tebuconazole (T1604)
Triticonazole (T7135)
Uniconazole (U5232)
Voriconazole (V5886)
Hexaconazole (H1992)

Imidazoles:
Ketoconazole (K1676)
Triflumizole (T6932)
Miconazole (M3309)
Tioconazole (T3357)
Clotrimazole (C4657)
Bifonazole (B3320)
Oxiconazole (O9234)
Butoconazole (B8278)
Fenticonazole (F1854)

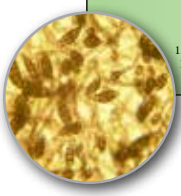

Spores of Alternaria alternata, *a common grain contaminant*

Fluoroquinolones

Fluoroquinolones are a group of broad-spectrum antibacterials. These compounds limit DNA synthesis by inhibiting activity of bacterial DNA gyrase as well as topoisomerase IV[1-2]. Fluoroquinolones are effective against both gram positive and gram negative bacteria.

Flouroquinolones can be classified into four generations according to antimicrobial activity[3]. First generation fluoroquinolones such as **Pipemidic Acid (P3461)** are mostly selective for DNA gyrase. Second generation fluoroquinolones such as **Norfloxacin (N5768)**, **Ofloxacin (O2144)**, and **Ciprofloxacin (C3262)** display improved efficacy against gram negative bacteria. **Pazufloxacin Mesylate (P0398), Sparfloxacin (S6000)**, and **Balofloxacin Dihydrate (B0246)** belong to third generation and show more significant activity against *Streptococcus*. **Clinafloxacin HCl (C4535), Moxifloxacin HCl (M5794)** are fourth generation fluoroquinolones that are less susciptible to the development of resistance.

Also available: **Levofloxacin HCl (L1786)**, **Orbifloxacin (O6805)**, **Enrofloxacin (E5369)**, **Besifloxacin HCl (B1973)** and others**.**

1. Levine C, Hiasa H, et al. Biochim. Biophys. Acta. 1998;1400:29-43.
2. Oliphant CM, Green GM. American Family Physician. 2002;65:455.
3. Owens RC Jr., Ambrose PG. Med. Clin. North. Am. 2000;84: 1447

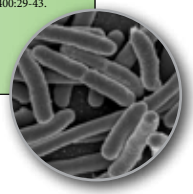

Escherichia coli, *a common target of antibiotics*

Dihydroartemisinin

Dihydroartemisinin (A6979) is a sesquiterpene lactone that can be found in *Artemesia*. Dihydroartemisinin is the active metbolite of all artemisinin compounds; this group of products is best known for their antimalarial activity. Commercial dihydroartemisinin is used in the treatment of malaria alone or in combination with piperaquine[1]. Dihydroartemisinin appears to have fewer systemic side effects than other malaria treatments, such as **Artesunate (A6982)**.

Dihydroartemisinin displays a variety of antimicrobial benefits, including anti-parasitic and antiviral activities. In addition to inhibiting growth and survival of *Plasmodium*, this compound also inhibits proliferation of *Schistosoma*[2].

Dihydroartemisinin also displays anticancer activity. In colorectal cancer cells, dihydroartemisinin induces mitochondria-dependent apoptosis and increases levels of reactive oxygen species and Bax[3]. This compound also inhibits mTORC1 in rhabdomyosarcoma cells[4].

Additionally, dihydroartemisinin decreases release of Th2 cytokines and infiltration of inflammatory cells in animal models of asthma, suppressing airway hyper-responsiveness[6].

1. Wanzira H, Kakuru A, Arinaitwe E, et al. Clin Infect Dis. 2014 May 13.
2. Li HJ, Xu FL, Wang YH, et al. Parasitol Res. 2014 Jan;113(1):239-41.
3. Ontikatze T, Rudner J, Handrick R, et al. Front Oncol. 2014 May 19;4:116.
4. Odaka Y, Xu B, Luo Y, et al. Carcinogenesis. 2014 Jan;35(1):192-200.
5. Cabello CM, Lamore SD, Bair WB 3rd, et al. Invest New Drugs. 2012 Aug;30(4):1289-301.
6. Wei M, Xie X, Chu X, et al. Immunopharmacol Immunotoxicol. 2013 Jun;35(3):382-9.

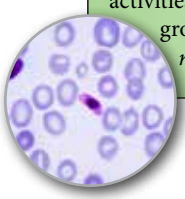

Dihydroartemisinin inhibits survival of Plasmodium falciparum

Soy Isoflavones

Many isoflavones can be found in soy, including **Genistein (G1652)** and **Daidzein (D0032)**; these compounds are also phenolic phytoestrogens. Isoflavones such as these can also be found in beans and other legumes.

Genistein induces activity of phase II enzymes such as superoxide dismutase, Nrf2, and heme oxygenase 1 in vitro[1]. In animals fed a high fat diet, genistein decreases body weight, liver weight, lipid levels, and insulin dysregulation by inhibiting S6K1 signaling[2]. In colon cancer cells, genistein induces G2/M phase cell cycle arrest and apoptosis[3].

Daidzein also displays antioxidative and anticancer benefits. In vivo, daidzein increases levels of superoxide dismutase, catalase, glutathione peroxidase, and glutathione-S-transferase, inhibiting DMBA-induced development of breast cancer[4].

Biochanin A (B3358) is another soy isoflavone. In pancreatic cancer cells, this compound inhibits cellular proliferation, migration, and invasion[5]. Biochanin A also improves cognitive deficits in animal models of Alzheimer's disease[6].

Formononetin (F5770) also exhibits antioxidative properties, increasing activity of superoxide dismutase and glutathione peroxidase in animal models of traumatic brain injury[7].

1. Lee SH, Kim JK, Jang HD. Int J Mol Sci. 2014 Jun 12;15(6):10605-21.
2. Arunkumar E, Karthik D, Anuradha CV. Pharm Biol. 2013 Jul;51(7):815-24
3. Wu J, Xu J, Han S, et al. Wei Sheng Yan Jiu. 2014 Jan;43(1):1-5.
4. Mishra P, Kar A, Kale RK. Mol Cell Biochem. 2009 May;325(1-2):149-57.
5. Bhardwaj V, Tadinada SM, Jain A, et al. Anticancer Drugs. 2014 Mar;25(3):296-302.
6. Biradar SM, Joshi H, Chheda TK. Hum Exp Toxicol. 2014 Apr;33(4):369-82.
7. Li Z, Dong X, Zhang J, et al. J Neurol Sci. 2014 Mar 15;338(1-2):112-7.

Soybeans and other legumes are significant sources of isoflavones

Green Tea Catechins

Green tea catechins are polyphenols that can be found in green tea (*Camellia sinensis*). Green tea catechins display a variety of known biological properties, including antioxidative, antimicrobial, anticancer, and anti-inflammatory activities.

Epigallocatechin Gallate (EGCG, G6234) is a flavonoid isolated from green tea. Epigallocatechin gallate directly inhibits the aryl hydrocarbon receptor and STAT3, two activities potentially linked to its chemopreventive properties[1]. In animal models of bladder cancer, this compound decreases tumor growth; in other cellular models of cancer, it indirectly inhibits EGFR and induces apoptosis[2-3].

Catechin (C0278, 99%) is a flavonoid isolated from green tea that displays similar activities. Catechin decreases tumor number and formation in animal models of colorectal cancer[4]. This compound also increases life span in *Caenorhabditis elegans* and inhibits MAO-B in vitro[5].

In animal models of myocardial ischemia and reperfusion, **Epicatechin (E6231)** decreases myocardial infarct size and improves mitochondrial respiration[6]. **Epicatechin Gallate (ECG, E6232)** and **Epigallocatechin (EGC, E6233)** exhibit agonist activity at cannabinoid 1 receptors[7]. **Gallocatechin (G0243)** exhibits antiviral activity, inhibiting HIV-1 reverse transcriptase and integrase[8]. Gallocatechin also inhibits α-amylase, decreasing absorption of carbohydrates and limiting increases in blood glucose levels[9].

1. Wang Y, Ren X, Deng C, et al. Oncol Rep. 2013 Dec;30(6):2691-6.
2. Ma YC, Li C, Gao F, et al. Oncol Rep. 2014 Mar;31(3):1343-9.
3. Jankun J, Keck RW, Selman SH. Int J Oncol. 2014 Jan;44(1):147-52.
4. Weyant MJ, Carothers AM, Dannenberg AJ, et al. Cancer Res. 2001 Jan 1;61(1):118-25.
5. Saul N, Pietsch K, Menzel R, et al. Mech Ageing Dev. 2009 Aug;130(8):477-86.
6. Yamazaki KG, Andreyev AY, Ortiz-Vilchis P, et al. Int J Cardiol. 2014 Aug 1;175(2):297-306.
7. Korte G, Dreiseitel A, Schreier P, et al. Phytomedicine. 2010 Jan;17(1):19-22.
8. Jiang Y, Ng TB, Liu Z, et al. Biosci Rep. 2010 Nov 30.
9. Tsujita T, Shintani T, Sato H. J Agric Food Chem. 2013 May 15;61(19):4570-6.

Green tea contains a wide variety of catechins

7,8-Dihydroxyflavone Hydrate

7,8-Dihydroxyflavone Hydrate (D3329) is a flavone that can be found in *Godmania aesculifolia*, *Tridax procumbens*, and primula tree leaves. This compound exhibits a wide variety of biological activities in research models, including neuromodulatory, anti-obesity, antioxidative, anti-inflammatory, anti-cancer, and antihypertensive properties.

7,8-Dihydroxyflavone hydrate (DHF) is a brain-derived neurotrophic factor (BDNF) mimetic that activates TrkB receptors; it promotes synaptic plasticity and improves cognitive function in models of schizophrenia and neurodegenerative diseases such as Parkinson's disease, Alzheimer's disease, and amyotrophic lateral sclerosis (ALS)[1-4].

DHF not only prevents the induction of diet-induced obesity in animal models but also decreases adiposity, increases energy expenditure, and improves insulin sensitivity in already-obese animals[5].

In other research models, DHF induces apoptosis and inhibits cell growth in oral squamous cell carcinoma cells[6]. This compound also protects keratinocytes against hydrogen peroxide- and UV light-induced oxidative damage[7].

1. Sconce MD, Churchill MJ, Moore C, et al. 2015 Apr 2;290:454-71.
2. Yang YJ, Li YK, Wang W, et al. Pharmacol Biochem Behav. 2014 Jul;122:30-6.
3. Korkmaz OT, Aytan N, Carreras I, et al. Neurosci Lett. 2014 Apr 30;566:286-91.
4. Castello NA, Nguyen MH, Tran JD, et al. PLoS One. 2014 Mar 10;9(3):e91453.
5. Chan CB, Tse MC, Liu X, et al. 2015 Mar 19;22(3):355-68.
6. Lee RH, Shin JC, Kim KH, et al. Oncol Rep. 2015 Feb;33(2):631-8.
7. Ryu MJ, Kang KA, Piao MJ, et al. Int J Mol Med. 2014 Apr;33(4):964-70.

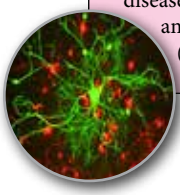

7,8-Dihydroxyflavone activates Trk receptors on neurons

Luteolin

Luteolin (L8377) is a flavone that can be found in many sources, including celery, broccoli, dandelion, thyme, rosemary, oranges, and carrots. Many flavonoids, including luteolin, have a yellow crystalline appearance.

Luteolin exhibits a broad range of biological activities, including anti-inflammatory, antihypertensive, anticancer, anti-diabetic, antioxidative, and neuromodulatory properties. This compound inhibits HSP90, IGF-1R, and phosphodiesterases 1-5; it also potentiates activity at dopamine and norepinephrine transporters[1-4].

Likely related to these targets, luteolin decreases tumor volume and weight in animal models with gastric carcinoma xenografts[5]. Luteolin also inhibits LPS-induced production of IL-6 in the brain by suppressing phosphorylation of JNK and activation of AP-1[6].

In animal models of diet-induced obesity, luteolin suppresses high fat diet-induced body weight gain, fat deposition, and adipocyte hypertrophy; it also improves glucose intolerance and insulin sensitivity and reduces infiltration of mast cells and macrophages as well as levels of pro-inflammatory cytokines[7].

1. Chen D, Bi A, Dong X, et al. Biochem Biophys Res Commun. 2014 Jan 3;443(1):326-32.
2. Yang Y, Shen J, Yu X, et al. Chembiochem. 2013 May 27;14(8):929-33.
3. Yu MC, Chen JH, Lai CY, et al. Eur J Pharmacol. 2010 Feb 10;627(1-3):269-75.
4. Zhao G, Qin GW, Wang J, et al. Neurochem Int. 2010 Jan;56(1):168-76.
5. Lu XY, Li YH, Xiao XW, et al. Zhonghua Yi Xue Za Zhi. 2013 Jan 8;93(2):142-6.
6. Jang S, Kelley KW, Johnson RW. Proc Natl Acad Sci U S A. 2008 May 27;105(21):7534-9.
7. Xu N, Zhang L, Dong J, et al. Mol Nutr Food Res. 2014 Jun;58(6):1258-68.

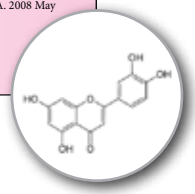

Luteolin features a distinctive flavone ring structure

Immunosuppressive Agents

Immunosuppressive compounds inhibit the immune response and are used to treat diseases related to autoimmunity, inflammation, and transplant rejection.

Agents such as **Rapamycin (R0161)** bind cytosolic protein FK-binding protein 12 (FKBP12), preventing it from associating with mTORC1. This inhibits the activity of IL-2, preventing activation of B and T cells and limiting the ability of the immune system to mount an effective response against non-host entities[1]. As a result, rapamycin is primarily used to prevent the rejection of transplanted tissues and organs[2].

Tacrolimus (T0008) is used to lower transplant rejection rates by utilizing a similar mechanism of action. Tacrolimus also binds FKBP12, but interacts with and inhibits calcineurin, preventing T cell signal transduction and IL-2 production[3].

Mitomycin C (M3377) is a cytostatic DNA cross-linking agent that inhibits cell division; it suppresses proliferation of B and T cells and is used to limit cancer cell growth and prevent host reactions during eye sugeries[4].

Dexamethasone (D1963) is a glucocorticoid (GC) receptor agonist that is used to treat inflammatory and autoimmune diseases such as rheumatoid arthritis and asthma[5]. Activation of the GC receptor stimulates a negative feedback loop that suppresses immune signaling. Also available: **Dexamethasone Sodium Phosphate (D1965)** and **Dexamethasone Acetate (D1694)**.

1. Morris RE. Immunol Today. 1991 May;12(5):137-40.
2. Klintmalm GB, Nashan B. J Transplant. 2014;2014:845438.
3. Azzi JR, Sayegh MH, Mallat SG. J Immunol. 2013 Dec 15;191(12):5785-91.
4. Santhiago MR, Netto MV, Wilson SE. Cornea. 2012 Mar;31(3):311-21.
5. Reeves EK, Rayavarapu S, Damsker JM, et al. Endocr Metab Immune Disord Drug Targets. 2012 Mar;12(1):95-103.

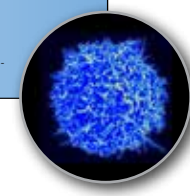

Immunosuppressants prevent activation of T cells

All-trans Retinol

All-trans Retinol (R1876) is a retinoic acid receptor (RAR) and retinoid X receptor (RXR) agonist and one of many forms of vitamin A. Vitamin A is an essential nutrient necessary for effective vision, skin health, and bone growth.

All-trans retinol induces cell differentiation, playing a significant role in embryonic growth and development. This compound is also used in research models to induce differentiation of stem cells to study development and function of various cell lineages[1].

The ability of all-trans retinol to induce cell differentiation shows benefit in cancer models. All-trans retinol induces differentiation of glioblastoma multiforme cancer stem cells, decreasing cancer cell migration and proliferation[2].

In the immune system, retinol appears to play a protective role in autoimmune diseases such as multiple sclerosis. In animal models of experimental autoimmune encephalitis (EAE), this compound downregulates pro-inflammatory responses stimulated by Th1 and Th17 cells and reduces disease severity[3].

Other retinoids available include:
All-trans Retinol, high purity (R1877)
Trans-retinoic Acid (R1870)
13-Cis Retinoic Acid (R1779)
9-Cis Retinoic Acid (R1777)
Retinyl Palmitate (R1879)
Retinyl Acetate (R1878)
N-(4-carbethoxyphenyl)retinamide (C0170)
N-(4-hydroxyphenyl)retinamide (H9613)
Etretinate (E7668)
Adapalene (A1202)
Acitretin (A0933)

1. Duester G. Cell. 2008 Sep 19;134(6):921-31.
2. Friedman MD, Jeevan DS, Tobias M, et al. Oncol Rep. 2013 Oct;30(4):1645-50.
3. Zhan XX, Liu Y, Yang JF, et al. Immunology. 2013 Apr;138(4):333-45.

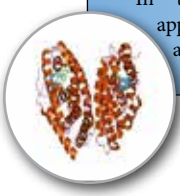

All-trans retinol activates retinoid X receptors

Cathepsin K Inhibitors

Cathepsin K is a lysosomal cysteine protease involved in bone remodeling and resorption. Cathepsin K is produced by osteoclasts and secreted to break down bone and cartilage by catabolizing elastin, collagen, and gelatin[1]. This protease plays a major role in the development of osteoporosis.

Osteoporosis is a bone disease characterized by decreased bone density and increased risk of fracture or breakage. Under normal conditions, bone mass undergoes remodeling continually by osteoclasts, which degrade the bone matrix, and osteoblasts, which rebuild the bone matrix.

Osteoclasts are activated by a number of signaling mediators from NF-κB, Wnt, and eicosanoid pathways[2]. These are all involved in several signaling pathways, making them poor targets in the treatment of osteoporosis. Because the primary role of cathepsin K is in the management of bone remodeling and it is highly localized in osteoclasts, it makes an excellent target for bone disease management.

Cathepsin K inhibitors such as **Odanacatib (O1200)** and **Balicatib (B0245)** increase bone mineral density and formation rates and decrease bone resorption, protecting against the development of osteoporosis-related bone fractures[3-5].

1. Inaoka T, Bilbe G, Ishibashi O, et al. Biochem Biophys Res Commun. 1995 Jan 5;206(1):89-96.
2. Wu S, Liu Y, Zhang L, et al. Genome Med. 2013 May 29;5(5):44.
3. Bone HG, Dempster DW, Eisman JA, et al. Osteoporos Int. 2015 Feb;26(2):699-712.
4. Gauthier JY, Chauret N, Cromlish W, et al. Bioorg Med Chem Lett. 2008 Feb 1;18(3):923-8.
5. Jerome C, Missbach M, Gamse R. 2012 Jan;23(1):339-49.

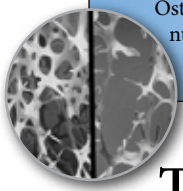

Osteoporosis (right) involves the degradation of normal bone structure (left)

Toll-like Receptor Modulators

Toll-like receptors (TLRs) are pattern recognition receptors expressed in immune cells such as macrophages and dendritic cells; they play a significant role in the development of the innate immune response.

These receptors recognize structurally conserved molecules shared by classes of pathogens. These structures are referred to as pathogen-associated molecular patterns. Although associated with pathogens, some structures can also be found endogenously. There are 11 isoforms of TLRs, and each recognizes distinct ligands, including single-stranded RNA, double-stranded RNA, lipopolysaccharides, CpG DNA, and bacterial peptidoglycans[1].

TLRs are involved in propagation of signals for inflammation, phagocytosis, antigen presentation, and other immune responses, making them good targets for compounds that regulate inflammation, allergic reactions, and autoimmune diseases.

VGX-1027 (V2792) is an inhibitor of TLR4, a receptor that recognizes many endogenous structures. This compound inhibits antigen presentation in models of systemic lupus erythmatosus[2].

TLR7 and TLR8 recognize viral RNA sequences. **Imiquimod (I5034)** is an agonist at these receptors, stimulating a Th1-based immune response against Japanese encephalitis virus[3].

Limonin (L3550) is a natural product isolated from citrus fruits that down-regulates expression of TLR2 and TLR4, suppressing pro-inflammatory cytokine release[4].

1. Roach JC, Glusman G, Rowen L, et al. Proc Natl Acad Sci U S A. 2005 Jul 5;102(27):9577-82.
2. Fagone P, Muthumani K, Mangano K, et al. Immunology. 2014 Aug;142(4):594-602.
3. Nazmi A, Mukherjee S, Kundu K, et al. 2014 Sep;69:235-47.
4. Mahmoud MF, Gamal S, El-Fayoumi HM. 2014 Oct 5;740:676-82.

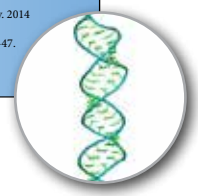

Some toll-like receptors can recognize double-stranded RNA

Aflatoxins

Aflatoxins are mycotoxins initially produced by *Aspergillus flavus* and *Aspergillus parasiticus*. These toxins often occur in poorly stored grains and nuts. Commercially, aflatoxins have been found in peanut butter and various cooking oils. Aflatoxins are highly cytotoxic and carcinogenic; with chronic exposure, cirrhosis of the liver and hepatocellular carcinoma may develop[1]. Aflatoxins form DNA adducts, preventing replication of DNA and inducing cell cycle arrest.

Aflatoxin M1 (A2052) and **Aflatoxin M2 (A2054)** are hydroxylated metabolites of **Aflatoxin B1 (A2044)** and **Aflatoxin B2 (A2046)** produced by metabolic enzymes in the liver[2].

Aflatoxin B1 is considered the most cytotoxic of all aflatoxins as it is skin-permeable, highlighting potential risk for agricultural workers exposed to contaminated harvests[3]. Additionally, aflatoxin B1 displays immunosuppressive activity, inhibiting humoral and cell-mediated immune responses[4].

Also available: **Aflatoxicol (A2244)**, **Aflatoxin G1 (A2048)**, and **Aflatoxin G2 (A2050)**.

1. Miliță NM, Mihăescu G, Chifiriuc C. Bacteriol Virusol Parazitol Epidemiol. 2010 Jan-Mar;55(1):19-24.
2. Dutton MF, Ehrlich K, Bennett JW. Appl Environ Microbiol. 1985 Jun;49(6):1392-5.
3. Boonen J, Malysheva SV, Taevernier L, et al. Toxicology. 2012 Nov 15;301(1-3):21-32.
4. Sirajudeen M, Gopi K, Tyagi JS, et al. Environ Toxicol. 2011 Apr;26(2):153-60.

Some aflatoxins are produced by Aspergillus flavus

Trichothecene Mycotoxins

Trichothecene mycotoxins were first produced by various species of *Fusarium, Trichoderma, Myrothecium, Trichothecium, Cephalosporium, Verticimonosporium*, and *Stachybotrys*.

These toxins can be found in grains used in cereals and livestock feed. Trichothecenes can be absorbed through the skin as well as in the intestinal mucosa, making them highly toxic. Unlike many other toxins, this group of compounds does not require metabolic activation to exert biological activity. These mycotoxins bind ribosomes and inhibit protein synthesis[1].

Type A trichothecenes, including **T-2 Toxin (T0002), HT-2 Toxin (T7676)**, and **Diacetoxyscirpenol (D3200)**, are more potent than type B trichothecenes such as **15-Acetyl-deoxynivalenol (D1761), Nivalenol (N3584), 3-Acetyl-deoxynivalenol (D1760)**, and **Deoxynivalenol (D1759)**.

Interest in trichothecene toxins is on the rise as new studies are published examining the abilities of these compounds to impair the immune response, disrupt oocyte maturation, and inhibit production of hormones such as growth hormone and testosterone[2-5]. Other research highlights the high frequency with which trichothecenes contaminate grain products; in some studies, up to 80% of grain samples exhibit trichothecene contamination[6].

Also available: **Neosolaniol (N1858), 15-Acetoxyscirpenol (A0818), T2 Triol (T0004), Fusarenon X (F8272),** and **T2 Tetraol (T0003)**.

1. Hassan YI, Watts C, Li XZ, et al. Toxins (Basel). 2015 Jun 2;7(6):1989-2005.
2. Savard C, Gagnon CA, Chorfi Y. Vaccine. 2015 Jul 31;33(32):3881-6.
3. Zhu CC, Zhang Y, Duan X, et al. Arch Toxicol. 2015 Jul 3.
4. Wan D, Wang X, Wu Q, et al. Toxicol Sci. 2015 Jul 2.
5. Yang JY, Zhang YF, Li YX, et al. Toxicol Ind Health. 2015 Jun 17.
6. Rodrigues I, Naehrer K. Toxins (Basel). 2012 Sep; 4(9):663-75.

Trichothecene mycotoxins are present in grains such as wheat

Marine Toxins

Many microorganisms produce toxins capable of causing disease through interaction with biological macromolecules such as enzymes or cellular receptors. Marine organisms such as algae and sea sponges produce a wide variety of toxins, some of which are responsible for shellfish poisoning.

12-Desmethyl Spirolide C (S6236) is a cyclic imine marine toxin produced by species of the dinoflagellate *Alexandrium*; this compound blocks nicotinic acetylcholine receptors (nAChRs), inducing neuromuscular block and muscle paralysis[1].

Microcystin LR (M3406) is a cyclic heptapeptide produced by species of cyanobacteria *Microcystis*; like other cyanotoxins, microcystin LR inhibits serine phosphatases PP1 and PP2A[2].

Another inhibitor of serine phosphatases is **Okadaic Acid (O4101)**, a neurotoxin that is also produced by dinoflagellates and sea sponges[3].

α-Conotoxin GI (C5655) is a toxin produced by sea snails that inhibits nAChRs. This peptide binds nAChRs at αγ and αδ interfaces, inhibiting signaling at the neuromuscular junction and inducing muscle paralysis[4].

Microginins such as **Microginin 527 (M3208), Microginin 690 (M3210)**, and **Microginin 704 (M3212)** are inhibitors of protein phosphatases and are produced by species of cyanobacteria *Microcystis*. These compounds also inhibit leucine aminopeptidase and angiotensin-converting enzyme (ACE)[5].

Brevetoxins are lipid-soluble polyether neurotoxins produced by the dinoflagellate *Karenia*. Brevetoxins act as sodium channel agonists, binding neurotoxin site 5 on Nav1.4 and Nav1.5 voltage-gated sodium channels in skeletal muscle and cardiac tissue[6]. This action opens the channels, resulting in bronchoconstriction and airway inflammation in vivo[7]. **Brevetoxin 2 (B6917)** and **Brevetoxin 3 (B6918)** are likely a cause of neurotoxic shellfish poisoning.

Oscillamide Y (O7213) is a marine toxin isolated from species of the cyanobacterium *Planktothrix* (*Oscillatoria*). Like microcystins, this toxin is also a cyclic peptide that inhibits protein phosphatases such as PP1 and PP2A[8].

Anabaenopeptins are cyclopentapeptides isolated from cyanobacteria such as *Microcystis aeruginosa* and *Oscillatoria agardhii*. Like other cyanotoxins, anabaenopeptins are typically inhibitors of serine proteases and protein phosphatases[9]. Anabaenopeptins may also inhibit carboxypeptidases. **Anabaenopeptin B (A5201)** and **Anabaenopeptin F (A5203)** are considered "nontoxic" variants.

Also available: other **Microcystins, Anabaenopeptins, Oscilloginins, Aeruginosamides, Cyanopeptolins,** and **Microginins.**

1. Marrouchi R, Rome G, Kharrat R, et al. Toxicon. 2013 Dec 1;75:27-34.
2. Liang J, Li T, Zhang YL, et al. J Zhejiang Univ Sci B. 2011 Dec;12(12):951-60.
3. Mori N, Ishikawa C, Uchihara JN, et al. Curr Cancer Drug Targets. 2013 Oct;13(8):829-42.
4. Hann RM, Pagán OR, Gregory LM, et al. Biochemistry. 1997 Jul 22;36(29):9051-6.
5. Schatz D, Keren Y, Vardi A, et al. Environ Microbiol. 2007 Apr;9(4):965-70.
6. Bottein Dechraoui MY, Ramsdell JS. Toxicon. 2003 Jun;41(7):919-27.
7. Zaias J, Fleming LE, Baden DG, et al. Inhal Toxicol. 2011 Mar;23(4):205-11.
8. Sano T, Usui T, Ueda K, et al. J Nat Prod. 2001 Aug;64(8):1052-5.
9. Gesner-Apter S, Carmeli S. J Nat Prod. 2009 Aug;72(8):1429-36.

Microcystis aeruginosa, *a source of many marine toxins*

Sodium Channel Modulators

Sodium channels are transmembrane ion channels. The majority of sodium channels are voltage-gated channels involved in propagation of action potentials. In response to electrical current, activation gates open and sodium ions flow into the cell; this increases membrane voltage, forming the start of an action potential.

Sodium channels are found primarily on neurons, cardiac myocytes, gastrointestinal smooth muscle cells, and skeletal muscle cells[1]. Mutations or other alterations in sodium channels are associated with epilepsy, seizures, pain, and cardiac arrhythmia.

Aconitine (A0958) is a toxin that can be found in *Aconitum* that binds neurotoxin binding site 2 of sodium channels. This prevents channel closure, allowing continual depolarization and eventually paralysis[3].

Sodium channel blockers such as **Proxymetacaine HCl (P7059)** and **Propofol (P6870)** are often clinically used as anesthetics[3-4].

Duloxetine HCl (D8145), a serotonin-norepinephrine reuptake inhibitor, exhibits benefit as a potential treatment for neuropathy and fibromyalgia. This activity is likely due to its ability to block voltage-gated $Na_v1.7$ sodium channels, which are involved in fibromyalgia and pain signaling[5].

1. Yu FH and Catterall WA. Genome Biol. 2003;4(3):207.
2. Chan TY. Aconite poisoning. Clin Toxicol (Phila). 2009 Apr;47(4):279-85.
3. Jauregui MJ, Sanders TJ, Polse KA. J Am Optom Assoc. 1980 Jan;51(1):37-41.
4. Kotani Y, Shimazawa M, Yoshimura S, et al. CNS Neurosci Ther. 2008 Summer;14(2):95-106.
5. Wang SY, Calderon J, Kuo Wang G. Anesthesiology. 2010 Sep;113(3):655-65.

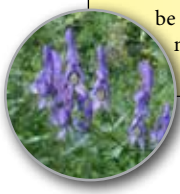

Aconitine is a sodium channel modulator found in Aconitum

Levetiracetam

Levetiracetam (L1784) is the S-enantiomer of etiracetam; it is used as an anticonvulsant in the prevention of seizures and epilepsy. Levetiracetam also exhibits potential as a treatment for other psychiatric and neurological disorders, including anxiety disorder, autism, and Tourette syndrome[1].

Levetiracetam alters calcium signaling, although it does not directly interact with calcium channels. Instead, this compound binds a particular synaptic vesicle glycoprotein (SV2A) common to all synaptic and endocrine vesicles[2]. SV2A plays a role in calcium-induced vesicle fusion, action potential proliferation, normal CNS function, and survival. Altering SV2A function suppresses presynaptic calcium release, reduces excitatory postsynaptic potentials, and inhibits synaptic transmission[3]. This also alters synaptic release of neurotransmitters and other signaling molecules.

Levetiracetam also exhibits activity in models of Alzheimer's disease. Administration of levetiracetam reverses behavioral abnormalities, synaptic dysfunction, hippocampal remodeling, and learning and memory deficits in animal models[4].

1. Farooq MU, Bhatt A, Majid A, et al. Am J Health Syst Pharm. 2009 Mar 15;66(6):541-61.
2. Lynch BA, Lambeng N, Nocka K, et al. Proc Natl Acad Sci U S A. 2004 Jun 29;101(26):9861-6.
3. Vogl C, Mochida S, Wolff C, et al. Mol Pharmacol. 2012 Aug;82(2):199-208.
4. Sanchez PE, Zhu L, Verret L, et al. Proc Natl Acad Sci U S A. 2012 Oct 16;109(42):E2895-903.

Synaptic vesicles help transmit signals across synapses

Antidepressants

Antidepressants are clinically used to treat major depressive disorder; they can be grouped in several categories by their mechanism of action: selective serotonin reuptake inhibitors (SSRIs) inhibit the serotonin transporter (SERT), serotonin-norepinephrine reuptake inhibitors (SNRIs) inhibit SERT and the norepinephrine transporter (NET), monoamine oxidase inhibitors (MAOIs) inhibit monoamine oxidase (MAO), and tricyclic antidepressants (TCAs) typically inhibit SERT, NET, and various serotonin receptors.

In addition to its antidepressant activity, **Fluoxetine HCl (F4780)** also increases abstinence rates in former heroin-dependent subjects when combined with naltrexone versus naltrexone alone[1]. **Paroxetine HCl (P0297)** decreases amyloid-β levels when administered to subjects with Alzheimer's disease[2].

Amitriptyline HCl (A5235) is a TCA that increases neurite outgrowth and decreases cell death in neurons[3]. **Moclobemide (M5610)** displays similar neuroprotective activity, inducing hippocampal neurogenesis and increasing progenitor cell proliferation and expression of BDNF in vitro[4].

Venlafaxine HCl (V1854) inhibits SERT, NET, and MAO. This compound also improves cognitive performance and decreases oxidative stress parameters in animal models of Huntington's disease[5].

1. Krupitsky EM, Zvartau EE, Masalov DV, et al. J Subst Abuse Treat. 2006 Dec;31(4):319-28.
2. Aboukhatwa M, Luo Y. J Alzheimers Dis. 2011;24(2):221-34.
3. Jang SW, Liu X, Chan CB, et al. Chem Biol. 2009 Jun 26;16(6):644-56.
4. Li YF, Zhang YZ, Liu YQ, et al. Acta Pharmacol Sin. 2004 Nov;25(11):1408-12.
5. Kumar P, Kalonia H, Kumar A. Behav Pharmacol. 2010 May;21(3):217-30.

There are many different antidepressants, all targeting different receptors and enzymes

TRP Channel Modulators

Transient receptor potential (TRP) channels are ion channels located on the plasma membrane of many different cell types. TRP channels play a significant role in sensory transduction, pain signal relay, temperature, taste, and pressure.

TRP vanilloid (TRPV) channels are the most well-studied of these channels. **Capsaicin (C0266)** and **Piperine (P3465)** are TRPV channel activators that can be found in plant sources and are responsible for the hot or spicy flavor of some peppers[1].

TRP canonical (TRPC) channels are often found on cardiomyocytes and nerves; TRPC channels play a role in cardiac hypertrophy[2]. Amyotrophic lateral sclerosis (ALS) treatment **Riluzole (R3347)** activates TRPC5 channels. **Clemizole (C4417)**, an NS4B and histamine receptor blocker, inhibits TRPC5 channels, potentially regulating neurite length[3].

TRP melastatin-like (TRPM) channels are involved in temperature and taste transduction as well as cell adhesion. **Ginsenoside Rd (G3456)** inhibits TRPM7 channels and **Pregnenolone (P7023)** activates TRPM3 channels[4-5]. **Icillin (I0933)** activates TRPM8 channels and inhibits TRPV3 channels, acting as a cooling agent[6].

TRP ankyrin (TRPA) channels are mechanical stress sensors expressed in the spinal cord and on hair cells. Activators of TRPA channels include **1'-Acetoxychavicol Acetate (A0817), Parthenolide (P0270),** and **Etodolac (E7556)**[7-9].

Other TRP channels include TRP polycystin (TRPP) channels and TRP mucolipin (TRPML) channels.

1. Kissin I. Anesth Analg. 2008 Jul;107(1):271-81.
2. Bush EW, Hood DB, Papst PJet al. J Biol Chem. 2006 Nov 3;281(44):33487-96.
3. Richter JM, Schaefer M, Hill K. Mol Pharmacol. 2014 Nov;86(5):514-21.
4. Kim BJ. J Ginseng Res. 2013 Apr;37(2):201-9.
5. Wagner TF, Loch S, Lambert S, et al. Nat Cell Biol. 2008 Dec;10(12):1421-30.
6. Sherkheli MA, Gisselmann G, Hatt H. ScientificWorldJournal. 2012;2012:982725.
7. Narukawa M, Koizumi K, Iwasaki Y, et al. Biosci Biotechnol Biochem. 2010;74(8):1694-6.
8. Materazzi S, Benemei S, Fusi C, et al. Pain. 2013 Dec;154(12):2750-8.
9. Wang S, Dai Y, Kogure Y, et al. J Neurosci Res. 2013 Dec;91(12):1591-8.

TRP channels were initially discovered in Drosophila

Fluoxetine Hydrochloride

Selective serotonin reuptake inhibitors (SSRIs) are antidepressants. These compounds increase central serotonin levels by blocking serotonin transporters (SERTs); this increase in extracellular serotonin activates serotonin receptors. Serotonin is a neurotransmitter that plays a key role in mood, arousal, learning, and cardiovascular function. **Fluoxetine HCl (F4780)** is one SSRI that is commonly used to treat a wide variety of mood disorders.

Fluoxetine also boosts extracellular concentrations of norepinephrine as well as dopamine in the prefrontal cortex of animal models[1]. Fluoxetine inhibits SERT, acts as an antagonist at 5-HT2A/2C receptors, and acts as an agonist at σ1 receptors[2-3].

SSRIs such as fluoxetine also display analgesic activity. Systemic administration of fluoxetine inhibits nociception in animals undergoing tail immersion and hot plate assays[4]. Fluoxetine-induced antinociception likely involves both central opioid as well as serotoninergic pathways[5]. This compound's ability to indirectly modulate opioid signaling also suggests potential efficacy as a heroin relapse prevention agent[6].

1. Bymaster FP, Zhang W, Carter PA, et al. Psychopharmacologia. 2002;160(4):353-61.
2. Pälvimäki EP, Roth BL, Majasuo H, et al. Psychopharmacology (Berl). 1996 Aug;126(3):234-40.
3. Narita N, Hashimoto K, Tomitaka S, et al. Eur J Pharmacol. 1996 Jun 20;307(1):117-9.
4. Anjaneyulu M and Chopra K. Eur J Pharmacol. 2006 May 24;538(1-3):80-4.
5. Singh VP, Jain NK, Kulkarni SK. Brain Res. 2001;915(2):218-26.
6. Krupitsky EM, Zvartau EE, Masalov DV, et al. J Subst Abuse Treat. 2006 Dec;31(4):319-28.

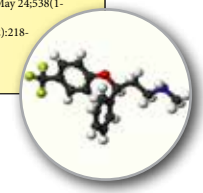

Fluoxetine is a commonly used antidepressant

LRRK2 Inhibitors

Leucine-rich repeat kinase 2 (LRRK2) is a protein that can be found in the cytoplasm and the mitochondrial outer membrane.

LRRK2 gain-of-function mutants are associated with increased risk for Parkinson's disease as well as Crohn's disease. Research models of Parkinson's disease show that LRRK2 mutations affect vesicular trafficking, autophagy, protein synthesis, and cytoskeletal function[1]. LRRK2 interacts with Parkin, one component of a multi-protein E3 ubiquitin ligase complex involved in protein degradation; mutant forms of Parkin are associated with the development of a juvenille familial form of Parkinson's disease[2].

Expression of LRRK2 mutants results in shortening of dendrites in neurons in vitro[3].

Inhibition of LRRK2 suppresses its kinase activity, lessening pathologies associated with Parkinson's disease in cellular and animal models.

PF-06447475 (P2100) prevents α-synuclein-induced neurodegeneration and neuroinflammation in animal models[4]. In vitro, **CZC-54252 (C9808)** limits mutant LRRK2-induced injury of rodent and human neurons[5]. **GNE-7915 (G5216)** is an aminopyrimidine in early stages of development that inhibits LRRK2 with high potency across several species[6].

1. Martin I, Kim JW, Dawson VL, et al. J Neurochem. 2014 Dec;131(5):554-65.
2. Smith WW, Pei Z, Jiang H, Moore DJ, et al. Proc Natl Acad Sci U S A. 2005 Dec 20;102(51):18676-81.
3. MacLeod D, Dowman J, Hammond R, et al. Neuron. 2006 Nov 22;52(4):587-93.
4. Daher JP, Abdelmotilib HA, Hu X, et al. 2015 Jun 15. [Epub ahead of print].
5. Ramsden N, Perrin J, Ren Z, et al. ACS Chem Biol. 2011 Oct 21;6(10):1021-8.
6. Estrada AA, Liu X, Baker-Glenn C, et al. J Med Chem. 2012 Nov 26;55(22):9416-33.

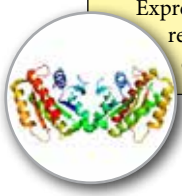

LRRK2 can be found in the mitochondrial outer membrane

γ-Secretase Inhibitors

γ-Secretase is a multi-subunit protein responsible for cleaving transmembrane proteins such as amyloid precursor protein and Notch. Cleavage of amyloid precursor protein eventually results in the formation of 42-amino acid peptide amyloid-β, the main component of amyloid plaques characteristic of Alzheimer's disease[1]. Cleavage of Notch allows for gene transcription and other downstream signal transduction necessary for cell-cell communications involved in embryogenesis, cell differentiation, endocrine development, and potentially tumorigenesis[2].

In animal models of Alzheimer's disease, **LY-450139 (L9701)** prevents formation of new amyloid plaques[3]. Similarly, **MK-0752 (M4200)** also decreases the formation of amyloid plaques; this compound displays potential as a treatment for brain and CNS-centric cancers as well[4-5].

FLI-06 (F4432) inhibits protein secretion prior to endoplasmic reticulum exit, displaying neuroprotective benefit[6].

Additional representative γ-secretase inhibitors include: **DAPT (D0260)** and **Deshydroxy LY-411575 (D1773)**.

1. Tharp WG and Sarkar IN. BMC Genomics. 2013 Apr 30;14:290.
2. Artavanis-Tsakonas S, Rand MD, Lake RJ. Science. 1999 Apr 30;284(5415):770-6.
3. Beggiato S, Giuliani A, Sivilia S, et al. Neuroscience. 2014 Apr 25;266:13-22.
4. Olson RE, Albright CF. Curr Top Med Chem. 2008;8(1):17-33.
5. Hoffman LM, Fouladi M, Olson J, et al. 2015 Aug;31(8):1283-9.
6. Krämer A, Mentrup T, Kleizen B, et al. 2013 Nov;9(11):731-8.

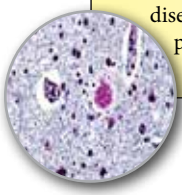

Amyloid plaque formation is a feature of Alzheimer's disease

GABA Modulators

γ-Aminobutyric acid (GABA) is the primary inhibitory neurotransmitter found in the central nervous system; it plays a major role in neuronal excitability and regulates muscle tone. In vertebrates, GABA binds GABA receptors at inhibitory synapses, inducing the flow of negatively charged chloride ions into the cell or positively charged potassium ions out of the cell, inhibiting action potential propagation.

Etomidate (E7758) is a GABA-A positive modulator that is clinically used to induce short term sedation or anesthesia[1].

Flumenazil (F4681) is an antagonist at GABA-A receptors that is used as a stimulant to counteract the effects GABA-A agonists and potentiators[2].

(+)-Bicuculline (B3211) is another GABA-A receptor antagonist used to study regional variation of GABA receptors and their role in various disease pathologies[3].

Baclofen (B0110) is a GABA derivative that displays GABA-B agonist activity; it is occasionally used to treat spastic movement disorders but is also used in research models to study the GABA-B receptor[4].

Gabapentin (G0106) is an analog of GABA that does not directly bind GABA receptors but indirectly potentiates GABA signaling through voltage-gated calcium channels. Like other GABA modulators, this compound is clinically used to prevent seizures and to treat neuropathic pain[5].

Valproic Acid Sodium Salt (V0147) potentiates GABA signaling but does not act directly on GABA receptors; instead, it inhibits GABA transaminase, increasing extracellular GABA concentrations[6].

1. Martin LJ, Oh GH, Orser BA. Anesthesiology. 2009 Nov;111(5):1025-35.
2. Lader M. Addiction. 2011 Dec;106(12):2086-109.
3. Torkaman-Boutorabi A, Soltani S, Oryan S, et al. Pharmacol Biochem Behav. 2013 Apr;105:142-50.
4. Uchiyama T, Nakanishi K, Fukawa N, et al. Neurol Med Chir (Tokyo). 2012;52(7):463-9.
5. Kukkar A, Bali A, Singh N, et al. Arch Pharm Res. 2013 Mar;36(3):237-51.
6. Rosenberg G. Cell Mol Life Sci. 2007 Aug;64(16):2090-103.

GABA is the most common inhibitory neurotransmitter in the brain

Clopidogrel Sulfate

Clopidogrel Sulfate (C4658) is a first generation thienopyridine P2Y12 receptor antagonist that is used as an antithrombotic. Clopidogrel prevents myocardial infarction and stroke in high risk subjects with coronary artery disease, peripheral vascular disease, or other cardiovascular diseases that involve narrowing of the blood vessels[1].

Clopidogrel is a prodrug; through oxidation and hydrolysis, cytochrome P2C19 produces the active metabolite. Once activated, this compound forms a disulfide bridge with the platelet ADP receptor, P2Y12, preventing platelet activation and fibrin cross-linking[2]. The P2Y12 receptor is present on platelet cell membranes, where it plays a significant role in the regulation of blood clotting.

Clopidogrel is also combined with acetylsalicylic acid to prevent thrombosis in patients that have received a coronary stent; this combination decreases the risk of stent thrombosis and other cardiovascular complications[3].

Additional ADP P2Y12 receptor inhibitors include: **Ticlopidine HCl (T3310), Prasugrel (P6903),** and **Ticagrelor (T3200).**

1. Cohen MV, Downey JM. J Cardiovasc Pharmacol Ther. 2014 Mar;19(2):179-90.
2. Ferri N, Corsini A, Bellosta S. Drugs. 2013 Oct;73(15):1681-709.
3. Mauri L, Kereiakes DJ, Yeh RW, et al. N Engl J Med. 2014 Dec 4;371(23):2155-66.

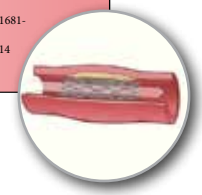

Clopidogrel reduces the risk of coronary stent thrombosis

Statins

Statins display antihyperlipidemic activity[1]. Statins are commonly used in clinical settings to lower levels of low-density lipoprotein (LDL) cholesterol and to increase levels of high-density lipoprotein (HDL) cholesterol.

Statins inhibit 3-hydroxy-3-methyl-glutaryl-coenzyme A (HMG-CoA) reductase, preventing the formation of cholesterol[2]. Most circulating cholesterol stems from endogenous production rather than dietary intake, so inhibition of this enzyme can have a significant effect on plasma cholesterol levels.

Statins can be categorized into two primary groups: compounds that can be produced by plant sources and synthetic products.

Statins that can be found naturally include: **Lovastatin (M1687), Simvastatin (S3449), Pravastatin Sodium (P6801),** and **Mevastatin (M1685).**

Statins that are produced only by synthetic means include: **Atorvastatin Calcium Trihydrate (A7658), Fluvastatin Sodium (F4482), Cerivastatin Sodium (C1668), Rosuvastatin Calcium (R5974),** and **Pitavastatin Calcium (P3576).**

Many statins also exhibit anticancer activity, limiting cellular proliferation and tumor growth in preclinical models and increasing survival rates in clinical settings[3-4].

1. Blumenthal, R.S. Am. Heart J. 2000;139:577-83.
2. Krause, B.R., Newton, R.S. Atherosclerosis 1995;117:237-44.
3. Ishikawa S, Hayashi H, Kinoshita K, et al. Int J Cancer. 2013 Dec 17.
4. Zhang W, Wu J, Zhou L, et al. Indian J Exp Biol. 2010 Dec;48(12):1167-74.

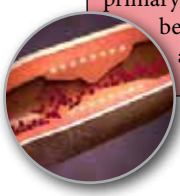

Lowering cholesterol levels helps reduce the possibility of cardiovascular disease

ACE Inhibitors

Angiotensin-converting enzyme (ACE) inhibitors are commonly used to treat hypertension and congestive heart failure. ACE inhibitors block the conversion of angiotensin I to angiotensin II. Angiotensin II induces vasoconstriction, increases water retention stimulated by vasopressin, and contributes to ventricular hypertrophy; by decreasing the production of angiotensin II, these effects can be minimized. Overall, the consequences of suppressing angiotensin II production include decreasing blood pressure, reducing the progress of diabetic nephropathy, and decreasing cardiac output and stroke volume[1-2].

In addition to their cardiovascular activities, some ACE inhibitors have also displayed other biological activities, including anticancer properties. **Captopril (C0261)** decreases tumor growth and metastasis in animal models of lung cancer[3]. **Perindopril Erbumine (P1869)** inhibits VEGF expression and tubule formation in vivo, preventing angiogenesis and tumor development[4].

Other ACE inhibitors include: **Ramipril (R0249), Temocapril HCl (T1750), Trandolapril (T6803), Spirapril HCl (S6168), Fosinopril Sodium (F5773), Lisinopril Dihydrate (L3374), Quinapril HCl (Q8134),** and **Enalapril (E5202).**

1. Jandeleit-Dahm K and Cooper ME. Endocrinol Metab Clin North Am. 2006 Sep;35(3):469-90, vii.
2. Ajayi AA, Campbell BC, Howie CA, et al. J Hypertens. 1985 Feb;3(1):47-53.
3. Attoub S, Gaben AM, Al-Salam S, et al. Ann N Y Acad Sci. 2008 Sep;1138:65-72.
4. Yoshiji H, Kuriyama S, Kawata M, et al. Clin Cancer Res. 2001 Apr;7(4):1073-8.

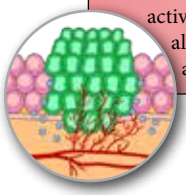

ACE inhibitors such as Perindopril can inhibit angiogenesis

Losartan Potassium

Losartan Potassium (L5873) is clinically used to treat hypertension and to delay the progression of diabetic nephropathy; it is an angiotensin II type 1 (AT1) receptor antagonist.

Activation of the AT1 receptor induces vasoconstriction, cardiac hypertrophy, and renal sodium re-uptake; it also increases secretion of vasopressin and aldosterone. Inhibiting AT1 receptors causes vasodilation and reduces secretion of vasopressin and aldosterone[1]. Together, these inhibitory effects cause a significant decrease in blood pressure.

In addition to its vasodilatory activity, losartan also prevents the endothelial-to-mesenchymal transition by indirectly suppressing ERK phosphorylation. This suggests that losartan may prevent the excessive growth and fibrosis that occurs post-myocardial infarction[2].

In animal models of obstructive nephropathy, losartan decreases levels of α-smooth muscle actin and collagen type 1 and inhibits phosphorylation of STAT3, suppressing renal tubular fibrosis and renal tubular cell apoptosis[3].

Other AT1 antagonists include: **Irbesartan (I6804), Olmesartan Medoxomil (O4549), Valsartan (V0146), Candesartan (C0253),** and **Candesartan Celexetil Ester (C0254).**

1. Siragy H. Am J Cardiol. 1999 Nov 18;84(10A):3S-8S.
2. Wylie-Sears J, Levine RA, Bischoff J. Biochem Biophys Res Commun. 2014 Apr 18;446(4):870-5.
3. He P, Li D, Zhang B. Mol Med Rep. 2014 Aug;10(2):638-44.
4. de las Heras N, Martín-Fernández B, Miana M, et al. J Hypertens Suppl. 2009 Aug;27(6):S37-41.

Losartan is used for the treatment of high blood pressure

Endogenous Natriuretic Peptides

Natriuretic peptides are endogenous peptides that induce natriuresis, the excretion of sodium. Natriuretic peptides are typically found in cardiac myocytes. Here, they control water, sodium, and adipose loads and regulate blood pressure[1].

A-type Natriuretic Peptide (ANP, A7669) is a 28-amino acid peptide released from atrial myocytes that activates the guanylyl cyclase A (GC-A) receptor. Activation of this receptor decreases sodium reabsorption in the kidneys and increases cGMP levels, relaxing vascular smooth muscle. This also causes a reduction in blood volume, cardiac output, and systemic blood pressure. A-type natriuretic peptide (ANP) may also display anticancer activity, inhibiting components of the Ras-MEK-ERK signaling pathway and inducing cell death and tumor regression in various cancer models[2].

B-type Natriuretic Peptide (BNP, B5561) is a 32-amino acid peptide secreted by the ventricles of the heart. Like ANP, B-type natriuretic peptide (BNP) also binds GC-A receptors, causing natriuresis and decreasing systemic vascular resistance and blood pressure. BNP has a significantly longer halflife than ANP, so it is often used as a clinical biomarker for heart failure or renal failure[3]. BNP inhibits de novo collagen synthesis as well, increasing expression of matrix metalloproteinases 1, 2, and 3 in vitro and preventing ventricular remodeling[4].

Nesiritide Acetate (N1873) is a recombinant form of BNP used to treat heart failure by decreasing blood volume and systemic blood pressure. In animal models, nesiritide decreases inflammation and prevents cardiac remodeling[5-6].

C-type Natriuretic Peptide (CNP, C7997) is a 22-amino acid peptide that binds guanylyl cyclase B (GC-B) receptors. C-type natriuretic peptide (CNP) does not have direct natriuretic activity. CNP instead contributes to cardiac function by playing a role in cardiac hypertrophy and remodeling[7]. In animal models, chronic administration of CNP attenuates angiotensin II-induced cardiac hypertrophy without altering systemic blood pressure[8]. This peptide also plays a role in fertility and bone growth. Activation of GC-B receptors stimulates long bone growth in animal models. Loss-of-function mutations that inhibit the ability of CNP to bind GC-B induce dwarfism and gain-of-function mutations result in an overgrowth syndrome[9-10].

Additional peptides and peptide fragments for various animal models are also available:

Rat ANP, 1-11 (A5460)
Frog ANP, 1-30 (A5461)
Rat BNP, 1-32 (B5560)
Chicken CNP, 1-22 (C7998)
Pig CNP, 1-22 (C5260)

1. Potter LR, Yoder AR, Flora DR, et al. Handb Exp Pharmacol. 2009;(191):341-66.
2. Vesely DL. Anticancer Res. 2012 Jul;32(7):2515-21.
3. García-Berrocoso T, Giralt D, Bustamante A, et al. Neurology. 2013 Dec 3;81(23):1976-85.
4. Tsuruda T, Boerrigter G, Huntley BK, et al. Circ Res. 2002 Dec 13;91(12):1127-34.
5. Shaw SM, Critchley WR, Puchalka CM, et al. Transpl Immunol. 2012 Mar;26(2-3):119-22.
6. Kishimoto I, Tokudome T, Horio T, et al. Curr Cardiol Rev. 2009 Jan;5(1):45-51.
7. Del Ry S. Peptides. 2013 Feb;40:93-8.
8. Izumiya Y, Araki S, Usuku H, et al. Int J Vasc Med. 2012;2012:246058.
9. Yoder AR, Kruse AC, Earhart CA, et al. Peptides. 2008 Sep;29(9):1575-81.
10. Miura K, Kim OH, Lee HR, et al. Am J Med Genet A. 2014 Jan;164A(1):156-63.

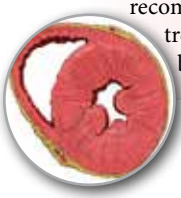

Natriuretic peptides can help prevent ventricular hypertrophy, the thickening of the ventricle walls in the heart

Flufenamic Acid

Flufenamic Acid (F4483) belongs to the class of N-phenylanthranilic acids and is considered a non-steroidal anti-inflammatory drug (NSAID) through its ability to inhibit cyclooxygenase (COX) enzymes. Cyclooxygenase is a key enzyme in the synthesis of prostaglandins, prostacyclins, and thromboxane. Two isoforms exist: COX-1 is constitutively expressed while COX-2 expression is induced by inflammatory mediators. Flufenamic acid is a non-selective inhibitor of both COX-1 and COX-2[1].

Like most NSAIDs, flufenamic acid is used to manage pain, fever, and inflammation. In addition to its anti-inflammatory, analgesic, and antipyretic properties, flufenamic acid also displays neuromodulatory activity. This compound inhibits voltage-gated sodium channels, transient receptor potential C3 channels, and transient receptor potential M2 channels; it also potentiates TREK1 potassium channel signaling[2-5].

Additionally, flufenamic acid is a reversible gap junction blocker that can be used to study the role of connexin 43-mediated gap junction communication in biological processes[6].

1. Ouellet M, Percival MD. Biochem. J. 306 (Pt 1):247-251 (1995).
2. Xie YF, Zhou F. Neurol Sci. 2014 May 21.
3. Veale EL, Al-Moubarak E, Bajaria N, et al. Mol Pharmacol. 2014 May;85(5):671-81.
4. Yau HJ, Baranauskas G, Martina M. J Physiol. 2010 Oct 15;588(Pt 20):3869-82.
5. Nazıroğlu M, Özgül C, Çelik Ö, et al. J Membr Biol. 2011 May;241(2):69-75.
6. Harks EG, et al. J. Pharmacol. Exp. Ther. 2001;298(3):1033-41.

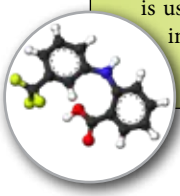

Flufenamic acid is a non-selective COX inhibitor

Cyclooxygenase-2 Inhibitors

Cyclooxygenase-2 (COX-2) inhibitors belong to a class of nonsteroidal anti-inflammatory drugs (NSAIDs) that directly target COX-2; COX-2 is an induceable enzyme involved in signal transduction of fever, pain, and inflammation[1-2]. COX-2 inhibitors are specific for the induceable isoform of COX and do not inhibit cyclooxygenase-1 (COX-1), a constitutively expressed isoform present throughout the body.

Blocking only COX-2 allows for a more targeted response, minimizing side effects such as gastric irritation and peptic ulceration.

COX-2 inhibitors also exhibit chemopreventive activity in research models, likely due to their ability to prevent inflammation[3-4].

Representative COX-2 inhibitors:

Rofecoxib (R5722)
Valdecoxib (V0245)
Celecoxib (C1644)
Lumiracoxib (L8248)
Deracoxib (D1869)
Etoracoxib (E7858)
Parecoxib (P0369)
Niflumic Acid (N3322)
Etodolac (E7556)
Diclofenac (D3209)
Aceclofenac (A1017)
Carprofen (C0351)
Nimesulide (N3450)
Meloxicam (M1644)
Nabumetone (N0205)

1. Reuben SS. Curr. Opin. Anaesthesiol. 2007;20:440-50.
2. Harris RC, Breyer MD. Clin. J. Am. Soc. Nephrol. 2006;1:236-45.
3. Das D, Arber N, Jankowski JA. Digestion 2007;76:51-67.
4. Howe LR. Breast Cancer Res. 2007;9:210.

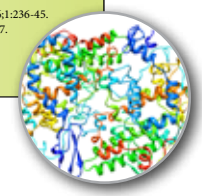

COX-2 inhibitors are specific for the induceable form of cyclooxygenase

Histone Methyltransferase Inhibitors

Histone methyltransferases (HMTs) catalyze the transfer of methyl groups to lysine and arginine residues of histone proteins. This modification regulates important processes such as gene expression and cell mitosis, altering gene transcription. Abnormal activity of HMTs has been associated with some cancers, including colorectal, ovarian, and lung cancers[1].

HMT enhancer of zeste homolog 2 (EZH2) is a an enzyme that acts mainly as a gene silencer, potentially preventing expression of tumor suppressor genes. **GSK126 (G7340)** is an inhibitor of EZH2 that displays anticancer activity by inhibiting cell proliferation in cellular and animal models of diffuse large B-cell lymphoma[2]. **GSK-343 (G7442)** also inhibits EZH2; this compound suppresses cell invasion and cell growth in epithelial ovarian cancer cells[3].

HMT disruptor of telomeric silencing 1-like (DOT1L) also methylates lysines on histone H3, similar to EZH2. Blockade of DOT1L by **EPZ-5676 (E6398)** and **EPZ-004777 (E6298)** increases survival rates in animal models of leukemia and induces tumor regression in other animal models[4-5].

Also available: **EPZ005687 (E6396)** and **EPZ6438 (E6397)**.

1. Hamamoto R, Furukawa Y, Morita M, et al. Nat Cell Biol. 2004 Aug;6(8):731-40.
2. McCabe MT, Ott HM, Ganji G, et al. Nature. 2012 Dec 6;492(7427):108-12.
3. Amatangelo MD, Garipov A, Li H, et al. Cell Cycle. 2013 Jul 1;12(13):2113-9.
4. Daigle SR, Olhava EJ, Therkelsen CA, et al. Blood. 2013 Aug 8;122(6):1017-25.
5. Yu W, Chory EJ, Wernimont AK, et al. Nat Commun. 2012;3:1288.

Histone methyltransferases can alter cell mitosis

Histone Deacetylase Inhibitors

Histone deacetylases (HDACs) are enzymes that remove acetyl groups from histones, allowing histones to wrap DNA more tightly, preventing transcription. Like other epigenetic enzymes, HDACs play a significant role in altering gene expression.

HDAC inhibitors such as **Valproic Acid Sodium Salt (V0147)** and **Butyric Acid Sodium Salt (B8276)** show benefit in the treatment of mood disorders and epilepsy[1-2].

Phenylbutyrate (P2815) is an HDAC inhibitor clinically used to treat urea cycle disorders. This compound also exhibits chemotherapeutic activity, suppressing tumor growth in animal models of pancreatic cancer[3-4].

Romidepsin (R5749) enhances natural killer cell cytotoxicity by increasing MIC A/B (NK ligand) expression on tumor cells in leukemia and lymphoma models[5].

Other HDAC inhibitors that display anticancer activity include **Tubacin (T8000), Tubastatin A Hydrochloride (T8006), Entinostat (E5477), Belinostat (B1746), LBH-589 (L0528), TMP-269 (T5060),** and **Vorinostat (V5734)**[6-10].

Compounds that target class III HDACs (sirtuins) often display neuroprotective activity. Compounds in this category include **AK-7 (A4002), AK-1 (A4000)**, and **SRT1720 (S7868)**.

1. Han A, Sung YB, Chung SY, et al. Neuropharmacology. 2014 Jun;81:292-302.
2. Zhao L, Chen CN, Hajji N, et al. Circulation. 2012 Jul 24;126(4):455-67.
3. Batshaw ML, MacArthur RB, Tuchman M. J Pediatr. 2001 Jan;138(1 Suppl):S46-54.
4. Dovzhanskiy DI, Hartwig W, Lázár NG, et al. Oncol Res. 2012;20(2-3):103-11.
5. Satwani P, Bavishi S, Saha A, et al. Cytotherapy. 2014 May 20. [Epub ahead of print].
6. Rao-Bindal K, Koshkina NV, Stewart J, et al. Curr Cancer Drug Targets. 2013 May;13(4):411-22.
7. Haggarty SJ, Koeller KM, Wong JC, et al. Proc Natl Acad Sci U S A. 2003 Apr 15;100(8):4389-94.
8. Gradilone SA, Radtke BN, Bogert PS, et al. Cancer Res. 2013 Apr 1;73(7):2259-70.
9. Zorzi AP, Bernstein M, Samson Y, et al. Pediatr Blood Cancer. 2013 Nov;60(11):1868-74.
10. Silva G, Cardoso BA, Belo H, et al. PLoS One. 2013;8(1):e53766.

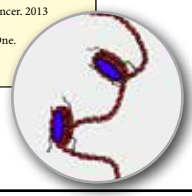

Removal of acetyl groups allows DNA to coil around histones more tightly

Custom Synthesis and Analytical Services

LKT Laboratories offers custom synthesis and analysis to fit your needs. The LKT analytical team can offer custom analysis of your compounds using our extensive range of analytical equipment. Our experienced chemists can produce milligram to kilogram quantities of high purity products at competitive prices.

Natural Product Isolation

LKT Laboratories can isolate your natural products using high performance counter current chromatography. This separation method has the advantage of nearly 100% sample recovery, no sample degradation, and full polarity coverage in one single run. Separation scales can range from a few milligrams to several grams.

Custom Synthesis

LKT Laboratories is equipped to carry out multistep organic synthesis on a milligram to kilogram scale. We fully characterize compounds and have access to a wide variety of analytical instrumentation. Quality control is performed in-house using UHPLC, HPLC, LC/MS, GC and NMR.

We Specialize In:

-Natural Product Isolation
-Product Purification
-Total Synthesis
-Natural Product Analog Development

Analytical Services:

-UHPLC with PDA (UV-VIS) Detection
-HPLC with UV, ELSD, or Mass Spec Detection
-GC with FID
-UV Spectrophotometry
-NMR Spectroscopy
-Mass Spectroscopy

For more information on custom services or to receive a quote from LKT please contact us by phone or email:

getinfo@lktlabs.com
888-558-5227

New: Kinase Inhibitors

Kinases are enzymes that transfer a phosphate group from ATP to a protein in a cell. These enzymes function as "on" or "off" switches in many cellular functions, including cell growth. Aberrant kinase activity or functional mutations in the enzymes can cause constitutive activation of cell growth and cell cycle pathways in cancer cells; this leads to the uncontrolled cell growth characteristic of tumors.

This faulty signaling may occur as a result of a mutation in the gene that expresses a particular kinase. In chronic myelogenous leukemia, a chromosomal translocation has been identified that creates a novel protein consisting of two fused tyrosine kinases, BCR and Abl; the kinase domains on this new protein are constitutively active. Normally, these two proteins are involved in regulation of cell differentiation, cell division, cell adhesion, and stress responses. Continuous activation of such processes leads to unregulated cell proliferation and the development of cancer.

There are nearly 100 tyrosine kinases in the human genome, many of which may be useful targets for developing new chemotherapeutics. Many kinase inhibitors inhibit serine and threonine kinases as well.

AMG-458 (A4926) is an inhibitor of c-MET that exhibits anticancer activity. AMG-458 enhances the radiosensitivity of lung adenocarcinoma cells, inducing apoptosis[1]. In vivo, this compound inhibits growth of glioblastoma tumors[2].

LDK378 (L1340) is an anaplastic lymphoma kinase (ALK) inhibitor that shows chemotherapeutic activity in the treatment of non-small cell lung cancer (NSCLC); it also inhibits IGF-1R[3].

OSI-906 (O7333) is an inhibitor of the insulin receptor (InsR) and IGF-1R that inhibits cell proliferation and tumor growth in animal models of cancer[4].

PCI-32765 (P0932) is an inhibitor of Bruton's tyrosine kinase (BTK), an enzyme that plays a significant role in B-cell malignancies, B-cell receptor signaling, and autoimmune diseases[5]. PCI-32765 also inhibits IL-2-inducible kinase[6].

Tozasertib (T5996) is a pan-aurora kinase (AurK) inhibitor that also inhibits FMS-like tyrosine kinase 3 (FLT3) and Abl; this compound shows promise as a potential treatment for prostate cancer and acute lymphoblastic leukemia[7].

(+)-JQ-1 (J6400) is a triazolothienodiazepine that inhibits BET bromodomain (BRD) proteins. JQ-1 exhibits chemotherapeutic activity in models of acute lymphoblastic leukemia; it also inhibits bromodomain testis-specific protein BRDT and chromatin remodeling during spermatogenesis, preventing sperm production[8-9].

NVP-BHG712 (N8460) inhibits ephrin receptor EphB4, which plays a significant role in vessel development, vascular development, and tumor angiogenesis[10].

ARRY-162 (A6971) is an inhibitor of MEK1/2 and ERK that exhibits anticancer activity, inhibiting proliferation in models of melanoma, non-small-cell lung cancer (NSCLC), head/neck cancer, and pancreatic cancer[11].

1. Li B, Torossian A, Sun Y, et al. Int J Radiat Oncol Biol Phys. 2012 Nov 15;84(4):e525-31.
2. Liu L, Siegmund A, Xi N, et al. J Med Chem. 2008 Jul 10;51(13):3688-91.
3. www.clinicaltrials.gov/show/NCT01685060
4. Mulvihill MJ, Cooke A, Rosenfeld-Franklin M, et al. Future Med Chem. 2009 Sep;1(6):1153-71.
5. Honigberg LA, Smith AM, Sirisawad M, et al. Proc Natl Acad Sci U S A. 2010 Jul 20;107(29):13075-80.
6. Dubovsky JA, Beckwith KA, Natarajan G, et al. Blood. 2013 Jul 25.
7. Giles FJ, Swords RT, Nagler A, et al. Leukemia. 2013 Jan;27(1):113-7.
8. Ott CJ, Kopp N, Bird L, et al. Blood. 2012 Oct 4;120(14):2843-52.
9. Filippakopoulos P, Qi J, Picaud S, et al. Nature. 2010 Dec 23;468(7327):1067-73.
10. Martiny-Baron G, Holzer P, Billy E, et al. Angiogenesis. 2010 Sep;13(3):259-67.
11. www.clinicaltrials.gov/show/NCT00959127

Kinase inhibitors can control unchecked cell growth in cancers

New: mTOR Inhibitors

Mechanistic target of rapamycin (mTOR) is a protein kinase that plays a role in cell growth, proliferation, motility, and survival. Important downstream targets of mTOR include p70SK6 and eIF-4EBP; interaction of mTOR with these targets induces translation and protein synthesis[1-2]. mTOR forms two different complexes, mTORC1 and mTORC2, through the binding of various other proteins. The mTORC1 complex contains Raptor, FKBP12, and PRAS40, whereas the mTORC2 complex contains Rictor, mSIN1, and PROTOR1/2.

mTOR signaling is dysregulated in several human diseases, including cancer, neurodegenerative disease, diabetes, and metabolic syndrome. mTOR inhibitors such as **Rapamycin (R0161)** and **Everolimus (E8419)** are used as immunosuppressants, preventing transplant rejection, minimizing angiogenesis in coronary stents, and suppressing immune signaling in cancer treatment[3-4].

New mTOR inhibitors such as **OSI-027 (O7332), GDC-0980 (G1209), GSK2126458 (G7342)**, and **INK128 (I5440)** are currently in development as cancer treatments, exhibiting anti-angiogenic, anti-metastatic, and chemotherapeutic activities in various cellular and animal models[5].

1. Hay N and Sonenberg N. Genes Dev. 2004 Aug 15;18(16):1926-45.
2. Dobashi Y, Watanabe Y, Miwa C, et al. Int J Clin Exp Pathol. 2011 Jun 20;4(5):476-95.
Hennig M, Bauer D, Wasmuth S, et al. Exp Eye Res. 2012 Dec;105:43-52.
2. Klintmalm GB, Nashan B.. J Transplant. 2014;2014:845438.
3. Maiso P, Liu Y, Morgan B, et al. Blood. 2011 Dec 22;118(26):6860-70.
4. Sampath D, Oeh J, Wyatt SK, et al. Neoplasia. 2013 Jul;15(7):694-711.
5. Falcon BL, Barr S, Gokhale PC, et al. Cancer Res. 2011 Mar 1;71(5):1573-83.

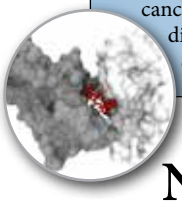

Many mTOR inhibitors prevent binding of mTOR and FKBP12

New: Wnt Signaling Modifiers

Wnt signaling pathways play a key role in the transmittance of signals from outside of a cell through cell surface receptors to the inside of the cell. There are three pathways involved in Wnt signaling: The canonical Wnt pathway regulates gene transcription, the noncanonical pathway regulates cytoskeleton structure, and the non-canonical Wnt/calcium pathway regulates intracellular calcium signaling. Wnt signaling pathways are important in embryonic development and cell proliferation and migration.

Wnt signaling is often dysregulated in many forms of cancer. Elevated activity of the canonical Wnt pathway and increased levels of β-catenin are implicated in the development of breast cancer, colorectal cancer, and melanoma[1]. New compounds displaying anticancer activity such as **C59 (C0800), IWP-2 (I9060)**, **GDC-0449 (G1408)**, and **LGK-974 (L2540)** target overactive Wnt signaling by inhibiting positive modulators of this signaling pathway, such as PORCN or Smo[2-4].

Other new Wnt signaling inhibitors include **IWP-3 (I9061), JW55 (J8800),** and **KY-02111 (K9600)**. These compounds promote differentiation of stem cells into cardiomyocytes and decrease body weight[5-7].

1. Logan CY and Nusse R. Annu Rev Cell Dev Biol. 2004;20:781-810.
2. Proffitt KD, Madan B, Ke Z, et al. Cancer Res. 2013 Jan 15;73(2):502-7.
3. Mo ML, Li MR, Chen Z, et al. Oncol Lett. 2013 May;5(5):1719-1723.
4. Willems E, Spiering S, Davidovics H, et al. Circ Res. 2011 Aug 5;109(4):360-4.
5. Liu J, Pan S, Hsieh MH, et al. Proc Natl Acad Sci U S A. 2013 Dec 10;110(50):20224-9.
6. Minami I, Yamada K, Otsuji TG, et al. Cell Rep. 2012 Nov 29;2(5):1448-60.
7. Mao J, Hu X, Xiao Y, et al. Diabetes. 2013 Nov;62(11):3736-46.

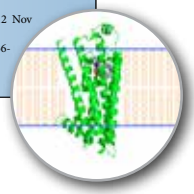

Proteins involved in Wnt pathways transmit messages across cell membranes

New: PARP Inhibitors

PARP (poly [ADP-ribose] polymerase) is a family of proteins involved in DNA repair and cell death found in the cell nucleus. PARP immediately transmits a signal to DNA repair machinery such as DNA ligase and DNA polymerase in response to metabolic, chemical, or radiation-induced single-stranded DNA damage[1].

Several forms of cancer are highly dependent upon PARP due to their lack of other DNA repair mechanisms. PARP can also stimulate the repair of DNA breaks induced by chemotherapeutics.

When PARP is inhibited in these repair-deficient cancer cells, they are overwhelmed with irreparable double strand DNA breaks. The unchecked damaged DNA eventually induces cell death, a key mechanism in prevention of fast-dividing tumor cell growth.

PARP inhibitors can act in two ways. These compounds prevent the enzymatic activity of PARP, suppressing DNA repair, and can also prevent PARP from separating from damaged DNA, inhibiting replication[2].

PARP inhibitors:
Iniparib (I5354)
Veliparib (V1745)
Olaparib (O4402)
3-Aminobenzamide (A4931)
AZD2461 (A9612)
PJ34 HCl (P3600)

1. Piskunova TS, Yurova MN, Ovsyannikov AI, et. al., Curr Gerontol Geriatr Res. 2008:754190
2. Murai J, Huang SY, Das BB, et al. Cancer Res. 2012 Nov 1;72(21):5588-99.

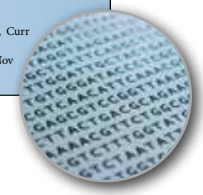

PARP proteins detect single strand breaks in DNA

New: PI3K Inhibitors

Phosphatidylinositol-3-kinase (PI3K) is an enzyme involved in cell growth, proliferation, differentiation, motility, and survival. PI3Ks are grouped into several different classes based on structure, function, and substrate specificity.

Class I PI3Ks are heterodimers composed of a regulatory subunit (p85) and a catalytic subunit (p110), both of which have several variants. This class of PI3Ks is likely the most well known, as it is responsible for activating Akt (PKB) and regulating signal transduction of mTOR and other kinases. Class I PI3Ks are involved in intracellular trafficking, cell proliferation, immune function, and insulin signaling[1-2].

Because of its broad spectrum of activity, PI3K is an excellent target in the development of immunosuppressants, anti-diabetic compounds, cardiovascular products, anti-inflammatories, and chemotherapeutics.

Representative PI3K inhibitors:
Wortmannin (W5769)
BYL719 (B9700)
GSK2334470 (G7344)
CAL101 (C0044)
TGX-221 (T2792)
TG100-115 (T2402)
PX-866 (P9200)
PIK-75 HCl (P3540)
AZD6482 (A9712)
AS-605240 (A7204)

1. Knight ZA, Gonzalez B, Feldman ME, et al. Cell. 2006 May 19;125(4):733-47.
2. Gómez Del Pulgar T, De Ceballos ML, Guzmán M, et al. J Biol Chem. 2002 Sep 27;277(39):36527-33.

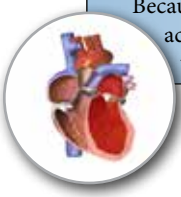

Many PI3K inhibitors exhibit cardioprotective activities

New Products

A0002	A66
A2420	A-769662
A0001	A-803467
A0401	Abacavir
A0402	Abacavir Sulfate
A0776	ABT-199
A0777	ABT-263
A0778	ABT-737
A0922	Acetyl-L-Carnitine Hydrochloride
A1592	ADX-47273
A1607	AEBSF Hydrochloride
A1895	Aeruginosamide B
A1896	Aeruginosamide C
A1897	Aeruginosamide D
A1898	Aeruginosamide E
A1890	Aeruginosin 722
A2077	Afatinib
A2401	AG-18
A2400	AG-1024
A2500	AG-1478
A2501	AG-1517
A2532	AGI-6780
A3080	AHU-377 Tris Salt
A4000	AK-1
A4002	AK-7
A4646	ALLN
A4777	Altiratinib
A4924	AMG-208
A4926	AMG-458
A5061	Ampalex
A5204	Anabaenopeptin 856
A5205	Anabaenopeptin 872
A5200	Anabaenopeptin A
A5201	Anabaenopeptin B
A5203	Anabaenopeptin F
A5353	Annexin V-FITC Apoptosis Detection Kit
A6000	AP-III-a4 (ENOblock)
A6058	Apoptosis Activator 2
A6269	Apremilast
A6396	APY0201
A6800	AR-A014418
A6818	Arenobufagin
A6925	L-Arginine Ethyl Ester Dihydrochloride
A7200	AS-252424
A7202	AS-604850
A7204	AS-605240
A7203	AS-703026
A7600	AT-56
A7604	ATB 346
A7725	Atglistatin
A7868	Atropine
A8644	AVL-292
A8812	AWD 131-138
A9708	AZD-1208
A9812	AZD-1480
A9710	AZD-2014
A9714	AZD-1152-HQPA
A9612	AZD-2461
A9814	AZD-4547
A9712	AZD-6482
A9912	AZD-7762 Hydrochloride
A9914	AZD-8055
A9715	AZD-8330
B0245	Balicatib
B0396	BAY80-6946
B1724	Begacestat
B1746	Belinostat
B1955	Benztropine Mesylate
B1754	N-Benzyl-2-(6-bromo-2-methylquinolin-4-yloxy)acetamide
B1954	N-benzyl-N-Methyl-1-(4-(trifluoromethyl) benzyl)piperidine-3-carboxamide
B1976	Betrixaban
B1977	Betulin
B1978	Betulin-3-Acetate
B1996	BEZ235
B3200	BI-2536
B3300	BI-6727
B3459	Bioymifi
B3472	4,4"-(1,1"-Biphenyl-4,4"-diyldioxy) dianiline
B4248	BKM120
B5044	BML-277
B5074	BMS-599626
B5075	BMS-708163
B5072	BMS-754807
B4974	BMS-777607
B5728	Bohemine
B5870	Borrelidin
B6902	B-Raf IN 1
B6959	Bromosporine
B8277	Butein
B8377	5-Tert-butoxyquinazoline-2,4-diamine
B8676	BVT-2733
B9200	BX-795
C0800	C59
C0044	CAL101
C0048	Cambinol
C0273	Casin
C0396	CAY10505
C0824	CCG1423
C1644	Celecoxib
C2540	CGK 733
C2802	CH5132799
C2900	CH5424802
C2932	Chidamide
C3200	CI-994
C3212	CID-2011756
C3214	CID-797718
C3352	Cinacalcet Hydrochloride
C4000	CK-636
C4417	Clemizole
C4418	Clemizole Hydrochloride
C4800	CM346 Hydrochloride
C5600	CO-1686
C5863	Coptisine Hydrochloride
C5970	Corydaline
C5972	Coryneline
C6000	CP-640186
C6818	Crenolanib
C7992	CTX-0294885
C8112	CUDC-907
C9200	CX-6258
C9603	Cyanopeptolin 1007 MB1

New Products

C9604	Cyanopeptolin 1007 MB2
C9605	Cyanopeptolin 1020
C9601	Cyanopeptolin 1040 MB
C9606	Cyanopeptolin 1054 MB1
C9607	Cyanopeptolin 1054 MB2
C9616	Cyanopeptolin 1068 MB
C9708	CYC-116
C9644	Cylindrospermopsin
C9748	CYM-5442
C9876	CYT-387
C9781	Basic Cytotoxicity Test Assay Kit
C9808	CZC-54252
D0261	Dapivirine
D0260	DAPT
D1722	Defactinib
D1720	Deferiprone
D1631	Dehydrocorydaline
D1746	Deltarasin Hydrochloride
D1869	Deracoxib
D1872	Des(benzylpyridyl) Atazanavir
D1773	Deshydroxy LY-411575
D1994	Dexrazoxane
D1995	Dexrazoxane Hydrochloride
D3428	Dihydrochelerythrine
D3430	Dihydrosanguinarine
D3329	7,8-Dihydroxyflavone Hydrate
D3349	Dimebon Dihydrochloride
D3448	Dimethyl Fumarate
D3451	Dimethyloxalylglycine
D3352	Dinaciclib
D5610	Docosahexaenoic Acid (all cis-4,7,10,13,16,19)
D5611	Docosahexaenoic Acid (all cis-4,7,10,13,16,19) Methyl Ester
D5747	Dolasetron Mesylate Hydrate
D6108	1,4-DPCA
D8276	Dutasteride
D9752	Dynasore
E0001	E64
E0003	E64-d
E2003	Efavirenz
E4668	ELR-510444
E4785	Elvitegravir
E5178	Emtricitabine
E6398	EPZ-5676
E7356	Esomeprazole Magnesium Trihydrate
E7857	Etofenamate
E7758	Etomidate
E7858	Etoricoxib
E9201	EX-527
E9603	Ezatiostat
F0121	FAM-DEVD-OPH in vitro Apoptosis Detection Reagent
F0118	Fam-Phe-DAP Green FLISP Assay™ Kit
F0119	FAM-VAD-OPH I in vitro Apoptosis Detection Reagent
F0120	FAM-VAD-OPH II in vitro Apoptosis Detection Reagent
F1768	Ferintoic Acid A
F1769	Methoxy Ferintoic Acid A
F1992	Fexaramine
F4432	FLI-06
F4532	Flibanserin
F4534	FLICA® 660 Caspase 1 Assay Kit
F4535	FLICA® 660 Caspase 3/7 Assay Kit
F4533	FLICA® 660 Poly Caspase Assay Kit
F5968	Foretinib
G0668	GBR 12935 Dihydrochloride
G1310	GDC-0349
G1408	GDC-0449
G1210	GDC-0623
G1209	GDC-0980
G3253	8-Gingerol
G3254	10-Gingerol
G4662	GLPG-0634
G5216	GNE-7915
G5320	GNF-2
G5322	GNF-5
G7200	GS-967
G7232	GS-9973
G7442	GSK-343
G7443	GSK-429286A
G7241	GSK-461364
G7242	GSK-690693
G7444	GSK-1070916
G7440	GSK-1120212
G7540	GSK-1838705A
G7541	GSK-1904529A
G7345	GSK-2606414
G7346	GSK-2636771
G7240	GSK-2830371
G7862	GTPL-5846
G8800	GW-788388
G9648	12-Methyl Gymnodimine
H6225	HPGDS-inhibitor-1
H9863	Hyperforin Dicyclohexylammonium
I0516	I-BET151
I0800	IC-87114
I0933	Icilin
I5203	Inauhzin
I5210	INCB018424
I5208	INCB-28060
I5212	Indirubin
I5992	IOX2
I6132	IPI-145
I7258	Isoflurane
I7155	Isoindigo
I0010	5-(9-Isopropyl-2-morpholino-9H-purin-6-yl)pyrimidin-2-amine
I7469	ISRIB
I7478	Istradefylline
I9060	IWP-2
J0001	J-147
J0240	JAK2 Inhibitor V
J0378	Jatrorrhizine
J0379	Jatrorrhizine Chloride
J3204	E-JIB-04
J3205	Z-JIB-04
J5237	JNJ-26854165
J8800	JW55
K0271	Kartogenin
K0552	Kb NB 77-78
K0652	Kb NB 142-70
K1679	(+)-Ketanserin Tartrate

New Products

K5604	Kobe 0065
K5606	Kobe 2602
K6276	KPT-330
K9200	KX1-004
L0400	LB-100
L0528	LBH-589
L1875	Lestaurtinib
L1982	Leupeptin Hemisulfate
L2540	LGK-974
L2800	LH846
L9600	LY-2090314
L9602	LY-2874455
L9800	LY-364947
L9700	LY-411575
L9701	LY-450139
L4796	LY-294002
L9610	Lycorine Hydrochloride
M0113	Madecassoside
M1335	Mdivi-1
M1444	MDL 29951
M1579	Methazolamide
M1874	3-Methyladenine
M3232	Methylisoindigotin
M2077	1-Methoxy-5-methylphenazinium Methyl Sulfate
M2400	MG-132
M2409	MGCD-0103
M3196	MHY-1485
M3406	Microcystin-LR
M3407	Microcystin-RR
M3411	[D-Asp3, (E)-Dhb7]-Microcystin-RR
M3412	[D-Asp3, (E)-Dhb7]-Microcystin-HphR
M3414	[D-Asp3, (E)-Dhb7]-Microcystin-HtyR
M3206	Microginin 511
M3207	Microginin 674
M3209	Microginin 688
M3430	Micropeptin 1106
M3380	MitoPT® TMRE Mitochondrial Depolarization Assay Kit
M3381	MitoPT® TMRM Mitochondrial Depolarization Assay Kit
M4200	MK-0752
M4102	MK-1775
M4004	MK-2461
M4400	ML-161
M4455	MLN-2238
M4652	MLN8237
M5610	Moclobemide
M5877	Motesanib Diphosphate
M7200	MS436
N1610	Necrostatin-1
N1894	Nexturastat A
N2400	NG-52
N3350	Nimorazole
N3577	Nitidine Chloride
N3476	Nitisinone
N4524	NLG919
N4972	NMS-873
N5072	NMS-1286937
N6272	NPS-2143 Hydrochloride
N7200	NS-11394
N7209	NSC-207895
N7208	NSC-74859
N7211	NSC 405020
N7332	NSI-189
N8277	Nutlin-3
N8660	NVP-AUY922
N8662	NVP-BGJ398
N8604	NVP-BGT226
N8663	NVP-LDE225 Diphosphate
N8760	NVP-TAE684
O1200	Odanacatib
O6845	Orlistat
O7208	Oscillaginin A
O7209	Oscillaginin A Methyl Ester
O7210	Oscillaginin B
O7211	Oscillaginin B Methyl Ester
O7212	Oscillaginin C
O7213	Oscillamide Y
O7332	OSI-027
O7333	OSI-906
O7992	OTX-015
P0109	P7C3A20
P0110	(R)-P7C3-OMe
P0344	Palbociclib Isethionate
P0246	Palomid 529
P0346	Palosuran
P0369	Parecoxib Sodium
P1969	Perifosine
P2000	PF-03758309 Dihydrochloride
P2012	PF-04217903
P2002	PF-04691502 Dihydrate
P2100	PF-06447475
P2133	PFI-1
P3018	Phellodendrine
P3076	PHT-427
P3198	Phytanic Acid
P3540	PIK-75 Hydrochloride
P3542	PIK-93
P3440	PIK-293
P3441	PIK-294
P3469	Pirfenidone
P3600	PJ34 Hydrochloride
P4132	PKI-402
P4782	PluriSln 1
P6002	PP-121
P6004	PP-242
P6264	PPQ-102
P7000	PR-619
P6870	Propofol
P7158	Protopine
P7218	Pseudoprotodioscin
P7608	PTC124
P8370	Purmorphamine
P9200	PX-866
P9870	Pyridostatin Trihydrochloride
R0247	Raltegravir
R1217	RDEA119
R1724	Regadenoson
R1885	Reversine
R2400	RG-108
R2788	RGW-611
R3476	RITA
R4132	RKI-1447

New Products

R5212	RN-486
R5600	RO-4929097
R5700	Ro 61-8048
R5749	Romidepsin
S0072	5S rRNA Modificator
S0001	S0859
S0344	Salermide
S0245	Salmeterol
S0253	Sanguinarine
S0501	SB-939
S0500	SB-203580
S0928	SCH-900776
S2792	SGX-523
S2957	Shogaol
S3568	Siramesine
S4244	SKLB 610
S4932	SMI-4a
S3368	S1RA
S5722	Sofosbuvir
S6236	13-Desmethyl Spirolide C
S6247	Splitomicin
S6800	SR1001
S7061	SRPIN340
S7184	SR-VAD-OPH in vitro Apoptosis Detection Reagent
S7868	SRT1720 Hydrochloride
S7601	Statil
S7618	StemRegenin 1
T0216	TAE-226
T0140	TAK-632
T0394	(+)-Taxifolin
T1852	Tenovin-1
T1953	Tenovin-3
T1853	Tenovin-6
T1968	Terpinen-4-ol
T1978	Tetrahydroberberine
T1979	Tetrahydrocoptisine
T2402	TG100-115
T2404	TG101348
T2668	TGR5 Receptor Agonist
T3132	Thiazovivin
T3196	Thymoquinone
T3461	Tiplaxtinin
T3568	Tirasemtiv
T3584	Tivantinib
T4400	TL-32711
T4800	TM3-0089 Sodium
T5060	TMP-269
T5720	Tofacitinib Citrate
T6276	TPT-260
T6931	Triclosan
T6930	Triclosan Methyl Ether
T7232	S-Trityl-L-cysteine
T7860	TTP 22
T8006	Tubastatin A Hydrochloride
T8269	(S)-ar-Turmerone
U5208	UNC0064-12
V1600	VE-821
V2792	VGX-1027
V3325	Virginiamycin M1
V3326	Virginiamycin S1
V3278	Vitamin E Acetate
V7200	VS-5584
V9201	VX-11e
V9202	VX-702
V9228	VX-765
W0247	Walrycin B
W2800	WH-4-023
W2934	WHI-P258
W7200	WS3
W7201	WS6
W9600	WZ-4002
X4400	XL-228
X4424	XL-765
Y0002	Y-320
Y4800	YM-155
Y4802	YM-201636
Z4552	ZLN005
Z4900	ZM-447439
Z7477	ZSTK474

Alphabetical Listing of our Life Science Biochemicals

Contact us:

Tel: 888-558-5227
Fax: 888-558-7329

Email: getinfo@lktlabs.com
Web: lktlabs.com

A0002

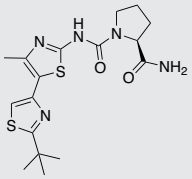

A66

NEW

1 mg
5 mg
10 mg

$C_{17}H_{23}N_5O_2S_2$ FW: 393.53 [1166227-08-2] ≥98%

Inhibitor of p110α PI3K. It decreases viability of endometrial cancer cells and impairs glucose and insulin tolerance.

Weigelt B, Warne PH, Lambros MB, et al. PI3K pathway dependencies in endometrioid endometrial cancer cell lines. Clin Cancer Res. 2013 Jul 1;19(13):3533-44. PMID: 23674493.

Smith GC, Ong WK, Rewcastle GW, et al. Effects of acutely inhibiting PI3K isoforms and mTOR on regulation of glucose metabolism in vivo. Biochem J. 2012 Feb 15;442(1):161-9. PMID: 22142257.

A0099

H-Asp-Arg-Val-Tyr-Ile-His-DAla-OH

A-779

1 mg
2 mg
5 mg

$C_{39}H_{60}N_{12}O_{11}$ FW: 872.99 ≥95%

Mas antagonist that inhibits signaling by angiotensin (1-7), preventing vasodilation and insulin sensitization.

Tao X, Fan J, Kao G, et al. Angiotensin-(1-7) attenuates angiotensin II-induced signaling associated with activation of a tyrosine phosphatase in Sprague-Dawley rats cardiac fibroblasts. Biol Cell. 2014 Mar 18. [Epub ahead of print]. PMID: 24641355.

Santos RA, Campagnole-Santos MJ, Baracho NC, et al. Characterization of a new angiotensin antagonist selective for angiotensin-(1-7): evidence that the actions of angiotensin-(1-7) are mediated by specific angiotensin receptors. Brain Res Bull. 1994;35(4):293-8. PMID: 7850477.

A2420

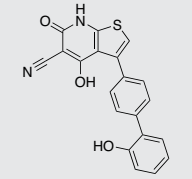

A-769662

NEW

5 mg
10 mg

$C_{20}H_{12}N_2O_3S$ FW: 360.39 [844499-71-4] ≥98%

AMPK activator used to study signaling mechanisms involved in cellular homeostasis. It inhibits cellular proliferation, migration, and invasion in prostate cancer cells, suppresses H_2O_2-induced apoptosis in osteoblasts, and decreases platelet aggregation.

Kim J, Shin J, Ha J. Screening methods for AMP-activated protein kinase modulators: a patent review. Expert Opin Ther Pat. 2015 Mar;25(3):261-77. PMID: 25535089.

Choudhury Y, Yang Z, Ahmad I, et al. AMP-activated protein kinase (AMPK) as a potential therapeutic target independent of PI3K/Akt signaling in prostate cancer. Oncoscience. 2014 Jun 4;1(6):446-56. PMID: 25594043.

Zhu Y, Zhou J, Ao R, et al. A-769662 protects osteoblasts from hydrogen dioxide-induced apoptosis through activating of AMP-activated protein kinase (AMPK). Int J Mol Sci. 2014 Jun 23;15(6):11190-203. PMID: 24960362.

A0001

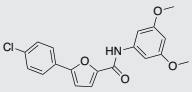

A-803467

NEW

10 mg
50 mg

$C_{19}H_{16}ClNO_4$ FW: 357.79 [944261-79-4] ≥98%

$Na_v1.8$ Na^+ channel blocker and potential $Na_v1.5$ Na^+ channel blocker. It suppresses mechanical and thermal pain nociception and alters action potential morphology in ventricular myocytes.

Rahman W, Dickenson AH. Osteoarthritis-dependent changes in antinociceptive action of $Na_v1.7$ and $Na_v1.8$ sodium channel blockers: An in vivo electrophysiological study in the rat. Neuroscience. 2015 Jun 4;295:103-16. PMID: 25818052.

Han Z, Jiang Y, Xiao F, et al. The effects of A-803467 on cardiac $Na_v1.5$ channels. Eur J Pharmacol. 2015 May 5;754:52-60. PMID: 25701724.

Liu XD, Yang JJ, Fang D, et al. Functional upregulation of $Na_v1.8$ sodium channels on the membrane of dorsal root Ganglia neurons contributes to the development of cancer-induced bone pain. PLoS One. 2014 Dec 11;9(12):e114623. PMID: 25503076.

A0101

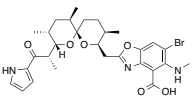

4-bromo-A23187

1 mg
5 mg

4-BrA23187

$C_{29}H_{36}BrN_3O_6$ FW: 602.52 [76455-82-8] ≥98%

Non-fluorescent halogenated A23187 analog and Ca^{2+} ionophore. It induces formation of endothelial microvesicles, increasing leakage of lactate dehydrogenase and decreasing cell viability. It also induces mast cell degranulation and stimulates the acrosome reaction in spermatozoa.

Kim DY, Kang TB, Shim DW, et al. Emodin attenuates A23187-induced mast cell degranulation and tumor necrosis factor-α secretion through protein kinase C and IκB kinase 2 signaling. Eur J Pharmacol. 2014 Jan 15;723:501-6. PMID: 24239713.

Shang M, Zhang Q, Zhang MX, et al. Effects of endothelial microvesicles induced by A23187 on H9c2 cardiomyocytes. Zhongguo Ying Yong Sheng Li Xue Za Zhi. 2013 Nov;29(6):559-64. PMID: 24654540.

Tateno H, Krapf D, Hino T, et al. Ca^{2+} ionophore A23187 can make mouse spermatozoa capable of fertilizing in vitro without activation of cAMP-dependent phosphorylation pathways. Proc Natl Acad Sci U S A. 2013 Nov 12;110(46):18543-8. PMID: 24128762.

A0102

A23187 Ca-Mg

5 mg
10 mg

$(C_{29}H_{36}N_3O_6)_2Mg \bullet (C_{29}H_{36}N_3O_6)_2Ca$ FW: 523.62 ≥98%

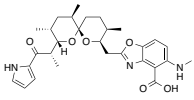

Ca^{2+} ionophore. It induces formation of endothelial microvesicles, increasing leakage of lactate dehydrogenase and decreasing cell viability. It also induces mast cell degranulation and stimulates the acrosome reaction in spermatozoa.

Kim DY, Kang TB, Shim DW, et al. Emodin attenuates A23187-induced mast cell degranulation and tumor necrosis factor-α secretion through protein kinase C and IκB kinase 2 signaling. Eur J Pharmacol. 2014 Jan 15;723:501-6. PMID: 24239713.

Shang M, Zhang Q, Zhang MX, et al. Effects of endothelial microvesicles induced by A23187 on H9c2 cardiomyocytes. Zhongguo Ying Yong Sheng Li Xue Za Zhi. 2013 Nov;29(6):559-64. PMID: 24654540.

Tateno H, Krapf D, Hino T, et al. Ca^{2+} ionophore A23187 can make mouse spermatozoa capable of fertilizing in vitro without activation of cAMP-dependent phosphorylation pathways. Proc Natl Acad Sci U S A. 2013 Nov 12;110(46):18543-8. PMID: 24128762.

A0401

Abacavir

NEW

10 mg
25 mg
50 mg

$C_{14}H_{18}N_6O$ FW: 286.33 [136470-78-5] ≥98%

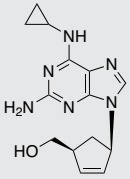

Guanosine analog and inhibitor of RT, guanylyl cyclase, and telomerase used to treat HIV infection.

Leeansyah E, Cameron PU, Solomon A, et al. Inhibition of telomerase activity by human immunodeficiency virus (HIV) nucleos(t)ide reverse transcriptase inhibitors: a potential factor contributing to HIV-associated accelerated aging. J Infect Dis. 2013 Apr;207(7):1157-65. PMID: 23303810.

Baum PD, Sullam PM, Stoddart CA, et al. Abacavir increases platelet reactivity via competitive inhibition of soluble guanylyl cyclase. AIDS. 2011 Nov 28;25(18):2243-8. PMID: 21941165.

Ribera E, Tuset M, Martín M, et al. Characteristics of antiretroviral drugs. Enferm Infecc Microbiol Clin. 2011 May;29(5):362-91. PMID: 21531048.

A0402

Abacavir Sulfate

NEW

5 mg
10 mg
25 mg
50 mg

$(C_{14}H_{18}N_6O)_2 \bullet H_2O_4S$ FW: 670.75 [188062-50-2] ≥98%

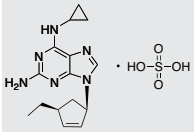

Guanosine analog and inhibitor of RT, guanylyl cyclase, and telomerase used to treat HIV infection.

Leeansyah E, Cameron PU, Solomon A, et al. Inhibition of telomerase activity by human immunodeficiency virus (HIV) nucleos(t)ide reverse transcriptase inhibitors: a potential factor contributing to HIV-associated accelerated aging. J Infect Dis. 2013 Apr;207(7):1157-65. PMID: 23303810.

Baum PD, Sullam PM, Stoddart CA, et al. Abacavir increases platelet reactivity via competitive inhibition of soluble guanylyl cyclase. AIDS. 2011 Nov 28;25(18):2243-8. PMID: 21941165.

Ribera E, Tuset M, Martín M, et al. Characteristics of antiretroviral drugs. Enferm Infecc Microbiol Clin. 2011 May;29(5):362-91. PMID: 21531048.

A0501

Abamectin

1 g
5 g
25 g

Avermectin B1

$C_{48}H_{72}O_{14}$(B1a) $C_{47}H_{70}O_{14}$(B1b) [71751-41-2] ≥70%

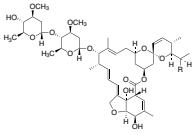

F0F1-ATPase and adenine nucleotide translocator inhibitor and GABA receptor antagonist. It prevents mitochondrial respiration and decreases sperm count and motility.

Castanha Zanoli JC, Maioli MA, Medeiros HC, et al. Abamectin affects the bioenergetics of liver mitochondria: A potential mechanism of hepatotoxicity. Toxicol In Vitro. 2012 Feb;26(1):51-6. PMID: 22024101.

Celik-Ozenci C, Tasatargil A, Tekcan M, et al. Effects of abamectin exposure on male fertility in rats: potential role of oxidative stress-mediated poly(ADP-ribose) polymerase (PARP) activation. Regul Toxicol Pharmacol. 2011 Dec;61(3):310-7. PMID: 21945325.

Holden-Dye L, Walker RJ. Avermectin and avermectin derivatives are antagonists at the 4-aminobutyric acid (GABA) receptor on the somatic muscle cells of *Ascaris*; is this the site of anthelmintic action? Parasitology. 1990 Oct;101 Pt 2:265-71. PMID: 2175874.

A0534

Abiraterone

5 mg
25 mg
100 mg

$C_{24}H_{31}NO$ FW: 349.51 [154229-19-3] ≥98%

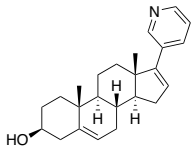

Progesterone derivative and Cyp17A1 inhibitor used to treat castration-resistant prostate cancer. It decreases androgen production and may inhibit eIF4F signaling.

Ryan CJ, Cheng ML. Abiraterone acetate for the treatment of prostate cancer. Expert Opin Pharmacother. 2013 Jan;14(1):91-6. PMID: 23199349.

Rehman Y, Rosenberg JE. Abiraterone acetate: oral androgen biosynthesis inhibitor for treatment of castration-resistant prostate cancer. Drug Des Devel Ther. 2012;6:13-8. PMID: 22291466.

Soifer HS, Souleimanian N, Wu S, et al. Direct regulation of androgen receptor activity by potent CYP17 inhibitors in prostate cancer cells. J Biol Chem. 2012 Feb 3;287(6):3777-87. PMID: 22174412.

A0776

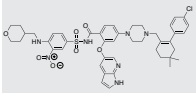

ABT-199

NEW

1 mg
5 mg
10 mg

GDC-0199

$C_{45}H_{50}ClN_7O_7S$ FW: 868.44 [1257044-40-8] ≥98%

BH3 mimetic and Bcl-2 inhibitor. It induces apoptosis in chronic lymphocytic leukemia cells.

Khaw SL, Mérino D, Anderson MA, et al. Both leukaemic and normal peripheral B lymphoid cells are highly sensitive to the selective pharmacological inhibition of prosurvival Bcl-2 with ABT-199. Leukemia. 2014 Jan 9. [Epub ahead of print]. PMID: 24402163.

Pan R, Hogdal LJ, Benito JM, et al. Selective BCL-2 Inhibition by ABT-199 Causes On-Target Cell Death in Acute Myeloid Leukemia. Cancer Discov. 2014 Feb 13. [Epub ahead of print]. PMID: 24346116.

Vandenberg CJ, Cory S. ABT-199, a new Bcl-2-specific BH3 mimetic, has in vivo efficacy against aggressive Myc-driven mouse lymphomas without provoking thrombocytopenia. Blood. 2013 Mar 21;121(12):2285-8. PMID: 23341542.

A0777

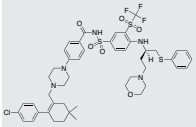

ABT-263

NEW

1 mg
5 mg
10 mg

Navitoclax; A-855071

$C_{47}H_{55}ClF_3N_5O_6S_3$ FW: 974.61 [923564-51-6] ≥98%

BH3 mimetic and inhibitor of Bcl-2, Bcl-ω, and Bcl-xl. It enhances the efficacy of co-administered chemotherapeutics and inhibits proliferation of chronic lymphocytic leukemia cells.

Debrincat MA, Pleines I, Lebois M, et al. BCL-2 is dispensable for thrombopoiesis and platelet survival. Cell Death Dis. 2015 Apr 16;6:e1721. PMID: 25880088.

Khaw SL, Mérino D, Anderson MA, et al. Both leukaemic and normal peripheral B lymphoid cells are highly sensitive to the selective pharmacological inhibition of prosurvival Bcl-2 with ABT-199. Leukemia. 2014 Jan 9. [Epub ahead of print]. PMID: 24402163.

Balakrishnan K, Gandhi V. Bcl-2 antagonists: a proof of concept for CLL therapy. Invest New Drugs. 2013 Oct;31(5):1384-94. PMID: 23907405.

A0778

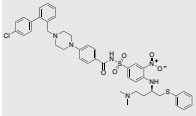

ABT-737

NEW

5 mg
10 mg

$C_{42}H_{45}ClN_6O_5S_2$ FW: 813.43 [852808-04-9] ≥98%

BH3 mimetic and inhibitor of Bcl-2, Bcl-xl, and Bcl-ω. It inhibits growth of acute myelogenous leukemia cells and induces apoptosis and clearance in platelets.

Lieber J, Armeanu-Ebinger S, Fuchs J. The Role of BH3-Mimetic Drugs in the Treatment of Pediatric Hepatoblastoma. Int J Mol Sci. 2015 Feb 16;16(2):4190-4208. PMID: 25690034.

Baev DV, Krawczyk J, O'Dwyer M, et al. The BH3-mimetic ABT-737 effectively kills acute myeloid leukemia initiating cells. Leuk Res Rep. 2014 Sep 1;3(2):79-82. PMID: 25379408.

Gyulkhandanyan AV, Mutlu A, Allen DJ, et al. BH3-mimetic ABT-737 induces strong mitochondrial membrane depolarization in platelets but only weakly stimulates apoptotic morphological changes, platelet shrinkage and microparticle formation. Thromb Res. 2014 Jan;133(1):73-9. PMID: 24268298.

A0812

Ac-D-E

5 mg
10 mg
25 mg

Isospaglumic acid; NAAG

Ac-Asp-Glu-OH

$C_{11}H_{16}N_2O_8$ FW: 304.3 [3106-85-2] ≥95%

Mast cell stabilizer used to treat seasonal allergic rhinitis.

Horak F. Seasonal allergic rhinitis. Newer treatment approaches. Drugs. 1993 Apr;45(4):518-27. PMID: 7684672.

C0375

Ac-DEVD-pNA

1 mg
2 mg
5 mg

Colorimetric caspase 3 substrate

Ac-Asp-Glu-Val-Asp-pNA

$C_{26}H_{34}N_6O_{13}$ FW: 638.6 ≥95%

Substrate used to measure activity of caspase 3.

Mahdavi M, Davoodi J, Zali MR, et al. Concomitant activation of caspase-9 and down-regulation of IAP proteins as a mechanism of apoptotic death in HepG2, T47D and HCT-116 cells upon exposure to a derivative from 4-aryl-4H-chromenes family. Biomed Pharmacother. 2011 Jun;65(3):175-82. PMID: 21565459.

Kluza J, Lansiaux A, Wattez N, et al. Apoptotic response of HL-60 human leukemia cells to the antitumor drug TAS-103. Cancer Res. 2000 Aug 1;60(15):4077-84. PMID: 10945613

A0825

Ac-GPK-pNA

25 mg

$C_{21}H_{30}N_6O_6$ FW: 462.5 ≥95%

Ac-Gly-Pro-Lys-pNA

Substrate used to measure caspase activity.

A0826

Ac-GPK(Ac)-pNA

25 mg

$C_{23}H_{32}N_6O_7$ FW: 504.5 ≥95%

Ac-Gly-Pro-Lys(Ac)-pNA

Substrate used to measure caspase activity.

A0832 Ac-IEAR-pNA — 25 mg

$C_{28}H_{43}N_9O_9$ FW: 649.7 ≥95%

Ac-Ile-Glu-Ala-Arg-pNA • HCl

Substrate used to measure caspase activity.

A0834 Ac-IETD-pNA — 25 mg

$C_{27}H_{38}N_6O_{12}$ FW: 638.6 ≥95%

Ac-Ile-Glu-Thr-Asp-pNA

Substrate used to measure caspase 8 activity.

Smith GK, Barrett DG, Blackburn K, et al. Expression, preparation, and high-throughput screening of caspase-8: discovery of redox-based and steroid diacid inhibition. Arch Biochem Biophys. 2002 Mar 15;399(2):195-205. PMID: 11888206.

Koeplinger KA, Mildner AM, Leone JW, et al. Caspase 8: an efficient method for large-scale autoactivation of recombinant procaspase 8 by matrix adsorption and characterization of the active enzyme. Protein Expr Purif. 2000 Apr;18(3):378-87. PMID: 10733893.

A1084 Ac-VEID-pNA — 25 mg

$C_{28}H_{40}N_6O_{11}$ FW: 636.6 ≥95%

Ac-Val-Glu-Ile-Asp-pNA

Substrate used to measure caspase 6 activity.

Kanazawa T, Kono T, Watanabe M, et al. Bcl-2 blocks apoptosis caused by pierisin-1, a guanine-specific ADP-ribosylating toxin from the cabbage butterfly. Biochem Biophys Res Commun. 2002 Aug 9;296(1):20-5. PMID: 12147221.

A1097 Ac-YVAD-pNA — 25 mg

$C_{29}H_{36}N_6O_{10}$ FW: 628.6 ≥95%

Ac-Tyr-Val-Ala-Asp-pNA

Substrate used to measure caspase 1 activity.

Pereira NA, Song Z. Some commonly used caspase substrates and inhibitors lack the specificity required to monitor individual caspase activity. Biochem Biophys Res Commun. 2008 Dec 19;377(3):873-7. PMID: 18976637.

Eckert A, Steiner B, Marques C, et al. Elevated vulnerability to oxidative stress-induced cell death and activation of caspase-3 by the Swedish amyloid precursor protein mutation. J Neurosci Res. 2001 Apr 15;64(2):183-92. PMID: 11288146.

A0802 Acarbose — 1 g, 5 g, 25 g

BAY G 5421

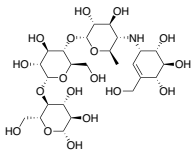

$C_{25}H_{43}NO_{18}$ FW: 645.6 [56180-94-0] ≥98%

α-Glucosidase inhibitor that decreases digestion of complex carbohydrates and prevents glucose absorption. It improves insulin sensitivity and decreases postprandial hyperglycemia.

Kalra S. Alpha glucosidase inhibitors. J Pak Med Assoc. 2014 Apr;64(4):474-6. PMID: 24864650.

Okada K, Yanagawa T, Warabi E, et al. The alpha-glucosidase inhibitor acarbose prevents obesity and simple steatosis in sequestosome 1/A170/p62 deficient mice. Hepatol Res. 2009 May;39(5):490-500. PMID: 19207582.

Hoffmann J, Spengler M. Efficacy of 24-week monotherapy with acarbose, metformin, or placebo in dietary-treated NIDDM patients: the Essen-II Study. Am J Med. 1997 Dec;103(6):483-90. PMID: 9428831.

A1017 Aceclofenac — 1 g, 5 g, 25 g, 100 g

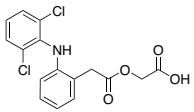

$C_{16}H_{13}Cl_2NO_4$ FW: 354.18 [89796-99-6] ≥98%

Diclofenac analog, NSAID, and COX-2 inhibitor used to treat arthritis. It also decreases neutrophil adhesion to endothelial cells.

Chopade AR, Sayyad FJ, Naikwade NS. Pharmacological characterization of carrageenan induced heat muscle hyperalgesia in rats using non-selective, preferential and selective COX-2 inhibitors. Pharmacol Rep. 2014 Jun;66(3):353-62. PMID: 24905509.

González-Alvaro I, Carmona L, Díaz-González F, et al. Aceclofenac, a new nonsteroidal antiinflammatory drug, decreases the expression and function of some adhesion molecules on human neutrophils. J Rheumatol. 1996 Apr;23(4):723-9. PMID: 8730134.

A0816 Acemetacin — 1 g, 5 g

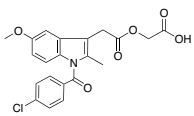

$C_{21}H_{18}ClNO_6$ FW: 415.83 [53164-05-9] ≥98%

Prodrug of indomethacin, NSAID, and COX-1/2 inhibitor used to treat pain and arthritis. It also scavenges ROS and RNS.

Chávez-Piña AE, McKnight W, Dicay M, et al. Mechanisms underlying the anti-inflammatory activity and gastric safety of acemetacin. Br J Pharmacol. 2007 Nov;152(6):930-8. PMID: 17876306.

Fernandes E, Costa D, Toste SA, et al. In vitro scavenging activity for reactive oxygen and nitrogen species by nonsteroidal anti-inflammatory indole, pyrrole, and oxazole derivative drugs. Free Radic Biol Med. 2004 Dec 1;37(11):1895-905. PMID: 15528048.

A0916

Acepromazine Maleate

25 mg
100 mg
250 mg

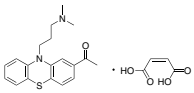

$C_{19}H_{22}N_2OS \cdot C_4H_4O_4$ FW: 442.53 [3598-37-6] ≥98%

Dopamine D1/2 receptor and 5-HT1A/2A receptor antagonist used to prevent nausea and induce sedation. It also prevents sudden cardiac death in models of status epilepticus and reduces vasopressor activity of dopamine during anesthesia.

Monteiro ER, Teixeira Neto FJ, et al. Effects of acepromazine on the cardiovascular actions of dopamine in anesthetized dogs. Vet Anaesth Analg. 2007 Sep;34(5):312-21. PMID: 17686118.

Harrigan T, Bureau YR, Persinger MA, et al. Prevention of sudden cardiac death by the atypical neuroleptic acepromazine following status epilepticus in rats. Life Sci. 1994;54(24):PL457-62. PMID: 8196501.

A0919

Acetyl-L-Carnitine

1 g
5 g

ALCAR

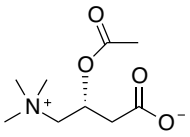

$C_9H_{17}NO_4$ FW: 203.24 [3040-38-8] ≥98%

Carnitine derivative involved in energy homeostasis. It displays a variety of biological activities, including acetylating p65 and upregulating expression of mGluR2s, suppressing cellular stress responses in neurons, and indirectly modulating activity of M1 mAChRs.

Cuccurazzu B, Bortolotto V, Valente MM, et al. Upregulation of mGlu2 receptors via NF-κB p65 acetylation is involved in the Proneurogenic and antidepressant effects of acetyl-l-carnitine. Neuropsychopharmacology. 2013 Oct;38(11):2220-30. PMID: 23670591.

Onofrj M, Ciccocioppo F, Varanese S, et al. Acetyl-L-carnitine: from a biological curiosity to a drug for the peripheral nervous system and beyond. Expert Rev Neurother. 2013 Aug;13(8):925-36. PMID: 23965166.

A0922

Acetyl-L-Carnitine Hydrochloride

NEW

1 g
5 g
25 g

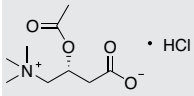

$C_9H_{17}NO_4 \cdot HCl$ FW: 239.7 [5080-50-2] ≥98%

Carnitine derivative involved in energy homeostasis. It acetylates p65, inhibits 3-NPA-produced cellular stress responses and neurotoxicity, normalizes brain levels of neurotrophic factors such as NGF, GDNF, and artemin, and indirectly modulates M1 mAChR activity.

Cuccurazzu B, Bortolotto V, Valente MM, et al. Upregulation of mGlu2 receptors via NF-κB p65 acetylation is involved in the Proneurogenic and antidepressant effects of acetyl-l-carnitine. Neuropsychopharmacology. 2013 Oct;38(11):2220-30. PMID: 23670591.

Onofrj M, Ciccocioppo F, Varanese S, et al. Acetyl-L-carnitine: from a biological curiosity to a drug for the peripheral nervous system and beyond. Expert Rev Neurother. 2013 Aug;13(8):925-36. PMID: 23965166.

A0819

Acetylsalicylic Acid

500 g
1 kg

Salicylic acid acetate; Aspirin

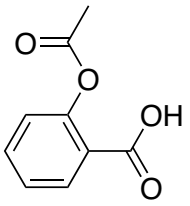

$C_9H_8O_4$ FW: 180.16 [50-78-2] ≥98%

NSAID and COX-1/2 inhibitor used to decrease inflammation. It inhibits platelet aggregation and prolongs bleeding time by decreasing levels of thromboxane A2. Chronic administration decreases risk of cancer and cardiovascular events.

Algra AM, Rothwell PM. Effects of regular aspirin on long-term cancer incidence and metastasis: a systematic comparison of evidence from observational studies versus randomised trials. Lancet Oncol. 2012 May;13(5):518-27. PMID: 22440112.

Antithrombotic Trialists' (ATT) Collaboration: Baigent C, Blackwell L, Collins R, et al. Aspirin in the primary and secondary prevention of vascular disease: collaborative meta-analysis of individual participant data from randomised trials. Lancet. 2009 May 30;373(9678):1849-60. PMID: 9482214.

A0817

D,L-1'-Acetoxychavicol Acetate

25 mg
100 mg
250 mg

CCRIS 7708

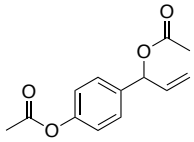

$C_{13}H_{14}O_4$ FW: 234.25 [52946-22-2] ≥98%

TRPA1 channel agonist and xanthine oxidase inhibitor. It increases levels of phase II enzymes in models of colon carcinogenesis and suppresses tumor growth in animal models of squamous cell carcinoma. In other cancer models, it prevents angiogenesis and metastasis. It also inhibits CRM1, preventing influenza virus replication.

Williams M, Tietzel I, Quick QA. 1'-Acetoxychavicol acetate promotes caspase 3-activated glioblastoma cell death by overcoming enhanced cytokine expression. Oncol Lett. 2013 Jun;5(6):1968-1972. PMID: 23833677.

Seo JW, Cho SC, Park SJ, et al. 1'-Acetoxychavicol acetate isolated from Alpinia galanga ameliorates ovalbumin-induced asthma in mice. PLoS One. 2013;8(2):e56447. PMID: 23451048.

Aziz AN, Ibrahim H, Rosmy Syamsir D, et al. Antimicrobial compounds from Alpinia conchigera. J Ethnopharmacol. 2013 Feb 13;145(3):798-802. PMID: 23266278.

A0818

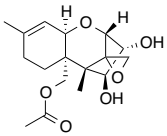

15-Acetoxyscirpenol

1 mg
5 mg

$C_{17}H_{24}O_6$ FW: 324.37 [2623-22-5] ≥97%

Mycotoxin found in *Fusarium*. It induces apoptosis in Jurkat T cells.

Lee DH, Park T, Kim HW. Induction of apoptosis by disturbing mitochondrial-membrane potential and cleaving PARP in Jurkat T cells through treatment with acetoxyscirpenol mycotoxins. Biol Pharm Bull. 2006 Apr;29(4):648-54. PMID: 16595895.

A0921

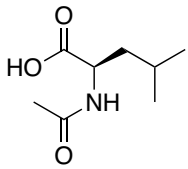

N-Acetyl-D-Leucine

1 g
5 g

$C_8H_{15}NO_3$ FW: 173.21 [19764-30-8] ≥98%

D-amino acid that inhibits bacterial biofilm formation when incorporated into bacterial cell walls.

Leiman SA, May JM, Lebar MD, et al. D-amino acids indirectly inhibit biofilm formation in *Bacillus* subtilis by interfering with protein synthesis. J Bacteriol. 2013 Dec;195(23):5391-5. PMID: 24097941.

Kolodkin-Gal I, Romero D, Cao S, et al. D-amino acids trigger biofilm disassembly. Science. 2010 Apr 30;328(5978):627-9. PMID: 20431016.

A0918

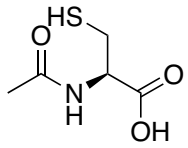

N-Acetyl-L-Cysteine

10 g
25 g
100 g

$C_5H_9NO_3S$ FW: 163.2 [616-91-1] ≥98%

Cysteine derivative and antioxidant used to treat acetaminophen overdose. It scavenges ROS and decreases oxidative stress, inhibits TNF-α-induced pro-inflammatory cytokine release, and inhibits hepatitis B virus replication by suppressing viral assembly.

Lim JH, Lee YM, Park SR, et al. Anticancer activity of hispidin via reactive oxygen species-mediated apoptosis in colon cancer cells. Anticancer Res. 2014 Aug;34(8):4087-93. PMID: 25075033.

Grosicka-Maciąg E, Szumiło M, Czeczot H, et al. Modulation of antioxidant defense system by the dithiocarbamate fungicides Maneb and Zineb in Chinese hamster V79 cells and the role of N-acetyl-L-cysteine. Food Chem Toxicol. 2013 Oct;60:130-4. PMID: 23871785.

A0820

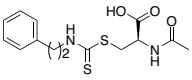

N-Acetyl-S-(N'-benzylthiocarbamoyl)-L-cysteine

10 mg
25 mg
100 mg

Acetyl benzylisothiocyanate-L-cysteine

$C_{13}H_{16}N_2O_3S_2$ FW: 312.41 ≥98%

Conjugate of N-acetyl-cysteine and benzylisothiocyanate. It may display a wide variety of biological activities, including inducing cell cycle arrest and apoptosis in glioma cells, suppressing mTOR activity and inducing autophagy in prostate cancer cells, and inhibiting growth of *Bacillus*, *Staphylococcus*, *Enterococcus*, *Salmonella*, and *Enterobacter*.

Dufour V, Stahl M, Rosenfeld E, et al. Insights into the mode of action of benzyl isothiocyanate on Campylobacter jejuni. Appl Environ Microbiol. 2013 Nov;79(22):6958-68. PMID: 24014524.

Ni WY, Hsiao YP, Hsu SC, et al. Oral administration of benzyl-isothiocyanate inhibits in vivo growth of subcutaneous xenograft tumors of human malignant melanoma A375.S2 cells. In Vivo. 2013 Sep-Oct;27(5):623-6. PMID: 23988897.

Zhu Y, Zhuang JX, Wang Q, et al. Inhibitory effect of benzyl isothiocyanate on proliferation in vitro of human glioma cells. Asian Pac J Cancer Prev. 2013;14(4):2607-10. PMID: 23725183.

A0822

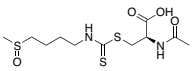

N-Acetyl-S-(N-methylsulfinylbutylthiocarbamoyl)-L-cysteine

5 mg
10 mg
25 mg

N-Acetyl cysteine sulforaphane

$C_{11}H_{20}N_2O_4S_3$ FW: 340.48 ≥98%

Conjugate of sulforaphane and N-acetyl cysteine. It may decrease oxidative damage.

A0823

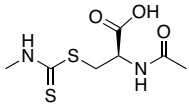

N-Acetyl-S-(N'-methylthiocarbamoyl)-L-cysteine

10 mg
25 mg
100 mg

Acetyl methylisothiocyanate-L-cysteine

$C_7H_{12}N_2O_3S_2$ FW: 236.31 ≥98%

Conjugate of N-acetyl-cysteine and methylisothiocyanate. It may display a wide variety of biological activities, including inhibiting hatch of *Heterodera*, increasing aldehyde levels in blood and brain, and inducing lipid peroxidation-mediated DNA damage.

Ren Y, Lee B, Mahon D, et al. Fumigation of wheat using liquid ethyl formate plus methyl isothiocyanate in 50-tonne farm bins. J Econ Entomol. 2008 Apr;101(2):623-30. PMID: 18459432.

Kassie F, Laky B, Nobis E, et al. Genotoxic effects of methyl isothiocyanate. Mutat Res. 2001 Jan 25;490(1):1-9. Erratum in: Mutat Res 2001 May 31;492(1-2):111-3. PMID: 11152966.

A0920

N-Acetyl-S-(N'-phenethylthiocarbamoyl)-L-cysteine

25 mg
100 mg
500 mg

Acetyl phenethylisothiocyanate-L-cysteine

$C_{14}H_{18}N_2O_3S_2$ FW: 326.43 ≥95%

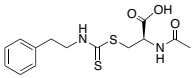

N-acetyl cysteine conjugate of phenethylisothiocyanate. It increases activation of JNK, p53, and MAPKs and induces apoptosis in lung cancer cells and prostate cancer cells.

Kassie F, Melkamu T, Endalew A, et al. Inhibition of lung carcinogenesis and critical cancer-related signaling pathways by N-acetyl-S-(N-2-phenethylthiocarbamoyl)-l-cysteine, indole-3-carbinol and myo-inositol, alone and in combination. Carcinogenesis. 2010 Sep;31(9):1634-41. PMID: 20603442.

Yang YM, Conaway CC, Chiao JW, et al. Inhibition of benzo(a)pyrene-induced lung tumorigenesis in A/J mice by dietary N-acetylcysteine conjugates of benzyl and phenethyl isothiocyanates during the postinitiation phase is associated with activation of mitogen-activated protein kinases and p53 activity and induction of apoptosis. Cancer Res. 2002 Jan 1;62(1):2-7. PMID: 11782348.

Chiao JW, Chung F, Krzeminski J, et al. Modulation of growth of human prostate cancer cells by the N-acetylcysteine conjugate of phenethyl isothiocyanate. Int J Oncol. 2000 Jun;16(6):1215-9. PMID: 10811998.

A0902

N-Acetyl-S-(N'-phenylhexylthiocarbamoyl)-L-cysteine

10 mg
25 mg
100 mg

Acetyl phenylhexylisothiocyanate-L-cysteine

$C_{18}H_{26}N_2O_3S_2$ FW: 382.54 ≥98%

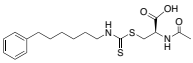

Conjugate of N-acetyl-cysteine and phenylhexylisothiocyanate. It may exhibit several biological activities, including inducing apoptosis in myeloma and leukemia cells, inhibiting HDAC activity, and suppressing activation of carcinogen NNK.

Lu Q, Lin X, Feng J, et al. Phenylhexyl isothiocyanate has dual function as histone deacetylase inhibitor and hypomethylating agent and can inhibit myeloma cell growth by targeting critical pathways. J Hematol Oncol. 2008 Jun 9;1:6. PMID: 18577263.

Lu L, Liu D, Ma X, et al. The phenylhexyl isothiocyanate induces apoptosis and inhibits leukemia cell growth in vivo. Oncol Rep. 2006 Dec;16(6):1363-7. PMID: 17089062.

A0910

N-Acetyl-S-(N'-phenylthiocarbamoyl)-L-cysteine

10 mg
25 mg
100 mg

$C_{12}H_{14}N_2O_3S_2$ FW: 298.38 ≥98%

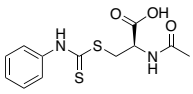

Conjugate of N-acetyl-cysteine and phenylisothiocyanate. It may inhibit lipid peroxidation, induce vasodilation, decrease release of pro-inflammatory cytokines, and increase total white blood cell count, antibody titer, and plaque-forming cell levels.

Martelli A, Testai L, Citi V, et al. Pharmacological characterization of the vascular effects of aryl isothiocyanates: Is hydrogen sulfide the real player? Vascul Pharmacol. 2013 Nov 25. pii: S1537-1891(13)00138-9. PMID: 24287004.

Abreu AC, Borges A, Simões LC, et al. Antibacterial activity of phenyl isothiocyanate on *Escherichia* coli and *Staphylococcus aureus*. Med Chem. 2013 Aug;9(5):756-61. PMID: 22974327.

Schroeder NE, Macguidwin AE. Mortality and behavior in *Heterodera* glycines juveniles following exposure to isothiocyanate compounds. J Nematol. 2010 Sep;42(3):194-200. PMID: 22736856.

A0833

Acipimox

1 g
5 g
10 g

$C_6H_6N_2O_3$ FW: 154.12 [51037-30-0] ≥98%

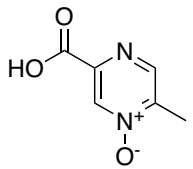

Niacin derivative that decreases levels of triglycerides, LDL, and free fatty acids. It also suppresses lipolysis.

Møller N, Gormsen LC, Schmitz O, et al. Free fatty acids inhibit growth hormone/signal transducer and activator of transcription-5 signaling in human muscle: a potential feedback mechanism. J Clin Endocrinol Metab. 2009 Jun;94(6):2204-7. PMID: 19276230.

Christie AW, McCormick DK, Emmison N, et al. Mechanism of anti-lipolytic action of acipimox in isolated rat adipocytes. Diabetologia. 1996 Jan;39(1):45-53. PMID: 8720602.

A0933

Acitretin

25 mg
100 mg
250 mg

Neotigason

$C_{21}H_{26}O_3$ FW: 326.43 [55079-83-9] ≥98%

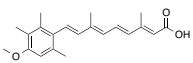

RARα/β/γ agonist used to treat psoriasis. It decreases inflammation and increases cAMP-PKA binding in erythrocytes.

Niu X, Cao W, Ma H, et al. Acitretin exerted a greater influence on T-helper (Th)1 and Th17 than on Th2 cells in treatment of psoriasis vulgaris. J Dermatol. 2012 Nov;39(11):916-21. PMID: 22913391.

Saurat JH. Retinoids and psoriasis: novel issues in retinoid pharmacology and implications for psoriasis treatment. J Am Acad Dermatol. 1999 Sep;41(3 Pt 2):S2-6. PMID: 10459139.

Raynaud F, Gerbaud P, Bouloc A, et al. Rapid effect of treatment of psoriatic erythrocytes with the synthetic retinoid acitretin to increase 8-azido cyclic AMP binding to the RI regulatory subunit. J Invest Dermatol. 1993 Jan;100(1):77-81. PMID: 8380830.

A0934

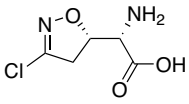

Acivicin

10 mg
25 mg
100 mg

ACIA

$C_5H_7ClN_2O_3$ FW: 178.57 [42228-92-2] ≥98%

Glutamine analog and inhibitor of γ-glutamyl transferase, CTP synthetase, GMP synthetase, and FGAM synthetase. It prevents purine synthesis, inhibits pancreatic cancer cell proliferation, and suppresses growth of *Alternaria*, *Magnaporthe*, and *Botrytis*.

Maeda K, Nakajima Y, Motoyama T, et al. Effects of acivicin on growth, mycotoxin production and virulence of phytopathogenic fungi. Lett Appl Microbiol. 2014 May 27. [Epub ahead of print]. PMID: 24863673.

Hidalgo M, Rodriguez G, Kuhn JG, et al. A Phase I and pharmacological study of the glutamine antagonist acivicin with the amino acid solution aminosyn in patients with advanced solid malignancies. Clin Cancer Res. 1998 Nov;4(11):2763-70. PMID: 9829740.

Lyons SD, Sant ME, Christopherson RI. Cytotoxic mechanisms of glutamine antagonists in mouse L1210 leukemia. J Biol Chem. 1990 Jul 5;265(19):11377-81. PMID: 2358467.

A0958

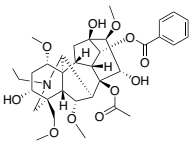

Aconitine

10 mg
25 mg
100 mg

Acetylbenzoylaconine

$C_{34}H_{47}NO_{11}$ FW: 645.74 [302-27-2] ≥88%

Voltage-gated Na^+ channel modulator found in *Aconitum*. It induces muscle paralysis, decreases pain, and acts as a positive inotrope.

Chan TY. Aconite poisoning. Clin Toxicol (Phila). 2009 Apr;47(4):279-85. PMID: 19514874.

Gutser UT, Friese J, Heubach JF, et al. Mode of antinociceptive and toxic action of alkaloids of *Aconitum* spec. Naunyn Schmiedebergs Arch Pharmacol. 1998 Jan;357(1):39-48. PMID: 9459571.

Okazaki M, Kimura I, Kimura M. Aconitine-induced increase and decrease of acetylcholine release in the mouse phrenic nerve-hemidiaphragm muscle preparation. Jpn J Pharmacol. 1994 Dec;66(4):421-6. PMID: 7723217.

A0977

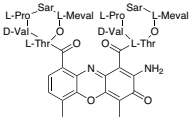

Actinomycin

5 mg
10 mg

Actinomycin D

$C_{62}H_{86}N_{12}O_{16}$ FW: 1255.41 [50-76-0] ≥98%

RNA polymerase and topoisomerase inhibitor. It binds DNA, preventing chain elongation and inhibiting cellular proliferation and tumor growth in several cancers.

Merkel O, Wacht N, Sifft E, et al. Actinomycin D induces p53-independent cell death and prolongs survival in high-risk chronic lymphocytic leukemia. Leukemia. 2012 Dec;26(12):2508-16. PMID: 22743622.

Koba M, Konopa J. Actinomycin D and its mechanisms of action. Postepy Hig Med Dosw (Online). 2005;59:290-8. PMID: 15995596.

Sobell HM. Actinomycin and DNA transcription. Proc Natl Acad Sci U S A. 1985 Aug;82(16):5328-31. PMID: 2410919.

A0978

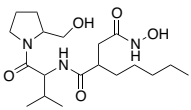

Actinonin

5 mg

$C_{19}H_{35}N_3O_5$ FW: 385.5 [13434-13-4] ≥98%

Inhibitor of peptide deformylase, MMP meprin A, and aminopeptidase N (CD13). It induces apoptosis in Burkitt's lymphoma cells, prevents alterations in renal capillary profusion and sepsis, and inhibits growth of gram positive bacteria.

Sheth A, Escobar-Alvarez S, Gardner J, et al. Inhibition of human mitochondrial peptide deformylase causes apoptosis in c-myc-overexpressing hematopoietic cancers. Cell Death Dis. 2014 Mar 27;5:e1152. PMID: 24675470.

Goemaere E, Melet A, Larue V, et al. New peptide deformylase inhibitors and cooperative interaction: a combination to improve antibacterial activity. J Antimicrob Chemother. 2012 Jun;67(6):1392-400. PMID: 22378679.

Wang Z, Herzog C, Kaushal GP, et al. Actinonin, a meprin A inhibitor, protects the renal microcirculation during sepsis. Shock. 2011 Feb;35(2):141-7. PMID: 20577148.

A1096

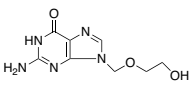

Acyclovir

50 mg
100 mg
500 mg

$C_8H_{11}N_5O_3$ FW: 225.2 [59277-89-3] ≥98%

Guanosine analog and viral DNA polymerase and D-amino oxidase inhibitor that prevents DNA chain elongation. It is used to treat herpes virus infections.

James SH, Prichard MN. Current and future therapies for herpes simplex virus infections: mechanism of action and drug resistance. Curr Opin Virol. 2014 Jul 15;8C:54-61. PMID: 25036916.

Katane M, Matsuda S, Saitoh Y, et al. The antiviral drug acyclovir is a slow-binding inhibitor of (D)-amino acid oxidase. Biochemistry. 2013 Aug 20;52(33):5665-74. PMID: 23859606.

Elion GB. Mechanism of action and selectivity of acyclovir. Am J Med. 1982 Jul 20;73(1A):7-13. PMID: 6285736.

A1202 Adapalene

100 mg
250 mg
1 g

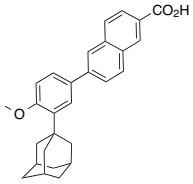

$C_{28}H_{28}O_3$ FW: 412.52 [106685-40-9] ≥98%

Tretinoin analog and RARα/β/γ agonist used to treat acne and pityriasis versicolor. It decreases expression of Ki67, α2-integrin, α6-integrin, TLR2, IL-8, and β-defensin.

Tirado-Sánchez A, Espíndola YS, Ponce-Olivera RM, et al. Efficacy and safety of adapalene gel 0.1% and 0.3% and tretinoin gel 0.05% for acne vulgaris: results of a single-center, randomized, double-blinded, placebo-controlled clinical trial on Mexican patients (skin type III-IV). J Cosmet Dermatol. 2013 Jun;12(2):103-7. PMID: 23725303.

Shi TW, Ren XK, Yu HX, et al. Roles of adapalene in the treatment of pityriasis versicolor. Dermatology. 2012;224(2):184-8. PMID: 22572567.

Zuliani T, Khammari A, Chaussy H, et al. Ex vivo demonstration of a synergistic effect of Adapalene and benzoyl peroxide on inflammatory acne lesions. Exp Dermatol. 2011 Oct;20(10):850-3. PMID: 21793939.

A1217 Adefovir

10 mg
50 mg
250 mg

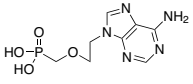

$C_8H_{12}N_5O_4P$ FW: 273.19 [106941-25-7] ≥98%

Adenosine analog, viral DNA polymerase inhibitor, and DNA chain terminator used to treat hepatitis B infection. It also decreases levels of Treg cells and increases levels of IL-4, IL-2, TNF-α, and IFN-γ.

Jiang Y, Li W, Yu L, et al. Enhancing the antihepatitis B virus immune response by adefovir dipivoxil and entecavir therapies. Cell Mol Immunol. 2011 Jan;8(1):75-82. PMID: 20921939

Rodriguez-Frias F, Jardi R, Schaper M, et al. Adefovir for chronic hepatitis B treatment: identification of virological markers linked to therapy response. Antivir Ther. 2008;13(8):991-9. PMID: 19195324.

Zídek Z, Franková D, Holý A. Chemokines, nitric oxide and antiarthritic effects of 9-(2-phosphonomethoxyethyl) adenine (Adefovir). Eur J Pharmacol. 1999 Jul 2;376(1-2):91-100. PMID: 10440094.

A1218 Adefovir Dipivoxil

10 mg
50 mg
250 mg

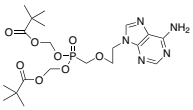

$C_{20}H_{32}N_5O_8P$ FW: 501.47 [142340-99-6] ≥98%

Adenosine analog, viral DNA polymerase inhibitor, and DNA chain terminator used to treat hepatitis B infection. It also decreases levels of Treg cells and increases levels of IL-4, IL-2, TNF-α, and IFN-γ.

Jiang Y, Li W, Yu L, et al. Enhancing the antihepatitis B virus immune response by adefovir dipivoxil and entecavir therapies. Cell Mol Immunol. 2011 Jan;8(1):75-82. PMID: 20921939

Rodriguez-Frias F, Jardi R, Schaper M, et al. Adefovir for chronic hepatitis B treatment: identification of virological markers linked to therapy response. Antivir Ther. 2008;13(8):991-9. PMID: 19195324.

Zídek Z, Franková D, Holý A. Chemokines, nitric oxide and antiarthritic effects of 9-(2-phosphonomethoxyethyl) adenine (Adefovir). Eur J Pharmacol. 1999 Jul 2;376(1-2):91-100. PMID: 10440094.

A1318 Adenine

10 g
25 g

1,6-Dihydro-6-iminopurine; Leuco-4; Vitamin B4

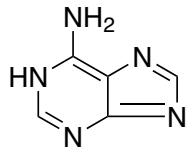

$C_5H_5N_5$ FW: 135.13 [73-24-5] ≥98%

Endogenous nucleotide base required for synthesis of ATP, NAD, FAD, DNA, and RNA.

Nakamura M, Bhatnagar A, Sadoshima J. Overview of pyridine nucleotides review series. Circ Res. 2012 Aug 17;111(5):604-10. PMID: 22904040.

Klingenberg M. Molecular aspects of the adenine nucleotide carrier from mitochondria. Arch Biochem Biophys. 1989 Apr;270(1):1-14. PMID: 2648994.

A1319 Adenosine Triphosphate Disodium

1 g
5 g
10 g
25 g

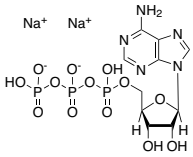

$C_{10}H_{16}N_5Na_2O_{13}P_3$ FW: 551.14 [987-65-5] ≥95%

Endogenous coenzyme and unit of cellular energy, required for production of nucleic acids, cAMP, and other signal transduction molecules. It is used to inhibit reperfusion injury after myocardial infarction during percutaneous coronary intervention and to improve left ventricular function.

Sakuma T, Motoda C, Tokuyama T, et al. Exogenous adenosine triphosphate disodium administration during primary percutaneous coronary intervention reduces no-reflow and preserves left ventricular function in patients with acute anterior myocardial infarction: a study using myocardial contrast echocardiography. Int J Cardiol. 2010 Apr 15;140(2):200-9. PMID: 19081151.

Tokuyama T, Sakuma T, Motoda C, et al. Intravenous administration of adenosine triphosphate disodium during primary percutaneous coronary intervention attenuates the transient rapid improvement of myocardial wall motion, not myocardial stunning, shortly after recanalization in acute anterior myocardial infarction. J Cardiol. 2009 Oct;54(2):289-96. PMID: 19782267.

Törnroth-Horsefield S, Neutze R. Opening and closing the metabolite gate. Proc Natl Acad Sci U S A. 2008 Dec 16;105(50):19565-6. PMID: 19073922.

A1330 Adipokinetic Hormone

1 mg
2 mg
5 mg

AKH

pGlu-Leu-Thr-Phe-Thr-Ser-Trp-Gly-NH_2

$C_{44}H_{60}N_{10}O_{12}$ FW: 921 ≥95%

Found in insects and involved in circadian rhythms. It increases activity of peptidase, lipase, amylase, and polygalacturonase in the salivary glands and decreases lipid peroxidation in brain samples.

Metaxakis A, Tain LS, Grönke S, et al. Lowered insulin signalling ameliorates age-related sleep fragmentation in *Drosophila*. PLoS Biol. 2014 Apr 1;12(4):e1001824. PMID: 24690889.

Vinokurov K, Bednářová A, Tomčala A, et al. Role of adipokinetic hormone in stimulation of salivary gland activities: the fire bug Pyrrhocoris apterus L. (Heteroptera) as a model species. J Insect Physiol. 2014 Jan;60:58-67. PMID: 24269343.

Bednářová A, Kodrík D, Krishnan N. Adipokinetic hormone exerts its anti-oxidative effects using a conserved signal-transduction mechanism involving both PKC and cAMP by mobilizing extra- and intracellular Ca^{2+} stores. Comp Biochem Physiol C Toxicol Pharmacol. 2013 Sep;158(3):142-9. PMID: 23845878.

A1332 Adipokinetic Hormone II from *Locusta migratoria*

1 mg
2 mg
5 mg

$C_{43}H_{58}N_{11}O_{11}$ FW: 903.9 ≥98%

pGlu-Leu-Asn-Phe-Thr-Pro-Asn-Trp-Gly-Thr-NH_2

Neuroregulator and hormone found in *Locusta migratoria*.

Siegert K, Morgan P, Mordue W. Primary structures of locust adipokinetic hormones II. Biol Chem Hoppe Seyler. 1985 Aug;366(8):723-7. PMID: 4063072.

A1333 Adipokinetic Hormone II from *Schistocera gregaria*

1 mg
2 mg
5 mg

$C_{44}H_{60}N_{11}O_{12}$ FW: 934.02 ≥95%

pGlu-Leu-Asn-Phe-Ser-Ala-Gly-Trp-NH_2

Neuroregulator and hormone found in *Schistocera gregaria*.

Siegert K, Morgan P, Mordue W. Primary structures of locust adipokinetic hormones II. Biol Chem Hoppe Seyler. 1985 Aug;366(8):723-7. PMID: 4063072.

A1331 Adipokinetic Hormone, locust

1 mg
2 mg
5 mg

AKH

H-Arg-Pro-Val-Lys-Val-Tyr-Pro-Asn-Gly-Ala-Glu-Asp-Glu-Ser-Ala-Glu-Ala-Phe-Pro-Leu-Glu-Phe-OH

$C_{54}H_{74}N_{14}O_{15}$ FW: 1159.3 ≥95%

Found in insects and involved in circadian rhythms. It increases activity of peptidase, lipase, amylase, and polygalacturonase in the salivary glands and decreases lipid peroxidation in brain samples.

Metaxakis A, Tain LS, Grönke S, et al. Lowered insulin signalling ameliorates age-related sleep fragmentation in *Drosophila*. PLoS Biol. 2014 Apr 1;12(4):e1001824. PMID: 24690889.

Vinokurov K, Bednářová A, Tomčala A, et al. Role of adipokinetic hormone in stimulation of salivary gland activities: the fire bug Pyrrhocoris apterus L. (Heteroptera) as a model species. J Insect Physiol. 2014 Jan;60:58-67. PMID: 24269343.

Bednářová A, Kodrík D, Krishnan N. Adipokinetic hormone exerts its anti-oxidative effects using a conserved signal-transduction mechanism involving both PKC and cAMP by mobilizing extra- and intracellular Ca^{2+} stores. Comp Biochem Physiol C Toxicol Pharmacol. 2013 Sep;158(3):142-9. PMID: 23845878.

A0963 Adrenocorticotropic Hormone (1-10), human

1 mg
2 mg
5 mg

ACTH

H-Ser-Tyr-Ser-Met-Glu-His-Phe-Arg-Trp-Gly-OH

$C_{59}H_{78}N_{16}O_{16}S_1$ FW: 1299.4 ≥95%

Endogenous melanocortin 2 receptor agonist involved in stress signaling. It stimulates adrenal cortisol production, decreases inflammatory cytokine levels, and stimulates proliferation of osteoblasts.

Berkovich R, Agius MA. Mechanisms of action of ACTH in the management of relapsing forms of multiple sclerosis. Ther Adv Neurol Disord. 2014 Mar;7(2):83-96. PMID: 24587825.

Isales CM, Zaidi M, Blair HC. ACTH is a novel regulator of bone mass. Ann N Y Acad Sci. 2010 Mar;1192:110-6. PMID: 20392225.

A0964 Adrenocorticotropic Hormone (1-13), human

0.5 mg
1 mg
2.5 mg

ACTH

H-Ser-Tyr-Ser-Met-Glu-His-Phe-Arg-Trp-Gly-Lys-Pro-Val-OH

$C_{75}H_{106}N_{20}O_{19}S_1$ FW: 1623.9 ≥95%

Endogenous melanocortin 2 receptor agonist involved in stress signaling. It stimulates adrenal cortisol production, decreases inflammatory cytokine levels, and stimulates proliferation of osteoblasts.

Berkovich R, Agius MA. Mechanisms of action of ACTH in the management of relapsing forms of multiple sclerosis. Ther Adv Neurol Disord. 2014 Mar;7(2):83-96. PMID: 24587825.

Isales CM, Zaidi M, Blair HC. ACTH is a novel regulator of bone mass. Ann N Y Acad Sci. 2010 Mar;1192:110-6. PMID: 20392225.

A0965

Adrenocorticotropic Hormone (1-14)

1 mg
2 mg
5 mg

ACTH

H-Ser-Tyr-Ser-Met-Glu-His-Phe-Arg-Trp-Gly-Lys-Pro-Val-Gly-OH

$C_{77}H_{169}N_{21}O_{20}S_1$ FW: 1680.9 ≥95%

Endogenous melanocortin 2 receptor agonist involved in stress signaling. It stimulates adrenal cortisol production, decreases inflammatory cytokine levels, and stimulates proliferation of osteoblasts.

Berkovich R, Agius MA. Mechanisms of action of ACTH in the management of relapsing forms of multiple sclerosis. Ther Adv Neurol Disord. 2014 Mar;7(2):83-96. PMID: 24587825.

Isales CM, Zaidi M, Blair HC. ACTH is a novel regulator of bone mass. Ann N Y Acad Sci. 2010 Mar;1192:110-6. PMID: 20392225.

A0966

Adrenocorticotropic Hormone (1-16), human

0.5 mg
1 mg
2.5 mg

ACTH

H-Ser-Tyr-Ser-Met-Glu-His-Phe-Arg-Trp-Gly-Lys-Pro-Val-Gly-Lys-Lys-OH

$C_{89}H_{133}N_{25}O_{22}S$ FW: 1937.27 ≥95%

Endogenous melanocortin 2 receptor agonist involved in stress signaling. It stimulates adrenal cortisol production, decreases inflammatory cytokine levels, and stimulates proliferation of osteoblasts.

Berkovich R, Agius MA. Mechanisms of action of ACTH in the management of relapsing forms of multiple sclerosis. Ther Adv Neurol Disord. 2014 Mar;7(2):83-96. PMID: 24587825.

Isales CM, Zaidi M, Blair HC. ACTH is a novel regulator of bone mass. Ann N Y Acad Sci. 2010 Mar;1192:110-6. PMID: 20392225.

A0967

Adrenocorticotropic Hormone (1-17), human

0.5 mg
1 mg
2.5 mg

ACTH

H-Ser-Tyr-Ser-Met-Glu-His-Phe-Arg-Trp-Gly-Lys-Pro-Val-Gly-Lys-Lys-Arg-OH

$C_{95}H_{145}N_{29}O_{23}S$ FW: 2093.5 ≥95%

Endogenous melanocortin 2 receptor agonist involved in stress signaling. It stimulates adrenal cortisol production, decreases inflammatory cytokine levels, and stimulates proliferation of osteoblasts.

Berkovich R, Agius MA. Mechanisms of action of ACTH in the management of relapsing forms of multiple sclerosis. Ther Adv Neurol Disord. 2014 Mar;7(2):83-96. PMID: 24587825.

Isales CM, Zaidi M, Blair HC. ACTH is a novel regulator of bone mass. Ann N Y Acad Sci. 2010 Mar;1192:110-6. PMID: 20392225.

A0968

Adrenocorticotropic Hormone (1-24), human

0.5 mg
1 mg
2.5 mg

ACTH

H-Ser-Tyr-Ser-Met-Glu-His-Phe-Arg-Trp-Gly-Lys-Pro-Val-Gly-Lys-Lys-Arg-Arg-Pro-Val-Lys-Val-Tyr-Pro-OH

$C_{136}H_{210}N_{40}O_{31}S$ FW: 2933.5 ≥95%

Endogenous melanocortin 2 receptor agonist involved in stress signaling. It stimulates adrenal cortisol production, decreases inflammatory cytokine levels, and stimulates proliferation of osteoblasts.

Berkovich R, Agius MA. Mechanisms of action of ACTH in the management of relapsing forms of multiple sclerosis. Ther Adv Neurol Disord. 2014 Mar;7(2):83-96. PMID: 24587825.

Isales CM, Zaidi M, Blair HC. ACTH is a novel regulator of bone mass. Ann N Y Acad Sci. 2010 Mar;1192:110-6. PMID: 20392225.

A0960

Adrenocorticotropic Hormone (1-39), human

1 mg

ACTH

H-Ser-Tyr-Ser-Met-Glu-His-Phe-Arg-Trp-Gly-Lys-Pro-Val-Gly-Lys-Lys-Arg-Arg-Pro-Val-Lys-Val-Tyr-Pro-Asn-Gly-Ala-Glu-Asp-Glu-Ser-Ala-Glu-Ala-Phe-Pro-Leu-Glu-Phe-OH

$C_{207}H_{308}N_{56}O_{58}S$ FW: 4541.1 [12279-41-3] ≥95%

Endogenous melanocortin 2 receptor agonist involved in stress signaling. It stimulates adrenal cortisol production, decreases inflammatory cytokine levels, and stimulates proliferation of osteoblasts.

Berkovich R, Agius MA. Mechanisms of action of ACTH in the management of relapsing forms of multiple sclerosis. Ther Adv Neurol Disord. 2014 Mar;7(2):83-96. PMID: 24587825.

Isales CM, Zaidi M, Blair HC. ACTH is a novel regulator of bone mass. Ann N Y Acad Sci. 2010 Mar;1192:110-6. PMID: 20392225.

A0961

Adrenocorticotropic Hormone (1-39), rat

0.5 mg
1 mg
2.5 mg

ACTH

H-Ser-Tyr-Ser-Met-Glu-His-Phe-Arg-Trp-Gly-Lys-Pro-Val-Gly-Lys-Lys-Arg-Arg-Pro-Val-Lys-Val-Tyr-Pro-Asn-Val-Ala-Glu-Asn-Glu-Ser-Ala-Glu-Ala-Phe-Pro-Leu-Glu-Phe-OH

$C_{210}H_{315}N_{57}O_{57}S$ FW: 4582.3 [77465-10-2] ≥95%

Endogenous melanocortin 2 receptor agonist involved in stress signaling. It stimulates adrenal cortisol production, decreases inflammatory cytokine levels, and stimulates proliferation of osteoblasts.

Berkovich R, Agius MA. Mechanisms of action of ACTH in the management of relapsing forms of multiple sclerosis. Ther Adv Neurol Disord. 2014 Mar;7(2):83-96. PMID: 24587825.

Isales CM, Zaidi M, Blair HC. ACTH is a novel regulator of bone mass. Ann N Y Acad Sci. 2010 Mar;1192:110-6. PMID: 20392225.

A0962

Adrenocorticotropic Hormone (1-4)

1 mg
2 mg
5 mg

ACTH

H-Ser-Tyr-Ser-Met-OH

$C_{20}H_{30}N_4O_8S$ FW: 486.6 ≥95%

Endogenous melanocortin 2 receptor agonist involved in stress signaling. It stimulates adrenal cortisol production, decreases inflammatory cytokine levels, and stimulates proliferation of osteoblasts.

Berkovich R, Agius MA. Mechanisms of action of ACTH in the management of relapsing forms of multiple sclerosis. Ther Adv Neurol Disord. 2014 Mar;7(2):83-96. PMID: 24587825.

Isales CM, Zaidi M, Blair HC. ACTH is a novel regulator of bone mass. Ann N Y Acad Sci. 2010 Mar;1192:110-6. PMID: 20392225.

A0970

Adrenocorticotropic Hormone (18-39), human

1 mg
2 mg
5 mg

ACTH

H-Arg-Pro-Val-Lys-Val-Tyr-Pro-Asn-Gly-Ala-Glu-Asp-Glu-Ser-Ala-Glu-Ala-Phe-Pro-Leu-Glu-Phe-OH

$C_{112}H_{165}N_{27}O_{36}$ FW: 2465.7 ≥95%

Endogenous melanocortin 2 receptor agonist involved in stress signaling. It stimulates adrenal cortisol production, decreases inflammatory cytokine levels, and stimulates proliferation of osteoblasts.

Berkovich R, Agius MA. Mechanisms of action of ACTH in the management of relapsing forms of multiple sclerosis. Ther Adv Neurol Disord. 2014 Mar;7(2):83-96. PMID: 24587825.

Isales CM, Zaidi M, Blair HC. ACTH is a novel regulator of bone mass. Ann N Y Acad Sci. 2010 Mar;1192:110-6. PMID: 20392225.

A0971

Adrenocorticotropic Hormone (4-10), human

1 mg
2 mg
5 mg

ACTH

H-Met-Glu-His-Phe-Arg-Trp-Gly-OH

$C_{44}H_{59}N_{13}O_{10}S_1$ FW: 962.1 ≥95%

Endogenous melanocortin 2 receptor agonist involved in stress signaling. It stimulates adrenal cortisol production, decreases inflammatory cytokine levels, and stimulates proliferation of osteoblasts.

Berkovich R, Agius MA. Mechanisms of action of ACTH in the management of relapsing forms of multiple sclerosis. Ther Adv Neurol Disord. 2014 Mar;7(2):83-96. PMID: 24587825.

Isales CM, Zaidi M, Blair HC. ACTH is a novel regulator of bone mass. Ann N Y Acad Sci. 2010 Mar;1192:110-6. PMID: 20392225.

A1368

Adrenomedullin (1-52), human

0.5 mg
1 mg
2.5 mg

H-Tyr-Arg-Gln-Ser-Met-Asn-Asn-Phe-Gln-Gly-Leu-Arg-Ser-Phe-Gly-Cys-Arg-Phe-Gly-Thr-Cys-Thr-Val-Gln-Lys-Leu-Ala-His-Gln-Ile-Tyr-Gln-Phe-Thr-Asp-Lys-Asp-Lys-Asp-Asn-Val-Ala-Pro-Arg-Ser-Lys-Ile-Ser-Pro-Gln-Gly-Tyr-NH_2 (Disulfide Bridge Cys16-Cys21)

$C_{264}H_{406}N_{80}O_{77}S_3$ FW: 6028.9 ≥95%

Endogenous CLR-RAMP2/3 receptor agonist involved in cell growth and differentiation. It decreases blood pressure, increases neovascularization, and binds microtubule-associated proteins in the cytoskeleton.

Larráyoz IM, Martínez-Herrero S, Ochoa-Callejero L, et al. Is the cytoskeleton an intracellular receptor for adrenomedullin and PAMP? Curr Protein Pept Sci. 2013 Aug;14(5):429-43. PMID: 23745706.

Chang CL, Hsu SY. Roles of CLR/RAMP receptor signaling in reproduction and development. Curr Protein Pept Sci. 2013 Aug;14(5):393-406. PMID: 23745703.

A1369

Adrenomedullin (13-52), human

0.5 mg
1 mg
2.5 mg

H-Ser-Phe-Gly-Cys-Arg-Phe-Gly-Thr-Cys-Thr-Val-Gln-Lys-Leu-Ala-His-Gln-Ile-Tyr-Gln-Phe-Thr-Asp-Lys-Asp-Lys-Asp-Asn-Val-Ala-Pro-Arg-Ser-Lys-Ile-Ser-Pro-Gln-Gly-Tyr-NH_2 (Disulfide Bridge Cys16-Cys21)

$C_{200}H_{308}N_{58}O_{59}S_2$ FW: 4533.17 ≥95%

Endogenous CLR-RAMP2/3 receptor agonist involved in cell growth and differentiation. It decreases blood pressure, increases neovascularization, and binds microtubule-associated proteins in the cytoskeleton.

Larráyoz IM, Martínez-Herrero S, Ochoa-Callejero L, et al. Is the cytoskeleton an intracellular receptor for adrenomedullin and PAMP? Curr Protein Pept Sci. 2013 Aug;14(5):429-43. PMID: 23745706.

Chang CL, Hsu SY. Roles of CLR/RAMP receptor signaling in reproduction and development. Curr Protein Pept Sci. 2013 Aug;14(5):393-406. PMID: 23745703.

A1370

Adrenomedullin (22-52), human

0.5 mg
1 mg
2.5 mg

H-Thr-Val-Gln-Lys-Leu-Ala-His-Gln-Ile-Try-Gln-Phe-Thr-Asp-Lys-Asp-Lys-Asp-Asn-Val-Ala-Pro-Arg-Ser-Lys-Ile-Ser-Pro-Gln-Gly-Tyr-NH2

$C_{159}H_{252}N_{46}O_{48}$ FW: 3576.06 ≥95%

Endogenous CLR-RAMP2/3 receptor agonist involved in cell growth and differentiation. It decreases blood pressure, increases neovascularization, and binds microtubule-associated proteins in the cytoskeleton.

Larráyoz IM, Martínez-Herrero S, Ochoa-Callejero L, et al. Is the cytoskeleton an intracellular receptor for adrenomedullin and PAMP? Curr Protein Pept Sci. 2013 Aug;14(5):429-43. PMID: 23745706.

Chang CL, Hsu SY. Roles of CLR/RAMP receptor signaling in reproduction and development. Curr Protein Pept Sci. 2013 Aug;14(5):393-406. PMID: 23745703.

A1371

Adrenorphin

Metorphamide

H-Tyr-Gly-Gly-Phe-Met-Arg-Arg-Val-NH_2

$C_{44}H_{69}N_{15}O_9S$ FW: 984.2 ≥95%

1 mg
2 mg
5 mg

Endogenous μOR and κOR agonist. It induces respiratory depression, inhibits catecholamine secretion, and suppresses urinary bladder muscle contractions.

Yanase T, Nawata H, Kato K,et al. Studies on adrenorphin in pheochromocytoma. J Clin Endocrinol Metab. 1987 Apr;64(4):692-7. PMID: 3818899.

Xu SF, Lu WX, Zhou KR, et al. The analgesic and respiratory depressant actions of metorphamide in mice and rabbits. Neuropeptides. 1985 Apr;6(2):121-31. PMID: 4000426.

A1592

ADX-47273

NEW

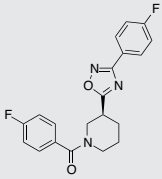

$C_{20}H_{17}F_2N_3O_2$ FW: 369.36 [851881-60-2] ≥98%

5 mg
25 mg

Positive allosteric modulator of mGluR5 receptors. It increases waking activity, stimulates late phase LTP, enhances adaptive learning, and decreases amphetamine- and phencyclidine-induced hyperlocomotion.

Ahnaou A, Langlois X, Steckler T, et al. Negative versus positive allosteric modulation of metabotropic glutamate receptors (mGluR5): indices for potential pro-cognitive drug properties based on EEG network oscillations and sleep-wake organization in rats. Psychopharmacology (Berl). 2015 Mar;232(6):1107-22. PMID: 25323624.

Xu J, Zhu Y, Kraniotis S, et al. Potentiating mGluR5 function with a positive allosteric modulator enhances adaptive learning. Learn Mem. 2013 Jul 18;20(8):438-45. PMID: 23869026.

Kroker KS, Rast G, Rosenbrock H. Differential effect of the mGlu5 receptor positive allosteric modulator ADX-47273 on early and late hippocampal LTP. Neuropharmacology. 2011 Sep;61(4):707-14. PMID: 21640734.

A1607

AEBSF Hydrochloride

NEW

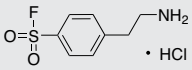

4-(2-Aminoethyl)benzenesulfonyl fluoride hydrochloride

$C_8H_{10}FNO_2S \cdot HCl$ FW: 239.69 [30827-99-7] ≥98%

25 mg
100 mg
500 mg

Serine protease substrate/inhibitor used to measure serine protease activity.

Monnappa AK, Dwidar M, Seo JK, et al. Bdellovibrio bacteriovorus inhibits *Staphylococcus aureus* biofilm formation and invasion into human epithelial cells. Sci Rep. 2014 Jan 22;4:3811. PMID: 24448451.

Wang R, Liu S, Wang J, et al. Purification, characterization and identification of a senescence related serine protease in dark-induced senescent wheat leaves. Phytochemistry. 2013 Nov;95:118-26. PMID: 23910959.

A1865

Aeroplysinin

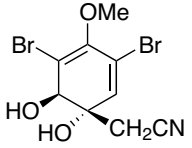

$C_9H_9Br_2NO_3$ FW: 338.98 [28656-91-9] ≥96%

100 μg
5x100 μg
1 mg

Found in marine sponges. It decreases levels of pro-inflammatory cytokines, inhibits capillary tube formation, and induces cell death in Ehrlich ascites tumor cells.

Martínez-Poveda B, García-Vilas JA, Cárdenas C, et al. The brominated compound aeroplysinin-1 inhibits proliferation and the expression of key pro- inflammatory molecules in human endothelial and monocyte cells. PLoS One. 2013;8(1):e55203. PMID: 23383109.

Rodríguez-Nieto S, González-Iriarte M, Carmona R, et al. Antiangiogenic activity of aeroplysinin-1, a brominated compound isolated from a marine sponge. FASEB J. 2002 Feb;16(2):261-3. PMID: 11772945.

Koulman A, Proksch P, Ebel R, et al. Cytotoxicity and mode of action of aeroplysinin-1 and a related dienonefrom the sponge Aplysina aerophoba. J Nat Prod. 1996 Jun;59(6):591-4. PMID: 8786366.

A1895

Aeruginosamide B

NEW

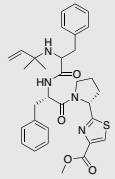

$C_{32}H_{38}N_4O_4S$ FW: 574.73 ≥95%

100 μg

Potential serine protease and PP inhibitor found in *Microcystis*. It is cytotoxic and may inhibit thrombin activity.

Leikoski N, Liu L, Jokela J, et al. Genome mining expands the chemical diversity of the cyanobactin family to include highly modified linear peptides. Chem Biol. 2013 Aug 22;20(8):1033-43. PMID: 23911585.

A1896

Aeruginosamide C

NEW

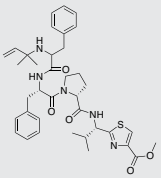

$C_{37}H_{47}N_5O_5S$ FW: 673.86 ≥95%

100 μg

Potential serine protease and PP inhibitor found in *Microcystis*. It is cytotoxic and may inhibit thrombin activity.

Leikoski N, Liu L, Jokela J, et al. Genome mining expands the chemical diversity of the cyanobactin family to include highly modified linear peptides. Chem Biol. 2013 Aug 22;20(8):1033-43. PMID: 23911585.

A1897 Aeruginosamide D

NEW **100 µg**

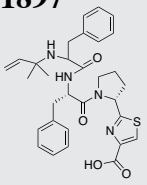

$C_{31}H_{36}N_4O_4S$ FW: 560.71 ≥95%

Potential serine protease and PP inhibitor found in *Microcystis*. It is cytotoxic and may inhibit thrombin activity.

Leikoski N, Liu L, Jokela J, et al. Genome mining expands the chemical diversity of the cyanobactin family to include highly modified linear peptides. Chem Biol. 2013 Aug 22;20(8):1033-43. PMID: 23911585.

A1898 Aeruginosamide E

NEW **100 µg**

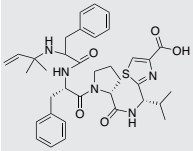

$C_{36}H_{45}N_5O_5S$ FW: 659.84 ≥95%

Potential serine protease and PP inhibitor found in *Microcystis*. It is cytotoxic and may inhibit thrombin activity.

Leikoski N, Liu L, Jokela J, et al. Genome mining expands the chemical diversity of the cyanobactin family to include highly modified linear peptides. Chem Biol. 2013 Aug 22;20(8):1033-43. PMID: 23911585.

A1890 Aeruginosin 722

NEW **100 µg**

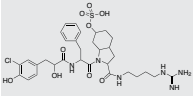

$C_{32}H_{43}ClN_6O_9S$ FW: 723.24 ≥95%

Serine protease and PP inhibitor found in *Microcystis*. It is cytotoxic, decreases levels of IL-8 and ICAM-1, and may inhibit thrombin activity.

Kapuścik A, Hrouzek P, Kuzma M, et al. Novel Aeruginosin-865 from Nostoc sp. as a potent anti-inflammatory agent. Chembiochem. 2013 Nov 25;14(17):2329-37. PMID: 24123716.

Silva-Stenico ME, Silva CS, Lorenzi AS, et al. Non-ribosomal peptides produced by Brazilian cyanobacterial isolates with antimicrobial activity. Microbiol Res. 2011 Mar 20;166(3):161-75. PMID: 20630723.

Wang G, Goyal N. Aeruginosin analogs and other compounds with rigid bicyclic structure as potential antithrombotic agents. Cardiovasc Hematol Agents Med Chem. 2009 Apr;7(2):147-65. PMID: 19355876.

A2077 Afatinib

NEW **5 mg** **10 mg** **25 mg** **100 mg**

BIBW 2992

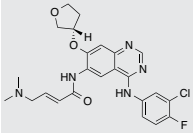

$C_{24}H_{25}ClFN_5O_3$ FW: 485.94 [850140-72-6] ≥98%

EGFR inhibitor used to treat non-small cell lung cancer. It downregulates expression of HER2/EGFR2 and induces apoptosis.

Yap TA, Popat S. The role of afatinib in the management of non-small cell lung carcinoma. Expert Opin Drug Metab Toxicol. 2013 Nov;9(11):1529-39. PMID: 23985030.

Janjigian YY, Viola-Villegas N, Holland JP, et al. Monitoring afatinib treatment in HER2-positive gastric cancer with 18F-FDG and 89Zr-trastuzumab PET. J Nucl Med. 2013 Jun;54(6):936-43. PMID: 23578997.

Solca F, Dahl G, Zoephel A, et al. Target binding properties and cellular activity of afatinib (BIBW 2992), an irreversible ErbB family blocker. J Pharmacol Exp Ther. 2012 Nov;343(2):342-50. PMID: 22888144.

A2244 Aflatoxicol

1 mg **5 mg**

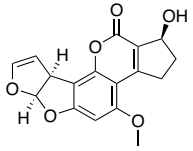

$C_{17}H_{14}O_6$ FW: 314.29 [29611-03-8] ≥98%

Mycotoxin, metabolite of aflatoxin B1, DNA synthesis inhibitor, and carcinogen found in *Aspergillus*. It may form DNA adducts.

Karabulut S, Paytakov G, Leszczynski J. Reduction of aflatoxin B1 to aflatoxicol: a comprehensive DFT study provides clues to its toxicity. J Sci Food Agric. 2014 Dec;94(15):3134-40. PMID: 24652695.

Cortés G, Carvajal M, Méndez-Ramírez I, et al. Identification and quantification of aflatoxins and aflatoxicol from poultry feed and their recovery in poultry litter. Poult Sci. 2010 May;89(5):993-1001. PMID: 20371852.

Bailey GS, Loveland PM, Pereira C, et al. Quantitative carcinogenesis and dosimetry in rainbow trout for aflatoxin B1 and aflatoxicol, two aflatoxins that form the same DNA adduct. Mutat Res. 1994 Aug;313(1):25-38. PMID: 7519308.

A2044 Aflatoxin B1

1 mg **5 mg**

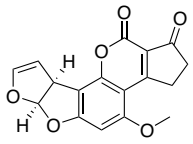

$C_{17}H_{12}O_6$ FW: 312.27 [1162-65-8] ≥98%

DNA synthesis inhibitor and carcinogen. It is the most cytotoxic of all aflatoxins. It induces cell cycle arrest and liver damage.

Miliţă NM, Mihăescu G, Chifiriuc C. Aflatoxins--health risk factors. Bacteriol Virusol Parazitol Epidemiol. 2010 Jan-Mar;55(1):19-24. PMID: 21038701.

Gabal MA, Hegazi SA, Hassanin N. Aflatoxin production by *Aspergillus* flavus field isolates. Vet Hum Toxicol. 1994 Dec;36(6):519-21. PMID: 7900269.

Dutton MF, Ehrlich K, Bennett JW. Biosynthetic relationship among aflatoxins B1, B2, M1, and M2. Appl Environ Microbiol. 1985 Jun;49(6):1392-5. PMID: 3925881.

A2046 Aflatoxin B2

1 mg
5 mg

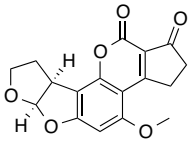

$C_{17}H_{14}O_6$ FW: 314.229 [7220-81-7] ≥98%

DNA synthesis inhibitor and carcinogen. It induces cell cycle arrest and liver damage.

Militã NM, Mihăescu G, Chifiriuc C. Aflatoxins--health risk factors. Bacteriol Virusol Parazitol Epidemiol. 2010 Jan-Mar;55(1):19-24. PMID: 21038701.

Gabal MA, Hegazi SA, Hassanin N. Aflatoxin production by *Aspergillus* flavus field isolates. Vet Hum Toxicol. 1994 Dec;36(6):519-21. PMID: 7900269.

A2048 Aflatoxin G1

1 mg
5 mg

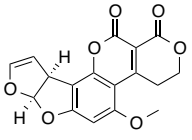

$C_{17}H_{12}O_7$ FW: 328.27 [1165-39-5] ≥98%

DNA synthesis inhibitor and carcinogen. It induces cell cycle arrest and liver damage.

Militã NM, Mihăescu G, Chifiriuc C. Aflatoxins--health risk factors. Bacteriol Virusol Parazitol Epidemiol. 2010 Jan-Mar;55(1):19-24. PMID: 21038701.

Gabal MA, Hegazi SA, Hassanin N. Aflatoxin production by *Aspergillus* flavus field isolates. Vet Hum Toxicol. 1994 Dec;36(6):519-21. PMID: 7900269.

A2050 Aflatoxin G2

1 mg
5 mg

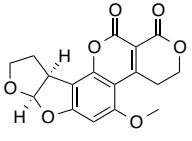

$C_{17}H_{14}O_7$ FW: 330.29 [7241-98-7] ≥98%

DNA synthesis inhibitor and carcinogen. It induces cell cycle arrest and liver damage.

Militã NM, Mihăescu G, Chifiriuc C. Aflatoxins--health risk factors. Bacteriol Virusol Parazitol Epidemiol. 2010 Jan-Mar;55(1):19-24. PMID: 21038701.

Gabal MA, Hegazi SA, Hassanin N. Aflatoxin production by *Aspergillus* flavus field isolates. Vet Hum Toxicol. 1994 Dec;36(6):519-21. PMID: 7900269.

A2052 Aflatoxin M1

100 µg
1 mg

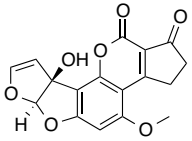

$C_{17}H_{12}O_7$ FW: 328.27 [6795-23-9] ≥98%

DNA synthesis inhibitor and carcinogen. It is a metabolite of aflatoxin B1 that induces cell cycle arrest and liver damage.

Bianco G, Russo R, Marzocco S, et al. Modulation of macrophage activity by aflatoxins B1 and B2 and their metabolites aflatoxins M1 and M2. Toxicon. 2012 May;59(6):644-50. PMID: 22402176.

Dutton MF, Ehrlich K, Bennett JW. Biosynthetic relationship among aflatoxins B1, B2, M1, and M2. Appl Environ Microbiol. 1985 Jun;49(6):1392-5. PMID: 3925881.

A2054 Aflatoxin M2

100 µg
1 mg

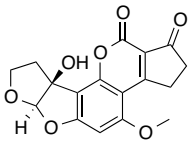

$C_{17}H_{14}O_7$ FW: 330.29 [6885-57-0] ≥98%

DNA synthesis inhibitor and carcinogen. It is a metabolite of aflatoxin B2 that induces cell cycle arrest and liver damage.

Bianco G, Russo R, Marzocco S, et al. Modulation of macrophage activity by aflatoxins B1 and B2 and their metabolites aflatoxins M1 and M2. Toxicon. 2012 May;59(6):644-50. PMID: 22402176.

Dutton MF, Ehrlich K, Bennett JW. Biosynthetic relationship among aflatoxins B1, B2, M1, and M2. Appl Environ Microbiol. 1985 Jun;49(6):1392-5. PMID: 3925881.

A2401 AG-18

NEW

5 mg
25 mg

Tyrphostin A23

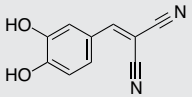

$C_{10}H_6N_2O_2$ FW: 186.17 [118409-57-7] ≥98%

Inhibitor of EGFR and PDGFR. It blocks Ca^{2+} currents in vascular smooth muscle and suppresses clathrin-mediated endocytosis.

Montezano AC, Callera GE, Yogi A, et al. Aldosterone and angiotensin II synergistically stimulate migration in vascular smooth muscle cells through c-Src-regulated redox-sensitive RhoA pathways. Arterioscler Thromb Vasc Biol. 2008 Aug;28(8):1511-8. PMID: 18467645.

Yaish P, Gazit A, Gilon C, et al. Blocking of EGF-dependent cell proliferation by EGF receptor kinase inhibitors. Science. 1988 Nov 11;242(4880):933-5. PMID: 3263702.

A2400 AG-1024

NEW

1 mg
5 mg

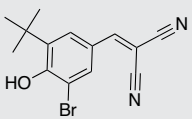

$C_{14}H_{13}BrN_2O$ FW: 305.17 [65678-07-1] ≥98%

Tyrphostin and IGF-1R inhibitor. It inhibits invasion and proliferation of hepatocellular carcinoma cells and breast cancer cells.

Yao WF, Liu JW, Sheng GL, et al. Blockade of IGF-IR exerts anticancer effects in hepatocellular carcinoma. Mol Med Rep. 2011 Jul-Aug;4(4):719-22. PMID: 21567089.

Chakraborty AK, Welsh A, Digiovanna MP. Co-targeting the insulin-like growth factor I receptor enhances growth-inhibitory and pro-apoptotic effects of anti-estrogens in human breast cancer cell lines. Breast Cancer Res Treat. 2010 Apr;120(2):327-35. PMID: 19337828.

A2500 AG-1478

NEW

5 mg
25 mg

Tyrphostin AG1478; NSC693255

$C_{16}H_{14}ClN_3O_2$ FW: 315.76 [153436-53-4] ≥98%

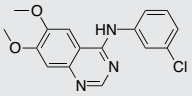

EGFR inhibitor. It inhibits proliferation of hepatocellular carcinoma cells, decreases mucus hypersecretion, and prevents airway inflammation and remodeling.

Parker JC, Douglas I, Bell J, et al. Epidermal Growth Factor Removal or Tyrphostin AG1478 Treatment Reduces Goblet Cells & Mucus Secretion of Epithelial Cells from Asthmatic Children Using the Air-Liquid Interface Model. PLoS One. 2015 Jun 9;10(6):e0129546. PMID: 26057128.

Bondì ML, Azzolina A, Craparo EF, et al. Entrapment of an EGFR inhibitor into nanostructured lipid carriers (NLC) improves its antitumor activity against human hepatocarcinoma cells. J Nanobiotechnology. 2014 May 12;12:21. PMID: 24886097.

Shimizu S, Kouzaki H, Ogawa T, et al. Eosinophil-epithelial cell interactions stimulate the production of MUC5AC mucin and profibrotic cytokines involved in airway tissue remodeling. Am J Rhinol Allergy. 2014 Mar-Apr;28(2):103-9. PMID: 24717945.

A2501 AG-1517

NEW

5 mg
25 mg

Tyrphostin AG1517; PD153035; SU5271

$C_{16}H_{14}BrN_3O_2$ FW: 360.21 [153436-54-5] ≥98%

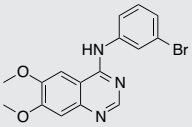

EGFR inhibitor. It inhibits growth of cholangiocarcinoma cells and suppresses DNA replication, cell cycle progression, and cell proliferation in keratinocytes.

Zhang Z, Oyesanya RA, Campbell DJ, et al. Preclinical assessment of simultaneous targeting of epidermal growth factor receptor (ErbB1) and ErbB2 as a strategy for cholangiocarcinoma therapy. Hepatology. 2010 Sep;52(3):975-86. PMID: 20607690.

Powell TJ, Ben-Bassat H, Klein BY, et al. Growth inhibition of psoriatic keratinocytes by quinazoline tyrosine kinase inhibitors. Br J Dermatol. 1999 Nov;141(5):802-10. PMID: 10583160.

A2412 AGDV

5 mg
10 mg
25 mg

$C_{14}H_{24}N_4O_7$ FW: 360.37 ≥95%

H-Ala-Gly-Asp-Val-OH

Fibrinogen fragment containing glycoprotein IIb/IIIa binding sequence necessary for platelet adhesion and aggregation.

Srokowski EM, Woodhouse KA. Evaluation of the bulk platelet response and fibrinogen interaction to elastin-like polypeptide coatings. J Biomed Mater Res A. 2014 Feb;102(2):540-51. PMID: 23505204.

Podolnikova NP, Gorkun OV, Loreth RM, et al. A cluster of basic amino acid residues in the gamma370-381 sequence of fibrinogen comprises a binding site for platelet integrin alpha(IIb)beta3 (glycoprotein IIb/IIIa). Biochemistry. 2005 Dec 27;44(51):16920-30. PMID: 16363805.

A2658 Agomelatine

50 mg
100 mg
500 mg

$C_{15}H_{17}NO_2$ FW: 243.3 [138112-76-2] ≥98%

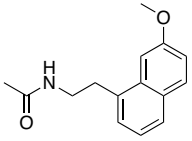

Melatonin analog, MT1/2 receptor agonist, and 5-HT2C receptor antagonist used to treat depression. It also improves sleep quality and enhances neuroplasticity and neurogenesis in the hippocampus and prefrontal cortex.

Smeraldi E, Delmonte D. Agomelatine in depression. Expert Opin Drug Saf. 2013 Nov;12(6):873-80. PMID: 24033095.

Pompili M, Serafini G, Innamorati M, et al. Agomelatine, a novel intriguing antidepressant option enhancing neuroplasticity: a critical review. World J Biol Psychiatry. 2013 Aug;14(6):412-31. PMID: 23530731.

Srinivasan V, Zakaria R, Othaman Z, et al. Melatonergic drugs for therapeutic use in insomnia and sleep disturbances of mood disorders. CNS Neurol Disord Drug Targets. 2012 Mar;11(2):180-9. PMID: 22483286.

A3080 AHU-377 Tris Salt

NEW

5 mg
10 mg

Sacubitril

$C_{24}H_{29}NO_5 \bullet C_4H_{11}NO_3$ FW: 532.63 [149709-62-6] ≥99%

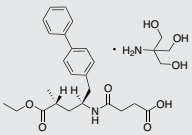

Neprilysin inhibitor and LBQ657 prodrug. It prevents degradation of atrial natriuretic peptide and brain-derived natriuretic peptide, stimulating vasodilation.

Vardeny O, Miller R, Solomon SD. Combined neprilysin and renin-angiotensin system inhibition for the treatment of heart failure. JACC Heart Fail. 2014 Dec;2(6):663-70. PMID: 25306450.

Monge M, Lorthioir A, Bobrie G, et al. New drug therapies interfering with the renin-angiotensin-aldosterone system for resistant hypertension. J Renin Angiotensin Aldosterone Syst. 2013 Dec;14(4):285-9. PMID: 24222656.

Ruilope LM, Dukat A, Böhm M, et al. Blood-pressure reduction with LCZ696, a novel dual-acting inhibitor of the angiotensin II receptor and neprilysin: a randomised, double-blind, placebo-controlled, active comparator study. Lancet. 2010 Apr 10;375(9722):1255-66. PMID: 20236700.

A4000 — AK-1

NEW

5 mg
10 mg
25 mg

SIRT2 inhibitor II

$C_{19}H_{21}N_3O_5S$ FW: 403.45 [330461-64-8] ≥98%

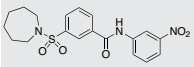

SIRT2 inhibitor. It prevents hippocampal neurodegeneration in models of Alzheimer's disease and induces cell cycle arrest in colon carcinoma cells.

Cheon MG, Kim W, Choi M, et al. AK-1, a specific SIRT2 inhibitor, induces cell cycle arrest by downregulating Snail in HCT116 human colon carcinoma cells. Cancer Lett. 2015 Jan 28;356(2 Pt B):637-45. PMID: 25312940.

Spires-Jones TL, Fox LM, Rozkalne A, et al. Inhibition of Sirtuin 2 with Sulfobenzoic Acid Derivative AK1 is Non-Toxic and Potentially Neuroprotective in a Mouse Model of Frontotemporal Dementia. Front Pharmacol. 2012 Mar 12;3:42. PMID: 22416232.

A4002 — AK-7

NEW

5 mg
25 mg

$C_{19}H_{21}BrN_2O_3S$ FW: 437.35 [420831-40-9] ≥98%

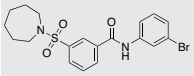

SIRT2 inhibitor. It decreases brain atrophy and improves motor function in models of Huntington's disease.

Chopra V, Quinti L, Kim J, et al. The sirtuin 2 inhibitor AK-7 is neuroprotective in Huntington's disease mouse models. Cell Rep. 2012 Dec 27;2(6):1492-7. PMID: 23200855.

A4369 — A-K-R-R-R-L-S-S-L-R-A

1 mg
2 mg
5 mg

$C_{54}H_{104}N_{24}O_{14}$ FW: 1313.58 ≥95%

H-Ala-Lys-Arg-Arg-Arg-Leu-Ser-Ser-Leu-Arg-Ala-OH

Substrate for ROCK-2.

Trauger JW, Lin FF, Turner MS, et al. Kinetic mechanism for human Rho-Kinase II (ROCK-II). Biochemistry. 2002 Jul 16;41(28):8948-53. PMID: 12102637.

A4401 — ALAL

1 mg
2 mg
5 mg

$C_{18}H_{34}N_4O_5$ FW: 386.5 ≥95%

H-Ala-Leu-Ala-Leu-OH

Used as a linker to conjugate two compounds together for more targeted delivery of chemotherapeutics.

Schmid B, Chung DE, Warnecke A, et al. Albumin-binding prodrugs of camptothecin and doxorubicin with an Ala-Leu-Ala-Leu-linker that are cleaved by cathepsin B: synthesis and antitumor efficacy. Bioconjug Chem. 2007 May-Jun;18(3):702-16. PMID: 17378599.

Mier W, Beijer B, Graham K, et al. Fluorescent somatostatin receptor probes for the intraoperative detection of tumor tissue with long-wavelength visible light. Bioorg Med Chem. 2002 Aug;10(8):2543-52. PMID: 12057643.

A4400 — Alamethicin

1 mg
5 mg

$C_{92}H_{150}N_{22}O_{25}$ FW: 1964.4 [27061-78-5] ≥95%

Ac-Aib-Pro-Aib-Ala-Aib-Ala-Gln-Aib-Val-Aib-Gly-Leu-Aib-Pro-Val-Aib-Aib-Glu-Gln-Phl

Aib=2-aminoisobutyric acid

Membrane pore formation inducer found in *Trichoderma*. It disturbs the lipid layer of the cell membrane.

Krauson AJ, He J, Wimley WC. Determining the mechanism of membrane permeabilizing peptides: identification of potent, equilibrium pore-formers. Biochim Biophys Acta. 2012 Jul;1818(7):1625-32. PMID: 22365969.

Huang HW. Molecular mechanism of antimicrobial peptides: the origin of cooperativity. Biochim Biophys Acta. 2006 Sep;1758(9):1292-302. PMID: 16542637.

A4402 — L-Alaninol

1 g
10 g

C_3H_9NO FW: 75.11 [2749-11-3] ≥98%

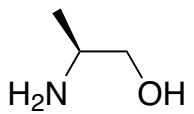

Amino acid derivative that inhibits proliferation of melanoma cells and increases levels of cytochrome c reductase and tau-glutamyl transpeptidase.

Landau O, Wasserman L, Deutsch AA, et al. Amino acid alcohols: growth inhibition and induction of differentiated features in melanoma cells. Cancer Lett. 1993 May 14;69(3):203-8. PMID: 8099846.

A4606 — Albendazole

10 g
50 g

$C_{12}H_{15}N_3O_2S$ FW: 265.33 [54965-21-8] ≥95%

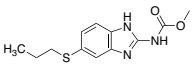

Microtubule polymerization inhibitor used to treat worm infections. It binds the colchine site of tubulin. It also induces cell cycle arrest and apoptosis in colorectal cancer models.

Pourgholami MH, Akhter J, Wang L, et al. Antitumor activity of albendazole against the human colorectal cancer cell line HT-29: in vitro and in a xenograft model of peritoneal carcinomatosis. Cancer Chemother Pharmacol. 2005 May;55(5):425-32. PMID: 15565325.

Theodorides VJ, Gyurik RJ, Kingsbury WD, et al. Anthelmintic activity of albendazole against liver flukes, tapeworms., lung and gastrointestinal roundworms. Experientia. 1976 Jun 15;32(6):702-3. PMID: 950011.

A4515

Alendronate Monosodium Trihydrate

100 mg
500 mg

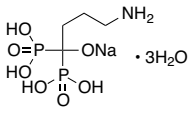

ABDP

$C_4H_{12}NNaO_7P_2 \bullet 3H_2O$ FW: 325.08 [121268-17-5] ≥98%

It is used to treat bone diseases such as osteoporosis. It inhibits bone resorption and osteoclast formation but does not have any effects on bone mineralization. It also increases δγ T cell activation and inhibits tumor growth.

Tsubaki M, Komai M, Itoh T, et al. Nitrogen-containing bisphosphonates inhibit RANKL- and M-CSF-induced osteoclast formation through the inhibition of ERK1/2 and Akt activation. J Biomed Sci. 2014 Feb 3;21:10. PMID: 24490900.

Sasaki O, Imamura M, Yamazumi Y, et al. Alendronate attenuates eosinophilic airway inflammation associated with suppression of Th2 cytokines, Th17 cytokines, and eotaxin-2. J Immunol. 2013 Sep 15;191(6):2879-89. PMID: 23935198.

Gutman D, Epstein-Barash H, Tsuriel M, et al. Alendronate liposomes for antitumor therapy: activation of γδ T cells and inhibition of tumor growth. Adv Exp Med Biol. 2012;733:165-79. PMID: 22101722.

A4521

Alfacalcidol

1 mg
5 mg

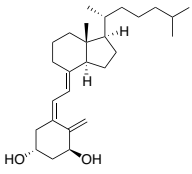

1-Hydroxyvitamin D3; 1-Hydroxycholecalciferol

$C_{27}H_{44}O_2$ FW: 400.64 [41294-56-8] ≥98%

Vitamin D analog used to treat osteoporosis. It increases bone strength and formation and prevents bone degradation.

Mazzaferro S, Goldsmith D, Larsson TE, et al. Vitamin D Metabolites and/or Analogs: Which D for Which Patient? Curr Vasc Pharmacol. 2014 Mar;12(2):339-49. PMID: 23713876.

Hara S, Kishimoto KN, Okuno H, et al. Effects of alfacalcidol on back extensor strength gained through back extensor exercise in postmenopausal women with osteoporosis. Am J Phys Med Rehabil. 2013 Feb;92(2):101-10. PMID: 23044701.

Chen H, Tian X, Liu X, et al. Alfacalcidol-stimulated focal bone formation on the cancellous surface and increased bone formation on the periosteal surface of the lumbar vertebrae of adult female rats. Calcif Tissue Int. 2008 Feb;82(2):127-36. PMID: 18175034.

A4523

Alfuzosin Hydrochloride

100 mg
500 mg
1 g

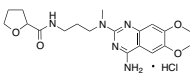

$C_{19}H_{27}N_5O_4 \bullet HCl$ FW: 425.91 [81403-68-1] ≥98%

α1-Adrenergic receptor antagonist used to treat BPH. It relaxes prostatic smooth muscle, increases urinary flow rate, and prolongs action potential duration and cardiac QT interval by increasing the probability of $hNa_v1.5$ channel openings and burst duration.

Lacerda AE, Kuryshev YA, Chen Y, et al. Alfuzosin delays cardiac repolarization by a novel mechanism. J Pharmacol Exp Ther. 2008 Feb;324(2):427-33. PMID: 17986649.

Lee M. Alfuzosin hydrochloride for the treatment of benign prostatic hyperplasia. Am J Health Syst Pharm. 2003 Jul 15;60(14):1426-39. Erratum in: Am J Health Syst Pharm. 2004 Mar 1;61(5):437. PMID: 12892027.

Dutkiewics S. Efficacy and tolerability of drugs for treatment of benign prostatic hyperplasia. Int Urol Nephrol. 2001;32(3):423-32. PMID: 11583366.

A4534

Aliskiren Hemifumarate

25 mg
100 mg
250 mg

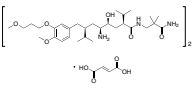

$(C_{30}H_{53}N_3O_6)_2 \bullet C_4H_4O_4$ FW: 609.83 [173334-58-2] ≥98%

Renin inhibitor used to treat hypertension. It binds to the S3bp binding site of renin, inhibiting its ability to cleave angiotensinin into angiotensin I. It decreases plasma volume and blood pressure, decreases pro-inflammatory cytokine levels, and improves insulin resistance.

Yen TH, Yang HY, Yeh YH, et al. Aliskiren attenuates proteinuria in mice with lupus nephritis by a blood pressure-independent mechanism. Lupus. 2013 Feb;22(2):180-9. PMID: 23257405.

Hermanowicz JM, Hermanowicz A, Buczko P, et al. Aliskiren inhibits experimental venous thrombosis in two-kidney one- clip hypertensive rats. Thromb Res. 2013 Jan;131(1):e39-44. PMID: 23174623.

Gandhi S, Srinivasan B, Akarte AS. Aliskiren improves insulin resistance and ameliorates diabetic renal vascular complications in STZ-induced diabetic rats. J Renin Angiotensin Aldosterone Syst. 2013 Mar;14(1):3-13. PMID: 22791702.

A4438

Allatostatin I

1 mg
2 mg
5 mg

H-Ala-Pro-Ser-Gly-Ala-Gln-Arg-Leu-Tyr-Gly-Phe-Gly-Leu-NH_2

$C_{61}H_{94}N_{18}O_{16}$ FW: 1335.54 ≥95%

Juvenile hormone synthesis inhibitor found in insects.

Lloyd GT, Woodhead AP, Stay B. Release of neurosecretory granules within the corpus allatum in relation to the regulation of juvenile hormone synthesis in Diploptera punctata. Insect Biochem Mol Biol. 2000 Aug-Sep;30(8-9):739-46. PMID: 10876117.

Skinner JR, Fairbairn SE, Woodhead AP, et al. Allatostatin in hemocytes of the cockroach Diploptera punctata. Cell Tissue Res. 1997 Oct;290(1):119-28. PMID: 9377632.

A4440

Allicin

1 mg
5 mg

Diallyl thiosulfinate

$C_6H_{10}OS_2$ FW: 162.27 [539-86-6] ≥98%

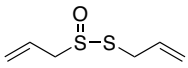

Synthetic compound found in garlic that binds nitrogen bases and phosphate backbones in DNA, activates inwardly rectifying K^+ channels, and blocks L-type Ca^{2+} channels. It exhibits a wide variety of biological activities, including inducing autophagy and apoptosis, lowering systolic blood pressure and triglyceride levels, decreasing anti-islet cell antibodies and insulin levels, and enhancing Nrf2 signaling. This product is a solution of methanol:water:formic acid (60:40:0.1) and allicin at 10mg/mL.

Chu YL, Ho CT, Chung JG, et al. Allicin Induces Anti-human Liver Cancer Cells through the p53 Gene Modulating Apoptosis and Autophagy. J Agric Food Chem. 2013 Oct 16;61(41):9839-9848. PMID: 24059278.

Tyagi G, Pradhan S, Srivastava T, et al. Nucleic acid binding properties of allicin: Spectroscopic analysis and estimation of anti-tumor potential. Biochim Biophys Acta. 2013 Sep 13;1840(1):350-356. PMID: 24041991.

Liu DS, Gao W, Liang ES, et al. Effects of allicin on hyperhomocysteinemia-induced experimental vascular endothelial dysfunction. Eur J Pharmacol. 2013 Aug 15;714(1-3):163-9. PMID: 23792140.

A4441

Allicin, aqueous

1 mg
5 mg

Diallyl thiosulfinate

$C_6H_{10}OS_2$ FW: 162.27 [539-86-6] ≥98%

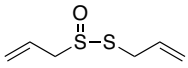

Synthetic compound found in garlic that binds nitrogen bases and phosphate backbones in DNA, activates inwardly rectifying K^+ channels, and blocks L-type Ca^{2+} channels. It exhibits a wide variety of biological activities, including inducing autophagy and apoptosis, lowering systolic blood pressure and triglyceride levels, decreasing anti-islet cell antibodies and insulin levels, and enhancing Nrf2 signaling. This product is an aqueous solution (with 0.1 % formic acid as a stabilizer) of allicin at 25 mg/mL.

Chu YL, Ho CT, Chung JG, et al. Allicin Induces Anti-human Liver Cancer Cells through the p53 Gene Modulating Apoptosis and Autophagy. J Agric Food Chem. 2013 Oct 16;61(41):9839-9848. PMID: 24059278.

Tyagi G, Pradhan S, Srivastava T, et al. Nucleic acid binding properties of allicin: Spectroscopic analysis and estimation of anti-tumor potential. Biochim Biophys Acta. 2013 Sep 13;1840(1):350-356. PMID: 24041991.

Liu DS, Gao W, Liang ES, et al. Effects of allicin on hyperhomocysteinemia-induced experimental vascular endothelial dysfunction. Eur J Pharmacol. 2013 Aug 15;714(1-3):163-9. PMID: 23792140.

A4443

L-(+)-Alliin

25 mg
50 mg
100 mg

EINECS 209-118-9; S-Allyl-L-cysteine-S-oxide

$C_6H_{11}NO_3S$ FW: 177.22 [556-27-4] ≥98%

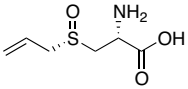

Optically active synthetic cysteine derivative, NMDA receptor agonist, and antioxidant. It increases activity of phase II enzymes in models of myocardial infarction and suppresses inflammation in adipocytes. It also inhibits VEGF-induced angiogenesis in fibrosarcoma cells.

Ieong Tou W, Chang SS, Wu D, et al. Molecular level activation insights from a NR2A/NR2B agonist. J Biomol Struct Dyn. 2014;32(5):683-93. PMID: 23600691.

Quintero-Fabián S, Ortuño-Sahagún D, Vázquez-Carrera M, et al. Alliin, a garlic (Allium sativum) compound, prevents LPS-induced inflammation in 3T3-L1 adipocytes. Mediators Inflamm. 2013;2013:381815. PMID: 24453416.

Nasim SA, Dhir B, Kapoor R, et al. Alliin obtained from leaf extract of garlic grown under in situ conditions possess higher therapeutic potency as analyzed in alloxan-induced diabetic rats. Pharm Biol. 2011 Apr;49(4):416-21. PMID: 21391887.

A4444

L-Alliin

100 mg
500 mg
1 g

$C_6H_{11}NO_3S$ FW: 177.22 ≥98%

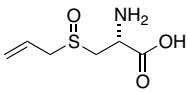

Synthetic NMDA receptor agonist and antioxidant. It increases activity of phase II enzymes in models of myocardial infarction and suppresses inflammation in adipocytes. It also inhibits VEGF-induced angiogenesis in fibrosarcoma cells.

Ieong Tou W, Chang SS, Wu D, et al. Molecular level activation insights from a NR2A/NR2B agonist. J Biomol Struct Dyn. 2014;32(5):683-93. PMID: 23600691.

Quintero-Fabián S, Ortuño-Sahagún D, Vázquez-Carrera M, et al. Alliin, a garlic (Allium sativum) compound, prevents LPS-induced inflammation in 3T3-L1 adipocytes. Mediators Inflamm. 2013;2013:381815. PMID: 24453416.

A4646

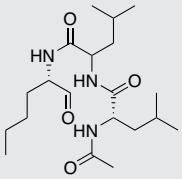

ALLN

NEW

5 mg
25 mg

Calpain inhibitor 1; MG-101

$C_{20}H_{37}N_3O_4$ FW: 383.53 [110044-82-1] ≥98%

Peptide calpain I/II inhibitor. It stimulates autophagy, suppresses IκB proteolysis, and induces apoptosis in colon cancer cells.

Kaneko Y, Murphy CR, Day ML. Calpain 2 activity increases at the time of implantation in rat uterine luminal epithelial cells and administration of calpain inhibitor significantly reduces implantation sites. Histochem Cell Biol. 2014 Apr;141(4):423-30. PMID: 24271063.

Chatterjee C, Sparks DL. Hepatic Lipase Release is Inhibited by a Purinergic Induction of Autophagy. Cell Physiol Biochem. 2014 Mar 28;33(4):883-894. PMID: 24713587.

Ariyadi B, Isobe N, Yoshimura Y. Toll-like receptor signaling for the induction of mucin expression by lipopolysaccharide in the hen vagina. Poult Sci. 2014 Mar;93(3):673-9. PMID: 24604861.

A4445

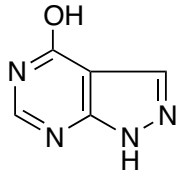

Allopurinol

5 g
10 g
25 g

$C_5H_4N_4O$ FW: 136.11 [315-30-0] ≥98%

Xanthine oxidase inhibitor used to treat hyperuricemia. It decreases inflammation in models of renal ischemia and suppresses oxidative stress, preventing atrial fibrillation.

Prieto-Moure B, Carabén-Redaño A, Aliena-Valero A, et al. Allopurinol in renal ischemia. J Invest Surg. 2014 Oct;27(5):304-16. PMID: 24914485.

Essawy SS, Elbaz AA. Role of adenosine receptors in the anti-nociceptive effects of allopurinol in mice. Eur Rev Med Pharmacol Sci. 2013 Jul;17(14):1857-63. PMID: 23877847.

Sakabe M, Fujiki A, Sakamoto T, et al. Xanthine oxidase inhibition prevents atrial fibrillation in a canine model of atrial pacing-induced left ventricular dysfunction. J Cardiovasc Electrophysiol. 2012 Oct;23(10):1130-5. PMID: 22587612.

A4547

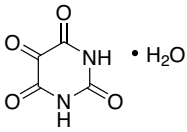

Alloxan Monohydrate

5 g
10 g
25 g

$C_4H_2N_2O_4 \bullet H_2O$ FW: 160.08 [2244-11-3] ≥98%

Glucose analog used to induce diabetes by destroying β cells.

Franzén S, Friederich-Persson M, Fasching A, et al. Differences in susceptibility to develop parameters of diabetic nephropathy in four mouse strains with type 1 diabetes. Am J Physiol Renal Physiol. 2014 May 15;306(10):F1171-8. PMID: 24623147.

Tyrberg B, Andersson A, Borg LA. Species differences in susceptibility of transplanted and cultured pancreatic islets to the beta-cell toxin alloxan. Gen Comp Endocrinol. 2001 Jun;122(3):238-51. PMID: 11356036.

Eizirik DL, Pipeleers DG, Ling Z, et al. Major species differences between humans and rodents in the susceptibility to pancreatic beta-cell injury. Proc Natl Acad Sci U S A. 1994 Sep 27;91(20):9253-6. PMID: 7937750.

A4544

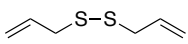

Allyl Disulfide

500 mg
1 g
5 g

Diallyl Disulfide; AI3-35128; BRN 1699241; CCRIS 6290

$C_6H_{10}S_2$ FW: 146.28 [2179-57-9] ≥98%

Lipid peroxidation inhibitor, free radical scavenger, and antioxidant. It induces phase II enzymes, limiting neurodegeneration in *Drosophila* models of Parkinson's disease. It also induces apoptosis in leukemia cells. In other cellular models, it inhibits 4α-methyl oxidase, suppressing cholesterol synthesis.

Schelkle B, Snellgrove D, Cable J. In vitro and in vivo efficacy of garlic compounds against Gyrodactylus turnbulli infecting the guppy (Poecilia reticulata). Vet Parasitol. 2013 Nov 15;198(1-2):96-101. PMID: 24074607.

Dasgupta P, Bandyopadhyay SS. Role of di-allyl disulfide, a garlic component in NF-κB mediated transient G2-M phase arrest and apoptosis in human leukemic cell-lines. Nutr Cancer. 2013;65(4):611-22. PMID: 23659453.

Trinh K, Moore K, Wes PD, et al. Induction of the phase II detoxification pathway suppresses neuron loss in *Drosophila* models of Parkinson's disease. J Neurosci. 2008 Jan 9;28(2):465-72. PMID: 18184789.

A0025

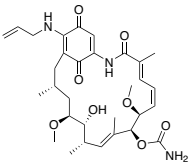

17-Allylaminogeldanamycin

0.5 mg
1 mg
5 mg
25 mg

17-AAG; Telatinib

$C_{31}H_{43}N_3O_8$ FW: 585.69 [75747-14-7] ≥97%

Geldanamycin derivative and HSP90 inhibitor. It induces apoptosis in cancer cells and inhibits replication of cytomegalovirus.

Thangjam GS, Dimitropoulou C, Joshi AD, et al. Novel mechanism of attenuation of LPS-induced NF-κB activation by the heat shock protein 90 inhibitor, 17-N-allylamino-17-demethoxygeldanamycin, in human lung microvascular endothelial cells. Am J Respir Cell Mol Biol. 2014 May;50(5):942-52. PMID: 24303801.

Powers MV, Valenti M, Miranda S, et al. Mode of cell death induced by the HSP90 inhibitor 17-AAG (tanespimycin) is dependent on the expression of pro-apoptotic BAX. Oncotarget. 2013 Nov;4(11):1963-75. PMID: 24185264.

A4617 Aloe Emodin

25 mg
100 mg
250 mg

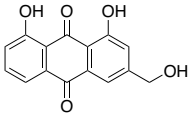

$C_{15}H_{10}O_5$ FW: 270.24 [481-72-1] ≥98%

CFTR Cl^- channel activator found in aloe. It increases colonic fluid secretion, decreases angiogenesis, and induces apoptosis in glioma cells.

Ismail S, Haris K, Abdul Ghani AR, et al. Enhanced induction of cell cycle arrest and apoptosis via the mitochondrial membrane potential disruption in human U87 malignant glioma cells by aloe emodin. J Asian Nat Prod Res. 2013 Jul 22. [Epub ahead of print]. PMID: 23869465.

Huang PH, Huang CY, Chen MC, et al. Emodin and Aloe-Emodin Suppress Breast Cancer Cell Proliferation through ER α Inhibition. Evid Based Complement Alternat Med. 2013; Epub 2013 Jun 24. PMID: 23864887.

Zhang W, Chen H, Liu DL, et al. Emodin sensitizes the gemcitabine-resistant cell line Bxpc-3/Gem to gemcitabine via downregulation of NF-κB and its regulated targets. Int J Oncol. 2013 Apr;42(4):1189-96. PMID: 23440366.

A4577 Alsterpaullone

1 mg
5 mg

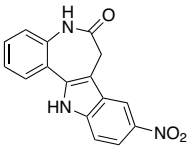

$C_{16}H_{11}N_3O_3$ FW: 293.28 [237430-03-4] ≥98%

GSK-3 and CDK inhibitor. It induces cell cycle arrest and apoptosis in leukemia cells, induces Wnt signaling to decrease egg hatching activity, and inhibits HIV-1 replication and proliferation.

Cui C, Wang Y, Wang Y, et al. Alsterpaullone, a Cyclin-Dependent Kinase Inhibitor, Mediated Toxicity in HeLa Cells through Apoptosis-Inducing Effect. J Anal Methods Chem. 2013;2013:602091. PMID: 23577282.

Windsor PJ, Leys SP. Wnt signaling and induction in the sponge aquiferous system: evidence for an ancient origin of the organizer. Evol Dev. 2010 Sep-Oct;12(5):484-93. PMID: 20883217.

Zahler S, Liebl J, Fürst R, et al. Anti-angiogenic potential of small molecular inhibitors of cyclin dependent kinases in vitro. Angiogenesis. 2010 Sep;13(3):239-49. PMID: 20706783.

A4675 Alternariol

1 mg
5 mg

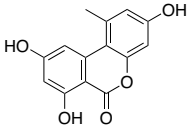

$C_{14}H_{10}O_5$ FW: 258.23 [641-38-3] ≥98%

Mycotoxin, topoisomerase I and II inhibitor, and potential ER agonist found in *Alternaria*. It increases production of estradiol and progesterone, induces oxidation of DNA bases and formation of DNA strand breaks, and induces cell cycle arrest in macrophages.

Frizzell C, Ndossi D, Kalayou S, et al. An in vitro investigation of endocrine disrupting effects of the mycotoxin alternariol. Toxicol Appl Pharmacol. 2013 Aug 15;271(1):64-71. PMID: 23665424.

Solhaug A, Holme JA, Haglund K, et al. Alternariol induces abnormal nuclear morphology and cell cycle arrest in murine RAW 264.7 macrophages. Toxicol Lett. 2013 May 10;219(1):8-17. PMID: 23454835.

Broggi L, Reynoso C, Resnik S, et al. Occurrence of alternariol and alternariol monomethyl ether in beverages from the Entre Rios Province market, Argentina. Mycotoxin Res. 2013 Feb;29(1):17-22. PMID: 23334721.

A4678 Alternariol-9-methyl Ether

1 mg
5 mg

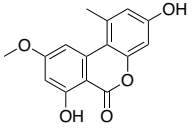

$C_{15}H_{12}O_5$ FW: 272.25 [23452-05-3] ≥98%

Mycotoxin, oxidative phosphorylation inhibitor, and potential ER agonist found in *Alternaria*. It prevents photosynthesis, induces apoptosis in colon carcinoma cells, and may exhibit mutagenic activity.

Demuner AJ, Barbosa LC, Miranda AC, et al. The Fungal Phytotoxin Alternariol 9-Methyl Ether and Some of Its Synthetic Analogues Inhibit the Photosynthetic Electron Transport Chain. J Nat Prod. 2013 Nov 18. [Epub ahead of print]. PMID: 24245962.

Broggi L, Reynoso C, Resnik S, et al. Occurrence of alternariol and alternariol monomethyl ether in beverages from the Entre Rios Province market, Argentina. Mycotoxin Res. 2013 Feb;29(1):17-22. PMID: 23334721.

Scott PM, Zhao W, Feng S, et al. *Alternaria* toxins alternariol and alternariol monomethyl ether in grain foods in Canada. Mycotoxin Res. 2012 Nov;28(4):261-6. PMID: 23087499.

A4679 Altrenogest

100 mg
250 mg
1 g

Allyltrenbolone

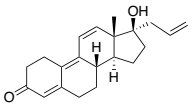

$C_{21}H_{26}O_2$ FW: 310.44 [850-52-2] ≥98%

Synthetic progestogen and progesterone receptor agonist used to suppress or control the estrous cycle of female animals.

Horsley BR, Estienne MJ, Harper AF, et al. Effect of P.G. 600 on the timing of ovulation in gilts treated with altrenogest. J Anim Sci. 2005 Jul;83(7):1690-5. PMID: 15956478.

dos Santos JM, Wentz I, Bortolozzo FP, et al. Early-weaned sows: altrenogest therapy, estrus, ovulation, and reproductive performance. Anim Reprod Sci. 2004 Sep;84(3-4):407-13. PMID: 15302382.

Webel SK, Squires EL. Control of the oestrous cycle in mares with altrenogest. J Reprod Fertil Suppl. 1982;32:193-8. PMID: 6962854.

A4578

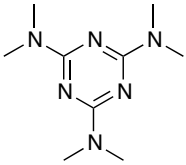

Altretamine

HMM; Hexamethylmelamine

$C_9H_{18}N_6$ FW: 210.28 [645-05-6] ≥98%

DNA alkylator used to treat refractory ovarian cancer. It forms DNA adducts and is metabolized to formaldehyde.

Chan JK, Loizzi V, Manetta A, et al. Oral altretamine used as salvage therapy in recurrent ovarian cancer. Gynecol Oncol. 2004 Jan;92(1):368-71. PMID: 14751188.

Coley HM, Brooks N, Phillips DH, et al. The role of the N-(hydroxymethyl)melamines as antitumour agents: mechanism of action studies. Biochem Pharmacol. 1995 May 11;49(9):1203-12. PMID: 7763301.

100 mg
500 mg
1 g
5 g

A4496

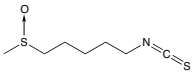

Alyssin

5-Methylsulfinylpentyl isothiocyanate

$C_7H_{13}NOS_2$ FW: 191.32 [646-23-1] ≥97%

Sulforaphane homolog and antioxidant. It induces phase II enzymes and increases Nrf2 levels in adenocarcinoma cells. It also decreases metabolism of polycyclic aromatic hydrocarbons, suppressing risk of carcinogenesis in vitro.

Lubelska K, Misiewicz-Krzemińska I, Milczarek M, et al. Isothiocyanate-drug interactions in the human adeno-carcinoma cell line Caco-2. Mol Cell Biochem. 2012 Aug;367(1-2):19-29. PMID: 22527941.

Kim MJ, Kim SH, Lim SJ. Comparison of the apoptosis-inducing capability of sulforaphane analogues in human colon cancer cells. Anticancer Res. 2010 Sep;30(9):3611-9. PMID: 20944144.

Skupinska K, Misiewicz-Krzeminska I, Stypulkowski R, et al. Sulforaphane and its analogues inhibit CYP1A1 and CYP1A2 activity induced by benzo[a]pyrene. J Biochem Mol Toxicol. 2009 Jan-Feb;23(1):18-28. PMID: 19202560.

25 mg
50 mg
100 mg
500 mg

A4497

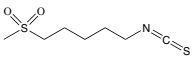

Alyssin Sulfone

$C_7H_{13}NO_2S_2$ FW: 207.31 ≥97%

Sulfonyl analog of sulforaphane and antioxidant. It induces phase II enzymes and increases Nrf2 levels in adenocarcinoma cells and inhibits cell growth in colon cancer cells.

Lubelska K, Misiewicz-Krzemińska I, Milczarek M, et al. Isothiocyanate-drug interactions in the human adeno-carcinoma cell line Caco-2. Mol Cell Biochem. 2012 Aug;367(1-2):19-29. PMID: 22527941.

Kim MJ, Kim SH, Lim SJ. Comparison of the apoptosis-inducing capability of sulforaphane analogues in human colon cancer cells. Anticancer Res. 2010 Sep;30(9):3611-9. PMID: 20944144.

25 mg
50 mg
100 mg
500 mg

A4498

pGlu-Gly-Arg-Leu-Gly-Thr-Gln-Trp-Ala-Val-Gly-His-leu-Met-NH_2

Alytesin

$C_{68}H_{106}N_{22}O_{17}S$ FW: 1535.8 [31078-12-3] ≥95%

Found in amphibian skin. It decreases gastric acid secretion and food intake.

König E, Zhou M, Wang L, et al. Antimicrobial peptides and alytesin are co-secreted from the venom of the Midwife toad, Alytes maurus (Alytidae, Anura): implications for the evolution of frog skin defensive secretions. Toxicon. 2012 Nov;60(6):967-81. PMID: 22800568

Cline MA, Fouse DN, Prall BC. Central and peripheral alytesin cause short-term anorexigenic effects in neonatal chicks. Neuropeptides. 2008 Jun;42(3):283-91. PMID: 18384875.

1 mg
2 mg
5 mg

A4802

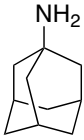

Amantadine Hydrochloride

$C_{10}H_{17}N \bullet HCl$ FW: 187.71 [665-66-7] ≥98%

Viral M2 proton channel blocker and inhibitor of MAO-A, NET, NMDA receptors, and α7 nAChRs used to treat Parkinson's disease. It has previously been used to treat influenza virus infection.

Sommerauer C, Rebernik P, Reither H, et al. The noradrenaline transporter as site of action for the anti-Parkinson drug amantadine. Neuropharmacology. 2012 Mar;62(4):1708-16. PMID: 22155208.

Jing X, Ma C, Ohigashi Y, et al. Functional studies indicate amantadine binds to the pore of the influenza A virus M2 proton-selective ion channel. Proc Natl Acad Sci U S A. 2008 Aug 5;105(31):10967-72. PMID: 18669647.

25 g
100 g

A4803

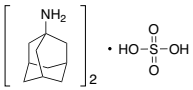

Amantadine Sulfate

$(C_{10}H_{17}N)_2 \bullet H_2SO_4$ FW: 400.58 [31377-23-8] ≥98%

Viral M2 proton channel blocker and inhibitor of MAO-A, NET, NMDA receptors, and α7 nAChRs used to treat Parkinson's disease. It has previously been used to treat influenza virus infection.

Sommerauer C, Rebernik P, Reither H, et al. The noradrenaline transporter as site of action for the anti-Parkinson drug amantadine. Neuropharmacology. 2012 Mar;62(4):1708-16. PMID: 22155208.

Jing X, Ma C, Ohigashi Y, et al. Functional studies indicate amantadine binds to the pore of the influenza A virus M2 proton-selective ion channel. Proc Natl Acad Sci U S A. 2008 Aug 5;105(31):10967-72. PMID: 18669647.

25 g
100 g

A4805

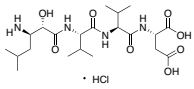

Amastatin Hydrochloride

$C_{21}H_{38}N_4O_8 \bullet HCl$ FW: 511.01 [100938-10-1] ≥98%

1 mg
5 mg
10 mg

Aminopeptidase inhibitor that also induces vasoconstriction.

Tobin VA, Arechaga G, Brunton PJ, et al. Oxytocinase in the female rat hypothalamus: a novel mechanism controlling oxytocin neurones during lactation. J Neuroendocrinol. 2014 Apr;26(4):205-16. PMID: 24612105.

Pillay D, Boulangé AF, Coustou V, et al. Recombinant expression and biochemical characterisation of two alanyl aminopeptidases of Trypanosoma congolense. Exp Parasitol. 2013 Dec;135(4):675-84. PMID: 24177338.

A4806

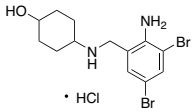

Ambroxol Hydrochloride

$C_{13}H_{18}Br_2N_2O \bullet HCl$ FW: 414.57 [23828-92-4] ≥98%

1 g
5 g
25 g

Expectorant used to treat respiratory diseases. It stimulates the ciliary beat frequency and increases mucous secretion in the lung and trachea. It also increases levels of thioredoxin and thioredoxin reductase, decreases oxidative stress, and inhibits sodium nitroprusside-induced activation of guanylate cyclase.

Huang J, Xu J, Tian L, et al. A thioredoxin reductase and/or thioredoxin system-based mechanism for antioxidant effects of ambroxol. Biochimie. 2014 Feb;97:92-103. PMID: 24103200.

Utsugi M, Dobashi K, Koga Y, et al. Ambroxol inhibits platelet-derived growth factor production in human monocytic cells. Eur J Pharmacol. 2002 Feb 1;436(1-2):47-51. PMID: 11834245.

A4924

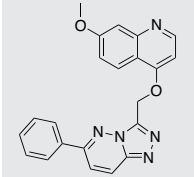

AMG-208

NEW

$C_{22}H_{17}N_5O_2$ FW: 383.4 [1002304-34-8] ≥98%

1 mg
5 mg

Inhibitor of c-MET and Ron. It suppresses proliferation of prostate cancer cells.

Liu X, Newton RC, Scherle PA. Developing c-MET pathway inhibitors for cancer therapy: progress and challenges. Trends Mol Med. 2010 Jan;16(1):37-45. PMID: 20031486.

Albrecht BK, Harmange JC, Bauer D, et al. Discovery and optimization of triazolopyridazines as potent and selective inhibitors of the c-Met kinase. J Med Chem. 2008 May 22;51(10):2879-82. PMID: 18426196.

A4926

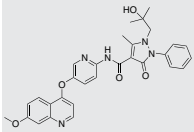

AMG-458

NEW

$C_{30}H_{29}N_5O_5$ FW: 539.58 [913376-83-7] ≥98%

1 mg
5 mg

Inhibitor of c-MET. It enhances radiosensitivity and induces apoptosis in lung adenocarcinoma cells.

Li B, Torossian A, Sun Y, et al. Higher levels of c-Met expression and phosphorylation identify cell lines with increased sensitivity to AMG-458, a novel selective c-Met inhibitor with radiosensitizing effects. Int J Radiat Oncol Biol Phys. 2012 Nov 15;84(4):e525-31. PMID: 22836051.

Liu L, Siegmund A, Xi N, et al. Discovery of a potent, selective, and orally bioavailable c-Met inhibitor: 1-(2-hydroxy-2-methylpropyl)-N-(5-(7-methoxyquinolin-4-yloxy)pyridin-2-yl)-5-methyl-3-oxo-2-phenyl-2,3-dihydro-1H-pyrazole-4-carboxamide (AMG 458). J Med Chem. 2008 Jul 10;51(13):3688-91. PMID: 18553959.

A4933

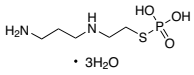

Amifostine Trihydrate

$C_5H_{15}N_2O_3PS \bullet 3H_2O$ FW: 268.27 [112901-68-5] ≥98%

50 mg
100 mg
500 mg

Thiol prodrug and antioxidant co-administered with chemotherapeutics. It scavenges free radicals, protecting normal tissue against chemotherapy- and radiation-induced damage.

Chen C, Tian L, Zhang M, et al. Protective effect of amifostine on high-dose methotrexate-induced small intestinal mucositis in mice. Dig Dis Sci. 2013 Nov;58(11):3134-43. PMID: 23979434.

Lv W, Zhang M, Zhang Z, et al. Amifostine acts upon mitochondria to stimulate growth of bone marrow and regulate cytokines. Adv Exp Med Biol. 2013;789:195-201. PMID: 23852495.

Wozniak K, Gloc E, Morawiec Z, et al. Amifostine can differentially modulate DNA double-strand breaks and apoptosis induced by idarubicin in normal and cancer cells. Exp Oncol. 2008 Mar;30(1):22-8. PMID: 18438337.

A5132

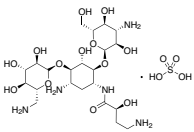

Amikacin Disulfate

$C_{22}H_{43}N_5O_{13} \bullet 2H_2SO_4$ FW: 781.76 [39831-55-5] ≥98%

250 mg
1 g
5 g

Protein translation inhibitor used to treat gram negative bacterial infections.

Barza M, Scheife RT. Drug therapy reviews: Antimicrobial spectrum, pharmacology and therapeutic use of antibiotics--part 4: aminoglycosides. Am J Hosp Pharm. 1977 Jul;34(7):723-37. PMID: 407790.

Kawaguchi H. Discovery, chemistry, and activity of amikacin. J Infect Dis. 1976 Nov;134 SUPPL:S242-8. PMID: 825583.

A5133

Amiloride Hydrochloride Dihydrate

500 mg
1 g
5 g

Amiprazidine

$C_6H_8ClN_7O \cdot HCl \cdot 2H_2O$ FW: 302.12 [17440-83-4] ≥98%

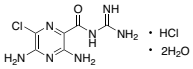

K^+-sparing diuretic that inhibits ENaC channels, acid-sensing ion channels, and Na^+/H^+ antiporters. It increases excretion of Na^+ and water and is used to treat hypertension and congestive heart failure. It also inhibits replication of Coxsackievirus B3 and poliovirus type 1.

Ogram SA, Boone CD, McKenna R, et al. Amiloride inhibits the initiation of Coxsackievirus and poliovirus RNA replication by inhibiting VPg uridylylation. Virology. 2014 Sep;464-465:87-97. PMID: 25058507.

Yu X, Hu Y, Yu S. Effects of acid on vagal nociceptive afferent subtypes in guinea pig esophagus. Am J Physiol Gastrointest Liver Physiol. 2014 Aug 15;307(4):G471-8. PMID: 24994852.

Paar M, Pavenstädt H, Kusche-Vihrog K, et al. Endothelial sodium channels trigger endothelial salt sensitivity with aging. Hypertension. 2014 Aug;64(2):391-6. PMID: 24866143.

A4930

7-Aminoactinomycin D

1 mg
5 mg

7-amino-AMD

$C_{62}H_{87}N_{13}O_{16}$ FW: 1270.43 [7240-37-1] ≥97%

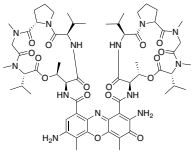

Actinomycin derivative and DNA binding agent used to study apoptosis and phagocytosis.

Su YJ, Cheng TT, Chen CJ, et al. The association among leukocyte apoptosis, autoantibodies and disease severity in systemic lupus erythematosus. J Transl Med. 2013 Oct 19;11:261. PMID: 24138706.

Ortega E, Algarra I, Serrano MJ, et al. The use of 7-amino-actinomycin D in the analysis of *Candida albicans* phagocytosis and opsonization. J Immunol Methods. 2001 Jul 1;253(1-2):189-93. PMID: 11384680.

A4931

3-Aminobenzamide

100 mg
250 mg
500 mg

3-AB; INO-1001

$C_7H_8N_2O$ FW: 136.15 [3544-24-9] ≥97%

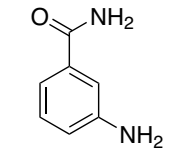

PARP inhibitor. It prevents UV-induced cell death, decreases atherosclerotic lesion size, and induces cell cycle arrest and differentiation in osteosarcoma cells.

Lakatos P, Szabó É, Hegedűs C, et al. 3-Aminobenzamide protects primary human keratinocytes from UV-induced cell death by a poly(ADP-ribosyl)ation independent mechanism. Biochim Biophys Acta. 2013 Mar;1833(3):743-51. PMID: 23246565.

Huang D, Wang Y, Wang L, et al. Poly(ADP-ribose) polymerase 1 is indispensable for transforming growth factor-β Induced Smad3 activation in vascular smooth muscle cell. PLoS One. 2011;6(10):e27123. PMID: 22073128.

A4935

6-Aminocaproic Acid

10 g
100 g

EACA

$C_6H_{13}NO_2$ FW: 131.17 [60-32-2] ≥98%

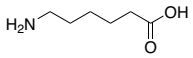

Protease inhibitor used to treat bleeding disorders. It inhibits plasmin, preventing fibrinolysis.

Lindner J, Guenther J, Nick H, et al. Modulation of granule cell migration by a glia-derived protein. Proc Natl Acad Sci U S A. 1986 Jun;83(12):4568-71. PMID: 3459192.

A5032

D,L-Aminoglutethimide

500 mg
1 g

$C_{13}H_{16}N_2O_2$ FW: 232.28 [125-84-8] ≥98%

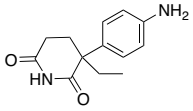

Aromatase inhibitor that prevents adrenal steroid synthesis. It is used to treat breast cancer and Cushing's disease.

Pozza C, Graziadio C, Giannetta E, et al. Management Strategies for Aggressive Cushing's Syndrome: From Macroadenomas to Ectopics. J Oncol. 2012;2012:685213. PMID: 22934113.

Dubrovsky B. Natural steroids counteracting some actions of putative depressogenic steroids on the central nervous system: potential therapeutic benefits. Med Hypotheses. 1997 Jul;49(1):51-5. PMID: 9247908.

A4940

6-Aminonicotinamide

1 g
5 g

6-Aminopyridine-3-carboxamide

$C_6H_7N_3O$ FW: 137.14 [329-89-5] ≥98%

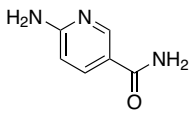

G6PDH inhibitor that suppresses pentose phosphate pathway signaling. It prevents oocyte maturation and induces apoptosis in cancer cells.

Parkhitko AA, Priolo C, Coloff JL, et al. Autophagy-dependent metabolic reprogramming sensitizes TSC2-deficient cells to the antimetabolite 6-aminonicotinamide. Mol Cancer Res. 2014 Jan;12(1):48-57. PMID: 24296756.

Alvarez GM, Ferretti EL, Gutnisky C, et al. Modulation of glycolysis and the pentose phosphate pathway influences porcine oocyte in vitro maturation. Reprod Domest Anim. 2013 Aug;48(4):545-53. PMID: 23189959.

Preuss J, Richardson AD, Pinkerton A, et al. Identification and characterization of novel human glucose-6-phosphate dehydrogenase inhibitors. J Biomol Screen. 2013 Mar;18(3):286-97. PMID: 23023104.

A5030

4-Aminophenylphosphate Monosodium

10 mg
50 mg
100 mg

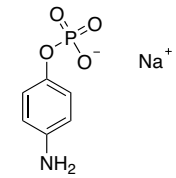

$C_6H_7NO_4PNa$ FW: 211.09 [52331-30-3] ≥97%

Alkaline phosphatase substrate used to quantify enzyme activity in research models.

Akanda MR, Tamilavan V, Park S, et al. Hydroquinone diphosphate as a phosphatase substrate in enzymatic amplification combined with electrochemical-chemical-chemical redox cycling for the detection of E. coli O157:H7. Anal Chem. 2013 Feb 5;85(3):1631-6. PMID: 23327094.

Pemberton RM, Hart JP, Stoddard P, et al. A comparison of 1-naphthyl phosphate and 4 aminophenyl phosphate as enzyme substrates for use with a screen-printed amperometric immunosensor for progesterone in cows' milk. Biosens Bioelectron. 1999 May 31;14(5):495-503. PMID: 10451917.

A5134

Aminophylline Anhydrous

25 g
100 g
500 g

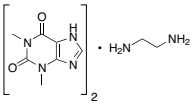

$C_{16}H_{24}N_{10}O_4$ FW: 420.43 [317-34-0] ≥98%

Adenosine receptor antagonist and PDE inhibitor used to treat COPD. It decreases levels of eosinophils and cytokines in allergen-induced lung inflammation models.

Nickels TJ, Schwartz AD, Blevins DE, et al. Effect of theophylline and aminophylline on transmitter release at the mammalian neuromuscular junction is not mediated by cAMP. Clin Exp Pharmacol Physiol. 2006 May-Jun;33(5-6):465-70. PMID: 16700879.

Danahay H, Broadley KJ, McCabe PJ, et al. The potential roles of cytokines, IL-5 and IL-8, and plasma cortisol in the anti-inflammatory actions of phosphodiesterase inhibitors in sensitized guinea-pig airways. Pulm Pharmacol Ther. 1997 Oct-Dec;10(5-6):277-85. PMID: 9778491.

A5135

Aminophylline Dihydrate

25 g
100 g
500 g

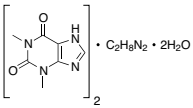

$C_{16}H_{24}N_{10}O_4 \cdot 2H_2O$ FW: 456.47 ≥98%

Xanthine derivative; adenosine receptor antagonist, and PDE inhibitor used to treat COPD. It also decreases levels of IL-5, IL-8, and eosinophils.

Nickels TJ, Schwartz AD, Blevins DE, et al. Effect of theophylline and aminophylline on transmitter release at the mammalian neuromuscular junction is not mediated by cAMP. Clin Exp Pharmacol Physiol. 2006 May-Jun;33(5-6):465-70. PMID: 16700879.

Danahay H, Broadley KJ, McCabe PJ, et al. The potential roles of cytokines, IL-5 and IL-8, and plasma cortisol in the anti-inflammatory actions of phosphodiesterase inhibitors in sensitized guinea-pig airways. Pulm Pharmacol Ther. 1997 Oct-Dec;10(5-6):277-85. PMID: 9778491.

A5001

Aminopterin

4-Aminofolic acid

25 mg
100 mg
500 mg

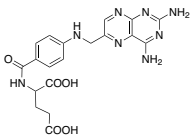

$C_{19}H_{20}N_8O_5$ FW: 440.41 [54-62-6] ≥95%

Folic acid analog, derivative of pterin, and dihydrofolate reductase inhibitor used to treat rheumatoid arthritis and leukemia. It depletes nucleotide pools and inhibits DNA and RNA synthesis.

Visentin M, Zhao R, Goldman ID. The antifolates. Hematol Oncol Clin North Am. 2012 Jun;26(3):629-48. PMID: 22520983.

McGuire JJ. Anticancer antifolates: current status and future directions. Curr Pharm Des. 2003;9(31):2593-613. PMID: 14529544.

A5033

4-Aminosalicylic Acid

25 g
100 g
500 g

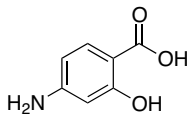

$C_7H_7NO_3$ FW: 153.14 [65-49-6] ≥98%

Dihydrofolate reductase inhibitor used to treat IBD, Crohn's disease, colitis, and tuberculosis. It is active in the small intestine and prevents growth of *Mycobacterium*.

Dhaneshwar SS. Colon-specific prodrugs of 4-aminosalicylic acid for inflammatory bowel disease. World J Gastroenterol. 2014 Apr 7;20(13):3564-71. PMID: 24707139.

Jensen KA, Rosdahl KG, Ingvorsen H. Tuberculostatic derivatives of rho-aminobenzoic acid; esters and amides of 4-aminosalicylic acid. Acta Chem Scand. 1948;2(3):220-4. PMID: 18098531.

A5034

4-Aminosalicylic Sodium Dihydrate

25 g
100 g
500 g

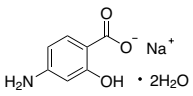

$C_7H_6NNaO_3 \cdot 2H_2O$ FW: 211.15 [6018-19-5] ≥98%

Dihydrofolate reductase inhibitor used to treat IBD, Crohn's disease, colitis, and tuberculosis. It is active in the colon and prevents growth of *Mycobacterium*.

Dhaneshwar SS. Colon-specific prodrugs of 4-aminosalicylic acid for inflammatory bowel disease. World J Gastroenterol. 2014 Apr 7;20(13):3564-71. PMID: 24707139.

A5035 5-Aminosalicylic Acid

5 g
25 g
100 g

Mesalamine

$C_7H_7NO_3$ FW: 153.14 [89-57-6] ≥98%

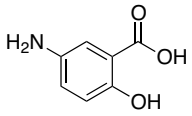

Salicylic acid derivative, PPARγ agonist, and potential COX-1/2 inhibitor used to treat IBD, Crohn's disease, and colitis. It is primarily active in the colon. It also decreases levels of ROS and inhibits proliferation of colorectal cancer cells.

Poh J, Knowles S. Safety of 5-Aminosalicylic Acid Derivatives in Patients with Sensitivity to Acetylsalicylic Acid and Nonsteroidal Anti-inflammatory Drugs. Can J Hosp Pharm. 2014 Jan;67(1):35-8. PMID: 24634525.

Managlia E, Katzman RB, Brown JB, et al. Antioxidant properties of mesalamine in colitis inhibit phosphoinositide 3-kinase signaling in progenitor cells. Inflamm Bowel Dis. 2013 Sep;19(10):2051-60. PMID: 23867870.

Baan B, Dihal AA, Hoff E, et al. 5-Aminosalicylic acid inhibits cell cycle progression in a phospholipase D dependent manner in colorectal cancer. Gut. 2012 Dec;61(12):1708-15. PMID: 22187071.

A5037 Amiodarone Hydrochloride

1 g
5 g
10 g

$C_{25}H_{29}I_2NO_3 \bullet HCl$ FW: 681.78 [19774-82-4] ≥98%

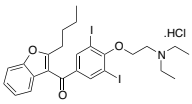

Voltage-gated Na^+, Ca^{2+}, and K^+ channel blocker, α/β-adrenergic receptor antagonist, and FIASMA used to treat ventricular fibrillation and tachycardia. It prolongs the duration of the action potential, increasing the length of the refractory period. It also inhibits cell entry by filovirus, guanarito virus, and hepatitis C.

Zoerner F, Semenas E. Resuscitation with amiodarone increases survival after hemorrhage and ventricular fibrillation in pigs. J Trauma Acute Care Surg. 2014 Jun;76(6):1402-8. PMID: 24854308.

Gehring G, Rohrmann K, Atenchong N, et al. The clinically approved drugs amiodarone, dronedarone and verapamil inhibit filovirus cell entry. J Antimicrob Chemother. 2014 Apr 7. [Epub ahead of print]. PMID: 24710028.

Cheng YL, Lan KH, Lee WP, et al. Amiodarone inhibits the entry and assembly steps of hepatitis C virus life cycle. Clin Sci (Lond). 2013 Nov;125(9):439-48. PMID: 23659500.

A5234 Amisulpride

25 mg
100 mg
500 mg

$C_{17}H_{27}N_3O_4S$ FW: 369.48 [71675-85-9] ≥98%

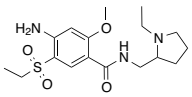

Antagonist at 5-HT7 receptors and dopamine D2/3 receptors. It modulates β2-arrestin signaling and increases neurite outgrowth.

Meltzer HY. Serotonergic mechanisms as targets for existing and novel antipsychotics. Handb Exp Pharmacol. 2012;(212):87-124. PMID: 23129329.

Park SW, Seo MK, Cho HY, et al. Differential effects of amisulpride and haloperidol on dopamine D2 receptor-mediated signaling in SH-SY5Y cells. Neuropharmacology. 2011 Sep;61(4):761-9. PMID: 21663752.

Möller HJ. Amisulpride: limbic specificity and the mechanism of antipsychotic atypicality. Prog Neuropsychopharmacol Biol Psychiatry. 2003 Oct;27(7):1101-11. PMID: 14642970.

A5039 Amitraz

5 g
25 g
100 g

$C_{19}H_{23}N_3$ FW: 293.41 [33089-61-1] ≥97%

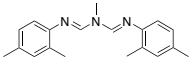

α-Adrenergic receptor agonist and MAO inhibitor used as an insecticide in the prevention of flea and tick infections. It prevents prostaglandin synthesis and may inhibit β-cell insulin release.

Chen AC, He H, Davey RB. Mutations in a putative octopamine receptor gene in amitraz-resistant cattle ticks. Vet Parasitol. 2007 Sep 30;148(3-4):379-83. PMID: 17662534.

Chen TH, Hsu WH. Inhibition of insulin release by a formamidine pesticide amitraz and its metabolites in a rat beta-cell line: an action mediated by alpha-2 adrenoceptors, a GTP-binding protein and a decrease in cyclic AMP. J Pharmacol Exp Ther. 1994 Dec;271(3):1240-5. PMID: 7527851.

A5235 Amitriptyline Hydrochloride

10 g
25 g
100 g

$C_{20}H_{23}N \bullet HCl$ FW: 313.86 [549-18-8] ≥98%

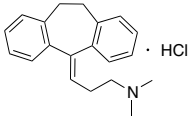

Activator of σ1 receptors, ryanodine 2 receptors, and TrkA/B receptors and inhibitor of 5-HT2/6/7 receptors, M1-5 mAChRs, histamine H1/4 receptors, α1-adrenergic receptors, SERT, NET, $K_V1.1/7.2/7.3$ K^+ channels, and L-type Ca^{2+} channels. It also acts as a FIASMA and increases neurite outgrowth.

Effects of chronic administration of amitriptyline, gabapentin and minocycline on spinal brain-derived neurotrophic factor expression and neuropathic pain behavior in a rat chronic constriction injury model.

Reg Anesth Pain Med. 2013 Mar-Apr;38(2):124-30. PMID: 23337936.

Ramakrishna D, Subhash MN. Differential modulation of α-1 adrenoceptor subtypes by antidepressants in the rat brain. J Neural Transm. 2010 Dec;117(12):1423-30. PMID: 21136124.

A4944 Amlexanox

500 mg
1 g
5 g

$C_{16}H_{14}N_2O_4$ FW: 298.29 [68302-57-8] ≥98%

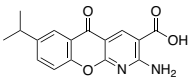

Inhibitor of TANK-binding kinase 1, S100A12, and S100A13 used to treat recurring aphthous ulcer and asthma. It attenuates actin stress fiber formation, increases energy expenditure, thermogenesis, and weight loss, minimizes mast cell release, and may inhibit 5-lipoxygenase activity.

Reilly SM, Chiang SH, Decker SJ, et al. An inhibitor of the protein kinases TBK1 and IKK-ε improves obesity-related metabolic dysfunctions in mice. Nat Med. 2013 Mar;19(3):313-21. PMID: 23396211.

Bell J. Amlexanox for the treatment of recurrent aphthous ulcers. Clin Drug Investig. 2005;25(9):555-66. PMID: 17532700.

A5045 Amlodipine

1 g
5 g
10 g

UK-48340

$C_{20}H_{25}ClN_2O_5$ FW: 408.88 [88150-42-9] ≥98%

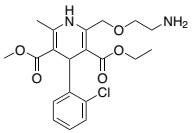

L-type Ca^{2+} channel blocker and FIASMA used to treat hypertension and angina. It induces relaxation of arterial smooth muscles, decreases blood pressure, and increases blood flow to the heart. It also improves smooth muscle hypertrophy and collagen deposition and prevents arterial remodeling.

Chen JL, Shang QH, Hu W, et al. Role of TGF-β1/Smads pathway in carotid artery remodeling in renovascular hypertensive rats and prevention by Enalapril and Amlodipine. J Geriatr Cardiol. 2012 Jun;9(2):185-91. PMID: 22916067.

Kornhuber J, Tripal P, Reichel M, et al. Functional Inhibitors of Acid Sphingomyelinase (FIASMAs): a novel pharmacological group of drugs with broad clinical applications. Cell Physiol Biochem. 2010;26(1):9-20. PMID: 20502000.

A5044 Amlodipine Besylate

1 g
5 g
10 g

$C_{20}H_{25}ClN_2O_5 \bullet C_6H_5SO_3H$ FW: 567.06 [111470-99-6] ≥98%

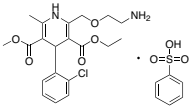

L-type Ca^{2+} channel blocker and FIASMA used to treat hypertension and angina. It induces relaxation of arterial smooth muscles, decreases blood pressure, and increases blood flow to the heart. It also improves smooth muscle hypertrophy and collagen deposition and prevents arterial remodeling.

Chen JL, Shang QH, Hu W, et al. Role of TGF-β1/Smads pathway in carotid artery remodeling in renovascular hypertensive rats and prevention by Enalapril and Amlodipine. J Geriatr Cardiol. 2012 Jun;9(2):185-91. PMID: 22916067.

Kornhuber J, Tripal P, Reichel M, et al. Functional Inhibitors of Acid Sphingomyelinase (FIASMAs): a novel pharmacological group of drugs with broad clinical applications. Cell Physiol Biochem. 2010;26(1):9-20. PMID: 20502000.

A5056 Amorolfine Hydrochloride

100 mg
250 mg
1 g

$C_{21}H_{35}NO \bullet HCl$ FW: 353.97 [78613-38-4] ≥98.5%

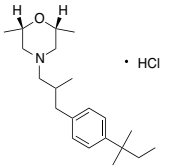

14-α Demethylase inhibitor that inhibits ergosterol synthesis and fungal cell wall formation. It also increases release of prostaglandin D2 metabolites and inhibits production of thymic stromal lymphopoietin in dermatitis models.

Ghelardi E, Celandroni F, Gueye SA, et al. Potential of Ergosterol Synthesis Inhibitors To Cause Resistance or Cross-Resistance in Trichophyton rubrum. Antimicrob Agents Chemother. 2014 May;58(5):2825-9. PMID: 24614379.

Hau CS, Kanda N, Watanabe S. Suppressive effects of antimycotics on thymic stromal lymphopoietin production in human keratinocytes. J Dermatol Sci. 2013 Sep;71(3):174-83. PMID: 23688403.

A5059 Amoxapine

250 mg
1 g
5 g

$C_{17}H_{16}ClN_3O$ FW: 313.78 [14028-44-5] ≥98%

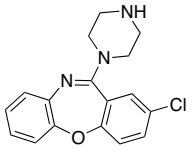

Inhibitor of 5-HT2/3/6/7 receptors, dopamine D2/3/4 receptors, histamine H1 receptors, α1-adrenergic receptors, SERT, NET, and hERG K^+ channels used to treat depression. It also inhibits bacterial β-glucuronidase and increases leu-enkephalin levels.

Ahmad S, Hughes MA, Yeh LA, et al. Potential repurposing of known drugs as potent bacterial β-glucuronidase inhibitors. J Biomol Screen. 2012 Aug;17(7):957-65. PMID: 22535688.

Yang G, Zhou MH, Ren Z, et al. Amoxapine inhibits delayed outward rectifier K(+) currents in cerebellar granule cells via dopamine receptor and protein kinase A activation. Cell Physiol Biochem. 2011;28(1):163-74. PMID: 21865859.

A5057 Amoxicillin

5 g
25 g
100 g

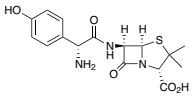

$C_{16}H_{19}N_3O_5S$ FW: 365.41 [26787-78-0] ≥98%

Penicillin binding protein inhibitor that inhibits cell wall synthesis. It is active against both gram negative and gram positive bacteria.

Astasov-Frauenhoffer M, Braissant O, Hauser-Gerspach I, et al. Microcalorimetric determination of the effects of amoxicillin, metronidazole, and their combination on in vitro biofilm. J Periodontol. 2014 Feb;85(2):349-57. PMID: 23594193.

Martin SI, Kaye KM. Beta-lactam antibiotics: newer formulations and newer agents. Infect Dis Clin North Am. 2004 Sep;18(3):603-19. PMID: 15308278.

A5061 Ampalex NEW

5 mg
10 mg
25 mg

CX-516

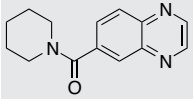

$C_{14}H_{15}N_3O$ FW: 241.29 [154235-83-3] ≥98%

AMPA receptor potentiator. It modulates fast synaptic plasticity and improves cognitive function in schizophrenia models.

O'Neill MJ, Witkin JM. AMPA receptor potentiators: application for depression and Parkinson's disease. Curr Drug Targets. 2007 May;8(5):603-20. PMID: 17504104.

Olsen CK, Kreilgaard M, Didriksen M. Positive modulation of glutamatergic receptors potentiates the suppressive effects of antipsychotics on conditioned avoidance responding in rats. Pharmacol Biochem Behav. 2006 Jun;84(2):259-65. PMID: 16782180.

A5130 Amphotericin B

100 mg
250 mg
500 mg
1 g

Fungilin

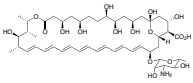

$C_{47}H_{73}NO_{17}$ FW: 924.08 [1397-89-3] ≥87%

Binds ergosterol and induces membrane pore formations, increasing ROS and suppressing fungal growth. It also increases expression of IL-1β, TNF-α, BDNF, and GDNF and protects against prion-induced neurodegeneration.

Serhan G, Stack CM, Perrone GG, et al. The polyene antifungals, amphotericin B and nystatin, cause cell death in *Saccharomyces* cerevisiae by a distinct mechanism to amphibian-derived antimicrobial peptides. Ann Clin Microbiol Antimicrob. 2014 May 12;13:18. PMID: 24884795.

Nakagawa Y, Umegawa Y, Takano T, et al. Effect of sterol side chain on ion channel formation by amphotericin B in lipid bilayers. Biochemistry. 2014 May 20;53(19):3088-94. PMID: 24762132.

Motoyoshi-Yamashiro A, Tamura M, Moriyama M, et al. Activation of cultured astrocytes by amphotericin B: stimulation of NO and cytokines production and changes in neurotrophic factors production. Neurochem Int. 2013 Aug;63(2):93-100. PMID: 23727061.

A5160 Ampicillin Trihydrate

5 g
25 g
100 g

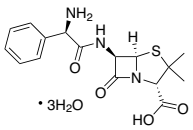

$C_{16}H_{19}N_3O_4S \bullet 3H_2O$ FW: 403.47 [7177-48-2] ≥97%

Transpeptidase inhibitor that prevents bacterial cell wall formation. It is effective against gram negative and gram positive bacteria.

Martin SI, Kaye KM. Beta-lactam antibiotics: newer formulations and newer agents. Infect Dis Clin North Am. 2004 Sep;18(3):603-19, ix. PMID: 15308278.

Demain AL. Production of beta-lactam antibiotics and its regulation. Proc Natl Sci Counc Repub China B. 1991 Oct;15(4):251-65. PMID: 1815263.

A5161 Ampiroxicam

1 g
5 g
25 g

CP-65703

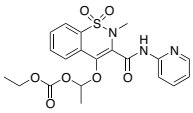

$C_{20}H_{21}N_3O_7S$ FW: 447.46 [99464-64-9] ≥98%

Piroxicam prodrug, NSAID, and COX-1/2 inhibitor that does not inhibit prostaglandin synthesis itself. It decreases pain and inflammation.

Sai S, Fujii K, Hiranuma K, et al. Preoperative ampiroxicam reduces postoperative pain after hand surgery. J Hand Surg Br. 2001 Aug;26(4):377-9. PMID: 11469844.

Carty TJ, Marfat A, Moore PF, et al. Ampiroxicam, an anti-inflammatory agent which is a prodrug of piroxicam. Agents Actions. 1993 Jul;39(3-4):157-65. PMID: 8304243.

A5162 Amprolium Hydrochloride

25 g
100 g

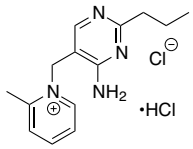

$C_{14}H_{19}ClN_4 \bullet HCl$ FW: 315.24 [137-88-2] ≥97%

Coccidiostat and thiamine transporter inhibitor. It inhibits thiamine transporters in species of *Eimeria*, preventing carbohydrate synthesis.

Young G, Alley ML, Foster DM, et al. Efficacy of amprolium for the treatment of pathogenic *Eimeria* species in Boer goat kids. Vet Parasitol. 2011 Jun 10;178(3-4):346-9. PMID: 21333448.

Dudeja PK, Tyagi S, Gill R, et al. Evidence for a carrier-mediated mechanism for thiamine transport to human jejunal basolateral membrane vesicles. Dig Dis Sci. 2003 Jan;48(1):109-15. PMID: 12645798.

A5170 Amrinone

250 mg
1 g

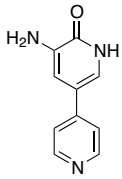

$C_{10}H_9N_3O$ FW: 187.2 [60719-84-8] ≥98%

PDE3 inhibitor used to treat congestive heart failure. It acts as a positive inotrope, inducing vasodilation and increasing cardiac contractility.

Coons JC, McGraw M, Murali S. Pharmacotherapy for acute heart failure syndromes. Am J Health Syst Pharm. 2011 Jan 1;68(1):21-35. PMID: 21164062.

van der Zypp A, Rechtman M, Majewski H. The role of cyclic nucleotides and calcium in the relaxation produced by amrinone in rat aorta. Gen Pharmacol. 2000 Apr;34(4):245-53. PMID: 11282218.

Hamada Y, Kawachi K, Yamamoto T, et al. Effects of single administration of a phosphodiesterase III inhibitor during cardiopulmonary bypass: comparison of milrinone and amrinone. Jpn Circ J. 1999 Aug;63(8):605-9. PMID: 10478810.

A5072 Amsacrine

10 mg
50 mg

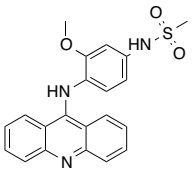

m-AMSA

$C_{21}H_{19}N_3O_3S$ FW: 393.46 [51264-14-3] ≥98%

Acridine derivative, DNA intercalator, topoisomerase II inhibitor, and hERG K^+ channel blocker used to treat acute myelogenous leukemia. It decreases expression of MMP2 and MMP9 to prevent invasion in leukemia cells and prolongs the cardiac QT interval.

Liu WH, Chen YJ, Chien JH, et al. Amsacrine suppresses matrix metalloproteinase-2 (MMP-2)/MMP-9 expression in human leukemia cells. J Cell Physiol. 2013 Oct 7. Epub ahead of print. PMID: 24122234.

Jangir DK, Dey SK, Kundu S, et al. Assessment of amsacrine binding with DNA using UV-visible, circular dichroism and Raman spectroscopic techniques. J Photochem Photobiol B. 2012 Sep 3;114:38-43. PMID: 22677564.

Thomas D, Hammerling BC, Wu K, et al. Inhibition of cardiac HERG currents by the DNA topoisomerase II inhibitor amsacrine: mode of action. Br J Pharmacol. 2004 Jun;142(3):485-94. PMID: 15148258.

A5193 Amygdalin

1 g
5 g
25 g

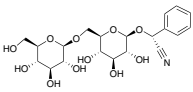

$C_{20}H_{27}NO_{11}$ FW: 457.43 [29883-15-6] ≥98%

Found in stone fruits and apples. It decreases formalin-induced pain, induces apoptosis in prostate cancer cells, and inhibits tumor xenograft growth.

Chen Y, Ma J, Wang F, et al. Amygdalin induces apoptosis in human cervical cancer cell line HeLa cells. Immunopharmacol Immunotoxicol. 2013 Feb;35(1):43-51. PMID: 23137229.

Hwang HJ, Kim P, Kim CJ, et al. Antinociceptive effect of amygdalin isolated from Prunus armeniaca on formalin-induced pain in rats. Biol Pharm Bull. 2008 Aug;31(8):1559-64. PMID: 18670089.

Chang HK, Shin MS, Yang HY, et al. Amygdalin induces apoptosis through regulation of Bax and Bcl-2 expressions in human DU145 and LNCaP prostate cancer cells. Biol Pharm Bull. 2006 Aug;29(8):1597-602. PMID: 16880611.

A4844 Amylin (8-37), human

H-Ala-Thr-Gln-Arg-Leu-Ala-Asn-Phe-Leu-Val-His-Ser-Ser-Asn-Asn-Phe-Gly-Ala-Ile-Leu-Ser-Ser-Thr-Asn-Val-Gly-Ser-Asn-Thr-Tyr-NH_2

0.5 mg
1 mg
2.5 mg

IAPP; Islet amyloid precursor peptide

$C_{138}H_{215}N_{41}O_{46}$ FW: 3184.5 ≥95%

Endogenous calcitonin-RAMP agonist involved in gastric emptying, gastric acid secretion, and enteric contraction. It slows food intake, suppresses gastric acid secretion, and inhibits osteoclast activity.

Paulsson JF, Westermark GT. Aberrant processing of human proislet amyloid polypeptide results in increased amyloid formation. Diabetes. 2005 Jul;54(7):2117-25. PMID: 15983213.

Ratner RE, Dickey R, Fineman M, et al. Amylin replacement with pramlintide as an adjunct to insulin therapy improves long-term glycaemic and weight control in Type 1 diabetes mellitus: a 1-year, randomized controlled trial. Diabet Med. 2004 Nov;21(11):1204-12. PMID: 15498087.

A4845 Amylin (8-37), rat

H-Ala-Thr-Gln-Arg-Leu-Ala-Asn-Phe-Leu-Val-Arg-Ser-Ser-Asn-Asn-Leu-Gly-Pro-Val-Leu-Pro-Pro-Thr-Asn-Val-Gly-Ser-Asn-Thr-Tyr-NH_2

0.5 mg
1 mg
2.5 mg

IAPP; Islet amyloid precursor peptide

$C_{140}H_{227}N_{43}O_{43}$ FW: 3200.63 ≥95%

Endogenous calcitonin-RAMP agonist involved in gastric emptying, gastric acid secretion, and enteric contraction. It slows food intake, suppresses gastric acid secretion, and inhibits osteoclast activity.

Paulsson JF, Westermark GT. Aberrant processing of human proislet amyloid polypeptide results in increased amyloid formation. Diabetes. 2005 Jul;54(7):2117-25. PMID: 15983213.

Ratner RE, Dickey R, Fineman M, et al. Amylin replacement with pramlintide as an adjunct to insulin therapy improves long-term glycaemic and weight control in Type 1 diabetes mellitus: a 1-year, randomized controlled trial. Diabet Med. 2004 Nov;21(11):1204-12. PMID: 15498087.

A4846

H-Lys-Cys-Asn-Thr-Ala-Thr-Cys-Ala-Thr-Gln-Arg-Leu-Ala-Asn-Phe-Leu-Ile-Arg-Ser-Ser-Asn-Asn- Leu-Gly-Ala-Ile-Leu-Ser-Pro-Thr-Asn-Val-Gly-Ser-Asn-Thr-Tyr-NH_2
(Disulfide Bridge Cys2-Cys7)

Amylin, cat

0.5 mg
1 mg
2.5 mg

IAPP; Islet amyloid precursor peptide

$C_{165}H_{270}N_{52}O_{54}S_2$ FW: 3910.45 ≥95%

Endogenous calcitonin-RAMP agonist involved in gastric emptying, gastric acid secretion, and enteric contraction. It slows food intake, suppresses gastric acid secretion, and inhibits osteoclast activity.

Paulsson JF, Westermark GT. Aberrant processing of human proislet amyloid polypeptide results in increased amyloid formation. Diabetes. 2005 Jul;54(7):2117-25. PMID: 15983213.

Ratner RE, Dickey R, Fineman M, et al. Amylin replacement with pramlintide as an adjunct to insulin therapy improves long-term glycaemic and weight control in Type 1 diabetes mellitus: a 1-year, randomized controlled trial. Diabet Med. 2004 Nov;21(11):1204-12. PMID: 15498087.

A4847

H-Lys-Cys-Asn-Thr-Ala-Thr-Cys-Ala-Thr-Gln-Arg-Leu-Ala-Asn-Phe-Leu-Val-His-Ser-Ser-Asn-Asn-Phe-Gly-Ala-Ile-Leu-Ser-Ser-Thr-Asn-Val-Gly-Ser-Asn-Thr-Tyr-NH_2

Amylin, human

0.5 mg
1 mg
2.5 mg

IAPP; Islet amyloid precursor peptide

$C_{165}H_{261}N_{51}O_{55}S_2$ FW: 3903.4 [122384-88-7] ≥95%

Endogenous calcitonin-RAMP agonist involved in gastric emptying, gastric acid secretion, and enteric contraction. It slows food intake, suppresses gastric acid secretion, and inhibits osteoclast activity.

Paulsson JF, Westermark GT. Aberrant processing of human proislet amyloid polypeptide results in increased amyloid formation. Diabetes. 2005 Jul;54(7):2117-25. PMID: 15983213.

Ratner RE, Dickey R, Fineman M, et al. Amylin replacement with pramlintide as an adjunct to insulin therapy improves long-term glycaemic and weight control in Type 1 diabetes mellitus: a 1-year, randomized controlled trial. Diabet Med. 2004 Nov;21(11):1204-12. PMID: 15498087.

A4850

H-Lys-Cys-Asn-Thr-Ala-Thr-Cys-Ala-Thr-Gln-Arg-Leu-Ala-Asn-Phe-Leu-Val-His-Ser-Ser-Asn-Asn-Leu-Gly-Pro-Val-Leu-Pro-Pro-Thr-Asn-Val-Gly-Ser-Asn-Thr-Tyr-NH_2
(Disulfide Bridge Cys2-Cys7)

Amylin, rat

0.5 mg
1 mg
2.5 mg

IAPP; Islet amyloid precursor peptide

$C_{167}H_{270}N_{52}O_{53}S_2$ FW: 3918.47 ≥95%

Endogenous calcitonin-RAMP agonist involved in gastric emptying, gastric acid secretion, and enteric contraction. It slows food intake, suppresses gastric acid secretion, and inhibits osteoclast activity.

Paulsson JF, Westermark GT. Aberrant processing of human proislet amyloid polypeptide results in increased amyloid formation. Diabetes. 2005 Jul;54(7):2117-25. PMID: 15983213.

A4848

Asp-Ala-Glu-Phe-Arg-His-Asp-Ser-Gly-Tyr-Glu-Val-His-His-Gln-Lys-Leu-Val-Phe-Phe-Ala-Glu-Asp-Val-Gly-Ser-Asn-Lys-Gly-Ala-Ile-Ile-Gly-Leu-Met-Val-Gly-Gly-Val-Val

Amyloid-β (1-40)

1 mg

Aβ (1-40)

$C_{194}H_{295}N_{53}O_{58}S$ FW: 4329.8 [131438-79-4] ≥98%

Endogenous APP peptide cleavage product and primary component in amyloid plaques typical of Alzheimer's disease. Aβ (1-40) is more common than other forms but less fibrillogenic.

Hu J, el-Fakahany EE. Neuroreport. 4(6):760-762 (1993).Jia J, Kang L, Li S, et al. Amelioratory effects of testosterone treatment on cognitive performance deficits induced by soluble Aβ1-42 oligomers injected into the hippocampus. Horm Behav. 2013 Aug;64(3):477-86. PMID: 23954394.

Yin YI, Bassit B, Zhu L, et al. gamma-Secretase Substrate Concentration Modulates the Abeta42/Abeta40 Ratio: Implications for Alzheimer's disease. J Biol Chem. 2007 Aug 10;282(32):23639-44. PMID: 17556361.

A4849

H-Gly-Ser-Asn-Lys-Gly-Ala-Ile-Ile-Gly-Leu-Met-OH

Amyloid-β (25-35)

1 mg
2 mg
5 mg

Aβ (25-35)

$C_{45}H_{81}N_{13}O_{14}S$ FW: 1060.27 [131602-53-4] ≥95%

Endogenous APP peptide cleavage product and primary component in amyloid plaques typical of Alzheimer's disease.

Hu J, el-Fakahany EE. Neuroreport. 4(6):760-762 (1993).Jia J, Kang L, Li S, et al. Amelioratory effects of testosterone treatment on cognitive performance deficits induced by soluble Aβ1-42 oligomers injected into the hippocampus. Horm Behav. 2013 Aug;64(3):477-86. PMID: 23954394.

Yin YI, Bassit B, Zhu L, et al. gamma-Secretase Substrate Concentration Modulates the Abeta42/Abeta40 Ratio: Implications for Alzheimer's disease. J Biol Chem. 2007 Aug 10;282(32):23639-44. PMID: 17556361.

A4851

H-Asp-Ala-Glu-Phe-Gly-His-Asp-Ser-Gly-Phe-Glu-Val-Arg-His-Gln-Lys-Leu-Val-Gly-Phe-Phe-Ala-Glu-Asp-Val-Gly-Ser-Asn-Lys-Gly-Ala-Ile-Ile-Gly-Leu-Met-Val-Gly-Gly-Val-Val-OH

β-Amyloid Peptide (1-40), rat

0.5 mg
1 mg
2.5 mg

Aβ (1-40)

$C_{190}H_{291}N_{51}O_{57}S_1$ FW: 4233.81 [131438-79-4] ≥95%

Endogenous APP peptide cleavage product and primary component in amyloid plaques typical of Alzheimer's disease. Aβ (1-40) is more common than other forms but less fibrillogenic.

Hu J, el-Fakahany EE. Neuroreport. 4(6):760-762 (1993).Jia J, Kang L, Li S, et al. Amelioratory effects of testosterone treatment on cognitive performance deficits induced by soluble Aβ1-42 oligomers injected into the hippocampus. Horm Behav. 2013 Aug;64(3):477-86. PMID: 23954394.

Yin YI, Bassit B, Zhu L, et al. gamma-Secretase Substrate Concentration Modulates the Abeta42/Abeta40 Ratio: Implications for Alzheimer's disease. J Biol Chem. 2007 Aug 10;282(32):23639-44. PMID: 17556361.

A4852

H-Asp-Ala-Glu-Phe-Arg-His-Asp-Ser-Gly-Tyr-Glu-Val-His-His-Gln-Lys-leu-Val-Phe-Phe-Ala-Glu-Asp-Val-Gly-Ser-Asn-Lys-Gly-Ala-Ile-Ile-Gly-Leu-Met-Val-Gly-Gly-Val-Val-OH

β-Amyloid Peptide (1-40)

0.5 mg
1 mg
2.5 mg

Aβ (1-40)

$C_{194}H_{295}N_{53}O_{58}S$ FW: 4329.9 ≥95%

Endogenous APP peptide cleavage product and primary component in amyloid plaques typical of Alzheimer's disease. Aβ (1-40) is more common than other forms but less fibrillogenic.

Jia J, Kang L, Li S, et al. Amelioratory effects of testosterone treatment on cognitive performance deficits induced by soluble Aβ1-42 oligomers injected into the hippocampus. Horm Behav. 2013 Aug;64(3):477-86. PMID: 23954394.

Yin YI, Bassit B, Zhu L, et al. gamma-Secretase Substrate Concentration Modulates the Abeta42/Abeta40 Ratio: Implications for Alzheimer's disease. J Biol Chem. 2007 Aug 10;282(32):23639-44. PMID: 17556361.

A4853

H-Asp-Ala-Glu-Phe-Arg-His-Asp-Ser-Gly-Tyr-Glu-Val-His-His-Gln-Lys-leu-Val-Phe-Phe-Ala-Glu-Asp-Val-Gly-Ser-Asn-Lys-Gly-Ala-Ile-Ile-Gly-Leu-Met-Val-Gly-Gly-Val-Val-Ile-Ala-OH

β-Amyloid Peptide (1-42), human

0.5 mg
1 mg
2.5 mg

Aβ (1-42)

$C_{203}H_{311}N_{55}O_{60}S$ FW: 4550.18 ≥95%

Endogenous APP peptide cleavage product and primary component in amyloid plaques typical of Alzheimer's disease. Aβ (1-42) is less common than other forms but more fibrillogenic.

Jia J, Kang L, Li S, et al. Amelioratory effects of testosterone treatment on cognitive performance deficits induced by soluble Aβ1-42 oligomers injected into the hippocampus. Horm Behav. 2013 Aug;64(3):477-86. PMID: 23954394.

Yin YI, Bassit B, Zhu L, et al. gamma-Secretase Substrate Concentration Modulates the Abeta42/Abeta40 Ratio: Implications for Alzheimer's disease. J Biol Chem. 2007 Aug 10;282(32):23639-44. PMID: 17556361.

A4854

H-Asp-Ala-Glu-Phe-Gly-His-Asp-Ser-Gly-Phe-Glu-Val-Arg-His-Gln-Lys-Leu-Val-Gly-Phe-Phe-Ala-Glu-Asp-Val-Gly-Ser-Asn-Lys-Gly-Ala-Ile-Ile-Gly-Leu-Met-Val-Gly-Gly-Val-Val-Ile-Ala-OH

β-Amyloid Peptide (1-42), rat

1 mg
2 mg
5 mg

Aβ (1-42)

$C_{199}H_{307}N_{53}O_{59}S$ FW: 4454.09 [107761-42-2] ≥95%

Endogenous APP peptide cleavage product and primary component in amyloid plaques typical of Alzheimer's disease. Aβ (1-42) is less common than other forms but more fibrillogenic.

Jia J, Kang L, Li S, et al. Amelioratory effects of testosterone treatment on cognitive performance deficits induced by soluble Aβ1-42 oligomers injected into the hippocampus. Horm Behav. 2013 Aug;64(3):477-86. PMID: 23954394.

A5204

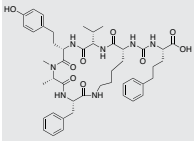

Anabaenopeptin 856

NEW **50 µg**

$C_{46}H_{61}N_7O_9$ FW: 856.02 ≥95%

Inhibitor of serine protease and PP and potential inhibitor of carboxypeptidases found in *Microcystis*. It is cytotoxic.

Gesner-Apter S, Carmeli S. Protease inhibitors from a water bloom of the cyanobacterium *Microcystis* aeruginosa. J Nat Prod. 2009 Aug;72(8):1429-36. PMID: 19650639.

Okumura HS, Philmus B, Portmann C, et al. Homotyrosine-containing cyanopeptolins 880 and 960 and anabaenopeptins 908 and 915 from Planktothrix agardhii CYA 126/8. J Nat Prod. 2009 Jan;72(1):172-6. PMID: 19115837.

Sedmak B, Carmeli S, Elersek T. "Non-toxic" cyclic peptides induce lysis of cyanobacteria-an effective cell population density control mechanism in cyanobacterial blooms. Microb Ecol. 2008 Aug;56(2):201-9. PMID: 18008101.

A5205

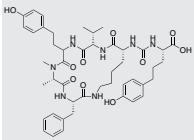

Anabaenopeptin 872

NEW **50 µg**

$C_{46}H_{61}N_7O_{10}$ FW: 872.02 ≥95%

Inhibitor of serine protease and PP and potential inhibitor of carboxypeptidases found in *Microcystis*. It is cytotoxic.

Gesner-Apter S, Carmeli S. Protease inhibitors from a water bloom of the cyanobacterium *Microcystis* aeruginosa. J Nat Prod. 2009 Aug;72(8):1429-36. PMID: 19650639.

Okumura HS, Philmus B, Portmann C, et al. Homotyrosine-containing cyanopeptolins 880 and 960 and anabaenopeptins 908 and 915 from Planktothrix agardhii CYA 126/8. J Nat Prod. 2009 Jan;72(1):172-6. PMID: 19115837.

Sedmak B, Carmeli S, Elersek T. "Non-toxic" cyclic peptides induce lysis of cyanobacteria-an effective cell population density control mechanism in cyanobacterial blooms. Microb Ecol. 2008 Aug;56(2):201-9. PMID: 18008101.

A5200

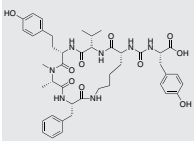

Anabaenopeptin A

NEW **100 µg**

$C_{44}H_{57}N_7O_{10}$ FW: 843.96 [161897-73-0] ≥95%

Inhibitor of serine protease and PP and potential inhibitor of carboxypeptidases found in *Microcystis*. It is cytotoxic.

Gesner-Apter S, Carmeli S. Protease inhibitors from a water bloom of the cyanobacterium *Microcystis* aeruginosa. J Nat Prod. 2009 Aug;72(8):1429-36. PMID: 19650639.

Okumura HS, Philmus B, Portmann C, et al. Homotyrosine-containing cyanopeptolins 880 and 960 and anabaenopeptins 908 and 915 from Planktothrix agardhii CYA 126/8. J Nat Prod. 2009 Jan;72(1):172-6. PMID: 19115837.

A5201 Anabaenopeptin B

NEW **100 µg**

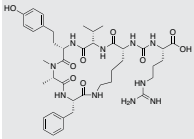

$C_{41}H_{60}N_{10}O_9$ FW: 836.98 [161897-74-1] ≥95%

Inhibitor of serine protease and PP and potential inhibitor of carboxypeptidases found in *Microcystis*. It is not cytotoxic.

Gesner-Apter S, Carmeli S. Protease inhibitors from a water bloom of the cyanobacterium *Microcystis* aeruginosa. J Nat Prod. 2009 Aug;72(8):1429-36. PMID: 19650639.

Okumura HS, Philmus B, Portmann C, et al. Homotyrosine-containing cyanopeptolins 880 and 960 and anabaenopeptins 908 and 915 from Planktothrix agardhii CYA 126/8. J Nat Prod. 2009 Jan;72(1):172-6. PMID: 19115837.

Sedmak B, Carmeli S, Elersek T. "Non-toxic" cyclic peptides induce lysis of cyanobacteria-an effective cell population density control mechanism in cyanobacterial blooms. Microb Ecol. 2008 Aug;56(2):201-9. PMID: 18008101.

A5203 Anabaenopeptin F

NEW **50 µg**

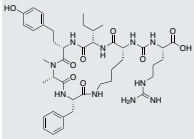

$C_{42}H_{62}N_{10}O_9$ FW: 851 [226416-60-0] ≥95%

Inhibitor of serine protease and PP and potential inhibitor of carboxypeptidases found in *Microcystis*. It is not cytotoxic.

Gesner-Apter S, Carmeli S. Protease inhibitors from a water bloom of the cyanobacterium *Microcystis* aeruginosa. J Nat Prod. 2009 Aug;72(8):1429-36. PMID: 19650639.

Okumura HS, Philmus B, Portmann C, et al. Homotyrosine-containing cyanopeptolins 880 and 960 and anabaenopeptins 908 and 915 from Planktothrix agardhii CYA 126/8. J Nat Prod. 2009 Jan;72(1):172-6. PMID: 19115837.

Sedmak B, Carmeli S, Elersek T. "Non-toxic" cyclic peptides induce lysis of cyanobacteria-an effective cell population density control mechanism in cyanobacterial blooms. Microb Ecol. 2008 Aug;56(2):201-9. PMID: 18008101.

A5202 Anabasine Hydrochloride

25 mg **100 mg**

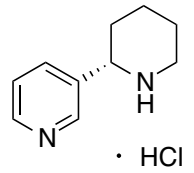

$C_{10}H_{14}N_2 \cdot HCl$ FW: 198.73 [15251-47-5] ≥98%

Depolarizing NMJ blocker, nAChR antagonist, aromatase inhibitor, and teratogen found in species of *Nicotiana*. It is used as an insecticide and as a clinical biomarker for tobacco smoke exposure.

Green BT, Lee ST, Welch KD, et al. Plant alkaloids that cause developmental defects through the disruption of cholinergic neurotransmission. Birth Defects Res C Embryo Today. 2013 Dec;99(4):235-46. PMID: 24339035.

Shimomura M, Yokota M, Ihara M, et al. Role in the selectivity of neonicotinoids of insect-specific basic residues in loop D of the nicotinic acetylcholine receptor agonist binding site. Mol Pharmacol. 2006 Oct;70(4):1255-63. PMID: 16868180.

Jacob P 3rd, Yu L, Shulgin AT, Benowitz NL. Minor tobacco alkaloids as biomarkers for tobacco use: comparison of users of cigarettes, smokeless tobacco, cigars, and pipes. Am J Public Health. 1999 May;89(5):731-6. PMID: 10224986.

A5327 Anagrelide

10 mg **25 mg** **100 mg**

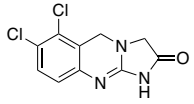

$C_{10}H_7Cl_2N_3O$ FW: 256.09 [68475-42-3] ≥98%

PDE3 inhibitor used to treat essential thrombocytosis and other chronic myeloproliferative disorders. It suppresses megakaryocytopoiesis and inhibits thombopoietin-mediated cell differentiation.

Ahluwalia M, Donovan H, Singh N, et al. Anagrelide represses GATA-1 and FOG-1 expression without interfering with thrombopoietin receptor signal transduction. J Thromb Haemost. 2010 Oct;8(10):2252-61. PMID: 20586925.

McCarty JM, Melone PD, Simanis JP, et al. A preliminary investigation into the action of anagrelide: thrombopoietin-c-Mpl receptor interactions. Exp Hematol. 2006 Jan;34(1):87-96. PMID: 16413395.

Wang G, Franklin R, Hong Y, et al. Comparison of the biological activities of anagrelide and its major metabolites in haematopoietic cell cultures. Br J Pharmacol. 2005 Oct;146(3):324-32. PMID: 16041400.

A5302 Anastrozole

100 mg **250 mg** **1 g**

ZD1033

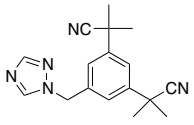

$C_{17}H_{19}N_5$ FW: 293.37 [120511-73-1] ≥99%

Aromatase inhibitor used to treat ER-positive breast cancer. It suppresses estrogen synthesis and induces apoptosis in breast cancer cells.

Kelly CM, Buzdar AU. Anastrozole. Expert Opin Drug Saf. 2010 Nov;9(6):995-1003. PMID: 20923259.

Hong Y, Chen S. Aromatase inhibitors: structural features and biochemical characterization. Ann N Y Acad Sci. 2006 Nov;1089:237-51. PMID: 17261771.

McCloskey E. Effects of third-generation aromatase inhibitors on bone. Eur J Cancer. 2006 May;42(8):1044-51. PMID: 16554149.

A5313 Andrographolide

10 mg
100 mg
250mg
1 g

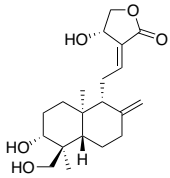

$C_{20}H_{30}O_5$ FW: 350.45 [5508-58-7] ≥98%

RIG1-like receptor antagonist found in *Andrographis*. It decreases TNF-α-induced generation of ROS, suppresses development of diabetes, and inhibits HSP90 activity and induces apoptosis in leukemia cells.

Lu CY, Yang YC, Li CC, et al. Andrographolide inhibits TNFα-induced ICAM-1 expression via suppression of NADPH oxidase activation and induction of HO-1 and GCLM expression through the PI3K/Akt/Nrf2 and PI3K/Akt/AP-1 pathways in human endothelial cells. Biochem Pharmacol. 2014 Sep 1;91(1):40-50. PMID: 24998495.

Yu B, Dai CQ, Jiang ZY, et al. Andrographolide as an anti-H1N1 drug and the mechanism related to retinoic acid-inducible gene-I-like receptors signaling pathway. Chin J Integr Med. 2014 Jul;20(7):540-5. PMID: 24972581.

Wang J, Tan XF, Nguyen VS, et al. A quantitative chemical proteomics approach to profile the specific cellular targets of andrographolide, a promising anticancer agent that suppresses tumor metastasis. Mol Cell Proteomics. 2014 Mar;13(3):876-86. PMID: 24445406.

A5314 Dehydroandrographolide

1 mg
5 mg
10 mg

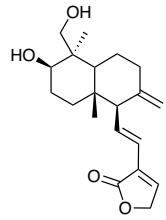

$C_{20}H_{28}O_4$ FW: 332.43 ≥98%

Found in *Andrographis*. It inhibits hepatitis B virus replication, decreases pro-inflammatory cytokine expression, and increases levels of superoxide dismutase.

Chen H, Ma YB, Huang XY, et al. Synthesis, structure-activity relationships and biological evaluation of dehydroandrographolide and andrographolide derivatives as novel anti-hepatitis B virus agents. Bioorg Med Chem Lett. 2014 May 15;24(10):2353-9. PMID: 24731274.

Zhu T, Guan X, Zhang W, et al. Dehydroandrographolide succinate inhibits oxidative stress in mice with lipopolysaccharide-induced acute lung injury by inactivating iNOS. Nan Fang Yi Ke Da Xue Xue Bao. 2012 Sep;32(9):1238-41. PMID: 22985554.

A5315 Deoxyandrographolide

1 mg
5 mg
10 mg

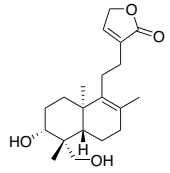

$C_{20}H_{30}O_4$ FW: 334.45 ≥98%

Activator of cNOS and adenylyl cyclase and inhibitor of PAF found in *Andrographis*. It may also block voltage-gated Ca^{2+} channels. It also lowers oxidative stress and ethanol-induced hepatic injury and decreases perfusion pressure and dilates vessels in vivo.

Mandal S, Nelson VK, Mukhopadhyay S, et al. 14-Deoxyandrographolide targets adenylate cyclase and prevents ethanol-induced liver injury through constitutive NOS dependent reduced redox signaling in rats. Food Chem Toxicol. 2013 Sep;59:236-48. PMID: 23764359.

Awang K, Abdullah NH, Hadi AH, et al. Cardiovascular activity of labdane diterpenes from *Andrographis* paniculata in isolated rat hearts. J Biomed Biotechnol. 2012;2012:876458. PMID: 22536026.

Burgos RA, Hidalgo MA, Monsalve J, et al. 14-deoxyandrographolide as a platelet activating factor antagonist in bovine neutrophils. Planta Med. 2005 Jul;71(7):604-8. PMID: 16041644.

A5217 *trans*-Anethole

50 ml
100 ml

trans-p-Propenylanisole; Anise camphor; Isoestragole

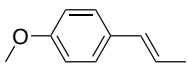

$C_{10}H_{12}O$ FW: 148.2 [4180-23-8] ≥98%

NMDA agonist found in essential oils. Protects against cerebral ischemia-induced neurodegeneration in vitro and decreases inflammatory cytokine production in animal models of hepatic ischemia/reperfusion injury.

Miyagawa M, Satou T, Yukimune C, et al. Anxiolytic-Like Effect of Illicium verum Fruit Oil, trans-Anethole and Related Compounds in Mice. Phytother Res. 2014 Jun 11. [Epub ahead of print]. PMID: 24919985.

Ryu S, Seol GH, Park H, et al. Trans-anethole protects cortical neuronal cells against oxygen-glucose deprivation/reoxygenation. Neurol Sci. 2014 Oct;35(10):1541-7. PMID: 24777545.

Fujita KI, Tatsumi M, Ogita A, et al. Anethole induces apoptotic cell death accompanied by reactive oxygen species production and DNA fragmentation in *Aspergillus* fumigatus and *Saccharomyces* cerevisiae. FEBS J. 2014 Jan 2. [Epub ahead of print]. PMID: 24393541.

A5219 Anethole Trithione

25 mg
100 mg
500 mg

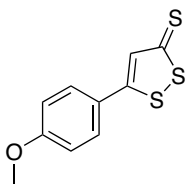

Trithioanethole; ADT

$C_{10}H_8OS_3$ FW: 240.37 [532-11-6] ≥98%

Oltipraz analog and salivary gland secretion enhancer used to treat xerostomia.

Nagano T, Takeyama M. Enhancement of salivary secretion and neuropeptide (substance P, alpha-calcitonin gene-related peptide) levels in saliva by chronic anethole trithione treatment. J Pharm Pharmacol. 2001 Dec;53(12):1697-702. PMID: 11804400.

Hamada T, Nakane T, Kimura T, et al. Treatment of xerostomia with the bile secretion-stimulating drug anethole trithione: a clinical trial. Am J Med Sci. 1999 Sep;318(3):146-51. PMID: 10487404.

A5225

α-ANP (1-28), human — 0.5 mg, 1 mg, 2.5 mg

Ser-Leu-Arg-Arg-Ser-Ser-Cys-Phe-Gly-Gly-Arg-Met-Asp-Arg-Ile-Gly-Ala-Gln-Ser-Gly-Leu-Gly-Cys-Asn-Ser-Phe-Arg-Tyr (Disulfide bridge Cys7-Cys23)

Atrial natriuretic peptide; hANF

$C_{127}H_{203}N_{45}O_{39}S_3$ FW: 3080.46 [91917-63-4] ≥95%

Endogenous NPR-A agonist. It increases cGMP levels and induces diuresis, natriuresis, and vasodilation. It may inhibit growth of cancer cells.

Vesely DL. New anticancer agents: hormones made within the heart. Anticancer Res. 2012 Jul;32(7):2515-21. PMID: 22753708.

Woodard GE, Rosado JA. Natriuretic peptides in vascular physiology and pathology. Int Rev Cell Mol Biol. 2008;268:59-93. PMID: 18703404.

A5228

Angiogenin — 50 µg

Ser-Leu-Arg-Arg-Ser-Ser-Cys-Phe-Gly-Gly-Arg-Met-Asp-Arg-Ile-Gly-Ala-Gln-Ser-Gly-Leu-Gly-Cys-Asn_Ser-Phe-Arg-Tyr (Disulfide bridge Cys7-Cys23)

14.4 kDa [97950-81-7] ≥98%

It stimulates development of new blood vessels and cleaves RNA. It also degrades basement membrane connective tissues to allow cell migration and invasion.

Gao X, Xu Z. Mechanisms of action of angiogenin. Acta Biochim Biophys Sin (Shanghai). 2008 Jul;40(7):619-24. PMID: 18604453.

A5070

Angiotensin Acetate — Please inquire

Asp-Arg-Val-Tyr-Val-His-Pro-Phe-OH

$C_{49}H_{69}N_{13}O_{12}$ FW: 1032.18 ≥95%

Derivative of AT I and precursor to AT II that displays vasoconstrictive activity.

Moon JY. Recent Update of Renin-angiotensin-aldosterone System in the Pathogenesis of Hypertension. Electrolyte Blood Press. 2013 Dec;11(2):41-45. PMID: 24627703.

Herichova I, Szantoova K. Renin-angiotensin system: upgrade of recent knowledge and perspectives. Endocr Regul. 2013 Jan;47(1):39-52. PMID: 23363256.

A5273

Angiotensin Converting Enzyme Inhibitor Peptide — 5 mg, 10 mg, 25 mg

ACE inhibitor peptide

H-pGlu-Trp-Pro-Arg-Pro-Gln-Ile-Pro-Pro-OH

$C_{53}H_{77}N_{14}O_{12}$ FW: 1102.29 ≥95%

ACE inhibitor. It decreases blood pressure and inhibits bradykinin hydrolysis and LHRH inactivation.

Martins AR, Caldo H, Coelho HL, et al. Screening for rabbit brain neuropeptide-metabolizing peptidases. Inhibition of endopeptidase B by bradykinin potentiating peptide 9a (SQ 20881). J Neurochem. 1980 Jan;34(1):100-7. PMID: 6161209.

A5276

Angiotensin I, human — 5 mg, 10 mg, 25 mg

Hypertensin I

Asp-Arg-Val-Tyr-Ile-His-Pro-Phe-His-Leu

$C_{62}H_{89}N_{17}O_{14}$ FW: 1296.49 [70937-97-2] ≥98%

Endogenous cleavage product of angiotensin and precursor to angiotensin II. It serves no endogenous biological purpose.

Gonzalez-Villalobos RA, Shen XZ, Bernstein EA, et al. Rediscovering ACE: novel insights into the many roles of the angiotensin-converting enzyme. J Mol Med (Berl). 2013 Oct;91(10):1143-54. PMID: 23686164.

A5279

Angiotensin II (1-4), human — 5 mg, 10 mg, 25 mg

H-Asp-Arg-Val-Tyr-OH

$C_{24}H_{37}N_7O_8$ FW: 551.6 ≥95%

Endogenous peptide involved in vasoconstriction, Na^+ reabsorption, and blood pressure. It activates AT1 receptors and Na^+/H^+ transporters. It increases intracellular Ca^{2+}, induces vasoconstriction, and raises blood pressure, volume, and pH.

De Giusti VC, Ciancio MC, Orlowski A, et al. Modulation of the cardiac sodium/bicarbonate cotransporter by the renin angiotensin aldosterone system: pathophysiological consequences. Front Physiol. 2014 Jan 17;4:411. PMID: 24478712.

Moon JY. Recent Update of Renin-angiotensin-aldosterone System in the Pathogenesis of Hypertension. Electrolyte Blood Press. 2013 Dec;11(2):41-45. PMID: 24627703.

A5280

Angiotensin II (3-8), human — 5 mg, 10 mg, 25 mg

H-Val-Tyr-Ile-His-Pro-Phe-OH

$C_{40}H_{54}N_8O_8$ FW: 774.93 [23025-68-5] ≥95%

Endogenous peptide involved in vasoconstriction, Na^+ reabsorption, and blood pressure. It activates AT1 receptors and Na^+/H^+ transporters. It increases intracellular Ca^{2+}, induces vasoconstriction, and raises blood pressure, volume, and pH.

De Giusti VC, Ciancio MC, Orlowski A, et al. Modulation of the cardiac sodium/bicarbonate cotransporter by the renin angiotensin aldosterone system: pathophysiological consequences. Front Physiol. 2014 Jan 17;4:411. PMID: 24478712.

A5281 Angiotensin II (4-8), human

5 mg
10 mg
25 mg

$C_{35}H_{45}N_7O_7$ FW: 675.79 ≥95%

H-Tyn-Ile-His-Pro-Phe-OH

Endogenous peptide involved in vasoconstriction, Na^+ reabsorption, and blood pressure. It activates AT1 receptors and Na^+/H^+ transporters. It increases intracellular Ca^{2+}, induces vasoconstriction, and raises blood pressure, volume, and pH.

A5277 Angiotensin II, human

5 mg
10 mg
25 mg

Hypertensin II

$C_{50}H_{71}N_{13}O_{12}$ FW: 1046.19 [68521-88-0] ≥95%

Asp-Arg-Val-Tyr-Ile-His-Pro-Phe-OH

Endogenous peptide involved in vasoconstriction, Na^+ reabsorption, and blood pressure. It activates AT1 receptors and Na^+/H^+ transporters. It increases intracellular Ca^{2+}, induces vasoconstriction, and raises blood pressure, volume, and pH.

De Giusti VC, Ciancio MC, Orlowski A, et al. Modulation of the cardiac sodium/bicarbonate cotransporter by the renin angiotensin aldosterone system: pathophysiological consequences. Front Physiol. 2014 Jan 17;4:411. PMID: 24478712.

Moon JY. Recent Update of Renin-angiotensin-aldosterone System in the Pathogenesis of Hypertension. Electrolyte Blood Press. 2013 Dec;11(2):41-45. PMID: 24627703.

A5278 Angiotensin III, human

5 mg
10 mg
25 mg

$C_{46}H_{66}N_{12}O_9$ FW: 931.1 [12687-51-3] ≥98%

H-Arg-Val-Tyr-Ile-His-Pro-Phe-OH

Endogenous cleavage product of AT II and AT1 receptor agonist. It is less active than AT II. It also increases aldosterone secretion and mean arterial pressure.

Yugandhar VG, Clark MA. Angiotensin III: a physiological relevant peptide of the renin angiotensin system. Peptides. 2013 Aug;46:26-32. PMID: 23692861.

Yang R, Smolders I, Dupont AG. Blood pressure and renal hemodynamic effects of angiotensin fragments. Hypertens Res. 2011 Jun;34(6):674-83. PMID: 21412242.

A5272 Angiotensin, dog/rat

5 mg
10 mg
25 mg

$C_{41}H_{62}N_{12}O_{11}$ FW: 899.03 ≥95%

H-Asp-Arg-Val-Tyr-Ile-His-Pro-Phe-His-Leu-OH

Derivative of AT I and precursor to AT II that displays vasoconstrictive activity.

Moon JY. Recent Update of Renin-angiotensin-aldosterone System in the Pathogenesis of Hypertension. Electrolyte Blood Press. 2013 Dec;11(2):41-45. PMID: 24627703.

Herichova I, Szantoova K. Renin-angiotensin system: upgrade of recent knowledge and perspectives. Endocr Regul. 2013 Jan;47(1):39-52. PMID: 23363256.

A5275 [Des-Asp1]-Angiotensin I, human

5 mg
10 mg
25 mg

$C_{58}H_{84}N_{16}O_{11}$ FW: 1181.42 ≥95%

H-Arg-Val-Tyr-Ile-His-Pro-Phe-His-Leu-OH

Derivative of endogenous cleavage product of angiotensin and precursor to angiotensin II. It serves no endogenous biological purpose.

Gonzalez-Villalobos RA, Shen XZ, Bernstein EA, et al. Rediscovering ACE: novel insights into the many roles of the angiotensin-converting enzyme. J Mol Med (Berl). 2013 Oct;91(10):1143-54. PMID: 23686164.

A5285 [Ile7]-Angiotensin III

1 mg
2 mg
5 mg

$C_{43}H_{68}N_{12}O_9$ FW: 897.1 ≥95%

H-Arg-Val-Tyr-Ile-His-Pro-Ile-OH

Derivative of endogenous derivative and cleavage product of AT II and AT1 receptor agonist. It is less active than AT II. It also increases aldosterone secretion and mean arterial pressure.

Yugandhar VG, Clark MA. Angiotensin III: a physiological relevant peptide of the renin angiotensin system. Peptides. 2013 Aug;46:26-32. PMID: 23692861.

A5282 [Sar1 Ile8]-Angiotensin II

5 mg
10 mg
25 mg

$C_{46}H_{74}N_{13}O_{10}$ FW: 968.1 [67724-27-0] ≥95%

H-Sar-Arg-Val-Tyr-Ile-His-Pro-Ile-OH

Endogenous peptide derivative involved in vasoconstriction, Na^+ reabsorption, and blood pressure. It activates AT1 receptors and Na^+/H^+ transporters. It increases intracellular Ca^{2+}, induces vasoconstriction, and raises blood pressure, volume, and pH.

De Giusti VC, Ciancio MC, Orlowski A, et al. Modulation of the cardiac sodium/bicarbonate cotransporter by the renin angiotensin aldosterone system: pathophysiological consequences. Front Physiol. 2014 Jan 17;4:411. PMID: 24478712.

A5283 [Sar1]-Angiotensin II

5 mg
10 mg
25 mg

$C_{49}H_{71}N_{13}O_{11}$ FW: 1018.19 ≥95%

H-Sar-Arg-Val-Tyr-Ile-His-Pro-Phe-OH

Endogenous peptide derivative involved in vasoconstriction, Na^+ reabsorption, and blood pressure. It activates AT1 receptors and Na^+/H^+ transporters. It increases intracellular Ca^{2+}, induces vasoconstriction, and raises blood pressure, volume, and pH.

De Giusti VC, Ciancio MC, Orlowski A, et al. Modulation of the cardiac sodium/bicarbonate cotransporter by the renin angiotensin aldosterone system: pathophysiological consequences. Front Physiol. 2014 Jan 17;4:411. PMID: 24478712.

Moon JY. Recent Update of Renin-angiotensin-aldosterone System in the Pathogenesis of Hypertension. Electrolyte Blood Press. 2013 Dec;11(2):41-45. PMID: 24627703.

A5284 [Val5]-Angiotensin II, human

5 mg
10 mg
25 mg

$C_{49}H_{69}N_{13}O_{12}$ FW: 1032.18 ≥95%

H-Asp-Arg-Val-Tyr-Val-His-Pro-Phe-OH

Endogenous peptide derivative involved in vasoconstriction, Na^+ reabsorption, and blood pressure. It activates AT1 receptors and Na^+/H^+ transporters. It increases intracellular Ca^{2+}, induces vasoconstriction, and raises blood pressure, volume, and pH.

De Giusti VC, Ciancio MC, Orlowski A, et al. Modulation of the cardiac sodium/bicarbonate cotransporter by the renin angiotensin aldosterone system: pathophysiological consequences. Front Physiol. 2014 Jan 17;4:411. PMID: 24478712.

Moon JY. Recent Update of Renin-angiotensin-aldosterone System in the Pathogenesis of Hypertension. Electrolyte Blood Press. 2013 Dec;11(2):41-45. PMID: 24627703.

A5287 Angiotensinogen (1-14), human

1 mg
2 mg
5 mg

$C_{83}H_{122}N_{24}O_{19}$ FW: 1760.05 ≥95%

H-Asp-Arg-Val-Tyr-Ile-His-Pro-Phe-His-Leu-Val-Ile-His-Asn-OH

Renin substrate and precursor to all angiotensin peptides. It is produced in the liver in response to estrogen, thyroid, or corticosteroid signaling.

Herichova I, Szantoova K. Renin-angiotensin system: upgrade of recent knowledge and perspectives. Endocr Regul. 2013 Jan;47(1):39-52. PMID: 23363256.

Kobori H, Urushihara M. Augmented intrarenal and urinary angiotensinogen in hypertension and chronic kidney disease. Pflugers Arch. 2013 Jan;465(1):3-12. PMID: 22918624.

A5326 Aniracetam

25 mg
100 mg
500 mg
1 g

Ro-13-5057

$C_{12}H_{13}NO_3$ FW: 219.24 [72432-10-1] ≥98%

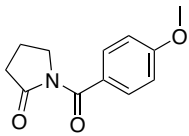

AMPA positive allosteric modulator and agonist at dopamine D2 receptors, 5-HT2A receptors, and nAChRs. It decreases anxiety-like behaviors and improves cognitive deficits associated with stroke and Alzheimer's disease.

Wang YF, Li CC, Cai JX. Aniracetam attenuates H_2O_2-induced deficiency of neuron viability, mitochondria potential and hippocampal long-term potentiation of mice in vitro. Neurosci Bull. 2006 Sep;22(5):274-80. PMID: 17690727.

Jin R, Clark S, Weeks AM, et al. Mechanism of positive allosteric modulators acting on AMPA receptors. J Neurosci. 2005 Sep 28;25(39):9027-36. PMID: 16192394.

Nakamura K. Aniracetam: its novel therapeutic potential in cerebral dysfunctional disorders based on recent pharmacological discoveries. CNS Drug Rev. 2002 Spring;8(1):70-89. PMID: 12070527.

A5334 Anisodamine

100 mg
500 mg
1 g
5 g

6-Hydroxy Hyoscyamine

$C_{17}H_{23}NO_4$ FW: 305.37 [55869-99-3] ≥98%

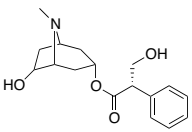

Inhibitor of α1-adrenergic receptors and mAChRs found in *Solanaceae* plants used to treat diabetic nephropathy, to induce atropinization in organophosphate poisoning subjects and to improve acute lung injury pathology.

Wang W, Chen QF, Li QB, et al. Efficiency of anisodamine for organophosphorus-poisoned patients when atropinization cannot be achieved with high doses of atropine. Environ Toxicol Pharmacol. 2014 Mar;37(2):477-81. PMID: 24561530.

Guoshou Z, Chengye Z, Zhihui L, et al. Effects of high dose of anisodamine on the respiratory function of patients with traumatic acute lung injury. Cell Biochem Biophys. 2013 Jun;66(2):365-9. PMID: 23504631.

Geng W, Fu XH, Gu XS, et al. Preventive effects of anisodamine against contrast-induced nephropathy in type 2 diabetics with renal insufficiency undergoing coronary angiography or angioplasty. Chin Med J (Engl). 2012 Oct;125(19):3368-72. PMID: 23044290.

A5373 Anisomycin

5 mg
25 mg
100 mg

Flagecidin

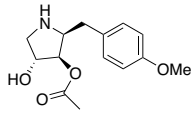

$C_{14}H_{19}NO_4$ FW: 265.31 [22862-76-6] ≥98%

Peptidyl transferase and protein translation inhibitor. It inhibits memory consolidation and reconsolidation, induces apoptosis in breast cancer cells, and suppresses proliferation of Jurkat T cells.

Monaghan D, O'Connell E, Cruickshank FL, et al. Inhibition of protein synthesis and JNK activation are not required for cell death induced by anisomycin and anisomycin analogues. Biochem Biophys Res Commun. 2014 Jan 10;443(2):761-7. PMID: 24333448.

Yu C, Xing F, Tang Z, et al. Anisomycin suppresses Jurkat T cell growth by the cell cycle-regulating proteins. Pharmacol Rep. 2013;65(2):435-44. PMID: 23744428.

You P, Xing F, Huo J, et al. In vitro and in vivo evaluation of anisomycin against Ehrlich ascites carcinoma. Oncol Rep. 2013 Jun;29(6):2227-36. PMID: 23525555.

A5353 Annexin V-FITC Apoptosis Detection Kit NEW

100 Tests

Apoptosis measuring kit.

A5458 Anorexigenic Peptide

1 mg
2 mg
5 mg

pGlu-His-Gly-OH

$C_{13}H_{17}N_5O_5$ FW: 323.4 [69275-10-1] ≥95%

Peptide that alters hormone secretion and decreases feeding behavior.

Blavet N, DeFeudis FV, Clostre F. Lack of effect of the peptide pyro-Glu-His-Gly-OH on food consumption in mice and rats. Gen Pharmacol. 1982;13(2):173-6. PMID: 6807743.

A5476 Antagonist G

0.5 mg
1 mg
2.5 mg

H-Arg-D-Trp-N-Me-Phe-D-Trp-Leu-Met-NH_2

$C_{49}H_{66}O_6N_{12}S$ FW: 951.2 [115150-59-9] ≥95%

Used to target and enhance the delivery of chemotherapeutics.

Moreira JN, Gaspar R. Antagonist G-mediated targeting and cytotoxicity of liposomal doxorubicin in NCI-H82 variant small cell lung cancer. Braz J Med Biol Res. 2004 Aug;37(8):1185-92. PMID: 15273819.

A5477 Antide Acetate

Please inquire

Ac-D-2-Nal-p-Chloro-D-Phe-£]-(3-pyridyl)-D-Ala-Ser-Lys (nicotinoyl)-D-Lys(nicotinoyl)-Leu-Lys (isopropyl)-Pro-D-Ala-NH_2

$C_{82}H_{108}ClN_{17}O_{14}$ FW: 1591.32 [112568-12-4] ≥95%

GnRH antagonist used to decrease LH levels. It decreases primordial follicle numbers and enhances spatial memory.

Attaman J, Arbogast LK, Friedman CI, et al. Effect of gonadotropin-releasing hormone antagonist on primordial follicle survival in the primate ovary. J Reprod Med. 2014 Mar-Apr;59(3-4):103-9. PMID: 24724216.

Ziegler SG, Thornton JE. Low luteinizing hormone enhances spatial memory and has protective effects on memory loss in rats. Horm Behav. 2010 Nov;58(5):705-13. PMID: 20691694.

A5479 Antiestrogen Peptide

0.5 mg
1 mg
2.5 mg

H-Cys-Asn-Val-Val-Pro-Leu-Tyr (PO_3H_2)-Asp-Leu-Leu-Leu-Glu-OH

$C_{64}H_{104}N_{13}O_{22}SP$ FW: 1470.64 ≥95%

Peptide that displays antiestrogenic activity.

A5378 Antimycin A

10 mg
50 mg

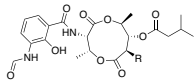

A1: R = C_6H_{13} A3: R = C_4H_9
A2: R = C_5H_{11} A4: R = C_3H_7

$C_{28}H_{40}N_2O_9$ FW: 548.63 [1397-94-0] ≥90%

Cytochrome C binding agent that inhibits electron transport chain activity, oxidative phosphorylation, and ATP synthesis.

Taddeo EP, Laker RC, Breen DS, et al. Opening of the mitochondrial permeability transition pore links mitochondrial dysfunction to insulin resistance in skeletal muscle. Mol Metab. 2013 Nov 26;3(2):124-34. PMID: 24634818.

Ma X, Jin M, Cai Y, et al. Mitochondrial electron transport chain complex III is required for antimycin A to inhibit autophagy. Chem Biol. 2011 Nov 23;18(11):1474-81. PMID: 22118681.

Quinlan CL, Gerencser AA, Treberg JR, et al. The mechanism of superoxide production by the antimycin-inhibited mitochondrial Q-cycle. J Biol Chem. 2011 Sep 9;286(36):31361-72. PMID: 21708945.

A5478 Antipain Dihydrochloride

1 mg
5 mg
25 mg

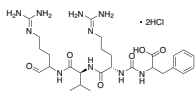

$C_{27}H_{44}N_{10}O_6 \cdot 2HCl$ FW: 677.62 [37691-11-5] ≥98%

Protease inhibitor found in *Actinomycetes*.

Anisuzzaman, Islam MK, Alim MA, et al. Longistatin is an unconventional serine protease and induces protective immunity against tick infestation. Mol Biochem Parasitol. 2012 Mar-Apr;182(1-2):45-53. PMID: 22206819.

He SH, Chen P, Chen HQ. Modulation of enzymatic activity of human mast cell tryptase and chymase by protease inhibitors. Acta Pharmacol Sin. 2003 Sep;24(9):923-9. PMID: 12956943.

Suda H, Aoyagi T, Hamada M, et al. Antipain, a new protease inhibitor isolated from *actinomycetes*. J Antibiot (Tokyo). 1972 Apr;25(4):263-6. PMID: 4559651.

A6002

Apamin

0.5 mg
1 mg
2.5 mg

H-Cys-Asn-Cys-Lys-Ala-Pro-Glu-Thr-Ala-Leu-Cys-Ala-Arg-Arg-Cys-Gln-Gln-His-Nh2 (Cys1-Cys11, Cys3-Cys15)

$C_{79}H_{131}N_{31}O_{24}S_4$ FW: 2027.37 [24345-16-2] ≥95%

Bee venom toxin and SK2/3/4 K^+ channel blocker. It prevents K^+ ion transport and lowers the threshold for action potential development. It also improves visiospatial learning deficits.

Dalaklioglu S, Ozbey G. Role of different types of potassium channels in the relaxation of corpus cavernosum induced by resveratrol. Pharmacogn Mag. 2014 Jan;10(37):47-52. PMID: 24696545.

Kallarackal AJ, Simard JM, Bailey AM. The effect of apamin, a small conductance calcium activated potassium (SK) channel blocker, on a mouse model of neurofibromatosis 1. Behav Brain Res. 2013 Jan 15;237:71-5. PMID: 22983217.

A6017

Apelin-13, human/cow

0.5 mg
1 mg
2.5 mg

H-Gln-Arg-Pro-Arg-Leu-Ser-His-Lys-Gly-Pro-Met-Pro-Phe-OH

$C_{69}H_{111}N_{23}O_{16}S$ FW: 1550.86 ≥95%

Apelin receptor agonist involved in vascular contraction, water homeostasis, and feeding behavior. It decreases brain edema, increases myocardial glucose uptake, and stimulates tube formation in myocardial microvascular endothelial cells.

Yang Y, Zhang X, Cui H, et al. Apelin-13 protects the brain against ischemia/reperfusion injury through activating PI3K/Akt and ERK1/2 signaling pathways. Neurosci Lett. 2014 Mar 29;568C:44-49. [Epub ahead of print]. PMID: 24686182.

Bo B, Lulu L, Ning Z, et al. Heterodimerization of human apelin and bradykinin 1 receptors: Novel signal transduction characteristics. Cell Signal. 2014 Mar 29. pii: S0898-6568(14)00124-7. [Epub ahead of print]. PMID: 24686079.

A6229

Aphidicolin

1 mg
5 mg
10 mg

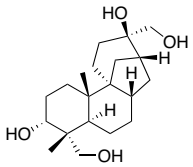

ICI-69653; NSC-234714

$C_{20}H_{34}O_4$ FW: 338.48 [38966-21-1] ≥98%

Eukaryotic and viral DNA polymerase inhibitor that induces S phase cell cycle arrest. It also inhibits vaccinia virus growth.

Willis J, DeStephanis D, Patel Y, et al. Study of the DNA damage checkpoint using Xenopus egg extracts. J Vis Exp. 2012 Nov 5;(69):e4449. PMID: 23149695.

Zhao YM, Li JY, Lan JP, et al. Cell cycle dependent telomere regulation by telomerase in human bone marrow mesenchymal stem cells. Biochem Biophys Res Commun. 2008 May 16;369(4):1114-9. PMID: 8339310.

DeFilippes FM. Effect of aphidicolin on vaccinia virus: isolation of an aphidicolin-resistant mutant. J Virol. 1984 Nov;52(2):474-82. PMID: 6436508.

A6132

Apicidin

1 mg
5 mg

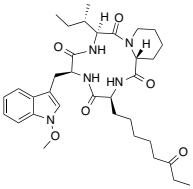

$C_{34}H_{49}N_5O_6$ FW: 623.78 [183506-66-3] ≥98%

HDAC inhibitor. It induces cell cycle arrest, apoptosis, and autophagy in oral squamous cell carcinoma cells and induces apoptosis in eosinophils and neutrophils.

Ahn MY, Ahn SG, Yoon JH. Apicidin, a histone deaceylase inhibitor, induces both apoptosis and autophagy in human oral squamous carcinoma cells. Oral Oncol. 2011 Nov;47(11):1032-8. PMID: 21856210.

Brazelle W, Kreahling JM, Gemmer J, et al. Histone deacetylase inhibitors downregulate checkpoint kinase 1 expression to induce cell death in non-small cell lung cancer cells. PLoS One. 2010 Dec 14;5(12):e14335. PMID: 21179472.

Kankaanranta H, Janka-Junttila M, Ilmarinen-Salo P, et al. Histone deacetylase inhibitors induce apoptosis in human eosinophils and neutrophils. J Inflamm (Lond). 2010 Feb 4;7:9. PMID: 20181093.

A6234

Apigenin

5 mg
25 mg
100 mg

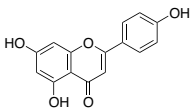

Spigenin; Versulin

$C_{15}H_{10}O_5$ FW: 270.24 [520-36-5] ≥98%

GABA-A receptor positive modulator and potential microtubule depolymerization inducer found in various plant sources. It displays a wide variety of biological activities, including inducing apoptosis in gastric cancer cells, inhibiting vascular contraction in aortic rings, reversing spinal cord injury-induced oxidative damage, and ameliorating amyloid-β-induced deficits in learning and cognition.

Chen J, Chen J, Li Z, et al. The apoptotic effect of apigenin on human gastric carcinoma cells through mitochondrial signal pathway. Tumour Biol. 2014 May 8. [Epub ahead of print]. PMID: 24805829.

Zhang F, Li F, Chen G. Neuroprotective effect of apigenin in rats after contusive spinal cord injury. Neurol Sci. 2014 Apr;35(4):583-8. PMID: 24166720.

Je HD, Kim HD, La HO. The Inhibitory Effect of Apigenin on the Agonist-Induced Regulation of Vascular Contractility via Calcium Desensitization-Related Pathways. Biomol Ther (Seoul). 2014 Feb;22(2):100-5. PMID: 24753814.

A6058 — Apoptosis Activator 2

NEW

5 mg
10 mg
50 mg

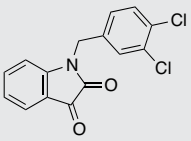

AA-2

$C_{15}H_9Cl_2NO_2$ FW: 306.14 [79183-19-0] ≥98%

It induces apoptosis and cell death in gastric adenocarcinoma cells and neurons.

Kim JH, Lee J. Induced neural stem cells protect neuronal cells against apoptosis. Med Sci Monit. 2014 Dec 22;20:2759-66. PMID: 25554259.

Farivar TN, Najafipour R, Johari P. Nano - drug Delivery of Apoptosis Activator 2 to AGS Cells by Liposomes Conjugated with Anti-TROP2 Antibody. N Am J Med Sci. 2012 Nov;4(11):582-5. PMID: 23181231.

Nguyen TV, Jayaraman A, Quaglino A, et al. Androgens selectively protect against apoptosis in hippocampal neurones. J Neuroendocrinol. 2010 Sep;22(9):1013-22. PMID: 20561156.

A6264 — Apramycin Sulfate

1 g
5 g

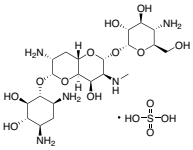

Nebramycin factor 2; EL-857

$C_{21}H_{41}N_5O_{11} \cdot H_2O_4S$ FW: 637.66 [65710-07-8] ≥98%

Protein translation inhibitor used to treat bacterial infections. It induces conformational changes in CA and GA base pairs and inhibits RNA translocation.

Witek MA, Conn GL. Expansion of the aminoglycoside-resistance 16S rRNA (m1A1408) methyltransferase family: Expression and functional characterization of four hypothetical enzymes of diverse bacterial origin. Biochim Biophys Acta. 2014 Jun 22. [Epub ahead of print]. PMID: 24963996.

Choi MJ, Lim SK, Nam HM, et al. Apramycin and gentamicin resistances in indicator and clinical *Escherichia* coli isolates from farm animals in Korea. Foodborne Pathog Dis. 2011 Jan;8(1):119-23. PMID: 21214385.

A6269 — Apremilast

NEW

5 mg
25 mg

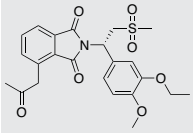

$C_{23}H_{25}NO_7S$ FW: 459.51 [608141-41-9] ≥98%

PDE4 inhibitor used to treat psoriasis and psoriatic arthritis. It also decreases levels of iNOS, IL-23, and TNF-α.

Schafer PH, Parton A, Capone L, et al. Apremilast is a selective PDE4 inhibitor with regulatory effects on innate immunity. Cell Signal. 2014 Sep;26(9):2016-29. PMID: 24882690.

Schafer P. Apremilast mechanism of action and application to psoriasis and psoriatic arthritis. Biochem Pharmacol. 2012 Jun 15;83(12):1583-90. PMID: 22257911.

A6368 — Aprepitant

5 mg
10 mg
25 mg

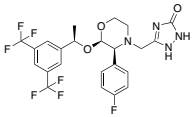

$C_{23}H_{21}F_7N_4O_3$ FW: 534.43 [170729-80-3] ≥98%

NK1 receptor antagonist used to treat nausea. It inhibits binding of substance P and prevents substance P's proliferative and pro-angiogenic signaling cascade. It also may decrease depression-like behaviors.

Muñoz M, Martinez-Armesto J, Coveñas R. NK-1 receptor antagonists as antitumor drugs: a survey of the literature from 2000 to 2011. Expert Opin Ther Pat. 2012 Jul;22(7):735-46. PMID: 22697287.

Massaro AM, Lenz KL. Aprepitant: a novel antiemetic for chemotherapy-induced nausea and vomiting. Ann Pharmacother. 2005 Jan;39(1):77-85. PMID: 15562136.

A6268 — Aprotinin

10 mg
50 mg

Pancreatic trypsin inhibitor; Trazinin

$C_{284}H_{432}N_{84}O_{79}S_7$ FW: 6511.44 [9087-70-1] ≥98%

Serine protease inhibitor that prevents formation of Factor XIIa and prevents breakdown of blood clots.

Shiga T, Wajima Z, Inoue T, et al. Aprotinin in major orthopedic surgery: a systematic review of randomized controlled trials. Anesth Analg. 2005 Dec;101(6):1602-7. PMID: 16301226.

Mahdy AM, Webster NR. Perioperative systemic haemostatic agents. Br J Anaesth. 2004 Dec;93(6):842-58. PMID: 15277296.

A6800 — AR-A014418

NEW

5 mg
10 mg
25 mg

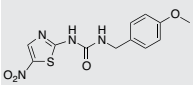

GSK-3β Inhibitor VIII

$C_{12}H_{12}N_4O_4S$ FW: 308.31 [487021-52-3] ≥98%

GSK-3β inhibitor. It decreases viability of glioma cells, inhibits thermal and mechanical pain signaling, and decreases inflammation in spinal cord injury models.

Yadav AK, Vashishta V, Joshi N, et al. AR-A 014418 Used against GSK3beta Downregulates Expression of hnRNPA1 and SF2/ASF Splicing Factors. J Oncol. 2014;2014:695325. PMID: 24550987.

Weng HR, Gao M, Maixner DW. Glycogen synthase kinase 3 beta regulates glial glutamate transporter protein expression in the spinal dorsal horn in rats with neuropathic pain. Exp Neurol. 2014 Feb;252:18-27. PMID: 24275526.

King MR, Anderson NJ, Guernsey LS, et al. Glycogen synthase kinase-3 inhibition prevents learning deficits in diabetic mice. J Neurosci Res. 2013 Apr;91(4):506-14. PMID: 23362012.

A6804 Arbutin

5 g
10 g
25 g

Hydroquinone glucose

$C_{12}H_{16}O_7$ FW: 272.25 [497-76-7] ≥98%

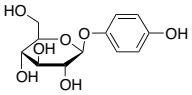

PLA2 and tyrosinase inhibitor found in *Bergenia* and *Arctostaphylos* used in skin whitening products. It decreases melanin production.

Inoue Y, Hasegawa S, Yamada T, et al. Analysis of the effects of hydroquinone and arbutin on the differentiation of melanocytes. Biol Pharm Bull. 2013;36(11):1722-30. PMID: 24189417.

Lim YJ, Lee EH, Kang TH, et al. Inhibitory effects of arbutin on melanin biosynthesis of alpha-melanocyte stimulating hormone-induced hyperpigmentation in cultured brownish guinea pig skin tissues. Arch Pharm Res. 2009 Mar;32(3):367-73. PMID: 19387580.

A6818 Arenobufagin

NEW

1 mg
5 mg
25 mg

$C_{24}H_{32}O_6$ FW: 416.51 [464-74-4] ≥98%

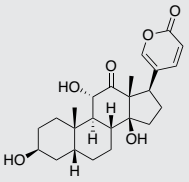

Inhibitor of VEGFR2 and cardiovascular Na^+/K^+ ATPase found in *Bufo arenarum*. It induces autophagy and apoptosis in hepatocellular carcinoma cells and suppresses angiogenesis.

Zhang DM, Liu JS, Deng LJ, et al. Arenobufagin, a natural bufadienolide from toad venom, induces apoptosis and autophagy in human hepatocellular carcinoma cells through inhibition of PI3K/Akt/mTOR pathway. Carcinogenesis. 2013 Jun;34(6):1331-42. PMID: 23393227.

Li M, Wu S, Liu Z, et al. Arenobufagin, a bufadienolide compound from toad venom, inhibits VEGF-mediated angiogenesis through suppression of VEGFR-2 signaling pathway. Biochem Pharmacol. 2012 May 1;83(9):1251-60. PMID: 22305746.

A6922 Arformoterol Tartrate

5 mg
10 mg
25 mg

$C_{19}H_{24}N_2O_4 \bullet C_4H_6O_6$ FW: 494.19 [200815-49-2] ≥98%

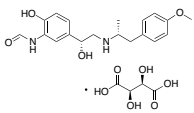

R,R enantiomer of formoterol and agonist at β2-adrenergic receptors and TAS2Rs used to treat COPD. It induces airway relaxation, inhibits migration of human airway smooth muscle cells, and suppresses phosphorylation of JNK, p38 MAPK, and the glucocorticoid receptor.

Grassin-Delyle S, Abrial C, Fayad-Kobeissi S, et al. The expression and relaxant effect of bitter taste receptors in human bronchi. Respir Res. 2013 Nov 22;14:134. PMID: 24266887.

Goncharova EA, Goncharov DA, Zhao H, et al. β2-adrenergic receptor agonists modulate human airway smooth muscle cell migration via vasodilator-stimulated phosphoprotein. Am J Respir Cell Mol Biol. 2012 Jan;46(1):48-54. PMID: 22210825.

Mercado N, To Y, Kobayashi Y, et al. p38 mitogen-activated protein kinase-γ inhibition by long-acting β2 adrenergic agonists reversed steroid insensitivity in severe asthma. Mol Pharmacol. 2011 Dec;80(6):1128-35. PMID: 21917909.

A6823 Argatroban

10 mg
25 mg
100 mg

$C_{23}H_{36}N_6O_5S$ FW: 508.64 [74863-84-6] ≥98%

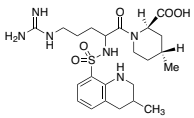

Thrombin inhibitor used to treat thrombosis and acute coronary syndrome.

Tardy-Poncet B, Combe M, Piot M, et al. Effects of argatroban, danaparoid, and fondaparinux on trombin generation in heparin-induced thrombocytopenia. Thromb Haemost. 2013 Mar;109(3):504-9. PMID: 23328916.

Cruz-González I, López-Jiménez R, Perez-Rivera A, et al. Pharmacokinetic evaluation of argatroban for the treatment of acute coronary syndrome. Expert Opin Drug Metab Toxicol. 2012 Nov;8(11):1483-93. PMID: 22970706.

A6825 L-Arginine

25 g
100 g
500 g

$C_6H_{14}N_4O_2$ FW: 174.2 [74-79-3] ≥98%

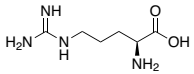

Endogenous amino acid also found in meat, dairy, grains, and legumes. It increases collagen deposition, decreases systolic and diastolic blood pressure, and improves cardiovascular and endothelial function.

Dong JY, Qin LQ, Zhang Z, et al. Effect of oral L-arginine supplementation on blood pressure: a meta-analysis of randomized, double-blind, placebo-controlled trials. Am Heart J. 2011 Dec;162(6):959-65. PMID: 22137067.

Stechmiller JK, Childress B, Cowan L. Arginine supplementation and wound healing. Nutr Clin Pract. 2005 Feb;20(1):52-61. PMID: 16207646.

A6925 L-Arginine Ethyl Ester Dihydrochloride

NEW

5 g
25 g

$C_8H_{18}N_4O_2 \bullet 2HCl$ FW: 275.18 [36589-29-4] ≥98%

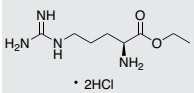

Arginine source used to study intracellular arginine signaling. It may increase production of NO and induce vasodilation.

Shin S, Mohan S, Fung HL. Intracellular L-arginine concentration does not determine NO production in endothelial cells: implications on the "L-arginine paradox". Biochem Biophys Res Commun. 2011 Nov 4;414(4):660-3. PMID: 21986532.

Knecht KR, Milam S, Wilkinson DA, et al. Time-dependent action of carbon monoxide on the newborn cerebrovascular circulation. Am J Physiol Heart Circ Physiol. 2010 Jul;299(1):H70-5. PMID: 20435844.

A6826 L-Arginine Hydrochloride

25 g
100 g
500 g

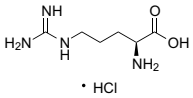

$C_6H_{14}N_4O_2 \cdot HCl$ FW: 210.66 [1119-34-2] ≥98%

Endogenous amino acid also found in meat, dairy, grains, and legumes. It increases collagen deposition, decreases systolic and diastolic blood pressure, and improves cardiovascular and endothelial function.

Dong JY, Qin LQ, Zhang Z, et al. Effect of oral L-arginine supplementation on blood pressure: a meta-analysis of randomized, double-blind, placebo-controlled trials. Am Heart J. 2011 Dec;162(6):959-65. PMID: 22137067.

Stechmiller JK, Childress B, Cowan L. Arginine supplementation and wound healing. Nutr Clin Pract. 2005 Feb;20(1):52-61. PMID: 16207646.

A6828 N(α),N(α)-Dimethyl-L-Arginine Ammonium

10 mg
25 mg
100 mg

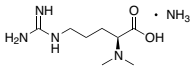

$C_8H_{18}N_4O_2 \cdot NH_3$ FW: 219.28 ≥98%

Endogenous amino acid derivative and NOS inhibitor that regulates water/Na^+ homeostasis. It aggravates gastric mucosal lesions and is associated with the development of cardiovascular diseases.

Mauricio MD, Aldasoro M, Ortega J, et al. Endothelial dysfunction in morbid obesity. Curr Pharm Des. 2013;19(32):5718-29. PMID: 23448493.

Szlachcic A, Krzysiek-Maczka G, Pajdo R, et al. The impact of asymmetric dimethylarginine (ADAMA), the endogenous nitric oxide (NO) synthase inhibitor, to the pathogenesis of gastric mucosal damage. Curr Pharm Des. 2013;19(1):90-7. PMID: 22950506.

A6829 NG,N'G-Dimethyl-L-Arginine Ammonium

10 mg
25 mg
100 mg

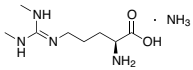

$C_8H_{18}N_4O_2 \cdot NH_3$ FW: 219.28 ≥98%

Amino acid derivative that competes with L-Arg for cellular uptake but does not inhibit NOS.

Surdacki A. L-arginine analogs--inactive markers or active agents in atherogenesis? Cardiovasc Hematol Agents Med Chem. 2008 Oct;6(4):302-11. PMID: 18855643.

Azuma H, Masuda H, Sato J, et al. A possible role of endogenous inhibitor for nitric oxide synthesis in the bovine ciliary muscle. Exp Eye Res. 1997 May;64(5):823-30. PMID: 9245913.

A6827 Argipressin Acetate

Please inquire

C[Cys-Tyr-Phe-Gln-Asn-Cys]Pro-Arg-Gly-NH_2

$C_{46}H_{65}N_{13}O_{12}S_2$ FW: 1084.23 [113-79-1] ≥95%

Endogenous vasopressin 1/2 receptor agonist involved in vascular contractility and water/Na^+ homeostasis. It increases blood pressure, vasoconstriction, and smooth muscle contraction.

Cao T, Feng Y. The (pro)renin receptor and body fluid homeostasis. Am J Physiol Regul Integr Comp Physiol. 2013 Jul 15;305(2):R104-6. PMID: 23678024.

Palazzuoli A, Ronco C. Cardio-renal syndrome: an entity cardiologists and nephrologists should be dealing with collegially. Heart Fail Rev. 2011 Nov;16(6):503-8. PMID: 21822604.

A7034 Aripiprazole

100 mg
250 mg
1 g

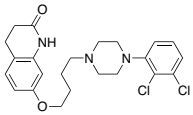

$C_{23}H_{27}Cl_2N_3O_2$ FW: 448.39 [129722-12-9] ≥98%

Partial agonist at dopamine D2 receptors and 5-HT1A receptors and inhibitor of SET and 5-HT2C/6/7 receptors used to treat schizophrenia and other mood disorders. It also potentiates NGF-induced neurite outgrowth and protects against H_2O_2-induced oxidative damage.

Lee JS, Lee JD, Park HJ, et al. Is the GABA System Related to the Social Competence Improvement Effect of Aripiprazole? An (18)F-Fluoroflumazenil PET Study. Psychiatry Investig. 2013 Mar;10(1):75-80. PMID: 23482902.

Miljević Č, Nikolić-Kokić A, Nikolić M, et al. Effect of atypical antipsychotics on antioxidant enzyme activities in human erythrocytes (in vitro study). Hum Psychopharmacol. 2013 Jan;28(1):1-6. PMID: 23124725.

Ishima T, Iyo M, Hashimoto K. Neurite outgrowth mediated by the heat shock protein Hsp90α: a novel target for the antipsychotic drug aripiprazole. Transl Psychiatry. 2012 Oct 16;2:e170. PMID: 23047241.

A6932 Aristolochic Acid A

1 mg
5 mg
10 mg

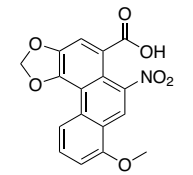

$C_{17}H_{11}NO_7$ FW: 341.27 [313-67-7] ≥95%

Carcinogen found in *Aristolochia* and *Radix*. It inhibits PLA2 and decreases GABA-induced release of arachidonic acid and phosphatidylcholine.

Chen WY, Ni Y, Pan YM, et al. GABA, progesterone and zona pellucida activation of PLA2 and regulation by MEK-ERK1/2 during acrosomal exocytosis in guinea pig spermatozoa. FEBS Lett. 2005 Aug 29;579(21):4692-700. PMID: 16098515.

Stiborová M, Frei E, Sopko B, et al. Human cytosolic enzymes involved in the metabolic activation of carcinogenic aristolochic acid: evidence for reductive activation by human NAD(P)H:quinone oxidoreductase. Carcinogenesis. 2003 Oct;24(10):1695-703. PMID: 12869422.

A6933 Aristolochic Acid B

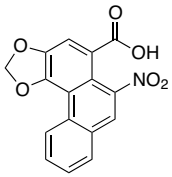

IIBRN 0329754; CCRIS 6497

$C_{16}H_9NO_6$ FW: 311.25 [475-80-9] ≥95%

1 mg
5 mg
10 mg

Carcinogen found in *Aristolochia* and *Radix*. It may inhibit PLA2.

Liu Y, Han S, Feng Q, et al. Determination of aristolochic acids A and B in Chinese herbals and traditional Chinese patent medicines using ultra high performance liquid chromatography-triple quadrupole mass spectrometry. Se Pu. 2011 Nov;29(11):1076-81. PMID: 22393694.

Stiborová M, Frei E, Sopko B, et al. Human cytosolic enzymes involved in the metabolic activation of carcinogenic aristolochic acid: evidence for reductive activation by human NAD(P)H:quinone oxidoreductase. Carcinogenesis. 2003 Oct;24(10):1695-703. PMID: 12869422.

A6934 Aristolochic Acid C

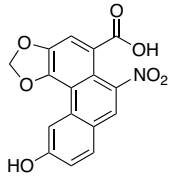

$C_{16}H_9NO_7$ FW: 327.25 [4849-90-5] ≥94%

1 mg
5 mg
10 mg

Carcinogen found in *Aristolochia* and *Radix*. It may inhibit PLA2.

Stiborová M, Frei E, Sopko B, et al. Human cytosolic enzymes involved in the metabolic activation of carcinogenic aristolochic acid: evidence for reductive activation by human NAD(P)H:quinone oxidoreductase. Carcinogenesis. 2003 Oct;24(10):1695-703. PMID: 12869422.

Wu TS, Ou LF, Teng CM. Aristolochic acids, aristolactam alkaloids and amides from *Aristolochia* kankauensis. Phytochemistry. 1994 Jul;36(4):1063-8. PMID: 7765207.

A6971 ARRY-162

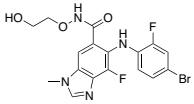

MEK162

$C_{17}H_{15}BrF_2N_4O_3$ FW: 441.23 [606143-89-9] ≥99%

5 mg
25 mg
100 mg

MEK1/2 and ERK inhibitor. It decreases proliferation of various cancer cells and suppresses downstream signaling of IL-1, IL-6, and TNF.

www.clinicaltrials.gov/show/NCT00959127

A6970 Artemether

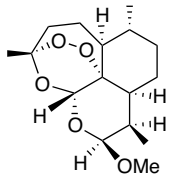

Dihydroartemisinin methyl ether; Dihydroqinghaosu methyl ether

$C_{16}H_{26}O_5$ FW: 298.37 [71963-77-4] ≥98%

50 mg
100 mg
500 mg
1 g

Derived from *Artemisia*. It inhibits growth of parasites such as *Plasmodium*, *Leishmania*, and *Schistosoma*.

Angus B. Novel anti-malarial combinations and their toxicity. Expert Rev Clin Pharmacol. 2014 May;7(3):299-316. PMID: 24716844.

Wang W, Li TY, Ji Y, et al. Efficacy of artemether and artesunate in mice infected with praziquantel non-susceptible isolate of *Schistosoma* japonicum. Parasitol Res. 2014 Mar;113(3):925-31. PMID: 24326467.

Ebrahimisadr P, Ghaffarifar F, Mohammad Hassan Z. In-vitro Evaluation of Antileishmanial Activity and Toxicity of Artemether with Focus on its Apoptotic Effect. Iran J Pharm Res. 2013 Fall;12(4):903-9. PMID: 24523770.

A6978 Artemisinin

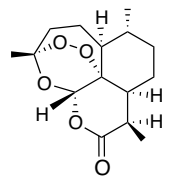

Arteannuin; Quinghaosu; QHS

$C_{15}H_{22}O_5$ FW: 282.35 [63968-64-9] ≥98%

100 mg
500 mg
1 g

Plasmodium growth inhibitor found in *Artemisia* (wormwood) used to treat malaria. It also decreases ventricular fibrillation threshold in animal models of myocardial infarction and inhibits growth of neuroblastoma cells, possibly through indirect activation of AMPK.

Gu Y, Wu G, Wang X, et al. Artemisinin prevents electric remodeling following myocardial infarction possibly by upregulating the expression of connexin 43. Mol Med Rep. 2014 Oct;10(4):1851-6. PMID: 25110145.

Tan WQ, Chen G, Jia B, et al. Artemisinin inhibits neuroblastoma proliferation through activation of AHP-activated protein kinase (AMPK) signaling. Pharmazie. 2014 Jun;69(6):468-72. PMID: 24974584.

Patel K, Batty KT, Moore BR, et al. Predicting the parasite killing effect of artemisinin combination therapy in a murine malaria model. J Antimicrob Chemother. 2014 Aug;69(8):2155-63. PMID: 24777899.

A6979 Dihydroartemisinin

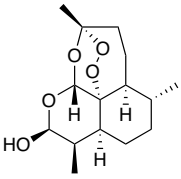

Dihydroqinghaosu

$C_{15}H_{24}O_5$ FW: 284.35 [71939-50-9] ≥96%

50 mg
100 mg
500 mg
1 g

mTORC1 inhibitor derived from *Artemisia*. It induces apoptosis in colorectal caner cells, inhibits growth of *Plasmodium*, *Schistosoma*, and cytomegalovirus, and decreases levels of inflammatory cells, Th2 cytokines, IgE, and mucus secretion in asthma models.

Ontikatze T, Rudner J, Handrick R, et al. Dihydroartemisinin is a Hypoxia-Active Anti-Cancer Drug in Colorectal Carcinoma Cells. Front Oncol. 2014 May 19;4:116. PMID: 24904829.

Wanzira H, Kakuru A, Arinaitwe E, et al. Longitudinal Outcomes in a Cohort of Ugandan Children Randomized to Artemether-lumefantrine Versus Dihydroartemisinin-piperaquine for the Treatment of Malaria. Clin Infect Dis. 2014 May 13. [Epub ahead of print]. PMID: 24825870.

A6982

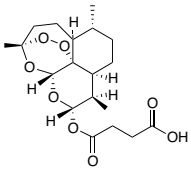

Artesunate

Dihydroqinghaosu hemisuccinate; Qinghaozhi

$C_{19}H_{28}O_8$ FW: 384.42 [88495-63-0] ≥98%

50 mg
100 mg
500 mg
1 g

Malaria treatment derived from *Artemisia*. It also induces cell cycle arrest in breast cancer cells, inhibits replication of Polyoma virus, and inhibits neovascularization and inflammation in corneas.

Zhang LX, Liu ZN, Ye J, et al. Artesunate exerts an anti-immunosuppressive effect on cervical cancer by inhibiting PGE2 production and Foxp3 expression. Cell Biol Int. 2014 May;38(5):639-46. PMID: 24446394.

Dong HY, Wang ZF. Antitumor effects of artesunate on human breast carcinoma MCF-7 cells and IGF-IR expression in nude mice xenografts. Chin J Cancer Res. 2014 Apr;26(2):200-7. PMID: 24826061.

A7085

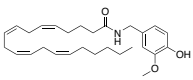

Arvanil

$C_{28}H_{41}NO_3$ FW: 439.63 [128007-31-8] ≥98%

5 mg

CB1 and TRPV1 agonist. It decreases immobility time in the forced swim test and tail suspension test, increases lung tidal volume, diaphragm activity, and mean arterial blood pressure, and inhibits lymphocyte proliferation.

Hayase T. Differential effects of TRPV1 receptor ligands against nicotine-induced depression-like behaviors. BMC Pharmacol. 2011 Jul 18;11:6. PMID: 21767384.

Kopczyńska B. Midcervical vagotomy precludes respiratory response to novel anti-inflammatory and anti-tumour drug arvanil in rats. Eur J Pharmacol. 2010 Sep 15;643(1):101-6. PMID: 20599930.

A7200

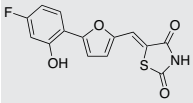

AS-252424

NEW

$C_{14}H_8FNO_4S$ FW: 305.28 [900515-16-4] ≥98%

1 mg
5 mg
10 mg

Inhibitor of p110γ PI3K and potential TRPC1/5/6 receptor negative modulator and TRPC3/7 receptor positive modulator. It decreases leukocyte recruitment and suppresses endothelin A receptor-mediated activity in vascular smooth muscle cells.

Shi J, Ju M, Large WA, et al. Pharmacological profile of phosphatidylinositol 3-kinases and related phosphatidylinositols mediating endothelin(A) receptor-operated native TRPC channels in rabbit coronary artery myocytes. Br J Pharmacol. 2012 Aug;166(7):2161-75. PMID: 22404177.

A7202

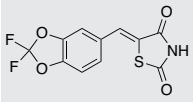

AS-604850

NEW

$C_{11}H_5F_2NO_4S$ FW: 285.22 [48449-76-7] ≥98%

1 mg
5 mg
10 mg

Inhibitor of p110γ PI3K. It decreases infiltration of leukocytes into the CNS in EAE models and suppresses chemotactic responses of eosinophils to platelet activating factor.

Li H, Park D, Abdul-Muneer PM, et al. PI3Kγ inhibition alleviates symptoms and increases axon number in experimental autoimmune encephalomyelitis mice. Neuroscience. 2013 Dec 3;253:89-99. PMID: 24012746.

Hasan AM, Mourtada-Maarabouni M, Hameed MS, et al. Phosphoinositide 3-kinase gamma mediates chemotactic responses of human eosinophils to platelet-activating factor. Int Immunopharmacol. 2010 Sep;10(9):1017-21. PMID: 20685403.

A7204

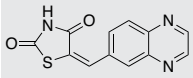

AS-605240

NEW

$C_{12}H_7N_3O_2S$ FW: 257.27 [648450-29-7] ≥98%

1 mg
5 mg
10 mg

Inhibitor of p110δ PI3K. It inhibits the development of EAE, decreases infiltration of dendritic cells in lung injury models, and suppresses expression of TLR4.

Comerford I, Litchfield W, Kara E, et al. PI3Kγ drives priming and survival of autoreactive CD4(+) T cells during experimental autoimmune encephalomyelitis. PLoS One. 2012;7(9):e45095. PMID: 23028778.

Azzi J, Moore RF, Elyaman W, et al. The novel therapeutic effect of phosphoinositide 3-kinase-γ inhibitor AS605240 in autoimmune diabetes. Diabetes. 2012 Jun;61(6):1509-18. PMID: 22403300.

Kim DI, Kim SR, Kim HJ, et al. PI3K-γ inhibition ameliorates acute lung injury through regulation of IκBα/NF-κB pathway and innate immune responses. J Clin Immunol. 2012 Apr;32(2):340-51. PMID: 22198681.

A7203

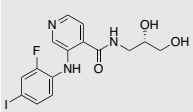

AS-703026

NEW

MSC1936369B

$C_{15}H_{15}FIN_3O_3$ FW: 431.2 [1236699-92-5] ≥98%

5 mg
25 mg

MEK1/2 inhibitor. It inhibits proliferation of melanoma cells and colorectal cancer cells and induces apoptosis in myeloma cells.

Park SJ, Hong SW, Moon JH, et al. The MEK1/2 inhibitor AS703026 circumvents resistance to the BRAF inhibitor PLX4032 in human malignant melanoma cells. Am J Med Sci. 2013 Dec;346(6):494-8. PMID: 24051957.

Yoon J, Koo KH, Choi KY. MEK1/2 inhibitors AS703026 and AZD6244 may be potential therapies for KRAS mutated colorectal cancer that is resistant to EGFR monoclonal antibody therapy. Cancer Res. 2011 Jan 15;71(2):445-53. PMID: 21118963.

A7208

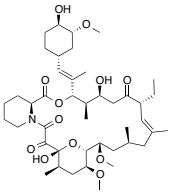

Ascomycin

1 mg
5 mg
25 mg
100 mg

$C_{43}H_{69}NO_{12}$ FW: 792.01 [104987-12-4] ≥98%

FK506 analog and calcineurin inhibitor used to treat organ transplant rejection and inflammatory skin diseases.

Liu F, Wang YQ, Meng L, et al. FK506-binding protein 12 ligands: a patent review. Expert Opin Ther Pat. 2013 Nov;23(11):1435-49. PMID: 23957229.

Sierra-Paredes G, Sierra-Marcuño G. Ascomycin and FK506: pharmacology and therapeutic potential as anticonvulsants and neuroprotectants. CNS Neurosci Ther. 2008 Spring;14(1):36-46. PMID: 18482098.

A7210

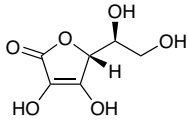

L-(+)-Ascorbic Acid

100 g
500 g

Vitamin C

$C_6H_8O_6$ FW: 176.12 [50-81-7] ≥98%

Vitamin C derivative found in various plant and food sources. It acts as a cofactor for prolyl hydroxylase and displays antioxidative activity.

Amaya I, Osorio S, Martinez-Ferri E, et al. Increased antioxidant capacity in tomato by ectopic expression of the strawberry D-galacturonate reductase gene. Biotechnol J. 2014 Aug 21. [Epub ahead of print]. PMID: 25143316.

Kotchey GP, Gaugler JA, Kapralov AA, et al. Effect of antioxidants on enzyme-catalysed biodegradation of carbon nanotubes. J Mater Chem B Mater Biol Med. 2013;1(3):302-309. PMID: 23626907.

Crescini E, Gualandi L, Uberti D, et al. Ascorbic acid rescues cardiomyocyte development in Fgfr1(-/-) murine embryonic stem cells. Biochim Biophys Acta. 2013 Jan;1833(1):140-7. PMID: 22735182.

A7309

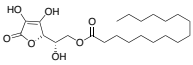

Ascorbyl Palmitate

25 g
100 g
500 g

Vitamin C palmitate; 6-Palmitoylascorbic acid

$C_{22}H_{38}O_7$ FW: 414.53 [137-66-6] ≥95%

Fat-soluble vitamin C derivative used as a dietary supplement and antioxidant. It decreases free radical formation in pig skin.

Zariwala MG, Farnaud S, Merchant Z, et al. Ascorbyl palmitate/DSPE-PEG nanocarriers for oral iron delivery: preparation, characterisation and in vitro evaluation. Colloids Surf B Biointerfaces. 2014 Mar 1;115:86-92. PMID: 24333557.

Let MB, Jacobsen C, Meyer AS. Ascorbyl palmitate, gamma-tocopherol, and EDTA affect lipid oxidation in fish oil enriched salad dressing differently. J Agric Food Chem. 2007 Mar 21;55(6):2369-75. PMID: 17319681.

Llabot JM, Palma SD, Manzo RH, et al. Design of novel antifungal mucoadhesive films. Part II. Formulation and in vitro biopharmaceutical evaluation. Int J Pharm. 2007 May 24;336(2):263-8. PMID: 17223291.

A7332

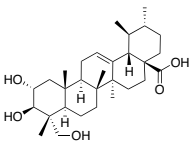

Asiatic Acid

100 mg
500 mg

NSC 166063

$C_{30}H_{48}O_5$ FW: 488.7 [464-92-6] ≥95%

Found in *Centella*. It exhibits several biological activities, including inhibiting TGF-β1-induced and overload-induced cardiac hypertrophy, inhibiting L-NAME-induced hypertension, modulating differentiation in bone marrow stromal cells, and decreasing tubular injury and fibroblast activation in fibrosis models.

Si L, Xu J, Yi C, et al. Asiatic acid attenuates cardiac hypertrophy by blocking transforming growth factor-β1-mediated hypertrophic signaling in vitro and in vivo. Int J Mol Med. 2014 Aug;34(2):499-506. PMID: 24827470.

Yan SL, Yang HT, Lee YJ, et al. Asiatic acid ameliorates hepatic lipid accumulation and insulin resistance in mice consuming a high-fat diet. J Agric Food Chem. 2014 May 21;62(20):4625-31. PMID: 24779966.

Bunbupha S, Pakdeechote P, Kukongviriyapan U, et al. Asiatic Acid Reduces Blood Pressure by Enhancing Nitric Oxide Bioavailability with Modulation of eNOS and p47 phox Expression in l-NAME-induced Hypertensive Rats. Phytother Res. 2014 Apr 11. [Epub ahead of print]. PMID: 24723332.

A7333

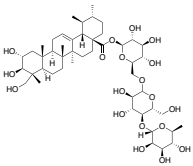

Asiaticoside

1 mg
5 mg
10 mg

$C_{48}H_{78}O_{19}$ FW: 959.12 [16830-15-2] ≥90%

Melanogenesis prevention (skin whitening) agent found in *Centella*. It decreases DNA binding by MITF. It also induces apoptosis in breast cancer cells, improves memory and learning deficits, decreases release of pro-inflammatory cytokines, and suppresses LPS-induced inflammation and fever.

Kwon KJ, Bae S, Kim K, et al. Asiaticoside, a component of *Centella* asiatica, inhibits melanogenesis in B16F10 mouse melanoma. Mol Med Rep. 2014 Jul;10(1):503-7. PMID: 24756377.

Chen S, Yin ZJ, Jiang C, et al. Asiaticoside attenuates memory impairment induced by transient cerebral ischemia-reperfusion in mice through anti-inflammatory mechanism. Pharmacol Biochem Behav. 2014 Jul;122:7-15. PMID: 24631487.

Al-Saeedi FJ. Study of the cytotoxicity of asiaticoside on rats and tumour cells. BMC Cancer. 2014 Mar 25;14:220. PMID: 24667059.

A7400

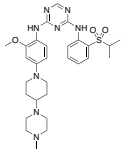

ASP3026

1 mg
5 mg
25 mg

$C_{29}H_{40}N_8O_3S$ FW: 580.74 [1097917-15-1] ≥99%

ALK inhibitor. It decreases tumor burden in lung and intrapleural tumor models.

www.clinicaltrials.gov/show/NCT01284192

www.clinicaltrials.gov/show/NCT014001504

A7460

Asparaginase

1 mg
5 mg
25 mg

$C_{1377}H_{2208}N_{382}O_{442}S_{17}$ FW: 31731.9 [9015-68-3] ≥98%

Catalyzes hydrolysis of asparagine to aspartate and ammonia. It treats leukemias by depleting asparagine levels and inhibiting cell growth. It also induces autophagy, decreases microvascular endothelial cell tube formation, and inhibits invasion of ovarian cancer cells.

He Y, Li B, Zhang H, et al. L-asparaginase induces in AML U937 cells apoptosis via an AIF-mediated mechanism. Front Biosci (Landmark Ed). 2014 Jan 1;19:515-27. PMID: 24389199.

Yu M, Henning R, Walker A, et al. L-asparaginase inhibits invasive and angiogenic activity and induces autophagy in ovarian cancer. J Cell Mol Med. 2012 Oct;16(10):2369-78. PMID: 22333033.

Nomme J, Su Y, Konrad M, et al. Structures of apo and product-bound human L-asparaginase: insights into the mechanism of autoproteolysis and substrate hydrolysis. Biochemistry. 2012 Aug 28;51(34):6816-26. PMID: 22861376.

A7462

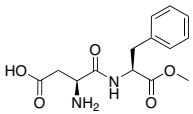

Aspartame

APM

1 g
5 g
25 g

$C_{14}H_{18}N_2O_5$ FW: 294.3 [22839-47-0] ≥98%

Artificial sweetener used in commercial food production. It inhibits growth of *Porphyromonas* and increasing latency times in pain assays.

Prashant GM, Patil RB, Nagaraj T, et al. The antimicrobial activity of the three commercially available intense sweeteners against common periodontal pathogens: an in vitro study. J Contemp Dent Pract. 2012 Nov 1;13(6):749-52. PMID: 23403996.

Rani S, Gupta MC. Evaluation and comparison of antinociceptive activity of aspartame with sucrose. Pharmacol Rep. 2012;64(2):293-8. PMID: 22661178.

Yagasaki M, Hashimoto S. Synthesis and application of dipeptides; current status and perspectives. Appl Microbiol Biotechnol. 2008 Nov;81(1):13-22. PMID: 18795289.

A7461

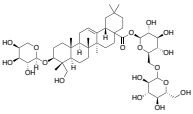

Asperosaponin VI

Akebia Saponin D

10 mg
25 mg
100 mg

$C_{47}H_{76}O_{18}$ FW: 929.1 [39524-08-8] ≥98.0%

Found in *Dipsacus asper*. It decreases levels of oxidative enzymes, improves left ventricle systolic pressure and left ventricle end-diastolic pressure, and suppresses expression of pro-inflammatory cytokines IL-6 and TNF-α.

Li C, Gao Y, Tian J, et al. Long-term oral Asperosaponin VI attenuates cardiac dysfunction, myocardial fibrosis in a rat model of chronic myocardial infarction. Food Chem Toxicol. 2012 May;50(5):1432-8. PMID: 22343037.

Li C, Tian J, Li G, et al. Asperosaponin VI protects cardiac myocytes from hypoxia-induced apoptosis via activation of the PI3K/Akt and CREB pathways. Eur J Pharmacol. 2010 Dec 15;649(1-3):100-7. PMID: 20863824.

Li C, Liu Z, Tian J, et al. Protective roles of Asperosaponin VI, a triterpene saponin isolated from *Dipsacus asper* Wall on acute myocardial infarction in rats. Eur J Pharmacol. 2010 Feb 10;627(1-3):235-41. PMID: 19909736.

A7577

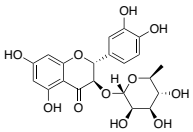

Astilbin

5 mg
10 mg
25 mg

$C_{21}H_{22}O_{11}$ FW: 450.39 [29838-67-3] ≥98.0%

Found in various plant sources. It decreases expression of IL-1β, IL-6, IL-10, MCP-1, and TNF-α, inhibits maturation of and antigen presentation by dendritic cells, and induces cell cycle arrest and apoptosis in hepatoma cells.

Li P, Gao S, Jie W, et al. Astilbin inhibits proliferation of rat aortic smooth muscle cells induced by angiotensin II and down-regulates expression of protooncogene. J Huazhong Univ Sci Technolog Med Sci. 2012 Apr;32(2):181-5. PMID: 22528217.

Huang H, Cheng Z, Shi H, et al. Isolation and characterization of two flavonoids, engeletin and astilbin, from the leaves of Engelhardia roxburghiana and their potential anti-inflammatory properties. J Agric Food Chem. 2011 May 11;59(9):4562-9. PMID: 21476602.

Petacci F, Freitas SS, Brunetti IL, et al. Inhibition of peroxidase activity and scavenging of reactive oxygen species by astilbin isolated from Dimorphandra mollis (*Fabaceae*, Caesalpinioideae). Biol Res. 2010;43(1):63-74. PMID: 21157633.

A7578 Astragaloside IV

10 mg
25 mg
100 mg

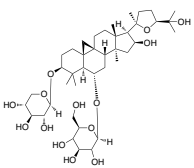

$C_{41}H_{68}O_{14}$ FW: 784.97 [83207-58-3] ≥98%

Found in *Astragalus membranaceus*. It inhibits the development of cardiac hypertrophy, prevents ischemia/reperfusion-induced myocardial infarction and myocardial apoptosis, and promotes tube and vessel formation in endothelial cells.

Lu M, Wang H, Wang J, et al. Astragaloside IV Protects against Cardiac Hypertrophy via Inhibiting the Ca^{2+}/CaN Signaling Pathway. Planta Med. 2013 Dec 11. [Epub ahead of print]. PMID: 24338553.

Wang SG, Xu Y, Chen JD, et al. Astragaloside IV stimulates angiogenesis and increases nitric oxide accumulation via JAK2/STAT3 and ERK1/2 pathway. Molecules. 2013 Oct 16;18(10):12809-19. PMID: 24135938.

He Y, Du M, Gao Y, et al. Astragaloside IV attenuates experimental autoimmune encephalomyelitis of mice by counteracting oxidative stress at multiple levels. PLoS One. 2013 Oct 4;8(10):e76495. PMID: 24124567.

A7604 ATB 346

NEW

1 mg
5 mg
25 mg

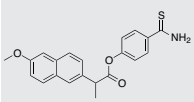

$C_{21}H_{19}NO_3S$ FW: 365.45 [1226895-20-0] ≥98%

NSAID and COX inhibitor. It attenuates zymosan-induced inflammation, nociception, and immune signaling and improves neurological function in animal models of traumatic brain injury.

Dief AE, Mostafa DK, Sharara GM, et al. Hydrogen sulfide releasing naproxen offers better anti-inflammatory and chondroprotective effect relative to naproxen in a rat model of zymosan induced arthritis. Eur Rev Med Pharmacol Sci. 2015 Apr;19(8):1537-46. PMID: 25967731.

Herrera BS, Coimbra LS, da Silva AR, et al. The H2S-releasing naproxen derivative, ATB-346, inhibits alveolar bone loss and inflammation in rats with ligature-induced periodontitis. Med Gas Res. 2015 Feb 27;5:4. PMID: 25755876.

Campolo M, Esposito E, Ahmad A, et al. Hydrogen sulfide-releasing cyclooxygenase inhibitor ATB-346 enhances motor function and reduces cortical lesion volume following traumatic brain injury in mice. J Neuroinflammation. 2014 Dec 4;11:196. PMID: 25472548.

A7618 Atenolol

1 g
5 g
25 g

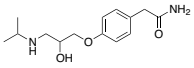

$C_{14}H_{22}N_2O_3$ FW: 266.34 [29122-68-7] ≥98%

β1-adrenergic receptor antagonist used to treat hypertension, angina, myocardial infarction, and tachycardia. It decreases cardiac output, lowering blood pressure.

Cockcroft JR, Pedersen ME. β-blockade: benefits beyond blood pressure reduction? J Clin Hypertens (Greenwich). 2012 Feb;14(2):112-20. PMID: 22277144.

Thadani U. Beta blockers in hypertension. Am J Cardiol. 1983 Nov 10;52(9):10D-15D. PMID: 6139008.

A7725 Atglistatin

NEW

5 mg
25 mg

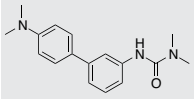

$C_{17}H_{21}N_3O$ FW: 283.38 [1469924-27-3] ≥98%

Adipose triglyceride lipase inhibitor. It decreases fatty acid mobilization and prevents triglyceride accumulation after acute myocardial infarction.

Zhang H, Sun T, Jiang X, et al. PEDF and PEDF-derived peptide 44mer stimulate cardiac triglyceride degradation via ATGL. J Transl Med. 2015 Feb 21;13:68. PMID: 25890298.

Cerk IK, Salzburger B, Boeszoermenyi A, et al. A peptide derived from G0/G1 switch gene 2 acts as noncompetitive inhibitor of adipose triglyceride lipase. J Biol Chem. 2014 Nov 21;289(47):32559-70. PMID: 25258314.

Mayer N, Schweiger M, Romauch M, et al. Development of small-molecule inhibitors targeting adipose triglyceride lipase. Nat Chem Biol. 2013 Dec;9(12):785-7. PMID: 24096302.

A7656 Atomoxetine Hydrochloride

25 mg
100 mg
250 mg

Tomoxetine

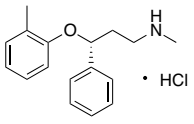

$C_{17}H_{21}NO \bullet HCl$ FW: 291.82 [82248-59-7] ≥98%

Inhibitor of NMDA receptors, NET, and SERT used to treat ADHD. It also prevents relapse in recently abstinent substance abuse subjects.

Isaksson J, Hogmark A, Nilsson KW, et al. Effects of stimulants and atomoxetine on cortisol levels in children with ADHD. Psychiatry Res. 2013 Jul 11. pii: S0165-1781 PMID: 23850434.

Ercan ES, Akyol Ardic U, Kabukcu Basay B, et al. Atomoxetine response in the inattentive and combined subtypes of attention deficit hyperactivity disorder: a retrospective chart review. Atten Defic Hyperact Disord. 2013 Jun 5. [Epub ahead of print]. PMID: 23737214.

Silverstone PH, Dadashova R. Atomoxetine treatment for nicotine withdrawal: a pilot double-blind, placebo-controlled, fixed-dose study in adult smokers. Ann Gen Psychiatry. 2012 Mar 9;11(1):6. PMID: 22405499.

A7658

Atorvastatin Calcium Trihydrate

10 mg
50 mg
100 mg

$(C_{33}H_{34}FN_2O_5)_2Ca \bullet 3H_2O$ FW: 1209.39 [344423-98-9] ≥98%

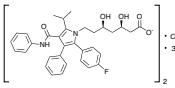

HMG-CoA reductase inhibitor used to lower cholesterol and lipid levels. It decreases levels of total cholesterol, triglycerides, and LDL, suppresses oxidative stress and inflammation, and inhibits development of left ventricular hypertrophy and cardiac fibrosis.

Cai J, Yu X, Zhang B, et al. Atorvastatin improves survival of implanted stem cells in a rat model of renal ischemia-reperfusion injury. Am J Nephrol. 2014;39(6):466-75. PMID: 24854145.

Akahori H, Tsujino T, Naito Y, et al. Atorvastatin ameliorates cardiac fibrosis and improves left ventricular diastolic function in hypertensive diastolic heart failure model rats. J Hypertens. 2014 Jul;32(7):1534-41. PMID: 24759122.

Lea AP, McTavish D. Atorvastatin. A review of its pharmacology and therapeutic potential in the management of hyperlipidaemias. Drugs. 1997 May;53(5):828-47. PMID: 9129869.

A7657

Atosiban Acetate

0.5 mg
1 mg
2.5 mg

$C_{43}H_{67}N_{11}O_{12}S_2$ FW: 994.2 [914453-95-5] ≥95%

c[Mpr-D-Tyr(OEt)-Ile-Thr-Asn-Cys-]-Pro-D-Arg-Gly-NH_2

Vasopressin 1/2 receptor and oxytocin receptor antagonist that alters uterine contractility and is used to prevent preterm birth.

Usta IM, Khalil A, Nassar AH. Oxytocin antagonists for the management of preterm birth: a review. Am J Perinatol. 2011 Jun;28(6):449-60. PMID: 21170825.

Pierzynski P. Oxytocin and vasopressin V(1A) receptors as new therapeutic targets in assisted reproduction. Reprod Biomed Online. 2011 Jan;22(1):9-16. PMID: 21130036.

A7668

Atracurium Besylate

50 mg
100 mg
500 mg

BW-33A; Tracrium

$C_{53}H_{72}N_2O_{12} \bullet (C_6H_5O_3S)_2$ FW: 1243.49 [64228-81-5] ≥95%

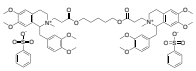

Non-depolarizing NMJ blocker and nonselective AChR antagonist used to induce anesthesia and skeletal muscle paralysis.

Shashank D, Singh NR, Singh LK. Effects of pretreatment with different neuromuscular blocking agents on facilitation of intubation with rocuronium: A prospective randomized comparative study. Indian J Anaesth. 2014 May;58(3):303-8. PMID: 25024474.

Jonsson M, Gurley D, Dabrowski M, et al. Distinct pharmacologic properties of neuromuscular blocking agents on human neuronal nicotinic acetylcholine receptors: a possible explanation for the train-of-four fade. Anesthesiology. 2006 Sep;105(3):521-33. PMID: 16931985.

Bowman WC. Neuromuscular block. Br J Pharmacol. 2006 Jan;147 Suppl 1:S277-86. PMID: 16402115.

A7670

Atriopeptin I

0.5 mg
1 mg
2.5 mg

$C_{83}H_{135}N_{29}O_{30}S_2$ FW: 2083.31 ≥95%

H-Ser-Ser-Cys-Phe-Gly-Gly-Arg-Ile-Asp-Arg-Ile-Gly-Ala-Gln-Ser-Gly-Leu-Gly-Cys-Asn-Ser-OH
(Disulfide Bridge Cys7-Cys23)

ANP analog and weak NPR-A agonist. It displays weak vasodilatory activity.

Stewart AG, Thompson JS, Rogers TK, et al. Atrial natriuretic peptide-induced relaxation of pre-constricted isolated rat perfused lungs: a comparison in control and hypoxia-adapted animals. Clin Sci (Lond). 1991 Aug;81(2):201-8. PMID: 1653664.

Numan NA, Gillespie MN, Altiere RJ. Pulmonary vasorelaxant activity of atrial peptides. Pulm Pharmacol. 1990;3(1):29-33. PMID: 1966900.

A7071

Atriopeptin II, rat/rabbit/mouse

0.5 mg
1 mg
2.5 mg

$C_{98}H_{156}N_{34}O_{32}S_2$ FW: 2386.67 ≥95%

H-Ser-Ser-Cys-Phe-Gly-Gly-Arg-Ile-Asp-Arg-Ile-Gly-Ala-Gln-Ser-Gly-Leu-Gly-Cys-Asn-Ser-Phe-Arg-OH
(Disulfide Bridge Cys7-Cys23)

ANP analog and NPR-A agonist. It decreases blood pressure and anxiety-like behaviors.

Ströhle A, Jahn H, Montkowski A, et al. Central and peripheral administration of atriopeptin is anxiolytic in rats. Neuroendocrinology. 1997 Mar;65(3):210-5. PMID: 9088002.

Prada JA, Ross R, Clark KE. Effect of atrial natriuretic peptide and other vasoactive compounds on the uterine vascular bed of the nonpregnant sheep. Proc Soc Exp Biol Med. 1992 Dec;201(3):261-6. PMID: 1438342.

A7072

Atriopeptin III

0.5 mg
1 mg
2.5 mg

$C_{107}H_{165}N_{35}O_{34}S_2$ FW: 2549.85 ≥95%

H-Ser-Ser-Cys-Phe-Gly-Gly-Arg-Ile-Asp-Arg-Ile-Gly-Ala-Gln-Ser-Gly-Leu-Gly-Cys-Asn-Ser-Phe-Arg-Tyr-OH
(Disulfide Bridge Cys7-Cys23)

ANP analog and NPR-A agonist. It decreases blood pressure.

Wang J, Shi P. Structure-function interrelation and clinical effect of atrial natriuretic peptide (ANP). Chin Med J (Engl). 1995 Apr;108(4):255-8. PMID: 7789210.

Lanese DM, Yuan BH, Falk SA, et al. Effects of atriopeptin III on isolated rat afferent and efferent arterioles. Am J Physiol. 1991 Dec;261(6 Pt 2):F1102-9. PMID: 1661082.

A7868 Atropine

NEW

1 g
5 g
25 g
100 g

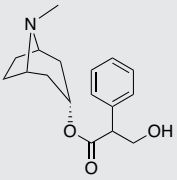

$C_{17}H_{23}NO_3$ FW: 289.37 [51-55-8] ≥98%

mAChR antagonist found in *Solanaceae* used to initiate mydriasis. It decreases thermal pain, inhibits histamine-induced increases in thromboxane A2, and acts as a positive inotrope.

Ghelardini C, Malmberg-Aiello P, Giotti A, et al. Investigation into atropine-induced antinociception. Br J Pharmacol. 1990 Sep;101(1):49-54. PMID: 2282466.

Alberts P, Ogren VR. Interaction of forskolin with the effect of atropine on [3H]acetylcholine secretion in guinea-pig ileum myenteric plexus. J Physiol. 1988 Jan;395:441-53. PMID: 2457681.

Berti F, Folco GC, Giachetti A, et al. Atropine inhibits thromboxane A2 generation in isolated lungs of the guinea-pig. Br J Pharmacol. 1980 Mar;68(3):467-72. PMID: 7052339.

A7672 Atropine Sulfate Monohydrate

5 g
10 g
25 g

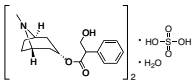

$(C_{17}H_{23}NO_3)_2 \cdot H_2SO_4 \cdot H_2O$ FW: 694.84 [5908-99-6] ≥98%

mAChR antagonist found in *Solanaceae* used to initiate mydriasis. It decreases thermal pain, inhibits histamine-induced increases in thromboxane A2, and acts as a positive inotrope.

Ghelardini C, Malmberg-Aiello P, Giotti A, et al. Investigation into atropine-induced antinociception. Br J Pharmacol. 1990 Sep;101(1):49-54. PMID: 2282466.

Alberts P, Ogren VR. Interaction of forskolin with the effect of atropine on [3H]acetylcholine secretion in guinea-pig ileum myenteric plexus. J Physiol. 1988 Jan;395:441-53. PMID: 2457681.

A5460 A-type Natriuretic Peptide (1-11), rat

1 mg
2 mg
5 mg

Atrial natriuretic peptide; ANP

H-Ser-Leu-Arg-Arg-Ser-Ser-Cys-Phe-Gly-Gly-Arg-OH

$C_{49}H_{83}N_{20}O_{15}S_1$ FW: 1224.4 ≥95%

Endogenous NPR-A agonist. It increases levels of cGMP and decreases blood pressure. It may also inhibit proliferation of cancer cells.

Vesely DL. New anticancer agents: hormones made within the heart. Anticancer Res. 2012 Jul;32(7):2515-21. PMID: 22753708.

Woodard GE, Rosado JA. Natriuretic peptides in vascular physiology and pathology. Int Rev Cell Mol Biol. 2008;268:59-93. PMID: 18703404.

A7669 A-type Natriuretic Peptide (1-28), rat

0.5 mg
1 mg
2.5 mg

ANP; Atrial natriuretic peptide

H-Ser-Leu-Arg-Arg-Ser-Ser-Cys-Phe-Gly-Gly-Arg-Ile-Asp-Arg-Ile-Gly-Ala-Gln-Ser-Gly-Leu-Gly-Cys-Asn-Ser-Phe-Arg-Tyr-OH
(Disulfide Bridge Cys7-Cys23)

$C_{128}H_{205}N_{45}O_{39}S_2$ FW: 3062.47 [88898-17-3] ≥95%

Endogenous NPR-A agonist. It increases levels of cGMP and decreases blood pressure. It may also inhibit proliferation of cancer cells.

Vesely DL. New anticancer agents: hormones made within the heart. Anticancer Res. 2012 Jul;32(7):2515-21. PMID: 22753708.

Woodard GE, Rosado JA. Natriuretic peptides in vascular physiology and pathology. Int Rev Cell Mol Biol. 2008;268:59-93. PMID: 18703404.

A5461 A-type Natriuretic Peptide (1-30), frog

0.5 mg
1 mg
2.5 mg

Atrial natriuretic peptide; ANP

H-Ala-Pro-Arg-Ser-Met-Arg-Arg-Ser-Ser-Asp-Cys-Phe-Gly-Ser-Arg-Ile-Asp-Arg-Ile-Gly-Ala-Gln-Ser-Gly-Met-Gly-Cys-Gly-Arg-Phe-OH
(Disulfide Bridge Cys11-Cys27)

$C_{131}H_{215}N_{49}O_{41}S_4$ FW: 3260.73 ≥95%

Endogenous NPR-A agonist. It increases levels of cGMP and decreases blood pressure. It may also inhibit proliferation of cancer cells.

Vesely DL. New anticancer agents: hormones made within the heart. Anticancer Res. 2012 Jul;32(7):2515-21. PMID: 22753708.

A8070 Auraptene

25 mg
100 mg
500 mg

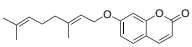

7-Geranyloxycoumarin

$C_{19}H_{22}O_3$ FW: 298.38 [495-02-3] ≥98%

PPARα agonist and ACAT inhibitor found in citrus plants. It displays several biological activities, including suppressing growth of *Leishmania*, decreasing mean arterial pressure, inducing expression of phase II enzymes, improving high fat diet-induced hyperglycemia, and preventing LPS-induced expression of COX-2.

Okuyama S, Yamamoto K, Mori H, et al. Auraptene in the Peels of Citrus kawachiensis (Kawachi Bankan) Ameliorates Lipopolysaccharide-Induced Inflammation in the Mouse Brain. Evid Based Complement Alternat Med. 2014;2014:408503. PMID: 24955102.

Imenshahidi M, Eghbal M, Sahebkar A, et al. Hypotensive activity of auraptene, a monoterpene coumarin from Citrus spp. Pharm Biol. 2013 May;51(5):545-9. PMID: 23368941.

Okuyama S, Minami S, Shimada N, et al. Anti-inflammatory and neuroprotective effects of auraptene, a citrus coumarin, following cerebral global ischemia in mice. Eur J Pharmacol. 2013 Jan 15;699(1-3):118-23. PMID: 23219792.

A8071

Auriculin A

0.5 mg
1 mg
2.5 mg

H-Arg-Ser-Ser-Cys-Phe-Gly-Gly-Arg-Ile-Asp-Arg-Ile-Gly-Ala-Gln-Ser-Gly-Leu-Gly-Cys-Asn-Ser-Phe-Arg-OH
(Disulfide Bridge Cys7-Cys23)

$C_{104}H_{168}N_{38}O_{33}S_2$ FW: 2542.86 ≥95%

Synthetic ANP analog and NPR-A agonist. It decreases blood pressure and increases Na^+ excretion.

Emmeluth C, Eiken P, Johannessen AC, et al. Effects of atrial natriuretic peptides and furosemide in conscious dogs. Proc Soc Exp Biol Med. 1987 Oct;186(1):103-12. PMID: 2957698.

Volpe M, Cuocolo A, Vecchione F, et al. Vagal mediation of the effects of atrial natriuretic factor on blood pressure and arterial baroreflexes in the rabbit. Circ Res. 1987 May;60(5):747-55. PMID: 2954718.

A8077

Autocamtide 2

0.5 mg
1 mg
2.5 mg

H-Lys-Lys-Ala-Leu-Arg-Arg-Gln-Glu-Thr-Val-Asp-Ala-Leu-OH

$C_{65}H_{118}N_{22}O_{20}$ FW: 1527.8 ≥95%

Substrate used to measure CamKII activity.

Cooper NG, Laabich A, Fan W, et al. The relationship between neurotrophic factors and CaMKII in the death and survival of retinal ganglion cells. Prog Brain Res. 2008;173:521-40. PMID: 18929132.

A8644

AVL-292

NEW

1 mg
5 mg
25 mg

CC-292

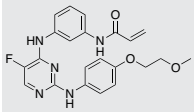

$C_{22}H_{22}FN_5O_3$ FW: 423.44 [1202757-89-8] ≥98%

BTK inhibitor. It suppresses proliferation of B-cell-related leukemia cells.

Burger JA. Bruton's tyrosine kinase (BTK) inhibitors in clinical trials. Curr Hematol Malig Rep. 2014 Mar;9(1):44-9. PMID: 24357428.

Robak T, Robak E. Tyrosine kinase inhibitors as potential drugs for B-cell lymphoid malignancies and autoimmune disorders. Expert Opin Investig Drugs. 2012 Jul;21(7):921-47. PMID: 22612424.

A8812

AWD 131-138

NEW

5 mg
10 mg
25 mg
50 mg

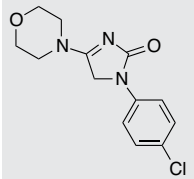

$C_{13}H_{14}ClN_3O_2$ FW: 279.72 [188116-07-6] ≥98%

GABA-A receptor positive allosteric modulator. It prevents the development of epilepsy and increases seizure thresholds in veterinary medicine.

Rundfeldt C, Löscher W. The pharmacology of imepitoin: the first partial benzodiazepine receptor agonist developed for the treatment of epilepsy. CNS Drugs. 2014 Jan;28(1):29-43. PMID: 24357084.

Löscher W, Hoffmann K, Twele F, et al. The novel antiepileptic drug imepitoin compares favourably to other GABA-mimetic drugs in a seizure threshold model in mice and dogs. Pharmacol Res. 2013 Nov;77:39-46. PMID: 24056205.

Yasar S, Bergman J, Munzar P, et al. Evaluation of the novel antiepileptic drug, AWD 131-138, for benzodiazepine-like discriminative stimulus and reinforcing effects in squirrel monkeys. Eur J Pharmacol. 2003 Apr 4;465(3):257-65. PMID: 12681437.

A9662

AZ-628

1 mg
5 mg

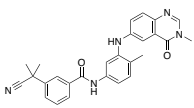

$C_{27}H_{25}N_5O_2$ FW: 451.52 [878739-06-1] ≥96%

Inhibitor of B-Raf and c-Raf. It is somewhat more selective for B-Raf in vivo and inhibits proliferation of melanoma cells.

Whittaker SR, Theurillat JP, Van Allen E, et al. A genome-scale RNA interference screen implicates NF1 loss in resistance to RAF inhibition. Cancer Discov. 2013 Mar;3(3):350-62. PMID: 23288408.

Montagut C, Sharma SV, Shioda T, et al. Elevated CRAF as a potential mechanism of acquired resistance to BRAF inhibition in melanoma. Cancer Res. 2008 Jun 15;68(12):4853-61. PMID: 18559533.

A9602

Azacitidine

100 mg
250 mg
1 g

Ladakamycin

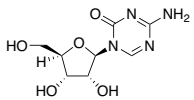

$C_8H_{12}N_4O_5$ FW: 244.2 [320-67-2] ≥98%

Cytidine analog and inhibitor of DNMT and protein synthesis used to treat myelodysplastic syndromes. It also induces differentiation of mesenchymal stem cells into cardiomyocytes, stimulates production of Treg and CD8+ T cells, increases glial cell differentiation, and inhibits replication of HIV.

Borodovsky A, Salmasi V, Turcan S, et al. 5-azacytidine reduces methylation, promotes differentiation and induces tumor regression in a patient-derived IDH1 mutant glioma xenograft. Oncotarget. 2013 Oct;4(10):1737-47. PMID: 24077805.

Solís-Paredes M, Eguía-Aguilar P, Chico-Ponce de León F, et al. Epigenetic modifications in cell lines of human astrocytoma differentially regulate expression of apoptotic genes. Childs Nerv Syst. 2013 Aug 13. Epub ahead of print. PMID: 23943192.

Tsujioka T, Yokoi A, Uesugi M, et al. Effects of DNA methyltransferase inhibitors (DNMTIs) on MDS-derived cell lines. Exp Hematol. 2013 Feb;41(2):189-97. PMID: 23085465.

A9603

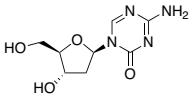

5-Aza-2'-deoxycytidine

2'-Deoxy-5-azacytidine

$C_8H_{12}N_4O_4$ FW: 228.21 [2353-33-5] ≥98%

5 mg
10 mg
50 mg

Deoxycytidine analog and inhibitor of DNMT and protein synthesis used to treat myelodysplastic syndromes. It also induces apoptosis in acute myelogenous leukemia cells and dopaminergic neurons, stimulates fetal hemoglobin production, and inhibits replication of HIV.

Zhou JH, Yao YS, Wang LX, et al. Demethylating agent decitabine induces autologous cancer testis antigen specific cytotoxic T lymphocytes in vivo. Chin Med J (Engl). 2013 Dec;126(23):4552-6. PMID: 24286424.

Wang Y, Wang X, Li R, et al. A DNA methyltransferase inhibitor, 5-aza-2'-deoxycytidine, exacerbates neurotoxicity and upregulates Parkinson's disease-related genes in dopaminergic neurons. CNS Neurosci Ther. 2013 Mar;19(3):183-90. PMID: 23441691.

Soncini M, Santoro F, Gutierrez A, et al. The DNA demethylating agent decitabine activates the TRAIL pathway and induces apoptosis in acute myeloid leukemia. Biochim Biophys Acta. 2013 Jan;1832(1):114-20. PMID: 23046813.

A9801

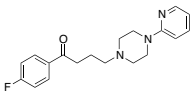

Azaperone

$C_{19}H_{22}FN_3O$ FW: 327.4 [1649-18-9] ≥98%

500 mg
1 g
5 g

Antagonist at α-adrenergic receptors, dopamine D2 receptors, and histamine receptors used as a tranquilizer.

Wolfe LL, Fisher MC, Davis TR, et al. Efficacy of a Low-Dosage Combination of Butorphanol, Azaperone, and Medetomidine (BAM) to Immobilize Rocky Mountain Elk. J Wildl Dis. 2014 Jul;50(3):676-80. PMID: 24807358.

McCormick AV, Wheeler JM, Guthrie CR, et al. Dopamine D2 receptor antagonism suppresses tau aggregation and neurotoxicity. Biol Psychiatry. 2013 Mar 1;73(5):464-71. PMID: 23140663.

A9803

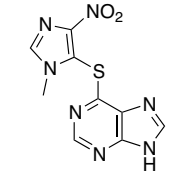

Azathioprine

AZA

$C_9H_7N_7O_2S$ FW: 277.26 [446-86-6] ≥98%

1 g
5 g
10 g

Purine analog, mercaptopurine prodrug, and potential PRPP transferase and HGPRT inhibitor used to suppress the immune response in organ transplant subjects. It also suppresses experimental autoimmune myasthenia gravis, prevents conjugation of antigen-presenting cells with T cells, and inhibits growth of bovine viral diarrhea virus.

Hernández-Breijo B, Monserrat J, Ramírez-Rubio S, et al. Preclinical evaluation of azathioprine plus buthionine sulfoximine in the treatment of human hepatocarcinoma and colon carcinoma. World J Gastroenterol. 2011 Sep 14;17(34):3899-911. PMID: 22025878.

Hoover S, Striker R. Thiopurines inhibit bovine viral diarrhea virus production in a thiopurine methyltransferase-dependent manner. J Gen Virol. 2008 Apr;89(Pt 4):1000-9. PMID: 18343842.

Poppe D, Tiede I, Fritz G, et al. Azathioprine suppresses ezrin-radixin-moesin-dependent T cell-APC conjugation through inhibition of Vav guanosine exchange activity on Rac proteins. J Immunol. 2006 Jan 1;176(1):640-51. PMID: 16365460.

A9708

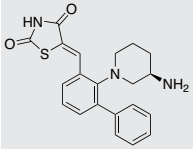

AZD-1208

NEW

$C_{21}H_{21}N_3O_2S$ FW: 379.48 [1204144-28-4] ≥98%

1 mg
5 mg
10 mg

Pim-1 inhibitor. It induces cell cycle arrest and apoptosis in acute myelogenous leukemia cells and inhibits phosphorylation of downstream targets such as Bcl-2, 4EBP1, p70S6K, and S6.

Kirschner AN, Wang J, van der Meer R, et al. PIM kinase inhibitor AZD1208 for treatment of MYC-driven prostate cancer. J Natl Cancer Inst. 2014 Dec 13;107(2). PMID: 25505253.

Keeton EK, McEachern K, Dillman KS, et al. AZD1208, a potent and selective pan-Pim kinase inhibitor, demonstrates efficacy in preclinical models of acute myeloid leukemia. Blood. 2014 Feb 6;123(6):905-13. PMID: 24363397.

A9812

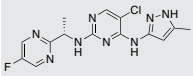

AZD-1480

NEW

$C_{14}H_{14}ClFN_8$ FW: 348.77 [935666-88-9] ≥98%

5 mg
10 mg

JAK1/2 inhibitor. It inhibits replication of hepatitis A virus, minimizes antigen presentation and T cell expansion in EAE models, and inhibits metastasis and tumor growth in prostate cancer models.

Jiang X, Kanda T, Nakamoto S, et al. The JAK2 inhibitor AZD1480 inhibits hepatitis A virus replication in Huh7 cells. Biochem Biophys Res Commun. 2015 Feb 19. [Epub ahead of print]. PMID: 25704089.

Gritsina G, Xiao F, O'Brien SW, et al. Targeted blockade of JAK/STAT3 signaling inhibits ovarian carcinoma growth. Mol Cancer Ther. 2015 Feb 2. [Epub ahead of print]. PMID: 25646015.

Suryani S, Bracken LS, Harvey RC, et al. Evaluation of the In Vitro and In Vivo Efficacy of the JAK Inhibitor AZD1480 against JAK-Mutated Acute Lymphoblastic Leukemia. Mol Cancer Ther. 2015 Feb;14(2):364-74. PMID: 25504635.

A9710 AZD-2014

NEW

1 mg
5 mg
10 mg

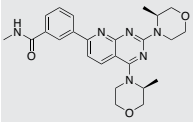

$C_{25}H_{30}N_6O_3$ FW: 462.54 [1009298-59-2] ≥98%

Inhibitor of mTORC1/2. It induces autophagy and inhibits growth without causing apoptosis in colorectal cancer cells.

Huo HZ, Zhou ZY, Wang B, et al. Dramatic suppression of colorectal cancer cell growth by the dual mTORC1 and mTORC2 inhibitor AZD-2014. Biochem Biophys Res Commun. 2014 Jan 10;443(2):406-12. PMID: 24309100.

A9714 AZD-1152-HQPA

NEW

1 mg
5 mg
10 mg

Barasertib

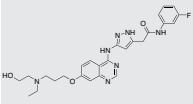

$C_{26}H_{30}FN_7O_3$ FW: 507.56 [722544-51-6] ≥98%

Aurora kinase A/B inhibitor. It prevents mitotic spindle formation and induces apoptosis in glioma cells and leukemia cells.

Hartsink-Segers SA, Zwaan CM, Exalto C, et al. Aurora kinases in childhood acute leukemia: the promise of aurora B as therapeutic target. Leukemia. 2013 Mar;27(3):560-8. PMID: 22940834.

Diaz RJ, Golbourn B, Shekarforoush M, et al. Aurora kinase B/C inhibition impairs malignant glioma growth in vivo. J Neurooncol. 2012 Jul;108(3):349-60. PMID: 22382783.

Boss DS, Witteveen PO, van der Sar J,et al. Clinical evaluation of AZD1152, an i.v. inhibitor of Aurora B kinase, in patients with solid malignant tumors. Ann Oncol. 2011 Feb;22(2):431-7. PMID: 20924078.

A9612 AZD-2461

NEW

5 mg
25 mg

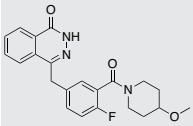

$C_{22}H_{22}FN_3O_3$ FW: 395.43 [1174043-16-3] ≥98%

PARP1 inhibitor. It limits cell proliferation in models of homologous recombination-deficient tumors and does not incur Pgp-related drug resistance.

Jaspers JE, Kersbergen A, Boon U, et al. Loss of 53BP1 causes PARP inhibitor resistance in Brca1-mutated mouse mammary tumors. Cancer Discov. 2013 Jan;3(1):68-81. PMID: 23103855.

A9600 AZD-3463

1 mg
5 mg
25 mg

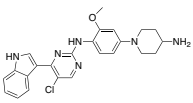

$C_{24}H_{25}ClN_6O$ FW: 448.95 [1356962-20-3] ≥99%

ALK and IGF-1R inhibitor. It alters ERK/Akt/STAT3 signaling, suppresses cell proliferation, and induces regression or stasis in tumor models.

Abstract: Yang B. Discovery of AZD3463 as a novel ALK/IGFR dual inhibitor and its ability in overcoming acquired resistance to crizotinib. Protein Kinases in Drug Discovery Conference. 2013.

A9814 AZD-4547

NEW

5 mg
10 mg

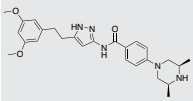

$C_{26}H_{33}N_5O_3$ FW: 463.57 [1035270-39-3] ≥98%

FGFR inhibitor somewhat selective for FGFR2. It induces apoptosis and inhibits proliferation, invasion, and migration of breast cancer cells.

Liu L, Ye TH, Han YP, et al. Reductions in myeloid-derived suppressor cells and lung metastases using AZD4547 treatment of a metastatic murine breast tumor model. Cell Physiol Biochem. 2014;33(3):633-45. PMID: 24642893.

Zhang J, Zhang L, Su X, et al. Translating the therapeutic potential of AZD4547 in FGFR1-amplified non-small cell lung cancer through the use of patient-derived tumor xenograft models. Clin Cancer Res. 2012 Dec 15;18(24):6658-67. Erratum in: Clin Cancer Res. 2013 Jul 1;19(13):3714. Schöttle, Jakob [added]. PMID: 23082000.

Gavine PR, Mooney L, Kilgour E, et al. AZD4547: an orally bioavailable, potent, and selective inhibitor of the fibroblast growth factor receptor tyrosine kinase family. Cancer Res. 2012 Apr 15;72(8):2045-56. PMID: 22369928.

A9601 AZD-5363

1 mg
5 mg
25 mg

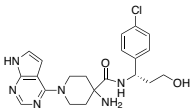

$C_{21}H_{25}ClN_6O_2$ FW: 428.92 [1143532-39-1] ≥99%

Inhibitor of AKT and potential inhibitor of ROCK, p70S6K, PKA, MKK1, MSK1, MSK2, PKC, PKG, PRKX, and RSK2/3. It inhibits cell proliferation and induces tumor regression in breast cancer and prostate cancer models.

Addie M, Ballard P, Buttar D, et al. Discovery of 4-amino-N-[(1S)-1-(4-chlorophenyl)-3-hydroxypropyl]-1-(7H-pyrrolo[2,3-d]pyrimidin-4-yl)piperidine-4-carboxamide (AZD5363), an orally bioavailable, potent inhibitor of Akt kinases. J Med Chem. 2013 Mar 14;56(5):2059-73. PMID: 23394218.

Lamoureux F, Thomas C, Crafter C, et al. Blocked autophagy using lysosomotropic agents sensitizes resistant prostate tumor cells to the novel Akt inhibitor AZD5363. Clin Cancer Res. 2013 Feb 15;19(4):833-44. PMID: 23258740.

Davies BR, Greenwood H, Dudley P, et al. Preclinical pharmacology of AZD5363, an inhibitor of AKT: pharmacodynamics, antitumor activity, and correlation of monotherapy activity with genetic background. Mol Cancer Ther. 2012 Apr;11(4):873-87. PMID: 22294718.

A9712

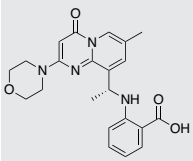

AZD-6482

NEW

1 mg
5 mg
10 mg

$C_{22}H_{24}N_4O_4$ FW: 408.45 [1173900-33-8] ≥98%

Inhibitor of p110β PI3K. It inhibits insulin-induced adipocyte glucose uptake and decreases thrombin activity without increasing bleeding time or blood loss.

Weigelt B, Warne PH, Lambros MB, et al. PI3K pathway dependencies in endometrioid endometrial cancer cell lines. Clin Cancer Res. 2013 Jul 1;19(13):3533-44. PMID: 23674493.

Nylander S, Kull B, Björkman JA, et al. Human target validation of phosphoinositide 3-kinase (PI3K)β: effects on platelets and insulin sensitivity, using AZD6482 a novel PI3Kβ inhibitor. J Thromb Haemost. 2012 Oct;10(10):2127-36. PMID: 22906130.

A9912

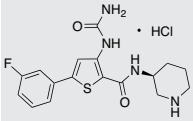

AZD-7762 Hydrochloride

NEW

5 mg
10 mg

$C_{17}H_{19}FN_4O_2S \bullet HCl$ FW: 398.88 [860352-01-8] ≥98%

CHK1 inhibitor. It increases sensitivity to DNA-damaging compounds and inhibits proliferation of breast cancer and ovarian cancer cells.

Bryant C, Rawlinson R, Massey AJ. Chk1 inhibition as a novel therapeutic strategy for treating triple-negative breast and ovarian cancers. BMC Cancer. 2014 Aug 7;14:570. PMID: 25104095.

Sausville E, Lorusso P, Carducci M, et al. Phase I dose-escalation study of AZD7762, a checkpoint kinase inhibitor, in combination with gemcitabine in US patients with advanced solid tumors. Cancer Chemother Pharmacol. 2014 Mar;73(3):539-49. PMID: 24448638.

Ma CX, Cai S, Li S, et al. Targeting Chk1 in p53-deficient triple-negative breast cancer is therapeutically beneficial in human-in-mouse tumor models. J Clin Invest. 2012 Apr;122(4):1541-52. Erratum in: J Clin Invest. 2012 Jul 2;122(7):2702. PMID: 22446188.

A9914

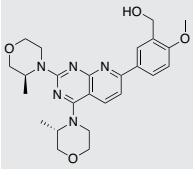

AZD-8055

NEW

5 mg
25 mg
50 mg

$C_{25}H_{31}N_5O_4$ FW: 465.55 [1009298-09-2] ≥98%

Inhibitor of mTORC1/2. It promotes antibody class switching in B cells at low doses and decreases B cell proliferation and differentiation at high doses. It also increases survival in transplant recipients and suppresses viability of brain tumor cells.

Limon JJ, So L, Jellbauer S, et al. mTOR kinase inhibitors promote antibody class switching via mTORC2 inhibition. Proc Natl Acad Sci U S A. 2014 Nov 25;111(47):E5076-85. PMID: 25385646.

Luchman HA, Stechishin OD, Nguyen SA, et al. Dual mTORC1/2 blockade inhibits glioblastoma brain tumor initiating cells in vitro and in vivo and synergizes with temozolomide to increase orthotopic xenograft survival. Clin Cancer Res. 2014 Nov 15;20(22):5756-67. PMID: 25316808.

Rosborough BR, Raïch-Regué D, Liu Q, et al. Adenosine triphosphate-competitive mTOR inhibitors: a new class of immunosuppressive agents that inhibit allograft rejection. Am J Transplant. 2014 Sep;14(9):2173-80. PMID: 25307040.

A9715

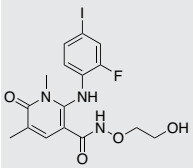

AZD-8330

NEW

1 mg
5 mg
10 mg

ARRY-704; ARRY-424704

$C_{16}H_{17}FIN_3O_4$ FW: 461.23 [869357-68-6] ≥98%

MEK 1/2 inhibitor. It inhibits proliferation of cancer cells.

Cohen RB, Aamdal S, Nyakas M, et al. A phase I dose-finding, safety and tolerability study of AZD8330 in patients with advanced malignancies. Eur J Cancer. 2013 May;49(7):1521-9. PMID: 23433846.

Akinleye A, Furqan M, Mukhi N, et al. MEK and the inhibitors: from bench to bedside. J Hematol Oncol. 2013 Apr 12;6:27. PMID: 23587417.

A9817

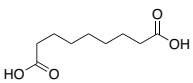

Azelaic Acid

5 g
25 g

Anchoic acid

$C_9H_{16}O_4$ FW: 188.22 [123-99-9] ≥98%

PPARγ agonist and kallikrein 5 inhibitor found in *Arabidopsis*. It is used to treat rosacea, acne, and hyperpigmentary disorders. It also suppresses activity of serine proteases, upregulates expression of antioxidative enzymes, inhibits proliferation of melanocytes, and suppresses DNA synthesis in cutaneous melanoma cells.

Coda AB, Hata T, Miller J, et al. Cathelicidin, kallikrein 5, and serine protease activity is inhibited during treatment of rosacea with azelaic acid 15% gel. J Am Acad Dermatol. 2013 Oct;69(4):570-7. PMID: 23871720.

Briganti S, Flori E, Mastrofrancesco A, et al. Azelaic acid reduced senescence-like phenotype in photo-irradiated human dermal fibroblasts: possible implication of PPARγ. Exp Dermatol. 2013 Jan;22(1):41-7. PMID: 23278893.

Fitton A, Goa KL. Azelaic acid. A review of its pharmacological properties and therapeutic efficacy in acne and hyperpigmentary skin disorders. Drugs. 1991 May;41(5):780-98. PMID: 1712709.

A9818

Azelastine Hydrochloride

100 mg
500 mg
1 g

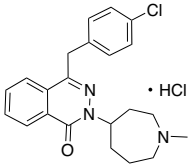

$C_{22}H_{23}N_3O \bullet HCl$ FW: 418.35 [79307-93-0] ≥98%

TRPV1 receptor agonist and histamine H1 receptor antagonist. Used to treat allergic rhinitis. It inhibits pro-inflammatory cytokine production in mast cells and decreases capsaicin-induced cough.

Singh U, Bernstein JA, Haar L, et al. Azelastine desensitization of transient receptor potential vanilloid 1: A potential mechanism explaining its therapeutic effect in nonallergic rhinitis. Am J Rhinol Allergy. 2014 May;28(3):215-24. PMID: 24980233.

Horak F, Zieglmayer UP. Azelastine nasal spray for the treatment of allergic and nonallergic rhinitis. Expert Rev Clin Immunol. 2009 Nov;5(6):659-69. PMID: 20477689.

Kempuraj D, Huang M, Kandere-Grzybowska K, et al. Azelastine inhibits secretion of IL-6, TNF-alpha and IL-8 as well as NF-kappaB activation and intracellular calcium ion levels in normal human mast cells. Int Arch Allergy Immunol. 2003 Nov;132(3):231-9. PMID: 14646384.

A3212

3'-Azido-3'-deoxythymidine

25 mg
100 mg
250 mg
1 g

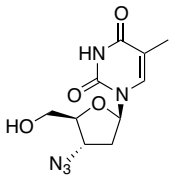

AZT; Azidothymidine

$C_{10}H_{13}N_5O_4$ FW: 267.24 [30516-87-1] ≥98%

Thymidine analog and DNA chain terminator used to treat HIV infection. It prevents DNA synthesis and viral replication and may inhibit DNA polymerase.

Banerjee A, Abdelmegeed MA, Jang S, et al. Zidovudine (AZT) and hepatic lipid accumulation: implication of inflammation, oxidative and endoplasmic reticulum stress mediators. PLoS One. 2013 Oct 11;8(10):e76850. PMID: 24146933.

Parker WB, White EL, Shaddix SC, et al. Mechanism of inhibition of human immunodeficiency virus type 1 reverse transcriptase and human DNA polymerases alpha, beta, and gamma by the 5'-triphosphates of carbovir, 3'-azido-3'-deoxythymidine, 2',3'-dideoxyguanosine and 3'-deoxythymidine. A novel RNA template for the evaluation of antiretroviral drugs. J Biol Chem. 1991 Jan 25;266(3):1754-62. PMID: 1703154.

A9834

Azithromycin Dihydrate

500 mg
1 g
5 g

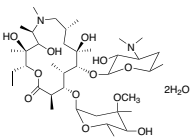

$C_{38}H_{72}N_2O_{12} \bullet 2H_2O$ FW: 785.02 [117772-70-0] ≥98%

Protein translation inhibitor used to treat bacterial infections. It also inhibits the epithelial-to-mesenchymal transition and suppresses LPS-stimulated production of pro-inflammatory cytokines in macrophages.

Bakheit AH, Al-Hadiya BM, Abd-Elgalil AA. Azithromycin. Profiles Drug Subst Excip Relat Methodol. 2014;39:1-40. PMID: 24794904.

Medina CA, Rowe AM, Yun H, et al. Azithromycin treatment increases survival of high-risk corneal allotransplants. Cornea. 2013 May;32(5):658-66. PMID: 23407315.

Banerjee B, Musk M, Sutanto EN, et al. Regional differences in susceptibiity of bronchial epithelium to mesenchymal transition and inhibition by the macrolide antibiotic azithromycin. PLoS One. 2012;7(12):e52309. PMID: 23284981.

A9978

Aztreonam

10 mg
50 mg
250 mg

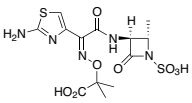

SQ-26776

$C_{13}H_{17}N_5O_8S_2$ FW: 435.43 [78110-38-0] ≥96%

Penicillin binding protein inhibitor that prevents cell wall synthesis. It inhibits growth of gram negative bacteria.

Dallal MM, Czachor JS. Aztreonam-induced myelosuppression during treatment of *Pseudomonas* aeruginosa pneumonia. DICP. 1991 Jun;25(6):594-7. PMID: 1877266.

A0248

BAM-12P

1 mg
2 mg
5 mg

H-Tyr-Gly-Gly-Phe-Met-Arg-Arg-Val-Gly-Arg-Pro-Glu-OH

Bovine adrenal medulla 12 peptide

$C_{62}H_{97}N_{21}O_{16}S$ FW: 1424.66 [75513-71-2] ≥95%

κOR agonist and cleavage product of proenkephalin.

Davis TP, Hoyer GL, Davis P, et al. Proenkephalin A-derived peptide E and its fragments alter opioid contractility in the small intestine. Eur J Pharmacol. 1990 Dec 4;191(3):253-61. PMID: 2086244.

Mizuno K, Minamino N, Kangawa K, et al. A new endogenous opioid peptide from bovine adrenal medulla: isolation and amino acid sequence of a dodecapeptide (BAM-12P). Biochem Biophys Res Commun. 1980 Aug 29;95(4):1482-8. PMID: 7417331.

A0249

BAM-22P

1 mg
2 mg
5 mg

H-Tyr-Gly-Gly-Phe-Met-Arg-Arg-Val-Gly-Arg-Pro-Glu-Trp-Trp-Met-Asp-Tyr-Gln-Lys-Arg-Tyr-Gly-OH

Bovine adrenal medulla 22 peptide

$C_{130}H_{184}N_{38}O_{31}S_2$ FW: 2839.28 ≥95%

κOR and μOR agonist and cleavage product of proenkephalin.

Cai M, Chen T, Quirion R, et al. The involvement of spinal bovine adrenal medulla 22-like peptide, the proenkephalin derivative, in modulation of nociceptive processing. Eur J Neurosci. 2007 Sep;26(5):1128-38. PMID: 17767492.

B0000 — 2B-(A)

1 mg
2 mg
5 mg

Biotin-Arg-Arg-Ala-Ala-Glu-Glu-Leu-Asp-Ser-Arg-Ala-Gly-Ala-Pro-Gln-Leu-OH

$C_{81}H_{137}N_{28}O_{28}S$ FW: 1983.23 ≥95%

Peptide-biotin conjugate.

B0072 — 2B-(S)

1 mg
2 mg
5 mg

Biotin-Arg-Arg-Ala-Ala-Glu-Glu-Leu-Asp-Ser-Arg-Ala-Gly-Ala-Pro-Gln-Leu-OH

$C_{81}H_{137}N_{28}O_{28}S$ FW: 1983.23 ≥95%

Peptide-biotin conjugate.

B0110 — Baclofen

1 g
5 g
10 g

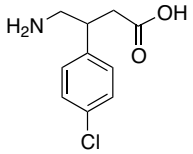

$C_{10}H_{12}ClNO_2$ FW: 213.66 [1134-47-0] ≥98%

GABA derivative and GABA-B receptor agonist used to study GABAergic neurotransmission and to treat spasticity and dystonia. It decreases frequency and amplitude of excitatory post-synaptic currents and mediates alcohol craving during withdrawal.

Fukuhara K, Katafuchi T, Yoshimura M. Effects of baclofen on mechanical noxious and innocuous transmission in the spinal dorsal horn of the adult rat: in vivo patch-clamp analysis. Eur J Neurosci. 2013 Aug 20. [Epub ahead of print]. PMID: 23961926.

Kumru H, Kofler M, Flores MC, et al. Effect of intrathecal baclofen on evoked pain perception: an evoked potentials and quantitative thermal testing study. Eur J Pain. 2013 Aug;17(7):1039-47. PMID: 23239275.

B0108 — Bactenecin

0.5 mg
1 mg

Bac7

H-Arg-Leu-Cys-Arg-Ile-Val-Val-Ile-Arg-Val-Cys-Arg-OH (Disulfide Bridge Cys3-Cys11)

$C_{63}H_{118}N_{24}O_{13}S_2$ FW: 1483.9 [116229-36-8] ≥95%

Cathelicidin derivative found in bovine neutrophils that alters bacterial membrane permeability. It inhibits growth of *Burkholderia*, *Escherichia*, *Pseudomonas*, *Salmonella*, *Staphylococcus*, and *Enterobacter*.

Madhongsa K, Pasan S, Phophetleb O, et al. Antimicrobial action of the cyclic peptide bactenecin on *Burkholderia* pseudomallei correlates with efficient membrane permeabilization. PLoS Negl Trop Dis. 2013 Jun 13;7(6):e2267. PMID: 23785532.

B0025 — Bafilomycin A1

1 mg

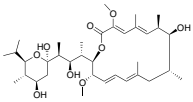

$C_{35}H_{58}O_9$ FW: 622.83 [88899-55-2] ≥90%

Vacuolar H^+ ATPase inhibitor. It suppresses autophagy, prevents tumor growth in breast cancer models, and inhibits growth of *Plasmodium*.

Graham RM, Thompson JW, Webster KA. Inhibition of the vacuolar ATPase induces Bnip3-dependent death of cancer cells and a reduction in tumor burden and metastasis. Oncotarget. 2014 Mar 15;5(5):1162-73. PMID: 24811485.

Xu MY, Lee SY, Kang SS, et al. Antitumor activity of jujuboside B and the underlying mechanism via induction of apoptosis and autophagy. J Nat Prod. 2014 Feb 28;77(2):370-6. PMID: 24547878.

B0026 — Bafilomycin B1

1 mg

Setamycin

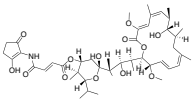

$C_{44}H_{65}NO_{13}$ FW: 815.99 [88899-56-3] ≥97%

Vacuolar H^+ ATPase inhibitor that also indirectly inhibits Foxo1 and induces β cell apoptosis.

Schachtschabel D, Arentshorst M, Lagendijk EL, et al. Vacuolar H(+)-ATPase plays a key role in cell wall biosynthesis of *Aspergillus* niger. Fungal Genet Biol. 2012 Apr;49(4):284-93. PMID: 22222772.

Hettiarachchi KD, Zimmet PZ, Danial NN, et al. Transplacental exposure to the vacuolar-ATPase inhibitor bafilomycin disrupts survival signaling in beta cells and delays neonatal remodeling of the endocrine pancreas. Exp Toxicol Pathol. 2008 Aug;60(4-5):295-306. PMID: 18486461.

B0133 — Baicalin

1 mg
5 mg
10 mg
25 mg
100 mg

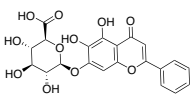

$C_{21}H_{18}O_{11}$ FW: 446.36 [21967-41-9] ≥95%

Prolyl oligopeptidase and neuraminidase inhibitor found in *Scutellaria*. It prevents influenza infection, decreases systolic blood pressure and inhibits ventricular remodeling, and suppresses UV-induced skin aging responses in fibroblasts.

Ding Y, Dou J, Teng Z, et al. Antiviral activity of baicalin against influenza A (H1N1/H3N2) virus in cell culture and in mice and its inhibition of neuraminidase. Arch Virol. 2014 Jul 31. [Epub ahead of print]. PMID: 25078390.

Min W, Liu X, Qian Q, et al. The effects of baicalin against UVA-induced photoaging in skin fibroblasts. Am J Chin Med. 2014;42(3):709-27. PMID: 24871661.

Zhang L, Pu Z, Wang J, et al. Baicalin inhibits hypoxia-induced pulmonary artery smooth muscle cell proliferation via the AKT/HIF-1α/p27-associated pathway. Int J Mol Sci. 2014 May 9;15(5):8153-68. PMID: 24821539.

B0109

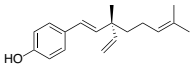

Bakuchiol

10 mg
25 mg
100 mg

UP 256

$C_{18}H_{24}O$ FW: 256.38 [10309-37-2] ≥98%

ERα agonist found in various plant sources. It exhibits a wide variety of biological activities, including inhibiting growth of *Streptococcus*, *Enterococcus*, *Lactobacillus*, Actinomyces, and *Porphyromonas*, suppressing LPS-stimulated production of pro-inflammatory cytokines, decreasing plasma glucose and triglyceride levels, and potentially inhibiting PP1B.

Lim SH, Ha TY, Ahn J, et al. Estrogenic activities of Psoralea corylifolia L. seed extracts and main constituents. Phytomedicine. 2011 Mar 15;18(5):425-30. PMID: 21382704.

Choi SY, Lee S, Choi WH, et al. Isolation and anti-inflammatory activity of Bakuchiol from Ulmus davidiana var. japonica. J Med Food. 2010 Aug;13(4):1019-23. PMID: 20553183.

B0245

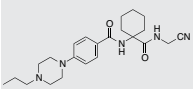

Balicatib

NEW

5 mg
25 mg

AAE-581

$C_{23}H_{33}N_5O_2$ FW: 411.55 [354813-19-7] ≥98%

Cathepsin K inhibitor. It inhibits osteoclast activity, decreasing bone turnover and increasing bone mineral density and bone formation rates.

Jerome C, Missbach M, Gamse R. Balicatib, a cathepsin K inhibitor, stimulates periosteal bone formation in monkeys. Osteoporos Int. 2012 Jan;23(1):339-49. PMID: 21380636.

Chappard D, Libouban H, Mindeholm L, et al. The cathepsin K inhibitor AAE581 induces morphological changes in osteoclasts of treated patients. Microsc Res Tech. 2010 Jul;73(7):726-32. PMID: 20025055.

B0246

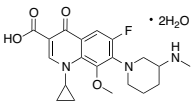

Balofloxacin Dihydrate

10 mg
50 mg
250 mg

$C_{20}H_{24}FN_3O_4 \cdot 2H_2O$ FW: 425.45 [151060-21-8] ≥98.0%

Bacterial DNA gyrase inhibitor used primarily to treat gram positive bacteria infections. It is also active against *Mycoplasma pneumoniae*.

Iwasaki H, Miyazaki S, Tsuji A, et al. In vitro and in vivo antibacterial activities of Q-35, a novel fluoroquinolone. Chemotherapy. 1995 Mar-Apr;41(2):100-12. PMID: 7758353.

Ito T, Kojima K, Koizumi K, et al. Inhibitory activity on DNA gyrase and intracellular accumulation of quinolones: structure-activity relationship of Q-35 analogs. Biol Pharm Bull. 1994 Jul;17(7):927-30. PMID: 8000379.

B0150

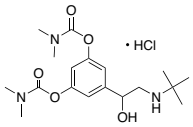

Bambuterol Hydrochloride

100 mg
500 mg
1 g
5 g

KWD-2183

$C_{18}H_{29}N_3O_5 \cdot HCl$ FW: 403.91 [81732-46-9] ≥98%

BChE inhibitor and β2-adrenergic receptor agonist that decreases bronchoconstriction. It is also a terbutaline prodrug.

Mohr F, Zimmermann M, Klein J. Mice heterozygous for AChE are more sensitive to AChE inhibitors but do not respond to BuChE inhibition. Neuropharmacology. 2013 Apr;67:37-45. PMID: 23147415.

Bosak A, Gazić I, Vinković V, et al. Stereoselective inhibition of human, mouse, and horse cholinesterases by bambuterol enantiomers. Chem Biol Interact. 2008 Sep 25;175(1-3):192-5. PMID: 18582854.

Waldeck B. Beta-adrenoceptor agonists and asthma--100 years of development. Eur J Pharmacol. 2002 Jun 7;445(1-2):1-12. PMID: 12065188.

B0396

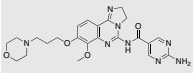

BAY80-6946

NEW

1 mg
5 mg
10 mg

Copanlisib

$C_{23}H_{28}N_8O_4$ FW: 480.52 [1032568-63-0] ≥98%

Inhibitor of p110α PI3K. It induces cell cycle arrest and apoptosis in multiple myeloma cells.

Glauer J, Pletz N, Schön M, et al. A novel selective small-molecule PI3K inhibitor is effective against human multiple myeloma in vitro and in vivo. Blood Cancer J. 2013 Sep 6;3:e141. PMID: 24013662.

Cheng H, Merika E, Syrigos KN, et al. Novel agents for the treatment of pancreatic adenocarcinoma. Highlights from the "2011 ASCO Annual Meeting". Chicago, IL, USA; June 3-7, 2011. JOP. 2011 Jul 8;12(4):334-8. PMID: 21737890.

B1603

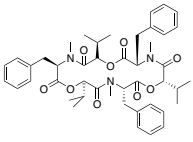

Beauvericin

1 mg
5 mg

$C_{45}H_{57}N_3O_9$ FW: 783.95 [26048-05-5] ≥95%

Mycotoxin found in *Cordyceps*. It induces apoptosis in colon adenocarcinoma cells and non-small cell lung cancer cells and stimulates intracellular influx of Ca^{2+}.

Prosperini A, Juan-García A, Font G, et al. Beauvericin-induced cytotoxicity via ROS production and mitochondrial damage in Caco-2 cells. Toxicol Lett. 2013 Oct 24;222(2):204-11. PMID: 23850777.

Chen BF, Tsai MC, Jow GM. Induction of calcium influx from extracellular fluid by beauvericin in human leukemia cells. Biochem Biophys Res Commun. 2006 Feb 3;340(1):134-9. PMID: 16343425.

B1746 Belinostat

NEW

5 mg
10 mg

PXD101

$C_{15}H_{14}N_2O_4S$ FW: 318.35 [414864-00-9] ≥98%

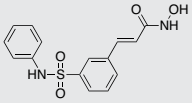

HDAC inhibitor used to treat T cell lymphoma. It also induces apoptosis in pancreatic cancer cells and decreases HIV release from macrophages.

Campbell GR, Bruckman RS, Chu YL, et al. Autophagy Induction by Histone Deacetylase Inhibitors Inhibits HIV Type 1. J Biol Chem. 2015 Feb 20;290(8):5028-40. PMID: 25540204.

Foss F, Advani R, Duvic M, et al. A Phase II trial of Belinostat (PXD101) in patients with relapsed or refractory peripheral or cutaneous T-cell lymphoma. Br J Haematol. 2014 Nov 17. [Epub ahead of print].

B1545 Benzalkonium Bromide

100 g
500 g

[91080-29-4] ≥96%

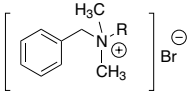

$R = C_8H_{17}$ to $C_{18}H_{37}$

Cationic surfactant used as a disinfectant. It dissociates bacterial lipid membranes, allowing cellular leakage. It is most effective against gram positive bacteria.

Larsen ST, Verder H, Nielsen GD. Airway effects of inhaled quaternary ammonium compounds in mice. Basic Clin Pharmacol Toxicol. 2012 Jun;110(6):537-43. PMID: 22188809.

Saito K, Hayakawa T, Kawabata R, et al. In vitro antibacterial and cytotoxicity assessments of an orthodontic bonding agent containing benzalkonium chloride. Angle Orthod. 2009 Mar;79(2):331-7. PMID: 19216609.

B1853 1,4-Benzoquinone

100 g
500 g

Quinone

$C_6H_4O_2$ FW: 108.09 [106-51-4] ≥98%

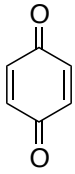

Hydroquinone synthesis precursor and inhibitor of 5-lipoxygenase used as a hydrogen acceptor and oxidant. It prevents leukotriene synthesis and inhibits growth of *Staphylococcus*, *Salmonella*, and *Bacillus*.

Schaible AM, Filosa R, Temml V, et al. Elucidation of the molecular mechanism and the efficacy in vivo of a novel 1,4-benzoquinone that inhibits 5-lipoxygenase. Br J Pharmacol. 2014 May;171(9):2399-412. PMID: 24467325.

Kim MH, Jo SH, Ha KS, et al. Antimicrobial activities of 1,4-benzoquinones and wheat germ extract. J Microbiol Biotechnol. 2010 Aug;20(8):1204-9. PMID: 20798583.

B1753 Benfotiamine

250 mg
1 g
5 g

$C_{19}H_{23}N_4O_6PS$ FW: 466.453 [22457-89-2] ≥98%

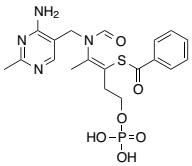

Thiamine/vitamin B derivative and antioxidant. It displays several biological activities, including inhibiting pain neurotransmission, decreasing production of production of amyloid-β, and inhibiting LPS-induced release of leukotrienes, prostaglandins, and thromboxane B2.

Hurt JK, Coleman JL, Fitzpatrick BJ, et al. Prostatic acid phosphatase is required for the antinociceptive effects of thiamine and benfotiamine. PLoS One. 2012;7(10):e48562. PMID: 23119057.

Sun XJ, Zhao L, Zhao N, et al. Benfotiamine prevents increased β-amyloid production in HEK cells induced by high glucose. Neurosci Bull. 2012 Oct;28(5):561-6. PMID: 22961478.

Shoeb M, Ramana KV. Anti-inflammatory effects of benfotiamine are mediated through the regulation of the arachidonic acid pathway in macrophages. Free Radic Biol Med. 2012 Jan 1;52(1):182-90. PMID: 22067901.

B1755 Benzimidazole

5 g
50 g
250 g

$C_7H_6N_2$ FW: 118.14 [51-17-2] ≥98%

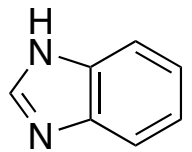

Microtubule polymerization inhibitor and potential topoisomerase I inhibitor. It binds the minor groove of DNA, cleaves supercoiled DNA, and inhibits proliferation of cancer cells when complexed with Cu(II).

Song WJ, Cheng JP, Jiang DH, et al. Synthesis, interaction with DNA and antiproliferative activities of two novel Cu(II) complexes with Schiff base of benzimidazole. Spectrochim Acta A Mol Biomol Spectrosc. 2013 Oct 14;121C:70-76. PMID: 24220672

Molecular basis for benzimidazole resistance from a novel β-tubulin binding site model. J Mol Graph Model. 2013 Sep;45:26-37. PMID: 23995453.

B1652 Benzo[a]pyrene

500 mg
1 g

BP

$C_{20}H_{12}$ FW: 252.32 [50-32-8] ≥98%

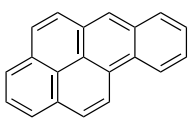

Polycyclic aromatic hydrocarbon found in coal tar, cigarette smoke, and wood smoke. Induces carcinogenesis in research models.

Gao L, Mai A, Li X, et al. LncRNA-DQ786227-mediated cell malignant transformation induced by benzo(a) pyrene. Toxicol Lett. 2013 Nov 25;223(2):205-10. PMID: 24084393.

Naveenkumar C, Raghunandakumar S, Asokkumar S, et al. Mitigating role of baicalein on lysosomal enzymes and xenobiotic metabolizing enzyme status during lung carcinogenesis of Swiss albino mice induced by benzo(a) pyrene. Fundam Clin Pharmacol. 2014 Jun;28(3):310-22. PMID: 23834621.

B1955 Benztropine Mesylate

NEW

1 g
5 g
25 g

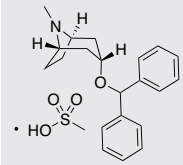

$C_{21}H_{25}NO \bullet CH_4O_3S$ FW: 403.53 [132-17-2] ≥98%

DAT inhibitor. It potentiates dopamine overflow in rat brain slices.

Ukairo OT, Bondi CD, Newman AH, et al. Recognition of benztropine by the dopamine transporter (DAT) differs from that of the classical dopamine uptake inhibitors cocaine, methylphenidate, and mazindol as a function of a DAT transmembrane 1 aspartic acid residue. J Pharmacol Exp Ther. 2005 Aug;314(2):575-83. PMID: 15879005.

Wieczorek WJ, Kruk ZL. A quantitative comparison on the effects of benztropine, cocaine and nomifensine on electrically evoked dopamine overflow and rate of re-uptake in the caudate putamen and nucleus accumbens in the rat brain slice. Brain Res. 1994 Sep 19;657(1-2):42-50. PMID: 7820642.

B1640 Benzydamine Hydrochloride

5 g
25 g

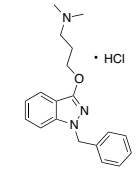

$C_{19}H_{23}N_3O \bullet HCl$ FW: 345.87 [132-69-4] ≥98%

NSAID and prostaglandin synthetase inhibitor used to treat mucositis and sore throat. It does not inhibit COX.

Chen CY, Kuo CJ, Lee YW, et al. Benzydamine hydrochloride on postoperative sore throat: a meta-analysis of randomized controlled trials. Can J Anaesth. 2014 Mar;61(3):220-8. PMID: 24263969.

Karavana Hizarcioğlu SY, Sezer B, Güneri P, et al. Efficacy of topical benzydamine hydrochloride gel on oral mucosal ulcers: an in vivo animal study. Int J Oral Maxillofac Surg. 2011 Sep;40(9):973-8. PMID: 21549562.

B1855 O6-Benzylguanine

50 mg
250 mg
1 g

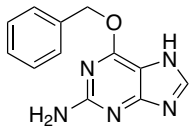

$C_{12}H_{11}N_5O$ FW: 241.25 [19916-73-5] ≥98%

MGMT inhibitor that prevents repair of DNA damage induced by chemotherapeutics. It allows apoptosis and other mechanisms of cell death to occur.

Qian L, Zheng J, Wang K, et al. Cationic core-shell nanoparticles with carmustine contained within O6-benzyl-guanine shell for glioma therapy. Biomaterials. 2013 Nov;34(35):8968-78. PMID: 23953782.

Quinn JA, Jiang SX, Reardon DA, et al. Phase II trial of temozolomide plus o6-benzylguanine in adults with recurrent, temozolomide-resistant malignant glioma. J Clin Oncol. 2009 Mar 10;27(8):1262-7. PMID: 19204199.

B1653 Benzyl Isothiocyanate

5 g
10 g

Isothiocyanic acid benzyl ester

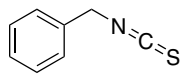

C_8H_7NS FW: 149.22 [622-78-6] ≥97%

Antioxidant. Induces apoptosis and autophagy and suppresses tumor growth in cancer models. It also increases activity of phase II enzymes and suppresses generation of ROS, decreasing oxidative stress in cardiovascular disease models.

Tang Y, Abe N, Yoshimoto M, et al. Benzyl isothiocyanate inhibits IL-13 expression in human basophilic KU812 cells. Biosci Biotechnol Biochem. 2014 Sep 25:1-5. PMID: 25253661.

Kim M, Cho HJ, Kwon GT, et al. Benzyl isothiocyanate suppresses high-fat diet-stimulated mammary tumor progression via the alteration of tumor microenvironments in obesity-resistant BALB/c mice. Mol Carcinog. 2014 Apr 11. [Epub ahead of print]. PMID: 24729546.

B1654 Benzyl Selenocyanate

50 mg
100 mg
500 mg

Selenocyanic acid benzyl ester

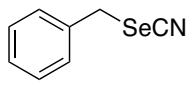

C_8H_7NSe FW: 196.11 [4671-93-6] ≥98%

DNA cytosine methyltransferase inhibitor found in selenium-enriched garlic; may inhibit PKA and PKC. It prevents carcinogenesis induced by DMBA, azoxymethane, and benzo[a]pyrene.

El-Bayoumy K, Sinha R, Pinto JT, et al. Cancer chemoprevention by garlic and garlic-containing sulfur and selenium compounds. J Nutr. 2006 Mar;136(3 Suppl):864S-869S. PMID: 16484582.

Fiala ES, Staretz ME, Pandya GA, et al. Inhibition of DNA cytosine methyltransferase by chemopreventive selenium compounds, determined by an improved assay for DNA cytosine methyltransferase and DNA cytosine methylation. Carcinogenesis. 1998 Apr;19(4):597-604. PMID: 9600343.

B1655 S-(N-Benzylthiocarbamoyl)-L-cysteine

500 mg
1 g
5 g

Benzyl isothiocyanate cysteine conjugate

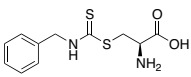

$C_{11}H_{14}N_2O_2S_2$ FW: 270.37 [35446-36-7] ≥98%

Cysteine conjugate of benzyl isothiocyanate, N-dimethylnitrosamine demethylase inhibitor. It induces apoptosis in bladder cancer cells and inhibits cell growth in leukemia cells.

Tang L, Li G, Song L, et al. The principal urinary metabolites of dietary isothiocyanates, N-acetylcysteine conjugates, elicit the same anti-proliferative response as their parent compounds in human bladder cancer cells. Anticancer Drugs. 2006 Mar;17(3):297-305. PMID: 16520658.

Jiao D, Conaway CC, Wang MH, et al. Inhibition of N-nitrosodimethylamine demethylase in rat and human liver microsomes by isothiocyanates and their glutathione, L-cysteine, and N-acetyl-L-cysteine conjugates. Chem Res Toxicol. 1996 Sep;9(6):932-8. PMID: 8870979.

B1656 Benzyl Thiocyanate

50 g
100 g

Benzyl rhodanide

C_8H_7NS FW: 149.21 [3012-37-1] ≥98%

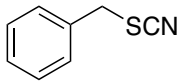

Chemopreventive. It inhibits cell proliferation in colorectal cancer cells and suppresses MAM acetate-induced carcinogenesis in vivo.

Musk SR, Stephenson P, Smith TK, et al. Selective toxicity of compounds naturally present in food toward the transformed phenotype of human colorectal cell line HT29. Nutr Cancer. 1995;24(3):289-98. PMID: 8610048.

Sugie S, Okamoto K, Okumura A, et al. Inhibitory effects of benzyl thiocyanate and benzyl isothiocyanate on methylazoxymethanol acetate-induced intestinal carcinogenesis in rats. Carcinogenesis. 1994 Aug;15(8):1555-60. PMID: 8055633.

B1870 Berberine Chloride

5 g
10 g

$C_{20}H_{17}NO_4 \bullet Cl$ FW: 371.82 [633-65-8] ≥97%

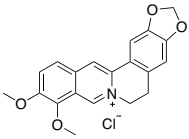

Inhibitor of oligopeptidase and AChE and potential σ receptor modulator found in various plant sources. It is used to stain heparin in mast cells. It also increases levels of 5-HT, DA, and NE and displays protective effects in Alzheimer's disease, cerebral ischemia, and depression.

Huang L, Shi A, He F, et al. Synthesis, biological evaluation, and molecular modeling of berberine derivatives as potent acetylcholinesterase inhibitors. Bioorg Med Chem. 2010 Feb;18(3):1244-51. PMID: 20056426.

Tarrago T, Kichik N, Seguí J, et al. The natural product berberine is a human prolyl oligopeptidase inhibitor. ChemMedChem. 2007 Mar;2(3):354-9. PMID: 17295371.

Kulkarni SK, Dhir A. Berberine: a plant alkaloid with therapeutic potential for central nervous system disorders. Phytother Res. 2010 Mar;24(3):317-24. PMID: 19998323.

B1769 Bergenin

1 mg
5 mg
10 mg

$C_{14}H_{16}O_9$ FW: 328.27 [477-90-7 ≥98%

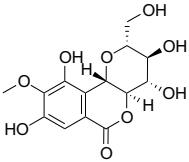

Found in *Bergenia*. It displays many activities, including suppressing pro-inflammatory cytokine release and edema, limiting growth of *Plasmodium*, preventing mechanical hyperalgesia, and inhibiting TPA- and DMBA-induced tumor development.

Jain SK, Singh S, Khajuria A, et al. Pyrano-isochromanones as IL-6 Inhibitors: Synthesis, in Vitro and in Vivo Antiarthritic Activity. J Med Chem. 2014 Aug 28;57(16):7085-97. PMID: 25111439.

Liang J, Li Y, Liu X, et al. In vivo and in vitro antimalarial activity of bergenin. Biomed Rep. 2014 Mar;2(2):260-264. PMID: 24649107.

Zhang J, Nishimoto Y, Tokuda H, et al. Cancer chemopreventive effect of bergenin from Peltophorum pterocarpum wood. Chem Biodivers. 2013 Oct;10(10):1866-75. PMID: 24130029.

B1668 Berteroin

25 mg
50 mg
100 mg
500 mg

5-Methylthiopentyl isothiocyanate

$C_7H_{13}NS_2$ FW: 175.43 [4430-42-6] ≥97%

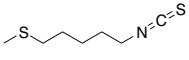

Erucin homolog and potential antioxidant. It decreases expression of androgen receptors in prostate cancer cells. It also decreases release of pro-inflammatory cytokines in LPS-stimulated macrophages.

Jung YJ, Jung JI, Cho HJ, et al. Berteroin present in cruciferous vegetables exerts potent anti-inflammatory properties in murine macrophages and mouse skin. Int J Mol Sci. 2014 Nov 11;15(11):20686-705. PMID: 25393510.

Kim MJ, Kim SH, Lim SJ. Comparison of the apoptosis-inducing capability of sulforaphane analogues in human colon cancer cells. Anticancer Res. 2010 Sep;30(9):3611-9. PMID: 20944144.

Kim SH, Singh SV. D,L-Sulforaphane causes transcriptional repression of androgen receptor in human prostate cancer cells. Mol Cancer Ther. 2009 Jul;8(7):1946-54. PMID: 19584240.

B1973 Besifloxacin Hydrochloride

25 mg
100 mg
250 mg

$C_{19}H_{22}ClFN_3O_3 \bullet HCl$ FW: 430.31 [405165-61-9] ≥98%

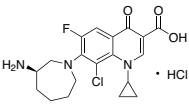

Topoisomerase IV and bacterial DNA gyrase inhibitor. It also inhibits production of IL-1R, IL-6, IL-1-β, and MCP-1.

Miller D, Chang JS, Flynn HW, et al. Comparative in vitro susceptibility of besifloxacin and seven comparators against ciprofloxacin- and methicillin-susceptible/nonsusceptible staphylococci. J Ocul Pharmacol Ther. 2013 Apr;29(3):339-44. PMID: 23289847.

Lan W, Petznick A, Heryati S, et al. Nuclear Factor-κB: central regulator in ocular surface inflammation and diseases. Ocul Surf. 2012 Jul;10(3):137-48. PMID: 22814642.

Cambau E, Matrat S, Pan XS, et al. Target specificity of the new fluoroquinolone besifloxacin in *Streptococcus* pneumoniae, *Staphylococcus aureus* and *Escherichia* coli. J Antimicrob Chemother. 2009 Mar;63(3):443-50. PMID: 19147516.

B1874 Bestatin Hydrochloride

1 mg
5 mg
10 mg
25 mg

Ubenimex hydrochloride

$C_{16}H_{24}N_2O_4 \cdot HCl$ FW: 344.87 [65391-42-6] ≥98%

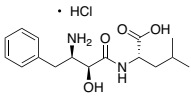

Aminopeptidase (N/CD13) inhibitor. It induces differentiation of acute promyelocytic leukemia cells, enhances proliferation of bone marrow macrophage progenitor cells, and inhibits catabolism of opioid endopeptides.

Hitzerd SM, Verbrugge SE, Ossenkoppele G, et al. Positioning of aminopeptidase inhibitors in next generation cancer therapy. Amino Acids. 2014 Apr;46(4):793-808. PMID: 24385243.

Qian X, He J, Zhao Y, et al. Inhibition of p38 MAPK Phosphorylation Is Critical for Bestatin to Enhance ATRA-Induced Cell Differentiation in Acute Promyelocytic Leukemia NB4 Cells. Am J Ther. 2013 Oct 17. [Epub ahead of print]. PMID: 24141198.

Jia MR, Wei T, Xu WF. The Analgesic Activity of Bestatin as a Potent APN Inhibitor. Front Neurosci. 2010 Jun 28;4:50. PMID: 20631848.

B1876 Betamethasone

100 mg
500 mg

$C_{22}H_{29}FO_5$ FW: 392.46 [378-44-9] ≥98%

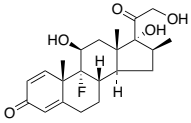

Glucocorticoid receptor agonist used to treat skin irritation and to accelerate preterm fetal lung development.

Shepherd J, Taheri A, Feldman SR. Once-daily topical treatment for psoriasis: calcipotriene + betamethasone two-compound topical formulation. Clin Cosmet Investig Dermatol. 2013 Dec 19;7:19-22. PMID: 24379688.

Waffarn F, Davis EP. Effects of antenatal corticosteroids on the hypothalamic-pituitary-adrenocortical axis of the fetus and newborn: experimental findings and clinical considerations. Am J Obstet Gynecol. 2012 Dec;207(6):446-54. PMID: 22840973.

B1878 Betamethasone 21-Phosphate Sodium

250 mg
1 g

$C_{22}H_{28}FNa_2O_8P$ FW: 516.4 [151-73-5] ≥98%

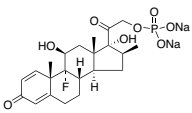

Derivative of betamethasone and glucocorticoid receptor agonist used to treat skin irritation and to accelerate preterm fetal lung development.

Shepherd J, Taheri A, Feldman SR. Once-daily topical treatment for psoriasis: calcipotriene + betamethasone two-compound topical formulation. Clin Cosmet Investig Dermatol. 2013 Dec 19;7:19-22. PMID: 24379688.

Waffarn F, Davis EP. Effects of antenatal corticosteroids on the hypothalamic-pituitary-adrenocortical axis of the fetus and newborn: experimental findings and clinical considerations. Am J Obstet Gynecol. 2012 Dec;207(6):446-54. PMID: 22840973.

B1879 Betamethasone Valerate

25 mg
100 mg
500 mg

$C_{27}H_{37}FO_6$ FW: 476.58 [2152-44-5] ≥98%

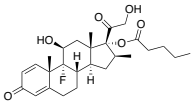

Synthetic glucocorticoid receptor agonist used to treat skin irritation and to accelerate preterm fetal lung development. It impairs maturation and viability of Langerhans and epidermal cells and inhibits vasodilatory responses in skin.

Naldi L, Yawalkar N, Kaszuba A, et al. Efficacy and safety of the Betamethasone valerate 0.1% plaster in mild-to-moderate chronic plaque psoriasis: a randomized, parallel-group, active-controlled, phase III study. Am J Clin Dermatol. 2011 Jun 1;12(3):191-201. PMID: 21284407.

Meindl S, Vaculik C, Meingassner JG, et al. Differential effects of corticosteroids and pimecrolimus on the developing skin immune system in humans and mice. J Invest Dermatol. 2009 Sep;129(9):2184-92. PMID: 19295616.

Leivo T, Arjomaa P, Oivula J, et al. Differential modulation of transforming growth factor-beta by betamethasone-17- valerate and isotretinoin: corticosteroid decreases and isotretinoin increases the level of transforming growth factor-beta in suction blister fluid. Skin Pharmacol Appl Skin Physiol. 2000 May-Aug;13(3-4):150-6. PMID: 10859533.

B1977 Betulin

NEW

500 mg
1 g
5 g

$C_{30}H_{50}O_2$ FW: 442.72 [473-98-3] ≥98%

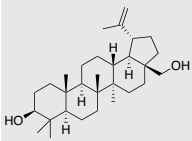

Found in various plant sources. It displays many biological activities, including decreasing symptoms of ethanol-induced fatty liver, inhibiting acidophilic necrosis, suppressing production and migration of ROS, and inducing apoptosis in cancer cells.

Wan Y, Jiang S, Lian LH, et al. Betulinic acid and betulin ameliorate acute ethanol-induced fatty liver via TLR4 and STAT3 in vivo and in vitro. Int Immunopharmacol. 2013 Jun 28;17(2):184-190. [Epub ahead of print] PMID: 23816536.

Jonnalagadda SC, Corsello MA, Sleet CE. Betulin-Betulinic Acid Natural Product Based Analogs as Anti-Cancer Agents. Anticancer Agents Med Chem. 2013 Jun 11. [Epub ahead of print] PubMed PMID: 23848199.

Szuster-Ciesielska A, Plewka K, Kandefer-Szerszeń M. Betulin, betulinic acid and butein are inhibitors of acetaldehyde-induced activation of liver stellate cells. Pharmacol Rep. 2011;63(5):1109-23. PMID: 22180353.

B1978 Betulin-3-Acetate

NEW — Please inquire

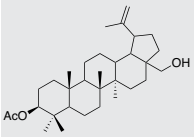

$C_{32}H_{52}O_3$ FW: 484.75 ≥97%

Betulin derivative found in various plant sources. It decreases inflammation, potentially induces apoptosis in cancer cells, and inhibits alphavirus replication.

Pohjala L, Alakurtti S, Ahola T, et al. Betulin-derived compounds as inhibitors of alphavirus replication. J Nat Prod. 2009 Nov;72(11):1917-26. PMID: 19839605.

B1979 Betulinic Acid

10 mg
50 mg
250 mg

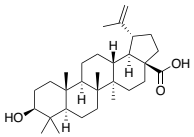

$C_{30}H_{48}O_3$ FW: 456.7 [472-15-1] ≥98%

It prevents platelet aggregation, promotes cholesterol efflux in macrophages, decreases atherosclerotic lesion size, and induces cell cycle arrest and apoptosis in cancer cells.

Zhao GJ, Tang SL, Lv YC, et al. Antagonism of Betulinic Acid on LPS-Mediated Inhibition of ABCA1 and Cholesterol Efflux through Inhibiting Nuclear Factor-kappaB Signaling Pathway and miR-33 Expression. PLoS One. 2013 Sep 25;8(9):e74782. PMID: 24086374.

Hsu TI, Wang MC, Chen SY, et al. Betulinic acid decreases specificity protein 1 (Sp1) level via increasing the sumoylation of sp1 to inhibit lung cancer growth. Mol Pharmacol. 2012 Dec;82(6):1115-28. PMID: 22956772.

Qian LB, Fu JY, Cai X, et al. Betulinic acid inhibits superoxide anion-mediated impairment of endothelium-dependent relaxation in rat aortas. Indian J Pharmacol. 2012 Sep-Oct;44(5):588-92. PMID: 23112419.

B1992 Bexarotene

25 mg
100 mg
250 mg

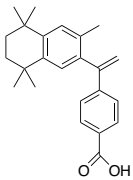

LGD-1069

$C_{24}H_{28}O_2$ FW: 348.48 [153559-49-0] ≥98%

RXR agonist used to treat cutaneous T cell lymphoma. It also induces apoptosis in cancer cells, decreases serum triglyceride levels, reverses behavioral deficits induced by 6-OH DA, and induces ApoE-dependent clearance of amyloid-β plaques.

McFarland K, Spalding TA, Hubbard D, et al. Low Dose Bexarotene Treatment Rescues Dopamine Neurons and Restores Behavioral Function in Models of Parkinson's Disease. ACS Chem Neurosci. 2013 Oct 11. [Epub ahead of print]. PMID: 24117438.

Schadt CR. Topical and oral bexarotene. Dermatol Ther. 2013 Sep;26(5):400-3. PMID: 24099070.

Aicardi G. New Hope from an Old Drug: Fighting Alzheimer's Disease with the Cancer Drug Bexarotene (Targretin)? Rejuvenation Res. 2013 Sep 19. [Epub ahead of print]. PMID: 24047423.

B1996 BEZ235

NEW

10 mg
25 mg
100 mg

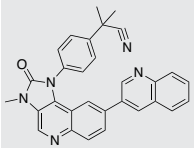

NVP-BEZ235; Dactolisib

$C_{30}H_{23}N_5O$ FW: 469.54 [915019-65-7] ≥98%

PI3K and mTOR inhibitor. It induces cell cycle arrest and apoptosis in nasopharyngeal cancer cells and induces apoptosis and autophagy in hepatocellular carcinoma cells.

Ma BB, Lui VW, Hui CW, et al. Preclinical evaluation of the mTOR-PI3K inhibitor BEZ235 in nasopharyngeal cancer models. Cancer Lett. 2014 Feb 1;343(1):24-32. PMID: 24041865.

Yothaisong S, Dokduang H, Techasen A, et al. Increased activation of PI3K/AKT signaling pathway is associated with cholangiocarcinoma metastasis and PI3K/mTOR inhibition presents a possible therapeutic strategy. Tumour Biol. 2013 Dec;34(6):3637-48. PMID: 23832540.

Chang Z, Shi G, Jin J, et al. Dual PI3K/mTOR inhibitor NVP-BEZ235-induced apoptosis of hepatocellular carcinoma cell lines is enhanced by inhibitors of autophagy. Int J Mol Med. 2013 Jun;31(6):1449-56. PMID: 23588698.

B1898 Bezafibrate

1 g
5 g
25 g

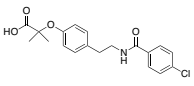

$C_{19}H_{20}ClNO_4$ FW: 361.82 [41859-67-0] ≥98%

PPARα agonist used to lower LDL and triglyceride levels. It also decreases risk of myocardial infarction, delays the onset of type 2 diabetes, promotes bone formation, and suppresses angiogenesis and tumor growth in models of non-small cell lung cancer.

Skrypnyk N, Chen X, Hu W, et al. PPARα activation can help prevent and treat non-small cell lung cancer. Cancer Res. 2014 Jan 15;74(2):621-31. PMID: 24302581.

Zhong X, Xiu LL, Wei GH, et al. Bezafibrate enhances proliferation and differentiation of osteoblastic MC3T3-E1 cells via AMPK and eNOS activation. Acta Pharmacol Sin. 2011 May;32(5):591-600. PMID: 21499286.

Tenenbaum A, Motro M, Fisman EZ, et al. Bezafibrate for the secondary prevention of myocardial infarction in patients with metabolic syndrome. Arch Intern Med. 2005 May 23;165(10):1154-60. PMID: 15911729.

B3200 BI-2536

NEW

5 mg
10 mg

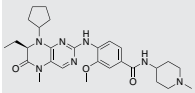

$C_{28}H_{39}N_7O_3$ FW: 521.65 [755038-02-9] ≥98%

PLK1 inhibitor. It disrupts mitosis and cell division and may induce apoptosis in cancer cells.

Colnaghi R, Wheatley SP. Liaisons between survivin and Plk1 during cell division and cell death. J Biol Chem. 2010 Jul 16;285(29):22592-604. PMID: 20427271.

Zhang J, Yang PL, Gray NS. Targeting cancer with small molecule kinase inhibitors. Nature Reviews Cancer. 2009 Jan;9:28-39.

B3300 BI-6727

NEW

5 mg
10 mg

Volasertib

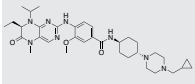

$C_{34}H_{50}N_8O_3$ FW: 618.81 [755038-65-4] ≥99%

PLK1 inhibitor. It induces apoptosis in acute myelogenous leukemia cells.

Münch C, Dragoi D, Frey AV, et al. Therapeutic polo-like kinase 1 inhibition results in mitotic arrest and subsequent cell death of blasts in the bone marrow of AML patients and has similar effects in non-neoplastic cell lines. Leuk Res. 2015 Jan 28. [Epub ahead of print]. PMID: 25697066.

Gjertsen BT, Schöffski P. Discovery and development of the Polo-like kinase inhibitor volasertib in cancer therapy. Leukemia. 2015 Jan;29(1):11-9. PMID: 25027517.

Lin CC, Su WC, Yen CJ, et al. A phase I study of two dosing schedules of volasertib (BI 6727), an intravenous polo-like kinase inhibitor, in patients with advanced solid malignancies. Br J Cancer. 2014 May 13;110(10):2434-40. PMID: 24755882.

B3203 Biapenem

10 mg
25 mg
100 mg

L-627; CL-186,815; LJ-C10,627

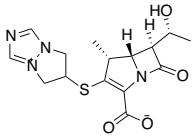

$C_{15}H_{18}N_4O_4S$ FW: 350.39 [120410-24-4] ≥98%

Penicillin binding protein inhibitor that prevents cell wall synthesis and is used to treat respiratory and urinary tract infections. It inhibits growth of *Bacteriodes*, *Prevotella*, *Clostridium*, and *Pseudomonas*.

Wang X, Zhang X, Zong Z, et al. Biapenem versus meropenem in the treatment of bacterial infections: a multicenter, randomized, controlled clinical trial. Indian J Med Res. 2013 Dec;138(6):995-1002. PMID: 24521647.

Yamachika S, Sugihara C, Kamai Y, et al. Correlation between penicillin-binding protein 2 mutations and carbapenem resistance in *Escherichia* coli. J Med Microbiol. 2013 Mar;62(Pt 3):429-36. PMID: 23222859.

B3209 Bicalutamide

100 mg
250 mg
1 g

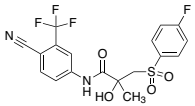

$C_{18}H_{14}F_4N_2O_4S$ FW: 430.37 [90357-06-5] ≥98%

Androgen receptor antagonist used to treat prostate cancer and hirsutism. It binds the androgen receptor in two sites, distorting coactivator binding and inhibiting transcription. It also induces apoptosis in prostate cancer cells and decreases plasma PSA levels.

Squillace RM, Miller D, Wardwell SD, et al. Synergistic activity of the mTOR inhibitor ridaforolimus and the antiandrogen bicalutamide in prostate cancer models. Int J Oncol. 2012 Aug;41(2):425-32. PMID: 22614157.

Yan J, Xie B, Capodice JL, et al. Zyflamend inhibits the expression and function of androgen receptor and acts synergistically with bicalutimide to inhibit prostate cancer cell growth. Prostate. 2012 Feb;72(3):244-52. PMID: 21656835.

B3210 R-Bicalutamide

100 mg
250 mg
1 g

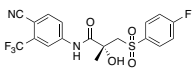

$C_{18}H_{14}F_4N_2O_4S$ FW: 430.37 [113299-40-4] ≥98%

Androgen receptor antagonist used to treat prostate cancer and hirsutism. It binds the androgen receptor in two sites, distorting coactivator binding and inhibiting transcription. It also induces apoptosis in prostate cancer cells and decreases plasma PSA levels.

Squillace RM, Miller D, Wardwell SD, et al. Synergistic activity of the mTOR inhibitor ridaforolimus and the antiandrogen bicalutamide in prostate cancer models. Int J Oncol. 2012 Aug;41(2):425-32. PMID: 22614157.

B3211 (+)-Bicuculline

25 mg
100 mg
500 mg

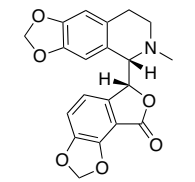

$C_{20}H_{17}NO_6$ FW: 367.35 [485-49-4] ≥98%

GABA-A receptor antagonist and NMDA receptor potentiator used to study GABA signaling. It induces membrane depolarization and prolongs Ca^{2+}-dependent action potentials in neurons.

Dela Peña IJ, Lee HL, Yoon SY, et al. The ethanol extract of Cirsium japonicum increased chloride ion influx through stimulating GABA(A) receptor in human neuroblastoma cells and exhibited anxiolytic-like effects in mice. Drug Discov Ther. 2013 Feb;7(1):18-23. PMID: 23524939.

Torkaman-Boutorabi A, Soltani S, Oryan S, et al. Involvement of the dorsal hippocampal GABA-A receptors in histamine-induced facilitation of memory in the Morris water maze. Pharmacol Biochem Behav. 2013 Apr;105:142-50. PMID: 23438692.

B3320

Bifonazole

1 g
5 g
25 g

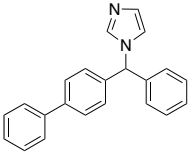

$C_{22}H_{18}N_2$ FW: 310.39 [60628-96-8] ≥98%

Inhibitor of 14-α demethylase, HMG-CoA reductase, and calmodulin-that inhibits ergosterol synthesis and fungal cell wall formation. It also reduces viability of prostate cancer cells and melanoma cells.

Cheng JS, Chou CT, Liang WZ, et al. The mechanism of bifonazole-induced [Ca^{2+}]i rises and non-Ca^{2+}-trig-gered cell death in PC3 human prostate cancer cells. J Recept Signal Transduct Res. 2014 May 22:1-7. PMID: 24849495.

Penso J, Beitner R. Clotrimazole and bifonazole detach hexokinase from mitochondria of melanoma cells. Eur J Pharmacol. 1998 Jan 19;342(1):113-7. PMID: 9544799.

Hegemann L, Toso SM, Lahijani KI, et al. Direct interaction of antifungal azole-derivatives with calmodulin: a possible mechanism for their therapeutic activity. J Invest Dermatol. 1993 Mar;100(3):343-6. PMID: 8440921.

B3324

Big Endothelin-1 (1-38), human

0.5 mg
1 mg
2.5 mg

H-Cys-Ser-Cys-Ser-Ser-Leu-Met-Asp-Lys-Glu-Cys-Val-Tyr-Phe-Cys-His-Leu-Asp-Ile-Ile-Trp-Val-Asn-Thr-Pro-Glu-His-Val-Val-Pro-Tyr-Gly-Leu-Gly-Ser-Pro-Arg-Ser-OH
(Cys1-Cys15, Cys3-Cys11)

$C_{189}H_{282}N_{48}O_{56}S_5$ FW: 4282.96 [124363-98-0] ≥95%

Endogenous endothelin-1 precursor and endothelin-A/B/C receptor agonist. It increases arteriolar constriction and decreases blood flow.

Lawrence E, Brain SD. Big endothelin-1 and big endothelin-3 are constrictor agents in the microvasculature: evidence for the local phosphoramidon-sensitive conversion of big endothelin-1. Eur J Pharmacol. 1993 Mar 23;233(2-3):243-50. PMID: 8467870.

Kohno M, Yasunari K, Yokokawa K, et al. Inhibition by atrial and brain natriuretic peptides of endothelin-1 secretion after stimulation with angiotensin II and thrombin of cultured human endothelial cells. J Clin Invest. 1991 Jun;87(6):1999-2004. PMID: 1645748.

B3345

(−)-Bilobalide

5 mg
10 mg
25 mg

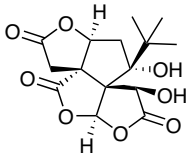

$C_{15}H_{18}O_8$ FW: 326.3 [33570-04-6] ≥98%

GABA-A receptor antagonist found in *Ginkgo*. It decreases anxiety and improves spatial learning and memory, lowers edema and infarct volume in cerebral ischemia/reperfusion models, and inhibits carrageenan- and capsaicin-induced hyperalgesia.

A P, V M N, S S A, et al. Bilobalide attenuates hypoxia induced oxidative stress, inflammation, and mitochondrial dysfunctions in 3T3 L1 adipocytes via its antioxidant potential. Free Radic Res. 2014 Jul 21:1-31. PMID: 25039303.

Goldie M, Dolan S. Bilobalide, a unique constituent of *Ginkgo* biloba, inhibits inflammatory pain in rats. Behav Pharmacol. 2013 Aug;24(4):298-306. PMID: 23838965.

Ma L, Wang S, Tai F, et al. Effects of bilobalide on anxiety, spatial learning, memory and levels of hippocampal glucocorticoid receptors in male Kunming mice. Phytomedicine. 2012 Dec 15;20(1):89-96. PMID: 23083816.

B3358

Biochanin A

100 mg
250 mg
1 g

4'-Methylgenistein

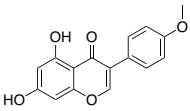

$C_{16}H_{12}O_5$ FW: 284.27 [491-80-5] ≥98%

Potential PPARα and PPARγ agonist found in *Fabaceae* plants such as clover, soy, and alfalfa. It prevents replication of influenza virus, improves cognitive deficits, induces osteoblast differentiation, inhibits migration, invasion, and proliferation of pancreatic cancer cells, and suppresses production of pro-inflammatory cytokines.

Wang L, Waltenberger B, Pferschy-Wenzig EM, et al. Natural product agonists of peroxisome proliferator-activated receptor gamma (PPARγ): a review. Biochem Pharmacol. 2014 Jul 30. [Epub ahead of print]. PMID: 25083916.

Biradar SM, Joshi H, Chheda TK. Biochanin-A ameliorates behavioural and neurochemical derangements in cognitive-deficit mice for the betterment of Alzheimer's disease. Hum Exp Toxicol. 2014 Apr;33(4):369-82. PMID: 23900307.

Bhardwaj V, Tadinada SM, Jain A, et al. Biochanin A reduces pancreatic cancer survival and progression. Anticancer Drugs. 2014 Mar;25(3):296-302. PMID: 24201306.

B3458

Biopterin

5 mg
10 mg
25 mg

Pterin HB2

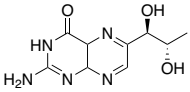

$C_9H_{11}N_5O_3$ FW: 237.22 [22150-76-1] ≥98%

Endogenous pterin coenzyme required for production of neurotransmitters and release of NO.

Longo N. Disorders of biopterin metabolism. J Inherit Metab Dis. 2009 Jun;32(3):333-42. Erratum in: J Inherit Metab Dis. 2009 Jun;32(3):457. PMID: 19234759.

Li HY, Yao YM, Shi ZG. The biological effect of tetrahydrobiopterin and its potential role in sepsis. Sheng Li Ke Xue Jin Zhan. 1999 Oct;30(4):303-8. PMID: 12532822.

B3278 Biotin

500 mg
1 g
5 g
10 g

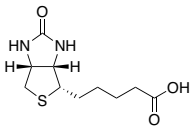

Biodermatin; Coenzyme R; Vitamin H

$C_{10}H_{16}N_2O_3S$ FW: 244.31 [58-85-5] ≥98%

Water-soluble coenzyme vitamin (B7) found in various foods, It is involved in synthesis of fatty acids and amino acids and is important in gluconeogenesis. It is found attached to lysine residues on histones and modulates gene expression.

Lietzan AD, St Maurice M. Functionally diverse biotin-dependent enzymes with oxaloacetate decarboxylase activity. Arch Biochem Biophys. 2014 Feb 15;544:75-86. PMID: 24184447.

Trippier PC. Synthetic strategies for the biotinylation of bioactive small molecules. ChemMedChem. 2013 Feb;8(2):190-203. PMID: 23303486.

Zempleni J, Wijeratne SS, Hassan YI. Biotin. Biofactors. 2009 Jan-Feb;35(1):36-46. PMID: 19319844.

B3374 Bisacodyl

10 g
25 g

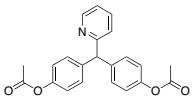

$C_{22}H_{19}NO_4$ FW: 361.39 [603-50-9] ≥98%

Diphenylmethane derivative and Na^+/K^+ ATPase inhibitor that stimulates colonic muscle contractions. It indirectly activates PKC, downregulates the expression of aquaporin 3 channels, stimulates enteric nerves, and increases NaCl secretion.

Ikarashi N, Baba K, Ushiki T, et al. The laxative effect of bisacodyl is attributable to decreased aquaporin-3 expression in the colon induced by increased PGE2 secretion from macrophages. Am J Physiol Gastrointest Liver Physiol. 2011 Nov;301(5):G887-95.PMID: 21868635.

Manabe N, Cremonini F, Camilleri M, et al. Effects of bisacodyl on ascending colon emptying and overall colonic transit in healthy volunteers. Aliment Pharmacol Ther. 2009 Nov 1;30(9):930-6. PMID: 19678812.

Beubler E, Schirgi-Degen A. Stimulation of enterocyte protein kinase C by laxatives in-vitro. J Pharm Pharmacol. 1993 Jan;45(1):59-62. PMID: 8094448.

B3472 4,4'-(1,1'-Biphenyl-4,4'-diyldioxy)dianiline NEW

5 g
25 g
100 g

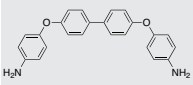

4,4'-Bis(4-aminophenoxy)biphenyl

$C_{24}H_{20}N_2O_2$ FW: 368.43 [13080-85-8] ≥98%

Potential inhibitor of VEGFR2, Met, RET, Axl, Ron, PDGFR, FGFR1, and FLT1/3/4. It may decrease angiogenesis and suppress proliferation in cancer cells.

B3373 Bis(aziridinyl)methylamino Phosphine Sulfide

500 mg
1 g
5 g

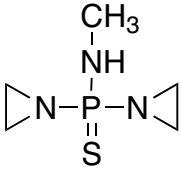

Bisazir

$C_3H_{12}N_3PS$ FW: 177.21 [13687-09-7] ≥98%

Mutagen used to sterilize male insects and lamprey eels. It induces DNA fragmentation in spermatozoa.

Ciereszko A, Wolfe TD, Dabrowski K. Analysis of DNA damage in sea lamprey (Petromyzon marinus) spermatozoa by UV, hydrogen peroxide, and the toxicant bisazir. Theriogenology. Aquat Toxicol. 2005 Jun 15;73(2):128-38. PMID: 15885821.

Ciereszko A, Babiak I, Dabrowski K. Efficacy of animal anti-fertility compounds against sea lamprey (Petromyzon marinus) spermatozoa. Theriogenology. 2004 Apr 15;61(6):1039-50. PMID: 15036993.

Srivastava VK, Kumar K. Effect of the chemosterilant bisazir on the testes of the spotted bollworm Earias fabia stoll. Toxicology. 1984 Jun;31(3-4):335-42. PMID: 6740707.

B3573 Bisdemethoxycurcumin

5 mg
10 mg
25 mg

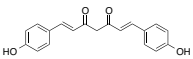

$C_{19}H_{16}O_4$ FW: 308.33 [24939-16-0] ≥98%

Curcumin derivative, inhibitor of DNMT1, α-amylase, and WIF-1 promoter demethylation, and potential activator of SIRT1 and AMPK. It inhibits Wnt signaling, induces apoptosis in non-small cell lung cancer cells, inhibits PDGF signaling in smooth muscle cells, and inhibits growth of gram positive bacteria.

Li YB, Zhong ZF, Chen MW, et al. Bisdemethoxycurcumin Increases Sirt1 to Antagonize t-BHP-Induced Premature Senescence in WI38 Fibroblast Cells. Evid Based Complement Alternat Med. 2013;2013:851714. Epub 2013 Sep 2. PMID: 24078830.

Li YB, Gao JL, Zhong ZF, et al. Bisdemethoxycurcumin suppresses MCF-7 cells proliferation by inducing ROS accumulation and modulating senescence-related pathways. Pharmacol Rep. 2013;65(3):700-9. PMID: 23950593.

Hua Y, Dolence J, Ramanan S, et al. Bisdemethoxycurcumin inhibits PDGF-induced vascular smooth muscle cell motility and proliferation. Mol Nutr Food Res. 2013 Sep;57(9):1611-8. PMID: 23554078.

B3272 Bis(3,5-dibromosalicyl) Fumarate

100 mg
500 mg
1 g
5 g

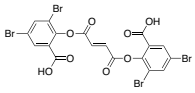

$C_{18}H_8O_8Br_4$ FW: 671.87 [71337-53-6] ≥91%

Aspirin analog, induces hemoglobin chain cross-linking. It is used to study hemoglobin function in research models. It also decreases carageenan-induced inflammation in animal models.

Macdonald VW, Motterlini R. Vasoconstrictor effects in isolated rabbit heart perfused with bis(3,5-dibromosalicyl)fumarate cross-linked hemoglobin (alpha alpha Hb). Artif Cells Blood Substit Immobil Biotechnol. 1994;22(3):565-75. PMID: 7994376.

Thompson EB, Klotz IM. Pharmacological actions of diaspirins, potential antisickling agents: analgesic and anti-inflammatory effects. Res Commun Chem Pathol Pharmacol. 1985 Jun;48(3):381-8. PMID: 4023420.

B3275 Bis(3,5-dibromosalicyl) Succinate

100 mg
500 mg
1 g
5 g

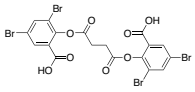

$C_{18}H_{10}O_8Br_4$ FW: 673.89 [71337-52-5] ≥95%

Aspirin analog, induces hemoglobin chain cross-linking. It is used to study hemoglobin function in research models. It also decreases carageenan-induced inflammation in animal models.

Macdonald VW, Motterlini R. Vasoconstrictor effects in isolated rabbit heart perfused with bis(3,5-dibromosalicyl)fumarate cross-linked hemoglobin (alpha alpha Hb). Artif Cells Blood Substit Immobil Biotechnol. 1994;22(3):565-75. PMID: 7994376.

Thompson EB, Klotz IM. Pharmacological actions of diaspirins, potential antisickling agents: analgesic and anti-inflammatory effects. Res Commun Chem Pathol Pharmacol. 1985 Jun;48(3):381-8. PMID: 4023420.

B3280 Bis(salicyl) Fumarate

100 mg
500 mg
1 g
5 g

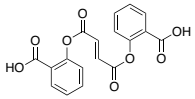

$C_{18}H_{12}O_8$ FW: 356.29 ≥98%

Aspirin analog, induces hemoglobin chain cross-linking. It is used to study hemoglobin function in research models. It may decrease carageenan-induced inflammation in animal models.

Macdonald VW, Motterlini R. Vasoconstrictor effects in isolated rabbit heart perfused with bis(3,5-dibromosalicyl)fumarate cross-linked hemoglobin (alpha alpha Hb). Artif Cells Blood Substit Immobil Biotechnol. 1994;22(3):565-75. PMID: 7994376.

B3577 Bitertanol

1 g
5 g
25 g

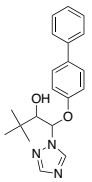

$C_{20}H_{23}N_3O_2$ FW: 337.42 [55179-31-2] ≥95%

Pesticide and demethylation inhibitor that disrupts membrane function and prevents sterol synthesis. It also increases activity of antioxidative enzymes and alters operant behavior in animal models.

Chan PK, Lu SY, Liao JW, et al. Induction and inhibition of cytochrome P450-dependent monooxygenases of rats by fungicide bitertanol. Food Chem Toxicol. 2006 Dec;44(12):2047-57. PMID: 16971034.

Allen AR, MacPhail RC. Bitertanol, a triazole fungicide, increases operant responding but not motor activity. Neurotoxicol Teratol. 1993 Jul-Aug;15(4):237-42. PMID: 8413077.

B4248 BKM120

NEW

1 mg
5 mg
25 mg

Buparlisib; NVP-BKM120

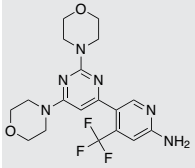

$C_{18}H_{21}F_3N_6O_2$ FW: 410.39 [944396-07-0] ≥98%

Inhibitor of PI3K and microtubule polymerization. It induces cell cycle arrest, polyploidy, and apoptosis in glioblastoma cells and suppresses invasiveness of squamous cell lung cancer cells.

Bonelli MA, Cavazzoni A, Saccani F, et al. Inhibition of PI3K pathway reduces invasiveness and epithelial-to-mesenchymal transition in squamous lung cancer cell lines harboring PIK3CA gene alterations. Mol Cancer Ther. 2015 May 26. [Epub ahead of print]. PMID: 26013318.

Wachsberger PR, Lawrence YR, Liu Y, et al. Hsp90 inhibition enhances PI-3 kinase inhibition and radiosensitivity in glioblastoma. J Cancer Res Clin Oncol. 2014 Feb 6. [Epub ahead of print]. PMID: 24500492.

Ando Y, Inada-Inoue M, Mitsuma A, et al. Phase I dose-escalation study of buparlisib (BKM120), an oral pan-class I PI3K inhibitor, in Japanese patients with advanced solid tumors. Cancer Sci. 2014 Jan 10. [Epub ahead of print]. PMID: 24405565.

B4402 Blasticidin S Hydrochloride

25 mg
50 mg
100 mg

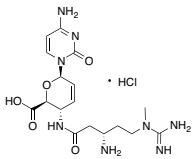

$C_{17}H_{26}N_8O_5 \cdot HCl$ FW: 458.5 [3513-03-9] ≥98%

Protein translation inhibitor that induces deformations in P-site tRNA. It inhibits aflatoxin production in species of *Aspergillus*.

Yoshinari T, Sakuda S, Watanabe M, et al. New metabolic pathway for converting blasticidin S in *Aspergillus* flavus and inhibitory activity of aflatoxin production by blasticidin S metabolites. J Agric Food Chem. 2013 Aug 21;61(33):7925-31. PMID: 23879927.

Svidritskiy E, Ling C, Ermolenko DN, et al. Blasticidin S inhibits translation by trapping deformed tRNA on the ribosome. Proc Natl Acad Sci U S A. 2013 Jul 23;110(30):12283-8. PMID: 23824292.

B4517

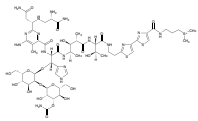

Bleomycin A5 Hydrochloride

Pingyangmycin hydrochloride

$C_{57}H_{89}N_{19}O_{21}S_2 \bullet HCl$ FW: 1477.02 [55658-47-4] ≥90%

1 mg
5 mg
10 mg
25 mg

DNA cleavage inducer use to treat various cancers. It induces cell cycle arrest and apoptosis in hemangioma. It may inhibit thioredoxin reductase.

Li P, Li DF, Guo ZT, et al. Therapeutic mechanism of bleomycin A5 on infancy hemangioma: an experimental study. Zhonghua Kou Qiang Yi Xue Za Zhi. 2013 Jan;48(1):18-22. PMID: 23534516.

Yang Y, Sun M, Ma Q, et al. Bleomycin A5 sclerotherapy for cervicofacial lymphatic malformations. J Vasc Surg. 2011 Jan;53(1):150-5. PMID: 20843632.

B4518

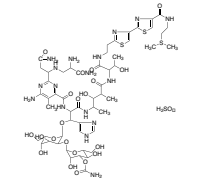

Bleomycin Sulfate

Blenoxane; Blexane

$C_{55}H_{84}N_{17}O_{21}S_3 \bullet H_2SO_4$ FW: 1512.63 [9041-93-4] ≥90%

5 mg
10 mg
25 mg
100 mg

Mixture of glycopeptide bleomycin sulfate salts that induces DNA strand breaks and is used to treat various cancers. It induces apoptosis and cell cycle arrest in hemangioma models. It also inhibits reproduction of human papilloma virus, cleaves DNA at 5'-GT sequences, and induces tRNA cleavage.

Ramírez-Fort MK, Au SC, Javed SA, et al. Management of cutaneous human papillomavirus infection: pharmacotherapies. Curr Probl Dermatol. 2014;45:175-85. PMID: 24643186.

Li P, Li DF, Guo ZT, et al. Therapeutic mechanism of bleomycin A5 on infancy hemangioma: an experimental study. Zhonghua Kou Qiang Yi Xue Za Zhi. 2013 Jan;48(1):18-22. PMID: 23534516.

Nguyen HT, Murray V. The DNA sequence specificity of bleomycin cleavage in telomeric sequences in human cells. J Biol Inorg Chem. 2012 Dec;17(8):1209-15. PMID: 22961398.

B5044

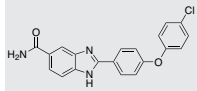

BML-277

NEW

$C_{20}H_{14}ClN_3O_2$ FW: 363.8 [516480-79-8] ≥98%

5 mg
25 mg

Chk2 inhibitor. It protects CD4+ and CD8+ T cells against radiation-induced apoptosis.

Arienti KL, Brunmark A, Axe FU, et al. Checkpoint kinase inhibitors: SAR and radioprotective properties of a series of 2-arylbenzimidazoles. J Med Chem. 2005 Mar 24;48(6):1873-85. PMID: 15771432.

B5074

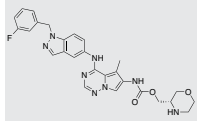

BMS-599626

AC480

NEW

$C_{27}H_{27}FN_8O_3$ FW: 530.55 [714971-09-2] ≥98%

5 mg
10 mg

Pan-HER (VEGFR/EGFR) inhibitor. It induces cell cycle arrest and inhibits growth of head and neck squamous cell carcinoma cells.

Soria JC, Cortes J, Massard C, et al. Phase I safety, pharmacokinetic and pharmacodynamic trial of BMS-599626 (AC480), an oral pan-HER receptor tyrosine kinase inhibitor, in patients with advanced solid tumors. Ann Oncol. 2012 Feb;23(2):463-71. PMID: 21576284.

Torres MA, Raju U, Molkentine D, et al. AC480, formerly BMS-599626, a pan Her inhibitor, enhances radiosensitivity and radioresponse of head and neck squamous cell carcinoma cells in vitro and in vivo. Invest New Drugs. 2011 Aug;29(4):554-61. PMID: 20119866.

B5072

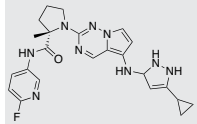

BMS-754807

NEW

$C_{23}H_{26}FN_9O$ FW: 463.51 [1001350-96-4] ≥98%

5 mg
10 mg
25 mg

InsR and IGF-1R inhibitor. It inhibits cell proliferation and tumor growth in models of pancreatic ductal adenocarcinoma and breast cancer.

Awasthi N, Zhang C, Ruan W, et al. BMS-754807, a small-molecule inhibitor of insulin-like growth factor-1 receptor/insulin receptor, enhances gemcitabine response in pancreatic cancer. Mol Cancer Ther. 2012 Dec;11(12):2644-53. PMID: 23047891.

Hou X, Huang F, Macedo LF, et al. Dual IGF-1R/InsR inhibitor BMS-754807 synergizes with hormonal agents in treatment of estrogen-dependent breast cancer. Cancer Res. 2011 Dec 15;71(24):7597-607. PMID: 22042792.

B4974

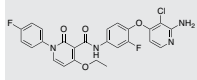

BMS-777607

NEW

$C_{25}H_{19}ClF_2N_4O_4$ FW: 512.89 [1196681-44-3] ≥98%

1 mg
5 mg

Inhibitor of MET and Ron. It induces polyploidy in breast cancer cells and inhibits motility and invasion of sarcoma cells.

Sharma S, Zeng JY, Zhuang CM, et al. Small-molecule inhibitor BMS-777607 induces breast cancer cell polyploidy with increased resistance to cytotoxic chemotherapy agents. Mol Cancer Ther. 2013 May;12(5):725-36. PMID: 23468529.

Dai Y, Bae K, Pampo C, et al. Impact of the small molecule Met inhibitor BMS-777607 on the metastatic process in a rodent tumor model with constitutive c-Met activation. Clin Exp Metastasis. 2012 Mar;29(3):253-61. PMID: 22286523.

B5000 BMS-911543

1 mg
5 mg

$C_{23}H_{28}N_8O$ FW: 432.52 [1271022-90-2] ≥99%

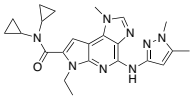

JAK2 inhibitor. It inhibits cell proliferation in models of myeloproliferative neoplasms.

Purandare AV, McDevitt TM, Wan H, et al. Characterization of BMS-911543, a functionally selective small-molecule inhibitor of JAK2. Leukemia. 2012 Feb;26(2):280-8. PMID: 22015772.

Tibes R, Bogenberger JM, Geyer HL, et al. JAK2 inhibitors in the treatment of myeloproliferative neoplasms. Expert Opin Investig Drugs. 2012 Dec;21(12):1755-74. PMID: 22991927.

B5608 Boc-FAAGRK-AMC

20 mg

$C_{44}H_{63}N_{11}O_6$ FW: 906 ≥98%

Boc-Phe-Ala-Ala-Gly-Arg-Lys-AMC

Substrate used to measure protease activity.

Santoni M, Amantini C, Morelli MB, et al. Pazopanib and sunitinib trigger autophagic and non-autophagic death of bladder tumour cells. Br J Cancer. 2013 Aug 20;109(4):1040-50. PMID: 23887605.

B5609 Boc-GRR-AMC

20 mg

$C_{29}H_{44}N_{10}O_7$ FW: 644.7 ≥98%

Boc-Gly-Arg-Arg-AMC

Substrate used to measure activity of serine proteases such as cathepsins.

Santoni M, Amantini C, Morelli MB, et al. Pazopanib and sunitinib trigger autophagic and non-autophagic death of bladder tumour cells. Br J Cancer. 2013 Aug 20;109(4):1040-50. PMID: 23887605.

B5610 Boc-PRR-AMC

20 mg

$C_{32}H_{48}N_{10}O_7$ FW: 684.8 ≥98%

Boc-Pro-Arg-Arg-AMC

Substrate used to measure activity of serine proteases such as cathepsins.

Santoni M, Amantini C, Morelli MB, et al. Pazopanib and sunitinib trigger autophagic and non-autophagic death of bladder tumour cells. Br J Cancer. 2013 Aug 20;109(4):1040-50. PMID: 23887605.

B5611 Boc-RRR-AMC

20 mg

$C_{33}H_{53}N_{13}O_7$ FW: 743.8 ≥98%

Boc-Arg-Arg-Arg-AMC

Substrate used to measure activity of serine proteases such as cathepsins.

Santoni M, Amantini C, Morelli MB, et al. Pazopanib and sunitinib trigger autophagic and non-autophagic death of bladder tumour cells. Br J Cancer. 2013 Aug 20;109(4):1040-50. PMID: 23887605.

B5648 Bombesin

1 mg
2 mg
5 mg

$C_{71}H_{111}N_{24}O_{18}S$ FW: 1619.86 [31362-50-2] ≥95%

pGlu-Gln-Arg-Leu-Gly-Asn-Gln-Trp-Ala-Val-Gly-His-Leu-Met-NH_2

GRP analog, bombesin and GRP receptor agonist, and hERG K^+ channel blocker found in *Bombina*. It potentiates GABA release, decreases food intake, and stimulates carcinogenic signaling pathways.

Zhang HP, Xiao Z, Cilz NI, et al. Bombesin facilitates GABAergic transmission and depresses epileptiform activity in the entorhinal cortex. Hippocampus. 2014 Jan;24(1):21-31. PMID: 23966303.

B5649 [Tyr4]-Bombesin

1 mg
2 mg
5 mg

$C_{74}H_{108}N_{24}O_{19}S$ FW: 1669.9 ≥95%

pGlu-Gln-Arg-Tyr-Gly-Asn-Gln-Trp-Ala-Val-Gly-His-Leu-Met-NH_2

Bombesin derivative, bombesin and GRP receptor agonist, and hERG K^+ channel blocker found in *Bombina*. It potentiates GABA release, decreases food intake, and stimulates carcinogenic signaling pathways.

Zhang HP, Xiao Z, Cilz NI, et al. Bombesin facilitates GABAergic transmission and depresses epileptiform activity in the entorhinal cortex. Hippocampus. 2014 Jan;24(1):21-31. PMID: 23966303.

Okarvi SM, Jammaz IA. Preparation and evaluation of bombesin peptide derivatives as potential tumor imaging agents: effects of structure and composition of amino acid sequence on in vitro and in vivo characteristics. Nucl Med Biol. 2012 Aug;39(6):795-804. PMID: 22381782.

B5753 Bongkrekic Acid

100 µg

$C_{28}H_{38}O_7$ FW: 486.6 [11076-19-0] ≥98%

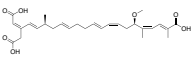

Respiratory toxin and mitochondrial permeability transition inhibitor. It suppresses transport of ADP/ATP across the mitochondrial inner membrane, decreasing oxidative stress.

Nolly MB, Caldiz CI, Yeves AM, et al. The signaling pathway for aldosterone-induced mitochondrial production of superoxide anion in the myocardium. J Mol Cell Cardiol. 2014 Feb;67:60-8. PMID: 24355174.

Rey M, Forest E, Pelosi L. Exploring the conformational dynamics of the bovine ADP/ATP carrier in mitochondria. Biochemistry. 2012 Dec 4;51(48):9727-35. PMID: 23136955.

B5870 Borrelidin

NEW

1 mg
5 mg

$C_{28}H_{43}NO_6$ FW: 489.64 [7184-60-3] ≥99%

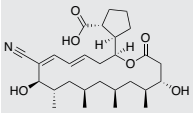

Threonyl-tRNA synthetase/ligase inhibitor. It inhibits growth of Trypanosoma, *Plasmodium*, and *Phytophthora*, induces cell cycle arrest and apoptosis in acute lymphocytic leukemia cells, and prevents formation of new capillary tubes in endothelial cells.

Kalidas S, Cestari I, Monnerat S, et al. Genetic validation of aminoacyl-tRNA synthetases as drug targets in *Trypanosoma brucei*. Eukaryot Cell. 2014 Apr;13(4):504-16. PMID: 24562907.

Azcárate IG, Marín-García P, Camacho N, et al. Insights into the preclinical treatment of blood-stage malaria by the antibiotic borrelidin. Br J Pharmacol. 2013 Jun;169(3):645-58. PMID: 23488671.

Gao YM, Wang XJ, Zhang J, et al. Borrelidin, a potent antifungal agent: insight into the antifungal mechanism against *Phytophthora* sojae. J Agric Food Chem. 2012 Oct 3;60(39):9874-81. PMID: 22967236.

B5875 Bosutinib, structural isomer

10 mg
25 mg
100 mg

$C_{26}H_{29}Cl_2N_5O_3$ FW: 530.45 ≥98%

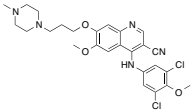

Structural isomer of bosutinib. Src and Abl inhibitor used to treat chronic myeloid leukemia. It does not induce apoptosis but suppresses cell proliferation. It also clears β-amyloid plaques and increases cognitive function in Alzheimer's disease models.

Rassi FE, Khoury HJ. Bosutinib: a SRC-ABL tyrosine kinase inhibitor for treatment of chronic myeloid leukemia. Pharmgenomics Pers Med. 2013 Aug 5;6:57-62. PMID: 24019749.

Lonskaya I, Hebron ML, Desforges NM, et al. Tyrosine kinase inhibition increases functional parkin-Beclin-1 interaction and enhances amyloid clearance and cognitive performance. EMBO Mol Med. 2013 Aug;5(8):1247-62. PMID: 23737459.

Ulmer A, Tabea Tauer J, Glauche I, et al. TK inhibitor treatment disrupts growth hormone axis: clinical observations in children with CML and experimental data from a juvenile animal model. Klin Padiatr. 2013 May;225(3):120-6. PMID: 23716272.

B6802 Bradykinin (1-3)

5 mg
10 mg
25 mg

$C_{16}H_{28}N_6O_4$ FW: 368.4 [58-82-2] ≥95%

H-Arg-Pro-Pro-OH

Natriuretic and vasodilatory B1/2 receptor agonist and bradykinin fragment. It inhibits distal nephron Na^+ transport, decreases H_2O_2-induced senescence, suppresses DNA damage and oxidative stress, and increases expression of VEGF and promotes tube formation.

Mamenko M, Zaika O, Pochynyuk O. Direct regulation of ENaC by bradykinin in the distal nephron. Implications for renal sodium handling. Curr Opin Nephrol Hypertens. 2014 Mar;23(2):122-9. PMID: 24378775.

Yu HS, Wang SW, Chang AC, et al. Bradykinin promotes vascular endothelial growth factor expression and increases angiogenesis in human prostate cancer cells. Biochem Pharmacol. 2014 Jan 15;87(2):243-53. PMID: 24225154.

B6803 Bradykinin (1-5)

5 mg
10 mg
25 mg

$C_{27}H_{40}N_8O_6$ FW: 572.67 ≥95%

H-Arg-Pro-Pro-Gly-Phe-OH

Natriuretic and vasodilatory B1/2 receptor agonist and bradykinin fragment. It inhibits distal nephron Na^+ transport, decreases H_2O_2-induced senescence, suppresses DNA damage and oxidative stress, and increases expression of VEGF and promotes tube formation.

Mamenko M, Zaika O, Pochynyuk O. Direct regulation of ENaC by bradykinin in the distal nephron. Implications for renal sodium handling. Curr Opin Nephrol Hypertens. 2014 Mar;23(2):122-9. PMID: 24378775.

Yu HS, Wang SW, Chang AC, et al. Bradykinin promotes vascular endothelial growth factor expression and increases angiogenesis in human prostate cancer cells. Biochem Pharmacol. 2014 Jan 15;87(2):243-53. PMID: 24225154.

B6804 Bradykinin (1-6)

5 mg
10 mg
25 mg

$C_{30}H_{45}N_9O_8$ FW: 659.75 ≥95%

H-Arg-Pro-Pro-Gly-Phe-Ser-OH

Natriuretic and vasodilatory B1/2 receptor agonist and bradykinin fragment. It inhibits distal nephron Na^+ transport, decreases H_2O_2-induced senescence, suppresses DNA damage and oxidative stress, and increases expression of VEGF and promotes tube formation.

Mamenko M, Zaika O, Pochynyuk O. Direct regulation of ENaC by bradykinin in the distal nephron. Implications for renal sodium handling. Curr Opin Nephrol Hypertens. 2014 Mar;23(2):122-9. PMID: 24378775.

Yu HS, Wang SW, Chang AC, et al. Bradykinin promotes vascular endothelial growth factor expression and increases angiogenesis in human prostate cancer cells. Biochem Pharmacol. 2014 Jan 15;87(2):243-53. PMID: 24225154.

B6805 Bradykinin (1-7)

5 mg
10 mg
25 mg

$C_{35}H_{52}N_{10}O_9$ FW: 756.87 ≥95%

H-Arg-Pro-Pro-Gly-Phe-Ser-Pro-OH

Natriuretic and vasodilatory B1/2 receptor agonist and bradykinin fragment. It inhibits distal nephron Na^+ transport, decreases H_2O_2-induced senescence, suppresses DNA damage and oxidative stress, and increases expression of VEGF and promotes tube formation.

Mamenko M, Zaika O, Pochynyuk O. Direct regulation of ENaC by bradykinin in the distal nephron. Implications for renal sodium handling. Curr Opin Nephrol Hypertens. 2014 Mar;23(2):122-9. PMID: 24378775.

Yu HS, Wang SW, Chang AC, et al. Bradykinin promotes vascular endothelial growth factor expression and increases angiogenesis in human prostate cancer cells. Biochem Pharmacol. 2014 Jan 15;87(2):243-53. PMID: 24225154.

B6806 Bradykinin (2-9)

5 mg
10 mg
25 mg

$C_{44}H_{61}N_{11}O_{10}$ FW: 904.04 ≥95%

H-Pro-Pro-Gly-Phe-Ser-Pro-Phe-Arg-OH

Natriuretic and vasodilatory B1/2 receptor agonist and bradykinin fragment. It inhibits distal nephron Na^+ transport, decreases H_2O_2-induced senescence, suppresses DNA damage and oxidative stress, and increases expression of VEGF and promotes tube formation.

Mamenko M, Zaika O, Pochynyuk O. Direct regulation of ENaC by bradykinin in the distal nephron. Implications for renal sodium handling. Curr Opin Nephrol Hypertens. 2014 Mar;23(2):122-9. PMID: 24378775.

Yu HS, Wang SW, Chang AC, et al. Bradykinin promotes vascular endothelial growth factor expression and increases angiogenesis in human prostate cancer cells. Biochem Pharmacol. 2014 Jan 15;87(2):243-53. PMID: 24225154.

B6812 Bradykinin Potentiator B

5 mg
10 mg
25 mg

$C_{56}H_{91}N_{15}O_{13}$ FW: 1182.46 ≥95%

pGlu-Gly-Leu-Pro-Pro-Arg-Pro-Lys-Ile-Pro-Pro-OH

Inhibitor of bradykinin inhibiting peptidase and ACE found in *Agkistrodon*.

Matsui H, Takahashi T. Presence of angiotensin-converting enzyme in follicular fluids of porcine ovaries and its possible involvement in the intrafollicular breakdown of bradykinin. Mol Reprod Dev. 2002 May;62(1):99-105. PMID: 11933166.

B6813 Bradykinin Potentiator C

5 mg
10 mg
25 mg

$C_{51}H_{77}N_{11}O_{13}$ FW: 1052.26 ≥95%

pGlu-Gly-Leu-Pro-Pro-Gly-Pro-Pro-Ile-Pro-Pro-OH

Inhibitor of bradykinin inhibiting peptidase and ACE found in *Agkistrodon*.

Matsui H, Takahashi T. Presence of angiotensin-converting enzyme in follicular fluids of porcine ovaries and its possible involvement in the intrafollicular breakdown of bradykinin. Mol Reprod Dev. 2002 May;62(1):99-105. PMID: 11933166.

Kariya K, Okamoto H, Kira K. Kinin-forming enzyme in rat brain mitochondria fraction and biological activity of a kinin released from rat plasma kininogen by this enzyme. Jpn J Pharmacol. 1984 Feb;34(2):203-10. PMID: 6748370.

B6800 Bradykinin Triacetate

10 mg
20 mg
50 mg

$C_{50}H_{73}N_{15}O_{11}$ FW: 1240.38 [5979-11-3] ≥95%

Arg-Pro-Pro-Gly-Phe-Ser-Pro-Phe-Arg

Natriuretic and vasodilatory B1/2 receptor agonist. It inhibits distal nephron Na^+ transport, decreases H_2O_2-induced senescence, suppresses DNA damage and oxidative stress, and increases expression of VEGF and promotes tube formation.

Mamenko M, Zaika O, Pochynyuk O. Direct regulation of ENaC by bradykinin in the distal nephron. Implications for renal sodium handling. Curr Opin Nephrol Hypertens. 2014 Mar;23(2):122-9. PMID: 24378775.

Yu HS, Wang SW, Chang AC, et al. Bradykinin promotes vascular endothelial growth factor expression and increases angiogenesis in human prostate cancer cells. Biochem Pharmacol. 2014 Jan 15;87(2):243-53. PMID: 24225154.

B6807 [Des-Arg9]-Bradykinin

5 mg
10 mg
25 mg

$C_{44}H_{61}N_{11}O_{10}$ FW: 904.04 ≥95%

H-Arg-Pro-Pro-Gly-Phe-Ser-Pro-Phe-OH

Natriuretic and vasodilatory B1/2 receptor agonist and bradykinin derivative. It inhibits distal nephron Na^+ transport, decreases H_2O_2-induced senescence, suppresses DNA damage and oxidative stress, and increases expression of VEGF and promotes tube formation.

Mamenko M, Zaika O, Pochynyuk O. Direct regulation of ENaC by bradykinin in the distal nephron. Implications for renal sodium handling. Curr Opin Nephrol Hypertens. 2014 Mar;23(2):122-9. PMID: 24378775.

Yu HS, Wang SW, Chang AC, et al. Bradykinin promotes vascular endothelial growth factor expression and increases angiogenesis in human prostate cancer cells. Biochem Pharmacol. 2014 Jan 15;87(2):243-53. PMID: 24225154.

B6808 [Des-Pro2]-Bradykinin

5 mg
10 mg
25 mg

$C_{45}H_{66}N_{14}O_{10}$ FW: 963.12 ≥95%

H-Arg-Pro-Gly-Phe-Ser-Pro-Phe-Arg-OH

Natriuretic and vasodilatory B1/2 receptor agonist and bradykinin derivative. It inhibits distal nephron Na^+ transport, decreases H_2O_2-induced senescence, suppresses DNA damage and oxidative stress, and increases expression of VEGF and promotes tube formation.

Mamenko M, Zaika O, Pochynyuk O. Direct regulation of ENaC by bradykinin in the distal nephron. Implications for renal sodium handling. Curr Opin Nephrol Hypertens. 2014 Mar;23(2):122-9. PMID: 24378775.

Yu HS, Wang SW, Chang AC, et al. Bradykinin promotes vascular endothelial growth factor expression and increases angiogenesis in human prostate cancer cells. Biochem Pharmacol. 2014 Jan 15;87(2):243-53. PMID: 24225154.

B6809 [DPhe7]-Bradykinin

1 mg
2 mg
5 mg

$C_{54}H_{75}N_{15}O_{11}$ FW: 1110.29 ≥95%

H-Arg-Pro-Pro-Gly-Phe-Ser-DPhe-Phe-Arg-OH

Natriuretic and vasodilatory B1/2 receptor agonist and bradykinin derivative. It inhibits distal nephron Na^+ transport, decreases H_2O_2-induced senescence, suppresses DNA damage and oxidative stress, and increases expression of VEGF and promotes tube formation.

Mamenko M, Zaika O, Pochynyuk O. Direct regulation of ENaC by bradykinin in the distal nephron. Implications for renal sodium handling. Curr Opin Nephrol Hypertens. 2014 Mar;23(2):122-9. PMID: 24378775.

Yu HS, Wang SW, Chang AC, et al. Bradykinin promotes vascular endothelial growth factor expression and increases angiogenesis in human prostate cancer cells. Biochem Pharmacol. 2014 Jan 15;87(2):243-53. PMID: 24225154.

B6810 [Hyp3]-Bradykinin

0.5 mg
1 mg
2.5 mg

$C_{30}H_{72}N_{15}O_{10}$ FW: 1077.23 ≥95%

H-Arg-Pro-Hyp-Gly-Phe-Ser-Pro-Phe-Arg-OH

Natriuretic and vasodilatory B1/2 receptor agonist and bradykinin derivative. It inhibits distal nephron Na^+ transport, decreases H_2O_2-induced senescence, suppresses DNA damage and oxidative stress, and increases expression of VEGF and promotes tube formation.

Mamenko M, Zaika O, Pochynyuk O. Direct regulation of ENaC by bradykinin in the distal nephron. Implications for renal sodium handling. Curr Opin Nephrol Hypertens. 2014 Mar;23(2):122-9. PMID: 24378775.

Yu HS, Wang SW, Chang AC, et al. Bradykinin promotes vascular endothelial growth factor expression and increases angiogenesis in human prostate cancer cells. Biochem Pharmacol. 2014 Jan 15;87(2):243-53. PMID: 24225154.

B6811 [Tyr8]-Bradykinin

5 mg
10 mg
50 mg

$C_{50}H_{73}N_{15}O_{12}$ FW: 1076.23 ≥95%

H-Arg-Pro-Pro-Gly-Phe-Ser-Pro-Tyr-Arg-OH

Natriuretic and vasodilatory B1/2 receptor agonist and bradykinin derivative. It inhibits distal nephron Na^+ transport, decreases H_2O_2-induced senescence, suppresses DNA damage and oxidative stress, and increases expression of VEGF and promotes tube formation.

Mamenko M, Zaika O, Pochynyuk O. Direct regulation of ENaC by bradykinin in the distal nephron. Implications for renal sodium handling. Curr Opin Nephrol Hypertens. 2014 Mar;23(2):122-9. PMID: 24378775.

B3346 Brain Injury-derived Neurotrophic Peptide (3)

1 mg
2 mg
5 mg

BINP

$C_{62}H_{101}N_{17}O_{19}$ FW: 1388.58 ≥98%

Glu-Ala-Leu-Glu-Leu-Ala-Arg-Gly-Ala-Ile-Phe-Gln-Ala

Supports neuronal survival and protects against glutamate-induced neurotoxicity.

Hama T, Maruyama M, Katoh-Semba R, et al. Identification and molecular cloning of a novel brain-specific receptor protein that binds to brain injury-derived neurotrophic peptide. Possible role for neuronal survival. J Biol Chem. 2001 Aug 24;276(34):31929-35. PMID: 11399754.

B6801 Brassinin

50 mg
100 mg
250 mg

$C_{11}H_{12}N_2S_2$ FW: 236.36 [105748-59-2] ≥98%

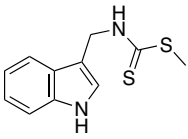

Indoleamine-2,3-dioxygenase inhibitor found in cruciferous vegetables. It induces cell cycle arrest and apoptosis in prostate cancer cells and inhibits DMBA-induced skin tumor formation in vivo.

Kim SM, Park JH, Kim KD, et al. Brassinin induces apoptosis in PC-3 human prostate cancer cells through the suppression of PI3K/Akt/mTOR/S6K1 signaling cascades. Phytother Res. 2014 Mar;28(3):423-31. PMID: 23686889.

Banerjee T, Duhadaway JB, Gaspari P, et al. A key in vivo antitumor mechanism of action of natural product-based brassinins is inhibition of indoleamine 2,3-dioxygenase. Oncogene. 2008 May 1;27(20):2851-7. PMID: 18026137.

B6816

Brefeldin A

5 mg
10 mg

Ascotoxin; Cyanein; Decumbin

$C_{16}H_{24}O_4$ FW: 280.36 [20350-15-6] ≥97%

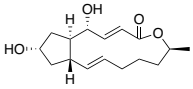

Guanine nucleotide exchange factor inhibitor found in fungi such as *Eupenicillium*. It suppresses protein transport from the endoplasmic reticulum to the Golgi apparatus. It also inhibits poliovirus replication and induces cell cycle arrest and apoptosis in prostate cancer cells.

Zhou C, Li C, Li D, et al. BIG1, a brefeldin A-inhibited guanine nucleotide-exchange protein regulates neurite development via PI3K-AKT and ERK signaling pathways. Neuroscience. 2013 Dec 19;254:361-8. PMID: 24090963.

Rouhana J, Padilla A, Estaran S, et al. Kinetics of interaction between ADP-ribosylation factor-1 (Arf1) and the Sec7 domain of Arno guanine nucleotide exchange factor, modulation by allosteric factors, and the uncompetitive inhibitor brefeldin A. J Biol Chem. 2013 Feb 15;288(7):4659-72. PMID: 23255605.

B6917

Brevetoxin 2

100 µg
1 mg
5 mg

PbTx-2

$C_{50}H_{70}O_{14}$ FW: 895.2 [79580-28-2] ≥95%

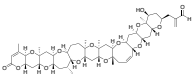

Na_v1.4/1.5 Na^+ channel activator and neurotoxin found in *Karenia brevis*. It induces bronchoconstriction and airway inflammation, stimulates NMDA receptor-mediated release of L-glutamate and L-aspartate in neurons, and forms DNA adducts with cytidine in isolated lung cells.

Zaias J, Fleming LE, Baden DG, et al. Repeated exposure to aerosolized brevetoxin-3 induces prolonged airway hyperresponsiveness and lung inflammation in sheep. Inhal Toxicol. 2011 Mar;23(4):205-11. PMID: 21456953.

Liberona JL, Cárdenas JC, Reyes R, et al. Sodium-dependent action potentials induced by brevetoxin-3 trigger both IP3 increase and intracellular Ca^{2+} release in rat skeletal myotubes. Cell Calcium. 2008 Sep;44(3):289-97. PMID: 18276006.

B6918

Brevetoxin 3

100 µg
1 mg
5 mg

PbTx-3

$C_{50}H_{72}O_{14}$ FW: 897.2 [85079-48-7] ≥95%

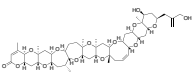

Na_v1.4/1.5 Na^+ channel activator and neurotoxin found in *Karenia brevis*. It induces bronchoconstriction and airway inflammation and stimulates NMDA receptor-mediated release of L-glutamate and L-aspartate in neurons. It is a metabolite of brevetoxin 2.

Zaias J, Fleming LE, Baden DG, et al. Repeated exposure to aerosolized brevetoxin-3 induces prolonged airway hyperresponsiveness and lung inflammation in sheep. Inhal Toxicol. 2011 Mar;23(4):205-11. PMID: 21456953.

Liberona JL, Cárdenas JC, Reyes R, et al. Sodium-dependent action potentials induced by brevetoxin-3 trigger both IP3 increase and intracellular Ca^{2+} release in rat skeletal myotubes. Cell Calcium. 2008 Sep;44(3):289-97. PMID: 18276006.

Cao Z, George J, Baden DG, et al. Brevetoxin-induced phosphorylation of Pyk2 and Src in murine neocortical neurons involves distinct signaling pathways. Brain Res. 2007 Dec 12;1184:17-27. PMID: 17963734.

B6935

Brivudine

10 mg
25 mg
100 mg

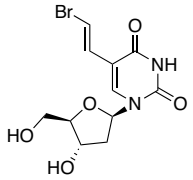

$C_{11}H_{13}BrN_2O_5$ FW: 333.13 [69304-47-8] ≥98%

Thymidine analog, DNA chain terminator, HSV-1 thymidine kinase inhibitor, and HSP27 modulator used to treat herpesvirus infections. It prevents DNA chain elongation, improves the efficacy of co-administered chemotherapeutics, and slows larval growth and development of *Spodoptera* worms.

Heinrich JC, Tuukkanen A, Schroeder M, et al. RP101 (brivudine) binds to heat shock protein HSP27 (HSPB1) and enhances survival in animals and pancreatic cancer patients. J Cancer Res Clin Oncol. 2011 Sep;137(9):1349-61. PMID: 21833720.

Breuer M, De Loof A, Balzarini J, et al. Insecticidal activity of the pyrimidine nucleoside analogue (E)-5-(2-bromovinyl)-2'-deoxyuridine (BVDU). Pest Manag Sci. 2005 Aug;61(8):737-41. PMID: 15838935.

B6957

Bromhexine Hydrochloride

25 g
100 g
500 g

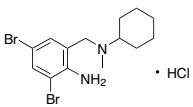

$C_{14}H_{20}Br_2N_2 \cdot HCl$ FW: 412.6 [611-75-6] ≥98%

Synthetic vasicine derivative used to treat mucus-related respiratory disorders. It increases production of serous mucus, decreases mucus viscosity, and helps cilia transport mucus out of the lungs.

Winsel K, Grollmuss H, Unger U, et al. Modulation of alveolar macrophage activity by ambroxol, bromhexine and exogenous arachidonic acid. Z Erkr Atmungsorgane. 1985;165(2):149-62. PMID: 3002048.

Takeda H, Abe Y, Misawa M, et al. The role of vagal reflex in mechanism of secretagogic action of bromhexine. Jpn J Pharmacol. 1984 Aug;35(4):445-50. PMID: 6503040.

B6856

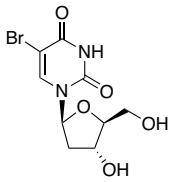

5-Bromo-2'-Deoxyuridine

250 mg
500 mg
1 g
5 g

Broxuridine; 5-bromouracil deoxyriboside; BUdR

$C_9H_{11}BrN_2O_5$ FW: 307.11 [59-14-3] ≥98%

Thymidine analog used to label actively proliferating cells. It is incorporated into DNA but does not prevent DNA replication.

Zhang R, Zhang J, Fang L, et al. Neuroprotective effects of sulforaphane on cholinergic neurons in mice with Alzheimer's disease-like lesions. Int J Mol Sci. 2014 Aug 18;15(8):14396-410. PMID: 25196440.

Jeong CH, Kim SM, Lim JY, et al. Mesenchymal stem cells expressing brain-derived neurotrophic factor enhance endogenous neurogenesis in an ischemic stroke model. Biomed Res Int. 2014;2014:129145. PMID: 24672780.

B6857

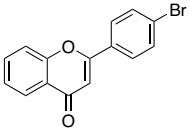

4-Bromoflavone

1 g
5 g
10 g

$C_{15}H_9BrO_2$ FW: 301.13 [1218-80-0] ≥98%

Nrf2-Keap1-ARE complex activator. It induces expression of phase II enzymes and prevents development of mammary tumors.

Lee JS, Surh YJ. Nrf2 as a novel molecular target for chemoprevention. Cancer Lett. 2005 Jun 28;224(2):171-84. PMID: 15914268.

Mehta RG, Pezzuto JM. Discovery of cancer preventive agents from natural products: from plants to prevention. Curr Oncol Rep. 2002 Nov;4(6):478-86. PMID: 12354359.

Song LL, Kosmeder JW 2nd, Lee SK, et al. Cancer chemopreventive activity mediated by 4'-bromoflavone, a potent inducer of phase II detoxification enzymes. Cancer Res. 1999 Feb 1;59(3):578-85. PMID: 9973203.

B6959

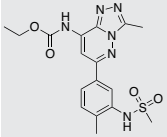

Bromosporine

NEW

1 mg
5 mg

$C_{17}H_{20}N_6O_4S$ FW: 404.44 ≥98%

Inhibitor of BRD2/4/9 and CECR2. It may inhibit proliferation of cancer cells.

B7058

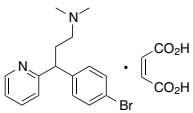

Brompheniramine Maleate

10 mg
25 mg
100 mg

$C_{16}H_{19}BrN_2 \cdot C_4H_4O_4$ FW: 435.31 ≥98%

Pheniramine derivative, histamine H1 receptor and mAChR antagonist, and potential SERT and MAO-B inhibitor used to treat allergic rhinitis and symptoms of the common cold. It inhibits histamine-induced vasodilation and potentiates the effects of opioid analgesics.

Egashira T, Takayama F, Yamanaka Y. The inhibition of monoamine oxidase activity by various antidepressants: differences found in various mammalian species. Jpn J Pharmacol. 1999 Sep;81(1):115-21. PMID: 10580379.

Yasuda SU, Yasuda RP. Affinities of brompheniramine, chlorpheniramine, and terfenadine at the five human muscarinic cholinergic receptor subtypes. Pharmacotherapy. 1999 Apr;19(4):447-51. PMID: 10212017.

B6998

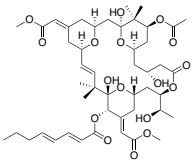

Bryostatin 1

10 µg

$C_{47}H_{68}O_{17}$ FW: 905.03 [83314-01-6] ≥98%

TLR4 activator and PKC modulator found in *Bugula*. It activates PKC at low doses and inhibits PKC at high doses. It also increases memory acquisition and storage, improves MHC class II antigen presentation by CD4+ T cells, and activates APP processing by α-secretase.

Irie K, Yanagita RC. Synthesis and biological activities of simplified analogs of the natural PKC ligands, bryostatin-1 and aplysiatoxin. Chem Rec. 2014 Apr;14(2):251-67. PMID: 24677503.

Yi P, Schrott L, Castor TP, et al. Bryostatin-1 vs. TPPB: dose-dependent APP processing and PKC-α, -δ, and -ε isoform activation in SH-SY5Y neuronal cells. J Mol Neurosci. 2012 Sep;48(1):234-44. PMID: 22700373.

Hossain A, God JM, Radwan FF, et al. HLA class II defects in Burkitt lymphoma: bryostatin-1-induced 17 kDa protein restores CD4+ T-cell recognition. Clin Dev Immunol. 2011;2011:780839. PMID: 22162713.

B5561

H-Ser-Pro-Lys-Met-Val-Gln-Gly-Ser-Gly-Cys-Phe-Gly-Arg- Lys-Met-Asp-Arg-Ile-Ser-Ser-Ser-Ser-Gly-Leu-Gly-Cys-Lys- Val-Leu-Arg-Arg-His-OH
(Disulfide Bridge Cys10-Cys26)

B-type Natriuretic Peptide (1-32), human

0.5 mg
1 mg
2.5 mg

Brain natriuretic peptide; BNP

$C_{143}H_{244}N_{50}O_{42}S_4$ FW: 3464.1 [114471-18-0] ≥97%

Endogenous NPR-A agonist secreted by the heart. It induces lipolysis and inhibits de novo collagen synthesis. It is associated with the development of cardiovascular diseases.

García-Berrocoso T, Giralt D, Bustamante A, et al. B-type natriuretic peptides and mortality after stroke: a systematic review and meta-analysis. Neurology. 2013 Dec 3;81(23):1976-85. PMID: 24186915.

Polak J, Kotrc M, Wedellova Z, et al. Lipolytic effects of B-type natriuretic peptide 1-32 in adipose tissue of heart failure patients compared with healthy controls. J Am Coll Cardiol. 2011 Sep 6;58(11):1119-25. PMID: 21884948.

B5560

B-type Natriuretic Peptide (1-32), rat

0.5 mg
1 mg
2.5 mg

H-Asn-Ser-Lys-Met-Ala-His-Ser-Ser-Ser-Cys-Phe-Gly-Gln-Lys-Ile-Asp-Arg-Ile-Gly-Ala-Val-Ser-Arg-Leu-Gly-Cys-Asp- Gly-Leu-Arg-Leu-Phe-OH
(Disulfide Bridge Cys10-Cys26)

Brain natriuretic peptide; BNP

$C_{146}H_{239}N_{47}O_{44}S_3$ FW: 3453.01 [133448-20-1] ≥95%

Endogenous NPR-A agonist secreted by the heart. It induces lipolysis and inhibits de novo collagen synthesis. It is associated with the development of cardiovascular diseases.

García-Berrocoso T, Giralt D, Bustamante A, et al. B-type natriuretic peptides and mortality after stroke: a systematic review and meta-analysis. Neurology. 2013 Dec 3;81(23):1976-85. PMID: 24186915.

Polak J, Kotrc M, Wedellova Z, et al. Lipolytic effects of B-type natriuretic peptide 1-32 in adipose tissue of heart failure patients compared with healthy controls. J Am Coll Cardiol. 2011 Sep 6;58(11):1119-25. PMID: 21884948.

B8010

Buccalin

1 mg
2 mg
5 mg

Gly-Met-Asp-Ser-Leu-Ala-Phe-Ser-Gly-Gly-Leu-NH_2

$C_{45}H_{72}N_{12}O_{15}S$ FW: 1053.2 [116844-51-0] ≥95%

Found in mollusks. It modulates neuromuscular transmission and decreases motor neuron-induced muscular contractions.

Veenstra JA. Neurohormones and neuropeptides encoded by the genome of Lottia gigantea, with reference to other mollusks and insects. Gen Comp Endocrinol. 2010 May 15;167(1):86-103. PMID: 20171220.

B8112

Budesonide

100 mg
250 mg
1 g

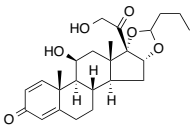

$C_{25}H_{34}O_6$ FW: 430.53 [51333-22-3] ≥97%

Glucocorticoid receptor agonist used to treat Crohn's disease, IBD, and COPD. It induces pulmonary vasoconstriction, decreases TGF-β1-induced VEGF secretion in lung fibroblasts, improves pulmonary function, and induces DNA hypermethylation.

Deng X, Zhang Z, Gu W, et al. Budesonide inhibits interleukin-32 expression in a rat model of chronic obstructive pulmonary disease. Exp Lung Res. 2012 Aug;38(6):295-301. PMID: 22646473.

Orta ML, Domínguez I, Pastor N, et al. The role of the DNA hypermethylating agent Budesonide in the decatenating activity of DNA topoisomerase II. Mutat Res. 2010 Dec 10;694(1-2):45-52. PMID: 20883705.

B8144

Bulleyaconitine A

10 mg
100 mg

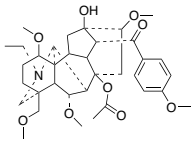

$C_{35}H_{49}NO_9$ FW: 627.76 [107668-79-1] ≥96%

Voltage-gated Na^+ channel blocker found in *Aconitum bulleyanum* used to treat pain and inflammation. It also reduces absorption and prolongs drug effect when co-administered with anesthetics.

Wang CF, Gerner P, Schmidt B, et al. Use of bulleyaconitine A as an adjuvant for prolonged cutaneous analgesia in the rat. Anesth Analg. 2008 Oct;107(4):1397-405. PMID: 18806059.

Wang CF, Gerner P, Wang SY, et al. Bulleyaconitine A isolated from *aconitum* plant displays long-acting local anesthetic properties in vitro and in vivo. Anesthesiology. 2007 Jul;107(1):82-90. PMID: 17585219.

B8248

Bumetanide

250 mg
1 g

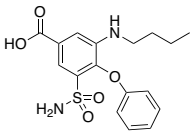

$C_{17}H_{20}N_2O_5S$ FW: 364.42 [28395-03-1] ≥98%

Loop diuretic, NKCC symporter and KCC2 co-transporter inhibitor, and potential GABA-A receptor antagonist. It also induces hyperpolarization in kidney cells, inhibits upregulation of low-affinity NGF/pan-neurotrophin receptor p75NTR, and suppresses facilitation of recurrent seizures.

Wang T, Yang YQ, Karasawa T, et al. Bumetanide hyperpolarizes madin-darby canine kidney cells and enhances cellular gentamicin uptake by elevating cytosolic $Ca^{(2+)}$ thus facilitating intermediate conductance $Ca^{(2+)}$--activated potassium channels. Cell Biochem Biophys. 2013 Apr;65(3):381-98. PMID: 23109177.

Krystal AD, Sutherland J, Hochman DW. Loop diuretics have anxiolytic effects in rat models of conditioned anxiety. PLoS One. 2012;7(4):e35417. PMID: 22514741.

Shulga A, Magalhães AC, Autio H, et al. The loop diuretic bumetanide blocks posttraumatic p75NTR upregulation and rescues injured neurons. J Neurosci. 2012 Feb 1;32(5):1757-70. PMID: 22302815.

B8261

Bupivacaine

1 g
5 g
25 g

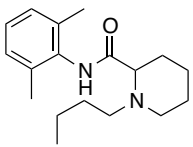

$C_{18}H_{28}N_2O$ FW: 288.43 [38396-39-3] ≥98%

BK/SK, Kv1, Kv3, TASK-2 K^+ channel and voltage-gated Na^+ channel blocker used as an anesthetic. It may be neurotoxic at high doses, inducing apoptosis in neuroblastoma cells.

Harato M, Huang L, Kondo F, et al. Bupivacaine-induced apoptosis independently of WDR35 expression in mouse neuroblastoma Neuro2a cells. BMC Neurosci. 2012 Dec 10;13:149. PMID: 23227925.

Martín P, Enrique N, Palomo AR, et al. Bupivacaine inhibits large conductance, voltage- and Ca^{2+}- activated K^+ channels in human umbilical artery smooth muscle cells. Channels (Austin). 2012 May-Jun;6(3):174-80. PMID: 22688134.

B8262

Bupivacaine Hydrochloride Monohydrate

1 g
5 g
25 g

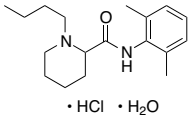

$C_{18}H_{28}N_2O \cdot HCl \cdot H_2O$ FW: 342.91 [73360-54-0] ≥98%

Voltage-gated Na^+, BK/SK, Kv1, Kv3, and TASK-2 K^+ channel inhibitor used as an anesthetic. It may cause depolarization of the mitochondrial membrane potential, increase levels of ROS, and induces apoptosis.

Harato M, Huang L, Kondo F, et al. Bupivacaine-induced apoptosis independently of WDR35 expression in mouse neuroblastoma Neuro2a cells. BMC Neurosci. 2012 Dec 10;13:149. PMID: 23227925.

Martín P, Enrique N, Palomo AR, et al. Bupivacaine inhibits large conductance, voltage- and Ca^{2+}- activated K^+ channels in human umbilical artery smooth muscle cells. Channels (Austin). 2012 May-Jun;6(3):174-80. PMID: 22688134.

B8363

Bupropion Hydrochloride

50 mg
250 mg
1 g

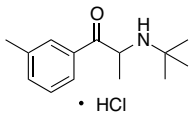

$C_{13}H_{18}ClNO \cdot HCl$ FW: 276.2 [31677-93-7] ≥98%

α3β2, α3β4, α4β2 nAChR antagonist and indirect DA and NE reuptake inhibitor used to treat depression and to increase smoking cessation rates. It suppresses firing of NE neurons due to activation of their inhibitory somatodendritic α2-adrenoreceptors by circulating NE.

Shah TH, Moradimehr A. Bupropion for the treatment of neuropathic pain. Am J Hosp Palliat Care. 2010 Aug;27(5):333-6. PMID: 20185402.

Arias HR. Is the inhibition of nicotinic acetylcholine receptors by bupropion involved in its clinical actions? Int J Biochem Cell Biol. 2009 Nov;41(11):2098-108. PMID: 19497387.

B8271

Bursin

5 mg
10 mg
25 mg

Bursopoietin; KHG-NH2

H-Lys-His-Gly-NH_2

$C_{14}H_{25}N_7O_3$ FW: 339.39 [60267-34-7] ≥95%

Adjuvant that induces B-cell differentiation.

Wang C, Wen WY, Su CX, et al. Bursin as an adjuvant is a potent enhancer of immune response in mice immunized with the JEV subunit vaccine. Vet Immunol Immunopathol. 2008 Apr 15;122(3-4):265-74. PMID: 18191231.

Otsubo Y, Chen N, Kajiwara E, et al. Role of bursin in the development of B lymphocytes in chicken embryonic Bursa of Fabricius. Dev Comp Immunol. 2001 Jun-Jul;25(5-6):485-93. PMID: 11356228.

B8274

Buspirone Hydrochloride

1 g
5 g

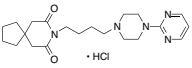

$C_{21}H_{31}N_5O_2 \cdot HCl$ FW: 421.97 [33386-08-2] ≥98%

α1-Adrenergic receptor and 5-HT1A receptor partial agonist, and dopamine D2/3/4 receptor antagonist used to treat anxiety. It also inhibits MMPP-induced enhancements in memory acquisition and formation.

Navarrete A, Flores-Machorro FX, Téllez-Ballesteros RI, et al. Study on action mechanism of 1-(4-methoxy-2-methylphenyl)piperazine (MMPP) in acquisition, formation, and consolidation of memory in mice. Drug Dev Res. 2014 Mar;75(2):59-67. PMID: 24648132.

B7973

Busulfan

10 g
25 g

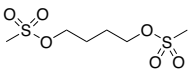

$C_6H_{14}O_6S_2$ FW: 246.3 [55-98-1] ≥98%

DNA alkylator used to treat chronic myelogenous leukemia. It may induce senescence by modulating ERK and p38 MAPK signaling.

Galaup A, Paci A. Pharmacology of dimethanesulfonate alkylating agents: busulfan and treosulfan. Expert Opin Drug Metab Toxicol. 2013 Mar;9(3):333-47. PMID: 23157726.

Probin V, Wang Y, Zhou D. Busulfan-induced senescence is dependent on ROS production upstream of the MAPK pathway. Free Radic Biol Med. 2007 Jun 15;42(12):1858-65. PMID: 17512465.

B8277

Butein

NEW

5 mg
10 mg
25 mg

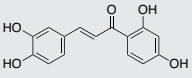

$C_{15}H_{12}O_5$ FW: 272.25 [487-52-5] ≥98%

Found in *Rhus verniciflua* and *Butea monosperma*. It induces cell cycle arrest and apoptosis in lung cancer cells, inhibits vessel sprouting from aortic rings, and prevents hepatic stellate cell activation.

Li Y, Ma C, Qian M, et al. Butein induces cell apoptosis and inhibition of cyclooxygenase 2 expression in A549 lung cancer cells. Mol Med Rep. 2014 Feb;9(2):763-7. PMID: 24337484.

Chung CH, Chang CH, Chen SS, et al. Butein Inhibits Angiogenesis of Human Endothelial Progenitor Cells via the Translation Dependent Signaling Pathway. Evid Based Complement Alternat Med. 2013;2013:943187. PMID: 23840271.

Lu M, Wang S, Han X, et al. Butein inhibits NF-κB activation and reduces infiltration of inflammatory cells and apoptosis after spinal cord injury in rats. Neurosci Lett. 2013 May 10;542:87-91. PMID: 23499960.

B8278

Butoconazole Nitrate

100 mg
250 mg
1 g

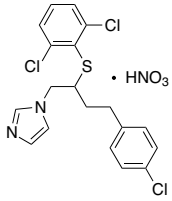

$C_{19}H_{17}Cl_3N_2S \bullet HNO_3$ FW: 474.79 [64872-77-1] ≥98%

14-α demethylase inhibitor that inhibits ergosterol synthesis and fungal cell wall formation. It inhibits growth of *Candida*, *Saccharomyces*, and *Trichomonas*.

Seidman LS, Skokos CK. An evaluation of butoconazole nitrate 2% site release vaginal cream (Gynazole-1) compared to fluconazole 150 mg tablets (Diflucan) in the time to relief of symptoms in patients with vulvovaginal candidiasis. Infect Dis Obstet Gynecol. 2005 Dec;13(4):197-206. PMID: 16338779.

Bourée P, Issoire C. In vitro evaluation of the activity of butoconazole against *Trichomonas* vaginalis. Pathol Biol (Paris). 1992 May;40(5):492-4. PMID: 1495832.

B8174

Butylated Hydroxyanisole

50 g
100 g

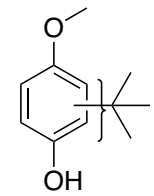

BHA; Antrancine 12

$C_{11}H_{16}O_2$ FW: 180.24 [25013-16-5] ≥96%

Commercial food additive and antioxidant. It scavenges free radicals and inhibits proliferation of breast cancer cells. It may also induce carcinogenesis.

Singh B, Bhat HK. Superoxide dismutase 3 is induced by antioxidants, inhibits oxidative DNA damage and is associated with inhibition of estrogen-induced breast cancer. Carcinogenesis. 2012 Dec;33(12):2601-10. PMID: 23027624.

Criado S, Allevi C, Ceballos C, et al. Visible-light promoted degradation of the commercial antioxidants butylated hydroxyanisole (BHA) and butylated hydroxytoluene (BHT): a kinetic study. Redox Rep. 2007;12(6):282-8. PMID: 17961300.

B7977

Butylated Hydroxytoluene

100 g
500 g

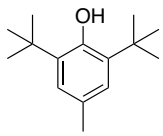

BHT; Antracine 8

$C_{15}H_{24}O$ FW: 220.35 [128-37-0] ≥98%

Food and cosmetics additive used to prevent oxidation. It also suppresses ethanol-induced neurodegeneration and COX-2 expression.

Lee JH, Jung MY. Direct spectroscopic observation of singlet oxygen quenching and kinetic studies of physical and chemical singlet oxygen quenching rate constants of synthetic antioxidants (BHA, BHT, and TBHQ) in methanol. J Food Sci. 2010 Aug 1;75(6):C506-13. PMID: 20722904.

Crews F, Nixon K, Kim D, et al. BHT blocks NF-kappaB activation and ethanol-induced brain damage. Alcohol Clin Exp Res. 2006 Nov;30(11):1938-49. PMID: 17067360.

B8070

2-*tert*-Butyl-4-Hydroxyanisole

100 mg
500 mg
1 g

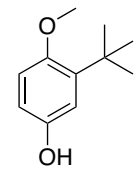

2-BHA

$C_{11}H_{16}O_2$ FW: 180.25 [88-32-4] ≥99%

Derivative of BHA and food and cosmetics additive used to prevent oxidation. It also induces phase II enzyme activity.

Hwang GH, Jeon YJ, Han HJ, et al. Protective effect of butylated hydroxylanisole against hydrogen peroxide-induced apoptosis in primary cultured mouse hepatocytes. J Vet Sci. 2014 Oct 8. [Epub ahead of print]. PMID: 25293491.

Nishiya H, Haga T, Nozue N, et al. Effects of 2(3)-tert-butyl-4-hydroxyanisole pretreatment on cefpiramide binding to mouse glutathione S-transferases. Pharmacology. 1989;39(4):213-23. PMID: 2608720.

B8071

3-*tert*-Butyl-4-Hydroxyanisole

5 g
10 g
50 g

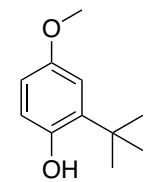

3-BHA

$C_{11}H_{16}O_2$ FW: 180.25 [121-00-6] ≥99%

Derivative of BHA and food and cosmetics additive used to prevent oxidation. It induces apoptosis and DNA damage in leukemia cells and increases phase II enzyme activity in vivo.

Hwang GH, Jeon YJ, Han HJ, et al. Protective effect of butylated hydroxylanisole against hydrogen peroxide-induced apoptosis in primary cultured mouse hepatocytes. J Vet Sci. 2014 Oct 8. [Epub ahead of print]. PMID: 25293491.

Okubo T, Yokoyama Y, Kano K, et al. Molecular mechanism of cell death induced by the antioxidant tert-butylhydroxyanisole in human monocytic leukemia U937 cells. Biol Pharm Bull. 2004 Mar;27(3):295-302. PMID: 14993791.

B8072

3-*tert*-Butyl-5-Methoxycatechol

10 mg
50 mg
100 mg

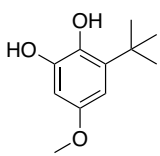

$C_{11}H_{16}O_3$ FW: 196.25 [80284-15-7] ≥98%

Derivative of BHA. It inhibits proliferation of leukemia cells and may also induce cellular differentiation.

Tsuchiya T, Ishida A, Miyata N, et al. Effects of 3-tert-Butyl-4-hydroxyanisole and its hydroquinone and quinone metabolites on rat and human embryonic cells in culture. Toxicol In Vitro. 1988;2(4):291-6. PMID: 20837439.

Lam LK, Garg PK, Swanson SM, et al. Evaluation of the cytotoxic potential of catechols and quinones structurally related to butylated hydroxyanisole. J Pharm Sci. 1988 May;77(5):393-5. PMID: 3411459.

B8073 4-*tert*-Butyl-5-Methoxycatechol

10 mg
50 mg
100 mg

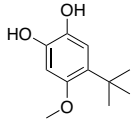

$C_{11}H_{16}O_3$ FW: 196.25 [91352-66-8] ≥98%

BHA derivative. It inhibits proliferation of leukemia cells.

Lam LK, Garg PK, Swanson SM, et al. Evaluation of the cytotoxic potential of catechols and quinones structurally related to butylated hydroxyanisole. J Pharm Sci. 1988 May;77(5):393-5. PMID: 3411459.

B8074 3-*tert*-Butyl-5-Methoxy-1,2-quinone

50 mg
100 mg
500 mg

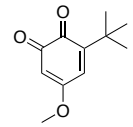

$C_{11}H_{14}O_3$ FW: 194.25 [2940-63-8] ≥98%

BHA derivative. It inhibits proliferation of leukemia cells.

Lam LK, Garg PK, Swanson SM, et al. Evaluation of the cytotoxic potential of catechols and quinones structurally related to butylated hydroxyanisole. J Pharm Sci. 1988 May;77(5):393-5. PMID: 3411459.

B8075 4-*tert*-Butyl-5-Methoxy-1,2-quinone

50 mg
100 mg
500 mg

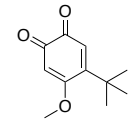

$C_{11}H_{14}O_3$ FW: 194.25 [36122-03-9] ≥98%

BHA derivative. It inhibits proliferation of leukemia cells.

Lam LK, Garg PK, Swanson SM, et al. Evaluation of the cytotoxic potential of catechols and quinones structurally related to butylated hydroxyanisole. J Pharm Sci. 1988 May;77(5):393-5. PMID: 3411459.

B8176 2-n-Butylthiophene

5 g
10 g

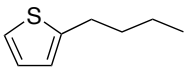

$C_8H_{12}S$ FW: 140.25 [1455-20-5] ≥98%

It induces phase II enzyme activity and prevents benzo[a]pyrene-induced tumor formation.

Lam LK, Zheng BL. Inhibitory effects of 2-n-heptylfuran and 2-n-butylthiophene on benzo[a]pyrene-induced lung and forestomach tumorigenesis in A/J mice. Nutr Cancer. 1992;17(1):19-26. PMID: 1574441.

B8275 n-Butyric Acid

10 ml
100 ml

Butanoic acid; Ethylacetic acid

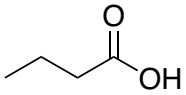

$C_4H_8O_2$ FW: 88.1 [107-92-6] ≥98%

HDAC inhibitor found in dairy products. It induces cell cycle arrest and apoptosis in glioma cells. It also stimulates epithelial cell proliferation at low doses and inhibits proliferation at high doses.

Kim SW, Hooker JM, Otto N, et al. Whole-body pharmacokinetics of HDAC inhibitor drugs, butyric acid, valproic acid and 4-phenylbutyric acid measured with carbon-11 labeled analogs by PET. Nucl Med Biol. 2013 Oct;40(7):912-8. PMID: 23906667.

Inagaki A, Sakata T. Dose-dependent stimulatory and inhibitory effects of luminal and serosal n-butyric acid on epithelial cell proliferation of pig distal colonic mucosa. J Nutr Sci Vitaminol (Tokyo). 2005 Jun;51(3):156-60. PMID: 16161765.

B8276 Butyric Acid Sodium

5 g
25 g

Sodium Butyrate

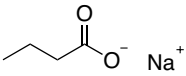

C_4H_7NaO2 FW: 110.09 [156-54-7] ≥97%

HDAC inhibitor and RNA splicing modulator. It decreases restraint stress-induced depression, induces apoptosis and inhibits proliferation in prostate cancer cells, and decreases release of IL-12 and increases production of IL-23 in dendritic cells.

Han A, Sung YB, Chung SY, et al. Possible additional antidepressant-like mechanism of sodium butyrate: targeting the hippocampus. Neuropharmacology. 2014 Jun;81:292-302. PMID: 24607816.

Mu D, Gao Z, Guo H, et al. Sodium butyrate induces growth inhibition and apoptosis in human prostate cancer DU145 cells by up-regulation of the expression of annexin A1. PLoS One. 2013 Sep 23;8(9):e74922. PMID: 24086397.

Berndt BE, Zhang M, Owyang SY, et al. Butyrate increases IL-23 production by stimulated dendritic cells. Am J Physiol Gastrointest Liver Physiol. 2012 Dec 15;303(12):G1384-92. PMID: 23086919.

B8676 BVT-2733

NEW

5 mg
25 mg

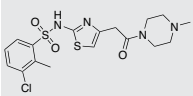

$C_{17}H_{21}ClN_4O_3S_2$ FW: 428.96 [376640-41-4] ≥98%

Inhibitor of 11βHSD1. It decreases blood glucose and serum insulin levels in animal models of hyperglycemia, suppresses pro-inflammatory cytokine production, and prevents 11βHSD-induced osteogenic differentiation.

Zhang L, Dong Y, Zou F, et al. 11β-Hydroxysteroid dehydrogenase 1 inhibition attenuates collagen-induced arthritis. Int Immunopharmacol. 2013 Nov;17(3):489-94. PMID: 23938253.

Wu L, Qi H, Zhong Y, et al. 11β-Hydroxysteroid dehydrogenase type 1 selective inhibitor BVT.2733 protects osteoblasts against endogenous glucocorticoid induced dysfunction. Endocr J. 2013;60(9):1047-58. PMID: 23759754.

B9200 BX-795

NEW

5 mg
10 mg

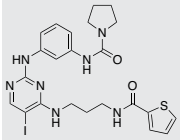

$C_{23}H_{26}IN_7O_2S$ FW: 591.47 [702675-74-9] ≥98%

PDK1 inhibitor. It induces apoptosis and suppresses tumor growth in cancer models.

Feldman RI, Wu JM, Polokoff MA, et al. Novel small molecule inhibitors of 3-phosphoinositide-dependent kinase-1. J Biol Chem. 2005 May 20;280(20):19867-74. PMID: 15772071.

B9700 BYL719

1 mg
5 mg
25 mg

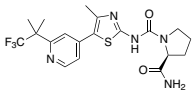

$C_{19}H_{22}F_3N_5O_2S$ FW: 441.47 [1217486-61-7] ≥99%

p110α PI3K inhibitor selective for p110 isoform activated in HER2+ breast cancers and gastric cancers. It inhibits proliferation of breast cancer cells and decreases invasiveness of squamous cell lung cancer cells.

Bonelli MA, Cavazzoni A, Saccani F, et al. Inhibition of PI3K pathway reduces invasiveness and epithelial-to-mesenchymal transition in squamous lung cancer cell lines harboring PIK3CA gene alterations. Mol Cancer Ther. 2015 May 26. [Epub ahead of print]. PMID: 26013318.

Elkabets M, Vora S, Juric D, et al. mTORC1 Inhibition Is Required for Sensitivity to PI3K p110α Inhibitors in PIK3CA-Mutant Breast Cancer. Sci Transl Med. 2013 Jul 31;5(196):196ra99. PMID: 23903756.

C0800 C59

NEW

1 mg
5 mg

Wnt-C59

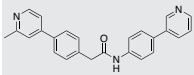

$C_{25}H_{21}N_3O$ FW: 379.45 [1243243-89-1] ≥98%

PORCN inhibitor. It downregulates Wnt signaling and inhibits mammary tumor progression.

Proffitt KD, Madan B, Ke Z, et al. Pharmacological inhibition of the Wnt acyltransferase PORCN prevents growth of WNT-driven mammary cancer. Cancer Res. 2013 Jan 15;73(2):502-7. PMID: 23188502.

C0006 Cabozantinib

10 mg
25 mg
100 mg
250 mg

XL-184; BMS-907351

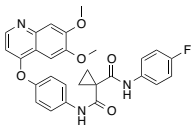

$C_{28}H_{24}FN_3O_5$ FW: 501.51 [849217-68-1] ≥98%

Inhibitor of VEGFR2, c-Met, and RET used to treat medullary thyroid cancer. It induces apoptosis and inhibits cell growth in cancer cells and suppresses proliferation of osteoclasts.

Dai J, Zhang H, Karatsinides A, et al. Cabozantinib inhibits prostate cancer growth and prevents tumor-induced bone lesions. Clin Cancer Res. 2013 Oct 4. [Epub ahead of print]. PMID: 24097861.

Elisei R, Schlumberger MJ, Müller SP, et al. Cabozantinib in progressive medullary thyroid cancer. J Clin Oncol. 2013 Oct 10;31(29):3639-46. PMID: 24002501.

Bentzien F, Zuzow M, Heald N, et al. In Vitro and In Vivo Activity of Cabozantinib (XL184), an Inhibitor of RET, MET, and VEGFR2, in a Model of Medullary Thyroid Cancer. Thyroid. 2013 Sep 17. [Epub ahead of print]. PMID: 23705946.

C0016 Caerulomycin A

1 mg

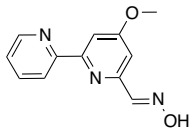

$C_{12}H_{11}N_3O_2$ FW: 229.23 [21802-37-9] ≥96%

Toxin that inhibits growth of *Entamoeba*, may prevent proliferation of cancer cells, and suppresses immune responses.

Zhu Y, Zhang Q, Li S, et al. Insights into Caerulomycin A Biosynthesis: A Two-Component Monooxygenase CrmH-Catalyzed Oxime Formation. J Am Chem Soc. 2013 Dec 5. [Epub ahead of print]. PMID: 24295370.

Cristalli G, Franchetti P, Grifantini M, et al. 2,2'-Bipyridyl-6-carboxamidoximes with potential antitumor and antimicrobial properties. Farmaco Sci. 1986 Jul;41(7):499-507. PMID: 3743743

C0020 Cafestol

50 mg
100 mg
500 mg

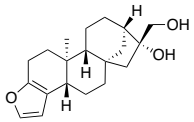

$C_{20}H_{28}O_3$ FW: 316.44 [469-83-0] ≥98%

Natural product found in brewed, unfiltered coffee. Inhibitor of ERK2 and MEK1, agonist at FXR and PXR receptors. It displays a wide variety of biological activities, including inhibiting angiogenesis, inducing apoptosis and cell cycle arrest in renal carcinoma cells, and suppressing neurodegeneration in Parkinson's disease models.

Wang S, Yoon YC, Sung MJ, et al. Antiangiogenic properties of cafestol, a coffee diterpene, in human umbilical vein endothelial cells. Biochem Biophys Res Commun. 2012 May 11;421(3):567-71. PMID: 22525673.

Choi MJ, Park EJ, Oh JH, et al. Cafestol, a coffee-specific diterpene, induces apoptosis in renal carcinoma Caki cells through down-regulation of anti-apoptotic proteins and Akt phosphorylation. Chem Biol Interact. 2011 Apr 25;190(2-3):102-8. PMID: 21334318.

Trinh K, Andrews L, Krause J, et al. Decaffeinated coffee and nicotine-free tobacco provide neuroprotection in *Drosophila* models of Parkinson's disease through an NRF2-dependent mechanism. J Neurosci. 2010 Apr 21;30(16):5525-32. PMID: 20410106.

C0021 Cafestol Acetate

50 mg
100 mg
500 mg

$C_{22}H_{30}O_4$ FW: 358.48 [81760-48-7] ≥98%

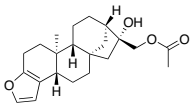

Semi-synthetic derivative of cafestol, a natural product found in brewed, unfiltered coffee. Inhibitor of ERK2 and MEK1, agonist at FXR and PXR receptors. It displays a wide variety of biological activities, including inhibiting angiogenesis, inducing apoptosis and cell cycle arrest in renal carcinoma cells, and suppressing neurodegeneration in Parkinson's disease models.

Wang S, Yoon YC, Sung MJ, et al. Antiangiogenic properties of cafestol, a coffee diterpene, in human umbilical vein endothelial cells. Biochem Biophys Res Commun. 2012 May 11;421(3):567-71. PMID: 22525673.

Choi MJ, Park EJ, Oh JH, et al. Cafestol, a coffee-specific diterpene, induces apoptosis in renal carcinoma Caki cells through down-regulation of anti-apoptotic proteins and Akt phosphorylation. Chem Biol Interact. 2011 Apr 25;190(2-3):102-8. PMID: 21334318.

C0025 Cafestol Eicosanate

25 mg
50 mg
100 mg

$C_{40}H_{66}O_4$ FW: 610.95 ≥98%

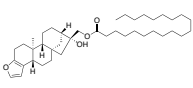

Semi-synthetic derivative of cafestol, a natural product found in brewed, unfiltered coffee. Inhibitor of ERK2 and MEK1, agonist at FXR and PXR receptors. It displays a wide variety of biological activities, including inhibiting angiogenesis, inducing apoptosis and cell cycle arrest in renal carcinoma cells, and suppressing neurodegeneration in Parkinson's disease models.

Wang S, Yoon YC, Sung MJ, et al. Antiangiogenic properties of cafestol, a coffee diterpene, in human umbilical vein endothelial cells. Biochem Biophys Res Commun. 2012 May 11;421(3):567-71. PMID: 22525673.

Choi MJ, Park EJ, Oh JH, et al. Cafestol, a coffee-specific diterpene, induces apoptosis in renal carcinoma Caki cells through down-regulation of anti-apoptotic proteins and Akt phosphorylation. Chem Biol Interact. 2011 Apr 25;190(2-3):102-8. PMID: 21334318.

C0027 Cafestol Linoleate

25 mg
50 mg
100 mg

$C_{38}H_{58}O_4$ FW: 578.87 ≥98%

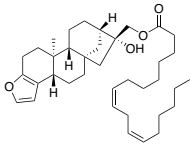

Semi-synthetic derivative of cafestol, a natural product found in brewed, unfiltered coffee. Inhibitor of ERK2 and MEK1, agonist at FXR and PXR receptors. It displays a wide variety of biological activities, including inhibiting angiogenesis, inducing apoptosis and cell cycle arrest in renal carcinoma cells, and suppressing neurodegeneration in Parkinson's disease models.

Wang S, Yoon YC, Sung MJ, et al. Antiangiogenic properties of cafestol, a coffee diterpene, in human umbilical vein endothelial cells. Biochem Biophys Res Commun. 2012 May 11;421(3):567-71. PMID: 22525673.

Choi MJ, Park EJ, Oh JH, et al. Cafestol, a coffee-specific diterpene, induces apoptosis in renal carcinoma Caki cells through down-regulation of anti-apoptotic proteins and Akt phosphorylation. Chem Biol Interact. 2011 Apr 25;190(2-3):102-8. PMID: 21334318.

C0029 Cafestol Oleate

25 mg
50 mg
100 mg

$C_{38}H_{60}O_4$ FW: 580.88 ≥98%

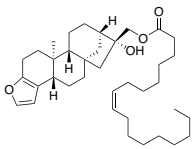

Semi-synthetic derivative of cafestol, a natural product found in brewed, unfiltered coffee. Inhibitor of ERK2 and MEK1, agonist at FXR and PXR receptors. It displays a wide variety of biological activities, including inhibiting angiogenesis, inducing apoptosis and cell cycle arrest in renal carcinoma cells, and suppressing neurodegeneration in Parkinson's disease models.

Wang S, Yoon YC, Sung MJ, et al. Antiangiogenic properties of cafestol, a coffee diterpene, in human umbilical vein endothelial cells. Biochem Biophys Res Commun. 2012 May 11;421(3):567-71. PMID: 22525673.

C0022 Cafestol Palmitate

50 mg
100 mg
500 mg

$C_{36}H_{58}O_4$ FW: 554.43 [81760-46-5] ≥98%

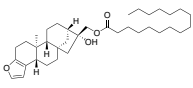

Semi-synthetic derivative of cafestol, a natural product found in brewed, unfiltered coffee. Inhibitor of ERK2 and MEK1, agonist at FXR and PXR receptors. It displays a wide variety of biological activities, including inhibiting angiogenesis, inducing apoptosis and cell cycle arrest in renal carcinoma cells, and suppressing neurodegeneration in Parkinson's disease models.

Wang S, Yoon YC, Sung MJ, et al. Antiangiogenic properties of cafestol, a coffee diterpene, in human umbilical vein endothelial cells. Biochem Biophys Res Commun. 2012 May 11;421(3):567-71. PMID: 22525673.

C0033 Cafestol Stearate

25 mg
50 mg
100 mg

$C_{38}H_{62}O_4$ FW: 582.9 ≥98%

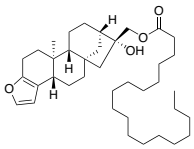

Semi-synthetic derivative of cafestol, a natural product found in brewed, unfiltered coffee. Inhibitor of ERK2 and MEK1, agonist at FXR and PXR receptors. It displays a wide variety of biological activities, including inhibiting angiogenesis, inducing apoptosis and cell cycle arrest in renal carcinoma cells, and suppressing neurodegeneration in Parkinson's disease models.

Wang S, Yoon YC, Sung MJ, et al. Antiangiogenic properties of cafestol, a coffee diterpene, in human umbilical vein endothelial cells. Biochem Biophys Res Commun. 2012 May 11;421(3):567-71. PMID: 22525673.

C0121 Caffeic Acid

5 g
25 g

3,4-Dihydroxycinnamic acid

$C_9H_8O_4$ FW: 180.16 [331-39-5] ≥98%

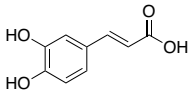

α-Amylase and α-glucosidase inhibitor found in coffee, argan oil, *Eucaplyptus*, *Salvinia*, and *Phellinus*. It exhibits a wide variety of biological activities, including inhibiting LPS-stimulated inflammatory cytokine release, inducing cell cycle arrest and apoptosis in colon cancer cells, and decreasing membrane stability and inhibiting proliferation of *Staphylococcus*.

Oboh G, Agunloye OM, Adefegha SA, et al. Caffeic and chlorogenic acids inhibit key enzymes linked to type 2 diabetes (in vitro): a comparative study. J Basic Clin Physiol Pharmacol. 2014 May 12. [Epub ahead of print]. PMID: 24825096.

Liu M, Song S, Li H, et al. The protective effect of caffeic acid against inflammation injury of primary bovine mammary epithelial cells induced by lipopolysaccharide. J Dairy Sci. 2014 May;97(5):2856-65. PMID: 24612802.

C0221 Caffeine

10 g
50 g
100 g

Thein; Guaranine; Methyltheobromine

$C_8H_{10}N_4O_2$ FW: 194.19 [58-08-2] ≥98%

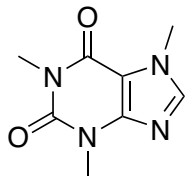

Adenosine agonist and PDE inhibitor found in coffee, tea, and other plant sources. It prevents fibrosis by decreasing release of STGF, collagen I, TGF-β1, and pro-inflammatory cytokines. It also increases vasoconstriction, decreases UV radiation-dependent skin damage, and may limit risk of cardiovascular and neurological disease development.

Qi H, Li S. Dose-response meta-analysis on coffee, tea and caffeine consumption with risk of Parkinson's disease. Geriatr Gerontol Int. 2014 Apr;14(2):430-9. PMID: 23879665.

Gordillo-Bastidas D, Oceguera-Contreras E, Salazar-Montes A, et al. Nrf2 and Snail-1 in the prevention of experimental liver fibrosis by caffeine. World J Gastroenterol. 2013 Dec 21;19(47):9020-33. PMID: 24379627.

C0044 CAL101

NEW

1 mg
5 mg
10 mg

Idelalisib; GS1101

$C_{22}H_{18}FN_7O$ FW: 415.42 [870281-82-6] ≥98%

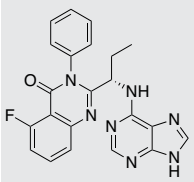

Inhibitor of p110δ PI3K used to treat chronic lymphocytic leukemia. It induces cell cycle arrest and apoptosis in mantle cell lymphoma cells and inhibits chemotaxis and migration in chronic lymphocytic leukemia cells.

Sanford DS, Wierda WG, Burger JA, et al. Three Newly Approved Drugs for Chronic Lymphocytic Leukemia: Incorporating Ibrutinib, Idelalisib, and Obinutuzumab into Clinical Practice. Clin Lymphoma Myeloma Leuk. 2015 Feb 19. [Epub ahead of print]. PMID: 25817936.

Chiron D, Martin P, Di Liberto M, et al. Induction of prolonged early G1 arrest by CDK4/CDK6 inhibition reprograms lymphoma cells for durable PI3Kδ inhibition through PIK3IP1. Cell Cycle. 2013 Jun 15;12(12):1892-900. PMID: 23676220.

Meadows SA, Vega F, Kashishian A, Johnson D, et al. PI3Kδ inhibitor, GS-1101 (CAL-101), attenuates pathway signaling, induces apoptosis, and overcomes signals from the microenvironment in cellular models of Hodgkin lymphoma. Blood. 2012 Feb 23;119(8):1897-900. PMID: 22210877.

C0246 Calcimycin

1 mg
5 mg
10 mg

A-23187

$C_{29}H_{37}N_3O_6$ FW: 523.62 [52665-69-7] ≥98%

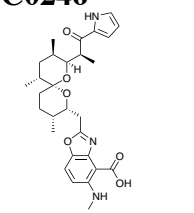

Divalent cation ionophore that increases intracellular Ca^{2+} levels, uncouples oxidative phosphorylation, and inhibits mitochondrial ATPase activity. In mast cells, it induces degranulation and pro-inflammatory cytokine production.

Hosokawa J, Suzuki K, Nakagomi D, et al. Role of calcium ionophore A23187-induced activation of IkappaB kinase 2 in mast cells. Int Arch Allergy Immunol. 2013;161 Suppl 2:37-43. PMID: 23711852.

C0247

Calcineurin Autoinhibitory Peptide

0.5 mg
1 mg
2.5 mg

H-Ile-Thr-Ser-Phe-Glu-Glu-Ala-Lys-Gly-Leu-Asp-Arg-Ile-Asn-Glu-Arg-Met-Pro-Pro-Arg-Arg-Asp-Ala-Met-Pro-OH

$C_{124}H_{205}N_{39}O_{39}S_2$ FW: 2930.38 ≥95%

Calcineurin inhibitor. It inhibits glutamate-mediated neuronal cell death and decreases L-type Ca^{2+} channel currents.

Terada H, Matsushita M, Lu YF, et al. Inhibition of excitatory neuronal cell death by cell-permeable calcineurin autoinhibitory peptide. J Neurochem. 2003 Dec;87(5):1145-51. PMID: 14622094.

Norris CM, Blalock EM, Chen KC, et al. Calcineurin enhances L-type $Ca^{(2+)}$ channel activity in hippocampal neurons: increased effect with age in culture. Neuroscience. 2002;110(2):213-25. PMID: 11958864.

C0248

Calcineurin Substrate

0.5 mg
1 mg
2.5 mg

Asp-Leu-Asp-Val-Pro-Ile-Pro-Gly-Arg-Phe-Asp-Arg-Arg-Val-Ser-Val-Ala-Ala-Glu

$C_{92}H_{150}N_{28}O_{29}S$ FW: 2112.4 [113873-67-9] ≥96%

Used to measure in vitro calcineurin activity.

Namgaladze D, Hofer HW, Ullrich V. Redox control of calcineurin by targeting the binuclear $Fe^{(2+)}$-$Zn^{(2+)}$ center at the enzyme active site. J Biol Chem. 2002 Feb 22;277(8):5962-9. PMID: 11741966.

Perrino BA, Fong YL, Brickey DA, et al. Characterization of the phosphatase activity of a baculovirus-expressed calcineurin A isoform. J Biol Chem. 1992 Aug 5;267(22):15965-9. PMID: 1322410.

C0243

Calcitonin Gene Related Peptide (8-37), human

0.5 mg
1 mg
2.5 mg

H-Val-Thr-His-Arg-Leu-Ala-Gly-Leu-Leu-Ser-Arg-Ser-Gly-Gly-Val-Val-Lys-Asn-Asn-Phe-Val-Pro-Thr-Asn-Val-Gly-Ser-Lys-Ala-Phe-NH_2

CGRP

$C_{139}H_{230}N_{44}O_{38}$ FW: 3125.65 [119911-68-1] ≥95%

Calcitonin-family peptide fragment used to study CGRP function. It likely activates RAMP1 and CGRP receptors. It also inhibits ghrelin signaling and induces apoptosis in retinal cells.

Nguyen VT, Wu Y, Guillory AN, et al. Delta-opioid augments cardiac contraction through β-adrenergic and CGRP-receptor co-signaling. Peptides. 2012 Jan;33(1):77-82. PMID: 22108711.

Yang JH, Zhang YQ, Guo Z. Endogenous CGRP protects retinal cells against stress induced apoptosis in rats. Neurosci Lett. 2011 Aug 26;501(2):83-5. PMID: 21763400.

C0249

Calcitonin Gene Related Peptide (8-37), rat

0.5 mg
1 mg
2.5 mg

H-Val-Thr-His-Arg-Leu-Ala-Gly-Leu-Leu-Ser-Arg-Ser-Gly-Gly-Val-Val-Lys-Asn-Asn-Phe-Val-Pro-Thr-Asn-Val-Gly-Ser-Lys-Ala-Phe-NH_2

CGRP

$C_{138}H_{224}N_{42}O_{41}$ FW: 3127.58 ≥95%

Calcitonin-family peptide fragment used to study CGRP function. It likely activates RAMP1 and CGRP receptors. It also inhibits ghrelin signaling and induces apoptosis in retinal cells.

Nguyen VT, Wu Y, Guillory AN, et al. Delta-opioid augments cardiac contraction through β-adrenergic and CGRP-receptor co-signaling. Peptides. 2012 Jan;33(1):77-82. PMID: 22108711.

Yang JH, Zhang YQ, Guo Z. Endogenous CGRP protects retinal cells against stress induced apoptosis in rats. Neurosci Lett. 2011 Aug 26;501(2):83-5. PMID: 21763400.

C0250

Calcitonin Gene Related Peptide II, human

0.5 mg
1 mg
2.5 mg

Ala-Cys-Asn-Thr-Ala-Thr-Cys-Val-Thr-His-Arg-Leu-Ala-Gly-Leu-Leu-Ser-Arg-Ser-Gly-Gly-Met-Val-Lys-Ser-Asn-Phe-Val-Pro-Thr-Asn-Val-Gly-Ser-Lys-Ala-Phe-NH_2
(Disulfide Bridge Cys2-Cys7)

CGRP II

$C_{162}H_{267}N_{51}O_{48}S_3$ FW: 3793.38 ≥95%

Calcitonin-family peptide that likely activates RAMP1 and CGRP receptors. It also dilates arterioles, inhibits gastric acid secretion, and is associated with inflammatory diseases.

Vanner S. Mechanism of action of capsaicin on submucosal arterioles in the guinea pig ileum. Am J Physiol. 1993 Jul;265(1 Pt 1):G51-5. PMID: 8338172.

Hernanz A, De Miguel E, Romera N, et al. Calcitonin gene-related peptide II, substance P and vasoactive intestinal peptide in plasma and synovial fluid from patients with inflammatory joint disease. Br J Rheumatol. 1993 Jan;32(1):31-5. PMID: 7678534.

C0251

Calcitonin Gene Related Peptide II, rat

0.5 mg
1 mg
2.5 mg

H-Ser-Cys-Asn-Thr-Ala-Thr-Cys-Val-Thr-His-Arg-Leu-Ala-Gly-Leu-Leu-Ser-Arg-Ser-Gly-Gly-Val-Val-Lys-Asp-Asn-Phe-Val-Pro-Thr-Asn-Val-Gly-Ser-Lys-Ala-Phe-NH_2
(Disulfide Bridge Cys2-Cys7)

CGRP II

$C_{163}H_{265}N_{51}O_{50}S_2$ FW: 3803.39 ≥95%

Calcitonin-family peptide that likely activates RAMP1 and CGRP receptors. It also dilates arterioles, inhibits gastric acid secretion, and is associated with inflammatory diseases.

Vanner S. Mechanism of action of capsaicin on submucosal arterioles in the guinea pig ileum. Am J Physiol. 1993 Jul;265(1 Pt 1):G51-5. PMID: 8338172.

Hernanz A, De Miguel E, Romera N, et al. Calcitonin gene-related peptide II, substance P and vasoactive intestinal peptide in plasma and synovial fluid from patients with inflammatory joint disease. Br J Rheumatol. 1993 Jan;32(1):31-5. PMID: 7678534.

C0245

Calcitonin Gene Related Peptide, rat

0.5 mg
1 mg
2.5 mg

H-Ser-Cys-Asn-Thr-Ala-Thr-Cys-Val-Thr-His-Arg-Leu-Ala-Gly-Leu-Leu-Ser-Arg-Ser-Gly-Gly-Val-Val-Lys-Asp-Asn-Phe-Val-Pro-Thr-Asn-Val-Gly-Ser-Glu-Ala-Phe-NH_2
(Disulfide Bridge Cys2-Cys7)

CGRP

$C_{162}H_{260}N_{50}O_{52}S_2$ FW: 3804.33 ≥95%

Endogenous calcitonin-family peptide involved in vasodilation and pain transmission. It activates RAMP1 and CGRP receptors, decreases pro-inflammatory cytokine levels, stimulates proliferation of osteoblasts, inhibits apoptosis in retinal cells, and increases capillary density in ischemia models.

Ma W, Zhang X, Shi S, et al. Neuropeptides stimulate human osteoblast activity and promote gap junctional intercellular communication. Neuropeptides. 2013 Jun;47(3):179-86. PMID: 23726661.

Yang JH, Zhang YQ, Guo Z. Endogenous CGRP protects retinal cells against stress induced apoptosis in rats. Neurosci Lett. 2011 Aug 26;501(2):83-5. PMID: 21763400.

C0146

Calcitonin, chicken

0.5 mg
1 mg
2.5 mg

H-Cys-Ala-Ser-Leu-Ser-Thr-Cys-Val-Leu-Gly-Lys-Leu-Ser-Gln-Glu-Leu-His-Lys-Leu-Gln-Thr-Tyr-Pro-Arg-Thr-Asp-Val-Gly-Ala-Gly-Thr-Pro-NH_2
(Disulfide Bridge Cys1-Cys7)

$C_{145}H_{240}N_{42}O_{46}S_2$ FW: 3371.91 [9007-12-9] ≥95%

Endogenous hormone that lowers extracellular Ca^{2+} levels. It increases growth of osteosarcoma cells, improves medial femoral condyle osteoarthritis, and inhibits SCDP-induced apoptosis of osteoclasts.

Tsagaraki I, Phenekos C, Tsilibary E, et al. Calcitonin-induced NF-κB activation up-regulates fibronectin expression in MG63 osteosarcoma cells. Anticancer Res. 2013 Nov;33(11):4901-6. PMID: 24222127.

Armagan O, Serin DK, Calisir C, et al. Inhalation therapy of calcitonin relieves osteoarthritis of the knee. J Korean Med Sci. 2012 Nov;27(11):1405-10. PMID: 23166425.

C0140

Calcitonin, eel

1 mg
2 mg
5 mg

H-Cys-Ser-Asn-Leu-Ser-Thr-Cys-Val-Leu-Gly-Lys-Leu-Ser-Gln-Glu-Leu-His-Lys-Leu-Gln-Thr-Tyr-Pro-Arg-Thr-AspVal-Gly-Ala-Gly-Thr-Pro-NH_2
(Disulfide Bridge Cys1-Cys7)

$C_{146}H_{241}N_{43}O_{47}S_2$ FW: 3414.94 ≥95%

Endogenous hormone that lowers extracellular Ca^{2+} levels. It increases growth of osteosarcoma cells, improves medial femoral condyle osteoarthritis, and inhibits SCDP-induced apoptosis of osteoclasts.

Tsagaraki I, Phenekos C, Tsilibary E, et al. Calcitonin-induced NF-κB activation up-regulates fibronectin expression in MG63 osteosarcoma cells. Anticancer Res. 2013 Nov;33(11):4901-6. PMID: 24222127.

Armagan O, Serin DK, Calisir C, et al. Inhalation therapy of calcitonin relieves osteoarthritis of the knee. J Korean Med Sci. 2012 Nov;27(11):1405-10. PMID: 23166425.

C0148

Calcitonin, human

0.5 mg
1 mg
2.5 mg

Cys-Gly-Asn-Leu-Ser-Thr-Cys-Met-Leu-Gly-Thr-Tyr-Thr-Gln-Asp-Phe-Asn-Lys-Phe-His-Thr-Phe-Pro-Gln-Thr-Ala-Ile-Gly-Val-Gly-Ala-Pro-NH_2
(Disulfide bridge Cys1-Cys7)

hCT; Thyrocalcitonin

$C_{145}H_{240}N_{44}O_{48}S_2$ FW: 3417.88 [21215-62-3] ≥95%

Endogenous hormone that lowers extracellular Ca^{2+} levels. It increases growth of osteosarcoma cells, improves medial femoral condyle osteoarthritis, and inhibits SCDP-induced apoptosis of osteoclasts.

Tsagaraki I, Phenekos C, Tsilibary E, et al. Calcitonin-induced NF-κB activation up-regulates fibronectin expression in MG63 osteosarcoma cells. Anticancer Res. 2013 Nov;33(11):4901-6. PMID: 24222127.

Armagan O, Serin DK, Calisir C, et al. Inhalation therapy of calcitonin relieves osteoarthritis of the knee. J Korean Med Sci. 2012 Nov;27(11):1405-10. PMID: 23166425.

C0153

Calcitonin, rat

0.5 mg
1 mg
2.5 mg

H-Cys-Gly-Asn-Leu-Ser-Thr-Cys-Met-Leu-Gly-Thr-Tyr-Thr-Gln-Asp-Leu-Asn-Lys-Phe-His-Thr-Phe-Pro-Gln-Thr-Ser-Ile-Gly-Val-Gly-Ala-Pro-NH_2
(Disulfide Bridge Cys1-Cys7)

$C_{148}H_{228}N_{40}O_{46}S_3$ FW: 3399.9 ≥95%

Endogenous hormone that lowers extracellular Ca^{2+} levels. It increases growth of osteosarcoma cells, improves medial femoral condyle osteoarthritis, and inhibits SCDP-induced apoptosis of osteoclasts.

Tsagaraki I, Phenekos C, Tsilibary E, et al. Calcitonin-induced NF-κB activation up-regulates fibronectin expression in MG63 osteosarcoma cells. Anticancer Res. 2013 Nov;33(11):4901-6. PMID: 24222127.

Armagan O, Serin DK, Calisir C, et al. Inhalation therapy of calcitonin relieves osteoarthritis of the knee. J Korean Med Sci. 2012 Nov;27(11):1405-10. PMID: 23166425.

C0149

Calcitonin, salmon

0.5 mg
1 mg
2.5 mg

Cys-Ser-Asn-Leu-Ser-Thr-Cys-Val-Leu-Gly-Lys-Leu-Ser-Gln-Glu-Leu-His-Lys-Leu-Gln-Thr-Tyr-Pro-Arg-Thr-Asn-Thr-Gly-Ser-Gly-Thr-Pro-NH_2
(Disulfide bridge Cys1-Cys7)

$C_{151}H_{226}N_{40}O_{45}S_3$ FW: 3431.85 [47931-85-1] ≥98%

Endogenous hormone that lowers extracellular Ca^{2+} levels. It increases growth of osteosarcoma cells, improves medial femoral condyle osteoarthritis, and inhibits SCDP-induced apoptosis of osteoclasts.

Tsagaraki I, Phenekos C, Tsilibary E, et al. Calcitonin-induced NF-κB activation up-regulates fibronectin expression in MG63 osteosarcoma cells. Anticancer Res. 2013 Nov;33(11):4901-6. PMID: 24222127.

C0244

α-Calcitonin Gene Related Peptide, chicken

0.5 mg
1 mg
2.5 mg

H-Ala-Cys-Asn-Thr-Ala-Thr-Cys-Val-Thr-His-Arg-Leu-Ala-Asp-Phe-Leu-Ser-Arg-Ser-Gly-Gly-Val-Gly-Lys-Asn-Asn-Phe-Val-Pro-Thr-Asn-Val-Gly-Ser-Lys-Ala-Phe-NH_2
(Disulfide Bridge Cys2-Cys7)

CGRP

$C_{165}H_{260}N_{52}O_{50}S_2$ FW: 3836.37 ≥95%

Endogenous calcitonin-family peptide involved in vasodilation and pain transmission. It activates RAMP1 and CGRP receptors, decreases pro-inflammatory cytokine levels, stimulates proliferation of osteoblasts, inhibits apoptosis in retinal cells, and increases capillary density in ischemia models.

Ma W, Zhang X, Shi S, et al. Neuropeptides stimulate human osteoblast activity and promote gap junctional intercellular communication. Neuropeptides. 2013 Jun;47(3):179-86. PMID: 23726661.

Yang JH, Zhang YQ, Guo Z. Endogenous CGRP protects retinal cells against stress induced apoptosis in rats. Neurosci Lett. 2011 Aug 26;501(2):83-5. PMID: 21763400.

C0151

α-Calcitonin Gene Related Peptide, human

0.5 mg
1 mg
2.5 mg

Ala-Cys-Asp-Thr-Ala-Thr-Cys-Val-Thr-His-Arg-Leu-Ala-Gly-Leu-Leu-Ser-Arg-Ser-Gly-Gly-Val-Val-Lys-Asn-Asn-Phe-Val-Pro-Thr-Asn-Val-Gly-Ser-Lys-Ala-Phe-NH_2
(Disulfide bridge Cys2-Cys7)

α-CGRP

$C_{163}H_{267}N_{51}O_{49}S_2$ FW: 3789.31 [90954-53-3] ≥95%

Endogenous calcitonin-family peptide involved in vasodilation and pain transmission. It activates RAMP1 and CGRP receptors, decreases pro-inflammatory cytokine levels, stimulates proliferation of osteoblasts, inhibits apoptosis in retinal cells, and increases capillary density in ischemia models.

Ma W, Zhang X, Shi S, et al. Neuropeptides stimulate human osteoblast activity and promote gap junctional intercellular communication. Neuropeptides. 2013 Jun;47(3):179-86. PMID: 23726661.

Yang JH, Zhang YQ, Guo Z. Endogenous CGRP protects retinal cells against stress induced apoptosis in rats. Neurosci Lett. 2011 Aug 26;501(2):83-5. PMID: 21763400.

C2468

β-Calcitonin Gene Related Peptide, human

1 mg

Ala-Cys-Asn-Thr-Ala-Thr-Cys-Val-Thr-His-Arg-Leu-Ala-Gly-Leu-Leu-Ser-Arg-Ser-Gly-Gly-Met-Val-Lys-Ser-Asn-Phe-Val-Pro-Thr-Asn-Val-Gly-Ser-Lys-Ala-Phe-NH_2
(Disulfide bridge Cys2-Cys7)

β–CGRP

$C_{162}H_{267}N_{51}O_{48}S_3$ FW: 3793.38 [98824-26-1] ≥98%

Endogenous calcitonin-family peptide involved in vasodilation and pain transmission. It activates RAMP1 and CGRP receptors, decreases pro-inflammatory cytokine levels, stimulates proliferation of osteoblasts, inhibits apoptosis in retinal cells, and increases capillary density in ischemia models.

Ma W, Zhang X, Shi S, et al. Neuropeptides stimulate human osteoblast activity and promote gap junctional intercellular communication. Neuropeptides. 2013 Jun;47(3):179-86. PMID: 23726661.

Yang JH, Zhang YQ, Guo Z. Endogenous CGRP protects retinal cells against stress induced apoptosis in rats. Neurosci Lett. 2011 Aug 26;501(2):83-5. PMID: 21763400.

C0145

Calcitriol

50 µg
5 x 50 µg
1 mg

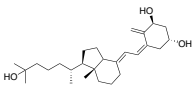

1α,25-Dihydroxyvitamin D3

$C_{27}H_{44}O_3$ FW: 416.64 [32222-06-3] ≥97%

Hormonally active form of vitamin D. It activates VDR and regulates dietary Ca^{2+} absorption. It is used as a dietary supplement to prevent osteoporosis. It also decreases hedgehog signaling, suppressing cancer progression, and stimulates differentiation of skin cells, preventing skin tumor formation.

Albert B, Hahn H. Interaction of hedgehog and vitamin D signaling pathways in basal cell carcinomas. Adv Exp Med Biol. 2014;810:329-41. PMID: 25207374.

Bikle DD. The vitamin D receptor: a tumor suppressor in skin. Adv Exp Med Biol. 2014;810:282-302. PMID: 25207372.

Adamczak DM, Nowak JK, Frydrychowicz M, et al. The role of Toll-like receptors and vitamin D in diabetes mellitus type 1--a review. Scand J Immunol. 2014 Aug;80(2):75-84. PMID: 24845558.

C0147

Calcium Folinate Pentahydrate

100 mg
500 mg
1 g

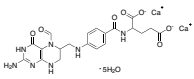

Leucovorin

$C_{20}H_{21}CaN_7O_7 \bullet 5H_2O$ FW: 601.59 [6035-45-6] ≥95%

Folate source often co-administered with methotrexate. It may inhibit thymidylate synthase.

Chen C, Tian L, Zhang M, et al. Protective effect of amifostine on high-dose methotrexate-induced small intestinal mucositis in mice. Dig Dis Sci. 2013 Nov;58(11):3134-43. PMID: 23979434.

Payet B, Fabre G, Tubiana N, et al. Plasma kinetic study of folinic acid and 5-methyltetrahydrofolate in healthy volunteers and cancer patients by high-performance liquid chromatography. Cancer Chemother Pharmacol. 1987;19(4):319-25. PMID: 3496173.

C0344 Calphostin C

100 µg

UCN-1028c

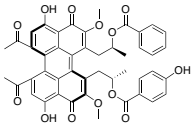

$C_{44}H_{38}O_{14}$ FW: 790.76 [121263-19-2] ≥98%

PKC inhibitor found in *Cladosporium*. It induces apoptosis and increases activation of JNK in breast cancer cells.

De Vita F, Riccardi M, Malanga D, et al. PKC-dependent phosphorylation of p27 at T198 contributes to p27 stabilization and cell cycle arrest. Cell Cycle. 2012 Apr 15;11(8):1583-92. PMID: 22441823.

Robitaille K, Daviau A, Lachance G, et al. Calphostin C-induced apoptosis is mediated by a tissue transglutaminase-dependent mechanism involving the DLK/JNK signaling pathway. Cell Death Differ. 2008 Sep;15(9):1522-31. PMID: 18497756.

Kobayashi E, Ando K, Nakano H, et al. Calphostins (UCN-1028), novel and specific inhibitors of protein kinase C. I. Fermentation, isolation, physico-chemical properties and biological activities. J Antibiot (Tokyo). 1989 Oct;42(10):1470-4. PMID: 2478514.

C0346 Calyculin A

10 µg
50 µg

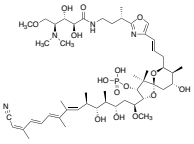

$C_{50}H_{81}N_4O_{15}P$ FW: 1009.17 [101932-71-2] ≥98%

PP1 and PP2A inhibitor found in *Discodermia*.

Iida Y, Yamamori S, Itakura M, et al. Protein phosphatase 2A dephosphorylates SNAP-25 through two distinct mechanisms in mouse brain synaptosomes. Neurosci Res. 2013 Mar;75(3):184-9. PMID: 23376809.

Palfrey HC, Pewitt EB. The ATP and Mg^{2+} dependence of $Na(^+)$-$K(^+)$-$2Cl^-$ cotransport reflects a requirement for protein phosphorylation: studies using calyculin A. Pflugers Arch. 1993 Nov;425(3-4):321-8. PMID: 8309793.

C0048 Cambinol

NEW

5 mg
25 mg

SIRT 1/2 inhibitor IV; SIRT1 Inhibitor II; NSC112546; SIRT2 Inhibitor VI

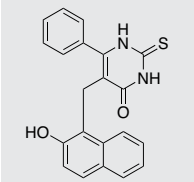

$C_{21}H_{16}N_2O_2S$ FW: 360.43 [14513-15-6] ≥98%

SIRT inhibitor. It inhibits expression of pro-inflammatory cytokines, improves survival in models of endotoxic shock and septic shock, and prevents proliferation and increases differentiation and senescence in hepatocellular carcinoma cells.

Lugrin J, Ciarlo E, Santos A, et al. The sirtuin inhibitor cambinol impairs MAPK signaling, inhibits inflammatory and innate immune responses and protects from septic shock. Biochim Biophys Acta. 2013 Jun;1833(6):1498-510. PMID: 23499872.

Portmann S, Fahrner R, Lechleiter A, et al. Antitumor effect of SIRT1 inhibition in human HCC tumor models in vitro and in vivo. Mol Cancer Ther. 2013 Apr;12(4):499-508. PMID: 23339189.

Heltweg B, Gatbonton T, Schuler AD, et al. Antitumor activity of a small-molecule inhibitor of human silent information regulator 2 enzymes. Cancer Res. 2006 Apr 15;66(8):4368-77. PMID: 16618762.

C0150 Camptothecin

25 mg
100 mg
250 mg
500 mg

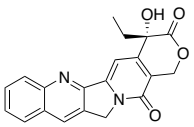

$C_{20}H_{16}N_2O_4$ FW: 348.35 [7689-03-4] ≥98%

Highly toxic synthetic precursor of irinotecan originally found in *Camptotheca*. It inhibits topoisomerase I and induces double-stranded DNA breaks.

Rodríguez-Berna G, Mangas-Sanjuán V, Gonzalez-Alvarez M, et al. A promising camptothecin derivative: Semisynthesis, antitumor activity and intestinal permeability. Eur J Med Chem. 2014 Jun 25;83C:366-373. PMID: 24980118.

Berniak K, Rybak P, Bernas T, et al. Relationship between DNA damage response, initiated by camptothecin or oxidative stress, and DNA replication, analyzed by quantitative 3D image analysis. Cytometry A. 2013 Jul 11. [Epub ahead of print]. PMID: 23846844.

Redinbo MR, Stewart L, Kuhn P, et al. Crystal structures of human topoisomerase I in covalent and noncovalent complexes with DNA. Science. 1998 Mar 6;279(5356):1504-13. PMID: 9488644.

C0152 9-Aminocamptothecin

1 mg
10 mg
25 mg
50 mg

9-AC

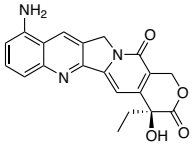

$C_{20}H_{17}N_3O_4$ FW: 363.37 [91421-43-1] ≥98%

Synthetic camptothecin derivative and topoisomerase I inhibitor. It inhibits growth of cancer cells and is highly cytotoxic.

Rodríguez-Berna G, Mangas-Sanjuán V, Gonzalez-Alvarez M, et al. A promising camptothecin derivative: Semisynthesis, antitumor activity and intestinal permeability. Eur J Med Chem. 2014 Jun 25;83C:366-373. PMID: 24980118.

Berniak K, Rybak P, Bernas T, et al. Relationship between DNA damage response, initiated by camptothecin or oxidative stress, and DNA replication, analyzed by quantitative 3D image analysis. Cytometry A. 2013 Jul 11. [Epub ahead of print]. PMID: 23846844.

Redinbo MR, Stewart L, Kuhn P, et al. Crystal structures of human topoisomerase I in covalent and noncovalent complexes with DNA. Science. 1998 Mar 6;279(5356):1504-13. PMID: 9488644.

C0154

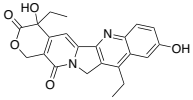

7-Ethyl-10-hydroxycamptothecin

SN-38; 7-ethyl-10-hydroxy-CPT

$C_{22}H_{20}N_2O_5$ FW: 392.4 [86639-52-3] ≥98%

10 mg
50 mg
100 mg

Synthetic camptothecin derivative and topoisomerase I inhibitor. It inhibits growth of cancer cells and is highly cytotoxic.

Rodríguez-Berna G, Mangas-Sanjuán V, Gonzalez-Alvarez M, et al. A promising camptothecin derivative: Semisynthesis, antitumor activity and intestinal permeability. Eur J Med Chem. 2014 Jun 25;83C:366-373. PMID: 24980118.

Berniak K, Rybak P, Bernas T, et al. Relationship between DNA damage response, initiated by camptothecin or oxidative stress, and DNA replication, analyzed by quantitative 3D image analysis. Cytometry A. 2013 Jul 11. [Epub ahead of print]. PMID: 23846844.

C0155

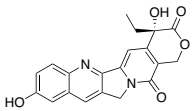

10-Hydroxycamptothecin

$C_{20}H_{16}N_2O_5$ FW: 364.35 [19685-09-7] ≥96%

25 mg
100 mg

Synthetic precursor of irinotecan originally found in *Camptotheca*. It inhibits topoisomerase I and induces double-stranded DNA breaks.

Rodríguez-Berna G, Mangas-Sanjuán V, Gonzalez-Alvarez M, et al. A promising camptothecin derivative: Semisynthesis, antitumor activity and intestinal permeability. Eur J Med Chem. 2014 Jun 25;83C:366-373. PMID: 24980118.

Berniak K, Rybak P, Bernas T, et al. Relationship between DNA damage response, initiated by camptothecin or oxidative stress, and DNA replication, analyzed by quantitative 3D image analysis. Cytometry A. 2013 Jul 11. [Epub ahead of print]. PMID: 23846844.

C0156

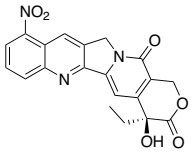

9-Nitro-20S-camptothecin

Rubitecan; 9-nitro-CPT

$C_{20}H_{15}N_3O_6$ FW: 393.35 [91421-42-0] ≥98%

25 mg
50 mg
100 mg

Synthetic camptothecin derivative and topoisomerase I inhibitor that induces double-stranded DNA breaks. It is highly cytotoxic.

Rodríguez-Berna G, Mangas-Sanjuán V, Gonzalez-Alvarez M, et al. A promising camptothecin derivative: Semisynthesis, antitumor activity and intestinal permeability. Eur J Med Chem. 2014 Jun 25;83C:366-373. PMID: 24980118.

Berniak K, Rybak P, Bernas T, et al. Relationship between DNA damage response, initiated by camptothecin or oxidative stress, and DNA replication, analyzed by quantitative 3D image analysis. Cytometry A. 2013 Jul 11. [Epub ahead of print]. PMID: 23846844.

C0253

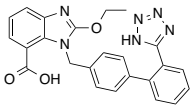

Candesartan

$C_{24}H_{20}N_6O_3$ FW: 440.45 [139481-59-7] ≥98%

100 mg
250 mg
1 g

AT1 receptor inhibitor used to treat hypertension. It decreases renal vascular resistance, glomerular filtration rate, and filtration fraction, suppresses calcium oxalate crystal deposition and kidney stone formation, and decreases retinal neovascularization without inhibiting total angiogenesis.

Patinha D, Fasching A, Pinho D, et al. Angiotensin II contributes to glomerular hyperfiltration in diabetic rats independently of adenosine type I receptors. Am J Physiol Renal Physiol. 2013 Mar 1;304(5):F614-22. PMID: 23283998.

Hu G, Li X, Sun X, et al. Identification of old drugs as potential inhibitors of HIV-1 integrase - human LEDGF/p75 interaction via molecular docking. J Mol Model. 2012 Dec;18(12):4995-5003. PMID: 22733274.

Nakamura S, Tsuruma K, Shimazawa M, et al. Candesartan, an angiotensin II type 1 receptor antagonist, inhibits pathological retinal neovascularization by downregulating VEGF receptor-2 expression. Eur J Pharmacol. 2012 Jun 15;685(1-3):8-14. PMID: 22543084.

C0254

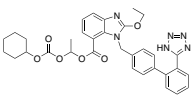

Candesartan Celexetil Ester

$C_{33}H_{34}N_6O_6$ FW: 610.66 [145040-37-5] ≥98%

100 mg
250 mg
1 g

AT1 receptor inhibitor used to treat hypertension. It decreases renal vascular resistance, glomerular filtration rate, and filtration fraction, suppresses calcium oxalate crystal deposition and kidney stone formation, and decreases retinal neovascularization without inhibiting total angiogenesis.

Patinha D, Fasching A, Pinho D, et al. Angiotensin II contributes to glomerular hyperfiltration in diabetic rats independently of adenosine type I receptors. Am J Physiol Renal Physiol. 2013 Mar 1;304(5):F614-22. PMID: 23283998.

Hu G, Li X, Sun X, et al. Identification of old drugs as potential inhibitors of HIV-1 integrase - human LEDGF/p75 interaction via molecular docking. J Mol Model. 2012 Dec;18(12):4995-5003. PMID: 22733274.

Nakamura S, Tsuruma K, Shimazawa M, et al. Candesartan, an angiotensin II type 1 receptor antagonist, inhibits pathological retinal neovascularization by downregulating VEGF receptor-2 expression. Eur J Pharmacol. 2012 Jun 15;685(1-3):8-14. PMID: 22543084.

C0252

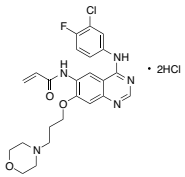

Canertinib Dihydrochloride

CI1033

$C_{24}H_{23}ClFN_5O_3 \bullet 2HCl$ FW: 558.86 [289499-45-2] ≥98%

25 mg
100 mg
250 mg

EGFR inhibitor. It induces cell cycle arrest in melanoma cells and inhibits Akt and ERK1/2 in cells lacking ErbB/EGFR receptors.

Djerf Severinsson EA, Trinks C, Gréen H, et al. The pan-ErbB receptor tyrosine kinase inhibitor canertinib promotes apoptosis of malignant melanoma in vitro and displays anti-tumor activity in vivo. Biochem Biophys Res Commun. 2011 Oct 28;414(3):563-8. PMID: 21982771.

Trinks C, Severinsson EA, Holmlund B, et al. The pan-ErbB tyrosine kinase inhibitor canertinib induces caspase-mediated cell death in human T-cell leukemia (Jurkat) cells. Biochem Biophys Res Commun. 2011 Jul 8;410(3):422-7. PMID: 21669187.

C0160

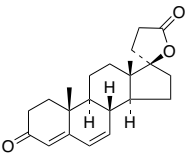

Canrenone

$C_{22}H_{28}O_3$ FW: 340.46 [976-71-6] ≥98%

1 g
5 g
25 g

Metabolite of spironolactone, Na^+/K^+ ATPase partial agonist and aldosterone and androgen receptor antagonist used as a diuretic.

Cargnelli G, Trevisi L, Debetto P, et al. Effects of canrenone on aorta and right ventricle of the rat. J Cardiovasc Pharmacol. 2001 May;37(5):540-7. PMID: 11336105.

Corvol P, Claire M, Oblin ME, et al. Mechanism of the antimineralocorticoid effects of spirolactones. Kidney Int. 1981 Jul;20(1):1-6. PMID: 7029118.

C0255

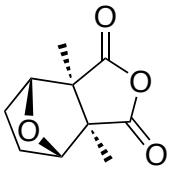

Cantharidin

$C_{10}H_{12}O_4$ FW: 196.2 [56-25-7] ≥98%

25 mg
100 mg
500 mg

PP1/2A inhibitor found in *Canarthis vesicatoria*. It inhibits proliferation of colorectal cancer cells, increases MCP-1, IL-6, and IL-1β levels, and inhibits differentiation and resorptive activity of osteoclasts.

Chen X, Liu J, Zhang Y. Cantharidin impedes the activity of protein serine/threonine phosphatase in Plutella xylostella. Mol Biosyst. 2013 Nov 19. [Epub ahead of print]. PMID: 24253262.

Kadioglu O, Kermani NS, Kelter G, et al. Pharmacogenomics of Cantharidin in Tumor Cells. Biochem Pharmacol. 2013 Nov 11. pii: S0006-2952(13)00709-0. Epub ahead of print]. PMID: 24231507.

Kim JA, Kim Y, Kwon BM, et al. The natural compound cantharidin induces cancer cell death through inhibition of heat shock protein 70 (HSP70) and Bcl-2-associated athanogene domain 3 (BAG3) expression by blocking heat shock factor 1 (HSF1) binding to promoters. J Biol Chem. 2013 Oct 4;288(40):28713-26. PMID: 23983126.

C0168

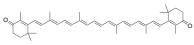

Canthaxanthin

$C_{40}H_{52}O_2$ FW: 564.84 [514-78-3] ≥9%

5 g
10 g
25 g

Carotenoid devoid of vitamin A activity. It stimulates cell-mediated and humoral immune responses, suppresses MCA-induced carcinogenesis, and inhibits t-BOOH-induced oxidative damage.

Chew BP, Park JS. Carotenoid action on the immune response. J Nutr. 2004 Jan;134(1):257S-261S. PMID: 14704330.

Stahl W, Sies H. The role of carotenoids and retinoids in gap junctional communication. Int J Vitam Nutr Res. 1998;68(6):354-9. PMID: 9857261.

C0162

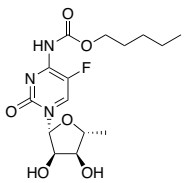

Capecitabine

$C_{15}H_{22}FN_3O_6$ FW: 359.35 [154361-50-9] ≥98%

250 mg
1 g
5 g

Prodrug of 5-FU and inhibitor of thymidylate synthase that is used to treat various cancers. It inhibits DNA synthesis.

Wilson PM, Fazzone W, LaBonte MJ, et al. Novel opportunities for thymidylate metabolism as a therapeutic target. Mol Cancer Ther. 2008 Sep;7(9):3029-37. PMID: 18790783.

Ishikawa T, Utoh M, Sawada N, et al. Tumor selective delivery of 5-fluorouracil by capecitabine, a new oral fluoropyrimidine carbamate, in human cancer xenografts. Biochem Pharmacol. 1998 Apr 1;55(7):1091-7. PMID: 9605432.

C0266

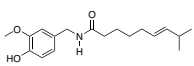

Capsaicin, natural

$C_{18}H_{27}NO_3$ FW: 305.41 [404-86-4] ≥95%

100 mg
250 mg
1 g

TRPV agonist found in *Capsicum*. It inhibits thermal and mechanical hyperalgesia, suppresses weight gain and fat deposition, and induces apoptosis in several cancer cell lines.

Díaz-Laviada I, Rodríguez-Henche N. The potential antitumor effects of capsaicin. Prog Drug Res. 2014;68:181-208. PMID: 24941670.

Leung FW. Capsaicin as an anti-obesity drug. Prog Drug Res. 2014;68:171-9. PMID: 24941669.

Kissin I. Vanilloid-induced conduction analgesia: selective, dose-dependent, long-lasting, with a low level of potential neurotoxicity. Anesth Analg. 2008 Jul;107(1):271-81. PMID: 18635498.

C0260

Capsanthin

50 g
100 g

Paprika extract

$C_{40}H_{56}O_3$ FW: 584.87 [465-42-9]

Found in *Capsicum*. It induces apoptosis and inhibits cell proliferation in leukemia cells and increases HDL levels.

Zhang X, Zhao WE, Hu L, et al. Carotenoids inhibit proliferation and regulate expression of peroxisome proliferators-activated receptor gamma (PPARγ) in K562 cancer cells. Arch Biochem Biophys. 2011 Aug 1;512(1):96-106. PMID: 21620794.

Aizawa K, Inakuma T. Dietary capsanthin, the main carotenoid in paprika (Capsicum annuum), alters plasma high-density lipoprotein-cholesterol levels and hepatic gene expression in rats. Br J Nutr. 2009 Dec;102(12):1760-6. PMID: 19646292.

Maoka T, Mochida K, Kozuka M, et al. Cancer chemopreventive activity of carotenoids in the fruits of red paprika Capsicum annuum L. Cancer Lett. 2001 Oct 30;172(2):103-9. PMID: 11566483.

C0261

Captopril

1 g
5 g
25 g

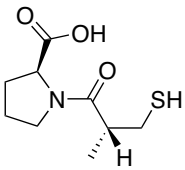

$C_9H_{15}NO_3S$ FW: 217.29 [62571-86-2] ≥81%

ACE inhibitor used to treat hypertension, diabetic nephropathy, and CHF. It also induces apoptosis and decreases tumor growth in lung cancer models.

Zidane F, Zeder-Lutz G, Altschuh D, et al. Surface plasmon resonance analysis of the binding mechanism of pharmacological and peptidic inhibitors to human somatic angiotensin I-converting enzyme. Biochemistry. 2013 Dec 3;52(48):8722-31. PMID: 24168709.

Attoub S, Gaben AM, Al-Salam S, et al. Captopril as a potential inhibitor of lung tumor growth and metastasis. Ann N Y Acad Sci. 2008 Sep;1138:65-72. PMID: 18837885.

C0268

Carbadox

25 g
100 g

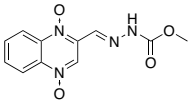

$C_{11}H_{10}N_4O_4$ FW: 262.22 [6804-07-5] ≥98%

Livestock antibiotic and growth promoter. It may be mutagenic. It is particularly effective against Lawsonia and Treponema.

Wattanaphansak S, Singer RS, Gebhart CJ. In vitro antimicrobial activity against 10 North American and European Lawsonia intracellularis isolates. Vet Microbiol. 2009 Mar 2;134(3-4):305-10. PMID: 18823723.

Laine T, Yliaho M, Myllys V, et al. The effect of antimicrobial growth promoter withdrawal on the health of weaned pigs in Finland. Prev Vet Med. 2004 Dec 15;66(1-4):163-74. PMID: 15579342.

C0270

Carbamazepine

1 g
5 g
25 g

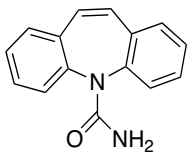

$C_{15}H_{12}N_2O$ FW: 236.27 [298-46-4] ≥98%

GABA receptor potentiator and voltage-gated Na^+ and ATP-sensitive K^+ channel blocker used to treat epilepsy, bipolar disorder, neuralgia/neuropathic pain, ADHD, schizophrenia, and PTSD. It also decreases LPS-induced expression of TNF-α and IL-1β.

Gómez CD, Buijs RM, Sitges M. The anti-seizure drugs vinpocetine and carbamazepine, but not valproic acid, reduce inflammatory IL-1β and TNF-α expression in rat hippocampus. J Neurochem. 2014 Jun 5. [Epub ahead of print]. PMID: 24903676.

Zhou Q, Chen PC, Devaraneni PK, et al. Carbamazepine inhibits ATP-sensitive potassium channel activity by disrupting channel response to MgADP. Channels (Austin). 2014 May 21;8(4). [Epub ahead of print]. PMID: 24849284.

Rahman W, Dickenson AH. Voltage gated sodium and calcium channel blockers for the treatment of chronic inflammatory pain. Neurosci Lett. 2013 Dec 17;557 Pt A:19-26. PMID: 23941888.

C0167

Carbenoxolone

1 g
5 g
25 g

$C_{34}H_{50}O_7$ FW: 570.76 [5697-56-3] ≥97%

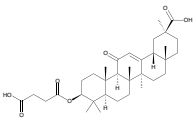

Glycyrrhetinic acid derivative and inhibitor of 11β-HSD inhibitor and gap junction connexin channels. It displays a wide variety of biological properties, including decreasing infarction size in cerebral ischemia models, decreasing production of IL-23 and Th17 cells, inhibiting macrophage migration into atria, and preventing development of fatty liver disease.

Beraki S, Litrus L, Soriano L, et al. A pharmacological screening approach for discovery of neuroprotective compounds in ischemic stroke. PLoS One. 2013 Jul 18;8(7):e69233. PMID: 23874920.

Okuda H, Nishida K, Higashi Y, et al. NAD(+) influx through connexin hemichannels prevents poly(ADP-ribose) polymerase-mediated astrocyte death. Life Sci. 2013 Apr 19;92(13):808-14. PMID: 23454167.

Oishi S, Sasano T, Tateishi Y, et al. Stretch of atrial myocytes stimulates recruitment of macrophages via ATP released through gap-junction channels. J Pharmacol Sci. 2012;120(4):296-304. PMID: 23196902.

C0169

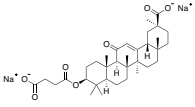

Carbenoxolone Disodium

18β-Glycyrrhetic acid hydrogen succinate

$C_{34}H_{48}Na_2O_7$ FW: 614.7 [7421-40-1] ≥97%

1 g
5 g
25 g

Synthetic derivative of glycyrrhizin and inhibitor of connexins and 11β-HSD. It is used to treat ulcers and inflammation but also displays other biological activities. It suppresses gap junction communication, delays onset of EAE in vivo, and decreases infarct volume in models of cerebral ischemia/reperfusion.

Chen G, Park CK, Xie RG, et al. Connexin-43 induces chemokine release from spinal cord astrocytes to maintain late-phase neuropathic pain in mice. Brain. 2014 Aug;137(Pt 8):2193-209. PMID: 24919967.

Beraki S, Litrus L, Soriano L, et al. A pharmacological screening approach for discovery of neuroprotective compounds in ischemic stroke. PLoS One. 2013 Jul 18;8(7):e69233. PMID: 23874920.

C0170

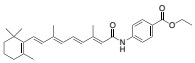

N-(4-Carbethoxyphenyl)retinamide

$C_{29}H_{37}NO_3$ FW: 447.62 [53839-71-7] ≥98%

100 mg
500 mg
1 g

It induces differentiation in leukemia cells and suppresses carcinogenesis in vivo.

Han J. Highlights of the cancer chemoprevention studies in China. Prev Med. 1993 Sep;22(5):712-22. PMID: 8234211.

C0175

Butyryl-Tyr(Me)-Ile-Gln-Asn-Cys-Pro-Leu-Gly-NH_2 (Sulfide bond: Butyryl-4-yl and Cys)

Carbetocin Acetate

$C_{45}H_{69}N_{11}O_{12}S$ FW: 988.17 ≥95%

Please inquire

Oxytocin analog and potential oxytocin receptor agonist used to prevent postpartum hemorrhaging. It also attenuates the negative aspects of withdrawal, prevents stress-induced reinstatement of drug self-administration, and suppresses depression-like behaviors.

Zanos P, Georgiou P, Wright SR, et al. The oxytocin analogue carbetocin prevents emotional impairment and stress-induced reinstatement of opioid-seeking in morphine-abstinent mice. Neuropsychopharmacology. 2014 Mar;39(4):855-65. PMID: 24129263.

C0367

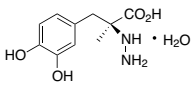

S-(−)-Carbidopa Monohydrate

$C_{10}H_{14}N_2O_4 \cdot H_2O$ FW: 244.24 [38821-49-7] ≥98%

25 mg
100 mg
1 g
5 g

L-amino acid decarboxylase inhibitor. It inhibits formation of dopamine granules and inhibits restoration of norepinephrine and other catecholamine production in models with mutant isoforms of dopamine β-hydroxylase.

Katow H, Suyemitsu T, Ooka S, et al. Development of a dopaminergic system in sea urchin embryos and larvae. J Exp Biol. 2010 Aug 15;213(Pt 16):2808-19. PMID: 20675551.

Thomas SA, Marck BT, Palmiter RD, et al. Restoration of norepinephrine and reversal of phenotypes in mice lacking dopamine beta-hydroxylase. J Neurochem. 1998 Jun;70(6):2468-76. PMID: 9603211.

C0172

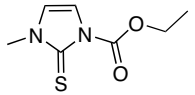

Carbimazole

Athyromazole

$C_7H_{10}N_2O_2S$ FW: 186.23 [22232-54-8] ≥98%

1 g
5 g
10 g

Methimazole prodrug and thyroid peroxidase inhibitor used to treat hyperthyroidism and Graves' disease. It decreases production of thyroid hormones and increases levels of IL-2.

Manna D, Roy G, Mugesh G. Antithyroid drugs and their analogues: synthesis, structure, and mechanism of action. Acc Chem Res. 2013 Nov 19;46(11):2706-15. PMID: 23883148.

Wilson R, McKillop JH, Buchanan LM, et al. The effect of carbimazole therapy on interleukin 2, interleukin 2 receptors and free radicals. Autoimmunity. 1990;8(1):3-7. PMID: 2129783.

C0171

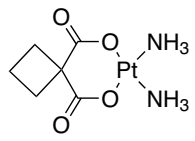

Carboplatin

$C_6H_{12}N_2O_4Pt$ FW: 371.25 [41575-94-4] ≥98%

25 mg
100 mg
250 mg

Platinum-based DNA cross-linker that inhibits DNA transcription and replication. It also modulates STAT signaling.

Hato SV, Khong A, de Vries IJ, et al. Molecular pathways: the immunogenic effects of platinum-based chemotherapeutics. Clin Cancer Res. 2014 Jun 1;20(11):2831-7. PMID: 24879823.

Chen X, Wu Y, Dong H, et al. Platinum-based agents for individualized cancer treatment. Curr Mol Med. 2013 Dec;13(10):1603-12. PMID: 24206132.

Ang WH, Myint M, Lippard SJ. Transcription inhibition by platinum-DNA cross-links in live mammalian cells. J Am Chem Soc. 2010 Jun 2;132(21):7429-35. PMID: 20443565.

C1600 Carcinoembryonic Antigen (605-613)

1 mg
2 mg
5 mg

CEA

Tyr-Leu-Ser-Gly-Ala-Asn-Leu-Asn-Leu

$C_{43}H_{69}N_{11}O_{14}$ FW: 964.09 ≥95%

Carcinoembryonic antigen epitope recognized by T cells.

Hou Y, Kavanagh B, Fong L. Distinct CD8+ T cell repertoires primed with agonist and native peptides derived from a tumor-associated antigen. J Immunol. 2008 Feb 1;180(3):1526-34. PMID: 18209048.

Tosi D, Valenti R, Cova A, et al. Role of cross-talk between IFN-alpha-induced monocyte-derived dendritic cells and NK cells in priming CD8+ T cell responses against human tumor antigens. J Immunol. 2004 May 1;172(9):5363-70. PMID: 15100276.

C1601 Carcinoembryonic Antigen (605-613) analog

1 mg
2 mg
5 mg

CEA

Tyr-Leu-Ser-Gly-Ala-Asp-Leu-Asn-Leu

$C_{43}H_{68}N_{10}O_{15}$ FW: 965.08 ≥95%

Carcinoembryonic antigen epitope analog recognized by T cells.

Hou Y, Kavanagh B, Fong L. Distinct CD8+ T cell repertoires primed with agonist and native peptides derived from a tumor-associated antigen. J Immunol. 2008 Feb 1;180(3):1526-34. PMID: 18209048.

C0271 Carfilzomib

1 mg
5 mg
25 mg

PR-171

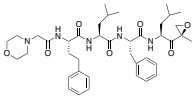

$C_{40}H_{57}N_5O_7$ FW: 719.91 [868540-17-4] ≥98%

Epoxomicin analog and proteasome inhibitor used to treat multiple myeloma. It prevents protein degradation, inducing cell cycle arrest and apoptosis.

Gu JJ, Hernandez-Ilizaliturri FJ, Kaufman GP, et al. The novel proteasome inhibitor carfilzomib induces cell cycle arrest, apoptosis and potentiates the anti-tumour activity of chemotherapy in rituximab-resistant lymphoma. Br J Haematol. 2013 Jul 4. Epub ahead of print] PMID: 23826755.

Lee HC, Shah JJ, Orlowski RZ. Novel approaches to treatment of double-refractory multiple myeloma. Am Soc Clin Oncol Educ Book. 2013;2013:302-6. doi: E10.1200/EdBook_AM.2013.33.e302. PMID: 23714530.

C0174 Carmofur

1 g
5 g

HCFU

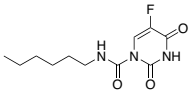

$C_{11}H_{16}FN_3O_3$ FW: 257.26 [61422-45-5] ≥97%

Pyrimidine analog, fluorouracil derivative, and inhibitor of thymidylate synthase and acid ceramidase used to treat resected colon cancer and breast cancer.

Pizzirani D, Pagliuca C, Realini N, et al. Discovery of a new class of highly potent inhibitors of acid ceramidase: synthesis and structure-activity relationship (SAR). J Med Chem. 2013 May 9;56(9):3518-30. PMID: 23614460.

Sakamoto J, Hamada C, Rahman M, et al. An individual patient data meta-analysis of adjuvant therapy with carmofur in patients with curatively resected colon cancer. Jpn J Clin Oncol. 2005 Sep;35(9):536-44. PMID: 16155120.

C0173 Carmustine

25 mg
100 mg

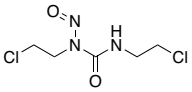

$C_5H_9Cl_2N_3O_2$ FW: 214.05 [154-93-8] ≥98%

DNA alkylator used to treat brain cancers, lymphomas, and multiple myeloma. It also induces apoptosis in platelets, increasing bleeding time.

Zhang J, Chen M, Zhang Y, et al. Carmustine induces platelet apoptosis. Platelets. 2014 Jun 23:1-6. [Epub ahead of print]. PMID: 24955606.

Drabløs F, Feyzi E, Aas PA, et al. Alkylation damage in DNA and RNA--repair mechanisms and medical significance. DNA Repair (Amst). 2004 Nov 2;3(11):1389-407. PMID: 15380096.

C0262 L-Carnitine

1 g
5 g
25 g

Vitamin B_T

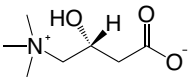

$C_7H_{15}NO_3$ FW: 161.2 [541-15-1] ≥98%

Endogenous quaternary ammonium required for fatty acid transport. It is used in dietary supplements and increases muscle carnitine content and work output while decreasing glycogen utilization during exercise. It also improves biomarkers of exercise stress, increases bone mineral density, and decreases ventricular arrhythmias and symptoms of angina.

DiNicolantonio JJ, Lavie CJ, Fares H, et al. L-carnitine in the secondary prevention of cardiovascular disease: systematic review and meta-analysis. Mayo Clin Proc. 2013 Jun;88(6):544-51. PMID: 23597877.

Wall BT, Stephens FB, Constantin-Teodosiu D, et al. Chronic oral ingestion of L-carnitine and carbohydrate increases muscle carnitine content and alters muscle fuel metabolism during exercise in humans. J Physiol. 2011 Feb 15;589(Pt 4):963-73. PMID: 21224234.

C0263

L-Carnitine Hydrochloride

1 g
5 g
25 g

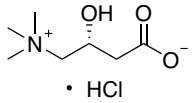

$C_7H_{15}NO_3$ HCl FW: 197.66 [6645-46-1] ≥98%

Endogenous quaternary ammonium required for fatty acid transport. It is used in dietary supplements and increases muscle carnitine content and work output while decreasing glycogen utilization during exercise. It also improves biomarkers of exercise stress, increases bone mineral density, and decreases ventricular arrhythmias and symptoms of angina.

DiNicolantonio JJ, Lavie CJ, Fares H, et al. L-carnitine in the secondary prevention of cardiovascular disease: systematic review and meta-analysis. Mayo Clin Proc. 2013 Jun;88(6):544-51. PMID: 23597877.

Wall BT, Stephens FB, Constantin-Teodosiu D, et al. Chronic oral ingestion of L-carnitine and carbohydrate increases muscle carnitine content and alters muscle fuel metabolism during exercise in humans. J Physiol. 2011 Feb 15;589(Pt 4):963-73. PMID: 21224234.

Volek JS, Judelson DA, Silvestre R, et al. Effects of carnitine supplementation on flow-mediated dilation and vascular inflammatory responses to a high-fat meal in healthy young adults. Am J Cardiol. 2008 Nov 15;102(10):1413-7. PMID: 18993165.

C0264

L-Carnitine Tartrate

1 g
5 g
25 g

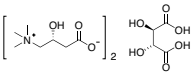

$2(C_7H_{15}NO_3)_2 \bullet C_4H_6O_6$ FW: 472.49 [36687-82-8] ≥98%

Endogenous quaternary ammonium required for fatty acid transport. It is used in dietary supplements and increases muscle carnitine content and work output while decreasing glycogen utilization during exercise. It also improves biomarkers of exercise stress, increases bone mineral density, and decreases ventricular arrhythmias and symptoms of angina.

DiNicolantonio JJ, Lavie CJ, Fares H, et al. L-carnitine in the secondary prevention of cardiovascular disease: systematic review and meta-analysis. Mayo Clin Proc. 2013 Jun;88(6):544-51. PMID: 23597877.

Wall BT, Stephens FB, Constantin-Teodosiu D, et al. Chronic oral ingestion of L-carnitine and carbohydrate increases muscle carnitine content and alters muscle fuel metabolism during exercise in humans. J Physiol. 2011 Feb 15;589(Pt 4):963-73. PMID: 21224234.

Volek JS, Judelson DA, Silvestre R, et al. Effects of carnitine supplementation on flow-mediated dilation and vascular inflammatory responses to a high-fat meal in healthy young adults. Am J Cardiol. 2008 Nov 15;102(10):1413-7. PMID: 18993165.

C0265

Carnosic Acid

5 mg
25 mg
50 mg

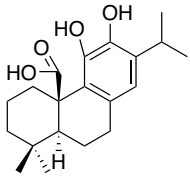

Salvin

$C_{20}H_{28}O_4$ FW: 332.43 [3650-09-7] ≥98%

Found in *Rosmarinus*. It displays a variety of biological activities, including inhibiting growth of colon adenocarcinoma cells, inducing autophagy in hepatoma cells, suppressing amyloid β-induced spatial memory and learning deficits, and upregulating activity of phase II enzymes.

Kim YJ, Kim JS, Seo YR, et al. Carnosic acid suppresses colon tumor formation in association with anti-adipogenic activity. Mol Nutr Food Res. 2014 Sep 9. [Epub ahead of print]. PMID: 25204550.

Gao Q, Liu H, Yao Y, et al. Carnosic acid induces autophagic cell death through inhibition of the Akt/mTOR pathway in human hepatoma cells. J Appl Toxicol. 2014 Sep 1. [Epub ahead of print]. PMID: 25178877.

Sahu BD, Putcha UK, Kuncha M, et al. Carnosic acid promotes myocardial antioxidant response and prevents isoproterenol-induced myocardial oxidative stress and apoptosis in mice. Mol Cell Biochem. 2014 Sep;394(1-2):163-76. PMID: 24903830.

C0267

Carnosol

1 mg
5 mg
25 mg

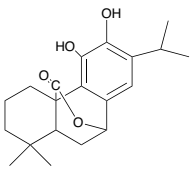

CCRIS 7122

$C_{20}H_{26}O_4$ FW: 330.42 [5957-80-2] ≥98%

Prostaglandin E2 synthase inhibitor found in *Rosmarinus*. It prevents PMA-induced edema, decreases expression of IL-1β and TNF-α, inhibits androgen and estrogen receptors, and suppresses epithelial-to-mesenchymal transition in ovarian cancer cells.

Vergara D, Simeone P, Bettini S, et al. Antitumor activity of the dietary diterpene carnosol against a panel of human cancer cell lines. Food Funct. 2014 Jun 28;5(6):1261-9. PMID: 24733049.

Park KW, Kundu J, Chae IG, et al. Carnosol induces apoptosis through generation of ROS and inactivation of STAT3 signaling in human colon cancer HCT116 cells. Int J Oncol. 2014 Apr;44(4):1309-15. PMID: 24481553.

López-Jiménez A, García-Caballero M, Medina MÁ, et al. Anti-angiogenic properties of carnosol and carnosic acid, two major dietary compounds from rosemary. Eur J Nutr. 2013 Feb;52(1):85-95. PMID: 22173778.

C0269 β-Carotene

1 g
5 g
25 g
50 g

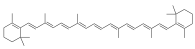

$C_{40}H_{56}$ FW: 536.87 [7235-40-7] ≥97%

Vitamin A prodrug used to quantify antioxidative activity. It exhibits a wide variety of activities, including preventing radiation-induced DNA damage, inducing cell cycle arrest and apoptosis in breast cancer cells, and decreasing levels of total cholesterol, VLDL, and LDL in vivo.

Abdel-Mageed WM, Bayoumi SA, Salama AA, et al. Antioxidant lipoxygenase inhibitors from the leaf extracts of Simmondsia chinensis. Asian Pac J Trop Med. 2014 Sep;7S1:S521-6. PMID: 25312177.

Berti AP, Düsman E, Mariucci RG, et al. Antimutagenic and radioprotective activities of beta-carotene against the biological effects of iodine-131 radiopharmaceutical in Wistar rats. Genet Mol Res. 2014 Mar 31;13(1):2248-58. PMID: 24737473.

Gloria NF, Soares N, Brand C, et al. Lycopene and beta-carotene induce cell-cycle arrest and apoptosis in human breast cancer cell lines. Anticancer Res. 2014 Mar;34(3):1377-86. PMID: 24596385.

C0351 Carprofen

1 g
5 g

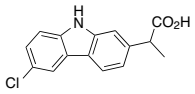

$C_{15}H_{12}ClNO_2$ FW: 273.71 [53716-49-7] ≥98%

NSAID and COX-2 inhibitor used to treat inflammation.

Lees P, Delatour P, Foster AP, et al. Evaluation of carprofen in calves using a tissue cage model of inflammation. Br Vet J. 1996 Mar;152(2):199-211. PMID: 8680842.

C0365 Carvedilol

1 g
5 g
10 g

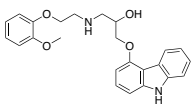

$C_{24}H_{26}N_2O_4$ FW: 406.47 [72956-09-3] ≥98%

Antagonist at α1- and β1/2-adrenergic receptors and FIASMA used to treat congestive heart failure. It decreases force, pressure, and cardiac workload. It also inhibits release of pro-inflammatory cytokines and alleviates oxidative stress.

Arab HH, El-Sawalhi MM. Carvedilol alleviates adjuvant-induced arthritis and subcutaneous air pouch edema: modulation of oxidative stress and inflammatory mediators. Toxicol Appl Pharmacol. 2013 Apr 15;268(2):241-8. PMID: 23360886.

Kornhuber J, Muehlbacher M, Trapp S, et al. Identification of novel functional inhibitors of acid sphingomyelinase. PLoS One. 2011;6(8):e23852. PMID: 21909365.

C0366 Carvedilol Phosphate Hemihydrate

1 g
5 g
10 g

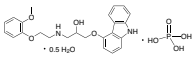

$C_{24}H_{26}N_2O_4 \bullet H_3O_4P \bullet 1/2H_2O$ FW: 513.47 [610309-89-2] ≥98%

Inhibitor of α1- and β1/2-adrenergic receptors and FIASMA used to treat congestive heart failure. It decreases force, pressure, and cardiac workload. It also inhibits release of pro-inflammatory cytokines and decreases oxidative stress.

Arab HH, El-Sawalhi MM. Carvedilol alleviates adjuvant-induced arthritis and subcutaneous air pouch edema: modulation of oxidative stress and inflammatory mediators. Toxicol Appl Pharmacol. 2013 Apr 15;268(2):241-8. PMID: 23360886.

Kornhuber J, Muehlbacher M, Trapp S, et al. Identification of novel functional inhibitors of acid sphingomyelinase. PLoS One. 2011;6(8):e23852. PMID: 21909365.

C0368 Carveol

5 g
25 g

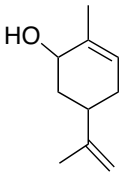

$C_{10}H_{16}O$ FW: 152.23 [99-48-9] ≥98%

TRPV3 agonist found in spearmint oil used commercially as a food additive and fragrance. It suppresses cell proliferation in prostate cancer cells and inhibits growth of *Dermatophagoides*.

Yang JY, Kim MG, Lee SE, et al. Acaricidal activities against house dust mites of spearmint oil and its constituents. Planta Med. 2014 Feb;80(2-3):165-70. PMID: 24488719.

Bhatia SP, McGinty D, Letizia CS, et al. Fragrance material review on carveol. Food Chem Toxicol. 2008 Nov;46 Suppl 11:S85-7. PMID: 18640224.

Vogt-Eisele AK, Weber K, Sherkheli MA, et al. Monoterpenoid agonists of TRPV3. Br J Pharmacol. 2007 Jun;151(4):530-40. PMID: 17420775.

C0372 Casein Kinase 2 Assay Kit

1 mg
2 mg
5 mg

H-Arg-Arg-Arg-Asp-Asp-Asp-Ser-Asp-Asp-Asp-OH

$C_{45}H_{73}N_{19}O_{24}$ FW: 1264.2 ≥95%

Substrate used to measure casein kinase 2 activity.

Raüber C, Berger S. Saturation transfer difference NMR studies of the interaction of the proteinkinase CK2 with peptides. Protein Pept Lett. 2012 Sep;19(9):934-9. PMID: 22486610.

Gratz A, Kuckländer U, Bollig R, et al. Identification of novel CK2 inhibitors with a benzofuran scaffold by novel non-radiometric in vitro assays. Mol Cell Biochem. 2011 Oct;356(1-2):83-90. PMID: 21750981.

C0374

β-Casomorphin, human

5 mg
10 mg
25 mg

H-Tyr-Pro-Phe-Val-Glu-Pro-Ile-OH

$C_{44}H_{61}N_7O_{11}$ FW: 864.02 ≥95%

Casein fragment that improves high glucose-induced oxidative damage and prevents the development of renal interstitial fibrosis.

Zhang W, Miao J, Wang S, et al. The protective effects of beta-casomorphin-7 against glucose -induced renal oxidative stress in vivo and vitro. PLoS One. 2013 May 3;8(5):e63472. PMID: 23658831.

Zhang W, Miao J, Ma C, et al. β-Casomorphin-7 attenuates the development of nephropathy in type I diabetes via inhibition of epithelial-mesenchymal transition of renal tubular epithelial cells. Peptides. 2012 Aug;36(2):186-91. PMID: 22687367.

C0274

Caspofungin Diacetate

5 mg
25 mg
100 mg

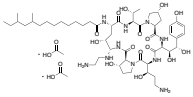

$C_{52}H_{88}N_{10}O_{15} \bullet C_4H_8O_4$ FW: 1213.42 [179463-17-3] ≥95%

1,3-β-Glucan synthase inhibitor that suppresses growth of *Aspergillus* and *Candida* by decreasing cell wall mechanical strength, altering cell surface hydrophobicity, and triggering cell aggregation.

El-Kirat-Chatel S, Beaussart A, Alsteens D, et al. Nanoscale analysis of caspofungin-induced cell surface remodelling in *Candida albicans*. Nanoscale. 2013 Feb 7;5(3):1105-15. PMID: 23262781.

Pacetti SA, Gelone SP. Caspofungin acetate for treatment of invasive fungal infections. Ann Pharmacother. 2003 Jan;37(1):90-8. PMID: 12503942.

C0275

Castanospermine

10 mg
50 mg
100 mg

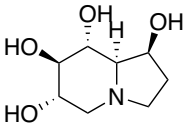

$C_8H_{15}NO_4$ FW: 189.21 [79831-76-8] ≥98%

O-GlcNAcase inhibitor. It decreases expression of cellular adhesion molecules in leukocytes and endothelial cells, inhibits metastasis of melanoma cells, and prevents viral replication of the Moloney murine leukemia virus.

Hibberd AD, Trevillian PR, Clark DA, et al. The effects of Castanospermine, an oligosaccharide processing inhibitor, on mononuclear/endothelial cell binding and the expression of cell adhesion molecules. Transpl Immunol. 2012 Aug;27(1):39-47. PMID: 22647882.

Macauley MS, He Y, Gloster TM, et al. Inhibition of O-GlcNAcase using a potent and cell-permeable inhibitor does not induce insulin resistance in 3T3-L1 adipocytes. Chem Biol. 2010 Sep 24;17(9):937-48. Erratum in: Chem Biol. 2010 Oct 29;17(10):1161. PMID: 20851343.

C0379

Catch-Relaxing Peptide

1 mg
2 mg
5 mg

CARP

H-Ala-Met-Pro-Met-Leu-Arg-Leu-NH_2

$C_{36}H_{67}N_{11}O_7S_2$ FW: 830.13 ≥95%

BK/SK K^+ channel modulator found in mollusks. It decreases heart rate and modulates muscle contractility.

Fujiwara-Sakata M, Kobayashi M. Neuropeptides regulate the cardiac activity of a prosobranch mollusk, Rapana thomasiana. Cell Tissue Res. 1992 Aug;269(2):241-7. PMID: 1423492.

C0278

(+)-Catechin

1 mg
5 mg

Cyanidol, Catechuic acid

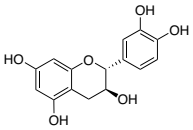

$C_{15}H_{14}O_6$ FW: 290.27 [154-23-4] ≥99%

MAO-B inhibitor found in *Camilla* (green tea). It displays a variety of biological activities, including increasing life span in *Caenorhabditis elegans*, suppressing LDL oxidation and uptake, activating phase II enzymes, inhibiting histidine decarboxylase, and decreasing tumor number and formation in colorectal cancer models.

Chang CF, Cho S, Wang J. (-)-Epicatechin protects hemorrhagic brain via synergistic Nrf2 pathways. Ann Clin Transl Neurol. 2014 Apr 1;1(4):258-271. PMID: 24741667.

Nogueira L, Ramirez-Sanchez I, Perkins GA, et al. (-)-Epicatechin enhances fatigue resistance and oxidative capacity in mouse muscle. J Physiol. 2011 Sep 15;589(Pt 18):4615-31. PMID: 21788351.

Saul N, Pietsch K, Menzel R, et al. Catechin induced longevity in C. elegans: from key regulator genes to disposable soma. Mech Ageing Dev. 2009 Aug;130(8):477-86. PMID: 19501612.

C0376

Catharanthine base

25 mg
100 mg
500 mg

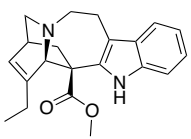

$C_{21}H_{24}N_2O_2$ FW: 336.43 [2468-21-5] ≥98%

Voltage-gated Ca^{2+} channel blocker found in *Catharanthus* and precursor in synthesis of vinca alkaloids. It binds tubulin poorly, suppresses growth of *Plasmodium*, and decreases blood pressure and heart rate.

Munigunti R, Becker K, Brun R, et al. Determination of antiplasmodial activity and binding affinity of selected natural products towards PfTrxR and PfGR. Nat Prod Commun. 2013 Aug;8(8):1135-6. PMID: 24079187.

Jadhav A, Liang W, Papageorgiou PC, et al. Catharanthine dilates small mesenteric arteries and decreases heart rate and cardiac contractility by inhibition of voltage-operated calcium channels on vascular smooth muscle cells and cardiomyocytes. J Pharmacol Exp Ther. 2013 Jun;345(3):383-92. PMID: 23532933.

C0377

Catharanthine Sulfate

25 mg
100 mg
500 mg

$C_{21}H_{24}N_2O_2 \bullet H_2SO_4$ FW: 434.51 ≥98%

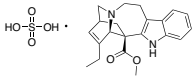

Voltage-gated Ca^{2+} channel blocker found in *Catharanthus* and precursor in synthesis of vinca alkaloids. It binds tubulin poorly, suppresses growth of *Plasmodium*, and decreases blood pressure and heart rate.

Munigunti R, Becker K, Brun R, et al. Determination of antiplasmodial activity and binding affinity of selected natural products towards PfTrxR and PfGR. Nat Prod Commun. 2013 Aug;8(8):1135-6. PMID: 24079187.

Jadhav A, Liang W, Papageorgiou PC, et al. Catharanthine dilates small mesenteric arteries and decreases heart rate and cardiac contractility by inhibition of voltage-operated calcium channels on vascular smooth muscle cells and cardiomyocytes. J Pharmacol Exp Ther. 2013 Jun;345(3):383-92. PMID: 23532933.

C0378

Catharanthine Tartrate

25 mg
100 mg
500 mg

$C_{21}H_{24}N_2O_2 \bullet C_4H_6O_6$ FW: 486.52 ≥97%

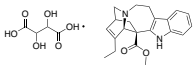

Voltage-gated Ca^{2+} channel blocker found in *Catharanthus* and precursor in synthesis of vinca alkaloids. It binds tubulin poorly, suppresses growth of *Plasmodium*, and decreases blood pressure and heart rate.

Munigunti R, Becker K, Brun R, et al. Determination of antiplasmodial activity and binding affinity of selected natural products towards PfTrxR and PfGR. Nat Prod Commun. 2013 Aug;8(8):1135-6. PMID: 24079187.

Jadhav A, Liang W, Papageorgiou PC, et al. Catharanthine dilates small mesenteric arteries and decreases heart rate and cardiac contractility by inhibition of voltage-operated calcium channels on vascular smooth muscle cells and cardiomyocytes. J Pharmacol Exp Ther. 2013 Jun;345(3):383-92. PMID: 23532933.

C0396

CAY10505

NEW

5 mg
10 mg
25 mg

$C_{14}H_8FNO_3S$ FW: 289.28 [1218777-13-9] ≥98%

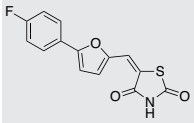

Inhibitor of p110γ PI3K. It increases endothelial relaxation, normalizes levels of glutathione, nitrate, and nitrite, and alters the vascular endothelial lining in hypertension models.

Tyagi S, Sharma S, Budhiraja RD. Effect of phosphatidylinositol 3-kinase-γ inhibitor CAY10505 in hypertension, and its associated vascular endothelium dysfunction in rats. Can J Physiol Pharmacol. 2012 Jul;90(7):881-5. PMID: 22731503.

C0476

CB-TH

1 mg
2 mg
5 mg

Arg-Trp-Lys-Ile-Phe-Lys-Lys-Ile-Glu-Lys-Met-Gly-Gly-Ser-Tyr-Cys-Asn-Arg-Arg-Thr-Gly-Lys-Cys-Gln-Arg-Met

$C_{138}H_{230}N_{46}O_{34}S_4$ FW: 3205.9 ≥95%

Cecropin B-thanatin conjugate that inhibits microbial growth.

Hongbiao W, Baolong N, Mengkui X, et al. Biological activities of cecropin B-thanatin hybrid peptides. J Pept Res. 2005 Dec;66(6):382-6. PMID: 16316454.

C0824

CCG1423

NEW

5 mg
25 mg

$C_{18}H_{13}ClF_6N_2O_3$ FW: 454.75 [285986-88-1] ≥98%

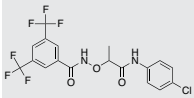

Serum response factor inhibitor that suppresses Rho signaling. It binds myocardin-related transcription factor A, improves glucose uptake and tolerance, and inhibits invasiveness of prostate cancer cells.

Hayashi K, Watanabe B, Nakagawa Y, et al. RPEL proteins are the molecular targets for CCG-1423, an inhibitor of Rho signaling. PLoS One. 2014 Feb 18;9(2):e89016. PMID: 24558465.

Bell JL, Haak AJ, Wade SM, et al. Optimization of novel nipecotic bis(amide) inhibitors of the Rho/MKL1/SRF transcriptional pathway as potential anti-metastasis agents. Bioorg Med Chem Lett. 2013 Jul 1;23(13):3826-32. PMID: 23707258.

Jin W, Goldfine AB, Boes T, et al. Increased SRF transcriptional activity in human and mouse skeletal muscle is a signature of insulin resistance. J Clin Invest. 2011 Mar;121(3):918-29. PMID: 21393865.

C1609

Cecropin B

1 mg
2 mg
5 mg

H-Lys-Trp-Lys-Val-Phe-Lys-Lys-Ile-Glu-Lys-Met-Gly-Arg-Asn-Ile-Arg-Asn-Gly-Ile-Val-Lys-Ala-Gly-Pro-Ala-Ile-Ala-Val-Leu-Gly-Glu-Ala-Lys-Ala-Leu-NH_2

$C_{176}H_{302}N_{51}O_{41}S$ FW: 3834.76 [80451-05-4] ≥95%

Found in *Hyalophora cecropia* and *Bombyx mori*. It inhibits growth of *Haemophilus*, *Staphylococcus*, and *Escherichia*.

Hu H, Wang C, Guo X, et al. Broad activity against porcine bacterial pathogens displayed by two insect antimicrobial peptides moricin and cecropin B. Mol Cells. 2013 Feb;35(2):106-14. PMID: 23456332.

Luo CC, Yin DY, Gao XJ, et al. Goat mammary gland expression of Cecropin B to inhibit bacterial pathogens causing mastitis. Anim Biotechnol. 2013 Jan;24(1):66-78. PMID: 23394371.

C1613

Cediranib

AZD2171

$C_{25}H_{27}FN_4O_3$ FW: 450.51 [288383-20-0] ≥98%

25 mg
100 mg
250 mg

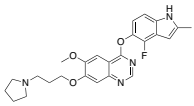

VEGFR inhibitor. It decreases tumor vascular bed volume in brain metastasis models and lowers lesion number and polyp size in intestinal cancer models.

Kummar S, Allen D, Monks A, et al. Cediranib for metastatic alveolar soft part sarcoma. J Clin Oncol. 2013 Jun 20;31(18):2296-302. PMID: 23630200.

JuanYin J, Tracy K, Zhang L, et al. Noninvasive imaging of the functional effects of anti-VEGF therapy on tumor cell extravasation and regional blood volume in an experimental brain metastasis model. Clin Exp Metastasis. 2009;26(5):403-14. PMID: 19277878.

Goodlad RA, Ryan AJ, Wedge SR, et al. Inhibiting vascular endothelial growth factor receptor-2 signaling reduces tumor burden in the ApcMin/+ mouse model of early intestinal cancer. Carcinogenesis. 2006 Oct;27(10):2133-9. PMID: 16782971.

C1623

CEF10

H-Cys-Leu-Gly-Gly-Leu-Leu-Thr-Met-Val-OH

$C_{39}H_{71}N_9O_{11}S$ FW: 906.2 ≥95%

1 mg
2 mg
5 mg

vSrc-induced cytokine from chicken embryo fibroblasts.

Bojović B, Rodrigues N, Dehbi M, et al. Multiple signaling pathways control the activation of the CEF-4/9E3 cytokine gene by pp60v-src. J Biol Chem. 1996 Sep 13;271(37):22528-37. PMID: 8798420.

Gonneville L, Martins TJ, Bédard PA. Complex expression pattern of the CEF-4 cytokine in transformed and mitogenically stimulated cells. Oncogene. 1991 Oct;6(10):1825-33. PMID: 1656364.

C1619

CEF3

H-Ser-Ile-Ile-Pro-Ser-Gly-Pro-Leu-Lys-OH

$C_{42}H_{74}N_{10}O_{12}$ FW: 911.12 ≥95%

1 mg
2 mg
5 mg

vSrc-induced cytokine from chicken embryo fibroblasts.

Bojović B, Rodrigues N, Dehbi M, et al. Multiple signaling pathways control the activation of the CEF-4/9E3 cytokine gene by pp60v-src. J Biol Chem. 1996 Sep 13;271(37):22528-37. PMID: 8798420.

Gonneville L, Martins TJ, Bédard PA. Complex expression pattern of the CEF-4 cytokine in transformed and mitogenically stimulated cells. Oncogene. 1991 Oct;6(10):1825-33. PMID: 1656364.

C1621

CEF4

H-Arg-Val-Leu-Ser-Phe-Ile-Lys-Gly-Thr-Lys-OH

$C_{53}H_{93}N_{15}O_{13}$ FW: 1148.42 ≥95%

1 mg
2 mg
5 mg

vSrc-induced cytokine from chicken embryo fibroblasts.

Bojović B, Rodrigues N, Dehbi M, et al. Multiple signaling pathways control the activation of the CEF-4/9E3 cytokine gene by pp60v-src. J Biol Chem. 1996 Sep 13;271(37):22528-37. PMID: 8798420.

Gonneville L, Martins TJ, Bédard PA. Complex expression pattern of the CEF-4 cytokine in transformed and mitogenically stimulated cells. Oncogene. 1991 Oct;6(10):1825-33. PMID: 1656364.

C1622

CEF6

H-Leu-Pro-Phe-Asp-Lys-Thr-Thr-Val-Met-OH

$C_{48}H_{78}N_{10}O_{14}S$ FW: 1051.28 ≥95%

1 mg
2 mg
5 mg

vSrc-induced cytokine from chicken embryo fibroblasts.

Bojović B, Rodrigues N, Dehbi M, et al. Multiple signaling pathways control the activation of the CEF-4/9E3 cytokine gene by pp60v-src. J Biol Chem. 1996 Sep 13;271(37):22528-37. PMID: 8798420.

Gonneville L, Martins TJ, Bédard PA. Complex expression pattern of the CEF-4 cytokine in transformed and mitogenically stimulated cells. Oncogene. 1991 Oct;6(10):1825-33. PMID: 1656364.

C1627

Cefaclor Monohydrate

$C_{15}H_{13}ClN_3O_4S \bullet H_2O$ FW: 385.83 [70356-03-5] ≥97%

500 mg
1 g
5 g

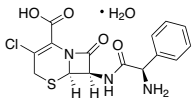

Penicillin binding protein inhibitor that prevents peptidoglycan synthesis and bacterial cell wall formation. It also enhances phagocytosis and bactericidal activity of granulocytes and macrophages and slows gastric emptying and intestinal transit.

Berti AD, Sakoulas G, Nizet V, et al. β-Lactam antibiotics targeting PBP1 selectively enhance daptomycin activity against methicillin-resistant *Staphylococcus aureus*. Antimicrob Agents Chemother. 2013 Oct;57(10):5005-12. PMID: 23896478.

Dabrowski MP, Stankiewicz W. Desirable and undesirable immunotropic effects of antibiotics: immunomodulating properties of cefaclor. J Chemother. 2001 Dec;13(6):615-20. PMID: 11806622.

Bozkurt A, Deniz M, Yegen BC. Cefaclor, a cephalosporin antibiotic, delays gastric emptying rate by a CCK-A receptor-mediated mechanism in the rat. Br J Pharmacol. 2000 Oct;131(3):399-404. PMID: 11015288.

C1629

Cefoperazone Acid

1 g
5 g

$C_{25}H_{27}N_9O_8S_2$ FW: 645.47 [62893-19-0] ≥98%

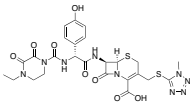

Penicillin binding protein inhibitor and mammalian mRNA splicing inhibitor that prevents peptidoglycan synthesis and bacterial cell wall formation.

Aukema KG, Chohan KK, Plourde GL, et al. Small molecule inhibitors of yeast pre-mRNA splicing. ACS Chem Biol. 2009 Sep 18;4(9):759-68. PMID: 19634919.

Mohanty S, Singhal R, Sood S, et al. Comparative in vitro activity of beta-lactam/beta-lactamase inhibitor combinations against gram negative bacteria. Indian J Med Res. 2005 Nov;122(5):425-8. PMID: 16456257.

C1630

Cefoperazone Sodium

1 g
5 g

$C_{25}H_{26}N_9NaO_8S_2$ FW: 667.65 [62893-20-3] ≥98%

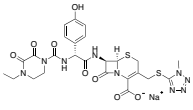

Penicillin binding protein inhibitor and mammalian mRNA splicing inhibitor that prevents peptidoglycan synthesis and bacterial cell wall formation.

Aukema KG, Chohan KK, Plourde GL, et al. Small molecule inhibitors of yeast pre-mRNA splicing. ACS Chem Biol. 2009 Sep 18;4(9):759-68. PMID: 19634919.

Mohanty S, Singhal R, Sood S, et al. Comparative in vitro activity of beta-lactam/beta-lactamase inhibitor combinations against gram negative bacteria. Indian J Med Res. 2005 Nov;122(5):425-8. PMID: 16456257.

C1632

Cefotaxime Acid

500 mg
1 g
5 g

$C_{16}H_{17}N_5O_7S_2$ FW: 455.47 [63527-52-6] ≥91%

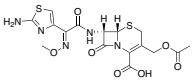

Penicillin binding protein inhibitor that prevents peptidoglycan synthesis and bacterial cell wall formation. It is mostly resistant to β-lactamase activity.

Philpott-Howard J, Williams JD. Activity of cephalosporin antibiotics against *Haemophilus* influenzae. Scand J Infect Dis Suppl. 1983;39:109-11. PMID: 6606223.

LeFrock JL, Prince RA, Leff RD. Mechanism of action, antimicrobial activity, pharmacology, adverse effects, and clinical efficacy of cefotaxime. Pharmacotherapy. 1982 Jul-Aug;2(4):174-84. PMID: 6302641.

C1633

Cefotaxime Sodium

500 mg
1 g
5 g

$C_{16}H_{16}N_5O_7S_2Na$ FW: 477.45 [64485-93-4] ≥96%

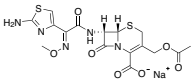

Penicillin binding protein inhibitor that prevents peptidoglycan synthesis and bacterial cell wall formation. It is mostly resistant to β-lactamase activity.

Philpott-Howard J, Williams JD. Activity of cephalosporin antibiotics against *Haemophilus* influenzae. Scand J Infect Dis Suppl. 1983;39:109-11. PMID: 6606223.

LeFrock JL, Prince RA, Leff RD. Mechanism of action, antimicrobial activity, pharmacology, adverse effects, and clinical efficacy of cefotaxime. Pharmacotherapy. 1982 Jul-Aug;2(4):174-84. PMID: 6302641.

C1635

Ceftazidime Hydrate

1 g
5 g

GR-20263

$C_{22}H_{22}N_6O_7S_2 \cdot xH_2O$ FW: 546.58 [78439-06-2] ≥97%

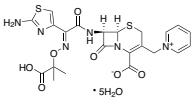

Penicillin binding protein inhibitor that prevents peptidoglycan synthesis and bacterial cell wall formation.

Chantratita N, Rholl DA, Sim B, et al. Antimicrobial resistance to ceftazidime involving loss of penicillin-binding protein 3 in *Burkholderia* pseudomallei. Proc Natl Acad Sci U S A. 2011 Oct 11;108(41):17165-70. PMID: 21969582.

Phelps DJ, Carlton DD, Farrell CA, et al. Affinity of cephalosporins for beta-lactamases as a factor in antibacterial efficacy. Antimicrob Agents Chemother. 1986 May;29(5):845-8. PMID: 3524432.

C1620

Ceftiofur Hydrochloride

500 mg
1 g
5 g

$C_{19}H_{17}N_5O_7S_3 \cdot HCl$ FW: 560.02 [104010-37-9] ≥90%

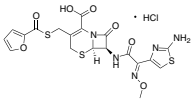

Penicillin binding protein inhibitor that prevents synthesis of bacterial cell walls. It also decreases LPS-induced expression of pro-inflammatory cytokines in endotoxemia models.

Li X, Zheng W, Machesky ML, et al. Degradation kinetics and mechanism of antibiotic ceftiofur in recycled water derived from a beef farm. J Agric Food Chem. 2011 Sep 28;59(18):10176-81. PMID: 21863813.

Ci X, Li H, Song Y, et al. Ceftiofur regulates LPS-induced production of cytokines and improves LPS-induced survival rate in mice. Inflammation. 2008 Dec;31(6):422-7. PMID: 18989766.

C1637 Ceftriaxone Sodium

250 mg
500 mg
1 g

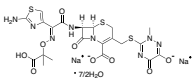

$C_{18}H_{16}N_8O_7S_3Na_2 \cdot 7/2H_2O$ FW: 598.54 [104376-79-6] ≥98%

Penicillin binding protein inhibitor that prevents peptidoglycan synthesis and bacterial cell wall formation. It also decreases neuronal autophagy, improves traumatic brain injury-induced brain edema and cognitive function deficits, and attenuates the development of dependence and abstinence-induced withdrawal.

Cui C, Cui Y, Gao J, et al. Neuroprotective effect of ceftriaxone in a rat model of traumatic brain injury. Neurol Sci. 2014 May;35(5):695-700. PMID: 24277205.

Sari Y, Prieto AL, Barton SJ, et al. Ceftriaxone-induced up-regulation of cortical and striatal GLT1 in the R6/2 model of Huntington's disease. J Biomed Sci. 2010 Jul 27;17:62. PMID: 20663216.

C1624 Cefuroxime Sodium

1 g
5 g

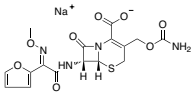

$C_{16}H_{15}N_4O_8SNa$ FW: 446.37 [56238-63-2] ≥98%

Penicillin binding protein inhibitor that inhibits bacterial cell wall synthesis. It displays activity against *Haemophilus*, *Enterobacteriaceae*, *Staphylococcus*, and *Klebsiella*. It also downregulates expression of genes associated with Th2 and Treg differentiation.

Mor F, Cohen IR. Beta-lactam antibiotics modulate T-cell functions and gene expression via covalent binding to cellular albumin. Proc Natl Acad Sci U S A. 2013 Feb 19;110(8):2981-6. PMID: 23382225.

Abdullah FE, Mushtaq A, Irshad M, et al. Current efficacy of antibiotics against *Klebsiella* isolates from urine samples - a multi-centric experience in Karachi. Pak J Pharm Sci. 2013 Jan;26(1):11-5. PMID: 23261722.

C1644 Celecoxib

NEW

100 mg
500 mg
1 g

SC-58635

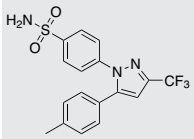

$C_{17}H_{14}F_3N_3O_2S$ FW: 381.37 [169590-42-5] ≥98%

NSAID and COX-2 inhibitor used to treat pain and inflammation. It also induces apoptosis in hepatoma cells and indirectly activates SIRT1.

Shao D, Kan M, Qiao P, et al. Celecoxib induces apoptosis via a mitochondria dependent pathway in the H22 mouse hepatoma cell line. Mol Med Rep. 2014 Oct;10(4):2093-8. PMID: 25109418.

Annamanedi M, Kalle AM. Celecoxib sensitizes *Staphylococcus aureus* to antibiotics in macrophages by modulating SIRT1. PLoS One. 2014 Jun 20;9(6):e99285. PMID: 24950067.

Li WW, Long GX, Liu DB, et al. Cyclooxygenase-2 inhibitor celecoxib suppresses invasion and migration of nasopharyngeal carcinoma cell lines through a decrease in matrix metalloproteinase-2 and -9 activity. Pharmazie. 2014 Feb;69(2):132-7. PMID: 24640603.

C1648 α-Cembrenediol

10 mg

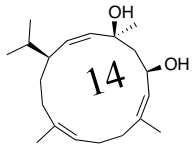

$C_{20}H_{34}O_2$ FW: 306.48 [57605-80-8] ≥98%

Found in *Anisomeles*. It inhibits growth of *Mycobacterium* and *Colletotrichum*.

Kulkarni RR, Shurpali K, Gawde RL, et al. Phyllocladane diterpenes from *Anisomeles* heyneana. J Asian Nat Prod Res. 2012;14(12):1162-8. PMID: 23157282.

Kennedy BS, Nielsen MT, Severson RF. Biorationals from *Nicotiana* protect cucumbers against *Colletotrichum* lagenarium (Pass.) ell. & halst disease development. J Chem Ecol. 1995 Feb;21(2):221-31. PMID: 24234021.

C1649 β-Cembrenediol

10 mg

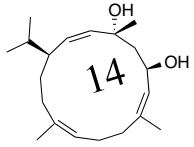

$C_{20}H_{34}O_2$ FW: 306.48 [57605-81-9] ≥98%

Found in *Anisomeles*. It inhibits growth of *Mycobacterium* and *Colletotrichum*.

Kulkarni RR, Shurpali K, Gawde RL, et al. Phyllocladane diterpenes from *Anisomeles* heyneana. J Asian Nat Prod Res. 2012;14(12):1162-8. PMID: 23157282.

Kennedy BS, Nielsen MT, Severson RF. Biorationals from *Nicotiana* protect cucumbers against *Colletotrichum* lagenarium (Pass.) ell. & halst disease development. J Chem Ecol. 1995 Feb;21(2):221-31. PMID: 24234021.

C1650 β-Cembrenediol Methyl Ether

10 mg

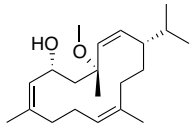

$C_{21}H_{36}O_2$ FW: 320.51 ≥98%

Found in tobacco plants and cigarette smoke. It is cytotoxic in cancer cells and some microbes.

Kulkarni RR, Shurpali K, Gawde RL, et al. Phyllocladane diterpenes from *Anisomeles* heyneana. J Asian Nat Prod Res. 2012;14(12):1162-8. PMID: 23157282.

Wright AD, Nielson JL, Tapiolas DM, et al. A great barrier reef Sinularia sp. yields two new cytotoxic diterpenes. Mar Drugs. 2012 Aug;10(8):1619-30. PMID: 23015765.

C1660 CEP-32496

1 mg
5 mg

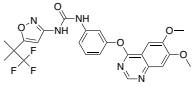

$C_{24}H_{22}F_3N_5O_5$ FW: 517.46 [1188910-76-0] ≥98%

V600E mutant B-Raf inhibitor. It also inhibits MEK and ERK, inhibiting proliferation in several cancer cell lines.

James J, Ruggeri B, Armstrong RC, et al. CEP-32496: a novel orally active BRAF(V600E) inhibitor with selective cellular and in vivo antitumor activity. Mol Cancer Ther. 2012 Apr;11(4):930-41. PMID: 22319199.

Rowbottom MW, Faraoni R, Chao Q, et al. Identification of 1-(3-(6,7-dimethoxyquinazolin-4-yloxy)phenyl)-3-(5-(1,1,1-trifluoro-2-methylpropan-2-yl)isoxazol-3-yl)urea hydrochloride (CEP-32496), a highly potent and orally efficacious inhibitor of V-RAF murine sarcoma viral oncogene homologue B1 (BRAF) V600E. J Med Chem. 2012 Feb 9;55(3):1082-105. PMID: 22168626.

C1718 Cepharanthine

100 mg
500 mg
1 g

O-Methylcepharanoline

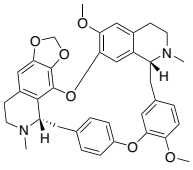

$C_{37}H_{38}N_2O_6$ FW: 606.71 [481-49-2] ≥95%

Found in *Stephania*. It inhibits the development of *Plasmodium*, prevents cell fusion and entry of HIV-1, induces cell cycle arrest and apoptosis in osteosarcoma cells, and decreases LPS-stimulated expression of pro-inflammatory cytokines in macrophages.

Desgrouas C, Chapus C, Desplans J, et al. In vitro antiplasmodial activity of cepharanthine. Malar J. 2014 Aug 22;13(1):327. PMID: 25145413.

Matsuda K, Hattori S, Komizu Y, et al. Cepharanthine inhibited HIV-1 cell-cell transmission and cell-free infection via modification of cell membrane fluidity. Bioorg Med Chem Lett. 2014 May 1;24(9):2115-7. PMID: 24704028.

C1867 Ceramide

5 mg
25 mg

N-Palmitoyl-D-sphingosine

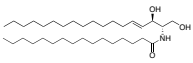

C_{16} ($C_{34}H_{67}NO_3$) FW: 537.9 [24696-26-2] ≥98%

Endogenous lipid component of sphingomyelin required for cell membrane lipid bilayer production. It is involved in differentiation, proliferation, programmed cell death, and apoptosis.

Hannun YA, Obeid LM. Principles of bioactive lipid signalling: lessons from sphingolipids. Nat Rev Mol Cell Biol. 2008 Feb;9(2):139-50. PMID: 18216770.

Wu D, Ren Z, Pae M, et al. Aging up-regulates expression of inflammatory mediators in mouse adipose tissue. J Immunol. 2007 Oct 1;179(7):4829-39. PMID: 17878382.

C1868 Cerebellin

1 mg
2 mg
5 mg

H-Ser-Gly-Ser-Ala-Lys-Val-Ala-Phe-Ser-Ala-Ile-Arg-Ser-Thr-Asn-His-OH

$C_{69}H_{113}N_{23}O_{23}$ FW: 1632.81 [94071-26-8] ≥95%

Neurexin-family cell adhesion peptide involved in synapse formation.

Lee SJ, Uemura T, Yoshida T, et al. GluRδ2 assembles four neurexins into trans-synaptic triad to trigger synapse formation. J Neurosci. 2012 Mar 28;32(13):4688-701. PMID: 22457515.

Rong Y, Wei P, Parris J, et al. Comparison of Cbln1 and Cbln2 functions using transgenic and knockout mice. J Neurochem. 2012 Feb;120(4):528-40. PMID: 22117778.

C1668 Cerivastatin Sodium

5 mg
10 mg
25 mg

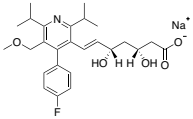

$C_{26}H_{33}FNO_5Na$ FW: 481.53 [143201-11-0] ≥98%

HMG-CoA reductase inhibitor used to lower cholesterol and lipid levels. Use is associated with the development of rhabdomyolysis. It also decreases production of pro-inflammatory cytokines and PAI-1, preventing atherosclerosis, fibrosis, and inflammation.

Takeshita Y, Takamura T, Hamaguchi E, et al. Tumor necrosis factor-alpha-induced production of plasminogen activator inhibitor 1 and its regulation by pioglitazone and cerivastatin in a nonmalignant human hepatocyte cell line. Metabolism. 2006 Nov;55(11):1464-72. PMID: 17046548.

Schachter M. Chemical, pharmacokinetic and pharmacodynamic properties of statins: an update. Fundam Clin Pharmacol. 2005 Feb;19(1):117-25. PMID: 15660968.

C1869 Cerulenin

1 mg
5 mg
10 mg

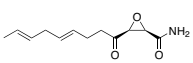

$C_{12}H_{17}NO_3$ FW: 223.27 [17397-89-6] ≥98%

Fatty acid synthase inhibitor found in Cephalosporium. It induces apoptosis and cellular death in colon cancer cells. It may also inhibit insulin secretion.

Straub SG, Sharp GW. Inhibition of insulin secretion by cerulenin might be due to impaired glucose metabolism. Diabetes Metab Res Rev. 2007 Feb;23(2):146-51. PMID: 16705622.

Price AC, Choi KH, Heath RJ, et al. Inhibition of beta-ketoacyl-acyl carrier protein synthases by thiolactomycin and cerulenin. Structure and mechanism. J Biol Chem. 2001 Mar 2;276(9):6551-9. PMID: 11050088.

C1876

Cetirizine Dihydrochloride

1 g
5 g
10 g
25 g

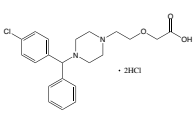

$C_{21}H_{25}ClN_2O_3 \cdot 2HCl$ FW: 461.82 [83881-52-1] ≥99%

Histamine H1 receptor antagonist used to treat dermatitis. It also inhibits its DNA binding activity of NF-κB, suppresses expression of adhesion molecules on immunocytes and endothelial cells, and increases release of prostaglandin E2.

Namazi MR. Cetirizine and allopurinol as novel weapons against cellular autoimmune disorders. Int Immunopharmacol. 2004 Mar;4(3):349-53. PMID: 15037212.

Bruno G, Andreozzi P, Magrini L, et al. Serum tryptase in allergic rhinitis: effect of cetirizine treatment. Int J Immunopathol Pharmacol. 2001 Sep-Dec;14(3):147-152. PMID: 12604015.

Slater JW, Zechnich AD, Haxby DG. Second-generation antihistamines: a comparative review. Drugs. 1999 Jan;57(1):31-47. PMID: 9951950.

C1878

Cetrimide

50 g
250 g

Cetrimonium Bromide

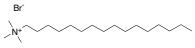

$C_{19}H_{42}BrN$ FW: 364.45 [57-09-0] ≥98%

Mixture of quaternary ammonium salts, cationic detergent, and H^+ ATP synthase inhibitor. It induces pore formation in bacterial membranes and inhibits proliferation of head and neck cancer cells.

Ito E, Yip KW, Katz D, et al. Potential use of cetrimonium bromide as an apoptosis-promoting anticancer agent for head and neck cancer. Mol Pharmacol. 2009 Nov;76(5):969-83. PMID: 19654225.

Bragadin M, Dell'Antone P. Mitochondrial bioenergetics as affected by cationic detergents. Arch Environ Contam Toxicol. 1996 Feb;30(2):280-4. PMID: 8593085.

C1879

Cetrorelix Acetate

50 mg
100 mg

Ac-3-(2-naphthyl)-D-Ala-4Chloro-D-Phe-3(3-pyridyl)-D-Ala-Ser-Tyr-D-Cit-Leu-Arg-Pro-D-Ala-OH

$C_{70}H_{92}N_{17}O_{14}$ FW: 1431.06 [130143-01-0] ≥95%

GnRH analog and GnRH receptor agonist used as a treatment for infertility. It also decreases prostate size and weight in BPH models, inhibits activity of LHRH and GnRH, and induces apoptosis in granulosa cells.

Rick FG, Schally AV, Block NL, et al. LHRH antagonist Cetrorelix reduces prostate size and gene expression of proinflammatory cytokines and growth factors in a rat model of benign prostatic hyperplasia. Prostate. 2011 May 15;71(7):736-47. PMID: 20945403.

Zhao XJ, Huang YH, Yu YC, et al. GnRH antagonist cetrorelix inhibits mitochondria-dependent apoptosis triggered by chemotherapy in granulosa cells of rats. Gynecol Oncol. 2010 Jul;118(1):69-75. PMID: 20417958.

C2540

CGK 733

NEW

5 mg
10 mg
25 mg

ATM/ATR Kinase Inhibitor

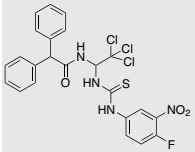

$C_{23}H_{18}Cl_3FN_4O_3S$ FW: 555.83 [905973-89-9] ≥98%

ATM and ATR kinase inhibitor. It prevents double-stranded DNA strand break repair and induces cell death in cancer cells.

Jekimovs C, Bolderson E, Suraweera A, et al. Chemotherapeutic compounds targeting the DNA double-strand break repair pathways: the good, the bad, and the promising. Front Oncol. 2014 Apr 22;4:86. PMID: 24795863.

Alao JP, Sunnerhagen P. The ATM and ATR inhibitors CGK733 and caffeine suppress cyclin D1 levels and inhibit cell proliferation. Radiat Oncol. 2009 Nov 10;4:51. PMID: 19903334.

C2802

CH5132799

NEW

1 mg
5 mg
25 mg

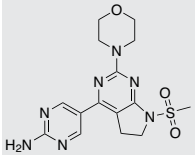

$C_{15}H_{19}N_7O_3S$ FW: 377.42 [1007207-67-1] ≥98%

Inhibitor of p110α PI3K. It inhibits cell proliferation and tumor growth in several cancer models.

Tanaka H, Yoshida M, Tanimura H, et al. The selective class I PI3K inhibitor CH5132799 targets human cancers harboring oncogenic PIK3CA mutations. Clin Cancer Res. 2011 May 15;17(10):3272-81. PMID: 21558396.

Ohwada J, Ebiike H, Kawada H, et al. Discovery and biological activity of a novel class I PI3K inhibitor, CH5132799. Bioorg Med Chem Lett. 2011 Mar 15;21(6):1767-72. PMID: 21316229.

C2900

CH5424802

NEW

5 mg
10 mg

Alectinib

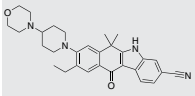

$C_{30}H_{34}N_4O_2$ FW: 482.62 [1256580-46-7] ≥99%

Inhibitor of WT and L1196M ALK. It inhibits proliferation and metastasis in non-small cell lung cancer cells.

Santarpia M, Altavilla G, Rosell R. Alectinib: a selective, next-generation ALK inhibitor for treatment of ALK-rearranged non-small-cell lung cancer. Expert Rev Respir Med. 2015 Feb 5:1-14. [Epub ahead of print]. PMID: 25652176.

Kodama T, Hasegawa M, Takanashi K, et al. Antitumor activity of the selective ALK inhibitor alectinib in models of intracranial metastases. Cancer Chemother Pharmacol. 2014 Nov;74(5):1023-8. PMID: 25205428.

Kodama T, Tsukaguchi T, Yoshida M, et al. Selective ALK inhibitor alectinib with potent antitumor activity in models of crizotinib resistance. Cancer Lett. 2014 Sep 1;351(2):215-21. PMID: 24887559.

C2800 Chalcone

25 g
100 g
500 g

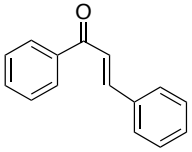

$C_{15}H_{12}O$ FW: 208.26 [94-41-7] ≥97%

Chalcone and its derivatives typically display a wide variety of biological activities, including suppressing inflammation, limiting oxidative damage, and inhibiting growth of cancer cells.

Wu JZ, Cheng CC, Shen LL, et al. Synthetic Chalcones with Potent Antioxidant Ability on H_2O_2-Induced Apoptosis in PC12 Cells. Int J Mol Sci. 2014 Oct 14;15(10):18525-18539. PMID: 25318055.

Jantan I, Bukhari SN, Adekoya OA, et al. Studies of synthetic chalcone derivatives as potential inhibitors of secretory phospholipase A2, cyclooxygenases, lipoxygenase and pro-inflammatory cytokines. Drug Des Devel Ther. 2014 Sep 16;8:1405-18. PMID: 25258510.

Abdellatif KR, Elshemy HA, Salama SA, et al. Synthesis, characterization and biological evaluation of novel 4'-fluoro-2'-hydroxy-chalcone derivatives as antioxidant, anti-inflammatory and analgesic agents. J Enzyme Inhib Med Chem. 2014 Sep 8:1-8. PMID: 25198887.

C2803 Chartreusin

5 mg
25 mg

Lambdamycin; NSC-5159

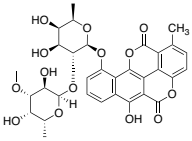

$C_{32}H_{32}O_{14}$ FW: 640.6 [6377-18-0] ≥98%

RNA synthesis inhibitor that binds DNA. It induces accumulation of free radicals.

Portugal J. Chartreusin, elsamicin A and related anti-cancer antibiotics. Curr Med Chem Anticancer Agents. 2003 Nov;3(6):411-20. PMID: 14529449.

Uramoto M, Kusano T, Nishio T, et al. Specific binding of chartreusin, an antitumor antibiotic, to DNA. FEBS Lett. 1983 Mar 21;153(2):325-8. PMID: 6311618.

C2816 Cheirolin

25 mg
50 mg
100 mg
500 mg

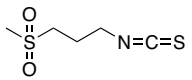

$C_5H_9NO_2S_2$ FW: 179.26 [505-34-0] ≥97%

Antioxidant and sulfonyl analog of sulforaphane. It induces phase II enzyme activity and expression.

Ernst IM, Palani K, Esatbeyoglu T, et al. Synthesis and Nrf2-inducing activity of the isothiocyanates iberverin, iberin and cheirolin. Pharmacol Res. 2013 Apr;70(1):155-62. PMID: 23403058.

C2818 Chelerythrine Chloride

1 mg
5 mg

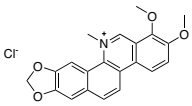

$C_{21}H_{18}ClNO_4$ FW: 383.82 [3895-92-9] ≥98%

Inhibitor of PKC and Na^+/K^+ ATPase found in *Chelidonium* and *Zanthoxylum*. It decreases LPS-stimulated pro-inflammatory cytokine expression and induces apoptosis in hepatoma cells.

Niu X, Mu Q, Li W, et al. Protective Effects of Chelerythrine Against Lipopolysaccharide-Induced Endotoxic Shock in Mice. Inflammation. 2014 Jun 14. [Epub ahead of print]. PMID: 24928629.

Dorney KM, Sizemore IE, Alqahtani T, et al. Surface-enhanced Raman spectroscopy (SERS) tracking of chelerythrine, a Na(+)/K(+) pump inhibitor, into cytosol and plasma membrane fractions of human lens epithelial cell cultures. Cell Physiol Biochem. 2013;32(7):146-56. PMID: 24429821.

Zhang ZF, Guo Y, Zhang JB, et al. Induction of apoptosis by chelerythrine chloride through mitochondrial pathway and Bcl-2 family proteins in human hepatoma SMMC-7721 cell. Arch Pharm Res. 2011 May;34(5):791-800. PMID: 21656365.

C2916 Chenodeoxycholic Acid

1 g
5 g
25 g

CDC

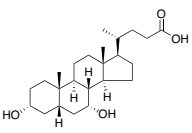

$C_{24}H_{40}O_4$ FW: 392.57 [474-25-9] ≥98%

Endogenous bile acid and FXR agonist used to treat constipation. It prevents NSAID-induced gastrointestinal injury and decreases PKC activity and induces apoptosis in ovarian cancer cells.

Fiorucci S, Mencarelli A, Cipriani S, et al. Activation of the farnesoid-X receptor protects against gastrointestinal injury caused by non-steroidal anti-inflammatory drugs in mice. Br J Pharmacol. 2011 Dec;164(8):1929-38. PMID: 21564085.

Horowitz NS, Hua J, Powell MA, et al. Novel cytotoxic agents from an unexpected source: bile acids and ovarian tumor apoptosis. Gynecol Oncol. 2007 Nov;107(2):344-9. PMID: 17720233.

C2946 Chlorambucil

100 mg
500 mg
1 g
10 g

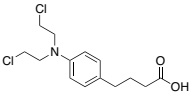

$C_{14}H_{19}Cl_2NO_2$ FW: 304.21 [305-03-3] ≥98%

DNA alkylator used to treat chronic lymphocytic leukemia. It inhibits DNA replication.

Begleiter A, Mowat M, Israels LG, et al. Chlorambucil in chronic lymphocytic leukemia: mechanism of action. Leuk Lymphoma. 1996 Oct;23(3-4):187-201. PMID: 9031099.

Kundu GC, Schullek JR, Wilson IB. The alkylating properties of chlorambucil. Pharmacol Biochem Behav. 1994 Nov;49(3):621-4. PMID: 7862715.

C2844 Chloramphenicol

5 g
10 g
50 g

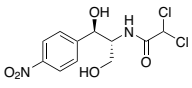

$C_{11}H_{12}Cl_2N_2O_5$ FW: 323.13 [56-75-7] ≥98%

Protein translation and peptidyl transferase inhibitor. It is particularly active against *Streptomyces*.

Sheth A, Escobar-Alvarez S, Gardner J, et al. Inhibition of human mitochondrial peptide deformylase causes apoptosis in c-myc-overexpressing hematopoietic cancers. Cell Death Dis. 2014 Mar 27;5:e1152. PMID: 24675470.

Rajesh T, Song E, Lee BR, et al. Increased sensitivity to chloramphenicol by inactivation of manB in *Streptomyces* coelicolor. J Microbiol Biotechnol. 2012 Oct;22(10):1324-9. PMID: 23075781.

Wilson DN. On the specificity of antibiotics targeting the large ribosomal subunit. Ann N Y Acad Sci. 2011 Dec;1241:1-16. PMID: 22191523.

C2845 Levo-Chloramphenicol

5 g
10 g
50 g

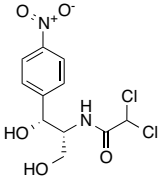

$C_{11}H_{12}Cl_2N_2O_5$ FW: 323.13 [56-75-7] ≥98%

Protein translation and peptidyl transferase inhibitor. It is particularly active against *Streptomyces*.

Sheth A, Escobar-Alvarez S, Gardner J, et al. Inhibition of human mitochondrial peptide deformylase causes apoptosis in c-myc-overexpressing hematopoietic cancers. Cell Death Dis. 2014 Mar 27;5:e1152. PMID: 24675470.

Rajesh T, Song E, Lee BR, et al. Increased sensitivity to chloramphenicol by inactivation of manB in *Streptomyces* coelicolor. J Microbiol Biotechnol. 2012 Oct;22(10):1324-9. PMID: 23075781.

C2847 Chlormadinone Acetate

1 g
5 g

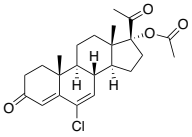

$C_{23}H_{29}ClO_4$ FW: 404.93 [302-22-7] ≥96%

Synthetic steroid hormone and antagonist at androgen and estrogen receptors used to treat BPH and polycystic ovary syndrome. It also promotes osteoblast differentiation and Ca^{2+} deposition in bone marrow stem cells.

Kim JM, Lee JE, Ryu SH, et al. Chlormadinone acetate promotes osteoblast differentiation of human mesenchymal stem cells through the ERK signaling pathway. Eur J Pharmacol. 2014 Mar 5;726:1-8. PMID: 24440171.

Fujimoto K, Hirao Y, Ohashi Y, et al. The effects of chlormadinone acetate on lower urinary tract symptoms and erectile functions of patients with benign prostatic hyperplasia: a prospective multicenter clinical study. Adv Urol. 2013;2013:584678. PMID: 23762042.

Gomes VA, Vieira CS, Jacob-Ferreira AL, et al. Oral contraceptive containing chlormadinone acetate and ethinylestradiol reduces plasma concentrations of matrix metalloproteinase-2 in women with polycystic ovary syndrome. Basic Clin Pharmacol Toxicol. 2012 Sep;111(3):211-6. PMID: 22510229.

C2942 Mechlorethamine Hydrochloride

5 g
10 g
25 g

Nitrogen mustard; Bis(2-chloroethyl)methylamine

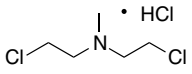

$C_5H_{11}Cl_2N \bullet HCl$ FW: 192.51 [55-86-7] ≥98%

DNA alkylator used to treat various cancers. It forms a reactive aziridinium ion intermediate and induces 5'-GNC-3' DNA crosslinks. It also increases oxidative stress and apoptosis in B-cell chronic lymphocytic leukemia cells.

Polavarapu A, Stillabower JA, Stubblefield SG, et al. The mechanism of guanine alkylation by nitrogen mustards: a computational study. J Org Chem. 2012 Jul 20;77(14):5914-21. PMID: 22681226.

Wang F, Li F, Ganguly M, et al. A bridging water anchors the tethered 5-(3-aminopropyl)-2'-deoxyuridine amine in the DNA major groove proximate to the N'2 C.G base pair: implications for formation of interstrand 5'-GNC-3' cross-links by nitrogen mustards. Biochemistry. 2008 Jul 8;47(27):7147-57. PMID: 18549246.

Crater J, Kannan S. Molecular mechanism of nitrogen mustard induced leukocyte(s) chemotaxis. Med Hypotheses. 2007;68(2):318-9. PMID: 16997491.

C2948 Chloroadenosine

5 mg
10 mg
50 mg

2-CADO

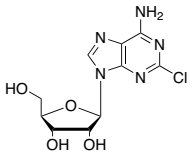

$C_{10}H_{12}ClN_5O_4$ FW: 301.69 [146-77-0] ≥98%

Adenosine analog and adenosine receptor agonist that terminates DNA chain elongation. It induces double-stranded DNA breaks and apoptosis in lung cancer cells. It also stimulates arterial dilation and decreases expression of TNF-α.

Duan HY, Cao JX, Qi JJ, et al. E2F1 enhances 8-chloro-adenosine-induced G2/M arrest and apoptosis in A549 and H1299 lung cancer cells. Biochemistry (Mosc). 2012 Mar;77(3):261-9. PMID: 22803943.

Bender SB, Tune JD, Borbouse L, et al. Altered mechanism of adenosine-induced coronary arteriolar dilation in early-stage metabolic syndrome. Exp Biol Med (Maywood). 2009 Jun;234(6):683-92. PMID: 19307464.

Sakamaki F, Ishizaka A, Urano T, et al. Attenuation by intravenous 2-chloroadenosine of acute lung injury induced by live *escherichia* coli or latex particles added to endotoxin in the neutropenic state. J Lab Clin Med. 2003 Aug;142(2):128-35. PMID: 12960960.

C2943

Chlorogenic Acid (from *Eucommia*)

250 mg
1 g

$C_{16}H_{18}O_9$ FW: 354.31 [327-97-9] ≥98%

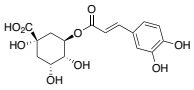

Derivative of caffeic acid found in *Eucommia* and inhibitor of DNMT. It inhibits oxidative stress in acetaminophen-induced liver injury, suppresses inflammation and mast cell activation, and inhibits glioma cell migration.

Zeng HJ, Liang HL, You J, et al. Study on the binding of chlorogenic acid to pepsin by spectral and molecular docking. Luminescence. 2013 Dec 12. [Epub ahead of print]. PMID: 24339327.

Luís A, Silva F, Sousa S, et al. Antistaphylococcal and biofilm inhibitory activities of gallic, caffeic, and chlorogenic acids. Biofouling. 2014 Jan;30(1):69-79. PMID: 24228999.

Shi H, Dong L, Jiang J, et al. Chlorogenic acid reduces liver inflammation and fibrosis through inhibition of toll-like receptor 4 signaling pathway. Toxicology. 2013 Jan 7;303:107-14. PMID: 23146752.

C2944

Chlorogenic Acid (from *Lonicera*)

100 mg
250 mg
1 g

3-Caffeoylquinic acid

$C_{16}H_{18}O_9$ FW: 354.31 [327-97-9] ≥98%

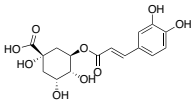

Derivative of caffeic acid found in *Lonicera* and inhibitor of DNMT. It inhibits oxidative stress in acetaminophen-induced liver injury, suppresses inflammation and mast cell activation, and inhibits glioma cell migration.

Zeng HJ, Liang HL, You J, et al. Study on the binding of chlorogenic acid to pepsin by spectral and molecular docking. Luminescence. 2013 Dec 12. [Epub ahead of print]. PMID: 24339327.

Luís A, Silva F, Sousa S, et al. Antistaphylococcal and biofilm inhibitory activities of gallic, caffeic, and chlorogenic acids. Biofouling. 2014 Jan;30(1):69-79. PMID: 24228999.

C2945

Chlorophyllin Sodium-Copper Salt

5 g
25 g
100 g

$C_{32}H_{40}CuN_4Na_2O_4$ FW: 654.21 [15611-43-5] ≥98%

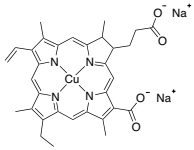

Semi-synthetic derivative of chlorophyll commercially used as a food additive and coloring agent. Induces apoptosis and autophagy under UV light in bladder cancer cells and suppresses benzo[a]pyrene- and DBP-induced carcinogenesis.

Lihuan D, Jingcun Z, Ning J, et al. Photodynamic therapy with the novel photosensitizer chlorophyllin f induces apoptosis and autophagy in human bladder cancer cells. Lasers Surg Med. 2014 Apr;46(4):319-34. PMID: 24464873.

Nagini S, Vidya Priyadarsini R, Veeravarmal V, et al. Chlorophyllin abrogates canonical Wnt/β-catenin signaling and angiogenesis to inhibit the development of DMBA-induced hamster cheek pouch carcinomas. Cell Oncol (Dordr). 2012 Oct;35(5):385-95. Erratum in: Cell Oncol (Dordr). 2013 Apr;36(2):179. PMID: 22983718.

Keshava C, Divi RL, Einem TL, et al. Chlorophyllin significantly reduces benzo[a]pyrene-DNA adduct formation and alters cytochrome P450 1A1 and 1B1 expression and EROD activity in normal human mammary epithelial cells. Environ Mol Mutagen. 2009 Mar;50(2):134-44. PMID: 19152381.

C2950

Chloroquine Diphosphate

25 g
50 g
100 g

$C_{18}H_{26}ClN_3 2H_3PO_4$ FW: 515.87 [50-63-5] ≥98%

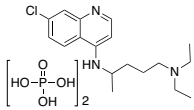

It binds heme and causes cell lysis and is used to treat malaria. It also inhibits replication of many viruses, decreases pro-inflammatory cytokine production, and suppresses the induction of autophagy.

Liang X, Tang J, Liang Y, et al. Suppression of autophagy by chloroquine sensitizes 5-fluorouracil-mediated cell death in gallbladder carcinoma cells. Cell Biosci. 2014 Mar 3;4(1):10. PMID: 24581180.

Hempelmann E. Hemozoin biocrystallization in *Plasmodium falciparum* and the antimalarial activity of crystallization inhibitors. Parasitol Res. 2007 Mar;100(4):671-6. PMID: 17111179.

Savarino A, Boelaert JR, Cassone A, et al. Effects of chloroquine on viral infections: an old drug against today's diseases? Lancet Infect Dis. 2003 Nov;3(11):722-7. PMID: 14592603.

C2949

Chlorpheniramine Maleate

5 g
25 g
100 g

$C_{16}H_{19}ClN_2 \bullet C_4H_4O_4$ FW: 390.87 [113-92-8] ≥98%

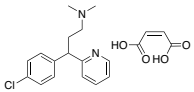

Histamine H1 receptor antagonist and SERT and NET inhibitor used to treat allergic rhinitis and urticaria. It also modulates memory consolidation.

Gianlorenço AC, Serafim KR, Canto-de-Souza A, et al. Emotional memory consolidation impairment induced by histamine is mediated by H1 but not H2 receptors. Brain Res Bull. 2012 Dec 1;89(5-6):197-202. PMID: 22986235.

Hellbom E. Chlorpheniramine, selective serotonin-reuptake inhibitors (SSRIs) and over-the-counter (OTC) treatment. Med Hypotheses. 2006;66(4):689-90. PMID: 16413139.

C2947 Chlorpromazine Hydrochloride

10 g
25 g
100 g

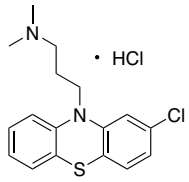

$C_{17}H_{19}ClN_2S \bullet HCl$ FW: 355.33 [69-09-0] ≥98%

Antagonist at D1/2/3/4 receptors, 5-HT1/2 receptors, M1/2 mAChRs, and α1/2-adrenergic receptors. It also acts as a FIASMA, prevents oligomerization by stabilizing misfolding motifs of prions, and induces autophagy and apoptosis in glioma tumor models.

Baral PK, Swayampakula M, Rout MK, et al. Structural basis of prion inhibition by phenothiazine compounds. Structure. 2014 Feb 4;22(2):291-303. PMID: 24373770.

Ramos MA. Drugs in context: a historical perspective on theories of psychopharmaceutical efficacy. J Nerv Ment Dis. 2013 Nov;201(11):926-33. PMID: 24177478.

Shin SY, Lee KS, Choi YK, et al. The antipsychotic agent chlorpromazine induces autophagic cell death by inhibiting the Akt/mTOR pathway in human U-87MG glioma cells. Carcinogenesis. 2013 Sep;34(9):2080-9. PMID: 23689352.

C2951 Chlortetracycline Hydrochloride

5 g
25 g
100 g

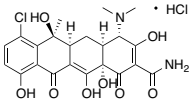

$C_{22}H_{23}ClN_2O_8 \bullet HCl$ FW: 515.35 [64-72-2] ≥85%

Inhibitor of protein translation, MMPs, calpain, and NMDA receptors. It also acts as a free radical scavenger and protects against cerebral ischemia.

Nguyen F, Starosta AL, Arenz S, et al. Tetracycline antibiotics and resistance mechanisms. Biol Chem. 2014 May;395(5):559-75. PMID: 24497223.

Kładna A, Michalska T, Berczyński P, et al. Evaluation of the antioxidant activity of tetracycline antibiotics in vitro. Luminescence. 2012 Jul-Aug;27(4):249-55. PMID: 22887986.

C2956 Cholecalciferol

1 g
5 g
25 g

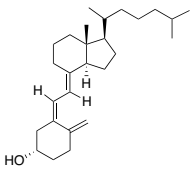

Oleovitamin D3; Vitamin D3

$C_{27}H_{44}O$ FW: 384.64 [67-97-0] ≥98%

Vitamin D prodrug synthesized in the skin under UV-B exposure. It is used as a dietary supplement to prevent bone loss. It may also decrease skin cancer risk.

Bendik I, Friedel A, Roos FF, et al. Vitamin D: a critical and essential micronutrient for human health. Front Physiol. 2014 Jul 11;5:248. PMID: 25071593.

Moukayed M, Grant WB. Molecular link between vitamin D and cancer prevention. Nutrients. 2013 Sep 30;5(10):3993-4021. PMID: 24084056.

Geddes JA, Inderjeeth CA. Evidence for the treatment of osteoporosis with vitamin D in residential care and in the community dwelling elderly. Biomed Res Int. 2013;2013:463589. PMID: 24058907.

C2957 Cholesterol

5 g
25 g
100 g

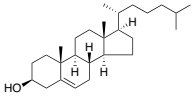

$C_{27}H_{46}O$ FW: 386.65 [57-88-5] ≥97%

Endogenous sterol component of animal cell membranes and precursor to steroid hormones, bile acids, and vitamin D compounds. It is also involved in vesicular transport, nerve conduction, and antioxidative activity.

Labrie F, Simard J, Luu-The V, et al. Structure, function and tissue-specific gene expression of 3β-hydroxysteroid dehydrogenase/5-ene-4-ene isomerase enzymes in classical and peripheral intracrine steroidogenic tissues. J Steroid Biochem Mol Biol. 1992 Dec;43(8):805-26. PMID: 22217825.

Smith LL. Another cholesterol hypothesis: cholesterol as antioxidant. Free Radic Biol Med. 1991;11(1):47-61. PMID: 1937129.

C2961 Chondroitin Sulfate, chicken

5 g
25 g

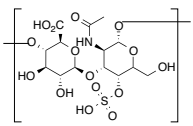

$C_{13}H_{21}NO_{15}S$ ~50,000 Da [9007-28-7] ≥90%

Endogenous compound used in dietary supplements to improve connective tissue resistance and elasticity. It suppresses expression of pro-inflammatory cytokines, increases synthesis of collagen, proteoglycan, and hyaluronic acid, and decreases levels of ROS.

Henrotin Y, Mathy M, Sanchez C, et al. Chondroitin sulfate in the treatment of osteoarthritis: from in vitro studies to clinical recommendations. Ther Adv Musculoskelet Dis. 2010 Dec;2(6):335-48. PMID: 22870459.

Campo GM, Avenoso A, Campo S, et al. Glycosaminoglycans modulate inflammation and apoptosis in LPS-treated chondrocytes. J Cell Biochem. 2009 Jan 1;106(1):83-92. PMID: 19009563.

Campo GM, Avenoso A, Campo S, et al. Chondroitin-4-sulphate inhibits NF-kB translocation and caspase activation in collagen-induced arthritis in mice. Osteoarthritis Cartilage. 2008 Dec;16(12):1474-83. PMID: 18501644.

C2960 Chondroitin Sulfate, cow

5 g
25 g

$C_{13}H_{21}NO_{15}S$ ~50,000 Da [9007-28-7] ≥90%

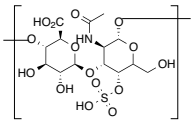

Endogenous compound used in dietary supplements to improve connective tissue resistance and elasticity. It suppresses expression of pro-inflammatory cytokines, increases synthesis of collagen, proteoglycan, and hyaluronic acid, and decreases levels of ROS.

Henrotin Y, Mathy M, Sanchez C, et al. Chondroitin sulfate in the treatment of osteoarthritis: from in vitro studies to clinical recommendations. Ther Adv Musculoskelet Dis. 2010 Dec;2(6):335-48. PMID: 22870459.

Campo GM, Avenoso A, Campo S, et al. Glycosaminoglycans modulate inflammation and apoptosis in LPS-treated chondrocytes. J Cell Biochem. 2009 Jan 1;106(1):83-92. PMID: 19009563.

C2965 Chromium Picolinate

5 g
25 g

Chromium(III) trispicolinate

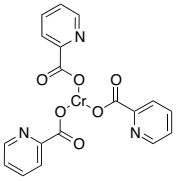

$C_{18}H_{12}CrN_3O_6$ FW: 418.3 [14639-25-9] ≥98%

Used to prevent chromium deficiency and to decrease serum glucose and insulin levels. It also decreases plasma lipid levels and platelet aggregation and improves myocardial contractility.

Seif AA. Chromium picolinate inhibits cholesterol-induced stimulation of platelet aggregation in hypercholesterolemic rats. Ir J Med Sci. 2014 Mar 15. [Epub ahead of print]. PMID: 24633441.

Amooee S, Parsanezhad ME, Ravanbod Shirazi M, et al. Metformin versus chromium picolinate in clomiphene citrate-resistant patients with PCOs: A double-blind randomized clinical trial. Iran J Reprod Med. 2013 Aug;11(8):611-8. PMID: 24639797.

Abebe W, Liu JY, Wimborne H, et al. Effects of chromium picolinate on vascular reactivity and cardiac ischemia-reperfusion injury in spontaneously hypertensive rats. Pharmacol Rep. 2010 Jul-Aug;62(4):674-82. PMID: 20885007.

C2969 Chromomycin A3

1 mg
5 mg
10 mg

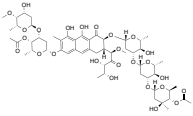

$C_{57}H_{82}O_{26}$ FW: 1183.2488 [7059-24-7] ≥97%

Mg^{2+}/Zn^{2+} chelator, bacterial DNA gyrase and RNA polymerase inhibitor, and potential alcohol dehydrogenase inhibitor. It inhibits growth of *Bacillus* and suppresses tumor growth of breast cancer xenografts.

Devi PG, Chakraborty PK, Dasgupta D. Inhibition of a Zn(II)-containing enzyme, alcohol dehydrogenase, by anticancer antibiotics, mithramycin and chromomycin A3. J Biol Inorg Chem. 2009 Mar;14(3):347-59. PMID: 19034537.

Mir MA, Dasgupta D. Association of the anticancer antibiotic chromomycin A(3) with the nucleosome: role of core histone tail domains in the binding process. Biochemistry. 2001 Sep 25;40(38):11578-85. PMID: 11560508.

Simon H, Wittig B, Zimmer C. Effect of netropsin, distamycin A and chromomycin A3 on the binding and cleavage reaction of DNA gyrase. FEBS Lett. 1994 Oct 10;353(1):79-83. PMID: 7926028.

C2971 Chromostatin, cow

0.5 mg
1 mg
2.5 mg

H-Ser-Asp-Glu-Asp-Ser-Asp-Gly-Asp-Arg-Pro-Gln-Ala-Ser-Pro-Gly-Leu-Gly-Pro-Gly-Pro-OH

$C_{78}H_{120}N_{24}O_{35}$ FW: 1953.97 ≥95%

Chromogranin A fragment and PP2A activator. It inhibits vasoconstriction in thoracic arteries and saphenous veins induced by K^+, norepinephrine, and endothelin-1 and suppresses catecholamine secretion in chromaffin cells.

Garcia GE, Gabbai FB, O'Connor DT, et al. Does chromostatin influence catecholamine release or blood pressure in vivo? Peptides. 1994 Jan;15(1):195-7. PMID: 8015978.

Aardal S, Galindo E, Aunis D, et al. Human chromostatin inhibits endothelin-1-induced contractures in human blood vessels. Regul Pept. 1993 Aug 13;47(1):25-32. PMID: 8210519.

C2968 Chrysin

5 g
25 g

5,7-Dihydroxyflavone

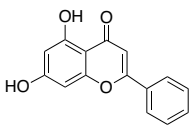

$C_{15}H_{10}O_4$ FW: 254.2 [480-40-0] ≥98%

HDAC2/8 inhibitor found in *Passiflora*, *Oroxylum*, and *Pleurotis*. It may also inhibitor aromatase. It displays a wide variety of biological activities, including suppressing LPS-stimulated inflammation in macrophages, increasing levels of antioxidative enzymes, and preventing DEN-induced renal carcinogenesis in vivo.

Li R, Zang A, Zhang L, et al. Chrysin ameliorates diabetes-associated cognitive deficits in Wistar rats. Neurol Sci. 2014 Oct;35(10):1527-32. PMID: 24737349.

Lirdprapamongkol K, Sakurai H, Abdelhamed S, et al. A flavonoid chrysin suppresses hypoxic survival and metastatic growth of mouse breast cancer cells. Oncol Rep. 2013 Nov;30(5):2357-64. PMID: 23969634.

Rehman MU, Tahir M, Khan AQ, et al. Chrysin suppresses renal carcinogenesis via amelioration of hyperproliferation, oxidative stress and inflammation: plausible role of NF-κB. Toxicol Lett. 2013 Feb 4;216(2-3):146-58. PMID: 23194824.

C2970 Chrysophanol

10 mg
25 mg
100 mg

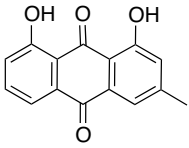

$C_{15}H_{10}O_4$ FW: 254.24 [481-74-3] ≥98%

Found in *Rheum*. It inhibits activation of the NALP3 inflammasome, ameliorates stroke-related pathology, decreases proliferation of Japanese encephalitis virus, and induces necrotic cell death in lung cancer cells.

Zhang N, Zhang X, Liu X, et al. Chrysophanol Inhibits NALP3 Inflammasome Activation and Ameliorates Cerebral Ischemia/Reperfusion in Mice. Mediators Inflamm. 2014;2014:370530. PMID: 24876671.

Ni CH, Yu CS, Lu HF, et al. Chrysophanol-induced cell death (necrosis) in human lung cancer A549 cells is mediated through increasing reactive oxygen species and decreasing the level of mitochondrial membrane potential. Environ Toxicol. 2014 May;29(7):740-9. PMID: 22848001.

Chang SJ, Huang SH, Lin YJ, et al. Antiviral activity of *Rheum* palmatum methanol extract and chrysophanol against Japanese encephalitis virus. Arch Pharm Res. 2014 Jan 7. [Epub ahead of print]. PMID: 24395532.

C2997 Chymostatin

1 mg
5 mg
25 mg
50 mg

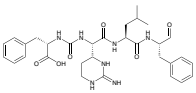

$C_{20}H_{16}N_2O_4$ FW: 1809.1 [9076-44-2] ≥98%

Protease inhibitor used in research models.

Paliwal D, Panda SK, Kapur N, et al. Hepatitis E virus (HEV) protease: a chymotrypsin-like enzyme that processes both non-structural (pORF1) and capsid (pORF2) protein. J Gen Virol. 2014 Aug;95(Pt 8):1689-700. PMID: 24795447.

Wang T, Han SX, Zhang SF, et al. Role of chymase in cigarette smoke-induced pulmonary artery remodeling and pulmonary hypertension in hamsters. Respir Res. 2010 Mar 31;11:36. PMID: 20356378.

C3208 Ciclopirox Olamine

1 g
5 g

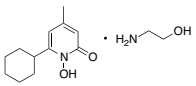

$C_{12}H_{17}NO_2 \bullet C_2H_7NO$ FW: 268.36 [41621-49-2] ≥98%

Metal ion chelator and mTOR inhibitor. It induces DNA damage and cell death in *Candida* and *Saccharomyces*, induces cell cycle arrest and apoptosis in various cancer cells, and prevents tube formation.

Sen S, Hassane DC, Corbett C, et al. Novel mTOR inhibitory activity of ciclopirox enhances parthenolide antileukemia activity. Exp Hematol. 2013 Sep;41(9):799-807.e4. PMID: 23660068.

Belenky P, Camacho D, Collins JJ. Fungicidal drugs induce a common oxidative-damage cellular death pathway. Cell Rep. 2013 Feb 21;3(2):350-8. PMID: 23416050.

Luo Y, Zhou H, Liu L, et al. The fungicide ciclopirox inhibits lymphatic endothelial cell tube formation by suppressing VEGFR-3-mediated ERK signaling pathway. Oncogene. 2011 May 5;30(18):2098-107. PMID: 21217783.

C3214 CID-797718

NEW

5 mg
25 mg

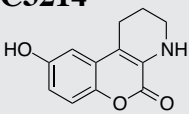

$C_{12}H_{11}NO_3$ FW: 217.22 [370586-05-3] ≥98%

Potential PKD binding agent.

C3210 Ciglitazone

1 mg
5 mg
25 mg

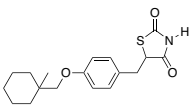

$C_{18}H_{23}NO_3S$ FW: 333.45 [74772-77-3] ≥98%

PPARγ agonist. It decreasing insulin levels, VEGF production, and blood pressure and induces cell cycle arrest in stomach cancer cells.

Shah DK, Menon KM, Cabrera LM, et al. Thiazolidinediones decrease vascular endothelial growth factor (VEGF) production by human luteinized granulosa cells in vitro. Fertil Steril. 2010 Apr;93(6):2042-7. PMID: 19342033.

Cheon CW, Kim DH, Kim DH, et al. Effects of ciglitazone and troglitazone on the proliferation of human stomach cancer cells. World J Gastroenterol. 2009 Jan 21;15(3):310-20. PMID: 19140230.

C3446 Cilnidipine

100 mg
250 mg
1 g

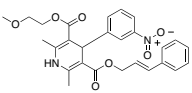

$C_{27}H_{26}N_2O_7$ FW: 490.525 [132203-70-4] ≥98%

L-type and N-type Ca^{2+} channel blocker used to treat hypertension. It also improves insulin sensitivity, suppresses nociception, and inhibits progression of glomerulonephritis.

Soeki T, Kitani M, Kusunose K, et al. Renoprotective and antioxidant effects of cilnidipine in hypertensive patients. Hypertens Res. 2012 Nov;35(11):1058-62. PMID: 22763473.

Fan L, Yang Q, Xiao XQ, et al. Dual actions of cilnidipine in human internal thoracic artery: inhibition of calcium channels and enhancement of endothelial nitric oxide synthase. J Thorac Cardiovasc Surg. 2011 Apr;141(4):1063-9. PMID: 20599230.

Koganei H, Shoji M, Iwata S. Suppression of formalin-induced nociception by cilnidipine, a voltage-dependent calcium channel blocker. Biol Pharm Bull. 2009 Oct;32(10):1695-700. PMID: 19801830.

C3246 Cilostazol

OPC-13013

$C_{20}H_{27}N_5O_2$ FW: 369.46 [73963-72-1] ≥98%

50 mg
100 mg
500 mg

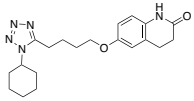

PDE 3B inhibitor used to treat intermittent claudication associated with peripheral vascular disease. It also inhibits TNF-α-induced inflammation, improves glucose tolerance and insulin resistance, and upregulates production of G-CSF and VEGF.

Biscetti F, Pecorini G, Straface G, et al. Cilostazol promotes angiogenesis after peripheral ischemia through a VEGF-dependent mechanism. Int J Cardiol. 2013 Aug 10;167(3):910-6. PMID: 22473072.

Wada T, Onogi Y, Kimura Y, et al. Cilostazol ameliorates systemic insulin resistance in diabetic db/db mice by suppressing chronic inflammation in adipose tissue via modulation of both adipocyte and macrophage functions. Eur J Pharmacol. 2013 May 5;707(1-3):120-9. PMID: 23528355.

Patel DS, Anand IS, Bhatt PA. Evaluation of antidepressant and anxiolytic activity of phosphodiesterase 3 inhibitor - cilostazol. Indian J Psychol Med. 2012 Apr;34(2):124-8. PMID: 23162186.

C3250 Cimetidine

$C_{10}H_{16}N_6S$ FW: 252.34 [51481-61-9] ≥98%

5 g
10 g
25 g

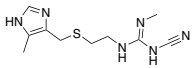

Inhibitor of catalase, histamine H2 receptors and androgen receptors used to treat ulcers. It also increases the efficacy of co-administered chemotherapeutics.

Masoud M, Ebrahimi F, Minai-Tehrani D. Effect of Cimetidine on Catalase Activity of *Pseudomonas* aeruginosa: A Suggested Mechanism of Action. J Mol Microbiol Biotechnol. 2014 Jul 2;24(3):196-201. PMID: 24993120.

Zheng Y, Xu M, Li X, et al. Cimetidine suppresses lung tumor growth in mice through proapoptosis of myeloid-derived suppressor cells. Mol Immunol. 2013 May;54(1):74-83. PMID: 23220070.

Matsumoto S, Imaeda Y, Umemoto S, et al. Cimetidine increases survival of colorectal cancer patients with high levels of sialyl Lewis-X and sialyl Lewis-A epitope expression on tumour cells. Br J Cancer. 2002 Jan 21;86(2):161-7. PMID: 11870500.

C3352 Cinacalcet Hydrochloride NEW

$C_{22}H_{22}F_3N \bullet HCl$ FW: 393.87 [364782-34-3] ≥98%

5 mg
25 mg
100 mg

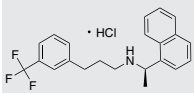

Ca^{2+}-sensing receptor agonist used to treat secondary hyperparathyroidism with chronic kidney disease. It decreases parathyroid hormone secretion and prevents the development of renal fibrosis.

Kuczera P, Adamczak M, Machnik G, et al. Treatment with Cinacalcet Increases Plasma Adiponectin Concentration in Hemodialysed Patients with Chronic Kidney Disease and Secondary Hyperparathyroidism. Endocr Pract. 2015 Mar 18:1-22. [Epub ahead of print]. PMID: 25786554.

Wu M, Tang RN, Liu H, et al. Cinacalcet attenuates the renal endothelial-to-mesenchymal transition in rats with adenine-induced renal failure. Am J Physiol Renal Physiol. 2014 Jan 1;306(1):F138-46. PMID: 24154694.

C3251 Cinnarizine

$C_{26}H_{28}N_2$ FW: 368.51 [298-57-7] ≥98%

10 g
100 g

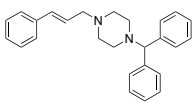

L-type Ca^{2+} channel blocker and dopamine D2 receptor antagonist. It acts as a FIASMA, suppresses stimulant-induced locomotor activity, and limits seizure development.

Taghdiri F, Togha M, Razeghi Jahromi S, et al. Cinnarizine for the prophylaxis of migraine associated vertigo: a retrospective study. Springerplus. 2014 May 7;3:231. PMID: 24834377.

Brahmane RI, Wanmali VV, Pathak SS, et al. Role of cinnarizine and nifedipine on anticonvulsant effect of sodium valproate and carbamazepine in maximal electroshock and pentylenetetrazole model of seizures in mice. J Pharmacol Pharmacother. 2010 Jul;1(2):78-81. PMID: 21350614.

Dall'Igna OP, Tort AB, Souza DO, et al. Cinnarizine has an atypical antipsychotic profile in animal models of psychosis. J Psychopharmacol. 2005 Jul;19(4):342-6. PMID: 15982988.

C3260 Ciprofibrate

$C_{13}H_{14}Cl_2O_3$ FW: 289.16 [52214-84-3] ≥98%

25 mg
100 mg

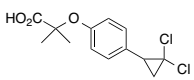

PPARα agonist used to decrease levels of triglycerides and total cholesterol and increase levels of HDL. It also induces depolarization of the mitochondrial membrane potential and enhances peroxisome proliferation.

Aguilar-Salinas CA, Assis-Luores-Vale A, Stockins B, et al. Ciprofibrate therapy in patients with hypertriglyceridemia and low high density lipoprotein (HDL)-cholesterol: greater reduction of non-HDL cholesterol in subjects with excess body weight (The CIPROAMLAT study). Cardiovasc Diabetol. 2004 Jul 23;3:8. PMID: 15272932.

Li Y, Glauert HP, Spear BT. Activation of nuclear factor-kappaB by the peroxisome proliferator ciprofibrate in H4IIEC3 rat hepatoma cells and its inhibition by the antioxidants N-acetylcysteine and vitamin E. Biochem Pharmacol. 2000 Feb 15;59(4):427-34. PMID: 10644051.

C3262

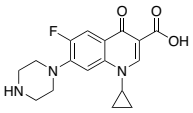

Ciprofloxacin

BAY Q 3939

$C_{17}H_{18}FN_3O_3$ FW: 331.34 [85721-33-1] ≥98%

5 g
25 g
50 g

Inhibitor of topoisomerase IV and bacterial DNA gyrase. It inhibits prevents DNA replication, inhibiting growth of gram negative and gram positive bacteria.

Rajendram M, Hurley KA, Foss MH, et al. Gyramides Prevent Bacterial Growth by Inhibiting DNA Gyrase and Altering Chromosome Topology. ACS Chem Biol. 2014 Apr 22. [Epub ahead of print]. PMID: 24712739.

Oliphant CM, Green GM. Quinolones: a comprehensive review. Am Fam Physician. 2002 Feb 1;65(3):455-64. PMID: 11858629.

Drlica K, Zhao X. DNA gyrase, topoisomerase IV, and the 4-quinolones. Microbiol Mol Biol Rev. 1997 Sep;61(3):377-92. PMID: 9293187.

C3263

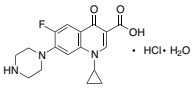

Ciprofloxacin Hydrochloride Monohydrate

$C_{17}H_{18}FN_3O_3 \bullet HCl \bullet H_2O$ FW: 385.82 [86393-32-0] ≥98%

5 g
25 g
50 g

Topoisomerase IV and bacterial DNA gyrase inhibitor. It prevents DNA replication in gram negative and gram positive bacteria.

Rajendram M, Hurley KA, Foss MH, et al. Gyramides Prevent Bacterial Growth by Inhibiting DNA Gyrase and Altering Chromosome Topology. ACS Chem Biol. 2014 Apr 22. [Epub ahead of print]. PMID: 24712739.

Oliphant CM, Green GM. Quinolones: a comprehensive review. Am Fam Physician. 2002 Feb 1;65(3):455-64. PMID: 11858629.

Drlica K, Zhao X. DNA gyrase, topoisomerase IV, and the 4-quinolones. Microbiol Mol Biol Rev. 1997 Sep;61(3):377-92. PMID: 9293187.

C3472

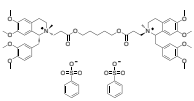

Cisatracurium Besylate

$C_{53}H_{72}N_2O_{12} \bullet 2C_6H_5O_3S$ FW: 1243.48 [96946-42-8] ≥95%

25 mg
100 mg
500 mg

Non-depolarizing NMJ blocker and antagonist at nAChRs and M2 mAChRs used to induce anesthesia. It relaxes skeletal muscles, prevents action potential shortening, and suppresses atrial fibrillation.

Liu M, Dilger JP. Synergy between pairs of competitive antagonists at adult human muscle acetylcholine receptors. Anesth Analg. 2008 Aug;107(2):525-33. PMID: 18633030.

Patterson E, Scherlag BJ, Zhou J, et al. Antifibrillatory actions of cisatracurium: an atrial specific M2 receptor antagonist. J Cardiovasc Electrophysiol. 2008 Aug;19(8):861-8. PMID: 18363689.

Dilger JP, Vidal AM, Liu M, et al. Roles of amino acids and subunits in determining the inhibition of nicotinic acetylcholine receptors by competitive antagonists. Anesthesiology. 2007 Jun;106(6):1186-95. PMID: 17525594.

C3374

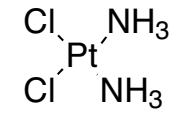

Cisplatin

CDDP; *cis*-diamminedichloroplatinum

$Cl_2H_6N_2Pt$ FW: 300.04 [15663-27-1] ≥98%

50 mg
100 mg
500 mg
1 g

Platinum-based DNA cross-linker used to treat various cancers. It decreases phosphorylation of PI3K, Akt, and FOXO3a and induces apoptosis in lung cancer cells and modulates STAT signaling and immune responses in other models.

Hato SV, Khong A, de Vries IJ, et al. Molecular pathways: the immunogenic effects of platinum-based chemotherapeutics. Clin Cancer Res. 2014 Jun 1;20(11):2831-7. PMID: 24879823.

Liu H, Yin J, Wang C, et al. FOXO3a mediates the cytotoxic effects of cisplatin in lung cancer cells. Anticancer Drugs. 2014 Sep;25(8):898-907. PMID: 24814195.

Stordal B, Davey M. Understanding cisplatin resistance using cellular models. IUBMB Life. 2007 Nov;59(11):696-9. PMID: 17885832.

C3477

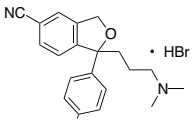

Citalopram Hydrobromide

$C_{20}H_{21}FN_2O \bullet HBr$ FW: 405.31 [59729-32-7] ≥98%

25 mg
100 mg
500 mg

SERT inhibitor used to treat depression and anxiety. It also inhibits neuronal apoptosis, suppresses arthritis progression by decreasing pro-inflammatory cytokine production, and potentially prolongs the cardiac QT interval.

Tan Y, Duan J, Li Y, et al. Effects of citalopram on serum deprivation induced PC12 cell apoptosis and BDNF expression. Pharmazie. 2010 Nov;65(11):845-8. PMID: 21155393.

Sacre S, Medghalchi M, Gregory B, et al. Fluoxetine and citalopram exhibit potent antiinflammatory activity in human and murine models of rheumatoid arthritis and inhibit toll-like receptors. Arthritis *Rheum*. 2010 Mar;62(3):683-93. PMID: 20131240.

Apparsundaram S, Stockdale DJ, Henningsen RA, et al. Antidepressants targeting the serotonin reuptake transporter act via a competitive mechanism. J Pharmacol Exp Ther. 2008 Dec;327(3):982-90. PMID: 18801947.

C3576

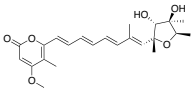

Citreoviridin A

1 mg
5 mg

$C_{23}H_{30}O_6$ FW: 402.48 [25425-12-1] ≥95%

Mycotoxin and F1F0 ATP synthase inhibitor found in grain products. It induces oxidative stress and DNA damage, increases TNF-α-induced cellular adhesion to monocytes, and suppresses growth of *Bacillus* and *Candida* and replication of HIV-1.

Bai Y, Jiang LP, Liu XF, et al. The role of oxidative stress in citreoviridin-induced DNA damage in human liver-derived HepG2 cells. Environ Toxicol. 2013 Dec 6. [Epub ahead of print]. PMID: 24318808.

Wu YH, Hu CW, Chien CW, et al. Quantitative proteomic analysis of human lung tumor xenografts treated with the ectopic ATP synthase inhibitor citreoviridin. PLoS One. 2013 Aug 21;8(8):e70642. PMID: 23990911.

Hou H, Zhou R, Jia Q, et al. Citreoviridin enhances tumor necrosis factor-α-induced adhesion of human umbilical vein endothelial cells. Toxicol Ind Health. 2013 Mar 22. PMID: 23524880.

C3479

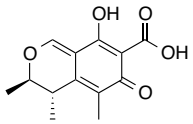

Citrinin

1 mg
5 mg
10 mg

$C_{13}H_{14}O_5$ FW: 250.249 [518-75-2] ≥98%

Mycotoxin found in *Penicillum*, *Aspergillus*, and *Monascus*. It inhibits testosterone production and induces caspase-mediated apoptosis in leydig cells, increases generation of ROS and superoxide anions, and causes malformations, edema, and red cell accumulation in embryos.

Wu TS, Yang JJ, Yu FY, et al. Cardiotoxicity of mycotoxin citrinin and involvement of microRNA-138 in zebrafish embryos. Toxicol Sci. 2013 Dec;136(2):402-12. PMID: 24052562.

Liu S, Wang D, Zhang J, et al. Citrinin reduces testosterone secretion by inducing apoptosis in rat Leydig cells. Toxicol In Vitro. 2012 Sep;26(6):856-61. PMID: 22564900.

Flajs D, Peraica M. Toxicological properties of citrinin. Arh Hig Rada Toksikol. 2009 Dec;60(4):457-64. PMID: 20061247.

C3578

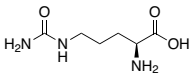

L-Citrulline

1 g
5 g
25 g
100 g

$C_6H_{13}N_3O_3$ FW: 175.19 [372-75-8] ≥98%

By product of L-arginine metabolism also found in watermelon. It decreases uterine contractile force, reverses NOS inhibitor-induced neurogenic vasodilation, and inhibits lipid peroxidation.

Munglue P, Eumkep G, Wray S, et al. The effects of watermelon (Citrullus lanatus) extracts and L-citrulline on rat uterine contractility. Reprod Sci. 2013 Apr;20(4):437-48. PMID: 22991380.

Gou L, Zhang L, Yin C, et al. Protective effect of L-citrulline against acute gastric mucosal lesions induced by ischemia-reperfusion in rats. Can J Physiol Pharmacol. 2011 May;89(5):317-27. PMID: 21619416.

Lee TJ, Sarwinski S, Ishine T, et al. Inhibition of cerebral neurogenic vasodilation by L-glutamine and nitric oxide synthase inhibitors and its reversal by L-citrulline. J Pharmacol Exp Ther. 1996 Feb;276(2):353-8. PMID: 8632296.

C4000

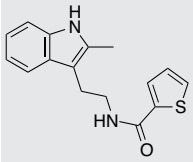

CK-636

NEW

5 mg
25 mg

CK-0944636

$C_{16}H_{16}N_2OS$ FW: 284.38 [442632-72-6] ≥98%

Actin-related protein 2/3 inhibitor that suppresses the formation of lamellipodia and cellular movement. It inhibits the production of tight junctions, cell-cell adhesion, and epidermal differentiation.

Zhou K, Muroyama A, Underwood J, et al. Actin-related protein2/3 complex regulates tight junctions and terminal differentiation to promote epidermal barrier formation. Proc Natl Acad Sci U S A. 2013 Oct 1;110(40):E3820-9. PMID: 24043783.

Kwon KW, Park H, Doh J. Migration of T cells on surfaces containing complex nanotopography. PLoS One. 2013 Sep 12;8(9):e73960. PMID: 24069255.

Nolen BJ, Tomasevic N, Russell A, et al. Characterization of two classes of small molecule inhibitors of Arp2/3 complex. Nature. 2009 Aug 20;460(7258):1031-4. PMID: 19648907.

C4274

H-Leu-Gln-Asn-Arg-Arg-Gly-Leu-Asp-Leu-Leu-Phe-Leu-Lys-Glu-Gly-Gly-Leu-OH

CKS-17

0.5 mg
1 mg
2.5 mg

$C_{87}H_{148}N_{26}O_{24}$ FW: 1942.31 [99273-04-8] ≥95%

Synthetic retroviral envelope protein sequence analog. It inhibits Th1-centric immune responses.

Haraguchi S, Good RA, Day-Good NK. A potent immunosuppressive retroviral peptide: cytokine patterns and signaling pathways. Immunol Res. 2008;41(1):46-55. PMID: 18506644.

Fan Tx, Day NK, Luangwedchakarn V, et al. The phosphorylation of phospholipase C-gamma1, Raf-1, MEK, and ERK1/2 induced by a conserved retroviral peptide. Peptides. 2005 Nov;26(11):2165-74. PMID: 15978701.

C4402

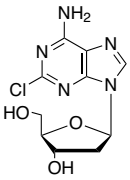

Cladribine

2-CdA; 2-Chlorodeoxyadenosine

$C_{10}H_{12}ClN_5O_3$ FW: 285.69 [4291-63-8] ≥98%

5 mg
10 mg
25 mg

Deoxyadenosine analog, DNA chain terminator, and inhibitor of ribonucleotide reductase and DNA polymerase used to treat hairy cell leukemia. It induces apoptosis in monocyte-derived dendritic cells and decreases levels of circulating B and T lymphocytes.

Singh V, Prajeeth CK, Gudi V, et al. 2-Chlorodeoxyadenosine (cladribine) induces apoptosis in human monocyte-derived dendritic cells. Clin Exp Immunol. 2013 Aug;173(2):288-97. PMID: 23607690.

Comi G, Hartung HP, Kurukulasuriya NC, et al. Cladribine tablets for the treatment of relapsing-remitting multiple sclerosis. Expert Opin Pharmacother. 2013 Jan;14(1):123-36. PMID: 23256518.

C4502

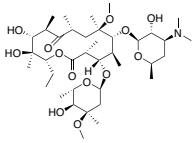

Clarithromycin

$C_{38}H_{69}NO_{13}$ FW: 747.95 [81103-11-9] ≥95%

100 mg
250 mg
1 g

Protein translation inhibitor used to treat respiratory infections. It is primarily effective against gram positive bacteria and *Helicobacter pylori*.

Cobos-Trigueros N, Ateka O, Pitart C, et al. Macrolides and ketolides. Enferm Infecc Microbiol Clin. 2009 Aug-Sep;27(7):412-8. PMID: 19625112.

Hao Q, Li Y, Zhang ZJ, et al. New mutation points in 23S rRNA gene associated with *Helicobacter pylori* resistance to clarithromycin in northeast China. World J Gastroenterol. 2004 Apr 1;10(7):1075-7. PMID: 15052698.

C4417

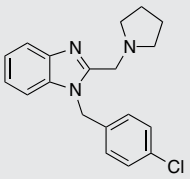

Clemizole

NEW

$C_{19}H_{20}ClN_3$ FW: 325.84 [442-52-4] ≥98%

5 mg
10 mg
25 mg

Inhibitor of NS4B, H1 histamine receptors, and TRPC5 channels. It suppresses replication of hepatitis C virus, decreases convulsive behaviors, and limits histamine-induced inflammation and allergy responses.

Richter JM, Schaefer M, Hill K. Clemizole hydrochloride is a novel and potent inhibitor of transient receptor potential channel TRPC5. Mol Pharmacol. 2014 Nov;86(5):514-21. PMID: 25140002.

Baraban SC, Dinday MT, Hortopan GA. Drug screening in Scn1a zebrafish mutant identifies clemizole as a potential Dravet syndrome treatment. Nat Commun. 2013;4:2410. PMID: 24002024.

Einav S, Sobol HD, Gehrig E, et al. The hepatitis C virus (HCV) NS4B RNA binding inhibitor clemizole is highly synergistic with HCV protease inhibitors. J Infect Dis. 2010 Jul 1;202(1):65-74. PMID: 20486856.

C4418

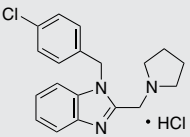

Clemizole Hydrochloride

NEW

$C_{19}H_{20}ClN_3 \bullet HCl$ FW: 362.3 [1163-36-6] ≥98%

5 mg
25 mg

Inhibitor of histamine H1 receptors, NS4B, and TRPC5 channels. It suppresses HCV replication and prevents the development of seizures.

Richter JM, Schaefer M, Hill K. Clemizole hydrochloride is a novel and potent inhibitor of transient receptor potential channel TRPC5. Mol Pharmacol. 2014 Nov;86(5):514-21. PMID: 25140002.

Baraban SC, Dinday MT, Hortopan GA. Drug screening in Scn1a zebrafish mutant identifies clemizole as a potential Dravet syndrome treatment. Nat Commun. 2013;4:2410. PMID: 24002024.

C4517

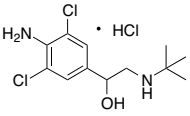

Clenbuterol Hydrochloride

$C_{12}H_{18}Cl_2N_2O \bullet HCl$ FW: 313.65 [21898-19-1] ≥98%

25 mg
100 mg
250 mg

β2-Adrenergic receptor agonist used to treat asthma. It also decreases adipose cell size and increases muscle fiber size, induces hypertrophy in skeletal muscle, and kainic acid-induced apoptosis of hippocampal neurons.

Li Y, He J, Sui S, et al. Clenbuterol upregulates histone demethylase JHDM2a via the β2-adrenoceptor/cAMP/PKA/p-CREB signaling pathway. Cell Signal. 2012 Dec;24(12):2297-306. PMID: 22820505.

Abo T, Iida RH, Kaneko S, et al. IGF and myostatin pathways are respectively induced during the earlier and the later stages of skeletal muscle hypertrophy induced by clenbuterol, a β2-adrenergic agonist. Cell Biochem Funct. 2012 Dec;30(8):671-6. PMID: 22696074.

C4510

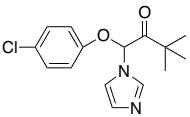

Climbazole

$C_{15}H_{17}ClN_2O_2$ FW: 292.76 [38083-17-9] ≥98%

5 g
10 g
25 g

14-α Demethylase inhibitor that inhibits ergosterol synthesis and fungal cell wall formation. It is used to treat dandruff and eczema as it displays activity against *Malassezia*.

Turner GA, Matheson JR, Li GZ, et al. Enhanced efficacy and sensory properties of an anti-dandruff shampoo containing zinc pyrithione and climbazole. Int J Cosmet Sci. 2013 Feb;35(1):78-83. PMID: 22970742.

Schmidt A. In vitro activity of climbazole, clotrimazole and silver-sulphadiazine against isolates of *Malassezia* pachydermatis. Zentralbl Veterinarmed B. 1997 Jun;44(4):193-7. PMID: 9230670.

C4535

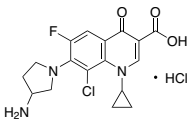

Clinafloxacin Hydrochloride

AM-1091; CI-960; PD-12739

$C_{17}H_{17}ClFN_3O_3 \cdot HCl$ FW: 402.24 [105956-99-8] ≥98%

100 mg
250 mg
1 g

Topoisomerase IV and bacterial DNA gyrase inhibitor used to treat bacterial respiratory infections. It inhibits growth of *Actinobacillus*, *Pasturella*, *Mannheima*, and *Histophilus*.

Sweeney MT, Quesnell R, Tiwari R, et al. In vitro activity and rodent efficacy of clinafloxacin for bovine and swine respiratory disease. Front Microbiol. 2013 Jun 14;4:154. PMID: 23785362.

Ball P, Fernald A, Tillotson G. Therapeutic advances of new fluoroquinolones. Expert Opin Investig Drugs. 1998 May;7(5):761-83. PMID: 15991967.

C4532

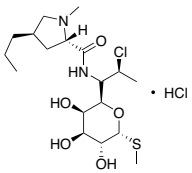

Clindamycin Hydrochloride

7(S)-Chloro-7-deoxylincomycin hydrochloride

$C_{18}H_{34}Cl_2N_2O_5S \cdot HCl$ FW: 461.44 [21462-39-5] ≥87%

10 mg
50 mg
100 mg

Ribosomal translocation and protein synthesis inhibitor that displays efficacy against MRSA. It is also occasionally used to treat *Plasmodium* infection.

Takem EN, D'Alessandro U. Malaria in pregnancy. Mediterr J Hematol Infect Dis. 2013;5(1):e2013010. PMID: 23350023.

Sireesha P, Setty CR. Detection of various types of resistance patterns and their correlation with minimal inhibitory concentrations against clindamycin among methicillin-resistant *Staphylococcus aureus* isolates. Indian J Med Microbiol. 2012 Apr-Jun;30(2):165-9. PMID: 22664431.

C4534

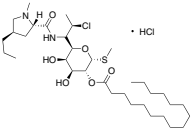

Clindamycin Palmitate Hydrochloride

$C_{34}H_{63}ClN_2O_6S \cdot HCl$ FW: 699.85 [25507-04-4] ≥98%

10 mg
50 mg
100 mg

Ribosomal translocation and protein synthesis inhibitor that displays efficacy against MRSA. It is also occasionally used to treat *Plasmodium* infection.

Takem EN, D'Alessandro U. Malaria in pregnancy. Mediterr J Hematol Infect Dis. 2013;5(1):e2013010. PMID: 23350023.

Sireesha P, Setty CR. Detection of various types of resistance patterns and their correlation with minimal inhibitory concentrations against clindamycin among methicillin-resistant *Staphylococcus aureus* isolates. Indian J Med Microbiol. 2012 Apr-Jun;30(2):165-9. PMID: 22664431.

C4533

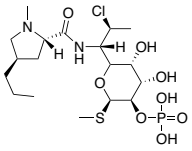

Clindamycin Phosphate

7(S)-Chloro-7-deoxylincomycin 2-phosphate

$C_{18}H_{34}ClN_2O_8PS$ FW: 504.96 [24729-96-2] ≥95%

10 mg
50 mg
100 mg

Ribosomal translocation and protein synthesis inhibitor that displays efficacy against MRSA. It is also occasionally used to treat *Plasmodium* infection.

Takem EN, D'Alessandro U. Malaria in pregnancy. Mediterr J Hematol Infect Dis. 2013;5(1):e2013010. PMID: 23350023.

C4659

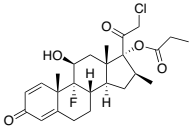

Clobetasol Propionate

$C_{25}H_{32}ClFO_5$ FW: 466.98 [25122-46-7] ≥98%

100 mg
500 mg
1 g

Glucocorticoid receptor agonist used to treat eczema, psoriasis, contact dermatitis, and several autoimmune diseases. It also inhibits TNF-α- and CD40L-induced activation of NF-ϰB.

Cechin SR, Buchwald P. Effects of representative glucocorticoids on TNFα- and CD40L-induced NF-ϰB activation in sensor cells. Steroids. 2014 Jul;85:36-43. PMID: 24747770.

Lenane P, Macarthur C, Parkin PC, et al. Clobetasol propionate, 0.05%, vs hydrocortisone, 1%, for alopecia areata in children: a randomized clinical trial. JAMA Dermatol. 2014 Jan;150(1):47-50. PMID: 24226568.

C3449

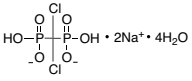

Clodronate Disodium Tetrahydrate

$CH_2Cl_2Na_2O_6P_2 \cdot 4H_2O$ FW: 360.92 [22560-50-5] ≥98%

10 mg
50 mg
100 mg

Mitochondrial ATP/ADP translocase inhibitor used to prevent bone resorption. It generates a non-hydrolysable β-γ ATP analog that prevents mitochondrial oxygen consumption and function and induces apoptosis in osteoblasts. It also decreases severity of experimental autoimmune neuritis and inhibits proliferation of renal cell carcinoma cells.

Katzav A, Bina H, Aronovich R, et al. Treatment for experimental autoimmune neuritis with clodronate (Bonefos). Immunol Res. 2013 Jul;56(2-3):334-40. PMID: 23579773.

Soltau J, Zirrgiebel U, Esser N, et al. Antitumoral and antiangiogenic efficacy of bisphosphonates in vitro and in a murine RENCA model. Anticancer Res. 2008 Mar-Apr;28(2A):933-41. PMID: 18507039.

C4646 Clofarabine

10 mg
25 mg
100 mg

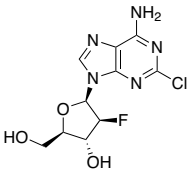

$C_{10}H_{11}ClFN_5O_3$ FW: 303.68 [123318-82-1] ≥98%

Adenosine analog, DNA chain terminator, ribonucleotide reductase and DNA polymerase inhibitor, and adenosine A1/2/3 receptor modulator used to treat acute lymphoblastic leukemia.

Robak P, Robak T. Older and new purine nucleoside analogs for patients with acute leukemias. Cancer Treat Rev. 2013 Dec;39(8):851-61. PMID: 23566572.

Jensen K, Johnson LA, Jacobson PA, et al. Cytotoxic purine nucleoside analogues bind to A1, A2A, and A3 adenosine receptors. Naunyn Schmiedebergs Arch Pharmacol. 2012 May;385(5):519-25. PMID: 22249336.

C4557 Clofibrate

1 g
5 g

Chlorophenoxyisobutyrate; CPIB

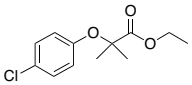

$C_{12}H_{15}ClO_3$ FW: 242.7 [637-07-0] ≥98%

PPARα agonist used to lower cholesterol levels. It also induces cell cycle arrest and differentiation in leukemia cells.

Laurora S, Pizzimenti S, Briatore F, et al. Peroxisome proliferator-activated receptor ligands affect growth-related gene expression in human leukemic cells. J Pharmacol Exp Ther. 2003 Jun;305(3):932-42. PMID: 12649303.

Nicholls-Grzemski FA, Calder IC, Priestly BG, et al. Clofibrate-induced in vitro hepatoprotection against acetaminophen is not due to altered glutathione homeostasis. Toxicol Sci. 2000 Jul;56(1):220-8. PMID: 10869471.

C4556 Clofibric Acid

10 g
50 g

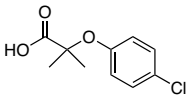

$C_{10}H_{11}ClO_3$ FW: 214.65 [882-09-7] ≥98%

PPARα agonist, auxin inhibitor and metabolite of clofibrate used as a plant growth regulator. It also decreases production of cholesterol and activity of HMG-CoA reductase and ACAT. It also suppresses microvessel growth in ovarian cancer models.

Yokoyama Y, Xin B, Shigeto T, et al. Clofibric acid, a peroxisome proliferator-activated receptor alpha ligand, inhibits growth of human ovarian cancer. Mol Cancer Ther. 2007 Apr;6(4):1379-86. PMID: 17431116.

C4559 Clomiphene Citrate

1 g
5 g
10 g

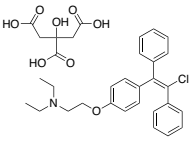

$C_{26}H_{28}ClNO \bullet C_6H_8O_7$ FW: 598.09 [50-41-9] ≥98%

SERM and FIASMA used for in vitro fertilization. It inhibits estrogen receptors in the hypothalamus, upregulating release of LH and FSH.

Amita M, Takahashi T, Tsutsumi S, et al. Molecular mechanism of the inhibition of estradiol-induced endometrial epithelial cell proliferation by clomiphene citrate. Endocrinology. 2010 Jan;151(1):394-405. PMID: 19934375.

Shoham Z, Schacter M, Loumaye E, et al. The luteinizing hormone surge--the final stage in ovulation induction: modern aspects of ovulation triggering. Fertil Steril. 1995 Aug;64(2):237-51. PMID: 7615097.

C4457 Clomipramine Hydrochloride

1 g
5 g

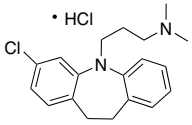

$C_{19}H_{23}ClN_2 \bullet HCl$ FW: 351.32 [17321-77-6] ≥98%

Inhibitor of mAChRs, 5-HT2/3/6/7 receptors, α1/2-adrenergic receptors, SERT, NET, and hERG K^+ and L-type Ca^{2+} channels used to treat depression, anxiety, narcolepsy, and obsessive-compulsive disorder. It also acts as a FIASMA, decreases thermal and mechanical pain, and may prolong the cardiac QT interval.

Kostadinov ID, Delev DP, Kostadinova II. Antinociceptive effect of clomipramine through interaction with serotonin 5-HT2 and 5-HT3 receptor subtypes. Folia Med (Plovdiv). 2012 Oct-Dec;54(4):69-77. PMID: 23441472.

Jo SH, Hong HK, Chong SH, et al. Clomipramine block of the hERG K^+ channel: accessibility to F656 and Y652. Eur J Pharmacol. 2008 Sep 11;592(1-3):19-25. PMID: 18634780.

C4558 Clonidine Hydrochloride

250 mg
1 g

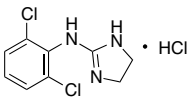

$C_9H_9Cl_2N_3 \bullet HCl$ FW: 266.55 [4205-91-8] ≥98%

α2-Adrenergic receptor and imidazoline 1 receptor agonist and $Na_v1.7$ Na^+ channel blocker used to treat mood disorders, migraines, and hypertension. It also inhibits long term potentiation, decreases excitatory postsynaptic potentials, suppresses mechanical and thermal pain, and induces downstream activation of histamine H2 receptors.

Li CJ, Zhou M, Li HG, et al. Clonidine suppresses the induction of long-term potentiation by inhibiting HCN channels at the schaffer collateral-CA1 synapse in anesthetized adult rats. Cell Mol Neurobiol. 2013 Nov;33(8):1075-86. PMID: 23975095.

Maruta T, Nemoto T, Satoh S, et al. Dexmedetomidine and clonidine inhibit the function of Na(v)1.7 independent of α(2)-adrenoceptor in adrenal chromaffin cells. J Anesth. 2011 Aug;25(4):549-57. PMID: 21607767.

C4658 Clopidogrel Sulfate

500 mg
1 g
5 g

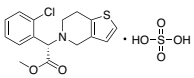

$C_{16}H_{16}ClNO_2S \bullet H_2SO_4$ FW: 419.9 [135046-48-9] ≥98%

P2Y12 receptor antagonist used to treat coronary artery disease and peripheral vascular disease and to prevent myocardial infarction and stroke.

Thomas MR, Storey RF. Impact of aspirin dosing on the effects of P2Y12 inhibition in patients with acute coronary syndromes. J Cardiovasc Transl Res. 2014 Feb;7(1):19-28. PMID: 24309957.

Ferri N, Corsini A, Bellosta S. Pharmacology of the new P2Y12 receptor inhibitors: insights on pharmacokinetic and pharmacodynamic properties. Drugs. 2013 Oct;73(15):1681-709. PMID: 24114622.

C4656 Clopidol

1 g
5 g
25 g

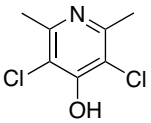

$C_7H_7Cl_2NO$ FW: 192.04 [2971-90-6] ≥98%

Coccidiostat used to treat parasite infections in veterinary medicine.

Gerhold RW, Fuller AL, Lollis L, et al. The efficacy of anticoccidial products against *Eimeria* spp. in northern bobwhites. Avian Dis. 2011 Mar;55(1):59-64. PMID: 21500637.

Arakawa A, Tanaka Y, Baba E, et al. Effects of clopidol on sporulation and infectivity of *Eimeria* tenella oocysts. Vet Parasitol. 1991 Jan;38(1):55-60. PMID: 2024430.

C4758 Closantel Sodium

1 g
5 g
25 g

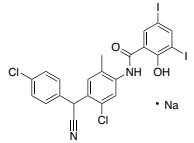

$C_{22}H_{14}Cl_2I_2N_2O_2Na$ FW: 686.06 [61438-64-0] ≥98%

Protonophore and chitinase OvCHT1 inhibitor that inhibits nematode development and parasite survival.

Gooyit M, Tricoche N, Lustigman S, et al. Dual Protonophore-Chitinase Inhibitors Dramatically Affect O. volvulus Molting. J Med Chem. 2014 Jun 20. [Epub ahead of print]. PMID: 24918716.

C4657 Clotrimazole

5 g
10 g
25 g

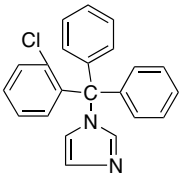

Mycosporin

$C_{22}H_{17}ClN_2$ FW: 344.84 [23593-75-1] ≥97%

Inhibitor of 14-α demethylase, H^+/K^+ ATPase, and Na^+/K^+ ATPase that prevents ergosterol synthesis and fungal cell wall formation and is used to treat fungal infections. It also induces cell cycle arrest and apoptosis in cancer cells and prevents heme degradation and *Plasmodium* growth.

Wang J, Jia L, Kuang Z, et al. The in vitro and in vivo antitumor effects of clotrimazole on oral squamous cell carcinoma. PLoS One. 2014 Jun 3;9(6):e98885. PMID: 24892421.

Witzke A, Lindner K, Munson K, et al. Inhibition of the gastric H,K-ATPase by clotrimazole. Biochemistry. 2010 Jun 1;49(21):4524-32. PMID: 20423050.

Huy NT, Takano R, Hara S, et al. Enhancement of heme-induced membrane damage by the anti-malarial clotrimazole: the role of colloid-osmotic forces. Biol Pharm Bull. 2004 Mar;27(3):361-5. PMID: 14993803.

C4756 Cloxacillin Sodium Monohydrate

1 g
5 g
25 g

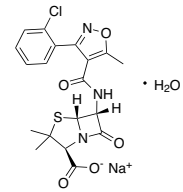

Methocillin-S

$C_{19}H_{18}ClN_3NaO_5S \bullet H_2O$ FW: 475.88 [7081-44-9] ≥98%

Penicillin binding protein inhibitor that prevents cell wall synthesis and is especially active versus *Staphylococcus*.

Sawai T, Yamaguchi A. Mechanism of beta-lactamase inhibition: differences between sulbactam and other inhibitors. Diagn Microbiol Infect Dis. 1989 Jul-Aug;12(4 Suppl):121S-129S. PMID: 2591172.

Barza M. Antimicrobial spectrum, pharmacology and therapeutic use of antibiotics. Part 2: penicillins. Am J Hosp Pharm. 1977 Jan;34(1):57-67. PMID: 318800.

C4757 Clozapine

25 mg
100 mg
250 mg

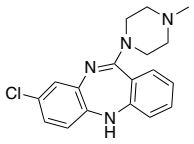

$C_{18}H_{19}ClN_4$ FW: 326.82 [5786-21-0] ≥97%

M4 mAChR agonist, 5-HT1A receptor partial agonist, and inhibitor of M1/2/3/5 mAChRs, dopamine D2 receptors, and $K_v1.1$ K^+ channels used to treat mood disorders. It also prolongs the cardiac QT interval, induces granulocytosis, and potentiates GABAergic neurotransmission.

Hill AP, Perrin MJ, Heide J, et al. Kinetics of drug interaction with the Kv11.1 potassium channel. Mol Pharmacol. 2014 May;85(5):769-76. PMID: 24586056.

Tanahashi S, Yamamura S, Nakagawa M, et al. Clozapine, but not haloperidol, enhances glial D-serine and L-glutamate release in rat frontal cortex and primary cultured astrocytes. Br J Pharmacol. 2012 Mar;165(5):1543-55. PMID: 21880034.

Wu Y, Blichowski M, Daskalakis ZJ, et al. Evidence that clozapine directly interacts on the GABAB receptor. Neuroreport. 2011 Sep 14;22(13):637-41. PMID: 21753741.

C4759

Clozapine *N*-oxide

5 mg
25 mg

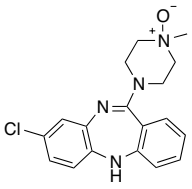

CNO

$C_{18}H_{19}ClN_4O$ FW: 342.82 [34233-69-7] ≥98%

Pharmacologically inert clozapine analog that activates specialized GPCRs.

Li JH, Jain S, McMillin SM, et al. A novel experimental strategy to assess the metabolic effects of selective activation of a G(q)-coupled receptor in hepatocytes in vivo. Endocrinology. 2013 Oct;154(10):3539-51. PMID: 23861369.

Wess J, Nakajima K, Jain S. Novel designer receptors to probe GPCR signaling and physiology. Trends Pharmacol Sci. 2013 Jul;34(7):385-92. PMID: 23769625.

Farrell MS, Pei Y, Wan Y, et al. A Gαs DREADD mouse for selective modulation of cAMP production in striatopallidal neurons. Neuropsychopharmacology. 2013 Apr;38(5):854-62. PMID: 23303063.

C4800

CM346 Hydrochloride

NEW

5 mg
25 mg

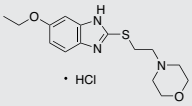

Obenoxazine

$C_{15}H_{21}N_3O_2S \bullet HCl$ FW: 343.87 [173352-39-1] ≥98%

Potential anxiolytic.

C5196

C-Myc Peptide

1 mg
2 mg
5 mg

H-Glu-Gln-Lys-Leu-Ile-Ser-Glu-Glu-Asp-Leu-OH

$C_{51}H_{86}N_{12}O_1$ FW: 1203.32 ≥95%

C-Myc fragment, PAC1 receptor agonist, and CK2 activator used in protein activity measurement assays.

Yaylim I, Ozkan NE, Isitmangil T, et al. CK2 enzyme affinity against c-myc 424-434 substrate in human lung cancer tissue. Asian Pac J Cancer Prev. 2012;13(10):5233-6. PMID: 23244141.

Smith WC, Dinculescu A, Peterson JJ, et al. The surface of visual arrestin that binds to rhodopsin. Mol Vis. 2004 Jun 15;10:392-8. PMID: 15215746.

C5600

CO-1686

NEW

1 mg
5 mg
10 mg

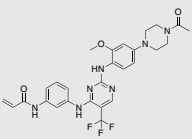

AVL-301; Rociletinib; CNX-419

$C_{27}H_{28}F_3N_7O_3$ FW: 555.55 [1374640-70-6] ≥98%

Inhibitor of WT and T790M EGFR. It sensitizes cancer cells to other chemotherapeutics and induces tumor regression in models of non-small cell lung cancer.

Walter AO, Sjin RT, Haringsma HJ, et al. Discovery of a mutant-selective covalent inhibitor of EGFR that overcomes T790M-mediated resistance in NSCLC. Cancer Discov. 2013 Dec;3(12):1404-15. PMID: 24065731.

Yu HA, Riely GJ. Second-generation epidermal growth factor receptor tyrosine kinase inhibitors in lung cancers. J Natl Compr Canc Netw. 2013 Feb 1;11(2):161-9. PMID: 23411383.

C5618

Coelenterazine, natural

1 mg
5 mg

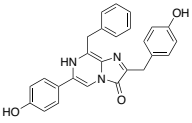

$C_{26}H_{21}N_3O_3$ FW: 423.46 [55779-48-1] ≥98%

Light-emitting luciferin analog found in aquatic organisms used to measure cell activity. It is one of two components of aequorin, a calcium-sensitive photoprotein found in bioluminescent jellyfish. It oxidizes in organic solvents such as DMSO.

Schill WB. Immunofluorescent localization of acrosin in spermatozoa by boar acrosin antibodies. Naturwissenschaften. 1975 Nov;62(11):540-1. PMID: 765844.

Shimomura O, Johnson FH. Chemical nature of bioluminescence systems in coelenterates. Proc Natl Acad Sci U S A. 1975 Apr;72(4):1546-9. PMID: 236561.

C5645

Colchicine, 97%

500 mg
1 g

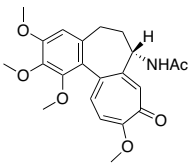

$C_{22}H_{25}NO_6$ FW: 399.44 [64-86-8] ≥97%

Microtubule polymerization inhibitor found in *Colchicum* that is used to treat gout. It also inhibits neutrophil motility, inflammasome activation, cytokine generation, and chemotaxis.

Dalbeth N, Lauterio TJ, Wolfe HR. Mechanism of Action of Colchicine in the Treatment of Gout. Clin Ther. 2014 Aug 21. [Epub ahead of print]. PMID: 25151572.

Ching JK, Ju JS, Pittman SK, et al. Increased autophagy accelerates colchicine-induced muscle toxicity. Autophagy. 2013 Dec;9(12):2115-25. PMID: 24184927.

C5647

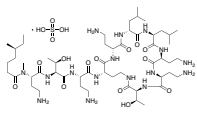

Colistin Sulphate

Belcomycin; Polymixin E

$C_{45}H_{85}N_{13}O_{10} \bullet H_2O_4S$ FW: 1267.55 [1264-72-8]

NADH quinone oxidoreductase inhibitor that induces formation of pores in membranes of gram negative bacteria. It is highly neurotoxic and nephrotoxic.

Deris ZZ, Akter J, Sivanesan S, et al. A secondary mode of action of polymyxins against Gram-negative bacteria involves the inhibition of NADH-quinone oxidoreductase activity. J Antibiot (Tokyo). 2014 Feb;67(2):147-51. PMID: 24169795.

Dai C, Zhang D, Gao R, et al. In vitro toxicity of colistin on primary chick cortex neurons and its potential mechanism. Environ Toxicol Pharmacol. 2013 Sep;36(2):659-66. PMID: 23892071.

Manning AJ, Kuehn MJ. Contribution of bacterial outer membrane vesicles to innate bacterial defense. BMC Microbiol. 2011 Dec 1;11:258. PMID: 22133164.

100 mg
500 mg
1 g
5 g

C5646

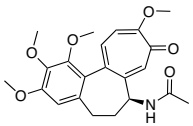

Collagen Binding Fragment

$C_{52}H_{75}N_{14}O_{20}S$ FW: 1248.32 ≥95%

Fibronectin fragment used as a negative control to study fibronectin effects on cell migration and gastrulation.

Boucaut JC, Darribère T, Poole TJ, et al. Biologically active synthetic peptides as probes of embryonic development: a competitive peptide inhibitor of fibronectin function inhibits gastrulation in amphibian embryos and neural crest cell migration in avian embryos. J Cell Biol. 1984 Nov;99(5):1822-30. PMID: 6490722.

1 mg
2 mg
5 mg

C5654

Concanavalin A

ConA

[11028-71-0] ≥98%

Plant mitogen found in *Canavelia* that binds α-D-mannosyl and α-D-glucosyl residues and is used to study cell adhesion. It induces fibrosis and stimulates autophagy in hepatoma models.

Wan Y, Tang MH, Chen XC, et al. Inhibitory effect of liposomal quercetin on acute hepatitis and hepatic fibrosis induced by concanavalin A. Braz J Med Biol Res. 2014 Aug;47(8):655-61. PMID: 25098714.

Lei HY, Chang CP. Lectin of Concanavalin A as an anti-hepatoma therapeutic agent. J Biomed Sci. 2009 Jan 19;16:10. PMID: 19272170.

50 mg
250 mg
500 mg
1 g

C5655

α-Conotoxin GI

H-Glu-Cys-Cys-Asn-Pro-Ala-Cys-Gly-Arg-His-Tyr-Ser-Cys-NH_2
(Cys2-Cys7, Cys3-Cys13)

$C_{55}H_{76}N_{20}O_{18}S_4$ FW: 1433.63 ≥95%

Toxin and nAChR inhibitor found in *Conus* snails. It decreases peak amplitude and induces tetanic and train-of-four fades, causing neuromuscular junction block.

Hann RM, Pagán OR, Gregory LM, et al. The 9-arginine residue of alpha-conotoxin GI is responsible for its selective high affinity for the alphagamma agonist site on the electric organ acetylcholine receptor. Biochemistry. 1997 Jul 22;36(29):9051-6. PMID: 9220994.

Blount K, Johnson A, Prior C, et al. alpha-Conotoxin GI produces tetanic fade at the rat neuromuscular junction. Toxicon. 1992 Aug;30(8):835-42. PMID: 1355934.

0.5 mg
1 mg
2.5 mg

C5656

α-Conotoxin IMI

H-Gly-Cys-Cys-Ser-Asp-Pro-Arg-Cys-Ala-Trp-Arg-Cys-NH_2
(Cys2-Cys8, Cys3-Cys12)

$C_{52}H_{74}N_{20}O_{15}S_4$ FW: 1347.58 ≥95%

Toxin and α7 nAChR inhibitor found in *Conus* snails. It disrupts motor coordination.

Yu R, Craik DJ, Kaas Q. Blockade of neuronal α7-nAChR by α-conotoxin ImI explained by computational scanning and energy calculations. PLoS Comput Biol. 2011 Mar;7(3):e1002011. PMID: 21390272.

Wagenaar DA, Gonzalez R, Ries DC, et al. Alpha-conotoxin ImI disrupts central control of swimming in the medicinal leech. Neurosci Lett. 2010 Nov 26;485(3):151-6. PMID: 20833225.

0.5 mg
1 mg
2.5 mg

C5662

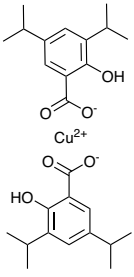

Copper Bis-3,5-diisopropylsalicylate

$C_{26}H_{34}O_6Cu$ FW: 506.11 [21246-18-4] ≥98%

Antioxidant that decreases hyperglycemia and DNA damage in diabetes models, suppresses lung fibrosis development, and inhibits mammary tumor growth.

Qazzaz M, Abdul-Ghani R, Metani M, et al. The antioxidant activity of copper(II) (3,5-diisopropyl salicylate)4 and its protective effect against streptozotocin-induced diabetes mellitus in rats. Biol Trace Elem Res. 2013 Jul;154(1):88-96. PMID: 23677849.

Baquial JG, Sorenson JR. Down-regulation of NADPH-diaphorase (nitric oxide synthase) may account for the pharmacological activities of Cu(II)2 (3,5-diisopropylsalicylate)4. J Inorg Biochem. 1995 Nov 1;60(2):133-48. Erratum in: J Inorg Biochem. 1997 Nov 15;68(3):233. PMID: 8530918.

Denis M. Antioxidant therapy partially blocks immune-induced lung fibrosis. Inflammation. 1995 Apr;19(2):207-19. PMID: 7601506.

1 g
5 g

C5863

Coptisine Chloride

NEW

1 mg
5 mg

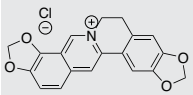

$C_{19}H_{14}ClNO_4$ FW: 355.77 [6020-18-4] ≥98%

MAO-A inhibitor found in a variety of plant sources. It attenuates mitochondrial respiratory dysfunction, inhibits expression of RhoA and ROCK, suppresses proliferation of hepatoma and leukemia cells, and decreases myocardial apoptosis.

Guo J, Wang SB, Yuan TY, et al. Coptisine protects rat heart against myocardial ischemia/reperfusion injury by suppressing myocardial apoptosis and inflammation. Atherosclerosis. 2013 Dec;231(2):384-91. PMID: 24267256.

Gong LL, Fang LH, Wang SB, et al. Coptisine exert cardioprotective effect through anti-oxidative and inhibition of RhoA/Rho kinase pathway on isoproterenol-induced myocardial infarction in rats. Atherosclerosis. 2012 May;222(1):50-8. PMID: 22387061.

Suzuki H, Tanabe H, Mizukami H, et al. Differential gene expression in rat vascular smooth muscle cells following treatment with coptisine exerts a selective antiproliferative effect. J Nat Prod. 2011 Apr 25;74(4):634-8. PMID: 21401114.

C5768

Corazonin

1 mg
2 mg
5 mg

pGlu-Thr-Phe-Gln-Tyr-Ser-Arg-Gly-Trp-Thr-Asn-NH_2

$C_{62}H_{86}N_{18}O_{19}$ FW: 1369.49 [122984-73-0] ≥95%

Found in insects. It stimulates cardiovascular function and promotes transfer of sperm and mating behavior.

Tayler TD, Pacheco DA, Hergarden AC, et al. A neuropeptide circuit that coordinates sperm transfer and copulation duration in *Drosophila*. Proc Natl Acad Sci U S A. 2012 Dec 11;109(50):20697-702. PMID: 23197833.

Hillyer JF, Estévez-Lao TY, Funkhouser LJ, et al. *Anopheles* gambiae corazonin: gene structure, expression and effect on mosquito heart physiology. Insect Mol Biol. 2012 Jun;21(3):343-55. PMID: 22404523.

C5968

Cordycepin

10 mg
25 mg
100 mg

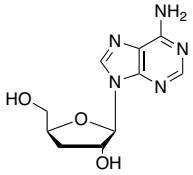

$C_{10}H_{13}N_5O_3$ FW: 251.24 [73-03-0] ≥98%

Deoxyadenosine analog and RNA and DNA synthesis inhibitor found in *Cordyceps*. It induces double-stranded DNA breaks and apoptosis in cancer cells, decreases the amplitude of excitatory presynaptic membrane potentials, indirectly inhibits AMPA receptor- and NMDA receptor-mediated responses, and terminates RNA chains in cells infected with picornavirus.

Yao LH, Huang JN, Li CH, et al. Cordycepin suppresses excitatory synaptic transmission in rat hippocampal slices via a presynaptic mechanism. CNS Neurosci Ther. 2013 Apr;19(4):216-21. PMID: 23419191.

Lee HJ, Burger P, Vogel M, et al. The nucleoside antagonist cordycepin causes DNA double strand breaks in breast cancer cells. Invest New Drugs. 2012 Oct;30(5):1917-25. PMID: 22821173.

Jeong JW, Jin CY, Park C, et al. Induction of apoptosis by cordycepin via reactive oxygen species generation in human leukemia cells. Toxicol In Vitro. 2011 Jun;25(4):817-24. PMID: 21310227.

C5870

Corosolic Acid

10 mg
25 mg
100 mg

2α-Hydroxyursolic acid; Glucosol

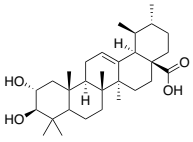

$C_{30}H_{48}O_4$ FW: 472.7 [4547-24-4] ≥98%

Found in *Lagerstroemia speciosa*. It decreases blood sugar, increases glucose uptake, induces apoptosis in lung adenocarcinoma cells, and inhibits expression of STAT3, NF-kB activity, and MCP-1.

Nho KJ, Chun JM, Kim HK. Corosolic acid induces apoptotic cell death in human lung adenocarcinoma A549 cells in vitro. Food Chem Toxicol. 2013 Jun;56:8-17. PMID: 23454206.

Horlad H, Fujiwara Y, Takemura K, et al. Corosolic acid impairs tumor development and lung metastasis by inhibiting the immunosuppressive activity of myeloid-derived suppressor cells. Mol Nutr Food Res. 2013 Jun;57(6):1046-54. PMID: 23417831.

Miura T, Takagi S, Ishida T. Management of Diabetes and Its Complications with Banaba (*Lagerstroemia speciosa* L.) and Corosolic Acid. Evid Based Complement Alternat Med. 2012;2012:871495. PMID: 23082086.

C5771

Corticosterone

100 mg
250 mg
500 mg

Kendall's compound B; Reichstein's substance H; 17-Deoxycortisol

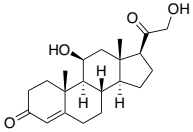

$C_{21}H_{30}O_4$ FW: 346.46 [50-22-6] ≥96%

Endogenous steroid hormone involved in immune responses, stress responses, and energy homeostasis. It activates mineralocorticoid and glucocorticoid receptors.

Angelier F, Wingfield JC. Importance of the glucocorticoid stress response in a changing world: theory, hypotheses and perspectives. Gen Comp Endocrinol. 2013 Sep 1;190:118-28. PMID: 23770214.

Silverman MN, Sternberg EM. Glucocorticoid regulation of inflammation and its functional correlates: from HPA axis to glucocorticoid receptor dysfunction. Ann N Y Acad Sci. 2012 Jul;1261:55-63. PMID: 22823394.

Williams GH. Aldosterone biosynthesis, regulation, and classical mechanism of action. Heart Fail Rev. 2005 Jan;10(1):7-13. PMID: 15947886.

C5770

Corticotropin Releasing Factor, cow

0.5 mg
1 mg
2.5 mg

H-Ser-Gln-Glu-Pro-Pro-Ile-Ser-Leu-Asp-Leu-Thr-Phe-His-Leu-Leu-Arg-Glu-Val-Leu-Glu-Met-Thr-Lys-Ala-Asp-Gln-Leu-Ala-Gln-Gln-Ala-His-Asn-Asn-Arg-Lys-Leu-Leu-Asp-Ile-Ala-NH_2

CRF; CRH

$C_{206}H_{340}N_{60}O_{63}S$ FW: 4697.44 ≥95%

Endogenous CRF agonist involved in stress response and mood. It stimulates release of cortisol, ACTH, DHEA, and β-endorphin.

Lowry CA, Moore FL. Regulation of behavioral responses by corticotropin-releasing factor. Gen Comp Endocrinol. 2006 Mar;146(1):19-27. PMID: 16426606.

Arborelius L, Owens MJ, Plotsky PM, et al. The role of corticotropin-releasing factor in depression and anxiety disorders. J Endocrinol. 1999 Jan;160(1):1-12. PMID: 9854171.

C5772

Corticotropin Releasing Factor, human/rat

0.5 mg
1 mg
2.5 mg

Ser-Glu-Glu-Pro-Pro-Ile-Ser-Leu-Asp-Leu-Thr-Phe-His-Leu-Leu-Arg-Glu-Val-Leu-Glu-Met-Ala-Arg-Ala-Glu-Gln-Leu-Ala-Gln-Gln-Ala-His-Ser-Asn-Arg-Lys-Leu-Met-Glu-Ile-Ile-NH_2

CRF; CRH

$C_{208}H_{344}N_{60}O_{63}S_2$ FW: 4757.49 [86784-80-7] ≥98%

Endogenous CRF agonist involved in stress response and mood. It stimulates release of cortisol, ACTH, DHEA, and β-endorphin.

Lowry CA, Moore FL. Regulation of behavioral responses by corticotropin-releasing factor. Gen Comp Endocrinol. 2006 Mar;146(1):19-27. PMID: 16426606.

Arborelius L, Owens MJ, Plotsky PM, et al. The role of corticotropin-releasing factor in depression and anxiety disorders. J Endocrinol. 1999 Jan;160(1):1-12. PMID: 9854171.

C5774

Corticotropin Releasing Factor, sheep

0.5 mg
1 mg
2.5 mg

H-Ser-Gln-Glu-Pro-Pro-Ile-Ser-Leu-Asp-Leu-Thr-Phe-His-Leu-Leu-Arg-Glu-Val-Leu-Glu-Met-Thr-Lys-Ala-Asp-Gln-Leu-Ala-Gln-Gln-Ala-His-Ser-Asn-Arg-Lys-Leu-Leu-Asp-Ile-Ala-NH_2

CRF; CRH

$C_{205}H_{339}N_{59}O_{63}S$ FW: 4370.41 ≥95%

Endogenous CRF agonist involved in stress response and mood. It stimulates release of cortisol, ACTH, DHEA, and β-endorphin.

Lowry CA, Moore FL. Regulation of behavioral responses by corticotropin-releasing factor. Gen Comp Endocrinol. 2006 Mar;146(1):19-27. PMID: 16426606.

Arborelius L, Owens MJ, Plotsky PM, et al. The role of corticotropin-releasing factor in depression and anxiety disorders. J Endocrinol. 1999 Jan;160(1):1-12. PMID: 9854171.

C5773

Cortistatin-14

0.5 mg
1 mg
2.5 mg

H-Pro-Cys-Lys-Asn-Phe-Phe-Trp-Lys-Thr-Phe-Ser-Ser-Cys-Lys-OH
(Disulfide Bridge Cys2-Cys13)

CST-14

$C_{81}H_{113}N_{19}O_{19}S_2$ FW: 1721.02 [186901-48-4] ≥95%

Endogenous somatostatin analog that activates somatostatin and ghrelin receptors. It also decreases seizure duration, inhibits production of IL-1β in macrophages, and suppresses carrageenan-induced edema.

Aourz N, Portelli J, Coppens J, et al. Cortistatin-14 Mediates its Anticonvulsant Effects Via sst₂ and sst₃ but Not Ghrelin Receptors. CNS Neurosci Ther. 2014 Mar 31. [Epub ahead of print]. PMID: 24685142.

Markovics A, Szoke É, Sándor K, et al. Comparison of the anti-inflammatory and anti-nociceptive effects of cortistatin-14 and somatostatin-14 in distinct in vitro and in vivo model systems. J Mol Neurosci. 2012 Jan;46(1):40-50. PMID: 21695504.

C5970

Corydaline

NEW

1 mg
5 mg

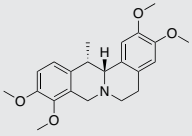

$C_{22}H_{27}NO_4$ FW: 369.45 [518-69-4] ≥95%

Found in *Corydalis*. It exhibits many activities, including increasing gastric emptying and small intestine transit speed, decreasing chemically-induced pain, and potentially suppressing mast cell-dependent smooth muscle contraction of the aorta.

Lee TH, Son M, Kim SY. Effects of corydaline from *Corydalis* tuber on gastric motor function in an animal model. Biol Pharm Bull. 2010;33(6):958-62. PMID: 20522959.

Wang C, Wang S, Fan G, et al. Screening of antinociceptive components in *Corydalis* yanhusuo W.T. Wang by comprehensive two-dimensional liquid chromatography/tandem mass spectrometry. Anal Bioanal Chem. 2010 Mar;396(5):1731-40. PMID: 20101504.

Saito SY, Tanaka M, Matsunaga K, et al. The combination of rat mast cell and rabbit aortic smooth muscle is the simple bioassay for the screening of anti-allergic ingredient from methanolic extract of *Corydalis* tuber. Biol Pharm Bull. 2004 Aug;27(8):1270-4. PMID: 15305035.

C5972

Corynoline

NEW

1 mg
5 mg

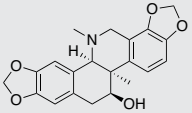

$C_{21}H_{21}NO_5$ FW: 367.4 [18797-79-0] ≥98%

AChE inhibitor found in *Corydalis*. It displays cytotoxicity in various cancer cell lines.

Choi SU, Baek NI, Kim SH, et al. Cytotoxic isoquinoline alkaloids from the aerial parts of *Corydalis* incisa. Arch Pharm Res. 2007 Feb;30(2):151-4. PMID: 17366734.

Kim DK. Inhibitory effect of corynoline isolated from the aerial parts of *Corydalis* incisa on the acetylcholinesterase. Arch Pharm Res. 2002 Dec;25(6):817-9. PMID: 12510831.

C5782

Coumarin

10 g
50 g

Tonka bean camphor

$C_9H_6O_2$ FW: 146.14 [91-64-5] ≥98%

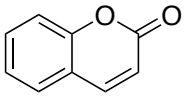

Vitamin K inhibitor and warfarin synthesis precursor found in various plants. It is commercially used in perfumes, dyes, and bio-imaging and is also used to treat edema. It stimulates macrophages to degrade extracellular albumen and increase fluid reabsorption.

Kontogiorgis C, Detsi A, Hadjipavlou-Litina D. Coumarin-based drugs: a patent review (2008 -- present). Expert Opin Ther Pat. 2012 Apr;22(4):437-54. PMID: 22475457.

Farinola N, Piller N. Pharmacogenomics: its role in re-establishing coumarin as treatment for lymphedema. Lymphat Res Biol. 2005 Summer;3(2):81-6. PMID: 16000056.

C5680

Coumestrol

10 mg
25 mg

$C_{15}H_8O_5$ FW: 268.2 [479-13-0] ≥96%

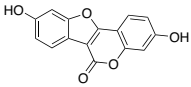

ERβ agonist and inhibitor of aromatase and 3α-HSD found in plants such as soy and clover. It decreases immobility in animals undergoing the forced swim test, suppresses pro-inflammatory cytokine release, and limits T cell differentiation and activation.

Karieb S, Fox SW. Suppression of T cell-induced osteoclast formation. Biochem Biophys Res Commun. 2013 Jul 12;436(4):619-24. PMID: 23764400.

Blomquist CH, Lima PH, Hotchkiss JR. Inhibition of 3alpha-hydroxysteroid dehydrogenase (3alpha-HSD) activity of human lung microsomes by genistein, daidzein, coumestrol and C(18)-, C(19)- and C(21)-hydroxysteroids and ketosteroids. Steroids. 2005 Jul;70(8):507-14. PMID: 15894034.

Walf AA, Rhodes ME, Frye CA. Antidepressant effects of ERbeta-selective estrogen receptor modulators in the forced swim test. Pharmacol Biochem Behav. 2004 Jul;78(3):523-9. PMID: 15251261.

C6018

C-Peptide, dog

0.5 mg
1 mg
2.5 mg

H-Glu-Val-Glu-Asp-Leu-Gln-Val-Arg-Asp-Val-Glu-Leu-Ala-Gly-Ala-Pro-Gly-Glu-Gly-Gly-Leu-Gln-Pro-Leu-Ala-Leu-Glu-Gly-Ala-Leu-Gln-OH

$C_{137}H_{225}N_{37}O_{49}$ FW: 3174.54 ≥95%

Endogenous peptide that connects A and B chains of insulin. It binds cell surfaces, activating Ca^{2+}-dependent signaling pathways and improving neuropathy symptoms and kidney function.

Hills CE, Brunskill NJ. Intracellular signalling by C-peptide. Exp Diabetes Res. 2008;2008:635158. PMID: 18382618.

Samnegård B, Jacobson SH, Jaremko G, et al. Effects of C-peptide on glomerular and renal size and renal function in diabetic rats. Kidney Int. 2001 Oct;60(4):1258-65. PMID: 11576340.

C6019

C-Peptide, human

0.5 mg
1 mg
2.5 mg

H-Glu-Ala-Glu-Asp-Leu-Gln-Val-Gly-Gln-Val-Glu-Leu-Gly-Gly-Gly-Pro-Gly-Ala-Gly-Ser-Leu-Gln-Pro-Leu-Ala-Leu-Glu-Gly-Ser-Leu-Gln-OH

$C_{129}H_{211}N_{35}O_{48}$ FW: 3020.33 ≥95%

Endogenous peptide that connects A and B chains of insulin. It binds cell surfaces, activating Ca^{2+}-dependent signaling pathways and improving neuropathy symptoms and kidney function.

Hills CE, Brunskill NJ. Intracellular signalling by C-peptide. Exp Diabetes Res. 2008;2008:635158. PMID: 18382618.

Samnegård B, Jacobson SH, Jaremko G, et al. Effects of C-peptide on glomerular and renal size and renal function in diabetic rats. Kidney Int. 2001 Oct;60(4):1258-65. PMID: 11576340.

C6132

CPI-203

1 mg
5 mg
25 mg

$C_{19}H_{18}ClN_5OS$ FW: 399.9 ≥99%

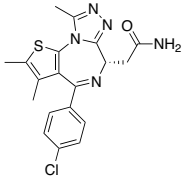

JQ-1 derivative and BRD inhibitor. It decreases production of IL-6, downregulates expression of Myc, and inhibits phosphorylation of the carboxyl-terminus domain of RNA polymerase II.

King B, Trimarchi T, Reavie L, et al. The ubiquitin ligase FBXW7 modulates leukemia-initiating cell activity by regulating MYC stability. Cell. 2013 Jun 20;153(7):1552-66. PMID: 23791182.

Devaiah BN, Lewis BA, Cherman N, et al. BRD4 is an atypical kinase that phosphorylates serine2 of the RNA polymerase II carboxy-terminal domain. Proc Natl Acad Sci U S A. 2012 May 1;109(18):6927-32. PMID: 22509028.

C6916

CREBtide

1 mg
2 mg
5 mg

H-Lys-Arg-Arg-Glu-Ile-Leu-Ser-Arg-Arg-Pro-Ser-Tyr-Arg

$C_{73}H_{127}N_{29}O_{18}$ FW: 1699.01 ≥95%

Synthetic CREB analog and PKD1 and PKA substrate.

Rybin VO, Guo J, Harleton E, et al. Regulatory domain determinants that control PKD1 activity. J Biol Chem. 2012 Jun 29;287(27):22609-15. PMID: 22582392.

Colbran JL, Roach PJ, Fiol CJ, et al. cAMP-dependent protein kinase, but not the cGMP-dependent enzyme, rapidly phosphorylates delta-CREB, and a synthetic delta-CREB peptide. Biochem Cell Biol. 1992 Oct-Nov;70(10-11):1277-82. PMID: 1338414.

C6818 Crenolanib

NEW

5 mg
10 mg

CP-868596

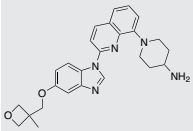

$C_{26}H_{29}N_5O_2$ FW: 443.54 [670220-88-9] ≥98%

FLT3 and PDGFR inhibitor. It inhibits proliferation and induces apoptosis in non-small cell lung cancer cells and acute myelogenous leukemia cells.

Wang P, Song L, Ge H, et al. Crenolanib, a PDGFR inhibitor, suppresses lung cancer cell proliferation and inhibits tumor growth in vivo. Onco Targets Ther. 2014 Sep 26;7:1761-8. PMID: 25328409.

Smith CC, Lasater EA, Lin KC, et al. Crenolanib is a selective type I pan-FLT3 inhibitor. Proc Natl Acad Sci U S A. 2014 Apr 8;111(14):5319-24. PMID: 24623852.

Zimmerman EI, Turner DC, Buaboonnam J, et al. Crenolanib is active against models of drug-resistant FLT3-ITD-positive acute myeloid leukemia. Blood. 2013 Nov 21;122(22):3607-15. PMID: 24046014.

C6935 Crizotinib

5 mg
10 mg
25 mg
100 mg

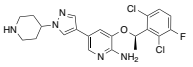

$C_{21}H_{22}Cl_2FN_5O$ FW: 450.34 [877399-52-5] ≥98%

Inhibitor of ALK, ROS1, and c-MET used to treat non-small cell lung cancer. It downregulates expression of survivin, induces apoptosis, and inhibits cell proliferation.

Timm A, Kolesar JM. Crizotinib for the treatment of non-small-cell lung cancer. Am J Health Syst Pharm. 2013 Jun 1;70(11):943-7. PMID: 23686600.

Okamoto W, Okamoto I, Arao T, et al. Antitumor action of the MET tyrosine kinase inhibitor crizotinib (PF-02341066) in gastric cancer positive for MET amplification. Mol Cancer Ther. 2012 Jul;11(7):1557-64. PMID: 22729845.

Tanizaki J, Okamoto I, Okamoto K, et al. MET tyrosine kinase inhibitor crizotinib (PF-02341066) shows differential antitumor effects in non-small cell lung cancer according to MET alterations. J Thorac Oncol. 2011 Oct;6(10):1624-31. PMID: 21716144.

C6955 Cromolyn Sodium

1 g
5 g

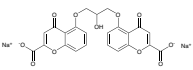

$C_{23}H_{14}O_{11}Na_2$ FW: 512.3 [15826-37-6] ≥98%

Mast cell destabilizer and potential TRP antagonist and Cl^- channel blocker used to treat asthma. It also activates phosphorylation of PKC and release of annexin A1, inhibits release of pro-inflammatory cytokines, and prevents left ventricular remodeling and dysfunction.

Zhang A, Chi X, Luo G, et al. Mast cell stabilization alleviates acute lung injury after orthotopic autologous liver transplantation in rats by downregulating inflammation. PLoS One. 2013 Oct 8;8(10):e75262. PMID: 24116032.

Yazid S, Sinniah A, Solito E, et al. Anti-allergic cromones inhibit histamine and eicosanoid release from activated human and murine mast cells by releasing Annexin A1. PLoS One. 2013;8(3):e58963. PMID: 23527056.

Mina Y, Rinkevich-Shop S, Konen E, et al. Mast cell inhibition attenuates myocardial damage, adverse remodeling, and dysfunction during fulminant myocarditis in the rat. J Cardiovasc Pharmacol Ther. 2013 Mar;18(2):152-61. PMID: 23172937.

C6956 Crotamiton

25 g
100 g

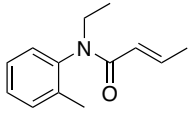

$C_{13}H_{17}NO$ FW: 203.28 [483-63-6] ≥98%

Antipruritic used to treat scabies and and demodicosis. It kills disease-causing mites.

Sekine R, Satoh T, Takaoka A, et al. Anti pruritic effects of topical crotamiton, capsaicin, and a corticosteroid on pruritogen-induced scratching behavior. Exp Dermatol. 2012 Mar;21(3):201-4. PMID: 22379965.

Hsu CK, Hsu MM, Lee JY. Demodicosis: a clinicopathological study. J Am Acad Dermatol. 2009 Mar;60(3):453-62. PMID: 19231642.

C6957 Croton Oil

100 mL
500 mL
1 L

Oleum tiglii

[8001-28-3] ≥98%

Mixture found in species of *Croton* used to induce inflammation, edema, and skin tumor development. It also repels mosquitos and inhibits growth of *Candida*, *Lactobaccilus*, *Staphylococcus*, *Streptococcus*, and *Porphyromonas*.

Boukhatem MN, Ferhat MA, Kameli A, et al. Lemon grass (Cymbopogon citratus) essential oil as a potent anti-inflammatory and antifungal drugs. Libyan J Med. 2014 Sep 19;9:25431. PMID: 25242268.

Liju VB, Jeena K, Kuttan R. Chemopreventive activity of turmeric essential oil and possible mechanisms of action. Asian Pac J Cancer Prev. 2014;15(16):6575-80. PMID: 25169490.

Vongsombath C, Pålsson K, Björk L, et al. Mosquito (Diptera: Culicidae) repellency field tests of essential oils from plants traditionally used in Laos. J Med Entomol. 2012 Nov;49(6):1398-404. PMID: 23270168.

C6982

Crustacean Cardioactive Peptide

1 mg
2 mg
5 mg

CCAP

H-Pro-Phe-Cys-Asn-Ala-Phe-Thr-Gly-Cys-OH
(Disulfide Bridge Cys3-Cys9)

$C_{42}H_{56}N_{10}O_{12}S_2$ FW: 957.1 ≥95%

Hormone found in arthropods that modulates heart rate, cardiac contractility, cardiac output, muscle contractions, and ecdysis.

Lee D, Orchard I, Lange AB. Evidence for a conserved CCAP-signaling pathway controlling ecdysis in a hemimetabolous insect, Rhodnius prolixus. Front Neurosci. 2013 Nov 5;7:207. PMID: 24204330.

Lee D, Vanden Broeck J, Lange AB. Identification and expression of the CCAP receptor in the Chagas' disease vector, Rhodnius prolixus, and its involvement in cardiac control. PLoS One. 2013 Jul 9;8(7):e68897. PMID: 23874803.

C7097

Cryptotanshinone

10 mg
25 mg
100 mg

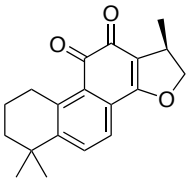

$C_{19}H_{20}O_3$ FW: 296.36 [35825-57-1] ≥90%

STAT3 inhibitor found in species of *Salvia*. It downregulates expression of VEGF and inhibits HIF-1α signaling and induces cell cycle arrest in rhabdomyosarcoma cells.

Lu L, Li C, Li D, et al. Cryptotanshinone inhibits human glioma cell proliferation by suppressing STAT3 signaling. Mol Cell Biochem. 2013 Sep;381(1-2):273-82. PMID: 23740516.

Lee HJ, Jung DB, Sohn EJ, et al. Inhibition of Hypoxia Inducible Factor Alpha and Astrocyte-Elevated Gene-1 Mediates Cryptotanshinone Exerted Antitumor Activity in Hypoxic PC-3 Cells. Evid Based Complement Alternat Med. 2012;2012:390957. rratum in: Evid Based Complement Alternat Med. 2013;2013:267352. PMID: 23243443.

C7098

Crystalline

1 mg
2 mg
5 mg

H-Trp-Gly-OH

$C_{13}H_{15}N_3O_3$ FW: 261.28 ≥95%

Dipeptide containing tryptophan and glycine.

C7602

CTAP

0.5 mg
1 mg
2.5 mg

H-D-Phe-Cys-Tyr-D-Trp-Arg-Thr-Pen-Thr-NH_2
(Disulfide bridge Cys2-Pen7)

$C_{51}H_{67}N_{13}O_{11}S$ FW: 1102.33 ≥95%

μOR agonist. It prevents reinstatement of drug seeking and inhibits opioid-induced analgesia.

Perry CJ, McNally GP. A role for the ventral pallidum in context-induced and primed reinstatement of alcohol seeking. Eur J Neurosci. 2013 Sep;38(5):2762-73. PMID: 23773238.

Saccani F, Anselmi L, Jaramillo I, et al. Protective role of μ opioid receptor activation in intestinal inflammation induced by mesenteric ischemia/reperfusion in mice. J Neurosci Res. 2012 Nov;90(11):2146-53. PMID: 22806643.

C7618

C-Telopeptide

0.5 mg
1 mg
2.5 mg

H-Glu-Lys-Ala-His-Asp-Gly-Gly-Arg-OH

$C_{34}H_{56}N_{14}O_{13}$ FW: 868.91 ≥95%

Structural component of collagen.

Kwansa AL, De Vita R, Freeman JW. Mechanical recruitment of N- and C-crosslinks in collagen type I. Matrix Biol. 2013 Nov 21. pii: S0945-053X(13)00141-8. PMID: 24269790.

Wu JJ, Eyre DR. Structural analysis of cross-linking domains in cartilage type XI collagen. Insights on polymeric assembly. J Biol Chem. 1995 Aug 11;270(32):18865-70. PMID: 7642541.

C7997

C-Type Natriuretic Peptide (1-22), human

0.5 mg
1 mg
2.5 mg

CNP

H-Gly-Leu-Ser-Lys-Gly-Cys-Phe-Gly-Leu-Lys-Leu-Asp-Arg-Ile-Gly-Ser-Met-Ser-Gly-Leu-Gly-Cys-OH
(Disulfide bridge Cys6-Cys22)

$C_{93}H_{157}N_{27}O_{28}S_3$ FW: 2197.64 ≥95%

Endogenous NPR-B agonist. It increases conduction velocity in the sinoatrial node and decreases basal ATP-sensitive K^+ channel openings and currents. It also plays a role in the regulation of skeletal growth and inflammation.

Burley DS, Cox CD, Zhang J, et al. Natriuretic peptides modulate ATP-sensitive K(+) channels in rat ventricular cardiomyocytes. Basic Res Cardiol. 2014 Mar;109(2):402. PMID: 24477916.

Azer J, Hua R, Krishnaswamy PS, et al. Effects of natriuretic peptides on electrical conduction in the sinoatrial node and atrial myocardium of the heart. J Physiol. 2014 Mar 1;592(Pt 5):1025-45. PMID: 24344164.

C5260

C-type Natriuretic Peptide (1-22), pig/human/rat

1 mg

CNP

Gly-Leu-Ser-Lys-Gly-Cys-Phe-Gly-Leu-lys-Leu-Asp-Arg-Ile-Gly-Ser-Met-Ser-Gly-Leu-Gly-Cys
(Disulfide bridge Cys6-Cys22)

$C_{93}H_{157}N_{27}O_{28}S_3$ FW: 2797.61 ≥95%

Endogenous cardiomodulatory NPR-B agonist. It regulates cardiac hypertrophy and remodeling, inhibits the renin-angiotensin system, and plays a role in bone growth.

Del Ry S. C-type natriuretic peptide: a new cardiac mediator. Peptides. 2013 Feb;40:93-8. PMID: 23262354.

Calvieri C, Rubattu S, Volpe M. Molecular mechanisms underlying cardiac antihypertrophic and antifibrotic effects of natriuretic peptides. J Mol Med (Berl). 2012 Jan;90(1):5-13. PMID: 21826523.

C7998

C-Type Natriuretic Peptide, chicken

0.5 mg
1 mg
2.5 mg

H-Gly-Leu-Ser-Arg-Ser-Cys-Phe-Gly-Val-Lys-Leu-Asp-Arg-Ile-Gly-Ser-Met-Ser-Gly-Leu-Gly-Cys-OH
(Disulfide bridge Cys6-Cys22)

CNP

$C_{93}H_{157}N_{29}O_{29}S_3$ FW: 2241.66 ≥95%

Endogenous NPR-B agonist. It increases conduction velocity in the sinoatrial node and decreases basal ATP-sensitive K^+ channel openings and currents. It also plays a role in the regulation of skeletal growth and inflammation.

Burley DS, Cox CD, Zhang J, et al. Natriuretic peptides modulate ATP-sensitive K(+) channels in rat ventricular cardiomyocytes. Basic Res Cardiol. 2014 Mar;109(2):402. PMID: 24477916.

Azer J, Hua R, Krishnaswamy PS, et al. Effects of natriuretic peptides on electrical conduction in the sinoatrial node and atrial myocardium of the heart. J Physiol. 2014 Mar 1;592(Pt 5):1025-45. PMID: 24344164.

C7992

CTX-0294885

NEW

5 mg
25 mg

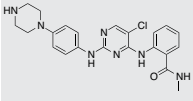

$C_{22}H_{24}ClN_7O$ FW: 437.93 [1439934-41-4] ≥98%

Inhibitor of many kinases.

Zhang L, Holmes IP, Hochgräfe F, et al. Characterization of the novel broad-spectrum kinase inhibitor CTx-0294885 as an affinity reagent for mass spectrometry-based kinome profiling. J Proteome Res. 2013 Jul 5;12(7):3104-16. PMID: 23692254.

C7692

CTX IV (6-12)

1 mg
2 mg
5 mg

Leu-Ile-Pro-Pro-Phe-Trp-Lys-NH_2

$C_{48}H_{70}N_{10}O_7$ FW: 899.14 ≥98%

Snake venom cardiotoxin found in *Naja naja atra*.

Jayaraman G, Kumar TK, Tsai CC, et al. Elucidation of the solution structure of cardiotoxin analogue V from the Taiwan cobra (*Naja naja atra*)--identification of structural features important for the lethal action of snake venom cardiotoxins. Protein Sci. 2000 Apr;9(4):637-46. PMID: 10794406.

Jang JY, Krishnaswamy T, Kumar S, et al. Comparison of the hemolytic activity and solution structures of two snake venom cardiotoxin analogues which only differ in their N-terminal amino acid. Biochemistry. 1997 Dec 2;36(48):14635-41. PMID: 9398182.

C7693

[Arg3,14] CTX IV (3-14)

1 mg
2 mg
5 mg

Arg-Asn-Arg-Leu-Ile-Pro-Pro-Phe-Trp-Lys-Thr-Arg-NH_2

$C_{74}H_{119}N_{25}O_{14}$ FW: 1582.91 ≥98%

Snake venom cardiotoxin found in *Naja naja atra*.

Jayaraman G, Kumar TK, Tsai CC, et al. Elucidation of the solution structure of cardiotoxin analogue V from the Taiwan cobra (*Naja naja atra*)--identification of structural features important for the lethal action of snake venom cardiotoxins. Protein Sci. 2000 Apr;9(4):637-46. PMID: 10794406.

C8112

CUDC-907

NEW

1 mg
5 mg
25 mg

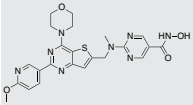

$C_{23}H_{24}N_8O_4S$ FW: 508.55 [1339928-25-4] ≥98%

PI3K and HDAC inhibitor. It inhibits cell proliferation and tumor growth in various cancer models.

Qian C, Lai CJ, Bao R, et al. Cancer network disruption by a single molecule inhibitor targeting both histone deacetylase activity and phosphatidylinositol 3-kinase signaling. Clin Cancer Res. 2012 Aug 1;18(15):4104-13. PMID: 22693356.

C8017

Cuelure

100 mg
250 mg
1 g

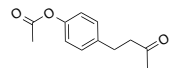

$C_{12}H_{14}O_3$ FW: 206.24 [3572-06-3] ≥97%

Hormonal attractant for male *Bactrocera* flies.

C8069

Curcumin

5 g
10 g
50 g

Turmeric yellow

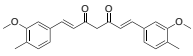

$C_{21}H_{20}O_6$ FW: 368.38 [458-37-7] ≥97%

Found in *Zingiberaceae*. It displays a wide variety of biological activities, including decreasing oxidative stress in vivo, activating MST1 and inducing apoptosis in cancer models, inhibiting cell wall biosynthesis of *Candida albicans*, and protecting against amyloid-β-induced hippocampal damage.

Kawanishi N, Kato K, Takahashi M, et al. Curcumin attenuates oxidative stress following downhill running-induced muscle damage. Biochem Biophys Res Commun. 2013 Nov 22;441(3):573-8. PMID: 24184481.

Du WZ, Feng Y, Wang XF, et al. Curcumin Suppresses Malignant Glioma Cells Growth and Induces Apoptosis by Inhibition of SHH/GLI1 Signaling Pathway in Vitro and Vivo. CNS Neurosci Ther. 2013 Dec;19(12):926-36. PMID: 24165291.

Tian N, Li X, Luo Y, et al. Curcumin regulates the metabolism of low density lipoproteins by improving the C-to-U RNA editing efficiency of apolipoprotein B in primary rat hepatocytes. Mol Med Rep. 2013 Oct 24. [Epub ahead of print]. PMID: 24173373.

C8070 Curcumin, high purity

10 mg
25 mg
100 mg

Turmeric yellow

$C_{21}H_{20}O_6$ FW: 368.38 [458-37-7] ≥98%

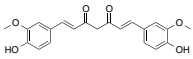

Natural product found in turmeric, MST1 activator, and CRMP2 inhibitor. It displays a wide variety of biological activities, including decreasing oxidative stress, increasing levels of APOBEC1, facilitating increased clearance of lipid particles from plasma, inducing apoptosis in cancer cells, and protecting against amyloid-β-induced hippocampal damage.

Kawanishi N, Kato K, Takahashi M, et al. Curcumin attenuates oxidative stress following downhill running-induced muscle damage. Biochem Biophys Res Commun. 2013 Oct 30. [Epub ahead of print]. PMID: 24184481.

Du WZ, Feng Y, Wang XF, et al. Curcumin Suppresses Malignant Glioma Cells Growth and Induces Apoptosis by Inhibition of SHH/GLI1 Signaling Pathway in Vitro and Vivo. CNS Neurosci Ther. 2013 Oct 25. [Epub ahead of print]. PMID: 24165291.

Tian N, Li X, Luo Y, et al. Curcumin regulates the metabolism of low density lipoproteins by improving the C-to-U RNA editing efficiency of apolipoprotein B in primary rat hepatocytes. Mol Med Rep. 2013 Oct 24. [Epub ahead of print]. PMID: 24173373.

C8500 CV-65

100 µg
1 mg

$C_{13}H_7N_2O_4$ FW: 270.24 ≥60%

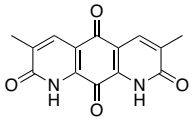

JNK and ERK5 inhibitor. It suppresses proliferation of various cancer cells.

Pipaón C, Gutierrez P, Montero JC, et al. Mitogen-activated protein kinase routes as targets in the action of diaza-anthracene compounds with a potent growth-inhibitory effect on cancer cells. Mol Cancer Ther. 2002 Aug;1(10):811-9. PMID: 12492114.

C8501 CV-66

100 µg
1 mg

$C_{14}H_{10}N_2O_4$ FW: 270.24 ≥95%

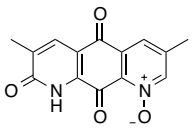

JNK and ERK5 inhibitor. It suppresses proliferation of various cancer cells.

Pipaón C, Gutierrez P, Montero JC, et al. Mitogen-activated protein kinase routes as targets in the action of diaza-anthracene compounds with a potent growth-inhibitory effect on cancer cells. Mol Cancer Ther. 2002 Aug;1(10):811-9. PMID: 12492114.

C8502 CV-70

100 µg
1 mg

$C_{16}H_{14}N_2O_4$ FW: 298.29 ≥90%

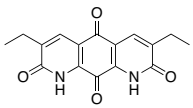

JNK and ERK5 inhibitor that inhibits proliferation of cancer cells.

Pipaón C, Gutierrez P, Montero JC, et al. Mitogen-activated protein kinase routes as targets in the action of diaza-anthracene compounds with a potent growth-inhibitory effect on cancer cells. Mol Cancer Ther. 2002 Aug;1(10):811-9. PMID: 12492114.

C9200 CX-6258

NEW

5 mg
25 mg

$C_{26}H_{24}ClN_3O_3$ FW: 461.95 [1202916-90-2] ≥98%

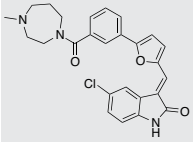

Pim kinase inhibitor. It decreases tumor growth in animal models of cancer.

Padmanabhan A, Gosc EB, Bieberich CJ. Stabilization of the prostate-specific tumor suppressor NKX3.1 by the oncogenic protein kinase Pim-1 in prostate cancer cells. J Cell Biochem. 2013 May;114(5):1050-7. PMID: 23129228.

Haddach M, Michaux J, Schwaebe MK, et al. Discovery of CX-6258. A Potent, Selective, and Orally Efficacious pan-Pim Kinases Inhibitor. ACS Med Chem Lett. 2011 Dec 27;3(2):135-9. PMID: 24900437.

C9600 Cyanopeptolin 1007

50 µg

CYP1007

$C_{49}H_{70}N_{10}O_{13}$ FW: 1007.14 [791104-89-7] ≥95%

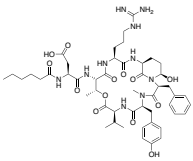

Serine protease inhibitor found in *Microcystis*. It may also inhibit growth of gram negative and gram positive bacteria.

Silva-Stenico ME, Rigonato J, Leal MG, et al. Non-ribosomal halogenated protease inhibitors from cyanobacterial isolates as attractive drug targets. Curr Med Chem. 2012;19(30):5205-13. PMID: 22934766.

Gademann K, Portmann C, Blom JF, et al. Multiple toxin production in the cyanobacterium *microcystis*: isolation of the toxic protease inhibitor cyanopeptolin 1020. J Nat Prod. 2010 May 28;73(5):980-4. PMID: 20405925.

Choi H, Oh SK, Yih W, et al. Cyanopeptoline CB071: a cyclic depsipeptide isolated from the freshwater cyanobacterium Aphanocapsa sp. Chem Pharm Bull (Tokyo). 2008 Aug;56(8):1191-3. PMID: 18670126.

C9603 Cyanopeptolin 1007 MB1 NEW 50 µg

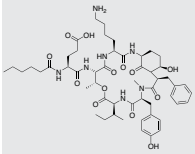

$C_{51}H_{74}N_8O_{13}$ FW: 1007.18 [912460-65-2] ≥95%

Serine protease inhibitor found in *Microcystis*. It is cytotoxic and may inhibit growth of gram negative and gram positive bacteria.

Silva-Stenico ME, Rigonato J, Leal MG, et al. Non-ribosomal halogenated protease inhibitors from cyanobacterial isolates as attractive drug targets. Curr Med Chem. 2012;19(30):5205-13. PMID: 22934766.

Gademann K, Portmann C, Blom JF, et al. Multiple toxin production in the cyanobacterium *microcystis*: isolation of the toxic protease inhibitor cyanopeptolin 1020. J Nat Prod. 2010 May 28;73(5):980-4. PMID: 20405925.

C9604 Cyanopeptolin 1007 MB2 NEW 25 µg

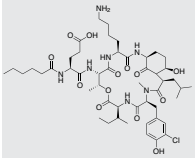

$C_{48}H_{75}ClN_8O_{13}$ FW: 1007.61 ≥95%

Serine protease inhibitor found in *Microcystis*. It is cytotoxic and may inhibit growth of gram negative and gram positive bacteria.

Silva-Stenico ME, Rigonato J, Leal MG, et al. Non-ribosomal halogenated protease inhibitors from cyanobacterial isolates as attractive drug targets. Curr Med Chem. 2012;19(30):5205-13. PMID: 22934766.

Gademann K, Portmann C, Blom JF, et al. Multiple toxin production in the cyanobacterium *microcystis*: isolation of the toxic protease inhibitor cyanopeptolin 1020. J Nat Prod. 2010 May 28;73(5):980-4. PMID: 20405925.

C9605 Cyanopeptolin 1020 NEW 25 µg

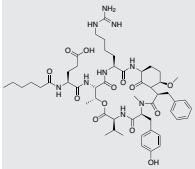

$C_{50}H_{72}N_{10}O_{13}$ FW: 1021.17 ≥95%

Serine protease inhibitor found in *Microcystis*. It is cytotoxic and may inhibit growth of gram negative and gram positive bacteria.

Silva-Stenico ME, Rigonato J, Leal MG, et al. Non-ribosomal halogenated protease inhibitors from cyanobacterial isolates as attractive drug targets. Curr Med Chem. 2012;19(30):5205-13. PMID: 22934766.

Gademann K, Portmann C, Blom JF, et al. Multiple toxin production in the cyanobacterium *microcystis*: isolation of the toxic protease inhibitor cyanopeptolin 1020. J Nat Prod. 2010 May 28;73(5):980-4. PMID: 20405925.

C9601 Cyanopeptolin 1040 MB NEW 100 µg

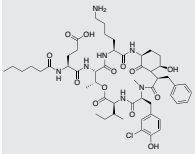

$C_{51}H_{73}ClN_8O_{13}$ FW: 1041.62 ≥95%

Serine protease inhibitor found in *Microcystis*. It is cytotoxic and may inhibit growth of gram negative and gram positive bacteria.

Silva-Stenico ME, Rigonato J, Leal MG, et al. Non-ribosomal halogenated protease inhibitors from cyanobacterial isolates as attractive drug targets. Curr Med Chem. 2012;19(30):5205-13. PMID: 22934766.

Gademann K, Portmann C, Blom JF, et al. Multiple toxin production in the cyanobacterium *microcystis*: isolation of the toxic protease inhibitor cyanopeptolin 1020. J Nat Prod. 2010 May 28;73(5):980-4. PMID: 20405925.

C9602 Cyanopeptolin 1041 100 µg

CYP1041

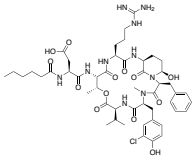

$C_{49}H_{69}ClN_{10}O_{13}$ FW: 1041.7 ≥95%

Serine protease inhibitor found in *Microcystis*. It may also inhibit growth of gram negative and gram positive bacteria.

Silva-Stenico ME, Rigonato J, Leal MG, et al. Non-ribosomal halogenated protease inhibitors from cyanobacterial isolates as attractive drug targets. Curr Med Chem. 2012;19(30):5205-13. PMID: 22934766.

Gademann K, Portmann C, Blom JF, et al. Multiple toxin production in the cyanobacterium *microcystis*: isolation of the toxic protease inhibitor cyanopeptolin 1020. J Nat Prod. 2010 May 28;73(5):980-4. PMID: 20405925.

C9606 Cyanopeptolin 1054 MB1 NEW 50 µg

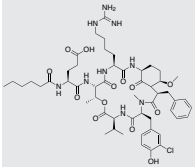

$C_{50}H_{71}ClN_{10}O_{13}$ FW: 1055.61 ≥95%

Serine protease inhibitor found in *Microcystis*. It is cytotoxic and may inhibit growth of gram negative and gram positive bacteria.

Silva-Stenico ME, Rigonato J, Leal MG, et al. Non-ribosomal halogenated protease inhibitors from cyanobacterial isolates as attractive drug targets. Curr Med Chem. 2012;19(30):5205-13. PMID: 22934766.

Gademann K, Portmann C, Blom JF, et al. Multiple toxin production in the cyanobacterium *microcystis*: isolation of the toxic protease inhibitor cyanopeptolin 1020. J Nat Prod. 2010 May 28;73(5):980-4. PMID: 20405925.

C9607 Cyanopeptolin 1054 MB2 NEW 25 µg

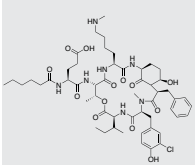

$C_{52}H_{75}ClN_8O_{13}$ FW: 1055.65 ≥95%

Serine protease inhibitor found in *Microcystis*. It is cytotoxic and may inhibit growth of gram negative and gram positive bacteria.

Silva-Stenico ME, Rigonato J, Leal MG, et al. Non-ribosomal halogenated protease inhibitors from cyanobacterial isolates as attractive drug targets. Curr Med Chem. 2012;19(30):5205-13. PMID: 22934766.

Gademann K, Portmann C, Blom JF, et al. Multiple toxin production in the cyanobacterium *microcystis*: isolation of the toxic protease inhibitor cyanopeptolin 1020. J Nat Prod. 2010 May 28;73(5):980-4. PMID: 20405925.

C9616 Cyanopeptolin 1068 MB

NEW **25 µg**

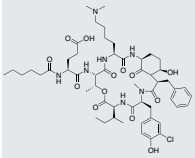

$C_{53}H_{77}ClN_8O_{13}$ FW: 1069.68 ≥95%

Serine protease inhibitor found in *Microcystis*. It is cytotoxic and may inhibit growth of gram negative and gram positive bacteria.

Silva-Stenico ME, Rigonato J, Leal MG, et al. Non-ribosomal halogenated protease inhibitors from cyanobacterial isolates as attractive drug targets. Curr Med Chem. 2012;19(30):5205-13. PMID: 22934766.

Gademann K, Portmann C, Blom JF, et al. Multiple toxin production in the cyanobacterium *microcystis*: isolation of the toxic protease inhibitor cyanopeptolin 1020. J Nat Prod. 2010 May 28;73(5):980-4. PMID: 20405925.

C9708 CYC-116

NEW **5 mg** **25 mg**

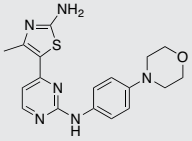

$C_{18}H_{20}N_6OS$ FW: 368.46 [693228-63-6] ≥98%

Aurora kinase B/C inhibitor. It prevents mitotic spindle formation and inhibits proliferation of a variety of cancer cells.

Kamei H, Jackson RC, Zheleva D, et al. An integrated pharmacokinetic-pharmacodynamic model for an Aurora kinase inhibitor. J Pharmacokinet Pharmacodyn. 2010 Aug;37(4):407-34. PMID: 20694801.

Wang S, Midgley CA, Scaërou F, et al. Discovery of N-phenyl-4-(thiazol-5-yl)pyrimidin-2-amine aurora kinase inhibitors. J Med Chem. 2010 Jun 10;53(11):4367-78. PMID: 20462263.

C9677 Cyclocytidine Hydrochloride

1 g **5 g**

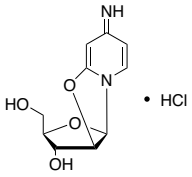

Ancitabine hydrochloride

$C_9H_{11}N_3O_4 \cdot HCl$ FW: 261.66 [10212-25-6] ≥98%

Pyrimidine analog and DNA synthesis inhibitor previously used to treat leukemias. It inhibits proliferation of HSV-1 and CMV and induces degranulation of granular tubules.

Thomopoulos GN, Garrett JR, Proctor GB. Ultrastructural histochemical studies of secretory granule replenishment in rat submandibular granular tubules after cyclocytidine-induced secretion. J Submicrosc Cytol Pathol. 2002 Jul;34(3):279-89. PMID: 12408361.

Chen Z, Song J, Chen K. Anti-herpes simplex virus action of combined therapy with cyclocytidine and ganciclovir. Zhonghua Yan Ke Za Zhi. 1996 Jan;32(1):25-8. PMID: 8758385.

C9709 Cycloheximide

1 g **5 g**

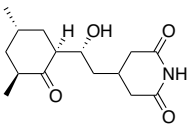

Naramycin A; Actidione

$C_{15}H_{23}NO_4$ FW: 281.35 [66-81-9] ≥95%

Eukaryotic protein synthesis inhibitor that prevents tRNA translocation and elongation. It is used to measure protein lifespan.

Bohnert M, Scherer O, Wiechmann K, et al. Melleolides induce rapid cell death in human primary monocytes and cancer cells. Bioorg Med Chem. 2014 Aug 1;22(15):3856-61. PMID: 25028062.

Ren Y, D'Ambrosio MA, Garvin JL, et al. Aldosterone sensitizes connecting tubule glomerular feedback via the aldosterone receptor GPR30. Am J Physiol Renal Physiol. 2014 Aug 15;307(4):F427-34. PMID: 24966088.

C9710 Cyclopamine

1 mg **5 mg** **25 mg** **100 mg** **500 mg** **1 g**

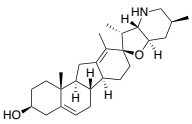

11-Deoxyjervine; HSDB 3505

$C_{27}H_{41}NO_2$ FW: 411.62 [4449-51-8] ≥98%

Smoothened inhibitor found in *Veratrum*. It inhibits hedgehog signaling pathways and induces birth defects. It also induces apoptosis and inhibits proliferation in adenoma cells and neuroblastoma cells.

Song M, Ou X, Xiao C, et al. Hedgehog signaling inhibitor cyclopamine induces apoptosis by decreasing Gli2 and Bcl2 expression in human salivary pleomorphic adenoma cells. Biomed Rep. 2013 Mar;1(2):325-329. PMID: 24648943.

Xu L, Wang X, Wan J, et al. Sonic Hedgehog pathway is essential for neuroblastoma cell proliferation and tumor growth. Mol Cell Biochem. 2012 May;364(1-2):235-41. PMID: 22350753.

Stanton BZ, Peng LF. Small-molecule modulators of the Sonic Hedgehog signaling pathway. Mol Biosyst. 2010 Jan;6(1):44-54. PMID: 20024066.

C9609 Cyclophosphamide Monohydrate

1 g **5 g**

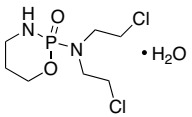

$C_7H_{15}Cl_2N_2O_2P \cdot H_2O$ FW: 279.1 [6055-19-2] ≥98%

Nitrogen mustard and DNA alkylator that inhibits DNA repair and replication. It is highly toxic and is used to treat various cancers and autoimmune diseases.

Sistigu A, Viaud S, Chaput N, et al. Immunomodulatory effects of cyclophosphamide and implementations for vaccine design. Semin Immunopathol. 2011 Jul;33(4):369-83. PMID: 21611872.

Makhani N, Gorman MP, Branson HM, et al. Cyclophosphamide therapy in pediatric multiple sclerosis. Neurology. 2009 Jun 16;72(24):2076-82. PMID: 19439723.

C9809

Cyclopiazonic Acid

5 mg
10 mg

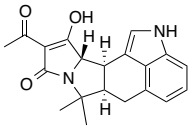

$C_{20}H_{20}N_2O_3$ FW: 336.39 [18172-33-3] ≥98%

SERCA inhibitor that alters contractility in smooth muscle tissues. It also inhibits proliferation of *Plasmodium*.

Pulcini S, Staines HM, Pittman JK, et al. Expression in yeast links field polymorphisms in PfATP6 to in vitro artemisinin resistance and identifies new inhibitor classes. J Infect Dis. 2013 Aug 1;208(3):468-78. PMID: 23599312.

Chericoni S, Testai L, Campeol E, et al. Vasodilator activity of Michelia figo Spreng. (Magnoliaceae) by in vitro functional study. J Ethnopharmacol. 2004 Apr;91(2-3):263-6. PMID: 15120449.

C9610

D-Cycloserine

250 mg
1 g
5 g

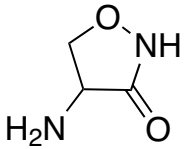

$C_3H_6N_2O_2$ FW: 102.09 [68-41-7] ≥98%

NMDA partial agonist and D-Ala-D-Ala ligase inhibitor. It enhances memory and learning and suppresses growth of *Mycobacterium*.

Dang YH, Ma XC, Zhang JC, et al. Targeting of NMDA Receptors in the Treatment of Major Depression. Curr Pharm Des. 2014 Jan 10. [Epub ahead of print]. PMID: 24410564.

Prosser GA, de Carvalho LP. Metabolomics Reveal d-Alanine:d-Alanine Ligase As the Target of d-Cycloserine in *Mycobacterium* tuberculosis. ACS Med Chem Lett. 2013 Dec 12;4(12):1233-1237. PMID: 24478820.

Portero-Tresserra M, Martí-Nicolovius M, Guillazo-Blanch G, et al. D-cycloserine in the basolateral amygdala prevents extinction and enhances reconsolidation of odor-reward associative learning in rats. Neurobiol Learn Mem. 2013 Feb;100:1-11. PMID: 23200640.

C9611

Cyclosporin A

10 mg
50 mg
100 mg

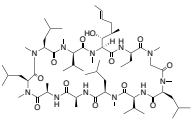

$C_{62}H_{111}N_{11}O_{12}$ FW: 1202.61 [59865-13-3] ≥98%

Calcineurin inhibitor used to prevent transplant rejection and graft-versus-host disease. It binds cyclophilin, inhibiting calcineurin and decreasing levels of IL-2 and activated T cells.

Lulic D, Burns J, Bae EC, et al. A review of laboratory and clinical data supporting the safety and efficacy of cyclosporin A in traumatic brain injury. Neurosurgery. 2011 May;68(5):1172-86. PMID: 21307793.

Reynolds NJ, Al-Daraji WI. Calcineurin inhibitors and sirolimus: mechanisms of action and applications in dermatology. Clin Exp Dermatol. 2002 Oct;27(7):555-61. PMID: 12464150.

C9615

Cyclosporin B

1 mg
5 mg

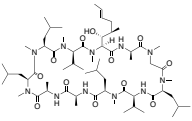

$C_{61}H_{109}N_{11}O_{12}$ FW: 1188.59 [63775-95-1] ≥95%

Calcineurin inhibitor. It inhibits entry of hepatitis B into hepatocytes and induces apoptosis in osteoclasts. It is less immunosuppressive than other cyclosporins.

Iwamoto M, Watashi K, Tsukuda S, et al. Evaluation and identification of hepatitis B virus entry inhibitors using HepG2 cells overexpressing a membrane transporter NTCP. Biochem Biophys Res Commun. 2014 Jan 17;443(3):808-13. PMID: 24342612.

Igarashi K, Hirotani H, Woo JT, et al. Cyclosporine A and FK506 induce osteoclast apoptosis in mouse bone marrow cell cultures. Bone. 2004 Jul;35(1):47-56. PMID: 15207740.

C9612

Cyclosporin C

1 mg
5 mg

Thr2-cyclosporine

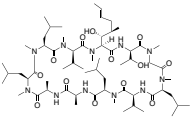

$C_{62}H_{111}N_{11}O_{13}$ FW: 1218.61 [59787-61-0] ≥98%

Cyclosporin metabolite and weak calmodulin inhibitor. It inhibits *Plasmodium* development and suppresses growth of filamentous phytopathogenic fungi.

Moussaïf M, Jacques P, Schaarwächter P, et al. Cyclosporin C is the main antifungal compound produced by Acremonium luzulae. Appl Environ Microbiol. 1997 May;63(5):1739-43. PMID: 9143111.

Uadia PO, Ezeamuzie IC, Ladan MJ, et al. Antimalarial activity of cyclosporins A, C and D. Afr J Med Med Sci. 1994 Mar;23(1):47-51. PMID: 7839946.

C9613

Cyclosporin D

1 mg
5 mg

Val2-cyclosporine

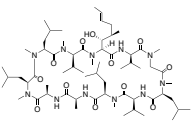

$C_{63}H_{113}N_{11}O_{12}$ FW: 1216.64 [63775-96-2] ≥98%

Cyclosporin metabolite and weak calmodulin inhibitor. It inhibits *Plasmodium* development.

Uadia PO, Ezeamuzie IC, Ladan MJ, et al. Antimalarial activity of cyclosporins A, C and D. Afr J Med Med Sci. 1994 Mar;23(1):47-51. PMID: 7839946.

Sadeg N, Pham-Huy C, Rucay P, et al. In vitro and in vivo comparative studies on immunosuppressive properties of cyclosporines A, C, D and metabolites M1, M17 and M21. Immunopharmacol Immunotoxicol. 1993 Mar-Jun;15(2-3):163-77. PMID: 8349948.

C9614

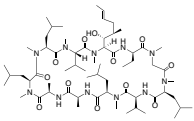

Cyclosporin H

Csh cyclosporin

$C_{62}H_{111}N_{11}O_{12}$ FW: 1202.61 [83602-39-5] ≥96%

1 mg
5 mg

Cyclosporin metabolite and formyl peptide inhibitor. It inhibits basophil activation but does not display significant immunosuppressive activity.

Stenfeldt AL, Karlsson J, Wennerås C, et al. Cyclosporin H, Boc-MLF and Boc-FLFLF are antagonists that preferentially inhibit activity triggered through the formyl peptide receptor. Inflammation. 2007 Dec;30(6):224-9. PMID: 17687636.

Yan P, Nanamori M, Sun M, et al. The immunosuppressant cyclosporin A antagonizes human formyl peptide receptor through inhibition of cognate ligand binding. J Immunol. 2006 Nov 15;177(10):7050-8. PMID: 17082621.

C9711

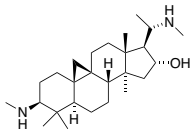

Cyclovirobuxine D

Bebuxine

$C_{26}H_{46}N_2O$ FW: 402.66 [860-79-7] ≥98%

25 mg
100 mg
500 mg

hERG K^+ channel inhibitor found in *Buxus*. It induces autophagy in breast cancer cells, improves heart failure pathology, and decreases infarct size and venous thrombus size in models of myocardial ischemia.

Lu J, Sun D, Gao S, et al. Cyclovirobuxine D induces autophagy-associated cell death via the Akt/mTOR pathway in MCF-7 human breast cancer cells. J Pharmacol Sci. 2014;125(1):74-82. PMID: 24758922.

Yu B, Fang TH, Lü GH, et al. Beneficial effect of Cyclovirobuxine D on heart failure rats following myocardial infarction. Fitoterapia. 2011 Sep;82(6):868-77. PMID: 21575690.

Zhao J, Wang Q, Xu J, et al. Cyclovirobuxine D inhibits the currents of HERG potassium channels stably expressed in HEK293 cells. Eur J Pharmacol. 2011 Jun 25;660(2-3):259-67. PMID: 21497594.

C9644

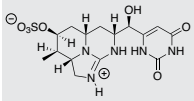

Cylindrospermopsin

NEW

$C_{15}H_{21}N_5O_7S$ FW: 415.42 [143545-90-8] ≥95%

100 µg

Protein and glutathione synthesis inhibitor found in *Cylindrospermopsis*. It induces oxidative stress and double-stranded DNA breaks, causes degeneration and steatosis in the liver, glomerulopathy in the kidney, and myofibrolysis and edema in the heart, and may be carcinogenic.

Gutiérrez-Praena D, Risalde MA, Pichardo S, et al. Histopathological and immunohistochemical analysis of Tilapia (Oreochromis niloticus) exposed to cylindrospermopsin and the effectiveness of N-Acetylcysteine to prevent its toxic effects. Toxicon. 2013 Nov 28;78C:18-34. [Epub ahead of print]. PMID: 24291634.

Guzmán-Guillén R, Prieto AI, Moreno I, et al. Cyanobacterium producing cylindrospermopsin cause histopathological changes at environmentally relevant concentrations in subchronically exposed tilapia (Oreochromis niloticus). Environ Toxicol. 2013 Sep 2. [Epub ahead of print]. PMID: 24000190.

Alja Š, Filipič M, Novak M, et al. Double strand breaks and cell-cycle arrest induced by the cyanobacterial toxin cylindrospermopsin in HepG2 cells. Mar Drugs. 2013 Aug 21;11(8):3077-90. PMID: 23966038.

C9660

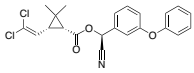

Cypermethrin

$C_{22}H_{19}Cl_2NO_3$ FW: 416.3 [52315-07-8] ≥98%

10 mg
25 mg
100 mg
1 g

Synthetic type II pyrethroid insecticide and protein phosphatase inhibitor. It inhibits protein phosphatases, inducing nerve blockade and paralysis

Maurya SK, Mishra J, Tripathi VK, et al. Cypermethrin induces astrocyte damage: role of aberrant $Ca^{(2+)}$, ROS, JNK, P38, matrix metalloproteinase 2 and migration related reelin protein. Pestic Biochem Physiol. 2014 May;111:51-9. PMID: 24861934.

Gammon DW. Correlations between in vitro and in vivo mechanisms of pyrethroid insecticide action. Fundam Appl Toxicol. 1985 Feb;5(1):9-23. PMID: 2985459.

C9863

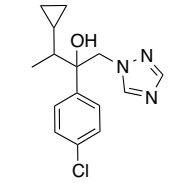

Cyproconazole

$C_{15}H_{18}ClN_3O$ FW: 291.78 [94361-06-5] ≥95%

5 g
10 g
100 g

14-α Demethylase inhibitor that inhibits ergosterol synthesis and fungal cell wall formation. It also inhibits voltage-gated Ca^{2+} channels, potentially inhibits aromatase, and may be a carcinogen. It alters hepatic cell proliferation, serum cholesterol, and hepatic retinoic acid levels in an androgen receptor-dependent manner.

Heusinkveld HJ, Molendijk J, van den Berg M, et al. Azole fungicides disturb intracellular Ca^{2+} in an additive manner in dopaminergic PC12 cells. Toxicol Sci. 2013 Aug;134(2):374-81. PMID: 23708404.

Hester S, Moore T, Padgett WT, et al. The hepatocarcinogenic conazoles: cyproconazole, epoxiconazole, and propiconazole induce a common set of toxicological and transcriptional responses. Toxicol Sci. 2012 May;127(1):54-65. PMID: 22334560.

Peffer RC, Moggs JG, Pastoor T, et al. Mouse liver effects of cyproconazole, a triazole fungicide: role of the constitutive androstane receptor. Toxicol Sci. 2007 Sep;99(1):315-25. PMID: 17557908.

C9662

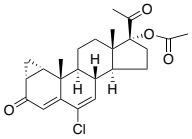

Cyproterone Acetate

100 mg
250 mg
1 g

CPA

$C_{24}H_{29}ClO_4$ FW: 416.94 [427-51-0] ≥98%

Androgen receptor antagonist that inhibits androgen entry into the prostate.

Guadalix FJ, Botella Llusiá J. The action mechanism of cyproterone. Acta Ginecol (Madr). 1975 Jul 1;27(1):7-11. PMID: 1146472.

Giorgi EP, Shirley IM, Grant JK, et al. Androgen dynamics in vitro in the human prostate gland. Effect of cyproterone and cyproterone acetate. Biochem J. 1973 Mar;132(3):465-74. PMID: 4125095.

C9876

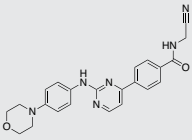

CYT-387

NEW

5 mg
10 mg
25 mg

CYT-11387; Momelotinib

$C_{23}H_{22}N_6O_2$ FW: 414.46 [1056634-68-4] ≥99%

JAK2 inhibitor. It induces cell cycle arrest and decreases tumor burden in multiple myeloma models.

Abubaker K, Luwor RB, Zhu H, et al. Inhibition of the JAK2/STAT3 pathway in ovarian cancer results in the loss of cancer stem cell-like characteristics and a reduced tumor burden. BMC Cancer. 2014 May 6;14:317. PMID: 24886434.

Geyer HL, Tibes R, Mesa RA. JAK2 inhibitors and their impact in myeloproliferative neoplasms. Hematology. 2012 Apr;17 Suppl 1:S129-32. PMID: 22507800.

Monaghan KA, Khong T, Burns CJ, et al. The novel JAK inhibitor CYT387 suppresses multiple signalling pathways, prevents proliferation and induces apoptosis in phenotypically diverse myeloma cells. Leukemia. 2011 Dec;25(12):1891-9. PMID: 21788946.

C9670

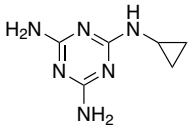

Cyromazine

25 g
100 g

$C_6H_{10}N_6$ FW: 166.18 [66215-27-8] ≥98%

Melamine derivative and insect growth regulator. It inhibits chitin synthesis and prevents growth of *Anopheles*, *Culex*, and *Aedes*.

Darriet F, Zaim M, Corbel V. Laboratory evaluation of cyromazine against insecticide-susceptible and -resistant mosquito larvae. J Am Mosq Control Assoc. 2008 Mar;24(1):123-6. PMID: 18437826.

Mommaerts V, Sterk G, Smagghe G. Hazards and uptake of chitin synthesis inhibitors in bumblebees Bombus terrestris. Pest Manag Sci. 2006 Aug;62(8):752-8. PMID: 16786494.

C9673

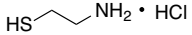

Cysteamine Hydrochloride

25 g
100 g

Mercaptamine; Decarboxycysteine; MEA

$C_2H_7NS \cdot HCl$ FW: 113.61 [156-57-0] ≥98%

Component of endogenous coenzyme A. It is used to induce ulcer formation and to treat cystinosis and other disorders of cysteine excretion. It also suppresses metastasis in pancreatic cancer models and displays therapeutic benefit in models of schizophrenia, neurodegenerative disease, and depression.

Khomenko T, Deng X, Ahluwalia A, et al. STAT3 and importins are novel mediators of early molecular and cellular responses in experimental duodenal ulceration. Dig Dis Sci. 2014 Feb;59(2):297-306. PMID: 24385009.

Fujisawa T, Rubin B, Suzuki A, et al. Cysteamine suppresses invasion, metastasis and prolongs survival by inhibiting matrix metalloproteinases in a mouse model of human pancreatic cancer. PLoS One. 2012;7(4):e34437. PMID: 22532830.

Shieh CH, Hong CJ, Huang YH, et al. Potential antidepressant properties of cysteamine on hippocampal BDNF levels and behavioral despair in mice. Prog Neuropsychopharmacol Biol Psychiatry. 2008 Aug 1;32(6):1590-4. PMID: 18582526.

C9778

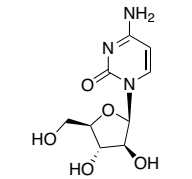

Cytarabine

100 mg
500 mg
1 g

Ara-C

$C_9H_{13}N_3O_5$ FW: 243.22 [147-94-4] ≥98%

Cytidine analog and inhibitor of DNA polymerase and RNA polymerase. It terminates DNA chain elongation and is used to treat leukemias and lymphomas. It also inhibits growth or replication of herpesviruses.

Abdel-Aziz W, Jiang HY, Hickey RJ, et al. Ara-C affects formation of cancer cell DNA synthesome replication intermediates. Cancer Chemother Pharmacol. 2000;45(4):312-9. PMID: 10755320.

Hiddemann W. Cytosine arabinoside in the treatment of acute myeloid leukemia: the role and place of high-dose regimens. Ann Hematol. 1991 Apr;62(4):119-28. PMID: 2031974.

Lauter CB, Bailey EJ, Lerner AM. Assessment of cytosine arabinoside as an antiviral agent in humans. Antimicrob Agents Chemother. 1974 Nov;6(5):598-602. PMID: 15825312.

C9779 Cytisine

5 mg
25 mg
100 mg

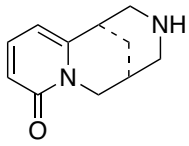

$C_{11}H_{14}N_2O$ FW: 190.24 [485-35-8] ≥98%

α3β4 nAChR agonist and α4β2 nAChR partial agonist found in *Laburnum*, and *Cytisus*. It decreases depression-like behaviors and increases smoking cessation rates.

Hajek P, McRobbie H, Myers K. Efficacy of cytisine in helping smokers quit: systematic review and meta-analysis. Thorax. 2013 Nov;68(11):1037-42. PMID: 23404838.

Simeonova R, Vitcheva V, Mitcheva M. Effect of cytisine on some brain and hepatic biochemical parameters in spontaneously hypertensive rats. Interdiscip Toxicol. 2010 Mar;3(1):21-5. PMID: 21217867.

C9878 Cytochalasin A

1 mg
5 mg

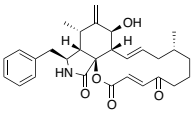

$C_{29}H_{35}NO_5$ FW: 477.6 [14110-64-6] ≥98%

Actin polymerization inhibitor and $K_v1.5$ K^+ channel blocker found in *Aspergillus*. It inhibits platelet-mediated adhesion of tumor cells and prevents phagocytosis in macrophages.

Choi BH, Park JA, Kim KR, et al. Direct block of cloned hKv1.5 channel by cytochalasins, actin-disrupting agents. Am J Physiol Cell Physiol. 2005 Aug;289(2):C425-36. PMID: 15800051.

Menter DG, Sloane BF, Steinert BW, et al. Platelet enhancement of tumor cell adhesion to subendothelial matrix: role of platelet cytoskeleton and platelet membrane. J Natl Cancer Inst. 1987 Nov;79(5):1077-90. PMID: 3479634.

C9879 Cytochalasin B

1 mg
5 mg

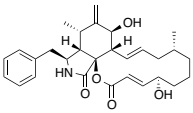

$C_{29}H_{37}NO_5$ FW: 479.61 [14930-96-2] ≥98%

Actin polymerization inhibitor found in *Aspergillus*. It inhibits secretion of corticosterone and aldosterone, suppresses FGF- and PDGF-induced mitogenesis, and prevents phagocytosis in macrophages.

Delarue C, Esneu M, Fournier A, et al. Role of the cytoskeleton in the secretory response of the frog adrenal gland to calcitonin gene-related peptide. J Steroid Biochem Mol Biol. 1997 Sep-Oct;63(1-3):21-7. PMID: 9449202.

Reist RH, Dey RD, Durham JP, et al. Inhibition of proliferative activity of pulmonary fibroblasts by tetrandrine. Toxicol Appl Pharmacol. 1993 Sep;122(1):70-6. PMID: 8104360.

C9880 Cytochalasin C

1 mg
5 mg

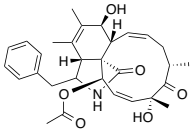

$C_{30}H_{37}NO_6$ FW: 507.62 [22144-76-9] ≥98%

Actin polymerization inhibitor found in *Aspergillus*. It inhibits motility of spermatozoa and increases transcription of TGF-β, collagenase, fibronectin, and procollagens 1 and 2.

Varedi M, Ghahary A, Scott PG, et al. Cytoskeleton regulates expression of genes for transforming growth factor-beta 1 and extracellular matrix proteins in dermal fibroblasts. J Cell Physiol. 1997 Aug;172(2):192-9. PMID: 9258340.

Glinsukon T, Sinlapanapaporn S, Chulasamaya M. Inhibitory effect of cytochalasins on the motility of rat epididymal spermatozoa in vitro. Res Commun Chem Pathol Pharmacol. 1986 Feb;51(2):265-8. PMID: 3961270.

C9881 Cytochalasin D

1 mg
5 mg

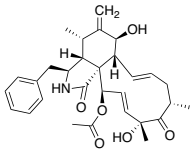

$C_{30}H_{37}NO_6$ FW: 507.62 [22144-77-0] ≥98%

Actin polymerization inhibitor found in *Aspergillus*. It inhibits FGF- and VEGF-induced angiogenesis, increases production of ROS, and increases levels of PPARγ, lipoprotein lipase, and FABP4.

Wilkins JR, Pike DB, Gibson CC, et al. Differential effects of cyclic stretch on bFGF- and VEGF-induced sprouting angiogenesis. Biotechnol Prog. 2014 Feb 14. [Epub ahead of print]. PMID: 24574264.

Choy JS, Lu X, Yang J, et al. Endothelial actin depolymerization mediates NADPH oxidase-superoxide production during flow reversal. Am J Physiol Heart Circ Physiol. 2014 Jan 1;306(1):H69-77. PMID: 24186098.

Schiller ZA, Schiele NR, Sims JK, et al. Adipogenesis of adipose-derived stem cells may be regulated via the cytoskeleton at physiological oxygen levels in vitro. Stem Cell Res Ther. 2013 Jul 9;4(4):79. PMID: 23838354.

C9882 Cytochalasin E

1 mg
5 mg

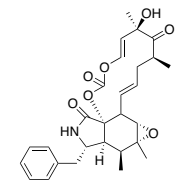

$C_{28}H_{33}NO_7$ FW: 495.57 [36011-19-5] ≥98%

Actin polymerization inhibitor found in *Aspergillus*. It inhibits FGF-induced angiogenesis, suppresses lung tumor growth, and increases levels of IL-8, ICAM-1, and CD-54.

Ikewaki N, Yamada A, Inoko H. Depolymerization of actin filament by cytochalasin E induces interleukin-8 production and up-regulates CD54 in the HeLa epithelial cell line. Microbiol Immunol. 2003;47(10):775-83. PMID: 14605444.

Udagawa T, Yuan J, Panigrahy D, et al. Cytochalasin E, an epoxide containing *Aspergillus*-derived fungal metabolite, inhibits angiogenesis and tumor growth. J Pharmacol Exp Ther. 2000 Aug;294(2):421-7. PMID: 10900214.

C9781 Basic Cytotoxicity Test Assay Kit

NEW

125 tests
250 tests

Cytotoxicity measuring kit.

C9782 Total Cytotoxicity Test Assay Kit

125 Tests
250 Tests

Cytotoxicity measuring kit.

C9773 L-Cystine

25 g
100 g
500 g

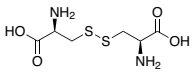

$C_6H_{12}N_2O_4S_2$ FW: 240.3 [56-89-3] ≥98%

Endogenous amino acid that forms disulfide bridges in proteins.

Kolmar H. Biological diversity and therapeutic potential of natural and engineered cystine knot miniproteins. Curr Opin Pharmacol. 2009 Oct;9(5):608-14. PMID: 19523876.

Dröge W, Holm E. Role of cysteine and glutathione in HIV infection and other diseases associated with muscle wasting and immunological dysfunction. FASEB J. 1997 Nov;11(13):1077-89. PMID: 9367343.

C9808 CZC-54252

NEW

5 mg
25 mg

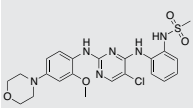

$C_{22}H_{25}ClN_6O_4S$ FW: 504.99 [1191911-27-9] ≥98%

LRRK2 inhibitor. It may decrease neuronal injury in models of neurodegenerative diseases.

Kramer T, Lo Monte F, Göring S, et al. Small molecule kinase inhibitors for LRRK2 and their application to Parkinson's disease models. ACS Chem Neurosci. 2012 Mar 21;3(3):151-60. PMID: 22860184.

Ramsden N, Perrin J, Ren Z, et al. Chemoproteomics-based design of potent LRRK2-selective lead compounds that attenuate Parkinson's disease-related toxicity in human neurons. ACS Chem Biol. 2011 Oct 21;6(10):1021-8. PMID: 21812418.

D0004 Dabrafenib

5 mg
25 mg

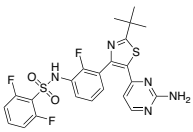

$C_{23}H_{20}F_3N_5O_2S_2$ FW: 519.56 [1195765-45-7] ≥98%

Inhibitor of V600E/V600K/V600D mutant B-Raf and c-Raf used to treat metastatic melanoma.

Ballantyne AD, Garnock-Jones KP. Dabrafenib: First Global Approval. Drugs. 2013 Jul 24. [Epub ahead of print] PMID: 23881668.

Huang T, Karsy M, Zhuge J, et al. B-Raf and the inhibitors: from bench to bedside. J Hematol Oncol. 2013 Apr 25;6:30. PMID: 23617957.

Klinac D, Gray ES, Millward M, et al. Advances in personalized targeted treatment of metastatic melanoma and non-invasive tumor monitoring. Front Oncol. 2013;3:54. PMID: 23515890.

D0005 Dabrafenib Mesylate

5 mg
25 mg

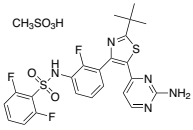

$C_{23}H_{20}F_3N_5O_2S_2 \bullet CH_3SO_3H$ FW: 615.67 [1195768-06-9] ≥98%

Inhibitor of V600E/V600K/V600D mutant B-Raf and c-Raf used to treat metastatic melanoma.

Ballantyne AD, Garnock-Jones KP. Dabrafenib: First Global Approval. Drugs. 2013 Jul 24. [Epub ahead of print] PMID: 23881668.

Huang T, Karsy M, Zhuge J, et al. B-Raf and the inhibitors: from bench to bedside. J Hematol Oncol. 2013 Apr 25;6:30. PMID: 23617957.

Klinac D, Gray ES, Millward M, et al. Advances in personalized targeted treatment of metastatic melanoma and non-invasive tumor monitoring. Front Oncol. 2013;3:54. PMID: 23515890.

D0011 Dacarbazine

100 mg
1 g

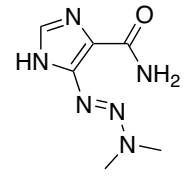

$C_6H_{10}N_6O$ FW: 182.18 [4342-03-4] ≥98%

DNA alkylator used to treat various cancers.

Gallamini A, Di Raimondo F, La Nasa G, et al. Standard therapies versus novel therapies in Hodgkin lymphoma. Immunol Lett. 2013 Sep-Oct;155(1-2):56-9. PMID: 24140162.

Koprowska K, Czyż M. Dacarbazine, a chemotherapeutic against metastatic melanoma and a reference drug for new treatment modalities. Postepy Hig Med Dosw (Online). 2011 Nov 23;65:734-51. PMID: 22173438.

D0006

Dacomitinib Monohydrate

1 mg
5 mg
25 mg

PF-00299804

$C_{24}H_{25}ClFN_5O_2 \cdot H_2O$ FW: 487.95 [1042385-75-0] ≥99%

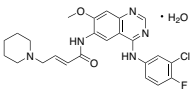

EGFR inhibitor that covalently modifies cytosine residues in the catalytic domain of EGFR. It induces cell cycle arrest and apoptosis in squamous cell carcinoma cells, ovarian carcinoma cells, and non-small-cell lung cancer cells.

Kalous O, Conklin D, Desai AJ, et al. Dacomitinib (PF-00299804), an irreversible Pan-HER inhibitor, inhibits proliferation of HER2-amplified breast cancer cell lines resistant to trastuzumab and lapatinib. Mol Cancer Ther. 2012 Sep;11(9):1978-87. PMID: 22761403.

Gonzales AJ, Hook KE, Althaus IW, et al. Antitumor activity and pharmacokinetic properties of PF-00299804, a second-generation irreversible pan-erbB receptor tyrosine kinase inhibitor. Mol Cancer Ther. 2008 Jul;7(7):1880-9. PMID: 18606718.

D0032

Daidzein

250 mg
1 g
5 g

7,4'-Dihydroxyisoflavone

$C_{15}H_{10}O_4$ FW: 254.24 [486-66-8] ≥97%

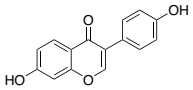

Found in many plant sources, including soy. It exhibits a variety of biological activities, including activating TGF-β/Smad signaling to increase collagen synthesis in fibroblasts, decreasing TNF-α-induced inflammation in vivo, increasing antioxidative enzyme activity to inhibit DMBA-induced carcinogenesis, and neurite growth.

Li HY, Pan L, Ke YS, et al. Daidzein suppresses pro-inflammatory chemokine Cxcl2 transcription in TNF-α-stimulated murine lung epithelial cells via depressing PARP-1 activity. Acta Pharmacol Sin. 2014 Apr;35(4):496-503. PMID: 24632845.

Zhao D, Shi Y, Dang Y, et al. Daidzein stimulates collagen synthesis by activating the TGF-β/smad signal pathway. Australas J Dermatol. 2014 Mar 19. [Epub ahead of print]. PMID: 24645968.

Park HJ, Jeon YK, You DH, et al. Daidzein causes cytochrome c-mediated apoptosis via the Bcl-2 family in human hepatic cancer cells. Food Chem Toxicol. 2013 Oct;60:542-9. PMID: 23959101.

D0033

Daidzin

1 mg
5 mg

$C_{21}H_{20}O_9$ FW: 416.38 [552-66-9] ≥98%

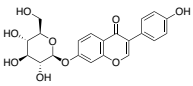

Phytoestrogen found in soy that displays a variety of biological activities, including reversing scopolamine-induced memory impairments, promoting proliferation of osteoblasts and bone marrow stromal cells, and inhibiting adipocytic differentiation in osteoblasts.

Kim DH, Jung HA, Park SJ, et al. The effects of daidzin and its aglycon, daidzein, on the scopolamine-induced memory impairment in male mice. Arch Pharm Res. 2010 Oct;33(10):1685-90. PMID: 21052945.

Kim SH, Heo JH, Kim YS, et al. Protective effect of daidzin against D-galactosamine and lipopolysaccharide-induced hepatic failure in mice. Phytother Res. 2009 May;23(5):701-6. PMID: 19107740.

Li XH, Zhang JC, Sui SF, et al. Effect of daidzin, genistin, and glycitin on osteogenic and adipogenic differentiation of bone marrow stromal cells and adipocytic transdifferentiation of osteoblasts. Acta Pharmacol Sin. 2005 Sep;26(9):1081-6. PMID: 16115375.

D0044

D-Ala-D-Ala

250 mg

D-Ala-D-Ala

$C_6H_{12}N_2O_3$ FW: 160.17 [923-16-0] ≥98%

Peptidoglycan cell wall component targeted by antibacterials such as vancomycin.

Kwun MJ, Novotna G, Hesketh AR, et al. In vivo studies suggest that induction of VanS-dependent vancomycin resistance requires binding of the drug to D-Ala-D-Ala termini in the peptidoglycan cell wall. Antimicrob Agents Chemother. 2013 Sep;57(9):4470-80. PMID: 23836175.

D0025

DAMGO

1 mg
2 mg
5 mg

H-Try-D-Ala-Gly-N-MePhe-Gly-OH

$C_{26}H_{35}N_5O_6$ FW: 513.0 ≥95%

μOR agonist that decreases pain transmission, motor activity, and GABA-A current.

Wu Q, Xia S, Lin J, et al. Effects of the altered activity of δ-opioid receptor on the expression of glutamate transporter type 3 induced by chronic exposure to morphine. J Neurol Sci. 2013 Dec 15;335(1-2):174-81. PMID: 24120272.

Alexeeva EV, Nazarova GA, Sudakov SK. Effects of peripheral μ, δ, and K-opioid receptor agonists on the levels of anxiety and motor activity of rats. Bull Exp Biol Med. 2012 Sep;153(5):720-1. PMID: 23113268.

D0253

Danazol

100 mg
250 mg
1 g

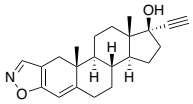

$C_{22}H_{27}NO_2$ FW: 337.46 [17230-88-5] ≥98%

Synthetic ethisterone derivative and weak androgen receptor agonist used for in vitro fertilization and to treat endometriosis and hereditary angioedema. It inhibits production of FSH and LH.

Füst G, Farkas H, Csuka D, et al. Long-term efficacy of danazol treatment in hereditary angioedema. Eur J Clin Invest. 2011 Mar;41(3):256-62. PMID: 20955212.

Kusakabe K, Morishima S, Nakamuta N, et al. Effect of danazol on NK cells and cytokines in the mouse uterus. J Reprod Dev. 2007 Feb;53(1):87-94. PMID: 17077583.

Murakami K, Nomura K, Shinohara K, et al. Danazol inhibits aromatase activity of endometriosis-derived stromal cells by a competitive mechanism. Fertil Steril. 2006 Aug;86(2):291-7. PMID: 16806212.

D0353

Danofloxacin Mesylate

500 mg
1 g
5 g

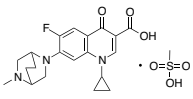

$C_{19}H_{20}FN_3O_3 \bullet CH_3SO_3H$ FW: 453.48 [119487-55-6] ≥98%

Bacterial DNA gyrase inhibitor. It increases activity of antioxidative enzymes and suppresses growth of *Mycoplasma*, *Actinobacillus*, *Mannheima*, *Escherichia*, and *Pasturella*.

Kawai K, Higuchi H, Iwano H, et al. Antimicrobial susceptibilities of Mycoplasma isolated from bovine mastitis in Japan. Anim Sci J. 2013 Nov 21. [Epub ahead of print]. PMID: 24261609.

Yu CH, Liu ZY, Sun LS, et al. Effect of Danofloxacin on Reactive Oxygen Species Production, Lipid Peroxidation and Antioxidant Enzyme Activities in Kidney Tubular Epithelial Cell Line, LLC-PK1. Basic Clin Pharmacol Toxicol. 2013 Jul 15. [Epub ahead of print]. PMID: 23855763.

Archambault M, Harel J, Gouré J, et al. Antimicrobial susceptibilities and resistance genes of Canadian isolates of *Actinobacillus* pleuropneumoniae. Microb Drug Resist. 2012 Apr;18(2):198-206. PMID: 22204596.

D0254

Dansyl-YVG

25 mg
50 mg
125 mg

Dansyl-Tyr-Val-Gly

$C_{28}H_{34}N_4O_7S$ FW: 571.63 ≥95%

Substrate of peptidylglycine monooxygenase and peptidylglycine α-amidating enzyme.

Bauman AT, Yukl ET, Alkevich K, et al. The hydrogen peroxide reactivity of peptidylglycine monooxygenase supports a Cu(II)-superoxo catalytic intermediate. J Biol Chem. 2006 Feb 17;281(7):4190-8. PMID: 16330540.

Miller DA, Sayad KU, Kulathila R, et al. Characterization of a bifunctional peptidylglycine alpha-amidating enzyme expressed in Chinese hamster ovary cells. Arch Biochem Biophys. 1992 Nov 1;298(2):380-8. PMID: 1384431.

D0255

Dantrolene Sodium Heptahydrate

100 mg
250 mg
1 g

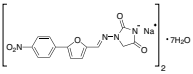

$(C_{14}H_9N_4O_5Na)_2 \bullet 7H_2O$ FW: 399.29 [24868-20-0] ≥98%

Hydantoin derivative and inhibitor of ryanodine receptors and L-type Ca^{2+} channels used to treat malignant hyperthermia. It also decreases apoptosis and TNF-α levels in ischemia/reperfusion models.

Jakob R, Beutner G, Sharma VK, et al. Molecular and functional identification of a mitochondrial ryanodine receptor in neurons. Neurosci Lett. 2014 May 23. [Epub ahead of print]. PMID: 24861510.

Bannister RA. Dantrolene-induced inhibition of skeletal L-type Ca^{2+} current requires RyR1 expression. Biomed Res Int. 2013;2013:390493. PMID: 23509717.

Boys JA, Toledo AH, Anaya-Prado R, et al. Effects of dantrolene on ischemia-reperfusion injury in animal models: a review of outcomes in heart, brain, liver, and kidney. J Investig Med. 2010 Oct;58(7):875-82. PMID: 20517166.

D0262

Dapiprazole Hydrochloride

10 mg
25 mg
100 mg

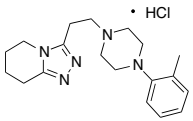

$C_{19}H_{23}N_5 \bullet HCl$ FW: 357.89 [72822-13-0] ≥98%

α1-Adrenergic receptor antagonist used to reverse mydriasis. It also decreases mean intraocular pressure, suppresses pigment shedding, and increases outflow facility.

Eltze M. Affinity of the miotic drug, dapiprazole, at alpha 1-adrenoceptor subtypes A, B and D. J Pharm Pharmacol. 1997 Nov;49(11):1091-5. PMID: 9401944.

Hogan TS, McDaniel DD, Bartlett JD, et al. Dose-response study of dapiprazole HCl in the reversal of mydriasis induced by 2.5% phenylephrine. J Ocul Pharmacol Ther. 1997 Aug;13(4):297-302. PMID: 9261765.

Mastropasqua L, Carpineto P, Ciancaglini M, et al. The usefulness of dapiprazole, an alpha-adrenergic blocking agent, in pigmentary glaucoma. Ophthalmic Surg Lasers. 1996 Sep;27(9):806-9. PMID: 8878205.

D0261

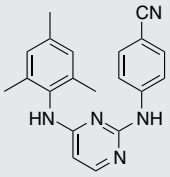

Dapivirine

NEW

5 mg
25 mg

TMC120

$C_{20}H_{19}N_5$ FW: 329.41 [244767-67-7] ≥98%

RT inhibitor that suppresses HIV replication in dendritic cells and T cells.

Devlin B, Nuttall J, Wilder S, et al. Development of dapivirine vaginal ring for HIV prevention. Antiviral Res. 2013 Dec;100 Suppl:S3-8. PMID: 24188702.

Gupta SK, Nutan. Clinical use of vaginal or rectally applied microbicides in patients suffering from HIV/AIDS. HIV AIDS (Auckl). 2013 Oct 22;5:295-307. PMID: 24174883.

Njai HF, Lewi PJ, Janssen CG, et al. Pre-incubation of cell-free HIV-1 group M isolates with non-nucleoside reverse transcriptase inhibitors blocks subsequent viral replication in co-cultures of dendritic cells and T cells. Antivir Ther. 2005;10(2):255-62. PMID: 15865220.

D0263

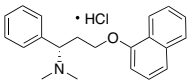

Dapoxetine Hydrochloride

10 mg
50 mg
100 mg

$C_{21}H_{23}NO \cdot HCl$ FW: 341.87 [129938-20-1] ≥99%

SERT inhibitor and potential voltage-gated K^+ channel blocker used to treat premature ejaculation. It does not exhibit significant antidepressant activity.

McMahon CG. Dapoxetine: a new option in the medical management of premature ejaculation. Ther Adv Urol. 2012 Oct;4(5):233-51. PMID: 23024705.

Jeong I, Yoon SH, Hahn SJ. Effects of dapoxetine on cloned Kv1.5 channels expressed in CHO cells. Naunyn Schmiedebergs Arch Pharmacol. 2012 Jul;385(7):707-16. PMID: 22568341.

Jeong I, Kim SW, Yoon SH, et al. Block of cloned Kv4.3 potassium channels by dapoxetine. Neuropharmacology. 2012 Jun;62(7):2261-6. PMID: 22192593.

D0260

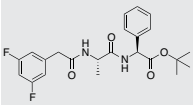

DAPT

NEW

5 mg
25 mg

GSI-IX

$C_{23}H_{26}F_2N_2O_4$ FW: 432.47 [208255-80-5] ≥98%

Inhibitor of γ-secretase and Notch signaling. It inhibits proliferation of cancer stem cells.

Liu J, Mao Z, Huang J, et al. Blocking the NOTCH pathway can inhibit the growth of CD133-positive A549 cells and sensitize to chemotherapy. Biochem Biophys Res Commun. 2014 Feb 21;444(4):670-5. PMID: 24502949.

D0363

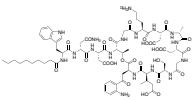

Daptomycin

25 mg
100 mg

$C_{72}H_{101}N_{17}O_{26}$ FW: 1620.67 [103060-53-3] ≥90%

Cell membrane organization modulator used to treat gram positive bacterial infections. It prevents cell wall synthesis and induces release of intracellular Ca^{2+}.

Pogliano J, Pogliano N, Silverman JA. Daptomycin-mediated reorganization of membrane architecture causes mislocalization of essential cell division proteins. J Bacteriol. 2012 Sep;194(17):4494-504. PMID: 22661688.

Vilhena C, Bettencourt A. Daptomycin: a review of properties, clinical use, drug delivery and resistance. Mini Rev Med Chem. 2012 Mar;12(3):202-9. PMID: 22356191

D0169

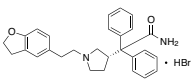

Darifenacin Hydrobromide

10 mg
25 mg
100 mg

$C_{28}H_{30}N_2O_2 \cdot HBr$ FW: 507.46 [133099-07-7] ≥98%

M3 mAChR antagonist used to treat overactive bladder. It inhibits smooth muscle contraction.

Matsumoto Y, Miyazato M, Yokoyama H, et al. Role of M2 and M3 muscarinic acetylcholine receptor subtypes in activation of bladder afferent pathways in spinal cord injured rats. Urology. 2012 May;79(5):1184.e15-20. PMID: 22386753.

Hegde SS. Muscarinic receptors in the bladder: from basic research to therapeutics. Br J Pharmacol. 2006 Feb;147 Suppl 2:S80-7. PMID: 16465186.

D0375

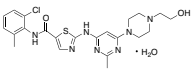

Dasatinib Monohydrate

10 mg
25 mg
100 mg
500 mg

$C_{22}H_{26}ClN_7O_2S \cdot H_2O$ FW: 506.02 [863127-77-9] ≥98%

Inhibitor of Abl, PDGFR, EphR, Src, k-Kit, FYN, LCK, and HCK clinically used to treat leukemias. It induces myeloid differentiation and autophagy in acute myelogenous leukemia cells. It also inhibits dengue virus infection.

Xie N, Zhong L, Liu L, et al. Autophagy contributes to dasatinib-induced myeloid differentiation of human acute myeloid leukemia cells. Biochem Pharmacol. 2014 May 1;89(1):74-85. PMID: 24607273.

de Wispelaere M, LaCroix AJ, Yang PL. The small molecules AZD0530 and dasatinib inhibit dengue virus RNA replication via Fyn kinase. J Virol. 2013 Jul;87(13):7367-81. PMID: 23616652.

Montero JC, Seoane S, Ocaña A, et al. Inhibition of SRC family kinases and receptor tyrosine kinases by dasatinib: possible combinations in solid tumors. Clin Cancer Res. 2011 Sep 1;17(17):5546-52. PMID: 21670084.

D0182

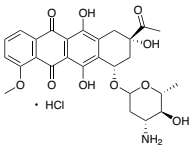

Daunorubicin Hydrochloride

10 mg
50 mg
100 mg

Leukaemomycin C; Rubidomycin; RP-13057

$C_{27}H_{29}NO_{10} \cdot HCl$ FW: 564 [23541-50-6] ≥98%

DNA intercalator and topoisomerase II inhibitor used to treat various cancers. It also promotes histone H2AX eviction from chromatin, inhibiting DNA repair.

Pang B, Qiao X, Janssen L, et al. Drug-induced histone eviction from open chromatin contributes to the chemotherapeutic effects of doxorubicin. Nat Commun. 2013;4:1908. PMID: 23715267.

Quigley GJ, Wang AH, Ughetto G, et al. Molecular structure of an anticancer drug-DNA complex: daunomycin plus d(CpGpTpApCpG). Proc Natl Acad Sci U S A. 1980 Dec;77(12):7204-8. PMID: 6938965.

D0808

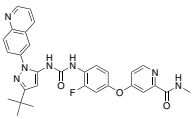

DCC-2036

5 mg
10 mg

Rebastinib

$C_{30}H_{28}FN_7O_3$ FW: 553.59 [1020172-07-9] ≥98%

Abl inhibitor that binds the switch control pocket of Abl that is involved in conformational regulation of the kinase domain. It induces apoptosis in chronic myelogenous leukemia cells.

Shen Y, Shi X, Pan J. The conformational control inhibitor of tyrosine kinases DCC-2036 is effective for imatinib-resistant cells expressing T674I FIP1L1-PDGFRα. PLoS One. 2013 Aug 29;8(8):e73059. PMID: 24009732.

Eide CA, Adrian LT, Tyner JW, et al. The ABL switch control inhibitor DCC-2036 is active against the chronic myeloid leukemia mutant BCR-ABLT315I and exhibits a narrow resistance profile. Cancer Res. 2011 May 1;71(9):3189-95. PMID: 21505103.

D1722

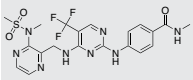

Defactinib

NEW

5 mg
25 mg
100 mg

VS-6063; PF-04554878

$C_{20}H_{21}F_3N_8O_3S$ FW: 510.49 [1073154-85-4] ≥98%

FAK inhibitor. It induces apoptosis and inhibits proliferation of ovarian cancer cells.

Lee BY, Timpson P, Horvath LG, et al. FAK signaling in human cancer as a target for therapeutics. Pharmacol Ther. 2015 Feb;146C:132-149. PMID: 25316657.

Kang Y, Hu W, Ivan C, et al. Role of focal adhesion kinase in regulating YB-1-mediated paclitaxel resistance in ovarian cancer. J Natl Cancer Inst. 2013 Oct 2;105(19):1485-95. PMID: 24062525.

D1621

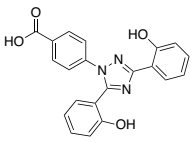

Deferasirox

25 mg
100 mg
250 mg

ICL670A; CGP 72 670

$C_{21}H_{15}N_3O_4$ FW: 373.63 [201530-41-8] ≥98%

Iron chelator used to treat iron-overload disease. It increases expression of metastasis suppressing genes, decreases tumor growth in cancer models, and limits stroke damage in cerebral ischemia models.

Vazana-Barad L, Granot G, Mor-Tzuntz R, et al. Mechanism of the antitumoral activity of deferasirox, an iron chelation agent, on mantle cell lymphoma. Leuk Lymphoma. 2013 Apr;54(4):851-9. PMID: 23020673.

Lui GY, Obeidy P, Ford SJ, et al. The iron chelator, deferasirox, as a novel strategy for cancer treatment: oral activity against human lung tumor xenografts and molecular mechanism of action. Mol Pharmacol. 2013 Jan;83(1):179-90. PMID: 23074173.

Zhao Y, Rempe DA. Prophylactic neuroprotection against stroke: low-dose, prolonged treatment with deferoxamine or deferasirox establishes prolonged neuroprotection independent of HIF-1 function. J Cereb Blood Flow Metab. 2011 Jun;31(6):1412-23. PMID: 21245873.

D1720

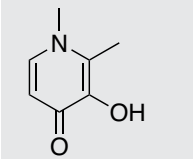

Deferiprone

NEW

5 g
25 g

$C_7H_9NO_2$ FW: 139.15 [30652-11-0] ≥97%

Iron chelator. It decreases plasma iron and cholesterol levels, phosphorylation of tau protein, and levels of amyloid-β, suppresses T cell survival, and reverses iron-overload cardiomyopathy in clinical heart failure.

Prasanthi JR, Schrag M, Dasari B, et al. Deferiprone reduces amyloid-β and tau phosphorylation levels but not reactive oxygen species generation in hippocampus of rabbits fed a cholesterol-enriched diet. J Alzheimers Dis. 2012;30(1):167-82. PMID: 22406440.

Sweeney ME, Slusser JG, Lynch SG, et al. Deferiprone modulates in vitro responses by peripheral blood T cells from control and relapsing-remitting multiple sclerosis subjects. Int Immunopharmacol. 2011 Nov;11(11):1796-801. PMID: 21807124.

Kolnagou A, Michaelides Y, Kontos C, et al. Myocyte damage and loss of myofibers is the potential mechanism of iron overload toxicity in congestive cardiac failure in thalassemia. Complete reversal of the cardiomyopathy and normalization of iron load by deferiprone. Hemoglobin. 2008;32(1-2):17-28. PMID: 18274979.

D1624 Deflazacort

100 mg
250 mg
1 g

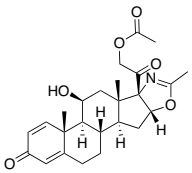

$C_{25}H_{31}NO_6$ FW: 441.52 [14484-47-0] ≥98%

Glucocorticoid receptor agonist used to treat Duchenne muscular dystrophy. It improves motor function, slows disease progression, and decreases the development of myocardial fibrosis.

Hoffman EP, Reeves E, Damsker J, et al. Novel approaches to corticosteroid treatment in Duchenne muscular dystrophy. Phys Med Rehabil Clin N Am. 2012 Nov;23(4):821-8. PMID: 23137739.

Silva EC, Machado DL, Resende MB, et al. Motor function measure scale, steroid therapy and patients with Duchenne muscular dystrophy. Arq Neuropsiquiatr. 2012 Mar;70(3):191-5. PMID: 22392111.

D1731 15,16-Dehydrocafestol

5 mg
10 mg
25 mg

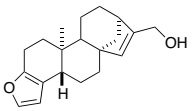

$C_{20}H_{26}O_2$ FW: 298.42 ≥98%

Reduction product of cafestol found in roasted coffee. It potentially inhibits the development of liver fibrosis and induces apoptosis in malignant pleural mesothelioma cells.

Arauz J, Moreno MG, Cortés-Reynosa P, et al. Coffee attenuates fibrosis by decreasing the expression of TGF-β and CTGF in a murine model of liver damage. J Appl Toxicol. 2013 Sep;33(9):970-9. PMID: 22899499.

Lee KA, Chae JI, Shim JH. Natural diterpenes from coffee, cafestol and kahweol induce apoptosis through regulation of specificity protein 1 expression in human malignant pleural mesothelioma. J Biomed Sci. 2012 Jun 26;19:60. PMID: 22734486.

D1631 Dehydrocorydaline NEW

1 mg
5 mg

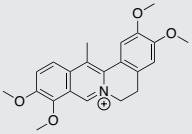

$C_{22}H_{24}NO_4$ FW: 366.43 [30045-16-0] ≥95%

AChE inhibitor found in *Corydalis*. It induces DNA fragmentation in breast cancer cells, inhibits LPS-induced increases in IL-6 and IL-1β in macrophages, and suppresses the development of passive cutaneous anaphylaxis, contact dermatitis, and mast cell degranulation in models of allergies.

Xu Z, Chen X, Fu S, et al. Dehydrocorydaline inhibits breast cancer cells proliferation by inducing apoptosis in MCF-7 cells. Am J Chin Med. 2012;40(1):177-85. Erratum in: Am J Chin Med. 2012;40(6):1323. PMID: 22298457.

Ishiguro K, Ando T, Maeda O, et al. Dehydrocorydaline inhibits elevated mitochondrial membrane potential in lipopolysaccharide-stimulated macrophages. Int Immunopharmacol. 2011 Sep;11(9):1362-7. PMID: 21575743.

D1627 Dehydrocostus Lactone

5 mg
10 mg
25 mg

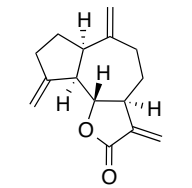

$C_{15}H_{18}O_2$ FW: 230.3 [477-43-0] ≥98%

Sesquiterpene lactone found in *Saussurea*. It exhibits several biological activities, including inhibiting growth of *Mycobacterium*, preventing mitochondrial dysfunction induced by antimycin A, activating cAMP-activated CFTR Cl^- channels, and inducing G0/G1 phase cell cycle arrest and preventing capillary tube formation.

Wang X, Zhang YF, Yu B, et al. Dehydrocostuslactone, a sesquiterpene lactone activates wild-type and ΔF508 mutant CFTR chloride channel. J Asian Nat Prod Res. 2013;15(8):855-66. PMID: 23799322.

Lohberger B, Rinner B, Stuendl N, et al. Sesquiterpene lactones downregulate G2/M cell cycle regulator proteins and affect the invasive potential of human soft tissue sarcoma cells. PLoS One. 2013 Jun 14;8(6):e66300. PMID: 23799090.

Wang CY, Tsai AC, Peng CY, et al. Dehydrocostuslactone suppresses angiogenesis in vitro and in vivo through inhibition of Akt/GSK-3β and mTOR signaling pathways. PLoS One. 2012;7(2):e31195. PMID: 22359572.

D1629 Dehydroepiandrosterone

5 g
25 g
100 g

Prasterone; DHEA; Androstenolone

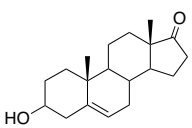

$C_{19}H_{28}O_2$ FW: 288.42 [53-43-0] ≥98%

Endogenous steroid hormone that acts as an agonist at ERβ, NMDA, and σ1 receptors, a partial agonist at ERα and AR, and antagonist at GABA-A receptors. It displays a variety of biological activities, including enhancing working memory and cognition, inhibiting proliferation and migration of cervical cancer cells, increasing expression of various glutamate transporters to suppress seizures, and minimizing gastric acid secretion, lipid peroxidation, and ulcer formation.

do Vale S, Selinger L, Martins JM, et al. The relationship between dehydroepiandrosterone (DHEA), working memory and distraction--a behavioral and electrophysiological approach. PLoS One. 2014 Aug 8;9(8):e104869. PMID: 25105970.

Ortega-Calderón YN, López-Marure R. Dehydroepiandrosterone inhibits proliferation and suppresses migration of human cervical cancer cell lines. Anticancer Res. 2014 Aug;34(8):4039-44. PMID: 25075027.

Xu L, Xiang X, Ji X, et al. Effects and mechanism of dehydroepiandrosterone on epithelial-mesenchymal transition in bronchial epithelial cells. Exp Lung Res. 2014 Jun;40(5):211-21. PMID: 24784499.

D1628

5,6-Dehydrokawain

5 mg
10 mg

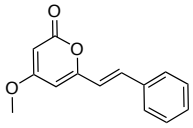

$C_{14}H_{12}O_3$ FW: 228.25 [1952-41-6] ≥98%

Found in *Piper methysticum* (kava plant). It inhibits aggregation and ATP release of platelets, thromboxane B2 formation, and H_2O_2-induced oxidative stress.

Rao YK, Shih HN, Lee YC, et al. Purification of kavalactones from Alpinia zerumbet and their protective actions against hydrogen peroxide-induced cytotoxicity in PC12 cells. J Biosci Bioeng. 2014 Jun 11. [Epub ahead of print]. PMID: 24929995.

Teng CM, Hsu SY, Lin CH, et al. Antiplatelet action of dehydrokawain derivatives isolated from Alpinia speciosa rhizoma. Chin J Physiol. 1990;33(1):41-8. PMID: 2376215.

D1643

Delta Sleep Inducing Peptide

1 mg
2 mg
5 mg

H-Trp-Ala-Gly-Gly-Asp-Ala-Ser-Gly-Glu-OH

$C_{35}H_{48}N_{10}O_{15}$ FW: 848.83 [62568-57-4] ≥95%

GABA signaling potentiator and NMDA receptor negative allosteric modulator. It decreases the incidence, severity, and duration of metaphit-induced seizures, inhibits non-enzymatic glycosylation of hemoglobin, and suppresses expression of HSP70 in myoleukemia cells.

Bondarenko TI, Sorokina IA, Mayboroda EA, et al. Effect of delta sleep-inducing peptide on oxidative modification of proteins in rat tissues and blood during physiological aging. Bull Exp Biol Med. 2012 Jul;153(3):371-4. PMID: 22866315.

D1746

Deltarasin Hydrochloride Trihydrate

NEW

5 mg
10 mg

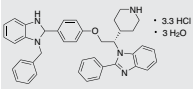

$C_{40}H_{37}N_5O$ • 3.3HCl • $3H_2O$ FW: 778.1 [1440898-82-7] ≥98%

PDEδ inhibitor and indirect K-Ras inhibitor that binds PDEδ at the farnesyl binding pocket. It inhibits proliferation in pancreatic ductal adenocarcinoma cells.

Zimmermann G, Schultz-Fademrecht C, Küchler P, et al. Structure guided design and kinetic analysis of highly potent benzimidazole inhibitors targeting the PDEδ prenyl binding site. J Med Chem. 2014 Jun 26;57(12):5435-48. PMID: 24884780.

Zimmermann G, Papke B, Ismail S, et al. Small molecule inhibition of the KRAS-PDEδ interaction impairs oncogenic KRAS signalling. Nature. 2013 May 30;497(7451):638-42. PMID: 23698361.

D1644

Deltorphin I

5 mg
10 mg
25 mg

Deltorphin C

Tyr-D-Ala-Phe-Asp-Val-Val-Gly-NH_2

$C_{37}H_{52}N_8O_{10}$ FW: 768.87 [122752-15-2] ≥98%

δOR agonist that decreases nociception and stimulates proliferation, migration, adhesion, and tube formation.

Dai X, Song HJ, Cui SG, et al. The stimulative effects of endogenous opioids on endothelial cell proliferation, migration and angiogenesis in vitro. Eur J Pharmacol. 2010 Feb 25;628(1-3):42-50. PMID: 19932695.

D1748

Demeclocycline Hydrochloride

100 mg
250 mg
1 g

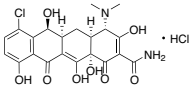

$C_{21}H_{21}ClN_2O_8$ • HCl FW: 501.3 [64-73-3] ≥85%

Protein translation inhibitor and potential calpain inhibitor used to treat bacterial infections. It also decreases expression of aquaporin 2 (AQP2) and adenylate cyclase 5/6 to prevent hyponatremia in SIADH and suppresses glutamate-induced neuronal death in models of cerebral ischemia.

Kortenoeven ML, Sinke AP, Hadrup N, et al. Demeclocycline attenuates hyponatremia by reducing aquaporin-2 expression in the renal inner medulla. Am J Physiol Renal Physiol. 2013 Dec 15;305(12):F1705-18. PMID: 24154696.

Jiang SX, Lertvorachon J, Hou ST, et al. Chlortetracycline and demeclocycline inhibit calpains and protect mouse neurons against glutamate toxicity and cerebral ischemia. J Biol Chem. 2005 Oct 7;280(40):33811-8. PMID: 16091365.

D1749

Demecolcine

1 mg
5 mg
10 mg
50 mg

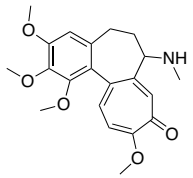

$C_{21}H_{25}NO_5$ FW: 371.43 [477-30-5] ≥97%

Microtubule polymerization inhibitor used to study embryonic cloning. It forces ejection of the nucleus.

Yang H, Ganguly A, Cabral F. Inhibition of cell migration and cell division correlates with distinct effects of microtubule inhibiting drugs. J Biol Chem. 2010 Oct 15;285(42):32242-50. PMID: 20696757.

Lan GC, Wu YG, Han D, et al. Demecolcine-assisted enucleation of goat oocytes: protocol optimization, mechanism investigation, and application to improve the developmental potential of cloned embryos. Cloning Stem Cells. 2008 Jun;10(2):189-202. PMID: 18373477.

D1849

4'-Demethylepipodophyllotoxin

500 mg
1 g
5 g

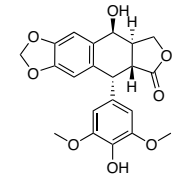

$C_{21}H_{20}O_8$ FW: 400.38 [6559-91-7] ≥98%

Podophyllotoxin derivative and topoisomerase II inhibitor found in *Podophyllum*. It may inhibit proliferation of cancer cells.

Xiao L, Zhao W, Li HM, et al. Design and synthesis of the novel DNA topoisomerase II inhibitors: esterification and amination substituted 4'-demethylepipodophyllotoxin derivates exhibiting anti-tumor activity by activating ATM/ATR signaling pathways. Eur J Med Chem. 2014 Jun 10;80:267-77. PMID: 24793877.

Yang TM, Guo SF, Chen CR, et al. Anti-osteosarcoma effects and mechanisms of 4-O-amino-phenol-4'-demethyl-epipodophyllotoxin ether. J Pharm Pharmacol. 2008 Feb;60(2):179-88. PMID: 18237465.

D1850

Demethoxycurcumin

5 mg
10 mg
25 mg

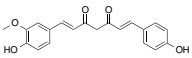

$C_{20}H_{18}O_5$ FW: 338.35 [24939-17-1] ≥98%

Curcumin derivative, AMPK activator, STAT3 and eIF4E-BP3 inhibitor, and potential AChE and EGFR inhibitor. It inhibits proliferation, migration, and invasion in cancer cells, suppresses phosphorylation of tau, and prevents migration of vascular smooth muscle cells.

Sheu MJ, Lin HY, Yang YH, et al. Demethoxycurcumin, a major active curcuminoid from Curcuma longa, suppresses balloon injury induced vascular smooth muscle cell migration and neointima formation: an in vitro and in vivo study. Mol Nutr Food Res. 2013 Sep;57(9):1586-97. PMID: 23520190.

Shieh JM, Chen YC, Lin YC, et al. Demethoxycurcumin inhibits energy metabolic and oncogenic signaling pathways through AMPK activation in triple-negative breast cancer cells. J Agric Food Chem. 2013 Jul 3;61(26):6366-75. PMID: 23777448.

Villaflores OB, Chen YJ, Chen CP, et al. Curcuminoids and resveratrol as anti-Alzheimer agents. Taiwan J Obstet Gynecol. 2012 Dec;51(4):515-25. PMID: 23276553.

D1757

L-Deoxyalliin

100 mg
250 mg
1 g
5 g

S-Allylcysteine

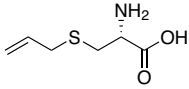

$C_6H_{11}NO_2S$ FW: 161.22 [21593-77-1] ≥98%

Found in garlic. It inhibits growth of *Staphylococcus*, *Escherichia*, and *Pseudomonas* when complexed with Pd(III). It may also induce phase II enzyme activity.

Spera MB, Quintão FA, Ferraresi DK, et al. Palladium(II) complex with S-allyl-L-cysteine: new solid-state NMR spectroscopic measurements, molecular modeling and antibacterial assays. Spectrochim Acta A Mol Biomol Spectrosc. 2011 Jan;78(1):313-8. PMID: 21050807.

Arnault I, Christidès JP, Mandon N, et al. High-performance ion-pair chromatography method for simultaneous analysis of alliin, deoxyalliin, allicin and dipeptide precursors in garlic products using multiple mass spectrometry and UV detection. J Chromatogr A. 2003 Mar 28;991(1):69-75. PMID: 12703902.

D1859

2-Deoxy-D-glucose

1 g
5 g
25 g

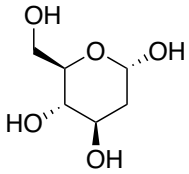

$C_6H_{12}O_5$ FW: 164.16 [154-17-6] ≥98%

Inhibitor of glucose metabolism and N-linked glycosylation used as a biomarker of glucose metabolism, hypoxia, and angiogenesis. It also mimics glucose deprivation and induces cell death in cancer cells.

Kaira K, Murakami H, Endo M, et al. Biological correlation of (18)F-FDG uptake on PET in pulmonary neuroendocrine tumors. Anticancer Res. 2013 Oct;33(10):4219-28. PMID: 24122985.

Andresen L, Skovbakke SL, Persson G, et al. 2-deoxy D-glucose prevents cell surface expression of NKG2D ligands through inhibition of N-linked glycosylation. J Immunol. 2012 Feb 15;188(4):1847-55. PMID: 22227571.

Shutt DC, O'Dorisio MS, Aykin-Burns N, et al. 2-deoxy-D-glucose induces oxidative stress and cell killing in human neuroblastoma cells. Cancer Biol Ther. 2010 Jun 1;9(11):853-61. PMID: 20364116.

D1759

Deoxynivalenol

1 mg
5 mg

Vomitoxin

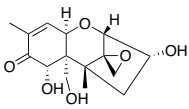

$C_{15}H_{20}O_6$ FW: 296.32 [51481-10-8] ≥98%

Mycotoxin found in *Fusarium*. It increases the formation of pores in the intestinal epithelial barrier of the jejunum, upregulates expression of pro-inflammatory cytokines, and induces apoptosis.

Ovando-Martínez M, Ozsisli B, Anderson J, et al. Analysis of deoxynivalenol and deoxynivalenol-3-glucoside in hard red spring wheat inoculated with *Fusarium* graminearum. Toxins (Basel). 2013 Dec 17;5(12):2522-32. PMID: 24351715.

Nossol C, Diesing AK, Kahlert S, et al. Deoxynivalenol affects the composition of the basement membrane proteins and influences en route the migration of CD16(+) cells into the intestinal epithelium. Mycotoxin Res. 2013 Nov;29(4):245-54. PMID: 23949948.

He K, Zhou HR, Pestka JJ. Targets and intracellular signaling mechanisms for deoxynivalenol-induced ribosomal RNA cleavage. Toxicol Sci. 2012 Jun;127(2):382-90. PMID: 22491426.

D1760

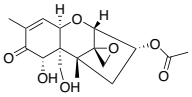

3-Acetyl-deoxynivalenol

1 mg
5 mg

3α-Acetylvomitoxin; 3-Acetyl DON; Deoxynivalenol monoacetate; NSC 26703

$C_{17}H_{22}O_7$ FW: 338.35 [50722-38-8 ≥98%

Mycotoxin found in *Fusarium*. It induces apoptosis in Jurkat T cells, modulates expression of IL-2, IL-4, and IL-5, and inhibits the plaque-forming cell response.

Puri KD, Zhong S. The 3ADON population of *Fusarium* graminearum found in North Dakota is more aggressive and produces a higher level of DON than the prevalent 15ADON population in spring wheat. Phytopathology. 2010 Oct;100(10):1007-14. PMID: 20839936.

Monbaliu S, Van Poucke C, Detavernier C, et al. Occurrence of mycotoxins in feed as analyzed by a multi-mycotoxin LC-MS/MS method. J Agric Food Chem. 2010 Jan 13;58(1):66-71. PMID: 19994896.

Gottschalk C, Barthel J, Engelhardt G, et al. Occurrence of type A trichothecenes in conventionally and organically produced oats and oat products. Mol Nutr Food Res. 2007 Dec;51(12):1547-53. PMID: 18030660.

D1761

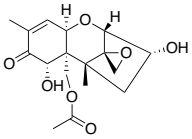

15-Acetyl-deoxynivalenol

1 mg
5 mg

15-A-DON

$C_{17}H_{22}O_7$ FW: 338.35 [88337-96-6] ≥98%

Mycotoxin found in *Fusarium*. It induces apoptosis in Jurkat T cells and modulates expression of IL-2, IL-4, and IL-5.

Puri KD, Zhong S. The 3ADON population of *Fusarium* graminearum found in North Dakota is more aggressive and produces a higher level of DON than the prevalent 15ADON population in spring wheat. Phytopathology. 2010 Oct;100(10):1007-14. PMID: 20839936.

Monbaliu S, Van Poucke C, Detavernier C, et al. Occurrence of mycotoxins in feed as analyzed by a multi-mycotoxin LC-MS/MS method. J Agric Food Chem. 2010 Jan 13;58(1):66-71. PMID: 19994896.

D1869

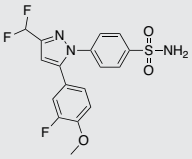

Deracoxib

NEW

10 mg
25 mg
100 mg

$C_{17}H_{14}F_3N_3O_3S$ FW: 397.37 [169590-41-4] ≥98%

NSAID and COX-2 inhibitor used to treat osteoarthritis. It induces cell cycle arrest and apoptosis in mammary tumor cells, decreases platelet aggregation, and lowers inflammatory responses.

Ustün Alkan F, Ustüner O, et al. The effects of piroxicam and deracoxib on canine mammary tumour cell line. ScientificWorldJournal. 2012;2012:976740. PMID: 23251109.

Bienhoff SE, Smith ES, Roycroft LM, et al. Efficacy and safety of deracoxib for control of postoperative pain and inflammation associated with soft tissue surgery in dogs. Vet Surg. 2012 Apr;41(3):336-44. PMID: 22225463.

McMillan SK, Boria P, Moore GE, et al. Antitumor effects of deracoxib treatment in 26 dogs with transitional cell carcinoma of the urinary bladder. J Am Vet Med Assoc. 2011 Oct 15;239(8):1084-9. PMID: 21985349.

D1768

Ala-Leu-Trp-Lys-Thr-Met-Leu-Lys-Lys-Leu-Gly-Thr-Met-Ala-Leu-His-Ala-Gly-Lys-Ala-Leu-Gly-Ala-Ala-Ala-Ala-Asp-ThrIle-Ser-Gln-Gly-Thr-Gln

Dermaseptin I

0.5 mg
1 mg
2.5 mg

$C_{152}H_{257}N_{43}O_{44}S_2$ FW: 3455.08 ≥96%

It alters bacterial membrane permeability and suppresses growth of *Acinetobacter* and *Pseudomonas*. It also inhibits capillary formation and tumor growth in prostate cancer models.

Jiang Z, Vasil AI, Vasil ML, et al. "Specificity Determinants" Improve Therapeutic Indices of Two Antimicrobial Peptides Piscidin 1 and Dermaseptin S4 Against the Gram-negative Pathogens *Acinetobacter* baumannii and *Pseudomonas* aeruginosa. Pharmaceuticals (Basel). 2014 Mar 25;7(4):366-91. PMID: 24670666.

Caillon L, Killian JA, Lequin O, et al. Biophysical investigation of the membrane-disrupting mechanism of the antimicrobial and amyloid-like peptide dermaseptin S9. PLoS One. 2013 Oct 11;8(10):e75528. PMID: 24146759.

D1767

H-Tyr-D-Met-Phe-His-Leu-Met-Asp-NH_2

Dermenkephalin

1 mg
2 mg
5 mg

$C_{44}H_{62}N_{10}O_{10}S_2$ FW: 955.17 ≥95%

Exogenous δOR-2 agonist. It increases pain response latency and induces conditioned place preference in animal models previously administered ethanol or cocaine.

Mitchell JM, Margolis EB, Coker AR, et al. Intra-VTA deltorphin, but not DPDPE, induces place preference in ethanol-drinking rats: distinct DOR-1 and DOR-2 mechanisms control ethanol consumption and reward. Alcohol Clin Exp Res. 2014 Jan;38(1):195-203. PMID: 24033469.

D1769

Tyr-D-Ala-Phe-Gly-Tyr-Pro-Ser-NH_2

Dermorphin

1 mg
2 mg
5 mg

$C_{40}H_{50}N_8O_{10}$ FW: 802.88 [77614-16-5] ≥96%

μOR agonist that increases pain thresholds in thermal, mechanical, and chemical pain models.

Mizoguchi H, Bagetta G, Sakurada T, et al. Dermorphin tetrapeptide analogs as potent and long-lasting analgesics with pharmacological profiles distinct from morphine. Peptides. 2011 Feb;32(2):421-7. PMID: 21126548.

Guzevatykh LS, Voronina TA, Emel'ianova TG, et al. Comparative analysis of analgesic activities of dermorphin, [DPro6]-dermorphin, and their C-terminal tripeptides. Izv Akad Nauk Ser Biol. 2007 Sep-Oct;(5):577-82. PMID: 18038625.

D1770

Dermorphin Analog

5 mg
10 mg
25 mg

$C_{44}H_{59}N_{11}O_{10}$ FW: 902.03 ≥95%

H-Tyr-D-Arg-Phe-Sar-Tyr-Pro-Ser-NH_2

Synthetic dermorphin analog and δOR and μOR agonist. It alters learning and memory, increases motor activity, and decreases pain nociception.

Vonhof S, Barone FC, Price WJ, et al. Receptor binding and biological activity of the dermorphin analog Tyr-D-Arg(2)-Phe-Sar (TAPS). Eur J Pharmacol. 2001 Mar 23;416(1-2):83-93. PMID: 11282116.

Ukai M, Kobayashi T, Mori K, et al. Attenuation of memory with Tyr-D-Arg-Phe-beta-Ala-NH2, a novel dermorphin analog with high affinity for mu-opioid receptors. Eur J Pharmacol. 1995 Dec 20;287(3):245-9. PMID: 8991797.

D1872

Des(benzylpyridyl) Atazanavir

NEW

5 mg
10 mg
25 mg

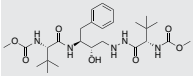

$C_{26}H_{43}N_5O_7$ FW: 537.66 [1192224-24-0] ≥98%

Dealkylated metabolite of atazanavir and inhibitor of HIV protease.

ter Heine R, Hillebrand MJ, Rosing H, et al. Identification and profiling of circulating metabolites of atazanavir, a HIV protease inhibitor. Drug Metab Dispos. 2009 Sep;37(9):1826-40. PMID: 19546238.

D1773

Deshydroxy LY-411575

NEW

5 mg
25 mg

YO-01027; Dibenzazepine

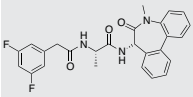

$C_{26}H_{23}F_2N_3O_3$ FW: 463.48 [209984-56-5] ≥98%

Inhibitor of γ-secretase and Notch signaling. It improves glucose tolerance and insulin response, suppresses the development of fibrosis in models of chronic kidney disease, and inhibits the formation of abdominal aortic aneurysms in aging models.

Petersen N, Reimann F, van Es JH, et al. Targeting development of incretin-producing cells increases insulin secretion. J Clin Invest. 2015 Jan;125(1):379-85. PMID: 25500886.

Xiao Z, Zhang J, Peng X, et al. The Notch γ-secretase inhibitor ameliorates kidney fibrosis via inhibition of TGF-β/Smad2/3 signaling pathway activation. Int J Biochem Cell Biol. 2014 Oct;55:65-71. PMID: 25150830.

Zheng YH, Li FD, Tian C, et al. Notch γ-secretase inhibitor dibenzazepine attenuates angiotensin II-induced abdominal aortic aneurysm in ApoE knockout mice by multiple mechanisms. PLoS One. 2013 Dec 16;8(12):e83310. PMID: 24358274.

D1774

Desloratadine

100 mg
500 mg
1 g

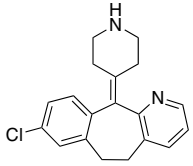

$C_{19}H_{19}ClN_2$ FW: 310.82 [100643-71-8] ≥97%

Loratadine metabolite, FIASMA, and histamine H1 receptor antagonist used to treat allergic rhinitis and chronic idiopathic urticaria. It is non-sedative and decreases allergy-related inflammation and immune responses.

Doetkotte R, Opitz K, Kiianmaa K, et al. Reduction of voluntary ethanol consumption in alcohol-preferring Alko alcohol (AA) rats by desoxypeganine and galanthamine. Eur J Pharmacol. 2005 Oct 17;522(1-3):72-7. PMID: 16209867.

Glass DJ, Harper AS. Assessing satisfaction with desloratadine and fexofenadine in allergy patients who report dissatisfaction with loratadine. BMC Fam Pract. 2003 Aug 13;4:10. PMID: 12917016.

D1775

Deslorelin Acetate

Please inquire

$C_{64}H_{83}N_{17}O_{12}$ FW: 1282.47 [57773-65-6] ≥95%

Pyr-His-Trp-Ser-Tyr-D-Trp-Leu-Arg-Pro-NHEt

GnRH receptor agonist used to treat BPH and control fertility. It decreases testosterone levels, instills sterility in male subjects, and induces estrous in female subjects.

Marino G, Rizzo S, Quartuccio M, et al. Deslorelin Implants in Pre-pubertal Female Dogs: Short- and Long-Term Effects on the Genital Tract. Reprod Domest Anim. 2014 Apr;49(2):297-301. PMID: 24467617.

Goericke-Pesch S, Georgiev P, Fasulkov I, et al. Basal testosterone concentrations after the application of a slow-release GnRH agonist implant are associated with a loss of response to buserelin, a short-term GnRH agonist, in the tom cat. Theriogenology. 2013 Jul 1;80(1):65-9. PMID: 23622940.

D1776

Desmopressin

1 mg
2 mg
5 mg

$C_{46}H_{64}N_{14}O_{12}S_2$ FW: 1069.1 [16679-58-6] ≥95%

Map-Tyr-Phe-Gln-Asn-Cys-Pro-D-Arg-Gly-NH_2
(Disulfide bridge, Map1-Cys6)

Synthetic vasopressin derivative and V2R agonist used to treat bleeding disorders. It enhances platelet coagulant activity and thrombin generation.

Colucci G, Stutz M, Rochat S, et al. The effect of desmopressin on platelet function: a selective enhancement of procoagulant COAT-platelets in patients with primary platelet function defects. Blood. 2014 Jan 17. [Epub ahead of print]. PMID: 24443440.

Leissinger C, Carcao M, Gill JC, et al. Desmopressin (DDAVP) in the management of patients with congenital bleeding disorders. Haemophilia. 2014 Mar;20(2):158-67. PMID: 23937614.

D1777

Desmopressin Acetate

1 mg
2 mg
5 mg

$C_{46}H_{64}N_{14}O_{12}S_2$ FW: 1069.24 [16679-58-6] ≥95%

c[Mpr-Tyr-Phe-Gln-Asn-Cys]-Pro-D-Arg-Gly-NH_2

Synthetic vasopressin derivative and V2 receptor agonist used to treat bleeding disorders. It increases platelet-dependent thrombin generation and pro-coagulant activity.

Colucci G, Stutz M, Rochat S, et al. The effect of desmopressin on platelet function: a selective enhancement of procoagulant COAT-platelets in patients with primary platelet function defects. Blood. 2014 Jan 17. [Epub ahead of print]. PMID: 24443440.

Leissinger C, Carcao M, Gill JC, et al. Desmopressin (DDAVP) in the management of patients with congenital bleeding disorders. Haemophilia. 2014 Mar;20(2):158-67. PMID: 23937614.

D0368

2-Epi-16-deoxysarcophine

10 mg

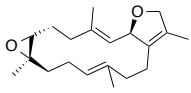

$C_{20}H_{30}O_2$ FW: 302.45 ≥98%

Found in *Sarcophyton*. It inhibits metastasis in melanoma cells.

Sawant SS, Youssef DT, Reiland J, et al. Biocatalytic and antimetastatic studies of the marine cembranoids sarcophine and 2-epi-16-deoxysarcophine. J Nat Prod. 2006 Jul;69(7):1010-3. PMID: 16872134.

D1874

Desvenlafaxine Succinate

100 mg
250 mg
1 g

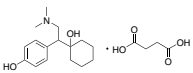

$C_{16}H_{25}NO_2 \cdot C_5H_8O_4$ FW: 395.49 [386750-22-7] ≥98%

Venlafaxine metabolite and inhibitor of SERT and NET used to treat depression. It also alters rates of gastric emptying and decreases symptoms of menopausal hot flashes.

Song J, Yin J, Chen JD. Acute and chronic effects of desvenlafaxine on gastrointestinal transit and motility in dogs. Neurogastroenterol Motil. 2013 Jul 19. [Epub ahead of print]. PMID: 23865827.

Sun Z, Hao Y, Zhang M. Efficacy and safety of desvenlafaxine treatment for hot flashes associated with menopause: a meta-analysis of randomized controlled trials. Gynecol Obstet Invest. 2013;75(4):255-62. PMID: 23548358.

DeMartinis NA, Yeung PP, Entsuah R, et al. A double-blind, placebo-controlled study of the efficacy and safety of desvenlafaxine succinate in the treatment of major depressive disorder. J Clin Psychiatry. 2007 May;68(5):677-88. PMID: 17503976.

D1693

Dexamethasone

100 mg
500 mg
1 g

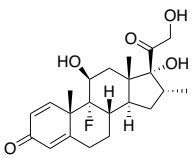

$C_{22}FH_{29}O_5$ FW: 392.46 [50-02-2] ≥97%

Glucocorticoid agonist used to treat respiratory diseases, skin diseases, and multiple myeloma. It decreases secretion of TNF, IL-6, and IL-1β, inhibiting migration and maturation of macrophages. It also upregulates expression of PTEN in models of asthma.

Bartneck M, Peters FM, Warzecha KT, et al. Liposomal encapsulation of dexamethasone modulates cytotoxicity, inflammatory cytokine response, and migratory properties of primary human macrophages. Nanomedicine. 2014 Mar 7. [Epub ahead of print]. PMID: 24607939.

Ni Z, Tang J, Cai Z, et al. A new pathway of glucocorticoid action for asthma treatment through the regulation of PTEN expression. Respir Res. 2011 Apr 14;12:47. PMID: 21489309.

Morgan G. Future drug developments in multiple myeloma: an overview of novel lenalidomide-based combination therapies. Blood Rev. 2010 Nov;24 Suppl 1:S27-32. PMID: 21126634.

D1694

Dexamethasone Acetate Monohydrate

100 mg
500 mg
1 g

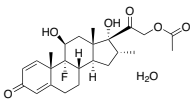

$C_{24}H_{31}FO_6 \cdot H_2O$ FW: 452.52 [55812-90-3] ≥98%

Glucocorticoid receptor agonist used to treat diseases of inflammation and the respiratory system. It decreases secretion of pro-inflammatory cytokines, upregulates expression of PTEN, and inhibits migration and maturation of macrophages.

Bartneck M, Peters FM, Warzecha KT, et al. Liposomal encapsulation of dexamethasone modulates cytotoxicity, inflammatory cytokine response, and migratory properties of primary human macrophages. Nanomedicine. 2014 Mar 7. [Epub ahead of print]. PMID: 24607939.

Ni Z, Tang J, Cai Z, et al. A new pathway of glucocorticoid action for asthma treatment through the regulation of PTEN expression. Respir Res. 2011 Apr 14;12:47. PMID: 21489309.

Morgan G. Future drug developments in multiple myeloma: an overview of novel lenalidomide-based combination therapies. Blood Rev. 2010 Nov;24 Suppl 1:S27-32. PMID: 21126634.

D1695 Dexamethasone Phosphate Sodium

100 mg
500 mg
1 g

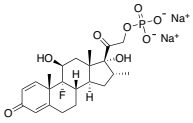

$C_{22}H_{28}FO_8PNa_2$ FW: 516.4 [2392-39-4] ≥98%

Glucocorticoid receptor agonist used to treat diseases of inflammation and the respiratory system. It decreases secretion of pro-inflammatory cytokines, upregulates expression of PTEN, and inhibits migration and maturation of macrophages.

Bartneck M, Peters FM, Warzecha KT, et al. Liposomal encapsulation of dexamethasone modulates cytotoxicity, inflammatory cytokine response, and migratory properties of primary human macrophages. Nanomedicine. 2014 Mar 7. [Epub ahead of print]. PMID: 24607939.

Ni Z, Tang J, Cai Z, et al. A new pathway of glucocorticoid action for asthma treatment through the regulation of PTEN expression. Respir Res. 2011 Apr 14;12:47. PMID: 21489309.

Morgan G. Future drug developments in multiple myeloma: an overview of novel lenalidomide-based combination therapies. Blood Rev. 2010 Nov;24 Suppl 1:S27-32. PMID: 21126634.

D1994 Dexrazoxane

NEW

5 mg
25 mg
100 mg

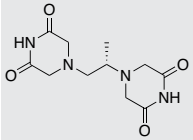

$C_{11}H_6N_4O_4$ FW: 268.27 [24584-09-6] ≥98%

Iron chelator used to prevent anthracycline-induced cardiotoxicity. It decreases infarct size, increases capillary density, and improves cardiac function in models of myocardial infarction and suppresses growth of *Plasmodium*.

Doroshow JH. Dexrazoxane for the prevention of cardiac toxicity and treatment of extravasation injury from the anthracycline antibiotics. Curr Pharm Biotechnol. 2012 Aug;13(10):1949-56. PMID: 22352729.

Zhou L, Sung RY, Li K, et al. Cardioprotective effect of dexrazoxane in a rat model of myocardial infarction: anti-apoptosis and promoting angiogenesis. Int J Cardiol. 2011 Oct 20;152(2):196-201. PMID: 20692056.

Jones RL. Utility of dexrazoxane for the reduction of anthracycline-induced cardiotoxicity. Expert Rev Cardiovasc Ther. 2008 Nov;6(10):1311-7. PMID: 19018683.

D1995 Dexrazoxane Hydrochloride

NEW

5 mg
25 mg
100 mg

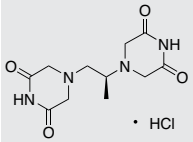

$C_{11}H_{16}N_4O_4 \bullet HCl$ FW: 304.73 [149003-01-0] ≥98%

Iron chelator used to prevent anthracycline-induced cardiotoxicity. It decreases infarct size, increases capillary density, and improves cardiac function in models of myocardial infarction and suppresses growth of *Plasmodium*.

Doroshow JH. Dexrazoxane for the prevention of cardiac toxicity and treatment of extravasation injury from the anthracycline antibiotics. Curr Pharm Biotechnol. 2012 Aug;13(10):1949-56. PMID: 22352729.

Zhou L, Sung RY, Li K, et al. Cardioprotective effect of dexrazoxane in a rat model of myocardial infarction: anti-apoptosis and promoting angiogenesis. Int J Cardiol. 2011 Oct 20;152(2):196-201. PMID: 20692056.

D1792 Dextromethorphan Hydrobromide Hydrate

δ-Methorphan

5 g
10 g
50 g

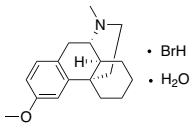

$C_{18}H_{25}NO \bullet HBr \bullet H_2O$ FW: 370.3 [6700-34-1] ≥98%

Agonist at σ1/2 and μ/κ/δ-OR receptors and antagonist at α3β4/α4β2/α7 nAChR, NMDA receptors, SERT, and NET. It is used to treat respiratory cough. It also prevents endotoxin-induced dopaminergic neurodegeneration, suppresses the development of seizures, and inhibits RANKL-induced osteoclastogenesis.

Burns JM, Boyer EW. Antitussives and substance abuse. Subst Abuse Rehabil. 2013 Nov 6;4:75-82. PMID: 24648790.

Wu K, Lin TH, Liou HC, et al. Dextromethorphan inhibits osteoclast differentiation by suppressing RANKL-induced nuclear factor-κB activation. Osteoporos Int. 2013 Aug;24(8):2201-14. PMID: 23400250.

Damaj MI, Flood P, Ho KK, et al. Effect of dextrometorphan and dextrorphan on nicotine and neuronal nicotinic receptors: in vitro and in vivo selectivity. J Pharmacol Exp Ther. 2005 Feb;312(2):780-5. PMID: 15356218.

D3303 Diacerein

Diacetylrhein

50 mg
250 mg

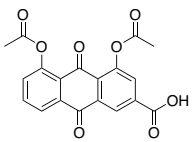

$C_{19}H_{12}O_8$ FW: 368.29 [13739-02-1] ≥98%

IL-1β inhibitor used to treat osteoarthritis. It also suppresses somatic nociception induced by glutamate, NMDA, and kainate and suppresses synthesis of resorptive factors and in osteoclast formation.

Gadotti VM, Martins DF, Pinto HF, et al. Diacerein decreases visceral pain through inhibition of glutamatergic neurotransmission and cytokine signaling in mice. Pharmacol Biochem Behav. 2012 Oct;102(4):549-54. PMID: 22750064.

Boileau C, Tat SK, Pelletier JP, et al. Diacerein inhibits the synthesis of resorptive enzymes and reduces osteoclastic differentiation/survival in osteoarthritic subchondral bone: a possible mechanism for a protective effect against subchondral bone remodelling. Arthritis Res Ther. 2008;10(3):R71. PMID: 18578867.

D3200 Diacetoxyscirpenol

1 mg
5 mg

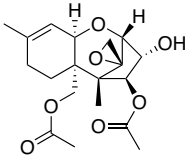

Anguidine

$C_{19}H_{26}O_7$ FW: 366.41 [2270-40-8] ≥98%

Mycotoxin found in *Fusarium*. It induces apoptosis in Jurkat T cells, inhibits the killing action of phagocytic cells, alters lysozyme abilities, and displays some cytotoxicity in more tissues and cell types.

Jun DY, Kim JS, Park HS, et al. Cytotoxicity of diacetoxyscirpenol is associated with apoptosis by activation of caspase-8 and interruption of cell cycle progression by down-regulation of cdk4 and cyclin B1 in human Jurkat T cells. Toxicol Appl Pharmacol. 2007 Jul 15;222(2):190-201. PMID: 17559898.

Nasri T, Bosch RR, Voorde St, et al. Differential induction of apoptosis by type A and B trichothecenes in Jurkat T-lymphocytes. Toxicol In Vitro. 2006 Sep;20(6):832-40. PMID: 16472964.

D3201 Diallyl Sulfide

25 ml
100 ml

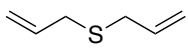

Diallyl thioether

$C_6H_{10}S$ FW: 114.21 [592-88-1] ≥97%

Found in garlic. It exhibits a variety of activities, including decreasing DES-induced DNA damage and carcinogenesis, inducing phase II enzyme activity, and VEGF levels, microvessel density, cellular invasion, and tumor growth in osteosarcoma models.

McCaskill ML, Rogan E, D Thomas R. Diallyl sulfide inhibits diethylstilbestrol induced DNA damage in human breast epithelial cells (MCF-10A). Steroids. 2014 Sep 30. [Epub ahead of print]. PMID: 25278253.

Ho CY, Weng CJ, Jhang JJ, et al. Diallyl sulfide as a potential dietary agent to reduce TNF-α- and histamine-induced proinflammatory responses in A7r5 cells. Mol Nutr Food Res. 2014 May;58(5):1069-78. PMID: 24415531.

Hu Y, Chen L, Yi C, et al. Experimental study on inhibitory effects of diallyl sulfide on growth and invasion of human osteosarcoma MG-63 cells. J Huazhong Univ Sci Technolog Med Sci. 2012 Aug;32(4):581-5. PMID: 22886974.

D3203 Diallyl Tetrasulfide

5 mg
25 mg
100 mg

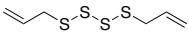

$C_6H_{10}S_4$ FW: 210.4 [2444-49-7] ≥90%

Synthetic microtubule polymerization inhibitor found in garlic. It induces mitotic arrest, suppresses growth of *Staphylococcus*, *Candida*, and *Aspergillus*, and decreases cadmium-mediated oxidative damage.

Saidu NE, Abu Asali I, Czepukojc B, et al. Comparison between the effects of diallyl tetrasulfide on human retina pigment epithelial cells (ARPE-19) and HCT116 cells. Biochim Biophys Acta. 2013 Nov;1830(11):5267-76. PMID: 23948592.

Kelkel M, Cerella C, Mack F, et al. ROS-independent JNK activation and multisite phosphorylation of Bcl-2 link diallyl tetrasulfide-induced mitotic arrest to apoptosis. Carcinogenesis. 2012 Nov;33(11):2162-71. PMID: 22822094.

Ponnusamy M, Pari L. Protective role of diallyl tetrasulfide on cadmium-induced testicular damage in adult rats: a biochemical and histological study. Toxicol Ind Health. 2011 Jun;27(5):407-16. PMID: 21245201.

D3202 Diallyl Trisulfide

100 mg
500 mg
1 g

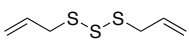

DATS

$C_6H_{10}S_3$ FW: 178.34 [2050-87-5] ≥98%

Synthetic compound found in garlic. It exhibits a wide variety of biological activities, including increasing phase II enzyme activity, decreasing collagen deposition and fibrosis, suppressing angiogenesis in osteosarcoma cells, and inducing cell cycle arrest and apoptosis in leukemia cells.

Suda S, Watanabe K, Tanaka Y, et al. Identification of molecular target of diallyl trisulfide in leukemic cells. Biosci Biotechnol Biochem. 2014;78(8):1415-7. PMID: 25130746.

Sumedha N, Miltonprabu S. Diallyl trisulfide ameliorates arsenic-induced hepatotoxicity by abrogation of oxidative stress, inflammation, and apoptosis in rats. Hum Exp Toxicol. 2014 Jul 25. [Epub ahead of print]. PMID: 25062976.

Hung FM, Shang HS, Tang NY, et al. Effects of diallyl trisulfide on induction of apoptotic death in murine leukemia WEHI-3 cells in vitro and alterations of the immune responses in normal and leukemic mice in vivo. Environ Toxicol. 2014 May 28. [Epub ahead of print]. PMID: 24890016.

D3301 Diaveridine

250 mg
1 g
10 g

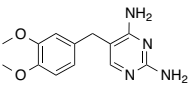

$C_{13}H_{16}N_4O_2$ FW: 260.29 [5355-16-8] ≥98%

Coccidiostat and dihydrofolate reductase inhibitor. It prevents folic acid synthesis in species of *Pneumocystis* and induces DNA damage.

Ono T, Sekiya T, Takahashi Y, et al. The genotoxicity of diaveridine and trimethoprim. Environ Toxicol Pharmacol. 1997 Sep;3(4):297-306. PMID: 21781790.

Cirioni O, Giacometti A, Scalise G. In-vitro activity of atovaquone, sulphamethoxazole and dapsone alone and combined with inhibitors of dihydrofolate reductase and macrolides against Pneumocystis carinii. J Antimicrob Chemother. 1997 Jan;39(1):45-51. PMID: 9044027.

D3302 Diaveridine Hydrochloride

250 mg
1 g
10 g

$C_{13}H_{16}N_4O_2 \bullet HCl$ FW: 296.74 ≥98%

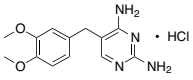

Coccidiostat and dihydrofolate reductase inhibitor. It prevents folic acid synthesis in species of *Pneumocystis* and induces DNA damage.

Ono T, Sekiya T, Takahashi Y, et al. The genotoxicity of diaveridine and trimethoprim. Environ Toxicol Pharmacol. 1997 Sep;3(4):297-306. PMID: 21781790.

Cirioni O, Giacometti A, Scalise G. In-vitro activity of atovaquone, sulphamethoxazole and dapsone alone and combined with inhibitors of dihydrofolate reductase and macrolides against Pneumocystis carinii. J Antimicrob Chemother. 1997 Jan;39(1):45-51. PMID: 9044027.

D3304 Dibenzoylmethane

10 g
25 g
100 g

γ-Hydroxychalkone

$C_{15}H_{12}O_2$ FW: 224.25 [120-46-7] ≥98%

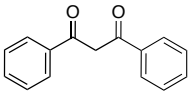

Cytoprotectant found in *Glycyrrhiza* (licorice) used in sunscreen components. It induces cell cycle arrest and inhibits proliferation in prostate cancer cells and activates phase II enzyme expression.

Hegedűs C, Lakatos P, Kiss-Szikszai A, et al. Cytoprotective dibenzoylmethane derivatives protect cells from oxidative stress-induced necrotic cell death. Pharmacol Res. 2013 Jun;72:25-34. PMID: 23523665.

Anand P, Sung B, Kunnumakkara AB, et al. Suppression of pro-inflammatory and proliferative pathways by diferuloylmethane (curcumin) and its analogues dibenzoylmethane, dibenzoylpropane, and dibenzylideneacetone: role of Michael acceptors and Michael donors. Biochem Pharmacol. 2011 Dec 15;82(12):1901-9. PMID: 21924245.

Lin W, Hong JL, Shen G, et al. Pharmacokinetics of dietary cancer chemopreventive compound dibenzoylmethane in rats and the impact of nanoemulsion and genetic knockout of Nrf2 on its disposition. Biopharm Drug Dispos. 2011 Mar;32(2):65-75. PMID: 21341276.

D3208 Diclazuril

500 mg
1 g
5 g

R-64433

$C_{17}H_{10}Cl_2N_4O_2$ FW: 407.64 [101831-37-2] ≥98%

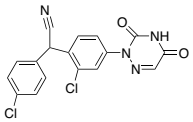

Coccidiostat and GAPDH inhibitor used to prevent parasitic contamination of livestock and poultry feed.

Oz HS, Tobin T. Diclazuril Protects against Maternal Gastrointestinal Syndrome and Congenital Toxoplasmosis. Int J Clin Med. 2014 Jan 1;5(3):93-101. PMID: 24851194.

Wang C, Han C, Li T, et al. Nuclear translocation and accumulation of glyceraldehyde-3-phosphate dehydrogenase involved in diclazuril-induced apoptosis in *Eimeria* tenella (E. tenella). Vet Res. 2013 May 7;44:29. PMID: 23651214.

D3209 Diclofenac Sodium

10 g
25 g
100 g

$C_{14}H_{10}Cl_2NO_2Na$ FW: 318.14 [15307-79-6] ≥98%

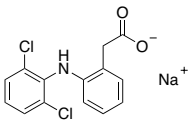

NSAID and inhibitor of COX-1/2 inhibitor used to treat pain and inflammation. It may modulate K^+ channel activity. It also inhibits DMH-induced colon carcinogenesis and suppresses epithelial-to-mesenchymal transition, decreasing squamous cell carcinoma tumor growth.

Arumugam A, Weng Z, Talwelkar SS, et al. Inhibiting cycloxygenase and ornithine decarboxylase by diclofenac and alpha-difluoromethylornithine blocks cutaneous SCCs by targeting Akt-ERK axis. PLoS One. 2013 Nov 8;8(11):e80076. PMID: 24260338.

Akbari E, Mirzaei E, Shahabi Majd N. Long-term Morphine-treated Rats are more Sensitive to Antinociceptive Effect of Diclofenac than the Morphine-naive rats. Iran J Pharm Res. 2013 Winter;12(1):175-84. PMID: 24250586.

Huang CW, Hung TY, Liao YK, et al. Underlying mechanism of regulatory actions of diclofenac, a nonsteroidal anti-inflammatory agent, on neuronal potassium channels and firing: an experimental and theoretical study. J Physiol Pharmacol. 2013 Jun;64(3):269-80. PMID: 23959723.

D3212 2',3'-Dideoxycytidine

25 mg
100 mg
250 mg
500 mg

$C_9H_{13}N_3O_3$ FW: 211.22 [7481-89-2] ≥98%

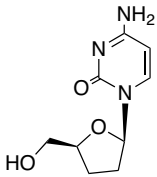

Cytidine analog and inhibitor of RT that terminates DNA chain elongation. It is used to treat HIV infection.

Shelton MJ, O'Donnell AM, Morse GD. Zalcitabine. Ann Pharmacother. 1993 Apr;27(4):480-9. PMID: 8097417.

Balzarini J. Anti-retroviral activity and molecular-biochemical action mechanism of 2',3'-dideoxynucleoside analogs and 9-(2-phosphonylmethoxyethyl) purine derivatives. Verh K Acad Geneeskd Belg. 1991;53(1):61-98. PMID: 1647085.

D3214

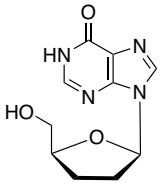

2',3'-Dideoxyinosine

Didanosine; ddI

$C_{10}H_{12}N_4O_3$ FW: 236.23 [69655-05-6] ≥98%

1 mg
5 mg
25 mg

Guanosine analog, DNA chain terminator, and RT inhibitor used to treat HIV infection. It also inhibits the humoral immune response by targeting B lymphocytes.

Ribera E, Tuset M, Martín M, et al. Characteristics of antiretroviral drugs. Enferm Infecc Microbiol Clin. 2011 May;29(5):362-91. PMID: 21531048.

Phillips KE, Munson AE. 2'3'-Dideoxyinosine inhibits the humoral immune response in female B6C3F1 mice by targeting the B lymphocyte. Toxicol Appl Pharmacol. 1997 Aug;145(2):260-7. PMID: 9266798.

D3215

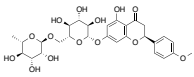

Didymin

Isosakuranetin

$C_{28}H_{34}O_{14}$ FW: 594.56 [14259-47-3] ≥98%

1 mg
5 mg
10 mg

Antioxidant found in citrus fruit. It induces apoptosis in non-small cell lung cancer cells and suppresses tumor growth in neuroblastoma models.

Singhal J, Nagaprashantha LD, Vatsyayan R, et al. Didymin induces apoptosis by inhibiting N-Myc and upregulating RKIP in neuroblastoma. Cancer Prev Res (Phila). 2012 Mar;5(3):473-83. PMID: 22174364.

Hung JY, Hsu YL, Ko YC, et al. Didymin, a dietary flavonoid glycoside from citrus fruits, induces Fas-mediated apoptotic pathway in human non-small-cell lung cancer cells in vitro and in vivo. Lung Cancer. 2010 Jun;68(3):366-74. PMID: 19733932.

D3218

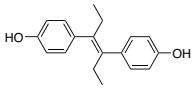

Diethylstilbestrol

DES

$C_{18}H_{20}O_2$ FW: 268.35 [56-53-1] ≥98%

1 g
5 g
10 g

Synthetic non-steroid endocrine disrupter and estrogen receptor agonist. It was previously used to treat hormonal cancers and disorders.

Ingle JN, Ahmann DL, Green SJ, et al. Randomized clinical trial of diethylstilbestrol versus tamoxifen in postmenopausal women with advanced breast cancer. N Engl J Med. 1981 Jan 1;304(1):16-21. PMID: 7001242.

Dieckmann WJ, Davis ME, Rynkiewicz LM, et al. Does the administration of diethylstilbestrol during pregnancy have therapeutic value? Am J Obstet Gynecol. 1953 Nov;66(5):1062-81. PMID: 13104505.

D3320

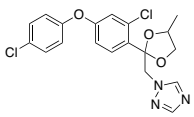

Difenoconazole

$C_{19}H_{17}Cl_2N_3O_3$ FW: 406.26 [119446-68-3] ≥98%

5 g
10 g
100 g

14-α Demethylase inhibitor that inhibits ergosterol synthesis and fungal cell wall formation. It may inhibit aromatase.

Kjærstad MB, Taxvig C, Nellemann C, et al. Endocrine disrupting effects in vitro of conazole antifungals used as pesticides and pharmaceuticals. Reprod Toxicol. 2010 Dec;30(4):573-82. PMID: 20708073.

Hinfray N, Porcher JM, Brion F. Inhibition of rainbow trout (Oncorhynchus mykiss) P450 aromatase activities in brain and ovarian microsomes by various environmental substances. Comp Biochem Physiol C Toxicol Pharmacol. 2006 Nov;144(3):252-62. PMID: 17081805.

D3223

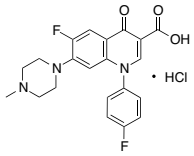

Difloxacin Hydrochloride

$C_{21}H_{19}F_2N_3O_3 \cdot HCl$ FW: 435.85 [91296-86-5] ≥98%

5 g
25 g
100 g

Bacterial DNA gyrase inhibitor. It suppresses growth of *Staphylococcus*, *Escherichia*, and *Pasturella*.

Schink AK, Kadlec K, Hauschild T, et al. Susceptibility of canine and feline bacterial pathogens to pradofloxacin and comparison with other fluoroquinolones approved for companion animals. Vet Microbiol. 2013 Feb 22;162(1):119-26. PMID: 22939523.

Awji EG, Tassew DD, Lee JS, et al. Comparative mutant prevention concentration and mechanism of resistance to veterinary fluoroquinolones in *Staphylococcus* pseudintermedius. Vet Dermatol. 2012 Aug;23(4):376-80, e68-9. PMID: 22409306.

D3219

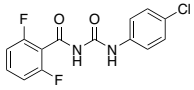

Diflubenzuron

$C_{14}H_9ClF_2N_2O_2$ FW: 310.68 [35367-38-5] ≥95%

1 g
10 g
25 g
100 g

Insect growth regulator and chitin synthesis inhibitor. It inhibits growth of *Tribolium*, *Anopheles*, *Ascaris*, and *Haemonchus*.

Merzendorfer H, Kim HS, Chaudhari SS, et al. Genomic and proteomic studies on the effects of the insect growth regulator diflubenzuron in the model beetle species *Tribolium* castaneum. Insect Biochem Mol Biol. 2012 Apr;42(4):264-76. PMID: 22212827.

Zhang J, Zhu KY. Characterization of a chitin synthase cDNA and its increased mRNA level associated with decreased chitin synthesis in *Anopheles* quadrimaculatus exposed to diflubenzuron. Insect Biochem Mol Biol. 2006 Sep;36(9):712-25. PMID: 16935220.

Fetterer RH, Urban JF Jr, Miller RW. Effects of the chitin synthesis inhibitor diflubenzuron on development of *Ascaris* suum and *Haemonchus* contortus. Vet Parasitol. 1989 Jul 15;32(2-3):181-92. PMID: 2505433.

D3322 Diflunisal

5 g
10 g
50 g

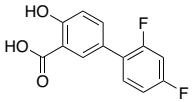

$C_{13}H_8F_2O_3$ FW: 250.2 [22494-42-4] ≥98%

NSAID and COX-1/2 inhibitor used to treat arthritis and dental pain. It also prevents viral integration of HIV-1 by inhibiting docking to LEDGF/p75.

Hu G, Li X, Sun X, et al. Identification of old drugs as potential inhibitors of HIV-1 integrase - human LEDGF/p75 interaction via molecular docking. J Mol Model. 2012 Dec;18(12):4995-5003. PMID: 22733274.

Lawton GM, Chapman PJ. Diflunisal--a long-acting non-steroidal anti-inflammatory drug. A review of its pharmacology and effectiveness in management of postoperative dental pain. Aust Dent J. 1993 Aug;38(4):265-71. PMID: 8216032.

D3420 3,4-Difluorobenzocurcumin

100 mg
250 mg
1 g

CDF

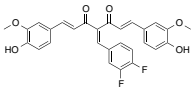

$C_{28}H_{22}F_2O_6$ FW: 492.47 [N/A] ≥95%

Curcumin derivative that may inhibit inflammation, oxidative stress, and bacterial growth.

D3221 Difluoromethylornithine Hydrochloride Monohydrate

10 mg
25 mg

Eflornithine; DFMO

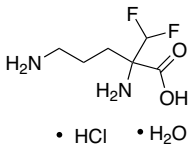

$C_6H_{12}F_2N_2O_2 \cdot HCl \cdot H_2O$ FW: 236.65 [96020-91-6] ≥98%

Ornithine decarboxylase inhibitor that is used to treat African sleeping sickness. It inhibits growth of *Leishmania* and *Trypanosoma*, suppresses breast cancer cell invasion by increasing PKA signaling, and decreases development of esophageal tumors in vivo.

Singh AK, Roberts S, Ullman B, et al. A quantitative proteomic screen to identify potential drug resistance mechanism in α-difluoromethylornithine (DFMO) resistant *Leishmania* donovani. J Proteomics. 2014 May 6;102:44-59. PMID: 24631822.

Tysoe C, Withers SG. Fluorinated mechanism-based inhibitors: common themes and recent developments. Curr Top Med Chem. 2014;14(7):865-74. PMID: 24484426.

Arumugam A, Weng Z, Talwelkar SS, et al. Inhibiting cycloxygenase and ornithine decarboxylase by diclofenac and alpha-difluoromethylornithine blocks cutaneous SCCs by targeting Akt-ERK axis. PLoS One. 2013 Nov 8;8(11):e80076. PMID: 24260338.

D3428 Dihydrochelerythrine NEW

1 mg
5 mg
25 mg

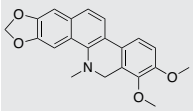

$C_{21}H_{19}NO_4$ FW: 349.38 [6880-91-7] ≥98%

Found in *Garcinia*. It displays many activities, including suppressing growth of *Trypanosoma*, *Leishmania*, *Botrytis*, *Erysiphe*, and *Candida*, inducing apoptosis and necrosis in leukemia cells, and binding DNA sequences containing contiguous G or C base pairs.

Yao JY, Zhou ZM, Li XL, et al. Antiparasitic efficacy of dihydrosanguinarine and dihydrochelerythrine from Macleaya microcarpa against Ichthyophthirius multifiliis in richadsin (Squaliobarbus curriculus). Vet Parasitol. 2011 Dec 29;183(1-2):8-13. PMID: 21813242.

Feng G, Zhang J, Liu YQ. Inhibitory activity of dihydrosanguinarine and dihydrochelerythrine against phytopathogenic fungi. Nat Prod Res. 2011 Jul;25(11):1082-9. PMID: 21500094.

Vrba J, Dolezel P, Vicar J, et al. Chelerythrine and dihydrochelerythrine induce G1 phase arrest and bimodal cell death in human leukemia HL-60 cells. Toxicol In Vitro. 2008 Jun;22(4):1008-17. PMID: 18358694.

D3430 Dihydrosanguinarine NEW

1 mg
5 mg
25 mg

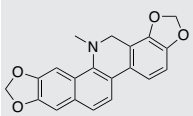

$C_{20}H_{15}NO_4$ FW: 333.34 [3606-45-9] ≥98%

Sanguinarine metabolite. It inhibits growth of *Leishmania*, *Botrytis*, *Erysiphe*, and *Candida*, induces apoptosis and necrosis in leukemia cells, suppresses LPS-induced production of NO and IL-6, and binds DNA sequences containing contiguous G or C base pairs.

Chae HS, Kang OH, Keum JH, et al. Anti-inflammatory effects of Hylomecon hylomeconoides in RAW 264.7 cells. Eur Rev Med Pharmacol Sci. 2012 Jul;16 Suppl 3:121-5. PMID: 22957426.

Yao JY, Zhou ZM, Li XL, et al. Antiparasitic efficacy of dihydrosanguinarine and dihydrochelerythrine from Macleaya microcarpa against Ichthyophthirius multifiliis in richadsin (Squaliobarbus curriculus). Vet Parasitol. 2011 Dec 29;183(1-2):8-13. PMID: 21813242.

Feng G, Zhang J, Liu YQ. Inhibitory activity of dihydrosanguinarine and dihydrochelerythrine against phytopathogenic fungi. Nat Prod Res. 2011 Jul;25(11):1082-9. PMID: 21500094.

D3429 Dihydrocytochalasin B

1 mg
5 mg

$C_{29}H_{39}NO_5$ FW: 481.62 [39156-67-7] ≥98%

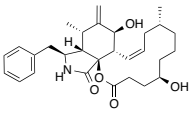

Mycotoxin derivative, actin polymerization inhibitor, and K_v1.1-to-A-type K^+ channel converter. It prevents mitosis and inhibits growth of *Entamoeba invadens*.

Makioka A, Kumagai M, Kobayashi S, et al. Different effects of cytochalasins on the growth and differentiation of *Entamoeba invadens*. Parasitol Res. 2004 May;93(1):68-71. PMID: 15103555.

Reshetnikova G, Barkan R, Popov B, et al. Disruption of the actin cytoskeleton leads to inhibition of mitogen-induced cyclin E expression, Cdk2 phosphorylation, and nuclear accumulation of the retinoblastoma protein-related p107 protein. Exp Cell Res. 2000 Aug 25;259(1):35-53. PMID: 10942577.

D3328 Dihydrokainic Acid

10 mg
25 mg

$C_{10}H_{17}NO_4$ FW: 215.25 [52497-36-6] ≥98%

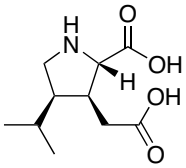

NMDA agonist and GLT-1 inhibitor. It attenuates alcohol intake and prevents cellular uptake of glutamate.

Smith KL, John CS, Sypek EI, et al. Exploring the role of central astrocytic glutamate uptake in ethanol reward in mice. Alcohol Clin Exp Res. 2014 May;38(5):1307-14. PMID: 24655029.

Nie H, Weng HR. Impaired glial glutamate uptake induces extrasynaptic glutamate spillover in the spinal sensory synapses of neuropathic rats. J Neurophysiol. 2010 May;103(5):2570-80. PMID: 20220084.

D3229 7,8-Dihydrokawain

5 mg
10 mg

DHK; Marindinin

$C_{14}H_{16}O_3$ FW: 232.28 [587-63-3] ≥98%

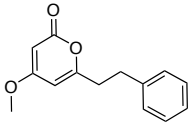

Found in *Piper methysticum* (kava plant). It activates neuronal Nrf2, protecting against amyloid-β-induced neurotoxicity.

Xuan TD, Elzaawely AA, Fukuta M, et al. Herbicidal and Fungicidal Activities of Lactones in Kava (*Piper methysticum*). J Agric Food Chem. 2006 Feb 8;54(3):720-5. PMID: 16448174.

D3227 Dihydromethysticin

5 mg
10 mg

$C_{15}H_{16}O_5$ FW: 276.28 [19902-91-1] ≥98%

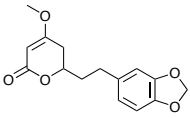

Voltage-gated Na^+ and L-type Ca^{2+} channel blocker found in *Piper methysticum* (kava plant). It inhibits the formation of NNK-induced tumors, suppresses growth of *Fusarium*, *Trichoderma*, and *Colletotrichum*, and protects against cerebral ischemia-induced damage.

Narayanapillai SC, Balbo S, Leitzman P, et al. Dihydromethysticin (DHM) from kava blocks tobacco carcinogen 4-(methylnitrosamino)-1-(3-pyridyl)-1-butanone (NNK)-induced lung tumorigenesis and differentially reduces DNA damage in A/J mice. Carcinogenesis. 2014 Jul 22. [Epub ahead of print]. PMID: 25053626.

Xuan TD, Elzaawely AA, Fukuta M, et al. Herbicidal and Fungicidal Activities of Lactones in Kava (*Piper methysticum*). J Agric Food Chem. 2006 Feb 8;54(3):720-5. PMID: 16448174.

Friese J, Gleitz J. Kavain, dihydrokavain, and dihydromethysticin non-competitively inhibit the specific binding of [3H]-batrachotoxinin-A 20-alpha-benzoate to receptor site 2 of voltage-gated Na^+ channels. Planta Med. 1998 Jun;64(5):458-9. PMID: 9690349.

D3228 Dihydromyristicin

100 mg
500 mg
1 g

$C_{11}H_{14}O_3$ FW: 194.23 [52811-28-6] ≥98%

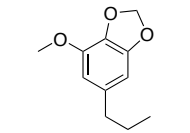

Antioxidant found in parsley. It induces phase II enzyme activity and inhibits benzo[a]pyrene-induced carcinogenesis.

Zheng GQ, Kenney PM, Zhang J, et al. Inhibition of benzo[a]pyrene-induced tumorigenesis by myristicin, a volatile aroma constituent of parsley leaf oil. Carcinogenesis. 1992 Oct;13(10):1921-3. PMID: 1423855.

D3331 α,β-Dihydroresveratrol

10 mg
25 mg
100 mg

$C_{14}H_{14}O_3$ FW: 230.26 [58436-28-5] ≥98%

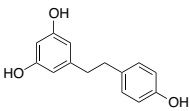

Resveratrol metabolite and potential voltage-gated K^+ channel modulator found in various plant sources. It features better bioavailability than resveratrol and may inhibit growth of cancer cells.

Bode LM, Bunzel D, Huch M, et al. In vivo and in vitro metabolism of trans-resveratrol by human gut microbiota. Am J Clin Nutr. 2013 Feb;97(2):295-309. PMID: 23283496.

Alfaras I, Juan ME, Planas JM. trans-Resveratrol reduces precancerous colonic lesions in dimethylhydrazine-treated rats. J Agric Food Chem. 2010 Jul 14;58(13):8104-10. PMID: 20521815.

Orsini F, Verotta L, Lecchi M, et al. Resveratrol derivatives and their role as potassium channels modulators. J Nat Prod. 2004 Mar;67(3):421-6. PMID: 15043422.

D3330 Dihydrotanshinone

10 mg
25 mg
100 mg

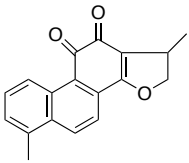

$C_{18}H_{14}O_3$ FW: 278.3 [87205-99-0] ≥90%

Inhibitor of fatty acid synthase, AChE, mineralocorticoid receptors, and glucocorticoid receptors found in *Salvia*. It displays many biological activities, including increasing activation of AMPK, suppressing passive cutaneous anaphylaxis, inhibiting collagen-induced thromboxane B2 production and platelet aggregation, and preventing angiogenesis.

Cheung J, Beri V, Shiomi K, et al. Acetylcholinesterase Complexes with the Natural Product Inhibitors Dihydrotanshinone I and Territrem B: Binding Site Assignment from Inhibitor Competition and Validation Through Crystal Structure Determination. J Mol Neurosci. 2014 Feb 27. [Epub ahead of print]. PMID: 24573600.

D3329 7,8-Dihydroxyflavone Hydrate

NEW

25 mg
100 mg
500 mg

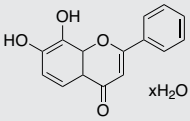

$C_{15}H_{10}O_4 \cdot xH_2O$ FW: 254.24 [38183-03-8] ≥98%

BDNF mimetic and TrkB agonist. It displays many biological activities, including improving cognitive and motor function, decreasing brain edema in traumatic brain injury models, improving insulin sensitivity, inducing apoptosis in oral squamous cell carcinoma cells, and decreasing blood pressure.

Chan CB, Tse MC, Liu X, et al. Activation of Muscular TrkB by its Small Molecular Agonist 7,8-Dihydroxyflavone Sex-Dependently Regulates Energy Metabolism in Diet-Induced Obese Mice. 2015 Mar 19;22(3):355-68. PMID: 25754472.

Sconce MD, Churchill MJ, Moore C, et al. Intervention with 7,8-dihydroxyflavone blocks further striatal terminal loss and restores motor deficits in a progressive mouse model of Parkinson's disease. Neuroscience. 2015 Apr 2;290:454-71. PMID: 25655214.

Lee RH, Shin JC, Kim KH, et al. Apoptotic effects of 7,8-dihydroxyflavone in human oral squamous cancer cells through suppression of Sp1. Oncol Rep. 2015 Feb;33(2):631-8. PMID: 25434704.

D3431 3,4-Dihydroxyphenyl Ethanol

10 mg
25 mg
100 mg

3-Hydroxytyrosol

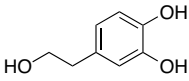

$C_8H_{10}O_3$ FW: 154.16 [10597-60-1] ≥95%

Antioxidant found in olive oil. It displays a wide variety of biological activities, including decreasing lipid peroxidation, lowering fasting glucose and serum lipid levels, preventing platelet aggregation, and inhibiting proliferation of cholangiocarcinoma cells.

Scoditti E, Nestola A, Massaro M, et al. Hydroxytyrosol suppresses MMP-9 and COX-2 activity and expression in activated human monocytes via PKCα and PKCβ1 inhibition. Atherosclerosis. 2014 Jan;232(1):17-24. PMID: 24401212.

D3231 1-(2,4-Dihydroxy-6-methoxy-phenyl)-3-hydroxy-3-(4-methoxy-phenyl)-propan-1-one

5 mg
10 mg

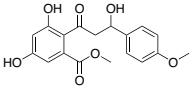

$C_{17}H_{18}O_6$ FW: 318.32 ≥98%

Synthetic compound found in *Piper methysticum* (kava plant).

Chantrapromma S, Jeerapong J, Kruahong T, et al. 1-(2,6-Dihydr-oxy-4-methoxy-phen-yl)-3-phenyl-propan-1-one. Acta Crystallogr Sect E Struct Rep Online. 2010 Apr 21;66(Pt 5):o1120-1. PMID: 21579171.

D3230 1-(2,4-Dihydroxy-6-methoxy-phenyl)-3-hydroxy-3-phenyl-propan-1-one

5 mg
10 mg

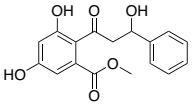

$C_{16}H_{16}O_5$ FW: 288.3 ≥98%

Synthetic compound found in *Piper methysticum* (kava plant).

Chantrapromma S, Jeerapong J, Kruahong T, et al. 1-(2,6-Dihydr-oxy-4-methoxy-phen-yl)-3-phenyl-propan-1-one. Acta Crystallogr Sect E Struct Rep Online. 2010 Apr 21;66(Pt 5):o1120-1. PMID: 21579171.

D3232 3,3'-Diindolylmethane

1 g
5 g
10 g

DIM

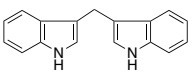

$C_{17}H_{14}N_2$ FW: 246.31 [1968-05-4] ≥98%

Antioxidant and AhR agonist found in cruciferous vegetables. It suppresses expression of TLR4 and Th17 cells to prevent liver inflammation and inhibits T cell activity to suppress EAE development in vivo. It also decreases activity of HDAC2 and inhibits cellular invasion, cellular metastasis, and tumor growth in nasopharyngeal carcinoma models.

Liu Y, She W, Wang F, et al. 3, 3'-diindolylmethane alleviates steatosis and the progression of NASH partly through shifting the imbalance of Treg/Th17 cells to Treg dominance. Int Immunopharmacol. 2014 Oct 1. [Epub ahead of print]. PMID: 25281898.

D3447

Diltiazem Hydrochloride

1 g
5 g
10 g

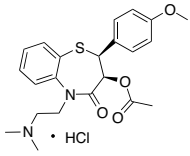

$C_{22}H_{26}N_2O_4S \bullet HCl$ FW: 450.98 [33286-22-5] ≥98%

L-type Ca^{2+} channel blocker and potential CNG channel blocker used to treat hypertension, angina, and arrhythmia. It also prevents formation of aortic aneurysms and limits dephosphorylation of connexin43 gap junction proteins in ischemia/reperfusion models.

Mieth A, Revermann M, Babelova A, et al. L-type calcium channel inhibitor diltiazem prevents aneurysm formation by blood pressure-independent anti-inflammatory effects. Hypertension. 2013 Dec;62(6):1098-104. PMID: 24082061.

Matsushita S, Kurihara H, Watanabe M, et al. Inhibition of connexin43 dephosphorylation is involved in protective effects of diltiazem on cardiac function during hypoxic injury. Histol Histopathol. 2011 Mar;26(3):315-22. PMID: 21210344.

Podda MV, D'Ascenzo M, Leone L, et al. Functional role of cyclic nucleotide-gated channels in rat medial vestibular nucleus neurons. J Physiol. 2008 Feb 1;586(3):803-15. PMID: 18048449.

D3349

Dimebon Dihydrochloride

NEW

5 mg
10 mg

Latrepirdine

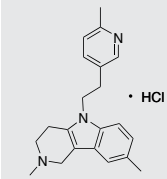

$C_{21}H_{25}N_3 \bullet 2HCl$ FW: 392.37 [97657-92-6] ≥98%

AMPK activator, AMPA receptor potentiator, and inhibitor of L-type Ca^{2+} channels, NMDA receptors, histamine H1/2 receptors, α-adrenergic receptors, and 5-HT2C/5A/6 receptors. It decreases neuronal excitability and glutamate release and prevents amyloid-β-induced mitochondrial swelling in the brain.

Coughlan KS, Mitchem MR, Hogg MC, et al. "Preconditioning" with latrepirdine, an adenosine 5'-monophosphate-activated protein kinase activator, delays amyotrophic lateral sclerosis progression in SOD1(G93A) mice. Neurobiol Aging. 2015 Feb;36(2):1140-50. PMID: 25443289.

Shevtsova EF, Vinogradova DV, Kireeva EG, et al. Dimebon attenuates the Aβ-induced mitochondrial permeabilization. Curr Alzheimer Res. 2014;11(5):422-9. PMID: 24801220.

Weisová P, Alvarez SP, Kilbride SM, et al. Latrepirdine is a potent activator of AMP-activated protein kinase and reduces neuronal excitability. Transl Psychiatry. 2013 Oct 22;3:e317. PMID: 24150226.

D4873

Meso-2,3-dimercaptosuccinic Acid

1 g
5 g
25 g

DMS; DMSA

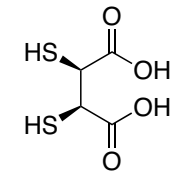

$C_4H_6O_4S_2$ FW: 182.22 [304-55-2] ≥98%

Chelating agent used to treat lead poisoning and to highlight imaging of renal tissue.

Wright JW, Duguid R, McKiddie F, et al. Automatic classification of DMSA scans using an artificial neural network. Phys Med Biol. 2014 Apr 7;59(7):1789-800. PMID: 24619240.

Rooney JP. The role of thiols, dithiols, nutritional factors and interacting ligands in the toxicology of mercury. Toxicology. 2007 May 20;234(3):145-56. Erratum in: Toxicology. 2007 Sep 5;238(2-3):216. PMID: 17408840.

D3348

11,12-Dimethoxydihydrokawain

5 mg
10 mg

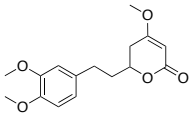

$C_{16}H_{20}O_5$ FW: 292.33 ≥97%

Kawain derivative found in *Piper methysticum* (kava plant).

He XG, Lin LZ, Lian LZ. Electrospray high performance liquid chromatography-mass spectrometry in phytochemical analysis of kava (*Piper methysticum*) extract. Planta Med. 1997 Feb;63(1):70-4. PMID: 17252331.

D4802

17-Dimethylaminoethylamino Demethoxygeldanamycin

1 mg
5 mg
10 mg

17-DMAG; Alvespimycin

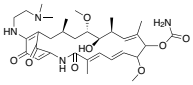

$C_{32}H_{48}N_4O_8$ FW: 616.75 [467214-20-6] ≥98%

Geldanamycin derivative and HSP90 inhibitor. It induces autophagy and improves motor dysfunction in Machado-Joseph disease models, induces cell cycle arrest and apoptosis in neuroblastoma cells, and prevents viral production by human T-lymphocytic virus type-1.

Silva-Fernandes A, Duarte-Silva S, Neves-Carvalho A, et al. Chronic Treatment with 17-DMAG Improves Balance and Coordination in A New Mouse Model of Machado-Joseph Disease. Neurotherapeutics. 2014 Jan 30. [Epub ahead of print]. PMID: 24477711.

Yi B, Yang J, Wang L. The growth inhibitory effect of 17-DMAG on ALK and MYCN double-positive neuroblastoma cell line. Tumour Biol. 2013 Nov 30. [Epub ahead of print]. PMID: 24293393.

Sun X, Bristol JA, Iwahori S, et al. Hsp90 inhibitor 17-DMAG decreases expression of conserved herpesvirus protein kinases and reduces virus production in Epstein-Barr virus-infected cells. J Virol. 2013 Sep;87(18):10126-38. PMID: 23843639.

D3351 — 4-Dimethylaminopyridine

10 g
25 g
100 g

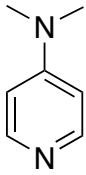

DMAP

$C_7H_{10}N_2$ FW: 122.17 [1122-58-3] ≥98%

Acyl transfer catalyst involved in peptide synthesis. It also acts as a positive inotrope.

Wang J, Niu S, Zhao B, et al. Catalytic synthesis of sulfated polysaccharides. II: comparative studies of solution conformation and antioxidant activities. Carbohydr Polym. 2014 Jul 17;107:221-31. PMID: 24702939.

Lahsasni SA. Microwave- and ultrasound-assisted synthesis of some acyclonucleobases based on a uracil moiety using dmap as base. Nucleosides Nucleotides Nucleic Acids. 2013;32(8):439-52. PMID: 23895354.

Hayashi T, Sun Y, Tamura T, et al. Semisynthetic lectin-4-dimethylaminopyridine conjugates for labeling and profiling glycoproteins on live cell surfaces. J Am Chem Soc. 2013 Aug 21;135(33):12252-8. PMID: 23889132.

D3449 — Dimethylcurcumin

5 mg
10 mg
25 mg

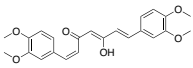

$C_{23}H_{24}O_6$ FW: 396.43 [160096-59-3] ≥98%

Curcumin derivative. It induces DNA damage and apoptosis in cancer cells, increases levels of ROS in cancer cells without affecting normal cells, suppresses expression of pro-inflammatory cytokines, and inhibits growth of gram negative and gram positive bacteria.

Kunwar A, Jayakumar S, Srivastava AK, et al. Dimethoxycurcumin-induced cell death in human breast carcinoma MCF7 cells: evidence for pro-oxidant activity, mitochondrial dysfunction, and apoptosis. Arch Toxicol. 2012 Apr;86(4):603-14. PMID: 22119759.

Patwardhan RS, Checker R, Sharma D, et al. Dimethoxycurcumin, a metabolically stable analogue of curcumin, exhibits anti-inflammatory activities in murine and human lymphocytes. Biochem Pharmacol. 2011 Sep 15;82(6):642-57. PMID: 21726543.

Kunwar A, Barik A, Sandur SK, et al. Differential antioxidant/pro-oxidant activity of dimethoxycurcumin, a synthetic analogue of curcumin. Free Radic Res. 2011 Aug;45(8):959-65. PMID: 21615275.

D3448 — Dimethyl Fumarate

NEW

25 g
100 g

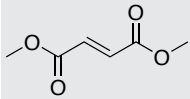

BG-12

$C_6H_8O_4$ FW: 144.13 [624-49-7] ≥98%

Agonist at nAChRs and indirect Nrf2 activator used to treat psoriasis. It decreases proliferation of T cells and release of inflammatory cytokines and improves neurologic outcomes in multiple sclerosis subjects.

Fox RJ, Miller DH, Phillips JT, et al. Placebo-controlled phase 3 study of oral BG-12 or glatiramer in multiple sclerosis. N Engl J Med. 2012 Sep 20;367(12):1087-97. Erratum in: N Engl J Med. 2012 Oct 25;367(17):1673. PMID: 22992072.

Scannevin RH, Chollate S, Jung MY, et al. Fumarates promote cytoprotection of central nervous system cells against oxidative stress via the nuclear factor (erythroid-derived 2)-like 2 pathway. J Pharmacol Exp Ther. 2012 Apr;341(1):274-84. PMID: 22267202.

Lehmann JC, Listopad JJ, Rentzsch CU, et al. Dimethylfumarate induces immunosuppression via glutathione depletion and subsequent induction of heme oxygenase 1. J Invest Dermatol. 2007 Apr;127(4):835-45. PMID: 17235328.

D3353 — Diminazene Aceturate

1 g
5 g
25 g

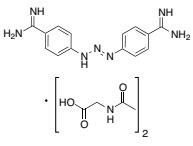

$C_{14}H_{15}N_7 \bullet 2C_4H_7NO_6$ FW: 515.52 [908-54-3] ≥98%

ACE2 activator and DNA polymerase inhibitor. It opposes the effects of AT II and inhibits growth of *Trypanosoma*, *Babesia*, *Brucella*, and *Streptococcus*.

Mecca AP, Regenhardt RW, O'Connor TE, et al. Cerebroprotection by angiotensin-(1-7) in endothelin-1-induced ischaemic stroke. Exp Physiol. 2011 Oct;96(10):1084-96. doi: 10.1113/expphysiol.2011.058578. Epub 2011 Jun 17.

D3352 — Dinaciclib

NEW

5 mg
10 mg

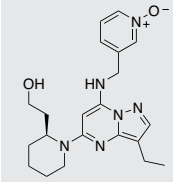

SCH 727965

$C_{21}H_{28}N_6O_2$ FW: 396.49 [779353-01-4] ≥98%

CDK1/2/5/9 inhibitor. It binds BRD proteins and inhibits cell proliferation, motility, and colony formation in pancreatic cancer models.

Flynn J, Jones J, Johnson AJ, et al. Dinaciclib is a novel cyclin dependent kinase inhibitor with significant clinical activity in relapsed and refractory chronic lymphocytic leukemia. Leukemia. 2015 Feb 24. [Epub ahead of print]. PMID: 25708835.

Martin MP, Olesen SH, Georg GI, et al. Cyclin-dependent kinase inhibitor dinaciclib interacts with the acetyl-lysine recognition site of bromodomains. ACS Chem Biol. 2013 Nov 15;8(11):2360-5. PMID: 24007471.

Gojo I, Sadowska M, Walker A, et al. Clinical and laboratory studies of the novel cyclin-dependent kinase inhibitor dinaciclib (SCH 727965) in acute leukemias. Cancer Chemother Pharmacol. 2013 Oct;72(4):897-908. PMID: 23949430.

D3355

Diosgenin

5 g
100 g

3β-Hydroxy-5-spirostene

$C_{27}H_{42}O_3$ FW: 414.62 [512-04-9] ≥98%

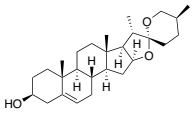

Found in *Dioscorea*. It exhibits many biological activities, including inhibiting actin polymerization and cell migration in breast cancer cells, suppressing production of pro-inflammatory cytokines in macrophages, and improving performance on object recognition memory tasks.

He Z, Chen H, Li G, et al. Diosgenin inhibits the migration of human breast cancer MDA-MB-231 cells by suppressing Vav2 activity. Phytomedicine. 2014 Mar 18. [Epub ahead of print]. PMID: 24656238.

Tohda C, Urano T, Umezaki M, et al. Diosgenin is an exogenous activator of 1,25D3-MARRS/Pdia3/ERp57 and improves Alzheimer's disease pathologies in 5XFAD mice. Sci Rep. 2012;2:535. PMID: 22837815.

Uemura T, Goto T, Kang MS, et al. Diosgenin, the main aglycon of fenugreek, inhibits LXRα activity in HepG2 cells and decreases plasma and hepatic triglycerides in obese diabetic mice. J Nutr. 2011 Jan;141(1):17-23. PMID: 21106928.

D3356

Diosmetin

250 mg
1 g
5 g
25 g

Cyanidenon-4'-methyl ether 1479; Luteolin-4'-methyl ether

$C_{16}H_{12}O_6$ FW: 300.26 [520-34-3] ≥98%

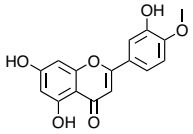

Found in vetch and various fruits. It exhibits many biological activities, including decreasing generation of ROS, inducing differentiation in osteoblasts, and causing cell cycle arrest in breast cancer cells.

Liao W, Ning Z, Chen L, et al. Intracellular Antioxidant Detoxifying Effects of Diosmetin on 2,2-Azobis(2-amidinopropane) Dihydrochloride (AAPH)-Induced Oxidative Stress through Inhibition of Reactive Oxygen Species Generation. J Agric Food Chem. 2014 Aug 27;62(34):8648-54. PMID: 25075433.

Yu G, Wan R, Yin G, et al. Diosmetin ameliorates the severity of cerulein-induced acute pancreatitis in mice by inhibiting the activation of the nuclear factor-κB. Int J Clin Exp Pathol. 2014 Apr 15;7(5):2133-42. PMID: 24966921.

D3357

Diosmin

1 g
5 g
25 g

$C_{28}H_{32}O_{15}$ FW: 608.54 [520-27-4] ≥95%

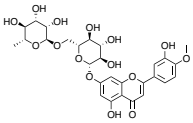

Found in *Teucrium*. It displays several biological activities, including alleviating neurological deficits and decreasing infarct volume in models of cerebral ischemia/reperfusion, increasing antioxidative enzyme activity, and inhibiting proliferation of hepatocellular carcinoma cells.

Senthamizhselvan O, Manivannan J, Silambarasan T, et al. Diosmin pretreatment improves cardiac function and suppresses oxidative stress in rat heart after ischemia/reperfusion. Eur J Pharmacol. 2014 Aug 5;736:131-7. PMID: 24769512.

Liu X, Zhang X, Zhang J, et al. Diosmin protects against cerebral ischemia/reperfusion injury through activating JAK2/STAT3 signal pathway in mice. Neuroscience. 2014 May 30;268:318-27. PMID: 24680937.

Queenthy SS, John B. Diosmin exhibits anti-hyperlipidemic effects in isoproterenol induced myocardial infarcted rats. Eur J Pharmacol. 2013 Oct 15;718(1-3):213-8. PMID: 24036254.

D3462

Diphenhydramine Hydrochloride

10 g
25 g
100 g

$C_{17}H_{21}NO \bullet HCl$ FW: 291.82 [147-24-0] ≥98%

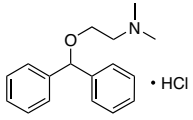

Voltage-gated Na^+ channel blocker, mAChR antagonist, and histamine H1 receptor inverse agonist used to treat inflammation and allergies. It also decreases leukocyte infiltration to injury sites.

Raphael GD, Angello JT, Wu MM, et al. Efficacy of diphenhydramine vs desloratadine and placebo in patients with moderate-to-severe seasonal allergic rhinitis. Ann Allergy Asthma Immunol. 2006 Apr;96(4):606-14. PMID: 16680933.

Yamashiro K, Kiryu J, Tsujikawa A, et al. Suppressive effects of histamine H1 receptor antagonist diphenhydramine on the leukocyte infiltration during endotoxin-induced uveitis. Exp Eye Res. 2001 Jul;73(1):69-80. PMID: 11428864.

D3261

Dipropyl Disulfide

25 g
100 g

4,5-Dithiaoctane

$C_6H_{14}S_2$ FW: 150.31 [629-19-6] ≥98%

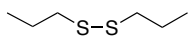

Cholesterol synthesis inhibitor found in *Allium*. It induces phase II enzyme activity, suppresses benzo[a]pyrene-induced carcinogenesis, and decreases N-nitrosamine-induced DNA damage.

Tsai CW, Liu KL, Lin CY, et al. Structure and function relationship study of allium organosulfur compounds on upregulating the pi class of glutathione S-transferase expression. J Agric Food Chem. 2011 Apr 13;59(7):3398-405. PMID: 21381664.

Arranz N, Haza AI, García A, et al. Protective effects of organosulfur compounds towards N-nitrosamine-induced DNA damage in the single-cell gel electrophoresis (SCGE)/HepG2 assay. Food Chem Toxicol. 2007 Sep;45(9):1662-9. PMID: 17434656.

D3262

Dipropyl Sulfide

10 g
25 g

4-Thiaheptane; Dipropyl thioether

$C_6H_{14}S$ FW: 118.24 [111-47-7] ≥98%

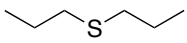

Cholesterol synthesis inhibitor found in *Allium*. It induces phase II enzyme activity, suppresses benzo[a]pyrene-induced carcinogenesis, and decreases N-nitrosamine-induced DNA damage.

Tsai CW, Liu KL, Lin CY, et al. Structure and function relationship study of allium organosulfur compounds on upregulating the pi class of glutathione S-transferase expression. J Agric Food Chem. 2011 Apr 13;59(7):3398-405. PMID: 21381664.

Arranz N, Haza AI, García A, et al. Protective effects of organosulfur compounds towards N-nitrosamine-induced DNA damage in the single-cell gel electrophoresis (SCGE)/HepG2 assay. Food Chem Toxicol. 2007 Sep;45(9):1662-9. PMID: 17434656.

Yeh YY, Liu L. Cholesterol-lowering effect of garlic extracts and organosulfur compounds: human and animal studies. J Nutr. 2001 Mar;131(3s):989S-93S. PMID: 11238803.

D3362

Dipyridamole

1 g
5 g
25 g

$C_{24}H_{40}N_8O_4$ FW: 504.63 [58-32-2] ≥98%

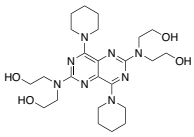

PDE and adenosine deaminase inhibitor used to prevent stroke and myocardial infarction. It inhibits vascular stenosis and prevents expression of MMP9.

Massaro M, Scoditti E, Carluccio MA, et al. Dipyridamole decreases inflammatory metalloproteinase-9 expression and release by human monocytes. Thromb Haemost. 2013 Feb;109(2):280-9. PMID: 23238437.

Alberts MJ. Antithrombotic therapy for secondary stroke prevention. Continuum (Minneap Minn). 2011 Dec;17(6 2ndary Stroke Prevention):1255-66. PMID: 22810029.

Zhuplatov SB, Masaki T, Blumenthal DK, et al. Mechanism of dipyridamole's action in inhibition of venous and arterial smooth muscle cell proliferation. Basic Clin Pharmacol Toxicol. 2006 Dec;99(6):431-9. PMID: 17169124.

D3372

Disodium Cycloheptylaminomethylene Diphosphate

25 mg
100 mg
250 mg

Incadronate disodium hydrate

$C_8H_{17}NNa_2O_6P_2$ FW: 331.15 [138330-18-4] ≥98%

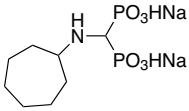

Squalene synthase inhibitor. It prevents bone resorption and suppresses bone loss due to immobilization. It also improves stiffness and ultimate load in fractured bones.

Miwa A, Takezako N, Hayakawa H, et al. YM-175 induces apoptosis of human native monocyte-lineage cells via inhibition of prenylation. Am J Hematol. 2012 Dec;87(12):1084-8. PMID: 23044853.

Li C, Mori S, Li J, et al. Long-term effect of incadronate disodium (YM-175) on fracture healing of femoral shaft in growing rats. J Bone Miner Res. 2001 Mar;16(3):429-36. PMID: 11277259.

Li J, Mori S, Mashiba T, et al. Preadministration of incadronate disodium can prevent bone loss in rat proximal tibial metaphysis when induced by hindlimb immobilization by bandage. Bone. 1998 Nov;23(5):459-63. PMID: 9823453.

D3374

Disulfiram

50 g
100 g
250 g

Tetraethylthiuram disulfide; Teturamin

$C_{10}H_{20}N_2S_4$ FW: 296.54 [97-77-8] ≥98%

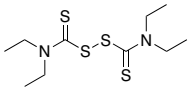

Inhibitor of aldehyde dehydrogenase, 26S proteasome, and MGMT used to treat chronic alcohol dependence. It prevents metabolism of alcohol and causes acetaldehyde buildup. It induces apoptosis in several cancer cell lines and inhibits the growth of *Trichomonas* and *Tritrichomonas*.

Paranjpe A, Zhang R, Ali-Osman F, et al. Disulfiram is a direct and potent inhibitor of human O6-methylguanine-DNA methyltransferase (MGMT) in brain tumor cells and mouse brain and markedly increases the alkylating DNA damage. Carcinogenesis. 2014 Mar;35(3):692-702. PMID: 24193513.

Wickström M, Danielsson K, Rickardson L, et al. Pharmacological profiling of disulfiram using human tumor cell lines and human tumor cells from patients. Biochem Pharmacol. 2007 Jan 1;73(1):25-33. PMID: 17026967.

D3575

2,5-Di-tert-butyl-4-hydroxyanisole

1 g
5 g

$C_{15}H_{24}O_2$ FW: 212.33 [1991-52-2] ≥98%

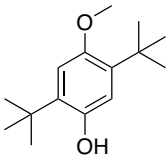

Derivative of BHA and potential Ca^{2+} ATPase inhibitor. It displays both cytoprotective and carcinogenic activities and may inhibit T cell adhesion.

Qu J, Adam J, Bloxham DM, et al. Phosphatidylserine-dependent adhesion of T cells to endothelial cells. Biochim Biophys Acta. 2000 Jun 15;1501(2-3):99-115. PMID: 10838184.

Lam LK, Garg P. Tumorigenicity of di-tert-butyl-substituted hydroquinone and hydroxyanisoles in the forestomach of Syrian golden hamsters. Carcinogenesis. 1991 Jul;12(7):1341-4. PMID: 2070501.

D0010

3H-1,2-Dithiole-3-thione

25 mg
100 mg
500 mg

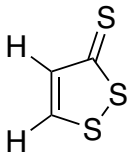

D3T

$C_3H_2S_3$ FW: 134.25 [534-25-8] ≥98%

Synthetic product found in cruciferous vegetables. It induces activation of Nrf2, inhibits apoptosis in neurons, and prevents the formation of DBP-induced DNA adducts.

Jia J, Xiao Y, Wang W, et al. Differential mechanisms underlying neuroprotection of hydrogen sulfide donors against oxidative stress. Neurochem Int. 2013 Jun;62(8):1072-8. PMID: 23587562.

Pazdro R, Burgess JR. The antioxidant 3H-1,2-dithiole-3-thione potentiates advanced glycation end-product-induced oxidative stress in SH-SY5Y cells. Exp Diabetes Res. 2012;2012:137607. PMID: 22675339.

Dong J, Yan D, Chen SY. Stabilization of Nrf2 protein by D3T provides protection against ethanol-induced apoptosis in PC12 cells. PLoS One. 2011 Feb 3;6(2):e16845. PMID: 21304811.

D5607

Dobutamine Hydrochloride

10 mg
50 mg
100 mg

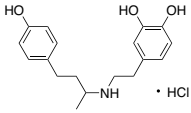

$C_{18}H_{23}NO_3 \cdot HCl$ FW: 337.85 [49745-95-1] ≥98%

β1-Adrenergic receptor agonist and β2- and α1-adrenergic receptor antagonist used to treat heart failure and cardiogenic shock. It decreases GABAergic, glycinergic, and glutamatergic neurotransmission to cardiac vagal neurons and acts as a positive inotrope.

Bateman RJ, Boychuk CR, Philbin KE, et al. β adrenergic receptor modulation of neurotransmission to cardiac vagal neurons in the nucleus ambiguus. Neuroscience. 2012 May 17;210:58-66. PMID: 22425752.

Coons JC, McGraw M, Murali S. Pharmacotherapy for acute heart failure syndromes. Am J Health Syst Pharm. 2011 Jan 1;68(1):21-35. PMID: 21164062.

D5709

Docetaxel

5 mg
10 mg
25 mg
100 mg

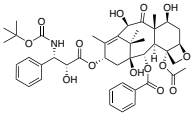

$C_{43}H_{53}NO_{14}$ FW: 807.89 [114977-28-5] ≥98%

Semi-synthetic microtubule depolymerization inhibitor and taxol analog used to treat various cancers.

Lyseng-Williamson KA, Fenton C. Docetaxel: a review of its use in metastatic breast cancer. Drugs. 2005;65(17):2513-31. PMID: 16296875.

Eisenhauer EA, Vermorken JB. The taxoids. Comparative clinical pharmacology and therapeutic potential. Drugs. 1998 Jan;55(1):5-30. PMID: 9463787.

D5610

Docosahexaenoic Acid (all cis-4,7,10,13,16,19) NEW

25 mg
100 mg

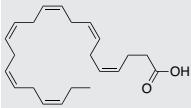

DHA

$C_{22}H_{32}O_2$ FW: 328.49 ≥99%

Essential fatty acid found in fish oil. It is involved in prostaglandin synthesis and inflammation.

Tapiero H, Ba GN, Couvreur P, et al. Polyunsaturated fatty acids (PUFA) and eicosanoids in human health and pathologies. Biomed Pharmacother. 2002 Jul;56(5):215-22. PMID: 12199620.

Hu PC, Chen BH. Effects of riboflavin and fatty acid methyl esters on cholesterol oxidation during illumination. J Agric Food Chem. 2002 Jun 5;50(12):3572-8. PMID: 12033831.

Liu W, Wang HJ, Wang LP, et al. Formation of high-molecular-weight protein adducts by methyl docosahexaenoate peroxidation products. Biochim Biophys Acta. 2007 Feb;1774(2):258-66. PMID: 17207667.

D5611

Docosahexaenoic Acid (all cis-4,7,10,13,16,19) Methyl Ester

25 mg
100 mg

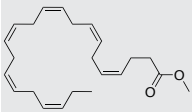

DHA methyl ester NEW

$C_{23}H_{34}O_2$ FW: 342.51 ≥99%

Derivative of essential fatty acid found in fish oil. It is involved in prostaglandin synthesis and inflammation and may form protein adducts in aging-related diseases.

Tapiero H, Ba GN, Couvreur P, et al. Polyunsaturated fatty acids (PUFA) and eicosanoids in human health and pathologies. Biomed Pharmacother. 2002 Jul;56(5):215-22. PMID: 12199620.

Hu PC, Chen BH. Effects of riboflavin and fatty acid methyl esters on cholesterol oxidation during illumination. J Agric Food Chem. 2002 Jun 5;50(12):3572-8. PMID: 12033831.

D5612

2-n-Dodecylfuran

1 g
5 g
10 g

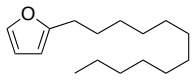

$C_{16}H_{28}O$ FW: 212.38 [75308-12-2] ≥98%

It may inhibit *Mycobacterium* growth or display other antibacterial activity.

Chen FC, Peng CF, Tsai IL, et al. Antitubercular constituents from the stem wood of Cinnamomum kotoense. J Nat Prod. 2005 Sep;68(9):1318-23. PMID: 16180806.

D5746

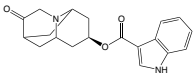

Dolasetron

5 mg
25 mg
100 mg

$C_{19}H_{20}N_2O_3$ FW: 324.37 [115956-12-2] ≥98%

5-HT3 receptor antagonist used to prevent nausea and emesis.

Hsu ES. A review of granisetron, 5-hydroxytryptamine3 receptor antagonists, and other antiemetics. Am J Ther. 2010 Sep-Oct;17(5):476-86. PMID: 20844345.

Birmingham SD, Mecklenburg BW, Lujan E, et al. Dolasetron versus ondansetron as single-agent prophylaxis for patients at increased risk for postoperative nausea and vomiting: a prospective, double-blind, randomized trial. Mil Med. 2006 Sep;171(9):913-6. PMID: 17036618.

D5747

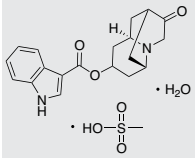

Dolasetron Mesylate Hydrate

NEW

10 mg
50 mg

$C_{19}H_{20}N_2O_3 \bullet CH_4O_3S \bullet xH_2O$ FW: 420.48 ≥98%

5-HT3 receptor antagonist used to treat nausea. It also decreases pain sensitivity in fibromyalgia subjects.

Roberts SM, Bezinover DS, Janicki PK. Reappraisal of the role of dolasetron in prevention and treatment of nausea and vomiting associated with surgery or chemotherapy. Cancer Manag Res. 2012;4:67-73. PMID: 22427733.

Vergne-Salle P, Dufauret-Lombard C, Bonnet C, et al. A randomised, double-blind, placebo-controlled trial of dolasetron, a 5-hydroxytryptamine 3 receptor antagonist, in patients with fibromyalgia. Eur J Pain. 2011 May;15(5):509-14. PMID: 21036635.

D5649

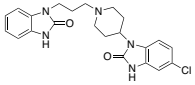

Domperidone

50 mg
250 mg
1 g

$C_{22}H_{24}ClN_5O_2$ FW: 425.91 [57808-66-9] ≥98%

Dopamine D2/3 receptor antagonist and hERG K^+ channel blocker used to treat nausea, induce prolactin release, and increase gastrointestinal transit speed. It also decreases pain and prolongs the cardiac QT interval.

Claassen S, Zünkler BJ. Comparison of the effects of metoclopramide and domperidone on HERG channels. Pharmacology. 2005 Apr;74(1):31-6. PMID: 15640612.

Sivasanker M, Reddy PM, Shashindran CH, et al. Formalin assay parameters differ in confirming the antinociceptive mechanism of domperidone in mice. Indian J Exp Biol. 2004 Apr;42(4):429-31. PMID: 15088695.

D5753

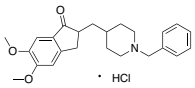

Donepezil Hydrochloride

25 mg
100 mg
500 mg

$C_{24}H_{29}NO_3 \bullet HCl$ FW: 415.95 [120011-70-3] ≥98%

GSK3 and AChE inhibitor and potential σ1 receptor agonist used to treat Alzheimer's disease. It also improves learning and memory, downregulates expression of the NR1 subunit of NMDA receptors, decreases left ventricular end diastolic pressure, and increases left ventricular contractility.

Jiang Y, Zou Y, Chen S, et al. The anti-inflammatory effect of donepezil on experimental autoimmune encephalomyelitis in C57 BL/6 mice. Neuropharmacology. 2013 Oct;73:415-24. PMID: 23831366.

Xia Z, Zhang R, Wu P, et al. Memory defect induced by β-amyloid plus glutamate receptor agonist is alleviated by catalpol and donepezil through different mechanisms. Brain Res. 2012 Mar 2;1441:27-37. PMID: 22305339.

D5662

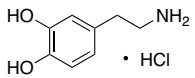

Dopamine Hydrochloride

5 g
25 g
100 g

$C_8H_{11}NO_2 \bullet HCl$ FW: 189.64 [62-31-7] ≥98%

Endogenous dopamine D1-5 receptor agonist involved in motor control, mood, cognition, reward, and nausea. It also activates naïve and resting T cells and inhibits activated T cells.

Cachope R, Cheer JF. Local control of striatal dopamine release. Front Behav Neurosci. 2014 May 23;8:188. PMID: 24904339.

Pacheco R, Contreras F, Zouali M. The dopaminergic system in autoimmune diseases. Front Immunol. 2014 Mar 21;5:117. PMID: 24711809.

D5868

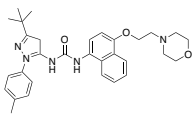

Doramapimod

BIRB796

10 mg
25 mg
100 mg

$C_{31}H_{37}N_5O_3$ FW: 527.66 [2859873-48-4] ≥98%

Inhibitor of JNK, ALK, and p38 MAPK. It inhibits expression of pro-inflammatory cytokines, decreases release of prostaglandin E2, and inhibits growth of cancer cells.

Hoogendijk AJ, Pinhanços SS, van der Poll T, et al. Intrapulmonary administration of a p38 mitogen activated protein kinase inhibitor partially prevents pulmonary inflammation. Immunobiology. 2013 Apr;218(4):435-42. PMID: 22727776.

af Gennäs GB, Mologni L, Ahmed S, et al. Design, synthesis, and biological activity of urea derivatives as anaplastic lymphoma kinase inhibitors. ChemMedChem. 2011 Sep 5;6(9):1680-92. PMID: 21721129.

D5869

Doripenem Hydrate

10 mg
25 mg
100 mg

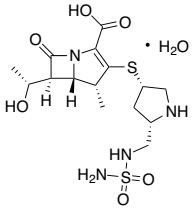

$C_{15}H_{24}N_4O_6S_2 \bullet H_2O$ FW: 438.52 [364622-82-2] ≥98%

Penicillin binding protein inhibitor that inhibits bacterial cell wall synthesis. It is especially active against *Pseudomonas* and *Enterobacteriaceae*.

Schneider KD, Ortega CJ, Renck NA, et al. Structures of the class D carbapenemase OXA-24 from *Acinetobacter* baumannii in complex with doripenem. J Mol Biol. 2011 Mar 4;406(4):583-94. PMID: 21215758.

Davies TA, Shang W, Bush K, et al. Affinity of doripenem and comparators to penicillin-binding proteins in *Escherichia* coli and *Pseudomonas* aeruginosa. Antimicrob Agents Chemother. 2008 Apr;52(4):1510-2. PMID: 18250190.

Jones RN, Huynh HK, Biedenbach DJ, et al. Doripenem (S-4661), a novel carbapenem: comparative activity against contemporary pathogens including bactericidal action and preliminary in vitro methods evaluations. J Antimicrob Chemother. 2004 Jul;54(1):144-54. PMID: 15190031.

D5992

Doxapram Hydrochloride Hydrate

25 mg
100 mg
500 mg

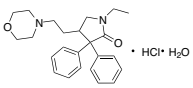

$C_{24}H_{30}N_2O_2 \bullet HCl \bullet H_2O$ FW: 432.98 [7081-53-0] ≥98%

K^+ channel blocker. It stimulates catecholamine release from carotid bodies, facilitates presynaptic activity, and inhibits postsynaptic activity.

Anderson-Beck R, Wilson L, Brazier S, et al. Doxapram stimulates dopamine release from the intact rat carotid body in vitro. Neurosci Lett. 1995 Feb 24;187(1):25-8. PMID: 7617294.

Peers C. Effects of doxapram on ionic currents recorded in isolated type I cells of the neonatal rat carotid body. Brain Res. 1991 Dec 24;568(1-2):116-22. PMID: 1667613.

Pollard BJ, Randall NP, Pleuvry BJ. Doxapram and the neuromuscular junction. Br J Anaesth. 1989 Jun;62(6):664-8. PMID: 2751921.

D5690

Doxazosin Mesylate

50 mg
250 mg
1 g

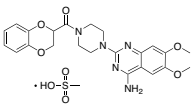

$C_{23}H_{25}N_5O_5 \bullet CH_3SO_3H$ FW: 547.59 [77883-43-3] ≥98%

α1-Adrenergic receptor antagonist used to treat hypertension and BPH. It also induces Fas-mediated apoptosis in benign and malignant prostate cells.

Shannon R, Chaudhry M. Effect of alpha1-adrenergic receptors in cardiac pathophysiology. Am Heart J. 2006 Nov;152(5):842-50. PMID: 17070143.

Garrison JB, Kyprianou N. Doxazosin induces apoptosis of benign and malignant prostate cells via a death receptor-mediated pathway. Cancer Res. 2006 Jan 1;66(1):464-72. PMID: 16397262.

Kyprianou N. Doxazosin and terazosin suppress prostate growth by inducing apoptosis: clinical significance. J Urol. 2003 Apr;169(4):1520-5. PMID: 12629407.

D5994

Doxepin Hydrochloride

1 g
5 g
25 g

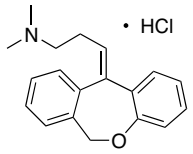

$C_{19}H_{21}NO \bullet HCl$ FW: 315.84 [1229-29-4] ≥98%

Inhibitor of 5-HT1/2 receptors, M1-5 mAChRs, α1-adrenergic receptors, histamine H1/2 receptors, SERT, NET, and H^+/K^+ ATPase. It is used to treat depression, anxiety, insomnia, and dermatological itch. It also acts as a FIASMA and decreases stress-induced corticosterone release.

Hassanzadeh P, Hassanzadeh A. The Role of the Endocannabinoids in Suppression of the Hypothalamic-pituitary-adrenal Axis Activity by Doxepin. Iran J Basic Med Sci. 2011 Sep;14(5):414-21. PMID: 23493814.

Cheng BC, Chan BR, Chen YW, et al. Doxepin has a potent and long-acting spinal anesthetic effect in rats. Kaohsiung J Med Sci. 2006 Feb;22(2):68-74. PMID: 16568723.

Hajak G, Rodenbeck A, Voderholzer U et al. Doxepin in the treatment of primary insomnia: a placebo-controlled, double-blind, polysomnographic study. J Clin Psychiatry. 2001 Jun;62(6):453–63. PMID: 11465523.

D5692

Doxifluridine

50 mg
100 mg
250 mg

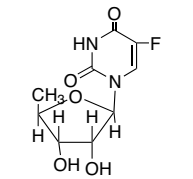

5'-DFUR

$C_9H_{11}FN_2O_5$ FW: 246.19 [3094-09-5] ≥98%

Prodrug of 5-FU and inhibitor of thymidylate synthase that is used to treat various cancers. It inhibits DNA synthesis and induces apoptosis in gastric carcinoma models by downregulating expression of FasL and PD-ECGF.

Zhao WH, Wang SF, Ding W, et al. Apoptosis induced by preoperative oral 5'-DFUR administration in gastric adenocarcinoma and its mechanism of action. World J Gastroenterol. 2006 Mar 7;12(9):1356-61. PMID: 16552801.

Saurat JH. Retinoids and psoriasis: novel issues in retinoid pharmacology and implications for psoriasis treatment. J Am Acad Dermatol. 1999 Sep;41(3 Pt 2):S2-6. PMID: 10459139.

D5792

Doxofylline

1 g
5 g
25 g

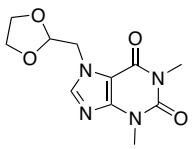

$C_{11}H_{14}N_4O_4$ FW: 266.25 [69975-86-6] ≥98%

Xanthine derivative and PDE inhibitor used to treat asthma. It decreases bronchoconstriction and does not activate adenosine receptors.

Shukla D, Chakraborty S, Singh S, et al. Doxofylline: a promising methylxanthine derivative for the treatment of asthma and chronic obstructive pulmonary disease. Expert Opin Pharmacother. 2009 Oct;10(14):2343-56. PMID: 19678793.

Cirillo R, Barone D, Franzone JS. Doxofylline, an antiasthmatic drug lacking affinity for adenosine receptors. Arch Int Pharmacodyn Ther. 1988 Sep-Oct;295:221-37. PMID: 3245738.

D5794

Doxorubicin Hydrochloride

5 mg
10 mg
50 mg

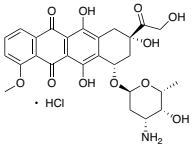

$C_{27}H_{29}NO_{11} \bullet HCl$ FW: 579.99 [25316-40-9] ≥98%

DNA intercalator and topoisomerase II inhibitor used to treat various cancers. It inhibits DNA repair by promoting histone H2AX eviction from chromatin. It also inhibits growth of *Plasmodium*.

Pang B, Qiao X, Janssen L, et al. Drug-induced histone eviction from open chromatin contributes to the chemotherapeutic effects of doxorubicin. Nat Commun. 2013;4:1908. PMID: 23715267.

Tacar O, Sriamornsak P, Dass CR. Doxorubicin: an update on anticancer molecular action, toxicity and novel drug delivery systems. J Pharm Pharmacol. 2013 Feb;65(2):157-70. PMID: 23278683.

Gamo FJ, Sanz LM, Vidal J, et al. Thousands of chemical starting points for antimalarial lead identification. Nature. 2010 May 20;465(7296):305-10. PMID: 20485427.

D5897

Doxycycline Hyclate

1 g
5 g
10 g
25 g

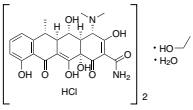

$(C_{22}H_{24}N_2O_8)_2 \bullet 2HCl \bullet H_2O \bullet C_2H_6O$ FW: 512.9 [24390-14-5] ≥97%

Inhibitor of MMPs and protein translation. It also inhibits expression of the apicoplast genome, induces sterilization in *Wolbachia* endosymbionts from *Wucheria*, improves pulmonary function and parameters of COPD, and inhibits migration and proliferation of breast adenocarcinoma cells

Joks R, Durkin HG. Non-antibiotic properties of tetracyclines as anti-allergy and asthma drugs. Pharmacol Res. 2011 Dec;64(6):602-9. PMID: 21501686.

Dalvi PS, Singh A, Trivedi HR, et al. Effect of doxycycline in patients of moderate to severe chronic obstructive pulmonary disease with stable symptoms. Ann Thorac Med. 2011 Oct;6(4):221-6. PMID: 21977068.

Errami M, Galindo CL, Tassa AT, et al. Doxycycline attenuates isoproterenol- and transverse aortic banding-induced cardiac hypertrophy in mice. J Pharmacol Exp Ther. 2008 Mar;324(3):1196-203. PMID: 18089841.

D5898

Doxycycline Monohydrate

1 g
5 g
10 g
25 g

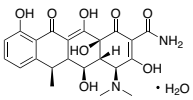

$C_{22}H_{24}N_2O_8 \bullet H_2O$ FW: 462.45 [17086-28-1] ≥97%

Inhibitor of protein translation inhibitor and MMPs used to treat bacterial infections and inflammatory diseases. It also inhibits expression of the apicoplast genome and induces loss of function in parasites, improves pulmonary function and parameters of COPD, and suppresses migration and proliferation of breast adenocarcinoma cells.

Joks R, Durkin HG. Non-antibiotic properties of tetracyclines as anti-allergy and asthma drugs. Pharmacol Res. 2011 Dec;64(6):602-9. PMID: 21501686.

Dalvi PS, Singh A, Trivedi HR, et al. Effect of doxycycline in patients of moderate to severe chronic obstructive pulmonary disease with stable symptoms. Ann Thorac Med. 2011 Oct;6(4):221-6. PMID: 21977068.

Errami M, Galindo CL, Tassa AT, et al. Doxycycline attenuates isoproterenol- and transverse aortic banding-induced cardiac hypertrophy in mice. J Pharmacol Exp Ther. 2008 Mar;324(3):1196-203. PMID: 18089841.

D6108

1,4-DPCA

NEW

5 mg
25 mg

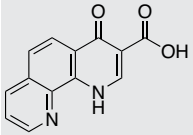

$C_{13}H_8N_2O_3$ FW: 240.22 [331830-20-7] ≥98%

Prolyl hydroxylase inhibitor that stabilizes expression of HIF-1α. It inhibits proliferation of breast cancer cells and limits growth of connective tissue on biomaterials and implanted medical devices.

Zhang Y, Strehin I, Bedelbaeva K, et al. Drug-induced regeneration in adult mice. Sci Transl Med. 2015 Jun 3;7(290):290ra92. PMID: 26041709.

Xiong G, Deng L, Zhu J, et al. Prolyl-4-hydroxylase α subunit 2 promotes breast cancer progression and metastasis by regulating collagen deposition. BMC Cancer. 2014 Jan 2;14:1. PMID: 24383403.

Love RJ, Jones KS. Transient inhibition of connective tissue infiltration and collagen deposition into porous poly(lactic-co-glycolic acid) discs. J Biomed Mater Res A. 2013 Dec;101(12):3599-606. PMID: 23766241.

D6957 Droloxifene

25 mg
100 mg
250 mg

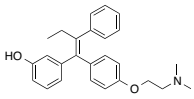

$C_{26}H_{29}NO_2$ FW: 387.51 [82413-20-5] ≥98%

Tamoxifen analog and SERM that acts as an ER agonist in bone and as an ER antagonist in breast tissue. It increases apoptosis in luteal cells, inhibits bone resorption and turnover, and decreases levels of E-selectin.

Shelly W, Draper MW, Krishnan V, et al. Selective estrogen receptor modulators: an update on recent clinical findings. Obstet Gynecol Surv. 2008 Mar;63(3):163-81. PMID: 18279543.

Martin JH, Symonds A, Chohan S. Down-regulation of nitric oxide production by droloxifene and toremifene in human breast cancer cells. Oncol Rep. 2003 Jul-Aug;10(4):979-84. PMID: 12792756

Herrington DM, Brosnihan KB, Pusser BE, et al. Differential effects of E and droloxifene on C-reactive protein and other markers of inflammation in healthy postmenopausal women. J Clin Endocrinol Metab. 2001 Sep;86(9):4216-22. PMID: 11549652.

D6958 Droloxifene Citrate

25 mg
100 mg
250 mg

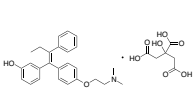

$C_{26}H_{29}NO_2 \bullet C_6H_8O_7$ FW: 579.64 [97752-20-0] ≥98%

Tamoxifen analog and SERM that acts as an ER agonist in bone and as an ER antagonist in breast tissue. It increases apoptosis in luteal cells, inhibits bone resorption and turnover, and decreases levels of E-selectin.

Shelly W, Draper MW, Krishnan V, et al. Selective estrogen receptor modulators: an update on recent clinical findings. Obstet Gynecol Surv. 2008 Mar;63(3):163-81. PMID: 18279543.

Martin JH, Symonds A, Chohan S. Down-regulation of nitric oxide production by droloxifene and toremifene in human breast cancer cells. Oncol Rep. 2003 Jul-Aug;10(4):979-84. PMID: 12792756

D8014 DU-14

5 mg
25 mg

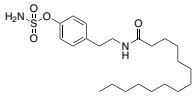

$C_{22}H_{38}N_2O_4S$ FW: 426.6 [186303-55-9] ≥98%

Steroid sulfatase inhibitor. It increases levels of excitatory neurosteroids, enhances cognitive function,and improves memory acquisition and learning associated with contextual fear and spatial memory.

Babalola PA, Fitz NF, Gibbs RB, et al. The effect of the steroid sulfatase inhibitor (p-O-sulfamoyl)-tetradecanoyl tyramine (DU-14) on learning and memory in rats with selective lesion of septal-hippocampal cholinergic tract. Neurobiol Learn Mem. 2012 Oct;98(3):303-10. PMID: 23022361.

Johnson DA, Wu T, Li P, et al. The effect of steroid sulfatase inhibition on learning and spatial memory. Brain Res. 2000 May 26;865(2):286-90. PMID: 10821934.

Johnson DA, Rhodes ME, Boni RL, et al. Chronic steroid sulfatase inhibition by (p-O-sulfamoyl)-N-tetradecanoyl tyramine increases dehydroepiandrosterone sulfate in whole brain. Life Sci. 1997;61(24):PL 355-9. PMID: 9399636.

D8145 Duloxetine Hydrochloride

100 mg
250 mg
1 g

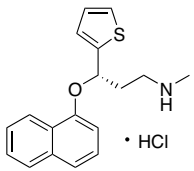

LY-248686 hydrochloride

$C_{18}H_{19}NOS \bullet HCl$ FW: 333.88 [136434-34-9] ≥98%

Inhibitor of SERT, NET, and Nav1.7 Na^+ channels used to treat mood disorders, neuropathy, fibromyalgia, and stress urinary incontinence. It also decreases pain transmission and alters downstream signaling mediated by NMDA receptors and NO.

Wang SY, Calderon J, Kuo Wang G. Block of neuronal Na^+ channels by antidepressant duloxetine in a state-dependent manner. Anesthesiology. 2010 Sep;113(3):655-65. PMID: 20693878.

Carter NJ, McCormack PL. Duloxetine: a review of its use in the treatment of generalized anxiety disorder. CNS Drugs. 2009;23(6):523-41. PMID: 19480470.

Apparsundaram S, Stockdale DJ, Henningsen RA, et al. Antidepressants targeting the serotonin reuptake transporter act via a competitive mechanism. J Pharmacol Exp Ther. 2008 Dec;327(3):982-90. PMID: 18801947.

D8276 Dutasteride

NEW

5 mg
25 mg

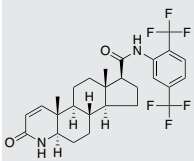

$C_{27}H_{30}F_6N_2O_2$ FW: 528.53 [164656-23-9] ≥98%

5-α-reductase inhibitor used to treat benign prostatic hyperplasia. It induces apoptosis and inhibits proliferation of prostate cells and suppresses growth of prostate tumors.

Tsujimura A, Fukuhara S, Soda T, et al. Histologic evaluation of human benign prostatic hyperplasia treated by dutasteride: a study by xenograft model with improved severe combined immunodeficient mice. Urology. 2015 Jan;85(1):274.e1-8. PMID: 25444635.

Barkin J. Review of dutasteride/tamsulosin fixed-dose combination for the treatment of benign prostatic hyperplasia: efficacy, safety, and patient acceptability. Patient Prefer Adherence. 2011;5:483-90. PMID: 22003286.

Arena F. Dutasteride in the treatment of hormone refractory prostate cancer. Minerva Urol Nefrol. 2008 Jun;60(2):71-6. PMID: 18500220.

D9752

Dynasore

NEW

5 mg
25 mg

$C_{18}H_{14}N_2O_4$ FW: 322.32 [304448-55-3] ≥98%

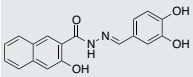

Dynamin inhibitor that prevents endocytosis-mediated membrane fission. It inhibits bone resorption and suppresses HSV viral entry and infectivity.

Mues MB, Cheshenko N, Wilson DW, et al. Dynasore disrupts trafficking of herpes simplex virus proteins. J Virol. 2015 Jul 1;89(13):6673-84. PMID: 25878109.

Thirukonda GJ, Uehara S, Nakayama T, et al. The dynamin inhibitor dynasore inhibits bone resorption by rapidly disrupting actin rings of osteoclasts. J Bone Miner Metab. 2015 Jun 11. [Epub ahead of print]. PMID: 26063501.

Preta G, Cronin JG, Sheldon IM. Dynasore - not just a dynamin inhibitor. Cell Commun Signal. 2015 Apr 10;13:24. PMID: 25889964.

E0001

E64

NEW

5 mg
25 mg
100 mg

$C_{15}H_{27}N_5O_5$ FW: 357.41 [66701-25-5] ≥98%

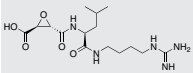

Cysteine protease inhibitor. It decreases production of IL-8.

Quain MD, Makgopa ME, Márquez-García B, et al. Ectopic phytocystatin expression leads to enhanced drought stress tolerance in soybean (Glycine max) and *Arabidopsis* thaliana through effects on strigolactone pathways and can also result in improved seed traits. Plant Biotechnol J. 2014 Apr 22. [Epub ahead of print]. PMID: 24754628.

Lee YA, Nam YH, Min A, et al. *Entamoeba* histolytica-secreted cysteine proteases induce IL-8 production in human mast cells via a PAR2-independent mechanism. Parasite. 2014;21:1. PMID: 24502918.

Shin SP, Han SY, Han JE, et al. Expression and characterization of cathepsin L-like cysteine protease from Philasterides dicentrarchi. Parasitol Int. 2014 Apr;63(2):359-65. PMID: 24361286.

E0003

E64-d

NEW

1 mg
5 mg

Aloxistatin

$C_{17}H_{30}N_2O_5$ FW: 342.43 [88321-09-9] ≥98%

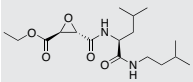

Cathepsin inhibitor. It decreases brain amyloid-β plaque formation and aggravates left ventricular dysfunction in models of myocardial infarction.

Hook G, Yu J, Toneff T, et al. Brain Pyroglutamate Amyloid-Beta is Produced by Cathepsin B and is Reduced by the Cysteine Protease Inhibitor E64d, Representing a Potential Alzheimer's Disease Therapeutic. J Alzheimers Dis. 2014 Mar 4. [Epub ahead of print]. PMID: 24595198.

Chen H, Wang J, Xiang MX, et al. Cathepsin S-mediated fibroblast trans-differentiation contributes to left ventricular remodelling after myocardial infarction. Cardiovasc Res. 2013 Oct 1;100(1):84-94. PMID: 23771947.

E0403

Ebastine

1 g
5 g

$C_{32}H_{39}NO_2$ FW: 469.66 [90729-43-4] ≥98%

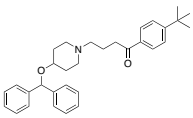

Histamine H1 receptor antagonist used to treat allergic rhinitis. It is minimally sedative. It also increases production of IFN-γ.

Ciprandi G. Clinical utility and patient adherence with ebastine for allergic rhinitis. Patient Prefer Adherence. 2010 Oct 14;4:389-95. PMID: 21206514.

Ciprandi G, Cirillo I, Pistorio A, et al. Ebastine increases IFN-gamma production in patients with persistent allergic rhinitis. J Biol Regul Homeost Agents. 2009 Jan-Mar;23(1):31-6. PMID: 19321044.

Tagawa M, Kano M, Okamura N, et al. Neuroimaging of histamine H1-receptor occupancy in human brain by positron emission tomography (PET): a comparative study of ebastine, a second-generation antihistamine, and (+)-chlorpheniramine, a classical antihistamine. Br J Clin Pharmacol. 2001 Nov;52(5):501-9. PMID: 11736858.

E0073

Ebselen

5 mg
25 mg

$C_{13}H_9NOSe$ FW: 274.18 [60940-34-3] ≥98%

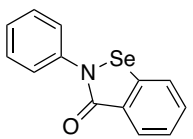

Synthetic glutathione peroxidase mimetic and yeast sporulation inhibitor. It displays a variety of biological activities, including inhibiting GDH function, preventing outer membrane synthesis in *Mycobacterium*, and decreasing decreases glucose levels, Hb1Ac, and oxidative stress.

Azad GK, Singh V, Mandal P, et al. Ebselen induces reactive oxygen species (ROS)-mediated cytotoxicity in *Saccharomyces* cerevisiae with inhibition of glutamate dehydrogenase being a target. FEBS Open Bio. 2014 Jan 6;4:77-89. PMID: 24490132.

Favrot L, Grzegorzewicz AE, Lajiness DH, et al. Mechanism of inhibition of *Mycobacterium* tuberculosis antigen 85 by ebselen. Nat Commun. 2013;4:2748. PMID: 24193546.

Mahadevan J, Parazzoli S, Oseid E, et al. Ebselen treatment prevents islet apoptosis, maintains intranuclear Pdx-1 and MafA levels, and preserves β-cell mass and function in ZDF rats. Diabetes. 2013 Oct;62(10):3582-8. PMID: 23801580.

E0813

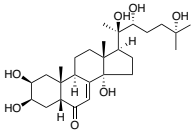

Ecdysterone

5 mg
10 mg
25 mg

20-Hydroxyecdysone; Polypodine A

$C_{27}H_{44}O_7$ FW: 480.64 [5289-74-7] ≥96%

Ecdysone agonist produced by arthropods involved in ecdysis and metamorphosis. It induces autophagy in *Drosophila*, decreases chronic nerve and muscle fatigue, and increases microvessel density in cerebral ischemia models.

Liu H, Jia Q, Tettamanti G, et al. Balancing crosstalk between 20-hydroxyecdysone-induced autophagy and caspase activity in the fat body during *Drosophila* larval-prepupal transition. Insect Biochem Mol Biol. 2013 Nov;43(11):1068-78. PMID: 24036278.

Volodin VV, Sidorova IuS, Mazo VK. 20-Hydroxyecdysone--plant adaptogen: an anabolic effect, possible use in sports nutrition. Vopr Pitan. 2013;82(6):24-30. PMID: 24741953.

Luo C, Yi B, Fan W, et al. Enhanced angiogenesis and astrocyte activation by ecdysterone treatment in a focal cerebral ischemia rat model. Acta Neurochir Suppl. 2011;110(Pt 1):151-5. PMID: 21116931.

E0929

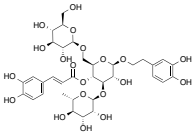

Echinacoside

5 mg
10 mg
25 mg

$C_{35}H_{46}O_{20}$ FW: 786.73 [82854-37-3] ≥98.0%

Found in *Echinacea*. It induces vasodilation, inhibits suppression of dopamine and DAT levels in Parkinson's disease models, and improves bone mineral density and microarchitecture.

Yang X, Li F, Yang Y, et al. Efficacy and safety of echinacoside in a rat osteopenia model. Evid Based Complement Alternat Med. 2013;2013:926928. PMID: 23573159.

Zhu M, Lu C, Li W. Transient exposure to echinacoside is sufficient to activate Trk signaling and protect neuronal cells from rotenone. J Neurochem. 2013 Feb;124(4):571-80. PMID: 23189969.

Wei LL, Chen H, Jiang Y, et al. Effects of echinacoside on histio-central levels of active mass in middle cerebral artery occlusion rats. Biomed Environ Sci. 2012 Apr;25(2):238-44.PMID: 22998833.

E2002

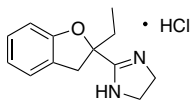

Efaroxan Hydrochloride

25 mg
100 mg
250 mg

$C_{13}H_{16}N_2O \cdot HCl$ FW: 252.74 [89197-00-2] ≥99%

Inhibitor of α2-adrenergic receptors, imidazoline-1 receptors, and ATP-sensitive K^+ channels. It improves glucose tolerance, alters opioid-mediated tolerance and antinociception signaling pathways, and decreases symptoms of Parkinson's Disease.

Milne B, Jhamandas K, Sutak M, et al. Stereo-selective inhibition of spinal morphine tolerance and hyperalgesia by an ultra-low dose of the alpha-2-adrenoceptor antagonist efaroxan. Eur J Pharmacol. 2013 Feb 28;702(1-3):227-34. PMID: 23376415.

Lehner Z, Stadlbauer K, Adorjan I, et al. Mechanisms of antihyperglycaemic action of efaroxan in mice: time for reappraisal of α2A-adrenergic antagonism in the treatment of type 2 diabetes? Diabetologia. 2012 Nov;55(11):3071-82. PMID: 22898767.

Le Brigand L, Virsolvy A, Manechez D, et al. In vitro mechanism of action on insulin release of S-22068, a new putative antidiabetic compound. Br J Pharmacol. 1999 Nov;128(5):1021-6. PMID: 10556939.

E2003

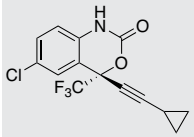

Efavirenz

NEW

10 mg
25 mg
50 mg

$C_{14}H_9ClF_3NO_2$ FW: 315.67 [154598-52-4] ≥98%

Non-nucleoside RT inhibitor used to treat HIV infection. It also induces autophagy in neurons and inhibits cellular proliferation and increases activation of p53 in cancer cells.

Schauer GD, Huber KD, Leuba SH, et al. Mechanism of allosteric inhibition of HIV-1 reverse transcriptase revealed by single-molecule and ensemble fluorescence. Nucleic Acids Res. 2015 Feb 1;42(18):11687-96. PMID: 25232099.

Purnell PR, Fox HS. Efavirenz induces neuronal autophagy and mitochondrial alterations. J Pharmacol Exp Ther. 2014 Nov;351(2):250-8. PMID: 25161171.

Hecht M, Harrer T, Büttner M, et al. Cytotoxic effect of efavirenz is selective against cancer cells and associated with the cannabinoid system. AIDS. 2013 Aug 24;27(13):2031-40. PMID: 23612009.

E2424

H-Ile-Ser-Ile-Asn-Gln-Asp-Leu-Lys-Ala-Ile-Thr-Asp-Met-Leu-Leu-Thr-Glu-Gln-Ile-Arg-Glu-Arg-Gln-Arg-Tyr-Leu-Ala-Asp-Leu-Arg-Gln-Arg-Leu-Leu-Glu-Lys-NH_2

Egg Laying Hormone (from *Aplysia*)

0.5 mg
1 mg
2.5 mg

$C_{190}H_{329}N_{59}O_{57}S_1$ FW: 4384.17 [117680-39-4] ≥95%

Found in *Aplysia*. It is released from bag cell neurons and triggers ovulation.

Hickey CM, Groten CJ, Sham L, et al. Voltage-gated Ca^{2+} influx and mitochondrial Ca^{2+} initiate secretion from *Aplysia* neuroendocrine cells. Neuroscience. 2013 Oct 10;250:755-72. PMID: 23876326.

Li L, Garden RW, Floyd PD, et al. Egg-laying hormone peptides in the aplysiidae family. J Exp Biol. 1999 Nov;202(Pt 21):2961-73. PMID: 10518477.

E4408 Elcatonin Acetate

Please inquire

Ser-Asn-Leu-Ser-Thr-Asu-Val-Leu-Gly-Lys-Leu-Ser-Gln-Glu-Leu-His-Lys-Leu-Gln-Thr-Tyr-Pro-Arg-Thr-Asp-Val-Gly-Ala-Gly-Thr-Pro-Ser---Asu

$C_{148}H_{244}N_{42}O_{47}$ FW: 3363.8 [60731-46-6] ≥95%

Synthetic calcitonin analog. It inhibits thermal and chemical pain transmission, decreases symptoms of gastroesophageal reflux disease, induces osteoblast proliferation, and prevents bone resorption.

Aoki M, Kurauchi Y, Mori A, et al. Comparison of the effects of single doses of elcatonin and pregabalin on oxaliplatin-induced cold and mechanical allodynia in rats. Biol Pharm Bull. 2014;37(2):322-6. PMID: 24492729.

Ito A, Takeda M, Yoshimura T, et al. Anti-hyperalgesic effects of calcitonin on neuropathic pain interacting with its peripheral receptors. Mol Pain. 2012 Jun 7;8:42. PMID: 22676202.

E4416 Eledoisin

1 mg
2 mg
5 mg

pGlu-Pro-Ser-Lys-Asp-Ala-Phe-Ile-Gly-Leu-Met-NH_2

$C_{54}H_{85}N_{13}O_{15}S_1$ FW: 1188.44 [69-25-0] ≥95%

Substance P analog and NK receptor agonist. It modulates gastric acid secretion, induces gastric muscle contractions, and dilates blood vessels.

Tucci P, Bolle P, Severini C. Effects of natural tachykinins on ovine lower urinary tract smooth muscle. J Auton Pharmacol. 2001 Apr;21(2):79-84. PMID: 11679016.

Ito S, Ohta T, Honda H, et al. Gastric vasodilator and motor responses to splanchnic stimulation and tachykinins in the dog. Gen Pharmacol. 1993 Mar;24(2):291-8. PMID: 7683299.

E4417 Eledoisin Related Peptide

5 mg
10 mg
25 mg

ERP

H-Lys-Phe-Ile-Gly-Leu-Met-NH_2

$C_{34}H_{58}N_8O_6S$ FW: 706.96 ≥95%

Substance P analog and NK receptor agonist. It decreases pain thresholds in thermal pain models, induces bronchoconstriction, stimulates gastric acid secretion, and inhibits M-currents.

Clint BD, Lipton JM, Giesecke AH Jr. Analgesic and cardiovascular effects of centrally administered substance P. Peptides. 1988 May-Jun;9(3):619-23. PMID: 2458573.

E4418 β-Elemene

25 mg
100 mg
500 mg

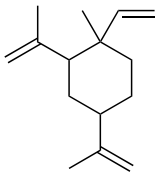

$C_{15}H_{24}$ FW: 204.35 [515-13-9] ≥98%

Found in various plant sources. It suppresses Notch-1 signaling, decreases differentiation of Th17 cells, prevents expression of pro-inflammatory cytokines, and induces apoptosis in various cancer cell lines.

Yan B, Zhou Y, Feng S, et al. β -Elemene-Attenuated Tumor Angiogenesis by Targeting Notch-1 in Gastric Cancer Stem-Like Cells. Evid Based Complement Alternat Med. 2013;2013:268468. PMID: 23710217.

Zhang X, Li Y, Zhang Y, et al. Beta-elemene blocks epithelial-mesenchymal transition in human breast cancer cell line MCF-7 through Smad3-mediated down-regulation of nuclear transcription factors. PLoS One. 2013;8(3):e58719. PMID: 23516540.

E4444 Ellagic Acid

1 g
5 g
10 g
50 g

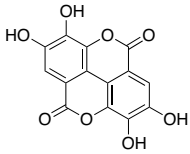

Benzoaric acid

$C_{14}H_6O_8$ FW: 302.2 [476-66-4] ≥98%

HDAC modulator found in fruit. It displays a variety of activities, including suppressing neovascularization and angiogenesis, preventing airway hyperresponsiveness in allergy models, inhibiting cellular proliferation and inducing apoptosis in pancreatic adenocarcinoma cells, and limiting proliferation of *Plasmodium* and *Rhinovirus*.

Zhou E, Fu Y, Wei Z, et al. Inhibition of allergic airway inflammation through the blockage of NF-κB activation by ellagic acid in an ovalbumin-induced mouse asthma model. Food Funct. 2014 Sep;5(9):2106-12. PMID: 24998475.

Kang I, Okla M, Chung S. Ellagic acid inhibits adipocyte differentiation through coactivator-associated arginine methyltransferase 1-mediated chromatin modification. J Nutr Biochem. 2014 Sep;25(9):946-53. PMID: 24929439.

Kowshik J, Giri H, Kiran Kishore TK, et al. Ellagic Acid Inhibits VEGF/VEGFR2, PI3K/Akt and MAPK Signaling Cascades in the Hamster Cheek Pouch Carcinogenesis Model. Anticancer Agents Med Chem. 2014 Jul 23. [Epub ahead of print]. PMID: 25060902.

E4668 ELR-510444

NEW

Please inquire

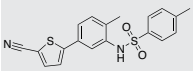

$C_{19}H_{16}N_2O_2S_2$ FW: 368.47 [1233948-35-0] ≥98%

Microtubule polymerization inhibitor. It inhibits cell proliferation and tumor growth in models of breast cancer and suppresses expression of HIF-1α in models of renal cell carcinoma.

Carew JS, Esquivel JA 2nd, Espitia CM, et al. ELR510444 inhibits tumor growth and angiogenesis by abrogating HIF activity and disrupting microtubules in renal cell carcinoma. PLoS One. 2012;7(1):e31120. PMID: 22295124.

Risinger AL, Westbrook CD, Encinas A, et al. ELR510444, a novel microtubule disruptor with multiple mechanisms of action. J Pharmacol Exp Ther. 2011 Mar;336(3):652-60. PMID: 21148249.

E4785 Elvitegravir

NEW

10 mg
25 mg
50 mg

$C_{23}H_{23}ClFNO_5$ FW: 447.88 [697761-98-1] ≥98%

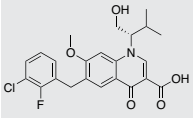

Integrase inhibitor used to treat HIV infection.

Reviriego C. Elvitegravir for the treatment of HIV infection. Drugs Today (Barc). 2014 Mar;50(3):209-17. PMID: 24696866.

Shimura K, Kodama E, Sakagami Y, et al. Broad antiretroviral activity and resistance profile of the novel human immunodeficiency virus integrase inhibitor elvitegravir (JTK-303/GS-9137). J Virol. 2008 Jan;82(2):764-74. PMID: 17977962.

E4902 Emamectin B1 Benzoate

100 mg
250 mg
1 g

MK-244

$C_{49}H_{75}NO_{13}$ FW: 886.12 [137512-74-4] ≥80%

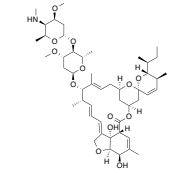

Semi-synthetic GABA signaling potentiator used to treat worm and parasite infections. It induces neuromuscular paralysis in microbes and parasites.

Yen TH, Lin JL. Acute poisoning with emamectin benzoate. J Toxicol Clin Toxicol. 2004;42(5):657-61. PMID: 15462160.

E4912 EMD 1214063

5 mg
10 mg

MSC2156119J

$C_{29}H_{28}N_6O_2$ FW: 492.57 [1100598-32-0] ≥98%

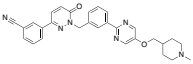

c-MET inhibitor. It inhibits tumor growth and induces regression in models of hepatocellular carcinoma, pancreatic cancer, and glioblastoma.

Bladt F, Friese-Hamim M, Ihling C, et al. The c-Met Inhibitor MSC2156119J Effectively Inhibits Tumor Growth in Liver Cancer Models. Cancers (Basel). 2014 Aug 19;6(3):1736-52. PMID: 25256830.

Bladt F, Faden B, Friese-Hamim M, et al. EMD 1214063 and EMD 1204831 constitute a new class of potent and highly selective c-Met inhibitors. Clin Cancer Res. 2013 Jun 1;19(11):2941-51. PMID: 23553846.

E5057 Emodin

100 mg
250 mg
1 g

$C_{15}H_{10}O_5$ FW: 270.24 [518-82-1] ≥95%

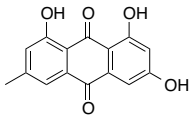

CFTR Cl^- channel activator found in various plant sources. It displays a variety of activities, including increasing fluid secretion and inducing mitochondria-dependent apoptosis.

Ismail S, Haris K, Abdul Ghani AR, et al. Enhanced induction of cell cycle arrest and apoptosis via the mitochondrial membrane potential disruption in human U87 malignant glioma cells by aloe emodin. J Asian Nat Prod Res. 2013 Jul 22. [Epub ahead of print]. PMID: 23869465.

Huang PH, Huang CY, Chen MC, et al. Emodin and Aloe-Emodin Suppress Breast Cancer Cell Proliferation through ER α Inhibition. Evid Based Complement Alternat Med. 2013; Epub 2013 Jun 24. PMID: 23864887.

Zhang W, Chen H, Liu DL, et al. Emodin sensitizes the gemcitabine-resistant cell line Bxpc-3/Gem to gemcitabine via downregulation of NF-κB and its regulated targets. Int J Oncol. 2013 Apr;42(4):1189-96. PMID: 23440366.

E5178 Emtricitabine

NEW

10 mg
25 mg
50 mg

$C_8H_{10}FN_3O_3S$ FW: 247.25 [143491-57-0] ≥98%

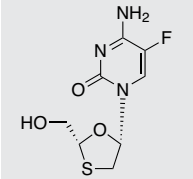

Cytidine analog and inhibitor of RT and telomerase used to treat HIV infection. It also decreases proliferation of hepatitis B virus.

Kulkarni R, Hluhanich R, McColl DM, et al. The combined anti-HIV-1 activities of emtricitabine and tenofovir plus the integrase inhibitor elvitegravir or raltegravir show high levels of synergy in vitro. Antimicrob Agents Chemother. 2014 Oct;58(10):6145-50. PMID: 25092710.

Arribas JR, Eron J. Advances in antiretroviral therapy. Curr Opin HIV AIDS. 2013 Jul;8(4):341-9. PMID: 23666392.

E5202 Enalapril

1 g
5 g

$C_{20}H_{28}N_2O_5$ FW: 376.45 [75847-73-3] ≥98%

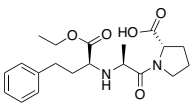

ACE inhibitor used to treat hypertension, heart failure, and diabetic nephropathy. It prevents and reverses atrial remodeling and improves endothelial function by increasing levels of NO.

Chen JL, Shang QH, Hu W, et al. Role of TGF-β1/Smads pathway in carotid artery remodeling in renovascular hypertensive rats and prevention by Enalapril and Amlodipine. J Geriatr Cardiol. 2012 Jun;9(2):185-91. PMID: 22916067.

Bilan VP, Salah EM, Bastacky S, et al. Diabetic nephropathy and long-term treatment effects of rosiglitazone and enalapril in obese ZSF1 rats. J Endocrinol. 2011 Sep;210(3):293-308. PMID: 21680617.

Javanmard SH, Sonbolestan SA, Heshmat-Ghahdarijani K, et al. Enalapril improves endothelial function in patients with migraine: A randomized, double-blind, placebo-controlled trial. J Res Med Sci. 2011 Jan;16(1):26-32. PMID: 21448379.

E5201 Enalapril Maleate

1 g
5 g

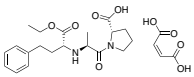

$C_{20}H_{28}N_2O_5 \bullet C_4H_4O_4$ FW: 492.52 [76095-16-4] ≥98%

ACE inhibitor used to treat hypertension, heart failure, and diabetic nephropathy. It prevents and reverses atrial remodeling and improves endothelial function by increasing levels of NO.

Chen JL, Shang QH, Hu W, et al. Role of TGF-β1/Smads pathway in carotid artery remodeling in renovascular hypertensive rats and prevention by Enalapril and Amlodipine. J Geriatr Cardiol. 2012 Jun;9(2):185-91. PMID: 22916067.

Bilan VP, Salah EM, Bastacky S, et al. Diabetic nephropathy and long-term treatment effects of rosiglitazone and enalapril in obese ZSF1 rats. J Endocrinol. 2011 Sep;210(3):293-308. PMID: 21680617.

Javanmard SH, Sonbolestan SA, Heshmat-Ghahdarijani K, et al. Enalapril improves endothelial function in patients with migraine: A randomized, double-blind, placebo-controlled trial. J Res Med Sci. 2011 Jan;16(1):26-32. PMID: 21448379.

E5200 Enalaprilat Dihydrate

10 mg
50 mg
100 mg

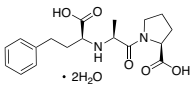

$C_{18}H_{24}N_2O_5 \bullet 2H_2O$ FW: 384.42 [84680-54-6] ≥98%

Enalapril metabolite and ACE inhibitor used to treat hypertension, heart failure, and diabetic nephropathy. It prevents and reverses atrial remodeling and improves endothelial function by increasing levels of NO.

Chen JL, Shang QH, Hu W, et al. Role of TGF-β1/Smads pathway in carotid artery remodeling in renovascular hypertensive rats and prevention by Enalapril and Amlodipine. J Geriatr Cardiol. 2012 Jun;9(2):185-91. PMID: 22916067.

Bilan VP, Salah EM, Bastacky S, et al. Diabetic nephropathy and long-term treatment effects of rosiglitazone and enalapril in obese ZSF1 rats. J Endocrinol. 2011 Sep;210(3):293-308. PMID: 21680617.

E5210 Endomorphin-1

5 mg
10 mg
25 mg

H-Tyr-Pro-Trp-Phe-NH_2

$C_{34}H_{38}N_6O_5$ FW: 610.72 [189388-22-5] ≥95%

Endogenous μOR agonist. It increases pain thresholds and stimulates proliferation, migration, adhesion, and tube formation in endothelial cells.

Dai X, Song HJ, Cui SG, et al. The stimulative effects of endogenous opioids on endothelial cell proliferation, migration and angiogenesis in vitro. Eur J Pharmacol. 2010 Feb 25;628(1-3):42-50. PMID: 19932695.

Anton B, Leff P, Calva JC, et al. Endomorphin 1 and endomorphin 2 suppress in vitro antibody formation at ultra-low concentrations: anti-peptide antibodies but not opioid antagonists block the activity. Brain Behav Immun. 2008 Aug;22(6):824-32. PMID: 18374539.

E5211 Endomorphin-2

5 mg
10 mg
25 mg

H-Tyr-Pro-Phe-Phe-NH_2

$C_{32}H_{37}N_5O_5$ FW: 571.68 [141801-26-5] ≥95%

Endogenous μOR agonist. It increases pain thresholds and stimulates proliferation, migration, adhesion, and tube formation in endothelial cells.

Liu NJ, Gintzler AR. Spinal endomorphin 2 antinociception and the mechanisms that produce it are both sex- and stage of estrus cycle-dependent in rats. J Pain. 2013 Nov;14(11):1522-30. PMID: 24084000.

Dai X, Song HJ, Cui SG, et al. The stimulative effects of endogenous opioids on endothelial cell proliferation, migration and angiogenesis in vitro. Eur J Pharmacol. 2010 Feb 25;628(1-3):42-50. PMID: 19932695.

E5212 Endonuclease Antigenic Site

1 mg
2 mg
5 mg

Glu-Thr-Gly-Gln-Glu-Thr-Ala-Tyr-Phe-Leu-Leu-Lys-Leu-Ala-Gly-Arg-Trp-Pro-Val-Lys

$C_{108}H_{167}N_{27}O_{29}$ FW: 2307.67 ≥98%

HIV-1 endonuclease cytotoxic T lymphocyte binding pocket fragment.

Rahman MA, Kuse N, Murakoshi H, et al. Raltegravir and elvitegravir-resistance mutation E92Q affects HLA-B*40:02-restricted HIV-1-specific CTL recognition. Microbes Infect. 2014 May;16(5):434-8. PMID: 24657622.

E5214 α-Endorphin

1 mg
2 mg
5 mg

H-Tyr-Gly-Gly-Phe-Met-Thr-Ser-Glu-Lys-Ser-Gln-Thr-Pro-Leu-Val-Thr-OH

$C_{77}H_{120}N_{18}O_{26}S$ FW: 1745.98 [61512-76-3] ≥95%

Endogenous μOR agonist that plays a significant role in reward and reinforcement signaling. It increases pain thresholds and decreases depression-like behaviors.

Charbogne P, Kieffer BL, Befort K. 15 years of genetic approaches in vivo for addiction research: Opioid receptor and peptide gene knockout in mouse models of drug abuse. Neuropharmacology. 2014 Jan;76 Pt B:204-17. PMID: 24035914.

Dinas PC, Koutedakis Y, Flouris AD. Effects of exercise and physical activity on depression. Ir J Med Sci. 2011 Jun;180(2):319-25. PMID: 21076975.

E5215

Ac-Tyr-Gly-Gly-Phe-Met-Thr-Ser-Glu-Lys-Ser-Gln-Thr-Pro-Leu-Val-Thr-OH

Acetyl-α-Endorphin

1 mg
2 mg
5 mg

$C_{79}H_{122}N_{18}O_{27}S$ FW: 1788.02 ≥95%

α-Endorphin derivative and μOR agonist that is involved in reward and reinforcement signaling. It increases pain thresholds and decreases depression-like behaviors.

Charbogne P, Kieffer BL, Befort K. 15 years of genetic approaches in vivo for addiction research: Opioid receptor and peptide gene knockout in mouse models of drug abuse. Neuropharmacology. 2014 Jan;76 Pt B:204-17. PMID: 24035914.

Dinas PC, Koutedakis Y, Flouris AD. Effects of exercise and physical activity on depression. Ir J Med Sci. 2011 Jun;180(2):319-25. PMID: 21076975.

E5216

H-Tyr-Gly-Gly-Phe-Met-Thr-Ser-Glu-Lys-Ser-Gln-Thr-Pro-Leu-Val-Thr-Leu-Phe-Lys-Asn-Ala-Ile-Ile-Lys-Asn-Ala-His-Lys-Lys-Gly-Gln-OH

β-Endorphin, camel

1 mg
2 mg
5 mg

$C_{155}H_{250}N_{42}O_{44}S$ FW: 3438.04 ≥95%

Endogenous μOR agonist. It plays a role in reward and reinforcement signaling, increases B cell levels and antibody production, and decreases depression-like behaviors.

Charbogne P, Kieffer BL, Befort K. 15 years of genetic approaches in vivo for addiction research: Opioid receptor and peptide gene knockout in mouse models of drug abuse. Neuropharmacology. 2014 Jan;76 Pt B:204-17. PMID: 24035914.

Gein SV, Baeva TA, Nebogatikov VO, et al. β-Endorphin effects on antibody production, proliferation, and secretion of Th1/Th2 cytokines in vivo. Bull Exp Biol Med. 2012 Mar;152(5):595-9. PMID: 22803142.

E5217

H-Tyr-Gly-Gly-Phe-Met-Thr-Ser-Glu-Lys-Ser-Gln-Thr-Pro-Leu-Val-Thr-Leu-Phe-Lys-Asn-Ala-Ile-Ile-Lys-Asn-Ala-Tyr-Lys-Lys-Gly-Glu-OH

β-Endorphin, human

1 mg
2 mg
5 mg

$C_{158}H_{251}N_{39}O_{46}S$ FW: 3465.06 ≥95%

Endogenous μOR agonist. It plays a role in reward and reinforcement signaling, increases B cell levels and antibody production, and decreases depression-like behaviors.

Charbogne P, Kieffer BL, Befort K. 15 years of genetic approaches in vivo for addiction research: Opioid receptor and peptide gene knockout in mouse models of drug abuse. Neuropharmacology. 2014 Jan;76 Pt B:204-17. PMID: 24035914.

Gein SV, Baeva TA, Nebogatikov VO, et al. β-Endorphin effects on antibody production, proliferation, and secretion of Th1/Th2 cytokines in vivo. Bull Exp Biol Med. 2012 Mar;152(5):595-9. PMID: 22803142.

E5218

H-Tyr-Gly-Gly-Phe-Met-Thr-Ser-Glu-Lys-Ser-Gln-Thr-Pro-Leu-Val-Thr-Leu-Phe-Lys-Asn-Ala-Ile-Ile-Lys-Asn-Val-His-Lys-Lys-Gly-Gln-OH

β-Endorphin, rat

1 mg
2 mg
5 mg

$C_{157}H_{254}N_{42}O_{44}S$ FW: 3466.09 ≥95%

Endogenous μOR agonist. It plays a role in reward and reinforcement signaling, increases B cell levels and antibody production, and decreases depression-like behaviors.

Charbogne P, Kieffer BL, Befort K. 15 years of genetic approaches in vivo for addiction research: Opioid receptor and peptide gene knockout in mouse models of drug abuse. Neuropharmacology. 2014 Jan;76 Pt B:204-17. PMID: 24035914.

Gein SV, Baeva TA, Nebogatikov VO, et al. β-Endorphin effects on antibody production, proliferation, and secretion of Th1/Th2 cytokines in vivo. Bull Exp Biol Med. 2012 Mar;152(5):595-9. PMID: 22803142.

E5219

H-Cys-Ser-Cys-Ser-Ser-Leu-Met-Asp-Lys-Glu-Cys-Val-Tyr-Phe-Cys-His-Leu-Asp-Ile-Ile-Trp-OH
(Cys1-Cys15, Cys3-Cys11)

Endothelin-1, human

0.5 mg
1 mg
2.5 mg

$C_{109}H_{159}N_{25}O_{32}S_5$ FW: 2491.95 ≥95%

Endogenous endothelin A/B receptor agonist involved in vascular contraction. It induces proliferation in osteoblasts and decreases tube formation and PPARγ expression in pulmonary artery endothelial cells.

Zhong X, Wang H, Huang S. Endothelin-1 induces interleukin-18 expression in human osteoblasts. Arch Oral Biol. 2014 Mar;59(3):289-96. PMID: 24581851.

Osmond JM, Gonzalez Bosc LV, Walker BR, et al. Endothelin-1-induced vasoconstriction does not require intracellular Ca^{2+} waves in arteries from rats exposed to intermittent hypoxia. Am J Physiol Heart Circ Physiol. 2014 Mar;306(5):H667-73. PMID: 24414066.

E5221

H-Cys-Ser-Cys-Ser-Ser-Trp-Leu-Asp-Lys-Glu-Cys-Val-Tyr-Phe-Cys-His-Leu-Asp-Ile-Ile-Trp-OH
(Cys1-Cys15, Cys3-Cys11)

Endothelin-2, human

0.5 mg
1 mg
2.5 mg

$C_{115}H_{160}N_{26}O_{32}S_4$ FW: 2546.97 [123562-20-9] ≥95%

Endogenous endothelin A/B receptor agonist involved in vascular contraction. It inhibits endothelial cell migration and invasion and promotes myelination.

Compeer MG, Janssen GM, De Mey JG. Endothelin-1 and endothelin-2 initiate and maintain contractile responses by different mechanisms in rat mesenteric and cerebral arteries. Br J Pharmacol. 2013 Nov;170(6):1199-209. PMID: 23941276.

Rattner A, Yu H, Williams J, et al. Endothelin-2 signaling in the neural retina promotes the endothelial tip cell state and inhibits angiogenesis. Proc Natl Acad Sci U S A. 2013 Oct 1;110(40):E3830-9. PMID: 24043815.

E5222 — Endothelin-3, human

0.5 mg
1 mg
2.5 mg

H-Cys-Thr-Cys-Phe-Thr-Tyr-Lys-Asp-Lys-Glu-Cys-Val-Tyr-Tyr-Cys-His-Leu-Asp-Ile-Ile-Trp-OH
(Cys1-Cys15, Cys3-Cys11)

$C_{121}H_{168}N_{26}O_{33}S_4$ FW: 2643.1 [117399-93-6] ≥95%

Endogenous endothelin B receptor agonist involved in vascular contraction. It also inhibits platelet-activating factor-induced edema, suppresses hypothalamic release of norepinephrine, and increases expression of VEGF, COX1/2, HIF-1α, and prostaglandin E2.

Sato A, Ebina K. Endothelin-3 at low concentrations attenuates inflammatory responses via the endothelin B2 receptor. Inflamm Res. 2013 Apr;62(4):417-24. PMID: 23370722.

Spinella F, Rosanò L, Di Castro V, et al. Endothelin-1 and endothelin-3 promote invasive behavior via hypoxia-inducible factor-1alpha in human melanoma cells. Cancer Res. 2007 Feb 15;67(4):1725-34. PMID: 17308114.

E5220 — Enfuvirtide (T-20)

1 mg
2 mg
5 mg

CH_3CO-Tyr-Thr-Ser-Leu-Ile-His-Ser-Leu-Ile-Glu-Glu-Ser-Gln-Asn-Gln-Gln-Glu-Lys-Asn-Glu-Gln-Glu-Leu-Leu-Glu-Leu-Asp-Lys-Trp-Ala-Ser-Leu-Trp-Asn-Trp-Phe-NH_2

T20; DP178

$C_{204}H_{301}N_{51}O_{64}$ FW: 4462 [159519-65-0] ≥95%

Viral fusion inhibitor derived from HIV-1 used to treat HIV infection. It mimics the sequence of gp41, preventing fusion of the virus to the host cell membrane. It may also induce apoptosis in other cells.

Tan JJ, Ma XT, Liu C, et al. The current status and challenges in the development of fusion inhibitors as therapeutics for HIV-1 infection. Curr Pharm Des. 2013;19(10):1810-7. PMID: 23092283.

Cai L, Gochin M, Liu K. Biochemistry and biophysics of HIV-1 gp41 - membrane interactions and implications for HIV-1 envelope protein mediated viral-cell fusion and fusion inhibitor design. Curr Top Med Chem. 2011 Dec;11(24):2959-84. PMID: 22044229.

E5240 — Leu-Enkephalin

25 mg
50 mg
125 mg

H-Tyr-Gly-Gly-Phe-Leu-OH

$C_{28}H_{37}N_5O_7$ FW: 555.62 [58822-25-6] ≥95%

Endogenous δOR and μOR agonist involved in reward and reinforcement signaling. It also increases pain thresholds and inhibits gastrointestinal muscle contractility.

Popov M, Abu Hammad I, Bachar T, et al. Delivery of analgesic peptides to the brain by nano-sized bolaamphiphilic vesicles made of monolayer membranes. Eur J Pharm Biopharm. 2013 Nov;85(3 Pt A):381-9. PMID: 23791683.

Crayton R, Soller W, Mattiasson A, et al. Exogenously administered opioids contract the female rat intrinsic urethral sphincter in vivo. Neurourol Urodyn. 2010 Jun;29(5):777-82. PMID: 19899147.

E5241 — Met-Enkephalin

25 mg
50 mg
125 mg

H-Tyr-Gly-Gly-Phe-Met-OH

Opioid growth factor; Adrenorphin (1-5)

$C_{27}H_{35}N_5O_7S$ FW: 573.67 [58569-55-4] ≥95%

Endogenous δOR and μOR agonist involved in reward and reinforcement signaling. It also increases pain thresholds, decreases depression-like behaviors, and inhibits gastrointestinal muscle contractility.

Gonzalez-Nunez V, Jimenez González A, Barreto-Valer K, et al. In vivo regulation of the μ opioid receptor: role of the endogenous opioid agents. Mol Med. 2013 Mar 5;19:7-17. PMID: 23348513.

Fanning RA, McMorrow JP, Campion DP, et al. Opioid mediated activity and expression of mu and delta opioid receptors in isolated human term non-labouring myometrium. Eur J Pharmacol. 2013 Jan 5;698(1-3):170-7. PMID: 23051674.

E2542 — Met-Enkephalin Amide

10 mg
20 mg
50 mg

H-Tyr-Gly-Gly-Phe-Met-NH_2

$C_{27}H_{36}N_6O_6S$ FW: 572.69 [60117-17-1] ≥95%

Endogenous δOR and μOR agonist involved in reward and reinforcement signaling. It also increases pain thresholds, decreases depression-like behaviors, and inhibits gastrointestinal muscle contractility.

Gonzalez-Nunez V, Jimenez González A, Barreto-Valer K, et al. In vivo regulation of the μ opioid receptor: role of the endogenous opioid agents. Mol Med. 2013 Mar 5;19:7-17. PMID: 23348513.

E5456 — Enocitabine

25 mg
100 mg
250 mg

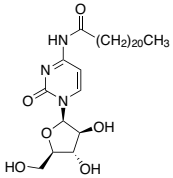

BH-AC

$C_{31}H_{55}N_3O_6$ FW: 565.78 [55726-47-1] ≥98%

Cytarabine derivative, cytosine analog, and DNA chain terminator. It also also inhibits replication and growth of cytomegalovirus.

Ito Y, Wakita A, Takada S, et al. Phase 1 trial of gemtuzumab ozogamicin in combination with enocitabine and daunorubicin for elderly patients with relapsed or refractory acute myeloid leukemia: Japan Adult Leukemia Study Group (JALSG)-GML208 study. Int J Hematol. 2012 Oct;96(4):485-91. PMID: 22956429.

Hamada A, Kawaguchi T, Nakano M. Clinical pharmacokinetics of cytarabine formulations. Clin Pharmacokinet. 2002;41(10):705-18. PMID: 12162758.

Nakamura K, Eizuru Y, Kumura K, et al. Antiviral effect of antileukemic drugs N4-behenoyl-1-beta-D-arabinofuranosylcytosine (BH-AC) and 2,2'-anhydro-1-beta-D-arabinofuranosylcytosine (cyclo-C) against human cytomegalovirus. J Med Virol. 1990 Jun;31(2):141-7. PMID: 1696958.

E5358 Enoxacin

500 mg
1 g
5 g

$C_{15}H_{17}FN_4O_3$ FW: 320.32 [74011-58-8] ≥98%

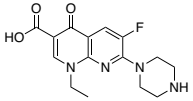

Vacuolar H^+ ATPase, topoisomerase IV,and bacterial DNA gyrase inhibitor used to treat bacterial infections. It also inhibits osteoclast formation by decreasing RANKL-induced JNK signaling.

Liu X, Qu X, Wu C, et al. The effect of enoxacin on osteoclastogenesis and reduction of titanium particle-induced osteolysis via suppression of JNK signaling pathway. Biomaterials. 2014 Jul;35(22):5721-30. PMID: 24767789.

Toro EJ, Zuo J, Ostrov DA, et al. Enoxacin directly inhibits osteoclastogenesis without inducing apoptosis. J Biol Chem. 2012 May 18;287(21):17894-904. PMID: 22474295.

Zuma AA, Cavalcanti DP, Maia MC, et al. Effect of topoisomerase inhibitors and DNA-binding drugs on the cell proliferation and ultrastructure of Trypanosoma cruzi. Int J Antimicrob Agents. 2011 May;37(5):449-56. PMID: 21292448.

E5568 Enramycin A

1 mg
5 mg
25 mg

[34438-27-2] ≥95%

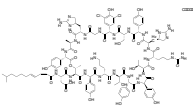

Peptidoglycan inhibitor that prevents cell wall synthesis and is used as a livestock feed additive to prevent bacterial infection, accelerate growth rates, and relieve stress reactions.

Pedroso AA, Menten JF, Lambais MR, et al. Intestinal bacterial community and growth performance of chickens fed diets containing antibiotics. Poult Sci. 2006 Apr;85(4):747-52. PMID: 16615359.

Ohya T, Sato S. Effects of dietary antibiotics on intestinal microflora in broiler chickens. Natl Inst Anim Health Q (Tokyo). 1983 Summer;23(2):49-60. PMID: 6680771.

Kariyama R. Increase of cardiolipin content in *Staphylococcus aureus* by the use of antibiotics affecting the cell wall. J Antibiot (Tokyo). 1982 Dec;35(12):1700-4. PMID: 7166534.

E5569 Enramycin B

1 mg
5 mg
25 mg

[34304-21-7] ≥83%

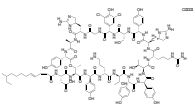

Peptidoglycan inhibitor that prevents cell wall synthesis and is used as a livestock feed additive to prevent bacterial infection, accelerate growth rates, and relieve stress reactions.

Pedroso AA, Menten JF, Lambais MR, et al. Intestinal bacterial community and growth performance of chickens fed diets containing antibiotics. Poult Sci. 2006 Apr;85(4):747-52. PMID: 16615359.

Ohya T, Sato S. Effects of dietary antibiotics on intestinal microflora in broiler chickens. Natl Inst Anim Health Q (Tokyo). 1983 Summer;23(2):49-60. PMID: 6680771.

Kariyama R. Increase of cardiolipin content in *Staphylococcus aureus* by the use of antibiotics affecting the cell wall. J Antibiot (Tokyo). 1982 Dec;35(12):1700-4. PMID: 7166534.

E5369 Enrofloxacin

5 g
10 g
50 g

$C_{19}H_{22}FN_3O_3$ FW: 359.39 [93106-60-6] ≥98%

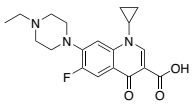

Bacterial DNA gyrase inhibitor used to treat gram positive and gram negative infection in veterinary medicine.

Cengiz M, Sahinturk P, Sonal S, et al. In vitro bactericidal activity of enrofloxacin against gyrA mutant and qnr-containing *Escherichia* coli isolates from animals. Vet Rec. 2013 May 4;172(18):474. PMID: 23605176.

Rzedzicki J, Boś M, Kolasa A. Influence of antibiotics on growth dynamics and movement ability of *Salmonella* rods. Pol J Vet Sci. 2004;7(4):267-74. PMID: 15633786.

E5575 Entacapone

25 mg
100 mg
500 mg

$C_{14}H_{15}N_3O_5$ FW: 305.29 [116314-67-1] ≥98%

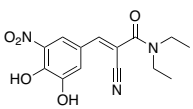

COMT inhibitor used to treat Parkinson's disease. It reduces clearance of L-DOPA, improves motor function, and prevents α-synuclein and amyloid-β oligomerization and fibril formation.

Di Giovanni S, Eleuteri S, Paleologou KE, et al. Entacapone and tolcapone, two catechol O-methyltransferase inhibitors, block fibril formation of alpha-synuclein and beta-amyloid and protect against amyloid-induced toxicity. J Biol Chem. 2010 May 14;285(20):14941-54. PMID: 20150427.

Hamaue N, Ogata A, Terado M, et al. Entacapone, a catechol-O-methyltransferase inhibitor, improves the motor activity and dopamine content of basal ganglia in a rat model of Parkinson's disease induced by Japanese encephalitis virus. Brain Res. 2010 Jan 14;1309:110-5. PMID: 19879254.

Deleu D, Northway MG, Hanssens Y. Clinical pharmacokinetic and pharmacodynamic properties of drugs used in the treatment of Parkinson's disease. Clin Pharmacokinet. 2002;41(4):261-309. PMID: 11978145.

E5576 Entecavir

1 mg
5 mg
25 mg

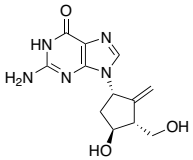

$C_{12}H_{15}N_5O_3$ FW: 277.28 [142217-69-4] ≥97%

Deoxyguanosine analog, DNA chain terminator, and RT inhibitor used to treat hepatitis B infections. It prevents DNA synthesis and may inhibit HIV-1 RT.

Yurdaydin C. Entecavir: a step forward in combating hepatitis B disease. Expert Opin Pharmacother. 2008 Dec;9(17):3095-109. PMID: 19006481.

Cheng PN, Chang TT. Entecavir: a potent antiviral with minimal long-term resistance in nucleoside-naive chronic hepatitis B patients. Expert Rev Anti Infect Ther. 2008 Oct;6(5):569-79. PMID: 18847396.

E5276 Enterostatin, human

1 mg
2 mg
5 mg

Ala-Pro-Gly-Pro-Arg

$C_{21}H_{86}N_3O_6$ FW: 496.57 [117830-79-2] ≥97%

Endogenous F1-ATPase inhibitor involved in dietary fat intake. It decreases serum cholesterol and inhibits insulin secretion.

Erlanson-Albertsson C. Fat-Rich Food Palatability and Appetite Regulation. In: Montmayeur JP, le Coutre J, editors. Fat Detection: Taste, Texture, and Post Ingestive Effects. Boca Raton (FL): CRC Press; 2010. Chapter 14. PMID: 21452478.

Takenaka Y, Shimano T, Mori T, et al. Enterostatin reduces serum cholesterol levels by way of a CCK(1) receptor-dependent mechanism. Peptides. 2008 Dec;29(12):2175-8. PMID: 18824202.

E5277 Enterostatin, pig/rat

1 mg
2 mg
5 mg

Val-Pro-Asp-Pro-Arg

$C_{25}H_4N_8O_8$ FW: 582.66 ≥98%

Endogenous F1-ATPase inhibitor involved in dietary fat intake. It decreases serum cholesterol and inhibits insulin secretion.

Erlanson-Albertsson C. Fat-Rich Food Palatability and Appetite Regulation. In: Montmayeur JP, le Coutre J, editors. Fat Detection: Taste, Texture, and Post Ingestive Effects. Boca Raton (FL): CRC Press; 2010. Chapter 14. PMID: 21452478.

E5477 Entinostat

1 mg
5 mg
25 mg

SNDX-275; MS-275

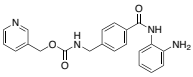

$C_{21}H_{20}N_4O_3$ FW: 376.41 [209783-80-2] ≥98%

HDAC1 inhibitor. It decreases formation of tubulin-based microtentacles, prevents epithelial-to-mesenchymal transition, improves the ability of natural killer cells to destroy cancer cells, and decreases amyloid-β deposition in the hippocampus and cortex.

Shah P, Gau Y, Sabnis G. Histone deacetylase inhibitor entinostat reverses epithelial to mesenchymal transition of breast cancer cells by reversing the repression of E-cadherin. Breast Cancer Res Treat. 2013 Dec 5. [Epub ahead of print]. PMID: 24305977.

Zhu S, Denman CJ, Cobanoglu ZS, et al. The Narrow-Spectrum HDAC Inhibitor Entinostat Enhances NKG2D Expression Without NK Cell Toxicity, Leading to Enhanced Recognition of Cancer Cells. Pharm Res. 2013 Nov 8. [Epub ahead of print]. PMID: 24203492.

E6231 (−)-Epicatechin

1 mg
5 mg
25 mg

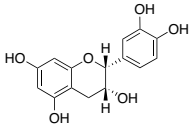

$C_{15}H_{14}O_6$ FW: 290.27 [490-46-0] ≥93%

Catechin found in *Camilla* (green tea). It decreases levels of amyloid-β in the brain, minimizes atherosclerotic lesion area, and decreases infarct size in models of myocardial ischemia/reperfusion.

Yamazaki KG, Andreyev AY, Ortiz-Vilchis P, et al. Intravenous (-)-epicatechin reduces myocardial ischemic injury by protecting mitochondrial function. Int J Cardiol. 2014 Aug 1;175(2):297-306. PMID: 24908200.

Zeng YQ, Wang YJ, Zhou XF. Effects of (-)Epicatechin on the Pathology of APP/PS1 Transgenic Mice. Front Neurol. 2014 May 9;5:69. PMID: 24847308.

Morrison M, van der Heijden R, Heeringa P, et al. Epicatechin attenuates atherosclerosis and exerts anti-inflammatory effects on diet-induced human-CRP and NFκB in vivo. Atherosclerosis. 2014 Mar;233(1):149-56. PMID: 24529136.

E6232 (−)-Epicatechin gallate

1 mg
5 mg
25 mg

ECG

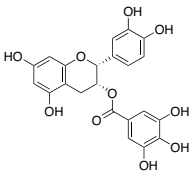

$C_{22}H_{18}O_{10}$ FW: 442.37 [1257-08-5] ≥98%

CB1 agonist found in *Camilla* (green tea). It suppresses proliferation in acute myelogenous leukemia cells and inhibits LPS- and peptidoglycan-induced production of VEGF and expression of COX-2.

Nakanishi T, Mukai K, Hosokawa Y, et al. Catechins inhibit vascular endothelial growth factor production and cyclooxygenase-2 expression in human dental pulp cells. Int Endod J. 2014 May 21. [Epub ahead of print]. PMID: 24847951.

Ly BT, Chi HT, Yamagishi M, et al. Inhibition of FLT3 expression by green tea catechins in FLT3 mutated-AML cells. PLoS One. 2013 Jun 20;8(6):e66378. PMID: 23840454.

E6233

(−)-Epigallocatechin

1 mg
5 mg

EGC

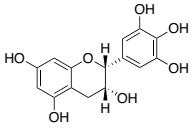

$C_{15}H_{14}O_7$ FW: 306.27 [970-74-1] ≥98%

CB1 agonist found in *Camilla* (green tea). It decreases platelet aggregation, inhibits cell migration and invasion of breast cancer cells, suppresses adipocyte formation, and increases osteogenic differentiation.

Chen XQ, Wang XB, Guan RF, et al. Blood anticoagulation and antiplatelet activity of green tea (-)-epigallocatechin (EGC) in mice. Food Funct. 2013 Oct;4(10):1521-5. PMID: 24056410.

Ly BT, Chi HT, Yamagishi M, et al. Inhibition of FLT3 expression by green tea catechins in FLT3 mutated-AML cells. PLoS One. 2013 Jun 20;8(6):e66378. PMID: 23840454.

E6234

Epigallocatechin Gallate

25 mg
50 mg
100 mg

EGCG; 3-O-gallate

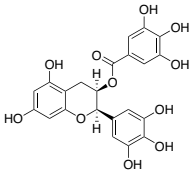

$C_{22}H_{18}O_{11}$ FW: 458.37 [989-51-5] ≥98%

Found in *Camilla* (green tea). It inhibits HSP90, AhR, STAT3, α-amylase, and α-glucosidase. It displays many biological activities, including suppressing α-synuclein oligomerization and amyloid-β aggregation, limiting ROS-mediated DNA damage and oxidative stress, inducing cell cycle arrest and apoptosis in hepatocarcinoma cells, and stimulating apoptosis in *Candida*.

Moses MA, Henry EC, Ricke WA, et al. The heat shock protein 90 inhibitor, (-)-epigallocatechin gallate, has anticancer activity in a novel human prostate cancer progression model. Cancer Prev Res (Phila). 2015 Mar;8(3):249-57. PMID: 25604133.

Lorenzen N, Nielsen SB, Yoshimura Y, et al. How epigallocatechin gallate can inhibit α-synuclein oligomer toxicity in vitro. J Biol Chem. 2014 Aug 1;289(31):21299-310. PMID: 24907278.

Bao S, Cao Y, Fan C, et al. Epigallocatechin gallate improves insulin signaling by decreasing toll-like receptor 4 (TLR4) activity in adipose tissues of high-fat diet rats. Mol Nutr Food Res. 2014 Apr;58(4):677-86. PMID: 24259392

E6236

Epigallocatechin Gallate Octaacetate

10 mg
25 mg
100 mg

Peracetylated epigallocatechin gallate; Octaacetyl epigallocatechin gallate

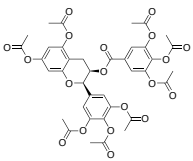

$C_{38}H_{34}O_{19}$ FW: 794.67 ≥98%

Green tea catechin and derivative of EGCG. It inhibits acetylation of histone H3K9, suppresses dextran sulfate sodium-induced colitis and colon tumorigenesis, and activates ERK1/2 signaling.

Chiou YS, Sang S, Cheng KH, et al. Peracetylated (-)-epigallocatechin-3-gallate (AcEGCG) potently prevents skin carcinogenesis by suppressing the PKD1-dependent signaling pathway in CD34+ skin stem cells and skin tumors. Carcinogenesis. 2013 Jun;34(6):1315-22. PMID: 23385063.

E6134

Epimedin C

5 mg
10 mg
25 mg

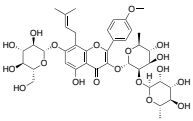

$C_{39}H_{50}O_{19}$ FW: 822.8 [110642-44-9] ≥98.0%

Found in *Epimedium sagittatum*. It inhibits proliferation of hepatoma cells and enhances lymphocyte proliferation and increased IL-2 production in hydrocortisone acetate-mediated immunosuppression models.

Liu TZ, Chen CY, Yiin SJ, et al. Molecular mechanism of cell cycle blockage of hepatoma SK-Hep-1 cells by Epimedin C through suppression of mitogen-activated protein kinase activation and increased expression of CDK inhibitors p21(Cip1) and p27(Kip1). Food Chem Toxicol. 2006 Feb;44(2):227-35. PMID: 16112786.

Liang HR, Vuorela P, Vuorela H, et al. Isolation and immunomodulatory effect of flavonol glycosides from *Epimedium* hunanense. Planta Med. 1997 Aug;63(4):316-9. PMID: 9270375.

E6432

(−)-Epinephrine

1 g
5 g
10 g
100 g

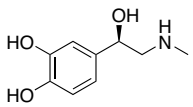

$C_9H_{13}NO_3$ FW: 183.2 [51-43-4] ≥98%

Active isomer of epinephrine, endogenous hormone neurotransmitter, and α/β-adrenergic receptor agonist involved in sympathetic nervous system signaling. It is used to treat cardiac arrest and anaphylaxis. It increases cardiac output and peripheral resistance, decreases edema, inhibits insulin secretion, increases glucagon and adrenocorticotropic hormone (ACTH) secretion, and induces glycogenolysis, glycolysis, and lipolysis.

Seravalle G, Dimitriadis K, Dell'Oro R, et al. How to assess sympathetic nervous system activity in clinical practice. Curr Clin Pharmacol. 2013 Aug;8(3):182-8. PMID: 23173963.

Busse PJ, Buckland MS. Non-histaminergic angioedema: focus on bradykinin-mediated angioedema. Clin Exp Allergy. 2013 Apr;43(4):385-94. PMID: 23517034.

E6235

Epirubicin Hydrochloride

1 mg
5 mg
10 mg

Epiadriamycin

$C_{27}H_{29}NO_{11} \cdot HCl$ FW: 579.99 [56390-09-1] ≥90%

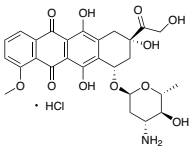

DNA intercalator and topoisomerase II inhibitor used to treat breast cancer. It inhibits DNA and RNA synthesis and increases levels of ROS.

Monteiro LJ, Khongkow P, Kongsema M, et al. The Forkhead Box M1 protein regulates BRIP1 expression and DNA damage repair in epirubicin treatment. Oncogene. 2013 Sep 26;32(39):4634-45. PMID: 23108394.

Conte PF, Gennari A, Landucci E, et al. Role of epirubicin in advanced breast cancer. Clin Breast Cancer. 2000 Sep;1 Suppl 1:S46-51. PMID: 11970749.

E6245

Eplerenone

10 mg
25 mg
100 mg

$C_{24}H_{30}O_6$ FW: 414.29 [107724-20-9] ≥98%

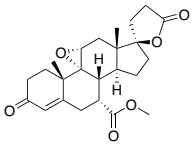

Mineralocorticoid receptor antagonist used to treat congestive heart failure. It prevents COX expression and high salt diet-induced kidney damage, decreases oxidative stress, and suppresses nephrotic VEGF expression.

Yasuoka S, Kai H, Kajimoto H, et al. Blood pressure variability activates cardiac mineralocorticoid receptor and induces cardiac remodeling in hypertensive rats. Circ J. 2013;77(6):1474-81. PMID: 23470864.

Bayorh M, Rollins-Hairston A, Adiyiah J, et al. Eplerenone inhibits aldosterone-induced renal expression of cyclooxygenase. J Renin Angiotensin Aldosterone Syst. 2012 Sep;13(3):353-9. PMID: 22554826.

Bayorh MA, Rollins-Hairston A, Adiyiah J, et al. Eplerenone suppresses aldosterone/ salt-induced expression of NOX-4. J Renin Angiotensin Aldosterone Syst. 2011 Sep;12(3):195-201. PMID: 21292834.

E6256

Epothilone A

1 mg
5 mg
10 mg
25 mg

$C_{26}H_{39}NO_6S$ FW: 493.66 [152044-53-6] ≥95%

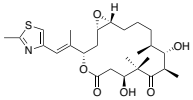

Microtubule depolymerization inhibitor that binds β-tubulin and induces formation of a short helix. It inhibits growth of lung cancer and prostate cancer cells. It is the most active of the epothilone subtypes.

Prota AE, Bargsten K, Zurwerra D, et al. Molecular mechanism of action of microtubule-stabilizing anticancer agents. Science. 2013 Feb 1;339(6119):587-90. PMID: 23287720.

Entwistle RA, Rizk RS, Cheng DM, et al. Differentiating between models of epothilone binding to microtubules using tubulin mutagenesis, cytotoxicity, and molecular modeling. ChemMedChem. 2012 Sep;7(9):1580-6. PMID: 22807375.

Edelman MJ, Shvartsbeyn M. Epothilones in development for non--small-cell lung cancer: novel anti-tubulin agents with the potential to overcome taxane resistance. Clin Lung Cancer. 2012 May;13(3):171-80. PMID: 22133291

E6257

Epothilone B

1 mg
5 mg
10 mg
25 mg

$C_{27}H_{41}NO_6S$ FW: 507.68 [152044-54-7] ≥98%

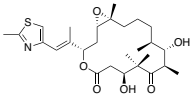

Microtubule depolymerization inhibitor that binds β-tubulin and induces formation of a short helix. It inhibits growth of lung cancer and prostate cancer cells and stimulates axonal regeneration in spinal cord injury models.

Ruschel J, Hellal F, Flynn KC, et al. Systemic administration of epothilone B promotes axon regeneration after spinal cord injury. Science. 2015 Mar 12. [Epub ahead of print]. PMID: 25765066.

Prota AE, Bargsten K, Zurwerra D, et al. Molecular mechanism of action of microtubule-stabilizing anticancer agents. Science. 2013 Feb 1;339(6119):587-90. PMID: 23287720.

Entwistle RA, Rizk RS, Cheng DM, et al. Differentiating between models of epothilone binding to microtubules using tubulin mutagenesis, cytotoxicity, and molecular modeling. ChemMedChem. 2012 Sep;7(9):1580-6. PMID: 22807375.

E6356

Epothilone D

1 mg
5 mg
10 mg
25 mg

$C_{27}H_{41}NO_5S$ FW: 491.68 [189453-10-9] ≥98%

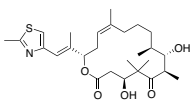

Microtubule depolymerization inhibitor that binds β-tubulin and induces formation of a short helix. It inhibits growth of lung cancer and prostate cancer cells. It is the least active of the epothilone subtypes.

Prota AE, Bargsten K, Zurwerra D, et al. Molecular mechanism of action of microtubule-stabilizing anticancer agents. Science. 2013 Feb 1;339(6119):587-90. PMID: 23287720.

Entwistle RA, Rizk RS, Cheng DM, et al. Differentiating between models of epothilone binding to microtubules using tubulin mutagenesis, cytotoxicity, and molecular modeling. ChemMedChem. 2012 Sep;7(9):1580-6. PMID: 22807375.

Edelman MJ, Shvartsbeyn M. Epothilones in development for non--small-cell lung cancer: novel anti-tubulin agents with the potential to overcome taxane resistance. Clin Lung Cancer. 2012 May;13(3):171-80. PMID: 22133291

E6259

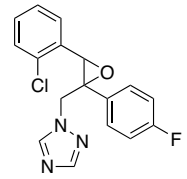

Epoxiconazole

5 g
10 g
100 g

$C_{17}H_{13}ClFN_3O$ FW: 329.76 [106325-08-0] ≥95%

14-α Demethylase inhibitor that inhibits ergosterol synthesis and fungal cell wall formation. It may inhibit aromatase and act as an endocrine disrupter.

Schneider S, Hofmann T, Stinchcombe S, et al. Species differences in developmental toxicity of epoxiconazole and its relevance to humans. Birth Defects Res B Dev Reprod Toxicol. 2013 Jun;98(3):230-46. PMID: 23630118.

Kjærstad MB, Taxvig C, Nellemann C, et al. Endocrine disrupting effects in vitro of conazole antifungals used as pesticides and pharmaceuticals. Reprod Toxicol. 2010 Dec;30(4):573-82. PMID: 20708073.

Taxvig C, Vinggaard AM, Hass U, et al. Endocrine-disrupting properties in vivo of widely used azole fungicides. Int J Androl. 2008 Apr;31(2):170-7. PMID: 18067565.

E6470

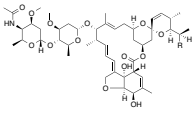

Eprinomectin

100 mg
250 mg
1 g

B_{1a}: C_2H_5 $C_{50}H_{75}NO_{14}$; B_{1b}: CH_3 $C_{49}H_{73}NO_{14}$ [123997-26-2] ≥45%

Semi-synthetic GABA signaling potentiator used to inhibit bacterial infections. It causes neuromuscular paralysis in microbes and parasites.

Knaus M, Chester ST, Rosentel J, et al. Efficacy of a novel topical combination of fipronil, (S)-methoprene, eprinomectin and praziquantel against larval and adult stages of the cat lungworm, Aelurostrongylus abstrusus. Vet Parasitol. 2014 Apr 28;202(1-2):64-8. PMID: 24703080.

Nazir T, Katoch R, Godara R, et al. Efficacy of eprinomectin pour-on against Rhipicephalus (Boophilus) microplus on buffaloes. J Parasit Dis. 2013 Oct;37(2):166-7. PMID: 24431562.

E6376

Map-Har-Gly-Asp-Trp-Pro-Cys-NH_2
(Disulfide bridge, Map1-Cys6)

Eptifibatide

5 mg
10 mg
25 mg

$C_{35}H_{49}N_{11}O_9S_2$ FW: 832.4 [188627-80-7] ≥98%

Glycoprotein IIb/IIIa inhibitor that inhibits fibrinogen-mediated platelet aggregation and is used to treat cute coronary syndrome.

Angiolillo DJ. The evolution of antiplatelet therapy in the treatment of acute coronary syndromes: from aspirin to the present day. Drugs. 2012 Nov 12;72(16):2087-116. PMID: 23083110.

Gurbel PA, Galbut B, Bliden KP, et al. Effect of eptifibatide for acute coronary syndromes: rapid versus late administration--therapeutic yield on platelets (The EARLY Platelet Substudy). J Thromb Thrombolysis. 2002 Dec;14(3):213-9. PMID: 12913401.

E6398

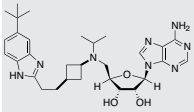

EPZ-5676

NEW

1 mg
5 mg
10 mg

$C_{30}H_{42}N_8O_3$ FW: 562.71 [1380288-87-8] ≥98%

DOT1L HMT inhibitor. It induces cell death in acute myelogenous leukemia cells.

Basavapathruni A, Olhava EJ, Daigle SR, et al. Nonclinical pharmacokinetics and metabolism of EPZ-5676, a novel DOT1L histone methyltransferase inhibitor. Biopharm Drug Dispos. 2014 Jan 10. [Epub ahead of print]. PMID: 24415392.

Daigle SR, Olhava EJ, Therkelsen CA, et al. Potent inhibition of DOT1L as treatment of MLL-fusion leukemia. Blood. 2013 Aug 8;122(6):1017-25. PMID: 23801631.

E6396

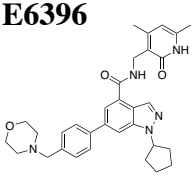

EPZ005687

1 mg
5 mg
25 mg

$C_{32}H_{37}N_5O_3$ FW: 539.67 [1396772-26-1] ≥99%

EZH2 HMT inhibitor active against Y641 and A677 EZH2 mutants. It induces apoptosis and controls gene transcription fidelity in cells.

Knutson SK, Wigle TJ, Warholic NM, et al. A selective inhibitor of EZH2 blocks H3K27 methylation and kills mutant lymphoma cells. Nat Chem Biol. 2012 Nov;8(11):890-6. PMID: 23023262.

E6397

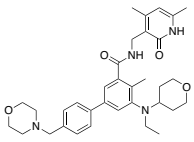

EPZ6438

E7438

1 mg
5 mg
25 mg

$C_{34}H_{44}N_4O_4$ FW: 572.74 [1403254-99-8] ≥99%

EZH2 HMT inhibitor. It induces regression in malignant or atypical teratoid rhabdoid tumors containing altered or mutant SWI/SNF ATP-dependent chromatin remodelers.

Knutson SK, Warholic NM, Wigle TJ, et al. Durable tumor regression in genetically altered malignant rhabdoid tumors by inhibition of methyltransferase EZH2. Proc Natl Acad Sci U S A. 2013 May 7;110(19):7922-7. PMID: 23620515.

E6781 (±)-Equol

10 mg
25 mg
100 mg

$C_{15}H_{14}O_3$ FW: 242.27 [94105-90-5] ≥98%

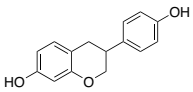

Phytoestrogen and ER agonist found in soy. It is the major metabolite of daidzein. It increases expression of extracellular matrix proteins collagen and elastin, decreases expression of pro-inflammatory cytokines, and induces apoptosis in cancer models.

Lephart ED. Protective effects of equol and their polyphenolic isomers against dermal aging: microarray/protein evidence with clinical implications and unique delivery into human skin. Pharm Biol. 2013 Nov;51(11):1393-400. PMID: 23862588.

Richardson TE, Simpkins JW. R- and S-equol have equivalent cytoprotective effects in Friedreich's ataxia. BMC Pharmacol Toxicol. 2012 Oct 22;13:12. PMID: 23088310.

Choi EJ, Kim GH. Anticancer mechanism of equol in 7,12-dimethylbenz(a)anthracene-treated animals. Int J Oncol. 2011 Sep;39(3):747-54. PMID: 21667019.

E6814 Erdosteine

100 mg
500 mg
1 g

RV-144

$C_8H_{11}NO_4S_2$ FW: 249.31 [84611-23-4] ≥98%

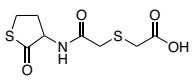

Thiol derivative and antioxidant used to treat bronchitis and COPD. It inhibits H_2O_2-induced oxidative stress and DNA damage, scavenges free radicals, and decreases levels of leukotrienes.

Marabini L, Calò R, Braga PC. Protective effect of erdosteine metabolite I against hydrogen peroxide-induced oxidative DNA-damage in lung epithelial cells. Arzneimittelforschung. 2011;61(12):700-6. PMID: 22282957.

Dal Negro RW, Visconti M, Tognella S, et al. Erdosteine affects eicosanoid production in COPD. Int J Clin Pharmacol Ther. 2011 Jan;49(1):41-5. PMID: 21176724.

E6825 Ergosterol

5 g
10 g
25 g
100 g

Provitamin D2

$C_{28}H_{44}O$ FW: 396.65 [57-87-4] ≥96%

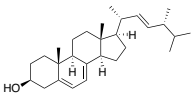

Sterol cell membrane component found in yeast and fungi. It inhibits bladder cancer tumor promotion and suppresses neovascularization in sarcoma models.

Roberts CW, McLeod R, Rice DW, et al. Fatty acid and sterol metabolism: potential antimicrobial targets in apicomplexan and trypanosomatid parasitic protozoa. Mol Biochem Parasitol. 2003 Feb;126(2):129-42. PMID: 12615312.

Takaku T, Kimura Y, Okuda H. Isolation of an antitumor compound from Agaricus blazei Murill and its mechanism of action. J Nutr. 2001 May;131(5):1409-13. PMID: 11340091.

E6846 Erlotinib Monohydrochloride

10 mg
25 mg
100 mg
500 mg

$C_{22}H_{23}N_3O_4 \bullet HCl$ FW: 429.9 [183319-69-9] ≥98%

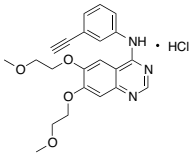

EGFR inhibitor. It induces autophagy and cell cycle arrest in non-small cell lung cancer cells.

Li YY, Lam SK, Mak JC, et al. Erlotinib-induced autophagy in epidermal growth factor receptor mutated non-small cell lung cancer. Lung Cancer. 2013 Sep;81(3):354-61. PMID: 23769318.

Miyabayashi K, Ijichi H, Mohri D, et al. Erlotinib prolongs survival in pancreatic cancer by blocking gemcitabine-induced MAPK signals. Cancer Res. 2013 Apr 1;73(7):2221-34. PMID: 23378339.

Weickhardt AJ, Price TJ, Chong G, et al. Dual targeting of the epidermal growth factor receptor using the combination of cetuximab and erlotinib: preclinical evaluation and results of the phase II DUX study in chemotherapy-refractory, advanced colorectal cancer. J Clin Oncol. 2012 May 1;30(13):1505-12. PMID: 22412142.

E6880 Erucin

25 mg
50 mg
100 mg

4-Methylthiobutyl isothiocyanate

$C_6H_{11}NS_2$ FW: 161.29 [4430-36-8] ≥98%

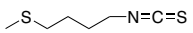

Sulforaphane analog and telomerase inhibitor found in cruciferous vegetables. It induces phase II enzyme activity, suppresses cellular proliferation in hepatocellular carcinoma cells, prevents 6-OHDA-induced neurodegeneration, and inhibits LPS-stimulated pro-inflammatory cytokine expression in vivo.

Herz C, Hertrampf A, Zimmermann S, et al. The isothiocyanate erucin abrogates telomerase in hepatocellular carcinoma cells in vitro and in an orthotopic xenograft tumour model of HCC. J Cell Mol Med. 2014 Sep 25. [Epub ahead of print]. PMID: 25256442.

Cho HJ, Lee KW, Park JH. Erucin exerts anti-inflammatory properties in murine macrophages and mouse skin: possible mediation through the inhibition of NFκB signaling. Int J Mol Sci. 2013 Oct 15;14(10):20564-77. dPMID: 24132147.

Tarozzi A, Morroni F, Bolondi C, et al. Neuroprotective Effects of Erucin against 6-Hydroxydopamine-Induced Oxidative Damage in a Dopaminergic-like Neuroblastoma Cell Line. Int J Mol Sci. 2012;13(9):10899-910. PMID: 23109827.

E6896 Erysolin, 97%

25 mg
50 mg
100 mg
500 mg

$C_6H_{11}NO_2S_2$ FW: 193.29 [504-84-7] ≥97%

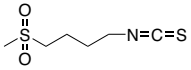

Sulforaphane analog found in cruciferous vegetables. It induces phase II enzyme activity and inhibits growth of colon cancer cells.

Kim MJ, Kim SH, Lim SJ. Comparison of the apoptosis-inducing capability of sulforaphane analogues in human colon cancer cells. Anticancer Res. 2010 Sep;30(9):3611-9. PMID: 20944144.

Zhang Y, Talalay P, Cho CG, et al. A major inducer of anticarcinogenic protective enzymes from broccoli: isolation and elucidation of structure. Proc Natl Acad Sci U S A. 1992 Mar 15;89(6):2399-403. PMID: 1549603.

E6994 Erythromycin

5 g
25 g
100 g

$C_{37}H_{67}NO_{13}$ FW: 733.93 [114-07-8] ≥94%

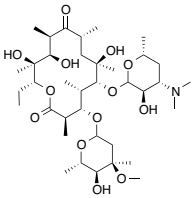

Inhibitor of protein translation and mammalian mRNA splicing. It inhibits growth of gram negative and gram positive bacteria.

Hertweck M, Hiller R, Mueller MW. Inhibition of nuclear pre-mRNA splicing by antibiotics in vitro. Eur J Biochem. 2002 Jan;269(1):175-83. PMID: 11784311.

Menninger JR, Otto DP. Erythromycin, carbomycin, and spiramycin inhibit protein synthesis by stimulating the dissociation of peptidyl-tRNA from ribosomes. Antimicrob Agents Chemother. 1982 May;21(5):811-8. PMID: 6179465.

E6995 Erythromycin Ethylsuccinate

5 g
25 g
100 g

$C_{43}H_{75}NO_{16}$ FW: 862.05 [41342-53-4] ≥97%

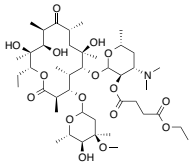

Inhibitor of protein translation and mammalian mRNA splicing. It inhibits growth of gram negative and gram positive bacteria.

Hertweck M, Hiller R, Mueller MW. Inhibition of nuclear pre-mRNA splicing by antibiotics in vitro. Eur J Biochem. 2002 Jan;269(1):175-83. PMID: 11784311.

Menninger JR, Otto DP. Erythromycin, carbomycin, and spiramycin inhibit protein synthesis by stimulating the dissociation of peptidyl-tRNA from ribosomes. Antimicrob Agents Chemother. 1982 May;21(5):811-8. PMID: 6179465.

E6993 Erythromycin Resistance Peptide MRLFV

1 mg
2 mg
5 mg

E-peptide

Met-Arg-Leu-Phe-Val

$C_{31}H_{52}N_8O_6S$ FW: 664.86 ≥95%

It confers resistance against macrolide antibiotics such as erythromycin by preventing antibiotic-ribosome interactions.

Verdier L, Gharbi-Benarous J, Bertho G, et al. Antibiotic resistance peptides: interaction of peptides conferring macrolide and ketolide resistance with *Staphylococcus aureus* ribosomes: conformation of bound peptides as determined by transferred NOE experiments. Biochemistry. 2002 Apr 2;41(13):4218-29. PMID: 11914067.

E6996 Erythromycin Thiocyanate

5 g
25 g
100 g

$C_{37}H_{67}NO_{13} \bullet HSCN$ FW: 793.02 [7704-67-8] ≥90%

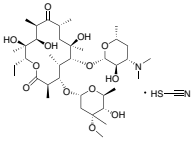

Protein translation and mammalian mRNA splicing inhibitor. It is active against both gram negative and gram positive bacteria.

Hertweck M, Hiller R, Mueller MW. Inhibition of nuclear pre-mRNA splicing by antibiotics in vitro. Eur J Biochem. 2002 Jan;269(1):175-83. PMID: 11784311.

Menninger JR, Otto DP. Erythromycin, carbomycin, and spiramycin inhibit protein synthesis by stimulating the dissociation of peptidyl-tRNA from ribosomes. Antimicrob Agents Chemother. 1982 May;21(5):811-8. PMID: 6179465.

E6997 Erythropoietin

50 U

Hemopoietine; ESF; Epo

[11096-26-7] ≥97%

Endogenous glycoprotein hormone and EpoR agonist involved in red blood cell production. It is used to treat anemia. It also increases absorption of iron, increases proliferation of smooth muscle fibers, stimulates angiogenesis, and improves memory and mood.

Liu S, Ren J, Hong Z, et al. Efficacy of erythropoietin combined with enteral nutrition for the treatment of anemia in Crohn's disease: a prospective cohort study. Nutr Clin Pract. 2013 Feb;28(1):120-7. PMID: 23064018.

Ashby DR, Gale DP, Busbridge M, et al. Erythropoietin administration in humans causes a marked and prolonged reduction in circulating hepcidin. Haematologica. 2010 Mar;95(3):505-8. PMID: 19833632.

Miskowiak K, Inkster B, Selvaraj S, et al. Erythropoietin improves mood and modulates the cognitive and neural processing of emotion 3 days post administration. Neuropsychopharmacology. 2008 Feb;33(3):611-8. PMID: 17473836.

E7209

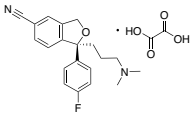

Escitalopram Oxalate

10 mg
50 mg
100 mg

$C_{22}H_{21}FN_2O \bullet C_2H_2O_4$ FW: 414.43 [219861-08-2] ≥99%

S-enantiomer of citalopram and inhibitor of SERT used to treat depression. It also decreases weight gain, suppresses formation of osteoclasts and osteoblasts, prevents production of NO and TNF-α, and potentially prolongs the cardiac QT interval.

Hodge JM, Wang Y, Berk M, et al. Selective serotonin reuptake inhibitors inhibit human osteoclast and osteoblast formation and function. Biol Psychiatry. 2013 Jul 1;74(1):32-9. PMID: 23260229.

Tynan RJ, Weidenhofer J, Hinwood M, et al. A comparative examination of the anti-inflammatory effects of SSRI and SNRI antidepressants on LPS stimulated microglia. Brain Behav Immun. 2012 Mar;26(3):469-79. PMID: 22251606.

E7309

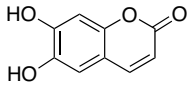

Esculetin

500 mg
1 g

6,7-Dihydroxycoumarin; Cichorigenin

$C_9H_6O_4$ FW: 178.14 [305-01-1] ≥98%

β-catenin inhibitor found in chicory and other plant sources. It displays a wide variety of activities, including inhibiting MPTP-induced neurotoxicity and neuronal apoptosis, decreasing body weight, triglyceride levels, total cholesterol, and glucose levels in high-fat diet-fed animals, and suppressing proliferation of colon cancer cells.

Kim Y, Park Y, Namkoong S, et al. Esculetin inhibits the inflammatory response by inducing heme oxygenase-1 in cocultured macrophages and adipocytes. Food Funct. 2014 Aug 20;5(9):2371-7. PMID: 25088305.

Rubio V, Calviño E, García-Pérez A, et al. Human acute promyelocytic leukemia NB4 cells are sensitive to esculetin through induction of an apoptotic mechanism. Chem Biol Interact. 2014 Jul 1;220C:129-139. PMID: 24995577.

E7310

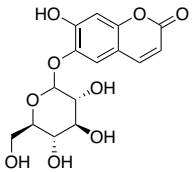

Esculin

5 g
10 g

Bicolorin

$C_{15}H_{16}O_9$ FW: 340.28 [531-75-9] ≥97%

Antioxidant found in *Aesculus*, *Daphne*, and *Bursaria*. It is hydrolyzed by species of *Streptococcus*, *Enterococcus*, *Listeria*, and *Aerococcus*. It also decreases lipid peroxidation and lowers blood glucose and glucose-6-phosphatase levels in diabetes models.

Kang KS, Lee W, Jung Y, et al. Protective effect of esculin on streptozotocin-induced diabetic renal damage in mice. J Agric Food Chem. 2014 Mar 5;62(9):2069-76. PMID: 24484395.

Naaz F, Abdin MZ, Javed S. Protective effect of esculin against prooxidant aflatoxin B1-induced nephrotoxicity in mice. Mycotoxin Res. 2014 Feb;30(1):25-32. PMID: 24326591.

E7356

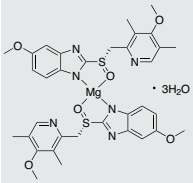

Esomeprazole Magnesium Trihydrate

NEW

50 mg
250 mg
1 g

$2(C_{17}H_{18}N_3O_3S)\ Mg \bullet 3H_2O$ FW: 767.17 [217087-09-7] ≥98%

S-isomer of omeprazole and H^+/K^+ ATPase and MAO-A/B inhibitor used to treat ulcers and gastroesophageal reflux disease. It also decreases mTOR activity and induces autophagy in melanoma cells, increases gastric antioxidant capacity, and induces apoptosis in osteoclasts and osteoblasts.

Sugano K, Choi MG, Lin JT, et al. Multinational, double-blind, randomised, placebo-controlled, prospective study of esomeprazole in the prevention of recurrent peptic ulcer in low-dose acetylsalicylic acid users: the LAVENDER study. Gut. 2013 Dec 10. [Epub ahead of print]. PMID: 24326741.

Costa-Rodrigues J, Reis S, Teixeira S, et al. Dose-dependent inhibitory effects of proton pump inhibitors on human osteoclastic and osteoblastic cell activity. FEBS J. 2013 Oct;280(20):5052-64. PMID: 23937530.

Petzer A, Pienaar A, Petzer JP. The inhibition of monoamine oxidase by esomeprazole. Drug Res (Stuttg). 2013 Sep;63(9):462-7. PMID: 23677700.

E7357

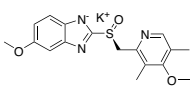

Esomeprazole Potassium

25 mg
100 mg
500 mg

(S)-Omeprazole potassium

$C_{17}H_{18}N_3O_3S\ K$ FW: 383.51 [161796-84-5] ≥98%

(S)-isomer of omeprazole and inhibitor of H^+/K^+ ATPase and MAO-A/B used to treat ulcers. It also induces autophagy and apoptosis in melanoma cells, decreases bone turnover, and increases antioxidative enzyme expression.

Sugano K, Choi MG, Lin JT, et al. Multinational, double-blind, randomised, placebo-controlled, prospective study of esomeprazole in the prevention of recurrent peptic ulcer in low-dose acetylsalicylic acid users: the LAVENDER study. Gut. 2013 Dec 10. [Epub ahead of print]. PMID: 24326741.

Costa-Rodrigues J, Reis S, Teixeira S, et al. Dose-dependent inhibitory effects of proton pump inhibitors on human osteoclastic and osteoblastic cell activity. FEBS J. 2013 Oct;280(20):5052-64. PMID: 23937530.

E7376 Estradiol

1 g
5 g
25 g

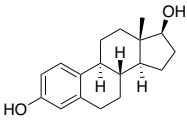

$C_{18}H_{24}O_2$ FW: 272.38 [50-28-2] ≥97%

Endogenous steroid hormone involved in regulation of menstrual cycle and growth of reproductive organs. It is an ER agonist used in HRT. It also inhibits acetylcholine-induced vascular constriction, prevents sperm apoptosis, and limits glutamate-induced neurotoxicity.

Pentikäinen V, Erkkilä K, Suomalainen L, et al. Estradiol acts as a germ cell survival factor in the human testis in vitro. J Clin Endocrinol Metab. 2000 May;85(5):2057-67. PMID: 10843196.

Behl C, Widmann M, Trapp T, et al. 17-beta estradiol protects neurons from oxidative stress-induced cell death in vitro. Biochem Biophys Res Commun. 1995 Nov 13;216(2):473-82. PMID: 7488136.

Collins P, Rosano GM, Sarrel PM, et al. 17 beta-Estradiol attenuates acetylcholine-induced coronary arterial constriction in women but not men with coronary heart disease. Circulation. 1995 Jul 1;92(1):24-30. PMID: 7788912.

E7578 Estramustine

100 mg
250 mg
1 g

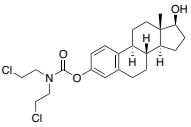

$C_{23}H_{31}Cl_2NO_3$ FW: 440.4 [2998-57-4] ≥98%

Estradiol derivative and microtubule depolymerization inducer used to treat prostate cancer. It induces apoptosis in various cancer cells and increases DNA fragmentation in glioma cells without affecting normal tissue.

Matsumoto K, Tanaka N, Hayakawa N, et al. Efficacy of estramustine phosphate sodium hydrate (EMP) monotherapy in castration-resistant prostate cancer patients: report of 102 cases and review of literature. Med Oncol. 2013 Dec;30(4):717. PMID: 24005812.

Mohan R, Panda D. Kinetic stabilization of microtubule dynamics by estramustine is associated with tubulin acetylation, spindle abnormalities, and mitotic arrest. Cancer Res. 2008 Aug 1;68(15):6181-9. PMID: 18676841.

Yoshida D, Hoshino S, Shimura T, et al. Drug-induced apoptosis by anti-microtubule agent, estramustine phosphate on human malignant glioma cell line, U87MG; in vitro study. J Neurooncol. 2000 Apr;47(2):133-40. PMID: 10982154.

E7579 Estramustine Phosphate Sodium

25 mg
100 mg
250 mg
1 g

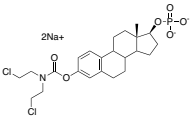

$C_{23}H_{32}Cl_2NO_6PNa_2$ FW: 564.35 [52205-73-9] ≥95%

Estradiol derivative and microtubule depolymerization inducer used to treat prostate cancer. It induces apoptosis in various cancer cells and increases DNA fragmentation in glioma cells without affecting normal tissue.

Matsumoto K, Tanaka N, Hayakawa N, et al. Efficacy of estramustine phosphate sodium hydrate (EMP) monotherapy in castration-resistant prostate cancer patients: report of 102 cases and review of literature. Med Oncol. 2013 Dec;30(4):717. PMID: 24005812.

Mohan R, Panda D. Kinetic stabilization of microtubule dynamics by estramustine is associated with tubulin acetylation, spindle abnormalities, and mitotic arrest. Cancer Res. 2008 Aug 1;68(15):6181-9. PMID: 18676841.

E7377 Estriol

100 mg
500 mg
1 g

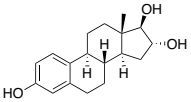

$C_{18}H_{24}O_3$ FW: 288.38 [50-27-1] ≥97%

Endogenous steroid hormone, estradiol metabolite, and ER agonist used in HRT. It decreases pro-inflammatory cytokine production, improves neuronal pathology, and inhibits platelet aggregation.

Jana P, Maiti S, Kahn NN, et al. Estriol-induced fibrinolysis due to the activation of plasminogen to plasmin by nitric oxide synthesis in platelets. Blood Coagul Fibrinolysis. 2014 Apr 2. [Epub ahead of print]. PMID: 24695088.

Tiwari-Woodruff S, Voskuhl RR. Neuroprotective and anti-inflammatory effects of estrogen receptor ligand treatment in mice. J Neurol Sci. 2009 Nov 15;286(1-2):81-5. PMID: 19442988.

Huang R, Kaji Y, Fukuda S, et al. Experimental use of estriol for visualizing the vitreous body in the anterior chamber after posterior capsule rupture in animal models. J Cataract Refract Surg. 2009 Jul;35(7):1260-5. PMID: 19545818.

E7378 Estrone

1 g
5 g
25 g

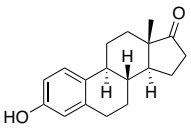

$C_{18}H_{22}O_2$ FW: 270.37 [53-16-7] ≥97%

Endogenous steroid hormone, estriol precursor, and ER agonist. It may be carcinogenic, as it forms DNA adducts.

Rizzati V, Rathahao E, Gamet-Payrastre L, et al. In vitro aromatic bioactivation of the weak estrogen E(2)alpha and genesis of DNA adducts. Steroids. 2005 Mar;70(3):161-72. PMID: 15763594.

Borges C, Lemière F, Embrechts J, et al. Characterisation of estrone-nucleic acid adducts formed by reaction of 3,4-estrone-o-quinone with 2'-deoxynucleosides/deoxynucleotides using capillary liquid chromatography/electrospray ionization mass spectrometry. Rapid Commun Mass Spectrom. 2004;18(19):2191-200. PMID: 15384136.

E7228 Ethacridine Lactate Monohydrate

25 g
50 g
100 g

$C_{15}H_{15}N_{3O} \bullet C_3H_6O_3 \bullet H_2O$ FW: 361.39 [6402-23-9] ≥98%

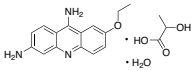

Acridine derivative and DNA intercalator used as an antiseptic. It increases levels of prostaglandin E, decreases excretion of estriol, and may induce fetal death in pregnant females.

Mei Q, Li X, Liu H, et al. Effectiveness of mifepristone in combination with ethacridine lactate for second trimester pregnancy termination. Eur J Obstet Gynecol Reprod Biol. 2014 Jul;178:12-5. PMID: 24948048.

Oie S, Kamiya A. Microbial contamination of antiseptic-soaked cotton balls. Biol Pharm Bull. 1997 Jun;20(6):667-9. PMID: 9212987.

E7230 Ethambutol Dihydrochloride

25 g
100 g

EMB

$C_{10}H_{24}N_2O_2 \bullet 2HCl$ FW: 277.24 [1070-11-7] ≥98%

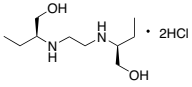

Arabinosyl transferase inhibitor that prevents bacterial cell wall formation and is used to treat tuberculosis.

Plinke C, Walter K, Aly S, et al. *Mycobacterium* tuberculosis embB codon 306 mutations confer moderately increased resistance to ethambutol in vitro and in vivo. Antimicrob Agents Chemother. 2011 Jun;55(6):2891-6. PMID: 21444710.

Kahana LM. Ethambutol in tuberculosis. Biomed Pharmacother. 1990;44(1):21-3. PMID: 1369688.

E7324 Ethisterone

1 g
5 g
25 g
100 g

$C_{21}H_{28}O_2$ FW: 312.45 [434-03-7] ≥98%

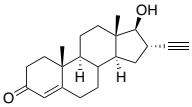

Synthetic contraceptive and progesterone receptor agonist previously used in contraceptives. Derivatives inhibit prostate cancer cell growth.

Levine PM, Imberg K, Garabedian MJ, et al. Multivalent peptidomimetic conjugates: a versatile platform for modulating androgen receptor activity. J Am Chem Soc. 2012 Apr 25;134(16):6912-5. PMID: 22509763.

Forinash AB, Evans SL. New hormonal contraceptives: a comprehensive review of the literature. Pharmacotherapy. 2003 Dec;23(12):1573-91. PMID: 14695038.

E7329 Ethoxyquin

100 g
250 g
1 kg

$C_{14}H_{19}NO$ FW: 217.31 [91-53-2] ≥75%

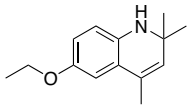

HSP90 inhibitor and antioxidant used as a pesticide and preservative in animal feed.

Sadikot T, Swink M, Eskew JD, et al. Development of a high-throughput screening cancer cell-based luciferase refolding assay for identifying Hsp90 inhibitors. Assay Drug Dev Technol. 2013 Oct;11(8):478-88. PMID: 24127661.

Ørnsrud R, Arukwe A, Bohne V, et al. Investigations on the metabolism and potentially adverse effects of ethoxyquin dimer, a major metabolite of the synthetic antioxidant ethoxyquin in salmon muscle. J Food Prot. 2011 Sep;74(9):1574-80. PMID: 21902931.

E7731 17-α-Ethynylestradiol

1 g
5 g
10 g

$C_{20}H_{24}O_2$ FW: 296.4 [77538-56-8] ≥98%

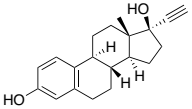

Synthetic ER agonist used as a contraceptive. It decreases platelet activating factor acetylhydrolase activity, leads to feminization of males after chronic exposure, and may induce preterm birth.

Kidd KA, Blanchfield PJ, Mills KH, et al. Collapse of a fish population after exposure to a synthetic estrogen. Proc Natl Acad Sci U S A. 2007 May 22;104(21):8897-901. PMID: 17517636.

Schultz IR, Skillman A, Nicolas JM, et al. Short-term exposure to 17 alpha-ethynylestradiol decreases the fertility of sexually maturing male rainbow trout (Oncorhynchus mykiss). Environ Toxicol Chem. 2003 Jun;22(6):1272-80. PMID: 12785584.

E7433 Etidronate Disodium

1 g
5 g

$C_2H_6Na_2O_7P_2$ FW: 249.99 [7414-83-7] ≥98%

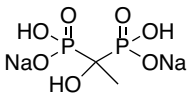

Metal chelating agent used in detergents and cleaning agents. It inhibits bone calcification and resorption and is used to treat osteoporosis. It also decreases production of pro-inflammatory cytokines in macrophages.

Asano S, Suzuki A, Itoh M. Etidronate for treatment of osteoporosis. Nihon Rinsho. 2009 May;67(5):938-42. PMID: 19432113.

Lomashvili KA, Monier-Faugere MC, Wang X, et al. Effect of bisphosphonates on vascular calcification and bone metabolism in experimental renal failure. Kidney Int. 2009 Mar;75(6):617-25. PMID: 19129793.

Suzuki Y, Nishiyama T, Hasuda K, et al. Effect of etidronate on COX-2 expression and PGE(2) production in macrophage-like RAW 264.7 cells stimulated by titanium particles. J Orthop Sci. 2007 Nov;12(6):568-77. PMID: 18040640.

E7556

Etodolac

100 mg
250 mg
1 g

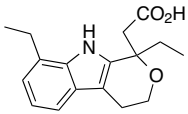

$C_{17}H_{21}NO_3$ FW: 287.35 [41340-25-4] ≥98%

NSAID, TRPA1 receptor agonist, and COX-2 inhibitor used to treat pain and inflammation. It also decreases incidence of intraductal papillary carcinoma, displays radical scavenging activity, and induces cell cycle arrest in hepatocellular carcinoma cells.

Wang S, Dai Y, Kogure Y, et al. Etodolac activates and desensitizes transient receptor potential ankyrin 1. J Neurosci Res. 2013 Dec;91(12):1591-8. PMID: 24027177.

Adachi T, Tajima Y, Kuroki T, et al. Chemopreventive effects of a selective cyclooxygenase-2 inhibitor (etodolac) on chemically induced intraductal papillary carcinoma of the pancreas in hamsters. Carcinogenesis. 2008 Apr;29(4):830-3. PMID: 18296437.

E7758

Etomidate

NEW

10 mg
25 mg
100 mg

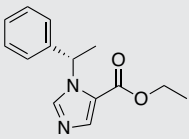

$C_{14}H_{16}N_2O_2$ FW: 244.29 [33125-97-2] ≥98%

GABA-A receptor agonist used to induce anesthesia and sedation. It inhibits presynaptic excitatory synaptic transmission in a SNARE-dependent manner. It also attenuates acetylcholine-induced relaxation in aortic endothelial tissue and impairs memory performance in several tasks.

Herring BE, McMillan K, Pike CM, et al. Etomidate and propofol inhibit the neurotransmitter release machinery at different sites. J Physiol. 2011 Mar 1;589(Pt 5):1103-15. Erratum in: J Physiol. 2011 Sep 15;589(Pt 18):4633. PMID: 21173083.

Martin LJ, Oh GH, Orser BA. Etomidate targets alpha5 gamma-aminobutyric acid subtype A receptors to regulate synaptic plasticity and memory blockade. Anesthesiology. 2009 Nov;111(5):1025-35. PMID: 19809285.

E7657

Etoposide

25 mg
100 mg
500 mg

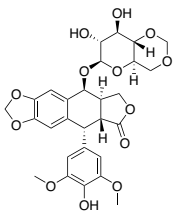

$C_{29}H_{32}O_{13}$ FW: 588.56 [33419-42-0] ≥98%

Derivative of podophyllin and inhibitor of topoisomerase II that prevents DNA replication and repair. It induces autophagy and apoptosis in hepatoma cells and decreases release of pro-inflammatory cytokines and suppresses T cell activity in hemophagocytic lymphohistiocytosis.

Johnson TS, Terrell CE, Millen SH, et al. Etoposide selectively ablates activated T cells to control the immunoregulatory disorder hemophagocytic lymphohistiocytosis. J Immunol. 2014 Jan 1;192(1):84-91. PMID: 24259502.

Mir Mohammadrezaei F, Mohseni kouchesfehani H, Montazeri H, et al. Signaling crosstalk of FHIT, CHK2 and p38 in etoposide induced growth inhibition in MCF-7 cells. Cell Signal. 2013 Jan;25(1):126-32. PMID: 23000346.

Yoo SH, Yoon YG, Lee JS, et al. Etoposide induces a mixed type of programmed cell death and overcomes the resistance conferred by Bcl-2 in Hep3B hepatoma cells. Int J Oncol. 2012 Oct;41(4):1443-54. PMID: 22895528.

E7658

Etoposide Phosphate

25 mg
100 mg
250 mg

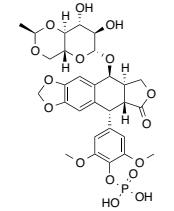

$C_{29}H_{33}O_{16}P$ FW: 668.54 [117091-64-2] ≥98%

Epipodophyllotoxin derivative and topoisomerase II inhibitor used to treat various cancers and hemophagocytic lymphohistiocytosis. It prevents DNA repair and causes cell death in breast cancer cells, induces autophagy and apoptosis in hepatoma cells, decreases release of pro-inflammatory cytokines, and inhibits activated T cells.

Johnson TS, Terrell CE, Millen SH, et al. Etoposide selectively ablates activated T cells to control the immunoregulatory disorder hemophagocytic lymphohistiocytosis. J Immunol. 2014 Jan 1;192(1):84-91. PMID: 24259502.

Mir Mohammadrezaei F, Mohseni kouchesfehani H, Montazeri H, et al. Signaling crosstalk of FHIT, CHK2 and p38 in etoposide induced growth inhibition in MCF-7 cells. Cell Signal. 2013 Jan;25(1):126-32. PMID: 23000346.

E7858

Etoricoxib

NEW

25 mg
100 mg

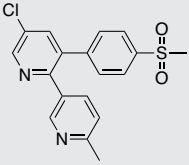

$C_{18}H_{15}ClN_2O_2S$ FW: 358.84 [202409-33-4] ≥98%

NSAID and COX-2 inhibitor used to treat arthritis, pain, and gout. It also decreases levels of oxidative enzymes, decreases aberrant crypt foci and lesion formation, and suppresses colon carcinogenesis.

Nadda N, Vaish V, Setia S, et al. Angiostatic role of the selective cyclooxygenase-2 inhibitor etoricoxib (MK0663) in experimental lung cancer. Biomed Pharmacother. 2012 Sep;66(6):474-83. PMID: 22681911.

Sharma P, Kaur J, Sanyal SN. Effect of etoricoxib, a cyclooxygenase-2 selective inhibitor on aberrant crypt formation and apoptosis in 1,2 dimethyl hydrazine induced colon carcinogenesis in rat model. Nutr Hosp. 2010 Jan-Feb;25(1):39-48. PMID: 20204254.

Kanwar SS, Vaiphei K, Nehru B, et al. Antioxidative effects of nonsteroidal anti-inflammatory drugs during the initiation stages of experimental colon carcinogenesis in rats. J Environ Pathol Toxicol Oncol. 2008;27(2):89-100. PMID: 18540845.

E7668 Etretinate

25 mg
100 mg
500 mg

$C_{25}H_{30}O_3$ FW: 354.49 [54350-48-0] ≥98%

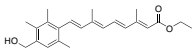

RAR and RXR agonist previously used to treat psoriasis. It induces birth defects and suppresses proliferation in cutaneous T-cell lymphoma models.

Burg G, Dummer R. Historical perspective on the use of retinoids in cutaneous T-cell lymphoma (CTCL). Clin Lymphoma. 2000 Nov;1 Suppl 1:S41-4. PMID: 11707863.

Saurat JH. Retinoids and psoriasis: novel issues in retinoid pharmacology and implications for psoriasis treatment. J Am Acad Dermatol. 1999 Sep;41(3 Pt 2):S2-6. PMID: 10459139.

E8419 Everolimus

1 mg
5 mg
25 mg

$C_{53}H_{83}NO_{14}$ FW: 958.22 [159351-69-6] ≥98%

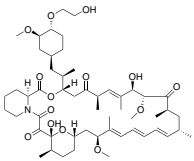

mTOR1 inhibitor used as an immunosuppressant in renal transplant subjects. It also induces autophagy and apoptosis in nasopharyngeal carcinoma cells, decreases levels of Th1, Th2, and Th17 cytokines, and improves renal function in models of nephrotic syndrome.

Sendur MA, Zengin N, Aksoy S, et al. Everolimus: a new hope for patients with breast cancer. Curr Med Res Opin. 2014 Jan;30(1):75-87. PMID: 24050600.

Cai Y, Xia Q, Su Q, et al. mTOR inhibitor RAD001 (everolimus) induces apoptotic, not autophagic cell death, in human nasopharyngeal carcinoma cells. Int J Mol Med. 2013 Apr;31(4):904-12. PMID: 23426850.

E8657 Evodiamine

100 mg
250 mg
1 g

$C_{19}H_{17}N_3O$ FW: 303.36 [518-17-2] ≥98%

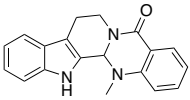

Topoisomerase I and II inhibitor found in *Evodia rutaecarpa*. It displays a wide variety of biological activities, including enhancing TRAIL-induced apoptosis in bladder cancer cells, inducing cell cycle arrest in leukemia cells, improving glucose tolerance, and inhibiting viral replication of influenza virus A.

Zhang T, Qu S, Shi Q, et al. Evodiamine Induces Apoptosis and Enhances TRAIL-Induced Apoptosis in Human Bladder Cancer Cells through mTOR/S6K1-Mediated Downregulation of Mcl-1. Int J Mol Sci. 2014 Feb 21;15(2):3154-71. PMID: 24566141.

Wang T, Kusudo T, Takeuchi T, et al. Evodiamine inhibits insulin-stimulated mTOR-S6K activation and IRS1 serine phosphorylation in adipocytes and improves glucose tolerance in obese/diabetic mice. PLoS One. 2013 Dec 31;8(12):e83264. PMID: 24391749.

Dai JP, Li WZ, Zhao XF, et al. A drug screening method based on the autophagy pathway and studies of the mechanism of evodiamine against influenza A virus. PLoS One. 2012;7(8):e42706. PMID: 22900043.

E9201 EX-527

NEW

5 mg
25 mg

Selisistat

$C_{13}H_{13}ClN_2O$ FW: 248.71 [49843-98-3] ≥98%

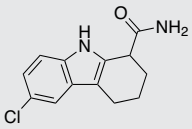

SIRT1 inhibitor that binds the NAD+ site of sirtuin 1, stabilizing a closed conformation. It delays renal cyst formation and growth in models of polycystic kidney disease, improves myocardial histology, and increases the number of Foxp3+ Treg cells in gastrointestinal inflammatory diseases.

Akimova T, Xiao H, Liu Y, et al. Targeting sirtuin-1 alleviates experimental autoimmune colitis by induction of Foxp3+ T-regulatory cells. Mucosal Immunol. 2014 Feb 19. [Epub ahead of print]. PMID: 24549276.

Gertz M, Fischer F, Nguyen GT, et al. Ex-527 inhibits Sirtuins by exploiting their unique NAD+-dependent deacetylation mechanism. Proc Natl Acad Sci U S A. 2013 Jul 23;110(30):E2772-81. PMID: 23840057.

Zhou X, Fan LX, Sweeney WE Jr, et al. Sirtuin 1 inhibition delays cyst formation in autosomal-dominant polycystic kidney disease. J Clin Invest. 2013 Jul 1;123(7):3084-98. PMID: 23778143.

E9317 Exemestane

25 mg
100 mg

FCE-24304

$C_{20}H_{24}O_2$ FW: 296.4 [107868-30-4] ≥98%

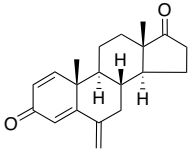

Aromatase inhibitor used to treat ER+ breast cancer. It prevents estrogen synthesis and induces cell cycle arrest, autophagy, and apoptosis in breast cancer cells.

Amaral C, Borges M, Melo S, et al. Apoptosis and autophagy in breast cancer cells following exemestane treatment. PLoS One. 2012;7(8):e42398. PMID: 22912703.

Hong Y, Rashid R, Chen S. Binding features of steroidal and nonsteroidal inhibitors. Steroids. 2011 Jul;76(8):802-6. PMID: 21420422.

Bertelli G, Hall E, Ireland E, et al. Long-term endometrial effects in postmenopausal women with early breast cancer participating in the Intergroup Exemestane Study (IES)--a randomised controlled trial of exemestane versus continued tamoxifen after 2-3 years tamoxifen. Ann Oncol. 2010 Mar;21(3):498-505. PMID: 19717534.

E9418

Exendin 3 (9-39)

0.5 mg
1 mg
2.5 mg

H-Asp-Leu-Ser-Lys-Gln-Met-Glu-Glu-Glu-Ala-Val-Arg-Leu-Phe-Ile-Glu-Trp-Leu-Lys-Asn-Gly-Gly-Pro-Ser-Ser-Gly-Ala-Pro-Pro-Pro-Ser-NH_2

$C_{149}H_{234}N_{40}O_{47}S$ FW: 3369.83 [133514-43-9] ≥95%

Exendin 3 derivative and GLP-1 receptor antagonist found in *Heloderma*. It induces spontaneous contractions in colon circular muscle.

Amato A, Baldassano S, Liotta R, et al. Exogenous glucagon-like peptide-1 reduces contractions in human colon circular muscle. J Endocrinol. 2014 Jan 17. [Epub ahead of print]. PMID: 24443715.

Hu G, Zhang Y, Jiang H, et al. Exendin-4 attenuates myocardial ischemia and reperfusion injury by inhibiting high mobility group box 1 protein expression. Cardiol J. 2013;20(6):600-4. PMID: 24338536.

E9416

Exendin-3

0.5 mg
1 mg
2.5 mg

H-His-Ser-Asp-Gly-Thr-Phe-Thr-Ser-Asp-Leu-Ser-Lys-Gln-Met-Glu-Glu-Glu-Ala-Val-Arg-Leu-Phe-Ile-Glu-Trp-Leu-Lys-Asn-Gly-Gly-Pro-Ser-Ser-Gly-Ala-Pro-Pro-Pro-Ser-NH_2

$C_{184}H_{282}N_{50}O_{61}S$ FW: 4202.66 [130391-54-7] ≥95%

GLP-1 analog and GLP-1 receptor agonist found in *Heloderma*. It may display anti-diabetic activities.

Zhang Y, Chen W. Radiolabeled glucagon-like peptide-1 analogues: a new pancreatic β-cell imaging agent. Nucl Med Commun. 2012 Mar;33(3):223-7.PMID: 22262216.

Eng J, Andrews PC, Kleinman WA, et al. Purification and structure of exendin-3, a new pancreatic secretagogue isolated from *Heloderma* horridum venom. J Biol Chem. 1990 Nov 25;265(33):20259-62. PMID: 1700785.

E9417

Exendin-4

0.5 mg
1 mg
2.5 mg

H-His-Gly-Glu-Gly-Thr-Phe-Thr-Ser-Asp-Leu-Ser-Lys-Gln-Met-Glu-Glu-Glu-Ala-Val-Arg-Leu-Phe-Ile-Glu-Trp-Leu-Lys-Asn-Gly-Gly-Pro-Ser-Ser-Gly-Ala-Pro-Pro-Pro-Ser-NH_2

$C_{184}H_{282}N_{50}O_{60}S$ FW: 4186.03 [141758-74-9] ≥95%

GLP-1 analog and GLP-1 receptor agonist found in *Heloderma*. It inhibits fibronectin secretion, suppresses ox-LDL-induced migration of macrophages, and prevents oxidative damage.

Xu WW, Guan MP, Zheng ZJ, et al. Exendin-4 Alleviates High Glucose-Induced Rat Mesangial Cell Dysfunction through the AMPK Pathway. Cell Physiol Biochem. 2014;33(2):423-32. PMID: 24556697.

Hu G, Zhang Y, Jiang H, et al. Exendin-4 attenuates myocardial ischemia and reperfusion injury by inhibiting high mobility group box 1 protein expression. Cardiol J. 2013;20(6):600-4. PMID: 24338536.

E9819

Ezetimibe

25 mg
100 mg
250 mg

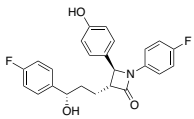

$C_{24}H_{21}F_2NO_3$ FW: 409.43 [163222-33-1] ≥98%

NPC1L1 inhibitor. It induces autophagy and decreases free cholesterol in hepatocytes, prevents THP-1 cells from differentiating into macrophage-like cells, and improves fibrosis and steatosis in models of nonalcoholic fatty liver disease.

F0010

FAM FLICA® Poly Caspases Assay Kit

25 Tests
100 Tests

Caspase activity measuring kit.

F0011

FAM FLICA™ Caspase 1 Assay Kit

25 Tests
100 Tests

Caspase 1 activity measuring kit.

F0012

FAM FLICA™ Caspase 2 Assay Kit

25 Tests
100 Tests

Caspase 2 activity measuring kit.

F0013

FAM FLICA™ Caspase 3 & 7 Assay Kit

25 Tests
100 Tests

Caspase 3/7 activity measuring kit.

F0014

FAM FLICA™ Caspase 6 Assay Kit

25 Tests
100 Tests

Caspase 6 activity measuring kit.

F0015	**FAM FLICA™ Caspase 8 Assay Kit** Caspase 8 activity measuring kit.	**25 Tests** **100 Tests**
F0016	**FAM FLICA™ Caspase 9 Assay Kit** Caspase 9 activity measuring kit.	**25 Tests** **100 Tests**
F0017	**FAM FLICA™ Caspase 10 Assay Kit** Caspase 10 activity measuring kit.	**25 Tests** **100 Tests**
F0018	**FAM FLICA™ Caspase 13 Assay Kit** Caspase 13 activity measuring kit.	**25 Tests** **100 Tests**
F0121	**FAM-DEVD-OPH in vitro Apoptosis Detection Reagent** **NEW** Apoptosis measuring kit.	**4 vial Pack**
F0021	**FAM-Leu-CMK Green FLISP™ Assay Kit** Leucine-specific serine protease activity measuring kit.	**25 Tests** **100 Tests**
F0024	**FAM-Leu-DAP Green FLISP™ Assay Kit** Serine protease activity measuring kit.	**25 Tests** **100 Tests**
F0019	**FAM-Phe-CMK Green FLISP™ Assay Kit** Phenylalanine-specific serine protease activity measuring kit.	**25 Tests** **100 Tests**
F0118	**Fam-Phe-DAP Green FLISP Assay™ Kit** **NEW** Serine protease activity measuring kit.	**25 Tests** **100 Tests**
F0023	**FAM-Spacer-Leu-CMK Green FLISP™ Assay Kit** Serine protease activity measuring kit.	**25 Tests** **100 Tests**
F0022	**FAM-Spacer-Phe-CMK Green FLISP™ Assay Kit** Serine protease activity measuring kit.	**25 Tests** **100 Tests**
F0119	**FAM-VAD-OPH I in vitro Apoptosis Detection Reagent** **NEW** Apoptosis measuring kit.	**4 vial Pack**
F0120	**FAM-VAD-OPH II in vitro Apoptosis Detection Reagent** **NEW** Apoptosis measuring kit.	**4 vial Pack**

F0048 Famciclovir

50 mg
100 mg
500 mg

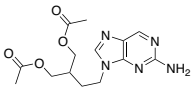

$C_{14}H_{19}N_5O_4$ FW: 321.33 [104227-87-4] ≥98%

Penciclovir prodrug and guanosine analog. It terminates DNA chain synthesis and is used to treat herpes virus infection.

Modi S, Van L, Gewirtzman A, et al. Single-day treatment for orolabial and genital herpes: a brief review of pathogenesis and pharmacology. Ther Clin Risk Manag. 2008 Apr;4(2):409-17. PMID: 18728852.

Luber AD, Flaherty JF Jr. Famciclovir for treatment of herpesvirus infections. Ann Pharmacother. 1996 Sep;30(9):978-85. PMID: 8876860.

F0150 Famotidine

500 mg
1 g
5 g

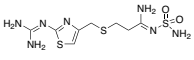

$C_8H_{15}N_7O_2S_3$ FW: 337.45 [76824-35-6] ≥98%

Histamine H2 receptor antagonist and GSK-3β inhibitor used to treat ulcers. It also suppresses radiation-induced DNA damage.

Mohammad M, Al-Masri IM, Issa A, et al. Famotidine inhibits glycogen synthase kinase-3β: an investigation by docking simulation and experimental validation. J Enzyme Inhib Med Chem. 2013 Aug;28(4):690-4. PMID: 22512725.

Mozdarani H, Nasirian B, Haeri SA. In vivo gamma-rays induced initial DNA damage and the effect of famotidine in mouse leukocytes as assayed by the alkaline comet assay. J Radiat Res. 2007 Mar;48(2):129-34. PMID: 17299251.

F0268 Farnesol

50 ml
100 ml

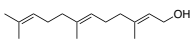

$C_{15}H_{26}O$ FW: 222.37 [4602-84-0] ≥97%

Found in various essential oils. It regulates the volatility of odorants in perfumes. It displays a variety of biological activities, including inducing cell cycle arrest and stimulating p21 and p27 expression in pancreatic adenocarcinoma cells, increasing latency to tumor formation in TPA-induced skin carcinogenesis, and inhibiting growth of *Aspergillus* and *Candida*.

Wang X, Wang YZ, Zhou Y, et al. Farnesol induces apoptosis-like cell death in the pathogenic fungus *Aspergillus* flavus. Mycologia. 2014 Jun 3. [Epub ahead of print]. PMID: 24895430.

F0275 Fasudil Hydrochloride

100 mg
250 mg
1 g

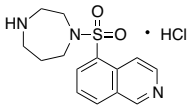

$C_{14}H_{17}N_3O_2S \bullet HCl$ FW: 327.83 [105628-07-7] ≥98%

ROCK inhibitor used to treat cerebral vasospasm and hypertension. It decreases myocardial infarction size, inhibits progression of existing aneurysms, and suppresses motor neuron loss in ALS models.

Peng C, Gu P, Zhou J, et al. Inhibition of rho-kinase by fasudil suppresses formation and progression of experimental abdominal aortic aneurysms. PLoS One. 2013 Nov 14;8(11):e80145. PMID: 24244631.

Takata M, Tanaka H, Kimura M, et al. Fasudil, a rho kinase inhibitor, limits motor neuron loss in experimental models of amyotrophic lateral sclerosis. Br J Pharmacol. 2013 Sep;170(2):341-51.PMID: 23763343.

F1607 Febuxostat

250 mg
1 g

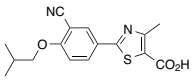

$C_{16}H_{16}N_2O_3S$ FW: 316.37 [144060-53-7] ≥98%

Xanthine oxidase inhibitor used to treat gout. It prevents uric acid generation, decreases oxidative stress, and suppresses the development of fibrosis in models of renal ischemia.

Nomura J, Busso N, Ives A, et al. Febuxostat, an Inhibitor of Xanthine Oxidase, Suppresses Lipopolysaccharide-Induced MCP-1 Production via MAPK Phosphatase-1-Mediated Inactivation of JNK. PLoS One. 2013 Sep 25;8(9):e75527. PMID: 24086554.

Karve AV, Jagtiani SS, Chitnis KA. Evaluation of effect of allopurinol and febuxostat in behavioral model of depression in mice. Indian J Pharmacol. 2013 May-Jun;45(3):244-7. PMID: 23833366.

F1745 Felodipine

50 mg
100 mg
250 mg

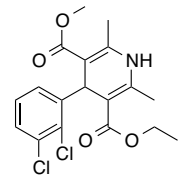

$C_{18}H_{19}Cl_2NO_4$ FW: 384.25 [72509-76-3] ≥98%

L-type Ca^{2+} channel blocker used to treat hypertension. It decreases blood pressure, serum insulin, and circulating macrophage levels.

Tan HW, Xing SS, Bi XP, et al. Felodipine attenuates vascular inflammation in a fructose-induced rat model of metabolic syndrome via the inhibition of NF-kappaB activation. Acta Pharmacol Sin. 2008 Sep;29(9):1051-9. PMID: 18718174.

Kal JE, Spaan JA, van Wezel HB. Calcium channel blockade with felodipine does not affect metabolic coronary vasodilation in patients with coronary artery disease. J Cardiovasc Pharmacol. 2002 Feb;39(2):225-33. PMID: 11791008.

F1650

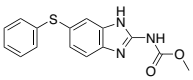

Fenbendazole

5 g
10 g
100 g

HOE-881v

$C_{15}H_{13}N_3O_2S$ FW: 299.35 [43210-67-9] ≥98%

Microtubule polymerization inhibitor to treat infections of *Giardia*, *Strongyloides*, and various worms. It binds fungal tubulin, inhibiting hyphal growth and nuclear division.

Küster T, Stadelmann B, Aeschbacher D, et al. Activities of fenbendazole in comparison with albendazole against Echinococcus multilocularis metacestodes in vitro and in a murine infection model. Int J Antimicrob Agents. 2014 Apr;43(4):335-42. PMID: 24646943.

Lubega GW, Prichard RK. Specific interaction of benzimidazole anthelmintics with tubulin: high-affinity binding and benzimidazole resistance in *Haemonchus* contortus. Mol Biochem Parasitol. 1990 Jan 15;38(2):221-32. PMID: 2325707.

Prichard RK. Anthelmintics for cattle. Vet Clin North Am Food Anim Pract. 1986 Jul;2(2):489-501. PMID: 3488116.

F1652

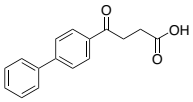

Fenbufen

1 g
5 g
10 g

$C_{16}H_{14}O_3$ FW: 254.28 [36330-85-5] ≥98%

NSAID and COX-1/2 inhibitor used to treat arthritis and tendinitis. It also scavenges oxygen radicals.

Moore RA, Derry S, McQuay HJ. Single dose oral fenbufen for acute postoperative pain in adults. Cochrane Database Syst Rev. 2009 Oct 7;(4):CD007547. PMID: 19821427.

Costa D, Moutinho L, Lima JL, et al. Antioxidant activity and inhibition of human neutrophil oxidative burst mediated by arylpropionic acid non-steroidal anti-inflammatory drugs. Biol Pharm Bull. 2006 Aug;29(8):1659-70. PMID: 16880623.

F1853

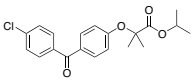

Fenofibrate

5 g
25 g
100 g

$C_{20}H_{21}ClO_4$ FW: 360.83 [49562-28-9] ≥98%

PPARα agonist used to decrease triglyceride, VLDL, and LDL levels. It stimulates lipoprotein lipase, decreases oxidative stress-induced pro-inflammatory cytokine expression, and induces cell cycle arrest in breast cancer cells.

Gao Y, Shen W, Zhang Q, et al. Up-regulation of Hepatic VLDLR via PPARα Is Required for the Triglyceride-Lowering Effect of Fenofibrate. J Lipid Res. 2014 Jun 4. [Epub ahead of print]. PMID: 24899625.

Li T, Zhang Q, Zhang J, et al. Fenofibrate induces apoptosis of triple-negative breast cancer cells via activation of NF-κB pathway. BMC Cancer. 2014 Feb 16;14:96. PMID: 24529079.

Xie C, Li L, Xu YP, et al. Anti-fibrosis effects of fenofibrate in mice with hepatic fibrosis. Zhonghua Gan Zang Bing Za Zhi. 2013 Dec;21(12):914-9. PMID: 24636293.

F1654

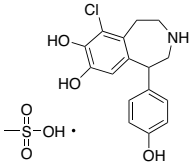

Fenoldopam Mesylate

25 mg
100 mg
500 mg

$C_{16}H_{16}ClNO_3S \bullet CH_3SO_3H$ FW: 401.87 [67227-57-0] ≥98%

Benzazepine derivative, dopamine D1 receptor partial agonist, and potential α1-adrenergic receptor antagonist. It promotes sodium excretion and decreases blood pressure, afterload, and blood flow.

Grider JS, Ott CE, Jackson BA. Dopamine D1 receptor-dependent inhibition of NaCl transport in the rat thick ascending limb: mechanism of action. Eur J Pharmacol. 2003 Jul 25;473(2-3):185-90. PMID: 12892837.

Schafer JA, Li L, Sun D. The collecting duct, dopamine and vasopressin-dependent hypertension. Acta Physiol Scand. 2000 Jan;168(1):239-44. PMID: 10691807.

Martin SW, Broadley KJ. Renal vasodilatation by dopexamine and fenoldopam due to alpha 1-adrenoceptor blockade. Br J Pharmacol. 1995 May;115(2):349-55. PMID: 7670737.

F1655

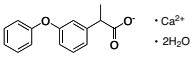

Fenoprofen Calcium Dihydrate

1 g
5 g
10 g

Lilly 53838

$2C_{30}H_{24}O_6Ca \bullet 2H_2O$ FW: 558.64 [53746-45-5] ≥97%

NSAID and COX-1/2 inhibitor used to treat arthritis. It also inhibits fatty acid oxidation and acts as a peroxisome proliferator.

Barissa GR, Poggi JC, Donadi EA, et al. Influence of rheumatoid arthritis in the enantioselective disposition of fenoprofen. Chirality. 2004 Nov;16(9):602-8. PMID: 15390088.

De Craemer D, Van den Branden C, Pauwels M, et al. Peroxisome-proliferating effects of fenoprofen in mice. Lipids. 1998 May;33(5):539-43. PMID: 9625603.

F1854 Fenticonazole Nitrate

100 mg
250 mg
1 g

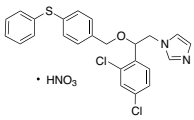

$C_{24}H_{20}Cl_2N_2OS \bullet HNO_3$ FW: 518.41 [73151-29-8] ≥98%

14-α Demethylase inhibitor and potential glucosamine-6-phosphate synthase inhibitor that inhibits ergosterol synthesis and fungal cell wall formation. It inhibits secretion of proteinase and suppresses growth of *Candida*, *Trichomonas*, and gram positive bacteria.

Veraldi S, Milani R. Topical fenticonazole in dermatology and gynaecology: current role in therapy. Drugs. 2008;68(15):2183-94. PMID: 18840006.

Fernández-Alba J, Valle-Gay A, Dibildox M, et al. Fenticonazole nitrate for treatment of vulvovaginitis: efficacy, safety, and tolerability of 1-gram ovules, administered as ultra-short 2-day regimen. J Chemother. 2004 Apr;16(2):179-86. PMID: 15216954.

F1768 Ferintoic Acid A

NEW

100 µg

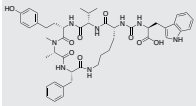

$C_{46}H_{58}N_8O_9$ FW: 867 [176327-91-6] ≥95%

Found in *Microcystis*.

Williams DE, Craig M, Holmes CFB, et al. Ferintoic Acids A and B, New Cyclic Hexapeptides from the Freshwater Cyanobacterium *Microcystis* aeruginosa. J Nat Prod. 1996;59(6): 570-575.

F1769 Methoxy Ferintoic Acid A

NEW

50 µg

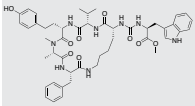

$C_{47}H_{60}N_8O_9$ FW: 881.03 ≥95%

Found in *Microcystis*.

Williams DE, Craig M, Holmes CFB, et al. Ferintoic Acids A and B, New Cyclic Hexapeptides from the Freshwater Cyanobacterium *Microcystis* aeruginosa. J Nat Prod. 1996;59(6): 570-575.

F1669 Ferulic Acid

5 g
25 g
100 g

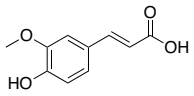

Caffeic acid 3-methyl ether; 4-Hydroxy-3-methoxy-cinnamic acid

$C_{10}H_{10}O_4$ FW: 194.18 [1135-24-6] ≥98%

Verbascoside metabolite found in various plant sources. It displays a variety of activities, including suppressing oxidative stress and inflammation, reversing pathology induced by amyloid-β dimers, inhibiting presynaptic glutamate release from cortical synaptosomes, and decreasing levels of NE, DA, 5-HT to limit nociception.

Quirantes-Piné R, Herranz-López M, Funes L, et al. Phenylpropanoids and their metabolites are the major compounds responsible for blood-cell protection against oxidative stress after administration of Lippia citriodora in rats. Phytomedicine. 2013 Sep 15;20(12):1112-8. PMID: 23827667.

Xu Y, Zhang L, Shao T, et al. Ferulic acid increases pain threshold and ameliorates depression-like behaviors in reserpine-treated mice: behavioral and neurobiological analyses. Metab Brain Dis. 2013 Dec;28(4):571-83. PMID: 23584961.

Picone P, Nuzzo D, Di Carlo M. Ferulic acid: a natural antioxidant against oxidative stress induced by oligomeric A-beta on sea urchin embryo. Biol Bull. 2013 Feb;224(1):18-28. PMID: 23493505.

F1670 Ferulic Acid Methyl Ester

1 g
5 g
25 g

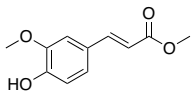

$C_{11}H_{12}O_4$ FW: 208.21 [2309-07-1] ≥98%

Verbascoside metabolite and ion chelator. It decreases oxidative stress and inflammation in diabetic nephropathy models, protects against oxidative damage, decreases levels of NE, DA, 5-HT, and substance P in the hippocampus and frontal cortex, and reverses amyloid-β-induced pathology.

Quirantes-Piné R, Herranz-López M, Funes L, et al. Phenylpropanoids and their metabolites are the major compounds responsible for blood-cell protection against oxidative stress after administration of Lippia citriodora in rats. Phytomedicine. 2013 Sep 15;20(12):1112-8. PMID: 23827667.

Xu Y, Zhang L, Shao T, et al. Ferulic acid increases pain threshold and ameliorates depression-like behaviors in reserpine-treated mice: behavioral and neurobiological analyses. Metab Brain Dis. 2013 Dec;28(4):571-83. PMID: 23584961.

F1895 Fexofenadine Hydrochloride

25 mg
100 mg
500 mg

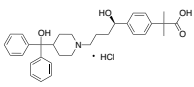

$C_{32}H_{39}NO_4 \bullet HCl$ FW: 538.12 [153439-40-8] ≥98%

Histamine H1 receptor antagonist used to treat seasonal allergic rhinitis.

Compalati E, Baena-Cagnani R, Penagos M, et al. Systematic review on the efficacy of fexofenadine in seasonal allergic rhinitis: a meta-analysis of randomized, double-blind, placebo-controlled clinical trials. Int Arch Allergy Immunol. 2011;156(1):1-15. PMID: 21969990.

Smith SM, Gums JG. Fexofenadine: biochemical, pharmacokinetic and pharmacodynamic properties and its unique role in allergic disorders. Expert Opin Drug Metab Toxicol. 2009 Jul;5(7):813-22. PMID: 19545214.

F3204 — Fibrinogen-binding Peptide — 5 mg

$C_{25}H_{39}H_7O_8$ FW: 565.63 ≥98%

Glu-His-Ile-Pro-Ala

GP IIb/IIIa analog and fibrinogen binding inhibitor.

Gartner TK, Loudon R, Taylor DB. The peptides APLHK, EHIPA and GAPL are hydropathically equivalent peptide mimics of a fibrinogen binding domain of glycoprotein IIb/IIIa. Biochem Biophys Res Commun. 1991 Nov 14;180(3):1446-52. PMID: 1953789.

F3205 — Fibrinogen γ-chain Dodecapeptide — 1 mg / 2 mg / 5 mg

$C_{50}H_{80}N_{18}O_{16}$ FW: 1189.29 ≥98%

His-His-Leu-Gly-Gly-Ala-Lys-Gln-Ala-Gly-Asp-Val

Platelet substitute and GP IIb/IIIa activator used as a platelet substitute. It enhances thrombus formation and rescues subjects from hemorrhage.

Tokutomi K, Tagawa T, Korenaga M, et al. Ability of fibrinogen γ-derived dodecapeptides with different sequences to bind to rat platelets. Int J Pharm. 2012 Nov 15;438(1-2):296-301. PMID: 22985603.

Nishikawa K, Hagisawa K, Kinoshita M, et al. Fibrinogen γ-chain peptide-coated, ADP-encapsulated liposomes rescue thrombocytopenic rabbits from non-compressible liver hemorrhage. J Thromb Haemost. 2012 Oct;10(10):2137-48. PMID: 22905905.

F3206 — Fibrinolysis Inhibiting Factor — 1 mg / 2 mg / 5 mg

$C_{18}H_{31}N_7O_5$ FW: 425.49 ≥98%

Gly-Pro-Arg-Pro

Fibrinolysis inhibitor that induces acute immune hemolysis in hepatectomy models.

Nakatsuji T. Acceleration of thrombosis and hemolysis by fibrinolysis inhibiting factor and suppression by Ia antigen expressed on T cells in partially hepatectomized Lewis rats. Int J Hematol. 1996 Oct;64(3-4):181-8. PMID: 8923779.

F3208 — Fibrinopeptide B, human — 1 mg / 2 mg / 5 mg

$C_{66}H_{93}N_{19}O_{25}$ FW: 1552.59 [36204-23-6] ≥95%

pGlu-Gly-Val-Asn-Asp-Asn-Glu-Glu-Gly-Phe-Phe-Ser-Ala-Arg-OH

Generated during the formation of fibrin. It is released from thrombin in platelets and may decrease procollagen levels.

Tang YQ, Yeaman MR, Selsted ME. Antimicrobial peptides from human platelets. Infect Immun. 2002 Dec;70(12):6524-33. PMID: 12438321.

Huang QQ, Teng MK, Niu LW. Purification and characterization of two fibrinogen-clotting enzymes from five-pace snake (*Agkistrodon* acutus) venom. Toxicon. 1999 Jul;37(7):999-1013. PMID: 10484747.

F3207 — Fibronectin CS-1 Peptide — 1 mg / 2 mg / 5 mg

$C_{38}H_{64}N_8O_{15}$ FW: 872.97 ≥98%

Glu-Ile-Leu-Asp-Val-Pro-Ser-Thr

α4β1 Integrin activator. It stimulates proliferation of T cells, decreases infarct size in cerebral ischemia/reperfusion models, and regulates migration and invasion of oral squamous cell carcinoma cells.

Kamarajan P, Garcia-Pardo A, D'Silva NJ, et al. The CS1 segment of fibronectin is involved in human OSCC pathogenesis by mediating OSCC cell spreading, migration, and invasion. BMC Cancer. 2010 Jun 25;10:330. PMID: 20579373.

Yakubenko VP, Lobb RR, Plow EF, et al. Differential induction of gelatinase B (MMP-9) and gelatinase A (MMP-2) in T lymphocytes upon alpha(4)beta(1)-mediated adhesion to VCAM-1 and the CS-1 peptide of fibronectin. Exp Cell Res. 2000 Oct 10;260(1):73-84. PMID: 11010812.

F3209 — Fibronectin-Binding Protein — 0.5 mg / 1 mg / 2.5 mg

$C_{190}H_{283}N_{49}O_{66}$ FW: 4309.66 [119977-20-7] ≥95%

H-Phe-Asn-Lys-His-Thr-Glu-Ile-Ile-Glu-Glu-Asp-Thr-Asn-Lys-Asp-Lys-Pro-Ser-Tyr-Gln-Phe-Gly-Gly-His-Asn-Ser-Val-Asp-Phe-Glu-Glu-Asp-Thr-Leu-Pro-Lys-Val-OH

Binds fibronectin. It is involved in T cell activation, cytokine release, and basophil degranulation.

Reginald K, Westritschnig K, Linhart B, et al. *Staphylococcus aureus* fibronectin-binding protein specifically binds IgE from patients with atopic dermatitis and requires antigen presentation for cellular immune responses. J Allergy Clin Immunol. 2011 Jul;128(1):82-91.e8. PMID: 21513970.

F3354 — Finasteride — 100 mg / 500 mg

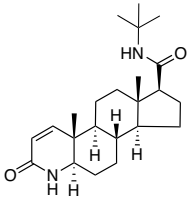

$C_{23}H_{36}N_2O_2$ FW: 372.54 [98319-26-7] ≥98%

Steroid 5-α-reductase inhibitor used to treat BPH and male pattern baldness. It decreases testosterone metabolism, inhibits growth of *Candida*, and suppresses regrowth of regressed prostate tumors

Chavez-Dozal AA, Lown L, Jahng M, et al. An in vitro analysis of finasteride activity against *Candida albicans* urinary biofilm formation and filamentation. Antimicrob Agents Chemother. 2014 Jul 21. [Epub ahead of print]. PMID: 25049253.

Masoodi KZ, Ramos Garcia R, Pascal LE, et al. 5α-reductase inhibition suppresses testosterone-induced initial regrowth of regressed xenograft prostate tumors in animal models. Endocrinology. 2013 Jul;154(7):2296-307. PMID: 23671262.

F3454 Fingolimod Hydrochloride

10 mg
25 mg
100 mg

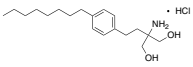

$C_{19}H_{32}NO_2 \bullet HCl$ FW: 343.93 [162359-56-0] ≥98%

Sphingosine 1-phosphate receptor antagonist used to treat autoimmune diseases. It prevents movement of autoreactive lymphocytes from the lymph nodes into circulation, decreases production of amyloid-β in Alzheimer's disease models, and induces cell death in neuroblastoma cells.

Li MH, Hla T, Ferrer F. FTY720 inhibits tumor growth and enhances the tumor-suppressive effect of topotecan in neuroblastoma by interfering with the sphingolipid signaling pathway. Pediatr Blood Cancer. 2013 Sep;60(9):1418-23. PMID: 23704073.

Takasugi N, Sasaki T, Ebinuma I, et al. FTY720/fingolimod, a sphingosine analogue, reduces amyloid-β production in neurons. PLoS One. 2013 May 7;8(5):e64050. PMID: 23667698.

Groves A, Kihara Y, Chun J. Fingolimod: direct CNS effects of sphingosine 1-phosphate (S1P) receptor modulation and implications in multiple sclerosis therapy. J Neurol Sci. 2013 May 15;328(1-2):9-18. PMID: 23518370.

F3473 Fisetin

100 mg
500 mg

3,3',4',7-Tetrahydroxyflavone

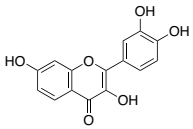

$C_{15}H_{10}O_6$ FW: 286.24 [528-48-3] ≥97%

Inhibitor of MMPs and topoisomerase I and II found in various plant sources. It displays many biological activities, including limiting the development of learning and memory deficits in Alzheimer's disease models, decreasing levels of H_2O_2-generated superoxide anions, hydroxyl radicals, and ROS, and inhibiting Th1/Th2 cytokine production.

Li R, Zhao Y, Chen J, et al. Fisetin inhibits migration, invasion and epithelial-mesenchymal transition of LMP1-positive nasopharyngeal carcinoma cells. Mol Med Rep. 2014 Feb;9(2):413-8. PMID: 24297333.

Currais A, Prior M, Dargusch R, et al. Modulation of p25 and inflammatory pathways by fisetin maintains cognitive function in Alzheimer's disease transgenic mice. Aging Cell. 2013 Dec 17. [Epub ahead of print]. PMID: 24341874.

Park JH, Jang YJ, Choi YJ, et al. Fisetin inhibits matrix metalloproteinases and reduces tumor cell invasiveness and endothelial cell tube formation. Nutr Cancer. 2013;65(8):1192-9. PMID: 24099040.

F4400 Flag Peptide

0.5 mg
1 mg
2.5 mg

Trypsinogen human pancreas isoenzyme 2 activation peptide; DYKDDDDK

H-Asp-Tyr-Lys-Asp-Asp-Asp-Asp-Lys-OH

$C_{41}H_{60}N_{10}O_{20}$ FW: 1012.99 [98849-88-8] ≥95%

Used to tag proteins for affinity chromatography, fluorescence, and gel electrophoresis.

Einhauer A, Jungbauer A. The FLAG peptide, a versatile fusion tag for the purification of recombinant proteins. J Biochem Biophys Methods. 2001 Oct 30;49(1-3):455-65. PMID: 11694294.

F4501 Flavanone

10 g
25 g

2,3-Dihydroflavone

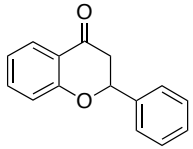

$C_{15}H_{12}O_2$ FW: 224.25 [487-26-3] ≥98%

Found in various plant sources. It inhibits proliferation of tumor cells and may decrease oxidative damage, inhibit angiogenesis, and suppress growth of bacteria.

Melliou E, Chinou I. Chemical analysis and antimicrobial activity of Greek propolis. Planta Med. 2004 Jun;70(6):515-9. PMID: 15229802.

Fotsis T, Pepper MS, Montesano R, et al. Phytoestrogens and inhibition of angiogenesis. Baillieres Clin Endocrinol Metab. 1998 Dec;12(4):649-66. PMID: 10384818.

F4502 Flavokawain A

5 mg
10 mg

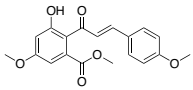

$C_{18}H_{18}O_5$ FW: 314.33 [64680-84-8] ≥98%

Found in *Piper methysticum* (kava plant). It suppresses expression of iNOS and COX-2 in macrophages, decreases expression of Ki67, XIAP, and survivin in urothelial cell carcinoma cells, and inhibits degradation of IκBα and activation of NF-κB.

Liu Z, Xu X, Li X, et al. Kava chalcone, flavokawain A, inhibits urothelial tumorigenesis in the UPII-SV40T transgenic mouse model. Cancer Prev Res (Phila). 2013 Dec;6(12):1365-75. PMID: 24121102.

Kwon DJ, Ju SM, Youn GS, et al. Suppression of iNOS and COX-2 expression by flavokawain A via blockade of NF-κB and AP-1 activation in RAW 264.7 macrophages. Food Chem Toxicol. 2013 Aug;58:479-86. PMID: 23727179.

Folmer F, Blasius R, Morceau F, et al. Inhibition of TNFalpha-induced activation of nuclear factor kappaB by kava (*Piper methysticum*) derivatives. Biochem Pharmacol. 2006 Apr 14;71(8):1206-18. PMID: 16464438.

F4503 Flavokawain B

5 mg
10 mg

$C_{17}H_{16}O_4$ FW: 284.31 [1775-97-9] ≥97%

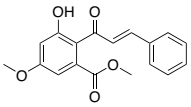

Found in *Piper methysticum* (kava plant). It suppresses inflammation and inhibits degradation of IκBα and activation of NF-κB.

Teschke R, Qiu SX, Lebot V. Herbal hepatotoxicity by kava: update on pipermethystine, flavokavain B, and mould hepatotoxins as primarily assumed culprits. Dig Liver Dis. 2011 Sep;43(9):676-81. PMID: 21377431.

Folmer F, Blasius R, Morceau F, et al. Inhibition of TNFalpha-induced activation of nuclear factor kappaB by kava (*Piper methysticum*) derivatives. Biochem Pharmacol. 2006 Apr 14;71(8):1206-18. PMID: 16464438.

F4518 Fleroxacin

5 g
10 g
25 g

AM-833

$C_{17}H_{18}F_3N_3O_3$ FW: 369.34 [79660-72-3] ≥98%

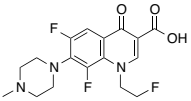

Bacterial DNA gyrase and helicase inhibitor. It inhibits growth of gram negative and gram positive bacteria, inhibits DNA unwinding and ATPase activities of Bloom helicase, and increases peroxidation of squalene when exposed to UVA light.

Luo H, Xu HQ, Chen X, et al. Potent in vitro interference of fleroxacin in DNA-binding, unwinding and ATPase activities of Bloom helicase. Biomed Environ Sci. 2013 Apr;26(4):231-42. PMID: 23534463.

Kawada A, Hatanaka K, Gomi H, et al. In vitro phototoxicity of new quinolones: production of active oxygen species and photosensitized lipid peroxidation. Photodermatol Photoimmunol Photomed. 1999 Dec;15(6):226-30. PMID: 10599972

F4420 Boc-FLFLF

5 mg
10 mg
25 mg

$C_{44}H_{59}N_5O_8$ FW: 785.99 [148182-34-7] ≥95%

Boc-Phe-Leu-Phe-Leu-Phe-OH

FPR1 receptor antagonist. It inhibits antinociceptive activity of annexin and suppresses muscle contractions induced by formyl peptides.

Pei L, Zhang J, Zhao F, et al. Annexin 1 exerts anti-nociceptive effects after peripheral inflammatory pain through formyl-peptide-receptor-like 1 in rat dorsal root ganglion. Br J Anaesth. 2011 Dec;107(6):948-58. PMID: 21990306.

Ma XJ, Kunimatsu M, Ozaki Y, et al. Putative mechanism for guinea pig ileum contraction by N-formyl peptides. A comparative study of N-formyl and N-acetyl peptides with the N-terminal sequence of the calpain small subunit. Life Sci. 1995;57(5):463-71. PMID: 7623613.

F4432 FLI-06

NEW

5 mg
25 mg

$C_{25}H_{30}N_2O_5$ FW: 438.52 [313967-18-9] ≥98%

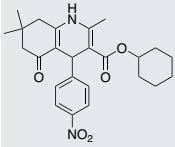

Inhibitor of γ-secretase and Notch signaling. It inhibits protein secretion prior to endoplasmic reticulum exit.

Krämer A, Mentrup T, Kleizen B, et al. Small molecules intercept Notch signaling and the early secretory pathway. Nat Chem Biol. 2013 Nov;9(11):731-8. PMID: 24077179.

F4532 Flibanserin

NEW

5 mg
25 mg
100 mg

$C_{20}H_{21}F_3N_4O$ FW: 390.4 [167933-07-5] ≥98%

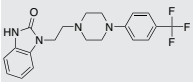

5-HT1A receptor agonist and 5-HT2A receptor antagonist used to treat hypoactive sexual disorder in females. It also decreases dystonia induced by L-DOPA and quinelorane in models of Parkinson's disease.

Gelez H, Clement P, Compagnie S, et al. Brain neuronal activation induced by flibanserin treatment in female rats. Psychopharmacology (Berl). 2013 Dec;230(4):639-52. PMID: 23857113.

Strecker K, Adamaszek M, Ohm S, et al. The 5-HT1A-receptor agonist flibanserin reduces drug-induced dyskinesia in RGS9-deficient mice. J Neural Transm. 2012 Nov;119(11):1351-9. PMID: 22569849.

Stahl SM, Sommer B, Allers KA. Multifunctional pharmacology of flibanserin: possible mechanism of therapeutic action in hypoactive sexual desire disorder. J Sex Med. 2011 Jan;8(1):15-27. PMID: 20840530.

F4534 FLICA® 660 Caspase 1 Assay Kit

NEW

25-50 Tests

Caspase 1 activity measuring kit.

F4535 FLICA® 660 Caspase 3/7 Assay Kit

NEW

25-50 Tests

Caspases 3/7 activity measuring kit.

F4533 FLICA® 660 Poly Caspase Assay Kit

NEW

25-50 Tests

Caspase activity measuring kit.

F4556

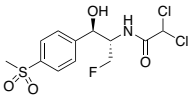

Florfenicol

Fluorothiamphenicol

$C_{12}H_{14}Cl_2FNO_4S$ FW: 358.21 [73231-34-2] ≥98%

1 g
5 g
10 g

Synthetic thiamphenicol analog and protein translation inhibitor. It is particularly active against *Shigella*, *Escherichia*, *Klebsiella*, *Enterobacter*, and *Haemophilus*.

Kehrenberg C, Schwarz S, Jacobsen L, et al. A new mechanism for chloramphenicol, florfenicol and clindamycin resistance: methylation of 23S ribosomal RNA at A2503. Mol Microbiol. 2005 Aug;57(4):1064-73. PMID: 16091044.

F4557

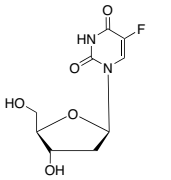

Floxuridine

NSC-27640; FUDR

$C_9H_{11}FN_2O_5$ FW: 246.19 [50-91-9] ≥98%

100 mg
500 mg
1 g

5-Fluorouracil derivative and pyrimidine nucleoside analog that inhibits thymidylate synthase. It induces apoptosis in cancer cells and inhibits replication of dengue virus.

Fischer MA, Smith JL, Shum D, et al. Flaviviruses are sensitive to inhibition of thymidine synthesis pathways. J Virol. 2013 Sep;87(17):9411-9. PMID: 23824813.

Muñoz-Pinedo C, Robledo G, López-Rivas A. Thymidylate synthase inhibition triggers glucose-dependent apoptosis in p53-negative leukemic cells. FEBS Lett. 2004 Jul 16;570(1-3):205-10. PMID: 15251465.

F4679

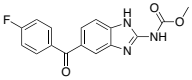

Flubendazole

$C_{16}H_{12}FN_3O_3$ FW: 313.28 [31430-15-6] ≥98%

10 g
25 g
100 g

Microtubule polymerization inhibitor. It suppresses growth of *Haemonchus* and *Trichomonas* and decreases viability of myeloma cells.

Spagnuolo PA, Hu J, Hurren R, et al. The antihelmintic flubendazole inhibits microtubule function through a mechanism distinct from Vinca alkaloids and displays preclinical activity in leukemia and myeloma. Blood. 2010 Jun 10;115(23):4824-33. PMID: 20348394.

F4682

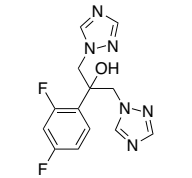

Fluconazole

$C_{13}H_{12}F_2N_6O$ FW: 306.27 [86386-73-4] ≥98%

500 mg
1 g
5 g

14-α Demethylase inhibitor that inhibits ergosterol synthesis and fungal cell wall formation. It is especially active against *Candida* and *Cryptococcus*.

Cuenca-Estrella M. Antifungal agents in the treatment of systemic infections: Relevance of mechanism of action, activity profile and resistances. Rev Esp Quimioter. 2010 Dec;23(4):169-76. PMID: 21191554.

Mansfield BE, Oltean HN, Oliver BG, et al. Azole drugs are imported by facilitated diffusion in *Candida albicans* and other pathogenic fungi. PLoS Pathog. 2010 Sep 30;6(9):e1001126. PMID: 20941354.

F4781

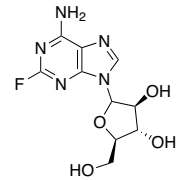

Fludarabine

$C_{10}H_{12}FN_5O_4$ FW: 285.23 [21679-14-1] ≥98%

5 mg
10 mg
25 mg

Adenosine analog, DNA chain terminator, and inhibitor of ribonucleotide reductase, DNA ligase, DNA primase, and adenosine A1 receptors. It is used to treat leukemias and graft-versus-host-disease in transplant patients. It also induces cell cycle arrest and apoptosis in alloreactive bone marrow stromal cells.

Jensen K, Johnson LA, Jacobson PA, et al. Cytotoxic purine nucleoside analogues bind to A1, A2A, and A3 adenosine receptors. Naunyn Schmiedebergs Arch Pharmacol. 2012 May;385(5):519-25. PMID: 22249336.

Nishioka C, Ikezoe T, Togitani K, et al. Fludarabine induces growth arrest and apoptosis of cytokine- or alloantigen-stimulated peripheral blood mononuclear cells, and decreases production of Th1 cytokines via inhibition of nuclear factor kappaB. Bone Marrow Transplant. 2008 Feb;41(3):303-9. PMID: 17994120.

F4782

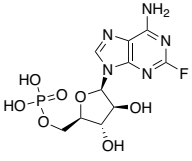

Fludarabine Phosphate

F-ara-A

$C_{10}H_{13}FN_5O_7P$ FW: 365.21 [75607-67-9] ≥98%

5 mg
10 mg
25 mg
100 mg

Adenosine analog, DNA chain terminator, and inhibitor of ribonucleotide reductase, DNA ligase, DNA primase, and adenosine A1 receptors used to treat various leukemias and to prevent graft-versus-host-disease during hematopoietic stem cell transplantation. It also inhibits TNF-α-stimulated production of IL-2 and IFN-γ.

Robak P and Robak T. Older and new purine nucleoside analogs for patients with acute leukemias. Cancer Treat Rev. 2013 Dec;39(8):851-61. PMID: 23566572.

Jensen K, Johnson LA, Jacobson PA, et al. Cytotoxic purine nucleoside analogues bind to A1, A2A, and A3 adenosine receptors. Naunyn Schmiedebergs Arch Pharmacol. 2012 May;385(5):519-25. PMID: 22249336.

F4483 Flufenamic Acid

10 g
50 g

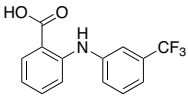

$C_{14}H_{10}F_3NO_2$ FW: 281.23 [530-78-9] ≥97%

NSAID, TREK1 K^+ potentiator, voltage-gated Na^+ channel blocker, TRPC3 and TRPM2 receptor antagonist, and COX-1/2 inhibitor. It decreases pain and inflammation and lowers glutamatergic excitatory activity and neuronal excitability.

Xie YF, Zhou F. TRPC3 channel mediates excitation of striatal cholinergic interneurons. Neurol Sci. 2014 May 21. [Epub ahead of print]. PMID: 24844791.

Veale EL, Al-Moubarak E, Bajaria N, et al. Influence of the N terminus on the biophysical properties and pharmacology of TREK1 potassium channels. Mol Pharmacol. 2014 May;85(5):671-81. PMID: 24509840.

Nazıroğlu M, Özgül C, Çelik Ö, et al. Aminoethoxydiphenyl borate and flufenamic acid inhibit Ca^{2+} influx through TRPM2 channels in rat dorsal root ganglion neurons activated by ADP-ribose and rotenone. J Membr Biol. 2011 May;241(2):69-75. PMID: 21509529.

F4580 FluM1 A2 Peptide (58-66)

1 mg
2 mg
5 mg

CEF1; Influenza matrix protein M1 (58-66)

Gly-Ile-Leu-Gly-Phe-Val-Phe-Thr-Leu

$C_{49}H_{75}N_9O_{11}$ FW: 966.2 [141368-69-6] ≥95%

Influenza matrix protein M1 epitope recognized by CD8+ T cells.

Zhou V, Yassai MB, Regunathan J, et al. The functional CD8 T cell memory recall repertoire responding to the influenza A M1(58-66) epitope is polyclonal and shows a complex clonotype distribution. Hum Immunol. 2013 Jul;74(7):809-17. PMID: 23295548.

F4681 Flumazenil

25 mg
100 mg

Anexate; Ro-15-1788

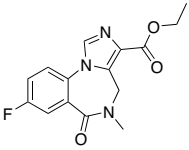

$C_{15}H_{14}FN_3O_3$ FW: 303.29 [78755-81-4] ≥98%

GABA-A receptor antagonist used as a stimulant to counteract the effects of benzodiazepines. It inhibits benzodiazepine-induced sedation, motor impairment, and ventilator depression.

Rye DB, Bliwise DL, Parker K, et al. Modulation of vigilance in the primary hypersomnias by endogenous enhancement of GABAA receptors. Sci Transl Med. 2012 Nov 21;4(161):161ra151. PMID: 23175709.

Lader M. Benzodiazepines revisited--will we ever learn? Addiction. 2011 Dec;106(12):2086-109. PMID: 21714826.

F4881 Flumequine Sodium

1 g
5 g
25 g

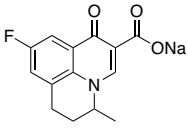

$C_{14}H_{11}FNNaO_3$ FW: 283.23 ≥98.0%

Bacterial DNA gyrase inhibitor and GABA-A receptor antagonist. It also displays both chemopreventive and carcinogenic activities.

Kuroiwa Y, Umemura T, Nishikawa A, et al. Lack of in vivo mutagenicity and oxidative DNA damage by flumequine in the livers of gpt delta mice. Arch Toxicol. 2007 Jan;81(1):63-9. PMID: 16802149.

Vik-Mo FT, Bergh O, Samuelsen OB. Efficacy of orally administered flumequine in the treatment of vibriosis caused by Listonella anguillarum in atlantic cod Gadus morhua. Dis Aquat Organ. 2005 Nov 9;67(1-2):87-92. PMID: 16385813.

F4582 Fluocinolone Acetonide

25 mg
100 mg
250 mg
1 g

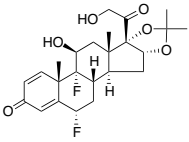

$C_{24}H_{30}F_2O_6$ FW: 452.49 [67-73-2] ≥98%

Synthetic hydrocortisone derivative and glucocorticoid receptor agonist used to treat ocular inflammation. It downregulates expression of pro-inflammatory cytokines and upregulates expression of PPARγ.

Cunha-Vaz J, Ashton P, Iezzi R, et al. Sustained Delivery Fluocinolone Acetonide Vitreous Implants: Long-Term Benefit in Patients with Chronic Diabetic Macular Edema. Ophthalmology. 2014 Jun 13. [Epub ahead of print]. PMID: 24935282.

Liu Z, Jiang T, Wang X, et al. Fluocinolone acetonide partially restores the mineralization of LPS-stimulated dental pulp cells through inhibition of NF-κB pathway and activation of AP-1 pathway. Br J Pharmacol. 2013 Nov;170(6):1262-71. PMID: 24024985.

F4480 5-Fluorouracil

1 g
5 g
25 g

5-FU; 2,4-dioxo-5-fluoropyrimidine

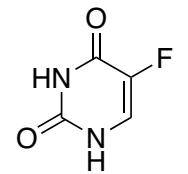

$C_4H_3FN_2O_2$ FW: 130.08 [51-21-8] ≥98%

Thymidylate synthase inhibitor that prevents DNA synthesis and is used to treat various cancers. It displays significant peripheral cytotoxicity.

Papanastasopoulos P, Stebbing J. Molecular basis of 5-fluorouracil-related toxicity: lessons from clinical practice. Anticancer Res. 2014 Apr;34(4):1531-5. PMID: 24692679.

Longley DB, Harkin DP, Johnston PG. 5-fluorouracil: mechanisms of action and clinical strategies. Nat Rev Cancer. 2003 May;3(5):330-8. PMID: 12724731.

F4780

Fluoxetine Hydrochloride

1 g
5 g

$C_{17}H_{18}F_3NO \bullet HCl$ FW: 345.79 [59333-67-4] ≥98%

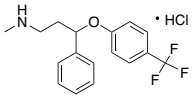

Inhibitor of SERT, 5-HT receptors, and σ1 receptors used to treat mood disorders. It also acts as a FIASMA, prevents cue- and stress-induced reinstatement of heroin administration, and reduces synthesis of cox-sackievirus RNA and protein.

Zuo J, Quinn KK, Kye S, et al. Fluoxetine is a potent inhibitor of coxsackievirus replication. Antimicrob Agents Chemother. 2012 Sep;56(9):4838-44. PMID: 22751539.

Apparsundaram S, Stockdale DJ, Henningsen RA, et al. Antidepressants targeting the serotonin reuptake transporter act via a competitive mechanism. J Pharmacol Exp Ther. 2008 Dec;327(3):982-90. PMID: 18801947.

Krupitsky EM, Zvartau EE, Masalov DV, et al. Naltrexone with or without fluoxetine for preventing relapse to heroin addiction in St. Petersburg, Russia. J Subst Abuse Treat. 2006 Dec;31(4):319-28. PMID: 17084785.

F4584

Fluphenazine Hydrochloride

1 g
5 g
25 g

Fluorophenazine

$C_{22}H_{26}F_3N_3OS \bullet 2HCl$ FW: 510.44 [146-56-5] ≥97%

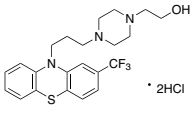

Inhibitor of dopamine D2 receptors and hERG K^+ channels used to treat dementia and mood disorders. It also acts as a FIASMA and prolongs the cardiac QT interval.

Hong HK, Lee BH, Park MH, et al. Block of hERG K^+ channel and prolongation of action potential duration by fluphenazine at submicromolar concentration. Eur J Pharmacol. 2013 Feb 28;702(1-3):165-73. PMID: 23395964.

Pickar D, Owen RR, Litman RE, et al. Clinical and biologic response to clozapine in patients with schizophrenia. Crossover comparison with fluphenazine. Arch Gen Psychiatry. 1992 May;49(5):345-53. PMID: 1375019.

F4583

Flupirtine Maleate

10 mg
25 mg
100 mg

$C_{15}H_{17}FN_4O_2 \bullet C_4H_4O_4$ FW: 304.32 [75507-68-5] ≥98%

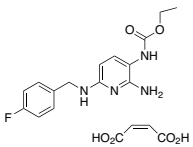

K_v7 K^+ channel activator, NMDA receptor antagonist, and GABA-A receptor negative modulator used to treat pain. It decreases axonal excitability and attenuates development of and reverses established pulmonary arterial hypertension.

Yadav G, Choupoo S, Das SK, et al. Evaluating the Role of Flupirtine for Postcraniotomy Pain and Compare it With Diclofenac Sodium: A Prospective, Randomized, Double Blind, Placebo-controlled Study. J Neurosurg Anesthesiol. 2013 Jun 11. [Epub ahead of print]. PMID: 23764718.

Fleckenstein J, Sittl R, Averbeck B, et al. Activation of axonal Kv7 channels in human peripheral nerve by flupirtine but not placebo - therapeutic potential for peripheral neuropathies: results of a randomised controlled trial. J Transl Med. 2013 Feb 8;11:34. PMID: 23394517.

Klinger F, Geier P, Dorostkar MM, et al. Concomitant facilitation of GABAA receptors and KV7 channels by the non-opioid analgesic flupirtine. Br J Pharmacol. 2012 Jul;166(5):1631-42. PMID: 22188423.

F4481

Flurbiprofen

1 g
5 g
25 g

$C_{15}H_{13}FO_2$ FW: 244.26 [5104-49-4] ≥98%

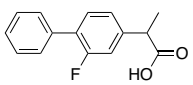

NSAID and COX-1/2 inhibitor used to treat pain and inflammation associated with arthritis. It also decreases infarct volume, apoptosis, and neurological deficits in models of cerebral ischemia/reperfusion and decreases cellular proliferation, metastasis, and tumor size in models of gastric cancer.

Sun B, Chen L, Wei X, et al. The Akt/GSK-3β pathway mediates flurbiprofen-induced neuroprotection against focal cerebral ischemia/reperfusion injury in rats. Biochem Biophys Res Commun. 2011 Jun 17;409(4):808-13. PMID: 21624354.

Jin H, Wang Z, Liu L, et al. R-flurbiprofen reverses multidrug resistance, proliferation and metastasis in gastric cancer cells by p75(NTR) induction. Mol Pharm. 2010 Feb 1;7(1):156-68. PMID: 19916560.

F4680

Flutamide

1 g
5 g

$C_{11}H_{11}F_3N_2O_3$ FW: 276.22 [13311-84-7] ≥98%

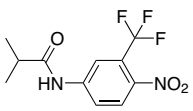

Non-steroidal androgen receptor antagonist used to treat prostate cancer and polycystic ovary syndrome. It induces cell cycle arrest in prostate cancer cells and suppresses release of pro-inflammatory cytokines.

Al-Saeedi F. Effects of flutamide on [methyl-(3)h]-choline uptake in human prostate cancer-3 cells: a pilot study. Curr Ther Res Clin Exp. 2007 Jul;68(4):226-41. PMID: 24683213.

Shimizu T, Yu HP, Hsieh YC, et al. Flutamide attenuates pro-inflammatory cytokine production and hepatic injury following trauma-hemorrhage via estrogen receptor-related pathway. Ann Surg. 2007 Feb;245(2):297-304. PMID: 17245185.

F4683

Fluticasone Propionate

10 mg
25 mg
100 mg

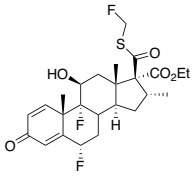

$C_{25}H_{31}F_3O_5S$ FW: 500.57 [80474-14-2] ≥98%

β2-Adrenergic receptor agonist used to treat asthma and COPD. It decreases lymphocyte activation and prevents eosinophilic inflammation and airway remodeling.

Kan-O K, Matsumoto K, Inoue H, et al. Corticosteroids plus long-acting β2-agonists prevent double-stranded RNA-induced upregulation of B7-H1 on airway epithelium. Int Arch Allergy Immunol. 2013;160(1):27-36. PMID: 22948082.

Mendes ES, Horvath G, Campos M, et al. Rapid corticosteroid effect on beta(2)-adrenergic airway and airway vascular reactivity in patients with mild asthma. J Allergy Clin Immunol. 2008 Mar;121(3):700-4. PMID: 18086493.

Lee SY, Kim JS, Lee JM, et al. Inhaled corticosteroid prevents the thickening of airway smooth muscle in murine model of chronic asthma. Pulm Pharmacol Ther. 2008;21(1):14-9. PMID: 17142077.

F4883

Flutriafol

500 mg
5 g
25 g

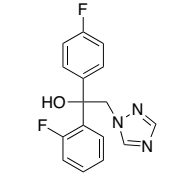

$C_{16}H_{13}F_2N_3O$ FW: 301.29 [76674-21-0] ≥95%

Pesticide, demethylation inhibitor, and NMDA receptor agonist that prevents sterol synthesis and disrupts membrane function. It also induces striatal dopamine release and decreases oxidative damage.

Faro LR, Alfonso M, Maués LA, et al. Role of ionotropic glutamatergic receptors and nitric oxide in the effects of flutriafol, a triazole fungicide, on the in vivo striatal dopamine release. J Toxicol Sci. 2012;37(6):1135-42. PMID: 23208429.

Santana MB, Rodrigues KJ, Durán R, et al. Evaluation of the effects and mechanisms of action of flutriafol, a triazole fungicide, on striatal dopamine release by using in vivo microdialysis in freely moving rats. Ecotoxicol Environ Saf. 2009 Jul;72(5):1565-71. PMID: 19232726.

Griffiths KM, Howlett BJ. Transcription of sterol Delta(5,6)-desaturase and sterol 14alpha-demethylase is induced in the plant pathogenic ascomycete, Leptosphaeria maculans, during treatment with a triazole fungicide. FEMS Microbiol Lett. 2002 Nov 19;217(1):81-7. PMID: 12445649.

F4482

Fluvastatin Sodium

10 mg
50 mg
100 mg

Fluindostatin; XU-62-320

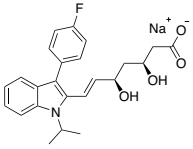

$C_{24}H_{25}FNNaO_4$ FW: 433.45 [93957-55-2] ≥98%

HMG-CoA reductase inhibitor used to lower cholesterol and lipid levels. It may inhibit RhoA. It also prevents viral replication of hepatitis C, decreases platelet activation, scavenges hydroxyl radicals, induces cell cycle arrest and apoptosis in hepatocellular carcinoma cells, and improves left ventricular function and prevents fibrosis in cardiac distress models.

Wuestenberg A, Kah J, Singethan K, et al. Matrix conditions and KLF2-dependent induction of heme oxygenase-1 modulate inhibition of HCV replication by fluvastatin. PLoS One. 2014 May 6;9(5):e96533. PMID: 24801208.

Moraes LA, Vaiyapuri S, Sasikumar P, et al. Antithrombotic actions of statins involve PECAM-1 signaling. Blood. 2013 Oct 31;122(18):3188-96. PMID: 24030383.

Vandjelovic N, Zhu H, Misra HP, et al. EPR studies on hydroxyl radical-scavenging activities of pravastatin and fluvastatin. Mol Cell Biochem. 2012 May;364(1-2):71-7. PMID: 22207075.

F4783

Fluvoxamine Maleate

25 mg
100 mg
500 mg

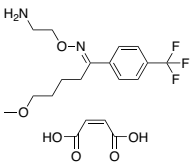

$C_{15}H_{21}O_2N_2F_3 \bullet C_4H_4O_4$ FW: 434.41 [61718-82-9] ≥97%

5-HT3 receptor and σ1 receptor agonist, SERT inhibitor, and FIASMA used to treat mood disorders. It also prevents transverse aortic constriction-induced myocardial hypertrophy, inhibits osteoclast formation and resorption, and decreases levels of oxidative enzymes.

Hodge JM, Wang Y, Berk M, et al. Selective serotonin reuptake inhibitors inhibit human osteoclast and osteoblast formation and function. Biol Psychiatry. 2013 Jul 1;74(1):32-9. PMID: 23260229.

Fu Y, Yu S, Guo X, et al. Fluvoxamine increased glutamate release by activating both 5-HT(3) and sigma-1 receptors in prelimbic cortex of chronic restraint stress C57BL/6 mice. Biochim Biophys Acta. 2012 Apr;1823(4):826-37. PMID: 22306004.

Tynan RJ, Weidenhofer J, Hinwood M, et al. A comparative examination of the anti-inflammatory effects of SSRI and SNRI antidepressants on LPS stimulated microglia. Brain Behav Immun. 2012 Mar;26(3):469-79. PMID: 22251606.

F4856

Fmoc-Lys(Boc)-Leu-Lys(Boc)

1 g

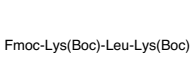

Fmoc-Lys(Boc)-Leu-Lys(Boc)

$C_{26}H_{35}N_8O_7S$ FW: 809.9 ≥98%

Highly reactive tripeptide used for glycation.

Mennella C, Visciano M, Napolitano A, et al. Glycation of lysine-containing dipeptides. J Pept Sci. 2006 Apr;12(4):291-6. PMID: 16180244.

F4859 FMRF

5 mg
10 mg
25 mg

$C_{29}H_{41}N_7O_5S$ FW: 599.76 ≥95%

H-Phe-Met-Arg-Phe-OH

Involved in reproductive behavior. It also increases the magnitude of delayed rectifier K^+ current (I(K)) in olfactory neurons.

Di Cristo C. Nervous control of reproduction in Octopus vulgaris: a new model. Invert Neurosci. 2013 Jun;13(1):27-34. PMID: 23558706.

Ringstad N, Horvitz HR. FMRFamide neuropeptides and acetylcholine synergistically inhibit egg-laying by C. elegans. Nat Neurosci. 2008 Oct;11(10):1168-76. PMID: 18806786.

F4857 FMRF Amide

1 mg

$C_{29}H_{42}N_8O_4S$ FW: 598.76 ≥95%

Phe-Met-Arg-Phe-NH_2

Cardiostimulatory delayed rectifier K^+ channel modulator. It inhibits Na^+ and Ca^{2+} exchange.

Di Cristo C. Nervous control of reproduction in Octopus vulgaris: a new model. Invert Neurosci. 2013 Jun;13(1):27-34. PMID: 23558706.

Ringstad N, Horvitz HR. FMRFamide neuropeptides and acetylcholine synergistically inhibit egg-laying by C. elegans. Nat Neurosci. 2008 Oct;11(10):1168-76. PMID: 18806786.

F4858 FMRF-like Peptide, snail

1 mg

$C_{44}H_{62}N_{11}O_{10}$ FW: 904.03 ≥98%

pGlu-Asp-Pro-Phe-Leu-Arg-Phe-NH_2

Cardiostimulatory delayed rectifier K^+ channel modulator found in *Lymnaea*. It inhibits Na^+ and Ca^{2+} exchange.

Di Cristo C. Nervous control of reproduction in Octopus vulgaris: a new model. Invert Neurosci. 2013 Jun;13(1):27-34. PMID: 23558706.

Ringstad N, Horvitz HR. FMRFamide neuropeptides and acetylcholine synergistically inhibit egg-laying by C. elegans. Nat Neurosci. 2008 Oct;11(10):1168-76. PMID: 18806786.

F5745 Folic Acid

10 g
50 g
100g

PGA; Vitamin M

$C_{19}H_{19}N_7O_6$ FW: 441.4 [59-30-3] ≥96%

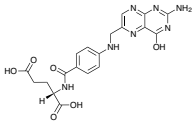

Non-endogenous essential vitamin (B9) found in leafy vegetables. It is required for synthesis and repair of DNA, division and growth of cells, and gamete maturation. It may prevent mood disorders such as depression and schizophrenia.

Reynolds EH. The neurology of folic acid deficiency. Handb Clin Neurol. 2014;120:927-43. PMID: 24365361.

Czeizel AE, Dudás I, Vereczkey A, et al. Folate deficiency and folic acid supplementation: the prevention of neural-tube defects and congenital heart defects. Nutrients. 2013 Nov 21;5(11):4760-75. PMID: 24284617.

F5766 Forchlorfenuron

500 mg
1 g
5 g

KT-30

$C_{12}H_{10}ClN_3O$ FW: 247.68 [68157-60-8] ≥98%

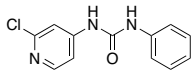

Synthetic cytokinin, plant growth regulator, and filament polymerization inducer. It induces paralysis in *Schistosoma* and inhibits proliferation and migration of prostate cancer cells.

Zeraik AE, Galkin VE, Rinaldi G, et al. Reversible paralysis of *Schistosoma* mansoni by forchlorfenuron, a phenylurea cytokinin that affects septins. Int J Parasitol. 2014 Apr 21. [Epub ahead of print]. PMID: 24768753.

Vardi-Oknin D, Golan M, Mabjeesh NJ. Forchlorfenuron disrupts SEPT9_i1 filaments and inhibits HIF-1. PLoS One. 2013 Aug 19;8(8):e73179. PMID: 23977378.

Hu Q, Nelson WJ, Spiliotis ET. Forchlorfenuron alters mammalian septin assembly, organization, and dynamics. J Biol Chem. 2008 Oct 24;283(43):29563-71. PMID: 18713753.

F5968 Foretinib

NEW

5 mg
10 mg
25 mg

GSK1363089

$C_{34}H_{34}F_2N_4O_6$ FW: 632.65 [849217-64-7] ≥98%

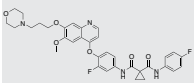

Inhibitor of ROS1, MET, Ron, Axl, TIE-2, and VEGFR2. It induces cell cycle arrest and inhibits growth and migration on hepatocellular carcinoma cells.

Shah MA, Wainberg ZA, Catenacci DV, et al. Phase II study evaluating 2 dosing schedules of oral foretinib (GSK1363089), cMET/VEGFR2 inhibitor, in patients with metastatic gastric cancer. PLoS One. 2013;8(3):e54014. PMID: 23516391.

Seiwert T, Sarantopoulos J, Kallender H, et al. Phase II trial of single-agent foretinib (GSK1363089) in patients with recurrent or metastatic squamous cell carcinoma of the head and neck. Invest New Drugs. 2013 Apr;31(2):417-24. PMID: 22918720.

Huynh H, Ong R, Soo KC. Foretinib demonstrates anti-tumor activity and improves overall survival in preclinical models of hepatocellular carcinoma. Angiogenesis. 2012 Mar;15(1):59-70. PMID: 22187171.

F5769 Formestane

100 mg
500 mg
1 g
5 g

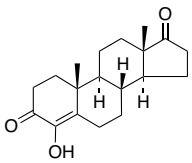

4-OHA

$C_{19}H_{26}O_3$ FW: 302.41 [566-48-3] ≥98%

Aromatase inhibitor used to treat ER+ breast cancer. It inhibits production of estrogens.

Miller WR. Aromatase inhibitors: mechanism of action and role in the treatment of breast cancer. Semin Oncol. 2003 Aug;30(4 Suppl 14):3-11. PMID: 14513432.

Dowsett M. Aromatase inhibition: basic concepts, and the pharmacodynamics of formestane. Ann Oncol. 1994;5 Suppl 7:S3-5. PMID: 7873460.

F5770 Formononetin

100 mg
500 mg
1 g

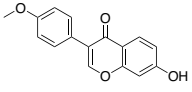

Biochanin B; Neochanin

$C_{16}H_{12}O_4$ FW: 268.26 [485-72-3] ≥90%

Found in *Fabaceae* (soy). It displays a wide variety of biological activities, including decreasing expression of pro-inflammatory cytokines, inducing apoptosis in prostate cancer cells, lowering systolic blood pressure, and inhibiting attachment and motility of *Giardia*.

Li Z, Dong X, Zhang J, et al. Formononetin protects TBI rats against neurological lesions and the underlying mechanism. J Neurol Sci. 2014 Mar 15;338(1-2):112-7. PMID: 24411660.

Huang WJ, Bi LY, Li ZZ, et al. Formononetin induces the mitochondrial apoptosis pathway in prostate cancer cells via downregulation of the IGF-1/IGF-1R signaling pathway. Pharm Biol. 2013 Dec 20. [Epub ahead of print]. PMID: 24359236.

F5868 Formoterol Fumarate Dihydrate

10 mg
50 mg

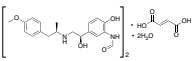

$(C_{19}H_{24}N_2O_4)_2 \cdot C_4H_4O_4 \cdot 2H_2O$ FW: 840.91 [43229-80-7] ≥98%

β2-Adrenergic receptor agonist used to treat asthma and COPD. It also increases resting energy expenditure, fat utilization, and mitochondrial biogenesis.

Lee P, Day RO, Greenfield JR, et al. Formoterol, a highly β2-selective agonist, increases energy expenditure and fat utilisation in men. Int J Obes (Lond). 2013 Apr;37(4):593-7. PMID: 22641064.

Wills LP, Trager RE, Beeson GC, et al. The β2-adrenoceptor agonist formoterol stimulates mitochondrial biogenesis. J Pharmacol Exp Ther. 2012 Jul;342(1):106-18. PMID: 22490378.

F5869 N-formyl-Met-Ala-Ser

1 mg
2 mg
5 mg

For-Met-Ala-Ser-OH

N-fMAS

$C_{12}H_{21}N_3O_6S$ FW: 335.38 [17351-32-5] ≥95%

FPR agonist involved in neutrophil activation.

He HQ, Troksa EL, Caltabiano G, et al. Structural determinants for the interaction of formyl Peptide receptor 2 with Peptide ligands. J Biol Chem. 2014 Jan 24;289(4):2295-306. PMID: 24285541.

F5870 N-formyl-Met-Leu-Phe

5 mg
10 mg
25 mg

For-Met-Leu-Phe-OH

N-fMLF

$C_{21}H_{31}N_3O_5S$ FW: 437.6 [59880-97-6] ≥95%

FPR agonist involved in neutrophil activation. It also generates ROS and inflammatory signaling cascades in neutrophils.

Hurtado-Nedelec M, Makni-Maalej K, Gougerot-Pocidalo MA, et al. Assessment of priming of the human neutrophil respiratory burst. Methods Mol Biol. 2014;1124:405-12. PMID: 24504964.

Andréasson E, Önnheim K, Forsman H. The subcellular localization of the receptor for platelet-activating factor in neutrophils affects signaling and activation characteristics. Clin Dev Immunol. 2013;2013:456407. PMID: 24069041.

F5871 N-formyl-Met-Leu-Phe-Lys

5 mg
10 mg
25 mg

For-Met-Leu-Phe-Lys-OH

Chemotactic peptide

$C_{27}H_{43}N_3O_6S$ FW: 565.74 [104180-18-9] ≥95%

FPR agonist involved in neutrophil activation.

He HQ, Troksa EL, Caltabiano G, et al. Structural determinants for the interaction of formyl Peptide receptor 2 with Peptide ligands. J Biol Chem. 2014 Jan 24;289(4):2295-306. PMID: 24285541.

F5872 N-formyl-Nle-Leu-Phe-Nle-Tyr-Lys

5 mg
10 mg
25 mg

For-Nle-Leu-Phe-Nle-Tyr-Lys-OH

F-Chemotactic peptide; F-Peptide

$C_{43}H_{65}O_7N_9$ FW: 824.04 [71901-21-8] ≥95%

FPR agonist involved in neutrophil activation.

Allen RA, Erickson RW, Jesaitis AJ. Identification of a human neutrophil protein of Mr 24 000 that binds N-formyl peptides: co-sedimentation with specific granules. Biochim Biophys Acta. 1989 Apr 25;991(1):123-33. PMID: 2653446.

F5668 Forskolin

1 mg
5 mg
10 mg

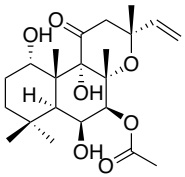

$C_{22}H_{34}O_7$ FW: 410.5 [66575-29-9] ≥98%

PP2A and adenylyl cyclase activator found in *Coleus*. It displays several biological activities, including increasing levels of cAMP, decreasing intraocular pressure in glaucoma models, enhancing proteasome activity, and suppressing Shh signaling to limit basal cell carcinoma tumor growth.

Rodriguez G, Ross JA, Nagy ZS, et al. Forskolin-inducible cAMP pathway negatively regulates T-cell proliferation by uncoupling the interleukin-2 receptor complex. J Biol Chem. 2013 Mar 8;288(10):7137-46. PMID: 23341462.

Makinodan E, Marneros AG. Protein kinase A activation inhibits oncogenic Sonic hedgehog signalling and suppresses basal cell carcinoma of the skin. Exp Dermatol. 2012 Nov;21(11):847-52. PMID: 23163650.

Alasbahi RH, Melzig MF. Forskolin and derivatives as tools for studying the role of cAMP. Pharmazie. 2012 Jan;67(1):5-13. PMID: 22393824.

F5873 Foscarnet Sodium

1 g
5 g
10 g

Phosphonoformic acid

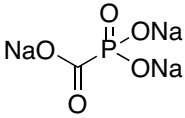

CNa_3O_5P FW: 191.95 [63585-09-1] ≥98%

Metal ion chelator and inhibitor of viral DNA polymerase, reverse transcriptase, and type II Pi transporter used to treat viral infections. It mimics the pyrophosphate leaving group in DNA polymerase. It also inhibits vascular calcification.

Zahn KE, Tchesnokov EP, Götte M, et al. Phosphonoformic acid inhibits viral replication by trapping the closed form of the DNA polymerase. J Biol Chem. 2011 Jul 15;286(28):25246-55. PMID: 21566148.

Villa-Bellosta R, Sorribas V. Phosphonoformic acid prevents vascular smooth muscle cell calcification by inhibiting calcium-phosphate deposition. Arterioscler Thromb Vasc Biol. 2009 May;29(5):761-6. PMID: 19213941.

Marchand B, Tchesnokov EP, Götte M. The pyrophosphate analogue foscarnet traps the pre-translocational state of HIV-1 reverse transcriptase in a Brownian ratchet model of polymerase translocation. J Biol Chem. 2007 Feb 2;282(5):3337-46. PMID: 17145704.

F5874 Fosfomycin Calcium

5 g
25 g

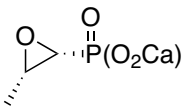

$C_3H_5CaO_4P$ FW: 176.12 [26016-98-8] ≥97%

MurA and isopentenyl mevalonate kinase inhibitor that prevents synthesis of bacterial cell walls. It also prevents aminoglycoside antibiotic-induced nephrotoxicity and lowers serum levels of TNF-α, IL-1β, and IL-6 in models of septic *Pseudomonas* infection.

Olesen SH, Ingles DJ, Yang Y, et al. Differential antibacterial properties of the MurA inhibitors terreic acid and fosfomycin. J Basic Microbiol. 2013 May 20. [Epub ahead of print]. PMID: 23686727.

Mabanglo MF, Serohijos AW, Poulter CD. The *Streptomyces*-produced antibiotic fosfomycin is a promiscuous substrate for archaeal isopentenyl phosphate kinase. Biochemistry. 2012 Jan 31;51(4):917-25. PMID: 22148590.

Yanagida C, Ito K, Komiya I, et al. Protective effect of fosfomycin on gentamicin-induced lipid peroxidation of rat renal tissue. Chem Biol Interact. 2004 Jul 20;148(3):139-47. PMID: 15276870.

F5773 Fosinopril Sodium

25 mg
100 mg
250 mg

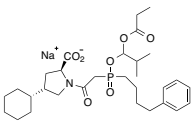

$C_{30}H_{45}NNaO_7P$ FW: 585.64 [88889-14-9] ≥98%

ACE inhibitor used to treat congestive heart failure. It suppresses the formation of atherosclerotic plaques and decreases left ventricular hypertrophy and blood pressure.

Yang S, Li R, Tang L, et al. TLR4-mediated anti-atherosclerosis mechanisms of angiotensin-converting enzyme inhibitor--fosinopril. Cell Immunol. 2013 Sep-Oct;285(1-2):38-41. PMID: 24044965.

Huang K, Dai G. The effect and mechanism of forsinopril on ventricular hypertrophy of SHR and left ventricular pressure overloading rat. J Huazhong Univ Sci Technolog Med Sci. 2002;22(1):17-20. PMID: 12658773.

F5976 Fotemustine

5 mg
25 mg
100 mg

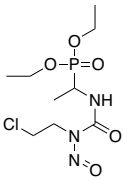

$C_9H_{19}ClN_3O_5P$ FW: 315.69 [92118-27-9] ≥98%

DNA alkylator and cross-linker. It induces cell cycle arrest and inhibits DNA repair mechanisms in cancer cells. It may also deactivate thioredoxin reductase, glutathione reductase, and ribonucleotide reductase by alkylating thiol active sites.

Hayes MT, Bartley J, Parsons PG. In vitro evaluation of fotemustine as a potential agent for limb perfusion in melanoma. Melanoma Res. 1998 Feb;8(1):67-75. PMID: 9508380.

Hayes MT, Bartley J, Parsons PG, et al. Mechanism of action of fotemustine, a new chloroethylnitrosourea anticancer agent: evidence for the formation of two DNA-reactive intermediates contributing to cytotoxicity. Biochemistry. 1997 Sep 2;36(35):10646-54. PMID: 9271495.

F6803 FRAX486

5 mg
10 mg

$(C_{25}H_{23}Cl_2FN_6O)_2 \bullet H_2O$ FW: 522.4 [1232030-35-1] ≥98%

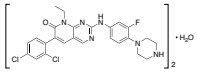

PAK inhibitor. It ameliorates synaptic deterioration induced by DISC1 knockdown and rescues seizures and other behavioral abnormalities in models of fragile X syndrome.

Hayashi-Takagi A, Araki Y, Nakamura M, et al. PAKs inhibitors ameliorate schizophrenia-associated dendritic spine deterioration in vitro and in vivo during late adolescence. Proc Natl Acad Sci U S A. 2014 Apr 29;111(17):6461-6. PMID: 24706880.

Dolan BM, Duron SG, Campbell DA, et al. Rescue of fragile X syndrome phenotypes in Fmr1 KO mice by the small-molecule PAK inhibitor FRAX486. Proc Natl Acad Sci U S A. 2013 Apr 2;110(14):5671-6. PMID: 23509247.

F7657 Ftorafur

250 mg
1 g

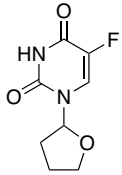

Tegafur; 5-Fluoro-1-(tetrahydro-2-furyl)uracil

$C_8H_9FN_2O_3$ FW: 200.17 [17902-23-7] ≥98%

Prodrug of 5-FU and inhibitor of thymidylate synthase that is used to treat various cancers. It inhibits DNA synthesis and displays significant peripheral toxicity.

Fukushima M. Antitumor activity and function of S-1, a new oral tegafur-based formulation. Gan To Kagaku Ryoho. 2006 Jun;33 Suppl 1:19-26. PMID: 16897968.

F8147 Fulvestrant

5 mg
25 mg
100 mg

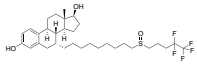

$C_{32}H_{47}F_5O_3S$ FW: 606.77 [129453-61-8] ≥98%

Anti-endocrine agent that Induces ER degradation and downregulates ER expression. It also lowers levels of LDL and total cholesterol.

Edavana VK, Penney RB, Yao-Borengasser A, et al. Fulvestrant up regulates UGT1A4 and MRPs through ERα and c-Myb pathways: a possible primary drug disposition mechanism. Springerplus. 2013 Nov 20;2:620. PMID: 24298433.

Krell J, Januszewski A, Yan K, et al. Role of fulvestrant in the management of postmenopausal breast cancer. Expert Rev Anticancer Ther. 2011 Nov;11(11):1641-52. PMID: 22050013.

Scott SM, Brown M, Come SE. Emerging data on the efficacy and safety of fulvestrant, a unique antiestrogen therapy for advanced breast cancer. Expert Opin Drug Saf. 2011 Sep;10(5):819-26. PMID: 21699443

F8048 Fumagillin

1 mg
5 mg

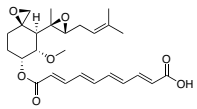

Amebacilin; Fumadil B

$C_{26}H_{34}O_7$ FW: 458.54 [23110-15-8] ≥98%

Type 2 methionine aminopeptidase inhibitor produced by *Aspergillus* used to treat microsporidiosis. It decreases pulmonary fibrosis, pulmonary hypertension, and ventricular remodeling, prevents endothelial tube and microvessel formation , and inhibits growth of *Plasmodium*, *Nosema*, and *Enterocytozoon*.

Kass DJ, Rattigan E, Kahloon R, et al. Early treatment with fumagillin, an inhibitor of methionine aminopeptidase-2, prevents Pulmonary Hypertension in monocrotaline-injured rats. PLoS One. 2012;7(4):e35388. PMID: 22509410.

Champion L, Durrbach A, Lang P, et al. Fumagillin for treatment of intestinal microsporidiosis in renal transplant recipients. Am J Transplant. 2010 Aug;10(8):1925-30. PMID: 20636462.

F8149 Fumonisin B1

1 mg
5 mg

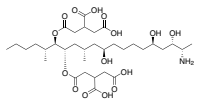

Macrofusine; FB1

$C_{34}H_{59}NO_{15}$ FW: 721.83 [116355-83-0] ≥98%

Mycotoxin and grain contaminant. It inhibits sphingosine acyltransferase and disrupts sphingolipid metabolism. It is less toxic than fumonisin B2.

Wei T, Zhu W, Pang M, et al. Natural occurrence of fumonisins B1 and B2 in corn in four provinces of China. Food Addit Contam Part B Surveill. 2013 Dec;6(4):270-4. PMID: 24779936.

Tardieu D, Bailly JD, Skiba F, et al. Chronic toxicity of fumonisins in turkeys. Poult Sci. 2007 Sep;86(9):1887-93. PMID: 17704375.

F8150 Fumonisin B2

1 mg
5 mg

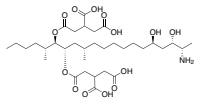

FB2

$C_{34}H_{59}NO_{14}$ FW: 705.8 [116355-84-1] ≥97%

Mycotoxin and grain contaminant. It inhibits sphingosine acyltransferase and disrupts sphingolipid metabolism. It is more toxic than fumonisin B1.

Wei T, Zhu W, Pang M, et al. Natural occurrence of fumonisins B1 and B2 in corn in four provinces of China. Food Addit Contam Part B Surveill. 2013 Dec;6(4):270-4. PMID: 24779936.

F8270 Furosemide

5 g
10 g
25 g

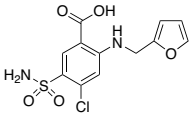

$C_{12}H_{11}ClN_2O_5S$ FW: 330.74 [54-31-9] ≥97%

Loop diuretic, NKCC symporter inhibitor, CFTR Cl^- channel blocker, and GABA-A receptor antagonist used to treat congestive heart failure, edema, and hypertension. It also decreases anxiety-like behaviors in contextual fear conditioning and fear-potentiated startle assays.

Ju M, Scott-Ward TS, Liu J, et al. Loop diuretics are open-channel blockers of the cystic fibrosis transmembrane conductance regulator with distinct kinetics. Br J Pharmacol. 2014 Jan;171(1):265-78. PMID: 24117047.

Krystal AD, Sutherland J, Hochman DW. Loop diuretics have anxiolytic effects in rat models of conditioned anxiety. PLoS One. 2012;7(4):e35417. PMID: 22514741.

Somasekharan S, Tanis J, Forbush B. Loop diuretic and ion-binding residues revealed by scanning mutagenesis of transmembrane helix 3 (TM3) of Na-K-Cl cotransporter (NKCC1). J Biol Chem. 2012 May 18;287(21):17308-17. PMID: 22437837.

F8272 Fusarenon X

1 mg
5 mg

Nivalenol monoacetate

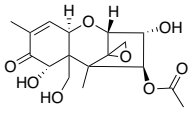

$C_{17}H_{22}O_8$ FW: 354.35 [23255-69-8] ≥98%

Mycotoxin found in *Fusarium*. It induces DNA strand breakage and decrease food intake.

Alassane-Kpembi I, Kolf-Clauw M, Gauthier T, et al. New insights into mycotoxin mixtures: the toxicity of low doses of Type B trichothecenes on intestinal epithelial cells is synergistic. Toxicol Appl Pharmacol. 2013 Oct 1;272(1):191-8. PMID: 23735874.

Wu W, Flannery BM, Sugita-Konishi Y, et al. Comparison of murine anorectic responses to the 8-ketotrichothecenes 3-acetyldeoxynivalenol, 15-acetyldeoxynivalenol, fusarenon X and nivalenol. Food Chem Toxicol. 2012 Jun;50(6):2056-61. PMID: 22465835.

G0000 G250.A2 Peptide

1 mg
2 mg
5 mg

His-Leu-Ser-Thr-Ala-Phe-Ala-Arg-Val

$C_{45}H_{72}N_{14}O_{12}$ FW: 1001.16 ≥95%

HLA-A2-restricted peptide epitope of carbonic anhydrase G250 that is recognized by T cells.

Socie G, Blazar BR. Immune Biology of Allogeneic Hematopoietic Stem Cell Transplantation. Elsevier, 2012. Web.

G0106 Gabapentin

10 mg
50 mg
250 mg

GOE-3450

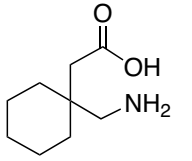

$C_9H_{17}NO_2$ FW: 171.24 [60142-96-3] ≥98%

GABA analog, GABA receptor potentiator, adenosine A1 receptor agonist, voltage-gated $\alpha 2\delta$ Ca^{2+} channel blocker, and NMDA receptor modulator used to prevent seizures and to treat neuropathic, inflammatory, and cancer-related pain.

Kukkar A, Bali A, Singh N, et al. Implications and mechanism of action of gabapentin in neuropathic pain. Arch Pharm Res. 2013 Mar;36(3):237-51. PMID: 23435945.

Davies A, Hendrich J, Van Minh AT, et al. Functional biology of the alpha(2)delta subunits of voltage-gated calcium channels. Trends Pharmacol Sci. 2007 May;28(5):220-8. PMID: 17403543.

G0104 Gabexate Mesylate

10 mg
100 mg
250 mg

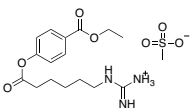

$C_{16}H_{24}N_3O_4 \bullet CH_3O_3S$ FW: 417.48 [56974-61-9] ≥98%

Proteasome inhibitor used to treat pancreatitis. It increases expression of PTEN, inhibits activity of tumor-associated trypsinogen and urokinase-type plasminogen activator, and prevents cleavage of hemagglutinin.

Brandi G, Tavolari S, Guarnieri T, et al. Antiprotease strategy in pancreatic cancer treatment: emergence from a preclinical study. Pancreas. 2014 Jan;43(1):53-63. PMID: 24201777.

Hsieh HP, Hsu JT. Strategies of development of antiviral agents directed against influenza virus replication. Curr Pharm Des. 2007;13(34):3531-42. PMID: 18220789.

G0048 γ-Amino Butyric Acid

10 g
25 g
100 g

Gammalon; GABA

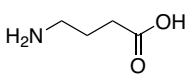

$C_4H_9NO_2$ FW: 103.12 [56-12-2] ≥98%

Endogenous neurotransmitter and GABA receptor agonist involved in neuronal excitability, muscle tone, stem cell growth, brain development, and mood. It decreases incidence of anxiety and seizures.

Li K, Xu E. The role and the mechanism of gamma-aminobutyric acid during central nervous system development. Neurosci Bull. 2008 Jun;24(3):195-200. PMID: 18500393.

Abdou AM, Higashiguchi S, Horie K, et al. Relaxation and immunity enhancement effects of gamma-aminobutyric acid (GABA) administration in humans. Biofactors. 2006;26(3):201-8. PMID: 16971751.

G0144

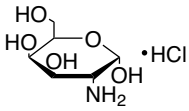

Galactosamine Hydrochloride

500 mg
1 g
5 g

Chondrosamine; GalN

$C_6H_{13}NO_5 \bullet HCl$ FW: 215.63 [1772-03-8] ≥98%

Galactose-derived hexosamine sugar and component of FSH and LH. It is used to induce endotoxic shock.

Capini CJ, Bertin-Maghit SM, Bessis N, et al. Active immunization against murine TNFalpha peptides in mice: generation of endogenous antibodies cross-reacting with the native cytokine and in vivo protection. Vaccine. 2004 Aug 13;22(23-24):3144-53. PMID: 15297067.

G0146

Gly-Trp-Thr-Leu-Asn-Ser-Ala-Gly-Tyr-Leu-Leu-Gly-Pro-His-Ala-Val-Gly-Asn-His-Arg-Ser-Phe-Ser-Asp-Lys-Asn-Gly-Leu-Thr-Ser

Galanin, human

1 mg

$C_{139}H_{210}N_{42}O_{43}$ FW: 3157.44 [119418-04-1] ≥98%

Endogenous GAP receptor agonist involved in nociception, sleep regulation, and feeding behavior. It also plays a role in action potential signaling and neuronal propagation.

Mitsukawa K, Lu X, Bartfai T. Galanin, galanin receptors and drug targets. Cell Mol Life Sci. 2008 Jun;65(12):1796-805. PMID: 18500647.

Counts SE, Perez SE, Mufson EJ. Galanin in Alzheimer's disease: neuroinhibitory or neuroprotective? Cell Mol Life Sci. 2008 Jun;65(12):1842-53. PMID: 18500641.

G0147

Gly-Trp-Thr-Leu-Asn-Ser-Ala-Gly-Tyr-Leu-Leu-Gly-Pro-His-Ala-Ile-Asp-Asn-His-Arg-Ser-Phe-His-Asp-Lys-Tyr-Gly-Leu-Ala-NH_2

Galanin, pig

1 mg

$C_{146}H_{213}N_{43}O_{40}$ FW: 3210.55 [88813-36-9] ≥98%

Endogenous GAP receptor agonist involved in nociception, sleep regulation, and feeding behavior. It also plays a role in action potential signaling and neuronal propagation.

Mitsukawa K, Lu X, Bartfai T. Galanin, galanin receptors and drug targets. Cell Mol Life Sci. 2008 Jun;65(12):1796-805. PMID: 18500647.

Counts SE, Perez SE, Mufson EJ. Galanin in Alzheimer's disease: neuroinhibitory or neuroprotective? Cell Mol Life Sci. 2008 Jun;65(12):1842-53. PMID: 18500641.

G0148

Gly-Trp-Thr-Leu-Asn-Ser-Ala-Gly-Tyr-Leu-Leu-Gly-Pro-His-Ala-Ile-Asp-Asn-His-Arg-Ser-Phe-Ser-Asp-Lys-His-Gly-Leu-Thr-NH_2

Galanin, rat

1 mg

$C_{141}H_{211}N_{43}O_{41}$ FW: 3164.48 [114547-31-8] ≥98%

Endogenous GAP receptor agonist involved in nociception, sleep regulation, and feeding behavior. It also plays a role in action potential signaling and neuronal propagation.

Mitsukawa K, Lu X, Bartfai T. Galanin, galanin receptors and drug targets. Cell Mol Life Sci. 2008 Jun;65(12):1796-805. PMID: 18500647.

G0246

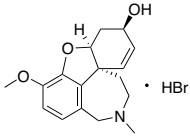

Galantamine Hydrobromide

5 mg
25 mg
100 mg

$C_{17}H_{21}NO_3 \bullet HBr$ FW: 368.27 [1953-04-4] ≥98%

AChE inhibitor, α7 nAChR agonist, and mAChR agonist found in *Galanthus*, *Narcissus*, *Leucojum*, and *Lycoris* used to improve cognitive deficits in subjects with Alzheimer's disease. It also promotes neurogenesis and may inhibit P2X7 receptors.

Kita Y, Ago Y, Higashino K, et al. Galantamine promotes adult hippocampal neurogenesis via M1 muscarinic and α7 nicotinic receptors in mice. Int J Neuropsychopharmacol. 2014 May 12:1-12. [Epub ahead of print]. PMID: 24818616.

Tsvetkova D, Obreshkova D, Zheleva-Dimitrova D, et al. Antioxidant activity of galantamine and some of its derivatives. Curr Med Chem. 2013;20(36):4595-608. PMID: 23834167.

Ago Y, Koda K, Takuma K, et al. Pharmacological aspects of the acetylcholinesterase inhibitor galantamine. J Pharmacol Sci. 2011;116(1):6-17. PMID: 21498956.

G0044

H-Gly-Trp-Thr-Leu-Asn-Ser-Ala-Gly-Tyr-Leu-Leu-Gly-Pro-Gln-Gln-Phe-Phe-Gly-Leu-Met-NH_2

Galantide

0.5 mg
1 mg
2.5 mg

M15

$C_{104}H_{151}N_{25}O_{26}S$ FW: 2199.58 [138579-66-5] ≥95%

Galanin receptor antagonist. It inhibits opioid-induced nociception, improves memory function, and induces contractions in gastric smooth muscle.

Sun YG, Yu LC. Interactions of galanin and opioids in nociceptive modulation in the arcuate nucleus of hypothalamus in rats. Regul Pept. 2005 Jan 15;124(1-3):37-43. PMID: 15544839.

Korolkiewicz RP, Konstanski Z, Rekowski P, et al. Mechanism of the contractile effects of galantide and Galanin(1-14) [alpha-aminobutyric acid]scyliorhinin-I in rat isolated fundus strips. Med Sci Monit. 2002 Jan;8(1):BR19-23. PMID: 11782668.

G0145 Gallic Acid

10 g
100 g
500 g

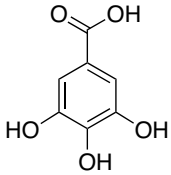

$C_7H_6O_5$ FW: 170.12 [149-91-7] ≥98%

Found in various plant sources and used to determine phenol content of analytes. It displays many biological activities, including inducing Fas-mediated apoptosis in breast cancer cells, inhibiting the production of α-hemolysin and cell adhesion in *Staphylococcus*, and increasing levels of antioxidative enzymes, limiting oxidative damage.

Sun J, Li YZ, Ding YH, et al. Neuroprotective effects of gallic acid against hypoxia/reoxygenation-induced mitochondrial dysfunctions in vitro and cerebral ischemia/reperfusion injury in vivo. Brain Res. 2014 Sep 22. [Epub ahead of print]. PMID: 25251593.

Wang K, Zhu X, Zhang K, et al. Investigation of gallic Acid induced anticancer effect in human breast carcinoma mcf-7 cells. J Biochem Mol Toxicol. 2014 Sep;28(9):387-93. PMID: 24864015.

Luís Â, Silva F, Sousa S, et al. Antistaphylococcal and biofilm inhibitory activities of gallic, caffeic, and chlorogenic acids. Biofouling. 2014 Jan;30(1):69-79. PMID: 24228999.

G0243 (−)-Gallocatechin

5 mg
10 mg
25 mg

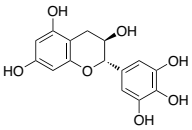

$C_{15}H_{14}O_7$ FW: 306.27 [3371-27-5] ≥98%

HIV integrase, RT, and α-amylase inhibitor found in *Camilla sinensis*. It exhibits several biological activities, including decreasing absorption of carbohydrates, upregulating expression of IL-2, downregulating expression of IL-10 and TNF-α, and inhibiting osteoclast differentiation.

Tsujita T, Shintani T, Sato H. α-Amylase inhibitory activity from nut seed skin polyphenols. 1. Purification and characterization of almond seed skin polyphenols. J Agric Food Chem. 2013 May 15;61(19):4570-6. PMID: 23614772.

Colon M, Nerin C. Role of catechins in the antioxidant capacity of an active film containing green tea, green coffee, and grapefruit extracts. J Agric Food Chem. 2012 Oct 3;60(39):9842-9. PMID: 22973940.

F Vale LH, Mendes MM, Fernandes RS, et al. Protective effect of schizolobium parahyba flavonoids against snake venoms and isolated toxins. Curr Top Med Chem. 2011;11(20):2566-77. PMID: 21682680

G0245 Gallocatechin Gallate

5 mg
10 mg

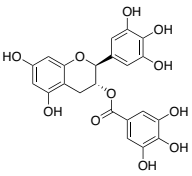

$C_{22}H_{18}O_{11}$ FW: 458.37 [4233-96-9] ≥98%

HIV integrase inhibitor found in *Camilla sinensis*. It displays a wide variety of biological activities, including suppressing amyloid formation by islet amyloid polypeptide, preventing nematode hatching, and inhibiting osteoclast differentiation.

Masler EP. Effects of catechin polyphenols and preparations from the plant-parasitic nematode *Heterodera* glycines on protease activity and behaviour in three nematode species. J Helminthol. 2013 May 2:1-8. [Epub ahead of print]. PMID: 23635519.

Timmel MA, Byl JA, Osheroff N. Epimerization of Green Tea Catechins during Brewing Does Not Affect the Ability to Poison Human Type II Topoisomerases. Chem Res Toxicol. 2013 Apr 4. [Epub ahead of print]. PMID: 23514406.

Boušová I, Hájek J, Dršata J, et al. Naturally occurring flavonoids as inhibitors of purified cytosolic glutathione S-transferase. Xenobiotica. 2012 Sep;42(9):872-9. PMID: 22458346.

G0247 2"O-Galloylhyperin

5 mg
10 mg
25 mg

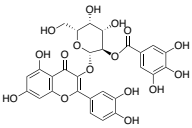

$C_{28}H_{24}O_{16}$ FW: 616.48 [53209-27-1] ≥98.0%

Found in *Pyrola*. It increases ruminal fiber fermentability by formed wall-bound lignin in primary maize cell walls.

Grabber JH, Ress D, Ralph J. Identifying new lignin bioengineering targets: impact of epicatechin, quercetin glycoside, and gallate derivatives on the lignification and fermentation of maize cell walls. J Agric Food Chem. 2012 May 23;60(20):5152-60. PMID: 22475000.

G0248 Gambogic Acid

5 mg
25 mg
100 mg

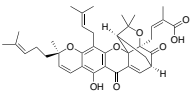

$C_{38}H_{44}O_8$ FW: 628.75 [2752-65-0] ≥98%

Found in *Garcinia hanburyi*. It induces apoptosis in several cancer cell lines, indirectly inhibits Akt signaling, suppresses telomerase activity, and potentially interacts with the transferrin receptor.

He XY, Liu XJ, Chen X, et al. Gambogic acid induces EGFR degradation and Akt/mTORC1 inhibition through AMPK dependent-LRIG1 upregulation in cultured U87 glioma cells. Biochem Biophys Res Commun. 2013 Jun 7;435(3):397-402. PMID: 23665322.

Gu H, Rao S, Zhao J, et al. Gambogic acid reduced bcl-2 expression via p53 in human breast MCF-7 cancer cells. J Cancer Res Clin Oncol. 2009 Dec;135(12):1777-82. PMID: 19582475.

Nie F, Zhang X, Qi Q, et al. Reactive oxygen species accumulation contributes to gambogic acid-induced apoptosis in human hepatoma SMMC-7721 cells. Toxicology. 2009 Jun 16;260(1-3):60-7. PMID: 19464570.

G0152

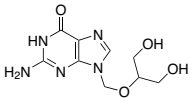

Ganciclovir

DHPG; 2'NDG; BIOLF

$C_9H_{13}N_5O_4$ FW: 255.23 [82410-32-0] ≥98%

50 mg
100 mg

Guanosine analog used to treat cytomegalovirus infection. It inhibits viral DNA polymerase and terminates DNA chain elongation.

Prichard MN, Kern ER. The search for new therapies for human cytomegalovirus infections. Virus Res. 2011 May;157(2):212-21. PMID: 21095209.

Abate-Daga D, Garcia-Rodríguez L, Sumoy L, et al. Cell cycle control pathways act as conditioning factors for TK/GCV sensitivity in pancreatic cancer cells. Biochim Biophys Acta. 2010 Oct;1803(10):1175-85. PMID: 20599444.

G0175

H-Tyr-Ala-Glu-Gly-Thr-Phe-Ile-Ser-Asp-Tyr-Ser-Ile-Ala-Met-Asp-Lys-Ile-His-Gln-Gln-Asp-Phe-Val-Asn-Trp-Leu-Leu-Ala-Gln-Lys-Gly-Lys-Lys-Asn-Asp-Trp-Lys-His-Asn-Ile-Thr-Gln-OH

Gastric Inhibitory Peptide, human

GIP

$C_{226}H_{338}N_{60}O_{66}S$ FW: 4983.64 [100040-31-1] ≥95%

0.5 mg
1 mg
2.5 mg

Endogenous somatostatin analog and GIP receptor agonist involved in insulin signaling. It enhances insulin secretion and increases plasma membrane translocation of GLUT4.

Mohammad S, Ramos LS, Buck J, et al. Gastric inhibitory peptide controls adipose insulin sensitivity via activation of cAMP-response element-binding protein and p110β isoform of phosphatidylinositol 3-kinase. J Biol Chem. 2011 Dec 16;286(50):43062-70. PMID: 22027830.

Adrian TE, Barnes AJ, Long RG, et al. The effect of somatostatin analogs on secretion of growth, pancreatic, and gastrointestinal hormones in man. J Clin Endocrinol Metab. 1981 Oct;53(4):675-81. PMID: 6116721.

G0180

pGlu-Gly-Pro-Trp-Leu-Glu-Glu-Glu-Glu-Ala-Tyr-Gly-Trp-Met-Asp-Phe-NH_2

Gastrin I, human

Big gastrin I (18-34); HG-17; Little gastrin I

$C_{130}H_{204}N_{38}O_{31}S$ FW: 2098.22 [10047-33-3] ≥98%

1 mg
2 mg
5 mg

Endogenous CCK2 receptor agonist and indirect H^+/K^+ ATPase activator involved in feeding behavior and enteric movement. It inhibits food intake, stimulates gastric acid production, and constricts the pyloric sphincter.

Furuse M, Ao R, Bungo T, et al. Central gastrin inhibits feeding behavior and food passage in neonatal chicks. Life Sci. 1999;65(3):305-11. PMID: 10447216.

Zimmerhackl B, Wünsch E, Classen M, et al. In man histamine and muscarinergic mechanisms are essential mediators of acid secretion in response to synthetic human gastrin (1-17). Regul Pept. 1993 Jul 23;46(3):583-92. PMID: 8105512.

G0181

Val-Pro-Leu-Pro-Ala-Gly-Gly-Gly-Thr-Val-Leu-Thr-Lys-Met-Tyr-Pro-Arg-Gly-Asn-His-Trp-Ala-Val-Gly-His-Leu-Met-NH_2

Gastrin Releasing Peptide, human

GRP

$C_{130}H_{204}N_{38}O_{31}S_2$ FW: 2859.4 [93755-85-2] ≥95%

1 mg

Endogenous bombesin-like GRP receptor agonist involved in feeding behavior, stress signaling, and circadian rhythms. It induces scratching behavior and stimulates angiogenesis in cancer models.

Kallingal GJ, Mintz EM. Site-specific effects of gastrin-releasing peptide in the suprachiasmatic nucleus. Eur J Neurosci. 2014 Feb;39(4):630-9. PMID: 24528136.

Lee KH, Koh SA, Kim JR. Hepatocyte growth factor-mediated gastrin-releasing peptide induces IL-8 expression through Ets-1 in gastric cancer cells. Oncol Res. 2013;20(9):393-402. PMID: 23924923.

G0182

Ala-Pro-Val-Ser-Val-Gly-Gly-Gly-Thr-Val-Leu-Ala-Lys-Met-Tyr-Pro-Arg-Gly-Asn-His-Trp-Ala-Val-Gly-His-Leu-Met-NH_2

Gastrin Releasing Peptide, pig

GRP

$C_{126}H_{198}N_{38}O_{31}S_2$ FW: 2805.4 [74815-57-9] ≥98%

1 mg

Endogenous bombesin-like GRP receptor agonist involved in feeding behavior, stress signaling, and circadian rhythms. It induces scratching behavior and stimulates angiogenesis in cancer models.

Kallingal GJ, Mintz EM. Site-specific effects of gastrin-releasing peptide in the suprachiasmatic nucleus. Eur J Neurosci. 2014 Feb;39(4):630-9. PMID: 24528136.

G0179

pGlu-Arg-Pro-Pro-Met-Glu-Glu-Glu-Glu-Glu-Ala-Tyr-Gly-Trp-Met-Asp-Phe-NH_2

Gastrin-1, rat

$C_{94}H_{128}N_{22}O_{31}S_2$ FW: 2126.32 [81123-06-0] ≥95%

0.5 mg
1 mg
2.5 mg

Endogenous CCK2 receptor agonist and indirect H^+/K^+ ATPase activator involved in feeding behavior and enteric movement. It inhibits food intake, stimulates gastric acid production, and constricts the pyloric sphincter.

Furuse M, Ao R, Bungo T, et al. Central gastrin inhibits feeding behavior and food passage in neonatal chicks. Life Sci. 1999;65(3):305-11. PMID: 10447216.

Zimmerhackl B, Wünsch E, Classen M, et al. In man histamine and muscarinergic mechanisms are essential mediators of acid secretion in response to synthetic human gastrin (1-17). Regul Pept. 1993 Jul 23;46(3):583-92. PMID: 8105512.

G0178 — Gastrin, chicken

0.5 mg
1 mg
2.5 mg

H-Phe-Leu-Pro-His-Val-Phe-Ala-Glu-Leu-Ser-Asp-Arg-Lys-Gly-Phe-Val-Gln-Gly-Asn-Gly-Ala-Val-Glu-Ala-Leu-His-Asp-Phe-Tyr-Pro-Asp-Trp-Met-Asp-Phe-NH_2

$C_{190}H_{265}N_{47}O_{51}S_1$ FW: 4055.58 ≥95%

Endogenous CCK2 receptor agonist and indirect H^+/K^+ ATPase activator involved in feeding behavior and enteric movement. It inhibits food intake, stimulates gastric acid production, and constricts the pyloric sphincter.

Furuse M, Ao R, Bungo T, et al. Central gastrin inhibits feeding behavior and food passage in neonatal chicks. Life Sci. 1999;65(3):305-11. PMID: 10447216.

G0278 — Gatifloxacin Sesquihydrate

500 mg
1 g
5 g

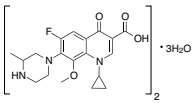

$(C_{19}H_{22}FN_3O_4)_2 \bullet (H_2O)_3$ FW: 402.42 [180200-66-2] ≥98%

Bacterial DNA gyrase inhibitor used to treat tuberculosis and pneumonia.

Pantel A, Petrella S, Veziris N, et al. Extending the definition of the GyrB quinolone resistance-determining region in *Mycobacterium* tuberculosis DNA gyrase for assessing fluoroquinolone resistance in M. tuberculosis. Antimicrob Agents Chemother. 2012 Apr;56(4):1990-6. PMID: 22290942.

Croisier D, Etienne M, Piroth L, et al. In vivo pharmacodynamic efficacy of gatifloxacin against *Streptococcus* pneumoniae in an experimental model of pneumonia: impact of the low levels of fluoroquinolone resistance on the enrichment of resistant mutants. J Antimicrob Chemother. 2004 Sep;54(3):640-7. PMID: 15317743.

G0096 — GAY

5 mg
10 mg
25 mg

Tyrosyl-alanyl-glycine Tag peptide

H-Gly-Ala-Tyr-OH

$C_{14}H_{19}N_3O_5$ FW: 309.18 [69537-64-0] ≥95%

Tripeptide used to tag and sort proteins.

G1200 — GDC-0068

1 mg
5 mg

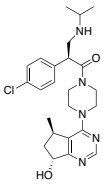

RG7440; Ipatasertib

$C_{24}H_{32}ClN_5O_2$ FW: 458 [1001264-89-6] ≥99%

Akt inhibitor that prevents inhibition of pro-apoptotic gene expression and suppresses proliferation of cancer cells.

Davies BR, Greenwood H, Dudley P, et al. Preclinical pharmacology of AZD5363, an inhibitor of AKT: pharmacodynamics, antitumor activity, and correlation of monotherapy activity with genetic background. Mol Cancer Ther. 2012 Apr;11(4):873-87. PMID: 22294718.

Markman B, Dienstmann R, Tabernero J. Targeting the PI3K/Akt/mTOR pathway--beyond rapalogs. Oncotarget. 2010 Nov;1(7):530-43. Review. PubMed PMID: 21317449.

G1310 — GDC-0349 NEW

1 mg
5 mg

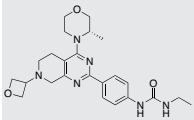

$C_{24}H_{32}N_6O_3$ FW: 452.55 [1207360-89-1] ≥98%

Inhibitor of mTOR. It inhibits cell proliferation and tumor growth in cancer models.

Pei Z, Blackwood E, Liu L, et al. Discovery and Biological Profiling of Potent and Selective mTOR Inhibitor GDC-0349. ACS Med Chem Lett. 2012 Nov 29;4(1):103-7. PMID: 24900569.

G1408 — GDC-0449 NEW

25 mg
100 mg

Vismodegib

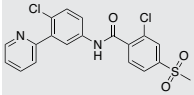

$C_{19}H_{14}Cl_2N_2O_3S$ FW: 421.3 [879085-55-9] ≥98%

Smo inhibitor used to treat basal cell carcinoma. It inhibits Wnt signaling and suppresses cell motility, invasion, and colony formation in basal cell carcinoma cells.

Islam SS, Mokhtari RB, Noman AS, et al. Sonic hedgehog (Shh) signaling promotes tumorigenicity and stemness via activation of epithelial-to-mesenchymal transition (EMT) in bladder cancer. Mol Carcinog. 2015 Mar 1. [Epub ahead of print]. PMID: 25728352.

Erdem GU, Sendur MA, Ozdemir NY, et al. A comprehensive review of the role of Hedgehog pathway and Vismodegib in the management of Basal Cell Carcinoma. Curr Med Res Opin. 2015 Feb 17:1-45. PMID: 25690490.

Kim EJ, Sahai V, Abel EV, et al. Pilot clinical trial of hedgehog pathway inhibitor GDC-0449 (vismodegib) in combination with gemcitabine in patients with metastatic pancreatic adenocarcinoma. Clin Cancer Res. 2014 Dec 1;20(23):5937-45. PMID: 25278454.

G1210 — GDC-0623 NEW

1 mg
5 mg
10 mg

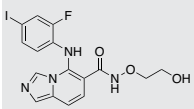

$C_{16}H_{14}FIN_4O_3$ FW: 456.21 [1168091-68-6] ≥98%

MEK inhibitor. It prevents prevents MEK-dependent B-Raf and KRAS signaling and suppresses proliferation in various cancer cell lines.

Hatzivassiliou G, Haling JR, Chen H, et al. Mechanism of MEK inhibition determines efficacy in mutant KRAS- versus BRAF-driven cancers. Nature. 2013 Sep 12;501(7466):232-6. PMID: 23934108.

G1208

GDC-0879

1 mg
5 mg

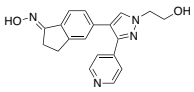

$C_{19}H_{18}N_4O_2$ FW: 334.37 [905281-76-7] ≥96%

V600E mutant B-Raf inhibitor. It decreases phosphorylation of MEK1 and downregulates expression of genes associated with cell proliferation.

Hoeflich KP, Herter S, Tien J, et al. Antitumor efficacy of the novel RAF inhibitor GDC-0879 is predicted by BRAFV600E mutational status and sustained extracellular signal-regulated kinase/mitogen-activated protein kinase pathway suppression. Cancer Res. 2009 Apr 1;69(7):3042-51. PMID: 19276360.

Wong H, Belvin M, Herter S, et al. Pharmacodynamics of 2-[4-[(1E)-1-(hydroxyimino)-2,3-dihydro-1H-inden-5-yl]-3-(pyridine-4-yl)-1H-pyrazol-1-yl]ethan-1-ol (GDC-0879), a potent and selective B-Raf kinase inhibitor: understanding relationships between systemic concentrations, phosphorylated mitogen-activated protein kinase kinase 1 inhibition, and efficacy. J Pharmacol Exp Ther. 2009 Apr;329(1):360-7. PMID: 19147858.

G1209

GDC-0980

NEW

RG7422

1 mg
5 mg
10 mg

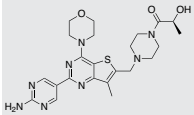

$C_{23}H_{30}N_8O_3S$ FW: 498.6 [1032754-93-0] ≥98%

PI3K and mTOR inhibitor. It inhibits cell growth in uterine serous carcinoma cells and decreases vascular density by altering vascular permeability parameter K.

English DP, Bellone S, Cocco E, et al. Oncogenic PIK3CA gene mutations and HER2/neu gene amplifications determine the sensitivity of uterine serous carcinoma cell lines to GDC-0980, a selective inhibitor of Class I PI3 kinase and mTOR kinase (TORC1/2). Am J Obstet Gynecol. 2013 Nov;209(5):465.e1-9. PMID: 23891627.

Sampath D, Oeh J, Wyatt SK, et al. Multimodal microvascular imaging reveals that selective inhibition of class I PI3K is sufficient to induce an antivascular response. Neoplasia. 2013 Jul;15(7):694-711. PMID: 23814482.

Wallin JJ, Edgar KA, Guan J, et al. GDC-0980 is a novel class I PI3K/mTOR kinase inhibitor with robust activity in cancer models driven by the PI3K pathway. Mol Cancer Ther. 2011 Dec;10(12):2426-36. PMID: 21998291.

G1721

Gefitinib

100 mg
250 mg
1 g

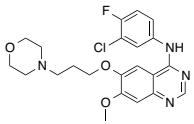

$C_{22}H_{24}ClFN_4O_3$ FW: 446.9 [184475-35-2] ≥98%

EGFR inhibitor. It induces apoptosis in various cancer cells, increases expression of PPARγ, indirectly inhibits HSP70 activity, and promotes differentiation of acute myelogenous leukemia cells.

Mansure JJ, Nassim R, Chevalier S, et al. A novel mechanism of PPAR gamma induction via EGFR signalling constitutes rational for combination therapy in bladder cancer. PLoS One. 2013;8(2):e55997. doi: 10.1371/journal.pone.0055997. Erratum in: PLoS One. 2013; 8(5). PMID: 23409107.

Yoshida T, Yamada K, Azuma K, et al. Comparison of adverse events and efficacy between gefitinib and erlotinib in patients with non-small-cell lung cancer: a retrospective analysis. Med Oncol. 2013 Mar;30(1):349. PMID: 23263831.

Wan S, Wright DW, Coveney PV. Mechanism of drug efficacy within the EGF receptor revealed by microsecond molecular dynamics simulation. Mol Cancer Ther. 2012 Nov;11(11):2394-400. PMID: 22863610.

G1646

Geldanamycin

100 μg
5x100 μg

BRN 1633093

1 mg

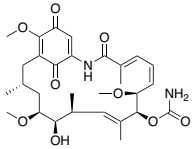

$C_{29}H_{40}N_2O_9$ FW: 560.64 [30562-34-6] ≥97%

HSP90 inhibitor. It decreases viral titers and inflammation in models of chikungunya virus infection, accelerates nerve regeneration, and sensitizes various cancer cell lines to the effects of co-administered chemotherapeutics.

Rathore AP, Haystead T, Das PK, et al. Chikungunya virus nsP3 & nsP4 interacts with HSP-90 to promote virus replication: HSP-90 inhibitors reduce CHIKV infection and inflammation in vivo. Antiviral Res. 2014 Mar;103:7-16. PMID: 24388965.

Sun HH, Saheb-Al-Zamani M, Yan Y, et al. Geldanamycin accelerated peripheral nerve regeneration in comparison to FK-506 in vivo. Neuroscience. 2012 Oct 25;223:114-23. PMID: 22835622.

G1745

Gemcitabine Hydrochloride

25 mg
100 mg
250 mg

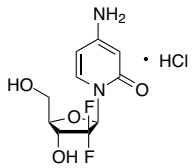

$C_9H_{11}F_2N_3O_4 \bullet HCl$ FW: 299.66 [122111-03-9] ≥98%

Deoxycytidine analog and inhibitor of ribonucleotide reductase and DNA synthesis. It inhibits survival of HIV-1 and FeLuk and induces cell death in pancreatic cancer cells via mitochondrial complexation of MST1 and cyclophilin D.

Chen SH, Li DL, Yang F, et al. Gemcitabine-induced pancreatic cancer cell death is associated with MST1/Cyclophilin D mitochondrial complexation. Biochimie. 2014 Apr 13. Epub ahead of print]. PMID: 24732633.

Su CH, Chu WC, Lan KH, et al. Gemcitabine causes telomere attrition by stabilizing TRF2. Eur J Cancer. 2012 Dec;48(18):3465-74. PMID: 22704123.

Greggs WM 3rd, Clouser CL, Patterson SE, et al. Discovery of drugs that possess activity against feline leukemia virus. J Gen Virol. 2012 Apr;93(Pt 4):900-5. PMID: 22258856.

G1749 Gemfibrozil

5 g
25 g

$C_{15}H_{22}O_3$ FW: 250.33 [25812-30-0] ≥98%

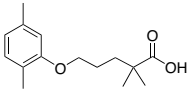

PPARα agonist and enoyl-CoA reductase inhibitor used to lower cholesterol levels. It increases synthesis of lipoprotein lipase, decreasing VLDL, LDL, and triglyceride levels. It also prevents fatty acid synthesis and suppresses growth of *Legionella* and *Mycobacterium*.

Reich-Slotky R, Kabbash CA, Della-Latta P, et al. Gemfibrozil inhibits *Legionella* pneumophila and *Mycobacterium* tuberculosis enoyl coenzyme A reductases and blocks intracellular growth of these bacteria in macrophages. J Bacteriol. 2009 Aug;191(16):5262-71. PMID: 19429621.

Sirtori CR, Franceschini G, Gianfranceschi G, et al. Activity profile of gemfibrozil on the major plasma lipoprotein parameters. Eur J Epidemiol. 1992 May;8 Suppl 1:120-4. PMID: 1505648.

G1849 Gemifloxacin Mesylate

250 mg
1 g
5 g
25 g

$C_{18}H_{21}FN_5O_4 \bullet CH_3SO_3H$ FW: 485.49 [210353-53-0] ≥98%

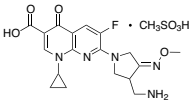

Bacterial DNA gyrase inhibitor that suppresses growth of gram negative and gram positive bacteria. It is used to treat bronchitis, COPD, and pneumonia.

Anzueto A, Miravitlles M. Short-course fluoroquinolone therapy in exacerbations of chronic bronchitis and COPD. Respir Med. 2010 Oct;104(10):1396-403. PMID: 20580215.

Lode HM, Schmidt-Ionas M, Stahlmann R. Gemifloxacin for community-acquired pneumonia. Expert Opin Investig Drugs. 2008 May;17(5):779-86. PMID: 18447602.

G1853 Genipin

25 mg
100 mg

$C_{11}H_{14}O_5$ FW: 226.23 [6902-77-8] ≥98%

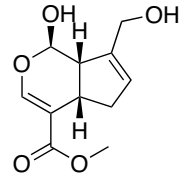

AChE inhibitor found in *Gardenia jasminoides*. It attenuates scopolamine-induced memory impairment, induces collagen cross-linking, delays progression of diabetic neuropathy, and suppresses pro-inflammatory cytokine expression.

Liu TX, Wang Z. Collagen crosslinking of porcine sclera using genipin. Acta Ophthalmol. 2013 Jun;91(4):e253-7. PMID: 23710671.

Nam Y, Lee D. Ameliorating effect of zhizi (Fructus gardeniae) extract and its glycosides on scopolamine-induced memory impairment. J Tradit Chin Med. 2013 Apr;33(2):223-7. PMID: 23789221.

Yang X, Yao J, Luo Y, et al. P38 MAP kinase mediates apoptosis after genipin treatment in non-small-cell lung cancer H1299 cells via a mitochondrial apoptotic cascade. J Pharmacol Sci. 2013;121(4):272-81. PMID: 23603895.

G1650 Geniposide

10 mg
25 mg
100 mg

$C_{17}H_{24}O_{10}$ FW: 388.37 [24512-63-8] ≥98%

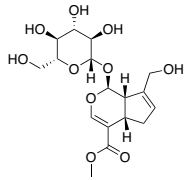

Found in *Gardenia*. It displays many biological activities, including inducing phase II enzyme expression, increasing insulin secretion in β cells, decreasing hippocampal levels of amyloid-β, and inhibiting collagen-induced platelet aggregation and activity of phospholipase A2.

Guo LX, Liu JH, Yin F. Regulation of insulin secretion by geniposide: possible involvement of phosphatidylinositol 3-phosphate kinase. Eur Rev Med Pharmacol Sci. 2014;18(9):1287-94. PMID: 24867506.

Song X, Zhang W, Wang T, et al. Geniposide Plays an Anti-inflammatory Role via Regulating TLR4 and Downstream Signaling Pathways in Lipopolysaccharide-Induced Mastitis in Mice. Inflammation. 2014 Apr 27. [Epub ahead of print]. PMID: 24771071.

Liu J, Guo L, Yin F, et al. Geniposide regulates glucose-stimulated insulin secretion possibly through controlling glucose metabolism in INS-1 cells. PLoS One. 2013 Oct 22;8(10):e78315. Erratum in: PLoS One. 2014;9(1). PMID: 24167617.

G1651 Geniposidic Acid

5 mg
25 mg

$C_{16}H_{22}O_{10}$ FW: 374.34 [27741-01-1] ≥98%

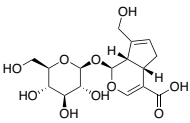

Found in *Eucommia*, *Castilleja*, *Plantago*, and *Gardenia*. It exhibits many biological properties, including promoting collagen synthesis, incresing osteoblast proliferation, and inhibiting survival of *Kalotermes flavicollis* and *Crematogaster scutellaris*.

Hirata T, Kobayashi T, Wada A, et al. Anti-obesity compounds in green leaves of *Eucommia* ulmoides. Bioorg Med Chem Lett. 2011 Mar 15;21(6):1786-91. PMID: 21324693.

Tzakou O, Mylonas P, Vagias C, et al. Iridoid glucosides with insecticidal activity from Galium melanantherum. Z Naturforsch C. 2007 Jul-Aug;62(7-8):597-602. PMID: 17913079.

G1652 Genistein

100 mg
500 mg
1 g

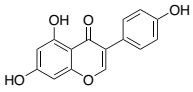

$C_{15}H_{10}O_5$ FW: 270.24 [446-72-0] ≥98%

Found in various plant sources such as soy. It exhibits a variety of biological activities, including inducing phase II enzyme activity, downregulating hedgehog signaling in hepatocarcinoma cells, inhibiting amyloid-β-induced neurotoxicity, and decreasing body weight, liver weight, lipid levels, and insulin dysregulation in high-fat diet models by inhibiting S6K1 signaling,

Lee SH, Kim JK, Jang HD. Genistein inhibits osteoclastic differentiation of RAW 264.7 cells via regulation of ROS production and scavenging. Int J Mol Sci. 2014 Jun 12;15(6):10605-21. PMID: 24927148.

Wang S, Wei H, Cai M, et al. Genistein attenuates brain damage induced by transient cerebral ischemia through up-regulation of ERK activity in ovariectomized mice. Int J Biol Sci. 2014 Apr 8;10(4):457-65. PMID: 24719563.

Li J, Li J, Yue Y, et al. Genistein suppresses tumor necrosis factor α-induced inflammation via modulating reactive oxygen species/Akt/nuclear factor κB and adenosine monophosphate-activated protein kinase signal pathways in human synoviocyte MH7A cells. Drug Des Devel Ther. 2014 Mar 17;8:315-23. PMID: 24669186.

G1653 Genistin

1 mg
5 mg

Genistein-7-O-glucoside

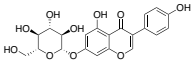

$C_{21}H_{20}O_{10}$ FW: 432.38 [529-59-9] ≥98%

SERM found in soy. It is the less active glycoside analog of genistein. It acts as a phytoestrogen, induces cell cycle arrest and apoptosis in ovarian cancer cells, improves bone density and strength, and decreases myosin light chain kinase levels.

Xiong YJ, Chen DP, Lv BC, et al. The characteristics of genistin-induced inhibitory effects on intestinal motility. Arch Pharm Res. 2013 Mar;36(3):345-52. PMID: 23435915.

Choi EJ, Kim T, Lee MS. Pro-apoptotic effect and cytotoxicity of genistein and genistin in human ovarian cancer SK-OV-3 cells. Life Sci. 2007 Mar 20;80(15):1403-8. PMID: 17291540.

G1658 Gentamycin Sulfate

500 mg
1 g
5 g
10 g

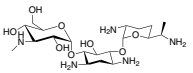

FW: 551.73 [1405-41-0] ≥98%

Protein translation inhibitor. It is primarily active against gram negative bacteria.

Cavallo G, Martinetto P. The mechanism of action of aminoglycosides. G Batteriol Virol Immunol. 1981 Jul-Dec;74(7-12):335-46. PMID: 6182050.

Hahn FE, Sarre SG. Mechanism of action of gentamicin. J Infect Dis. 1969 Apr-May;119(4):364-9. PMID: 4892389.

G1855 Gentiopicroside

10 mg
25 mg
100 mg

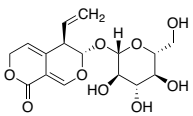

$C_{16}H_{20}O_9$ FW: 356.32 [20831-76-9] ≥97%

Found in *Gentiana* and *Cephalaria*. It displays many biological properties, including suppressing expression of NMDA receptors in the anterior cingulate cortex, inhibiting morphine conditioned place preference, and preventing arachidonic acid and PMA-induced superoxide generation.

Liu SB, Ma L, Guo HJ, et al. Gentiopicroside attenuates morphine rewarding effect through downregulation of GluN2B receptors in nucleus accumbens. CNS Neurosci Ther. 2012 Aug;18(8):652-8. PMID: 22621711.

Wei S, Chen G, He W, et al. Inhibitory effects of secoiridoids from the roots of *Gentiana* straminea on stimulus-induced superoxide generation, phosphorylation and translocation of cytosolic compounds to plasma membrane in human neutrophils. Phytother Res. 2012 Feb;26(2):168-73. PMID: 21584870.

Lian LH, Wu YL, Wan Y, et al. Anti-apoptotic activity of gentiopicroside in D-galactosamine/ lipopolysaccharide-induced murine fulminant hepatic failure. Chem Biol Interact. 2010 Oct 6;188(1):127-33. PMID: 20558151.

G1869 Geranylgeraniol

25 mg
100 mg

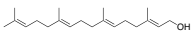

$C_{20}H_{34}O$ FW: 290.49 [24034-73-9] ≥95%

Geranylgeranyl pyrophosphate analog used in synthesis of vitamins E and K. It induces apoptosis and inhibits growth of various tumor cells, suppresses growth of *Mycobacterium*, and protects monocytes against statin-induced cytotoxicity.

Campia I, Lussiana C, Pescarmona G, et al. Geranylgeraniol prevents the cytotoxic effects of mevastatin in THP-1 cells, without decreasing the beneficial effects on cholesterol synthesis. Br J Pharmacol. 2009 Dec;158(7):1777-86. PMID: 19888963.

Vik A, James A, Gundersen LL. Screening of terpenes and derivatives for antimycobacterial activity; identification of geranylgeraniol and geranylgeranyl acetate as potent inhibitors of *Mycobacterium* tuberculosis in vitro. Planta Med. 2007 Oct;73(13):1410-2. PMID: 17924309.

G1975 Gestrinone

25 mg
100 mg
500 mg

$C_{21}H_{24}O_2$ FW: 308.41 [16320-04-0] ≥98%

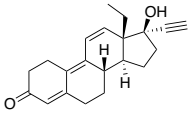

Synthetic androgen receptor agonist and ER and progesterone receptor antagonist used to treat endometriosis. It also downregulates expression of the progesterone receptor, estrogen receptor, and p-Src, inhibiting growth of uterine leiomyoma cells.

Zhu Y, Zhang T, Xie S, et al. Gestrinone inhibits growth of human uterine leiomyoma may relate to activity regulation of ERα, Src and P38 MAPK. Biomed Pharmacother. 2012 Dec;66(8):569-77. PMID: 23102719.

Wu S, Dong J, Cong J, et al. Gestrinone compared with mifepristone for emergency contraception: a randomized controlled trial. Obstet Gynecol. 2010 Apr;115(4):740-4. PMID: 20308833.

G2368 GFR

5 mg
10 mg
25 mg

$C_{17}H_{26}N_6O_4$ FW: 378.4 ≥95%

H-Gly-Phe-Arg-OH

Peptide hormone found in crustaceans. It induces abdominal contractions.

Pettis RJ, Erickson BW, Forward RB, et al. Superpotent synthetic tripeptide mimics of the mud-crab pumping pheromone. Int J Pept Protein Res. 1993 Oct;42(4):312-9. PMID: 8244626.

G2868 Ghrelin, human

1 mg
5 mg

$C_{149}H_{249}N_{47}O_{42}$ FW: 3370.9 [258279-04-8] ≥98%

Gly-Ser-Ser(n-octanoyl)-Phe-Leu-Ser-Pro-Glu-His-Gln-Arg-Val-Gln-Gln-Arg-Lys-Glu-Ser-Lys-Lys-Pro-Pro-Ala-Lys-Leu-Gln-Pro-Arg

Endogenous ghrelin receptor agonist involved in feeding behavior and energy homeostasis. It regulates secretion of GHRH, growth hormone, and somatostatin and counteracts the effects of leptin. It also enhances stress-induced fear responding and improves spatial learning and memory.

Meyer RM, Burgos-Robles A, Liu E, et al. A ghrelin-growth hormone axis drives stress-induced vulnerability to enhanced fear. Mol Psychiatry. 2013 Oct 15. [Epub ahead of print]. PMID: 24126924.

Xu X, Jhun BS, Ha CH, Jin ZG. Molecular mechanisms of ghrelin-mediated endothelial nitric oxide synthase activation. Endocrinology. 2008 Aug;149(8):4183-92. PMID: 18450953.

G2869 Ghrelin, rat

1 mg
5 mg

$C_{147}H_{245}N_{45}O_{42}$ FW: 3314.8 ≥95%

Gly-Ser-Ser(n-octanoyl)-Phe-Leu-Ser-Pro-Glu-His-Gln-Lys-Ala-Gln-Gln-Arg-Lys-Glu-Ser-Lys-Lys-Pro-Pro-Ala-Lys-Leu-Gln-Pro- Arg

Endogenous ghrelin receptor agonist involved in feeding behavior and energy homeostasis. It regulates secretion of GHRH, growth hormone, and somatostatin and counteracts the effects of leptin. It also enhances stress-induced fear responding and improves spatial learning and memory.

Meyer RM, Burgos-Robles A, Liu E, et al. A ghrelin-growth hormone axis drives stress-induced vulnerability to enhanced fear. Mol Psychiatry. 2013 Oct 15. [Epub ahead of print]. PMID: 24126924.

G3253 8-Gingerol NEW

5 mg
25 mg

$C_{19}H_{30}O_4$ FW: 322.44 [23513-08-8] ≥99%

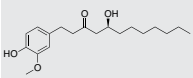

5-HT3 receptor antagonist found in *Zingiber*. It attenuates airway hyperresponsivenes, increases glucose uptake, decreases levels of CD19+ B cells, CD3+ T cells, and IgG, and inhibits proliferation of breast adenocarcinoma cells.

Townsend EA, Siviski ME, Zhang Y, et al. Effects of ginger and its constituents on airway smooth muscle relaxation and calcium regulation. Am J Respir Cell Mol Biol. 2013 Feb;48(2):157-63. PMID: 23065130.

Li Y, Tran VH, Duke CC, et al. Gingerols of *Zingiber* officinale enhance glucose uptake by increasing cell surface GLUT4 in cultured L6 myotubes. Planta Med. 2012 Sep;78(14):1549-55. PMID: 22828920.

G3254 10-Gingerol NEW

5 mg
25 mg

$C_{21}H_{34}O_4$ FW: 350.49 [23513-15-7] ≥99%

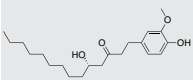

5-HT3 receptor antagonist found in *Zingiber*. It inhibits proliferation in breast adenocarcinoma cells, suppresses growth of gram negative bacteria, and increases radical scavenging of superoxide and hydroxyl radicals.

Almada da Silva J, Becceneri AB, Sanches Mutti H, et al. Purification and differential biological effects of ginger-derived substances on normal and tumor cell lines. J Chromatogr B Analyt Technol Biomed Life Sci. 2012 Aug 15;903:157-62. PMID: 22858304.

Dugasani S, Pichika MR, Nadarajah VD, et al. Comparative antioxidant and anti-inflammatory effects of [6]-gingerol, [8]-gingerol, [10]-gingerol and [6]-shogaol. J Ethnopharmacol. 2010 Feb 3;127(2):515-20. PMID: 19833188.

G3353 Ginkgolic Acid

1 mg
5 mg

Romanicardic acid

$C_{22}H_{34}O_3$ FW: 346.5 [22910-60-7] ≥98%

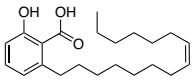

HIV protease and fatty acid synthase inhibitor found in *Ginkgo*. It suppresses HIV infection, inhibits growth of *Staphylococcus*, *Escherichia*, and *Bacillus*, increases activity of PP2C in neurons, and induces apoptosis in cancer cells.

Fu Y, Hong S, Li D, et al. Novel chemical synthesis of ginkgolic acid (13:0) and evaluation of its tyrosinase inhibitory activity. J Agric Food Chem. 2013 Jun 5;61(22):5347-52. PMID: 23701207.

Oh J, Hwang IH, Hong CE, et al. Inhibition of fatty acid synthase by ginkgolic acids from the leaves of *Ginkgo* biloba and their cytotoxic activity. J Enzyme Inhib Med Chem. 2013 Jun;28(3):565-8. PMID: 22380770.

Lü JM, Yan S, Jamaluddin S, et al. Ginkgolic acid inhibits HIV protease activity and HIV infection in vitro. Med Sci Monit. 2012 Aug;18(8):BR293-298. PMID: 22847190.

G3352 Ginkgolic Acid (13:0)

1 mg
5 mg

6-n-Tridecylsalicylic acid

$C_{20}H_{32}O_3$ FW: 320.47 [20261-38-5] ≥98%

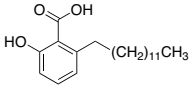

HIV protease inhibitor and indirect PP2C activator found in *Ginkgo*. It inhibits fatty acid synthase, induce apoptosis in cancer cells, and suppress growth of *Staphylococcus*, *Escherichia*, and *Bacillus*.

Fu Y, Hong S, Li D, et al. Novel chemical synthesis of ginkgolic acid (13:0) and evaluation of its tyrosinase inhibitory activity. J Agric Food Chem. 2013 Jun 5;61(22):5347-52. PMID: 23701207.

Oh J, Hwang IH, Hong CE, et al. Inhibition of fatty acid synthase by ginkgolic acids from the leaves of *Ginkgo* biloba and their cytotoxic activity. J Enzyme Inhib Med Chem. 2013 Jun;28(3):565-8. PMID: 22380770.

G3351 Ginkgolic Acid Mixture

5 mg
25 mg

≥98%

Mixture of compounds found in *Ginkgo* including HIV protease inhibitors and indirect PP2C activators.

Fu Y, Hong S, Li D, et al. Novel chemical synthesis of ginkgolic acid (13:0) and evaluation of its tyrosinase inhibitory activity. J Agric Food Chem. 2013 Jun 5;61(22):5347-52. PMID: 23701207.

Oh J, Hwang IH, Hong CE, et al. Inhibition of fatty acid synthase by ginkgolic acids from the leaves of *Ginkgo* biloba and their cytotoxic activity. J Enzyme Inhib Med Chem. 2013 Jun;28(3):565-8. PMID: 22380770.

G3354 Ginkgolide A

10 mg
25 mg
50 mg

$C_{20}H_{24}O_9$ FW: 408.4 [15291-75-5] ≥95%

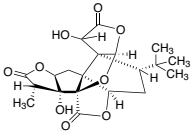

GSK-3β inhibitor and potential PXR agonist found in *Ginkgo*. It decreases phosphorylation of tau protein, prevents neointimal hyperplasia, and decreases anxiety.

Chen Y, Wang C, Hu M, et al. Effects of ginkgolide A on okadaic acid-induced tau hyperphosphorylation and the PI3K-Akt signaling pathway in N2a cells. Planta Med. 2012 Aug;78(12):1337-41. PMID: 22700047.

Weakley SM, Wang X, Mu H, et al. Ginkgolide A-gold nanoparticles inhibit vascular smooth muscle proliferation and migration in vitro and reduce neointimal hyperplasia in a mouse model. J Surg Res. 2011 Nov;171(1):31-9. PMID: 21571322.

Lau AJ, Yang G, Rajaraman G, et al. Human pregnane X receptor agonism by *Ginkgo* biloba extract: assessment of the role of individual ginkgolides. J Pharmacol Exp Ther. 2010 Dec;335(3):771-80. PMID: 20739453.

G3356 Ginkgolide AB

25 mg
50 mg

≥90%

Mixture of ginkgolides A and B found in *Ginkgo*.

G3355 Ginkgolide B

10 mg
25 mg
50 mg

$C_{20}H_{24}O_{10}$ FW: 424.4 [15291-77-7] ≥95%

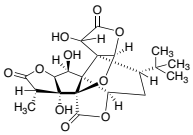

GlyR agonist found in *Ginkgo*. It inhibits ATP release from thrombin-activated platelets, protects neurons against ischemic injury, prevents edema and inflammation, and increases activation of PKA, Ca^{2+} signaling, and glutamate release.

Liu X, Yan Y, Bao L, et al. Ginkgolide B inhibits platelet release by blocking Syk and p38 MAPK phosphorylation in thrombin-stimulated platelets. Thromb Res. 2014 Sep 6. [Epub ahead of print]. PMID: 25223809.

Botao Y, Ma J, Xiao W, et al. Protective effect of ginkgolide B on high altitude cerebral edema of rats. High Alt Med Biol. 2013 Mar;14(1):61-4. PMID: 23537262.

Wu X, Qian Z, Ke Y, et al. Ginkgolide B preconditioning protects neurons against ischaemia-induced apoptosis. J Cell Mol Med. 2009 Nov-Dec;13(11-12):4474-83. PMID: 19602048.

G3357

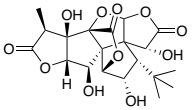

Ginkgolide C

BN-52022

$C_{20}H_{24}O_{11}$ FW: 440.4 [15291-76-6] ≥98%

10 mg
25 mg
50 mg

GABA-A receptor, α-1 GlyR, and PAF receptor antagonist found in *Ginkgo*. It suppresses production of TxA2 to inhibit platelet aggregation and inhibits formation of superoxide and hydroxyl radicals.

Cho HJ, Shon YH, Nam KS. Ginkgolide C inhibits platelet aggregation in cAMP- and cGMP-dependent manner by activating MMP-9. Biol Pharm Bull. 2007 Dec;30(12):2340-4. PMID: 18057723.

Huang SH, Duke RK, Chebib M, et al. Ginkgolides, diterpene trilactones of *Ginkgo* biloba, as antagonists at recombinant alpha1beta2gamma2L GABAA receptors. Eur J Pharmacol. 2004 Jun 28;494(2-3):131-8. PMID: 15212966.

Jaracz S, Nakanishi K, Jensen AA, et al. Ginkgolides and glycine receptors: a structure-activity relationship study. Chemistry. 2004 Mar 19;10(6):1507-18. PMID: 15034895.

G3359

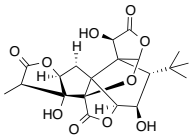

Ginkgolide J

$C_{20}H_{24}O_{10}$ FW: 424.4 [107438-79-9] ≥98%

1 mg
5 mg

Found in *Ginkgo*. It prevents amyloid-β-induced cell death and suppresses superoxide and hydroxyperoxyl radical formation.

Vitolo O, Gong B, Cao Z, et al. Protection against beta-amyloid induced abnormal synaptic function and cell death by Ginkgolide J. Neurobiol Aging. 2009 Feb;30(2):257-65. PMID: 17640772.

Ahlemeyer B, Krieglstein J. Pharmacological studies supporting the therapeutic use of *Ginkgo* biloba extract for Alzheimer's disease. Pharmacopsychiatry. 2003 Jun;36 Suppl 1:S8-14. PMID: 13130383.

Scholtyssek H, Damerau W, Wessel R, et al. Antioxidative activity of ginkgolides against superoxide in an aprotic environment. Chem Biol Interact. 1997 Oct 24;106(3):183-90. PMID: 9413545.

G3358

Ginkgolides

≥98%

25 mg
100 mg
500 mg
1 g

Mixture of Ginkgolides A, B, and C found in *Ginkgo*.

G3460

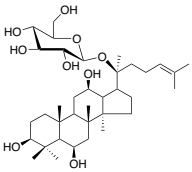

Ginsenoside F1

$C_{36}H_{62}O_{9}$ FW: 638.87 [53963-43-2] ≥98%

1 mg
5 mg
10 mg

Found in species of *Panax*. It decreases gap junction communication and inhibits UV-induced cell death and apoptosis.

Lee EH, Cho SY, Kim SJ, et al. Ginsenoside F1 protects human HaCaT keratinocytes from ultraviolet-B-induced apoptosis by maintaining constant levels of Bcl-2. J Invest Dermatol. 2003 Sep;121(3):607-13. PMID: 12925222.

Zhang YW, Dou DQ, Zhang L, et al. Effects of ginsenosides from *Panax* ginseng on cell-to-cell communication function mediated by gap junctions. Planta Med. 2001 Jul;67(5):417-22. PMID: 11488454.

G3461

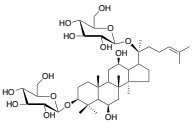

Ginsenoside F2

$C_{42}H_{72}O_{14}$ FW: 801.01 [62025-49-4] ≥98%

1 mg
5 mg
10 mg

Found in species of *Panax*. It inhibits hair cell apoptosis, decreases lipid accumulation in adipocytes, and induces formation of acidic vesicles, autophagy, and mitochondrial apoptosis in breast cancer stem cells.

Shin HS, Park SY, Hwang ES, et al. Ginsenoside F2 reduces hair loss by controlling apoptosis through the sterol regulatory element-binding protein cleavage activating protein and transforming growth factor-β pathways in a dihydrotestosterone-induced mouse model. Biol Pharm Bull. 2014;37(5):755-63. PMID: 24789999.

Siraj FM, Sathishkumar N, Kim YJ, et al. Ginsenoside F2 possesses anti-obesity activity via binding with PPARγ and inhibiting adipocyte differentiation in the 3T3-L1 cell line. J Enzyme Inhib Med Chem. 2014 Mar 25. [Epub ahead of print]. PMID: 24666293.

Mai TT, Moon J, Song Y, et al. Ginsenoside F2 induces apoptosis accompanied by protective autophagy in breast cancer stem cells. Cancer Lett. 2012 Aug 28;321(2):144-53. PMID: 22326284.

G3462

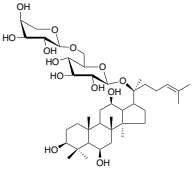

Ginsenoside F3

$C_{41}H_{70}O_{13}$ FW: 770.99 ≥98%

1 mg
5 mg
10 mg

Found in species of *Panax*. It increases levels of IL-2 and IFN-γ, stimulating proliferation of spleen cells.

Yu JL, Dou DQ, Chen XH, et al. Immunoenhancing activity of protopanaxatriol-type ginsenoside-F3 in murine spleen cells. Acta Pharmacol Sin. 2004 Dec;25(12):1671-6. PMID: 15569414.

G3454

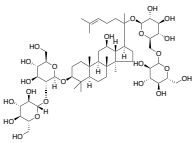

Ginsenoside Rb1

5 mg
10 mg
25 mg

Arasaponin E1; Gypenoside III; Sanchinoside E1

$C_{54}H_{92}O_{23}$ FW: 1109.29 [41753-43-9] ≥98%

Found in species of *Panax*. It displays several biological activities, including improving energy metabolism by increasing motor activity, food intake, and skeletal muscle ATP content, inhibiting glucose-induced neurotoxicity, and suppressing oxidative stress by activating antioxidative enzyme expression.

Tan SJ, Li N, Zhou F, et al. Ginsenoside Rb1 improves energy metabolism in the skeletal muscle of an animal model of postoperative fatigue syndrome. J Surg Res. 2014 May 2. [Epub ahead of print]. PMID: 24881470.

Wu LL, Jia BH, Sun J, et al. Protective effects of ginsenoside Rb1 on septic rats and its mechanism. Biomed Environ Sci. 2014 Apr;27(4):300-3. PMID: 24758759.

Liu D, Zhang H, Gu W, et al. Ginsenoside Rb1 protects hippocampal neurons from high glucose-induced neurotoxicity by inhibiting GSK3β-mediated CHOP induction. Mol Med Rep. 2014 Apr;9(4):1434-8. PMID: 24535619.

G3553

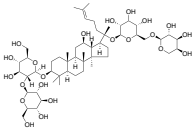

Ginsenoside Rb2

5 mg
10 mg
25 mg

Ginsenoside C

$C_{53}H_{90}O_{22}$ FW: 1079.27 [11021-13-9] ≥84%

Found in species of *Panax*. It exhibits several biological activities, including improving bone microarchitecture and bone mineral density, protecting against infection of hemagglutinating virus of Japan, decreasing triglyceride and cholesterol levels, and inhibiting neovascularization and tumor growth in animal models of melanoma.

Huang Q, Gao B, Jie Q, et al. Ginsenoside-Rb2 displays anti-osteoporosis effects through reducing oxidative damage and bone-resorbing cytokines during osteogenesis. Bone. 2014 Jun 13. [Epub ahead of print]. PMID: 24933344.

Yoo YC, Lee J, Park SR, et al. Protective effect of ginsenoside-Rb2 from Korean red ginseng on the lethal infection of haemagglutinating virus of Japan in mice. J Ginseng Res. 2013 Mar;37(1):80-6. PMID: 23717160.

G3554

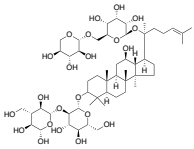

Ginsenoside Rb3

5 mg
10 mg
25 mg

$C_{53}H_{90}O_{22}$ FW: 1079.27 [68406-26-8] ≥98%

Found in species of *Panax*. It inhibits contractions in aortic rings, decreases blood glucose levels and improves oral glucose tolerance, improves immobility time in the forced swim, tail suspension, and learned helplessness tests, and inhibits oxidative damage.

Wang Y, Dong J, Liu P, et al. Ginsenoside Rb3 attenuates oxidative stress and preserves endothelial function in renal arteries from hypertensive rats. Br J Pharmacol. 2014 Jul;171(13):3171-81. PMID: 24571453.

Bu QT, Zhang WY, Chen QC, et al. Anti-diabetic effect of ginsenoside Rb(3) in alloxan-induced diabetic mice. Med Chem. 2012 Sep;8(5):934-41. PMID: 22741793.

G3455

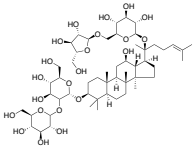

Ginsenoside Rc

1 mg
5 mg
10 mg

Panaxoside RC

$C_{53}H_{90}O_{22}$ FW: 1079.27 [11021-14-0] ≥98%

AMPK inhibitor and potential TRPV1 antagonist found in species of *Panax*. It exhibits many biological activities, including decreasing oxidative stress, suppressing formalin-induced nociception, and increasing the life span in *Caenorhabditis elegans*.

Kim DH, Park CH, Park D, et al. Ginsenoside Rc modulates Akt/FoxO1 pathways and suppresses oxidative stress. Arch Pharm Res. 2014 Jun;37(6):813-20. PMID: 23918648.

Lee MS, Hwang JT, Kim SH, et al. Ginsenoside Rc, an active component of *Panax* ginseng, stimulates glucose uptake in C2C12 myotubes through an AMPK-dependent mechanism. J Ethnopharmacol. 2010 Feb 17;127(3):771-6. PMID: 19961916.

G3456

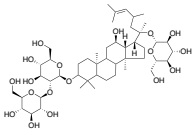

Ginsenoside Rd

1 mg
5 mg
10 mg

Gypenoside VIII

$C_{48}H_{82}O_{18}$ FW: 947.16 [52705-93-8] ≥98%

26S proteasome inhibitor and TRPM7 antagonist found in species of *Panax*. It shifts cytokine production toward Th2 phenotype, increases expression of BDNF and NGF, prevents tau phosphorylation, and decreases infarct size and myocyte apoptosis in myocardial ischemia/reperfusion models.

Zhu D, Liu M, Yang Y, et al. Ginsenoside Rd ameliorates experimental autoimmune encephalomyelitis in C57BL/6 mice. J Neurosci Res. 2014 Sep;92(9):1217-26. PMID: 24798871.

Zhang YX, Wang L, Xiao EL, et al. Ginsenoside-Rd exhibits anti-inflammatory activities through elevation of antioxidant enzyme activities and inhibition of JNK and ERK activation in vivo. Int Immunopharmacol. 2013 Dec;17(4):1094-100. PMID: 24455777.

G3457

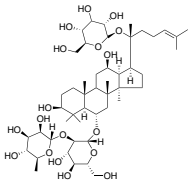

Ginsenoside Re

1 mg
5 mg
10 mg

Panaxoside RE; Ginsenoside B2

$C_{49}H_{84}O_{17}$ FW: 947.18 [52286-59-6] ≥98%

PPARγ agonist found in species of *Panax*. It inhibits formation of gastric mucosal lesions, decreases neutrophil infiltration, stimulates CD4+ T cell production, suppresses histamine release in mast cells, and prevents stress-induced anxiety, depression, and cognitive deficits.

Su X, Pei Z, Hu S. Ginsenoside Re as an adjuvant to enhance the immune response to the inactivated rabies virus vaccine in mice. Int Immunopharmacol. 2014 Jun;20(2):283-9. PMID: 24680943.

Lee S, Kim MG, Ko SK, et al. Protective effect of ginsenoside Re on acute gastric mucosal lesion induced by compound 48/80. J Ginseng Res. 2014 Apr;38(2):89-96. PMID: 24748832.

G3458

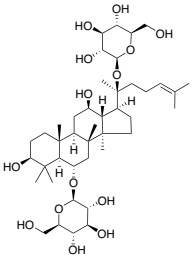

Ginsenoside Rg1

5 mg
10 mg
25 mg

Sanchinoside Rg1; Panaxoside A

$C_{42}H_{72}O_{14}$ FW: 801.01 [22427-39-0] ≥98%

Found in species of *Panax*. It exhibits several biological activities, including limiting decreases in cognitive capacity and neurogenesis, preventing platelet aggregation and fibrinogen binding, inhibiting inflammation and hepatic stellate cell activation, and inducing apoptosis in leukemia cells.

Zhu J, Mu X, Zeng J, et al. Ginsenoside rg1 prevents cognitive impairment and hippocampus senescence in a rat model of d-galactose-induced aging. PLoS One. 2014 Jun 30;9(6):e101291. PMID: 24979747.

Li JP, Gao Y, Chu SF, et al. Nrf2 pathway activation contributes to anti-fibrosis effects of ginsenoside Rg1 in a rat model of alcohol- and CCl4-induced hepatic fibrosis. Acta Pharmacol Sin. 2014 Jun 30. [Epub ahead of print]. PMID: 24976156.

G3459

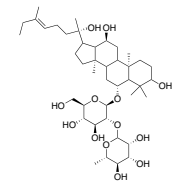

Ginsenoside Rg2

1 mg
5 mg
10 mg

$C_{42}H_{72}O_{13}$ FW: 785.01 [52286-74-5] ≥98%

Found in species of *Panax*. It inhibits LPS-stimulated production of VCAM-1 and ICAM-1, suppresses hepatic glucose production, and improves neural performance and cognition in animal models of vascular dementia.

Cho YS, Kim CH, Ha TS, et al. Ginsenoside rg2 inhibits lipopolysaccharide-induced adhesion molecule expression in human umbilical vein endothelial cell. Korean J Physiol Pharmacol. 2013 Apr;17(2):133-7. PMID: 23626475.

Yuan HD, Kim do Y, Quan HY, et al. Ginsenoside Rg2 induces orphan nuclear receptor SHP gene expression and inactivates GSK3β via AMP-activated protein kinase to inhibit hepatic glucose production in HepG2 cells. Chem Biol Interact. 2012 Jan 5;195(1):35-42. PMID: 22062806.

G3556

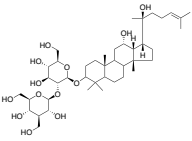

Ginsenoside Rg3

5 mg
10 mg
25 mg

$C_{42}H_{72}O_{13}$ FW: 785.01 [38243-03-7] ≥98%

γ2 GABA-A receptor agonist, K_v7.1 K^+ channel activator, α10 nAChR antagonist found in species of *Panax*. It displays many activities, including improving learning and memory deficits, preventing LPS-induced upregulation of pro-inflammatory cytokines, inhibiting tubular formation and migration of endothelial progenitor cells, and suppressing oxidative damage.

Zhang YH, Li HD, Li B, et al. Ginsenoside Rg3 induces DNA damage in human osteosarcoma cells and reduces MNNG-induced DNA damage and apoptosis in normal human cells. Oncol Rep. 2014 Feb;31(2):919-25. PMID: 24337872.

Lee B, Sur B, Park J, et al. Ginsenoside rg3 alleviates lipopolysaccharide-induced learning and memory impairments by anti-inflammatory activity in rats. Biomol Ther (Seoul). 2013 Sep 30;21(5):381-90. PMID: 24244826.

G3552

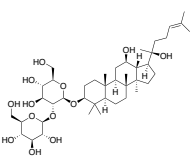

20S-Ginsenoside Rg3

5 mg
10 mg
25 mg

$C_{42}H_{72}O_{13}$ FW: 785.01 [14197-60-5] ≥98%

K_v7.1 K^+ channel activator, γ2 GABA-A receptor agonist, and α10 nAChR antagonist found in *Panax*. It exhibits a wide variety of biological activities, including decreasing expression of pro-inflammatory cytokines, reducing oxidative stress, and inhibiting tubular formation and migration of endothelial progenitor cells.

Zhang YH, Li HD, Li B, et al. Ginsenoside Rg3 induces DNA damage in human osteosarcoma cells and reduces MNNG-induced DNA damage and apoptosis in normal human cells. Oncol Rep. 2014 Feb;31(2):919-25. PMID: 24337872.

Lee B, Sur B, Park J, et al. Ginsenoside rg3 alleviates lipopolysaccharide-induced learning and memory impairments by anti-inflammatory activity in rats. Biomol Ther (Seoul). 2013 Sep 30;21(5):381-90. PMID: 24244826.

G3557

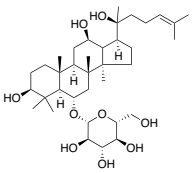

Ginsenoside Rh1

Sanchinoside Rh

$C_{36}H_{62}O_9$ FW: 638.87 [63223-86-9] ≥77%

5 mg
10 mg
25 mg

Found in species of *Panax*. It exhibits various biological activities, including enhancing memory and learning, decreasing adipocyte differentiation, inhibiting migration and invasion of hepatocellular carcinoma cells, and suppressing mast cell degranulation and anaphylaxis.

Hou J, Xue J, Lee M, et al. Long-term administration of ginsenoside Rh1 enhances learning and memory by promoting cell survival in the mouse hippocampus. Int J Mol Med. 2014 Jan;33(1):234-40. PMID: 24212564.

Gu W, Kim KA, Kim DH. Ginsenoside Rh1 ameliorates high fat diet-induced obesity in mice by inhibiting adipocyte differentiation. Biol Pharm Bull. 2013;36(1):102-7. PMID: 23302642.

G3453

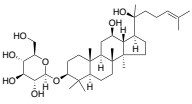

Ginsenoside Rh2

β-D-Glucopyranoside

$C_{36}H_{62}O_8 \cdot H_2O$ FW: 640.89 [78214-33-2] ≥98%

1 mg
5 mg
10 mg
25 mg

Aldose reductase inhibitor found in *Panax*. It also decreases ROS levels in keratinocytes, lowers levels of amyloid-β in Alzheimer's disease models, induces β-cell proliferation, and inhibits osteoclastogenesis by suppressing RANKL-induced osteoclast differentiation.

Fatmawati S, Ersam T, Yu H, et al. 20(S)-Ginsenoside Rh2 as aldose reductase inhibitor from *Panax* ginseng. Bioorg Med Chem Lett. 2014 Aug 12. [Epub ahead of print]. PMID: 25152999.

Shi Q, Li J, Feng Z, et al. Effect of ginsenoside Rh2 on the migratory ability of HepG2 liver carcinoma cells: Recruiting histone deacetylase and inhibiting activator protein 1 transcription factors. Mol Med Rep. 2014 Jul 18. [Epub ahead of print]. PMID: 25051397.

G3558

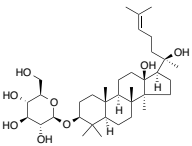

20R-Ginsenoside Rh2

$C_{36}H_{62}O_8$ FW: 622.87 ≥98%

1 mg
5 mg
10 mg
25 mg

Found in *Panax*. It increases proliferation of CD8+ T cells, improves spatial learning and memory, and modulates expression of inflammatory markers.

Lv S, Yi PF, Shen HQ, et al. Ginsenoside Rh2-B1 stimulates cell proliferation and IFN-γ production by activating the p38 MAPK and ERK-dependent signaling pathways in CTLL-2 cells. Immunopharmacol Immunotoxicol. 2013 Dec 3. [Epub ahead of print]. PMID: 24294901.

Hou J, Xue J, Lee M, et al. Ginsenoside Rh2 improves learning and memory in mice. J Med Food. 2013 Aug;16(8):772-6. PMID: 23957360.

G4400

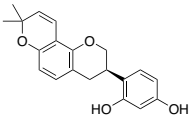

Glabridin

$C_{20}H_{20}O_4$ FW: 324.37 [59870-68-7] ≥98.0%

5 mg
10 mg
25 mg

GABA-A receptor positive modulator found in *Glycyrrhiza*. It promotes fatty acid oxidation, suppresses adipogenesis, improves learning and memory, and inhibits Rho signaling by decreasing FAK and Src activation.

Jin Z, Kim S, Cho S, et al. Potentiating Effect of Glabridin on GABAA Receptor-Mediated Responses in Dorsal Raphe Neurons. Planta Med. 2013 Aug 23. [Epub ahead of print]. PMID: 23975867.

Kim HS, Suh KS, Ko A, et al. The flavonoid glabridin attenuates 2-deoxy-D-ribose-induced oxidative damage and cellular dysfunction in MC3T3-E1 osteoblastic cells. Int J Mol Med. 2013 Jan;31(1):243-51. PMID: 23128413.

Ahn J, Lee H, Jang J, et al. Anti-obesity effects of glabridin-rich supercritical carbon dioxide extract of licorice in high-fat-fed obese mice. Food Chem Toxicol. 2013 Jan;51:439-45. PMID: 22967722.

G4532

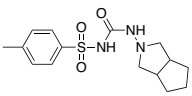

Gliclazide

$C_{15}H_{21}N_3O_3S$ FW: 323.41 [21187-98-4] ≥98%

1 g
5 g
10 g

SUR1 antagonist used to treat diabetes. It closes K^+ ion channels to stimulate insulin release and decreases H_2O_2-induced apoptosis and oxidative stress.

Proks P, de Wet H, Ashcroft FM. Molecular mechanism of sulphonylurea block of K(ATP) channels carrying mutations that impair ATP inhibition and cause neonatal diabetes. Diabetes. 2013 Nov;62(11):3909-19. PMID: 23835339.

Sliwinska A, Rogalska A, Szwed M, et al. Gliclazide may have an antiapoptotic effect related to its antioxidant properties in human normal and cancer cells. Mol Biol Rep. 2012 May;39(5):5253-67. PMID: 22183301.

Lawrence CL, Proks P, Rodrigo GC, et al. Gliclazide produces high-affinity block of KATP channels in mouse isolated pancreatic beta cells but not rat heart or arterial smooth muscle cells. Diabetologia. 2001 Aug;44(8):1019-25. PMID: 11484080.

G4535

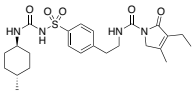

Glimepiride

HOE-490

$C_{24}H_{34}N_4O_5S$ FW: 490.62 [93479-97-1] ≥98%

500 mg
1 g
5 g

ATP-sensitive K^+ channel blocker used to treat diabetes. It increases insulin secretion and decreases expression and activity of BACE1 and amyloid-β.

Liu F, Wang Y, Yan M, et al. Glimepiride attenuates Aβ production via suppressing BACE1 activity in cortical neurons. Neurosci Lett. 2013 Dec 17;557 Pt B:90-4. PMID: 24184877.

Bashir MI, Pathan MF, Raza SA, et al. Role of oral hypoglycemic agents in the management of type 2 diabetes mellitus during Ramadan. Indian J Endocrinol Metab. 2012 Jul;16(4):503-7. PMID: 22837904.

Abdelmoneim AS, Hasenbank SE, Seubert JM, et al. Variations in tissue selectivity amongst insulin secretagogues: a systematic review. Diabetes Obes Metab. 2012 Feb;14(2):130-8. PMID: 21923736.

G4434

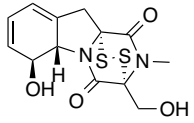

Gliotoxin

$C_{13}H_{14}N_2O_4S_2$ FW: 326.39 [67-99-2] ≥98%

1 mg
5 mg
10 mg

Toxin found in *Aspergillus*. It induces apoptosis in cervical cancer cells and chondrosarcoma cells, suppresses the adaptive immune response in leukocytes, and inhibits the proteasome in *Plasmodium falciparum*.

Nguyen VT, Lee JS, Qian ZJ, et al. Gliotoxin Isolated from Marine Fungus *Aspergillus* sp. Induces Apoptosis of Human Cervical Cancer and Chondrosarcoma Cells. Mar Drugs. 2013 Dec 24;12(1):69-87. PMID: 24368570.

Hur JM, Yun HJ, Yang SH, et al. Gliotoxin enhances radiotherapy via inhibition of radiation-induced GADD45a, p38, and NFkappaB activation. J Cell Biochem. 2008 Aug 15;104(6):2174-84. PMID: 18425744.

G4634

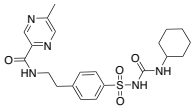

Glipizide

$C_{21}H_{27}N_5O_4S$ FW: 445.54 [29094-61-9] ≥98%

500 mg
1 g
5 g

ATP-sensitive K^+ channel blocker used to treat diabetes. It also decreases the metabolic clearance rate of insulin.

Barzilai N, Groop PH, Groop L, et al. A novel mechanism of glipizide sulfonylurea action: decreased metabolic clearance rate of insulin. Acta Diabetol. 1995 Dec;32(4):273-8. PMID: 8750768.

Weinhaus AJ, Poronnik P, Cook DI, et al. Insulin secretagogues, but not glucose, stimulate an increase in $[Ca^{2+}]i$ in the fetal rat beta-cell. Diabetes. 1995 Jan;44(1):118-24. PMID: 7529202.

G4662

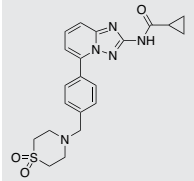

GLPG-0634

NEW

Filgotinib

$C_{21}H_{23}N_5O_3S$ FW: 425.5 [1206161-97-8] ≥98%

5 mg
10 mg

JAK1 inhibitor. It suppresses release of pro-inflammatory cytokines in models of rheumatoid arthritis and Crohn's disease.

Namour F, Diderichsen PM, Cox E, et al. Pharmacokinetics and Pharmacokinetic/Pharmacodynamic Modeling of Filgotinib (GLPG0634), a Selective JAK1 Inhibitor, in Support of Phase IIB Dose Selection. Clin Pharmacokinet. 2015 Feb 14. [Epub ahead of print]. PMID: 25681059.

Menet CJ, Fletcher SR, Van Lommen G, et al. Triazolopyridines as selective JAK1 inhibitors: from hit identification to GLPG0634. J Med Chem. 2014 Nov 26;57(22):9323-42. PMID: 25369270.

Norman P. Selective JAK inhibitors in development for rheumatoid arthritis. Expert Opin Investig Drugs. 2014 Aug;23(8):1067-77. PMID: 24818516.

G4479

Ala-Gln-Asp-Phe-Val-Gln-Trp-Leu-Met-Asn-Thr

Glucagon (19-29), human

Des(1-18) glucagon; Miniglucagon

$C_{61}H_{89}N_{15}O_{18}S$ FW: 1352.54 [64790-15-4] ≥95%

1 mg
2 mg
5 mg

Endogenous glucagon fragment and potential Ca^{2+} channel blocker. It is released with glucagon and inhibits β-cell insulin secretion.

Bataille D, Fontés G, Costes S, et al. The glucagon-miniglucagon interplay: a new level in the metabolic regulation. Ann N Y Acad Sci. 2006 Jul;1070:161-6. PMID: 16888159.

Dalle S, Fontés G, Lajoix AD, et al. Miniglucagon (glucagon 19-29): a novel regulator of the pancreatic islet physiology. Diabetes. 2002 Feb;51(2):406-12. PMID: 11812748.

G4482

H-His-Ala-Glu-Gly-Thr-Phe-Thr-Ser-Asp-Val-Ser-Ser-Tyr-Leu-Glu-Gly-Gln-Ala-Ala-Lys-Glu-Phe-Ile-Ala-Trp-Leu-Val-Lys-Gly-Arg-Gly-OH

Glucagon-like Peptide I (7-37)

Insulinotropin; Tglp-1; GLP-1

$C_{151}H_{228}N_{40}O_{47}$ FW: 3355.67 [106612-94-6] ≥95%

0.5 mg
1 mg
2.5 mg

Endogenous GLP-1 fragment and GLP1 receptor agonist involved in insulin secretion and feeding behavior. It decreases food intake and glucagon levels and slows gastric emptying.

Kim S, Wan Kim S, Bae YH. Synthesis, bioactivity and specificity of glucagon-like peptide-1 (7-37)/polymer conjugate to isolated rat islets. Biomaterials. 2005 Jun;26(17):3597-606. PMID: 15621250.

G4481

H-His-Ala-Glu-Gly-Thr-Phe-Thr-Ser-Asp-Val-Ser-Ser-Tyr-Leu-Glu-Gly-Gln-Ala-Ala-Lys-Glu-Phe-Ile-Ala-Trp-Leu-Val-Lys-Gly-Arg-NH_2

Glucagon-like Peptide I Amide (7-36), human

GLP-1

$C_{149}H_{229}N_{40}O_{45}$ FW: 3297.7 [107444-51-9] ≥95%

0.5 mg
1 mg
2.5 mg

Endogenous GLP-1 fragment and GLP1 receptor agonist involved in insulin secretion and feeding behavior. It decreases food intake and glucagon levels and slows gastric emptying.

Kim S, Wan Kim S, Bae YH. Synthesis, bioactivity and specificity of glucagon-like peptide-1 (7-37)/polymer conjugate to isolated rat islets. Biomaterials. 2005 Jun;26(17):3597-606. PMID: 15621250.

Vahl TP, Paty BW, Fuller BD, et al. Effects of GLP-1-(7-36)NH2, GLP-1-(7-37), and GLP-1- (9-36)NH2 on intravenous glucose tolerance and glucose-induced insulin secretion in healthy humans. J Clin Endocrinol Metab. 2003 Apr;88(4):1772-9. PMID: 12679472.

G4483

H-His-Ala-Asp-Gly-Ser-Phe-Ser-Asp-Glu-Met-Asn-Thr-Ile-Leu-Asp-Asn-Leu-Ala-Ala-Arg-Asp-Phe-Ile-Asn-Trp-Leu-Ile-Gln-Thr-Lys-Ile-Thr-Asp-Arg-OH

Glucagon-like Peptide II, human

GLP-2

$C_{171}H_{266}N_{48}O_{56}S$ FW: 3922.38 [223460-79-5] ≥95%

0.5 mg
1 mg
2.5 mg

Endogenous GLP-2 receptor agonist involved in intestinal function. It increases intestinal blood flow, decreases mean arterial pressure, potentiates L-type voltage-gated Ca^{2+} channels, and inhibits intestinal chemotherapy-induced mucosal atrophy.

Sasaki-Hamada S, Ito K, Oka JI. Neuronal Fos-like immunoreactivity associated with dexamethasone-induced hypertension in rats and effects of glucagon-like peptide-2. Life Sci. 2013 Oct 24. pii: S0024-3205(13)00618-8. [Epub ahead of print]. PMID: 24513200.

Hansen LB. GLP-2 and mesenteric blood flow. Dan Med J. 2013 May;60(5):B4634. PMID: 23673268.

G4484

H-His-Ala-Asp-Gly-Ser-Phe-Ser-Asp-Glu-Met-Asn-Thr-Ile-Leu-Asp-Asn-Leu-Ala-Thr-Arg-Asp-Phe-Ile-Asn-Trp-Leu-Ile-Gln-Thr-Lys-Ile-Thr-Asp-OH

Glucagon-like Peptide II, rat

GLP-2

$C_{166}H_{256}N_{44}O_{56}S$ FW: 3796.22 [195262-56-7] ≥95%

0.5 mg
1 mg
2.5 mg

Endogenous GLP-2 receptor agonist involved in intestinal function. It increases intestinal blood flow, decreases mean arterial pressure, potentiates L-type voltage-gated Ca^{2+} channels, and inhibits intestinal chemotherapy-induced mucosal atrophy.

Sasaki-Hamada S, Ito K, Oka JI. Neuronal Fos-like immunoreactivity associated with dexamethasone-induced hypertension in rats and effects of glucagon-like peptide-2. Life Sci. 2013 Oct 24. pii: S0024-3205(13)00618-8. [Epub ahead of print]. PMID: 24513200.

G4485

H-His-Ala-Asp-Gly-Ser-Phe-Ser-Asp-Glu-Met-Asn-Thr-Ile-Leu-Asp-Asn-Leu-Ala-Thr-Arg-Asp-Phe-Ile-Asn-Trp-Leu-Ile-Gln-Thr-Lys-Ile-Thr-Asp-OH

[Ala19]-Glucagon-like Peptide II, rat

GLP-2

$C_{165}H_{254}N_{44}O_{55}S$ FW: 3766.2 [89750-15-2] ≥95%

0.5 mg
1 mg
2.5 mg

GLP-2 derivative and GLP-2 receptor agonist involved in intestinal function. It increases intestinal blood flow, decreases mean arterial pressure, potentiates L-type voltage-gated Ca^{2+} channels, and inhibits intestinal chemotherapy-induced mucosal atrophy.

Hansen LB. GLP-2 and mesenteric blood flow. Dan Med J. 2013 May;60(5):B4634. PMID: 23673268.

G4480

His-Ser-Gln-Gly-Thr-Phe-Thr-Ser-Asp-Tyr-Ser-Lys-Tyr-Leu-Asp-Ser-Arg-Arg-Ala-Gln-Asp-Phe-Val-Gln-Trp-Leu-Met-Asn-Thr

Glucagon, human

HG-factor

$C_{153}H_{225}N_{43}O_{49}S$ FW: 3482.78 [16941-32-5] ≥98%

1 mg

Endogenous glucagon receptor agonist that counteracts insulin, increases glucose levels, and is used to treat severe hypoglycemia and anaphylactic shock. It also decreases blood pressure.

Xu E, Kumar M, Zhang Y, et al. Intra-islet insulin suppresses glucagon release via GABA-GABAA receptor system. Cell Metab. 2006 Jan;3(1):47-58. PMID: 16399504.

G4518

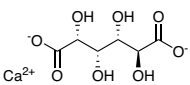

Glucaric Acid Calcium Tetrahydrate

D-Saccharic acid calcium salt

$C_6H_8O_8Ca \cdot 4H_2O$ FW: 320.3 [5793-89-5] ≥98%

25 g
100 g

Oxidized non-cylic hexose sugar. It may inhibit carcinogenesis and proliferation of cancer cells.

Shiue E, Prather KL. Improving D-glucaric acid production from myo-inositol in E. coli by increasing MIOX stability and myo-inositol transport. Metab Eng. 2014 Mar;22:22-31. PMID: 24333274.

Smith TN, Hash K, Davey CL, et al. Modifications in the nitric acid oxidation of D-glucose. Carbohydr Res. 2012 Mar 1;350:6-13. PMID: 22285512.

Bespalov VG, Aleksandrov VA. Anticarcinogenic effect of potassium salts of glucaric and glucuronic acid in induced models of cervical and esophageal tumors. Vopr Onkol. 2012;58(4):537-40. PMID: 23607211.

G4781 Glucoraphanin Potassium

5 mg
10 mg
25 mg

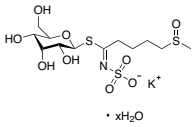

$C_{12}H_{22}KNO_{10}S_3 \bullet xH_2O$ FW: 475.6 ≥98%

Natural product found in cruciferous vegetables. It decreases inflammation in models of spinal cord injury, suppresses stress-induced expression of pro-inflammatory cytokines, and prevents DAT degradation and neuronal apoptosis.

Galuppo M, Giacoppo S, De Nicola GR, et al. RS-Glucoraphanin bioactivated with myrosinase treatment counteracts proinflammatory cascade and apoptosis associated to spinal cord injury in an experimental mouse model. J Neurol Sci. 2013 Nov 15;334(1-2):88-96. PMID: 23992921.

Galuppo M, Iori R, De Nicola GR, et al. Anti-inflammatory and anti-apoptotic effects of (RS)-glucoraphanin bioactivated with myrosinase in murine sub-acute and acute MPTP-induced Parkinson's disease. Bioorg Med Chem. 2013 Sep 1;21(17):5532-47. PMID: 23810671

Foti Cuzzola V, Galuppo M, Iori R, et al. Beneficial effects of (RS)-glucoraphanin on the tight junction dysfunction in a mouse model of restraint stress. Life Sci. 2013 Aug 28;93(7):288-305. PMID: 23871805.

G4782 Glucoraphenin Potassium

5 mg
10 mg
25 mg

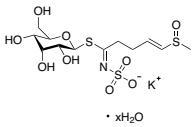

$C_{12}H_{20}KNO_{10}S_3\ xH_2O$ FW: 473.58 ≥98%

Natural product found in cruciferous vegetables. It increases activity and expression of antioxidative enzymes.

Abdull Razis AF, De Nicola GR, Pagnotta E, et al. A glucosinolate-rich extract of Japanese Daikon perturbs carcinogen-metabolizing enzyme systems in rat, being a potent inducer of hepatic glutathione S-transferase. Eur J Nutr. 2013 Apr;52(3):1279-85. PMID: 22710810.

Barillari J, Iori R, Broccoli M, et al. Glucoraphasatin and glucoraphenin, a redox pair of glucosinolates of *brassicaceae*, differently affect metabolizing enzymes in rats. J Agric Food Chem. 2007 Jul 11;55(14):5505-11. PMID: 17579433.

G4580 Glucosamine Hydrochloride

25 g
100 g
500 g

Chitosamine hydrochloride

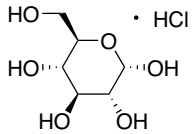

$C_6H_{13}NO_5 \bullet HCl$ FW: 215.6 [66-84-2] ≥96%

Endogenous amino acid sugar involved in cartilage development. It is used in dietary supplements to improve joint function. It also decreases N-glycosylation of gp130 to inhibit proliferation of prostate cancer cells and decreases TGF-β1-induced expression of collagen I, fibronectin, and α-SMA to prevent fibrosis.

Chesnokov V, Gong B, Sun C, et al. Anti-cancer activity of glucosamine through inhibition of N-linked glycosylation. Cancer Cell Int. 2014 May 28;14:45. PMID: 24932134.

Park J, Lee SY, Ooshima A, et al. Glucosamine hydrochloride exerts a protective effect against unilateral ureteral obstruction-induced renal fibrosis by attenuating TGF-β signaling. J Mol Med (Berl). 2013 Nov;91(11):1273-84. PMID: 24072041.

G4581 Glucosamine Sulfate Potassium

100 g
500 g
1 kg

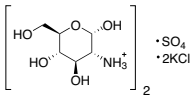

$C_6H_{14}NO_5SO_4 \bullet 2KCl$ FW: 425.34 ≥96%

Endogenous amino acid sugar involved in cartilage development. It is used in dietary supplements to improve joint function. It also decreases N-glycosylation of gp130 to inhibit proliferation of prostate cancer cells and decreases TGF-β1-induced expression of collagen I, fibronectin, and α-SMA to prevent fibrosis.

Chesnokov V, Gong B, Sun C, et al. Anti-cancer activity of glucosamine through inhibition of N-linked glycosylation. Cancer Cell Int. 2014 May 28;14:45. PMID: 24932134.

G4796 Glycerol Monolaurate

25 g
100 g

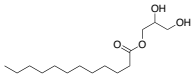

$C_{15}H_{30}O_4$ FW: 274.4 [142-18-7] ≥98%

Surfactant and emulsifier found in coconut oil. It inhibits growth of *Staphylococcus*, *Streptococcus*, *Gardnerella*, *Candida*, and *Haemophilus* and decreases production of pro-inflammatory cytokines.

Schlievert PM, Peterson ML. Glycerol monolaurate antibacterial activity in broth and biofilm cultures. PLoS One. 2012;7(7):e40350. PMID: 22808139.

Strandberg KL, Peterson ML, Lin YC, et al. Glycerol monolaurate inhibits *Candida* and *Gardnerella* vaginalis in vitro and in vivo but not *Lactobacillus*. Antimicrob Agents Chemother. 2010 Feb;54(2):597-601. PMID: 20008774.

Strandberg KL, Peterson ML, Schaefers MM, et al. Reduction in *Staphylococcus aureus* growth and exotoxin production and in vaginal interleukin 8 levels due to glycerol monolaurate in tampons. Clin Infect Dis. 2009 Dec 1;49(11):1711-7. PMID: 19863450.

G4596

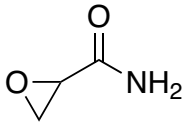

Glycidamide

Oxirane-2-carboxamide

$C_3H_5NO_2$ FW: 87.08 [5694-00-8] ≥98%

10 mg
25 mg
100 mg

Carcinogen and metabolite of acrylamide that induces DNA adduct formation and mutations.

Von Tungeln LS, Doerge DR, Gamboa da Costa G, et al. Tumorigenicity of acrylamide and its metabolite glycidamide in the neonatal mouse bioassay. Int J Cancer. 2012 Nov 1;131(9):2008-15. PMID: 22336951.

Von Tungeln LS, Churchwell MI, Doerge DR, et al. DNA adduct formation and induction of micronuclei and mutations in B6C3F1/Tk mice treated neonatally with acrylamide or glycidamide. Int J Cancer. 2009 May 1;124(9):2006-15. PMID: 19123476.

G4798

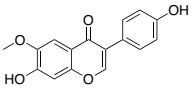

Glycitein

$C_{16}H_{12}O_5$ FW: 284.26 [40957-83-3] ≥98%

5 mg
10 mg
25 mg

Found in soy and red clover. It exhibits a variety of biological activities, including increasing Nrf2-related antioxidative signaling, preventing invasion in glioma cells, destabilizing amyloid-β aggregates and preventing fibril assembly, and inhibiting osteoclast generation.

Hirohata M, Ono K, Takasaki J, et al. Anti-amyloidogenic effects of soybean isoflavones in vitro: Fluorescence spectroscopy demonstrating direct binding to Aβ monomers, oligomers and fibrils. Biochim Biophys Acta. 2012 Aug;1822(8):1316-24. PMID: 22587837.

Park JS, Jung JS, Jeong YH, et al. Antioxidant mechanism of isoflavone metabolites in hydrogen peroxide-stimulated rat primary astrocytes: critical role of hemeoxygenase-1 and NQO1 expression. J Neurochem. 2011 Dec;119(5):909-19. PMID: 21781119.

Winzer M, Rauner M, Pietschmann P. Glycitein decreases the generation of murine osteoclasts and increases apoptosis. Wien Med Wochenschr. 2010 Sep;160(17-18):446-51. PMID: 20714813.

G4799

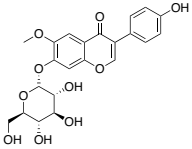

Glycitin

$C_{22}H_{22}O_{10}$ FW: 446.4 [40246-10-4] ≥98%

5 mg
25 mg

TAS2R agonist found in soy. It suppresses invasive activity of glioma cells, increases proliferation of mouse bone marrow stromal cells and osteoblasts, and inhibits adipocytic transdifferentiation of osteoblasts.

Roland WS, Vincken JP, Gouka RJ, et al. Soy isoflavones and other isoflavonoids activate the human bitter taste receptors hTAS2R14 and hTAS2R39. J Agric Food Chem. 2011 Nov 9;59(21):11764-71. PMID: 21942422.

Lee EJ, Kim SY, Hyun JW, et al. Glycitein inhibits glioma cell invasion through down-regulation of MMP-3 and MMP-9 gene expression. Chem Biol Interact. 2010 Apr 15;185(1):18-24. PMID: 20188714.

Li XH, Zhang JC, Sui SF, et al. Effect of daidzin, genistin, and glycitin on osteogenic and adipogenic differentiation of bone marrow stromal cells and adipocytic transdifferentiation of osteoblasts. Acta Pharmacol Sin. 2005 Sep;26(9):1081-6. PMID: 16115375.

G6000

H-Arg-Val-Thr-Ala-Ile-Glu-Lys-Tyr-Leu-Gln-Asp-Gln-Ala-Arg-Leu-Asn-Ser-Trp-Gly-Cys-Ala-Phe-Arg-Gln-Val-Cys-OH (Disulfide bridge Cys20-Cys26)

Glycoprotein 38

Podoplanin; gp38

$C_{133}H_{209}N_{41}O_{38}S_2$ FW: 3054.53 ≥95%

1 mg
2 mg
5 mg

Transmembrane O-glycoprotein that maintains barrier function in high endothelial venules and activates platelets to induce separation of lymphatic and blood vascular systems.

Herzog BH, Fu J, Wilson SJ, et al. Podoplanin maintains high endothelial venule integrity by interacting with platelet CLEC-2. Nature. 2013 Oct 3;502(7469):105-9. PMID: 23995678.

Krishnan H, Ochoa-Alvarez JA, Shen Y, et al. Serines in the intracellular tail of podoplanin (PDPN) regulate cell motility. J Biol Chem. 2013 Apr 26;288(17):12215-21. PMID: 23530051.

G6400

H-Gly-Gln-OH

Glycylglutamine

GQ

$C_7H_{13}N_3O_4$ FW: 203.2 [13115-71-4] ≥95%

5 mg
10 mg
25 mg

Endogenous beta-endorphin derivative. It decreases serum creatine kinase, lactate dehydrogenase, and lactic acid in burn injury models, improves cardiac contractility, suppresses IL-1β-induced thermogenesis and prostaglandin E2 production, and inhibits opioid-induced dopamine signaling.

Zhang Y, Yan H, Lv SG, et al. Effects of glycyl-glutamine dipeptide supplementation on myocardial damage and cardiac function in rats after severe burn injury. Int J Clin Exp Pathol. 2013 Apr 15;6(5):821-30. PMID: 23638213.

Jiang JW, Ren ZG, Chen LY, et al. Enteral supplementation with glycyl-glutamine improves intestinal barrier function after liver transplantation in rats. Hepatobiliary Pancreat Dis Int. 2011 Aug;10(4):380-5. PMID: 21813386.

G4597

18β-Glycyrrhetinic Acid

5 g
10 g
25 g

Enoxolone; Uralenic acid

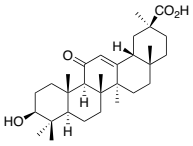

$C_{30}H_{46}O_4$ FW: 470.68 [471-53-4] ≥98%

Commercial flavorant found in *Glycyrrhiza*. It inhibits 15-HPGDH and blocks hERG and KCNA3/K_v1.3 K^+ channels. It prevents production of IL-2 and activation of T cells, induces apoptosis in non-small cell lung cancer cells, and decreases plasma lipid levels, fat weight, and body weight.

Jayasooriya RG, Dilshara MG, Park SR, et al. 18β-Glycyrrhetinic acid suppresses TNF-α induced matrix metalloproteinase-9 and vascular endothelial growth factor by suppressing the Akt-dependent NF-κB pathway. Toxicol In Vitro. 2014 Aug;28(5):751-8. PMID: 24613819.

Park M, Lee JH, Choi JK, et al. 18β-glycyrrhetinic acid attenuates anandamide-induced adiposity and high-fat diet induced obesity. Mol Nutr Food Res. 2014 Jul;58(7):1436-46. PMID: 24687644.

Song J, Ko HS, Sohn EJ, et al. Inhibition of protein kinase C α/βII and activation of c-Jun NH2-terminal kinase mediate glycyrrhetinic acid induced apoptosis in non-small cell lung cancer NCI-H460 cells. Bioorg Med Chem Lett. 2014 Feb 15;24(4):1188-91. PMID: 24461294.

G4598

Glycyrrhizic Acid Ammonium Trihydrate

10 g
25 g

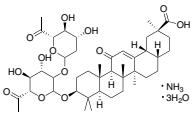

$C_{42}H_{65}NO_{16} \cdot 3H_2O$ FW: 894.03 [53956-04-0] ≥93%

Commercial flavorant and emulsifier found in *Glycyrrhiza*. It inhibits 11β-HSD and is used to treat herpes virus infection. It inhibits viral entry to host cells, prevents glial inflammation and kainic acid-induced neuronal death, and suppresses DMH-induced carcinogenesis.

Ye S, Zhu Y, Ming Y, et al. Glycyrrhizin protects mice against renal ischemia-reperfusion injury through inhibition of apoptosis and inflammation by downregulating p38 mitogen-activated protein kinase signaling. Exp Ther Med. 2014 May;7(5):1247-1252. PMID: 24940420.

Son M, Lee M, Sung GH, et al. Bioactive activities of natural products against herpesvirus infection. J Microbiol. 2013 Oct;51(5):545-51. Erratum in: J Microbiol. 2013 Dec;51(6):888. PMID: 24173639.

Luo L, Jin Y, Kim ID, et al. Glycyrrhizin attenuates kainic Acid-induced neuronal cell death in the mouse hippocampus. Exp Neurobiol. 2013 Jun;22(2):107-15. PMID: 23833559.

G5216

GNE-7915

NEW

5 mg
10 mg

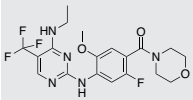

$C_{19}H_{21}F_4N_5O_3$ FW: 443.4 [1351761-44-8] ≥98%

LRRK2 inhibitor. It may suppress the development of neurodegenerative disorders.

Kavanagh ME, Doddareddy MR, Kassiou M. The development of CNS-active LRRK2 inhibitors using property-directed optimisation. Bioorg Med Chem Lett. 2013 Jul 1;23(13):3690-6. PMID: 23721803.

Estrada AA, Liu X, Baker-Glenn C, et al. Discovery of highly potent, selective, and brain-penetrable leucine-rich repeat kinase 2 (LRRK2) small molecule inhibitors. J Med Chem. 2012 Nov 26;55(22):9416-33. PMID: 22985112.

G5320

GNF-2

NEW

5 mg
25 mg

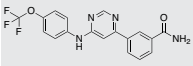

$C_{18}H_{13}F_3N_4O_2$ FW: 374.32 [778270-11-4] ≥98%

Abl inhibitor. It suppresses Bcr-abl-dependent cell proliferation, induces differentiation of osteoclasts, inhibits resorption of mature osteoclasts, and prevents phagocytosis in bone marrow-derived macrophages.

Kim HJ, Yoon HJ, Choi JY, et al. The tyrosine kinase inhibitor GNF-2 suppresses osteoclast formation and activity. J Leukoc Biol. 2014 Feb;95(2):337-45. PMID: 24130113.

Greuber EK, Pendergast AM. Abl family kinases regulate FcγR-mediated phagocytosis in murine macrophages. J Immunol. 2012 Dec 1;189(11):5382-92. PMID: 23100514.

Mian AA, Metodieva A, Najajreh Y, et al. p185(BCR/ABL) has a lower sensitivity than p210(BCR/ABL) to the allosteric inhibitor GNF-2 in Philadelphia chromosome-positive acute lymphatic leukemia. Haematologica. 2012 Feb;97(2):251-7. PMID: 22058195.

G5752

Gonadorelin Acetate

Please inquire

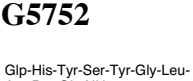

Glp-His-Tyr-Ser-Tyr-Gly-Leu-Arg-Pro-Gly-NH_2

$C_{55}H_{75}N_{17}O_{13} \cdot 2(C_2H_4O_2)$ FW: 1302.59 [71447-49-9] ≥95%

Synthetic GnRH derivative and GnRH receptor agonist used to treat endometriosis. It induces release of FSH and LH, inhibits testosterone activation of androgen receptors, and suppresses proliferation of prostate cancer cells.

Maudsley S, Davidson L, Pawson AJ, et al. Gonadotropin-releasing hormone functionally antagonizes testosterone activation of the human androgen receptor in prostate cells through focal adhesion complexes involving Hic-5. Neuroendocrinology. 2006;84(5):285-300. PMID: 17202804.

Maiti K, Oh DY, Moon JS, et al. Differential effects of gonadotropin-releasing hormone (GnRH)-I and GnRH-II on prostate cancer cell signaling and death. J Clin Endocrinol Metab. 2005 Jul;90(7):4287-98. PMID: 15870130.

G5772

Goserelin Acetate

1 mg
2.5 mg

$C_{59}H_{84}N_{18}O_{14}\ C_2H_4O_2$ FW: 1329.48 [145781-92-6] ≥95%

Pyr-His-Trp-Ser-Tyr-D-Ser(tBu)-Leu-Arg-Pro-AzaGly-NH_2

GnRH receptor agonist used to treat hormone-sensitive cancers and for in vitro fertilization. It induces release of FSH and LH, increases bone elongation, and suppresses proliferation of prostate cancer cells.

Detti L, Uhlmann RA, Zhang J, et al. Goserelin fosters bone elongation but does not prevent ovarian damage in cyclophosphamide-treated prepubertal mice. Fertil Steril. 2014 Jan 23. pii: S0015-0282(13)03460-2. [Epub ahead of print]. PMID: 24462062.

Zhang Y, Ding JX, Tao X, et al. Goserelin can inhibit ovarian cancer proliferation and simultaneously protect ovarian function from cisplatin: an in vitro and in vivo study. J Chemother. 2013 Apr;25(2):96-103. PMID: 23684357.

G5874

Gossypol

25 mg
100 mg
250 mg

$C_{30}H_{30}O_8$ FW: 518.55 [303-45-7] ≥98%

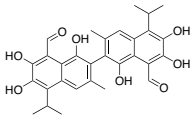

Calcineurin and PKC inhibitor found in *Gossypium*. It displays a variety of biological activities, including stimulating spermatogenesis arrest, inactivating HIV-1, suppressing T cell activation, and inducing apoptosis in myeloma cells.

Jang GH, Lee M. BH3-mimetic gossypol-induced autophagic cell death in mutant BRAF melanoma cells with high expression of p21Cip¹.). Life Sci. 2014 Apr 25;102(1):41-8. PMID: 24625733.

Song B, Huang G, Tong C, et al. Gossypol suppresses mouse T lymphocytes via inhibition of NFκB, NFAT and AP-1 pathways. Immunopharmacol Immunotoxicol. 2013 Oct;35(5):615-21. PMID: 23981004.

Lin J, Wu Y, Yang D, et al. Induction of apoptosis and antitumor effects of a small molecule inhibitor of Bcl-2 and Bcl-xl, gossypol acetate, in multiple myeloma in vitro and in vivo. Oncol Rep. 2013 Aug;30(2):731-8. PMID: 23708869.

G5875

Gossypol Acetic Acid

250 mg
1 g

$C_{30}H_{30}O_8 \bullet C_2H_4O_2$ FW: 578.61 [12542-36-8] ≥98%

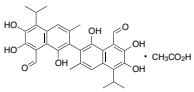

Inhibitor of Bcl-2, Bcl-xl, and sialyl transferase. It enhances apoptosis in breast cancer cells, delays the onset of androgen-independent prostate cancer, suppresses growth of gram negative bacteria, and inhibits spermatogenesis.

Deng S, Yuan H, Yi J, et al. Gossypol acetic acid induces apoptosis in RAW264.7 cells via a caspase-dependent mitochondrial signaling pathway. J Vet Sci. 2013;14(3):281-9. PMID: 23820203.

Hall C, Troutman SM, Price DK, et al. Bcl-2 family of proteins as therapeutic targets in genitourinary neoplasms. Clin Genitourin Cancer. 2013 Mar;11(1):10-9. PMID: 23083798.

Kisim A, Atmaca H, Cakar B, et al. Pretreatment with AT-101 enhances tumor necrosis factor-related apoptosis-inducing ligand (TRAIL)-induced apoptosis of breast cancer cells by inducing death receptors 4 and 5 protein levels. J Cancer Res Clin Oncol. 2012 Jul;138(7):1155-63. PMID: 22411600.

G6368

GPR

5 mg
10 mg
25 mg

$C_{13}H_{24}N_6O_4$ FW: 328.18 [47295-77-2] ≥95%

H-Gly-Pro-Arg-OH

Fibrinogen E analog and fibrin assembly inhibitor found in *Amaranthus*. It inhibits formation of amyloid-β fibrils and prevents neuronal apoptosis.

Montoya-Rodríguez A, de Mejía EG, Dia VP, et al. Extrusion improved the anti-inflammatory effect of amaranth (*Amaranthus* hypochondriacus) hydrolysates in LPS-induced human THP-1 macrophage-like and mouse RAW 264.7 macrophages by preventing activation of NF-κB signaling. Mol Nutr Food Res. 2014 Jan 15. [Epub ahead of print]. PMID: 24431078.

Zhou B, Li CL, Hao YQ, et al. Ferrocene tripeptide Gly-Pro-Arg conjugates: synthesis and inhibitory effects on Alzheimer's Aβ(1-42) fibrillogenesis and Aβ-induced cytotoxicity in vitro. Bioorg Med Chem. 2013 Jan 15;21(2):395-402. PMID: 23245572.

G6802

Granisetron Hydrochloride

25 mg
100 mg
500 mg

$C_{18}H_{24}N_4O \bullet HCl$ FW: 348.87 [107007-99-8] ≥98%

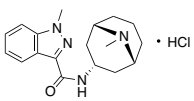

5-HT3 receptor antagonist that decreases nausea and post-inflammatory visceral sensitivity in colitis models.

Hsu ES. A review of granisetron, 5-hydroxytryptamine3 receptor antagonists, and other antiemetics. Am J Ther. 2010 Sep-Oct;17(5):476-86. PMID: 20844345.

Choi YD, Sung TS, Kim HJ, et al. Increased 5-hydroxytryptamine mediates post-inflammatory visceral hypersensitivity via the 5-hydroxytryptamine 3 receptor in rats. Dig Dis Sci. 2008 Nov;53(11):2909-16. PMID: 18357529.

Martin C, Roman V, Agay D, et al. Anti-emetic effect of ondansetron and granisetron after exposure to mixed neutron and gamma irradiation. Radiat Res. 1998 Jun;149(6):631-6. PMID: 9611102.

G6803 Granuliberin R

1 mg
2 mg
5 mg

H-Phe-Gly-Phe-Leu-Pro-Ile-Tyr-Arg-Arg-Pro-Ala-Ser-NH_2

$C_{69}H_{103}N_{19}O_{14}$ FW: 1422.71 [64704-41-2] ≥95%

Found in amphibian skin. It induces histamine release and increases K^+ efflux. It also inhibits basal gingival epithelial cell prolieration.

Nakao S, Komagoe K, Inoue T, et al. Comparative study of the membrane-permeabilizing activities of mastoparans and related histamine-releasing agents in bacteria, erythrocytes, and mast cells. Biochim Biophys Acta. 2011 Jan;1808(1):490-7. PMID: 20955685.

Kozakiewicz M, Godlewski A. Modulation of the mitotic activity and population of the mast cells in the oral mucosa by substance P. Cell Mol Biol Lett. 2003;8(3):727-34. PMID: 12949612.

G6817 Green Tea Polyphenols

10 g
20 g
100 g

[84650-60-2] ≥95%

Extract containing catechins and flavonoids found in *Camilla sinensis* (green tea). Components of this extract suppress microbial infection, inflammation, oxidative damage, and carcinogenesis.

Reygaert WC. The antimicrobial possibilities of green tea. Front Microbiol. 2014 Aug 20;5:434. PMID: 25191312.

Li MJ, Yin YC, Wang J, et al. Green tea compounds in breast cancer prevention and treatment. World J Clin Oncol. 2014 Aug 10;5(3):520-8. PMID: 25114865.

Kim HS, Quon MJ, Kim JA. New insights into the mechanisms of polyphenols beyond antioxidant properties; lessons from the green tea polyphenol, epigallocatechin 3-gallate. Redox Biol. 2014 Jan 10;2:187-95. PMID: 24494192.

G2870 Growth Hormone Releasing Factor (1-44), human

0.5 mg
1 mg
2.5 mg

Somatorelin; Somatoliberin; GHRF; GHRH

H-Tyr-Ala-Asp-Ala-Ile-Phe-Thr-Asn-Ser-Tyr-Arg-Lys-Val-Leu-Gly-Gln-Leu-Ser-Ala-Arg-Lys-Leu-Leu-Gln-Asp-Ile-Met-Ser-Arg-Gln-Gln-Gly-Glu-Ser-Asn-Gln-Glu-Arg-Gly-Ala-Arg-Ala-Arg-Leu-NH_2

$C_{215}H_{358}N_{72}O_{66}S_1$ FW: 5039.7 [83930-13-6] ≥95%

Endogenous peptide GHRH receptor agonist involved in growth hormone secretion. It promotes non-REM slow wave sleep, decreases fat synthesis in adipose tissue, and stimulates activity of plasminogen activator, playing a role in follicular development.

Obál F Jr, Krueger JM. The somatotropic axis and sleep. Rev Neurol (Paris). 2001 Nov;157(11 Pt 2):S12-5. PMID: 11924022.

Liesman JS, McNamara JP, Capuco AV, et al. Comparison of growth hormone-releasing factor and somatotropin: lipid and glucose metabolism in dairy cows. J Dairy Sci. 1995 Oct;78(10):2159-66. PMID: 8598400.

G2871 Growth Hormone Releasing Factor, cow

0.5 mg
1 mg
2.5 mg

GHRF; GHRH

H-Tyr-Ala-Asp-Ala-Ile-Phe-Thr-Asn-Ser-Tyr-Arg-Lys-Val-Leu-Gly-Gln-Leu-Ser-Ala-Arg-Lys-Leu-Leu-Gln-Asp-Ile-Met-Asn-Arg-Gln-Gln-Gly-Glu-Arg-Asn-Gln-Glu-Gln-Gly-Ala-Lys-Val-Arg-Leu-NH_2

$C_{220}H_{366}N_{72}O_{66}S_1$ FW: 5107.88 [88894-91-1] ≥95%

Endogenous GHRH receptor agonist involved in growth hormone secretion. It promotes non-REM slow wave sleep, decreases fat synthesis in adipose tissue, stimulates activity of plasminogen activator, and plays a role in follicular development.

Obál F Jr, Krueger JM. The somatotropic axis and sleep. Rev Neurol (Paris). 2001 Nov;157(11 Pt 2):S12-5. PMID: 11924022.

G6856 Growth Hormone Releasing Factor, human

1 mg

GHRF; GHRH

Tyr-Ala-Asp-Ala-Ile-Phe-Thr-Asn-Ser-Tyr-Arg-Lys-Val-Leu-Gly-Gln-Leu-Ser-Ala-Arg-Lys-Leu-Leu-Gln-Asp-Ile-Met-Ser-Arg-Gln-Gln-Gly-Glu-Ser-Asn-Gln-Glu-Arg-Gly-Ala-Arg-Ala-Arg-Leu-NH_2

$C_{215}H_{358}N_{72}O_{66}S$ FW: 5039.7 [83930-13-6] ≥98%

Endogenous GHRH receptor agonist that increases growth hormone production. It also increases locomotor activity, inhibits myosin light chain kinase activity, and enhances FSH-induced steroidogenesis.

Karakji EG, Tsang BK. Growth hormone releasing factor and vasoactive intestinal peptide stimulate rat granulosa cell plasminogen activator activity in vitro during follicular development. Mol Cell Endocrinol. 1995 Jan;107(1):105-12. PMID: 7796929.

Shiraga H, Stallwood D, Ebadi M, et al. Inhibition of calmodulin-dependent myosin light-chain kinase by growth-hormone-releasing factor and vasoactive intestinal peptide. Biochem J. 1994 Jun 15;300 (Pt 3):901-5. PMID: 8010976.

G2872 Growth Hormone Releasing Factor, mouse

0.5 mg
1 mg
2.5 mg

GHRF; GHRH

H-His-Val-Asp-Ala-Ile-Phe-Thr-Thr-Asn-Tyr-Arg-Lys-Leu-Leu-Ser-Gln-Leu-Tyr-Ala-Arg-Lys-Val-Ile-Gln-Asp-Ile-Met-Asn-Lys-Gln-Gly-Glu-Arg-Ile-Gln-Glu-Gln-Arg-Ala-Arg-Leu-Ser-OH

$C_{220}H_{365}N_{69}O_{64}S_1$ FW: 5032.85 ≥95%

Endogenous GHRH receptor agonist involved in growth hormone secretion. It promotes non-REM slow wave sleep, decreases fat synthesis in adipose tissue, stimulates activity of plasminogen activator, and plays a role in follicular development.

Obál F Jr, Krueger JM. The somatotropic axis and sleep. Rev Neurol (Paris). 2001 Nov;157(11 Pt 2):S12-5. PMID: 11924022.

G2874

Growth Hormone Releasing Factor, rat

0.5 mg
1 mg
2.5 mg

H-His-Ala-Asp-Ala-Ile-Phe-Thr-Ser-Ser-Tyr-Arg-Arg-Ile-Leu-Gly-Gln-Leu-Tyr-Ala-Arg-Lys-Leu-Leu-His-Glu-Ile-Met-Asn-Arg-Gln-Gln-Gly-Glu-Arg-Asn-Gln-Glu-Gln-Arg-Ser-Arg-Phe-Asn-OH

Somatotropin releasing hormone (1-43); Growth hormone releasing factor 43

$C_{225}H_{361}N_{77}O_{66}S$ FW: 5232.93 [86472-71-1] ≥95%

Endogenous GHRH receptor agonist involved in growth hormone secretion. It promotes non-REM slow wave sleep, decreases fat synthesis in adipose tissue, stimulates activity of plasminogen activator, and plays a role in follicular development..

Obál F Jr, Krueger JM. The somatotropic axis and sleep. Rev Neurol (Paris). 2001 Nov;157(11 Pt 2):S12-5. PMID: 11924022.

Liesman JS, McNamara JP, Capuco AV, et al. Comparison of growth hormone-releasing factor and somatotropin: lipid and glucose metabolism in dairy cows. J Dairy Sci. 1995 Oct;78(10):2159-66. PMID: 8598400.

G2873

Growth Hormone Releasing Factor, sheep

0.5 mg
1 mg
2.5 mg

H-Tyr-Ala-Asp-Ala-Ile-Phe-Thr-Asn-Ser-Tyr-Arg-Lys-Ile-Leu-Gly-Gln-Leu-Ser-Ala-Arg-Lys-Leu-Leu-Gln-Asp-Ile-Met-Asn-Arg-Gln-Gln-Gly-Glu-Arg-Asn-Gln-Glu-Gln-Gly-Ala-Lys-Val-Arg-Leu-NH_2

GHRF; GHRH

$C_{221}H_{368}N_{72}O_{66}S_1$ FW: 5121.9 [94948-82-0] ≥95%

Endogenous GHRH receptor agonist involved in growth hormone secretion. It promotes non-REM slow wave sleep, decreases fat synthesis in adipose tissue, stimulates activity of plasminogen activator, and plays a role in follicular development.

Obál F Jr, Krueger JM. The somatotropic axis and sleep. Rev Neurol (Paris). 2001 Nov;157(11 Pt 2):S12-5. PMID: 11924022.

G2969

Growth Hormone Releasing Hexapeptide

1 mg
2 mg
5 mg

H-His-DTrp-Ala-Trp-DPhe-Lys-NH_2

Growth hormone releasing hexapeptide; Skf 110679; GHRP-6

$C_{46}H_{56}N_{12}O_6$ FW: 873.04 [87616-84-0] ≥95%

Synthetic met-enkephalin analog and ghrelin agonist involved in growth hormone secretion. It also increases astrocyte proliferation, inhibits development of restraint stress-induced gastric lesions, increases food intake, and decreases locomotor activity.

Baquedano E, Chowen JA, Argente J, et al. Differential effects of GH and GH-releasing peptide-6 on astrocytes. J Endocrinol. 2013 Jul 29;218(3):263-74. PMID: 23792323.

G2968

Growth Hormone Releasing Peptide 2

0.5 mg
1 mg
2.5 mg

H-D-Ala-D-2-Nal-Ala-Trp-DPhe-Lys-NH_2

KP 102; GHRP-2

$C_{45}H_{54}O_6N_9$ FW: 818 [158861-67-7] ≥95%

Endogenous ghrelin receptor agonist involved in secretion of hormones and signaling mediators. It increases food intake, inhibits gastrointestinal contractility, decreases morphine-induced analgesia, and suppresses LPS-stimulated increases in pro-inflammatory cytokine levels.

Zeng P, Chen JX, Yang B, et al. Attenuation of systemic morphine-induced analgesia by central administration of ghrelin and related peptides in mice. Peptides. 2013 Dec;50:42-9. PMID: 24113541.

G7200

GS-967

NEW

5 mg
25 mg

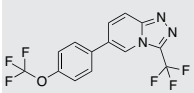

$C_{14}H_7F_6N_3O$ FW: 347.22 [1262618-39-2] ≥98%

Voltage-gated Na^+ channel blocker. It decreases seizure frequency and prevents ventricular tachycardia and fibrillation.

Anderson LL, Thompson CH, Hawkins NA, et al. Antiepileptic activity of preferential inhibitors of persistent sodium current. Epilepsia. 2014 Aug;55(8):1274-83. PMID: 24862204.

Pezhouman A, Madahian S, Stepanyan H, et al. Selective inhibition of late sodium current suppresses ventricular tachycardia and fibrillation in intact rat hearts. Heart Rhythm. 2014 Mar;11(3):492-501. PMID: 24291413.

Sicouri S, Belardinelli L, Antzelevitch C. Antiarrhythmic effects of the highly selective late sodium channel current blocker GS-458967. Heart Rhythm. 2013 Jul;10(7):1036-43. PMID: 23524321.

G7232

GS-9973

NEW

5 mg
10 mg

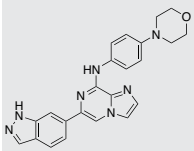

Entospletinib

$C_{23}H_{21}N_7O$ FW: 411.46 [1229208-44-9] ≥98%

Syk inhibitor. It decreases cell survival, inhibits cell growth, and disrupts chemokine signaling in models of chronic lymphocytic leukemia.

Sharman J, Hawkins M, Kolibaba K, et al. An open-label phase 2 trial of entospletinib (GS-9973), a selective Syk inhibitor, in chronic lymphocytic leukemia. Blood. 2015 Feb 18. Epub ahead of print]. PMID: 25696919.

Currie KS, Kropf JE, Lee T, et al. Discovery of GS-9973, a selective and orally efficacious inhibitor of spleen tyrosine kinase. J Med Chem. 2014 May 8;57(9):3856-73. PMID: 24779514.

Burke RT, Meadows S, Loriaux MM, et al. A potential therapeutic strategy for chronic lymphocytic leukemia by combining Idelalisib and GS-9973, a novel spleen tyrosine kinase (Syk) inhibitor. Oncotarget. 2014 Feb 28;5(4):908-15. PMID: 24659719.

G7340 GSK-126

1 mg
5 mg

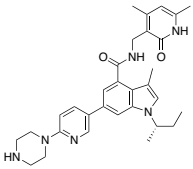

$C_{31}H_{38}N_6O_2$ FW: 526.67 [1346574-57-9] ≥99%

EZH2 HMT inhibitor active against Y641 and A677 EZH2 mutants. It inhibits proliferation of diffuse large B-cell lymphoma cells.

Tian X, Zhang S, Liu HM, et al. Histone lysine-specific methyltransferases and demethylases in carcinogenesis: new targets for cancer therapy and prevention. Curr Cancer Drug Targets. 2013 Jun 10;13(5):558-79. PMID: 23713993.

McCabe MT, Ott HM, Ganji G, et al. EZH2 inhibition as a therapeutic strategy for lymphoma with EZH2-activating mutations. Nature. 2012 Dec 6;492(7427):108-12. PMID: 23051747.

G7442 GSK-343

NEW

1 mg
5 mg
10 mg

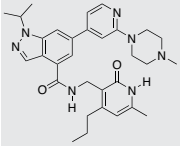

$C_{31}H_{39}N_7O_2$ FW: 541.69 [1346704-33-3] ≥98%

EZH2 HMT inhibitor. It inhibits cell invasion and cell growth in epithelial ovarian cancer cells.

Amatangelo MD, Garipov A, Li H, et al. Three-dimensional culture sensitizes epithelial ovarian cancer cells to EZH2 methyltransferase inhibition. Cell Cycle. 2013 Jul 1;12(13):2113-9. PMID: 23759589.

G7443 GSK-429286A

NEW

1 mg
5 mg

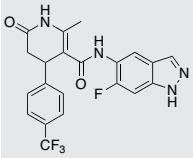

$C_{21}H_{16}F_4N_4O_2$ FW: 432.37 [864082-47-3] ≥98%

ROCK1/2 inhibitor and potential RSK and p70S6K inhibitor. It decreases mean arterial pressure in hypertension models.

Nichols RJ, Dzamko N, Hutti JE, et al. Substrate specificity and inhibitors of LRRK2, a protein kinase mutated in Parkinson's disease. Biochem J. 2009 Oct 23;424(1):47-60. PMID: 19740074.

Goodman KB, Cui H, Dowdell SE, et al. Development of dihydropyridone indazole amides as selective Rho-kinase inhibitors. J Med Chem. 2007 Jan 11;50(1):6-9. PMID: 17201405.

G7241 GSK-461364

NEW

5 mg
10 mg

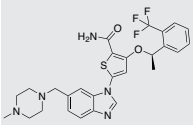

$C_{27}H_{28}F_3N_5O_2S$ FW: 543.6 [929095-18-1] ≥98%

PLK1 inhibitor. It inhibits cell proliferation, invasion, and colony formation and induces apoptosis and cell cycle arrest in glioblastoma cells.

Yim H. Current clinical trials with polo-like kinase 1 inhibitors in solid tumors. Anticancer Drugs. 2013 Nov;24(10):999-1006. PMID: 23949254.

Pezuk JA, Brassesco MS, Morales AG, et al. Polo-like kinase 1 inhibition causes decreased proliferation by cell cycle arrest, leading to cell death in glioblastoma. Cancer Gene Ther. 2013 Sep;20(9):499-506. PMID: 23887645.

Olmos D, Barker D, Sharma R, et al. Phase I study of GSK461364, a specific and competitive Polo-like kinase 1 inhibitor, in patients with advanced solid malignancies. Clin Cancer Res. 2011 May 15;17(10):3420-30. PMID: 21459796.

G7242 GSK-690693

NEW

5 mg
10 mg

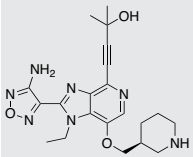

$C_{21}H_{27}N_7O_3$ FW: 425.48 [937174-76-0] ≥98%

Akt inhibitor. It induces apoptosis and inhibits cell growth in lung cancer models.

Nguyen T, Coover RA, Verghese J, et al. Phenylalanine-Based Inactivator of AKT Kinase: Design, Synthesis, and Biological Evaluation. ACS Med Chem Lett. 2014 Mar 7;5(5):462-7. PMID: 24900862.

Carol H, Morton CL, Gorlick R, et al. Initial testing (stage 1) of the Akt inhibitor GSK690693 by the pediatric preclinical testing program. Pediatr Blood Cancer. 2010 Dec 15;55(7):1329-37. PMID: 20740623.

Altomare DA, Zhang L, Deng J, et al. GSK690693 delays tumor onset and progression in genetically defined mouse models expressing activated Akt. Clin Cancer Res. 2010 Jan 15;16(2):486-96. PMID: 20075391.

G7444 GSK-1070916

NEW

5 mg
10 mg

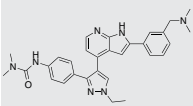

$C_{30}H_{33}N_7O$ FW: 507.63 [942918-07-2] ≥98%

Aurora kinase B/C inhibitor. It inhibits cell division, induces apoptosis, and suppresses tumor growth in models of breast cancer, colon cancer, and leukemia.

Adams ND, Adams JL, Burgess JL, et al. Discovery of GSK1070916, a potent and selective inhibitor of Aurora B/C kinase. J Med Chem. 2010 May 27;53(10):3973-4001. PMID: 20420387.

Hardwicke MA, Oleykowski CA, Plant R, et al. GSK1070916, a potent Aurora B/C kinase inhibitor with broad antitumor activity in tissue culture cells and human tumor xenograft models. Mol Cancer Ther. 2009 Jul;8(7):1808-17. PMID: 19567821.

G7440 GSK-1120212

NEW

5 mg
25 mg
100 mg

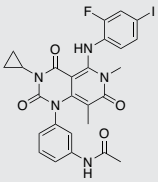

Trametinib; JTP-74057

$C_{26}H_{23}FIN_5O_4$ FW: 615.39 [871700-17-3] ≥98%

MEK1/2 inhibitor. It inhibits cell proliferation and tumor growth in colorectal cancer models.

Hartsough EJ, Basile K, Aplin AE. Beneficial Effects of RAF Inhibitor in Mutant BRAF Splice Variant-expressing Melanoma. Mol Cancer Res. 2014 Feb 11. [Epub ahead of print]. PMID: 24520098.

Kim KB, Kefford R, Pavlick AC, et al. Phase II study of the MEK1/MEK2 inhibitor Trametinib in patients with metastatic BRAF-mutant cutaneous melanoma previously treated with or without a BRAF inhibitor. J Clin Oncol. 2013 Feb 1;31(4):482-9. PMID: 23248257.

Yamaguchi T, Kakefuda R, Tajima N, et al. Antitumor activities of JTP-74057 (GSK1120212), a novel MEK1/2 inhibitor, on colorectal cancer cell lines in vitro and in vivo. Int J Oncol. 2011 Jul;39(1):23-31. PMID: 21523318.

G7540 GSK-1838705A

NEW

1 mg
5 mg
25 mg

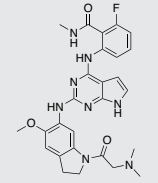

$C_{27}H_{29}FN_8O_3$ FW: 532.57 [1116235-49-7] ≥98%

ALK and IGF-1R inhibitor. It inhibits cell proliferation and tumor growth in models of large-cell lymphoma, neuroblastoma, and non-small cell lung cancer.

Sabbatini P, Korenchuk S, Rowand JL, et al. GSK1838705A inhibits the insulin-like growth factor-1 receptor and anaplastic lymphoma kinase and shows antitumor activity in experimental models of human cancers. Mol Cancer Ther. 2009 Oct;8(10):2811-20. PMID: 19825801.

G7541 GSK-1904529A

NEW

1 mg
5 mg
25 mg

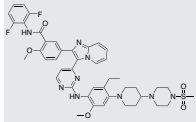

$C_{44}H_{47}F_2N_9O_5S$ FW: 851.96 [1089283-49-7] ≥98%

InsR and IGF-1R inhibitor. It induces cell cycle arrest and inhibits cellular proliferation and tumor growth in models of multiple myeloma and Ewing's sarcoma.

Sabbatini P, Rowand JL, Groy A, et al. Antitumor activity of GSK1904529A, a small-molecule inhibitor of the insulin-like growth factor-I receptor tyrosine kinase. Clin Cancer Res. 2009 May 1;15(9):3058-67. PMID: 19383820.

G7342 GSK-2126458

1 mg
5 mg
25 mg

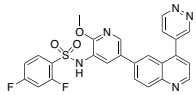

GSK458

$C_{25}H_{17}F_2N_5O_3S$ FW: 505.5 [1086062-66-9] ≥99%

p110α PI3K and mTOR inhibitor. It inhibits proliferation of various cancer cells.

Greger JG, Eastman SD, Zhang V, et al. Combinations of BRAF, MEK, and PI3K/mTOR inhibitors overcome acquired resistance to the BRAF inhibitor GSK2118436 dabrafenib, mediated by NRAS or MEK mutations. Mol Cancer Ther. 2012 Apr;11(4):909-20. PMID: 22389471.

G7344 GSK-2334470

1 mg
5 mg
25 mg

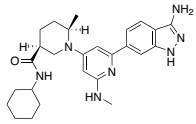

$C_{25}H_{34}N_8O$ FW: 462.59 [1227911-45-6] ≥99%

PI3K and PDK1 inhibitor. It inhibits T-loop phosphorylation of PI3K substrates SGK and S6K1, Akt and Akt substrates GSK3, FoxO, and PRAS40, and ERK substrate RSK2. It suppresses proliferation of cancer cells.

Najafov A, Sommer EM, Axten JM, et al. Characterization of GSK2334470, a novel and highly specific inhibitor of PDK1. Biochem J. 2011 Jan 15;433(2):357-69. PMID: 21087210.

G7345 GSK-2606414

NEW

1 mg
5 mg
25 mg

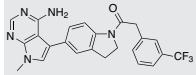

$C_{24}H_{20}F_3N_5O$ FW: 451.44 [1337531-89-1] ≥98%

PERK inhibitor. It suppresses growth of tumor xenografts.

Axten JM, Medina JR, Feng Y, et al. Discovery of 7-methyl-5-(1-{[3-(trifluoromethyl)phenyl]acetyl}-2,3-dihydro-1H-indol-5-yl)-7H-pyrrolo[2,3-d]pyrimidin-4-amine (GSK2606414), a potent and selective first-in-class inhibitor of protein kinase R (PKR)-like endoplasmic reticulum kinase (PERK). J Med Chem. 2012 Aug 23;55(16):7193-207. PMID: 22827572.

G7346 GSK-2636771

NEW

1 mg
5 mg

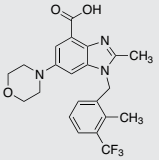

$C_{22}H_{22}F_3N_3O_3$ FW: 433.42 [1372540-25-4] ≥98.5%

p110β PI3K inhibitor. It suppresses proliferation of glioblastoma cells, prostate cancer cells, and endometrial cancer cells.

Weigelt B, Warne PH, Lambros MB, et al. PI3K Pathway Dependencies in Endometrioid Endometrial Cancer Cell Lines. Clin Cancer Res. 2013 Jul 1;19(13):3533-44. PMID: 23674493.

G7240 GSK-2830371 NEW

5 mg
10 mg

$C_{23}H_{29}ClN_4O_2S$ FW: 461.02 [1404456-53-6] ≥98%

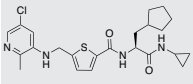

Wip1 inhibitor. It inhibits cell growth and tumor growth in lymphoma and neuroblastoma models.

Richter M, Dayaram T, Gilmartin AG, et al. WIP1 Phosphatase as a Potential Therapeutic Target in Neuroblastoma. PLoS One. 2015 Feb 6;10(2):e0115635. PMID: 25658463.

Gilmartin AG, Faitg TH, Richter M, et al. Allosteric Wip1 phosphatase inhibition through flap-subdomain interaction. Nat Chem Biol. 2014 Mar;10(3):181-7. PMID: 24390428.

G7862 GTPL-5846 NEW

5 mg
25 mg

6-N-Octylaminouracil; 6-OAU

$C_{12}H_{21}N_3O_2$ FW: 239.32 [83797-69-7] ≥98%

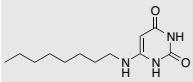

GPR84 agonist. It stimulates production of pro-inflammatory cytokines and increases macrophage chemotaxis.

Suzuki M, Takaishi S, Nagasaki M, et al. Medium-chain fatty acid-sensing receptor, GPR84, is a proinflammatory receptor. J Biol Chem. 2013 Apr 12;288(15):10684-91. PMID: 23449982.

G8101 Guaifenesin

25 g
100 g
500 g

Glycerol guaiacolate

$C_{10}H_{14}O_4$ FW: 198.22 [93-14-1] ≥98%

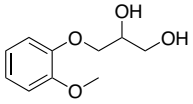

Expectorant used to treat respiratory cough. It inhibits mucin production, increases mucociliary transport, and decreases the viscoelasticity of mucus in airway epithelial cells.

Seagrave J, Albrecht H, Park YS, et al. Effect of guaifenesin on mucin production, rheology, and mucociliary transport in differentiated human airway epithelial cells. Exp Lung Res. 2011 Dec;37(10):606-14. PMID: 22044398.

Kagan L, Lavy E, Hoffman A. Effect of mode of administration on guaifenesin pharmacokinetics and expectorant action in the rat model. Pulm Pharmacol Ther. 2009 Jun;22(3):260-5. PMID: 19166957.

G8103 Guanylin, human

0.5 mg
1 mg
2.5 mg

H-Pro-Gly-Thr-Cys-Glu-Ile-Cys-Ala-Tyr-Ala-Ala-Cys-Thr-Gly-Cys-OH (Cys4-Cys12, Cys7-Cys15)

$C_{58}H_{87}N_{13}O_{21}S_4$ FW: 1458.68 [145319-90-0] ≥95%

Endogenous guanyl cyclase C receptor agonist. It increases cGMP levels and induces natriuresis and diuresis. It also suppresses proliferation of colonic cells.

Basu N, Saha S, Khan I, et al. Intestinal cell proliferation and senescence are regulated by receptor guanylyl cyclase C and p21. J Biol Chem. 2014 Jan 3;289(1):581-93. PMID: 24217248.

Fonteles MC, do Nascimento NR. Guanylin peptide family: history, interactions with ANP, and new pharmacological perspectives. Can J Physiol Pharmacol. 2011 Aug;89(8):575-85. PMID: 21815750.

G8104 Guanylin, rat/mouse

0.5 mg
1 mg
2.5 mg

H-Pro-Asn-Thr-Cys-Glu-Ile-Cys-Ala-Tyr-Ala-Ala-Cys-Thr-Gly-Cys-OH (Cys4-Cys12, Cys7-Cys15)

$C_{60}H_{90}N_{16}O_{22}S_4$ FW: 1515.74 [145257-03-0] ≥95%

Endogenous guanyl cyclase C receptor agonist. It increases cGMP levels and induces natriuresis and diuresis. It also suppresses proliferation of colonic cells.

Basu N, Saha S, Khan I, et al. Intestinal cell proliferation and senescence are regulated by receptor guanylyl cyclase C and p21. J Biol Chem. 2014 Jan 3;289(1):581-93. PMID: 24217248.

Fonteles MC, do Nascimento NR. Guanylin peptide family: history, interactions with ANP, and new pharmacological perspectives. Can J Physiol Pharmacol. 2011 Aug;89(8):575-85. PMID: 21815750.

G8225 Guggulsterone

5 mg
25 mg

$C_{21}H_{28}O_2$ FW: 312.45 [95975-55-6] ≥98%

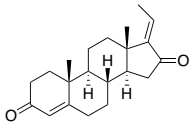

FXR antagonist found in myrrh. It displays a wide variety of biological activities, including disrupting cytoskeletal organization, inhibiting doxorubicin-induced toxicity in cardiomyocytes, inducing apoptosis in hepatic stellate cells, and preventing preadipocyte differentiation.

Macha MA, Rachagani S, Gupta S, et al. Guggulsterone decreases proliferation and metastatic behavior of pancreatic cancer cells by modulating JAK/STAT and Src/FAK signaling. Cancer Lett. 2013 Dec 1;341(2):166-77. PMID: 23920124.

Kim BH, Yoon JH, Yang JI, et al. Guggulsterone attenuates activation and survival of hepatic stellate cell by inhibiting nuclear factor kappa B activation and inducing apoptosis. J Gastroenterol Hepatol. 2013 Dec;28(12):1859-68. PMID: 23808824.

Wang WC, Uen YH, Chang ML, et al. Protective effect of guggulsterone against cardiomyocyte injury induced by doxorubicin in vitro..BMC Complement Altern Med. 2012 Aug 27;12:138. PMID: 22920231.

G8850

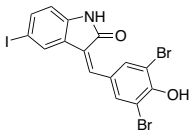

GW-5074

1 mg
5 mg

$C_{15}H_8Br_2INO2$ FW: 520.94 [220904-83-6] ≥98%

Inhibitor of c-Raf used to study Ras/Raf-1/ERK signaling. It prevents desuccinylation activity of Sirt5, alters DNA repair mechanisms, and suppresses 6-OHDA-induced neurotoxicity.

Suenkel B, Fischer F, Steegborn C. Inhibition of the human deacylase Sirtuin 5 by the indole GW5074. Bioorg Med Chem Lett. 2013 Jan 1;23(1):143-6. PMID: 23195732.

Li J, Fan Y, Zhang YN, et al. The Raf-1 inhibitor GW5074 and the ERK1/2 pathway inhibitor U0126 ameliorate PC12 cells apoptosis induced by 6-hydroxydopamine. Pharmazie. 2012 Aug;67(8):718-24. PMID: 22957439.

G8800

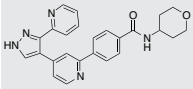

GW-788388

NEW

5 mg
25 mg

$C_{25}H_{23}N_5O_2$ FW: 425.49 [452342-67-5] ≥98%

Activin receptor-like kinase 5 inhibitor that suppresses TGF-β activity. It increases survival in studies of *Trypanosoma* infection, attenuates systolic dysfunction and left ventricular remodeling, and decreases the occurrence of renal fibrosis.

de Oliveira FL, Araújo-Jorge TC, de Souza EM, et al. Oral administration of GW788388, an inhibitor of transforming growth factor beta signaling, prevents heart fibrosis in Chagas disease. PLoS Negl Trop Dis. 2012;6(6):e1696. PMID: 22720109.

Tan SM, Zhang Y, Connelly KA, et al. Targeted inhibition of activin receptor-like kinase 5 signaling attenuates cardiac dysfunction following myocardial infarction. Am J Physiol Heart Circ Physiol. 2010 May;298(5):H1415-25. PMID: 20154262.

Petersen M, Thorikay M, Deckers M, et al. Oral administration of GW788388, an inhibitor of TGF-beta type I and II receptor kinases, decreases renal fibrosis. Kidney Int. 2008 Mar;73(6):705-15. PMID: 18075500.

G9648

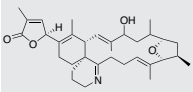

12-Methyl Gymnodimine

NEW

100 µg

$C_{33}H_{47}NO_4$ FW: 521.73 [1330004-64-2] ≥95%

Antagonist at nAChRs found in *Karenia*. It produces neuromuscular block and decreases accumulation of amyloid-β and phosphorylation of tau.

Marrouchi R, Rome G, Kharrat R, et al. Analysis of the action of gymnodimine-A and 13-desmethyl spirolide C on the mouse neuromuscular system in vivo. Toxicon. 2013 Dec 1;75:27-34. PMID: 23954513.

Hauser TA, Hepler CD, Kombo DC, et al. Comparison of acetylcholine receptor interactions of the marine toxins, 13-desmethylspirolide C and gymnodimine. Neuropharmacology. 2012 Jun;62(7):2239-50. PMID: 22306792.

Otero A, Chapela MJ, Atanassova M, et al. Cyclic imines: chemistry and mechanism of action: a review. Chem Res Toxicol. 2011 Nov 21;24(11):1817-29. PMID: 21739960.

H0001

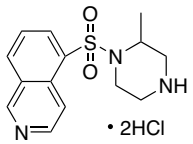

H7

10 mg
25 mg

$C_{14}H_{17}N_3O_2S \bullet 2HCl$ FW: 364.4 [108930-17-2] ≥98%

PKC and PKG inhibitor used to study protein kinase signaling.

Chen JJ, Zhang J, Cai Y, et al. C-type natriuretic peptide inhibiting vascular calcification might involve decreasing bone morphogenic protein 2 and osteopontin levels. Mol Cell Biochem. 2014 Jul;392(1-2):65-76. PMID: 24710639.

Zhang Y, Bao S, Kuang Z, et al. Urotensin II promotes monocyte chemoattractant protein-1 expression in aortic adventitial fibroblasts of rat. Chin Med J (Engl). 2014 May;127(10):1907-12. PMID: 24824254.

H0002

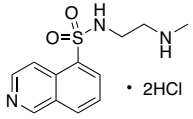

H8 dihydrochloride

5 mg
25 mg

$C_{12}H_{15}N_3O_2S$ 2HC1 FW: 338.25 [113276-94-1] ≥98%

PKA inhibitor that modulates Ca^{2+} signaling.

Sui HY, Luan HY, Liu YJ. Involvement of protein kinase A activation and phospholipase A(2) inhibition in the adenosine-activated basolateral 50 pS K(+) channels in the thick ascending limb of the rat kidney. Sheng Li Xue Bao. 2012 Aug 25;64(4):449-54. PMID: 22907306.

Hou L, Wang X. PKC and PKA, but not PKG mediate LPS-induced CGRP release and [Ca(2+)](i) elevation in DRG neurons of neonatal rats. J Neurosci Res. 2001 Nov 15;66(4):592-600. PMID: 11746379.

H0003

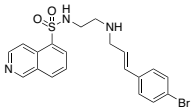

H89

1 mg
5 mg

$C_{20}H_{22}BrN_3O_2S$ FW: 446.36 [127243-85-0] ≥98%

Inhibitor of PKA used to study protein kinase signaling. It may also inhibit ROCK, S6K1, MSK1, MAPKAP-K1b, and PKBa.

Choi S, Kim MY, Joo KY, et al. Modafinil inhibits K(Ca)3.1 currents and muscle contraction via a cAMP-dependent mechanism. Pharmacol Res. 2012 Jul;66(1):51-9. PMID: 22414869.

Rogers RC, Hermann GE. Tumor necrosis factor activation of vagal afferent terminal calcium is blocked by cannabinoids. J Neurosci. 2012 Apr 11;32(15):5237-41. PMID: 22496569.

H0142

Haloperidol

1 g
5 g
10 g
25 g

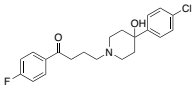

$C_{21}H_{23}ClFNO_2$ FW: 375.86 [52-86-8] ≥95%

Agonist at σ2 receptors and antagonist at α1-adrenergic receptors, dopamine D2 receptors, 5-HT2A receptors, and σ1 receptors. It is used to treat mood and personality disorders.

Cobos EJ, del Pozo E, Baeyens JM. Irreversible blockade of sigma-1 receptors by haloperidol and its metabolites in guinea pig brain and SH-SY5Y human neuroblastoma cells. J Neurochem. 2007 Aug;102(3):812-25. PMID: 17419803.

Colabufo NA, Berardi F, Contino M, et al. Antiproliferative and cytotoxic effects of some sigma2 agonists and sigma1 antagonists in tumour cell lines. Naunyn Schmiedebergs Arch Pharmacol. 2004 Aug;370(2):106-13. PMID: 15322732.

H0169

Harringtonine

5 mg
10 mg
25 mg

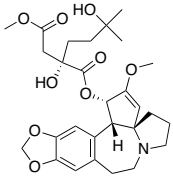

$C_{28}H_{37}NO_9$ FW: 531.59 [26833-85-2] ≥97%

Found in *Cephalotaxus*. It immobilizes initiated ribosomes, inhibiting protein translation by blocking the ribosomal A site. It suppresses viral replication and protein expression in chikungunya virus infection, inhibits cell growth in acute promyelocytic leukemia cells, and induces apoptosis in leukemia cells.

Wu C, Shen H, Xia D. Harringtonine induces apoptosis in NB4 cells through down-regulation of Mcl-1. Zhejiang Da Xue Xue Bao Yi Xue Ban. 2013 Jul;42(4):431-6. PMID: 24022932.

Kaur P, Thiruchelvan M, Lee RC, et al. Inhibition of chikungunya virus replication by harringtonine, a novel antiviral that suppresses viral protein expression. Antimicrob Agents Chemother. 2013 Jan;57(1):155-67. PMID: 23275491.

Ingolia NT, Brar GA, Rouskin S, et al. The ribosome profiling strategy for monitoring translation in vivo by deep sequencing of ribosome-protected mRNA fragments. Nat Protoc. 2012 Jul 26;7(8):1534-50. PMID: 22836135.

H1643

Helodermin

H-His-Ser-Asp-Ala-Ile-Phe-Thr-Glu-Glu-Tyr-Ser-Lys-Leu-Leu-Ala-Lys-Leu-Ala-Leu-Gln-Lys-Tyr-Leu-Ala-Ser-Ile-Leu-Gly-Ser-Arg-Thr-Ser-Pro-Pro-Pro-NH_2

0.5 mg
1 mg
2.5 mg

Exendin 2

$C_{176}H_{283}N_{45}O_{51}$ FW: 3845.49 [89468-62-2] ≥95%

Found in *Heloderma*. It decreases blood pressure and inhibits proliferation of small cell lung cancer cells.

Uddman R, Goadsby PJ, Jansen-Olesen I, et al. Helospectin-like peptides: immunochemical localization and effects on isolated cerebral arteries and on local cerebral blood flow in the cat. J Cereb Blood Flow Metab. 1999 Jan;19(1):61-7. PMID: 9886356.

Tanaka Y, Horikawa N, Ishiro H, et al. Glibenclamide-sensitive mechanism is involved in helodermin-produced vasodilatation in rat mesenteric artery. Res Commun Mol Pathol Pharmacol. 1997 Nov;98(2):141-56. PMID: 9467823.

H1644

Helodormin

His-Ser-Asp-Ala-Ile-Phe-Thr-Gln-Gln-Tyr-Ser-Lys-Leu-Leu-Ala-Lys-Leu-Ala-Leu-Gln-Lys-Tyr-Leu-Ala-Ser-Ile-Leu-Gly-Ser-Arg-Thr-Ser-Pro-Pro-Pro-NH_2

1 mg

$C_{176}H_{285}N_{47}O_{49}$ FW: 3843.47 [89468-62-2] ≥98%

Helodermin analog found in *Heloderma*. It decreases blood pressure and inhibits proliferation of small cell lung cancer cells.

Uddman R, Goadsby PJ, Jansen-Olesen I, et al. Helospectin-like peptides: immunochemical localization and effects on isolated cerebral arteries and on local cerebral blood flow in the cat. J Cereb Blood Flow Metab. 1999 Jan;19(1):61-7. PMID: 9886356.

H1645

Helospectin I

H-His-Ser-Asp-Ala-Thr-Phe-Thr-Ala-Glu-Tyr-Ser-Lys-Leu-Leu-Ala-Lys-Leu-Ala-Leu-Gln-Lys-Tyr-Leu-Glu-Ser-Ile-Leu-Gly-Ser-Ser-Thr-Ser-Pro-Arg-Pro-Pro-Ser-Ser-OH

1 mg
2 mg
5 mg

Exendin 1

$C_{183}H_{293}N_{47}O_{59}$ FW: 4095.66 [93438-37-0] ≥95%

VIP-family peptide found in *Heloderma*. It decreases blood pressure and increases plasma glucagon levels.

Tsueshita T, Onyükusel H, Sethi V, et al. Helospectin I and II evoke vasodilation in the intact peripheral microcirculation. Peptides. 2004 Jan;25(1):65-9. PMID: 15003357.

Uddman R, Goadsby PJ, Jansen-Olesen I, et al. Helospectin-like peptides: immunochemical localization and effects on isolated cerebral arteries and on local cerebral blood flow in the cat. J Cereb Blood Flow Metab. 1999 Jan;19(1):61-7. PMID: 9886356.

H1646

Helospectin II

H-His-Ser-Asp-Ala-Thr-Phe-Thr-Ala-Glu-Tyr-Ser-Lys-Leu-Leu-Ala-Lys-Leu-Ala-Leu-Gln-Lys-Tyr-Leu-Glu-Ser-Ile-Leu-Gly-Ser-Ser-Thr-Ser-Pro-Arg-Pro-Pro-Ser-OH

1 mg
2 mg
5 mg

$C_{180}H_{288}N_{46}O_{57}$ FW: 4008.58 [93585-83-2] ≥95%

VIP-family peptide found in *Heloderma*. It decreases blood pressure.

Tsueshita T, Onyükusel H, Sethi V, et al. Helospectin I and II evoke vasodilation in the intact peripheral microcirculation. Peptides. 2004 Jan;25(1):65-9. PMID: 15003357.

H0100 Hemagglutinin-1 Peptide

1 mg
2 mg
5 mg

HA1 fragment 98-106; HA tag peptide; Influenza Hemagglutinin Peptide

H-Tyr-Pro-Tyr-Asp-Val-Pro-Asp-Tyr-Ala-OH

$C_{53}H_{67}N_9O_{17}$ FW: 1102.18 [92000-76-5] ≥95%

Hemagglutinin epitope that binds B cells and T cells.

Hatzifoti C, Heath AW. CD40-mediated enhancement of immune responses against three forms of influenza vaccine. Immunology. 2007 Sep;122(1):98-106. PMID: 17472718.

H1648 Hemorphin-7

1 mg
2 mg
5 mg

Tyr-Pro-Trp-Thr-Gln-Arg-Phe

$C_{49}H_{64}N_{12}O_{11}$ FW: 997.12 ≥95%

Endogenous opioid receptor agonist and ACE inhibitor derived from the β-chain of hemoglobin. It decreases nociception and blood pressure.

Lantz I, Glämsta EL, Talbäck L, et al. Hemorphins derived from hemoglobin have an inhibitory action on angiotensin converting enzyme activity. FEBS Lett. 1991 Aug 5;287(1-2):39-41. PMID: 1652464.

Liebmann C, Schrader U, Brantl V. Opioid receptor affinities of the blood-derived tetrapeptides hemorphin and cytochrophin. Eur J Pharmacol. 1989 Aug 3;166(3):523-6. PMID: 2553436.

H1658 Heparin Sodium

1 g

4,000-6,000 Da [9041-08-1] ≥98%

Endogenous glycosaminoglycan produced by mast cells and basophils. It binds antithrombin III, activating the protein and inhibiting binding and activation of thrombin and Factor Xa. It also binds ALK.

Murray PB, Lax I, Reshetnyak A, et al. Heparin is an activating ligand of the orphan receptor tyrosine kinase ALK. Sci Signal. 2015 Jan 20;8(360):ra6. PMID: 25605972.

Brkljacic J, Pauk M, Erjavec I, et al. Exogenous heparin binds and inhibits bone morphogenetic protein 6 biological activity. Int Orthop. 2013 Mar;37(3):529-41. PMID: 23307015.

Chuang YJ, Swanson R, Raja SM, et al. Heparin enhances the specificity of antithrombin for thrombin and factor Xa independent of the reactive center loop sequence. Evidence for an exosite determinant of factor Xa specificity in heparin-activated antithrombin. J Biol Chem. 2001 May 4;276(18):14961-71. PMID: 11278930.

H1657 Heparin-binding Peptide

0.5 mg
1 mg
2.5 mg

Fibronectin Adhesion-Promoting Peptide

H-Trp-Gln-Pro-Pro-Arg-Ala-Arg-Ile-OH

$C_{47}H_{74}N_{16}O_{10}$ FW: 1023.22 [125720-21-0] ≥95%

It binds heparin and matches sequences found on various viral proteins.

Chen HL, Her SY, Huang KC, et al. Identification of a heparin binding peptide from the Japanese encephalitis virus envelope protein. Biopolymers. 2010;94(3):331-8. PMID: 20069543.

Chon JH, Chaikof EL. Soluble heparin-binding peptides regulate chemokinesis and cell adhesive forces. Am J Physiol Cell Physiol. 2001 Jun;280(6):C1394-402. PMID: 11350734.

H0207 Hepatitis B Virus Core Protein (128-140)

0.5 mg
1 mg
2.5 mg

HBV Core protein (128-140)

H-Thr-Pro-Pro-Ala-Tyr-Arg-Pro-Pro-Asn-Ala-Pro-Ile-Leu-OH

$C_{66}H_{103}N_{17}O_{17}$ FW: 1406.64 ≥95%

B cell epitope found on hepatitis B viral core protein (128-140). Represents a sequence used to form the viral capsid.

Yang J, Liu N, Zhang T, et al. Prediction and identification of B-cell linear epitopes of hepatitis B e antigen. Nan Fang Yi Ke Da Xue Xue Bao. 2013 Feb;33(2):253-7. PMID: 23443783.

H1862 Heptaplatin

1 mg
5 mg
10 mg
25 mg

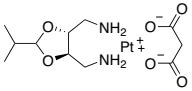

$C_{11}H_{20}N_2O_6Pt$ FW: 471.36 [146665-77-2] ≥98%

Platinum-based DNA cross-linker used to treat gastric cancer. It inhibits growth of head and neck squamous cell cancer cells.

Lee JW, Park JK, Lee SH, et al. Anti-tumor activity of heptaplatin in combination with 5-fluorouracil or paclitaxel against human head and neck cancer cells in vitro. Anticancer Drugs. 2006 Apr;17(4):377-84. PMID: 16549994.

Kim NK, Im SA, Kim DW, et al. Phase II clinical trial of SKI-2053R, a new platinum analog, in the treatment of patients with advanced gastric adenocarcinoma. Cancer. 1999 Oct 1;86(7):1109-15. PMID: 10506693.

Kim DK, Kim HT, Tai JH, et al. Pharmacokinetics and antitumor activity of a new platinum compound, cis-malonato[(4R,5R)-4,5-bis(aminomethyl)-2-isopropyl-1, 3- dioxolane]platinum(II), as determined by ex vivo pharmacodynamics. Cancer Chemother Pharmacol. 1995;37(1-2):1-6. PMID: 7497577.

H1662

HER2/neu (654-662) GP2

1 mg
2 mg
5 mg

ErbB2; EGFR2; CD340

Ile-Ile-Ser-Ala-Val-Val-Gly-Ile-Leu

$C_{42}H_{77}N_9O_{11}$ FW: 884.12 ≥95%

Peptide fragment of HER2/neu/erbB2 receptor. It is associated with breast cancer and other cancers.

Mitri Z, Constantine T, O'Regan R. The HER2 Receptor in Breast Cancer: Pathophysiology, Clinical Use, and New Advances in Therapy. Chemother Res Pract. 2012;2012:743193. PMID: 23320171.

Roy V, Perez EA. Beyond trastuzumab: small molecule tyrosine kinase inhibitors in HER-2-positive breast cancer. Oncologist. 2009 Nov;14(11):1061-9. PMID: 19887469.

H1663

HER2/neu Fragment (869-877)

1 mg
2 mg
5 mg

ErbB2; EGFR2

Leu-Leu-Asp-Ile-Asp-Glu-Thr-Glu-Tyr

$C_{49}H_{75}N_9O_{20}$ FW: 1110.19 ≥95%

HER2/neu/EGFR2 receptor fragment. This receptor is associated with breast cancer.

Mitri Z, Constantine T, O'Regan R. The HER2 Receptor in Breast Cancer: Pathophysiology, Clinical Use, and New Advances in Therapy. Chemother Res Pract. 2012;2012:743193. PMID: 23320171.

Roy V, Perez EA. Beyond trastuzumab: small molecule tyrosine kinase inhibitors in HER-2-positive breast cancer. Oncologist. 2009 Nov;14(11):1061-9. PMID: 19887469.

H1669

Herbimycin A

100 µg

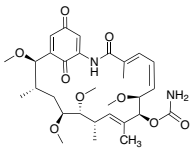

$C_{30}H_{42}N_2O_9$ FW: 574.66 [70563-58-5] ≥98%

Inhibitor of HSP90, PKC, Src, and Bcr-Abl. In inhibits proliferation of chronic myelogenous leukemia cells.

Kasai S, Kikuchi H. The inhibitory mechanisms of the tyrosine kinase inhibitors herbimycin a, genistein, and tyrphostin B48 with regard to the function of the aryl hydrocarbon receptor in Caco-2 cells. Biosci Biotechnol Biochem. 2010;74(1):36-43. PMID: 20057149.

Napolitano M, Bravo E. Activation of protein kinase C by phorbol esters in human macrophages reduces the metabolism of modified LDL by down-regulation of scavenger receptor activity. Int J Biochem Cell Biol. 2003 Jul;35(7):1127-43. PMID: 12672483.

Mucha DR, Myers CL, Schaeffer RC Jr. Endothelial contraction and monolayer hyperpermeability are regulated by Src kinase. Am J Physiol Heart Circ Physiol. 2003 Mar;284(3):H994-H1002. PMID: 12456392.

H1672

Hesperetin

1 g
5 g
10 g

Cyanidanon 4'-methyl ether 1626

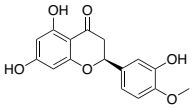

$C_{16}H_{14}O_6$ FW: 302.28 [520-33-2] ≥95%

L-type Ca^{2+} channel blocker found in citrus plants. It exhibits many activities, including inhibiting mechanical and thermal hyperalgesia and allodynia, increasing expression of antioxidative enzymes, preventing cardiac hypertrophy, cardiac dysfunction, and fibrosis, and inducing apoptosis in breast cancer cells.

Palit S, Kar S, Sharma G, et al. Hesperetin induces apoptosis in breast carcinoma by triggering accumulation of ROS and activation of ASK1/JNK pathway. J Cell Physiol. 2014 Sep 10. [Epub ahead of print]. PMID: 25204891.

Aswar M, Kute P, Mahajan S, et al. Protective effect of hesperetin in rat model of partial sciatic nerve ligation induced painful neuropathic pain: an evidence of anti-inflammatory and anti-oxidative activity. Pharmacol Biochem Behav. 2014 Sep;124:101-7. PMID: 24871567.

Liu Y, Niu L, Cui L, et al. Hesperetin inhibits rat coronary constriction by inhibiting $Ca^{(2+)}$ influx and enhancing voltage-gated $K^{(+)}$ channel currents of the myocytes. Eur J Pharmacol. 2014 Jul 15;735:193-201. PMID: 24751712.

H1673

Hesperidin

25 g
100 g

Cirantin

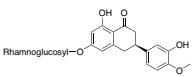

$C_{28}H_{34}O_{15}$ FW: 610.56 [520-26-3] ≥95%

COX-2 inhibitor found in citrus plants. It exhibits several biological activities, including decreasing levels of LDL, triglycerides, and total lipids, suppressing carrageenan-induced edema and inflammation, and preventing hormone-released changes in bone volume and thickness.

Guzmán-Gutiérrez SL, Navarrete A. Pharmacological exploration of the sedative mechanism of hesperidin identified as the active principle of Citrus *sinensis* flowers. Planta Med. 2009 Mar;75(4):295-301. PMID: 19219759.

Loscalzo LM, Wasowski C, Paladini AC, et al. Opioid receptors are involved in the sedative and antinociceptive effects of hesperidin as well as in its potentiation with benzodiazepines. Eur J Pharmacol. 2008 Feb 12;580(3):306-13. PMID: 18048026.

Hirata A, Murakami Y, Shoji M, et al. Kinetics of radical-scavenging activity of hesperetin and hesperidin and their inhibitory activity on COX-2 expression. Anticancer Res. 2005 Sep-Oct;25(5):3367-74. PMID: 16101151.

H1992

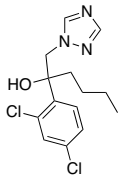

Hexaconazole

500 mg
5 g
25 g

$C_{14}H_{17}Cl_2N_3O$ FW: 314.21 [79983-71-4] ≥95%

Pesticide and demethylation inhibitor that prevents sterol synthesis and disrupts membrane function. It also induces production of apigenin-7-glucoside and other antioxidative compounds and inhibits growth of nitrogen-fixing bacteria.

Hojati M, Modarres-Sanavy SA, Ghanati F, et al. Hexaconazole induces antioxidant protection and apigenin-7-glucoside accumulation in Matricaria chamomilla plants subjected to drought stress. J Plant Physiol. 2011 May 15;168(8):782-91. PMID: 21208683.

Yilmaz S, Aksoy H, Unal F, et al. Genotoxic action of fungicide Conan 5FL (hexaconazole) on mammalian cells in vivo and in vitro. Genetika. 2008 Mar;44(3):323-8. PMID: 18664135.

Kalam A, Mukherjee AK. Influence of hexaconazole, carbofuran and ethion on soil microflora and dehydrogenase activities in soil and intact cell. Indian J Exp Biol. 2001 Jan;39(1):90-4. PMID: 11349536.

H1794

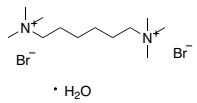

Hexamethonium Bromide Hydrate

10 g
25 g
100 g

C-6; Bistrium bromide

$C_{12}H_{30}Br_2N_2 \cdot xH_2O$ FW: 362.2 [55-97-0] ≥98%

Non-depolarizing NMJ blocker and nAChR antagonist. It has previously been used to treat hypertension. It inhibits sympathetic nervous system activity and acts as a skeletal muscle relaxant.

Barnett AJ, Fraser JR. The mechanism of arterial hypertension: a comparison of the effects of hexamethonium bromide in hypertensive and normotensive persons. Australas Ann Med. 1954 May;3(2):152-9. PMID: 13159745.

H1892

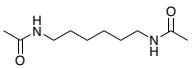

Hexamethylene Bisacetamide

25 g
50 g

HMBA

$C_{10}H_{20}N_2O_2$ FW: 200.28 [3073-59-4] ≥98%

HEXIM1 activator that inhibits transcription elongation factor b (P-TEFb) and modulates RNA polymerase II and mRNA synthesis. It induces differentiation and apoptosis in cancer cells.

Lew QJ, Chia YL, Chu KL, et al. Identification of HEXIM1 as a positive regulator of p53. J Biol Chem. 2012 Oct 19;287(43):36443-54. PMID: 22948151.

Dey A, Wong E, Kua N, et al. Hexamethylene bisacetamide (HMBA) simultaneously targets AKT and MAPK pathway and represses NF kappaB activity: implications for cancer therapy. Cell Cycle. 2008 Dec;7(23):3759-67. PMID: 19029824.

Zhang Z, Liong EC, Lau TY, et al. Induction of apoptosis by hexamethylene bisacetamide is p53-dependent associated with telomerase activity but not with terminal differentiation. Int J Oncol. 2000 May;16(5):887-92. PMID: 10762623.

H1893

His-D-2-Me-Trp-Ala-Trp-D-Phe-Lys-NH_2

Hexarelin

1 mg
5 mg
50 mg

Examorelin

$C_{47}H_{58}N_{12}O_6$ FW: 887 [140703-51-1] ≥95%

Synthetic ghrelin analog and ghrelin receptor agonist. It protects cardiac function in myocardial infarction models, prevents deposition of collagen and suppresses collagen expression, and decreases ovulation and number of offspring produced.

Mao Y, Tokudome T, Kishimoto I, et al. One dose of oral hexarelin protects chronic cardiac function after myocardial infarction. Peptides. 2014 Apr 18;56C:156-162. PMID: 24747279.

Xu X, Ding F, Pang J, et al. Chronic administration of hexarelin attenuates cardiac fibrosis in the spontaneously hypertensive rat. Am J Physiol Heart Circ Physiol. 2012 Sep 15;303(6):H703-11. PMID: 22842067.

H1894

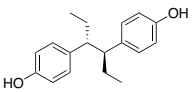

Hexestrol

1 g
5 g

Dihydrodiethylstilbestrol; Cycloestrol

$C_{18}H_{22}O_2$ FW: 270.37 [84-16-2] ≥98%

Synthetic ER agonist, microtubule polymerization inhibitor, and potential carcinogen. It induces mitotic arrest, aneuploidy, and DNA adduct formation.

Cavalieri EL, Rogan EG. A unifying mechanism in the initiation of cancer and other diseases by catechol quinones. Ann N Y Acad Sci. 2004 Dec;1028:247-57. PMID: 15650250.

Chaudoreille MM, Peyrot V, Braguer D, et al. Qualitative study of the interaction mechanism of estrogenic drugs with tubulin. Biochem Pharmacol. 1991 Mar 1;41(5):685-93. PMID: 1847811.

Wheeler WJ, Cherry LM, Downs T, et al. Mitotic inhibition and aneuploidy induction by naturally occurring and synthetic estrogens in Chinese hamster cells in vitro. Mutat Res. 1986 Jul;171(1):31-41. PMID: 3724781.

H1695

S-Hexylglutathione

100 mg
250 mg
1 g

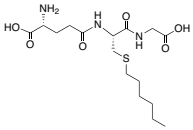

$C_{16}H_{29}N_3O_6S$ FW: 391.5 [24425-56-7] ≥98%

Glutathione-S-transferase inhibitor used to study the effects of phase II enzymes and glutathione.

Imaizumi N, Aniya Y. The role of a membrane-bound glutathione transferase in the peroxynitrite-induced mitochondrial permeability transition pore: formation of a disulfide-linked protein complex. Arch Biochem Biophys. 2011 Dec 15;516(2):160-72. PMID: 22050912.

Ulziikhishig E, Lee KK, Hossain QS, et al. Inhibition of mitochondrial membrane bound-glutathione transferase by mitochondrial permeability transition inhibitors including cyclosporin A. Life Sci. 2010 May 8;86(19-20):726-32. PMID: 20226794.

H3272

His Tag

5 mg

Polyhistidine tag; Hex histidine tag

His-His-His-His-His-His

$C_{36}H_{42}N_{18}O_6$ FW: 822.85 ≥98%

Six-histidine peptide used for affinity column purification of proteins and peptides.

Zhao C, Hellman LM, Zhan X, et al. Hexahistidine-tag-specific optical probes for analyses of proteins and their interactions. Anal Biochem. 2010 Apr 15;399(2):237-45. PMID: 20036207.

H3273

Histatin 5

0.5 mg
1 mg
2.5 mg

H-Asp-Ser-His-Ala-Lys-Arg-His-His-Gly-Tyr-Lys-Arg-Lys-Phe-His-Glu-Lys-His-His-Ser-His-Arg-Gly-Tyr-OH

$C_{133}H_{195}N_{51}O_{33}$ FW: 3036.36 [115966-68-2] ≥95%

Salivary gland peptide that binds bacterial DNA. It inhibits production of pro-inflammatory cytokines and causes ion flux-induced cell death of *Candida*.

Borgwardt DS, Martin AD, Van Hemert JR, et al. Histatin 5 binds to *Porphyromonas* gingivalis hemagglutinin B (HagB) and alters HagB-induced chemokine responses. Sci Rep. 2014 Jan 29;4:3904. PMID: 24473528.

Huo L, Zhang K, Ling J, et al. Antimicrobial and DNA-binding activities of the peptide fragments of human lactoferrin and histatin 5 against *Streptococcus* mutans. Arch Oral Biol. 2011 Sep;56(9):869-76. PMID: 21382611.

H3277

Histrelin Acetate

Please inquire

Pyr-His-Trp-Ser-Tyr-D-His(Bzl)-Leu-Arg-Pro-NHEt

$C_{66}H_{86}N_{18}O_{12}$ FW: 1323.52 [76712-82-8] ≥95%

GnRH analog and GnRH receptor agonist used to treat precocious puberty and to suppress estrogen and testosterone levels in prostate cancer patients. Over chronic administration, it decreases release of FSH and LH.

Lewis KA, Goldyn AK, West KW, et al. A single histrelin implant is effective for 2 years for treatment of central precocious puberty. J Pediatr. 2013 Oct;163(4):1214-6. PMID: 23809043.

Shore N, Cookson MS, Gittelman MC. Long-term efficacy and tolerability of once-yearly histrelin acetate subcutaneous implant in patients with advanced prostate cancer. BJU Int. 2012 Jan;109(2):226-32. PMID: 21851539.

H3275

HIV Integrase Protein Inhibitor HCKFWW

1 mg
2 mg
5 mg

$C_{46}H_{55}N_{11}O_7S$ FW: 906.1 ≥95%

His-Cys-Lys-Phe-Trp-Trp

Inhibitor of HIV integrase-mediated 3' processing and integration. It is active against HIV-1, HIV-2, FIV, and Moloney murine leukemia virus.

Puras Lutzke RA, Eppens NA, Weber PA, et al. Identification of a hexapeptide inhibitor of the human immunodeficiency virus integrase protein by using a combinatorial chemical library. Proc Natl Acad Sci U S A. 1995 Dec 5;92(25):11456-60. PMID: 8524782.

H3274

HIV p17 Gag (77-85)

1 mg
2 mg
5 mg

$C_{44}H_{72}N_{10}O_{15}$ FW: 981.1 ≥98%

Ser-Leu-Tyr-Asn-Thr-Val-Ala-Thr-Leu

Immunodominant HIV Gag epitope peptide used to prime activated CD8+ cytotoxic T cells.

Kan-Mitchell J, Bajcz M, Schaubert KL, et al. Degeneracy and repertoire of the human HIV-1 Gag p17(77-85) CTL response. J Immunol. 2006 Jun 1;176(11):6690-701. PMID: 16709828.

Kan-Mitchell J, Bisikirska B, Wong-Staal F, et al. The HIV-1 HLA-A2-SLYNTVATL is a help-independent CTL epitope. J Immunol. 2004 May 1;172(9):5249-61. PMID: 15100263.

H3276

HIV Protease Substrate ARVLAEA

1 mg

$C_{33}H_{59}N_{11}O_{10}$ FW: 769.9 ≥98%

Ac-Ala-Arg-Val-Leu-Ala-Glu-Ala-NH_2

HIV protease epitope that binds the capsid CA-p2 cleavage site.

Prabu-Jeyabalan M, Nalivaika E, Schiffer CA. How does a symmetric dimer recognize an asymmetric substrate? A substrate complex of HIV-1 protease. J Mol Biol. 2000 Sep 1;301(5):1207-20. PMID: 10966816.

H5748

D,L-Homocysteine Thiolactone Hydrochloride

50 g
100 g

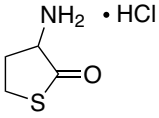

$C_4H_7NOS \bullet HCl$ FW: 153.63 [6038-19-3] ≥98%

Cysteine derivative that binds to and induces conformational changes in various plasma proteins, slowing coagulation and inducing oxidative stress. It decreases left ventricular systolic blood pressure and cardiac force and induces seizures in vivo.

Hrnčić D, Rašić-Marković A, Macut D, et al. Homocysteine thiolactone-induced seizures in adult rats are aggravated by inhibition of inducible nitric oxide synthase. Hum Exp Toxicol. 2014 May;33(5):496-503. PMID: 23760255.

Genoud V, Lauricella AM, Kordich LC, et al. Impact of homocysteine-thiolactone on plasma fibrin networks. J Thromb Thrombolysis. 2014 Mar 23. [Epub ahead of print]. PMID: 24659173.

Zivkovic V, Jakovljevic V, Pechanova O, et al. Effects of DL-homocysteine thiolactone on cardiac contractility, coronary flow, and oxidative stress markers in the isolated rat heart: the role of different gasotransmitters. Biomed Res Int. 2013;2013:318471. PMID: 24350259.

H5750

Homoharringtonine

1 mg
5 mg
10 mg

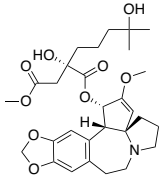

$C_{29}H_{39}NO_9$ FW: 545.62 [26833-87-4] ≥97%

Found in *Cephalotaxus* that blocks the A site of ribosomes, inhibiting ribosomal protein synthesis. It is used to treat chronic myelogenous leukemia. It also decreases CD34+ CD117+ cell levels.

Gandhi V, Plunkett W, Cortes JE. Omacetaxine: a protein translation inhibitor for treatment of chronic myelogenous leukemia. Clin Cancer Res. 2014 Apr 1;20(7):1735-40. PMID: 24501394.

Daver N, Vega-Ruiz A, Kantarjian HM, et al. A phase II open-label study of the intravenous administration of homoharringtonine in the treatment of myelodysplastic syndrome. Eur J Cancer Care (Engl). 2013 Sep;22(5):605-11. PMID: 23701251.

Li YF, Deng Z, Din BH, et al. Effect of homoharringtonine on bone marrow CD34 + CD117 + cells in patients with chronic myelogenous leukemia. Leuk Lymphoma. 2012 May;53(5):934-9. PMID: 22054289.

H5654

Honokiol

10 mg
25 mg
100 mg

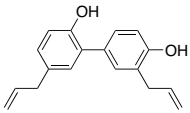

$C_{18}H_{18}O_2$ FW: 266.33 [35354-74-6] ≥98%

GABA-A receptor potentiator and PPARγ agonist found in species of *Magnolia*. It inhibits angiogenesis in epithelial cells, suppresses growth and proliferation in oral squamous cell carcinoma cells, decreases platelet aggregation, and suppresses cell entry and replication of hepatitis C virus and HIV-1.

Atanasov AG, Wang JN, Gu SP, et al. Honokiol: a non-adipogenic PPARγ agonist from nature. Biochim Biophys Acta. 2013 Oct;1830(10):4813-9. PMID: 23811337.

Zhang P, Liu X, Zhu Y, et al. Honokiol inhibits the inflammatory reaction during cerebral ischemia reperfusion by suppressing NF-κB activation and cytokine production of glial cells. Neurosci Lett. 2013 Feb 8;534:123-7. PMID: 23262090.

Lan KH, Wang YW, Lee WP, et al. Multiple effects of Honokiol on the life cycle of hepatitis C virus. Liver Int. 2012 Jul;32(6):989-97. PMID: 22098176.

H2876

H-Trp-Gly-OH

1 mg

Trp-Gly

$C_{13}H_{13}N_3O_2$ FW: 261.28 ≥98%

Used to study UV absorption and fluorescence.

Ehlerding A, Wyer JA, Zettergren H, et al. UV photodissociation of protonated Gly-Trp and Trp-Gly dipeptides and their complexes with crown ether in an electrostatic ion storage ring. J Phys Chem A. 2010 Jan 14;114(1):299-303. PMID: 19958010.

H8048

Human Follicular Gonadotropin Releasing Peptide

1 mg

hF-GRP

Thr-Asp-Thr-Ser-His-His-Asp-Gln-Asp-His-Pro-Thr-Phe-Asn

$C_{68}H_{94}N_{22}O_{27}$ FW: 1651.6 ≥98%

Stimulates release of LH and FSH.

Ramasharma K, Yamashiro D, Li CH. Human follicular gonadotropin releasing peptide analogs. Evaluation of biological (in vitro) and immunological activity. Int J Pept Protein Res. 1988 Dec;32(6):419-24. PMID: 3149951.

H3278

HIV Reverse Transcriptase A2.1 Peptide

1 mg
2 mg
5 mg

HIV-1 RT Peptide

H-Ile-Leu-Lys-Glu-Pro-Val-His-Gly-Val-OH

$C_{46}H_{78}N_{12}O_{12}$ FW: 991.21 ≥95%

HIV-1 reverse transcriptase A2.1 epitope recognizable by CD8+ T cells.

Peter K, Men Y, Pantaleo G, et al. Induction of a cytotoxic T-cell response to HIV-1 proteins with short synthetic peptides and human compatible adjuvants. Vaccine. 2001 Jul 20;19(30):4121-9. PMID: 11457536.

Shankar P, Sprang H, Lieberman J. Effective lysis of HIV-1-infected primary CD4+ T cells by a cytotoxic T-lymphocyte clone directed against a novel A2-restricted reverse-transcriptase epitope. J Acquir Immune Defic Syndr Hum Retrovirol. 1998 Oct 1;19(2):111-20. PMID: 9768618.

H2980

Humanin, human

0.5 mg
1 mg
2.5 mg

Met-Ala-Pro-Arg-Gly-Phe-Ser-Cys-Leu-Leu-Leu-Leu-Thr-Ser-Glu-Ile-Asp-Leu-Pro-Val-Lys-Arg-Arg-Ala

$C_{119}H_{204}N_{34}O_{32}S_2$ FW: 2687.28 [330936-69-1] ≥95%

Endogenous FPRL1/2 receptor agonist. It increases levels of antioxidative enzymes and inhibits amyloid-β-induced neuronal death.

Mottaghi-Dastjerdi N, Soltany-Rezaee-Rad M, Sepehrizadeh Z, et al. Genome expression analysis by suppression subtractive hybridization identified overexpression of Humanin, a target gene in gastric cancer chemoresistance. Daru. 2014 Jan 8;22(1):14. PMID: 24401285.

Zhao ST, Huang XT, Zhang C, et al. Humanin protects cortical neurons from ischemia and reperfusion injury by the increased activity of superoxide dismutase. Neurochem Res. 2012 Jan;37(1):153-60. PMID: 21935731.

H8162

(−)-Huperzine A

1 mg
5 mg

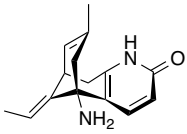

HupA

$C_{15}H_{18}N_2O$ FW: 242.32 [102518-79-6] ≥97%

AChE inhibitor and NMDA receptor antagonist found in *Huperzia serrata*. It exhibits a wide variety of biological activities, including improving cognition, memory, and mood, protecting against organophosphate-induced seizure and status epilepticus, and blocking chemical, thermal, and mechanical pain stimulation.

Yu D, Thakor DK, Han I, et al. Alleviation of chronic pain following rat spinal cord compression injury with multimodal actions of huperzine A. Proc Natl Acad Sci U S A. 2013 Feb 19;110(8):E746-55. PMID: 23386718.

Rafii MS, Walsh S, Little JT, et al. A phase II trial of huperzine A in mild to moderate Alzheimer disease. Neurology. 2011 Apr 19;76(16):1389-94. doi: PMID: 21502597.

Park P, Schachter S, Yaksh T. Intrathecal huperzine A increases thermal escape latency and decreases flinching behavior in the formalin test in rats. Neurosci Lett. 2010 Feb 5;470(1):6-9. PMID: 20026382.

H9801

Hyaluronic Acid Sodium

100 mg
500 mg
1 g

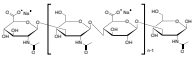

ARTZ

$(C_{14}H_{20}NO_{11}Na)_n$ FW: ~1,000,000 [9067-32-7] ≥95%

Endogenous anionic non-sulfated glycosaminoglycan found in connective tissue and synovial fluid. It binds cell surface proteins and causes inflammation.

Chen B, Miller RJ, Dhal PK. Hyaluronic acid-based drug conjugates: state-of-the-art and perspectives. J Biomed Nanotechnol. 2014 Jan;10(1):4-16. PMID: 24724495.

Rostami S, Parsian H. Hyaluronic Acid: from biochemical characteristics to its clinical translation in assessment of liver fibrosis. Hepat Mon. 2013 Dec 14;13(12):e13787. PMID: 24403913.

Yung S, Cheung KF, Zhang Q, et al. Mediators of inflammation and their effect on resident renal cells: implications in lupus nephritis. Clin Dev Immunol. 2013;2013:317682. PMID: 24171032.

H9614

Hydrochlorothiazide

5 g
25 g

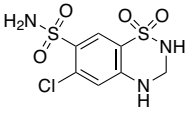

$C_7H_8ClN_3O_4S_2$ FW: 297.74 [58-93-5] ≥98%

Thiazide diuretic, NCCT inhibitor, and carbonic anhydrase I inhibitor used to treat hypertension and chronic kidney disease. It decreases Na^+ reabsorption and blood volume, increases reabsorption of Ca^{2+}, and enhances production of TT dimers under UVA light.

Kunisada M, Masaki T, Ono R, et al. Hydrochlorothiazide enhances UVA-induced DNA damage. Photochem Photobiol. 2013 May-Jun;89(3):649-54. PMID: 23331297.

Karadsheh F, Weir MR. Thiazide and thiazide-like diuretics: an opportunity to reduce blood pressure in patients with advanced kidney disease. Curr Hypertens Rep. 2012 Oct;14(5):416-20. PMID: 22886538.

Duarte JD, Cooper-DeHoff RM. Mechanisms for blood pressure lowering and metabolic effects of thiazide and thiazide-like diuretics. Expert Rev Cardiovasc Ther. 2010 Jun;8(6):793-802. PMID: 20528637.

H9611

Hydrocortisone

5 g
10 g
25 g

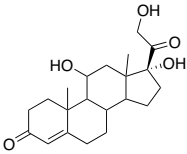

Cortisol

$C_{21}H_{30}O_5$ FW: 362.46 [50-23-7] ≥98%

Endogenous hormone and glucocorticoid receptor agonist involved in stress signaling. It is used to treat dermatologic diseases and severe allergic reactions. It stimulates gluconeogenesis, inhibits inflammatory cytokine production, and shifts the immune response from Th1 to Th2 subtype.

Angelier F, Wingfield JC. Importance of the glucocorticoid stress response in a changing world: theory, hypotheses and perspectives. Gen Comp Endocrinol. 2013 Sep 1;190:118-28. PMID: 23770214.

Tarchalska-Kryńska B. Glucocorticosteroids: mechanism of action, pharmacological effects, pharmacokinetics and adverse effects. Otolaryngol Pol. 1994;48 Suppl 17:41-8. PMID: 8090502.

H9612 Hydrocortisone 21-Acetate

1 g
5 g
10 g

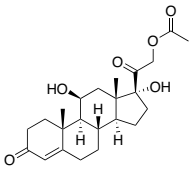

$C_{23}H_{32}O_6$ FW: 404.5 [50-03-3] ≥98%

Glucocorticoid receptor agonist involved in stress signaling used to treat skin diseases and allergic reactions. It stimulates gluconeogenesis, inhibits inflammatory cytokine production, and shifts the immune response from Th1 to Th2 subtype.

Angelier F, Wingfield JC. Importance of the glucocorticoid stress response in a changing world: theory, hypotheses and perspectives. Gen Comp Endocrinol. 2013 Sep 1;190:118-28. PMID: 23770214.

Tarchalska-Kryńska B. Glucocorticosteroids: mechanism of action, pharmacological effects, pharmacokinetics and adverse effects. Otolaryngol Pol. 1994;48 Suppl 17:41-8. PMID: 8090502.

H9618 Hydroquinone

50 g

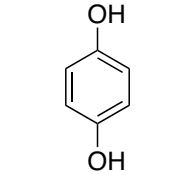

$C_6H_6O_2$ FW: 110.11 [123-31-9] ≥96%

Oxidoreductant and potential topoisomerase II inhibitor commercially used in skin whitening treatments and photography development. It may induce DNA damage.

Mondrala S, Eastmond DA. Topoisomerase II inhibition by the bioactivated benzene metabolite hydroquinone involves multiple mechanisms. Chem Biol Interact. 2010 Mar 19;184(1-2):259-68. PMID: 20034485.

Ji Z, Zhang L, Guo W, et al. The benzene metabolite, hydroquinone and etoposide both induce endoreduplication in human lymphoblastoid TK6 cells. Mutagenesis. 2009 Jul;24(4):367-72. PMID: 19491217.

H9712 (E)-4-Hydroxytamoxifen

5 mg
10 mg
25 mg

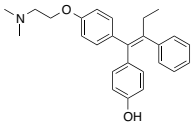

$C_{26}H_{29}NO_2$ FW: 387.51 [174592-47-3] ≥97%

SERM and active metabolite of tamoxifen. The E isomer is less active than the Z isomer. It induces autophagy, vacuole formation, and KRAS degradation in cancer cells and decreases contractility in myocytes.

Asp ML, Martindale JJ, Metzger JM. Direct, differential effects of tamoxifen, 4-hydroxytamoxifen, and raloxifene on cardiac myocyte contractility and calcium handling. PLoS One. 2013 Oct 24;8(10):e78768. PMID: 24205315.

Kohli L, Kaza N, Coric T, et al. 4-Hydroxytamoxifen induces autophagic death through K-Ras degradation. Cancer Res. 2013 Jul 15;73(14):4395-405. PMID: 23722551.

Schwartz JA, Zhong L, Deighton-Collins S, et al. Mutations targeted to a predicted helix in the extreme carboxyl-terminal region of the human estrogen receptor-alpha alter its response to estradiol and 4-hydroxytamoxifen. J Biol Chem. 2002 Apr 12;277(15):13202-9. Erratum in: J Biol Chem 2002 Jul 5;277(27):24842. PMID: 11823467.

H9711 (Z)-4-Hydroxytamoxifen

5 mg
10 mg
25 mg

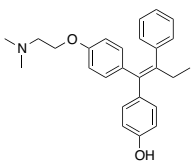

$C_{26}H_{29}NO_2$ FW: 387.51 [68047-06-3] ≥98%

SERM and active metabolite of tamoxifen. The Z isomer is more active than the E isomer. It induces autophagy, vacuole formation, and KRAS degradation in cancer cells and decreases contractility in myocytes.

Asp ML, Martindale JJ, Metzger JM. Direct, differential effects of tamoxifen, 4-hydroxytamoxifen, and raloxifene on cardiac myocyte contractility and calcium handling. PLoS One. 2013 Oct 24;8(10):e78768. PMID: 24205315.

Kohli L, Kaza N, Coric T, et al. 4-Hydroxytamoxifen induces autophagic death through K-Ras degradation. Cancer Res. 2013 Jul 15;73(14):4395-405. PMID: 23722551.

Schwartz JA, Zhong L, Deighton-Collins S, et al. Mutations targeted to a predicted helix in the extreme carboxyl-terminal region of the human estrogen receptor-alpha alter its response to estradiol and 4-hydroxytamoxifen. J Biol Chem. 2002 Apr 12;277(15):13202-9. Erratum in: J Biol Chem 2002 Jul 5;277(27):24842. PMID: 11823467.

H9716 (E,Z)-4-Hydroxytamoxifen

5 mg
10 mg
25 mg

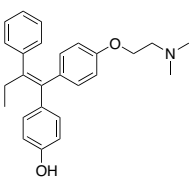

$C_{26}H_{29}NO_2$ FW: 387.51 [68392-35-8] ≥97%

SERM and active metabolite of tamoxifen. It is a mixture of cis and trans isomers. It induces autophagy, vacuole formation, and KRAS degradation in cancer cells and decreases contractility in myocytes.

Asp ML, Martindale JJ, Metzger JM. Direct, differential effects of tamoxifen, 4-hydroxytamoxifen, and raloxifene on cardiac myocyte contractility and calcium handling. PLoS One. 2013 Oct 24;8(10):e78768. PMID: 24205315.

Kohli L, Kaza N, Coric T, et al. 4-Hydroxytamoxifen induces autophagic death through K-Ras degradation. Cancer Res. 2013 Jul 15;73(14):4395-405. PMID: 23722551.

Schwartz JA, Zhong L, Deighton-Collins S, et al. Mutations targeted to a predicted helix in the extreme carboxyl-terminal region of the human estrogen receptor-alpha alter its response to estradiol and 4-hydroxytamoxifen. J Biol Chem. 2002 Apr 12;277(15):13202-9. Erratum in: J Biol Chem 2002 Jul 5;277(27):24842. PMID: 11823467.

H9715

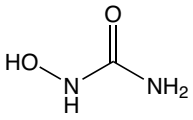

Hydroxyurea

Hydroxycarbamide

$CH_4N_2O_2$ FW: 76.06 [127-07-1] ≥98%

5 g
10 g
50 g
100 g

Fetal hemoglobin stimulator and ribonucleotide reductase inhibitor used to treat sickle cell anemia, myeloproliferative disorders, and leukemias. It decreases the production of deoxynucleotides and also increases levels of NO in the blood.

Amaru Calzada A, Pedrini O, Finazzi G, et al. Givinostat and hydroxyurea synergize in vitro to induce apoptosis of cells from JAK2(V617F) myeloproliferative neoplasm patients. Exp Hematol. 2013 Mar;41(3):253-60.e2. PMID: 23111067.

Vankayala SL, Hargis JC, Woodcock HL. Unlocking the binding and reaction mechanism of hydroxyurea substrates as biological nitric oxide donors. J Chem Inf Model. 2012 May 25;52(5):1288-97. PMID: 22519847.

H9717

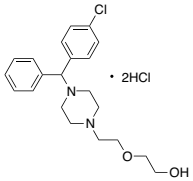

Hydroxyzine Dihydrochloride

$C_{21}H_{27}ClN_2O_2 \cdot 2HCl$ FW: 447.83 [2192-20-3] ≥98%

1 g
5 g
10 g

Histamine H1 receptor inverse agonist and antagonist at 5-HT2A receptors, dopamine D1/2 receptors, and α1-adrenergic receptors. It also acts as a FIASMA, decrease allergic responses, and induces sedation.

Llorca PM, Spadone C, Sol O, et al. Efficacy and safety of hydroxyzine in the treatment of generalized anxiety disorder: a 3-month double-blind study. J Clin Psychiatry. 2002 Nov;63(11):1020-7. PMID: 12444816.

Minogiannis P, El-Mansoury M, Betances JA, et al. Hydroxyzine inhibits neurogenic bladder mast cell activation. Int J Immunopharmacol. 1998 Oct;20(10):553-63. PMID: 9839659.

Haraguchi K, Ito K, Kotaki H, et al. Prediction of drug-induced catalepsy based on dopamine D1, D2, and muscarinic acetylcholine receptor occupancies. Drug Metab Dispos. 1997 Jun;25(6):675-84. PMID: 9193868.

H9726

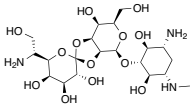

Hygromycin B

$C_{20}H_{37}N_3O_{13}$ FW: 527.52 [31282-04-9] ≥98.0%

50 mg
100 mg
250 mg
1 g

Protein translocation inhibitor that suppresses protein and RNA synthesis of bacteria and viruses by inducing misreadings during translation.

Brodersen DE, Clemons WM Jr, Carter AP, et al. The structural basis for the action of the antibiotics tetracycline, pactamycin, and hygromycin B on the 30S ribosomal subunit. Cell. 2000 Dec 22;103(7):1143-54. PMID: 11163189.

Ro YT, Scheffter SM, Patterson JL. Hygromycin B resistance mediates elimination of *Leishmania* virus from persistently infected parasites. J Virol. 1997 Dec;71(12):8991-8. PMID: 9371555.

Macintyre G, Woods DE, Anderson R. Hygromycin B inhibits synthesis of murine coronavirus RNA. Antimicrob Agents Chemother. 1991 Dec;35(12):2630-3. PMID: 1667257.

H9759

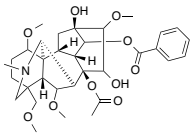

Hypaconitine

$C_{33}H_{45}NO_{10}$ FW: 615.71 [6900-87-4] ≥90%

10 mg
25 mg
100 mg

Voltage-gated Na^+ channel modulator found in *Aconitum*. It inhibits end plate potentials in isolated phrenic nerve-diaphragm muscles, blocking transmission at the neuromuscular junction.

Muroi M, Kimura I, Kimura M. Blocking effects of hypaconitine and aconitine on nerve action potentials in phrenic nerve-diaphragm muscles of mice. Neuropharmacology. 1990 Jun;29(6):567-72. PMID: 2385329.

Kimura M, Muroi M, Kimura I, et al. Hypaconitine, the dominant constituent responsible for the neuromuscular blocking action of the Japanese-sino medicine "bushi" (aconite root). Jpn J Pharmacol. 1988 Oct;48(2):290-3. PMID: 3210453.

H9863

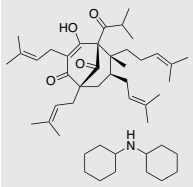

Hyperforin Dicyclohexylammonium

NEW

$C_{35}H_{52}O_4 \cdot C_{12}H_{23}N$ FW: 718.1 [238074-03-8] ≥97%

500 µg
1 mg

Stable salt form of hyperforin, a compound found in *Hypericum perforatum*. It induces cell cycle arrest and apoptosis in chronic myelogenous leukemia cells, prevents LPS- and substance P-induced release of IL-6 in astrocytoma cells, and suppresses the development of croton oil-induced edema.

Liu JY, Liu Z, Wang DM, et al. Induction of apoptosis in K562 cells by dicyclohexylammonium salt of hyperforin through a mitochondrial-related pathway. Chem Biol Interact. 2011 Apr 25;190(2-3):91-101. PMID: 21376709.

Sosa S, Pace R, Bornancin A, et al. Topical anti-inflammatory activity of extracts and compounds from *Hypericum perforatum* L. J Pharm Pharmacol. 2007 May;59(5):703-9. PMID: 17524236.

Gobbi M, Moia M, Funicello M, et al. In vitro effects of the dicyclohexylammonium salt of hyperforin on interleukin-6 release in different experimental models. Planta Med. 2004 Jul;70(7):680-2. PMID: 15303261.

H9861

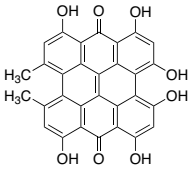

Hypericin

Hypericum red

$C_{30}H_{16}O_8$ FW: 504.44 [548-04-9] ≥97%

1 mg
5 mg

Inhibitor of dopamine β-hydroxylase, proteasomes and N-type and P/Q-type Ca^{2+} channels found in Hypericum. It decreases activation of PKC and neuropathic pain and induces apoptosis and cell death in epidermoid carcinoma cells when stimulated with UV light.

Chang Y, Wang SJ. Hypericin, the active component of St. John's wort, inhibits glutamate release in the rat cerebrocortical synaptosomes via a mitogen-activated protein kinase-dependent pathway. Eur J Pharmacol. 2010 May 25;634(1-3):53-61. PMID: 20193678.

Galeotti N, Vivoli E, Bilia AR, et al. St. John's Wort reduces neuropathic pain through a hypericin-mediated inhibition of the protein kinase Cgamma and epsilon activity. Biochem Pharmacol. 2010 May 1;79(9):1327-36. PMID: 20045676.

Berlanda J, Kiesslich T, Oberdanner CB, et al. Characterization of apoptosis induced by photodynamic treatment with hypericin in A431 human epidermoid carcinoma cells. J Environ Pathol Toxicol Oncol. 2006;25(1-2):173-88. PMID: 16566716.

H9661

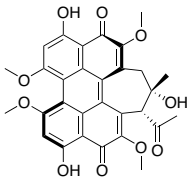

Hypocrellin A

$C_{30}H_{26}O_{10}$ FW: 546.52

1 mg
5 mg
10 mg
25 mg
100 mg

It prevents MHC II antigen presentation, increases levels of ROS, and induces cell wall damage in *Staphylococcus*, *Salmonella*, *Escherichia*, and *Bacillus*.

Du W, Sun C, Liang Z, et al. Antibacterial activity of hypocrellin A against *Staphylococcus aureus*. World J Microbiol Biotechnol. 2012 Nov;28(11):3151-7. PMID: 22864599.

Park S, Im SA, Kim KH, et al. Immunomodulatory Effects of Hypocrellin A on MHC-restricted Antigen Processing. Immune Netw. 2011 Dec;11(6):412-5. PMID: 22346783.

Su Y, Sun J, Rao S, et al. Photodynamic antimicrobial activity of hypocrellin A. J Photochem Photobiol B. 2011 Apr 4;103(1):29-34. PMID: 21300554.

H9662

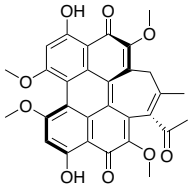

Hypocrellin B

$C_{30}H_{24}O_9$ FW: 528.51 [123940-54-5] ≥90%

1 mg
5 mg
10 mg
25 mg
100 mg

It causes DNA strand breakage, induces apoptosis in ovarian cancer cells, and inhibits proliferation of *Staphylococcus* by increasing ROS levels and damaging cell walls.

Jiang Y, Leung AW, Wang X, et al. Effect of photodynamic therapy with hypocrellin B on apoptosis, adhesion, and migration of cancer cells. Int J Radiat Biol. 2014 Jul;90(7):575-9. PMID: 24661233.

Jiang Y, Leung AW, Wang X, et al. Inactivation of *Staphylococcus aureus* by photodynamic action of hypocrellin B. Photodiagnosis Photodyn Ther. 2013 Dec;10(4):600-6. PMID: 24284117.

Babu A, Jeyasubramanian K, Gunasekaran P, et al. Gelatin nanocarrier enables efficient delivery and phototoxicity of hypocrellin B against a mice tumour model. J Biomed Nanotechnol. 2012 Feb;8(1):43-56. PMID: 22515093.

H9862

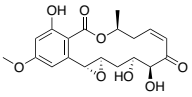

Hypothemycin

$C_{19}H_{22}O_8$ FW: 378.37 [76958-67-3] ≥96%

1 mg
5 mg

Found in *Setophoma*. It inhibits cell survival in melanoma and colon cancer cells and disrupts cell wall and endomembrane function in species of *Pernophythora*.

El-Elimat T, Figueroa M, Raja HA, et al. Biosynthetically Distinct Cytotoxic Polyketides from *Setophoma* terrestris. European J Org Chem. 2015 Jan 1;2015(1):109-121. PMID: 25574154.

Xu L, Xue J, Wu P, et al. Antifungal activity of hypothemycin against Peronophythora litchii in vitro and in vivo. J Agric Food Chem. 2013 Oct 23;61(42):10091-5. PMID: 24106914.

Nishino M, Choy JW, Gushwa NN, et al. Hypothemycin, a fungal natural product, identifies therapeutic targets in *Trypanosoma brucei* [corrected]. Elife. 2013 Jul 9;2:e00712. PMID: 23853713.

H9763

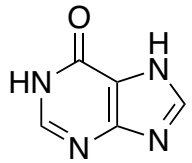

Hypoxanthine

Sarcine; Sarkin

$C_5H_4N_4O$ FW: 136.11 [68-94-0] ≥98%

5 g
25 g
100 g

Endogenous xanthine derivative. It is used as a biomarker to indicate freshness in commercial meat and fish consumption.

Ipata PL, Balestri F. The functional logic of cytosolic 5'-nucleotidases. Curr Med Chem. 2013;20(34):4205-16. PMID: 23992316.

Okamoto K, Kusano T, Nishino T. Chemical nature and reaction mechanisms of the molybdenum cofactor of xanthine oxidoreductase. Curr Pharm Des. 2013;19(14):2606-14. PMID: 23116398.

Lawal AT, Adeloju SB. Progress and recent advances in fabrication and utilization of hypoxanthine biosensors for meat and fish quality assessment: a review. Talanta. 2012 Oct 15;100:217-28. PMID: 23141330.

H9615

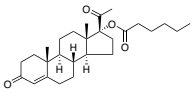

17α-Hydroxyprogesterone Caproate

1 g
5 g
10 g

$C_{27}H_{40}O_4$ FW: 428.6 [630-56-8] ≥98%

Synthetic ER antagonist used to prevent preterm birth.

Briery CM, Klauser CK, Martin RW, et al. The use of 17-hydroxy progesterone in women with arrested preterm labor: a randomized clinical trial. J Matern Fetal Neonatal Med. 2014 Mar 10. [Epub ahead of print]. PMID: 24512252.

Yemini M, Borenstein R, Dreazen E, et al. Prevention of premature labor by 17 alpha-hydroxyprogesterone caproate. Am J Obstet Gynecol. 1985 Mar 1;151(5):574-7. PMID: 3976757.

H9816

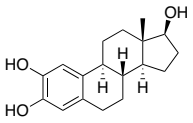

2-Hydroxyestradiol

1 mg
5 mg
10 mg

$C_{18}H_{24}O_3$ FW: 288.38 [362-05-0] ≥98%

Estradiol metabolite with low affinity for ERs. It decreases release of prostaglandin E2, suppresses H_2O_2-induced oxidative damage, and inhibits HIF-1α signaling.

Pavan B, Paganetto G, Dalpiaz A, et al. Estrogen metabolites in the release of inflammatory mediators from human amnion-derived cells. Life Sci. 2011 Mar 14;88(11-12):551-8. PMID: 21277863.

Becker CM, Rohwer N, Funakoshi T, et al. 2-methoxyestradiol inhibits hypoxia-inducible factor-1{alpha} and suppresses growth of lesions in a mouse model of endometriosis. Am J Pathol. 2008 Feb;172(2):534-44. PMID: 18202195.

Dubey RK, Jackson EK, Gillespie DG, et al. Catecholamines block the antimitogenic effect of estradiol on human coronary artery smooth muscle cells. J Clin Endocrinol Metab. 2004 Aug;89(8):3922-31. PMID: 15292328.

H9718

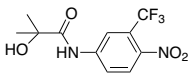

2-Hydroxyflutamide

10 mg
25 mg
100 mg

Hydroxyniphtholide

$C_{11}H_{11}F_3N_2O_4$ FW: 292.21 [52806-53-8] ≥98%

Non-steroidal androgen receptor antagonist. It inhibits IL-6 production in osteoblasts and enhances cytotoxicity of co-administered chemotherapeutics in prostate cancer cells.

Kawabata R, Oie S, Oka T, et al. Hydroxyflutamide enhances cellular sensitivity to 5-fluorouracil by suppressing thymidylate synthase expression in bicalutamide-resistant human prostate cancer cells. Int J Oncol. 2011 Mar;38(3):665-76. PMID: 21243325.

Hofbauer LC, Ten RM, Khosla S. The anti-androgen hydroxyflutamide and androgens inhibit interleukin-6 production by an androgen-responsive human osteoblastic cell line. J Bone Miner Res. 1999 Aug;14(8):1330-7. PMID: 10457265.

Furr BJ, Valcaccia B, Curry B, et al. ICI 176,334: a novel non-steroidal, peripherally selective antiandrogen. J Endocrinol. 1987 Jun;113(3):R7-9. PMID: 3625091.

H1660

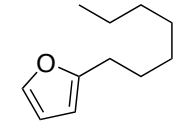

2-n-Heptylfuran

10 g
20 g

$C_{11}H_{18}O$ FW: 166.27 [3777-71-7] ≥98%

Antioxidant found in cooked meat. It induces phase II enzyme activity and inhibits benzo[a]pyrene-induced tumor development.

Lam LK, Zheng BL. Inhibitory effects of 2-n-heptylfuran and 2-n-butylthiophene on benzo[a]pyrene-induced lung and forestomach tumorigenesis in A/J mice. Nutr Cancer. 1992;17(1):19-26. PMID: 1574441.

H9620

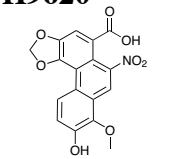

7-Hydroxyaristolochic Acid A

1 mg
5 mg
10 mg

$C_{17}H_{11}NO_8$ FW: 357.27 ≥95%

Aristolochic acid derivative found in *Asarum*. It may display carcinogenic activity.

Xie BB, Shang MY, Wang X, et al. A new aristolochic acid derivative from *Asarum* himalaicum. Yao Xue Xue Bao. 2011 Feb;46(2):188-92. PMID: 21542290.

H9613

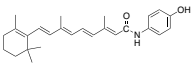

N-(4-Hydroxyphenyl)retinamide

1 mg
5 mg
10 mg

Fenretinide; 4-HPR

$C_{26}H_{33}NO_2$ FW: 391.55 [65646-68-6] ≥98%

Synthetic vitamin A analog that binds RBP4 and inhibits Des1. It increases ceramide levels, decreases levels of total cholesterol and triglycerides, and improves insulin sensitivity.

Durante S, Orienti I, Teti G, et al. Anti-tumor activity of fenretinide complexed with human serum albumin in lung cancer xenograft mouse model. Oncotarget. 2014 May 28. [Epub ahead of print]. PMID: 25015569.

Bikman BT, Guan Y, Shui G, et al. Fenretinide prevents lipid-induced insulin resistance by blocking ceramide biosynthesis. J Biol Chem. 2012 May 18;287(21):17426-37. PMID: 22474281.

H9714

L-5-Hydroxytryptophan

250 mg
1 g
5 g
25 g

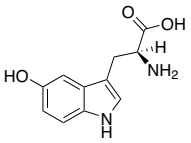

L-5HTP; Oxitriptan

$C_{11}H_{12}N_2O_3$ FW: 220.22 [4350-09-8] ≥98%

Endogenous amino acid and precursor of 5-HT and melatonin found in dietary supplements. It decreases depression- and anxiety-related behaviors, shifts circadian rhythms, and inhibits UV-induced apoptosis in monocytes.

Jangid P, Malik P, Singh P, et al. Comparative study of efficacy of l-5-hydroxytryptophan and fluoxetine in patients presenting with first depressive episode. Asian J Psychiatr. 2013 Feb;6(1):29-34. PMID: 23380314.

Basu P, Singaravel M, Haldar C. L-5-hydroxytryptophan resets the circadian locomotor activity rhythm of the nocturnal Indian pygmy field mouse, Mus terricolor. Naturwissenschaften. 2012 Mar;99(3):233-9. PMID: 22331255.

Lysek N, Kinscherf R, Claus R, et al. L-5-Hydroxytryptophan: antioxidant and anti-apoptotic principle of the intertidal sponge Hymeniacidon heliophila. Z Naturforsch C. 2003 Jul-Aug;58(7-8):568-72. PMID: 12939046.

H9812

5-Hydroxytryptophol

10 mg
25 mg
100 mg

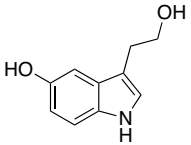

$C_{10}H_{11}NO_2$ FW: 177.2 [154-02-9] ≥98%

Serotonin/melatonin analog found in various plant and food sources and *Trypanosoma brucei*. It is used as a biomarker for recent alcohol consumption and causes sleeping sickness. It also inhibits oxidation of LDL.

Beck O, Helander A. 5-hydroxytryptophol as a marker for recent alcohol intake. Addiction. 2003 Dec;98 Suppl 2:63-72. PMID: 14984243.

Wang HX, Liu F, Ng TB. Examination of pineal indoles and 6-methoxy-2-benzoxazolinone for antioxidant and antimicrobial effects. Comp Biochem Physiol C Toxicol Pharmacol. 2001 Nov;130(3):379-88. PMID: 11701394.

H9814

25-Hydroxyvitamin D2

1 mg
5 mg

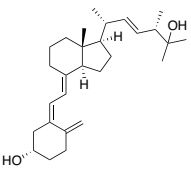

$C_{28}H_{44}O_2$ FW: 412.65 [21343-40-8] ≥90%

Ergocalciferol metabolite and VDR agonist used as a dietary supplement to restore bone mineralization and regulate Ca^{2+} homeostasis. Low levels of 25-OH D2 may be associated with the development of Alzheimer's disease.

Shah I, Petroczi A, Tabet N, et al. Low 25OH vitamin D2 levels found in untreated Alzheimer's patients, compared to acetylcholinesterase-inhibitor treated and controls. Curr Alzheimer Res. 2012 Nov;9(9):1069-76. PMID: 22876849.

Houghton LA, Vieth R. The case against ergocalciferol (vitamin D2) as a vitamin supplement. Am J Clin Nutr. 2006 Oct;84(4):694-7. PMID: 17023693.

H9815

25-Hydroxyvitamin D3

1 mg
5 mg
10 mg

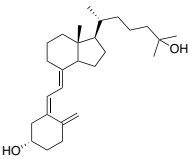

Calcifediol; Calcidiol; 25-Hydroxycholecalciferol

$C_{27}H_{44}O_2$ FW: 400.64 [19356-17-3] ≥98%

Calcitriol prodrug and VDR agonist. It restores bone mineralization and regulates Ca^{2+} homeostasis. It also modulates transcription of PTH, decreases levels of serum glucose, glycosylated hemoglobin, and TNF-α, and inhibits growth of prostate cancer cells.

Wang Q, Li H, Xie H, et al. 25-Hydroxyvitamin D3 attenuates experimental periodontitis through downregulation of TLR4 and JAK1/STAT3 signaling in diabetic mice. J Steroid Biochem Mol Biol. 2013 May;135:43-50. PMID: 23333931.

Li H, Xie H, Fu M, et al. 25-hydroxyvitamin D3 ameliorates periodontitis by modulating the expression of inflammation-associated factors in diabetic mice. Steroids. 2013 Feb;78(2):115-20. PMID: 23138030.

Ritter CS, Brown AJ. Direct suppression of Pth gene expression by the vitamin D prohormones doxercalciferol and calcidiol requires the vitamin D receptor. J Mol Endocrinol. 2011 Feb 15;46(2):63-6. PMID: 21169421.

I0502

Ibandronate Sodium Monohydrate

50 mg
100 mg

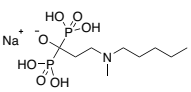

$C_9H_{22}NNaO_7P_2 \cdot H_2O$ FW: 359.21 [138926-19-9] ≥98%

It is used to treat osteoporosis. It increases bone mineral density, prevents resorption, and decreases osteoclast activity. It may inhibit angiogenesis.

Ziebart T, Pabst A, Klein MO, et al. Bisphosphonates: restrictions for vasculogenesis and angiogenesis: inhibition of cell function of endothelial progenitor cells and mature endothelial cells in vitro. Clin Oral Investig. 2011 Feb;15(1):105-11. PMID: 20024592.

Zhou Q, Zhao ZN, Cheng JT, et al. Ibandronate promotes osteogenic differentiation of periodontal ligament stem cells by regulating the expression of microRNAs. Biochem Biophys Res Commun. 2011 Jan 7;404(1):127-32. PMID: 21108928.

Epstein S, Zaidi M. Biological properties and mechanism of action of ibandronate: application to the treatment of osteoporosis. Bone. 2005 Oct;37(4):433-40. PMID: 16046205.

I0416

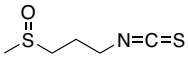

Iberin

3-Methylsulfinylpropyl isothiocyanate

$C_5H_9NOS_2$ FW: 163.26 [505-44-2] ≥97%

Sulforaphane homolog and antioxidant. It induces phase II enzyme activity and suppresses CDK expression, inducing apoptosis in cancer cells.

10 mg
25 mg
50 mg
100 mg

Ernst IM, Palani K, Esatbeyoglu T, et al. Synthesis and Nrf2-inducing activity of the isothiocyanates iberverin, iberin and cheirolin. Pharmacol Res. 2013 Apr;70(1):155-62. PMID: 23403058.

Barrera LN, Cassidy A, Wang W, et al. TrxR1 and GPx2 are potently induced by isothiocyanates and selenium, and mutually cooperate to protect Caco-2 cells against free radical-mediated cell death. Biochim Biophys Acta. 2012 Oct;1823(10):1914-24. PMID: 22820176.

Traka MH, Chambers KF, Lund EK, et al. Involvement of KLF4 in sulforaphane- and iberin-mediated induction of p21(waf1/cip1). Nutr Cancer. 2009;61(1):137-45. PMID: 19116884.

I0417

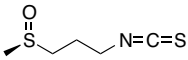

R-(−)-Iberin

3-Methylsulfinylpropyl isothiocyanate

$C_5H_9NOS_2$ FW: 163.26 ≥98%

Natural product and homolog of sulforaphane found in cruciferous vegetables. It stimulates activation of Nrf2, upregulates expression of p21, and induces apoptosis in cancer cells.

10 mg
25 mg
50 mg
100 mg

Ernst IM, Palani K, Esatbeyoglu T, et al. Synthesis and Nrf2-inducing activity of the isothiocyanates iberverin, iberin and cheirolin. Pharmacol Res. 2013 Apr;70(1):155-62. PMID: 23403058.

Barrera LN, Cassidy A, Wang W, et al. TrxR1 and GPx2 are potently induced by isothiocyanates and selenium, and mutually cooperate to protect Caco-2 cells against free radical-mediated cell death. Biochim Biophys Acta. 2012 Oct;1823(10):1914-24. PMID: 22820176.

I0418

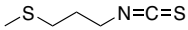

Iberverin

3-Methyl-mercaptopropyl isothiocyanate

$C_5H_9NS_2$ FW: 147.26 [505-79-3] ≥98%

Sulforaphane homolog and antioxidant found in cruciferous vegetables. It induces phase II enzyme activity and decreases expression of androgen receptors in prostate cancer cells.

25 mg
50 mg
100 mg
500 mg

Ernst IM, Palani K, Esatbeyoglu T, et al. Synthesis and Nrf2-inducing activity of the isothiocyanates iberverin, iberin and cheirolin. Pharmacol Res. 2013 Apr;70(1):155-62. PMID: 23403058.

Kim SH, Singh SV. D,L-Sulforaphane causes transcriptional repression of androgen receptor in human prostate cancer cells. Mol Cancer Ther. 2009 Jul;8(7):1946-54. PMID: 19584240.

Munday R, Munday CM. Induction of phase II detoxification enzymes in rats by plant-derived isothiocyanates: comparison of allyl isothiocyanate with sulforaphane and related compounds. J Agric Food Chem. 2004 Apr 7;52(7):1867-71. PMID: 15053522.

I0516

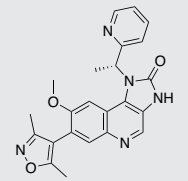

I-BET151

NEW

GSK1210151A

$C_{23}H_{21}N_5O_3$ FW: 415.44 [1300031-49-5] ≥98%

BRD2/3/4 inhibitor. It induces apoptosis and inhibits proliferation in various cancer cell lines and suppresses the development of bacteria-induced inflammation and sepsis.

5 mg
10 mg
25 mg

Chaidos A, Caputo V, Gouvedenou K, et al. Potent antimyeloma activity of the novel bromodomain inhibitors I-BET151 and I-BET762. Blood. 2014 Jan 30;123(5):697-705. PMID: 24335499.

Seal J, Lamotte Y, Donche F, et al. Identification of a novel series of BET family bromodomain inhibitors: binding mode and profile of I-BET151 (GSK1210151A). Bioorg Med Chem Lett. 2012 Apr 15;22(8):2968-72. PMID: 22437115.

I0480

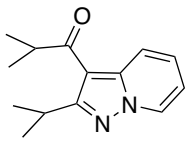

Ibudilast

$C_{14}H_{18}N_2O$ FW: 230.31 [50847-11-5] ≥98%

PDE3/5 inhibitor and LTD4 receptor antagonist used to treat asthma and stroke. It increases cerebral blood flow in several brain regions after ischemic stroke, prevents glial cell activation, and inhibits HIV-1 Tat-induced production of TNF-α.

10 mg
25 mg
100 mg

Inoue N, Fukuda S, Inada T, et al. Effect of ibudilast on the reciprocal inhibitory visual-vestibular interaction closely related to dizziness after cerebral ischemia. J Stroke Cerebrovasc Dis. 2014 Jan;23(1):51-5. PMID: 23085301.

Kiebala M, Maggirwar SB. Ibudilast, a pharmacologic phosphodiesterase inhibitor, prevents human immunodeficiency virus-1 Tat-mediated activation of microglial cells. PLoS One. 2011 Apr 8;6(4):e18633. PMID: 21494611.

Cho Y, Crichlow GV, Vermeire JJ, et al. Allosteric inhibition of macrophage migration inhibitory factor revealed by ibudilast. Proc Natl Acad Sci U S A. 2010 Jun 22;107(25):11313-8. PMID: 20534506.

I0481 Ibuprofen

1 g
5 g
10 g

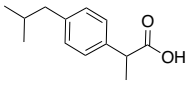

$C_{13}H_{18}O_2$ FW: 206.28 [15687-27-1] ≥98%

NSAID and COX-1/2 inhibitor used to treat pain, inflammation, and fever. Chronic administration decreases incidence of Alzheimer's disease.

Vlad SC, Miller DR, Kowall NW, et al. Protective effects of NSAIDs on the development of Alzheimer disease. Neurology. 2008 May 6;70(19):1672-7. PMID: 18458226.

Van Esch A, Van Steensel-Moll HA, Steyerberg EW, et al. Antipyretic efficacy of ibuprofen and acetaminophen in children with febrile seizures. Arch Pediatr Adolesc Med. 1995 Jun;149(6):632-7. PMID: 7767417.

I0482 S-(+)-Ibuprofen

1 g
5 g
25 g

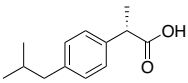

$C_{13}H_{18}O_2$ FW: 206.28 [51146-56-6] ≥98%

Optically active isomer of ibuprofen, NSAID and COX-1/2 inhibitor used to treat pain and inflammation. It also protects against the development of Alzheimer's disease.

Vlad SC, Miller DR, Kowall NW, et al. Protective effects of NSAIDs on the development of Alzheimer disease. Neurology. 2008 May 6;70(19):1672-7. PMID: 18458226.

Van Esch A, Van Steensel-Moll HA, Steyerberg EW, et al. Antipyretic efficacy of ibuprofen and acetaminophen in children with febrile seizures. Arch Pediatr Adolesc Med. 1995 Jun;149(6):632-7. PMID: 7767417.

I0800 IC-87114 NEW

1 mg
5 mg
10 mg

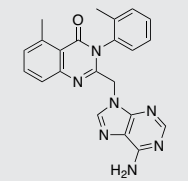

$C_{22}H_{19}N_7O$ FW: 397.43 [371242-69-2] ≥98%

Inhibitor of p110δ PI3K. It inhibits airway infiltration of lymphocytes, neutrophils, and eosinophils, impairs cardiac and vascular differentiation, and decreases infiltration of inflammatory cells into pancreatic islets.

Durand CA, Richer MJ, Brenker K, et al. Selective pharmacological inhibition of phosphoinositide 3-kinase p110delta opposes the progression of autoimmune diabetes in non-obese diabetic (NOD) mice. Autoimmunity. 2013 Feb;46(1):62-73. PMID: 23039284.

Bekhite MM, Finkensieper A, Binas S, et al. VEGF-mediated PI3K class IA and PKC signaling in cardiomyogenesis and vasculogenesis of mouse embryonic stem cells. J Cell Sci. 2011 Jun 1;124(Pt 11):1819-30. PMID: 21540297.

Park SJ, Lee KS, Kim SR, et al. Phosphoinositide 3-kinase δ inhibitor suppresses interleukin-17 expression in a murine asthma model. Eur Respir J. 2010 Dec;36(6):1448-59. PMID: 20351038.

I0901 Icariin

100 mg
500 mg
1 g

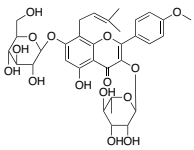

$C_{33}H_{40}O_{15}$ FW: 676.66 [489-32-7] ≥97%

PDE5 inhibitor found in *Epimedium*. It displays many activities, including inhibiting AAPH-induced oxidative DNA damage, decreasing immobility time in the forced swim test, and suppressing osteoclast growth and differentiation.

Zhao F, Tang YZ, Liu ZQ. Protective effect of icariin on DNA against radical-induced oxidative damage. J Pharm Pharmacol. 2007 Dec;59(12):1729-32. PMID: 18053336.

Luo Y, Nie J, Gong QH, et al. Protective effects of icariin against learning and memory deficits induced by aluminium in rats. Clin Exp Pharmacol Physiol. 2007 Aug;34(8):792-5. PMID: 17600559.

Chen KM, Ge BF, Liu XY, et al. Icariin inhibits the osteoclast formation induced by RANKL and macrophage-colony stimulating factor in mouse bone marrow culture. Pharmazie. 2007 May;62(5):388-91. PMID: 17557750.

I0902 Icaritin

1 mg
5 mg
25 mg

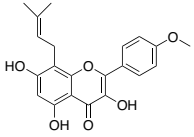

$C_{21}H_{20}O_6$ FW: 368.38 [118525-40-9] ≥98%

Phytoestrogen found in *Epimedium*. It increases glucocorticoid receptor and BDNF mRNA in the hippocampus, prevents development of social avoidance, and decreases levels of IL-6 and TNF-α.

Wu X, Wu J, Xia S, et al. Icaritin opposes the development of social aversion after defeat stress via increases of GR mRNA and BDNF mRNA in mice. Behav Brain Res. 2013 Sep 21;256C:602-608. PMID: 24064280.

Sheng H, Rui XF, Sheng CJ, et al. A novel semisynthetic molecule icaritin stimulates osteogenic differentiation and inhibits adipogenesis of mesenchymal stem cells. Int J Med Sci. 2013 Apr 23;10(6):782-9. PMID: 23630444.

Lai X, Ye Y, Sun C, et al. Icaritin exhibits anti-inflammatory effects in the mouse peritoneal macrophages and peritonitis model. Int Immunopharmacol. 2013 May;16(1):41-9. PMID: 23566810.

I0933 Icilin

NEW

10 mg
50 mg

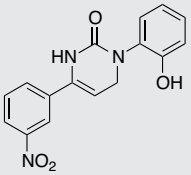

AG 3-5

$C_{16}H_{13}N_3O_4$ FW: 311.3 [36945-98-9] ≥98%

TRPM8 agonist and potential TRPV3 inhibitor. Induces short-term hyperalgesia and long-term analgesia. It also decreases levels of pro-inflammatory cytokines and induces cell cycle arrest in prostate cancer cells.

Burgos-Vega CC, Ahn DD, Bischoff C, et al. Meningeal transient receptor potential channel M8 activation causes cutaneous facial and hindpaw allodynia in a preclinical rodent model of headache. Cephalalgia. 2015 May 5. [Epub ahead of print]. PMID: 25944818.

Hosoya T, Matsumoto K, Tashima K, et al. TRPM8 has a key role in experimental colitis-induced visceral hyperalgesia in mice. Neurogastroenterol Motil. 2014 Aug;26(8):1112-21.PMID: 24832648.

Cucu D, Chiritoiu G, Petrescu S, et al. Characterization of functional transient receptor potential melastatin 8 channels in human pancreatic ductal adenocarcinoma cells. Pancreas. 2014 Jul;43(5):795-800. PMID: 24658318.

I1400 Idarubicin Hydrochloride

1 mg
5 mg
10 mg

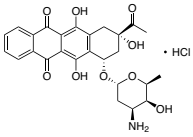

$C_{26}H_{27}NO_9 \bullet HCl$ FW: 533.96 [57852-57-0] ≥98%

DNA intercalator and topoisomerase II inhibitor used to treat leukemias. It induces double-stranded DNA breakage and causes histone eviction.

Eda Satana Kara H. Redox mechanism of anticancer drug idarubicin and in-situ evaluation of interaction with DNA using an electrochemical biosensor. Bioelectrochemistry. 2014 Oct;99:17-23. PMID: 24967755.

Pang B, Qiao X, Janssen L, et al. Drug-induced histone eviction from open chromatin contributes to the chemotherapeutic effects of doxorubicin. Nat Commun. 2013;4:1908. PMID: 23715267.

Crivellari D, Lombardi D, Spazzapan S, et al. New oral drugs in older patients: a review of idarubicin in elderly patients. Crit Rev Oncol Hematol. 2004 Feb;49(2):153-63. PMID: 15012975.

I1418 Idebenone

10 mg
25 mg
100 mg

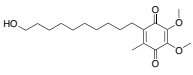

$C_{18}H_{28}O_5$ FW: 324.41 [58186-27-9] ≥98%

Synthetic quinone CoQ analog that promotes mitochondrial respiration, inhibits lipoperoxide formation, and stimulates ATP production. It also improves cognitive function and decreases cardiac inflammation and fibrosis.

Buyse GM, Van der Mieren G, Erb M, et al. Long-term blinded placebo-controlled study of SNT-MC17/idebenone in the dystrophin deficient mdx mouse: cardiac protection and improved exercise performance. Eur Heart J. 2009 Jan;30(1):116-24. PMID: 18784063.

Di Prospero NA, Baker A, Jeffries N, et al. Neurological effects of high-dose idebenone in patients with Friedreich's ataxia: a randomised, placebo-controlled trial. Lancet Neurol. 2007 Oct;6(10):878-86. PMID: 17826341.

Gutzmann H, Kühl KP, Hadler D, et al. Safety and efficacy of idebenone versus tacrine in patients with Alzheimer's disease: results of a randomized, double-blind, parallel-group multicenter study. Pharmacopsychiatry. 2002 Jan;35(1):12-8. PMID: 11819153.

I1257 Idoxuridine

500 mg
1 g
5 g

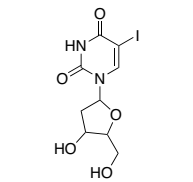

$C_9H_{11}IN_2O_5$ FW: 354.1 [54-42-2] ≥98%

Deoxyuridine analog and DNA chain terminator used to treat ocular herpes infections. It also increases radiation- and chemotherapy-induced damage in glioma cells.

Wilhelmus KR. Antiviral treatment and other therapeutic interventions for herpes simplex virus epithelial keratitis. Cochrane Database Syst Rev. 2010 Dec 8;(12):CD002898. PMID: 21154352.

Schultz CJ, Gaffney DK, Lindstrom MJ, et al. Iododeoxyuridine radiosensitization of human glioblastoma cells exposed to acute and chronic gamma irradiation: mechanistic implications and clinical relevance. Cancer J Sci Am. 1995 Jul-Aug;1(2):151-61. Erratum in: Cancer J Sci Am. 1996 Jan-Feb;2(1):15. PMID: 9166468.

I2056 Ifosfamide

25 mg
50 mg
250 mg
1 g

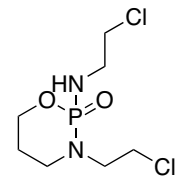

$C_7H_{15}Cl_2N_2O_2P$ FW: 261.09 [3778-73-2] ≥98%

DNA alkylator used to treat various cancers. It is highly cytotoxic.

Vincenzi B, Frezza AM, Santini D, et al. New therapies in soft tissue sarcoma. Expert Opin Emerg Drugs. 2010 Jun;15(2):237-48. PMID: 20465449.

Nissim I, Horyn O, Daikhin Y, et al. Ifosfamide-induced nephrotoxicity: mechanism and prevention. Cancer Res. 2006 Aug 1;66(15):7824-31. PMID: 16885387.

I4000 Ikarugamycin

0.5 mg
1 mg
5 mg

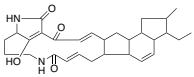

$C_{29}H_{40}N_2O_4$ FW: 480.64 [36531-78-9] ≥98%

Protein translation inhibitor. It also inhibits CCP-dependent phagocytosis and inhibits uptake of oxidized LDL in macrophages.

Popescu R, Heiss EH, Ferk F, et al. Ikarugamycin induces DNA damage, intracellular calcium increase, p38 MAP kinase activation and apoptosis in HL-60 human promyelocytic leukemia cells. Mutat Res. 2011 May 10;709-710:60-6. PMID: 21392513.

Luo T, Fredericksen BL, Hasumi K, et al. Human immunodeficiency virus type 1 Nef-induced CD4 cell surface downregulation is inhibited by ikarugamycin. J Virol. 2001 Mar;75(5):2488-92. PMID: 11160755.

Hasumi K, Shinohara C, Naganuma S, et al. Inhibition of the uptake of oxidized low-density lipoprotein in macrophage J774 by the antibiotic ikarugamycin. Eur J Biochem. 1992 Apr 15;205(2):841-6. PMID: 1572375.

I4659 Iloperidone

100 mg
250 mg
1 g

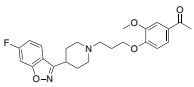

$C_{24}H_{27}FN_2O_4$ FW: 426.48 [133454-47-4] ≥98%

Antagonist at dopamine D2 receptors and 5-HT2A receptors and potential inhibitor of hERG K^+ channels used to treat schizophrenia. It may prolong the cardiac QT interval and induce ventricular tachyarrhythmia.

Dargani NV, Malhotra AK. Safety profile of iloperidone in the treatment of schizophrenia. Expert Opin Drug Saf. 2013 Nov 11. [Epub ahead of print]. PMID: 24206391.

Achalia R, Andrade C. Ventricular premature contractions associated with iloperidone. Indian J Psychiatry. 2013 Apr;55(2):195-6. PMID: 23825860.

Marino J, Caballero J. Iloperidone for the treatment of schizophrenia. Ann Pharmacother. 2010 May;44(5):863-70. PMID: 20388862.

I4802 Imatinib Mesylate

25 mg
100 mg
500 mg

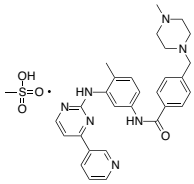

$C_{29}H_{31}N_7O \bullet CH_3SO_3H$ FW: 589.718 [220127-57-1] ≥98%

Inhibitor of Abl, c-Kit, and PDGFR used to treat Philadelphia chromosome-positive leukemias. It also accelerates erythroblast differentiation and inhibits melanogenesis.

Wang Y, Zhao Y, Liu L, et al. Inhibitory effects of imatinib mesylate on human epidermal melanocytes. Clin Exp Dermatol. 2014 Mar;39(2):202-8. PMID: 24479586.

D'allard D, Gay J, Descarpentries C, et al. Tyrosine kinase inhibitors induce down-regulation of c-Kit by targeting the ATP pocket. PLoS One. 2013 Apr 23;8(4):e60961. PMID: 23637779.

Gambacorti-Passerini CB, Gunby RH, Piazza R, et al. Molecular mechanisms of resistance to imatinib in Philadelphia-chromosome-positive leukaemias. Lancet Oncol. 2003 Feb;4(2):75-85. PMID: 12573349.

I5072 Imazalil

5 g
10 g
100 g

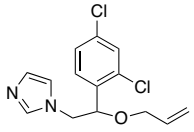

Enilconazole

$C_{14}H_{14}Cl_2N_2O$ FW: 297.18 [35554-44-0] ≥95%

Inhibitor of 14-α demethylase, aromatase, and androgen receptors that inhibits ergosterol synthesis and fungal cell wall formation. It also alters neural differentiation and displays teratogenic effects in vertebrate development.

Orton F, Rosivatz E, Scholze M, et al. Competitive androgen receptor antagonism as a factor determining the predictability of cumulative antiandrogenic effects of widely used pesticides. Environ Health Perspect. 2012 Nov;120(11):1578-84. PMID: 23008280.

Sun X, Wang J, Feng D, et al. PdCYP51B, a new putative sterol 14α-demethylase gene of Penicillium digitatum involved in resistance to imazalil and other fungicides inhibiting ergosterol synthesis. Appl Microbiol Biotechnol. 2011 Aug;91(4):1107-19. PMID: 21637936.

Zega G, De Bernardi F, Groppelli S, et al. Effects of the azole fungicide Imazalil on the development of the ascidian Ciona intestinalis (Chordata, Tunicata): morphological and molecular characterization of the induced phenotype. Aquat Toxicol. 2009 Feb 19;91(3):255-61. PMID: 19124165.

I4934 Imipenem Monohydrate

25 mg
100 mg
500 mg

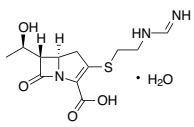

$C_{12}H_{17}N_3O_4S \bullet H_2O$ FW: 317.36 [74431-23-5] ≥98%

Penicillin binding protein inhibitor that inhibits bacterial cell wall synthesis. It is especially active against *Pseudomonas* and *Enterococcus*.

El-Gamal MI, Oh CH. Current status of carbapenem antibiotics. Curr Top Med Chem. 2010;10(18):1882-97. PMID: 20615191.

Clissold SP, Todd PA, Campoli-Richards DM. Imipenem/cilastatin. A review of its antibacterial activity, pharmacokinetic properties and therapeutic efficacy. Drugs. 1987 Mar;33(3):183-241. PMID: 3552595.

I5034 Imiquimod

100 mg
500 mg
1 g
5 g

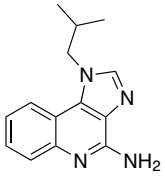

R-837

$C_{14}H_{16}N_4$ FW: 240.3 [99011-02-6] ≥99.5%

Imidazoquinoline nucleoside analog, TLR-7/8 agonist, KCNA1/K_v1.1 and KCNA2/Kv1.2 K^+ channel partial agonist, and TREK-1/K2P2 and TRAAK/K2P4 K^+ channel blocker used to modulate immune signaling. It stimulates Th1-based immune responses, induces apoptosis in squamous cell carcinoma cells, suppresses hedgehog signaling, and increases action potential duration and excitability of DRG neurons.

Nazmi A, Mukherjee S, Kundu K, et al. TLR7 is a key regulator of innate immunity against Japanese encephalitis virus infection. Neurobiol Dis. 2014 Sep;69:235-47. PMID: 24909816.

Sohn KC, Li ZJ, Choi DK, et al. Imiquimod induces apoptosis of squamous cell carcinoma (SCC) cells via regulation of A20. PLoS One. 2014 Apr 17;9(4):e95337. PMID: 24743316.

Wolff F, Loipetzberger A, Gruber W, et al. Imiquimod directly inhibits Hedgehog signalling by stimulating adenosine receptor/protein kinase A-mediated GLI phosphorylation. Oncogene. 2013 Dec 12;32(50):5574-81. PMID: 23995793.

I4961 Imperatorin

5 mg
25 mg
100 mg

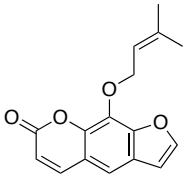

$C_{16}H_{14}O_4$ FW: 270.28 [482-44-0] ≥98%

Inhibitor of AChE, BChe, and voltage-gated Na^+ channels. It displays several activities, including decreasing levels of angiotensin II, inducing NO-regulated vasodilation, inhibiting growth of gram negative and gram positive bacteria, and improving memory acquisition and consolidation processes.

Granica S, Kiss AK, Jarończyk M, et al. Synthesis of Imperatorin Analogs and Their Evaluation as Acetylcholinesterase and Butyrylcholinesterase Inhibitors. Arch Pharm (Weinheim). 2013 Oct 14. [Epub ahead of print]. PMID: 24123207.

Wu KC, Chen YH, Cheng KS, et al. Suppression of voltage-gated Na(+) channels and neuronal excitability by imperatorin. Eur J Pharmacol. 2013 Dec 5;721(1-3):49-55. PMID: 24113522.

Budzynska B, Boguszewska-Czubara A, Kruk-Slomka M, et al. Effects of imperatorin on nicotine-induced anxiety- and memory-related responses and oxidative stress in mice. Physiol Behav. 2013 Oct 2;122:46-55. PMID: 23999469.

I5203 Inauhzin

NEW

5 mg
25 mg

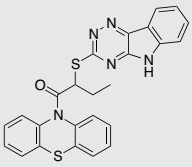

$C_{25}H_{19}N_5OS_2$ FW: 469.58 [309271-94-1] ≥98%

Inhibitor of SIRT1 and IMPDH that indirectly activates p53. It induces apoptosis and suppresses growth in non-small cell lung cancer cells and stimulates senescence in lung cancer and colon carcinoma models.

Zhang Q, Zhou X, Wu R, et al. The role of IMP dehydrogenase 2 in Inauhzin-induced ribosomal stress. Elife. 2014 Oct 27;3. PMID: 25347121.

Zhang Y, Zhang Q, Zeng SX, et al. Inauhzin sensitizes p53-dependent cytotoxicity and tumor suppression of chemotherapeutic agents. Neoplasia. 2013 May;15(5):523-34. PMID: 23633924.

I5210 INCB018424

NEW

5 mg
25 mg
50 mg

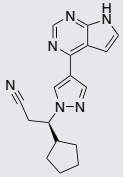

Ruxolitinib

$C_{17}H_{18}N_6$ FW: 306.37 [941678-49-5] ≥98%

JAK1/2 inhibitor. It prevents viral replication of HIV-1, HIV-2, and SHIV in lymphocytes, suppresses release of TNF-α, IL-10, and IL-1β in inflammation models, and inhibits growth of myeloma cells.

Springuel L, Hornakova T, Losdyck E, et al. Cooperating JAK1 and JAK3 mutants increase resistance to JAK inhibitors. Blood. 2014 Dec 18;124(26):3924-31. PMID: 25352124.

Hazem SH, Shaker ME, Ashamallah SA, et al. The novel Janus kinase inhibitor ruxolitinib confers protection against carbon tetrachloride-induced hepatotoxicity via multiple mechanisms. Chem Biol Interact. 2014 Sep 5;220:116-27. PMID: 24973641.

Gavegnano C, Detorio M, Montero C, et al. Ruxolitinib and tofacitinib are potent and selective inhibitors of HIV-1 replication and virus reactivation in vitro. Antimicrob Agents Chemother. 2014;58(4):1977-86. PMID: 24419350.

I5208 INCB-28060

NEW

1 mg
5 mg
10 mg

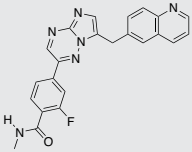

INC-280; Capmatinib

$C_{23}H_{17}FN_6O$ FW: 412.42 [1029712-80-8] ≥98%

c-MET inhibitor. It inhibits cell migration and induces apoptosis in various cancer cell lines.

Liu X, Wang Q, Yang G, et al. A novel kinase inhibitor, INCB28060, blocks c-MET-dependent signaling, neoplastic activities, and cross-talk with EGFR and HER-3. Clin Cancer Res. 2011 Nov 15;17(22):7127-38. PMID: 21918175.

I5414 Indapamide

250 mg
1 g
5 g

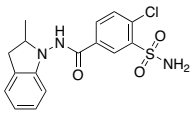

$C_{16}H_{16}ClN_3O_3S$ FW: 365.84 [26807-65-8] ≥98%

K_v7.1 and minK K^+ channel blocker and diuretic used to treat hypertension and heart failure. It prevents increases in systolic blood pressure, suppresses development of myocardial fibrosis, and may prolong the cardiac QT interval.

Janega P, Kojsová S, Jendeková L, et al. Indapamide-induced prevention of myocardial fibrosis in spontaneous hypertension rats is not nitric oxide-related. Physiol Res. 2007;56(6):825-8. PMID: 18197750.

Letsas KP, Alexanian IP, Pappas LK, et al. QT interval prolongation and torsade de pointes associated with indapamide. Int J Cardiol. 2006 Oct 10;112(3):373-4. PMID: 16260053.

I5313 Indinavir Sulfate

1 g
5 g
25 g

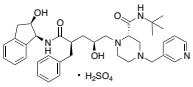

$C_{36}H_{47}N_5O_4 \bullet H_2O_4S$ FW: 711.87 [157810-81-6] ≥98%

Inhibitor of HIV protease, GLUT4, and calpain used to treat HIV infection. It also decreases phosphorylation of the insulin receptor β subunit, inhibits adenocarcinoma tumor growth, and may induce SOCS1 signaling.

Ismail WI, King JA, Anwar K, et al. Indinavir and nelfinavir inhibit proximal insulin receptor signaling and salicylate abrogates inhibition: potential role of the NFkappa B pathway. J Cell Biochem. 2013 Aug;114(8):1729-37. PMID: 23386514.

Toschi E, Sgadari C, Malavasi L, et al. Human immunodeficiency virus protease inhibitors reduce the growth of human tumors via a proteasome-independent block of angiogenesis and matrix metalloproteinases. Int J Cancer. 2011 Jan 1;128(1):82-93. PMID: 20617515.

I5212 Indirubin

NEW

5 mg
25 mg
100 mg

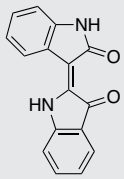

$C_{16}H_{10}N_2O_2$ FW: 262.26 [479-41-4] ≥98%

Potential EGFR and CDK inhibitor found in Indigo naturalis. It decreases levels of IgE and production of inflammatory cytokines, inhibits expression of pro-survival proteins in leukemia cells, and suppresses VEGFR2-mediated JAK/STAT signaling.

Kim MH, Choi YY, Yang G, et al. Indirubin, a purple 3,2- bisindole, inhibited allergic contact dermatitis via regulating T helper (Th)-mediated immune system in DNCB-induced model. J Ethnopharmacol. 2013 Jan 9;145(1):214-9. PMID: 23149289.

Hsieh WL, Lin YK, Tsai CN, et al. Indirubin, an acting component of indigo naturalis, inhibits EGFR activation and EGF-induced CDC25B gene expression in epidermal keratinocytes. J Dermatol Sci. 2012 Aug;67(2):140-6. PMID: 22721997.

Zhang X, Song Y, Wu Y, et al. Indirubin inhibits tumor growth by antitumor angiogenesis via blocking VEGFR2-mediated JAK/STAT3 signaling in endothelial cell. Int J Cancer. 2011 Nov 15;129(10):2502-11. PMID: 21207415.

I5213 Indole-3-carbinol

5 g
25 g

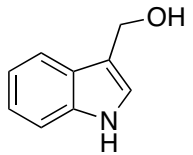

3-Indomethanol

C_9H_9NO FW: 147.17 [700-06-1] ≥98%

Found in cruciferous vegetables. It displays many biological activities, including inhibiting adipogenesis, preventing amyloid-β fibril formation, inducing hepatic stellate cell apoptosis, and modulating MCP-2 and ERK signaling to suppress migration and invasion of breast cancer cells.

Choi HS, Jeon HJ, Lee OH, et al. Indole-3-carbinol, a vegetable phytochemical, inhibits adipogenesis by regulating cell cycle and AMPKα signaling. Biochimie. 2014 Sep;104:127-36. PMID: 24952351.

Mao CG, Tao ZZ, Chen Z, et al. Indole-3-carbinol inhibits nasopharyngeal carcinoma cell growth in vivo and in vitro through inhibition of the PI3K/Akt pathway. Exp Ther Med. 2014 Jul;8(1):207-12. PMID: 24944623.

I5215 Indolicidin

0.5 mg
1 mg
2.5 mg

H-Ile-Leu-Pro-Trp-Lys-Trp-Pro-Trp-Trp-Pro-Trp-Arg-Arg-NH_2

$C_{100}H_{132}N_{26}O_{13}$ FW: 1906.33 [140896-21-5] ≥95%

It binds negatively charged lipid membranes and induces release of vesicle contents but does not form pores. It inhibits production of NO and iNOS in LPS-stimulated macrophages and suppresses growth of *Acinetobacter*, *Staphyloccocus*, and *Nocardia*.

Vila-Farres X, Garcia de la Maria C, López-Rojas R, et al. In vitro activity of several antimicrobial peptides against colistin-susceptible and colistin-resistant *Acinetobacter* baumannii. Clin Microbiol Infect. 2012 Apr;18(4):383-7. PMID: 21672084.

Végh AG, Nagy K, Bálint Z, et al. Effect of antimicrobial peptide-amide: indolicidin on biological membranes. J Biomed Biotechnol. 2011;2011:670589. PMID: 21765635.

I5315 Indomethacin

5 g
10 g
25 g
100 g

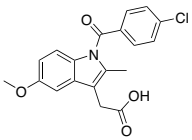

$C_{19}H_{16}ClNO_4$ FW: 357.79 [53-86-1] ≥98%

NSAID and COX-1/2 inhibitor used to treat pain, inflammation, and premature labor. It also decreases cancer cell migration by suppressing Ca^{2+} influx and induces intestinal damage and gastric lesions.

Adewoye EO, Salami AT. Anti-ulcerogenic mechanism of magnesium in indomethacin induced gastric ulcer in rats. Niger J Physiol Sci. 2013 Dec 20;28(2):193-9. PMID: 24937396.

Guo YC, Chang CM, Hsu WL, et al. Indomethacin inhibits cancer cell migration via attenuation of cellular calcium mobilization. Molecules. 2013 Jun 4;18(6):6584-96. PMID: 23736792.

Summ O, Evers S. Mechanism of action of indomethacin in indomethacin-responsive headaches. Curr Pain Headache Rep. 2013 Apr;17(4):327. PMID: 23423598.

I5354 Iniparib

5 mg

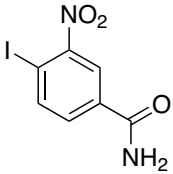

$C_7H_5IN_2O_3$ FW: 292.03 [160003-66-7] ≥98%

Cysteine adduct inducer and PARP-1 inhibitor. It is only minimally active in modulating PARP activity. It inhibits single-stranded DNA break repair mechanisms in cancer cells.

Mateo J, Ong M, Tan DS, et al. Appraising iniparib, the PARP inhibitor that never was-what must we learn? Nat Rev Clin Oncol. 2013 Dec;10(12):688-96. PMID: 24129347.

Wilkinson-Ryan I, Mutch D. A review of iniparib in ovarian cancer. Expert Opin Investig Drugs. 2013 Mar;22(3):399-405. PMID: 23394483.

Ma W, Halweg CJ, Menendez D, et al. Differential effects of poly(ADP-ribose) polymerase inhibition on DNA break repair in human cells are revealed with Epstein-Barr virus. Proc Natl Acad Sci U S A. 2012 Apr 24;109(17):6590-5. PMID: 22493268

I5440 INK128

1 mg
5 mg
25 mg

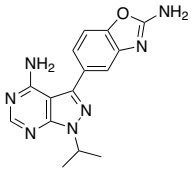

MLN-0128

$C_{15}H_{15}N_7O$ FW: 309.33 [1224844-38-5] ≥99%

Inhibitor of mTOR1/2. It suppresses migration and invasion of multiple myeloma cells and decreases colony formation in B cell acute lymphoblastic leukemia cells.

Janes MR, Vu C, Mallya S, et al. Efficacy of the investigational mTOR kinase inhibitor MLN0128/INK128 in models of B-cell acute lymphoblastic leukemia. Leukemia. 2013 Mar;27(3):586-94. PMID: 23090679.

Hsieh AC, Liu Y, Edlind MP, et al. The translational landscape of mTOR signalling steers cancer initiation and metastasis. Nature. 2012 Feb 22;485(7396):55-61. PMID: 22367541.

Maiso P, Liu Y, Morgan B, et al. Defining the role of TORC1/2 in multiple myeloma. Blood. 2011 Dec 22;118(26):6860-70. PMID: 22045983.

I5357 Inositol

100 g
500 g

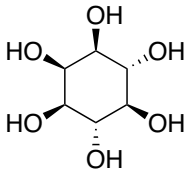

Cyclohexanehexol; Phaseomannite; Inosite

$C_6H_{12}O_6$ FW: 180.16 [6917-35-7] ≥98%

Endogenous sugar produced from glucose that is required for production of IMP and phosphatidyl inositol. It is involved in insulin sensitivity and glucose disposal.

Michell RH. Inositol lipids: from an archaeal origin to phosphatidylinositol 3,5-bisphosphate faults in human disease. FEBS J. 2013 Dec;280(24):6281-94. PMID: 23902363.

Larner J, Brautigan DL, Thorner MO. D-chiro-inositol glycans in insulin signaling and insulin resistance. Mol Med. 2010 Nov-Dec;16(11-12):543-52. PMID: 20811656.

Shen X, Xiao H, Ranallo R, et al. Modulation of ATP-dependent chromatin-remodeling complexes by inositol polyphosphates. Science. 2003 Jan 3;299(5603):112-4. PMID: 12434013.

I5476 Interleukin-6 Receptor Fragment

0.5 mg
1 mg
2.5 mg

IL-6R

H-Thr-Ser-Leu-Pro-Val-Gln-Asp-Ser-Ser-Ser-Val-Pro-OH

$C_{51}H_{85}N_{13}O_{21}$ FW: 1216.32 ≥95%

IL-6 receptor fragment that weakly binds IL-6 but does not display significant downstream signaling.

Bosze S, Hudecz F, Igaz P, et al. Interleukin-6 N-terminal peptides modulate the expression of junB protooncogene and the production of fibrinogen in HepG2 cells. Biol Chem. 2003 Mar;384(3):409-21. PMID: 12715892.

I5830 Iohexol

1 g
5 g
25 g

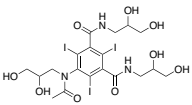

Win-39424

$C_{19}H_{26}I_3N_3O_9$ FW: 821.14 [66108-95-0] ≥98%

Low osmolarity contrast agent used for vascular imaging procedures.

McCormack PL. Iobitridol: a review of its use as a contrast medium in diagnostic imaging. Clin Drug Investig. 2013 Feb;33(2):155-66. PMID: 23341290.

I5753 Ionomycin Calcium

1 mg
5 mg
10 mg

ATCC 31005

$C_{41}H_{70}O_9Ca$ FW: 747.07 [56092-82-1] ≥98%

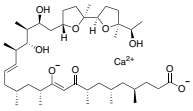

Polyether Ca^{2+} ionophore. Its depletion of intracellular Ca^{2+} stores may be linked to the induction of apoptosis.

Müller MS, Obel LF, Waagepetersen HS, et al. Complex actions of ionomycin in cultured cerebellar astrocytes affecting both calcium-induced calcium release and store-operated calcium entry. Neurochem Res. 2013 Jun;38(6):1260-5. PMID: 23519933.

Dedkova EN, Sigova AA, Zinchenko VP. Mechanism of action of calcium ionophores on intact cells: ionophore-resistant cells. Membr Cell Biol. 2000;13(3):357-68. PMID: 10768486

Reynolds JE, Eastman A. Intracellular calcium stores are not required for Bcl-2-mediated protection from apoptosis. J Biol Chem. 1996 Nov 1;271(44):27739-43. PMID: 8910367.

I5752 Ionomycin, Free Acid

1 mg
5 mg
10 mg

$C_{41}H_{72}O_9$ FW: 709 [56092-81-0] ≥98%

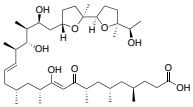

Ca^{2+} ionophore. Its depletion of intracellular Ca^{2+} stores may be linked to the induction of apoptosis.

Müller MS, Obel LF, Waagepetersen HS, et al. Complex actions of ionomycin in cultured cerebellar astrocytes affecting both calcium-induced calcium release and store-operated calcium entry. Neurochem Res. 2013 Jun;38(6):1260-5. PMID: 23519933.

Dedkova EN, Sigova AA, Zinchenko VP. Mechanism of action of calcium ionophores on intact cells: ionophore-resistant cells. Membr Cell Biol. 2000;13(3):357-68. PMID: 10768486

I5992 IOX2

NEW

5 mg
25 mg
100 mg

$C_{19}H_{16}N_2O_5$ FW: 352.34 [931398-72-0] ≥98%

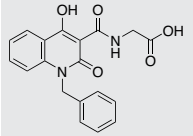

Prolyl hydroxylase inhibitor. It increases activation of HIF-1α and induces angiogenesis.

Sen A, Ren S, Lerchenmüller C, et al. MicroRNA-138 regulates hypoxia-induced endothelial cell dysfunction by targeting S100A1. PLoS One. 2013 Nov 11;8(11):e78684. PMID: 24244340.

I6132 IPI-145

NEW

1 mg
5 mg
10 mg

INK1197; Duvelisib

$C_{22}H_{17}ClN_6O$ FW: 416.86 [1201438-56-3] ≥98%

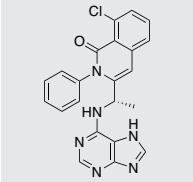

Inhibitor of p110δ PI3K. It induces apoptosis, inhibits proliferation of B and T cells, suppresses differentiation of Th17 cells, and decreases survival of chronic lymphocytic leukemia cells.

Balakrishnan K, Peluso M, Fu M, et al. The phosphoinositide-3-kinase (PI3K)-delta and gamma inhibitor, IPI-145 (Duvelisib), overcomes signals from the PI3K/AKT/S6 pathway and promotes apoptosis in CLL. Leukemia. 2015 Apr 28. [Epub ahead of print]. PMID: 25917267.

IPI-145 Shows Promise in CLL Patients. Cancer Discov. 2014 Feb;4(2):136. PMID: 24501284.

Boyle DL, Kim HR, Topolewski K, et al. Novel phosphoinositide 3-kinase δ,γ inhibitor: potent anti-inflammatory effects and joint protection in models of rheumatoid arthritis. J Pharmacol Exp Ther. 2014 Feb;348(2):271-80. PMID: 24244039.

I6068 Ipriflavone

1 g
5 g
10 g

$C_{18}H_{16}O_3$ FW: 280.32 [35212-22-7] ≥98%

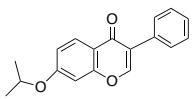

Decreases bone resorption and increases bone density and volume. It also protects against cyclophosphamide-induced DNA damage.

Lv WT, Yang YH, Ma LQ, et al. Ipriflavone reverses the adverse effects of a low-calcium diet on the histology of the tibia in caged layers. Br Poult Sci. 2014;55(2):207-14. PMID: 24404906.

Delarmelina JM, Dutra JC, Batitucci Mdo C. Antimutagenic activity of ipriflavone against the DNA-damage induced by cyclophosphamide in mice. Food Chem Toxicol. 2014 Mar;65:140-6. PMID: 24389340.

I6804 Irbesartan

1 g
5 g
25 g

$C_{25}H_{28}N_6O$ FW: 428.53 [138402-11-6] ≥98%

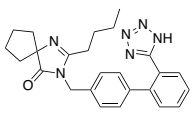

PPARγ agonist and AT1 receptor inhibitor. It decreases expression of TGF-β1, atrial natriuretic factor, and collagen in myocardial fibrosis models, lowers plasma levels of free fatty acids, triglycerides, and insulin, and upregulates expression of hepatic PPARα.

Zhang ZZ, Shang QH, Jin HY, et al. Cardiac protective effects of irbesartan via the PPAR-gamma signaling pathway in angiotensin-converting enzyme 2-deficient mice. J Transl Med. 2013 Sep 25;11(1):229. PMID: 24067190.

Iida Y, Xu B, Schultz GM, et al. Efficacy and mechanism of angiotensin II receptor blocker treatment in experimental abdominal aortic aneurysms. PLoS One. 2012;7(12):e49642. PMID: 23226500

Rong X, Li Y, Ebihara K, et al. Irbesartan treatment up-regulates hepatic expression of PPARalpha and its target genes in obese Koletsky (fa(k)/fa(k)) rats: a link to amelioration of hypertriglyceridaemia. Br J Pharmacol. 2010 Aug;160(7):1796-807. PMID: 20649581

I6932

Irinotecan

5 mg
10 mg
25 mg
100 mg
250 mg

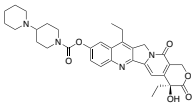

$C_{33}H_{38}N_4O_6$ FW: 586.68 [97682-44-5] ≥98%

Camptothecin analog and topoisomerase I inhibitor. It may inhibit AChE. It is used to treat colon cancer, but it also moderates inhibition of dendritic cell differentiation and decreases the number of tumor vessels in glioma models.

Hu J, Kinn J, Zirakzadeh AA, et al. The effects of chemotherapeutic drugs on human monocyte-derived dendritic cell differentiation and antigen presentation. Clin Exp Immunol. 2013 Jun;172(3):490-9. PMID: 23600838.

Pan P, Li Y, Yu H, et al. Molecular principle of topotecan resistance by topoisomerase I mutations through molecular modeling approaches. J Chem Inf Model. 2013 Apr 22;53(4):997-1006. PMID: 23521602.

Chen AY, Chen PM, Chen YJ. DNA topoisomerase I drugs and radiotherapy for lung cancer. J Thorac Dis. 2012 Aug;4(4):390-7. PMID: 22934142.

I6933

Irinotecan Hydrochloride Trihydrate

5 mg
10 mg
25 mg
100 mg

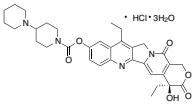

CPT-11

$C_{33}H_{38}N_4O_6 \cdot HCl \cdot 3H_2O$ FW: 677.19 [136572-09-3] ≥98%

Camptothecin analog, topoisomerase I inhibitor, and potential AChE inhibitor used to treat various cancers. It also decreases the number of tumor vessels and expression of VEGF and HIF-1α in glioma models and moderates inhibition of dendritic cell differentiation.

Hu J, Kinn J, Zirakzadeh AA, et al. The effects of chemotherapeutic drugs on human monocyte-derived dendritic cell differentiation and antigen presentation. Clin Exp Immunol. 2013 Jun;172(3):490-9. PMID: 23600838.

Pan P, Li Y, Yu H, et al. Molecular principle of topotecan resistance by topoisomerase I mutations through molecular modeling approaches. J Chem Inf Model. 2013 Apr 22;53(4):997-1006. PMID: 23521602.

I7074

Irsogladine Maleate

100 mg
500 mg
1 g

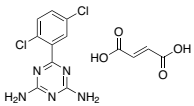

MN-1695

$C_9H_7Cl_2N_5 \cdot C_4H_4O_4$ FW: 372.17 [84504-69-8] ≥98%

Inhibitor of COX-1/2 and PDE. It decreases NSAID-induced mucosal injury, prevents fibrosis, and facilitates gap junction communication.

Kuramoto T, Umegaki E, Nouda S, et al. Preventive effect of irsogladine or omeprazole on non-steroidal anti-inflammatory drug-induced esophagitis, peptic ulcers, and small intestinal lesions in humans, a prospective randomized controlled study. BMC Gastroenterol. 2013 May 14;13:85. PMID: 23672202.

Akagi M, Amagase K, Murakami T, et al. Irsogladine: overview of the mechanisms of mucosal protective and healing- promoting actions in the gastrointestinal tract. Curr Pharm Des. 2013;19(1):106-14. PMID: 22950502.

Yamaguchi H, Suzuki K, Nagata M, et al. Irsogladine maleate ameliorates inflammation and fibrosis in mice with chronic colitis induced by dextran sulfate sodium. Med Mol Morphol. 2012 Jun;45(3):140-51. PMID: 23001296.

I7302

Isatin

100 g
500 g

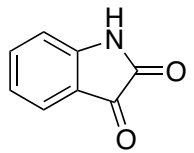

$C_8H_5NO_2$ FW: 147.13 [91-56-5] ≥97%

MAO-B and guanylate cyclase inhibitor found in *Isatis*, *Calanthe*, and *Couroupita*. It prevents TNBS-induced increases in pro-inflammatory cytokines and protects against colitis-induced injuries. Derivatives may inhibit cancer cell growth.

Liang C, Xia J, Lei D, et al. Synthesis, in vitro and in vivo antitumor activity of symmetrical bis-Schiff base derivatives of isatin. Eur J Med Chem. 2014 Mar 3;74:742-50. PMID: 24176732.

Socca EA, Luiz-Ferreira A, de Faria FM, et al. Inhibition of tumor necrosis factor-alpha and cyclooxigenase-2 by Isatin: a molecular mechanism of protection against TNBS-induced colitis in rats. Chem Biol Interact. 2014 Feb 25;209:48-55. PMID: 24316276.

Krishnegowda G, Prakasha Gowda AS, Tagaram HR, et al. Synthesis and biological evaluation of a novel class of isatin analogs as dual inhibitors of tubulin polymerization and Akt pathway. Bioorg Med Chem. 2011 Oct 15;19(20):6006-14. PMID: 21920762.

I7256

Isobavachalcone

1 mg
5 mg

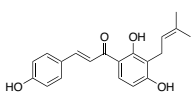

$C_{20}H_{20}O_4$ FW: 324.37 [20784-50-3] ≥98%

Cholesterol acyltransferase inhibitor found in *Psoraleae*. It inhibits platelet aggregation, suppresses growth of *Candida albicans* and *Cryptococcus neoformans*, prevents oligomerization and fibrillization of amyloid-β, and induces apoptosis in neuroblastoma cells.

Chen X, Yang Y, Zhang Y. Isobavachalcone and bavachinin from *Psoraleae* Fructus modulate Aβ42 aggregation process through different mechanisms in vitro. FEBS Lett. 2013 Sep 17;587(18):2930-5. PMID: 23907009.

Jing H, Zhou X, Dong X, et al. Abrogation of Akt signaling by Isobavachalcone contributes to its anti-proliferative effects towards human cancer cells. Cancer Lett. 2010 Aug 28;294(2):167-77. PMID: 20167420.

Choi JH, Rho MC, Lee SW, et al. Bavachin and isobavachalcone, acyl-coenzyme A: cholesterol acyltransferase inhibitors from Psoralea corylifolia. Arch Pharm Res. 2008 Nov;31(11):1419-23. PMID: 19023538.

I7258 Isoflurane

NEW

250 mg
1 g

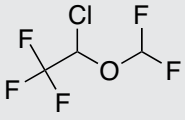

$C_3H_2ClF_5O$ FW: 184.49 [26675-46-7] ≥98%

Activator of Ca^{2+} ATPase and ATP-sensitive K^+ channels, potentiator of GABA-A receptors and GlyRs, and inhibitor of NMDA receptors and L-type Ca^{2+}, delayed rectifier K^+, and A-type K^+ channels used as an anesthetic. It decreases cardiac force, increases IL-6 levels, and lowers intracellular Ca^{2+} amplitude.

Shen X, Bhatt N, Xu J, et al. Effect of isoflurane on myocardial energetic and oxidative stress in cardiac muscle from zucker diabetic Fatty rat. J Pharmacol Exp Ther. 2014 Apr;349(1):21-8. PMID: 24431470.

Fanchaouy M, Cubano L, Maldonado H, et al. PKC independent inhibition of voltage gated calcium channels by volatile anesthetics in freshly isolated vascular myocytes from the aorta. Cell Calcium. 2013 Oct;54(4):257-65. PMID: 23948226.

Zhang L, Zhang J, Yang L, et al. Isoflurane and sevoflurane increase interleukin-6 levels through the nuclear factor-kappa B pathway in neuroglioma cells. Br J Anaesth. 2013 Jun;110 Suppl 1:i82-91. PMID: 23604542.

I4962 Isoimperatorin

5 mg
25 mg
100 mg

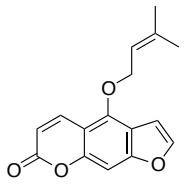

$C_{16}H_{14}O_4$ FW: 270.28 [482-45-1] ≥98.0%

COX-2 inhibitor. It induces cell cycle arrest and inhibits proliferation in melanoma cells, prevents activation of carcinogens, increases expression of PPAR-γ, and suppresses degranulation of bone marrow-derived mast cells.

Kimura Y, Sumiyoshi M, Sakanaka M, et al. In vitro and in vivo antiproliferative effect of a combination of ultraviolet-A and alkoxy furocoumarins isolated from Umbelliferae medicinal plants, in melanoma cells. Photochem Photobiol. 2013 Sep-Oct;89(5):1216-25. PMID: 23802687.

Marumoto S, Oda Y, Miyazawa M. Antigenotoxic activity of naturally occurring furanocoumarins. Environ Mol Mutagen. 2011 Oct;52(8):646-57. PMID: 21786339

I7155 Isoindigo

NEW

Please inquire

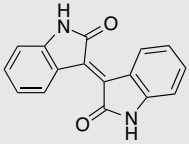

$C_{16}H_{10}N_2O_2$ FW: 262.27 [476-34-6] ≥98%

Aryl hydrocarbon receptor binding agent that inhibits cancer cell proliferation.

Wee XK, Yang T, Go ML. Exploring the anticancer activity of functionalized isoindigos: synthesis, drug-like potential, mode of action and effect on tumor-induced xenografts. ChemMedChem. 2012 May;7(5):777-91. PMID: 22416043.

Bouchikhi F, Anizon F, Moreau P. Synthesis and antiproliferative activities of isoindigo and azaisoindigo derivatives. Eur J Med Chem. 2008 Apr;43(4):755-62. PMID: 17628214.

Nishiumi S, Yamamoto N, Kodoi R, et al. Antagonistic and agonistic effects of indigoids on the transformation of an aryl hydrocarbon receptor. Arch Biochem Biophys. 2008 Feb 15;470(2):187-99. PMID: 18086550.

I7559 Isoliquiritigenin, natural

5 mg
10 mg
25 mg

4,2',4'-Trihydroxychalcone

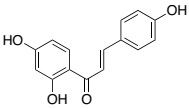

$C_{15}H_{12}O_4$ FW: 256.25 [961-29-5] ≥98%

SIRT activator, GABA-A receptor positive modulator, and inhibitor of NMDA receptors, VEGFR2, and HDACs. It increases Nrf2 expression, downregulates expression of COX-2 and PLA2, and induces apoptosis in breast cancer cells.

Chen H, Zhang B, Yuan X, et al. Isoliquiritigenin-induced effects on Nrf2 mediated antioxidant defence in the HL-60 cell monocytic differentiation. Cell Biol Int. 2013 Nov;37(11):1215-1224. PMID: 23881796.

Wang Z, Wang N, Han S, et al. Dietary compound isoliquiritigenin inhibits breast cancer neoangiogenesis via VEGF/VEGFR-2 signaling pathway. PLoS One. 2013 Jul 5;8(7):e68566. PMID: 23861918.

Li Y, Zhao H, Wang Y, et al. Isoliquiritigenin induces growth inhibition and apoptosis through downregulating arachidonic acid metabolic network and the deactivation of PI3K/Akt in human breast cancer. Toxicol Appl Pharmacol. 2013 Oct 1;272(1):37-48. PMID: 23747687.

I7341 Isoniazid

5 g
50 g
100 g

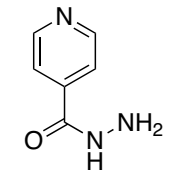

Isonicotinoylhydrazine

$C_6H_7N_3O$ FW: 137.14 [54-85-3] ≥98%

Nicotinic acid derivative and InhA inhibitor used to treat tuberculosis.

Bernardes-Génisson V, Deraeve C, Chollet A, et al. Isoniazid: an update on the multiple mechanisms for a singular action. Curr Med Chem. 2013;20(35):4370-85. PMID: 23931278.

Argyrou A, Vetting MW, Blanchard JS. New insight into the mechanism of action of and resistance to isoniazid: interaction of *Mycobacterium* tuberculosis enoyl-ACP reductase with INH-NADP. J Am Chem Soc. 2007 Aug 8;129(31):9582-3. PMID: 17636923.

Oliveira JS, Vasconcelos IB, Moreira IS, et al. Enoyl reductases as targets for the development of anti-tubercular and anti-malarial agents. Curr Drug Targets. 2007 Mar;8(3):399-411. PMID: 17348833.

I0010

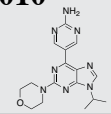

5-(9-Isopropyl-2-morpholino-9H-purin-6-yl)pyrimidin-2-amine

5 mg
25 mg

$C_{16}H_{20}N_8O$ FW: 340.39 [1246535-95-4] ≥98%

Intermediate purine analog and kinase inhibitor synthesis. **NEW**

I7356

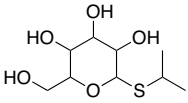

Isopropyl Thiogalactoside

IPTG

1 g
5 g
10 g

$C_9H_{18}O_5S$ FW: 238.3 [367-93-1] ≥98%

Galactose analog and allolactose mimic that induces activation of lac operon, stimulating protein expression.

Marbach A, Bettenbrock K. lac operon induction in *Escherichia* coli: Systematic comparison of IPTG and TMG induction and influence of the transacetylase LacA. J Biotechnol. 2012 Jan;157(1):82-8. PMID: 22079752.

Hansen LH, Knudsen S, Sørensen SJ. The effect of the lacY gene on the induction of IPTG inducible promoters, studied in *Escherichia* coli and *Pseudomonas* fluorescens. Curr Microbiol. 1998 Jun;36(6):341-7. PMID: 9608745.

I7259

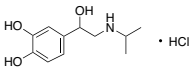

Isoproterenol Hydrochloride

5 g
25 g
100 g

$C_{11}H_{17}NO_3 \bullet HCl$ FW: 247.72 [51-30-9] ≥98%

β-Adrenergic receptor agonist used to treat bradycardia, heart block, and asthma. It increases systolic blood pressure, decreases diastolic blood pressure, and induces relaxation of airway smooth muscle.

Gong LL, Fang LH, Wang SB, et al. Coptisine exert cardioprotective effect through anti-oxidative and inhibition of RhoA/Rho kinase pathway on isoproterenol-induced myocardial infarction in rats. Atherosclerosis. 2012 May;222(1):50-8. PMID: 22387061.

Gump A, Haughney L, Fredberg J. Relaxation of activated airway smooth muscle: relative potency of isoproterenol vs. tidal stretch. J Appl Physiol (1985). 2001 Jun;90(6):2306-10. PMID: 11356796.

Green JF. Mechanism of action of isoproterenol on venous return. Am J Physiol. 1977 Feb;232(2):H152-6. PMID: 842647.

I7357

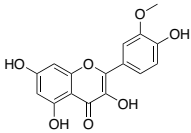

Isorhamnetin

3-Methylquercetin; Quercetin-3'-methyl ether

1 mg
5 mg
25 mg

$C_{16}H_{12}O_7$ FW: 316.26 [480-19-3] ≥98%

Found in *Tagetes*. It exhibits a variety of biological activities, including decreasing expression of COX-2 and production of ROS in edema, inducing cell cycle arrest in colon cancer cells, and suppressing activity of Src and β-catenin to prevent DSS- and azoxymethane-induced carcinogenesis.

Seo K, Yang JH, Kim SC, et al. The antioxidant effects of isorhamnetin contribute to inhibit COX-2 expression in response to inflammation: a potential role of HO-1. Inflammation. 2014 Jun;37(3):712-22. PMID: 24337631.

Li C, Yang X, Chen C, et al. Isorhamnetin suppresses colon cancer cell growth through the PI3K Akt mTOR pathway. Mol Med Rep. 2014 Mar;9(3):935-40. PMID: 24398569.

Saud SM, Young MR, Jones-Hall YL, et al. Chemopreventive activity of plant flavonoid isorhamnetin in colorectal cancer is mediated by oncogenic Src and β-catenin. Cancer Res. 2013 Sep 1;73(17):5473-84. PMID: 23824743.

I7360

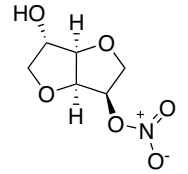

Isosorbide Mononitrate

5 g
10 g
25 g

$C_6H_9NO_6$ FW: 191.14 [16051-77-7] ≥98%

NO donor and vasodilator used to treat hydrocephalus, glaucoma, and angina pectoris.

Münzel T, Daiber A, Gori T. More answers to the still unresolved question of nitrate tolerance. Eur Heart J. 2013 Sep;34(34):2666-73. PMID: 23864131.

Cohn JN. Efficacy of vasodilators in the treatment of heart failure. J Am Coll Cardiol. 1993 Oct;22(4 Suppl A):135A-138A. PMID: 8376683.

Döring G. Antianginal and anti-ischemic efficacy of nicorandil in comparison with isosorbide-5-mononitrate and isosorbide dinitrate: results from two multicenter, double-blind, randomized studies with stable coronary heart disease patients. J Cardiovasc Pharmacol. 1992;20 Suppl 3:S74-81. PMID: 1282180.

I7447

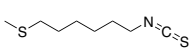

1-Isothiocyanato-6-(methylsulfenyl)-hexane

6-Methylsulfenylhexyl isothiocyanate

25 mg
50 mg
100 mg

$C_8H_{15}NS_2$ FW: 189.34 ≥98%

Potential antioxidant and synthetic analog of erucin.

Chen YJ, Huang YC, Tsai TH, et al. Effect of Wasabi Component 6-(Methylsulfinyl)hexyl Isothiocyanate and Derivatives on Human Pancreatic Cancer Cells. Evid Based Complement Alternat Med. 2014;2014:494739. PMID: 24575144.

I7457

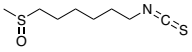

1-Isothiocyanato-6-(methylsulfinyl)-hexane

6-Methylsulfinylhexyl isothiocyanate

$C_8H_{15}NOS_2$ FW: 205.34 ≥98%

25 mg
50 mg
100 mg

Synthetic derivative of 6-methylsulfinyl-hexane isothiocyanate and analog of sulforaphane. It inhibits GSK-3β. It inhibits SOX2 signaling and induces cell cycle arrest in pancreatic cancer cells, suppresses oxidative stress in striatal cultures, and decreases pro-inflammatory cytokine release in macrophages.

Fuke Y, Hishinuma M, Namikawa M, et al. Wasabi-derived 6-(methylsulfinyl)hexyl isothiocyanate induces apoptosis in human breast cancer by possible involvement of the NF-κB pathways. Nutr Cancer. 2014;66(5):879-87. PMID: 24895898.

Chen YJ, Huang YC, Tsai TH, et al. Effect of Wasabi Component 6-(Methylsulfinyl)hexyl Isothiocyanate and Derivatives on Human Pancreatic Cancer Cells. Evid Based Complement Alternat Med. 2014;2014:494739. PMID: 24575144.

Uto T, Hou DX, Morinaga O, et al. Molecular Mechanisms Underlying Anti-Inflammatory Actions of 6-(Methylsulfinyl)hexyl Isothiocyanate Derived from Wasabi (Wasabia japonica). Adv Pharmacol Sci. 2012;2012:614046. PMID: 22927840.

I7557

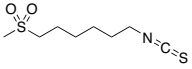

1-Isothiocyanato-6-(methylsulfonyl)-hexane

6-Methylsulfonylhexyl isothiocyanate

$C_8H_{15}NO_2S_2$ FW: 221.34 ≥98%

25 mg
50 mg
100 mg

Potential antioxidant and synthetic analog of erysolin. It inhibits SOX2 signaling and induces cell cycle arrest in pancreatic cancer cells.

Chen YJ, Huang YC, Tsai TH, et al. Effect of Wasabi Component 6-(Methylsulfinyl)hexyl Isothiocyanate and Derivatives on Human Pancreatic Cancer Cells. Evid Based Complement Alternat Med. 2014;2014:494739. PMID: 24575144.

I7746

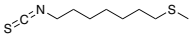

1-Isothiocyanato-7-(methylsulfenyl)-heptane

7-Methylsulfenylheptyl isothiocyanate

$C_9H_{17}NS_2$ FW: 203.37 ≥98%

10 mg
25 mg
50 mg

Potential antioxidant and synthetic analog of erucin.

I7456

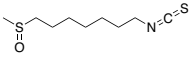

1-Isothiocyanato-7-(methylsulfinyl)-heptane

7-Methylsulfinylheptyl isothiocyanate

$C_9H_{17}NOS_2$ FW: 219.37 ≥98%

10 mg
25 mg
50 mg
100 mg

It induces phase II enzyme activity, inhibits MMP-9 signaling, and scavenges superoxide radicals. It also suppresses cell invasion in breast cancer cells.

Rose P, Huang Q, Ong CN, et al. Broccoli and watercress suppress matrix metalloproteinase-9 activity and invasiveness of human MDA-MB-231 breast cancer cells. Toxicol Appl Pharmacol. 2005 Dec 1;209(2):105-13. PMID: 15953625.

Kinae N, Masuda H, Shin IS, et al. Functional properties of wasabi and horseradish. Biofactors. 2000;13(1-4):265-9. PMID: 11237192.

Rose P, Faulkner K, Williamson G, et al. 7-Methylsulfinylheptyl and 8-methylsulfinyloctyl isothiocyanates from watercress are potent inducers of phase II enzymes. Carcinogenesis. 2000 Nov;21(11):1983-8. PMID: 11062158.

I7455

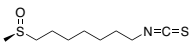

R-1-Isothiocyanato-7-(methylsulfinyl)-heptane

$C_9H_{17}NOS_2$ FW: 219.37 ≥98%

5 mg
10 mg
25 mg

Natural product and antioxidant. It increases phase II enzyme expression and suppresses MMP9 activity.

Rose P, Huang Q, Ong CN, et al. Broccoli and watercress suppress matrix metalloproteinase-9 activity and invasiveness of human MDA-MB-231 breast cancer cells. Toxicol Appl Pharmacol. 2005 Dec 1;209(2):105-13. PMID: 15953625.

Kinae N, Masuda H, Shin IS, et al. Functional properties of wasabi and horseradish. Biofactors. 2000;13(1-4):265-9. PMID: 11237192.

I7556

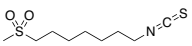

1-Isothiocyanato-7-(methylsulfonyl)-heptane

7-Methylsulfonylheptyl isothiocyanate

$C_9H_{17}NO_2S_2$ FW: 235.37 ≥98%

10 mg
25 mg
50 mg

Potential antioxidant and synthetic analog of erysolin.

I7359

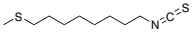

1-Isothiocyanato-8-(methylsulfenyl)-octane

8-Methylsulfenyloctyl isothiocyanate

$C_{10}H_{19}NS_2$ FW: 217.4 ≥98%

25 mg
50 mg
100 mg

Potential antioxidant and synthetic analog of erucin.

I7459 — 1-Isothiocyanato-8-(methylsulfinyl)-octane

25 mg
50 mg
100 mg

8-Methylsulfinyloctyl isothiocyanate

$C_{10}H_{19}NOS_2$ FW: 233.4 ≥98%

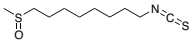

Synthetic antioxidant found in *Nasturtium officinale* (watercress). It induces phase II enzyme activity.

Rose P, Faulkner K, Williamson G, et al. 7-Methylsulfinylheptyl and 8-methylsulfinyloctyl isothiocyanates from watercress are potent inducers of phase II enzymes. Carcinogenesis. 2000 Nov;21(11):1983-8. PMID: 11062158.

I7460 — R-1-Isothiocyanato-8-(methylsulfinyl)-octane

5 mg
10 mg
25 mg

$C_{10}H_{19}NOS_2$ FW: 233.39 ≥98%

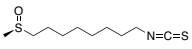

Natural product found in *Nasturtium officinale*. It induces phase II enzyme activity.

Rose P, Faulkner K, Williamson G, et al. 7-Methylsulfinylheptyl and 8-methylsulfinyloctyl isothiocyanates from watercress are potent inducers of phase II enzymes. Carcinogenesis. 2000 Nov;21(11):1983-8. PMID: 11062158.

I7659 — 1-Isothiocyanato-8-(methylsulfonyl)-octane

25 mg
50 mg
100 mg

8-Methylsulfonyloctyl isothiocyanate

$C_{10}H_{19}NO_2S_2$ FW: 249.4 ≥98%

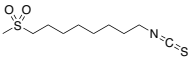

Potential antioxidant and synthetic analog of erysolin.

I7558 — 1-Isothiocyanato-9-(methylsulfenyl)-nonane

25 mg
50 mg
100 mg

9-Methylsulfenylnonyl isothiocyanate

$C_{11}H_{21}NS_2$ FW: 234.42 ≥97%

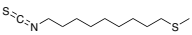

Potential antioxidant and synthetic analog of erucin.

I7458 — 1-Isothiocyanato-9-(methylsulfinyl)-nonane

25 mg
50 mg
100 mg

9-Methylsulfinylnonnyl isothiocyanate

$C_{11}H_{21}NOS_2$ FW: 247.42 ≥98%

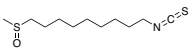

Potential antioxidant and synthetic analog of sulforaphane.

I7658 — 1-Isothiocyanato-9-(methylsulfonyl)-nonane

25 mg
50 mg
100 mg

9-Methylsulfonylnonyl isothiocyanate

$C_{11}H_{21}NO_2S_2$ FW: 263.42 ≥98%

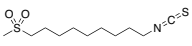

Potential antioxidant and synthetic analog of erysolin.

I7759 — Isoxanthohumol

1 mg
5 mg
10 mg

$C_{21}H_{22}O_5$ FW: 354.39 [70872-29-6] ≥98%

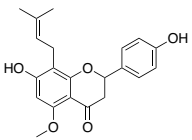

Less potent derivative of xanthohumol found in *Humulus lupulus*. It modulates signaling between endothelial cells and vascular smooth muscle cells, induces apoptosis in mature adipocytes, and inhibits differentiation of preadipocytes.

Negrão R, Duarte D, Costa R, et al. Isoxanthohumol modulates angiogenesis and inflammation via vascular endothelial growth factor receptor, tumor necrosis factor alpha and nuclear factor kappa B pathways. Biofactors. 2013 Aug 1. [Epub ahead of print] PMID: 23904052.

Negrão R, Costa R, Duarte D, et al. Angiogenesis and inflammation signaling are targets of beer polyphenols on vascular cells. J Cell Biochem. 2010 Dec 1;111(5):1270-9. PMID: 20803553.

Possemiers S, Rabot S, Espín JC, et al. Eubacterium limosum activates isoxanthohumol from hops (*Humulus lupulus* L.) into the potent phytoestrogen 8-prenylnaringenin in vitro and in rat intestine. J Nutr. 2008 Jul;138(7):1310-6. PMID: 18567753.

I7478 — Istradefylline NEW

5 mg
25 mg
100 mg

KW-6002

$C_{20}H_{24}N_4O_4$ FW: 384.43 [155270-99-8] ≥98%

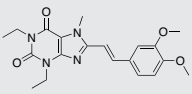

Caffeine analog and adenosine A2A receptor antagonist. It decreases "off" time in subjects with Parkinson's disease without worsening dyskinesia and decreases GABA release.

Kadowaki Horita T, Kobayashi M, Mori A, et al. Effects of the adenosine A2A antagonist istradefylline on cognitive performance in rats with a 6-OHDA lesion in prefrontal cortex. Psychopharmacology (Berl). 2013 Dec;230(3):345-52. PMID: 23748382.

Saki M, Yamada K, Koshimura E, et al. In vitro pharmacological profile of the A2A receptor antagonist istradefylline. Naunyn Schmiedebergs Arch Pharmacol. 2013 Nov;386(11):963-72. PMID: 23812646.

Mizuno Y, Hasegawa K, Kondo T, et al. Clinical efficacy of istradefylline (KW-6002) in Parkinson's disease: a randomized, controlled study. Mov Disord. 2010 Jul 30;25(10):1437-43. PMID: 20629136.

I7757 Itopride Hydrochloride

1 g
5 g
25 g

$C_{20}H_{26}N_2O_4 \bullet HCl$ FW: 394.88 [122892-31-3] ≥98%

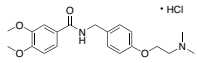

AChE inhibitor and dopamine D2 receptor antagonist used to treat functional dyspepsia and gastroesophageal reflux disease. It inhibits lower esophageal sphincter relaxation.

Huang X, Lv B, Zhang S, et al. Itopride therapy for functional dyspepsia: a meta-analysis. World J Gastroenterol. 2012 Dec 28;18(48):7371-7. PMID: 23326147.

Scarpellini E, Vos R, Blondeau K, et al. The effects of itopride on oesophageal motility and lower oesophageal sphincter function in man. Aliment Pharmacol Ther. 2011 Jan;33(1):99-105. PMID: 21083582.

Lim HC, Kim YG, Lim JH, et al. Effect of itopride hydrochloride on the ileal and colonic motility in guinea pig in vitro. Yonsei Med J. 2008 Jun 30;49(3):472-8. PMID: 18581598.

I7870 Itraconazole

50 mg
100 mg
250 mg
1 g

$C_{35}H_{38}Cl_2N_8O_4$ FW: 705.63 [84625-61-6] ≥98%

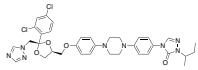

Inhibitor of Smoothened and 14-α demethylase that inhibits ergosterol synthesis and fungal cell wall formation. It also inhibits VEGF-induced angiogenesis and prevents growth of medulloblastoma tumors.

Kim J, Tang JY, Gong R, et al. Itraconazole, a commonly used antifungal that inhibits Hedgehog pathway activity and cancer growth. Cancer Cell. 2010 Apr 13;17(4):388-99. PMID: 20385363.

Chong CR, Xu J, Lu J, et al. Inhibition of angiogenesis by the antifungal drug itraconazole. ACS Chem Biol. 2007 Apr 24;2(4):263-70. PMID: 17432820.

I8618 Ivermectin

1 g
5 g

22,23-Dihydroavermectin B1; MK-933

$C_{48}H_{74}O_{14}$ FW: 875.09 [70288-86-7] ≥95%

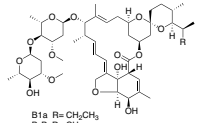

B1a R= CH_2CH_3
B_1B R= CH_3

Glu-gated Cl^- channel activator and agonist at GlyRs and GABA-A receptors. It interferes with neurotransmission and muscle function in arthropods and nematodes.

Chaccour CJ, Kobylinski KC, Bassat Q, et al. Ivermectin to reduce malaria transmission: a research agenda for a promising new tool for elimination. Malar J. 2013 May 7;12:153. PMID: 23647969.

Lynagh T, Lynch JW. Molecular mechanisms of Cys-loop ion channel receptor modulation by ivermectin. Front Mol Neurosci. 2012 May 7;5:60. PMID: 22586367.

I9060 IWP-2

NEW

5 mg
10 mg

$C_{22}H_{18}N_4O_2S_3$ FW: 466.6 [686770-61-6] ≥98%

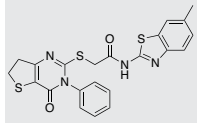

PORCN inhibitor. It suppresses Wnt signaling and inhibits proliferation, migration, and invasion of gastric cancer cells and colorectal cancer cells.

Frewer KA, Sanders AJ, Owen S, et al. A role for WISP2 in colorectal cancer cell invasion and motility. Cancer Genomics Proteomics. 2013 Jul-Aug;10(4):187-96. PMID: 23893926.

Mo ML, Li MR, Chen Z, et al. Inhibition of the Wnt palmitoyltransferase porcupine suppresses cell growth and downregulates the Wnt/β-catenin pathway in gastric cancer. Oncol Lett. 2013 May;5(5):1719-1723. PMID: 23761839.

J0001 J-147

NEW

5 mg
25 mg
100 mg

$C_{18}H_{17}F_3N_2O_2$ FW: 350.34 [1146963-51-0] ≥98%

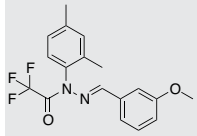

It decreases neuronal loss, oxidative stress, and glutamate-induced neurotoxicity.

Chen HY, Xu DP, Tan GL, et al. A Potent Multi-functional Neuroprotective Derivative of Tetramethylpyrazine. J Mol Neurosci. 2015 May 17. [Epub ahead of print]. PMID: 25982925.

Prior M, Dargusch R, Ehren JL, et al. The neurotrophic compound J147 reverses cognitive impairment in aged Alzheimer's disease mice. Alzheimers Res Ther. 2013 May 14;5(3):25. PMID: 23673233.

Chiruta C, Zhao Y, Tang F, et al. Metabolism of a potent neuroprotective hydrazide. Bioorg Med Chem. 2013 May 15;21(10):2733-41. PMID: 23582448.

J0240 JAK2 Inhibitor V

NEW

5 mg
25 mg

Z3

$C_{23}H_{24}N_2O$ FW: 344.46 [195371-52-9] ≥98%

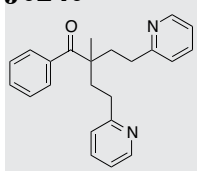

JAK2 inhibitor. It induces cell cycle arrest and suppresses cell proliferation in erythroleukemia cells.

Sayyah J, Magis A, Ostrov DA, et al. Z3, a novel Jak2 tyrosine kinase small-molecule inhibitor that suppresses Jak2-mediated pathologic cell growth. Mol Cancer Ther. 2008 Aug;7(8):2308-18. PMID: 18723478.

J0378 Jatrorrhizine

NEW

1 mg
5 mg

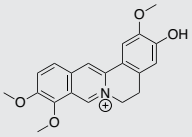

$C_{20}H_{20}NO_4$ FW: 338.38 [3621-38-3] ≥98%

AChE inhibitor found in *Corydalis* and *Coptydis*. It increases expression of p21 and p27 and induces cell cycle arrest in melanoma cells, suppresses amyloid-β-induced toxicity in neurons, inhibits growth of *Plasmodium*, *Leishmania*, and *Trypanosoma*, and increases gastric emptying rates.

Liu R, Cao Z, Pan Y, et al. Jatrorrhizine hydrochloride inhibits the proliferation and neovascularization of C8161 metastatic melanoma cells. Anticancer Drugs. 2013 Aug;24(7):667-76. PMID: 23695011.

Malebo HM, Wenzler T, Cal M, et al. Anti-protozoal activity of aporphine and protoberberine alkaloids from Annickia kummeriae (Engl. & Diels) Setten & Maas (Annonaceae). BMC Complement Altern Med. 2013 Feb 27;13:48. PMID: 23445637.

Luo T, Jiang W, Kong Y, et al. The protective effects of jatrorrhizine on β-amyloid (25-35)-induced neurotoxicity in rat cortical neurons. CNS Neurol Disord Drug Targets. 2012 Dec;11(8):1030-7. PMID: 23244426.

J0379 Jatrorrhizine Chloride

NEW

1 mg
5 mg

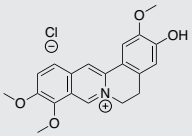

$C_{20}H_{20}NO_4$ Cl FW: 373.83 [6681-15-8] ≥95%

AChE inhibitor found in *Corydalis* and *Coptydis*. It increases expression of p21 and p27 and induces cell cycle arrest in melanoma cells, suppresses amyloid-β-induced toxicity in neurons, inhibits growth of *Plasmodium*, *Leishmania*, and *Trypanosoma*, and increases gastric emptying rates.

Liu R, Cao Z, Pan Y, et al. Jatrorrhizine hydrochloride inhibits the proliferation and neovascularization of C8161 metastatic melanoma cells. Anticancer Drugs. 2013 Aug;24(7):667-76. PMID: 23695011.

Malebo HM, Wenzler T, Cal M, et al. Anti-protozoal activity of aporphine and protoberberine alkaloids from Annickia kummeriae (Engl. & Diels) Setten & Maas (Annonaceae). BMC Complement Altern Med. 2013 Feb 27;13:48. PMID: 23445637.

J3204 E-JIB-04

NEW

5 mg
25 mg

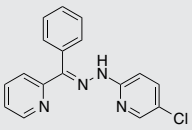

NSC 693627; JHDM inhibitor VII

$C_{17}H_{13}ClN_4$ FW: 308.77 [199596-05-9] ≥98%

E stereoisomer of JIB-04 and inhibitor of Jumonji family histone demethylases. It inhibits cell viability, decreases tumor burden, and increases survival rates in animal models of cancer.

Van Rechem C, Black JC, Boukhali M, et al. Lysine demethylase KDM4A associates with translation machinery and regulates protein synthesis. Cancer Discov. 2015 Mar;5(3):255-63. PMID: 25564516.

Wang L, Chang J, Varghese D, et al. A small molecule modulates Jumonji histone demethylase activity and selectively inhibits cancer growth. Nat Commun. 2013;4:2035. Erratum in: Nat Commun. 2013;4:2639. PMID: 23792809.

J3205 Z-JIB-04

NEW

5 mg
25 mg

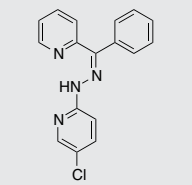

NSC 693627

$C_{17}H_{13}ClN_4$ FW: 308.77 [199596-24-2] ≥98%

Z stereoisomer of JIB-04 and inhibitor of Jumonji family histone demethylases. It inhibits cell viability, decreases tumor burden, and increases survival rates in animal models of cancer.

Van Rechem C, Black JC, Boukhali M, et al. Lysine demethylase KDM4A associates with translation machinery and regulates protein synthesis. Cancer Discov. 2015 Mar;5(3):255-63. PMID: 25564516.

J5237 JNJ-26854165

NEW

5 mg
25 mg

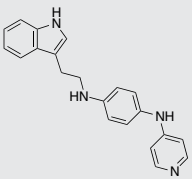

Serdemetan

$C_{21}H_{20}N_4$ FW: 328.42 [881202-45-5] ≥98%

E3 ligase MDM2 inhibitor. It delays tumor growth in animal models and prevents cholesterol efflux and transport in mantle cell lymphoma and multiple myeloma cells.

Jones RJ, Gu D, Bjorklund CC, et al. The novel anticancer agent JNJ-26854165 induces cell death through inhibition of cholesterol transport and degradation of ABCA1. J Pharmacol Exp Ther. 2013 Sep;346(3):381-92. Erratum in: J Pharmacol Exp Ther. 2013 Nov;347(2):540. PMID: 23820125.

Chargari C, Leteur C, Angevin E, et al. Preclinical assessment of JNJ-26854165 (Serdemetan), a novel tryptamine compound with radiosensitizing activity in vitro and in tumor xenografts. Cancer Lett. 2011 Dec 22;312(2):209-18. PMID: 21937165.

Kojima K, Burks JK, Arts J, et al. The novel tryptamine derivative JNJ-26854165 induces wild-type p53- and E2F1-mediated apoptosis in acute myeloid and lymphoid leukemias. Mol Cancer Ther. 2010 Sep;9(9):2545-57. PMID: 20736344.

J6400

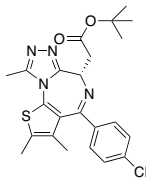

(+)-JQ-1

1 mg
5 mg
25 mg

$C_{23}H_{25}ClN_4O_2S$ FW: 456.99 [1268524-70-4] ≥99%

BRD inhibitor. It prevents sperm production, activates latent HIV-1, inhibits T cell proliferation, and induces cell cycle arrest in leukemia cells.

Cinar M, Rosenfelt F, Rokhsar S, et al. Concurrent inhibition of MYC and BCL2 is a potentially effective treatment strategy for double hit and triple hit B-cell lymphomas. Leuk Res. 2015 Apr 17. [Epub ahead of print]. PMID: 25916698.

Da Costa D, Agathanggelou A, Perry T, et al. BET inhibition as a single or combined therapeutic approach in primary paediatric B-precursor acute lymphoblastic leukaemia. Blood Cancer J. 2013 Jul 19;3:e126. PMID: 23872705.

Ott CJ, Kopp N, Bird L, et al. BET bromodomain inhibition targets both c-Myc and IL7R in high-risk acute lymphoblastic leukemia. Blood. 2012 Oct 4;120(14):2843-52. PMID: 22904298.

J8800

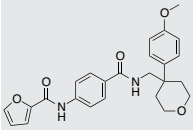

JW55

NEW

5 mg
25 mg

$C_{25}H_{26}N_2O_5$ FW: 434.49 [664993-53-7] ≥98%

TNKS inhibitor that suppresses Wnt signaling. It decreases body weight and intestinal epithelial stem cell proliferation in animal models of high-fat diet and diabetes.

Mao J, Hu X, Xiao Y, et al. Overnutrition stimulates intestinal epithelium proliferation through β-catenin signaling in obese mice. Diabetes. 2013 Nov;62(11):3736-46. PMID: 23884889.

Waaler J, Machon O, Tumova L, et al. A novel tankyrase inhibitor decreases canonical Wnt signaling in colon carcinoma cells and reduces tumor growth in conditional APC mutant mice. Cancer Res. 2012 Jun 1;72(11):2822-32. PMID: 22440753.

K0021

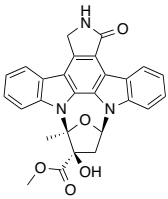

K252a

SF 2370

100 µg
1 mg
5 mg

$C_{27}H_{21}N_3O_5$ FW: 467.48 [99533-80-9] ≥98%

Staurosporine analog, PKC inhibitor, and TrkA/B receptor antagonist. It suppresses activity of neurotrophins.

El-Hashim AZ, Jaffal SM, Al-Rashidi FT, et al. Nerve growth factor enhances cough via a central mechanism of action. Pharmacol Res. 2013 Aug;74:68-77. PMID: 23742790.

Cardenas-Aguayo Mdel C, Kazim SF, Grundke-Iqbal I, et al. Neurogenic and neurotrophic effects of BDNF peptides in mouse hippocampal primary neuronal cell cultures. PLoS One. 2013;8(1):e53596. PMID: 23320097.

Sugiya H, Putney JW Jr. Protein kinase C-dependent and -independent mechanisms regulating the parotid substance P receptor as revealed by differential effects of protein kinase C inhibitors. Biochem J. 1988 Dec 1;256(2):677-80. PMID: 2464997.

K0022

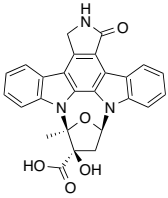

K252b

100 µg
1 mg

$C_{26}H_{16}N_3O_5$ FW: 453.13 [99570-78-2] ≥98%

Staurosporine analog and PKC inhibitor that suppresses DNA synthesis. It also inhibits microbial ectoprotein kinases and inhibits IgE cross-linking-dependent degranulation in basophils.

Lecht S, Arien-Zakay H, Kohan M, et al. Angiostatic effects of K252a, a Trk inhibitor, in murine brain capillary endothelial cells. Mol Cell Biochem. 2010 Jun;339(1-2):201-13. PMID: 20148355.

Okada M, Hojo Y, Ikeda U, et al. Interaction between monocytes and vascular smooth muscle cells induces expression of hepatocyte growth factor. J Hypertens. 2000 Dec;18(12):1825-31. PMID: 11132607.

Teshima R, Saito Y, Ikebuchi H, et al. Effect of an ectokinase inhibitor, K252b, on degranulation and Ca^{2+} signals of RBL-2H3 cells and human basophils. J Immunol. 1997 Jul 15;159(2):964-9. PMID: 9218617.

K0023

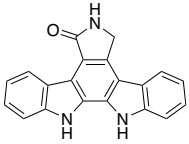

K252c

1 mg
5 mg

$C_{20}H_{13}N_3O$ FW: 311.34 [85753-43-1] ≥98%

Staurosporine analog and inhibitor of PKC and PKA. It inhibits proliferation of human cytomegalovirus and induces apoptosis in cancer cells.

Liu R, Zhu T, Li D, et al. Two indolocarbazole alkaloids with apoptosis activity from a marine-derived actinomycete Z(2)039-2. Arch Pharm Res. 2007 Mar;30(3):270-4. PMID: 17424930.

Zimmermann A, Wilts H, Lenhardt M, et al. Indolocarbazoles exhibit strong antiviral activity against human cytomegalovirus and are potent inhibitors of the pUL97 protein kinase. Antiviral Res. 2000 Oct;48(1):49-60. PMID: 11080540.

Fabre S, Prudhomme M, Rapp M. Protein kinase C inhibitors; structure-activity relationships in K252c-related compounds. Bioorg Med Chem. 1993 Sep;1(3):193-6. PMID: 8081852.

K0117

Kaempferol

1 mg
5 mg
10 mg
25 mg

Nimbecetin; Populnetin; Rhamnolutein; Robigenin; Swartziol; Trifolitin

$C_{15}H_{10}O_6$ FW: 286.24 [520-18-3] ≥98%

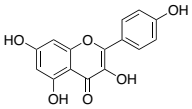

Found in various plant sources. It exhibits several biological activities, including inhibiting LPS-stimulated pro-inflammatory cytokine release, inducing apoptosis in bladder cancer cells, suppressing VEGF secretion and angiogenesis, and decreasing adipogenesis and triglyceride synthesis.

Tang XL, Liu JX, Dong W, et al. Protective Effect of Kaempferol on LPS plus ATP-Induced Inflammatory Response in Cardiac Fibroblasts. Inflammation. 2014 Sep 5. [Epub ahead of print]. PMID: 25189464.

Yang EJ, Kim GS, Jun M, et al. Kaempferol attenuates the glutamate-induced oxidative stress in mouse-derived hippocampal neuronal HT22 cells. Food Funct. 2014 Jul 25;5(7):1395-402. PMID: 24770605.

Dang Q, Song W, Xu D, et al. Kaempferol suppresses bladder cancer tumor growth by inhibiting cell proliferation and inducing apoptosis. Mol Carcinog. 2014 Apr 2. [Epub ahead of print]. PMID: 24700700.

K0030

Kahweol

10 mg
25 mg
100 mg
500 mg

$C_{20}H_{26}O_3$ FW: 314.42 [6894-43-5] ≥97%

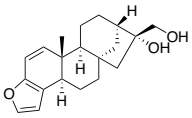

Natural product found in coffee beans. It exhibits a wide variety of biological activities, including inhibiting RANKL-induced osteoclast generation, inducing cell cycle arrest and apoptosis in oral squamous cell carcinoma cells, preventing aflatoxin B1-induced DNA adduct formation, and suppressing H_2O_2-induced DNA damage and oxidative stress.

Chae JI, Jeon YJ, Shim JH. Anti-Proliferative Properties of Kahweol in Oral Squamous Cancer Through the Regulation Specificity Protein 1. Phytother Res. 2014 Sep 8. [Epub ahead of print]. PMID: 25196544.

Wu KC, McDonald PR, Liu J, et al. Screening of natural compounds as activators of the keap1-nrf2 pathway. Planta Med. 2014 Jan;80(1):97-104. PMID: 24310212.

Fumimoto R, Sakai E, Yamaguchi Y, et al. The coffee diterpene kahweol prevents osteoclastogenesis via impairment of NFATc1 expression and blocking of Erk phosphorylation. J Pharmacol Sci. 2012;118(4):479-86. PMID: 22447306.

K0031

Kahweol Acetate

10 mg
25 mg
100 mg
500 mg

$C_{22}H_{28}O_4$ FW: 356.47 [81760-47-6] ≥98%

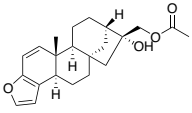

Semi-synthetic derivative of kahweol, a natural product found in coffee beans. It exhibits a wide variety of biological activities, including inhibiting RANKL-induced osteoclast generation, inducing cell cycle arrest and apoptosis in oral squamous cell carcinoma cells, preventing aflatoxin B1-induced DNA adduct formation, and suppressing H_2O_2-induced DNA damage and oxidative stress.

Chae JI, Jeon YJ, Shim JH. Anti-Proliferative Properties of Kahweol in Oral Squamous Cancer Through the Regulation Specificity Protein 1. Phytother Res. 2014 Sep 8. [Epub ahead of print]. PMID: 25196544.

K0034

Kahweol Eicosanate

10 mg
25 mg
100 mg

$C_{40}H_{64}O_4$ FW: 608.93 [108214-32-0] ≥98%

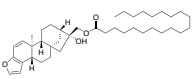

Semi-synthetic derivative of kahweol, a natural product found in coffee beans. It exhibits a wide variety of biological activities, including inhibiting RANKL-induced osteoclast generation, inducing cell cycle arrest and apoptosis in oral squamous cell carcinoma cells, preventing aflatoxin B1-induced DNA adduct formation, and suppressing H_2O_2-induced DNA damage and oxidative stress.

Chae JI, Jeon YJ, Shim JH. Anti-Proliferative Properties of Kahweol in Oral Squamous Cancer Through the Regulation Specificity Protein 1. Phytother Res. 2014 Sep 8. [Epub ahead of print]. PMID: 25196544.

K0036

Kahweol Linoleate

10 mg
25 mg
100 mg

$C_{38}H_{56}O_4$ FW: 576.85 [108214-29-5] ≥98%

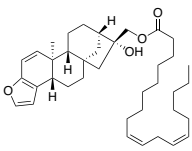

Semi-synthetic derivative of kahweol, a natural product found in coffee beans. It exhibits a wide variety of biological activities, including inhibiting RANKL-induced osteoclast generation, inducing cell cycle arrest and apoptosis in oral squamous cell carcinoma cells, preventing aflatoxin B1-induced DNA adduct formation, and suppressing H_2O_2-induced DNA damage and oxidative stress.

Chae JI, Jeon YJ, Shim JH. Anti-Proliferative Properties of Kahweol in Oral Squamous Cancer Through the Regulation Specificity Protein 1. Phytother Res. 2014 Sep 8. [Epub ahead of print]. PMID: 25196544.

K0038 Kahweol Oleate

10 mg
25 mg
100 mg

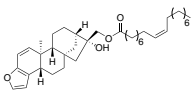

$C_{38}H_{58}O_4$ FW: 578.86 [108214-30-8] ≥98%

Semi-synthetic derivative of kahweol, a natural product found in coffee beans. It exhibits a wide variety of biological activities, including inhibiting RANKL-induced osteoclast generation, inducing cell cycle arrest and apoptosis in oral squamous cell carcinoma cells, preventing aflatoxin B1-induced DNA adduct formation, and suppressing H_2O_2-induced DNA damage and oxidative stress.

Chae JI, Jeon YJ, Shim JH. Anti-Proliferative Properties of Kahweol in Oral Squamous Cancer Through the Regulation Specificity Protein 1. Phytother Res. 2014 Sep 8. [Epub ahead of print]. PMID: 25196544.

K0032 Kahweol Palmitate

10 mg
25 mg
100 mg
500 mg

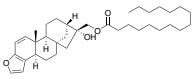

$C_{36}H_{56}O_4$ FW: 552.42 [81760-45-4] ≥97%

Semi-synthetic derivative of kahweol, a natural product found in coffee beans. It exhibits a wide variety of biological activities, including inhibiting RANKL-induced osteoclast generation, inducing cell cycle arrest and apoptosis in oral squamous cell carcinoma cells, preventing aflatoxin B1-induced DNA adduct formation, and suppressing H_2O_2-induced DNA damage and oxidative stress.

Chae JI, Jeon YJ, Shim JH. Anti-Proliferative Properties of Kahweol in Oral Squamous Cancer Through the Regulation Specificity Protein 1. Phytother Res. 2014 Sep 8. [Epub ahead of print]. PMID: 25196544.

K0040 Kahweol Stearate

10 mg
25 mg
100 mg

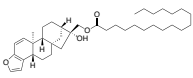

$C_{38}H_{60}O_4$ FW: 580.88 [108214-31-9] ≥98%

Semi-synthetic derivative of kahweol, a natural product found in coffee beans. It exhibits a wide variety of biological activities, including inhibiting RANKL-induced osteoclast generation, inducing cell cycle arrest and apoptosis in oral squamous cell carcinoma cells, preventing aflatoxin B1-induced DNA adduct formation, and suppressing H_2O_2-induced DNA damage and oxidative stress.

Chae JI, Jeon YJ, Shim JH. Anti-Proliferative Properties of Kahweol in Oral Squamous Cancer Through the Regulation Specificity Protein 1. Phytother Res. 2014 Sep 8. [Epub ahead of print]. PMID: 25196544.

K0133 Kainic Acid

10 mg
25 mg
100 mg

Digenin; Helminal

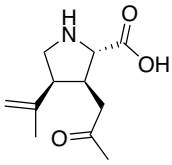

$C_{10}H_{15}NO_4$ FW: 213.23 [487-79-6] ≥98%

Excitatory amino acid and AMPA and kainate receptor agonist found in seaweed. It increases glutamate release and stimulates Na^+ channels, inducing seizures.

Fritsch B, Reis J, Gasior M, et al. Role of GluK1 kainate receptors in seizures, epileptic discharges, and epileptogenesis. J Neurosci. 2014 Apr 23;34(17):5765-75. PMID: 24760837.

Ben-Ari Y. Kainate and Temporal Lobe Epilepsies: 3 decades of progress. In: Noebels JL, Avoli M, Rogawski MA, et al. editors. Jasper's Basic Mechanisms of the Epilepsies [Internet]. 4th edition. Bethesda (MD): National Center for Biotechnology Information (US); 2012. PMID: 22787646.

K0144 Kallikrein Inhibitor

1 mg
2 mg
5 mg

KKI 5

Ac-Pro-Phe-Arg-Ser-Val-Gln-NH_2

$C_{35}H_{55}N_{11}O_9$ FW: 773.9 [97145-43-2] ≥95%

Serine protease inhibitor. It alters membrane potential and increases intracellular Ca^{2+}, inhibiting cell proliferation.

Bilgin M, Burgazli KM, Rafiq A, et al. Effect of bauhinia bauhinioides kallikrein inhibitor on endothelial proliferation and intracellular calcium concentration. Eur Rev Med Pharmacol Sci. 2014 Jan;18(1):46-51. PMID: 24452941.

Nakahata AM, Mayer B, Neth P, et al. Blocking the proliferation of human tumor cell lines by peptidase inhibitors from Bauhinia seeds. Planta Med. 2013 Mar;79(3-4):227-35. PMID: 23345168.

K0053 Kanamycin A

1 g
5 g
25 g

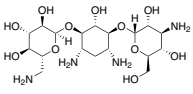

$C_{18}H_{36}N_4O_{11}$ FW: 484.5 [59-01-8] ≥98%

Inhibitor of protein translation and mammalian RNA splicing. It inhibits growth of gram negative bacteria and prevents formation of the initiation complex.

Romanowska J, Reuter N, Trylska J. Comparing aminoglycoside binding sites in bacterial ribosomal RNA and aminoglycoside modifying enzymes. Proteins. 2013 Jan;81(1):63-80. PMID: 22907688.

Patwardhan A, Cowan JA. Influence of charge and structure on the coordination chemistry of copper aminoglycosides. Dalton Trans. 2011 Feb 28;40(8):1795-801. PMID: 21218243.

K0054

Kanamycin B

100 mg
250 mg
1 g

Bekanamycin; NK-1006; Nebramycin V

$C_{18}H_{37}N_5O_{10}$ FW: 483.51 [4696-76-8] ≥98%

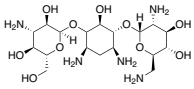

Inhibitor of protein translation and mammalian RNA splicing. It inhibits growth of gram negative bacteria, prevents formation of the initiation complex, and decreases action potential amplitude in cardiac pacemaker cells.

Patwardhan A, Cowan JA. Influence of charge and structure on the coordination chemistry of copper aminoglycosides. Dalton Trans. 2011 Feb 28;40(8):1795-801. PMID: 21218243.

Aukema KG, Chohan KK, Plourde GL, et al. Small molecule inhibitors of yeast pre-mRNA splicing. ACS Chem Biol. 2009 Sep 18;4(9):759-68. PMID: 19634919.

Morales MA, Castrillon JL, Hernandez DA. Effects of bekanamycin and dibekacin on the electrical activity of cardiac pacemaker cells. Arch Med Res. 1993 Winter;24(4):339-45. PMID: 8118157.

K0172

Kassinin

1 mg
2 mg
5 mg

$C_{59}H_{95}N_{15}O_{18}S$ FW: 1334.6 [63968-82-1] ≥95%

Asp-Val-Pro-Lys-Ser-Asp-Gln-Phe-Val-Gly-Leu-Met-NH_2

NK2 receptor agonist found in amphibians. It stimulates ion transport across skin membranes, induces contractions in bladder muscles, and inhibits both gastric acid secretion and gastric emptying.

Lippe C, Bellantuono V, Ardizzone C, et al. Eledoisin and Kassinin, but not Enterokassinin, stimulate ion transport in frog skin. Peptides. 2004 Nov;25(11):1971-5. PMID: 15501529.

Bolle P, Severini C, Falconieri-Erspamer G, et al. Effects of natural tachykinins on porcine lower urinary tract smooth muscle. J Auton Pharmacol. 2000 Jun;20(3):157-61. PMID: 11193004.

K0276

Katacalcin

0.5 mg
1 mg
2.5 mg

CCAP; CCP I; Calcitonin carboxyl-terminal flanking peptide

$C_{97}H_{154}N_{34}O_{36}S_2$ FW: 2436.64 [85916-47-8] ≥95%

H-Asp-Met-Ser-Ser-Asp-Leu-Glu-Arg-Asp-His-Arg-Pro-His-Val-Ser-Met-Pro-Gln-Asn-Ala-Asn-OH

PKA activator found in crustaceans. It induces migration of CD14+ peripheral blood mononuclear cells and deactivates chemotaxis.

Kaneider NC, Egger P, Wiedermann FJ, et al. Involvement of cyclic adenosine monophosphate-dependent protein kinase A and pertussis toxin-sensitive G proteins in the migratory response of human CD14+ mononuclear cells to katacalcin. J Bone Miner Res. 2002 Oct;17(10):1872-82. PMID: 12369791.

Angelucci F, Gruber SH, Mathé AA. A pilot study of rat brain regional distribution of calcitonin, katacalcin and calcitonin gene-related peptide before and after antipsychotic treatment. Neuropeptides. 2001 Oct-Dec;35(5-6):285-91. PMID: 12030813.

K0282

Kavalactones Mixture

1 ml

≥98%

Mixture of kavalactones found in *Piper methysticum* (kava plant).

Kormann EC, Amaral Pde A, David M, et al. Kavain analogues as potential analgesic agents. Pharmacol Rep. 2012;64(6):1419-26. PMID: 23406752.

Tsutsui R, Shinomiya K, Takeda Y, et al. Hypnotic and sleep quality-enhancing properties of kavain in sleep-disturbed rats. J Pharmacol Sci. 2009 Nov;111(3):293-8. PMID: 19881224.

Wruck CJ, Götz ME, Herdegen T, et al. Kavalactones protect neural cells against amyloid beta peptide-induced neurotoxicity via extracellular signal-regulated kinase 1/2-dependent nuclear factor erythroid 2-related factor 2 activation. Mol Pharmacol. 2008 Jun;73(6):1785-95. PMID: 18334601.

K0552

Kb NB 77-78

NEW

5 mg
10 mg
25 mg

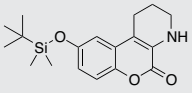

$C_{18}H_{25}NO_3Si$ FW: 331.49 [1350622-33-1] ≥98%

CID-797718 analog that may bind PKD1.

K0652

Kb NB 142-70

NEW

5 mg
25 mg

$C_{11}H_9NO_2S_2$ FW: 251.32 [1233533-04-4] ≥98%

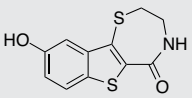

PKD inhibitor. It increases activation of Akt and inhibits migration of intestinal epithelial cells.

Sinnett-Smith J, Ni Y, Wang J, et al. Protein kinase D1 mediates class IIa histone deacetylase phosphorylation and nuclear extrusion in intestinal epithelial cells: role in mitogenic signaling. Am J Physiol Cell Physiol. 2014 May 15;306(10):C961-71. PMID: 24647541.

Ni Y, Sinnett-Smith J, Young SH, et al. PKD1 mediates negative feedback of PI3K/Akt activation in response to G protein-coupled receptors. PLoS One. 2013 Sep 9;8(9):e73149. Erratum in: PLoS One. 2014;9(1). PMID: 24039875.

Young SH, Rozengurt N, Sinnett-Smith J, et al. Rapid protein kinase D1 signaling promotes migration of intestinal epithelial cells. Am J Physiol Gastrointest Liver Physiol. 2012 Aug 1;303(3):G356-66. PMID: 22595992.

K0088

Kawain

5 mg
10 mg

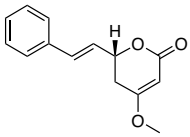

$C_{14}H_{14}O_3$ FW: 230.26 [3155-48-4] ≥98%

Voltage-gated Na^+ and L-type Ca^{2+} channel blocker found in *Piper methysticum* (kava plant). It displays a variety of biological activities, including protecting against amyloid-β-induced neurotoxicity, suppressing growth of *Fusarium*, *Trichoderma*, and *Colletotrichum*, increasing non-REM sleep time and delta activity during REM sleep, and inhibiting arachidonic acid-induced platelet aggregation and COX expression.

Tsutsui R, Shinomiya K, Takeda Y, et al. Hypnotic and sleep quality-enhancing properties of kavain in sleep-disturbed rats. J Pharmacol Sci. 2009 Nov;111(3):293-8. PMID: 19881224.

Wruck CJ, Götz ME, Herdegen T, et al. Kavalactones protect neural cells against amyloid beta peptide-induced neurotoxicity via extracellular signal-regulated kinase 1/2-dependent nuclear factor erythroid 2-related factor 2 activation. Mol Pharmacol. 2008 Jun;73(6):1785-95. PMID: 18334601.

Xuan TD, Elzaawely AA, Fukuta M, et al. Herbicidal and Fungicidal Activities of Lactones in Kava (*Piper methysticum*). J Agric Food Chem. 2006 Feb 8;54(3):720-5. PMID: 16448174.

K1650

Kemptide

1 mg
2 mg
5 mg

H-Leu-Arg-Arg-Ala-Ser-Leu-Gly-OH

$C_{32}H_{61}N_{13}O_9$ FW: 771.92 [65189-71-1] ≥95%

Substrate used to measure PKA activity.

Montenegro M, Garcia-Viloca M, González-Lafont A, et al. Comparative study of the prereactive protein kinase A Michaelis complex with kemptide substrate. J Comput Aided Mol Des. 2007 Oct-Nov;21(10-11):603-15. PMID: 18008170.

Benyo DF, Zeleznik AJ. Cyclic adenosine monophosphate signaling in the primate corpus luteum: maintenance of protein kinase A activity throughout the luteal phase of the menstrual cycle. Endocrinology. 1997 Aug;138(8):3452-8. PMID: 9231800.

K1653

Kendomycin

100 µg
500 µg

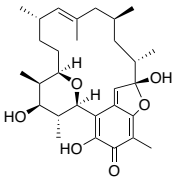

(–)-TAN 2162

$C_{29}H_{42}O_6$ FW: 486.64 [183202-73-5] ≥98%

Endothelin receptor antagonist and proteasome inhibitor. It induces apoptosis in lymphoma cells.

Janssen CO, Lim S, Lo EP, et al. Interaction of kendomycin and semi-synthetic analogues with the anti-apoptotic protein Bcl-xl. Bioorg Med Chem Lett. 2008 Nov 1;18(21):5771-3. PMID: 18845435.

Elnakady YA, Rohde M, Sasse F, et al. Evidence for the mode of action of the highly cytotoxic *Streptomyces* polyketide kendomycin. Chembiochem. 2007 Jul 23;8(11):1261-72. PMID: 17592829.

K1655

Kenpaullone

1 mg
5 mg

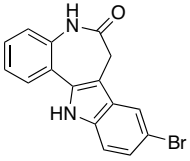

$C_{16}H_{11}BrN_2O$ FW: 327.18 [142273-20-9] ≥95%

GSK-3β, HGK, and CDK inhibitor. It increases expression of Foxp3 in T cells, improves motor neuron survival, and suppresses neuronal apoptosis.

Zhang Y, Welzig CM, Picard KL, et al. Glycogen synthase kinase-3β inhibition ameliorates cardiac parasympathetic dysfunction in type 1 diabetic akita mice. Diabetes. 2014 Jun;63(6):2097-113. PMID: 24458356.

Yoshida H, Kotani H, Kondo T, et al. CDK inhibitors suppress Th17 and promote iTreg differentiation, and ameliorate experimental autoimmune encephalomyelitis in mice. Biochem Biophys Res Commun. 2013 Jun 7;435(3):378-84. PMID: 23665028.

Yang YM, Gupta SK, Kim KJ, et al. A small molecule screen in stem-cell-derived motor neurons identifies a kinase inhibitor as a candidate therapeutic for ALS. Cell Stem Cell. 2013 Jun 6;12(6):713-26. PMID: 23602540.

K1678

Ketanserin

25 mg
100 mg
500 mg

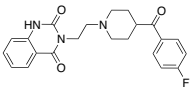

$C_{22}H_{22}F_3O_3$ FW: 395.43 [74050-98-9] ≥97%

5-HT2A receptor antagonist and potential α1-adrenergic receptor antagonist used to treat hypertension. It decreases blood pressure, improves left ventricular remodeling, increases capillary density in myocardial tissue, and may suppress TRPV1 channel-evoked thermal hyperalgesia.

Yu JG, Zhang EH, Liu AJ, et al. Ketanserin improves cardiac performance after myocardial infarction in spontaneously hypertensive rats partially through restoration of baroreflex function. Acta Pharmacol Sin. 2013 Dec;34(12):1508-14. PMID: 24241347.

Loyd DR, Chen PB, Hargreaves KM. Anti-hyperalgesic effects of anti-serotonergic compounds on serotonin- and capsaicin-evoked thermal hyperalgesia in the rat. Neuroscience. 2012 Feb 17;203:207-15. PMID: 22209919.

van Zwieten PA, Blauw GJ, van Brummelen P. Serotonergic receptors and drugs in hypertension. Pharmacol Toxicol. 1992 Jun;70(6 Pt 2):S17-22. PMID: 1354865.

K1679 (+)-Ketanserin Tartrate

NEW

10 mg
50 mg
250 mg
500 mg

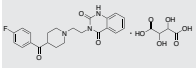

$C_{22}H_{22}FN_3O_3 \cdot C_4H_6O_6$ FW: 545.52 [83846-83-7] ≥98%

5-HT2A receptor and TRPV1 receptor antagonist and potential α1-adrenergic receptor antagonist used to treat hypertension. It increases capillary density in myocardial tissue, decreases blood pressure, and improves left ventricular remodeling and overall cardiac function.

Yu JG, Zhang EH, Liu AJ, et al. Ketanserin improves cardiac performance after myocardial infarction in spontaneously hypertensive rats partially through restoration of baroreflex function. Acta Pharmacol Sin. 2013 Dec;34(12):1508-14. PMID: 24241347.

Loyd DR, Chen PB, Hargreaves KM. Anti-hyperalgesic effects of anti-serotonergic compounds on serotonin- and capsaicin-evoked thermal hyperalgesia in the rat. Neuroscience. 2012 Feb 17;203:207-15. PMID: 22209919.

K1676 Ketoconazole

5 g
25 g

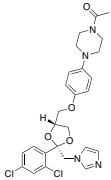

$C_{26}H_{28}Cl_2N_4O_4$ FW: 531.44 [65277-42-1] ≥98%

14-α Demethylase inhibitor used to treat fungal infections. It prevents ergosterol production and fungal cell wall synthesis. It also decreases testosterone and cortisol production and inhibits androgen receptors in prostate cancer models.

Tsuji G, Takahara M, Uchi H, et al. Identification of ketoconazole as an AhR-Nrf2 activator in cultured human keratinocytes: the basis of its anti-inflammatory effect. J Invest Dermatol. 2012 Jan;132(1):59-68. PMID: 21753779.

K1674 Ketolide Resistance Peptide MRFFV

1 mg
5 mg

Met-Arg-Phe-Phe-Val

$C_{34}H_{50}N_8O_6S$ FW: 698.9 ≥98%

Prevents ketolide antibiotic-ribosome binding and allows protein synthesis to continue.

Verdier L, Gharbi-Benarous J, Bertho G, et al. Antibiotic resistance peptides: interaction of peptides conferring macrolide and ketolide resistance with *Staphylococcus aureus* ribosomes: conformation of bound peptides as determined by transferred NOE experiments. Biochemistry. 2002 Apr 2;41(13):4218-29. PMID: 11914067.

K1677 Ketoprofen

5 g
25 g
100 g

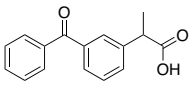

$C_{16}H_{14}O_3$ FW: 254.28 [22071-15-4] ≥98%

NSAID and inhibitor of COX-1/2 that is used to treat dental and arthritis pain and inflammation. It also decreases platelet counts by inhibiting lactate dehydrogenase and increases survival rates, macrophage phagocytosis, and neutrophil recruitment in septic lung infection models.

Razi MT, Javed I, Choudry MZ, et al. Effect of ketoprofen on lactic dehydrogenase from human platelets. Adv Clin Exp Med. 2014 May-Jun;23(3):377-80. PMID: 24979508.

Brogliato AR, Antunes CA, Carvalho RS, et al. Ketoprofen impairs immunosuppression induced by severe sepsis and reveals an important role for prostaglandin E2. Shock. 2012 Dec;38(6):620-9. PMID: 23143054.

K1978 Ketorolac Tromethamine

1 g
5 g
25 g

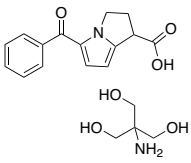

$C_{15}H_{13}N_2O_3 \cdot C_4H_{11}NO_3$ FW: 376.4 [74103-07-4] ≥98%

NSAID and COX-1/2 inhibitor. It also prevents spinal injury-induced increase of PAR1 and decreases expression of PDE4D.

Dong L, Smith JR, Winkelstein BA. Ketorolac reduces spinal astrocytic activation and PAR1 expression associated with attenuation of pain after facet joint injury. J Neurotrauma. 2013 May 15;30(10):818-25. PMID: 23126437.

Bendixen KH, Baad-Hansen L, Cairns BE, et al. Effects of low-dose intramuscular ketorolac on experimental pain in the masseter muscle of healthy women. J Orofac Pain. 2010 Fall;24(4):398-407. PMID: 21197512.

Wang XM, Hamza M, Gordon SM, et al. COX inhibitors downregulate PDE4D expression in a clinical model of inflammatory pain. Clin Pharmacol Ther. 2008 Jul;84(1):39-42. PMID: 18288087.

K1776 Ketotifen Fumarate

500 mg
1 g

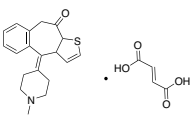

$C_{19}H_{19}NOS \cdot C_4H_4O_4$ FW: 425.5 [34580-14-8] ≥98%

Inhibitor of PDE and antagonist at H1 histamine and leukotriene receptors used to treat conjunctivitis and asthma. It stabilizes mast cells, downregulates expression of pro-inflammatory cytokines, and decreases humoral and cellular immune responses.

Zhang A, Chi X, Luo G, et al. Mast cell stabilization alleviates acute lung injury after orthotopic autologous liver transplantation in rats by downregulating inflammation. PLoS One. 2013 Oct 8;8(10):e75262. PMID: 24116032.

Doligalska M. Effect of ketotifen on the immune response in BALB/c mice infected with Trichinella spiralis. Wiad Parazytol. 2000;46(2):217-24. PMID: 16886340.

K2412 KGDS

1 mg
2 mg
5 mg

$C_{15}H_{27}N_5O_8$ FW: 405.41 ≥95%

H-Lys-Gly-Asp-Ser-OH

Synthetic fibrinogen derivative and glycoprotein IIb/IIIa receptor agonist. It inhibits fibrinogen-platelet binding and thrombin activity.

Knapp A, Degenhardt T, Dodt J. Hirudisins. Hirudin-derived thrombin inhibitors with disintegrin activity. J Biol Chem. 1992 Dec 5;267(34):24230-4. PMID: 1447173.

K3352 Kinetensin

1 mg
2 mg
5 mg

$C_{56}H_{85}N_{17}O_{11}$ FW: 1172.4 [103131-69-7] ≥95%

H-Ile-Ala-Arg-Arg-His-Pro-Tyr-Phe-Leu-OH

Neurotensin analog that induces histamine release in peritoneal mast cells.

Read D, Shulkes A, Fletcher D, et al. Pharmacokinetics and biological activity of kinetensin in conscious sheep. Agents Actions. 1993 Mar;38(3-4):231-9. PMID: 8213349.

K4401 KL-1 Peptide

1 mg
2 mg
5 mg

$C_{53}H_{90}N_{16}O_{18}$ FW: 1239.4 ≥95%

H-Leu-Pro-Pro-Val-Ala-Ala-Ser-Ser-Leu-Arg-Asn-Asp-OH

c-Kit ligand fragment that may stimulate cellular expansion or play a role in the development of inflammation and fibrosis.

El Kossi MM, Haylor JL, Johnson TS, et al. Stem cell factor in a rat model of serum nephrotoxic nephritis. Nephron Exp Nephrol. 2008;108(1):e1-e10. PMID: 18087173.

Koller MR, Oxender M, Brott DA, et al. flt-3 ligand is more potent than c-kit ligand for the synergistic stimulation of ex vivo hematopoietic cell expansion. J Hematother. 1996 Oct;5(5):449-59. PMID: 8938517.

K5604 Kobe 0065

NEW

5 mg
25 mg

$C_{15}H_{11}ClF_3N_5O_4S$ FW: 449.79 [436133-68-5] ≥98%

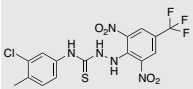

Ras inhibitor. It inhibits cell growth and induces apoptosis in cancer cells.

Shima F, Yoshikawa Y, Ye M, et al. In silico discovery of small-molecule Ras inhibitors that display antitumor activity by blocking the Ras-effector interaction. Proc Natl Acad Sci U S A. 2013 May 14;110(20):8182-7. PMID: 23630290.

Shima F, Yoshikawa Y, Matsumoto S, et al. Discovery of small-molecule Ras inhibitors that display antitumor activity by interfering with Ras-GTP-effector interaction. Enzymes. 2013;34 Pt. B:1-23. PMID: 25034098.

K5606 Kobe 2602

NEW

10 mg
50 mg
100 mg

$C_{14}H_9F_4N_5O_4S$ FW: 419.31 [454453-49-7] ≥98%

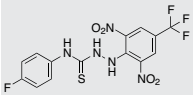

Ras inhibitor. It inhibits cell growth and induces apoptosis in cancer cells.

Shima F, Yoshikawa Y, Ye M, et al. In silico discovery of small-molecule Ras inhibitors that display antitumor activity by blocking the Ras-effector interaction. Proc Natl Acad Sci U S A. 2013 May 14;110(20):8182-7. PMID: 23630290.

Shima F, Yoshikawa Y, Matsumoto S, et al. Discovery of small-molecule Ras inhibitors that display antitumor activity by interfering with Ras-GTP-effector interaction. Enzymes. 2013;34 Pt. B:1-23. PMID: 25034098.

K6276 KPT-330

NEW

1 mg
5 mg
25 mg

$C_{17}H_{11}F_6N_7O$ FW: 443.31 [1421923-86-5] ≥98%

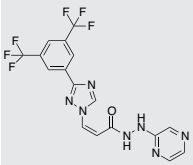

CRM1-selective inhibitor of nuclear export. It inhibits protein trafficking from the nucleus and induces cell cycle arrest and apoptosis in mesothelioma cells.

Ishizawa J, Kojima K, Hail N Jr, et al. Expression, function, and targeting of the nuclear exporter chromosome region maintenance 1 (CRM1) protein. Pharmacol Ther. 2015 Jun 3. [Epub ahead of print]. PMID: 26048327.

De Cesare M, Cominetti D, Doldi V, et al. Anti-tumor activity of selective inhibitors of XPO1/CRM1-mediated nuclear export in diffuse malignant peritoneal mesothelioma: the role of survivin. Oncotarget. 2015 May 30;6(15):13119-32. PMID: 25948791.

Parikh K, Cang S, Sekhri A, et al. Selective inhibitors of nuclear export (SINE)--a novel class of anti-cancer agents. J Hematol Oncol. 2014 Oct 15;7:78. PMID: 25316614.

K6864 KRQHPG

0.5 mg
1 mg
2.5 mg

Thyrotropin-releasing hormone progenitor peptide

$C_{30}H_{51}N_{13}O_8$ FW: 721.82 ≥95%

H-Lys-Arg-Gln-His-Pro-Gly-OH

Thyrotropin-releasing hormone progenitor fragment.

Aoki Y, Ono H, Yasuo S, et al. Molecular evolution of prepro-thyrotropin-releasing hormone in the chicken (Gallus gallus) and its expression in the brain. Zoolog Sci. 2007 Jul;24(7):686-92. PMID: 17824776.

Mitsuma T, Hirooka Y, Nogimori T. Effects of dexamethasone on TRH and TRH precursor peptide (Lys-Arg-Gln-His-Pro-Gly-Arg-Arg) levels in various rat organs. Endocr Regul. 1992 Mar;26(1):29-34. PMID: 1421205.

K7600

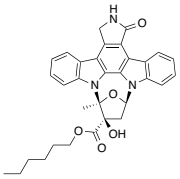

KT5720

100 µg
1 mg

$C_{32}H_{31}N_3O_5$ FW: 537.23 [108068-98-0] ≥98%

PKA and PDK1 inhibitor, HCN channel blocker, and potential GSK-3, MEK, MSK1, PKB inhibitor. It decreases intracellular Ca^{2+} levels and suppresses DRG neuron excitability.

Iwase K, Ishihara A, Yoshimura S, et al. The secretogranin II gene is a signal integrator of glutamate and dopamine inputs. J Neurochem. 2014 Jan;128(2):233-45. PMID: 24111984.

Hoffman MS, Mitchell GS. Spinal 5-HT7 receptors and protein kinase A constrain intermittent hypoxia-induced phrenic long-term facilitation. Neuroscience. 2013 Oct 10;250:632-43. PMID: 23850591.

Cheng Q, Zhou Y. Novel role of KT5720 on regulating hyperpolarization-activated cyclic nucleotide-gated channel activity and dorsal root ganglion neuron excitability. DNA Cell Biol. 2013 Jun;32(6):320-8. PMID: 23713946.

K7602

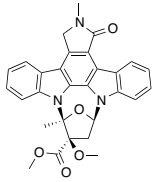

KT5823

100 µg
1 mg

$C_{28}H_{23}N_3O_5$ FW: 495.5 [126643-37-6] ≥98%

PKG inhibitor used to measure downstream effects of PKG/cGMP signaling.

Salloum FN, Das A, Samidurai A, et al. Cinaciguat, a novel activator of soluble guanylate cyclase, protects against ischemia/reperfusion injury: role of hydrogen sulfide. Am J Physiol Heart Circ Physiol. 2012 Mar 15;302(6):H1347-54. PMID: 22268103.

Moreno H, Vega-Saenz de Miera E, Nadal MS, et al. Modulation of Kv3 potassium channels expressed in CHO cells by a nitric oxide-activated phosphatase. J Physiol. 2001 Feb 1;530(Pt 3):345-58. PMID: 11281123.

K9200

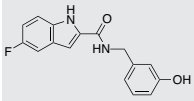

KX1-004

NEW

1 mg
5 mg
25 mg

$C_{16}H_{13}FN_2O_2$ FW: 284.29 [518058-84-9] ≥98%

Src inhibitor. It decreases apoptosis in hair cells.

Fetoni AR, Bielefeld EC, Paludetti G, et al. A putative role of p53 pathway against impulse noise induced damage as demonstrated by protection with pifithrin-alpha and a Src inhibitor. Neurosci Res. 2014 Apr-May;81-82:30-7. PMID: 24472721.

Bielefeld EC, Hangauer D, Henderson D. Protection from impulse noise-induced hearing loss with novel Src-protein tyrosine kinase inhibitors. Neurosci Res. 2011 Dec;71(4):348-54. PMID: 21840347.

Harris KC, Hu B, Hangauer D, et al. Prevention of noise-induced hearing loss with Src-PTK inhibitors. Hear Res. 2005 Oct;208(1-2):14-25. PMID: 15950415.

K9600

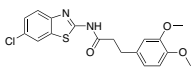

KY-02111

5 mg
10 mg

$C_{18}H_{17}ClN_2O_3S$ FW: 376.86 [1118807-13-8]

Wnt signaling inhibitor. It promotes differentiation of stem cells to form cardiomyocytes.

Minami I, Yamada K, Otsuji TG, et al. A small molecule that promotes cardiac differentiation of human pluripotent stem cells under defined, cytokine- and xeno-free conditions. Cell Rep. 2012 Nov 29;2(5):1448-60. PMID: 23103164.

K9858

H-Tyr-Arg-OH

Kyotorphin

5 mg
10 mg
25 mg

$C_{15}H_{23}N_5O_4$ FW: 337.4 [70904-56-2] ≥95%

Kyotorphin receptor agonist. It lowers blood pressure, induces nociception, and stimulates met-enkephalin release.

Miguel M, Manso M, Aleixandre A, et al. Vascular effects, angiotensin I-converting enzyme (ACE)-inhibitory activity, and antihypertensive properties of peptides derived from egg white. J Agric Food Chem. 2007 Dec 26;55(26):10615-21. PMID: 18047278.

Ueda H, Inoue M. In vivo signal transduction of nociceptive response by kyotorphin (tyrosine-arginine) through Galpha(i)- and inositol trisphosphate-mediated $Ca^{(2+)}$ influx. Mol Pharmacol. 2000 Jan;57(1):108-15. PMID: 10617685.

L0107

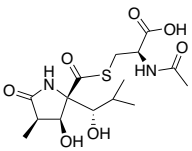

Lactacystin

200 µg

$C_{15}H_{24}N_2O_7S$ FW: 376.43 [133343-34-7] ≥98%

Proteasome inhibitor found in *Streptomyces*. It increases the Bax/Bcl-2 ratio and inhibits proliferation of glioma cells, inhibits growth and migration of smooth muscle cells, and suppresses infiltration of neutrophils and decreases levels of ICAM-1 in liver injury models.

Wang H, Zhang S, Zhong J, et al. The proteasome inhibitor lactacystin exerts its therapeutic effects on glioma via apoptosis: an in vitro and in vivo study. J Int Med Res. 2013 Feb;41(1):72-81. PMID: 23569132.

Barringhaus KG, Matsumura ME. The proteasome inhibitor lactacystin attenuates growth and migration of vascular smooth muscle cells and limits the response to arterial injury. Exp Clin Cardiol. 2007 Fall;12(3):119-24. PMID: 18650992.

Yao JH, Li YH, Wang ZZ, et al. Proteasome inhibitor lactacystin ablates liver injury induced by intestinal ischaemia-reperfusion. Clin Exp Pharmacol Physiol. 2007 Nov;34(11):1102-8. PMID: 17880361.

L0109 Lactalbumin

500 g
1 kg

[9013-90-5] ≥80%

Cation and fatty acid chelator found in milk and whey. It protects against stress-induced gastric injury.

Barbana C, Sánchez L, Pérez MD. Bioactivity of α-lactalbumin related to its interaction with fatty acids: a review. Crit Rev Food Sci Nutr. 2011 Sep;51(8):783-94. PMID: 21838558.

Matsumoto H, Shimokawa Y, Ushida Y, et al. New biological function of bovine alpha-lactalbumin: protective effect against ethanol- and stress-induced gastric mucosal injury in rats. Biosci Biotechnol Biochem. 2001 May;65(5):1104-11. PMID: 11440124.

L0209 Lactoferrin, cow

10 mg
50 mg
100 mg

90 kDa [146897-68-9] ≥92%

Endogenous glycoprotein and lactoferrin receptor agonist. It binds DNA and inhibits carcinogenesis in several cancer development models and suppresses growth of gram negative bacteria, *Candida*, rotavirus, herpesvirus, HIV, and cytomegalovirus.

Farnaud S, Evans RW. Lactoferrin--a multifunctional protein with antimicrobial properties. Mol Immunol. 2003 Nov;40(7):395-405. PMID: 14568385.

Viejo-Díaz M, Andrés MT, Fierro JF. Modulation of in vitro fungicidal activity of human lactoferrin against *Candida albicans* by extracellular cation concentration and target cell metabolic activity. Antimicrob Agents Chemother. 2004 Apr;48(4):1242-8. PMID: 15047526.

L0211 Lactulose

10 g
25 g

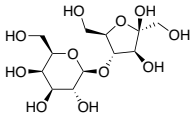

$C_{12}H_{22}O_{11}$ FW: 342.3 [4618-18-2] ≥98%

Synthetic non-digestible disaccharide used to treat constipation and hepatic encephalopathy-induced hyperammonemia. It induces water retention.

Panesar PS, Kumari S. Lactulose: production, purification and potential applications. Biotechnol Adv. 2011 Nov-Dec;29(6):940-8. PMID: 21856402.

Shukla S, Shukla A, Mehboob S, et al. Meta-analysis: the effects of gut flora modulation using prebiotics, probiotics and synbiotics on minimal hepatic encephalopathy. Aliment Pharmacol Ther. 2011 Mar;33(6):662-71. PMID: 21251030.

L0226 Lagochiline

25 mg
100 mg

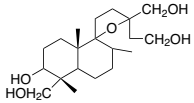

$C_{20}H_{36}O_5$ FW: 356.6 ≥98%

Found in *Lagochilus*. It may induce sedation and vasodilation.

Pulatova TP, Khazanovich RL. On the alkaloid content of some *Lagochilus* species and on the nature of lagochiline. Aptechn Delo. 1962 Nov-Dec;6:29-32. PMID: 13972488.

L0251 Laminin Peptide CDPGYIGSR

1 mg
5 mg

Cys-Asp-Pro-Gly-Tyr-Ile Gly-Ser-Arg

$C_{40}H_{62}N_{12}O_{14}S$ FW: 967.06 [110590-60-8] ≥98%

Peptide found on the B1 chain of laminin (925-933) that activates nonselective cation channels. It is used in combination with chemotherapeutics to deliver the drug to target tumor tissues. It inhibits angiogenesis and cancer cell growth and induces vasoconstriction in vascular smooth muscle cells.

Wenzel D, Koch M, Matthey M, et al. Identification of a novel vasoconstrictor peptide specific for the systemic circulation. Hypertension. 2012 Jun;59(6):1256-62. PMID: 22547445.

Sakamoto N, Iwahana M, Tanaka NG, et al. Inhibition of angiogenesis and tumor growth by a synthetic laminin peptide, CDPGYIGSR-NH2. Cancer Res. 1991 Feb 1;51(3):903-6. PMID: 1703042.

L0250 Laminin Peptide SIKVAV

1 mg
5 mg

Cys-Ser-Arg-Ala-Arg-Lys-Gln-Ala-Ala-Ser-Ile-Lys-Val-Ala-Val-Ser-Ala-Asp-Arg

$C_{82}H_{148}N_{31}O_{26}S$ FW: 2016.3 ≥98%

Peptide found on the A1 chain of laminin. It is used in combination with chemotherapeutics to deliver the drug to target tumor tissues. It increases vessel formation and migration.

Stevenson M, Hale AB, Hale SJ, et al. Incorporation of a laminin-derived peptide (SIKVAV) on polymer-modified adenovirus permits tumor-specific targeting via alpha6-integrins. Cancer Gene Ther. 2007 Apr;14(4):335-45. PMID: 17235355.

Freitas VM, Scheremeta B, Hoffman MP, et al. Laminin-1 and SIKVAV a laminin-1-derived peptide, regulate the morphology and protease activity of a human salivary gland adenoid cystic carcinoma cell line. Oral Oncol. 2004 May;40(5):483-9. PMID: 15006619.

L0248 Laminin Peptide YIGSR

1 mg
5 mg

$C_{26}H_{42}N_8O_8$ FW: 594.66 [110590-64-2] ≥98%

Tyr-Ile-Gly-Ser-Arg

Peptide found on the B1 chain of laminin (929-933). It is used in combination with chemotherapeutics to deliver the drug to target tumor tissues. It inhibits migration and growth of prostate cancer cells.

Yoon JH, Kim J, Lee H, et al. Laminin peptide YIGSR induces collagen synthesis in Hs27 human dermal fibroblasts. Biochem Biophys Res Commun. 2012 Nov 23;428(3):416-21. PMID: 23111328.

Dubey PK, Singodia D, Vyas SP. Polymeric nanospheres modified with YIGSR peptide for tumor targeting. Drug Deliv. 2010 Sep-Oct;17(7):541-51. PMID: 20560774.

L0249 Laminin Peptide YIGSR-NH2

1 mg
5 mg

$C_{26}H_{43}N_9O_7$ FW: 593.67 ≥98%

Tyr-Ile-Gly-Ser-Arg-NH2

Peptide amide found on the B1 chain of laminin (929-933). It is used in combination with chemotherapeutics to deliver the drug to target tumor tissues. It inhibits migration and growth of prostate cancer cells.

Yoon JH, Kim J, Lee H, et al. Laminin peptide YIGSR induces collagen synthesis in Hs27 human dermal fibroblasts. Biochem Biophys Res Commun. 2012 Nov 23;428(3):416-21. PMID: 23111328.

Dubey PK, Singodia D, Vyas SP. Polymeric nanospheres modified with YIGSR peptide for tumor targeting. Drug Deliv. 2010 Sep-Oct;17(7):541-51. PMID: 20560774.

L0350 Lamivudine

1 g
5 g
25 g

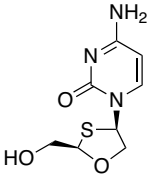

$C_8H_{11}N_3O_3S$ FW: 229.26 [134678-17-4] ≥98%

Thymidine analog and RT inhibitor used to treat hepatitis B infection. It also inhibits growth of HIV-infected cells and increases insulin resistance.

Blümer RM, van Vonderen MG, Sutinen J, et al. Zidovudine/lamivudine contributes to insulin resistance within 3 months of starting combination antiretroviral therapy. AIDS. 2008 Jan 11;22(2):227-36. PMID: 18097225.

Saavedra-Lozano J, McCoig CC, Cao Y, et al. Zidovudine, lamivudine, and abacavir have different effects on resting cells infected with human immunodeficiency virus in vitro. Antimicrob Agents Chemother. 2004 Aug;48(8):2825-30. PMID: 15273087

Balestrieri E, Forte G, Matteucci C, et al. Effect of lamivudine on transmission of human T-cell lymphotropic virus type 1 to adult peripheral blood mononuclear cells in vitro. Antimicrob Agents Chemother. 2002 Sep;46(9):3080-3. PMID: 12183277.

L0349 Lamotrigine

25 mg
100 mg
500 mg

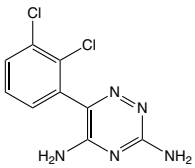

$C_9H_7Cl_2N_5$ FW: 255.01 [84057-84-1] ≥98%

R-type Ca^{2+} and voltage-gated Na^+ channel blocker used to treat epilepsy and bipolar disorder. It also decreases immobility time in the forced swim test, increases pain thresholds in the formalin test, and suppresses release of pro-inflammatory cytokines.

Himmerich H, Bartsch S, Hamer H, et al. Impact of mood stabilizers and antiepileptic drugs on cytokine production in-vitro. J Psychiatr Res. 2013 Nov;47(11):1751-9. PMID: 23978396.

Dibué M, Kamp MA, Alpdogan S, et al. Cav 2.3 (R-type) calcium channels are critical for mediating anticonvulsive and neuroprotective properties of lamotrigine in vivo. Epilepsia. 2013 Sep;54(9):1542-50. PMID: 23772876.

Munro G, Erichsen HK, Mirza NR. Pharmacological comparison of anticonvulsant drugs in animal models of persistent pain and anxiety. Neuropharmacology. 2007 Oct;53(5):609-18. PMID: 17714743.

L0254 Lansoprazole

250 mg
1 g

AG-1749

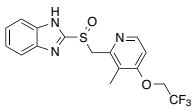

$C_{16}H_{14}F_3N_3O_2S$ FW: 369.36 [103577-45-3] ≥98%

H^+/K^+ ATPase inhibitor used to treat gastroesophageal reflux disease. It inhibits indomethacin-induced gastric damage, suppresses LPS-induced activation of p38 MAPK in neutrophils, and decreases levels of pro-inflammatory cytokines in macrophages.

Koshio O, Tansho S, Ubagai T, et al. Suppression of phosphorylation of extracellular-signal-regulated kinase and p38 mitogen-activated protein kinase in polymorphonuclear leukocytes by the proton pump inhibitor lansoprazole. J Infect Chemother. 2010 Apr;16(2):100-6. PMID: 20094750.

Maity P, Bindu S, Choubey V, et al. Lansoprazole protects and heals gastric mucosa from non-steroidal anti-inflammatory drug (NSAID)-induced gastropathy by inhibiting mitochondrial as well as Fas-mediated death pathways with concurrent induction of mucosal cell renewal. J Biol Chem. 2008 May 23;283(21):14391-401. PMID: 18375387.

Hinoki A, Yoshimura K, Fujita K, et al. Suppression of proinflammatory cytokine production in macrophages by lansoprazole. Pediatr Surg Int. 2006 Nov;22(11):915-23. PMID: 16932910.

L0360

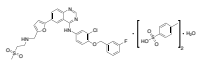

Lapatinib Ditosylate Monohydrate

10 mg
25 mg
100 mg

$C_{26}H_{26}ClFN_4O_4S \bullet 2C_7H_8O_3S \bullet H_2O$ FW: 925.46 [388082-78-8] ≥98%

EGFR inhibitor. It induces apoptosis in breast cancer cells and down-regulates expression of thymidylate synthase.

Janni W, Sarosiek T, Karaszewska B, et al. A phase II, randomized, multicenter study evaluating the combination of lapatinib and vinorelbine in women with ErbB2 overexpressing metastatic breast cancer. Breast Cancer Res Treat. 2014 Jan 9. [Epub ahead of print]. PMID: 24402830.

Kostyal D, Welt RS, Danko J, et al. Trastuzumab and lapatinib modulation of HER2 tyrosine/threonine phosphorylation and cell signaling. Med Oncol. 2012 Sep;29(3):1486-94. PMID: 21769502.

L0060

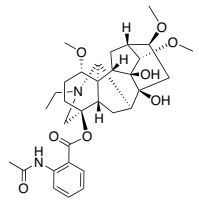

Lappaconitine

25 mg
100 mg
500 mg

$C_{32}H_{44}N_2O_8$ FW: 584.7 [32854-75-4] ≥98%

Cardiac Na^+ channel blocker found in species of *Aconitum*. It displays many biological activities, including increasing pain thresholds and downregulating expression of P2X3 receptors in DRG neurons, decreasing paw and ear edema, and inducing negative inotropic activity.

Ou S, Zhao YD, Xiao Z, et al. Effect of lappaconitine on neuropathic pain mediated by P2X3 receptor in rat dorsal root ganglion. Neurochem Int. 2011 Apr;58(5):564-73. PMID: 21272608.

Wang YZ, Xiao YQ, Zhang C, et al. Study of analgesic and anti-inflammatory effects of lappaconitine gelata. J Tradit Chin Med. 2009 Jun;29(2):141-5. PMID: 19663103.

L0284

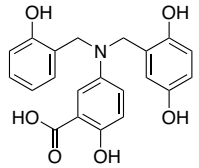

Lavendustin A

1 mg
5 mg

$C_{21}H_{19}NO_6$ FW: 381.38 [125697-92-9] ≥97%

Tyrosine kinase inhibitor that increases axonal outgrowth in neurons.

Rojas A, Wetherington J, Shaw R, et al. Activation of group I metabotropic glutamate receptors potentiates heteromeric kainate receptors. Mol Pharmacol. 2013 Jan;83(1):106-21. PMID: 23066089.

Kim HJ, Ahn HS, Choi BH, et al. Inhibition of Kv4.3 by genistein via a tyrosine phosphorylation-independent mechanism. Am J Physiol Cell Physiol. 2011 Mar;300(3):C567-75. PMID: 21148405.

L0528

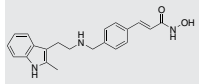

LBH-589

NEW

5 mg
25 mg
50 mg

Panobinostat

$C_{21}H_{23}N_3O_2$ FW: 349.43 [404950-80-7] ≥98%

Class I HDAC inhibitor used to treat multiple myeloma. It also reverses epithelial-to-mesenchymal transition and inhibits proliferation, invasion, and migration in breast cancer models.

Andreu-Vieyra CV, Berenson JR. The potential of panobinostat as a treatment option in patients with relapsed and refractory multiple myeloma. Ther Adv Hematol. 2014 Dec;5(6):197-210. PMID: 25469210.

Rhodes LV, Tate CR, Segar HC, et al. Suppression of triple-negative breast cancer metastasis by pan-DAC inhibitor panobinostat via inhibition of ZEB family of EMT master regulators. Breast Cancer Res Treat. 2014 Jun;145(3):593-604. PMID: 24810497.

Henrici A, Montalbano R, Neureiter D, et al. The pan-deacetylase inhibitor panobinostat suppresses the expression of oncogenic miRNAs in hepatocellular carcinoma cell lines. Mol Carcinog. 2013 Dec 23. [Epub ahead of print]. PMID: 24375802.

L1044

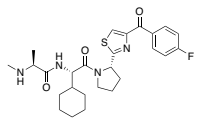

LCL-161

1 mg
5 mg

$C_{26}H_{33}FN_4O_3S$ FW: 500.63 [1005342-46-0] ≥99%

Smac mimetic, PXR agonist, and IAP inhibitor. It induces apoptosis in lymphoid cancer cells.

Dhuria S, Einolf H, Mangold J, et al. Time-dependent inhibition and induction of human cytochrome P4503A4/5 by an oral IAP antagonist, LCL161, in vitro and in vivo in healthy subjects. J Clin Pharmacol. 2013 Jun;53(6):642-53. PMID: 23585187.

Houghton PJ, Kang MH, Reynolds CP, et al. Initial testing (stage 1) of LCL161, a SMAC mimetic, by the Pediatric Preclinical Testing Program. Pediatr Blood Cancer. 2012 Apr;58(4):636-9. PMID: 21681929.

L1340

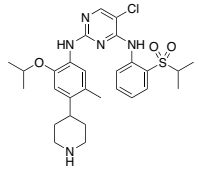

LDK378

1 mg
5 mg
25 mg

Ceritinib

$C_{28}H_{36}ClN_5O_3S$ FW: 558.13 [1032900-25-6] ≥99%

ALK and IGF-1R inhibitor. It decreases proliferation of non-small cell lung cancer cells.

Iams WT, Lovly CM. Anaplastic Lymphoma Kinase as a Therapeutic Target in Non-Small Cell Lung Cancer. Cancer J. 2015 Sep-Oct;21(5):378-82. PMID: 26389762.

Nishio M, Murakami H, Horiike A, et al. Phase I Study of Ceritinib (LDK378) in Japanese Patients with Advanced, Anaplastic Lymphoma Kinase-Rearranged Non-Small-Cell Lung Cancer or Other Tumors. J Thorac Oncol. 2015 Jul;10(7):1058-66. PMID: 26010125.

L1817

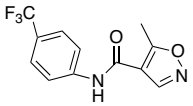

Leflunomide

HWA-486

$C_{12}H_9F_3N_2O_2$ FW: 270.21 [75706-12-6] ≥98%

100 mg
500 mg
1 g

AhR agonist and dihydroorotate dehydrogenase inhibitor used to treat rheumatoid arthritis. It prevents pyrimidine synthesis, inhibits replication of polyomavirus BK, and increases activity of aryl hydrocarbon receptors to suppress melanoma cell proliferation.

Qi R, Hua-Song Z, Xiao-Feng Z. Leflunomide inhibits the apoptosis of human embryonic lung fibroblasts infected by human cytomegalovirus. Eur J Med Res. 2013 Feb 1;18:3. PMID: 23369524.

O'Donnell EF, Kopparapu PR, Koch DC, et al. The aryl hydrocarbon receptor mediates leflunomide-induced growth inhibition of melanoma cells. PLoS One. 2012;7(7):e40926. PMID: 22815870.

Bernhoff E, Tylden GD, Kjerpeseth LJ, et al. Leflunomide inhibition of BK virus replication in renal tubular epithelial cells. J Virol. 2010 Feb;84(4):2150-6. PMID: 19955306.

L1628

Ac-Leu-Glu-His-Asp-pNA

Ac-LEHD-pNa

Chromogenic caspase-4, 5, 9 substrate

$C_{29}H_{38}N_8O_{11}$ FW: 674.7 ≥95%

1 mg
2 mg
5 mg

Substrate used to measure caspase 9 activity.

Yi HS, Pan C, Pan C, et al. BmICE-2 is a novel pro-apoptotic caspase involved in apoptosis in the silkworm, *Bombyx mori*. Biochem Biophys Res Commun. 2014 Jan 31. pii: S0006-291X(14)00174-0. [Epub ahead of print]. PMID: 24491540.

L1852

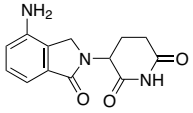

Lenalidomide

CC-5013

$C_{13}H_{13}N_3O_3$ FW: 259.26 [191732-72-6] ≥98%

50 mg
100 mg
250 mg

Thalidomide derivative and potential inhibitor of cereblon and TNF-α used to treat multiple myeloma and myelodysplastic syndromes associated with chromosome 5q deletions. It also inhibits VEGF-induced expression of HIF-1α.

Kim K, An S, Cha HJ, et al. Lenalidomide induces apoptosis and alters gene expression in non-small cell lung cancer cells. Oncol Lett. 2013 Feb;5(2):588-592. PMID: 23420263.

Chen Y, Borthakur G. Lenalidomide as a novel treatment of acute myeloid leukemia. Expert Opin Investig Drugs. 2013 Mar;22(3):389-97. PMID: 23316859.

L1661

H-Ser-Cys-Ser-Leu-Pro-Gln-Thr-Ser-Gly-Leu-Gln-Lys-Pro-Glu-Ser-OH

Leptin (116-130), mouse

$C_{64}H_{107}N_{18}O_{25}S_1$ FW: 1560.74 ≥95%

0.5 mg
1 mg
2.5 mg

Endogenous leptin receptor agonist involved in feeding behavior and energy homeostasis. It increases secretion of LH, prolactin, GnRH, and α-MSH, decreases blood pressure, inhibits myocardial muscle contractility, and decreases levels of tau and amyloid-β.

Rozhavskaya-Arena M, Lee DW, Leinung MC, et al. Design of a synthetic leptin agonist: effects on energy balance, glucose homeostasis, and thermoregulation. Endocrinology. 2000 Jul;141(7):2501-7. PMID: 10875251.

L1660

Val-Pro-Ile-Gln-Lys-Val-Gln-Asp-Asp-Thr-Lys-Thr-Leu-Ile-Lys-Thr-Ile-Val-Thr-Arg-Ile-Asn-Asp-Ile-Ser-His-Thr-Gln-Ser-Val-Ser-Ser-Lys-Gln-Lys

Leptin (22-56), human

OBGRP (22-56)

$C_{171}H_{298}N_{50}O_{56}$ FW: 3950.6 ≥98%

1 mg

Endogenous leptin receptor agonist involved in feeding behavior and energy homeostasis. It increases secretion of GnRH and α-MSH, decreases blood pressure, inhibits myocardial muscle contractility, and decreases levels of tau and amyloid-β.

Comninos AN, Jayasena CN, Dhillo WS. The relationship between gut and adipose hormones, and reproduction. Hum Reprod Update. 2014 Mar-Apr;20(2):153-74. PMID: 24173881.

L1761

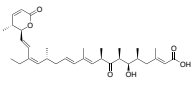

Leptomycin B

LMB; Elactocin; CI-940; CL-1957A; NSC-364372; PD-114720

$C_{33}H_{48}O_6$ FW: 540.74 [87081-35-4] ≥98%

1 μg
5 μg
10 μg
50 μg

CRM1 inhibitor that prevents nuclear export of proteins. It induces cell cycle arrest and apoptosis in cervical carcinoma cells.

Sun Q, Carrasco YP, Hu Y, et al. Nuclear export inhibition through covalent conjugation and hydrolysis of Leptomycin B by CRM1. Proc Natl Acad Sci U S A. 2013 Jan 22;110(4):1303-8. PMID: 23297231.

Abkallo HM, Kawano H, Watanabe K, et al. A new cell-based reporter system for sensitive screening of nuclear export inhibitors. Drug Discov Ther. 2011 Dec;5(6):286-92. PMID: 22466439.

Lu C, Shao C, Cobos E, et al. Chemotherapeutic sensitization of leptomycin B resistant lung cancer cells by pretreatment with doxorubicin. PLoS One. 2012;7(3):e32895. PMID: 22412944.

L1878 Letrozole

25 mg
50 mg
100 mg

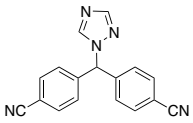

$C_{17}H_{11}N_5$ FW: 285.3 [112809-51-5] ≥98%

Aromatase inhibitor used to treat hormone-responsive breast cancer and infertility. It is also used to terminate pregnancy. It prevents the formation of estrogens and increases the secretion of LH.

Lee VC, Gao J, Lee KF, et al. The effect of letrozole with misoprostol for medical termination of pregnancy on the expression of steroid receptors in the placenta. Hum Reprod. 2013 Nov;28(11):2912-9. PMID: 23980056.

Tomao F, Spinelli G, Vici P, et al. Current role and safety profile of aromatase inhibitors in early breast cancer. Expert Rev Anticancer Ther. 2011 Aug;11(8):1253-63. PMID: 21916579.

L1980 Leucokinin I

1 mg
2 mg
5 mg

H-Asp-Pro-Ala-Phe-Asn-Ser-Trp-Gly-NH_2

$C_{41}H_{52}N_{11}O_{12}$ FW: 891.93 [104600-89-7] ≥95%

Diuretic found in insects that increases intracellular Ca^{2+} levels.

Radford JC, Terhzaz S, Cabrero P, et al. Functional characterisation of the *Anopheles* leucokinins and their cognate G-protein coupled receptor. J Exp Biol. 2004 Dec;207(Pt 26):4573-86. PMID: 15579553.

L1981 Leucokinin VIII

1 mg
2 mg
5 mg

H-Gly-Ala-Ser-Phe-Tyr-Ser-Trp-Gly-NH_2

$C_{42}H_{52}N_{10}O_{11}$ FW: 872.94 ≥95%

Diuretic found in insects. It decreases membrane resistance and increases permeability of gap junctions in *Anopheles* Malpighian tubes.

Weng XH, Piermarini PM, Yamahiro A, et al. Gap junctions in Malpighian tubules of *Aedes* aegypti. J Exp Biol. 2008 Feb;211(Pt 3):409-22. PMID: 18203997.

L1983 Leucomyosuppressin

0.5 mg
1 mg
2.5 mg

LMS

pGlu-Asp-Val-Asp-His-Val-Phe-Leu-Arg-Phe-NH_2

$C_{59}H_{84}N_{16}O_{15}$ FW: 1257.44 [106884-19-9] ≥95%

Peptide found in insects. It decreases food intake, suppresses weight gain, and inhibits peristalsis.

Maestro JL, Tobe SS, Belles X. Leucomyosuppressin modulates cardiac rhythm in the cockroach Blattella germanica. J Insect Physiol. 2011 Dec;57(12):1677-81. PMID: 21925505.

Matthews HJ, Audsley N, Weaver RJ. In vitro and in vivo effects of myo-active peptides on larvae of the tomato moth Lacanobia oleracea and the cotton leaf worm *Spodoptera* littoralis (Lepidoptera; Noctuidae). Arch Insect Biochem Physiol. 2008 Oct;69(2):60-9. PMID: 18780345.

L1982 Leupeptin Hemisulfate NEW

5 mg
10 mg
25 mg

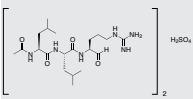

$C_{20}H_{38}N_6O_4 \bullet 1/2H_2SO_4$ FW: 475.59 [103476-89-7] ≥95%

Synthetic protease inhibitor used to study protease activity.

Ganapathi TR, Sunil Kumar GB, Srinivas L, et al. Analysis of the limitations of hepatitis B surface antigen expression in soybean cell suspension cultures. Plant Cell Rep. 2007 Sep;26(9):1575-84. PMID: 17534624.

Morejohn LC, Bureau TE, Fosket DE. Inhibition of plant cell proteolytic activities that degrade tubulin. Cell Biol Int Rep. 1985 Sep;9(9):849-57. PMID: 2864138.

L1881 Leuprolide Acetate

1 mg
5 mg

Leuprorelin

p-Pro-His-Trp-Ser-Tyr-D-Leu-Leu-Arg-Pro-NHEt

$C_{59}H_{84}N_{16}O_{12} \bullet C_2H_4O_2$ FW: 1269.65 [74381-53-6] ≥98%

Analog of GnRH and agonist at GnRH1 receptors used for in vitro fertilization and to treat various cancers. It stimulates release of reproductive hormones, prevents stress-induced immunosuppression, and suppresses expression of human telomerase reverse transcriptase.

Ko YH, Ha YR, Kim JW, et al. Silencing of the GnRH type 1 receptor blocks the antiproliferative effect of the GnRH agonist, leuprolide, on the androgen-independent prostate cancer cell line DU145. J Int Med Res. 2011;39(3):729-39. PMID: 21819703.

Tesone M, Bilotas M, Barañao RI, et al. The role of GnRH analogues in endometriosis-associated apoptosis and angiogenesis. Gynecol Obstet Invest. 2008;66 Suppl 1:10-8. PMID: 18936547.

L1682 Levamisole Hydrochloride

5 g
10 g

Tetramisole hydrochloride

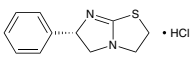

$C_{11}H_{12}N_2S \bullet HCl$ FW: 240.76 [16595-80-5] ≥98%

Alkaline phosphatase inhibitor and potential nAChR agonist used to treat worm infections and dermatologic conditions. It also induces DNA fragmentation in multiple myeloma cells and inhibits proliferation and differentiation of endothelial cells.

Ramanadham M, Nageshwari B. Anti-proliferative effect of levamisole on human myeloma cell lines in vitro. J Immunotoxicol. 2010 Oct-Dec;7(4):327-32. PMID: 20860474.

Friis T, Engel AM, Klein BM, et al. Levamisole inhibits angiogenesis in vitro and tumor growth in vivo. Angiogenesis. 2005;8(1):25-34. PMID: 16132615.

L1784 Levetiracetam

100 mg
250 mg
1 g

$C_8H_{14}N_2O_2$ FW: 170.21 [102767-28-2] ≥98%

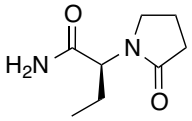

SV2A synaptic vesicle inhibitor used to treat epilepsy and seizure disorders. It prevents SV2A function, suppressing presynaptic Ca^{2+} release, reducing excitatory postsynaptic potentials, and inhibiting synaptic transmission. It also reduces memory and learning deficits in Alzheimer's disease models.

Vogl C, Mochida S, Wolff C, et al. The synaptic vesicle glycoprotein 2A ligand levetiracetam inhibits presynaptic Ca^{2+} channels through an intracellular pathway. Mol Pharmacol. 2012 Aug;82(2):199-208. PMID: 22554805.

Sanchez PE, Zhu L, Verret L, et al. Levetiracetam suppresses neuronal network dysfunction and reverses synaptic and cognitive deficits in an Alzheimer's disease model. Proc Natl Acad Sci U S A. 2012 Oct 16;109(42):E2895-903. PMID: 22869752.

L1735 Levitide

1 mg
2 mg
5 mg

$C_{66}H_{119}N_{21}O_{19}S$ FW: 1542.88 [114281-19-5] ≥95%

pGlu-Gly-Met-Ile-Gly-Thr-Leu-Thr-Ser-Lys-Arg-Ile-Lys-Gln-NH_2

Found in amphibian skin. It inhibits growth of microbes.

Langerveld AJ, Celestine R, Zaya R, et al. Chronic exposure to high levels of atrazine alters expression of genes that regulate immune and growth-related functions in developing Xenopus laevis tadpoles. Environ Res. 2009 May;109(4):379-89. PMID: 19272595.

L1780 Levocetirizine Dihydrochloride

1 g
5 g
25 g

(−)-Cetirizine

$C_{21}H_{25}ClN_2O_3 \cdot 2HCl$ FW: 461.81 [130018-87-0] ≥98%

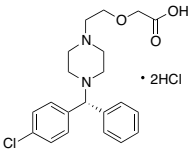

L-isomer of cetirizine and histamine H1 receptor antagonist. It increases levels of CD4+ CD25+ T cells and decreases levels of eosinophils, decreasing allergy symptoms.

García-Zepeda S, Estrada-Muñiz E, Elizondo G, et al. Levocetirizine inhibits migration of immune cells to lymph nodes and induces treg cells in a murine type I allergic conjunctivitis model. Open Ophthalmol J. 2012;6:129-36. PMID: 23284599.

Mahmoud F, Arifhodzic N, Haines D, et al. Levocetirizine modulates lymphocyte activation in patients with allergic rhinitis. J Pharmacol Sci. 2008 Oct;108(2):149-56. PMID: 18946193.

L1782 Levodopa

1 g
5 g
10 g

L-DOPA

$C_9H_{11}NO_4$ FW: 197.19 [59-92-7] ≥98%

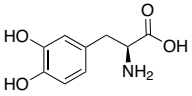

Endogenous catecholamine precursor found in *Mucuna* used to treat Parkinson's disease. It increases brain dopamine concentrations.

Pahwa R, Lyons KE. Treatment of early Parkinson's disease. Curr Opin Neurol. 2014 Jun 19. [Epub ahead of print]. PMID: 24950010.

Pd Med Collaborative Group. Long-term effectiveness of dopamine agonists and monoamine oxidase B inhibitors compared with levodopa as initial treatment for Parkinson's disease (PD MED): a large, open-label, pragmatic randomised trial. Lancet. 2014 Jun 10. [Epub ahead of print]. PMID: 24928805.

L1786 Levofloxacin Hydrochloride Monohydrate

500 mg
1 g
5 g

S-(−)-Ofloxacin

$C_{18}H_{20}FN_3O_4 \cdot HCl \cdot H_2O$ FW: 415.84 [100986-85-4] ≥90%

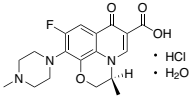

S-(−) isomer of ofloxacin and inhibitor of topoisomerase IV and bacterial DNA gyrase used to treat bacterial infections. It binds DNA and inhibits proliferation of cancer cells when complexed with gold(III).

Fu Y, Zhang W, Wang H, et al. Specific patterns of gyrA mutations determine the resistance difference to ciprofloxacin and levofloxacin in *Klebsiella* pneumoniae and *Escherichia* coli. BMC Infect Dis. 2013 Jan 7;13:8. PMID: 23295059.

Gouvea LR, Garcia LS, Lachter DR, et al. Atypical fluoroquinolone gold(III) chelates as potential anticancer agents: relevance of DNA and protein interactions for their mechanism of action. Eur J Med Chem. 2012 Sep;55:67-73. PMID: 22835721.

L1785 Levofloxacin Hemihydrate

500 mg
1 g
5 g

S-(−)-Ofloxacin

$(C_{18}H_{20}FN_3O_4)_2 \cdot H_2O$ FW: 370.4 ≥98%

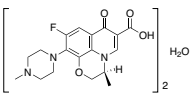

S-(−) isomer of ofloxacin and inhibitor of topoisomerase IV and bacterial DNA gyrase used to treat bacterial infections. It binds DNA and inhibits proliferation of cancer cells when complexed with gold(III).

Fu Y, Zhang W, Wang H, et al. Specific patterns of gyrA mutations determine the resistance difference to ciprofloxacin and levofloxacin in *Klebsiella* pneumoniae and *Escherichia* coli. BMC Infect Dis. 2013 Jan 7;13:8. PMID: 23295059.

Gouvea LR, Garcia LS, Lachter DR, et al. Atypical fluoroquinolone gold(III) chelates as potential anticancer agents: relevance of DNA and protein interactions for their mechanism of action. Eur J Med Chem. 2012 Sep;55:67-73. PMID: 22835721.

L1684 Levonorgestrel

100 mg
500 mg
1 g

D-(−)-Norgestrel

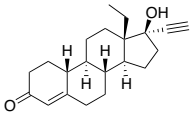

$C_{21}H_{28}O_2$ FW: 312.45 [797-63-7] ≥98%

Synthetic progestogen used as a contraceptive. It inhibits secretion of FSH and LH and increases expression of 17β-HSD.

Gemzell-Danielsson K, Berger C, P G L L. Emergency contraception -- mechanisms of action. Contraception. 2013 Mar;87(3):300-8. PMID: 23114735.

Yuan P, Chen B, Huang Y, et al. Long-term regression of experimental endometriosis in a rat model treated with local application of levonorgestrel-loaded biodegradable microspheres. Hum Reprod. 2012 Jul;27(7):2089-95. PMID: 22563024.

L1884 Levosimendan

100 mg
250 mg
1 g

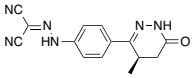

$C_{14}H_{12}N_6O$ FW: 280.28 [141505-33-1] ≥98%

Ca^{2+} sensitizer, ATP-sensitive K^+ channel activator, troponin C stabilizer, and PDE inhibitor used to treat heart failure. It improves cardiac performance and myocardial contractility without increasing oxygen consumption or decreasing preload or afterload.

Pathak A, Lebrin M, Vaccaro A, et al. Pharmacology of levosimendan: inotropic, vasodilatory and cardioprotective effects. J Clin Pharm Ther. 2013 Oct;38(5):341-9. PMID: 23594161.

Malmberg M, Vähäsilta T, Saraste A, et al. Intracoronary Levosimendan during Ischemia Prevents Myocardial Apoptosis. Front Physiol. 2012 Feb 14;3:17. PMID: 22347864.

L2540 LGK-974

NEW

1 mg
5 mg

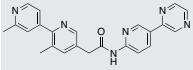

$C_{23}H_{20}N_6O$ FW: 396.44 [1243244-14-5] ≥98%

PORCN inhibitor. It inhibits proliferation and induces differentiation in pancreatic adenocarcinoma models.

Liu J, Pan S, Hsieh MH, et al. Targeting Wnt-driven cancer through the inhibition of Porcupine by LGK974. Proc Natl Acad Sci U S A. 2013 Dec 10;110(50):20224-9. PMID: 24277854.

Jiang X, Hao HX, Growney JD, et al. Inactivating mutations of RNF43 confer Wnt dependency in pancreatic ductal adenocarcinoma. Proc Natl Acad Sci U S A. 2013 Jul 30;110(31):12649-54. PMID: 23847203.

L2800 LH846

NEW

5 mg
25 mg

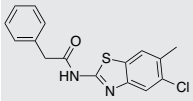

$C_{16}H_{13}ClN_2OS$ FW: 316.8 [639052-78-1] ≥98%

Casein kinase 1δ inhibitor. It lengthens the circadian period.

Lee JW, Hirota T, Peters EC, et al. A small molecule modulates circadian rhythms through phosphorylation of the period protein. Angew Chem Int Ed Engl. 2011 Nov 4;50(45):10608-11. PMID: 21954091.

L3250 D-Limonene

500 mL

(+)-Dipentene

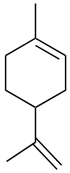

$C_{10}H_{16}$ FW: 136.23 [5989-27-5] ≥96%

Commercial flavorant, odorant, cleaning solvent, and insecticide found in the rind of various citrus plants. It displays a wide range of activities, including cell cycle arrest and apoptosis in gastric carcinoma cells, inducing phase II enzyme expression to limit oxidative damage, and suppressing cytokine production by CD4+ and CD8+ T cells.

Zhang XZ, Wang L, Liu DW, Tang GY, Zhang HY. Synergistic Inhibitory Effect of Berberine and d-Limonene on Human Gastric Carcinoma Cell Line MGC803. J Med Food. 2014 Sep;17(9):955-62. PMID: 25045784.

Rehman MU, Tahir M, Khan AQ, et al. D-limonene suppresses doxorubicin-induced oxidative stress and inflammation via repression of COX-2, iNOS, and NFκB in kidneys of Wistar rats. Exp Biol Med (Maywood). 2014 Apr;239(4):465-76. PMID: 24586096.

L3550 Limonin

50 mg
100 mg
500 mg

Evodine; Limonoic acid di-δ-lactone

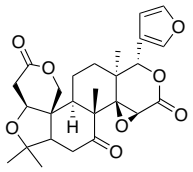

$C_{26}H_{30}O_8$ FW: 470.52 [1180-71-8] ≥98%

Natural product found in *Citrus* family fruits. It displays a variety of activities, including downregulating expression of TLR2, TLR4, and pro-inflammatory cytokines in models of hepatic ischemia/reperfusion, inducing apoptosis in colon adenocarcinoma cells, and inhibiting expression of HIV-1 and HTLV-1 in infected cells.

Mahmoud MF, Gamal S, El-Fayoumi HM. Limonin attenuates hepatocellular injury following liver ischemia and reperfusion in rats via toll-like receptor dependent pathway. Eur J Pharmacol. 2014 Oct 5;740:676-82. PMID: 24967531.

Hafeez F, Akram W, Shaalan EA. Mosquito larvicidal activity of citrus limonoids against *Aedes* albopictus. Parasitol Res. 2011 Jul;109(1):221-9. PMID: 21212981.

L3551 Limonin Glucoside

1 mg
5 mg

$C_{32}H_{42}O_{14}$ FW: 650.67 [123564-61-4] ≥95%

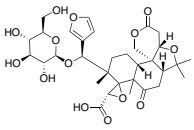

Found in citrus fruits. It induces apoptosis in colon adenocarcinoma cells, inhibits expression of HIV-1 and HTLV-1 in infected cells, and exhibits larvicidal activity against species of *Aedes*.

Mahmoud MF, Gamal S, El-Fayoumi HM. Limonin attenuates hepatocellular injury following liver ischemia and reperfusion in rats via toll-like receptor dependent pathway. Eur J Pharmacol. 2014 Jun 23. [Epub ahead of print]. PMID: 24967531.

Hafeez F, Akram W, Shaalan EA. Mosquito larvicidal activity of citrus limonoids against *Aedes* albopictus. Parasitol Res. 2011 Jul;109(1):221-9. PMID: 21212981.

Chidambara Murthy KN, Jayaprakasha GK, et al. Citrus limonin and its glucoside inhibit colon adenocarcinoma cell proliferation through apoptosis. J Agric Food Chem. 2011 Mar 23;59(6):2314-23. PMID: 21338095.

L3454 Lincomycin Hydrochloride Monohydrate

1 g
5 g
25 g

$C_{18}H_{34}N_2O_6S \cdot HCl \cdot H_2O$ FW: 461.01 [7179-49-9] ≥89%

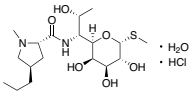

Peptidyl transferase and protein translation inhibitor used to treat bacterial infections. It also inhibits growth of *Plasmodium*.

Tenson T, Lovmar M, Ehrenberg M. The mechanism of action of macrolides, lincosamides and streptogramin B reveals the nascent peptide exit path in the ribosome. J Mol Biol. 2003 Jul 25;330(5):1005-14. PMID: 12860123.

Menninger JR. Mechanism of inhibition of protein synthesis by macrolide and lincosamide antibiotics. J Basic Clin Physiol Pharmacol. 1995;6(3-4):229-50. PMID: 8852269.

L3456 γ-Linolenic Acid (6c, 9c, 12c)

10 mg
25 mg
100 mg

GLA

$C_{18}H_{30}O_2$ FW: 278.43 [506-26-3] ≥98%

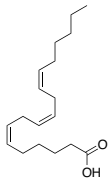

Omega-6 fatty acid and PPAR agonist found in vegetable oils. It is a precursor to prostaglandin E1 and eicosapentaenoic acid. It regulates insulin secretion, inhibits diabetes mellitus-induced albuminuria, and induces apoptosis in leukemia cells.

Lai MC, Teng TH, Yang C. The Natural PPAR Agonist Linoleic Acid Stimulated Insulin Release in Rat Pancreas. J Vet Med Sci. 2013 Jul 5. [Epub ahead of print] PMID: 23832628.

Kim DH, Yoo TH, Lee SH, et al. Gamma linolenic acid exerts anti-inflammatory and anti-fibrotic effects in diabetic nephropathy. Yonsei Med J. 2012 Nov 1;53(6):1165-75. PMID: 23074118.

L3561 D,L-α-Lipoic Acid

1 g
5 g
25 g

$C_8H_{14}O_2S_2$ FW: 206.33 [1077-28-7] ≥98%

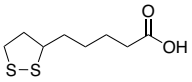

Endogenous antioxidant also found in meat and vegetables. It is required for aerobic metabolism, acting as a cofactor for the pyruvate dehydrogenase complex. It induces activation of phase II enzymes and protects against oxidative stress.

Shay KP, Moreau RF, Smith EJ, et al. Alpha-lipoic acid as a dietary supplement: molecular mechanisms and therapeutic potential. Biochim Biophys Acta. 2009 Oct;1790(10):1149-60. PMID: 19664690.

Petersen Shay K, Moreau RF, et al. Is alpha-lipoic acid a scavenger of reactive oxygen species in vivo? Evidence for its initiation of stress signaling pathways that promote endogenous antioxidant capacity. IUBMB Life. 2008 Jun;60(6):362-7. PMID: 18409172.

L3362 β-Lipotropin (61-64)

5 mg
10 mg
25 mg

$C_{22}H_{26}N_4O_6$ FW: 442.48 [60254-82-2] ≥95%

Tyr-Gly-Gly-Phe

β-lipotropin and met-enkephalin fragment. It activates melanin production, increases lipolysis, and stimulates steroidogenesis.

Spiess J, Mount CD, Nicholson WE, et al. NH2-terminal amino acid sequence and peptide mapping of purified human beta-lipotropin: comparison with previously proposed sequences. Proc Natl Acad Sci U S A. 1982 Aug;79(16):5071-5. PMID: 6956916.

L3374 Lisinopril Dihydrate

100 mg
1 g
5 g

$C_{21}H_{31}N_3O_5 \cdot 2H_2O$ FW: 441.52 [83915-83-7] ≥98%

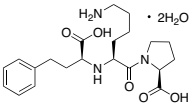

Enalapril analog and ACE inhibitor used to treat hypertension, congestive heart failure, myocardial infarction, and retinal disorders. It also inhibits left ventricular dilation, suppresses myocardial hypertrophy, and prevents the development of paraquat-induced lung fibrosis.

Brower GL, Levick SP, Janicki JS. Inhibition of matrix metalloproteinase activity by ACE inhibitors prevents left ventricular remodeling in a rat model of heart failure. Am J Physiol Heart Circ Physiol. 2007 Jun;292(6):H3057-64. PMID: 17308006.

Mohammadi-Karakani A, Ghazi-Khansari M, Sotoudeh M. Lisinopril ameliorates paraquat-induced lung fibrosis. Clin Chim Acta. 2006 May;367(1-2):170-4. PMID: 16458281.

L3577 — Litorin

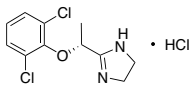

pGlu-Gln-Trp-Ala-Val-Gly-His-Phe-Met-NH_2

$C_{51}H_{68}N_{14}O_{11}S$ FW: 1085.28 [55749-97-8] ≥95%

Bombesin-like peptide found in amphibians. It binds bombesin receptors, decreases food intake and body temperature, and induces contractions in smooth muscle.

1 mg
2 mg
5 mg

L5822 — Lofexidine Hydrochloride

$C_{11}H_{12}Cl_2N_2O \bullet HCl$ FW: 295.6 [21498-08-8] ≥98%

α2-Adrenergic receptor agonist. It inhibits stress-induced reinstatement and self-administration of drug use.

Gowing L, Farrell MF, Ali R, et al. Alpha2-adrenergic agonists for the management of opioid withdrawal. Cochrane Database Syst Rev. 2014 Mar 31;3:CD002024. PMID: 24683051.

Lê AD, Harding S, Juzytsch W, et al. Role of alpha-2 adrenoceptors in stress-induced reinstatement of alcohol seeking and alcohol self-administration in rats. Psychopharmacology (Berl). 2005 May;179(2):366-73. PMID: 15551068.

1 g
5 g
25 g

L5624 — Loganin

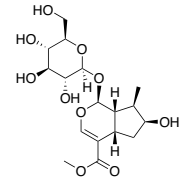

$C_{17}H_{26}O_{10}$ FW: 390.38 [18524-94-2] ≥98%

Inhibitor of β-secretase found in *Cornus officialis*. It improves memory impairment, downregulates expression of MCP-1, NF-κB, and iNOS, and modulates ERK signaling.

Youn K, Jeong WS, Jun M. β-Secretase (BACE1) inhibitory property of loganin isolated from Corni fructus. Nat Prod Res. 2013 Aug;27(16):1471-4. PMID: 22931211.

Jiang WL, Zhang SP, Hou J, et al. Effect of loganin on experimental diabetic nephropathy. Phytomedicine. 2012 Feb 15;19(3-4):217-22. PMID: 21978885.

Park CH, Tanaka T, Kim JH, et al. Hepato-protective effects of loganin, iridoid glycoside from Corni Fructus, against hyperglycemia-activated signaling pathway in liver of type 2 diabetic db/db mice. Toxicology. 2011 Nov 28;290(1):14-21. PMID: 21864639.

10 mg
25 mg
100 mg

L5749 — Lomefloxacin Hydrochloride

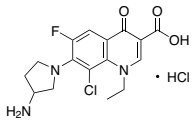

$C_{17}H_{19}F_2N_3O_3 \bullet HCl$ FW: 387.81 [98079-52-8] ≥98%

Topoisomerase IV and bacterial DNA gyrase inhibitor used to treat respiratory and urinary tract infections. It is primarily active against gram negative aerobic bacteria and may induce photocleavage of DNA

Martínez L, Chignell CF. Photocleavage of DNA by the fluoroquinolone antibacterials. J Photochem Photobiol B. 1998 Aug 21;45(1):51-9. PMID: 9819899.

Just PM. Overview of the fluoroquinolone antibiotics. Pharmacotherapy. 1993 Mar-Apr;13(2 Pt 2):4S-17S. PMID: 8386356.

1 g
5 g
10 g

L5750 — Lomeguatrib

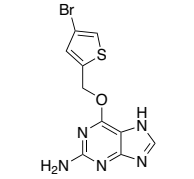

$C_{10}H_8BrN_5OS$ FW: 326.17 [192441-08-0] ≥98%

MGMT inhibitor that prevents repair of DNA damage induced by chemotherapeutics. It allows mechanisms of cell death to occur and induces apoptosis in glioblastoma cells.

Taspinar M, Ilgaz S, Ozdemir M, et al. Effect of lomeguatrib-temozolomide combination on MGMT promoter methylation and expression in primary glioblastoma tumor cells. Tumour Biol. 2013 Jun;34(3):1935-47. PMID: 23519841.

Tawbi HA, Villaruz L, Tarhini A, et al. Inhibition of DNA repair with MGMT pseudosubstrates: phase I study of lomeguatrib in combination with dacarbazine in patients with advanced melanoma and other solid tumours. Br J Cancer. 2011 Sep 6;105(6):773-7. PMID: 21811257.

10 mg
25 mg
100 mg

L5751 — Lomerizine Dihydrochloride

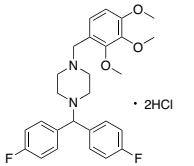

$C_{27}H_{30}F_2N_2O_3 \bullet 2HCl$ FW: 541.47 [101477-54-7] ≥98%

Antagonist at L-type and T-type Ca^{2+} channels and TRP5 channels used to treat migraines and vertigo. It also decreases glutamate excitotoxicity, Ca^{2+} overload, and mitochondrial dysfunction and protects against NMDA-induced retinal damage and neurodegeneration.

Tran LT, Gentil BJ, Sullivan KE, et al. The voltage-gated calcium channel blocker lomerizine is neuroprotective in motor neurons expressing mutant SOD1, but not TDP-43. J Neurochem. 2014 Apr 9. [Epub ahead of print]. PMID: 24716897.

Inoue Y, Yabe T. Lomerizine therapy for the treatment of benign paroxysmal vertigo of childhood transitioning into atypical basilar migraine: A case report. Exp Ther Med. 2013 Jun;5(6):1573-1575. PMID: 23837033.

Ito Y, Nakamura S, Tanaka H, et al. Lomerizine, a Ca^{2+} channel blocker, protects against neuronal degeneration within the visual center of the brain after retinal damage in mice. CNS Neurosci Ther. 2010 Apr;16(2):103-14. PMID: 19788586.

500 mg
1 g
5 g

L5648

Lomustine

50 mg
100 mg
500 mg

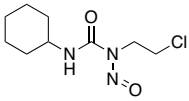

$C_9H_{16}ClN_3O_2$ FW: 233.7 [13010-47-4] ≥98%

DNA alkylator used to treat various cancers.

Buccheri G, Ferrigno D, Rosso A. A phase II study of methotrexate, doxorubicin, cyclophosphamide, and lomustine chemotherapy and lonidamine in advanced non-small cell lung cancer. Cancer. 1993 Sep 1;72(5):1564-72. PMID: 8394198.

Kamiya S. Synthesis of antitumor nitrosourea derivatives and chemical studies of their mechanism of action. Eisei Shikenjo Hokoku. 1986;(104):1-19. PMID: 3471287.

L5658

Lonidamine

5 mg
25 mg
100 mg

Diclondazolic acid; DICA; AF-1890

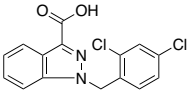

$C_{15}H_{10}Cl_2N_2O_2$ FW: 321.16 [50264-69-2] ≥98%

Inhibitor of hexokinase and aerobic glycolysis. It increases lifespan in *Caenorhabditis elegans*, inhibits growth of *Trypanosoma*, and decreases sperm count and testosterone levels.

Schmeisser S, Zarse K, Ristow M. Lonidamine extends lifespan of adult *Caenorhabditis elegans* by increasing the formation of mitochondrial reactive oxygen species. Horm Metab Res. 2011 Sep;43(10):687-92. PMID: 21932172.

Chambers JW, Fowler ML, Morris MT, et al. The anti-trypanosomal agent lonidamine inhibits *Trypanosoma brucei* hexokinase 1. Mol Biochem Parasitol. 2008 Apr;158(2):202-7. PMID: 18262292.

Traina ME, Guarino M, Natoli A, et al. Lonidamine affects testicular steroid hormones in immature mice. Toxicol Appl Pharmacol. 2007 May 15;221(1):95-101. PMID: 17442358.

L5660

Loperamide Hydrochloride

5 g
25 g

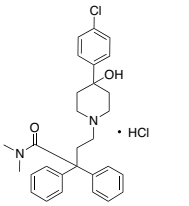

$C_{29}H_{33}ClN_2O_2 \bullet HCl$ FW: 513.51 [34552-83-5] ≥98%

μOR agonist, FIASMA, and potential HCN channel blocker used to treat diarrhea. It increases gastric emptying, decreases bowel water content, alters pain thresholds, and decreases foraging behavior and body weight.

Kumar R. Loperamide: from antidiarrheal to analgesic. J Opioid Manag. 2013 Jul-Aug;9(4):301-2. PMID: 24353024.

Kumar R, Reeta KH, Ray SB. Antinociceptive effect of intrathecal loperamide: role of mu-opioid receptor and calcium channels. Eur J Pharmacol. 2012 Dec 5;696(1-3):77-82. PMID: 23022331.

Placidi E, Marciani L, Hoad CL, et al. The effects of loperamide, or loperamide plus simethicone, on the distribution of gut water as assessed by MRI in a mannitol model of secretory diarrhoea. Aliment Pharmacol Ther. 2012 Jul;36(1):64-73. PMID: 22582872.

L5862

Lopinavir

500 mg
1 g
5 g

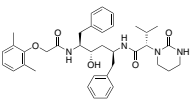

$C_{37}H_{48}N_4O_5$ FW: 321.16 [192725-17-0] ≥98%

HIV protease and SERCA inhibitor used to treat HIV infections. It decreases intracellular Ca^{2+} levels, upregulates ribonuclease L protein expression in HPV-positive cervical cancer cells, and induces cell cycle arrest in meningioma cells.

Kao E, Shinohara M, Feng M, et al. Human immunodeficiency virus protease inhibitors modulate Ca^{2+} homeostasis and potentiate alcoholic stress and injury in mice and primary mouse and human hepatocytes. Hepatology. 2012 Aug;56(2):594-604. PMID: 22407670.

Batman G, Oliver AW, Zehbe I, et al. Lopinavir up-regulates expression of the antiviral protein ribonuclease L in human papillomavirus-positive cervical carcinoma cells. Antivir Ther. 2011;16(4):515-25. PMID: 21685539.

Johnson MD, O'Connell M, Pilcher W. Lopinavir inhibits meningioma cell proliferation by Akt independent mechanism. J Neurooncol. 2011 Feb;101(3):441-8. PMID: 20596751.

L5767

Loratadine

500 mg
1 g
5 g

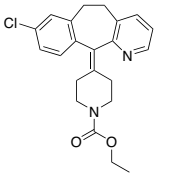

$C_{22}H_{23}ClN_2O_2$ FW: 382.88 [79794-75-5] ≥98%

Histamine H1 receptor antagonist and FIASMA used to treat allergic rhinitis, chronic idiopathic urticaria, and asthma. It also induces DNA damage and causes cell cycle arrest in colon cancer models.

Soule BP, Simone NL, DeGraff WG, et al. Loratadine dysregulates cell cycle progression and enhances the effect of radiation in human tumor cell lines. Radiat Oncol. 2010 Feb 3;5:8. PMID: 20128919.

DuBuske LM. Review of desloratadine for the treatment of allergic rhinitis, chronic idiopathic urticaria and allergic inflammatory disorders. Expert Opin Pharmacother. 2005 Nov;6(14):2511-23. PMID: 16259582.

L5769 Lorglumide Sodium

25 mg
100 mg

$C_{22}H_{31}Cl_2N_2O_4Na$ FW: 481.39 ≥98%

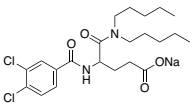

CCK antagonist used to treat various gastrointestinal pathologies. It also inhibits proliferation of colon cancer cells.

González-Puga C, García-Navarro A, Escames G, et al. Selective CCK-A but not CCK-B receptor antagonists inhibit HT-29 cell proliferation: synergism with pharmacological levels of melatonin. J Pineal Res. 2005 Oct;39(3):243-50. PMID: 16150104.

Makovec F, Bani M, Cereda R, et al. Antispasmodic activity on the gallbladder of the mouse of CR 1409 (lorglumide) a potent antagonist of peripheral CCK. Pharmacol Res Commun. 1987 Jan;19(1):41-51. PMID: 3575382.

Makovec F, Bani M, Cereda R, et al. Pharmacological properties of lorglumide as a member of a new class of cholecystokinin antagonists. Arzneimittelforschung. 1987 Nov;37(11):1265-8. PMID: 3440035.

L5870 Lornoxicam

100 mg
250 mg
1 g

$C_{13}H_{10}ClN_3O_4S_2$ FW: 371.82 [70374-39-9] ≥98%

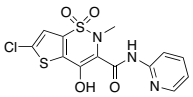

NSAID and COX-1/2 inhibitor. It also decreases herpetic stromal keratitis induced by herpes simplex virus HSV-1, attenuates Freund's adjuvant-induced hyperalgesia, and prevents neuronal apoptosis in models of brain injury.

Topcu I, Vatansever S, Bayram E, et al. The effects of lornoxicam on neuroprotection following diffuse traumatic brain injury in rats. Turk Neurosurg. 2013;23(6):764-71. PMID: 24310460.

Yin J, Huang Z, Xia Y, et al. Lornoxicam suppresses recurrent herpetic stromal keratitis through down-regulation of nuclear factor-kappaB: an experimental study in mice. Mol Vis. 2009 Jun 14;15:1252-9. PMID: 19547717.

Futaki N, Harada M, Sugimoto M, et al. The importance of brain PGE2 inhibition versus paw PGE2 inhibition as a mechanism for the separation of analgesic and antipyretic effects of lornoxicam in rats with paw inflammation. J Pharm Pharmacol. 2009 May;61(5):607-14. PMID: 19405999.

L5873 Losartan Potassium

1 g
5 g
25 g

$C_{22}H_{22}ClN_6O\ K$ FW: 461.01 [124750-99-8] ≥98%

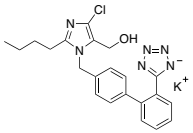

AT1 receptor antagonist used to treat hypertension. It suppresses renal tubular fibrosis, inhibits the epithelial-to-mesenchymal transition, and indirectly inhibits ERK activation.

He P, Li D, Zhang B. Losartan attenuates renal interstitial fibrosis and tubular cell apoptosis in a rat model of obstructive nephropathy. Mol Med Rep. 2014 Aug;10(2):638-44. PMID: 24912579.

Wylie-Sears J, Levine RA, Bischoff J. Losartan inhibits endothelial-to-mesenchymal transformation in mitral valve endothelial cells by blocking transforming growth factor-β-induced phosphorylation of ERK. Biochem Biophys Res Commun. 2014 Apr 18;446(4):870-5. PMID: 24632204.

Gibson TJ. Hypertension, its treatment, hyperuricaemia and gout. Curr Opin Rheumatol. 2013 Mar;25(2):217-22. PMID: 23370375.

L5993 Loxoprofen Sodium Dihydrate

100 mg
250 mg
1 g

$C_{15}H_{17}NaO_3 \bullet 2H_2O$ FW: 304.31 [80382-23-6] ≥98%

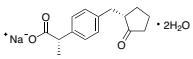

NSAID and COX-1/2 inhibitor. It decreases noxious heat-evoked neural responses, minimizes aortic atherosclerotic lesions, and suppresses nocturia in subjects with BPH.

Shin HI, Kim BH, Chang HS, et al. Long-term effect of loxoprofen sodium on nocturia in patients with benign prostatic hyperplasia. Korean J Urol. 2011 Apr;52(4):265-8. PMID: 21556213.

Hamaguchi M, Seno T, Yamamoto A, et al. Loxoprofen Sodium, a Non-Selective NSAID, Reduces Atherosclerosis in Mice by Reducing Inflammation. J Clin Biochem Nutr. 2010 Sep;47(2):138-47. PMID: 20838569.

Araki T, Yokoyama T, Araki M, et al. A clinical investigation of the mechanism of loxoprofen, a non-steroidal anti-inflammatory drug, for patients with nocturia. Acta Med Okayama. 2008 Dec;62(6):373-8. PMID: 19122682.

L8009 D-Luciferin 1-(4,5-dimethoxy-2-nitrophenyl) Ethyl Ester

1 mg
5 mg
10 mg

DMNPE-caged Luciferin

$C_{21}H_{19}N_3O_7S_2$ FW: 489.52 [223920-67-0] ≥95%

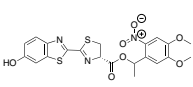

Heterocyclic light-emitting compound and natural ligand for luciferase used to detect cell activity. It requires ATP for its reaction, emitting a greenish-yellow luminescence at a peak wavelength of approximately 530 nm. DMNPE-caged luciferin crosses cell membranes easily.

Hastings JW. Chemistries and colors of bioluminescent reactions: a review. Gene 1996;173(1 Spec No):5–11. PMID: 8707056.

Green A, McElroy WD. Function of adenosine triphosphate in the activation of luciferin. Arch. Biochem. Biophys. 1956 Oct;64(2):257–71. PMID: 13363432.

L8010 D-Luciferin Potassium

5 mg
25 mg

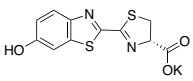

$C_{11}H_7KN_2O_3S_2$ FW: 318.42 [115144-35-9] ≥98%

Heterocyclic light-emitting compound and natural ligand for luciferase used to detect cell activity. It requires ATP for its reaction, emitting a greenish-yellow luminescence at a peak wavelength of approximately 530 nm. The salt form of luciferin dissolves in water or other typical buffers.

Hastings JW. Chemistries and colors of bioluminescent reactions: a review. Gene 1996;173(1 Spec No):5–11. PMID: 8707056.

L8011 D-Luciferin Sodium

5 mg
25 mg

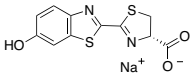

$C_{11}H_7N_2NaO_3S_2$ FW: 302.3 [103404-75-7] ≥99%

Heterocyclic light-emitting compound and natural ligand for luciferase used to detect cell activity. It requires ATP for its reaction, emitting a greenish-yellow luminescence at a peak wavelength of approximately 530 nm. The salt form of luciferin dissolves in water or other typical buffers.

Hastings JW. Chemistries and colors of bioluminescent reactions: a review. Gene 1996;173(1 Spec No):5–11. PMID: 8707056.

L8008 D-Luciferin, firefly, Free Acid

5 mg
25 mg

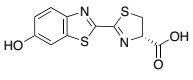

$C_{11}H_8N_2O_3S_2$ FW: 280.32 [2591-17-5] ≥98%

Heterocyclic light-emitting compound and natural ligand for luciferase used to detect cell activity. It requires ATP for its reaction, emitting a greenish-yellow luminescence at a peak wavelength of approximately 530 nm. The free acid form of luciferin requires addition of a dilute base such as NaOH or KOH to dissolve in water.

Hastings JW. Chemistries and colors of bioluminescent reactions: a review. Gene 1996;173(1 Spec No):5–11. PMID: 8707056.

L8248 Lumiracoxib

100 mg
250 mg
1 g

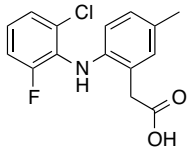

$C_{15}H_{13}ClFNO_2$ FW: 293.72 [220991-20-8] ≥98%

NSAID and COX-2 inhibitor. It displays many biological activities, including reversing vascular remodeling and inflammation in models of metabolic syndrome, inhibiting lymphocyte responses in EAE models, and inducing cell cycle arrest and apoptosis in non-small cell lung cancer cells.

Windsor MA, Valk PL, Xu S, et al. Exploring the molecular determinants of substrate-selective inhibition of cyclooxygenase-2 by lumiracoxib. Bioorg Med Chem Lett. 2013 Nov 1;23(21):5860-4. PMID: 24060487.

Renna NF, Diez ER, Lembo C, et al. Role of Cox-2 in vascular inflammation: an experimental model of metabolic syndrome. Mediators Inflamm. 2013;2013:513251. PMID: 23476105.

L8262 Lupinine

25 mg
100 mg

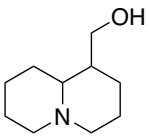

$C_{10}H_{19}NO$ FW: 169.26 [486-70-4] ≥98%

AChE and BChE inhibitor and potential CD69 activator found in species of *Loranthus*, *Calia*, and *Lupinus*. It may also inhibit heparin.

Basova NE, Kormilitsyn BN, Perchenok AIu, et al. Reversible lupininin inhibitors of cholinesterases of mammalian blood and of optical ganglia of individuals of the commander squid Berryteuthis magister from different zones of species areal. Zh Evol Biokhim Fiziol. 2012 May-Jun;48(3):213-8. PMID: 22827020.

Omeje EO, Osadebe PO, Nworu CS, et al. A novel sesquiterpene acid and an alkaloid from leaves of the Eastern Nigeria mistletoe, *Loranthus* micranthus with potent immunostimulatory activity on C57BL6 mice splenocytes and CD69 molecule. Pharm Biol. 2011 Dec;49(12):1271-6. PMID: 21988279.

L8276 Luteinizing Hormone Releasing Hormone

1 mg
2 mg
5 mg

LHRH

pGlu-His-Trp-Ser-Tyr-Gly-Leu-Arg-Pro-Gly-NH_2

$C_{55}H_{76}N_{17}O_{13}$ FW: 1182.3 [9034-40-6] ≥98%

Endogenous GnRH receptor agonist that stimulates secretion of LH and FSH. It is used to treat prostate and breast cancer, hyperplasia, and endometriosis.

Limonta P, Manea M. Gonadotropin-releasing hormone receptors as molecular therapeutic targets in prostate cancer: Current options and emerging strategies. Cancer Treat Rev. 2013 Oct;39(6):647-63. PMID: 23290320.

Millar RP, Newton CL. Current and future applications of GnRH, kisspeptin and neurokinin B analogues. Nat Rev Endocrinol. 2013 Aug;9(8):451-66. PMID: 23817290.

L2876

Luteinizing Hormone Releasing Hormone III, lamprey

1 mg
2 mg
5 mg

LHRH-III

pGlu-His-Trp-Ser-His-Asp-Trp-Lys-Pro-Gly-NH_2

$C_{59}H_{75}N_{18}O_{14}$ FW: 1259.4 ≥98%

GnRH receptor agonist and weak ERK1/2 and p38 MAPK activator found in eels. It induces secretion of FSH but not LH.

Yang D, Caraty A, Dupont J. Molecular mechanisms involved in LH release by the ovine pituitary cells. Domest Anim Endocrinol. 2005 Oct;29(3):488-507. PMID: 16153499.

Yu WH, Karanth S, Walczewska A, et al. A hypothalamic follicle-stimulating hormone-releasing decapeptide in the rat. Proc Natl Acad Sci U S A. 1997 Aug 19;94(17):9499-503. PMID: 9256511.

L8278

Luteinizing Hormone Releasing Hormone, salmon

1 mg
2 mg
5 mg

Gonadotropin-releasing hormone; LHRH; GnRH

pGlu-His-Trp-Ser-Tyr-Gly-Trp-Leu-Pro-Gly-NH_2

$C_{60}H_{73}N_{15}O_{13}$ FW: 1212.36 [86073-88-3] ≥95%

Endogenous GnRH receptor agonist involved in secretion of reproductive hormones. It may be used to treat hormone-dependent diseases such as prostate and breast cancer, hyperplasia, and endometriosis.

Limonta P, Manea M. Gonadotropin-releasing hormone receptors as molecular therapeutic targets in prostate cancer: Current options and emerging strategies. Cancer Treat Rev. 2013 Oct;39(6):647-63. PMID: 23290320.

Millar RP, Newton CL. Current and future applications of GnRH, kisspeptin and neurokinin B analogues. Nat Rev Endocrinol. 2013 Aug;9(8):451-66. PMID: 23817290.

L8277

[Gln8]-Luteinizing Hormone Releasing Hormone, chicken

1 mg
2 mg
5 mg

LHRH; GnRH

pGlu-His-Trp-Ser-Tyr-Gly-Leu-Gln-Pro-Gly-NH_2

$C_{54}H_{71}N_{15}O_{14}$ FW: 1154.28 [47922-48-5] ≥95%

GnRH derivative and GnRH receptor agonist involved in secretion of reproductive hormones. It may be used to treat hormone-dependent diseases such as prostate and breast cancer, hyperplasia, and endometriosis.

Limonta P, Manea M. Gonadotropin-releasing hormone receptors as molecular therapeutic targets in prostate cancer: Current options and emerging strategies. Cancer Treat Rev. 2013 Oct;39(6):647-63. PMID: 23290320.

L8377

Luteolin

100 mg
500 mg
1 g

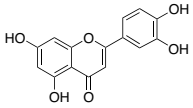

$C_{15}H_{10}O_6$ FW: 286.24 [491-70-3] ≥95%

Potentiator of DAT and NET, inhibitor of HSP90, IGF-1R, and PDE, and potential potential antagonist at α2-adrenergic receptors found in various plant sources. It displays several biological activities, including inhibiting LPS-stimulated expression of pro-inflammatory cytokines, suppressing mast cell activity and mast cell-dependent T cell activation, reversing xylazine/ketamine-induced anesthesia, decreasing systolic blood pressure, and lowering glucose tolerance and insulin sensitivity.

Xu N, Zhang L, Dong J, et al. Low-dose diet supplement of a natural flavonoid, luteolin, ameliorates diet-induced obesity and insulin resistance in mice. Mol Nutr Food Res. 2014 Jun;58(6):1258-68. PMID: 24668788.

Chen D, Bi A, Dong X, et al. Luteolin exhibits anti-inflammatory effects by blocking the activity of heat shock protein 90 in macrophages. Biochem Biophys Res Commun. 2014 Jan 3;443(1):326-32. PMID: 24321097.

Lv GY, Zhang YP, Gao JL, et al. Combined antihypertensive effect of luteolin and buddleoside enriched extracts in spontaneously hypertensive rats. J Ethnopharmacol. 2013 Nov 25;150(2):507-13. PMID: 24080032.

L9600

LY-2090314

NEW

1 mg
5 mg
10 mg

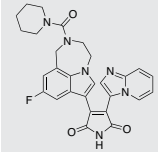

$C_{28}H_{25}FN_6O_3$ FW: 512.53 [603288-22-8] ≥98%

GSK-3 inhibitor.

Zamek-Gliszczynski MJ, Abraham TL, Alberts JJ, et al. Pharmacokinetics, metabolism, and excretion of the glycogen synthase kinase-3 inhibitor LY2090314 in rats, dogs, and humans: a case study in rapid clearance by extensive metabolism with low circulating metabolite exposure. Drug Metab Dispos. 2013 Apr;41(4):714-26. PMID: 23305709.

L9602

LY-2874455

NEW

1 mg
5 mg
10 mg

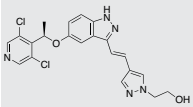

$C_{21}H_{19}Cl_2N_5O_2$ FW: 444.31 [1254473-64-7] ≥98%

FGFR inhibitor. It inhibits cell proliferation and tumor growth in models of lung cancer, gastric cancer, and multiple myeloma.

Zhao G, Li WY, Chen D, et al. A novel, selective inhibitor of fibroblast growth factor receptors that shows a potent broad spectrum of antitumor activity in several tumor xenograft models. Mol Cancer Ther. 2011 Nov;10(11):2200-10. PMID: 21900693.

L9800 — LY-364947

NEW

5 mg
25 mg

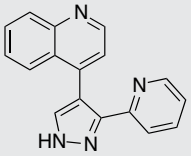

$C_{17}H_{12}N_4$ FW: 272.31 [396129-53-6] ≥98%

Activin receptor-like kinase 5 inhibitor that suppresses TGF-β activity. It improves radiosensitivity of non-small cell lung cancer cells and enhances liver regeneration, cell proliferation, and liver function.

Du S, Bouquet S, Lo CH, et al. Attenuation of the DNA damage response by transforming growth factor-beta inhibitors enhances radiation sensitivity of non-small-cell lung cancer cells in vitro and in vivo. Int J Radiat Oncol Biol Phys. 2015 Jan 1;91(1):91-9. PMID: 25835621.

Karkampouna S, Goumans MJ, Ten Dijke P, et al. Inhibition of TGFβ type I receptor activity facilitates liver regeneration upon acute CCl4 intoxication in mice. Arch Toxicol. 2015 Jan 8. [Epub ahead of print]. PMID: 25566828.

L9701 — LY-450139

NEW

5 mg
25 mg
50 mg

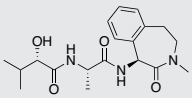

Semagacestat

$C_{19}H_{27}N_3O_4$ FW: 361.44 [425386-60-3] ≥98%

Inhibitor of γ-secretase and Notch signaling and activator of GHS-R1a receptors. It also increases glutamate levels in the prefrontal cortex.

Beggiato S, Giuliani A, Sivilia S, et al. CHF5074 and LY450139 sub-acute treatments differently affect cortical extracellular glutamate levels in pre-plaque Tg2576 mice. Neuroscience. 2014 Apr 25;266:13-22. PMID: 24530449.

Doody RS, Raman R, Farlow M, et al. A phase 3 trial of semagacestat for treatment of Alzheimer's disease. N Engl J Med. 2013 Jul 25;369(4):341-50. PMID: 23883379.

Schellekens H, McNamara O, Dinan TG, et al. Semagacestat, a γ-secretase inhibitor, activates the growth hormone secretagogue (GHS-R1a) receptor. J Pharm Pharmacol. 2013 Apr;65(4):528-38. PMID: 23488781.

L4796 — LY-294002

NEW

5 mg
25 mg
100 mg

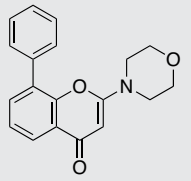

$C_{19}H_{17}NO_3$ FW: 307.34 [154447-36-6] ≥99%

PI3K inhibitor used to sensitize cancer cells to other co-administered chemotherapeutics. It inhibits LPS-induced expression of IL-10 in macrophages, prevents ruffled border formation in osteoclasts, and inhibits DNA-dependent protein kinase activity.

Avni D, Glucksam Y, Zor T. The phosphatidylinositol 3-kinase (PI3K) inhibitor LY294002 modulates cytokine expression in macrophages via p50 nuclear factor κB inhibition, in a PI3K-independent mechanism. Biochem Pharmacol. 2012 Jan 1;83(1):106-14. PMID: 22005520.

Salh B, Wagey R, Marotta A, et al. Activation of phosphatidylinositol 3-kinase, protein kinase B, and p70 S6 kinases in lipopolysaccharide-stimulated Raw 264.7 cells: differential effects of rapamycin, Ly294002, and wortmannin on nitric oxide production. J Immunol. 1998 Dec 15;161(12):6947-54. PMID: 9862729.

L9609 — Lycopene

1 mg
5 mg
10 mg

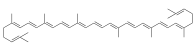

$C_{40}H_{56}$ FW: 536.88 [502-65-8] ≥90%

RAR agonist found in red and green fruits and vegetables. It inhibits hypertrophy and Akt/GSK-3β signaling, induces cell cycle arrest and apoptosis in breast cancer cells, and decreases oxidative stress in hepatic ischemia/reperfusion models.

Chao HH, Sung LC, Chen CH, et al. Lycopene Inhibits Urotensin-II-Induced Cardiomyocyte Hypertrophy in Neonatal Rat Cardiomyocytes. Evid Based Complement Alternat Med. 2014;2014:724670. PMID: 24971153.

Gloria NF, Soares N, Brand C, et al. Lycopene and beta-carotene induce cell-cycle arrest and apoptosis in human breast cancer cell lines. Anticancer Res. 2014 Mar;34(3):1377-86. PMID: 24596385.

Bayramoglu G, Bayramoglu A, Altuner Y, et al. The effects of lycopene on hepatic ischemia/reperfusion injury in rats. Cytotechnology. 2014 Mar 4. [Epub ahead of print]. PMID: 24590927.

L9610 — Lycorine Hydrochloride

NEW

10 mg
25 mg
100 mg

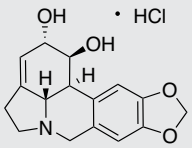

$C_{16}H_{17}NO_4 \bullet HCl$ FW: 323.77 [2188-68-3] ≥98%

Inhibitor of protein synthesis and potential inhibitor of peptidyltransferase and HDACs found in plants in the *Amaryllidaceae* family. It inhibits fungi growth, induces cell cycle arrest and apoptosis in *Trichomonas*, and suppresses proliferation of chromic myelogenous leukemia cells.

Shen JW, Ruan Y, Ren W, et al. Lycorine: a potential broad-spectrum agent against crop pathogenic fungi. J Microbiol Biotechnol. 2014 Mar 28;24(3):354-8. PMID: 24346469.

Li L, Dai HJ, Ye M, et al. Lycorine induces cell-cycle arrest in the G0/G1 phase in K562 cells via HDAC inhibition. Cancer Cell Int. 2012 Nov 23;12(1):49. PMID: 23176676.

Giordani RB, Vieira Pde B, Weizenmann M, et al. Lycorine induces cell death in the amitochondriate parasite, *Trichomonas* vaginalis, via an alternative non-apoptotic death pathway. Phytochemistry. 2011 May;72(7):645-50. PMID: 21324496.

L9874

L-(+)-Lysine Monohydrate

5 g
25 g
100 g

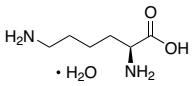

$C_6H_{14}N_2O_2 \bullet H_2O$ FW: 164.2 [39665-12-8] ≥97%

Non-endogenous essential amino acid found in meat, soy, dairy. It is required for production of collagen, acetyl-CoA, proteins, antibodies, and hormones. It may reduce stress-induced anxiety.

Sadoul K, Boyault C, Pabion M, et al. Regulation of protein turnover by acetyltransferases and deacetylases. Biochimie. 2008 Feb;90(2):306-12. PMID: 17681659.

Smriga M, Kameishi M, Uneyama H, et al. Dietary L-lysine deficiency increases stress-induced anxiety and fecal excretion in rats. J Nutr. 2002 Dec;132(12):3744-6. PMID: 12468617.

Young VR, Pellett PL. Plant proteins in relation to human protein and amino acid nutrition. Am J Clin Nutr. 1994 May;59(5 Suppl):1203S-1212S. PMID: 8172124.

L9875

Lys(Boc)-Leu-Lys(Boc)-Obzl

1 g

$C_{35}H_{59}N_5O_8$ FW: 667.9 ≥98%

Lys(Boc)-Leu-Lys(Boc)-Obzl

Proteinase substrate.

L9880

Lysipressin Acetate

Please inquire

(8-Lysine)vasopressin

C[Cys-Tyr-Phe-Gln-Asn-Cys]-Pro-Lys-Gly-NH_2

$C_{46}H_{65}N_{13}O_{12}S_2$ FW: 1056.22 [50-57-7] ≥95%

VP/V2 receptor agonist found in marsupials and pigs that is involved in vascular contraction.

László F, Karácsony G, Pávó I, et al. Aggressive role of vasopressin in development of different gastric lesions in rats. Eur J Pharmacol. 1994 Jun 2;258(1-2):15-22. PMID: 7925594.

Gorbulev V, Büchner H, Akhundova A, et al. Molecular cloning and functional characterization of V2 [8-lysine] vasopressin and oxytocin receptors from a pig kidney cell line. Eur J Biochem. 1993 Jul 1;215(1):1-7. PMID: 8393786.

M0035

M35

0.5 mg
1 mg
2.5 mg

Galanin-(1-13)-bradykinin-(2-9)-amide

H-Gly-Trp-Thr-Leu-Asn-Ser-Ala-Gly-Tyr-Leu-Leu-Gly-Pro-Pro-Pro-Gly-Phe-Ser-Pro-Phe-Arg-NH_2

$C_{107}H_{153}N_{27}O_{26}$ FW: 2233.58 [142846-71-7] ≥95%

Galanin receptor antagonist that decreases immobility time in the forced swim test, suppresses pancreatitis-induced necrosis, and attenuates insulin sensitivity.

Bu L, Liu Z, Zou J, et al. Blocking central galanin receptors attenuates insulin sensitivity in myocytes of diabetic trained rats. J Neurosci Res. 2013 Jul;91(7):971-7. PMID: 23653288.

Bhandari M, Kawamoto M, Thomas AC, et al. Galanin receptor antagonist m35 but not m40 or c7 ameliorates cerulein-induced acute pancreatitis in mice. Pancreatology. 2010;10(6):682-8. PMID: 21242707.

M0040

M40

0.5 mg
1 mg
2.5 mg

H-Gly-Trp-Thr-Leu-Asn-Ser-Ala-Gly-Tyr-Leu-Leu-Gly-Pro-Pro-Pro-Ala-Leu-Ala-Leu-Ala-NH_2

$C_{94}H_{145}N_{23}O_{24}$ FW: 1981.34 [143896-17-7] ≥95%

Galanin receptor antagonist that decreases stress-induced anxiety responses, suppresses food intake, and lowers reproductive behavior.

Silote GP, Rosal AB, de Souza MM, et al. Infusion of galanin into the mid-caudal portion of the dorsal raphe nucleus has an anxiolytic effect on rats in the elevated T-maze. Behav Brain Res. 2013 Sep 1;252:312-7. PMID: 23791934.

Echevarria DJ, Hernandez A, Diogenes A, et al. Administration of the galanin antagonist M40 into lateral septum attenuates shock probe defensive burying behavior in rats. Neuropeptides. 2005 Oct;39(5):445-51. PMID: 16084587.

M0009

Macitentan

1 mg
5 mg
25 mg

ACT-064992

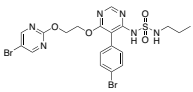

$C_{19}H_{20}Br_2N_6O_4S$ FW: 588.27 [441798-33-0] ≥99%

Endothelin receptor A/B antagonist used to treat pulmonary arterial hypertension. It decreases blood pressure and proteinuria, prevents right ventricle hypertrophy, and enhances cytotoxicity of co-administered chemotherapeutics.

Pulido T, Adzerikho I, Channick RN, et al. Macitentan and morbidity and mortality in pulmonary arterial hypertension. N Engl J Med. 2013 Aug 29;369(9):809-18. PMID: 23984728.

Corallo C, Pecetti G, Iglarz M, et al. Macitentan slows down the dermal fibrotic process in systemic sclerosis: in vitro findings. J Biol Regul Homeost Agents. 2013 Apr-Jun;27(2):455-62. PMID: 23830395.

Gatfield J, Mueller Grandjean C, Sasse T, et al. Slow receptor dissociation kinetics differentiate macitentan from other endothelin receptor antagonists in pulmonary arterial smooth muscle cells. PLoS One. 2012;7(10):e47662. PMID: 23077657.

M0114

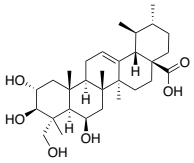

Madecassic Acid

Brahmic acid

$C_{30}H_{48}O_6$ FW: 504.7 [18449-41-7] ≥95%

500 mg
1 g
5 g

Found in *Centella*. It downregulates LPS-stimulated expression of pro-inflammatory cytokines and induces apoptosis in colon cancer models.

Zhang H, Zhang M, Tao Y, et al. Madecassic acid inhibits the mouse colon cancer growth by inducing apoptosis and immunomodulation. J BUON. 2014 Apr-Jun;19(2):372-6. PMID: 24965394.

Won JH, Shin JS, Park HJ, et al. Anti-inflammatory effects of madecassic acid via the suppression of NF-kappaB pathway in LPS-induced RAW 264.7 macrophage cells. Planta Med. 2010 Feb;76(3):251-7. PMID: 19774506.

M0113

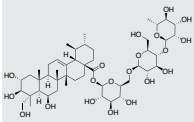

Madecassoside

NEW

$C_{48}H_{78}O_{20}$ FW: 975.12 [34540-22-2] ≥90%

25 mg
100 mg
250 mg
1 g

Found in *Centella*. It downregulates expression of pro-inflammatory cytokines and oxidative enzymes in cerebral ischemia/reperfusion models, protects neurons against amyloid-β-induced inflammation and autophagy, suppresses myocyte apoptosis, and prevents the development of pulmonary fibrosis.

Luo Y, Yang YP, Liu J, et al. Neuroprotective effects of madecassoside against focal cerebral ischemia reperfusion injury in rats. Brain Res. 2014 May 27;1565:37-47. PMID: 24735651.

Du B, Zhang Z, Li N. Madecassoside prevents Aβ(25-35)-induced inflammatory responses and autophagy in neuronal cells through the class III PI3K/Beclin-1/Bcl-2 pathway. Int Immunopharmacol. 2014 May;20(1):221-8. PMID: 24631516.

Lu GX, Bian DF, Ji Y, et al. Madecassoside Ameliorates Bleomycin-Induced Pulmonary Fibrosis in Mice by Downregulating Collagen Deposition. Phytother Res. 2014 Jan 23. [Epub ahead of print]. PMID: 24458872.

M0124

H-Gly-Ile-Gly-Lys-Phe-Leu-His-Ser-Ala-Gly-Lys-Phe-Gly-Lys-Ala-Phe-Val-Gly-Glu-Ile-Met-Lys-Ser-OH

Magainin 1

$C_{112}H_{177}N_{29}O_{28}S$ FW: 2409.9 [108433-99-4] ≥95%

0.5 mg
1 mg
2.5 mg

Found in frogs. It induces pore formation in cell membranes and inhibits growth of gram positive bacteria. It also induces apoptosis in leukemia cells.

Humblot V, Yala JF, Thebault P, et al. The antibacterial activity of Magainin I immobilized onto mixed thiols Self-Assembled Monolayers. Biomaterials. 2009 Jul;30(21):3503-12. PMID: 19345992.

Cruz-Chamorro L, Puertollano MA, Puertollano E, et al. In vitro biological activities of magainin alone or in combination with nisin. Peptides. 2006 Jun;27(6):1201-9. PMID: 16356589.

M0126

H-Gly-Ile-Gly-Lys-Phe-Leu-His-Ser-Ala-Lys-Lys-Phe-Gly-Lys-Ala-Phe-Val-Gly-Glu-Ile-Met-Asn-Ser-OH

Magainin 2

Z-12 Peptide; Mag-2

$C_{114}H_{180}N_{30}O_{29}S$ FW: 2466.95 [108433-95-0] ≥95%

0.5 mg
1 mg
2.5 mg

Found in frogs. It induces pore formation in cell membranes, inducing membrane leakage and inhibiting bacterial growth.

Last NB, Miranker AD. Common mechanism unites membrane poration by amyloid and antimicrobial peptides. Proc Natl Acad Sci U S A. 2013 Apr 16;110(16):6382-7. PMID: 23576726.

Miyazaki Y, Aoki M, Yano Y, et al. Interaction of antimicrobial peptide magainin 2 with gangliosides as a target for human cell binding. Biochemistry. 2012 Dec 21;51(51):10229-35. PMID: 23194027.

M0115

Magic Red™ Caspases 3 & 7 Assay Kit

25 Tests
100 Tests

Caspase 3 and 7 activity measuring kit.

M0116

Magic Red™ Cathepsin B Assay Kit

25 Tests
100 Tests

Cathepsin B activity measuring kit.

M0117

Magic Red™ Cathepsin K Assay Kit

25 Tests
100 Tests

Cathepsin K activity measuring kit.

M0118

Magic RedTM Cathepsin L Assay Kit

25 Tests
100 Tests

Cathepsin L activity measuring kit.

M0125

Magnolol

10 mg
25 mg
100 mg

Dehydrodichavicol

$C_{18}H_{18}O_2$ FW: 266.34 [528-43-8] ≥98%

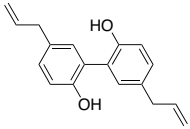

GABA-A receptor potentiator found in *Magnolia*. It inhibits scopolamine-induced oxidative dysfunction and learning and memory deficits, increases growth, collagen synthesis, and mineralization in osteoblasts, downregulates LPS-stimulated expression of pro-inflammatory cytokines, and decreases serum levels of glucose and lipids.

Wang JJ, Zhao R, Liang JC, et al. The antidiabetic and hepatoprotective effects of magnolol on diabetic rats induced by high-fat diet and streptozotocin. Yao Xue Xue Bao. 2014 Apr;49(4):476-81. PMID: 24974464.

Liu Y, Cao W, Zhang B, et al. The natural compound magnolol inhibits invasion and exhibits potential in human breast cancer therapy. Sci Rep. 2013 Nov 14;3:3098. PMID: 24226295.

Kim KM, Kim NS, Kim J, et al. Magnolol suppresses vascular endothelial growth factor-induced angiogenesis by inhibiting Ras-dependent mitogen-activated protein kinase and phosphatidylinositol 3-kinase/Akt signaling pathways. Nutr Cancer. 2013;65(8):1245-53. PMID: 24066970.

M0144

Malantide

1 mg
2 mg
5 mg

H-Arg-Thr-Lys-Arg-Ser-Gly-Ser-Val-Tyr-Glu-Pro-Leu-Lys-Ile-OH

$C_{72}H_{124}N_{22}O_{21}$ FW: 1633.93 [86555-35-3] ≥95%

Substrate used to measure PKA activity.

de Boer AR, Letzel T, Lingeman H, et al. Systematic development of an enzymatic phosphorylation assay compatible with mass spectrometric detection. Anal Bioanal Chem. 2005 Feb;381(3):647-55. PMID: 15703914.

Murray KJ, England PJ, Lynham JA, et al. Use of a synthetic dodecapeptide (malantide) to measure the cyclic AMP-dependent protein kinase activity ratio in a variety of tissues. Biochem J. 1990 May 1;267(3):703-8. PMID: 2160235.

M0248

Manidipine Dihydrochloride

25 mg
100 mg
250 mg

$C_{35}H_{38}N_4O_6 \cdot 2HCl$ FW: 683.62 [89226-75-5] ≥98%

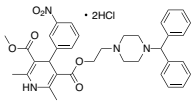

L-type and T-type Ca^{2+} channel blocker that decreases systemic blood pressure, glomerular capillary pressure, and renal vascular resistance. It also inhibits production of IL-6 and IL-8 in macrophages.

Costa S, Zimetti F, Pedrelli M, et al. Manidipine reduces pro-inflammatory cytokines secretion in human endothelial cells and macrophages. Pharmacol Res. 2010 Sep;62(3):265-70. PMID: 20347984.

Hayashi K, Ozawa Y, Fujiwara K, et al. Role of actions of calcium antagonists on efferent arterioles--with special references to glomerular hypertension. Am J Nephrol. 2003 Jul-Aug;23(4):229-44. PMID: 12840599.

Onuki T. Effects of a calcium channel blocker, manidipine hydrochloride, on the regulatory mechanism of glomerular capillary pressure in SHR. Nihon Jinzo Gakkai Shi. 1995 Feb;37(2):119-26. PMID: 7752503.

M0255

Manzamine A

1 mg
5 mg
10 mg

$C_{36}H_{44}N_4O$ FW: 548.76 [104196-68-1] ≥98%

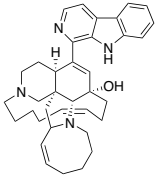

Vacuolar ATPase uncoupler and GSK-3 inhibitor found in marine sponges. It inhibits autophagy and tumor growth in cancer models, suppresses foam cell formation in macrophages, prevents growth of gram positive and gram negative bacteria, and decreases tau hyperphosphorylation.

Kallifatidis G, Hoepfner D, Jaeg T, et al. The marine natural product manzamine A targets vacuolar ATPases and inhibits autophagy in pancreatic cancer cells. Mar Drugs. 2013 Sep 17;11(9):3500-16. PMID: 24048269.

Eguchi K, Fujiwara Y, Hayashida A, et al. Manzamine A, a marine-derived alkaloid, inhibits accumulation of cholesterol ester in macrophages and suppresses hyperlipidemia and atherosclerosis in vivo. Bioorg Med Chem. 2013 Jul 1;21(13):3831-8. PMID: 23665143.

Aqil F, Zahin M, El Sayed KA, et al. Antimicrobial, antioxidant, and antimutagenic activities of selected marine natural products and tobacco cembranoids. Drug Chem Toxicol. 2011 Apr;34(2):167-79. PMID: 21314466.

M0262

Maprotiline Hydrochloride

1 g
5 g

$C_{20}H_{23}N \cdot HCl$ FW: 313.87 [10347-81-6] ≥98%

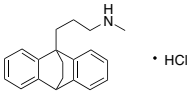

Inhibitor of histamine H1 receptors, 5-HT2 receptors, mAChRs, α1-adrenergic receptors, L-type Ca^{2+} channels, and NET used to treat depression. It also acts as a FIASMA and induces apoptosis in neuroblastoma cells.

Jan CR, Su JA, Teng CC, et al. Mechanism of maprotiline-induced apoptosis: role of [Ca^{2+}](i), ERK, JNK and caspase-3 signaling pathways. Toxicology. 2013 Feb 8;304:1-12. PMID: 23219590.

Zahradník I, Minarovic I, Zahradníková A. Inhibition of the cardiac L-type calcium channel current by antidepressant drugs. J Pharmacol Exp Ther. 2008 Mar;324(3):977-84. PMID: 18048694.

Mayers AG, Baldwin DS. Antidepressants and their effect on sleep. Hum Psychopharmacol. 2005 Dec;20(8):533-59. PMID: 16229049.

M0368 Marbofloxacin

250 mg
1 g

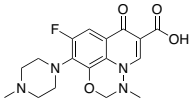

$C_{17}H_{19}FN_4O_4$ FW: 362.36 [115550-35-1] ≥98%

Bacterial DNA gyrase inhibitor. It suppresses growth of *Staphylococcus*, *Escherichia*, *Actinobacillus*, *Pasturella*, and *Mannheima*.

Damte D, Lee SJ, Yohannes SB, et al. Comparative activities of selected fluoroquinolones against dynamic populations of *Actinobacillus* pleuropneumoniae in an in vitro model of time-kill continuous culture experiment. Int J Antimicrob Agents. 2013 Dec;42(6):544-52. PMID: 24139884.

Illambas J, Potter T, Cheng Z, et al. Pharmacodynamics of marbofloxacin for calf pneumonia pathogens. Res Vet Sci. 2013 Jun;94(3):675-81. PMID: 23375665.

Awji EG, Tassew DD, Lee JS, et al. Comparative mutant prevention concentration and mechanism of resistance to veterinary fluoroquinolones in *Staphylococcus* pseudintermedius. Vet Dermatol. 2012 Aug;23(4):376-80, e68-9. PMID: 22409306.

M0374 Masitinib

5 mg
25 mg

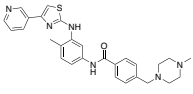

$C_{28}H_{30}N_6OS$ FW: 498.64 [790299-79-5] ≥98%

PDGFR and c-Kit inhibitor used to treat mast cell tumors. It induces apoptosis in cancer cells, decreases airway inflammation in allergic asthma models, and slows cognitive decline in Alzheimer's disease models.

Smrkovski OA, Essick L, Rohrbach BW, et al. Masitinib mesylate for metastatic and non-resectable canine cutaneous mast cell tumours. Vet Comp Oncol. 2013 Jul 12. [Epub ahead of print]. PMID: 23845124.

Fahey CE, Milner RJ, Kow K, et al. Apoptotic effects of the tyrosine kinase inhibitor, masitinib mesylate, on canine osteosarcoma cells. Anticancer Drugs. 2013 Jun;24(5):519-26. PMID: 23466652.

M0172 Mastoparan

1 mg

Ile-Asn-Leu-Lys-Ala-Leu-Ala-Ala-Leu-Ala-Lys-Lys-Ile-Leu-NH_2

$C_{70}H_{131}N_{19}O_{15}$ FW: 1478.92 [72093-21-1] ≥95%

Mast cell degranulation stimulator and GTPase potentiator found in *Vespula lewisii*. It increases Ca^{2+} influx, increases cell permeability, and inhibits production of TGF-β.

Brophy TM, Coller BS, Ahamed J. Identification of the thiol isomerase-binding peptide, mastoparan, as a novel inhibitor of shear-induced transforming growth factor β1 (TGF-β1) activation. J Biol Chem. 2013 Apr 12;288(15):10628-39. PMID: 23463512.

M0272 Mastoparan 7

1 mg
2 mg
5 mg

Mas7

H-Ile-Asn-Leu-Lys-Ala-Leu-Ala-Ala-Leu-Ala-Lys-Ala-Leu-Leu-NH_2

$C_{67}H_{124}N_{18}O_{15}$ FW: 1421.85 [145854-59-7] ≥95%

$G_{i/o}$ GPCR agonist and PLA2 activator found in bee and wasp venom. It restores neurotransmitter release from spinal cord cells treated with botulinum toxin serotype A.

Zhang P, Ray R, Singh BR, et al. Mastoparan-7 rescues botulinum toxin-A poisoned neurons in a mouse spinal cord cell culture model. Toxicon. 2013 Dec 15;76:37-43. PMID: 24047963.

Sprague RS, Bowles EA, Achilleus D, et al. A selective phosphodiesterase 3 inhibitor rescues low PO2-induced ATP release from erythrocytes of humans with type 2 diabetes: implication for vascular control. Am J Physiol Heart Circ Physiol. 2011 Dec;301(6):H2466-72. Erratum in: Am J Physiol Heart Circ Physiol. 2012 Jan;302(1):H378. PMID: 21963837.

M0273 Mastoparan 8

0.5 mg
1 mg
2.5 mg

Mas8

H-Ile-Asn-Leu-Lys-Ala-Leu-Ala-Ala-Leu-Ala-Lys-Arg-Leu-Leu-NH_2

$C_{70}H_{131}N_{21}O_{15}$ FW: 1506.96 ≥95%

$G_{i/o}$ GPCR agonist found in bee and wasp venom. It induces mast cell degranulation and insulin secretion.

dos Santos LD, Aparecido dos Santos Pinto JR, Menegasso AR, et al. Proteomic profiling of the molecular targets of interactions of the mastoparan peptide Protopolybia MP-III at the level of endosomal membranes from rat mast cells. Proteomics. 2012 Aug;12(17):2682-93. PMID: 22761183.

Cabrera MP, Alvares DS, Leite NB, et al. New insight into the mechanism of action of wasp mastoparan peptides: lytic activity and clustering observed with giant vesicles. Langmuir. 2011 Sep 6;27(17):10805-13. PMID: 21797216.

M0275 Mastoparan 17

1 mg
2 mg
5 mg

Mas17

H-Ile-Asn-Leu-Lys-Ala-Lys-Ala-Ala-Leu-Ala-Lys-Lys-Leu-Leu-NH_2

$C_{70}H_{132}N_{20}O_{15}$ FW: 1493.96 [145854-61-1] ≥95%

Inactive mastoparan analog used to measure mastoparan activity.

Amin RH, Chen HQ, Veluthakal R, et al. Mastoparan-induced insulin secretion from insulin-secreting betaTC3 and INS-1 cells: evidence for its regulation by Rho subfamily of G proteins. Endocrinology. 2003 Oct;144(10):4508-18. PMID: 12960065.

M0173 Mastoparan X

1 mg
2 mg
5 mg

H-Ile-Asn-Trp-Lys-Gly-Ile-Ala-Ala-Met-Ala-Lys-Lys-Leu-Leu-NH_2

$C_{73}H_{126}N_{20}O_{15}S$ FW: 1556.01 [72093-22-2] ≥95%

G_α GPCR agonist found in bee and wasp venom. It activates mast cells and also induces formation and leakage of giant unilamellar vesicles, causing barrier disruptions.

dos Santos LD, Aparecido dos Santos Pinto JR, Menegasso AR, et al. Proteomic profiling of the molecular targets of interactions of the mastoparan peptide Protopolybia MP-III at the level of endosomal membranes from rat mast cells. Proteomics. 2012 Aug;12(17):2682-93. PMID: 22761183.

Cabrera MP, Alvares DS, Leite NB, et al. New insight into the mechanism of action of wasp mastoparan peptides: lytic activity and clustering observed with giant vesicles. Langmuir. 2011 Sep 6;27(17):10805-13. PMID: 21797216.

M0278 Matrine

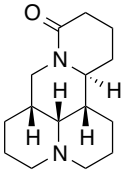

100 mg
500 mg
1 g

Sophocarpidine

$C_{15}H_{24}N_2O$ FW: 248.37 [519-02-8] ≥98%

Found in Sophora. It displays many biological activities, including inducing apoptosis in hepatoma cells and non-small cell lung cancer cells, decreasing pain responses in a opioid-dependent manner, regulating glutamate signaling, and decreasing seizures.

Kan QC, Zhang S, Xu YM, et al. Matrine regulates glutamate-related excitotoxic factors in experimental autoimmune encephalomyelitis. Neurosci Lett. 2014 Feb 7;560:92-7. PMID: 24368216.

Xiang J, Jiang Y. Antiepileptic potential of matrine via regulation the levels of gamma-aminobutyric acid and glutamic acid in the brain. Int J Mol Sci. 2013 Dec 5;14(12):23751-61. PMID: 24317434.

Ma X, Chen R, Liu X, et al. Effects of matrine on JAK-STAT signaling transduction pathways in bleomycin-induced pulmonary fibrosis. Afr J Tradit Complement Altern Med. 2013 Apr 12;10(3):442-8. PMID: 24146473.

M2460 Matrix GLa Protein - pNa

1 mg
10 mg

MGP-pNa

Met-Gly-Pro-pNA

$C_{18}H_{25}N_5O_5S$ FW: 423.4 ≥95%

Vascular calcification inhibitor. It may be used as a biomarker for renal failure, diabetes, and cardiovascular events.

McCarty MF, DiNicolantonio JJ. The molecular biology and pathophysiology of vascular calcification. Postgrad Med. 2014 Mar;126(2):54-64. PMID: 24685968.

Schurgers LJ, Uitto J, Reutelingsperger CP. Vitamin K-dependent carboxylation of matrix Gla-protein: a crucial switch to control ectopic mineralization. Trends Mol Med. 2013 Apr;19(4):217-26. PMID: 23375872.

M1335 Mdivi-1

NEW

5 mg
25 mg

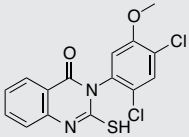

$C_{15}H_{10}Cl_2N_2O_2S$ FW: 353.2 [338967-87-6] ≥98%

Inhibitor of mitochondrial division that prevents mitochondrial fission. It decreases neuronal apoptosis, prevents oxidative damage in myocardial infarction models, and inhibits hypoxia-induced migration in breast cancer cells.

Li G, Jia Z, Cao Y, et al. Mitochondrial Division Inhibitor 1 Ameliorates Mitochondrial Injury, Apoptosis, and Motor Dysfunction After Acute Spinal Cord Injury in Rats. Neurochem Res. 2015 May 13. [Epub ahead of print]. PMID: 25968480.

Liu JM, Yi Z, Liu SZ, et al. The mitochondrial division inhibitor mdivi-1 attenuates spinal cord ischemia-reperfusion injury both in vitro and in vivo: Involvement of BK channels. Brain Res. 2015 Mar 24. [Epub ahead of print]. PMID: 25818100.

Sharp WW, Beiser DG, Fang YH, et al. Inhibition of the mitochondrial fission protein dynamin-related protein 1 improves survival in a murine cardiac arrest model. Crit Care Med. 2015 Feb;43(2):e38-47. PMID: 25599491.

M1444 MDL 29951

NEW

1 mg
5 mg
10 mg

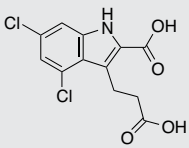

$C_{12}H_9Cl_2NO_4$ FW: 302.11 [130798-51-5] ≥98%

GRP17 agonist and inhibitor of NMDA receptors and fructose 1,6-bisphosphatase. It inhibits formalin-induced pain behavior, suppresses maturation of primary oligodendrocytes, and increases thresholds for the development of chemically-induced seizures.

Hennen S, Wang H, Peters L, et al. Decoding signaling and function of the orphan G protein-coupled receptor GPR17 with a small-molecule agonist. Sci Signal. 2013 Oct 22;6(298):ra93. PMID: 24150254.

Wright SW, Carlo AA, Danley DE, et al. 3-(2-carboxyethyl)-4,6-dichloro-1H-indole-2-carboxylic acid: an allosteric inhibitor of fructose-1,6-bisphosphatase at the AMP site. Bioorg Med Chem Lett. 2003 Jun 16;13(12):2055-8. PMID: 12781194.

Millan MJ, Seguin L. Chemically-diverse ligands at the glycine B site coupled to N-methyl-D-aspartate (NMDA) receptors selectively block the late phase of formalin-induced pain in mice. Neurosci Lett. 1994 Aug 29;178(1):139-43. PMID: 7816323.

M1605 Mebendazole

5 g
25 g

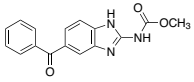

$C_{16}H_{13}N_3O_3$ FW: 295.29 [31431-39-7] ≥98%

Microtubule polymerization inhibitor used to treat worm infections. It also induces apoptosis in melanoma cells and decreases Bcl-2 and XIAP levels in vivo.

Doudican NA, Byron SA, Pollock PM, et al. XIAP downregulation accompanies mebendazole growth inhibition in melanoma xenografts. Anticancer Drugs. 2013 Feb;24(2):181-8. PMID: 23059386.

Doudican N, Rodriguez A, Osman I, et al. Mebendazole induces apoptosis via Bcl-2 inactivation in chemoresistant melanoma cells. Mol Cancer Res. 2008 Aug;6(8):1308-15. PMID: 18667591.

M1708 Mecamylamine Hydrochloride

5 mg
25 mg
100 mg

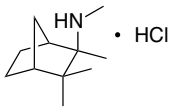

$C_{11}H_{21}N \bullet HCl$ FW: 203.75 [826-39-1] ≥98%

nAChR antagonist previously used to treat hypertension. It displays a wide variety of activities, including reducing depression-like behaviors in subjects with Tourette's syndrome and improving rates of smoking cessation.

Peng C, Kimbrell MR, Tian C, et al. Multiple modes of α7 nAChR noncompetitive antagonism of control agonist-evoked and allosterically enhanced currents. Mol Pharmacol. 2013 Sep;84(3):459-75. PMID: 23839567.

Sanberg PR, Vindrola-Padros C, Shytle RD. Translating laboratory discovery to the clinic: from nicotine and mecamylamine to Tourette's, depression, and beyond. Physiol Behav. 2012 Dec 5;107(5):801-8. PMID: 22776623.

LeSage MG, Shelley D, Pravetoni M, et al. Enhanced attenuation of nicotine discrimination in rats by combining nicotine-specific antibodies with a nicotinic receptor antagonist. Pharmacol Biochem Behav. 2012 Jul;102(1):157-62. PMID: 22503967.

M1613 Medroxyprogesterone 17-Acetate

500 mg
1 g
5 g

MAP

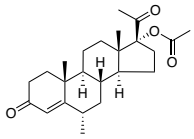

$C_{24}H_{34}O_4$ FW: 386.52 [71-58-9] ≥98%

Synthetic progesterone receptor, androgen receptor, and glucocorticoid receptor agonist agonist and 3α-HSD inhibitor used in HRT and to treat dysmenhorrea and breast cancer. It decreases levels of adrenocorticotropic hormone, cortisol, and other hormones.

Schindler AE, Campagnoli C, Druckmann R, et al. Classification and pharmacology of progestins. Maturitas. 2008 Sep-Oct;61(1-2):171-80. PMID: 19434889.

Meyer L, Venard C, Schaeffer V, et al. The biological activity of 3alpha-hydroxysteroid oxido-reductase in the spinal cord regulates thermal and mechanical pain thresholds after sciatic nerve injury. Neurobiol Dis. 2008 Apr;30(1):30-41. PMID: 18291663.

M1622 Mefenamic Acid

10 g
50 g
100 g

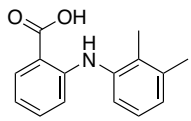

$C_{15}H_{15}NO_2$ FW: 241.29 [61-68-7] ≥98%

NSAID, GABA-A receptor potentiator, and COX-1/2 inhibitor used to treat pain. It inhibits proliferation in colon cancer cells and decreases infarct volume, edema, and ischemic brain damage.

Khansari PS, Halliwell RF. Evidence for neuroprotection by the fenamate NSAID, mefenamic acid. Neurochem Int. 2009 Dec;55(7):683-8. PMID: 19563851.

Weiss H, Amberger A, Widschwendter M, et al. Inhibition of store-operated calcium entry contributes to the anti-proliferative effect of non-steroidal anti-inflammatory drugs in human colon cancer cells. Int J Cancer. 2001 Jun 15;92(6):877-82. PMID: 11351310.

Halliwell RF, Thomas P, Patten D, et al. Subunit-selective modulation of GABAA receptors by the non-steroidal anti-inflammatory agent, mefenamic acid. Eur J Neurosci. 1999 Aug;11(8):2897-905. PMID: 10457186.

M1626 Megestrol Acetate

250 mg
1 g
5 g

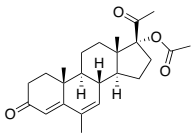

$C_{24}H_{32}O_4$ FW: 384.51 [595-33-5] ≥98%

Synthetic progestogen used to stimulate appetite and increase weight gain in cachexia-anorexia. It also induces cell cycle arrest and apoptosis in hepatocellular carcinoma cells.

Yeh SS, Lovitt S, Schuster MW. Usage of megestrol acetate in the treatment of anorexia-cachexia syndrome in the elderly. J Nutr Health Aging. 2009 May;13(5):448-54. PMID: 19390752.

Femia RA, Goyette RE. The science of megestrol acetate delivery: potential to improve outcomes in cachexia. BioDrugs. 2005;19(3):179-87. PMID: 15984902.

Zhang K, Chow PK. The effect of megestrol acetate on growth of HepG2 cells in vitro and in vivo. Clin Cancer Res. 2004 Aug 1;10(15):5226-32. PMID: 15297426.

M1826

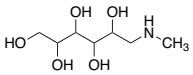

Meglumine — 100 g, 500 g, 1 kg

N-Methylglucamine

$C_7H_{17}NO_5$ FW: 195.21 [6284-40-8] ≥98%

Amino sugar and sorbitol derivative used as a bulking agent in the formulation of pharmaceutical drugs.

Borborema SE, Schwendener RA, Osso JA Jr, et al. Uptake and antileishmanial activity of meglumine antimoniate-containing liposomes in *Leishmania* (*Leishmania*) major-infected macrophages. Int J Antimicrob Agents. 2011 Oct;38(4):341-7. PMID: 21783345.

Rossetti RC, Perdigão A, Mesquita FS, et al. Effects of flunixin meglumine, recombinant bovine somatotropin and/or human chorionic gonadotropin on pregnancy rates in Nelore cows. Theriogenology. 2011 Sep 1;76(4):751-8. PMID: 21719091.

M1646

Asp-Phe-Asp-Met-Leu-Arg-Cys-Met-Leu-Gly-Arg-Val-Tyr-Arg-Pro-Cys-Trp-Gln-Val (Cys7-Cys16)

Melanin Concentrating Hormone, human/mouse/rat — 0.5 mg, 1 mg, 2.5 mg

MCH

$C_{105}H_{160}N_{30}O_{26}S_4$ FW: 2386.8 ≥98%

Endogenous MCH receptor agonist involved in energy homeostasis, circadian rhythms, and feeding behavior. It increases feeding behavior and modulates inflammation.

Palomba M, Seke Etet PF, Veronesi C. Effect of inflammatory challenge on hypothalamic neurons expressing orexinergic and melanin-concentrating hormone. Neurosci Lett. 2014 Jun 6;570:47-52. PMID: 24708924.

Ziogas DC, Karagiannis AK, Geiger BM, et al. Inflammation-induced functional connectivity of melanin-concentrating hormone and IL-10. Peptides. 2014 May;55:58-64. PMID: 24556508.

M1647

Asp-Thr-Met-Arg-Cys-Met-Val-Gly-Arg-Val-Tyr-Arg-Pro-Cys-Trp-Glu-Val (Cys5-Cys14)

Melanin Concentrating Hormone, salmon — 0.5 mg, 1 mg, 2.5 mg

MCH

$C_{89}H_{137}N_{27}O_{24}S_4$ FW: 2097.9 ≥98%

Endogenous MCH receptor agonist involved in energy homeostasis, circadian rhythms, and feeding behavior. It increases feeding behavior and modulates inflammation.

Palomba M, Seke Etet PF, Veronesi C. Effect of inflammatory challenge on hypothalamic neurons expressing orexinergic and melanin-concentrating hormone. Neurosci Lett. 2014 Jun 6;570:47-52. PMID: 24708924.

M7528

Ac-Ser-Tyr-Ser-Met-Glu-His-Phe-Arg-Trp-Gly-Lys-Pro-Val-NH_2

α-Melanocyte Stimulating Hormone — 1 mg

α-Melanotropin; α-MSH

$C_{77}H_{109}N_{21}O_{19}S$ FW: 1664.9 [581-05-5] ≥98%

Endogenous melanocortin receptor agonist derived from POMC and involved in energy homeostasis and melanin production. It also decreases the intensity of acetaminophen-induced liver lesions, prevents loss of GABAergic neurons, decreases anxiety levels, and improves spatial memory.

Ma K, McLaurin J. α-Melanocyte Stimulating Hormone Prevents GABAergic Neuronal Loss and Improves Cognitive Function in Alzheimer's Disease. J Neurosci. 2014 May 14;34(20):6736-45. PMID: 24828629.

Zhang L, Dong L, Liu X, et al. α-Melanocyte-stimulating hormone protects retinal vascular endothelial cells from oxidative stress and apoptosis in a rat model of diabetes. PLoS One. 2014 Apr 2;9(4):e93433. PMID: 24695675.

M7529

Ala-Glu-Lys-Lys-Asp-Glu-Gly-Pro-Tyr-Arg-Met-Glu-His-Phe-Arg-Trp-Gly-Ser-Pro-Pro-Lys-Asp

β-Melanocyte Stimulating Hormone, human — 1 mg

β-MSH

$C_{118}H_{174}N_{34}O_{35}S$ FW: 2660.9 [17908-57-5] ≥98%

Endogenous melanocortin 4 receptor agonist derived from POMC and involved in energy homeostasis and melanin production. It also decreases the intensity of acetaminophen-induced liver lesions and decreases food intake.

Blagaić V, Houra K, Turčić P, et al. The influence of alpha-, beta-, and gamma-melanocyte stimulating hormone on acetaminophen induced liver lesions in male CBA mice. Molecules. 2010 Mar 3;15(3):1232-41. PMID: 20335976.

M7530

Ac-Ser-Tyr-Ser-Nle-Glu-His-DPhe-Arg-Trp-Gly-Lys-Pro-Val-NH_2

[Nle4, D-Phe7]-α-Melanocyte Stimulating Hormone — 5 mg, 25 mg

NDP-MSH; Melanotan I; Afamelanotide

$C_{78}H_{111}N_{21}O_{19}$ FW: 1646.9 ≥98%

Melanocortin analog and melanocortin receptor agonist. It increases levels of IL-6, decreases neutrophil trafficking, and inhibits vascular leakage and leukocyte rolling and adhesion.

Lonati C, Carlin A, Leonardi P, et al. Modulatory effects of NDP-MSH in the regenerating liver after partial hepatectomy in rats. Peptides. 2013 Dec;50:145-52. PMID: 24446557.

Figueiredo J, Ferreira AE, Silva RL, et al. NDP-MSH inhibits neutrophil migration through nicotinic and adrenergic receptors in experimental peritonitis. Naunyn Schmiedebergs Arch Pharmacol. 2013 Apr;386(4):311-8. PMID: 23338711.

M7531

Tyr-Val-Met-Gly-His-Phe-Arg-Trp-Asp-Arg-Phe-NH_2

γ-1 Melanocyte Stimulating Hormone

γ-1 MSH

$C_{72}H_{97}N_{21}O_{14}S$ FW: 1512.8 ≥98%

1 mg

Endogenous melanocortin 3 receptor agonist derived from POMC and involved in energy homeostasis and melanin production. It also increases release of extracellular dopamine in the ventral tegmental area.

Jansone B, Bergstrom L, Svirskis S, et al. Opposite effects of gamma(1)- and gamma(2)-melanocyte stimulating hormone on regulation of the dopaminergic mesolimbic system in rats. Neurosci Lett. 2004 May 6;361(1-3):68-71. PMID: 15135895.

M7532

Tyr-Val-Met-Gly-His-Phe-Arg-Trp-Asp-Arg-Phe-Gly-Arg-Arg-Asn-Gly-Ser-Ser-Ser-Ser-Gly-Val-Gly-Gly-Ala-Ala-Gln

γ-3 Melanocyte Stimulating Hormone

γ-3 MSH

$C_{126}H_{188}N_{44}O_{37}S$ FW: 2943.2 ≥98%

1 mg

Endogenous melanocortin 3 receptor agonist derived from POMC and involved in energy homeostasis and melanin production. It also modulates ACTH-induced steroidogenesis.

Slominski A, Costantino R, Wortsman J, et al. Melanotropic activity of gamma MSH peptides in melanoma cells. Life Sci. 1992;50(15):1103-8. PMID: 1556905.

M0224

Phe-Leu-Trp-Gly-Pro-Arg-Ala-Leu-Val

Melanoma Antigen Gene-encoding Fragment 3 (271-279), human

MAGE-3

$C_{53}H_{79}N_{13}O_{10}$ FW: 1058.3 [160295-81-8] ≥95%

1 mg
2 mg
5 mg

Peptide antigen initially produced by hepatocellular carcinoma cells. It may be targeted by epitope-specific CD8+ T cells.

Zhou M, Peng JR, Zhang HG, et al. Identification of two naturally presented MAGE antigenic peptides from a patient with hepatocellular carcinoma by mass spectrometry. Immunol Lett. 2005 Jun 15;99(1):113-21. PMID: 15885805.

Zerbini A, Pilli M, Soliani P, et al. Ex vivo characterization of tumor-derived melanoma antigen encoding gene-specific CD8+cells in patients with hepatocellular carcinoma. J Hepatol. 2004 Jan;40(1):102-9. PMID: 14672620.

M1649

Ala-Ala-Gly-Ile-Gly-Ile-Leu-Thr-Val

Melanoma-associated Antigen Peptide 1 (27-35), human

MART-1 (27-35)

$C_{37}H_{67}N_9O_{11}$ FW: 814 ≥95%

1 mg
2 mg
5 mg

Melanoma-associated antigen used in vaccine development to induce an immune response against cancerous cells expressing melanoma antigens.

Chodon T, Comin-Anduix B, Chmielowski B, et al. Adoptive Transfer of MART-1 T-Cell Receptor Transgenic Lymphocytes and Dendritic Cell Vaccination in Patients with Metastatic Melanoma. Clin Cancer Res. 2014 May 1;20(9):2457-65. PMID: 24634374.

Romano E, Michielin O, Voelter V, et al. MART-1 peptide vaccination plus IMP321 (LAG-3Ig fusion protein) in patients receiving autologous PBMCs after lymphodepletion: results of a Phase I trial. J Transl Med. 2014 Apr 12;12:97. PMID: 24726012.

M1648

H-Tyr-Pro-Ser-Lys-Pro-Asp-Asn-Pro-Gly-Glu-Asp-Ala-Pro-Ala-Glu-Asp-Met-Ala-Lys-Tyr-Tyr-Ser-Ala-Leu-Arg-His-Tyr-Ile-Asn-Leu-Ile-Thr-Arg-Gln-Arg-Tyr-NH_2

Melanostatin, frog

MIF-1

$C_{189}H_{285}N_{53}O_{57}S_1$ FW: 4243.76 ≥95%

0.5 mg
1 mg
2.5 mg

Dopamine D2 receptor modulator. It potentiates antidepressant activity of amitriptyline and desipramine.

Pan W, Kastin AJ. From MIF-1 to endomorphin: the Tyr-MIF-1 family of peptides. Peptides. 2007 Dec;28(12):2411-34. PMID: 17988762.

Mishra RK, Makman MH, Costain WJ, et al. Modulation of agonist stimulated adenylyl cyclase and GTPase activity by L-pro-L-leu-glycinamide and its peptidomimetic analogue in rat striatal membranes. Neurosci Lett. 1999 Jul 2;269(1):21-4. PMID: 10821635.

M1650

Ac-Nle-Asp-His-D-Phe-Arg-Trp-Lys-NH_2
(Lactam bridge Asp2-Lys7)

Melanotan II

MT-II

$C_{50}H_{69}N_{15}O_9$ FW: 1024.2 [121062-08-6] ≥98%

5 mg
10 mg
25 mg

Synthetic melanocortin analog and melanocortin receptor agonist used to promote skin pigmentation. It also induces arousal and increases body temperatures, decreases pro-inflammatory cytokine levels, and increases aortic vasorelaxation.

Monge-Roffarello B, Labbé SM, Lenglos C, et al. The medial preoptic nucleus as a site of the thermogenic and metabolic actions of Melanotan II in male rats. Am J Physiol Regul Integr Comp Physiol. 2014 May 7. [Epub ahead of print]. PMID: 24808495.

Rinne P, Silvola JM, Hellberg S, et al. Pharmacological Activation of the Melanocortin System Limits Plaque Inflammation and Ameliorates Vascular Dysfunction in Atherosclerotic Mice. Arterioscler Thromb Vasc Biol. 2014 May 1. [Epub ahead of print]. PMID: 24790139.

M1745

Melatonin

1 g
5 g
10 g

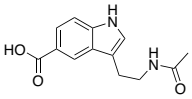

$C_{13}H_{16}N_2O_2$ FW: 232.27 [73-31-4] ≥98%

Endogenous hormone involved in circadian rhythms, activates MT receptors and decreases expression of FSH, LH, and leptin. It decreases body weight, adiposity, leptin levels, and insulin levels in obese animals, prevents tau hyperphosphorylation and amyloid-β fibrillogenesis in Alzheimer's disease models, and protects gastric mucosa from reflux-induced damage.

Kandil TS, Mousa AA, El-Gendy AA, et al. The potential therapeutic effect of melatonin in Gastro-Esophageal Reflux Disease. BMC Gastroenterol. 2010 Jan 18;10:7. PMID: 20082715.

Anisimov VN, Popovich IG, Zabezhinski MA, et al. Melatonin as antioxidant, geroprotector and anticarcinogen. Biochim Biophys Acta. 2006 May-Jun;1757(5-6):573-89. PMID: 16678784.

Mills E, Wu P, Seely D, et al. Melatonin in the treatment of cancer: a systematic review of randomized controlled trials and meta-analysis. J Pineal Res. 2005 Nov;39(4):360-6. PMID: 16207291.

M1845

Melitracen Hydrochloride

5 mg
25 mg
100 mg

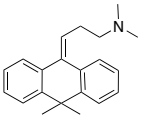

$C_{21}H_{25}N \bullet HCl$ FW: 327.89 [10563-70-9] ≥99%

Potential dopamine D1/2 receptor antagonist used to treat depression. It is often co-administered with flupenthixol as a treatment for trigeminal neuralgia. It does not affect cardiovascular function.

Liu EJ, Zhang WL, Bai YP. [Observation on clinical efficacy of depression treated with the alliance of acupuncture and medication]. Zhongguo Zhen Jiu. 2013 Jun;33(6):497-500. PMID: 23967634.

Hashash JG, Abdul-Baki H, Azar C, et al. Clinical trial: a randomized controlled cross-over study of flupenthixol + melitracen in functional dyspepsia. Aliment Pharmacol Ther. 2008 Jun 1;27(11):1148-55. PMID: 18331614.

Bin Yaacob H. Flupenthixol and Melitracen in the management of trigeminal neuralgia. Dent J Malays. 1985 Apr;8(2):37-8. PMID: 3917005.

M1744

Melittin

0.5 mg
1 mg
2.5 mg

Gly-Ile-Gly-Ala-Val-Leu-Lys-Val-Leu-Thr-Thr-Gly-Leu-Pro-Ala-Leu-Ile-Ser-Trp-Ile-Lys-Arg-Lys-Arg-Gln-Gln-NH_2

$C_{131}H_{229}N_{39}O_{31}$ FW: 2846.5 [20449-79-0] ≥98%

Found in *Apis mellifera* venom. It induces pore formation in cell membranes, causing ion leakage. It also increases formation of free radicals and induces apoptosis in *Candida* and induces autophagy and apoptosis in *Leishmania* and *Trypanosoma*.

Lee J, Lee DG. Melittin triggers apoptosis in *Candida albicans* through the reactive oxygen species-mediated mitochondria/caspase-dependent pathway. FEMS Microbiol Lett. 2014 Apr 27. [Epub ahead of print]. PMID: 24766524.

Lee MT, Sun TL, Hung WC, et al. Process of inducing pores in membranes by melittin. Proc Natl Acad Sci U S A. 2013 Aug 27;110(35):14243-8. PMID: 23940362.

M1644

Meloxicam

25 mg
100 mg
500 mg
1 g

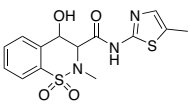

$C_{14}H_{13}N_3O_4S_2$ FW: 351.41 [71125-38-7] ≥98%

NSAID and COX-2 inhibitor used to treat pain and inflammation. It also inhibits MPTP-induced motor dysfunction, increases levels of tyrosine hydroxylase and stimulates expression of antioxidative enzymes.

Tasaki Y, Yamamoto J, Omura T, et al. Meloxicam ameliorates motor dysfunction and dopaminergic neurodegeneration by maintaining Akt-signaling in a mouse Parkinson's disease model. Neurosci Lett. 2012 Jul 11;521(1):15-9. PMID: 22617635.

Edfawy M, Hassan MH, Mansour A, et al. Meloxicam modulates oxidative stress status, inhibits prostaglandin E2, and abrogates apoptosis in carbon tetrachloride-induced rat hepatic injury. Int J Toxicol. 2012 Jun;31(3):276-86. PMID: 22556387.

M1746

Melphalan

100 mg
250 mg
1 g

L-PAM; L-Phenylalanine mustard; L-Sarcolysine

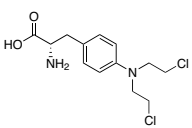

$C_{13}H_{18}Cl_2N_2O_2$ FW: 305.2 [148-82-3] ≥94%

DNA alkylator and derivative of mechlorethamine used to treat various cancers. It prevents DNA and RNA synthesis.

Polavarapu A, Stillabower JA, Stubblefield SG, et al. The mechanism of guanine alkylation by nitrogen mustards: a computational study.

M1749 Memantine Hydrochloride

25 mg
100 mg

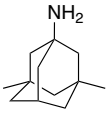

$C_{12}H_{21}N \bullet HCl$ FW: 215.77 [41100-52-1] ≥97%

Dopamine D2 receptor agonist, NMDA receptor antagonist, 5-HT3 receptor antagonist, and α7 nAChR antagonist used to treat Alzheimer's disease, dementia, and Parkinson's disease. It improves spatial learning and memory impairments and stimulates dendritic spine maturation and synapse formation.

Liu MY, Wang S, Yao WF, et al. Memantine improves spatial learning and memory impairments by regulating NGF signaling in APP/PS1 transgenic mice. Neuroscience. 2014 Jul 25;273:141-51. PMID: 24846616.

Wei H, Dobkin C, Sheikh AM, et al. The therapeutic effect of memantine through the stimulation of synapse formation and dendritic spine maturation in autism and fragile X syndrome. PLoS One. 2012;7(5):e36981. PMID: 22615862.

Aarsland D, Ballard C, Walker Z, et al. Memantine in patients with Parkinson's disease dementia or dementia with Lewy bodies: a double-blind, placebo-controlled, multicentre trial. Lancet Neurol. 2009 Jul;8(7):613-8. PMID: 19520613.

M1752 Men 10376

0.5 mg
1 mg
2.5 mg

Neurokinin A (4-10)

H-Asp-Tyr-D-Trp-Val-D-Trp-DTrp-Lys-NH_2

$C_{57}H_{68}N_{12}O_{10}$ FW: 1081.25 [135306-85-3] ≥95%

NK2 receptor antagonist. It decreases stretch-activated contractility in airway smooth muscle tissue and inhibits OVA-induced bronchoconstriction.

Hernandez JM, Cox G, Janssen LJ. Involvement of the neurokinin-2 receptor in airway smooth muscle stretch-activated contractions assessed in perfused intact bovine bronchial segments. J Pharmacol Exp Ther. 2008 Nov;327(2):503-10. PMID: 18719290.

M1774 2-Mercaptoethanesulfonate Sodium

5 g
10 g
25 g

MESNA

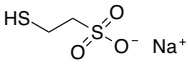

$C_2H_5O_3S_2Na$ FW: 164.18 [19767-45-4] ≥98%

Antioxidant used to decrease cytotoxicity of chemotherapeutics by detoxifying metabolites.

Bogiatzi S, Pagonopoulou O, Simopoulou M, et al. The cytogenetic action of ifosfamide, mesna, and their combination on peripheral rabbit lymphocytes: an in vivo/in vitro cytogenetic study. Cytotechnology. 2014 Oct;66(5):753-60. PMID: 23949582.

Vincenti V, Magnan J, Saccardi MS, et al. Chemically Assisted Dissection by Means of Mesna in Cholesteatoma Surgery. Otol Neurotol. 2014 Jul 14. [Epub ahead of print]. PMID: 25025536.

Li X, Yang S, Lv X, et al. The mechanism of mesna in protection from cisplatin-induced ovarian damage in female rats. J Gynecol Oncol. 2013 Apr;24(2):177-85. PMID: 23653836.

M1669 6-Mercaptopurine Monohydrate

1 g
5 g
25 g

Purine-6-thiol; 6MP

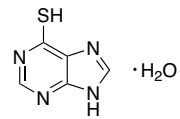

$C_5H_4N_4S \bullet H_2O$ FW: 170.2 [6112-76-1] ≥98%

Thiopurine inhibitor of PRPP amidotransferase used to treat autoimmune diseases, leukemias, and lymphomas. It inhibits IMP metabolism, preventing the synthesis of purines, DNA, and RNA.

Bradford K, Shih DQ. Optimizing 6-mercaptopurine and azathioprine therapy in the management of inflammatory bowel disease. World J Gastroenterol. 2011 Oct 7;17(37):4166-73. PMID: 22072847.

Nielsen OH, Vainer B, Rask-Madsen J. Review article: the treatment of inflammatory bowel disease with 6-mercaptopurine or azathioprine. Aliment Pharmacol Ther. 2001 Nov;15(11):1699-708. PMID: 11683683.

M1770 Meropenem Sodium Carbonate

25 mg
100 mg
500 mg
1 g

Merrem

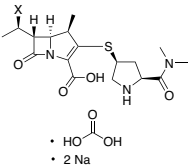

$C_{17}H_{25}N_3O_5S \bullet Na_2CO_3$ FW: 489.45 [96036-03-2] ≥81%

Penicillin binding protein inhibitor that prevents cell wall synthesis. It inhibits growth of *Morganella*, *Enterobacter*, *Klebsiella*, *Mycobacterium*, and *Bacillus*.

Guzek A, Tomaszewski D, Rybicki Z, et al. Comparison of in vitro efficacy of ertapenem, imipenem and meropenem in the infections caused by the *Enterobacteriaceae* strains family. Anaesthesiol Intensive Ther. 2013 Apr-Jun;45(2):67-72. PMID: 23877897.

Li WJ, Li DF, Hu YL, et al. Crystal structure of L,D-transpeptidase LdtMt2 in complex with meropenem reveals the mechanism of carbapenem against *Mycobacterium* tuberculosis. Cell Res. 2013 May;23(5):728-31. PMID: 23588382.

Louie A, VanScoy BD, Brown DL, et al. Impact of spores on the comparative efficacies of five antibiotics for treatment of *Bacillus* anthracis in an in vitro hollow fiber pharmacodynamic model. Antimicrob Agents Chemother. 2012 Mar;56(3):1229-39. PMID: 22155821.

M1769 Meropenem Trihydrate

10 mg
50 mg
100 mg

$C_{17}H_{25}N_3O_5S \bullet 3H_2O$ FW: 437.51 [119478-56-7] ≥98.0%

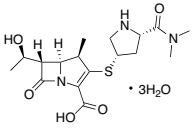

Penicillin binding protein inhibitor that inhibits bacterial cell wall synthesis and is used to treat bacterial meningitis, skin infections, and febrile neutropenia. It is most active against gram negative bacteria and is somewhat resistant to degradation by β-lactamases.

Mallick M, Odedra D, Vidyarthi AS, et al. Meropenem: a potent drug against superbug as unveiled through bioinformatics approaches. Int J Bioinform Res Appl. 2013;9(2):109-20. PMID: 23467058.

Pernot L, Frénois F, Rybkine T, et al. Crystal structures of the class D beta-lactamase OXA-13 in the native form and in complex with meropenem. J Mol Biol. 2001 Jul 20;310(4):859-74. PMID: 11453693.

Sumita Y, Fukasawa M. Potent activity of meropenem against *Escherichia* coli arising from its simultaneous binding to penicillin-binding proteins 2 and 3. J Antimicrob Chemother. 1995 Jul;36(1):53-64. PMID: 8537284.

M2076 Metformin Hydrochloride

5 g
25 g
100 g
250 g

$C_4H_{11}N_5 \bullet HCl$ FW: 165.62 [1115-70-4] ≥98%

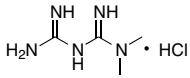

AMPK activator used to treat type 2 diabetes. It displays many biological activities, including reversing pathology of fatty liver disease, inhibiting expression of MHC molecules and co-stimulatory factors on dendritic cells, inducing cell cycle arrest in hepatocellular carcinoma cells, and preventing neoplasia initiation in prostate cancer models.

Fan C, Wang Y, Liu Z, et al. Metformin exerts anticancer effects through the inhibition of the Sonic hedgehog signaling pathway in breast cancer. Int J Mol Med. 2015 May 21. [Epub ahead of print]. PMID: 25999130.

Miyoshi H, Kato K, Iwama H, et al. Effect of the anti-diabetic drug metformin in hepatocellular carcinoma in vitro and in vivo. Int J Oncol. 2013 Dec 30. [Epub ahead of print]. PMID: 24378856.

Piwkowska A, Rogacka D, Jankowski M, et al. Metformin reduces NAD(P)H oxidase activity in mouse cultured podocytes through purinergic dependent mechanism by increasing extracellular ATP concentration. Acta Biochim Pol. 2013;60(4):607-12. PMID: 24432311.

M1579 Methazolamide

NEW

250 mg
1 g

$C_5H_8N_4O_3S_2$ FW: 236.27 [554-57-4] ≥98%

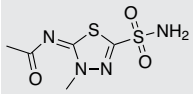

Carbonic anhydrase inhibitor used to treat glaucoma. It lowers intraocular pressure, decreases blood glucose and Hb1(Ac) levels, and may suppress the development of seizures.

Syrjänen L, Parkkila S, Scozzafava A, et al. Sulfonamide inhibition studies of the β carbonic anhydrase from *Drosophila* melanogaster. Bioorg Med Chem Lett. 2014 Jul 1;24(13):2797-801. PMID: 24852120.

Konstantopoulos N, Molero JC, McGee SL, et al. Methazolamide is a new hepatic insulin sensitizer that lowers blood glucose in vivo. Diabetes. 2012 Aug;61(8):2146-54. PMID: 22586591.

Friedman Z, Allen RC, Raph SM. Topical acetazolamide and methazolamide delivered by contact lenses. Arch Ophthalmol. 1985 Jul;103(7):963-6. PMID: 3860197.

M1976 Methimazole

10 g
25 g

$C_4H_6N_2S$ FW: 114.17 [60-56-0] ≥98%

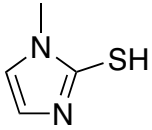

Thyroid peroxidase inhibitor used to treat hyperthyroidism and Graves' disease. It decreases levels of CXCL10 and downregulates expression of IFNγ receptors.

Rivkees SA. Pediatric Graves' disease: management in the post-propylthiouracil Era. Int J Pediatr Endocrinol. 2014;2014(1):10. PMID: 25089127.

Manna D, Roy G, Mugesh G. Antithyroid drugs and their analogues: synthesis, structure, and mechanism of action. Acc Chem Res. 2013 Nov 19;46(11):2706-15. PMID: 23883148.

Crescioli C, Cosmi L, Borgogni E, et al. Methimazole inhibits CXC chemokine ligand 10 secretion in human thyrocytes. J Endocrinol. 2007 Oct;195(1):145-55. PMID: 17911406.

M1978 S-(+)-Methoprene

ZR-515

25 mg
100 mg

$C_{19}H_{34}O_3$ FW: 310.47 [65733-16-6] ≥95%

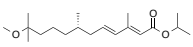

Juvenile insect growth hormone analog that prohibits the ability of the insect to change from pupae to adult. It is used to control mosquito populations. It alters Ca^{2+} signaling and redox activity of cytochrome oxidase and induces male sex differentiation.

Monteiro JP, Jurado AS, Moreno AJ, et al. Toxicity of methoprene as assessed by the use of a model microorganism. Toxicol In Vitro. 2005 Oct;19(7):951-6. PMID: 16081242.

Olmstead AW, LeBlanc GA. Insecticidal juvenile hormone analogs stimulate the production of male offspring in the crustacean Daphnia magna. Environ Health Perspect. 2003 Jun;111(7):919-24. PMID: 12782492.

M1676

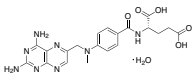

Methotrexate Hydrate

10 mg
50 mg
100 mg
500 mg

Amethopterin; MTX

$C_{20}H_{22}N_8O_5 \cdot H_2O$ FW: 472.45 [6745-93-3] ≥98%

DHF reductase inhibitor used to treat rheumatoid arthritis, ectopic pregnancy, and various cancers. It prevents synthesis of thymidine, RNA, and RNA. It also increases T cell apoptosis, decreases T cell activation, and suppresses cytokine production.

Herfarth HH, Long MD, Isaacs KL. Methotrexate: underused and ignored? Dig Dis. 2012;30 Suppl 3:112-8. doi: 10.1159/000342735. PMID: 23295701.

Mol F, Mol BW, Ankum WM, et al. Current evidence on surgery, systemic methotrexate and expectant management in the treatment of tubal ectopic pregnancy: a systematic review and meta-analysis. Hum Reprod Update. 2008 Jul-Aug;14(4):309-19. PMID: 18522946.

Wessels JA, Huizinga TW, Guchelaar HJ. Recent insights in the pharmacological actions of methotrexate in the treatment of rheumatoid arthritis. Rheumatology (Oxford). 2008 Mar;47(3):249-55. PMID: 18045808.

M1874

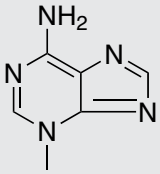

3-Methyladenine

NEW

25 mg
100 mg
500 mg

3-MA; NSC 66389

$C_6H_7N_5$ FW: 149.15 [5142-23-4] ≥98%

Adenine analog and DNA polymerase inhibitor. It inhibits autophagy and DNA synthesis.

Ramírez C, Pham K, Franco MF, et al. Hydroquinone induces oxidative and mitochondrial damage to human retinal Müller cells (MIO-M1). Neurotoxicology. 2013 Dec;39:102-8. PMID: 23994029.

Kumar S, Guru SK, Pathania AS, et al. Autophagy triggered by magnolol derivative negatively regulates angiogenesis. Cell Death Dis. 2013 Oct 31;4:e889. PMID: 24176847.

Johnson RE, Yu SL, Prakash S, et al. A role for yeast and human translesion synthesis DNA polymerases in promoting replication through 3-methyl adenine. Mol Cell Biol. 2007 Oct;27(20):7198-205. PMID: 17698580.

M1776

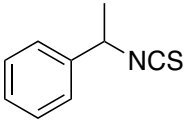

α-Methylbenzyl Isothiocyanate

5 g
10 g

C_9H_9NS FW: 163.24 [32393-32-1] ≥98%

Antioxidant that induces phase II enzyme activity.

Munday R, Zhang Y, Munday CM, et al. Structure-activity relationships and organ specificity in the induction of GST and NQO1 by alkyl-aryl isothiocyanates. Pharm Res. 2008 Sep;25(9):2164-70. PMID: 18563540.

M1777

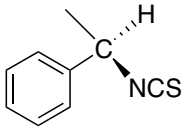

R-(−)-α-Methylbenzyl Isothiocyanate

1 g
5 g
10 g

C_9H_9NS FW: 163.24 [24277-44-9] ≥98%

Antioxidant that induces phase II enzyme activity. It is also used as a chiral agent.

Munday R, Zhang Y, Munday CM, et al. Structure-activity relationships and organ specificity in the induction of GST and NQO1 by alkyl-aryl isothiocyanates. Pharm Res. 2008 Sep;25(9):2164-70. PMID: 18563540.

M1778

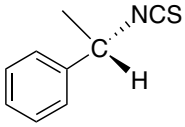

S-(+)-α–Methylbenzyl Isothiocyanate

1 g
5 g
10 g

C_9H_9NS FW: 163.24 [24277-43-8] ≥98%

Antioxidant that induces phase II enzyme activity. It is also used as a chiral agent.

Munday R, Zhang Y, Munday CM, et al. Structure-activity relationships and organ specificity in the induction of GST and NQO1 by alkyl-aryl isothiocyanates. Pharm Res. 2008 Sep;25(9):2164-70. PMID: 18563540.

M1560

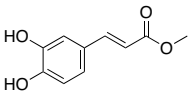

Methyl Caffeate

50 mg
100 mg
500 mg

3,4-Dihydroxycinnamic acid methylester

$C_{10}H_{10}O_4$ FW: 194.19 [3843-74-1] ≥98%

α-Glucosidase inhibitor found in species of *Solanum* and *Magnolia*. It exhibits several biological activities, including suppressing growth of *Pseudomonas*, *Klebsiella*, and *Mycobacterium*, inhibiting replication of HIV, and decreasing blood glucose levels in models of diabetes.

Balachandran C, Duraipandiyan V, Al-Dhabi NA, et al. Antimicrobial and Antimycobacterial Activities of Methyl Caffeate Isolated from *Solanum* torvum Swartz. Fruit. Indian J Microbiol. 2012 Dec;52(4):676-81. PMID: 24293730.

Gandhi GR, Ignacimuthu S, Paulraj MG, et al. Antihyperglycemic activity and antidiabetic effect of methyl caffeate isolated from *Solanum* torvum Swartz. fruit in streptozotocin induced diabetic rats. Eur J Pharmacol. 2011 Nov 30;670(2-3):623-31. PMID: 21963451.

Takahashi K, Yoshioka Y, Kato E, et al. Methyl caffeate as an alpha-glucosidase inhibitor from *Solanum* torvum fruits and the activity of related compounds. Biosci Biotechnol Biochem. 2010;74(4):741-5. PMID: 20378981.

M1876

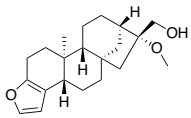

16-O-Methylcafestol

10 mg
25 mg
100 mg

$C_{21}H_{30}O_3$ FW: 330.46 ≥98%

Natural cafestol derivative found in coffee beans. It may prevent oxidative damage, inflammation, or cancer cell proliferation.

Liao XL, Chen XZ, Yu KB, et al. 16-O-Methyl-cafestol. Acta Crystallogr Sect E Struct Rep Online. 2010 Mar 6;66(Pt 4):o760. PMID: 21580605.

Mensink RP, Lebbink WJ, Lobbezoo IE, et al. Diterpene composition of oils from Arabica and Robusta coffee beans and their effects on serum lipids in man. J Intern Med. 1995 Jun;237(6):543-50. PMID: 7782725.

M1564

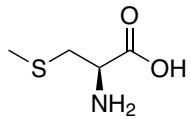

S-Methyl-L-cysteine

1 g
5 g
25 g

SMLC

$C_4H_9NO_2S$ FW: 135.18 [1187-84-4] ≥99%

Antioxidant found in *Brassicaceae* family plants. It decreases oxidative stress and inhibits oil drop formation in white pre-adipose tissue.

Ishiwata S, Ogata S, Umino A, et al. Increasing effects of S-methyl-L-cysteine on the extracellular D-serine concentrations in the rat medial frontal cortex. Amino Acids. 2013 May;44(5):1391-5. PMID: 23417484.

Yoshinari O, Shiojima Y, Igarashi K. Anti-obesity effects of onion extract in Zucker diabetic fatty rats. Nutrients. 2012 Oct 22;4(10):1518-26. PMID: 23201769.

Wassef R, Haenold R, Hansel A, et al. Methionine sulfoxide reductase A and a dietary supplement S-methyl-L-cysteine prevent Parkinson's-like symptoms. J Neurosci. 2007 Nov 21;27(47):12808-16. PMID: 18032652.

M1565

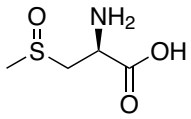

(±)-S-Methyl-L-cysteine-S-oxide

100 mg
250 mg
1 g

Methyiin; Pyrolyzate

$C_4H_9NO_3S$ FW: 151.19 [6853-87-8] ≥98%

Synthetic analog of alliin found in cruciferous vegetables.

Steventon GB. Diurnal variation in the metabolism of S-carboxymethyl-L-cysteine in humans. Drug Metab Dispos. 1999 Sep;27(9):1092-7. PMID: 10460812.

Synge RL, Wood JC. (+)-(S-methyl-L-cysteine S-oxide) in cabbage. Biochem J. 1956 Oct;64(2):252-9. PMID: 13363835.

M1566

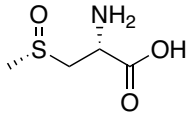

(+)-S-Methyl-L-cysteine-S-oxide

5 mg
25 mg
100 mg

Methyiin; Pyrolyzate

$C_4H_9NO_3S$ FW: 151.19 ≥98%

Alliin analog found in cruciferous vegetables. It decreases plasma glucose levels, suppresses endogenous lipogenesis, and increases lipid catabolism.

Kook S, Kim GH, Choi K. The antidiabetic effect of onion and garlic in experimental diabetic rats: meta-analysis. J Med Food. 2009 Jun;12(3):552-60. PMID: 19627203.

Kumari K, Augusti KT. Lipid lowering effect of S-methyl cysteine sulfoxide from Allium cepa Linn in high cholesterol diet fed rats. J Ethnopharmacol. 2007 Feb 12;109(3):367-71. PMID: 16987625.

Kumari K, Augusti KT. Antidiabetic and antioxidant effects of S-methyl cysteine sulfoxide isolated from onions (Allium cepa Linn) as compared to standard drugs in alloxan diabetic rats. Indian J Exp Biol. 2002 Sep;40(9):1005-9. PMID: 12587728.

M1779

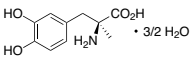

Methyldopa Sesquihydrate

1 g
5 g
10 g

Methyl-L-DOPA; MK-351

$C_{10}H_{13}NO_4 \bullet 3/2H_2O$ FW: 238.24 [41372-08-1] ≥98%

DOPA decarboxylase inhibitor and indirect α2-adrenergic receptor agonist used to treat hypertension. It inhibits the sympathetic nervous system, decreases production of dopamine, norepinephrine, and epinephrine, and exhibits NO-dependent sedative activity.

Sucak A, Kanat-Pektas M, Gungor T, et al. Leptin levels and antihypertensive treatment in preeclampsia. Singapore Med J. 2010 Jan;51(1):39-43. PMID: 20200774.

Soares de Moura R, Rios AA, et al. The effects of nitric oxide synthase inhibitors on the sedative effect of clonidine. Anesth Analg. 2001 Nov;93(5):1217-21. PMID: 11682401.

M1878

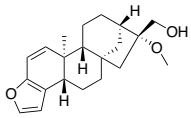

16-O-Methylkahweol

5 mg
10 mg
50 mg

$C_{21}H_{28}O_3$ FW: 328.45 ≥98%

Natural kahweol derivative found in coffee beans. It may prevent oxidative damage, inflammation, or cancer cell proliferation.

Mensink RP, Lebbink WJ, Lobbezoo IE, et al. Diterpene composition of oils from Arabica and Robusta coffee beans and their effects on serum lipids in man. J Intern Med. 1995 Jun;237(6):543-50. PMID: 7782725.

M3232

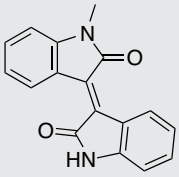

Methylisoindigotin

NEW

10 mg
50 mg

Meisoindigo

$C_{17}H_{12}N_2O_2$ FW: 276.3 [97207-47-1] ≥98%

Indirubin derivative. It inhibits proliferation of leukemia cells, induces apoptosis in colon cancer cells, and decreases production of pro-inflammatory cytokines.

Huang M, Lin HS, Lee YS, et al. Evaluation of meisoindigo, an indirubin derivative: in vitro antileukemic activity and in vivo pharmacokinetics. Int J Oncol. 2014 Oct;45(4):1724-34. PMID: 25050545.

Zhang HJ, Zhang Y, Jin J, et al. Mechanism about therapeutic effect of meisoindigo on psoriasis via down-regulation of the TLR4-TAK-NF-kappaB pathways. Yao Xue Xue Bao. 2013 Apr;48(4):503-7. PMID: 23833936.

Zuo MX, Li Y, Zhou JH, et al. Effect of Meisoindigo on Wnt signal pathway in K562 and HL-60 cells. Zhongguo Shi Yan Xue Ye Xue Za Zhi. 2010 Jun;18(3):579-82. PMID: 20561405.

M1575

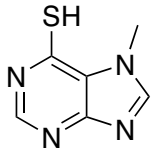

7-Methyl-6-mercaptopurine

10 mg
50 mg
100 mg
500 mg

$C_6H_6N_4S$ FW: 166.21 [3324-79-6] ≥87%

6-Mercaptopurine derivative and inhibitor of PRPP amidotransferase used to treat autoimmune diseases, leukemias, and lymphomas. It inhibits IMP metabolism, preventing the synthesis of purines, DNA, and RNA.

Bradford K, Shih DQ. Optimizing 6-mercaptopurine and azathioprine therapy in the management of inflammatory bowel disease. World J Gastroenterol. 2011 Oct 7;17(37):4166-73. PMID: 22072847.

Nielsen OH, Vainer B, Rask-Madsen J. Review article: the treatment of inflammatory bowel disease with 6-mercaptopurine or azathioprine. Aliment Pharmacol Ther. 2001 Nov;15(11):1699-708. PMID: 11683683.

M1678

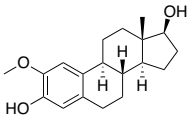

2-Methoxyestradiol

5 mg
10 mg
50 mg

$C_{19}H_{26}O_3$ FW: 302.41 [362-07-2] ≥98%

Estradiol metabolite and microtubule depolymerization inhibitor. It decreases tumor growth, VEGF expression, and angiogenesis in hepatocellular carcinoma models, lowers mean arterial blood pressure, and prevents TGF-β3-induced fibrosis.

Yuan W, Yu Y, Li J, et al. Estrogen metabolite 2-methoxyestradiol prevents hypertension in deoxycorticosterone acetate-salt rats. Cardiovasc Drugs Ther. 2013 Feb;27(1):17-22. PMID: 23229845.

Salama SA, Diaz-Arrastia CR, Kilic GS, et al. 2-Methoxyestradiol causes functional repression of transforming growth factor β3 signaling by ameliorating Smad and non-Smad signaling pathways in immortalized uterine fibroid cells. Fertil Steril. 2012 Jul;98(1):178-84. PMID: 22579131.

M1680

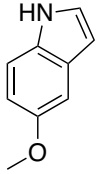

5-Methoxyindole

1 g
5 g
25 g

C_9H_9NO FW: 147.17 [1006-94-6] ≥98%

Melatonin derivative and potential PPARγ and 5-HT3 agonist.

Czimmerer Z, Varga T, Poliska S, et al. Identification of novel markers of alternative activation and potential endogenous PPARγ ligand production mechanisms in human IL-4 stimulated differentiating macrophages. Immunobiology. 2012 Dec;217(12):1301-14. PMID: 22954708.

Koike T, Hoashi Y, Takai T, et al. 1,6-Dihydro-2H-indeno[5,4-b]furan derivatives: design, synthesis, and pharmacological characterization of a novel class of highly potent MT2 -selective agonists. J Med Chem. 2011 May 12;54(9):3436-44. PMID: 21473625.

M1677

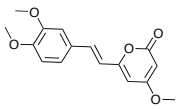

11-Methoxyyangonin

5 mg
10 mg

$C_{16}H_{16}O_5$ FW: 288.3 ≥98%

Found in *Piper methysticum* (kava plant).

Hänsel R, Klaproth L. Isolation of 11-methoxy-yangonin from the cava root. Arch Pharm Ber Dtsch Pharm Ges. 1966 Jun;299(6):503-6. PMID: 5228634.

M1877

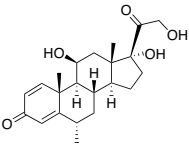

Methylprednisolone

100 mg
500 mg
1 g

$C_{22}H_{30}O_5$ FW: 374.47 [83-43-2] ≥96%

Synthetic glucocorticoid receptor agonist used to treat inflammation and autoimmune diseases. It decreases survival of activated CD4+ T cells, inhibits oxidative stress-induced apoptosis, and suppresses release of inflammatory cytokines.

Lu YS, Pu LY, Li XC, et al. Methylprednisolone inhibits activated CD4+ T cell survival promoted by toll-like receptor ligands. Hepatobiliary Pancreat Dis Int. 2010 Aug;9(4):376-83. PMID: 20688601.

Das A, Banik NL, Ray SK. Methylprednisolone and indomethacin inhibit oxidative stress mediated apoptosis in rat C6 glioblastoma cells. Neurochem Res. 2007 Nov;32(11):1849-56. PMID: 17570061.

M1979 Methyl Salicylate

250 mL
500 mL
1 L

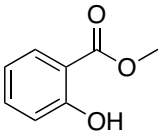

$C_8H_8O_3$ FW: 152.15 [119-36-8] ≥98%

TRPV1 modulator found in *Spiraea*, *Betula*, and *Gaultheria* commercially used as an antiseptic, flavorant, and fragrance. Derivatives of this compound inhibit pain and inflammation.

Tieman D, Zeigler M, Schmelz E, et al. Functional analysis of a tomato salicylic acid methyl transferase and its role in synthesis of the flavor volatile methyl salicylate. Plant J. 2010 Apr 1;62(1):113-23. PMID: 20070566.

Ohta T, Imagawa T, Ito S. Involvement of transient receptor potential vanilloid subtype 1 in analgesic action of methylsalicylate. Mol Pharmacol. 2009 Feb;75(2):307-17. PMID: 18987162.

M1875 S-(N-Methylsulfinylbutylthiocarbamoyl)-glutathione

5 mg
10 mg
25 mg

Sulforaphane glutathione conjugate

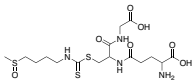

$C_{16}H_{28}N_4O_7S_3$ FW: 484.61 ≥98%

Glutathione-sulforaphane conjugate and antioxidant. It increases levels of HO-1 and Nrf2 and decreases levels of Bcl-xl, mTOR, and cyclin D1.

Keum YS, Khor TO, Lin W, et al. Pharmacokinetics and pharmacodynamics of broccoli sprouts on the suppression of prostate cancer in transgenic adenocarcinoma of mouse prostate (TRAMP) mice: implication of induction of Nrf2, HO-1 and apoptosis and the suppression of Akt-dependent kinase pathway. Pharm Res. 2009 Oct;26(10):2324-31. PMID: 19669099.

M1873 S-(N-Methylsulfinylbutylthiocarbamoyl)-L-cysteine

5 mg
10 mg
25 mg

L-Cysteine sulforaphane

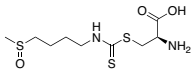

$C_9H_{18}N_2O_3S_3$ FW: 298.45 ≥98%

Conjugate of sulforaphane and L-cysteine. It may decrease oxidative damage.

M1975 S-(N-Methylthiocarbamoyl)-L-cysteine

10 mg
25 mg
100 mg

Methylsiothiocyanate-L-cysteine

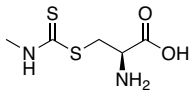

$C_5H_{10}N_2O_2S_2$ FW: 194.28 ≥98%

Cysteine-methylisothiocyanate conjugate, antioxidant, and aldehyde dehydrogenase inhibitor. It may display a wide variety of biological activities, including inhibiting hatch of *Heterodera*, increasing aldehyde levels in blood and brain, and inducing lipid peroxidation-mediated DNA damage.

M1679 Methysticin

5 mg
10 mg

Kavatin

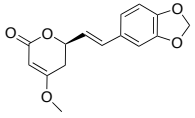

$C_{15}H_{14}O_5$ FW: 274.27 [495-85-2] ≥98%

Found in *Piper methysticum* (kava plant). It inhibits activation of NF-κB in lung adenocarcinoma tissue, activates Nrf2 in neurons and astroglia, decreases peak amplitude of voltage-gated Na^+ channels in hippocampal neurons, and suppresses growth of *Fusarium*, *Trichoderma*, and *Colletotrichum*.

Shaik AA, Hermanson DL, Xing C. Identification of methysticin as a potent and non-toxic NF-kappaB inhibitor from kava, potentially responsible for kava's chemopreventive activity. Bioorg Med Chem Lett. 2009 Oct 1;19(19):5732-6. PMID: 19716299.

Wruck CJ, Götz ME, Herdegen T, et al. Kavalactones protect neural cells against amyloid beta peptide-induced neurotoxicity via extracellular signal-regulated kinase 1/2-dependent nuclear factor erythroid 2-related factor 2 activation. Mol Pharmacol. 2008 Jun;73(6):1785-95. PMID: 18334601.

M1879 Metoprolol Tartrate

5 g
25 g

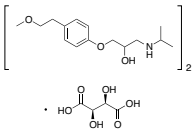

$(C_{15}H_{25}NO_3)_2 \bullet C_4H_6O_6$ FW: 684.82 [56392-17-7] ≥98%

β1-Adrenergic antagonist used to treat hypertension, myocardial infarction, tachycardia, and congestive heart failure. It decreases size of atherosclerotic plaques, inhibits seizures, and increases microvessel sprouting in aortic rings.

Ulleryd MA, Bernberg E, Yang LJ, et al. Metoprolol Reduces Proinflammatory Cytokines and Atherosclerosis in ApoE(-/-) Mice. Biomed Res Int. 2014;2014:548783. PMID: 25105129.

Borowicz KK, Banach M. Antiarrhythmic drugs and epilepsy. Pharmacol Rep. 2014 Aug;66(4):545-51. PMID: 24948053.

Stati T, Musumeci M, Maccari S, et al. β-Blockers promote angiogenesis in the mouse aortic ring assay. J Cardiovasc Pharmacol. 2014 Jul;64(1):21-7. PMID: 24621648.

M1977 Metronidazole

5 g
25 g
100 g

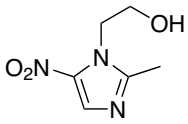

$C_6H_9N_3O_3$ FW: 171.15 [443-48-1] ≥98%

DNA synthesis inhibitor used to treat bacterial and protozoal infections. It is especially effective against *Clostridium* and *Trichomonas*.

Cohen SH, Gerding DN, Johnson S, et al. Clinical practice guidelines for *Clostridium difficile* infection in adults: 2010 update by the society for healthcare epidemiology of America (SHEA) and the infectious diseases society of America (IDSA). Infect Control Hosp Epidemiol. 2010 May;31(5):431-55. PMID: 20307191.

Raether W, Hänel H. Nitroheterocyclic drugs with broad spectrum activity. Parasitol Res. 2003 Jun;90 Supp 1:S19-39. PMID: 12811546.

M1685 Mevastatin

10 mg
50 mg
250 mg

6-Demethylmevinolin; CS-500; ML-236B

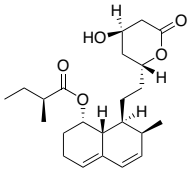

$C_{23}H_{34}O_5$ FW: 390.51 [73573-88-3] ≥98%

HMG-CoA reductase inhibitor used to lower cholesterol and lipid levels. It also induces apoptosis and inhibits growth of salivary adenoid cystic carcinoma cells and inhibits bisphosphonate-induced activation of γδ T cells.

Zhang S, Wang XL, Gan YH, et al. Activation of c-Jun N-terminal kinase is required for mevastatin-induced apoptosis of salivary adenoid cystic carcinoma cells. Anticancer Drugs. 2010 Aug;21(7):678-86. PMID: 20629200.

Thompson K, Rogers MJ. Statins prevent bisphosphonate-induced gamma,delta-T-cell proliferation and activation in vitro. J Bone Miner Res. 2004 Feb;19(2):278-88. PMID: 14969398.

Endo A, Kuroda M, Tsujita Y. ML-236A, ML-236B, and ML-236C, new inhibitors of cholesterogenesis produced by Penicillium citrinium. J Antibiot (Tokyo). 1976 Dec;29(12):1346-8. PMID: 1010803.

M1687 Mevinolin

50 mg
100 mg
500 mg

MK-803; Lovastatin

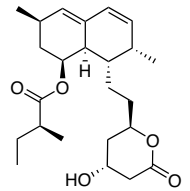

$C_{24}H_{36}O_5$ FW: 404.54 [75330-75-5] ≥97%

HMG-CoA reductase inhibitor used to lower cholesterol and lipid levels. It also prevents proliferation of lymphoma cells and inhibits coxsackievirus replication by decreasing expression of coxsackie and adenovirus receptors and preventing viral entry.

Song X, Liu BC, Lu XY, et al. Lovastatin inhibits human B lymphoma cell proliferation by reducing intracellular ROS and TRPC6 expression.

M2400 MG-132

NEW

5 mg
25 mg

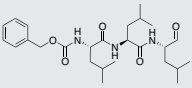

$C_{26}H_{41}N_3O_5$ FW: 475.62 [133407-82-6] ≥98%

Proteasome inhibitor. It induces apoptosis in renal interstitial fibroblasts, suppresses skeletal muscle atrophy in COPD models, and delays progression of osteoarthritis.

Zhu B, Jin Y, Han L, et al. Proteasome inhibitor inhibits proliferation and induces apoptosis in renal interstitial fibroblasts. Pharmacol Rep. 2013;65(5):1357-65. PMID: 24399732.

Ma BM, Liu ZH, Liang ZK, et al. The proteasome inhibitor MG132 attenuates skeletal muscle atrophy in a rat model of chronic obstructive pulmonary disease. Zhonghua Jie He He Hu Xi Za Zhi. 2013 Jun;36(6):441-6. PMID: 24103208.

Quan R, Huang Z, Yue Z, et al. Effects of a proteasome inhibitor on the NF-κB signalling pathway in experimental osteoarthritis. Scand J Rheumatol. 2013;42(5):400-7. PMID: 23826657.

M2409 MGCD-0103

NEW

5 mg
25 mg
50 mg

Mocetinostat

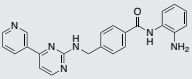

$C_{23}H_{20}N_6O$ FW: 396.44 [726169-73-9] ≥98%

HDAC inhibitor. It improves left ventricular and end diastolic pressure, decreases total collagen levels, increases transcription of NPR-A, and inhibits autophagy and induces apoptosis in chronic lymphocytic leukemia cells.

Nural-Guvener HF, Zakharova L, Nimlos J, et al. HDAC class I inhibitor, Mocetinostat, reverses cardiac fibrosis in heart failure and diminishes CD90+ cardiac myofibroblast activation. Fibrogenesis Tissue Repair. 2014 Jul 2;7:10. PMID: 25024745.

Kumar P, Tripathi S, Pandey KN. Histone deacetylase inhibitors modulate the transcriptional regulation of guanylyl cyclase/natriuretic peptide receptor-a gene: interactive roles of modified histones, histone acetyltransferase, p300, AND Sp1. J Biol Chem. 2014 Mar 7;289(10):6991-7002. PMID: 24451378.

El-Khoury V, Pierson S, Szwarcbart E, et al. Disruption of autophagy by the histone deacetylase inhibitor MGCD0103 and its therapeutic implication in B-cell chronic lymphocytic leukemia. Leukemia. 2014 Aug;28(8):1636-46. PMID: 24418989.

M3196 MHY-1485

NEW

5 mg
25 mg

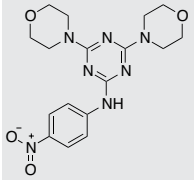

$C_{17}H_{21}N_7O_4$ FW: 387.4 [326914-06-1] ≥98%

Activator of mTOR. It inhibits autophagy and increases ovarian explant weights, follicle development, and production of viable, mature oocytes.

Li C, Siragy HM. (Pro)renin receptor regulates autophagy and apoptosis in podocytes exposed to high glucose. Am J Physiol Endocrinol Metab. 2015 Jun 16. [Epub ahead of print]. PMID: 26081285.

Cheng Y, Kim J, Li XX, et al. Promotion of ovarian follicle growth following mTOR activation: synergistic effects of AKT stimulators. PLoS One. 2015 Feb 24;10(2):e0117769. PMID: 25710488.

Choi YJ, Park YJ, Park JY, et al. Inhibitory effect of mTOR activator MHY1485 on autophagy: suppression of lysosomal fusion. PLoS One. 2012;7(8):e43418. Erratum in: PLoS One. 2013;8(1). PMID: 22927967.

M3309 Miconazole

1 g
5 g
25 g

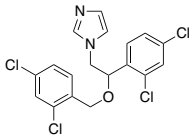

$C_{18}H_{14}Cl_4N_2O$ FW: 416.14 [22916-47-8] ≥98%

14-α Demethylase inhibitor and potential glucocorticoid antagonist that inhibits ergosterol synthesis and fungal cell wall formation. It is used to treat fungal infections by pathogens such as *Candida*. It also decreases expression of HIF-1α and VEGF in breast cancer and glioma cells.

Park JY, Jung HJ, Seo I, et al. Translational suppression of HIF-1α by miconazole through the mTOR signaling pathway. Cell Oncol (Dordr). 2014 Jul 29. [Epub ahead of print]. PMID: 25070654.

Niimi M, Firth NA, Cannon RD. Antifungal drug resistance of oral fungi. Odontology. 2010 Feb;98(1):15-25. PMID: 20155503.

Duret C, Daujat-Chavanieu M, Pascussi JM, et al. Ketoconazole and miconazole are antagonists of the human glucocorticoid receptor: consequences on the expression and function of the constitutive androstane receptor and the pregnane X receptor. Mol Pharmacol. 2006 Jul;70(1):329-39. PMID: 16608920.

M3310 Miconazole Nitrate

1 g
5 g
25 g

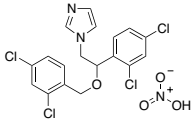

$C_{18}H_{14}Cl_4N_2 \bullet HNO_3$ FW: 479.15 [22832-87-7] ≥98%

14-α Demethylase inhibitor and potential glucocorticoid receptor antagonist that inhibits ergosterol synthesis and fungal cell wall formation. It is used to treat fungal infections and is especially active against *Candida*. It also decreases expression of HIF-1α and VEGF in breast cancer and glioma cells.

Park JY, Jung HJ, Seo I, et al. Translational suppression of HIF-1α by miconazole through the mTOR signaling pathway. Cell Oncol (Dordr). 2014 Jul 29. [Epub ahead of print]. PMID: 25070654.

Niimi M, Firth NA, Cannon RD. Antifungal drug resistance of oral fungi. Odontology. 2010 Feb;98(1):15-25. PMID: 20155503.

M3410 Microcystin (N-Me)-LR

25 µg

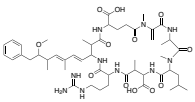

$C_{50}H_{76}N_{10}O_{12}$ FW: 1009.3 [1865776-22-2] ≥95%

Derivative of microcystin LR, PP1/2A inhibitor, and potential GSK-3β activator found in *Microcystis*. It induces apoptosis in testicular cells, stimulates cytoskeletal reorganization, causes oxidative damage, and produces cognitive deficits.

Zhou Y, Chen Y, Yuan M, et al. In vivo study on the effects of microcystin-LR on the apoptosis, proliferation and differentiation of rat testicular spermatogenic cells of male rats injected i.p. with toxins. J Toxicol Sci. 2013;38(5):661-70. PMID: 24025782.

Sun Y, Liu JH, Huang P, et al. Alterations of tau and VASP during microcystin-LR-induced cytoskeletal reorganization in a human liver cell line. Environ Toxicol. 2013 Aug 9. doi:. [Epub ahead of print]. PMID: 23929704.

Zhang H, Cai C, Fang W, et al. Oxidative damage and apoptosis induced by microcystin-LR in the liver of Rana nigromaculata in vivo. Aquat Toxicol. 2013 Sep 15;140-141:11-8. PMID: 23747548.

M3406 Microcystin-LR

NEW

100 µg

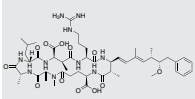

$C_{49}H_{74}N_{10}O_{12}$ FW: 995.17 [101043-37-2] ≥95%

PP1/2A inhibitor and potential GSK-3β activator found in *Microcystis*. It induces apoptosis in testicular cells, stimulates cytoskeletal reorganization, causes oxidative damage, and produces cognitive deficits.

Zhou Y, Chen Y, Yuan M, et al. In vivo study on the effects of microcystin-LR on the apoptosis, proliferation and differentiation of rat testicular spermatogenic cells of male rats injected i.p. with toxins. J Toxicol Sci. 2013;38(5):661-70. PMID: 24025782.

Sun Y, Liu JH, Huang P, et al. Alterations of tau and VASP during microcystin-LR-induced cytoskeletal reorganization in a human liver cell line. Environ Toxicol. 2013 Aug 9. doi:. [Epub ahead of print]. PMID: 23929704.

M3407 Microcystin-RR

NEW 100 µg

$C_{49}H_{75}N_{13}O_{12}$ FW: 1038.2 [111755-37-4] ≥95%

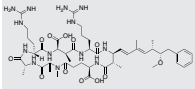

PP1/2A inhibitor and potential GSK-3β activator found in *Microcystis*. It induces endocrine disruption, alters cholesterol synthesis, stimulates oxidative stress, and causes apoptosis and liver damage.

Pavagadhi S, Natera S, Roessner U, et al. Insights into Lipidomic Perturbations in Zebrafish Tissues upon Exposure to Microcystin-LR and Microcystin-RR. Environ Sci Technol. 2013 Dec 17;47(24):14376-84. PMID: 24152164.

Zhao S, Xie P, Li G, et al. The proteomic study on cellular responses of the testes of zebrafish (Danio rerio) exposed to microcystin-RR. Proteomics. 2012 Jan;12(2):300-12. PMID: 22140076.

Huang P, Zheng Q, Xu LH. The apoptotic effect of oral administration of microcystin-RR on mice liver. Environ Toxicol. 2011 Oct;26(5):443-52. PMID: 20196164.

M3408 [D-Asp3]-Microcystin-LR

25 µg

$C_{48}H_{72}N_{10}O_{12}$ FW: 981.2 [120011-66-7] ≥95%

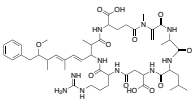

Derivative of microcystin LR, PP1/2A inhibitor, and potential GSK-3β activator found in *Microcystis*. It induces apoptosis in testicular cells, stimulates cytoskeletal reorganization, causes oxidative damage, and produces cognitive deficits.

Zhou Y, Chen Y, Yuan M, et al. In vivo study on the effects of microcystin-LR on the apoptosis, proliferation and differentiation of rat testicular spermatogenic cells of male rats injected i.p. with toxins. J Toxicol Sci. 2013;38(5):661-70. PMID: 24025782.

Sun Y, Liu JH, Huang P, et al. Alterations of tau and VASP during microcystin-LR-induced cytoskeletal reorganization in a human liver cell line. Environ Toxicol. 2013 Aug 9. doi:. [Epub ahead of print]. PMID: 23929704.

M3411 [D-Asp3, (E)-Dhb7]-Microcystin-RR

NEW 100 µg

$C_{49}H_{75}N_{13}O_{12}$ FW: 1038.2 [202120-08-9] ≥95%

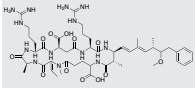

Microcystin RR derivative, PP1/2A inhibitor, and potential GSK-3β activator found in *Microcystis*. It induces endocrine disruption, alters cholesterol synthesis, stimulates oxidative stress, and causes apoptosis and liver damage.

Pavagadhi S, Natera S, Roessner U, et al. Insights into Lipidomic Perturbations in Zebrafish Tissues upon Exposure to Microcystin-LR and Microcystin-RR. Environ Sci Technol. 2013 Dec 17;47(24):14376-84. PMID: 24152164.

Zhao S, Xie P, Li G, et al. The proteomic study on cellular responses of the testes of zebrafish (Danio rerio) exposed to microcystin-RR. Proteomics. 2012 Jan;12(2):300-12. PMID: 22140076.

M3412 [D-Asp3, (E)-Dhb7]-Microcystin-HphR

NEW 25 µg

$C_{52}H_{72}N_{10}O_{12}$ FW: 1029.19 [1430108-50-1] ≥95%

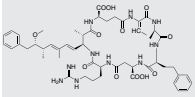

Microcystin HphR derivative and potential PP1/2A inhibitor and GSK-3β activator found in *Microcystis*. It is carcinogenic, pro-oxidative, and cytotoxic.

Namikoshi M, Sivonen K, Evans WR, et al. Structures of three new homotyrosine-containing microcystins and a new homophenylalanine variant from Anabaena sp. strain 66. Chem Res Toxicol. 1992 Sep-Oct;5(5):661-6. PMID: 1446006.

M3414 [D-Asp3, (E)-Dhb7]-Microcystin-HtyR

NEW 100 µg

$C_{52}H_{72}N_{10}O_{13}$ FW: 1045.19 [913178-65-1] ≥95%

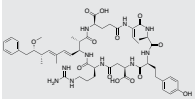

Microcystin HtyR derivative and potential PP1/2A inhibitor and GSK-3β activator found in *Microcystis*. It is carcinogenic, pro-oxidative, and cytotoxic.

Shimizu K, Sano T, Kubota R, et al. Effects of the amino Acid constituents of microcystin variants on cytotoxicity to primary cultured rat hepatocytes. Toxins (Basel). 2013 Dec 30;6(1):168-79. PMID: 24380975.

Hastie CJ, Borthwick EB, Morrison LF, et al. Inhibition of several protein phosphatases by a non-covalently interacting microcystin and a novel cyanobacterial peptide, nostocyclin. Biochim Biophys Acta. 2005 Nov 15;1726(2):187-93. PMID: 16046071.

M3206 Microginin 511

NEW 50 µg

$C_{25}H_{41}N_3O_6S$ FW: 511.67 ≥95%

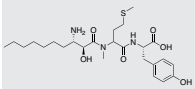

Inhibitor of protein phosphatase, ACE, and leucine aminopeptidase found in *Microcystis*.

Schatz D, Keren Y, Vardi A, et al. Towards clarification of the biological role of microcystins, a family of cyanobacterial toxins. Environ Microbiol. 2007 Apr;9(4):965-70. PMID: 17359268.

Kraft M, Schleberger C, Weckesser J, et al. Binding structure of the leucine aminopeptidase inhibitor microginin FR1. FEBS Lett. 2006 Dec 22;580(30):6943-7. PMID: 17157838.

M3208 Microginin 527 — 50 µg

$C_{25}H_{41}N_3O_7S$ FW: 527.67 [1135249-50-1] ≥95%

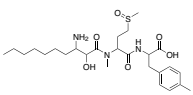

Inhibitor of protein phosphatase, ACE, and leucine aminopeptidase found in *Microcystis*.

Schatz D, Keren Y, Vardi A, et al. Towards clarification of the biological role of microcystins, a family of cyanobacterial toxins. Environ Microbiol. 2007 Apr;9(4):965-70. PMID: 17359268.

Kraft M, Schleberger C, Weckesser J, et al. Binding structure of the leucine aminopeptidase inhibitor microginin FR1. FEBS Lett. 2006 Dec 22;580(30):6943-7. PMID: 17157838.

Runnage ME, Burke AJ, Davies SG, et al. Asymmetric Synthesis of the N-terminal component of Microginin: (2S,3R)-3-Amino-2-Hydroxydecanoic Acid, its (2R,3R)-Epimer and (3R)-3-Aminodecanoic Acid. Tetrahedron: Asymmetry. 1995;6(1):165-176.

M3308 Microginin 527 Methyl Ester — 50 µg

$C_{26}H_{43}N_3O_7S$ FW: 541.7 ≥95%

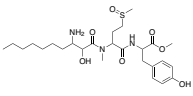

Inhibitor of protein phosphatase, ACE, and leucine aminopeptidase found in *Microcystis*.

Schatz D, Keren Y, Vardi A, et al. Towards clarification of the biological role of microcystins, a family of cyanobacterial toxins. Environ Microbiol. 2007 Apr;9(4):965-70. PMID: 17359268.

Kraft M, Schleberger C, Weckesser J, et al. Binding structure of the leucine aminopeptidase inhibitor microginin FR1. FEBS Lett. 2006 Dec 22;580(30):6943-7. PMID: 17157838.

M3207 Microginin 674 — NEW — 50 µg

$C_{34}H_{50}N_4O_8S$ FW: 674.85 ≥95%

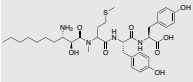

Inhibitor of protein phosphatase, ACE, and leucine aminopeptidase found in *Microcystis*.

Schatz D, Keren Y, Vardi A, et al. Towards clarification of the biological role of microcystins, a family of cyanobacterial toxins. Environ Microbiol. 2007 Apr;9(4):965-70. PMID: 17359268.

Kraft M, Schleberger C, Weckesser J, et al. Binding structure of the leucine aminopeptidase inhibitor microginin FR1. FEBS Lett. 2006 Dec 22;580(30):6943-7. PMID: 17157838.

M3209 Microginin 688 — NEW — 50 µg

$C_{35}H_{52}N_4O_8S$ FW: 688.87 ≥95%

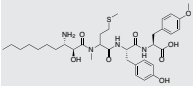

Inhibitor of protein phosphatase, ACE, and leucine aminopeptidase found in *Microcystis*.

Schatz D, Keren Y, Vardi A, et al. Towards clarification of the biological role of microcystins, a family of cyanobacterial toxins. Environ Microbiol. 2007 Apr;9(4):965-70. PMID: 17359268.

Kraft M, Schleberger C, Weckesser J, et al. Binding structure of the leucine aminopeptidase inhibitor microginin FR1. FEBS Lett. 2006 Dec 22;580(30):6943-7. PMID: 17157838.

M3210 Microginin 690 — 100 µg

$C_{34}H_{50}N_4O_9S$ FW: 690.85 [958961-34-7] ≥95%

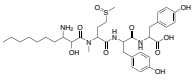

Inhibitor of protein phosphatase, ACE, and leucine aminopeptidase found in *Microcystis*.

Schatz D, Keren Y, Vardi A, et al. Towards clarification of the biological role of microcystins, a family of cyanobacterial toxins. Environ Microbiol. 2007 Apr;9(4):965-70. PMID: 17359268.

Kraft M, Schleberger C, Weckesser J, et al. Binding structure of the leucine aminopeptidase inhibitor microginin FR1. FEBS Lett. 2006 Dec 22;580(30):6943-7. PMID: 17157838.

M3312 Microginin 690 Methyl Ester — 100 µg

$C_{35}H_{52}N_4O_9S$ FW: 704.87 ≥95%

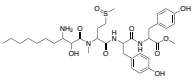

Inhibitor of protein phosphatase, ACE, and leucine aminopeptidase found in *Microcystis*.

Schatz D, Keren Y, Vardi A, et al. Towards clarification of the biological role of microcystins, a family of cyanobacterial toxins. Environ Microbiol. 2007 Apr;9(4):965-70. PMID: 17359268.

M3212 Microginin 704 — 50 µg

$C_{35}H_{52}N_4O_9S$ FW: 704.87 ≥95%

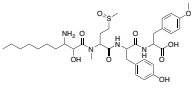

Inhibitor of protein phosphatase, ACE, and leucine aminopeptidase found in *Microcystis*.

Schatz D, Keren Y, Vardi A, et al. Towards clarification of the biological role of microcystins, a family of cyanobacterial toxins. Environ Microbiol. 2007 Apr;9(4):965-70. PMID: 17359268.

M3430 — Micropeptin 1106 — NEW — 100 µg

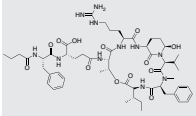

$C_{54}H_{79}N_{11}O_{14}$ FW: 1106.27 ≥95%

Serine protease and PP inhibitor found in *Microcystis*. It is cytotoxic.

Schwarzenberger A, Sadler T, Von Elert E. Effect of nutrient limitation of cyanobacteria on protease inhibitor production and fitness of Daphnia magna. J Exp Biol. 2013 Oct 1;216(Pt 19):3649-55. PMID: 23788705.

Yamaki H, Sitachitta N, Sano T, et al. Two new chymotrypsin inhibitors isolated from the Cyanobacterium *Microcystis* aeruginosa NIES-88. J Nat Prod. 2005 Jan;68(1):14-8. PMID: 15679310.

Ploutno A, Shoshan M, Carmeli S. Three novel protease inhibitors from a natural bloom of the cyanobacterium *Microcystis* aeruginosa. J Nat Prod. 2002 Jul;65(7):973-8. PMID: 12141855.

M3219 — Tyr-MIF-1 — 5 mg / 10 mg / 25 mg

(Tyr0)-Melanocyte-stimulating hormone-release inhibiting factor

H-Tyr-Pro-Leu-Gly-NH_2

$C_{22}H_{33}N_5O_5$ FW: 447.54 [77133-61-0] ≥95%

MIF-1 family μOR antagonist. It inhibits opioid-induced antinociception and analgesia and increases gastric motility.

Pan W, Kastin AJ. From MIF-1 to endomorphin: the Tyr-MIF-1 family of peptides. Peptides. 2007 Dec;28(12):2411-34. PMID: 17988762.

M3220 — Tyr-W-MIF-1 — 5 mg / 10 mg / 25 mg

(Tyr0, Trp2)-Melanocyte-stimulating hormone-release inhibiting factor

H-Tyr-Pro-Trp-Gly-NH_2

$C_{27}H_{32}N_6O_5$ FW: 520.59 [144450-13-5] ≥95%

MIF-1 family μOR-2 antagonist. It inhibits analgesic and antinociceptive activities of opioids, suppresses stress-induced secretion of corticosterone and ACTH, and potentially modulates reward processing.

Mizoguchi H, Takagi H, Watanabe C, et al. Involvement of multiple μ-opioid receptor subtypes on the presynaptic or postsynaptic inhibition of spinal pain transmission. Peptides. 2013 Oct 25. pii: S0196-9781(13)00344-6. PMID: 24512946.

Bocheva A, Dzambazova E, Hadjiolova R, et al. Effect of Tyr-MIF-1 peptides on blood ACTH and corticosterone concentration induced by three experimental models of stress. Auton Autacoid Pharmacol. 2008 Oct;28(4):117-23. PMID: 18798907.

M3321 — Mifepristone — 100 mg / 500 mg / 1 g

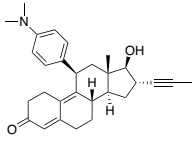

RU-486

$C_{29}H_{35}NO_2$ FW: 429.59 [84371-65-3] ≥98%

Synthetic progesterone and glucocorticoid receptor antagonist used in contraceptives to prevents ovulation and induce endometrial decidual degeneration. It also protects against against oxidative stress and cell death induced by amyloid-β, glutamate, and H_2O_2 and improves cognitive function, working memory, and spatial memory.

Fiala C, Gemzel-Danielsson K. Review of medical abortion using mifepristone in combination with a prostaglandin analogue. Contraception. 2006 Jul;74(1):66-86. PMID: 16781264.

Young AH, Gallagher P, Watson S, et al. Improvements in neurocognitive function and mood following adjunctive treatment with mifepristone (RU-486) in bipolar disorder. Neuropsychopharmacology. 2004 Aug;29(8):1538-45. PMID: 15127079.

M3344 — Milrinone — 10 mg / 50 mg / 100 mg

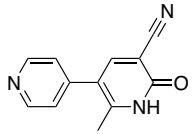

$C_{12}H_9N_3O$ FW: 211.22 [78415-72-2] ≥98%

PDE3 inhibitor used to treat heart failure. It inhibits platelet aggregation and increases cAMP, PKA activation, and Ca^{2+} influx.

Hiramatsu N, Kageyama K. Anti-thrombotic effect of milrinone is caused by inhibition of calcium release from the dense tubular system in human platelets. Acta Anaesthesiol Scand. 2003 Jan;47(1):53-7. PMID: 12492797.

M3353 — Minocycline Hydrochloride — 100 mg / 250 mg / 500 mg

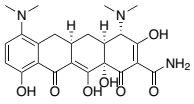

$C_{23}H_{27}N_3O_7 \bullet HCl$ FW: 493.94 [13614-98-7] ≥98%

Inhibitor of 5-lopoxygenase, MMPs, and protein translation used to treat bacterial skin infections. It also reduces hemorrhagic transformation after stroke, attenuates isofluorane-induced cognitive impairment, and inhibits T cell signaling in immune disorders.

Mora M, Medina-Leendertz SJ, Bonilla E, et al. Minocycline, but not ascorbic acid, increases motor activity and extends the life span of *Drosophila* melanogaster. Invest Clin. 2013 Jun;54(2):161-70. PMID: 23947005.

Blacker DJ, Prentice D, Alvaro A, et al. Reducing haemorrhagic transformation after thrombolysis for stroke: a strategy utilising minocycline. Stroke Res Treat. 2013;2013:362961. PMID: 23691430.

Kong F, Chen S, Cheng Y, et al. Minocycline attenuates cognitive impairment induced by isoflurane anesthesia in aged rats. PLoS One. 2013 Apr 17;8(4):e61385. PMID: 23613842.

M3453 Minoxidil

100 mg
500 mg
1 g

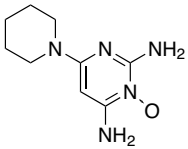

$C_9H_{15}N_5O$ FW: 209.25 [38304-91-5] ≥98%

NO donor and androgen receptor antagonist used to treat hair loss. It increases blood and nutrient flow to hair follicles.

Hsu CL, Liu JS, Lin AC, et al. Minoxidil may suppress androgen receptor-related functions. Oncotarget. 2014 Apr 30;5(8):2187-97. PMID: 24742982.

Rossi A, Cantisani C, Melis L, et al. Minoxidil use in dermatology, side effects and recent patents. Recent Pat Inflamm Allergy Drug Discov. 2012 May;6(2):130-6. PMID: 22409453.

M3368 Mirtazapine

10 mg
50 mg
250 mg

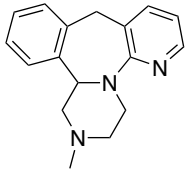

$C_{17}H_{19}N_3$ FW: 265.35 [61337-67-5] ≥98%

5-HT1 receptor agonist, 5-HT2/3 and α2-adrenergic receptor antagonist, and histamine H1 receptor inverse agonist used to treat depression and anxiety. It also acts as a sedative, prevents relapse in recently abstinent substance abuse subjects, and decreases behavioral complications associated with autism spectrum disorder.

Kongsakon R, Papadopoulos KI, Saguansiritham R. Mirtazapine in amphetamine detoxification: a placebo-controlled pilot study. Int Clin Psychopharmacol. 2005 Sep;20(5):253-6. PMID: 16096515.

Liappas J, Paparrigopoulos T, Malitas P, et al. Mirtazapine improves alcohol detoxification. J Psychopharmacol. 2004 Mar;18(1):88-93. PMID: 15107190.

Nutt DJ. Tolerability and safety aspects of mirtazapine. Hum Psychopharmacol. 2002 Jun;17 Suppl 1:S37-41. PMID: 12404669.

M3476 Mithramycin

1 mg
5 mg
10 mg

Plicamycin

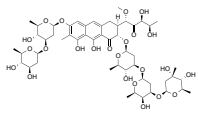

$C_{52}H_{76}O_{25}$ FW: 1084.47 [18378-89-7] ≥95%

Inhibitor of DNMT1 and RNA synthesis. It induces apoptosis in prostate cancer cells and prevents increases in H3 histone methylation in Huntington's disease models.

Choi ES, Chung T, Kim JS, et al. Mithramycin A induces apoptosis by regulating the mTOR/Mcl-1/tBid pathway in androgen-independent prostate cancer cells. J Clin Biochem Nutr. 2013 Sep;53(2):89-93. PMID: 24062605.

Choi ES, Jung JY, Lee JS, et al. Myeloid cell leukemia-1 is a key molecular target for mithramycin A-induced apoptosis in androgen-independent prostate cancer cells and a tumor xenograft animal model. Cancer Lett. 2013 Jan 1;328(1):65-72. PMID: 23000424.

Lin RK, Hsu CH, Wang YC. Mithramycin A inhibits DNA methyltransferase and metastasis potential of lung cancer cells. Anticancer Drugs. 2007 Nov;18(10):1157-64. PMID: 17893516.

M3577 Mitiglinide Calcium

100 mg
250 mg
1 g

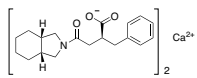

$2(C_{19}H_{24}NO_3)Ca$ FW: 668.88 [145375-43-5] ≥98%

ATP-sensitive K^+ channel blocker and potential ryanodine receptor agonist. It increases insulin secretion and decreases plasma glucose in pancreatic β cells and lowers levels of FGF-21, altering glucose metabolism.

Phillippe HM, Wargo KA. Mitiglinide for type 2 diabetes treatment. Expert Opin Pharmacother. 2013 Oct;14(15):2133-44. PMID: 23992284.

Wang B, Yang G, Yang M, et al. Mitiglinide treatment may decreases plasma fibroblast growth factor-21 levels in individuals with new-onset T2DM. Cytokine. 2012 Feb;57(2):300-3. PMID: 22129626.

Phillippe HM, Wargo KA. Mitiglinide: a novel agent for the treatment of type 2 diabetes mellitus. Ann Pharmacother. 2010 Oct;44(10):1615-23. PMID: 20841518.

M3377 Mitomycin C

1 mg
5 mg
10 mg
25 mg

MMC

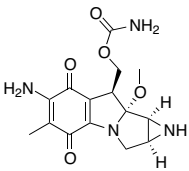

$C_{15}H_{18}N_4O_5$ FW: 334.33 [50-07-7] ≥98%

DNA cross-linker and thioredoxin reductase inhibitor used to treat various cancers. It also improves allograft transplant survival by decreasing CD4+ T cell activation and increasing Treg levels.

Liu L, Wang F, Zheng Y, et al. Pretreatment of transfused donor splenocytes and allografts with mitomycin C attenuates acute rejection in heart transplantation in mice. Transplant Proc. 2014 May;46(4):1169-74. PMID: 24815153.

Paz MM, Zhang X, Lu J, et al. A new mechanism of action for the anticancer drug mitomycin C: mechanism-based inhibition of thioredoxin reductase. Chem Res Toxicol. 2012 Jul 16;25(7):1502-11. PMID: 22694104.

Kang YH, Lee KA, Kim JH, et al. Mitomycin C modulates DNA-double strand break repair genes in cervical carcinoma cells. Amino Acids. 2010 Nov;39(5):1291-8. PMID: 20352460.

M3380 MitoPT® TMRE Mitochondrial Depolarization Assay Kit

500 Tests

NEW

Mitochondrial depolarization measuring kit.

M3381 MitoPT® TMRM Mitochondrial Depolarization Assay Kit

500 Tests

NEW

Mitochondrial depolarization measuring kit.

M3378 MitoPT™ JC-1 Assay kit

100 Tests
400 Tests

Cellular apoptosis measuring kit.

M3576 Mitotane

100 mg
500 mg
1 g

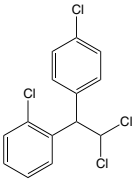

$C_{14}H_{10}Cl_4$ FW: 320.04 [53-19-0] ≥98%

It inhibits secretion of cortisol and is used to treat adrenocortical carcinoma. It inhibits proliferation of adrenocortical cells and increases serum levels of LDL, HDL, and triglycerides.

Shawa H, Deniz F, Bazerbashi H, et al. Mitotane-induced hyperlipidemia: a retrospective cohort study. Int J Endocrinol. 2013;2013:624962. PMID: 24348556.

Hescot S, Slama A, Lombès A, et al. Mitotane alters mitochondrial respiratory chain activity by inducing cytochrome c oxidase defect in human adrenocortical cells. Endocr Relat Cancer. 2013 May 21;20(3):371-81. PMID: 23696597.

M3379 Mitoxantrone Dihydrochloride

50 mg
100 mg
500 mg

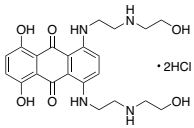

$C_{22}H_{28}N_4O_6 \cdot 2HCl$ FW: 517.41 [70476-82-3] ≥98%

DNA intercalator and Pim-1 inhibitor used to treat various cancers and multiple sclerosis. It cross-links DNA, preventing DNA synthesis.

Pendleton M, Lindsey RH Jr, Felix CA, et al. Topoisomerase II and leukemia. Ann N Y Acad Sci. 2014 Mar;1310:98-110. PMID: 24495080.

Wan X, Zhang W, Li L, et al. A new target for an old drug: identifying mitoxantrone as a nanomolar inhibitor of PIM1 kinase via kinome-wide selectivity modeling. J Med Chem. 2013 Mar 28;56(6):2619-29. PMID: 23442188.

Parker C, Waters R, Leighton C, et al. Effect of mitoxantrone on outcome of children with first relapse of acute lymphoblastic leukaemia (ALL R3): an open-label randomised trial. Lancet. 2010 Dec 11;376(9757):2009-17. PMID: 21131038.

M3584 Mivacurium Chloride

25 mg
100 mg
500 mg

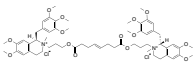

$C_{58}H_{80}N_2O_{14}Cl_2$ FW: 1100.18 [106861-44-3] ≥98%

Non-depolarizing NMJ blocker and nAChR antagonist used as an anesthetc. It inhibits skeletal muscle contractility and prevents atrial fibrillation.

Patterson E, Lu Z, Lin J, et al. Antifibrillatory properties of mivacurium in a canine model of atrial fibrillation. J Cardiovasc Pharmacol. 2008 Mar;51(3):293-303. PMID: 18356695.

Jonsson M, Gurley D, Dabrowski M, et al. Distinct pharmacologic properties of neuromuscular blocking agents on human neuronal nicotinic acetylcholine receptors: a possible explanation for the train-of-four fade. Anesthesiology. 2006 Sep;105(3):521-33. PMID: 16931985.

M3598 Mizoribine Hydrobromide

10 mg
25 mg
100 mg

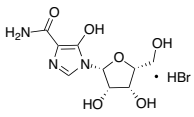

$C_9H_{13}N_3O_6 \cdot HBr$ FW: 340.13 [50924-49-7] ≥98%

IMPDH inhibitor used to treat autoimmune diseases such as lupus and rheumatoid arthritis. It inhibits proliferation of mesangial cells, decreases levels of pro-inflammatory cytokines in synovial cells, and may decrease proliferation of *Candida* and *Aspergillus*.

Sugiyama E, Ikemoto M, Taki H, et al. Mizoribine, an inhibitor of inosine monophosphate dehydrogenase, inhibits interleukin-6 production by freshly prepared rheumatoid synovial cells. Mod Rheumatol. 2001 Mar;11(1):28-33. PMID: 24387017.

Liu S, Xie Y, Lv Y, et al. A novel target of mizoribine inhibiting mesangial cell proliferation: S phase kinase-associated protein 2. Am J Nephrol. 2010;32(5):447-55. PMID: 20924167.

Rodriguez-Suarez R, Xu D, Veillette K, et al. Mechanism-of-action determination of GMP synthase inhibitors and target validation in *Candida albicans* and *Aspergillus* fumigatus. Chem Biol. 2007 Oct;14(10):1163-75. PMID: 17961828.

M4100

MK-0524

1 mg
5 mg
25 mg

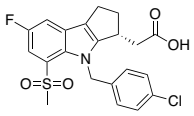

$C_{21}H_{19}ClFNO_4S$ FW: 435.9 [571170-77-9] ≥99%

DP1 receptor antagonist used to decrease niacin-induced flushing during niacin treatment of dyslipidemia. It also prevents PGD2-induced hyaluron synthesis and inhibits platelet activation.

Labrecque P, Roy SJ, Fréchette L, et al. Inverse agonist and pharmacochaperone properties of MK-0524 on the prostanoid DP1 receptor. PLoS One. 2013 Jun 10;8(6):e65767. PMID: 23762421.

Philipose S, Konya V, Lazarevic M, et al. Laropiprant attenuates EP3 and TP prostanoid receptor-mediated thrombus formation. PLoS One. 2012;7(8):e40222. PMID: 22870195.

Guo N, Baglole CJ, O'Loughlin CW, et al. Mast cell-derived prostaglandin D2 controls hyaluronan synthesis in human orbital fibroblasts via DP1 activation: implications for thyroid eye disease. J Biol Chem. 2010 May 21;285(21):15794-804. PMID: 20308056.

M4200

MK-0752

NEW

1 mg
5 mg
25 mg

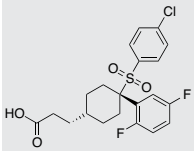

$C_{21}H_{21}ClF_2O_4S$ FW: 442.9 [471905-41-6] ≥98%

Inhibitor of γ-secretase and Notch signaling. It decreases the formation of amyloid-β plaques and may suppress growth of brain tumors.

Hoffman LM, Fouladi M, Olson J, et al. Phase I trial of weekly MK-0752 in children with refractory central nervous system malignancies: a pediatric brain tumor consortium study. Childs Nerv Syst. 2015 Aug;31(8):1283-9. PMID: 25930724.

Olson RE, Albright CF. Recent progress in the medicinal chemistry of gamma-secretase inhibitors. Curr Top Med Chem. 2008;8(1):17-33. PMID: 18220929.

M4102

MK-1775

NEW

5 mg
10 mg

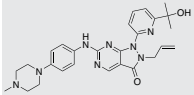

$C_{27}H_{32}N_8O_2$ FW: 500.6 [955365-80-7] ≥98%

Wee1 inhibitor that regulates the G2 mitosis checkpoint in response to DNA damage. It induces double-stranded DNA breaks in acute myelogenous leukemia cells and improves survival rates in other cancer models.

Qi W, Xie C, Li C, et al. CHK1 plays a critical role in the anti-leukemic activity of the wee1 inhibitor MK-1775 in acute myeloid leukemia cells. J Hematol Oncol. 2014 Aug 1;7:53. PMID: 25084614.

Van Linden AA, Baturin D, Ford JB, et al. Inhibition of Wee1 sensitizes cancer cells to antimetabolite chemotherapeutics in vitro and in vivo, independent of p53 functionality. Mol Cancer Ther. 2013 Dec;12(12):2675-84. PMID: 24121103.

M4004

MK-2461

NEW

1 mg
5 mg

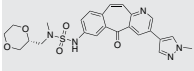

$C_{24}H_{25}N_5N_5S$ FW: 495.55 [917879-39-1] ≥98%

Inhibitor of MET, FGFR, and PDGFR. It decreases tumor growth and size in models of glioblastoma and gastric cancer.

Katz JD, Jewell JP, Guerin DJ, et al. Discovery of a 5H-benzo[4,5]cyclohepta[1,2-b]pyridin-5-one (MK-2461) inhibitor of c-Met kinase for the treatment of cancer. J Med Chem. 2011 Jun 23;54(12):4092-108. PMID: 21608528.

Pan BS, Chan GK, Chenard M, et al. MK-2461, a novel multitargeted kinase inhibitor, preferentially inhibits the activated c-Met receptor. Cancer Res. 2010 Feb 15;70(4):1524-33. PMID: 20145145.

M4000

MK-2206

1 mg
5 mg
25 mg

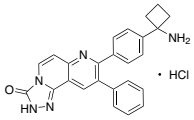

$C_{25}H_{22}ClN_5O$ FW: 443.93 [1032349-77-1] ≥99%

Akt inhibitor. It induces cell cycle arrest in hepatocellular carcinoma cells and inhibits proliferation of non-small cell lung cancer cells and thyroid cancer cells.

Zhao YY, Tian Y, Zhang J, et al. Effects of an oral allosteric AKT inhibitor (MK-2206) on human nasopharyngeal cancer in vitro and in vivo. Drug Des Devel Ther. 2014 Oct 10;8:1827-37. pMID: 25336925.

Burke JF, Schlosser L, Harrison AD, et al. MK-2206 Causes Growth Suppression and Reduces Neuroendocrine Tumor Marker Production in Medullary Thyroid Cancer Through Akt Inhibition. Ann Surg Oncol. 2013 Nov;20(12):3862-8. PMID: 23900743.

Jiao P, Zhou YS, Yang JX, et al. MK-2206 induces cell cycle arrest and apoptosis in HepG2 cells and sensitizes TRAIL-mediated cell death. Mol Cell Biochem. 2013 Jun 25. [Epub ahead of print] PMID: 23797319.

M4455

MLN-2238

NEW

1 mg
5 mg
10 mg

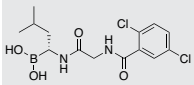

$C_{14}H_{19}BCl_2N_2O_4$ FW: 361.03 [1072833-77-2] ≥99%

Proteasome inhibitor and miR33b modulator. It downregulates Pim-1 activity in multiple myeloma cells.

Tian Z, Zhao JJ, Tai YT, et al. Investigational agent MLN9708/2238 targets tumor-suppressor miR33b in MM cells. Blood. 2012 Nov 8;120(19):3958-67. PMID: 22983447.

M4454

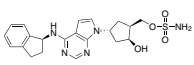

MLN-4924

Pevonedistat

$C_{21}H_{25}N_5O_4S$ FW: 443.16 [905579-51-3] ≥99%

1 mg
5 mg
25 mg

Nedd8-activating enzyme inhibitor that blocks proteasomal cullin protein neddylation by Cullin-RING E3 ubiquitin ligases. It induces cell cycle arrest, senescence, autophagy, and apoptosis in various cell lines. It also decreases release of pro-inflammatory cytokines and stimulates accumulation of HIF-1.

Yan ZH, Burkhardt A, Loke HK, et al. Quantifiable analysis of cellular pathway inhibition of a Nedd8-activating enzyme inhibitor, MLN4924, using AlphaScreen. Anal Biochem. 2013 Aug 15;439(2):109-15. PMID: 23624319.

Li L, Liu B, Dong T, et al. Neddylation pathway regulates the proliferation and survival of macrophages. Biochem Biophys Res Commun. 2013 Mar 15;432(3):494-8. PMID: 23416079.

Zhao Y, Xiong X, Jia L, et al. Targeting Cullin-RING ligases by MLN4924 induces autophagy via modulating the HIF1-REDD1-TSC1-mTORC1-DEPTOR axis. Cell Death Dis. 2012 Sep 6;3:e386. PMID: 22951983.

M4452

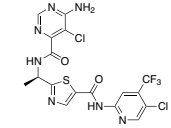

MLN2480

$C_{17}H_{12}Cl_2F_3N_7O_2S$ FW: 506.3 [1096708-71-2] ≥98%

1 mg
5 mg

Raf inhibitor that suppresses proliferation of cancer cells.

http://clinicaltrials.gov/show/NCT01425008

M4652

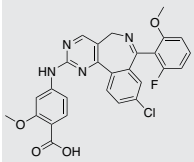

MLN8237

NEW

Alisertib

$C_{27}H_{20}ClFN_4O_4$ FW: 518.92 [1028486-01-2] ≥98%

1 mg
5 mg
10 mg

Aurora kinase A inhibitor. It prevents mitotic spindle formation, inhibits VEGF secretion, and induces cell cycle arrest, aneuploidy, and apoptosis in bladder cancer cells.

Romain C, Paul P, Kim KW, et al. Targeting Aurora kinase-A downregulates cell proliferation and angiogenesis in neuroblastoma. J Pediatr Surg. 2014 Jan;49(1):159-65. PMID: 24439602.

Kelly KR, Shea TC, Goy A, et al. Phase I study of MLN8237-investigational Aurora A kinase inhibitor-in relapsed/refractory multiple myeloma, Non-Hodgkin lymphoma and chronic lymphocytic leukemia. Invest New Drugs. 2013 Dec 20. [Epub ahead of print]. PMID: 24352795.

Zhou N, Singh K, Mir MC, et al. The investigational Aurora kinase A inhibitor MLN8237 induces defects in cell viability and cell-cycle progression in malignant bladder cancer cells in vitro and in vivo. Clin Cancer Res. 2013 Apr 1;19(7):1717-28. PMID: 23403633.

M5610

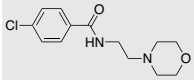

Moclobemide

NEW

$C_{13}H_{17}ClN_2O_2$ FW: 268.74 [71320-77-9] ≥98%

10 mg
25 mg
100 mg

MAO-A inhibitor used to treat depression and anxiety. It also suppresses LPS-induced increases in IL-1β and TNF-α expression in glial cells, increases latency time in animal models of thermal pain, and induces hippocampal neurogenesis.

Bielecka AM, Paul-Samojedny M, Obuchowicz E. Moclobemide exerts anti-inflammatory effect in lipopolysaccharide-activated primary mixed glial cell culture. Naunyn Schmiedebergs Arch Pharmacol. 2010 Dec;382(5-6):409-17. PMID: 20811738.

Li YF, Zhang YZ, Liu YQ, et al. Moclobemide up-regulates proliferation of hippocampal progenitor cells in chronically stressed mice. Acta Pharmacol Sin. 2004 Nov;25(11):1408-12. PMID: 15525460.

Schreiber S, Getslev V, Weizman A, et al. The antinociceptive effect of moclobemide in mice is mediated by noradrenergic pathways. Neurosci Lett. 1998 Sep 11;253(3):183-6. PMID: 9792241.

M5727

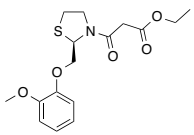

Moguisteine

$C_{16}H_{21}NO_5S$ FW: 339.41 [119637-67-1] ≥98%

100 mg
250 mg
1 g

Potential ATP-sensitive K^+ channel blocker and irritant receptor antagonist used to prevent chronic cough.

Luo YL, Li PB, Zhang CC, et al. Effects of four antitussives on airway neurogenic inflammation in a guinea pig model of chronic cough induced by cigarette smoke exposure. Inflamm Res. 2013 Dec;62(12):1053-61. PMID: 24085318.

Morita K, Onodera K, Kamei J. Inhaled pinacidil, an ATP-sensitive K^+ channel opener, and moguisteine have potent antitussive effects in guinea pigs. Jpn J Pharmacol. 2002 Jun;89(2):171-5. PMID: 12120760.

Sant'Ambrogio G, Sant'Ambrogio FB. Action of moguisteine on the activity of tracheobronchial rapidly adapting receptors in the dog. Eur Respir J. 1998 Feb;11(2):339-44. PMID: 9551735.

M5746

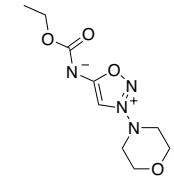

Molsidomine

500 mg
1 g
5 g

$C_9H_{14}N_4O_4$ FW: 242.23 [25717-80-0] ≥98%

NO donor and annexin A2 inhibitor. It inhibits PDGF-induced smooth muscle cell migration, suppresses carotid artery neointima formation, and prevents activated platelet adhesion.

Harnek J, Zoucas E, de Sá VP, et al. Intimal hyperplasia in balloon dilated coronary arteries is reduced by local delivery of the NO donor, SIN-1 via a cGMP-dependent pathway. BMC Cardiovasc Disord. 2011 Jun 11;11:30. PMID: 21663688.

Won KJ, Lee P, Jung SH, et al. 3-morpholinosydnonimine participates in the attenuation of neointima formation via inhibition of annexin A2-mediated vascular smooth muscle cell migration. Proteomics. 2011 Jan;11(2):193-201. PMID: 21204247.

Cardoso MH, Morganti RP, Lilla S, et al. The role of superoxide anion in the inhibitory effect of SIN-1 in thrombin-activated human platelet adhesion. Eur J Pharmacol. 2010 Feb 10;627(1-3):229-34. PMID: 19895807.

M5752

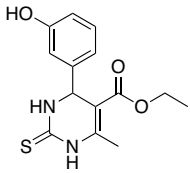

Monastrol

1 mg
5 mg

$C_{14}H_{16}N_2O_3S$ FW: 292.35 [254753-54-3] ≥95%

Pyrimidine derivative and kinesin Eg5 inhibitor. It prevents mitotic spindle formation, induces dendrite growth in neurons, and causes mitotic arrest in HeLa cells.

Chin GM, Herbst R. Induction of apoptosis by monastrol, an inhibitor of the mitotic kinesin Eg5, is independent of the spindle checkpoint. Mol Cancer Ther. 2006 Oct;5(10):2580-91. PMID: 17041103.

Maliga Z, Mitchison TJ. Small-molecule and mutational analysis of allosteric Eg5 inhibition by monastrol. BMC Chem Biol. 2006 Feb 27;6:2. PMID: 16504166.

Yoon SY, Choi JE, Huh JW, et al. Monastrol, a selective inhibitor of the mitotic kinesin Eg5, induces a distinctive growth profile of dendrites and axons in primary cortical neuron cultures. Cell Motil Cytoskeleton. 2005 Apr;60(4):181-90. PMID: 15751098.

M5753

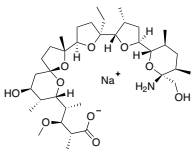

Monensin Sodium

500 mg
1 g
5 g

$C_{36}H_{61}O_{11}Na$ FW: 692.86 [22373-78-0] ≥98%

Ionophore and inhibitor of autophagy commercially used in livestock feed. It inhibits autophagy, interfering with the fusion of the autophagosome and the lysosome.

Choi HS, Jeong EH, Lee TG, et al. Autophagy Inhibition with Monensin Enhances Cell Cycle Arrest and Apoptosis Induced by mTOR or Epidermal Growth Factor Receptor Inhibitors in Lung Cancer Cells. Tuberc Respir Dis (Seoul). 2013 Jul;75(1):9-17. PMID: 23946753.

Lavine MD, Arrizabalaga G. Analysis of monensin sensitivity in Toxoplasma gondii reveals autophagy as a mechanism for drug induced death. PLoS One. 2012;7(7):e42107. PMID: 22848721.

M5853

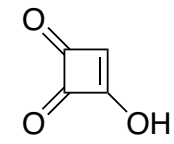

Moniliformin

1 mg
5 mg

$C_4H_2O_3$ FW: 98.06 [31876-38-7] ≥98%

Mycotoxin and potential pyruvate dehydrogenase inhibitor found in *Fusarium*. It decreases collagen synthesis,suppresses endocytosis, and may damage myocardial tissue.

Scarpino V, Blandino M, Negre M, et al. Moniliformin analysis in maize samples from North-West Italy using multifunctional clean-up columns and the LC-MS/MS detection method. Food Addit Contam Part A Chem Anal Control Expo Risk Assess. 2013;30(5):876-84. PMID: 23731218.

Ficheux AS, Sibiril Y, Parent-Massin D. Effects of beauvericin, enniatin b and moniliformin on human dendritic cells and macrophages: an in vitro study. Toxicon. 2013 Sep;71:1-10. PMID: 23685117.

von Bargen KW, Lohrey L, Cramer B, et al. Analysis of the *Fusarium* mycotoxin moniliformin in cereal samples using 13C2-moniliformin and high-resolution mass spectrometry. J Agric Food Chem. 2012 Apr 11;60(14):3586-91. PMID: 22428531.

M5756

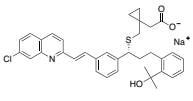

Montelukast Sodium

10 mg
25 mg
100 mg

$C_{35}H_{35}ClNO_3S\,Na$ FW: 608.17 [151767-02-1] ≥98%

CysLT1 antagonist used to treat allergic rhinitis and asthma. It also attenuates cough, decreases eosinophil infiltration, suppresses expression of pro-inflammatory cytokines, and lessens neuropathic pain in chronic constrictive injury models.

Zhou C, Shi X, Huang H, et al. Montelukast Attenuates Neuropathic Pain Through Inhibiting p38 Mitogen-Activated Protein Kinase and Nuclear Factor-Kappa B in a Rat Model of Chronic Constriction Injury. Anesth Analg. 2014 May;118(5):1090-6. PMID: 24686047.

Niimi A. Cough, asthma, and cysteinyl-leukotrienes. Pulm Pharmacol Ther. 2013 Oct;26(5):514-9. PMID: 23774534.

M5876

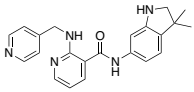

Motesanib

AMG-706

$C_{22}H_{23}N_5O$ FW: 373.45 [453562-69-1] ≥98%

5 mg
10 mg
25 mg

Inhibitor of VEGFR1/2/3, PDGFR, c-Kit, and RET. It inhibits cell proliferation and angiogenesis in breast cancer cells and non-small cell lung cancer cells.

Ellis PM, Al-Saleh K. Multitargeted anti-angiogenic agents and NSCLC: clinical update and future directions. Crit Rev Oncol Hematol. 2012 Oct;84(1):47-58. PMID: 22405734.

Coxon A, Ziegler B, Kaufman S, et al. Antitumor activity of motesanib alone and in combination with cisplatin or docetaxel in multiple human non-small-cell lung cancer xenograft models. Mol Cancer. 2012 Sep 19;11:70. PMID: 22992329.

Coxon A, Bready J, Kaufman S, et al. Anti-tumor activity of motesanib in a medullary thyroid cancer model. J Endocrinol Invest. 2012 Feb;35(2):181-90. PMID: 21422803.

M5877

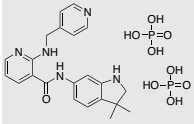

Motesanib Diphosphate

NEW

$C_{22}H_{23}N_5O \bullet 2H_3PO_4$ FW: 569.44 [857876-30-3] ≥98%

5 mg
25 mg
50 mg

Inhibitor of VEGFR1/2/3, PDGFR, c-Kit, and RET. It suppresses cell proliferation and tumor growth in models of non-small cell lung cancer, breast cancer, and medullary thyroid cancer.

Ellis PM, Al-Saleh K. Multitargeted anti-angiogenic agents and NSCLC: clinical update and future directions. Crit Rev Oncol Hematol. 2012 Oct;84(1):47-58. PMID: 22405734.

Coxon A, Ziegler B, Kaufman S, et al. Antitumor activity of motesanib alone and in combination with cisplatin or docetaxel in multiple human non-small-cell lung cancer xenograft models. Mol Cancer. 2012 Sep 19;11:70. PMID: 22992329.

M5675

H-Phe-Val-Pro-Ile-Phe-Thr-His-Ser-Glu-Leu-Gln-Lys-Ile-Arg-Glu-Lys-Glu-Arg-Asn-Lys-Gly-Gln-OH

Motilin, dog

$C_{120}H_{194}N_{36}O_{34}$ FW: 2685.1 [85490-53-5] ≥95%

0.5 mg
1 mg
2.5 mg

Endogenous motilin receptor agonist released during fasting. It modulates gastrointestinal motility, increases lipogenesis and expression of PPARγ, stimulates uptake of fatty acids and glucose, and facilitates GABAergic neurotransmission.

Sanger GJ, Wang Y, Hobson A, et al. Motilin: towards a new understanding of the gastrointestinal neuropharmacology and therapeutic use of motilin receptor agonists. Br J Pharmacol. 2013 Dec;170(7):1323-32. PMID: 23189978.

Feng B, Liu JC, Zhang J, et al. Anxiolytic actions of motilin in the basolateral amygdala. Mol Neurobiol. 2013 Jun;47(3):892-902. PMID: 23307330.

M5776

Phe-Val-Pro-Ile-Phe-Thr-Tyr-Gly-Glu-Leu-Gln-Arg-Met-Gln-Glu-Lys-Glu-Arg-Asn-Lys-Gly-Gln

Motilin, pig

$C_{120}H_{188}N_{34}O_{35}S$ FW: 2699.1 [52906-92-0] ≥98%

0.5 mg
1 mg
2.5 mg

Endogenous motilin agonist involved in enteric movement. It induces intestinal muscle contractions, increases lipogenesis, facilitates GABAergic neurotransmission, and increases uptake of fatty acids and glucose.

Sanger GJ, Wang Y, Hobson A, et al. Motilin: towards a new understanding of the gastrointestinal neuropharmacology and therapeutic use of motilin receptor agonists. Br J Pharmacol. 2013 Dec;170(7):1323-32. PMID: 23189978.

Feng B, Liu JC, Zhang J, et al. Anxiolytic actions of motilin in the basolateral amygdala. Mol Neurobiol. 2013 Jun;47(3):892-902. PMID: 23307330.

M5793

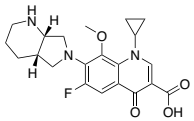

Moxifloxacin Free Base

$C_{21}H_{24}FN_3O_4$ FW: 401.43 [151096-09-2] ≥98%

100 mg
500 mg
1 g

Inhibitor of topoisomerase IV, topoisomerase II, and bacterial DNA gyrase used to treat bacterial ocular, sinus, and lung infections. It inhibits growth of gram negative and gram positive bacteria and suppresses proliferation of some cancer cells.

Wohlkonig A, Chan PF, Fosberry AP, et al. Structural basis of quinolone inhibition of type IIA topoisomerases and target-mediated resistance. Nat Struct Mol Biol. 2010 Sep;17(9):1152-3. PMID: 20802486.

Reuveni D, Halperin D, Shalit I, et al. Moxifloxacin enhances etoposide-induced cytotoxic, apoptotic and anti-topoisomerase II effects in a human colon carcinoma cell line. Int J Oncol. 2010 Aug;37(2):463-71. PMID: 20596674.

Reuveni D, Halperin D, Fabian I, et al. Moxifloxacin increases anti-tumor and anti-angiogenic activity of irinotecan in human xenograft tumors. Biochem Pharmacol. 2010 Apr 15;79(8):1100-7. PMID: 20025849.

M5794

Moxifloxacin Hydrochloride

100 mg
500 mg
1 g

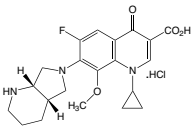

$C_{21}H_{24}FN_3O_4 \bullet HCl$ FW: 437.89 [186826-86-8] ≥98%

Inhibitor of topoisomerase IV, topoisomerase II, and bacterial DNA gyrase used to treat bacterial ocular, sinus, and lung infections. It also enhances cytotoxicity of concurrently administered chemotherapeutics.

Wohlkonig A, Chan PF, Fosberry AP, et al. Structural basis of quinolone inhibition of type IIA topoisomerases and target-mediated resistance. Nat Struct Mol Biol. 2010 Sep;17(9):1152-3. PMID: 20802486.

Reuveni D, Halperin D, Shalit I, et al. Moxifloxacin enhances etoposide-induced cytotoxic, apoptotic and anti-topoisomerase II effects in a human colon carcinoma cell line. Int J Oncol. 2010 Aug;37(2):463-71. PMID: 20596674.

Reuveni D, Halperin D, Fabian I, et al. Moxifloxacin increases anti-tumor and anti-angiogenic activity of irinotecan in human xenograft tumors. Biochem Pharmacol. 2010 Apr 15;79(8):1100-7. PMID: 20025849.

M7200

MS436

NEW

5 mg
25 mg
100 mg

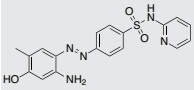

$C_{18}H_{17}N_5O_3S$ FW: 383.43 [1395084-25-9] ≥98%

BRD4 inhibitor. It decreases production of NO and pro-inflammatory cytokines.

Zhang G, Plotnikov AN, Rusinova E, et al. Structure-guided design of potent diazobenzene inhibitors for the BET bromodomains. J Med Chem. 2013 Nov 27;56(22):9251-64. PMID: 24144283.

M8007

Mubritinib, Free Base

5 mg
25 mg
100 mg

TAK-165

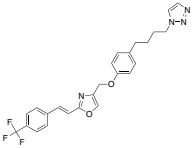

$C_{25}H_{23}F_3N_4O_2$ FW: 468.47 [366017-09-6] ≥98%

EGFR2 inhibitor that suppresses growth of bladder cancer, kidney cancer, and prostate cancer cells.

Nagasawa J, Mizokami A, Koshida K, et al. Novel HER2 selective tyrosine kinase inhibitor, TAK-165, inhibits bladder, kidney and androgen-independent prostate cancer in vitro and in vivo. Int J Urol. 2006 May;13(5):587-92. PMID: 16771730.

M9608

Myclobutanil

5 g
10 g
50 g

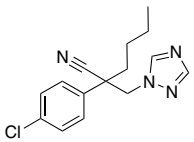

$C_{15}H_{17}ClN_4$ FW: 288.78 [88671-89-0] ≥97%

14-α demethylase inhibitor that inhibits ergosterol synthesis and fungal cell wall formation. It also weakly inhibits testosterone production.

Goetz AK, Rockett JC, Ren H, et al. Inhibition of rat and human steroidogenesis by triazole antifungals. Syst Biol Reprod Med. 2009 Dec;55(5-6):214-26. PMID: 19938956.

Schnabel G, Jones AL. The 14alpha-Demethylasse(CYP51A1) Gene is Overexpressed in Venturia inaequalis Strains Resistant to Myclobutanil. Phytopathology. 2001 Jan;91(1):102-10. PMID: 18944284.

M9710

Mycophenolic Acid

50 mg
250 mg
500 mg

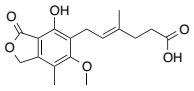

$C_{17}H_{20}O_6$ FW: 320.34 [24280-93-1] ≥98%

PPARγ agonist, IMPDH inhibitor, and microtubule polymerization inhibitor used to prevent transplant rejection. It inhibits B cell activation, induces necrotic cell death in B and T lymphocytes, induces cell cycle arrest in breast cancer cells, and decreases intracellular stores of GTP.

Rinaldelli E, Panattoni A, Luvisi A, et al. Effect of mycophenolic acid on trans-plasma membrane electron transport and electric potential in virus-infected plant tissue. Plant Physiol Biochem. 2012 Nov;60:137-40. PMID: 22935477.

Eickenberg S, Mickholz E, Jung E, et al. Mycophenolic acid counteracts B cell proliferation and plasmablast formation in patients with systemic lupus erythematosus. Arthritis Res Ther. 2012;14(3):R110. PMID: 22571761.

Zheng ZH, Yang Y, Lu XH, et al. Mycophenolic acid induces adipocyte-like differentiation and reversal of malignancy of breast cancer cells partly through PPARγ. Eur J Pharmacol. 2011 May 1;658(1):1-8. PMID: 21349264.

M9643

Myelin Basic Protein (1-11), human

1 mg
2 mg
5 mg

Ac-Ala-Ser-Gln-Lys-Arg-Pro-Ser-Gln-Arg-His-Gly-OH

$C_{52}H_{88}N_{22}O_{17}$ FW: 1293.42 [106128-98-7] ≥95%

Immunodominant peptide epitope occurring in multiple sclerosis. It is recognized by T cells and it decreases IL-12 expression in EAE models.

Buenafe AC, Sherwood C, Moes N, et al. Recombinase-activating gene 1-associated expression of the myelin basic protein 1-11-specific transgenic T-cell receptor in H-2b mice. J Neurosci Res. 2009 Jan;87(1):42-9. PMID: 18752298.

Zhang GX, Xu H, Kishi M, et al. The role of IL-12 in the induction of intravenous tolerance in experimental autoimmune encephalomyelitis. J Immunol. 2002 Mar 1;168(5):2501-7. PMID: 11859144.

M9646

Myelin Basic Protein (68-82), guinea pig

1 mg
2 mg
5 mg

MBP

H-Tyr-Gly-Ser-Leu-Pro-Gln-Lys-Ser-Gln-Arg-Ser-Gln-Asp-Glu-Asn-OH

$C_{71}H_{113}N_{23}O_{28}$ FW: 1736.8 ≥95%

Immunodominant peptide epitope occurring in multiple sclerosis. It may induce immune tolerance and downregulate T cell reactivity to myelin.

Mantzourani ED, Platts JA, Brancale A, et al. Molecular dynamics at the receptor level of immunodominant myelin basic protein epitope 87-99 implicated in multiple sclerosis and its antagonists altered peptide ligands: triggering of immune response. J Mol Graph Model. 2007 Sep;26(2):471-81. PMID: 17392002.

Liu JQ, Bai XF, Shi FD, et al. Inhibition of experimental autoimmune encephalomyelitis in Lewis rats by nasal administration of encephalitogenic MBP peptides: synergistic effects of MBP 68-86 and 87-99. Int Immunol. 1998 Aug;10(8):1139-48. PMID: 9723700.

M9644

Myelin Basic Protein (87-99), guinea pig/human

1 mg
2 mg
5 mg

MBP

H-Tyr-Gly-Ser-Leu-Pro-Gln-Lys-Ser-Gln-Arg-Ser-Gln-Asp-Glu-Asn-OH

$C_{74}H_{114}N_{20}O_{17}$ FW: 1555.8 ≥95%

Immunodominant peptide epitope occurring in multiple sclerosis. It may induce immune tolerance and downregulate T cell reactivity to myelin.

Mantzourani ED, Platts JA, Brancale A, et al. Molecular dynamics at the receptor level of immunodominant myelin basic protein epitope 87-99 implicated in multiple sclerosis and its antagonists altered peptide ligands: triggering of immune response. J Mol Graph Model. 2007 Sep;26(2):471-81. PMID: 17392002.

Liu JQ, Bai XF, Shi FD, et al. Inhibition of experimental autoimmune encephalomyelitis in Lewis rats by nasal administration of encephalitogenic MBP peptides: synergistic effects of MBP 68-86 and 87-99. Int Immunol. 1998 Aug;10(8):1139-48. PMID: 9723700.

M9645

Myelin Oligodendrocyte Glycoprotein (35-55), rat

1 mg
2 mg
5 mg

MOG (35-55)

Met-Glu-Val-Gly-Trp-Tyr-Arg-Ser-Pro-Phe-Ser-Arg-Val-Val-His-Leu-Tyr-Arg-Asn-Gly-Lys

$C_{118}H_{177}N_{35}O_{29}S$ FW: 2582 [163913-87-9] ≥98%

Oligodendrocyte antigen and peptide used to stimulate an immune response against myelin and induce EAE.

Zhu D, Liu M, Yang Y, et al. Ginsenoside Rd ameliorates experimental autoimmune encephalomyelitis in C57BL/6 mice. J Neurosci Res. 2014 May 2. [Epub ahead of print]. PMID: 24798871.

Sosa RA, Murphey C, Ji N, et al. The kinetics of myelin antigen uptake by myeloid cells in the central nervous system during experimental autoimmune encephalomyelitis. J Immunol. 2013 Dec 15;191(12):5848-57. PMID: 24227784.

M9356

Myomodulin

1 mg
2 mg
5 mg

Myomoduline A

H-Pro-Met-Ser-Met-Leu-Arg-Leu-NH_2

$C_{36}H_{67}N_{11}O_8S_2$ FW: 846.13 [110570-93-9] ≥95%

Na^+/K^+ pump inhibitor found in molluscs and insects. It alters heart neuron spike and burst frequency, modulates K^+, Na^+, and Ca^{2+} current amplitudes, and increases gut muscle contraction frequency.

Tobin AE, Calabrese RL. Myomodulin increases Ih and inhibits the NA/K pump to modulate bursting in leech heart interneurons. J Neurophysiol. 2005 Dec;94(6):3938-50. PMID: 16093342.

Britz FC, Deitmer JW. Membrane responses of the leech giant glial cell to the peptide transmitter myomodulin. Peptides. 2002 Dec;23(12):2117-25. PMID: 12535690.

M9367

Myricetin

10 mg
25 mg

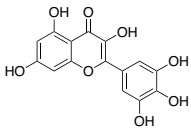

Cannabiscetin; Delphidenolon 1575

$C_{15}H_{10}O_8$ FW: 318.23 [529-44-2] ≥98%

COMT inhibitor found in fruits and vegetables. It exhibits a wide variety of biological activities, including decreasing cholesterol, triglyceride, and lipid levels, inhibiting amyloid-β-induced neurodegeneration, activating Wnt/β-catenin signaling to increase osteoclast differentiation, and inducing cell cycle arrest in oral squamous cell carcinoma cells.

Maggioni D, Nicolini G, Rigolio R, et al. Myricetin and Naringenin Inhibit Human Squamous Cell Carcinoma Proliferation and Migration In Vitro. Nutr Cancer. 2014 Sep 25:1-11. PMID: 25256786.

Kandasamy N, Ashokkumar N. Renoprotective effect of myricetin restrains dyslipidemia and renal mesangial cell proliferation by the suppression of sterol regulatory element binding proteins in an experimental model of diabetic nephropathy. Eur J Pharmacol. 2014 Sep 18. [Epub ahead of print]. PMID: 25240712.

Kandasamy N, Ashokkumar N. Protective effect of bioflavonoid myricetin enhances carbohydrate metabolic enzymes and insulin signaling molecules in streptozotocin-cadmium induced diabetic nephrotoxic rats. Toxicol Appl Pharmacol. 2014 Sep 1;279(2):173-85. PMID: 24923654.

M9634

Myriocin

1 mg
5 mg
10 mg

$C_{21}H_{39}NO_6$ FW: 401.54 [35891-70-4] ≥99%

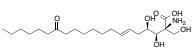

Atypical amino acid, parent compound of fingolimod, and serine palmitoyltransferase inhibitor found in *Isaria sinclairi*. It prevents sphingolipid formation, decreases levels of CD4+ lymphocytes, and induces cell cycle arrest in melanoma cells.

Wadsworth JM, Clarke DJ, McMahon SA, et al. The chemical basis of serine palmitoyltransferase inhibition by myriocin. J Am Chem Soc. 2013 Sep 25;135(38):14276-85. PMID: 23957439.

Lee YS, Choi KM, Choi MH, et al. Serine palmitoyltransferase inhibitor myriocin induces growth inhibition of B16F10 melanoma cells through G(2) /M phase arrest. Cell Prolif. 2011 Aug;44(4):320-9. PMID: 21645154.

Chiba K, Matsuyuki H, Maeda Y, et al. Role of sphingosine 1-phosphate receptor type 1 in lymphocyte egress from secondary lymphoid tissues and thymus. Cell Mol Immunol. 2006 Feb;3(1):11-9. PMID: 16549044.

M9368

Myristicin

100 mg
500 mg
1 g

$C_{11}H_{12}O_3$ FW: 192.21 [607-91-0] ≥97%

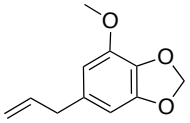

Natural product found in spices and umbelliferous plants. It induces apoptosis in leukemia cells, decreases pro-inflammatory cytokine expression in alveolar epithelial cells, and suppresses growth of *Clostridium*, *Enterococcus*, and *Candida*.

Martins C, Doran C, Silva IC, et al. Myristicin from nutmeg induces apoptosis via the mitochondrial pathway and down regulates genes of the DNA damage response pathways in human leukaemia K562 cells. Chem Biol Interact. 2014 Jul 25;218:1-9. PMID: 24792648.

Lim HJ, Woo KW, Lee KR, et al. Inhibition of Proinflammatory Cytokine Generation in Lung Inflammation by the Leaves of Perilla frutescens and Its Constituents. Biomol Ther (Seoul). 2014 Jan;22(1):62-7. PMID: 24596623.

Fraternale D, Genovese S, Ricci D. Essential oil composition and antimicrobial activity of aerial parts and ripe fruits of Echinophora spinosa (Apiaceae) from Italy. Nat Prod Commun. 2013 Apr;8(4):527-30. PMID: 23738471.

N0205

Nabumetone

5 g
25 g

$C_{15}H_{16}O_2$ FW: 228.29 [42924-53-8] ≥98%

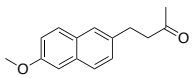

Derivative of 1-naphthalenacetic acid, NSAID, and COX-2 inhibitor used to treat pain and inflammation. It also inhibits intestinal carcinogenesis and induces apoptosis in colon cancer cells.

Paul S, Das N, Ghosh S. The effects of aceclofenac and nabumetone in osteoarthritis. JNMA J Nepal Med Assoc. 2009 Apr-Jun;48(174):121-5. PMID: 20387351.

Roy HK, Karoski WJ, Ratashak A, et al. Chemoprevention of intestinal tumorigenesis by nabumetone: induction of apoptosis and Bcl-2 downregulation. Br J Cancer. 2001 May 18;84(10):1412-6. PMID: 11355956.

N0114

Nadifloxacin

25 mg
100 mg
500 mg

$C_{19}H_{21}FN_2O_4$ FW: 360.38 [124858-35-1] ≥98%

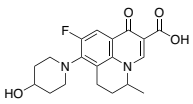

Bacterial DNA gyrase inhibitor used to treat acne vulgaris. It inhibits *Proponibacterium*-stimulated cytokine expression and decreases production of oxidative radicals by neutrophils.

Takenaka Y, Hayashi N, Takeda M, et al. Glycolic acid chemical peeling improves inflammatory acne eruptions through its inhibitory and bactericidal effects on Propionibacterium acnes. J Dermatol. 2012 Apr;39(4):350-4. PMID: 21950544.

Kuwahara K, Kitazawa T, Kitagaki H, et al. Nadifloxacin, an antiacne quinolone antimicrobial, inhibits the production of proinflammatory cytokines by human peripheral blood mononuclear cells and normal human keratinocytes. J Dermatol Sci. 2005 Apr;38(1):47-55. PMID: 15795123.

Akamatsu H, Sasaki H, Kurokawa I, et al. Effect of nadifloxacin on neutrophil functions. J Int Med Res. 1995 Jan-Feb;23(1):19-26. PMID: 7774755.

N0123

Naftopidil

25 mg
100 mg
500 mg

$C_{24}H_{28}N_2O_3$ FW: 392.49 [57149-07-2] ≥98%

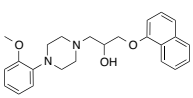

α1-Adrenergic receptor antagonist used to treat BPH. It improves nocturnal polyuria, increases bladder capacity, and inhibits collagen-induced Ca^{2+} mobilization and platelet aggregation.

Castiglione F, Benigni F, Briganti A, et al. Naftopidil for the treatment of benign prostate hyperplasia: a systematic review. Curr Med Res Opin. 2013 Dec 18. [Epub ahead of print]. PMID: 24188134.

Yokoyama O, Aoki Y, Tsujimura A, et al. α(1)-adrenoceptor blocker naftopidil improves sleep disturbance with reduction in nocturnal urine volume. World J Urol. 2011 Apr;29(2):233-8. PMID: 20387069.

Yokoyama O, Yusup A, Oyama N, et al. Improvement of bladder storage function by alpha1-blocker depends on the suppression of C-fiber afferent activity in rats. Neurourol Urodyn. 2006;25(5):461-7. PMID: 16673377.

N7604

Naltriben

0.5 mg
1 mg
2.5 mg

NTB

H-DPhe-Cys-Tyr-D-Trp-Orn-Thr-Pen-Thr-NH_2(Cys2-Pen7)

$C_{50}H_{65}N_{11}O_{11}S_2$ FW: 1060.29 ≥95%

δ2-OR antagonist. It induces anxiety, inhibits antinociceptive activities regulated by δORs, and suppresses opioid-induced reinforcement in conditioned place preference assays.

Sugiyama A, Nagase H, Oka JI, et al. DOR2-selective but not DOR1-selective antagonist abolishes anxiolytic-like effects of the δ opioid receptor agonist KNT-127. Neuropharmacology. 2013 Dec 12;79C:314-320. PMID: 24333676.

Billa SK, Xia Y, Morón JA. Disruption of morphine-conditioned place preference by a delta2-opioid receptor antagonist: study of mu-opioid and delta-opioid receptor expression at the synapse. Eur J Neurosci. 2010 Aug;32(4):625-31. PMID: 20626460.

N0160

NAP Peptide

0.5 mg
1 mg
2.5 mg

Davunetide

H-Asn-Ala-Pro-Val-Ser-Ile-Pro-Gln-OH

$C_{36}H_{60}N_{10}O_{12}$ FW: 824.94 [211439-12-2] ≥95%

Derived from activity-dependent neuroprotective protein. It displays a variety of biological activities, including preventing retinal apoptosis in diabetes models, protecting against oxidative stress, improving memory performance, and increasing life span in ALS models.

Scuderi S, D'Amico AG, Castorina A, et al. Davunetide (NAP) Protects the Retina Against Early Diabetic Injury by Reducing Apoptotic Death. J Mol Neurosci. 2014 Feb 2. [Epub ahead of print]. PMID: 24488575.

Jouroukhin Y, Ostritsky R, Assaf Y, et al. NAP (davunetide) modifies disease progression in a mouse model of severe neurodegeneration: protection against impairments in axonal transport. Neurobiol Dis. 2013 Aug;56:79-94. PMID: 23631872.

N0262

Naphazoline Hydrochloride

25 g
100 g

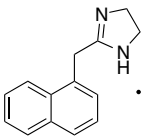

$C_{14}H_{14}N_2 \cdot HCl$ FW: 246.74 [550-99-2] ≥97%

α1-Adrenergic receptor agonist used to treat congestion and ocular pathologies. It also induces autophagy and necrotic cell death in erythroleukemia cells and inhibits erythroid differentiation.

Fuchs R, Schraml E, Leitinger G, et al. α1-Adrenergic drugs modulate differentiation and cell death of human erythroleukemia cells through non adrenergic mechanism. Exp Cell Res. 2011 Oct 1;317(16):2239-51. PMID: 21781962.

Nagane Y, Utsugisawa K, Suzuki S, et al. Topical naphazoline in the treatment of myasthenic blepharoptosis. Muscle Nerve. 2011 Jul;44(1):41-4. PMID: 21491460.

Rikimaru T. Therapeutic management of endobronchial tuberculosis. Expert Opin Pharmacother. 2004 Jul;5(7):1463-70. PMID: 15212597.

N0263

Naphazoline Nitrate

10 g
25 g
100 g

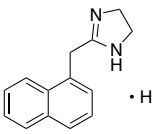

$C_{14}H_{14}N_2 \cdot HNO_3$ FW: 273.29 [5144-52-5] ≥97%

α1-Adrenergic receptor agonist used to treat congestion and ocular pathologies. It also induces autophagy and necrotic cell death in erythroleukemia cells and inhibits erythroid differentiation.

Fuchs R, Schraml E, Leitinger G, et al. α1-Adrenergic drugs modulate differentiation and cell death of human erythroleukemia cells through non adrenergic mechanism. Exp Cell Res. 2011 Oct 1;317(16):2239-51. PMID: 21781962.

Nagane Y, Utsugisawa K, Suzuki S, et al. Topical naphazoline in the treatment of myasthenic blepharoptosis. Muscle Nerve. 2011 Jul;44(1):41-4. PMID: 21491460.

Rikimaru T. Therapeutic management of endobronchial tuberculosis. Expert Opin Pharmacother. 2004 Jul;5(7):1463-70. PMID: 15212597.

N0161

β-Naphthoflavone

1 g
5 g

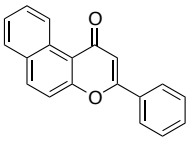

5,6-Benzoflavone

$C_{19}H_{12}O_2$ FW: 272.3 [6051-87-2] ≥98%

AhR agonist and antioxidant. It inhibits cigarette smoke-induced DNA damage and tumor development and induces cell cycle arrest in breast cancer cells.

Wang C, Xu CX, Bu Y, et al. Beta-naphthoflavone (DB06732) mediates estrogen receptor-positive breast cancer cell cycle arrest through AhR-dependent regulation of PI3K/AKT and MAPK/ERK signaling. Carcinogenesis. 2014 Mar;35(3):703-13. PMID: 24163404.

Tilton SC, Givan SA, Pereira CB, et al. Toxicogenomic profiling of the hepatic tumor promoters indole-3-carbinol, 17beta-estradiol and beta-naphthoflavone in rainbow trout. Toxicol Sci. 2006 Mar;90(1):61-72. PMID: 16192472.

Izzotti A, Bagnasco M, Cartiglia C, et al. Modulation of multigene expression and proteome profiles by chemopreventive agents. Mutat Res. 2005 Dec 11;591(1-2):212-23. PMID: 16083920.

N0163

2-(1,8-Naphthyridin-2-ly)phenol

100 mg
500 mg
1 g
5 g

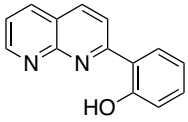

$C_{14}H_{10}N_2O$ FW: 222.24 [65182-56-1] ≥98%

Indirect STAT1 agonist that inhibits cell proliferation in fibrosarcoma cells and breast cancer cells.

Lynch RA, Etchin J, Battle TE, et al. A small-molecule enhancer of signal transducer and activator of transcription 1 transcriptional activity accentuates the antiproliferative effects of IFN-gamma in human cancer cells. Cancer Res. 2007 Feb 1;67(3):1254-61. PMID: 17283162.

N0061

D-Naproxen

5 g
25 g
50 g

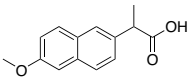

$C_{14}H_{14}O_3$ FW: 230.26 [22204-53-1] ≥98%

NSAID and COX-1/2 inhibitor used to treat pain, fever, and inflammation. It also inhibits influenza virus infection by preventing transcription initiation and replication.

Lejal N, Tarus B, Bouguyon E, et al. Structure-based discovery of the novel antiviral properties of naproxen against the nucleoprotein of influenza A virus. Antimicrob Agents Chemother. 2013 May;57(5):2231-42. PMID: 23459490.

Duggan KC, Walters MJ, Musee J, et al. Molecular basis for cyclooxygenase inhibition by the non-steroidal anti-inflammatory drug naproxen. J Biol Chem. 2010 Nov 5;285(45):34950-9. PMID: 20810665.

N0062

D,L-Naproxen

10 g
25 g
100 g

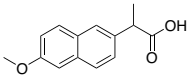

$C_{14}H_{14}O_3$ FW: 230.26 ≥96%

NSAID and COX-1/2 inhibitor used to treat fever, inflammation, and pain. It also inhibits influenza virus infection by preventing initiation of transcription and replication.

Lejal N, Tarus B, Bouguyon E, et al. Structure-based discovery of the novel antiviral properties of naproxen against the nucleoprotein of influenza A virus. Antimicrob Agents Chemother. 2013 May;57(5):2231-42. PMID: 23459490.

Duggan KC, Walters MJ, Musee J, et al. Molecular basis for cyclooxygenase inhibition by the non-steroidal anti-inflammatory drug naproxen. J Biol Chem. 2010 Nov 5;285(45):34950-9. PMID: 20810665.

N0068

Naringenin

5 g
10 g
25 g

4',5,7-Trihydroxyflavanone

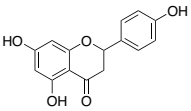

$C_{15}H_{12}O_5$ FW: 272.25 [480-41-1] ≥98%

Found in citrus fruits. It displays many biological activities, including increasing levels of Nrf2 to prevent 6-OHDA-induced neurodegeneration, inhibiting allergen-induced airway inflammation, inducing apoptosis in leukemia cells, suppressing α-SMA and collagen type I expression in fibroblasts, and increasing levels of antioxidative enzymes.

Esmaeili MA, Alilou M. Naringenin attenuates CCl4 -induced hepatic inflammation by the activation of an Nrf2-mediated pathway in rats. Clin Exp Pharmacol Physiol. 2014 Jun;41(6):416-22. PMID: 24684352.

Chtourou Y, Fetoui H, Gdoura R. Protective effects of naringenin on iron-overload-induced cerebral cortex neurotoxicity correlated with oxidative stress. Biol Trace Elem Res. 2014 Jun;158(3):376-83. PMID: 24682942.

Lou H, Jing X, Wei X, et al. Naringenin protects against 6-OHDA-induced neurotoxicity via activation of the Nrf2/ARE signaling pathway. Neuropharmacology. 2014 Apr;79:380-8. PMID: 24333330.

N0069

Naringin

25 g
100 g

Aurantiin

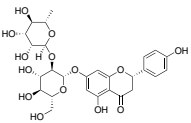

$C_{27}H_{32}O_{14}$ FW: 580.53 [10236-47-2] ≥97%

SERM found in citrus fruits. It exhibits a wide variety of biological activities, including inhibiting release of VEGF in ER+ breast cancer cells, improving colchicine-induced deficits in cognitive performance, attenuating oxidative damage, and suppressing gentamicin-induced pro-inflammatory cytokine expression.

Sahu BD, Tatireddy S, Koneru M, et al. Naringin ameliorates gentamicin-induced nephrotoxicity and associated mitochondrial dysfunction, apoptosis and inflammation in rats: possible mechanism of nephroprotection. Toxicol Appl Pharmacol. 2014 May 15;277(1):8-20. PMID: 24637089.

Li H, Yang B, Huang J, et al. Naringin inhibits growth potential of human triple-negative breast cancer cells by targeting β-catenin signaling pathway. Toxicol Lett. 2013 Jul 18;220(3):219-28. PMID: 23694763.

Wang DM, Yang YJ, Zhang L, et al. Naringin Enhances CaMKII Activity and Improves Long-Term Memory in a Mouse Model of Alzheimer's Disease. Int J Mol Sci. 2013 Mar 11;14(3):5576-86. PMID: 23478434.

N0075

Natamycin

25 mg
50 mg
100 mg

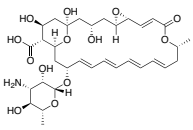

$C_{33}H_{47}NO_{13}$ FW: 665.73 [7681-93-8] ≥98%

Ergosterol inhibitor used to treat keratitis. It increases NALP3 inflammasome activation, activates polyclonal B cells, and inhibits growth of *Aspergillus* and *Fusarium*.

Kallinteri LD, Kostoula OK, Savvaidis IN. Efficacy of nisin and/or natamycin to improve the shelf-life of Galotyri cheese. Food Microbiol. 2013 Dec;36(2):176-81. PMID: 24010596.

Thomas PA, Kaliamurthy J. Mycotic keratitis: epidemiology, diagnosis and management. Clin Microbiol Infect. 2013 Mar;19(3):210-20. PMID: 23398543.

Darisipudi MN, Allam R, Rupanagudi KV, et al. Polyene macrolide antifungal drugs trigger interleukin-1β secretion by activating the NLRP3 inflammasome. PLoS One. 2011;6(5):e19588. PMID: 21625424.

N1610

Necrostatin-1

NEW

5 mg
25 mg
100 mg

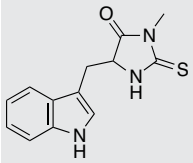

$C_{13}H_{13}N_3OS$ FW: 259.33 [4311-88-0] ≥98%

Receptor interacting protein 1 inhibitor that prevents necroptosis. It improves renal function and pathology in chronic kidney disease models and prevents death of hippocampal neurons in cerebral ischemia models.

Zhu Y, Cui H, Gan H, et al. Necroptosis mediated by receptor interaction protein kinase 1 and 3 aggravates chronic kidney injury of subtotal nephrectomised rats. Biochem Biophys Res Commun. 2015 Jun 12;461(4):575-81. PMID: 25907058.

Yin B, Xu Y, Wei RL, et al. Inhibition of receptor-interacting protein 3 upregulation and nuclear translocation involved in Necrostatin-1 protection against hippocampal neuronal programmed necrosis induced by ischemia/reperfusion injury. Brain Res. 2015 Jun 3;1609:63-71. PMID: 25801119.

Steinwascher S, Nugues AL, Schoeneberger H, et al. Identification of a novel synergistic induction of cell death by Smac mimetic and HDAC inhibitors in acute myeloid leukemia cells. Cancer Lett. 2015 May 28. [Epub ahead of print]. PMID: 26028172.

N0212

Nedaplatin

10 mg
25 mg
50 mg

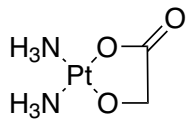

$C_2H_8N_2O_3Pt$ FW: 303.18 [95734-82-0] ≥98%

Platinum-based DNA cross-linker that inhibits DNA synthesis and repair.

Yuan G, Wu L, Huang M, et al. A phase II study of concurrent chemo-radiotherapy with weekly nedaplatin in advanced squamous cell carcinoma of the uterine cervix. Radiat Oncol. 2014 Feb 18;9:55. PMID: 24533532.

Ali I, Wani WA, Saleem K, et al. Platinum compounds: a hope for future cancer chemotherapy. Anticancer Agents Med Chem. 2013 Feb;13(2):296-306. PMID: 22583420.

N1822

Nefazodone Hydrochloride

1 g
5 g
25 g

BMY-13754; MJ-13754-1

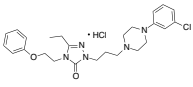

$C_{25}H_{32}ClN_5O_2 \cdot HCl$ FW: 506.48 [82752-99-6] ≥98%

Inhibitor of 5-HT2 receptors, SERT, NET, and hERG K^+ channels used to treat mood disorders. It decreases immobility time in the forced swim test.

Shin DS, Park MJ, Lee HA, et al. A novel assessment of nefazodone-induced hERG inhibition by electrophysiological and stereochemical method. Toxicol Appl Pharmacol. 2014 Feb 1;274(3):361-71. PMID: 24374264.

Clayton AH, Montejo AL. Major depressive disorder, antidepressants, and sexual dysfunction. J Clin Psychiatry. 2006;67 Suppl 6:33-7. PMID: 16848675.

Dremencov E, Gispan-Herman I, Rosenstein M, et al. The serotonin-dopamine interaction is critical for fast-onset action of antidepressant treatment: in vivo studies in an animal model of depression. Prog Neuropsychopharmacol Biol Psychiatry. 2004 Jan;28(1):141-7. PMID: 14687868.

N1721

Nefiracetam

100 mg
250 mg
1 g

DM-9384

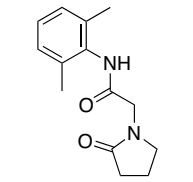

$C_{14}H_{18}N_2O_2$ FW: 246.3 [77191-36-7] ≥98%

NMDA receptor and mGluR5 agonist, N-type and L-type Ca^{2+} channel activator, and α4β2 nAChR potentiator. It decreases seizure frequency and duration, protects against neuronal death, and improves spatial memory and object recognition.

Lu XC, Dave JR, Chen Z, et al. Nefiracetam attenuates post-ischemic nonconvulsive seizures in rats and protects neuronal cell death induced by veratridine and glutamate. Life Sci. 2013 Jun 13;92(22):1055-63. PMID: 23603142.

Malykh AG, Sadaie MR. Piracetam and piracetam-like drugs: from basic science to novel clinical applications to CNS disorders. Drugs. 2010 Feb 12;70(3):287-312. PMID: 20166767.

Moriguchi S, Han F, Shioda N, et al. Nefiracetam activation of CaM kinase II and protein kinase C mediated by NMDA and metabotropic glutamate receptors in olfactory bulbectomized mice. J Neurochem. 2009 Jul;110(1):170-81. PMID: 19457128.

N1744

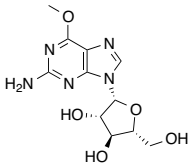

Nelarabine

506U78

$C_{11}H_{15}N_5O_5$ FW: 297.26 [121032-29-9] ≥98%

10 mg
25 mg
100 mg

Guanosine analog and DNA chain terminator used to treat T cell malignancies. It is a prodrug of 9-β-D-arabinofuranosylguanine that inhibits DNA synthesis.

Forcade E, Leguay T, Vey N, et al. Nelarabine for T cell acute lymphoblastic leukemia relapsing after allogeneic hematopoietic stem cell transplantation: an opportunity to improve survival. Biol Blood Marrow Transplant. 2013 Jul;19(7):1124-6. PMID: 23648236.

Robak T, Robak P. Purine nucleoside analogs in the treatment of rarer chronic lymphoid leukemias. Curr Pharm Des. 2012;18(23):3373-88. PMID: 22591387.

N1755

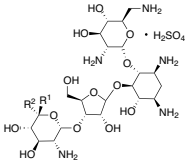

Neomycin B: R^1 = H, R^2 = CH_2NH_2
Neomycin C: R^2 = CH_2NH_2, R^1 = H

Neomycin Sulfate

$C_{23}H_{46}N_6O_{13} \cdot H_2SO_4$ FW: 908.9 [1405-10-3] ≥98%

1 g
5 g
10 g
25 g
100 g

Inhibitor of protein translation inhibitor, TRPV1 receptors, and P2X receptors. It also inhibits bacterial RNase P and bacterial T box antiterminator RNA, suppresses mammalian RNA splicing, and prevents presynaptic release of acetylcholine and norepinephrine in superior cervical ganglia.

Wang L, Pulk A, Wasserman MR, et al. Allosteric control of the ribosome by small-molecule antibiotics. Nat Struct Mol Biol. 2012 Sep;19(9):957-63. PMID: 22902368.

Bongartz EV, Rettinger J, Hausmann R. Aminoglycoside block of P2X2 receptors heterologously expressed in Xenopus laevis oocytes. Purinergic Signal. 2010 Dec;6(4):393-403. PMID: 21437010.

N1656

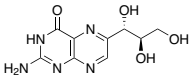

D-(+)-Neopterin

$C_9H_{11}N_5O_4$ FW: 253.21 [2009-64-5] ≥98%

10 mg

Endogenous pteridine metabolite of GTP used as an endogenous biomarker of cellular immune response and oxidative stress.

Ahmadzai H, Cameron B, Chui J, et al. Measurement of neopterin, TGF-β1 and ACE in the exhaled breath condensate of patients with sarcoidosis. J Breath Res. 2013 Dec;7(4):046003. PMID: 24091835.

Murr C, Widner B, Wirleitner B, et al. Neopterin as a marker for immune system activation. Curr Drug Metab. 2002 Apr;3(2):175-87. PMID: 12003349.

N1858

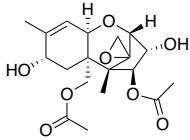

Neosolaniol

$C_{19}H_{26}O_8$ FW: 382.4 [36519-25-2] ≥98%

1 mg
5 mg

Mycotoxin found in *Fusarium*. It is cytotoxic to dividing cells and increases large platelet counts.

Monbaliu S, Van Poucke C, Detavernier C, et al. Occurrence of mycotoxins in feed as analyzed by a multi-mycotoxin LC-MS/MS method. J Agric Food Chem. 2010 Jan 13;58(1):66-71. PMID: 19994896.

Gottschalk C, Barthel J, Engelhardt G, et al. Occurrence of type A trichothecenes in conventionally and organically produced oats and oat products. Mol Nutr Food Res. 2007 Dec;51(12):1547-53. PMID: 18030660.

N1757

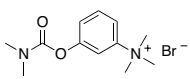

Neostigmine Bromide

$C_{12}H_{19}BrN_2O_2$ FW: 303.2 [114-80-7] ≥92%

250 mg
1 g

AChE inhibitor used to reverse the effects of NMJ blockers and to treat myasthenia gravis. It induces muscular contractions in muscle tissue and improves overall muscle tone.

Dahaba AA, Bornemann H, Hopfgartner E, et al. Effect of sugammadex or neostigmine neuromuscular block reversal on bispectral index monitoring of propofol/remifentanil anaesthesia. Br J Anaesth. 2012 Apr;108(4):602-6. PMID: 22315331.

Cellini J, Zaura Jukic AM, LePard KJ. Neostigmine-induced contraction and nitric oxide-induced relaxation of isolated ileum from STZ diabetic guinea pigs. Auton Neurosci. 2011 Dec 7;165(2):178-90. PMID: 21880552.

N1868

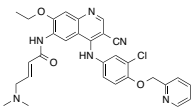

Neratinib

HKI-272

$C_{30}H_{29}ClN_6O_3$ FW: 557.04 [698387-09-6] ≥98%

5 mg
10 mg
25 mg
100 mg

EGFR inhibitor that prevents ligand-induced receptor dimerization by targeting a cysteine residue in the ATP binding pocket of EGFR. It induces cell cycle arrest ad inhibits proliferation in breast cancer cells.

López-Tarruella S, Jerez Y, Márquez-Rodas I, et al. Neratinib (HKI-272) in the treatment of breast cancer. Future Oncol. 2012 Jun;8(6):671-81. PMID: 22764764.

Sánchez-Martín M, Pandiella A. Differential action of small molecule HER kinase inhibitors on receptor heterodimerization: therapeutic implications. Int J Cancer. 2012 Jul 1;131(1):244-52. PMID: 21826647.

N1769

Nerolidol, synthetic

5 g
25 g

$C_{15}H_{26}O$ FW: 222.37 [7212-44-4] ≥96%

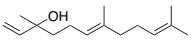

Synthetic AChE inhibitor and F0F1-ATP synthase modulator. It acts as a sedative, inhibits growth of bacteria and fungi, and decreases the mitochondrial transmembrane electric potential to induce cell death in hepatocarcinoma cells.

Nogueira Neto JD, de Almeida AA, da Silva Oliveira J, et al. Antioxidant effects of nerolidol in mice hippocampus after open field test. Neurochem Res. 2013 Sep;38(9):1861-70. PMID: 23765368.

Tao R, Wang CZ, Kong ZW. Antibacterial/antifungal activity and synergistic interactions between polyprenols and other lipids isolated from *Ginkgo* biloba L. leaves. Molecules. 2013 Feb 7;18(2):2166-82. PMID: 23434869.

Kang JS, Kim E, Lee SH, et al. Inhibition of acetylcholinesterases of the pinewood nematode, Bursaphelenchus xylophilus, by phytochemicals from plant essential oils. Pestic Biochem Physiol. 2013 Jan;105(1):50-6. PMID: 24238290.

N1873

Nesiritide Acetate

Please inquire

H-Ser-Pro-Lys-Met-Val-Gln-Gly-Ser-Gly-Cys-Phe-Gly-Arg-Lys-Met-Asp-Arg-Ile-Ser-Ser-Ser-Ser-Gly-Leu-Gly-Cys-Lys-Val-Leu-Arg-Arg-His-OH (Cys10-Cys26)

B-type natriuretic peptide; Brain natriuretic peptide; BNP

$C_{143}H_{244}N_{50}O_{42}S_4$ FW: 3464.1 [114471-18-0] ≥95%

Recombinant derivative of BNP and NPR-A agonist used to treat congestive heart failure. It decreases levels of CD8+ T cells and pro-inflammatory cytokines, suppresses generation of ROS, and inhibits cardiomyocyte apoptosis.

Shaw SM, Critchley WR, Puchalka CM, et al. Brain natriuretic peptide induces CD8+ T cell death via a caspase 3 associated pathway--implications following heart transplantation. Transpl Immunol. 2012 Mar;26(2-3):119-22. PMID: 22138041.

Gassanov N, Biesenbach E, Caglayan E, et al. Natriuretic peptides in therapy for decompensated heart failure. Eur J Clin Pharmacol. 2012 Mar;68(3):223-30. PMID: 21901345.

N1976

Netilmicin Pentasulfate

5 mg
10 mg
25 mg

Certomycin; Netromycin; Zetamicin

$(C_{21}H_{41}N_5O_7)_2\ 5H_2SO_4$ FW: 1441.56 [56391-57-2] ≥98%

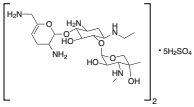

Protein translation inhibitor that displays activity against gram negative and gram positive bacteria. It also decreases melanocyte viability, tyrosinase activity, and melanin production.

Wrześniok D, Beberok A, Otreba M, et al. Netilmicin-induced modulation of melanogenesis in HEMa-LP melanocytes. Acta Pol Pharm. 2013 Sep-Oct;70(5):803-8. PMID: 24147358.

Liu TX, Xue XD, Wei LH, et al. Study of plasmid-mediated 16S rRNA methylase genes and drug-resistant transferability of *Acinetobacter* baumannii isolated from burn ward. Zhonghua Shao Shang Za Zhi. 2009 Apr;25(2):98-102. PMID: 19799032.

N1977

Neurokinin A (4-10)

1 mg
2 mg
5 mg

H-Asp-Ser-Phe-Val-Gly-Leu-Met-NH_2

Substance K

$C_{34}H_{54}N_8O_{10}S$ FW: 766.92 [97559-35-8] ≥95%

Endogenous NK1/2 receptor agonist. It induces contraction in ileal smooth muscle cells, contributes to nociceptive activity, expression of inflammatory cytokines, and induces bronchoconstriction.

Sun J, Ramnath RD, Tamizhselvi R, et al. Neurokinin A engages neurokinin-1 receptor to induce NF-kappaB-dependent gene expression in murine macrophages: implications of ERK1/2 and PI 3-kinase/Akt pathways. Am J Physiol Cell Physiol. 2008 Sep;295(3):C679-91. PMID: 18596216.

Fusco M, D'Andrea G, Miccichè F, et al. Neurogenic inflammation in primary headaches. Neurol Sci. 2003 May;24 Suppl 2:S61-4. PMID: 12811594.

N1978

Neurokinin B

1 mg
2 mg
5 mg

Asp-Met-His-Asp-Phe-Phe-Val-Gly-Leu-Met-NH_2

$C_{55}H_{79}N_{13}O_{14}S_2$ FW: 1210.45 [86933-75-7] ≥95%

Endogenous NK3 receptor agonist used as a biomarker to measure hypertension and pre-eclampsia. It is co-expressed with kisspeptin and dynorphin A. It induces contraction in ileal smooth muscle cells and decreases toxic effects of amyloid-β.

Ichiki T, Kuroishi KN, Gunjigake KK, et al. Neurokinin B activates the formation and bone resorption activity of rat osteoclasts. Neuropeptides. 2011 Jun;45(3):239-44. PMID: 21514667

Mantha AK, Moorthy K, Cowsik SM, et al. Neuroprotective role of neurokinin B (NKB) on beta-amyloid (25-35) induced toxicity in aging rat brain synaptosomes: involvement in oxidative stress and excitotoxicity. Biogerontology. 2006 Feb;7(1):1-17. PMID: 16518716.

N1979 Neuromedin

1 mg
2 mg
5 mg

Neuromedin N

H-Lys-Ile-Pro-Tyr-Ile-Leu-OH

$C_{38}H_{63}N_7O_8$ FW: 745.97 [102577-25-3] ≥95%

Endogenous proneurotensin peptide involved in energy homeostasis. It induces contraction in ileal smooth muscle cells, inhibits reward and reinforcement signaling, and is inactivated by dipeptidyl peptidases and aminopeptidases.

Basir YJ, Knoop FC, Dulka J, et al. Multiple antimicrobial peptides and peptides related to bradykinin and neuromedin N isolated from skin secretions of the pickerel frog, Rana palustris. Biochim Biophys Acta. 2000 Nov 30;1543(1):95-105. PMID: 11087945.

N1980 Neuromedin B, pig

1 mg
2 mg
5 mg

Gly-Asn-Leu-Trp-Ala-Thr-Gly-His-Phe-Met-NH_2

$C_{52}H_{73}N_{15}O_{12}S$ FW: 1132.3 [87096-84-2] ≥95%

Endogenous bombesin-related BB1 receptor agonist involved in endocrine signaling and feeding behavior. It decreases food intake, induces bradycardia, increases osteoblast proliferation and bone formation, and stimulates secretion of LH and FSH.

Boughton CK, Patel SA, Thompson EL, et al. Neuromedin B stimulates the hypothalamic-pituitary-gonadal axis in male rats. Regul Pept. 2013 Nov 10;187:6-11. PMID: 24120470.

N1981 Neuromedin C (18-27), pig

1 mg

Bombesin decapeptide; Gastrin releasing peptide; GRP

Gly-Asn-Leu-Trp-Ala-Thr-Gly-His-Phe-Met-NH_2

$C_{50}H_{73}N_{17}O_{11}S$ FW: 1120.3 [81608-30-2] ≥98%

Endogenous bombesin-related BB2 receptor agonist involved in endocrine signaling and feeding behavior. It decreases food intake and feeding time, stimulates mast cell degranulation, and induces bradycardia.

Sayegh AI. The role of bombesin and bombesin-related peptides in the short-term control of food intake. Prog Mol Biol Transl Sci. 2013;114:343-70. PMID: 23317790.

Andoh T, Kuwazono T, Lee JB, et al. Gastrin-releasing peptide induces itch-related responses through mast cell degranulation in mice. Peptides. 2011 Oct;32(10):2098-103. PMID: 21933692.

N1982 Neuromedin U, rat

1 mg
2 mg
5 mg

H-Tyr-Lys-Val-Asn-Glu-Tyr-Gln-Gly-Pro-Val-Ala-Pro-Ser-Gly-Gly-Phe-Phe-Leu-Phe-Arg-Pro-Arg-Asn-NH_2

$C_{124}H_{180}N_{34}O_{31}$ FW: 2643.03 [117505-80-3] ≥95%

Endogenous neuromedin receptor agonist involved in energy homeostasis. It increases core temperature, decreases food intake, activates Wnt/β-catenin signaling, stimulates production of progesterone in ovarian cells, and upregulates inflammation-related cytokine expression.

Helfer G, Ross AW, Morgan PJ. Neuromedin U partly mimics thyroid stimulating hormone and triggers Wnt/β-Catenin signalling in the photoperiodic response of F344 rats. J Neuroendocrinol. 2013 Oct 24. [Epub ahead of print]. PMID: 24164054.

Telegdy G, Adamik A. Anxiolytic action of neuromedin-U and neurotransmitters involved in mice. Regul Pept. 2013 Sep 10;186:137-40. PMID: 23892031.

N6020 Neuropeptide F

1 mg
2 mg
5 mg

NPF

H-Lys-Arg-Ser-Tyr(PO_3H_2)-Glu-Glu-His-Ile-Pro-OH

$C_{51}H_{80}N_{13}O_{19}P$ FW: 768.79 ≥95%

Neuropeptide Y analog found in insects. It is involved in circadian rhythms. It suppresses signaling of wake-promoting ventrolateral clock neurons and plays a role in learning, stress responses, feeding, and courtship behavior.

Shang Y, Donelson NC, Vecsey CG, et al. Short neuropeptide F is a sleep-promoting inhibitory modulator. Neuron. 2013 Oct 2;80(1):171-83. PMID: 24094110.

N1984 Neuropeptide FF

5 mg
10 mg
25 mg

NPFF; Octapeptide F8FA

Phe-Leu-Phe-Gln-Pro-Gln-Arg-Phe-NH_2

$C_{54}H_{76}N_{14}O_{10}$ FW: 1081.3 [99566-27-5] ≥95%

Endogenous NPFF1/2 receptor agonist involved in nociception and cardiovascular regulation. It decreases LPS-stimulated NO production in macrophages, suppresses carrageenan-induced edema, and inhibits opioid-induced stress-mediated analgesia.

Sun YL, Zhang XY, Sun T, et al. The anti-inflammatory potential of neuropeptide FF in vitro and in vivo. Peptides. 2013 Sep;47:124-32. PMID: 23856454.

Jhamandas JH, Goncharuk V. Role of neuropeptide FF in central cardiovascular and neuroendocrine regulation. Front Endocrinol (Lausanne). 2013 Feb 7;4:8. PMID: 23404625.

N1985

Neuropeptide K, pig

5 mg
10 mg
25 mg

Asp-Ala-Asp-Ser-Ser-Ile-Glu-Lys-Gln-Val-Ala-Leu-Leu-Lys-Ala-Leu-Tyr-Gly-His-Gly-Gln-Ile-Ser-His-Lys-Arg-His-Lys-Thr-Asp-Ser-Phe-Val-Gly-Leu-Met-NH_2

Neurokinin K

$C_{175}H_{284}N_{52}O_{52}S$ FW: 5980.6 ≥95%

Endogenous NK2 receptor agonist and N-terminal-extended neurokinin A analog. It decreases food intake and modulates cardiovascular activity.

Prall BC, Cline MA. Anorexigenic effects of central neuropeptide K are associated with hypothalamic changes in juvenile Gallus gallus. Gen Comp Endocrinol. 2008 Nov-Dec;159(2-3):130-5. PMID: 18786538.

N1983

Neuropeptide Y (3-36), human

0.5 mg
1 mg
2.5 mg

Ser-Lys-Pro-Asp-Asn-Pro-Gly-Glu-Asp-Ala-Pro-Ala-Glu-Asp-Met-Ala-Arg-Tyr-Tyr-Ser-Ala-Leu-Arg-His-Tyr-Ile-Asn-Leu-Ile-Thr-Arg-Gln-Arg-Tyr-NH_2

NPY

$C_{175}H_{269}N_{53}O_{54}S$ FW: 4011.48 [150138-78-6] ≥95%

Endogenous Y1-5 receptor agonist and neurotransmitter involved in feeding behavior, stress signaling, and circadian rhythms. It potentiates reward- and reinforcement-inducing effects of opioids, inhibits amyloid-β-induced depression and spatial memory deficits, decreases or prevents stress-induced development of anxiety, and promotes vascular growth.

Wang Q, Wang M, Whim MD. Neuropeptide y gates a stress-induced, long-lasting plasticity in the sympathetic nervous system. J Neurosci. 2013 Jul 31;33(31):12705-17. PMID: 23904607.

Desai SJ, Upadhya MA, Subhedar NK, et al. NPY mediates reward activity of morphine, via NPY Y1 receptors, in the nucleus accumbens shell. Behav Brain Res. 2013 Jun 15;247:79-91. PMID: 23511250

N1987

Neuropeptide Y (13-36), human

0.5 mg
1 mg
2.5 mg

H-Pro-Ala-Glu-Asp-Met-Ala-Arg-Tyr-Tyr-Ser-Ala-Leu-Arg-His-Tyr-Ile-Asn-Leu-Ile-Thr-Arg-Gln-Arg-Tyr-NH_2

NPY

$C_{134}H_{207}N_{41}O_{36}S$ FW: 3000.46 [122341-40-6] ≥95%

Endogenous Y1-5 receptor agonist and neurotransmitter involved in feeding behavior, stress signaling, and circadian rhythms. It potentiates reward- and reinforcement-inducing effects of opioids, inhibits amyloid-β-induced depression and spatial memory deficits, decreases or prevents stress-induced development of anxiety, and promotes vascular growth.

Wang Q, Wang M, Whim MD. Neuropeptide y gates a stress-induced, long-lasting plasticity in the sympathetic nervous system. J Neurosci. 2013 Jul 31;33(31):12705-17. PMID: 23904607.

N1986

Neuropeptide Y, human/rat

5 mg
10 mg
25 mg

Tyr-Pro-Ser-Lys-Pro-Asp-Asn-Pro-Gly-Glu-Asp-Ala-Pro-Ala-Glu-Asp-Met-Ala-Arg-Tyr-Tyr-Ser-Ala-Leu-Arg-His-Tyr-Ile-Asn-Leu-Ile-Thr-Arg-Gln-Arg-Tyr-NH_2

$C_{189}H_{285}N_{55}O_{57}S$ FW: 4271.7 ≥95%

Endogenous Y1-5 receptor agonist and neurotransmitter involved in feeding behavior, stress signaling, and circadian rhythms. It potentiates reward- and reinforcement-inducing effects of opioids, inhibits amyloid-β-induced depression and spatial memory deficits, decreases or prevents stress-induced development of anxiety, and promotes vascular growth.

Wang Q, Wang M, Whim MD. Neuropeptide y gates a stress-induced, long-lasting plasticity in the sympathetic nervous system. J Neurosci. 2013 Jul 31;33(31):12705-17. PMID: 23904607.

N1988

γ-Neuropeptide, rabbit

0.5 mg
1 mg
2.5 mg

H-Asp-Ala-Gly-His-Gly-Gln-Ile-Ser-His-Lys-Arg-His-Lys-Thr-Asp-Ser-Phe-Val-Gly-Leu-Met-NH_2

$C_{99}H_{158}N_{34}O_{29}S$ FW: 2320.64 [114882-65-4] ≥95%

Endogenous NK2 receptor agonist that mediates hypothalamic-pituitary-adrenal axis signaling and reproductive hormone release. It also stimulates smooth muscle contraction in the gastrointestinal tract and induces vasodilation.

Pietruszka M, Jankowska E, Kowalik-Jankowska T, et al. Complexation abilities of neuropeptide gamma toward copper(II) ions and products of metal-catalyzed oxidation. Inorg Chem. 2011 Aug 15;50(16):7489-99. PMID: 21770367.

N1989

Neurotensin

1 mg
2 mg
5 mg

pGlu-Leu-Tyr-Glu-Asn-Lys-Pro-Arg-Arg-Pro-Tyr-Ile-Leu

$C_{78}H_{122}N_{21}O_{20}$ FW: 1672.9 [39379-15-2] ≥95%

Endogenous NTS receptor agonist involved in hormone release. It induces contractions in smooth muscle cells, activates nonselective cation channels, and stimulates orexin neurons.

Kleczkowska P, Lipkowski AW. Neurotensin and neurotensin receptors: characteristic, structure-activity relationship and pain modulation--a review. Eur J Pharmacol. 2013 Sep 15;716(1-3):54-60. PMID: 23500196.

Degolier TF, Brown DR, Duke GE, et al. Neurotensin and cholecystokinin contract gallbladder circular muscle in chickens. Poult Sci. 2013 Aug;92(8):2156-62. PMID: 23873564.

N1991 [D-Trp11]-Neurotensin

5 mg
10 mg
25 mg

$C_{80}H_{122}N_{22}O_{19}$ FW: 1696 [75644-95-0] ≥95%

pGlu-Leu-Tyr-Glu-Asn-Lys-Pro-Arg-Arg-Pro-DTrp-Ile-Leu-OH

Derivative of endogenous neurotensin receptor agonist involved in hormone release. It induces contractions in smooth muscle cells, activates nonselective cation channels involved in gastrointestinal and colonic motility, and decreases blood pressure and heart rate.

Kleczkowska P, Lipkowski AW. Neurotensin and neurotensin receptors: characteristic, structure-activity relationship and pain modulation--a review. Eur J Pharmacol. 2013 Sep 15;716(1-3):54-60. PMID: 23500196.

Degolier TF, Brown DR, Duke GE, et al. Neurotensin and cholecystokinin contract gallbladder circular muscle in chickens. Poult Sci. 2013 Aug;92(8):2156-62. PMID: 23873564.

N1990 [Gln4]-Neurotensin

1 mg
2 mg
5 mg

$C_{78}H_{122}N_{22}O_{19}$ FW: 1671.9 [61445-54-3] ≥95%

pGlu-Leu-Tyr-Gln-Asn-Lys-Pro-Arg-Arg-Pro-Tyr-Ile-Leu-OH

Derivative of endogenous neurotensin receptor agonist involved in hormone release. It induces contractions in smooth muscle cells, activates nonselective cation channels involved in gastrointestinal and colonic motility, and decreases blood pressure and heart rate.

Kleczkowska P, Lipkowski AW. Neurotensin and neurotensin receptors: characteristic, structure-activity relationship and pain modulation--a review. Eur J Pharmacol. 2013 Sep 15;716(1-3):54-60. PMID: 23500196.

N1992 Neurotensin (1-11)

1 mg
2 mg
5 mg

$C_{66}H_{99}N_{19}O_{18}$ FW: 1446.66 [74032-89-6] ≥95%

pGlu-Leu-Tyr-Glu-Asn-Lys-Pro-Arg-Arg-Pro-Tyr-OH

Endogenous neurotensin receptor agonist involved in hormone release. It induces contractions in smooth muscle cells, activates nonselective cation channels involved in gastrointestinal and colonic motility, and decreases blood pressure and heart rate.

Kleczkowska P, Lipkowski AW. Neurotensin and neurotensin receptors: characteristic, structure-activity relationship and pain modulation--a review. Eur J Pharmacol. 2013 Sep 15;716(1-3):54-60. PMID: 23500196.

N1993 Neurotensin (9-13)

5 mg
10 mg
25 mg

$C_{32}H_{52}N_8O_7$ FW: 660.82 ≥95%

H-Arg-Pro-Tyr-Ile-Leu-OH

Endogenous neurotensin receptor agonist involved in hormone release. It induces contractions in smooth muscle cells, activates nonselective cation channels involved in gastrointestinal and colonic motility, and decreases blood pressure and heart rate.

Kleczkowska P, Lipkowski AW. Neurotensin and neurotensin receptors: characteristic, structure-activity relationship and pain modulation--a review. Eur J Pharmacol. 2013 Sep 15;716(1-3):54-60. PMID: 23500196.

N1994 Neurotensin, frog

0.5 mg
1 mg
2.5 mg

$C_{70}H_{115}N_{23}O_{17}$ FW: 1550.84 ≥95%

H-pGlu-Ser-His-Ile-Ser-Lys-Ala-Arg-Arg-Pro-Tyr-Ile-Leu-NH_2

Endogenous neurotensin receptor agonist involved in hormone release. It induces contractions in smooth muscle cells, activates nonselective cation channels involved in gastrointestinal and colonic motility, and decreases blood pressure and heart rate.

Kleczkowska P, Lipkowski AW. Neurotensin and neurotensin receptors: characteristic, structure-activity relationship and pain modulation--a review. Eur J Pharmacol. 2013 Sep 15;716(1-3):54-60. PMID: 23500196.

N1995 Neurotensin, guinea pig

1 mg
2 mg
5 mg

$C_{76}H_{119}N_{21}O_{21}$ FW: 1662.92 ≥95%

H-pGlu-Leu-Tyr-Glu-Asn-Lys-Ser-Arg-Arg-Pro-Tyr-Ile-Leu-OH

Endogenous neurotensin receptor agonist involved in hormone release. It induces contractions in smooth muscle cells, activates nonselective cation channels involved in gastrointestinal and colonic motility, and decreases blood pressure and heart rate.

Kleczkowska P, Lipkowski AW. Neurotensin and neurotensin receptors: characteristic, structure-activity relationship and pain modulation--a review. Eur J Pharmacol. 2013 Sep 15;716(1-3):54-60. PMID: 23500196.

N2400 NG-52

NEW

1 mg
5 mg
25 mg

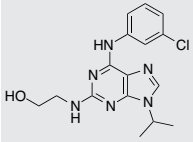

$C_{16}H_{19}ClN_6O$ FW: 346.81 [212779-48-1] ≥98%

Analog of purvalenol A and inhibitor of CDK2, Cdc28p, and Pho85p. It inhibits survival of *Saccharomyces*.

Gray NS, Wodicka L, Thunnissen AM, et al. Exploiting chemical libraries, structure, and genomics in the search for kinase inhibitors. Science. 1998 Jul 24;281(5376):533-8. PMID: 9677190.

N3301 Niacin

10 g
50 g

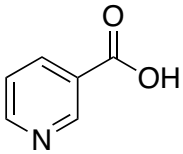

$C_6H_5NO_2$ FW: 123.11 [59-67-6] ≥98%

B vitamin, GPR109A agonist, and hepatic diacylglycerol acyltransferase-2 inhibitor required for formation of NAD and NADP. It induces cutaneous vasodilation and flushing and decreases secretion of VLDL and LDL.

Creider JC, Hegele RA, Joy TR. Niacin: another look at an underutilized lipid-lowering medication. Nat Rev Endocrinol. 2012 Sep;8(9):517-28. PMID: 22349076.

Kamanna VS, Ganji SH, Kashyap ML. The mechanism and mitigation of niacin-induced flushing. Int J Clin Pract. 2009 Sep;63(9):1369-77. PMID: 19691622.

N3208 Nicardipine

1 g
5 g
25 g

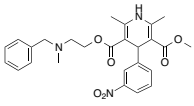

$C_{26}H_{29}N_3O_6$ FW: 479.52 [55985-32-5] ≥98%

L-type Ca^{2+} channel blocker used to treat angina and hypertension. It also inhibits amygdala kindling, enhances GABAergic signaling, and increases pain thresholds.

Yue W, Wang L, Zhang F, et al. Inhibition of nicardipine on amygdala kindling in rats. Acta Pharmacol Sin. 2001 Apr;22(4):365-8. PMID: 11742591.

Eraković V, Zupan G, Mrsić J, et al. The influence of nicardipine and ifenprodil on the brain free arachidonic acid level and behavior in hypoxia-exposed rats. Prog Neuropsychopharmacol Biol Psychiatry. 1997 May;21(4):633-47. PMID: 9194145.

N3310 Nicotinamide

50 g

Niacinamide; Vitamin PP; Vitamin B3

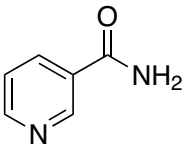

$C_6H_6N_2O$ FW: 122.12 [98-92-0] ≥98%

Amide form of vitamin B3 required for production of NAD and NADP. It modulates GABA activity and is used to treat acne vulgaris and rosacea. It is also used in commercial skin whitening treatments.

Navarrete-Solís J, Castanedo-Cázares JP, Torres-Álvarez B, et al. A Double-Blind, Randomized Clinical Trial of Niacinamide 4% versus Hydroquinone 4% in the Treatment of Melasma. Dermatol Res Pract. 2011;2011:379173. PMID: 21822427.

Niren NM. Pharmacologic doses of nicotinamide in the treatment of inflammatory skin conditions: a review. Cutis. 2006 Jan;77(1 Suppl):11-6. PMID: 16871774.

N3213 Nidulal

0.5 mg

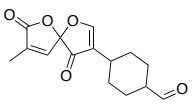

$C_{15}H_{16}O_5$ FW: 276.28 ≥95%

Found in *Nidula*. It induces differentiation of promyelocytic leukemia cells and activates expression of alkaline phosphatase.

Erkel G, Becker U, Anke T, et al. Nidulal, a novel inducer of differentiation of human promyelocytic leukemia cells from *Nidula candida*. J Antibiot (Tokyo). 1996 Dec;49(12):1189-95. PMID: 9031663.

N3228 Nifedipine

1 g
5 g
25 g

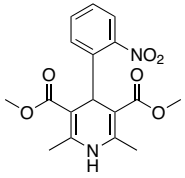

$C_{17}H_{18}N_2O_6$ FW: 346.33 [21829-25-4] ≥98%

L-type Ca^{2+} channel blocker used to prevent preterm labor and to treat angina. It also alters pain thresholds.

Gáspár R, Hajagos-Tóth J. Calcium channel blockers as tocolytics: principles of their actions, adverse effects and therapeutic combinations. Pharmaceuticals (Basel). 2013 May 23;6(6):689-99. PMID: 24276256.

Martín MI, del Val VL, Colado MI, et al. Behavioral and analgesic effects induced by administration of nifedipine and nimodipine. Pharmacol Biochem Behav. 1996 Sep;55(1):93-8. PMID: 8870043.

N3422 Nifekalant Hydrochloride

10 mg
25 mg

MS 551

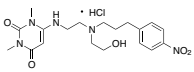

$C_{19}H_{27}N_5O_5 \bullet HCl$ FW: 441.91 [130656-51-8] ≥98%

Voltage-gated K^+ channel blocker used to treat ventricular tachyarrhythmia. It also increases right atrial monophasic action potential duration and the atrial effective refractory period.

Harayama N, Nihei SI, Nagata K, et al. Comparison of nifekalant and amiodarone for resuscitation of out-of-hospital cardiopulmonary arrest resulting from shock-resistant ventricular fibrillation. J Anesth. 2014 Jan 5. [Epub ahead of print]. PMID: 24389941.

Sonoda K, Watanabe I, Ohkubo K, et al. Rate-dependent electrophysiologic effects of the class III antiarrhythmic drugs nifekalant, amiodarone, and ibutilide on the atrium in patients with persistent atrial fibrillation. Int Heart J. 2013;54(5):279-84. PMID: 24097216.

Pantazopoulos IN, Troupis GT, Pantazopoulos CN, et al. Nifekalant in the treatment of life-threatening ventricular tachyarrhythmias. World J Cardiol. 2011 Jun 26;3(6):169-76. PMID: 21772943.

N3322 Niflumic Acid

10 g
25 g

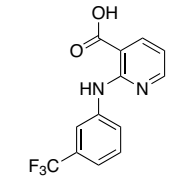

$C_{13}H_9F_3N_2O_2$ FW: 282.22 [4394-00-7] ≥98%

NSAID, NMDA receptor inverse agonist, T-type Ca^{2+} and Cl^- channel blocker, GABA-A receptor antagonist, and COX-2 inhibitor used to treat pain. It indirectly activates AMPK and inhibits TNF-α- and IL-1β-induced activation of NF-κB.

Balderas E, Ateaga-Tlecuitl R, Rivera M, et al. Niflumic acid blocks native and recombinant T-type channels. J Cell Physiol. 2012 Jun;227(6):2542-55. PMID: 21898399.

Chi Y, Li K, Yan Q, et al. Nonsteroidal anti-inflammatory drug flufenamic acid is a potent activator of AMP-activated protein kinase. J Pharmacol Exp Ther. 2011 Oct;339(1):257-66. PMID: 21765041.

N3323 Nifuratel

1 g
10 g
25 g
100 g

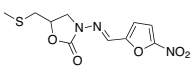

$C_{10}H_{11}N_3O_5S$ FW: 285.28 [4936-47-4] ≥98%

Nitrofuran derivative. It inhibits growth of gram negative and gram positive bacteria and fungi.

Togni G, Battini V, Bulgheroni A, et al. In vitro activity of nifuratel on vaginal bacteria: could it be a good candidate for the treatment of bacterial vaginosis? Antimicrob Agents Chemother. 2011 May;55(5):2490-2. PMID: 21321147.

N3520 Nifursol

5 g
25 g
100 g

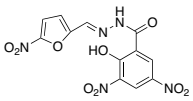

$C_{12}H_7N_5O_9$ FW: 365.21 [16915-70-1] ≥98%

Livestock feed additive and antibiotic used to prevent growth of *Histomonas*.

Verdon E, Couedor P, Sanders P. Multi-residue monitoring for the simultaneous determination of five nitrofurans (furazolidone, furaltadone, nitrofurazone, nitrofurantoine, nifursol) in poultry muscle tissue through the detection of their five major metabolites (AOZ, AMOZ, SEM, AHD, DNSAH) by liquid chromatography coupled to electrospray tandem mass spectrometry--in-house validation in line with Commission Decision 657/2002/EC. Anal Chim Acta. 2007 Mar 14;586(1-2):336-47. PMID: 17386733.

N3225 Nigericin Sodium

1 mg
5 mg
10 mg

Azalomycin M; Helixin C; Polyetherin A

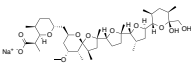

$C_{40}H_{67}O_{11}Na$ FW: 746.94 [28643-80-3] ≥98%

Cationic ionophore that inhibits Golgi function and suppresses growth of gram positive bacteria. It also prevents viral activation and triggers activation of the NALP3 inflammasome.

Heid ME, Keyel PA, Kamga C, et al. Mitochondrial reactive oxygen species induces NLRP3-dependent lysosomal damage and inflammasome activation. J Immunol. 2013 Nov 15;191(10):5230-8. PMID: 24089192.

Myskiw C, Piper J, Huzarewich R, et al. Nigericin is a potent inhibitor of the early stage of vaccinia virus replication. Antiviral Res. 2010 Dec;88(3):304-10. PMID: 20951746.

N3346 Nilotinib

10 mg
25 mg
100 mg

AMN 107

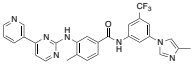

$C_{28}H_{22}F_3N_7O$ FW: 529.52 [641571-10-0] ≥98%

Abl, c-Kit, PDGFR, and PP2A inhibitor used to treat Bcr-Abl-positive chronic myelogenous leukemia. It induces autophagy in hepatocellular carcinoma cells, decreases expression of HDACs in hepatic stellate cells, and prevents mast cell histamine release and systemic anaphylaxis in allergy models.

Shaker ME, Ghani A, Shiha GE, et al. Nilotinib induces apoptosis and autophagic cell death of activated hepatic stellate cells via inhibition of histone deacetylases. Biochim Biophys Acta. 2013 Aug;1833(8):1992-2003. PMID: 23499874.

Yu HC, Lin CS, Tai WT, et al. Nilotinib induces autophagy in hepatocellular carcinoma through AMPK activation. J Biol Chem. 2013 Jun 21;288(25):18249-59. PMID: 23677989.

N3450 Nimesulide

1 g
5 g
10 g
25 g

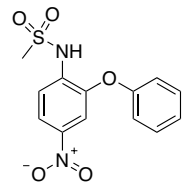

$C_{13}H_{12}N_2O_5S$ FW: 308.31 [51803-78-2] ≥98%

NSAID and COX-2 inhibitor used to treat pain, inflammation, and dysmenorrhea. It also downregulates expression of survivin and Bcl-2 and induces apoptosis in hypopharyngeal carcinoma cells.

Jia-Jun T, Su-Mei L, Liang Y, et al. Nimesulide inhibited the growth of hypopharyngeal carcinoma cells via suppressing Survivin expression. Head Neck Oncol. 2012 Mar 27;4:7. PMID: 22453101.

Vellani V, Franchi S, Prandini M, et al. Nimesulide inhibits protein kinase C epsilon and substance P in sensory neurons - comparison with paracetamol. J Pain Res. 2011;4:177-87. PMID: 21811393.

N3448 Nimodipine

500 mg
1 g
5 g

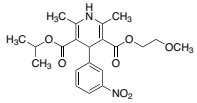

$C_{21}H_{26}N_2O_7$ FW: 418.44 [66085-59-4] ≥98%

L-type Ca^{2+} channel blocker used to treat hypertension. It also prevents cerebral ischemia and vasospasm, inhibits methylmercury-induced behavioral neurotoxicity, and attenuates neurological symptoms of drug-induced withdrawal.

Bia A GY, Polak P, Michalak A, et al. Influence of calcium channel antagonists on nonsomatic signs of nicotine and d-amphetamine withdrawal in mice. Pharmacol Rep. 2014 Apr;66(2):212-22. PMID: 24911072.

Bailey JM, Hutsell BA, Newland MC. Dietary nimodipine delays the onset of methylmercury neurotoxicity in mice. Neurotoxicology. 2013 Jul;37:108-17. PMID: 23583802.

Sanz JM, Chiozzi P, Colaianna M, et al. Nimodipine inhibits IL-1β release stimulated by amyloid β from microglia. Br J Pharmacol. 2012 Dec;167(8):1702-11. PMID: 22831460.

N3452 Nimustine Hydrochloride

100 mg
500 mg
1 g

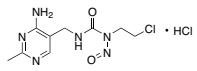

ACNU

$C_9H_{12}N_6O_2 \bullet HCl$ FW: 309.16 [55661-38-6] ≥97%

DNA cross-linker used to treat gliomas. It induces double-stranded DNA breakage and may downregulate expression of DNA ligase IV.

Kondo N, Takahashi A, Mori E, et al. DNA ligase IV is a potential molecular target in ACNU sensitivity. Cancer Sci. 2010 Aug;101(8):1881-5. PMID: 20487264.

N3577 Nitidine Chloride NEW

1 mg
5 mg
25 mg

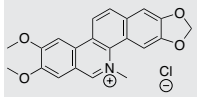

$C_{21}H_{18}ClNO_4$ FW: 383.82 [13063-04-2] ≥98%

Topoisomerase I inhibitor. It inhibits cell migration and invasion, binds to DNA sequences containing alternating G and C base pairs, decreases production of pro-inflammatory cytokines, and prevents growth of *Plasmodium*.

Fang Z, Tang Y, Jiao W, et al. Nitidine chloride inhibits renal cancer cell metastasis via suppressing AKT signaling pathway. Food Chem Toxicol. 2013 Oct;60:246-51. PMID: 23911800.

Liao J, Xu T, Zheng JX, et al. Nitidine chloride inhibits hepatocellular carcinoma cell growth in vivo through the suppression of the JAK1/STAT3 signaling pathway. Int J Mol Med. 2013 Jul;32(1):79-84. PMID: 23613111.

Wang Z, Jiang W, Zhang Z, et al. Nitidine chloride inhibits LPS-induced inflammatory cytokines production via MAPK and NF-kappaB pathway in RAW 264.7 cells. J Ethnopharmacol. 2012 Oct 31;144(1):145-50. PMID: 22971898.

N3476 Nitisinone NEW

10 mg
50 mg
250 mg

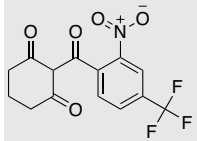

NTBC

$C_{14}H_{10}F_3NO_5$ FW: 329.23 [104206-65-7] ≥98%

HPPD inhibitor. It is used to slow the effects of hereditary type 1 tyrosinemia.

McKiernan PJ. Nitisinone in the treatment of hereditary tyrosinaemia type 1. Drugs. 2006;66(6):743-50. PMID: 16706549.

Kavana M, Moran GR. Interaction of (4-hydroxyphenyl)pyruvate dioxygenase with the specific inhibitor 2-[2-nitro-4-(trifluoromethyl)benzoyl]-1,3-cyclohexanedione. Biochemistry. 2003 Sep 2;42(34):10238-45. PMID: 12939152.

N3278 7-Nitroindazole

500 mg
1 g
5 g

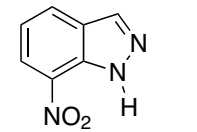

$C_7H_5N_3O_2$ FW: 163.14 [2942-42-9] ≥98%

nNOS inhibitor that prevents low salt diet- and pharmacologically-induced increases in COX-2 levels.

Cheng HF, Wang JL, Zhang MZ, et al. Nitric oxide regulates renal cortical cyclooxygenase-2 expression. Am J Physiol Renal Physiol. 2000 Jul;279(1):F122-9. PMID: 10894794.

N3276 Nitroso(acetoxymethyl)methylamine

10 mg
50 mg
100 mg

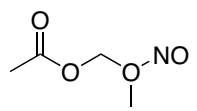

$C_4H_8N_2O_3$ FW: 132.12 [56856-83-8] ≥98%

Carcinogenic NNK precursor found in tobacco smoke. It also inhibits production of IL-8 and MCP-1 in alveolar and bronchial epithelial cells.

Proulx LI, Gaudreault M, Turmel V, et al. 4-(Methylnitrosamino)-1-(3-pyridyl)-1-butanone, a component of tobacco smoke, modulates mediator release from human bronchial and alveolar epithelial cells. Clin Exp Immunol. 2005 Apr;140(1):46-53. PMID: 15762874.

Cloutier JF, Drouin R, Castonguay A. Treatment of human cells with N-Nitroso(acetoxymethyl)methylamine: distribution patterns of piperidine-sensitive DNA damage at the nucleotide level of resolution are related to the sequence context. Chem Res Toxicol. 1999 Sep;12(9):840-9. PMID: 10490506.

N3378 S-Nitrosoglutathione

5 mg
10 mg
25 mg

$C_{10}H_{16}N_4O_7S$ FW: 336.32 [57564-91-7] ≥98%

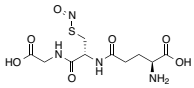

NO donor. It attenuates Pannexin-1 channel currents and ATP release, improves defective Cl^- transport in cystic fibrosis subjects, dilates blood vessels, and induces NO-related apoptosis in colon cancer cells.

Lohman AW, Weaver JL, Billaud M, et al. S-nitrosylation inhibits pannexin 1 channel function. J Biol Chem. 2012 Nov 16;287(47):39602-12. PMID: 23033481.

Servetnyk Z, Krjukova J, Gaston B, et al. Activation of chloride transport in CF airway epithelial cell lines and primary CF nasal epithelial cells by S-nitrosoglutathione. Respir Res. 2006 Oct 5;7:124. PMID: 17022806.

Carvalho-Filho MA, Ueno M, Hirabara SM, et al. S-nitrosation of the insulin receptor, insulin receptor substrate 1, and protein kinase B/Akt: a novel mechanism of insulin resistance. Diabetes. 2005 Apr;54(4):959-67. PMID: 15793233.

N3584 Nivalenol

1 mg
5 mg

$C_{15}H_{20}O_7$ FW: 312.32 [23282-20-4] ≥99%

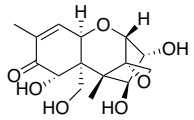

Peptide chain initiation inhibitor found in *Fusarium*. It inhibits proliferation of leukocytes, induces apoptosis in Jurkat T cells and macrophages, and stimulates polyribosome breakdown.

Alassane-Kpembi I, Kolf-Clauw M, Gauthier T, et al. New insights into mycotoxin mixtures: the toxicity of low doses of Type B trichothecenes on intestinal epithelial cells is synergistic. Toxicol Appl Pharmacol. 2013 Oct 1;272(1):191-8. PMID: 23735874.

Wu W, Flannery BM, Sugita-Konishi Y, et al. Comparison of murine anorectic responses to the 8-ketotrichothecenes 3-acetyldeoxynivalenol, 15-acetyldeoxynivalenol, fusarenon X and nivalenol. Food Chem Toxicol. 2012 Jun;50(6):2056-61. PMID: 22465835.

Nagashima H, Kushiro M, Nakagawa H. Nuclear factor-κB inhibitors alleviate nivalenol-induced cytotoxicity in HL60 cells. Environ Toxicol Pharmacol. 2011 Jan;31(1):258-61. PMID: 21787693.

N3496 Nizatidine

5 g
10 g

$C_{12}H_{21}N_5O_2S_2$ FW: 331.46 [76963-41-2] ≥98%

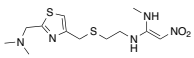

Histamine H2 receptor inverse agonist used to treat peptic ulcer disease and gastroesophageal reflux disease. It also boosts vaccine responses and stimulates maturation of dendritic cells.

Doi H, Sakakibara R, Sato M, et al. Nizatidine ameliorates gastroparesis in Parkinson's disease: a pilot study. Mov Disord. 2014 Apr;29(4):562-6. PMID: 24375669.

Wang S, Wu B, Xue J, et al. Nizatidine, a small molecular compound, enhances killed H5N1 vaccine cell-mediated responses and protects mice from lethal viral challenge. Hum Vaccin Immunother. 2014 Feb 1;10(2):461-8. PMID: 24253609.

Kurt A, Altun A, Bağcivan I, et al. Effects of proton pump inhibitors and h(2) receptor antagonists on the ileum motility. Gastroenterol Res Pract. 2011;2011:218342. PMID: 22216022.

N4972 NMS-873

NEW

5 mg
25 mg

$C_{27}H_{28}N_4O_3S_2$ FW: 520.67 [1418013-75-8] ≥98%

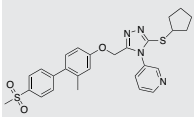

Valosin-containing protein inhibitor that alters endoplasmic reticulum-associated degradation. It activates the unfolded protein response and induces death in cancer cells.

Chou TF, Bulfer SL, Weihl CC, et al. Specific inhibition of p97/VCP ATPase and kinetic analysis demonstrate interaction between D1 and D2 ATPase domains. J Mol Biol. 2014 Jul 29;426(15):2886-99. PMID: 24878061.

Magnaghi P, D'Alessio R, Valsasina B, et al. Covalent and allosteric inhibitors of the ATPase VCP/p97 induce cancer cell death. Nat Chem Biol. 2013 Sep;9(9):548-56. PMID: 23892893.

N5072 NMS-1286937

NEW

5 mg
10 mg

NMS-P937

$C_{24}H_{27}F_3N_8O_3$ FW: 532.52 [1034616-18-6] ≥98%

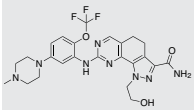

PLK1 inhibitor. It induces cell cycle arrest and apoptosis in osteosarcoma cells and colon cancer cells and improves survival rates in acute myelogenous leukemia models.

Sero V, Tavanti E, Vella S, et al. Targeting polo-like kinase 1 by NMS-P937 in osteosarcoma cell lines inhibits tumor cell growth and partially overcomes drug resistance. Invest New Drugs. 2014 Dec;32(6):1167-80. PMID: 25193492.

Casolaro A, Golay J, Albanese C, et al. The Polo-Like Kinase 1 (PLK1) inhibitor NMS-P937 is effective in a new model of disseminated primary CD56+ acute monoblastic leukaemia. PLoS One. 2013;8(3):e58424. PMID: 23520509.

Valsasina B, Beria I, Alli C, et al. NMS-P937, an orally available, specific small-molecule polo-like kinase 1 inhibitor with antitumor activity in solid and hematologic malignancies. Mol Cancer Ther. 2012 Apr;11(4):1006-16. PMID: 22319201.

N5605 Nobiletin

25 mg
100 mg

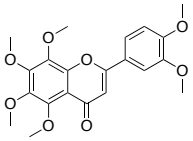

$C_{21}H_{22}O_8$ FW: 402.39 [478-01-3] ≥97%

Potential AMPA receptor positive modulator found in citrus fruits. It induces cell cycle arrest and inhibits cell proliferation in cancer cells, attenuates learning and memory impairments, decreases body weight gain, and stimulates phosphorylation of the GluR1 subunit of AMPA receptors.

Yoshigai E, Machida T, Okuyama T, et al. Citrus nobiletin suppresses inducible nitric oxide synthase gene expression in interleukin-1β-treated hepatocytes. Biochem Biophys Res Commun. 2013 Sep 13;439(1):54-9. PMID: 23958298.

Nakajima A, Aoyama Y, Nguyen TT, et al. Nobiletin, a citrus flavonoid, ameliorates cognitive impairment, oxidative burden, and hyperphosphorylation of tau in senescence-accelerated mouse. Behav Brain Res. 2013 Aug 1;250:351-60. PMID: 23714077.

Ma X, Jin S, Zhang Y, et al. Inhibitory Effects of Nobiletin on Hepatocellular Carcinoma In Vitro and In Vivo. Phytother Res. 2013 Jul 1. [Epub ahead of print]. PMID: 23818450.

N5210 Nociceptin

1 mg

Phe-Gly-Gly-Phe-Thr-Gly-Ala-Arg-Lys-Ser-Ala-Arg-Lys-Leu-Ala-Asn-Gln

$C_{79}H_{129}N_{27}O_{22}$ FW: 1809.1 [170713-75-4] ≥98%

Endogenous nociceptin receptor agonist involved in opioid signaling. It decreases glutamate release, inhibits activity of POMC neurons, and modulates GIRK channel signaling.

Borgquist A, Rivas VM, Kachani M, et al. Gonadal Steroids Differentially Modulate the Actions of Orphanin FQ/Nociceptin at A Physiologically Relevant Circuit Controlling Female Sexual Receptivity. J Neuroendocrinol. 2014 May;26(5):329-40. PMID: 24617903.

Kallupi M, Varodayan FP, Oleata CS, et al. Nociceptin/orphanin FQ decreases glutamate transmission and blocks ethanol-induced effects in the central amygdala of naive and ethanol-dependent rats. Neuropsychopharmacology. 2014 Apr;39(5):1081-92. PMID: 24169802.

N5211 Nocistatin

0.5 mg
1 mg
2.5 mg

H-Glu-Gln-Lys-Gln-Leu-Gln-OH

$C_{32}H_{56}N_{10}O_{12}$ FW: 772.86 ≥95%

TRPC receptor agonist and BK/SK K^+ channel modulator. It inhibits thermal hyperalgesia induced by nociceptin, suppresses memory acquisition impairment, and prevents release of 5-HT in synaptosomes.

Deák BH, Klukovits A, Tekes K, et al. Nocistatin inhibits pregnant rat uterine contractions in vitro: roles of calcitonin gene-related peptide and calcium-dependent potassium channel. Eur J Pharmacol. 2013 Aug 15;714(1-3):96-104. PMID: 23792038.

Chen YL, Li AH, Yeh TH, et al. Nocistatin and nociceptin exert opposite effects on the excitability of central amygdala nucleus-periaqueductal gray projection neurons. Mol Cell Neurosci. 2009 Jan;40(1):76-88. PMID: 18930828.

N5409 Nocodazole

10 mg
50 mg

Oncodazole; R 17934

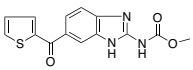

$C_{14}H_{11}N_3O_3S$ FW: 301.32 [31430-18-9] ≥98%

Microtubule polymerization inhibitor. It induces apoptosis in chronic lymphocytic leukemia cells and kills *Alveococcus* larvocysts.

Shkoliar NA, Kukhaleva IV, Legon'kov IuA, et al. Study of the therapeutic activity of nocodazole on experimental models of larval alveococcosis. Med Parazitol (Mosk). 2013 Apr-Jun;(2):20-7. PMID: 24003517.

Beswick RW, Ambrose HE, Wagner SD. Nocodazole, a microtubule de-polymerising agent, induces apoptosis of chronic lymphocytic leukaemia cells associated with changes in Bcl-2 phosphorylation and expression. Leuk Res. 2006 Apr;30(4):427-36. PMID: 16162358.

N5550 Nomilin

25 mg
100 mg
500 mg

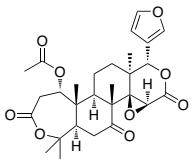

$C_{28}H_{34}O_9$ FW: 514.56 [1063-77-0] ≥98%

Natural product found in citrus fruits that inhibits HIV-1 protease and aromatase. It displays a variety of activities, including increasing glucose tolerance and decreasing body weight, glucose levels, and insulin levels in high-fat diet-fed animals, inhibiting pro-inflammatory cytokine release, suppressing proliferation, migration, and invasion of cancer cells, and preventing growth of *Aedes*.

Sato R. Nomilin as an anti-obesity and anti-hyperglycemic agent. Vitam Horm. 2013;91:425-39. PMID: 23374727.

Kim J, Jayaprakasha GK, Patil BS. Limonoids and their anti-proliferative and anti-aromatase properties in human breast cancer cells. Food Funct. 2013 Feb;4(2):258-65. PMID: 23117440.

Pratheeshkumar P, Kuttan G. Nomilin inhibits tumor-specific angiogenesis by downregulating VEGF, NO and proinflammatory cytokine profile and also by inhibiting the activation of MMP-2 and MMP-9. Eur J Pharmacol. 2011 Oct 15;668(3):450-8. PMID: 21839074.

N5652

Nonactin

1 mg
5 mg
10 mg

$C_{40}H_{64}O_{12}$ FW: 736.93 [6833-84-7] ≥95%

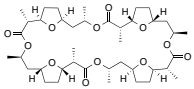

Neutral cyclic ionophore, metal ion carrier, and oxidative phosphorylation uncoupler. It suppresses intracellular glycosylation, inhibits several trafficking pathways in virus-infected cells, and uncouples oxidative phosphorylation in mitochondria.

Lee JM, Kim JG, Kim TH, et al. Nonactin hinders intracellular glycosylation in virus-infected baby hamster kidney cells. Mol Med Rep. 2010 Jan-Feb;3(1):115-9. PMID: 21472209.

Bala S, Kombrabail MH, Prabhananda BS. Effect of phloretin on ionophore mediated electroneutral transmembrane translocations of H(+), K(+) and Na(+) in phospholipid vesicles. Biochim Biophys Acta. 2001 Feb 9;1510(1-2):258-69. PMID: 11342163.

N5655

Nonoxynol-9

10 g
50 g
100 g

$C_{33}H_{60}O_{10}$ FW: 616.82 [26027-38-3] ≥98%

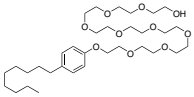

Nonoxynol surfactant used in contraceptives. It immobilizes sperm by altering acrosomal membranes.

Hillier SL, Moench T, Shattock R, et al. In vitro and in vivo: the story of nonoxynol 9. J Acquir Immune Defic Syndr. 2005 May 1;39(1):1-8. PMID: 15851907.

Maikhuri JP, Dwivedi AK, Dhar JD, et al. Mechanism of action of some acrylophenones, quinolines and dithiocarbamate as potent, non-detergent spermicidal agents. Contraception. 2003 May;67(5):403-8. PMID: 12742565.

N5669

Nordihydroguaiaretic Acid

500 mg
1 g
5 g

NDGA; Dihydronorguaiaretic acid

$C_{18}H_{22}O_4$ FW: 302.36 [500-38-9] ≥97%

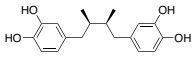

Inhibitor of 5-lipoxygenase, AChR, BChE, and mTORC1 found in creosote bush. It displays many biological activities, including preventing viral assembly in dengue virus samples, increasing life span, suppressing angiogenesis, invasion, and proliferation of glioma cells, and inhibiting osteoclastogenesis and bone destruction.

Hernández-Damián J, Andérica-Romero AC, Pedraza-Chaverri J. Paradoxical cellular effects and biological role of the multifaceted compound nordihydroguaiaretic Acid. Arch Pharm (Weinheim). 2014 Oct;347(10):685-97. PMID: 25100573.

Soto-Acosta R, Bautista-Carbajal P, Syed GH, et al. Nordihydroguaiaretic acid (NDGA) inhibits replication and viral morphogenesis of dengue virus. Antiviral Res. 2014 Sep;109:132-40. PMID: 25017471.

Harrison DE, Strong R, Allison DB, et al. Acarbose, 17-α-estradiol, and nordihydroguaiaretic acid extend mouse lifespan preferentially in males. Aging Cell. 2014 Apr;13(2):273-82. PMID: 24245565.

N5766

Norepinephrine Bitartrate Monohydrate

500 mg
1 g

Levarterenol bitartrate

$C_8H_{11}NO_3 \bullet C_4H_6O_6 \bullet H_2O$ FW: 337.28 [108341-18-0] ≥98%

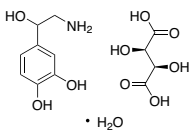

Endogenous hormone and neurotransmitter involved in sympathetic nervous system activity, reward, feeding, and other behaviors. It activates α/β-adrenergic receptors and is used to treat cardiac arrest, hypotension, and shock. It induces vascular vasoconstriction, increases blood pressure, stimulates choroidal neovascularization, and decreases core body temperature.

Lavine JA, Sang Y, Wang S, et al. Attenuation of choroidal neovascularization by β(2)-adrenoreceptor antagonism. JAMA Ophthalmol. 2013 Mar;131(3):376-82. PMID: 23303344.

Liang MJ, He LC, Yang GD. Screening, analysis and in vitro vasodilatation of effective components from Ligusticum Chuanxiong. Life Sci. 2005 Nov 26;78(2):128-33. PMID: 16154159.

Weiser M, Hilz MJ, Bronfin L, et al. Assessing microcirculation in familial dysautonomia by laser Doppler flowmeter. Clin Auton Res. 1998 Feb;8(1):13-23. PMID: 9532416.

N5767

Norethindrone

250 mg
1 g
5 g

$C_{20}H_{26}O_2$ FW: 298.42 [68-22-4] ≥98%

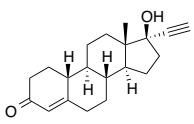

Progesterone receptor agonist used in contraceptives. It decreases levels of LH and FSH and increases lipid peroxidation due to its high lipophilicity.

Shoupe D. HRT dosing regimens: continuous versus cyclic-pros and cons. Int J Fertil Womens Med. 2001 Jan-Feb;46(1):7-15. PMID: 11294619.

Saha A, Roy K, De K, et al. Effects of oral contraceptive norethindrone on blood-lipid and lipid peroxidation parameters. Acta Pol Pharm. 2000 Nov-Dec;57(6):441-7. PMID: 11243250.

N5768 Norfloxacin

1 g
5 g
10 g
50 g

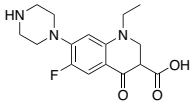

$C_{16}H_{18}FN_3O_3$ FW: 319.33 [70458-96-7] ≥98%

Topoisomerase IV and bacterial DNA gyrase inhibitor used to treat prostatitis and urinary tract infections. It decreases expression of pro-inflammatory cytokines and increases expression of antioxidative enzymes in neutrophils. It also inhibits proliferation of cancer cells when complexed with gold(III).

Gouvea LR, Garcia LS, Lachter DR, et al. Atypical fluoroquinolone gold(III) chelates as potential anticancer agents: relevance of DNA and protein interactions for their mechanism of action. Eur J Med Chem. 2012 Sep;55:67-73. PMID: 22835721.

Gómez-Hurtado I, Zapater P, Bellot P, et al. Interleukin-10-mediated heme oxygenase 1-induced underlying mechanism in inflammatory down-regulation by norfloxacin in cirrhosis. Hepatology. 2011 Mar;53(3):935-44. PMID: 21374664.

Padeĭskaia EN. Norfloxacin: more than 20 years of clinical use, the results and place among fluoroquinolones in modern chemotherapy for infections. Antibiot Khimioter. 2003;48(9):28-36. PMID: 15002177.

N5769 Norfloxacin Nicotinate

1 g
10 g
50 g

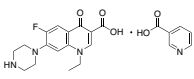

$C_{16}H_{18}FN_3O_3 \bullet C_6H_5NO_2$ FW: 442.44 [118803-81-9] ≥98%

Topoisomerase IV and bacterial DNA gyrase inhibitor used to treat urinary tract infections and prostatitis. It also decreases expression of pro-inflammatory cytokines and inhibits proliferation of several cancer cell lines when complexed with gold(III).

Gouvea LR, Garcia LS, Lachter DR, et al. Atypical fluoroquinolone gold(III) chelates as potential anticancer agents: relevance of DNA and protein interactions for their mechanism of action. Eur J Med Chem. 2012 Sep;55:67-73. PMID: 22835721.

Gómez-Hurtado I, Zapater P, Bellot P, et al. Interleukin-10-mediated heme oxygenase 1-induced underlying mechanism in inflammatory down-regulation by norfloxacin in cirrhosis. Hepatology. 2011 Mar;53(3):935-44. PMID: 21374664.

N5778 Notoginsenoside R1

5 mg
10 mg
25 mg

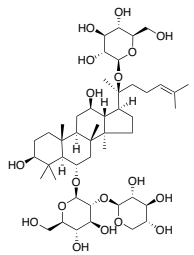

$C_{47}H_{80}O_{18}$ FW: 933.13 [80418-24-2] ≥98%

Found in species of *Panax*. It decreases amyloid-β-induced oxidative damage, lowers LDL, triglyceride, and cholesterol levels, increases expression of antioxidative enzymes, and stimulates antigen-induced spleenocyte proliferation.

Ma B, Meng X, Wang J, et al. Notoginsenoside R1 attenuates amyloid-β-induced damage in neurons by inhibiting reactive oxygen species and modulating MAPK activation. Int Immunopharmacol. 2014 Jun 24;22(1):151-159. PMID: 24975829.

Jia C, Xiong M, Wang P, et al. Notoginsenoside R1 Attenuates Atherosclerotic Lesions in ApoE Deficient Mouse Model. PLoS One. 2014 Jun 16;9(6):e99849. PMID: 24933211.

Sun HX, Chen Y, Ye Y. Ginsenoside Re and notoginsenoside R1: Immunologic adjuvants with low haemolytic effect. Chem Biodivers. 2006 Jul;3(7):718-26. PMID: 17193304.

N5986 Novobiocin Sodium

1 g
5 g

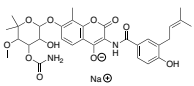

$C_{31}H_{35}N_2NaO_{11}$ FW: 634.61 [1476-53-5] ≥98%

Bacterial DNA gyrase inhibitor used to treat methicillin-resistant *Staphylococcus aureus*. It also inhibits HIF-1α binding to transcriptional coactivator p300/CBP.

Gunaherath GM, Marron MT, Wijeratne EM, et al. Synthesis and biological evaluation of novobiocin analogues as potential heat shock protein 90 inhibitors. Bioorg Med Chem. 2013 Sep 1;21(17):5118-29. PMID: 23859777.

Wu D, Zhang R, Zhao R, et al. A novel function of novobiocin: disrupting the interaction of HIF 1α and p300/CBP through direct binding to the HIF1α C-terminal activation domain. PLoS One. 2013 May 6;8(5):e62014. PMID: 23671581.

Walsh TJ, Standiford HC, Reboli AC, et al. Randomized Double-Blinded Trial of Rifampin with Either Novobiocin or Trimethoprim-Sulfamethoxazole against Methicillin-Resistant *Staphylococcus aureus* Colonization: Prevention of Antimicrobial Resistance and Effect of Host Factors on Outcome. Antimicrobial agents and chemotherapy 1993 Jun;37(6):1334–42. PMID: 8328783.

N6076 N(p-Tosyl)-GPR-pNA

100 mg

N(p-Tosyl)-Gly-Pro-Arg-pNA

$C_{26}H_{34}N_8O_7S$ FW: 602 ≥95%

Thrombin substrate used to measure thrombin activity.

Thiagarajan P, Dannenbring R, Matsuura K, et al. Monoclonal antibody light chain with prothrombinase activity. Biochemistry. 2000 May 30;39(21):6459-65. PMID: 10828960.

N6272

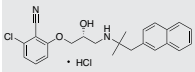

NPS-2143 Hydrochloride

NEW

5 mg
25 mg

$C_{24}H_{25}ClN_2O_2 \bullet HCl$ FW: 445.38 [324523-20-8] ≥98%

Ca^{2+}-sensing receptor antagonist. It increases bone turnover without decreasing bone mineral density, prevents development of pulmonary arterial hypertension, and inhibits production of amyloid-β and VEGF in Alzheimer's disease models.

Dal Prà I, Chiarini A, Pacchiana R, et al. Calcium-Sensing Receptors of Human Astrocyte-Neuron Teams: Amyloid-β-Driven Mediators and Therapeutic Targets of Alzheimer's Disease. Curr Neuropharmacol. 2014 Jul;12(4):353-64. PMID: 25342943.

Dal Prà I, Armato U, Chioffi F, et al. The Aβ peptides-activated calcium-sensing receptor stimulates the production and secretion of vascular endothelial growth factor-A by normoxic adult human cortical astrocytes. Neuromolecular Med. 2014 Dec;16(4):645-57. PMID: 24948534.

Yamamura A. Pathological function of Ca^{2+}-sensing receptor in pulmonary arterial hypertension. J Smooth Muscle Res. 2014;50:8-17. PMID: 24770445.

N7200

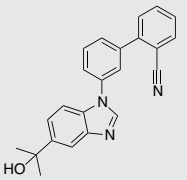

NS-11394

NEW

5 mg
25 mg

$C_{23}H_{19}N_3O$ FW: 353.43 [951650-22-9] ≥98%

GABA-A receptor positive allosteric modulator. It decreases formalin-induced pain and mechanical allodynia and suppresses anxiety in animal models.

Hofmann M, Kordás KS, Gravius A, et al. Assessment of the effects of NS11394 and L-838417, α2/3 subunit-selective GABA(A) [corrected] receptor-positive allosteric modulators, in tests for pain, anxiety, memory and motor function. Behav Pharmacol. 2012 Dec;23(8):790-801. Erratum in: Behav Pharmacol. 2013 Apr;24(2):153. PMID: 23075708.

Hansen RR, Erichsen HK, Brown DT, et al. Positive allosteric modulation of GABA-A receptors reduces capsaicin-induced primary and secondary hypersensitivity in rats. Neuropharmacology. 2012 Dec;63(8):1360-7. PMID: 22985969.

N7209

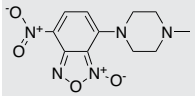

NSC-207895

NEW

1 mg
5 mg

$C_{11}H_{13}N_5O_4$ FW: 279.25 [58131-57-0] ≥98%

Benzofuroxan derivative and MDMX inhibitor. It induces apoptosis in breast cancer cells.

Wang H, Ma X, Ren S, et al. A small-molecule inhibitor of MDMX activates p53 and induces apoptosis. Mol Cancer Ther. 2011 Jan;10(1):69-79. PMID: 21075910.

N7208

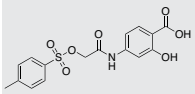

NSC-74859

NEW

5 mg

S3I-201

25 mg
100 mg

$C_{16}H_{15}NO_7S$ FW: 365.36 [501919-59-1] ≥95%

STAT3 inhibitor. It inhibits epithelial-to-mesenchymal transition, suppresses proliferation of hepatocellular carcinoma cells, and improves the efficacy of co-administered chemotherapeutics.

Kim CK, Ryu WS, Choi IY, et al. Detrimental effects of leptin on intracerebral hemorrhage via the STAT3 signal pathway. J Cereb Blood Flow Metab. 2013 Jun;33(6):944-53. PMID: 23462572.

Hu QD, Chen W, Yan TL, et al. NSC 74859 enhances doxorubicin cytotoxicity via inhibition of epithelial-mesenchymal transition in hepatocellular carcinoma cells. Cancer Lett. 2012 Dec 28;325(2):207-13. PMID: 22781398.

N7332

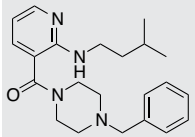

NSI-189

NEW

1 mg
5 mg
25 mg

$C_{22}H_{30}N_4O$ FW: 366.51 [1270138-40-3] ≥98%

Hippocampal volume increasing agent. It stimulates neurogenesis and improves memory consolidation.

https://clinicaltrials.gov/ct2/show/NCT01310881

https://clinicaltrials.gov/ct2/show/NCT01520649

N8277

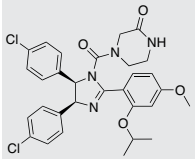

Nutlin-3

NEW

1 mg
5 mg

$C_{30}H_{30}Cl_2N_4O_4$ FW: 581.49 [548472-68-0] ≥98%

MDM2 inhibitor. It induces apoptosis in hepatocellular carcinoma cells, inhibits epithelial-to-mesenchymal transition, lowers hyperglycemia rates, and increases expression of antioxidative enzymes.

Shi X, Liu J, Ren L, et al. Nutlin-3 downregulates p53 phosphorylation on serine(392) and induces apoptosis in hepatocellular carcinoma cells. BMB Rep. 2014 Apr;47(4):221-6. PMID: 24286312.

Choe YJ, Lee SY, Ko KW, et al. Nutlin-3 induces HO-1 expression by activating JNK in a transcription-independent manner of p53. Int J Oncol. 2014 Mar;44(3):761-8. PMID: 24366007.

Wu Y, Fu Y, Zheng L, et al. Nutlin-3 inhibits epithelial-mesenchymal transition by interfering with canonical transforming growth factor-β1-Smad-Snail/Slug axis. Cancer Lett. 2014 Jan 1;342(1):82-91. PMID: 24001610.

N8660 NVP-AUY922

NEW

5 mg
10 mg

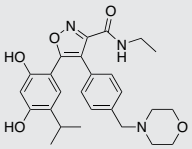

VER-52296

$C_{26}H_{31}N_3O_5$ FW: 465.54 [747412-49-3] ≥98%

HSP90 inhibitor. It induces cell cycle arrest and apoptosis in adult T-cell leukemia cells and suppresses tumor growth and decreases microvessel density in models of breast cancer, ovarian cancer, prostate cancer, and melanoma.

Kim SH, Kang JG, Kim CS, et al. Novel Heat Shock Protein 90 Inhibitor NVP-AUY922 Synergizes With the Histone Deacetylase Inhibitor PXD101 in Induction of Death of Anaplastic Thyroid Carcinoma Cells. J Clin Endocrinol Metab. 2015 Feb;100(2):E253-61. PMID: 25389633.

Taniguchi H, Hasegawa H, Sasaki D, et al. Heat shock protein 90 inhibitor NVP-AUY922 exerts potent activity against adult T-cell leukemia-lymphoma cells. Cancer Sci. 2014 Dec;105(12):1601-8. PMID: 25263741.

N8662 NVP-BGJ398

NEW

5 mg
25 mg
50 mg

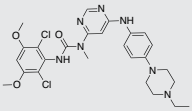

BGJ-398

$C_{26}H_{31}Cl_2N_7O_3$ FW: 560.48 [872511-34-7] ≥98%

FGFR inhibitor. It induces cell cycle arrest and inhibits growth of endometrial cancer cells, prevents progression and tumor formation in models of malignant rhabdoid tumors, and normalizes bone growth and mineralization in models of rickets disease.

Turkington RC, Longley DB, Allen WL, et al. Fibroblast growth factor receptor 4 (FGFR4): a targetable regulator of drug resistance in colorectal cancer. Cell Death Dis. 2014 Feb 6;5:e1046. PMID: 24503538.

Wöhrle S, Weiss A, Ito M, et al. Fibroblast growth factor receptors as novel therapeutic targets in SNF5-deleted malignant rhabdoid tumors. PLoS One. 2013 Oct 30;8(10):e77652. PMID: 24204904.

N8604 NVP-BGT226

NEW

1 mg
5 mg
10 mg

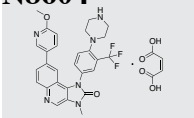

BGT226

$C_{32}H_{29}F_3N_6O_6$ FW: 650.6 [1245537-68-1] ≥98%

PI3K and mTOR inhibitor.

N8460 NVP-BHG712

1 mg
5 mg

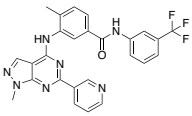

$C_{26}H_{20}F_3N_7O$ FW: 503.48 [940310-85-0] ≥98%

EphB4 inhibitor. It prevents VEGF-induced angiogenesis.

Wnuk M, Hlushchuk R, Janot M, et al. Podocyte EphB4 signaling helps recovery from glomerular injury. Kidney Int. 2012 Jun;81(12):1212-25. PMID: 22398409.

Martiny-Baron G, Holzer P, Billy E, et al. The small molecule specific EphB4 kinase inhibitor NVP-BHG712 inhibits VEGF driven angiogenesis. Angiogenesis. 2010 Sep;13(3):259-67. PMID: 20803239.

N8663 NVP-LDE225 Diphosphate

NEW

5 mg
10 mg

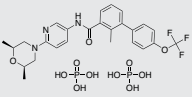

Erismodegib; Sonidegib

$C_{26}H_{26}F_3N_3O_3 \bullet 2H_3PO_4$ FW: 681.49 [1218778-77-8] ≥98%

Smo inhibitor that prevents Wnt signaling and is used to treat basal cell carcinoma. It also inhibits proliferation, migration, and invasion of renal cell carcinoma cells and induces apoptosis in prostate cancer cells.

Ferguson J, Hannam S, Toholka R, et al. Hair Loss and Hedgehog Inhibitors - A Class Effect? Br J Dermatol. 2014 Dec 18. [Epub ahead of print]. PMID: 25523648.

D'Amato C, Rosa R, Marciano R, et al. Inhibition of Hedgehog signalling by NVP-LDE225 (Erismodegib) interferes with growth and invasion of human renal cell carcinoma cells. Br J Cancer. 2014 Sep 9;111(6):1168-79. PMID: 25093491.

Nanta R, Kumar D, Meeker D, et al. NVP-LDE-225 (Erismodegib) inhibits epithelial-mesenchymal transition and human prostate cancer stem cell growth in NOD/SCID IL2Rγ null mice by regulating Bmi-1 and microRNA-128. Oncogenesis. 2013 Apr 8;2:e42. PMID: 23567619.

N8760 NVP-TAE684

NEW

5 mg
10 mg

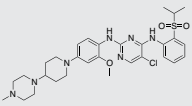

TAE684

$C_{30}H_{40}ClN_7O_3S$ FW: 614.21 [761439-42-3] ≥98%

Inhibitor of ALK, c-Fes, and LRRK2. It induces apoptosis in diffuse large B-cell lymphoma cells and stimulates cell cycle arrest and apoptosis in anaplastic large-cell lymphoma models.

Hellwig S, Miduturu CV, Kanda S, et al. Small-molecule inhibitors of the c-Fes protein-tyrosine kinase. Chem Biol. 2012 Apr 20;19(4):529-40. PMID: 22520759.

Zhang J, Deng X, Choi HG, et al. Characterization of TAE684 as a potent LRRK2 kinase inhibitor. Bioorg Med Chem Lett. 2012 Mar 1;22(5):1864-9. PMID: 22335897.

Cerchietti L, Damm-Welk C, Vater I, et al. Inhibition of anaplastic lymphoma kinase (ALK) activity provides a therapeutic approach for CLTC-ALK-positive human diffuse large B cell lymphomas. PLoS One. 2011 Apr 8;6(4):e18436. PMID: 21494621.

N9874

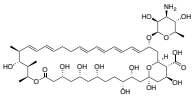

Nystatin

Fungicidin

$C_{47}H_{75}NO_{17}$ FW: 926.09 [1400-61-9] ≥98%

500 KU
1 MU
5 MU

It binds ergosterol and induces pore formation in fungal membranes. It is used to treat fungal infections.

Serhan G, Stack CM, Perrone GG, et al. The polyene antifungals, amphotericin B and nystatin, cause cell death in *Saccharomyces* cerevisiae by a distinct mechanism to amphibian-derived antimicrobial peptides. Ann Clin Microbiol Antimicrob. 2014 May 12;13:18. PMID: 24884795.

O0400

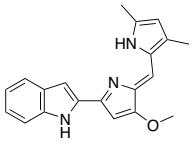

Obatoclax

GX15-070

$C_{20}H_{19}N_3O$ FW: 317.38 [803712-67-6] ≥98%

5 mg
25 mg
50 mg

BH3 mimetic and inhibitor of Bcl-2 and Bcl-xl. It induces autophagy and apoptosis in adenoid cystic carcinoma cells and suppresses proliferation, migration, and invasion of colorectal cancer cells.

Liang LZ, Ma B, Liang YJ, et al. Obatoclax induces Beclin 1- and ATG5-dependent apoptosis and autophagy in adenoid cystic carcinoma cells. Oral Dis. 2014 Dec 8. [Epub ahead of print]. PMID: 25482163.

Arellano ML, Borthakur G, Berger M, et al. A phase II, multicenter, open-label study of obatoclax mesylate in patients with previously untreated myelodysplastic syndromes with anemia or thrombocytopenia. Clin Lymphoma Myeloma Leuk. 2014 Dec;14(6):534-9. PMID: 25052051.

Koehler BC, Scherr AL, Lorenz S, et al. Pan-Bcl-2 inhibitor obatoclax delays cell cycle progression and blocks migration of colorectal cancer cells. PLoS One. 2014 Sep 5;9(9):e106571. PMID: 25192188.

O0829

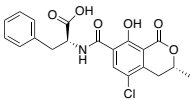

Ochratoxin A

$C_{20}H_{18}ClNO_6$ FW: 403.82 [303-47-9] ≥98%

1 mg
5 mg

Carcinogenic mycotoxin contaminant found in grains. It inhibits glial cell proliferation, induces kidney damage and collagen formation, and may increase the development of cancerous formations.

Hennemeier I, Humpf HU, Gekle M, et al. Role of microRNA-29b in the ochratoxin A-induced enhanced collagen formation in human kidney cells. Toxicology. 2014 Oct 3;324:116-22. PMID: 25091173.

Paradells S, Rocamonde B, Llinares C, et al. Neurotoxic effects of ochratoxin A on the subventricular zone of adult mouse brain. J Appl Toxicol. 2014 Sep 25. [Epub ahead of print]. PMID: 25256750.

Qi X, Yu T, Zhu L, et al. Ochratoxin A induces rat renal carcinogenicity with limited induction of oxidative stress responses. Toxicol Appl Pharmacol. 2014 Sep 8. [Epub ahead of print]. PMID: 25218026.

O1176

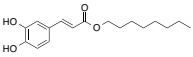

n-Octyl Caffeate

Caffeic acid n-octyl ester

$C_{17}H_{24}O_4$ FW: 292.37 ≥98%

5 mg
25 mg

Synthetic caffeic acid derivative that decreases lipid peroxidation, suppresses LPS-induced alterations in blood pressure, and limits formation of tumor nodules.

Nagaoka T, Banskota AH, Tezuka Y, et al. Inhibitory effects of caffeic acid phenethyl ester analogues on experimental lung metastasis of murine colon 26-L5 carcinoma cells. Biol Pharm Bull. 2003 May;26(5):638-41. PMID: 12736504.

Hsiao G, Shen MY, Chang WC, et al. A novel antioxidant, octyl caffeate, suppression of LPS/IFN-gamma-induced inducible nitric oxide synthase gene expression in rat aortic smooth muscle cells. Biochem Pharmacol. 2003 Apr 15;65(8):1383-92. PMID: 12694879.

O1177

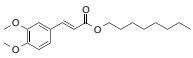

n-Octyl-3,4-Dimethylcaffeate

3,4-Dimethylcaffeic acid n-octyl ester

$C_{19}H_{28}O_4$ FW: 320.42 ≥98%

5 mg
25 mg

Synthetic derivative of n-octyl caffeate that decreases lipid peroxidation, suppresses LPS-induced alterations in blood pressure, and limits formation of tumor nodules.

Nagaoka T, Banskota AH, Tezuka Y, et al. Inhibitory effects of caffeic acid phenethyl ester analogues on experimental lung metastasis of murine colon 26-L5 carcinoma cells. Biol Pharm Bull. 2003 May;26(5):638-41. PMID: 12736504.

O1178

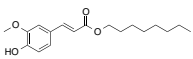

n-Octyl-3-methylcaffeate

3-Methylcaffeic acid n-octyl ester

$C_{18}H_{26}O_4$ FW: 306.4 ≥98%

5 mg
25 mg

Synthetic derivative of n-octyl caffeate that decreases lipid peroxidation, suppresses LPS-induced alterations in blood pressure, and limits formation of tumor nodules.

Nagaoka T, Banskota AH, Tezuka Y, et al. Inhibitory effects of caffeic acid phenethyl ester analogues on experimental lung metastasis of murine colon 26-L5 carcinoma cells. Biol Pharm Bull. 2003 May;26(5):638-41. PMID: 12736504.

O1179

n-Octyl-4-methylcaffeate

5 mg
25 mg

4-Methylcaffeic acid n-octyl ester

$C_{18}H_{26}O_4$ FW: 306.4 ≥98%

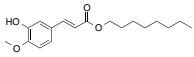

Synthetic derivative of n-octyl caffeate that decreases lipid peroxidation, suppresses LPS-induced alterations in blood pressure, and limits formation of tumor nodules.

Nagaoka T, Banskota AH, Tezuka Y, et al. Inhibitory effects of caffeic acid phenethyl ester analogues on experimental lung metastasis of murine colon 26-L5 carcinoma cells. Biol Pharm Bull. 2003 May;26(5):638-41. PMID: 12736504.

O0978

Octaneuropeptide

1 mg

$C_{41}H_{74}N_{12}O_{11}$ FW: 911.1 ≥98%

Arg-Pro-Gly-Leu-Leu-Asp-Leu-Lys

Diazepam-binding inhibitor derivative that increases intracellular Ca^{2+} levels in astrocytes in a PLC-dependent manner. It may stimulate the development of seizures.

Leprince J, Oulyadi H, Vaudry D, et al. Synthesis, conformational analysis and biological activity of cyclic analogs of the octadecaneuropeptide ODN. Design of a potent endozepine antagonist. Eur J Biochem. 2001 Dec;268(23):6045-57. PMID: 11732998.

Vezzani A, Serafini R, Stasi MA, et al. Epileptogenic activity of two peptides derived from diazepam binding inhibitor after intrahippocampal injection in rats. Epilepsia. 1991 Sep-Oct;32(5):597-603. PMID: 1655399.

O0977

Octopamine Hydrochloride

1 g
5 g
25 g

$C_8H_{11}NO_2 \bullet HCl$ FW: 189.64 [770-05-8] ≥98%

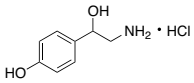

Endogenous biogenic amine, norepinephrine-like neurotransmitter, and potential α/β-adrenergic receptor agonist also found in various plant sources. It stimulates motor activity, inhibits LPS-stimulated release of NO, and decreases juvenile hormone degradation in female *Drosophila*.

Rand D, Knebel D, Ayali A. The effect of octopamine on the locust stomatogastric nervous system. Front Physiol. 2012 Jul 20;3:288. PMID: 22934040.

D'Andrea G, D'Arrigo A, Facchinetti F, et al. Octopamine, unlike other trace amines, inhibits responses of astroglia-enriched cultures to lipopolysaccharide via a β-adrenoreceptor-mediated mechanism. Neurosci Lett. 2012 May 23;517(1):36-40. PMID: 22507691.

Gruntenko NE, Karpova EK, Alekseev AA, et al. Effects of octopamine on reproduction, juvenile hormone metabolism, dopamine, and 20-hydroxyecdysone contents in *Drosophila*. Arch Insect Biochem Physiol. 2007 Jun;65(2):85-94. PMID: 17523171.

O1078

Octreotide Acetate

1 mg
5 mg
25 mg

$C_{49}H_{66}N_{10}O_{10}S_2 \bullet 2C_2H_4O_2$ FW: 1139.36 [79517-01-4] ≥98%

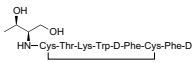

Somatostatin analog and agonist. It inhibits release of growth hormone, suppresses Wnt/β-catenin signaling, inhibits hepatic stellate cell proliferation, decreases peripheral blood mononuclear cell proliferation, and prevents fibrosis.

Wang S, Bao Z, Liang QM, et al. Octreotide stimulates somatostatin receptor-induced apoptosis of SW480 colon cancer cells by activation of glycogen synthase kinase-3β, A Wnt/β-catenin pathway modulator. Hepatogastroenterology. 2013 Oct;60(127):1639-46. PMID: 24634935.

Wang J, Wang L, Song G, et al. The mechanism through which octreotide inhibits hepatic stellate cell activity. Mol Med Rep. 2013 May;7(5):1559-64. PMID: 23525276.

Tug T, Kara H, Karaoglu A, et al. The effect of octreotide, an analog of somatostatin, on bleomycin-induced interstitial pulmonary fibrosis in rats. Drug Chem Toxicol. 2013 Apr;36(2):181-6. PMID: 22946449.

O1200

Odanacatib

NEW

5 mg
10 mg

MK0822

$C_{25}H_{27}F_4N_3O_3S$ FW: 525.56 [603139-19-1] ≥98%

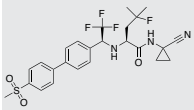

Cathepsin K inhibitor. It protects bone against periapical infection and disease, inhibits bone resorption, and increases bone mineral density.

Bone HG, Dempster DW, Eisman JA, et al. Odanacatib for the treatment of postmenopausal osteoporosis: development history and design and participant characteristics of LOFT, the Long-Term Odanacatib Fracture Trial. Osteoporos Int. 2015 Feb;26(2):699-712. PMID: 25432773.

Hao L, Chen W, McConnell M, et al. A small molecule, Odanacatib, inhibits inflammation and bone loss caused by endodontic disease. Infect Immun. 2015 Jan 12. [Epub ahead of print]. PMID: 25583522.

Gauthier JY, Chauret N, Cromlish W, et al. The discovery of odanacatib (MK-0822), a selective inhibitor of cathepsin K. Bioorg Med Chem Lett. 2008 Feb 1;18(3):923-8. PMID: 18226527.

O2144 Ofloxacin

5 g
10 g
50 g

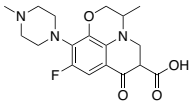

$C_{18}H_{20}FN_3O_4$ FW: 361.37 [82419-36-1] ≥98%

Topoisomerase IV and bacterial DNA gyrase inhibitor used to treat ocular and otic bacterial infections. It also induces ROS-mediated DNA damage under UV light.

Dwivedi A, Mujtaba SF, Yadav N, et al. Cellular and molecular mechanism of ofloxacin induced apoptotic cell death under ambient UV-A and sunlight exposure. Free Radic Res. 2014 Mar;48(3):333-46. PMID: 24286391.

Pantel A, Petrella S, Matrat S, et al. DNA gyrase inhibition assays are necessary to demonstrate fluoroquinolone resistance secondary to gyrB mutations in *Mycobacterium* tuberculosis. Antimicrob Agents Chemother. 2011 Oct;55(10):4524-9. PMID: 21768507.

Drlica K, Zhao X. DNA gyrase, topoisomerase IV, and the 4-quinolones. Microbiol Mol Biol Rev. 1997 Sep;61(3):377-92. PMID: 9293187.

O2145 Ofloxacin Hydrochloride

5 g
10 g
50 g

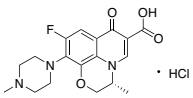

$C_{18}H_{20}FN_3O_4 \cdot HCl$ FW: 397.83 [118120-51-7] ≥98%

Topoisomerase IV and bacterial DNA gyrase inhibitor used to treat ocular and otic bacterial infections. It also induces ROS-mediated DNA damage under UV light.

Dwivedi A, Mujtaba SF, Yadav N, et al. Cellular and molecular mechanism of ofloxacin induced apoptotic cell death under ambient UV-A and sunlight exposure. Free Radic Res. 2014 Mar;48(3):333-46. PMID: 24286391.

Pantel A, Petrella S, Matrat S, et al. DNA gyrase inhibition assays are necessary to demonstrate fluoroquinolone resistance secondary to gyrB mutations in *Mycobacterium* tuberculosis. Antimicrob Agents Chemother. 2011 Oct;55(10):4524-9. PMID: 21768507.

O2146 R-(+)-Ofloxacin

1 mg
5 mg
10 mg

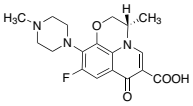

$C_{18}H_{20}FN_3O_4$ FW: 361.37 [100986-86-5] ≥98%

Optically active topoisomerase IV and bacterial DNA gyrase inhibitor used to treat ocular and otic bacterial infections. It also induces ROS-mediated DNA damage under UV light.

Dwivedi A, Mujtaba SF, Yadav N, et al. Cellular and molecular mechanism of ofloxacin induced apoptotic cell death under ambient UV-A and sunlight exposure. Free Radic Res. 2014 Mar;48(3):333-46. PMID: 24286391.

Pantel A, Petrella S, Matrat S, et al. DNA gyrase inhibition assays are necessary to demonstrate fluoroquinolone resistance secondary to gyrB mutations in *Mycobacterium* tuberculosis. Antimicrob Agents Chemother. 2011 Oct;55(10):4524-9. PMID: 21768507.

O4101 Okadaic Acid

25 µg
50 µg
100 µg
1 mg

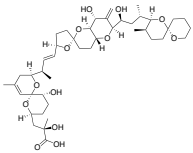

Halochondrine A

$C_{44}H_{68}O_{13}$ FW: 805 [78111-17-8] ≥98%

PP1 and PP2A inhibitor and toxin produced by dinoflagellates and sea sponges. It increases phosphorylation of tau protein, stimulates lipolysis, and increases expression of p21 and p27 in T cell leukemia cells.

Kamat PK, Rai S, Swarnkar S, et al. Molecular and Cellular Mechanism of Okadaic Acid (OKA)-Induced Neurotoxicity: A Novel Tool for Alzheimer's Disease Therapeutic Application. Mol Neurobiol. 2014 Apr 8. [Epub ahead of print]. PMID: 24710687.

Chang NC, Lin AC, Hsu CC, et al. Okadaic Acid, a Bioactive Fatty Acid from Halichondria okadai, Stimulates Lipolysis in Rat Adipocytes: The Pivotal Role of Perilipin Translocation. Evid Based Complement Alternat Med. 2013;2013:545739. PMID: 24319476.

Mori N, Ishikawa C, Uchihara JN, et al. Protein phosphatase 2A as a potential target for treatment of adult T cell leukemia. Curr Cancer Drug Targets. 2013 Oct;13(8):829-42. PMID: 24015987.

O4102 Okadaic Acid Ammonium

25 µg
100 µg
1 mg

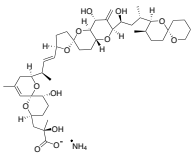

$C_{44}H_{67}O_{13}NH_4$ FW: 822.04 [155716-06-6] ≥98%

PP1 and PP2A inhibitor and toxin produced by dinoflagellates and sea sponges. It increases phosphorylation of tau protein, stimulates lipolysis, and increases expression of p21 and p27 in T cell leukemia cells.

Kamat PK, Rai S, Swarnkar S, et al. Molecular and Cellular Mechanism of Okadaic Acid (OKA)-Induced Neurotoxicity: A Novel Tool for Alzheimer's Disease Therapeutic Application. Mol Neurobiol. 2014 Apr 8. [Epub ahead of print]. PMID: 24710687.

Chang NC, Lin AC, Hsu CC, et al. Okadaic Acid, a Bioactive Fatty Acid from Halichondria okadai, Stimulates Lipolysis in Rat Adipocytes: The Pivotal Role of Perilipin Translocation. Evid Based Complement Alternat Med. 2013;2013:545739. PMID: 24319476.

O4104

Okadaic Acid Sodium

25 μg
100 μg
1 mg

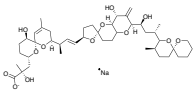

$C_{44}H_{67}O_{13}Na$ FW: 827 [209266-80-8] ≥98%

PP1 and PP2A inhibitor and toxin produced by dinoflagellates and sea sponges. It increases phosphorylation of tau protein, stimulates lipolysis, and increases expression of p21 and p27 in T cell leukemia cells.

Kamat PK, Rai S, Swarnkar S, et al. Molecular and Cellular Mechanism of Okadaic Acid (OKA)-Induced Neurotoxicity: A Novel Tool for Alzheimer's Disease Therapeutic Application. Mol Neurobiol. 2014 Apr 8. [Epub ahead of print]. PMID: 24710687.

Chang NC, Lin AC, Hsu CC, et al. Okadaic Acid, a Bioactive Fatty Acid from Halichondria okadai, Stimulates Lipolysis in Rat Adipocytes: The Pivotal Role of Perilipin Translocation. Evid Based Complement Alternat Med. 2013;2013:545739. PMID: 24319476.

O4400

Olanzapine

100 mg
250 mg
1 g

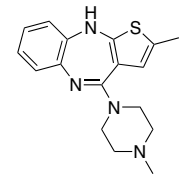

$C_{17}H_{20}N_4S$ FW: 312.43 [132539-06-1] ≥98%

AMPK activator and inhibitor of dopamine D1-4 receptors, 5-HT1A/2/3/6/7 receptors, M1-5 mAChRs, and α1/2-adrenergic receptors used to treat mood disorders and Tourette's syndrome. It also increases blood glucose levels and upregulates BDNF expression.

Ikegami M, Ikeda H, Ishikawa Y, et al. Olanzapine induces glucose intolerance through the activation of AMPK in the mouse hypothalamus. Eur J Pharmacol. 2013 Aug 22. [Epub ahead of print]. PMID: 23973646.

Cheon Y, Park JY, Modi HR, et al. Chronic olanzapine treatment decreases arachidonic acid turnover and prostaglandin E_2 concentration in rat brain. J Neurochem. 2011 Oct;119(2):364-76. PMID: 21812779.

O4402

Olaparib

5 mg
10 mg
25 mg

AZD2281; KU-0059436

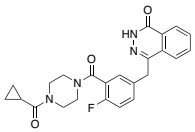

$C_{24}H_{23}FN_4O_3$ FW: 434.47 [763113-22-0] ≥98%

PARP1/2 inhibitor. It induces apoptosis and inhibits proliferation in ovarian cancer and breast cancer cells.

Lee JM, Ledermann JA, Kohn EC. PARP Inhibitors for BRCA1/2 mutation-associated and BRCA-like malignancies. Ann Oncol. 2013 Nov 12. [Epub ahead of print]. PMID: 24225019.

Olaparib Enters Phase III Clinical Testing. Cancer Discov. 2013 Nov;3(11):1210. PMID: 24203936.

Postel-Vinay S, Bajrami I, Friboulet L, et al. A high-throughput screen identifies PARP1/2 inhibitors as a potential therapy for ERCC1-deficient non-small cell lung cancer. Oncogene. 2013 Nov 21;32(47):5377-87. PMID: 23934192.

O4417

Oleanolic Acid

100 mg
500 mg
1 g

Astrantiagenin C; Caryophyllin; Giganteumgenin C; Virgaureagenin B

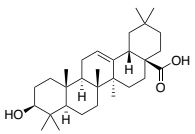

$C_{30}H_{48}O_3$ FW: 456.71 [508-02-1] ≥98%

Found in *Vigna angularis* and *Trigonella foenum-graecum*. It displays several biological activities, including inducing apoptosis in hypertrophic scar fibroblasts, inhibiting eosinophil infiltration and airway inflammation, preventing osteoclast differentiation, and suppressing LPS-induced bone erosion.

Chen JY, Zhang L, Zhang H, et al. Triggering of p38 MAPK and JNK Signaling is Important for Oleanolic Acid-Induced Apoptosis via the Mitochondrial Death Pathway in Hypertrophic Scar Fibroblasts. Phytother Res. 2014 Apr 6. [Epub ahead of print]. PMID: 24706573.

Ghosh S, Bishayee K, Khuda-Bukhsh AR. Oleanolic acid isolated from ethanolic extract of Phytolacca decandra induces apoptosis in A375 skin melanoma cells: drug-DNA interaction and signaling cascade. J Integr Med. 2014 Mar;12(2):102-14.PMID: 24666676.

Kim JY, Cheon YH, Oh HM, et al. Oleanolic acid acetate inhibits osteoclast differentiation by downregulating PLCγ2-$Ca^{(2+)}$-NFATc1 signaling, and suppresses bone loss in mice. Bone. 2014 Mar;60:104-11. PMID: 24361669.

O4533

Oligomycin

1 mg
5 mg
10 mg

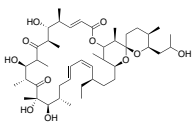

[1404-19-9] ≥97%

Mixture of oligomycins A, B, C. It is an oxidative phosphorylation inhibitor and potential Na^+/K^+ ATPase inhibitor that suppresses bacterial growth. It prevents intestinal epithelial barrier dysfunction induced by inflammatory cytokines and inhibits IFN-γ- and TNF-α-induced reductions in transepithelial resistance and paracellular permeability.

Liu H, Wang P, Cao M, et al. Protective role of oligomycin against intestinal epithelial barrier dysfunction caused by IFN-γ and TNF-α. Cell Physiol Biochem. 2012;29(5-6):799-808. PMID: 22613980.

Ding Y, Hao J, Rakowski RF. Effects of oligomycin on transient currents carried by Na^+ translocation of Bufo $Na^+/K^{(+)}$-ATPase expressed in Xenopus oocytes. J Membr Biol. 2011 Oct;243(1-3):35-46. PMID: 21877177.

O4531 Oligomycin A

1 mg
5 mg

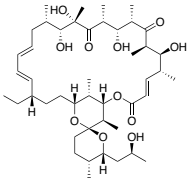

$C_{45}H_{74}O_{11}$ FW: 791.06 [579-13-5] ≥97%

F1F0 ATP synthase inhibitor. It suppresses growth of *Aspergillus*, *Alternaria*, *Botrytis*, and *Phytophthora* and induces apoptosis in cervical cancer cells.

He L, Jang JH, Choi HG, et al. Oligomycin A enhances apoptotic effect of TRAIL through CHOP-mediated death receptor 5 expression. Mol Carcinog. 2013 Feb;52(2):85-93. PMID: 23335397.

Ponnala S, Chetty C, Veeravalli KK, et al. Metabolic remodeling precedes mitochondrial outer membrane permeabilization in human glioma xenograft cells. Int J Oncol. 2012 Feb;40(2):509-18. PMID: 22076676.

Yang PW, Li MG, Zhao JY, et al. Oligomycins A and C, major secondary metabolites isolated from the newly isolated strain *Streptomyces* diastaticus. Folia Microbiol (Praha). 2010 Jan;55(1):10-6. PMID: 20336498.

O4532 Oligomycin B

1 mg
5 mg

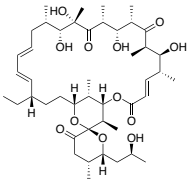

$C_{45}H_{72}O_{12}$ FW: 805.05 [11050-94-5] ≥97%

F1F0 ATP synthase inhibitor. It decreases contractile function under normoxic conditions and increases hypertension, bradycardia, increased arterial P_{O2}, and metabolic acidosis. It is used to mimic hypoxia-induced conditions.

Grover GJ, Malm J. Pharmacological profile of the selective mitochondrial F1F0 ATP hydrolase inhibitor BMS-199264 in myocardial ischemia. Cardiovasc Ther. 2008 Winter;26(4):287-96. PMID: 19035880.

Grover GJ, Atwal KS, Sleph PG, et al. Excessive ATP hydrolysis in ischemic myocardium by mitochondrial F1F0-ATPase: effect of selective pharmacological inhibition of mitochondrial ATPase hydrolase activity. Am J Physiol Heart Circ Physiol. 2004 Oct;287(4):H1747-55. Erratum in: Am J Physiol Heart Circ Physiol. 2006 Jul;291(1):H484. PMID: 15371268.

Koos BJ, Sameshima H, Power GG. Fetal breathing movement, sleep state and cardiovascular responses to an inhibitor of mitochondrial ATPase in sheep. J Dev Physiol. 1986 Feb;8(1):67-75. PMID: 2937831.

O4549 Olmesartan Medoxomil

25 mg
100 mg
250 mg

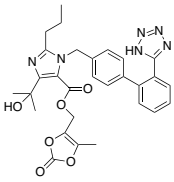

$C_{29}H_{30}N_6O_6$ FW: 558.59 [144689-63-4] ≥98%

AT1 receptor inhibitor used to treat hypertension. It decreases peripheral vascular resistance, increases cerebral blood flow, indirectly activates the DLL4/Notch1 signaling pathway, and attenuates vascular endothelial dysfunction.

You J, Wu J, Jiang G, et al. Olmesartan attenuates cardiac remodeling through DLL4/Notch1 pathway activation in pressure overload mice. J Cardiovasc Pharmacol. 2013 Feb;61(2):142-51. PMID: 23188126.

Verdecchia P, Angeli F, Repaci S, et al. Comparative assessment of angiotensin receptor blockers in different clinical settings. Vasc Health Risk Manag. 2009;5:939-48. PMID: 19997575.

Matsumoto S, Shimodozono M, Miyata R, et al. Benefits of the angiotensin II receptor antagonist olmesartan in controlling hypertension and cerebral hemodynamics after stroke. Hypertens Res. 2009 Nov;32(11):1015-21. PMID: 19745828.

O4556 Olomoucine

5 mg
25 mg
100 mg

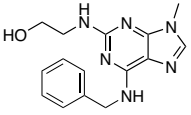

$C_{15}H_{18}N_6O$ FW: 298.34 [101622-51-9] ≥98%

Purine derivative and CDK inhibitor. it alters cell cycle progression in leukemia cells, prevents cathepsin L translocation and the induction of autophagy in neurons, and decreases levels of NO and iNOS in macrophages.

Wandl S, Wesierska-Gadek J. Is olomoucine, a weak CDK2 inhibitor, able to induce apoptosis in cancer cells? Ann N Y Acad Sci. 2009 Aug;1171:242-9. PMID: 19723061.

Fei XF, Qin ZH, Xiang B, et al. Olomoucine inhibits cathepsin L nuclear translocation, activates autophagy and attenuates toxicity of 6-hydroxydopamine. Brain Res. 2009 Apr 6;1264:85-97. PMID: 19368812.

O4658 Olopatadine Hydrochloride

10 mg
25 mg
100 mg

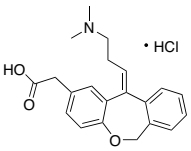

$C_{21}H_{23}NO_3 \cdot HCl$ FW: 373.87 [140462-76-6] ≥99%

Mast cell stabilizer and histamine H1/2/3 receptor antagonist used to treat allergic rhinitis and allergic conjunctivitis. It also suppresses allergy-related increases in substance P, NGF, and VEGF.

Tamura T. Olopatadine ophthalmic solution suppresses substance P release in the conjunctivitis models. Asia Pac Allergy. 2012 Apr;2(2):115-21. PMID: 22701861.

Tamura T. Investigation of the antiallergic activity of olopatadine on rhinitis induced by intranasal instillation of antigen in sensitized rats using thermography. Asia Pac Allergy. 2011 Oct;1(3):138-44. PMID: 22053310.

Roland PS, Ryan MW, Wall GM. Olopatadine nasal spray for the treatment of seasonal allergic rhinitis in patients aged 6 years and older. Expert Opin Pharmacother. 2010 Jun;11(9):1559-67. PMID: 20482305.

O4672 Olsalazine Sodium

25 mg
100 mg
250 mg

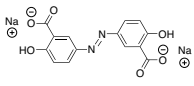

$C_{14}H_8N_2O_6Na_2$ FW: 346.2 [6054-98-4] ≥98%

5-Aminosalicylate prodrug, NSAID, and COX-1/2 inhibitor used to treat ulcerative colitis. It prevents binding of IFN-γ to its receptor in colonic epithelial cells and decreases risk of dysplasia and colorectal cancer.

Malewska K, Rychlik A, Nieradka R, et al. Treatment of inflammatory bowel disease (IBD) in dogs and cats. Pol J Vet Sci. 2011;14(1):165-71. PMID: 21528730.

Rubin DT, LoSavio A, Yadron N, et al. Aminosalicylate therapy in the prevention of dysplasia and colorectal cancer in ulcerative colitis. Clin Gastroenterol Hepatol. 2006 Nov;4(11):1346-50. PMID: 17059900.

O4578 Oltipraz

BRN 0978110

250 mg
500 mg
1 g

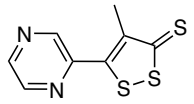

$C_8H_6N_2S_3$ FW: 226.34 [64224-21-1] ≥98%

Antioxidant and Nrf2 activator. It induces phase II enzyme expression, inhibits diet-induced development of hepatic fibrosis, decreases vessel density and tumor growth, and treats *Schistosoma* infection.

Shimozono R, Asaoka Y, Yoshizawa Y, et al. Nrf2 activators attenuate the progression of nonalcoholic steatohepatitis-related fibrosis in a dietary rat model. Mol Pharmacol. 2013 Jul;84(1):62-70. PMID: 23592516.

Yu Z, Shao W, Chiang Y, et al. Oltipraz upregulates the nuclear factor (erythroid-derived 2)-like 2 [corrected] (NRF2) antioxidant system and prevents insulin resistance and obesity induced by a high-fat diet in C57BL/6J mice. Diabetologia. 2011 Apr;54(4):922-34. Erratum in: Diabetologia. 2011 Apr;54(4):989. PMID: 21161163.

O4917 Omeprazole

500 mg
1 g
5 g
10 g

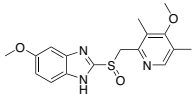

$C_{17}H_{19}N_3O_3S$ FW: 345.42 [73590-58-6] ≥98%

H^+/K^+ ATPase and mitochondrial carnitine/acylcarnitine transporter inhibitor used to treat GERD, dyspepsia, and peptic ulcer disease. It also decreases blood glucose levels and Hb1Ac, improves glucose tolerance, and induces β cell neogenesis and activation.

Tonazzi A, Eberini I, Indiveri C. Molecular mechanism of inhibition of the mitochondrial carnitine/acylcarnitine transporter by omeprazole revealed by proteoliposome assay, mutagenesis and bioinformatics. PLoS One. 2013 Dec 9;8(12):e82286. PMID: 24349247.

Ward RM, Kearns GL. Proton pump inhibitors in pediatrics : mechanism of action, pharmacokinetics, pharmacogenetics, and pharmacodynamics. Paediatr Drugs. 2013 Apr;15(2):119-31. PMID: 23512128.

Mefford IN, Mefford JT, Burris CA. Improved diabetes control and pancreatic function in a type 2 diabetic after omeprazole administration. Case Rep Endocrinol. 2012;2012:468609. PMID: 22937295.

O5212 Ondansetron Hydrochloride Dihydrate

100 mg
500 mg

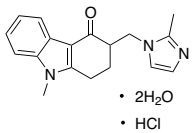

• $2H_2O$
• HCl

$C_{18}H_{19}N_3O \bullet HCl \bullet 2H_2O$ FW: 365.86 [99614-01-4] ≥98%

5-HT3 antagonist used to treat nausea. It also decreases immobility time in the forced swim test and increases open arm entries in the elevated plus maze.

Kurhe Y, Radhakrishnan M, Gupta D. Ondansetron attenuates depression co-morbid with obesity in obese mice subjected to chronic unpredictable mild stress; an approach using behavioral battery tests. Metab Brain Dis. 2014 Jun 27. [Epub ahead of print]. PMID: 24964970.

Rojas C, Raje M, Tsukamoto T, et al. Molecular mechanisms of 5-HT(3) and NK(1) receptor antagonists in prevention of emesis. Eur J Pharmacol. 2014 Jan 5;722:26-37. PMID: 24184669.

O6132 Opioid Receptor Antagonist Ac-RFMWMK-NH2

1 mg

Ac-Arg-Phe-Met-Trp-Met-Lys-NH_2

$C_{44}H_{66}N_{12}O_7S_2$ FW: 939.2 ≥98%

μ/δ/κ-OR inhibitor that increases contractility in the guinea pig ileum assay.

Dooley CT, Chung NN, Schiller PW, et al. Acetalins: opioid receptor antagonists determined through the use of synthetic peptide combinatorial libraries. Proc Natl Acad Sci U S A. 1993 Nov 15;90(22):10811-5. PMID: 8248174.

O6805 Orbifloxacin

100 mg
500 mg
5 g

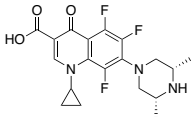

$C_{19}H_{20}F_3N_3O_3$ FW: 395.38 [113617-63-3] ≥98%

Bacterial DNA gyrase inhibitor used to suppress growth of gram negative and gram positive bacteria.

Scott DW, Peters J, Miller WH Jr. Efficacy of orbifloxacin tablets for the treatment of superficial and deep pyoderma due to *Staphylococcus* intermedius infection in dogs. Can Vet J. 2006 Oct;47(10):999-1002. PMID: 17078249.

Ganière JP, Médaille C, Etoré F. In vitro antimicrobial activity of orbifloxacin against *Staphylococcus* intermedius isolates from canine skin and ear infections. Res Vet Sci. 2004 Aug;77(1):67-71. PMID: 15120955.

O7116

Orexin B, human

1 mg

Arg-Ser-Gly-Pro-Pro-Gly-Leu-Gln-Gly-Arg-Leu-Gln-Arg-Leu-Leu-Gln-Ala-Ser-Gly-Asn-His-Ala-Ala-Gly-Ile-Leu-Thr-Met-NH_2

$C_{123}H_{212}N_{44}O_{35}S$ FW: 2899.4 ≥95%

Endogenous neurotransmitter and orexin 2 receptor agonist involved in circadian rhythms and feeding behaviors. It increases secretion of LH and FSH, improves neuronal viability, decreases anxiety, and stimulates insulin secretion.

Cataldi NI, Lux Lantos VA, Libertun C. Orexin A and B in vitro modify orexins receptors expression and gonadotropins secretion of anterior pituitary cells of proestrous rats. Regul Pept. 2014 Jan 10;188:25-30. PMID: 24333629.

Sokołowska P, Urbańska A, Biegańska K, et al. Orexins protect neuronal cell cultures against hypoxic stress: an involvement of Akt signaling. J Mol Neurosci. 2014 Jan;52(1):48-55. PMID: 24243084.

O6932

Oridonin

5 mg
25 mg
100 mg

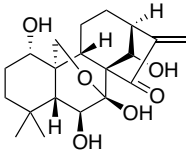

Isodonol; Rubescensin A

$C_{20}H_{28}O_6$ FW: 364.43 [28957-04-2] ≥98%

Potential HSP70 activator found in *Rabdosia rubescens*. It induces cell cycle arrest, apoptosis, and autophagy in several cancer cell lines.

Chen Z, Wang Z, Chen J, et al. Resonance light scattering technique as a new tool to determine the binding mode of anticancer drug oridonin to DNA. Eur J Med Chem. 2013 Aug;66:380-7. PMID: 23827178.

Dal Piaz F, Cotugno R, Lepore L, et al. Chemical proteomics reveals HSP70 1A as a target for the anticancer diterpene oridonin in Jurkat cells. J Proteomics. 2013 Apr 26;82:14-26. PMID: 23416714.

Yin B, Sheng H, Lin J, et al. The cell death of C6 astrocytoma cells induced by oridonin and its mechanism. Int J Clin Exp Pathol. 2012;5(6):562-8. PMID: 22949939.

O6845

Orlistat

NEW

100 mg
500 mg
1 g

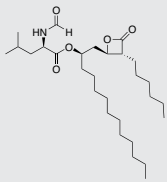

$C_{29}H_{53}NO_5$ FW: 495.73 [96829-58-2] ≥98%

Fatty acid synthase inhibitor used as a weight loss aid. It also inhibits tumor growth in T cell lymphoma and colorectal carcinoma models.

Kant S, Kumar A, Singh SM. Tumor growth retardation and chemosensitizing action of fatty acid synthase inhibitor orlistat on T cell lymphoma: implication of reconstituted tumor microenvironment and multidrug resistance phenotype. Biochim Biophys Acta. 2014 Jan;1840(1):294-302. PMID: 24060750.

Chuang HY, Chang YF, Hwang JJ. Antitumor effect of orlistat, a fatty acid synthase inhibitor, is via activation of caspase-3 on human colorectal carcinoma-bearing animal. Biomed Pharmacother. 2011 Jul;65(4):286-92. PMID: 21723078.

Halpern A, Pepe RB, Monegaglia AP, et al. Efficacy and tolerability of the association of sibutramine and orlistat for six months in overweight and obese patients. J Obes. 2010;2010. pii: 602537. PMID: 20871858.

O6953

Ornidazole

5 g
50 g

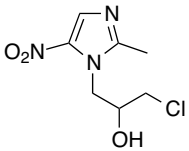

$C_7H_{10}ClN_3O_3$ FW: 219.63 [16773-42-5] ≥98%

Genotoxic 5-nitroimidazole derivative used to treat dysentery and other symptoms of bacterial infections. It increases sister chromatid exchange and micronuclei formation in peripheral lymphocytes.

Thulkar J, Kriplani A, Agarwal N. A comparative study of oral single dose of metronidazole, tinidazole, secnidazole and ornidazole in bacterial vaginosis. Indian J Pharmacol. 2012 Mar;44(2):243-5. PMID: 22529484.

Ikbal M, Yilmaz G, Dogan H, et al. The evaluation of genotoxic potential of ornidazole, nitroimidazole, in lymphocyte culture of patients with amebiasis. Drug Chem Toxicol. 2011 Apr;34(2):162-6. PMID: 21314465.

O7053

L-Ornithine Hydrochloride

10 g
25 g
100 g
1 kg

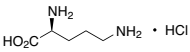

$C_5H_{12}N_2O_2 \cdot HCl$ FW: 168.62 [3184-13-2] ≥98%

Non-proteinogenic amino acid and L-arginine metabolite involved in the urea cycle. It increases efficiency of energy consumption, promotes excretion of ammonia, and decreases the symptoms of hepatic encephalopathy associated with liver cirrhosis.

Ivanenkov YA, Chufarova NV. Small-molecule arginase inhibitors. Pharm Pat Anal. 2014 Jan;3(1):65-85. PMID: 24354980.

Sikorska H, Cianciara J, Wiercińska-Drapało A. Physiological functions of L-ornithine and L-aspartate in the body and the efficacy of administration of L-ornithine-L-aspartate in conditions of relative deficiency. Pol Merkur Lekarski. 2010 Jun;28(168):490-5. PMID: 20642112.

O7208

Oscillaginin A

NEW

100 μg

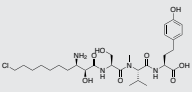

$C_{29}H_{47}ClN_4O_8$ FW: 615.16 [189438-19-5] ≥95%

Potential PP inhibitor found in *Oscillatoria*. It is likely cytotoxic.

Sano T and Kaya K. A 3-amino-10-chloro-2-hydroxydecanoic acid-containing tetrapeptide from Oscillatoria agardhii. Phytochemistry.1997 Apr;44(8):1503-05.

O7209 Oscillaginin A Methyl Ester — NEW — 100 µg

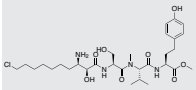

$C_{30}H_{49}ClN_4O_8$ FW: 629.19 ≥95%

Potential PP inhibitor found in *Oscillatoria*. It is likely cytotoxic.

Sano T and Kaya K. A 3-amino-10-chloro-2-hydroxydecanoic acid-containing tetrapeptide from Oscillatoria agardhii. Phytochemistry.1997 Apr;44(8):1503-05.

O7210 Oscillaginin B — NEW — 100 µg

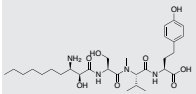

$C_{29}H_{48}N_4O_8$ FW: 580.71 [189438-21-9] ≥95%

Potential PP inhibitor found in *Oscillatoria*. It is likely cytotoxic.

Sano T and Kaya K. A 3-amino-10-chloro-2-hydroxydecanoic acid-containing tetrapeptide from Oscillatoria agardhii. Phytochemistry.1997 Apr;44(8):1503-05.

O7211 Oscillaginin B Methyl Ester — NEW — 100 µg

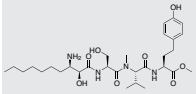

$C_{30}H_{50}N_4O_8$ FW: 594.74 ≥95%

Potential PP inhibitor found in *Oscillatoria*. It is likely cytotoxic.

Sano T and Kaya K. A 3-amino-10-chloro-2-hydroxydecanoic acid-containing tetrapeptide from Oscillatoria agardhii. Phytochemistry.1997 Apr;44(8):1503-05.

O7212 Oscillaginin C — NEW — 25 µg

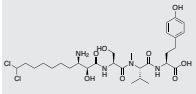

$C_{29}H_{46}Cl_2N_4O_8$ FW: 649.6 ≥95%

Potential PP inhibitor found in *Oscillatoria*. It is likely cytotoxic.

Sano T and Kaya K. A 3-amino-10-chloro-2-hydroxydecanoic acid-containing tetrapeptide from Oscillatoria agardhii. Phytochemistry.1997 Apr;44(8):1503-05.

O7213 Oscillamide Y — NEW — 100 µg

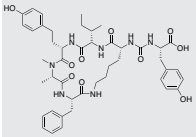

$C_{45}H_{59}N_7O_{10}$ FW: 857.99 [189438-19-5] ≥95%

PP1/2A inhibitor found in *Oscillatoria*. It is likely cytotoxic.

Barco M, Flores C, Rivera J, et al. Determination of microcystin variants and related peptides present in a water bloom of Planktothrix (Oscillatoria) rubescens in a Spanish drinking water reservoir by LC/ESI-MS. Toxicon. 2004 Dec 15;44(8):881-6. PMID: 15530970.

Sano T, Usui T, Ueda K, et al. Isolation of new protein phosphatase inhibitors from two cyanobacteria species, Planktothrix spp. J Nat Prod. 2001 Aug;64(8):1052-5. PMID: 11520225.

O7218 Oseltamivir Phosphate — 10 mg, 25 mg, 100 mg

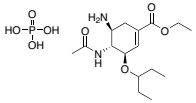

$C_{16}H_{28}N_2O_4 \cdot H_3PO_4$ FW: 410.4 [204255-11-8] ≥98%

Viral neuraminidase inhibitor and potential MAO-A inhibitor used to treat influenza infection. It also increases dopamine levels in the brain.

Huang L, Cao Y, Zhou J, et al. A conformational restriction in influenza A virus neuraminidase binding site by R152 caused the combinational effect of I222T with H274Y on oseltamivir resistance. Antimicrob Agents Chemother. 2013 Dec 23. [Epub ahead of print]. PMID: 24366752.

Vavricka CJ, Liu Y, Kiyota H, et al. Influenza neuraminidase operates via a nucleophilic mechanism and can be targeted by covalent inhibitors. Nat Commun. 2013;4:1491. PMID: 23422659.

O7332 OSI-027 — NEW — 1 mg, 5 mg, 10 mg

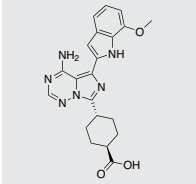

$C_{21}H_{22}N_6O_3$ FW: 406.44 [936890-98-1] ≥98%

Inhibitor of mTOR. It induces apoptosis and inhibits proliferation of various lymphoid cancer cells.

Li H, Lin J, Wang X, et al. Targeting of mTORC2 prevents cell migration and promotes apoptosis in breast cancer. Breast Cancer Res Treat. 2012 Aug;134(3):1057-66. PMID: 22476852.

Gupta M, Hendrickson AE, Yun SS, et al. Dual mTORC1/mTORC2 inhibition diminishes Akt activation and induces Puma-dependent apoptosis in lymphoid malignancies. Blood. 2012 Jan 12;119(2):476-87. PMID: 22080480.

O7333 OSI-906 — NEW — 5 mg, 25 mg, 50 mg

Linsitinib

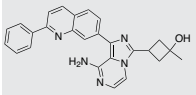

$C_{26}H_{23}N_5O$ FW: 421.49 [867160-71-2] ≥98%

IGF-1R and InsR inhibitor. It inhibits cell proliferation and tumor growth in models of ovarian cancer, colorectal cancer, breast cancer, and prostate cancer.

Bendell JC, Jones SF, Hart L, et al. A phase Ib study of linsitinib (OSI-906), a dual inhibitor of IGF-1R and IR tyrosine kinase, in combination with everolimus as treatment for patients with refractory metastatic colorectal cancer. Invest New Drugs. 2015 Feb;33(1):187-93. PMID: 25335932.

Rao W, Li H, Song F, et al. OVA66 increases cell growth, invasion and survival via regulation of IGF-1R-MAPK signaling in human cancer cells. Carcinogenesis. 2014 Jul;35(7):1573-81. PMID: 24667688.

O7377 Osthole

250 mg
1 g
5 g

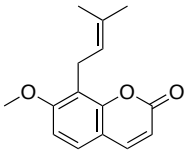

$C_{15}H_{16}O_3$ FW: 244.29 [484-12-8] ≥98%

Ca^{2+} channel blocker. It inhibits IGF-1-induced epithelial-to-mesenchymal transition, suppresses migration and invasion of lung cancer cells, decreases carrageenan-induced lung inflammation, and prevents lipid peroxidation.

Lin YC, Lin JC, Hung CM, et al. Osthole inhibits insulin-like growth factor-1-induced epithelial to mesenchymal transition via the inhibition of PI3K/Akt signaling pathway in human brain cancer cells. J Agric Food Chem. 2014 May 14. [Epub ahead of print]. PMID: 24828835.

Li Z, Ji H, Song X, et al. Osthole attenuates the development of carrageenan-induced lung inflammation in rats. Int Immunopharmacol. 2014 May;20(1):33-6. PMID: 24576740.

Mo LQ, Chen Y, Song L, et al. Osthole prevents intestinal ischemia-reperfusion-induced lung injury in a rodent model. J Surg Res. 2014 Mar 15. [Epub ahead of print]. PMID: 24726060.

O7992 OTX-015

NEW

5 mg
10 mg

Y-803

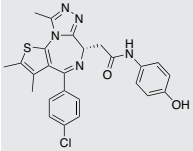

$C_{25}H_{22}ClN_5O_2S$ FW: 491.99 [202590-98-5] ≥98%

BRD inhibitor. It inhibits cell and tumor growth in models of anaplastic large cell lymphoma and induces apoptosis in diffuse large B-cell lymphoma cells.

Boi M, Gaudio E, Bonetti P, et al. The BET Bromodomain Inhibitor OTX015 Affects Pathogenetic Pathways in Preclinical B-cell Tumor Models and Synergizes with Targeted Drugs. Clin Cancer Res. 2015 Apr 1;21(7):1628-38.PMID: 25633213.

Noel JK, Iwata K, Ooike S, et al. Development of the BET bromodomains inhibitor OTX015. Mol Cancer Ther. 2013 Nov:12;C244.

Boi M, Todaro M, Vurchio V, et al. OTX015, a bromodomains and extraterminal inhibitor, represents a novel agent for ALK positive anaplastic large cell lymphoma. Mol Cancer Ther. 2013 Nov:12;A219.

O8500 Ovalbumin Fragment (257-264)

1 mg

OVA (257-264)

Ser-Ile-Ile-Asn-Phe-Glu-Lys-Leu

$C_{45}H_{74}N_{10}O_{13}$ FW: 963.2 ≥98%

OVA antigen containing a CD8+ T cell epitope used to stimulate a Th1 immune response.

Cheng WK, Wee K, Kollmann TR, et al. Topical CpG adjuvantation of a protein-based vaccine induces protective immunity to Listeria monocytogenes. Clin Vaccine Immunol. 2014 Mar;21(3):329-39. PMID: 24391136.

Xie Y, Wang L, Freywald A, et al. A novel T cell-based vaccine capable of stimulating long-term functional CTL memory against B16 melanoma via CD40L signaling. Cell Mol Immunol. 2013 Jan;10(1):72-7. PMID: 23042534.

O8503 Ovalbumin Fragment (323-339)

5 mg

OVA (323-339)

Ile-Ser-Gln-Ala-Val-His-Ala-Ala-His-Ala-Glu-Ile-Asn-Glu-Ala-Gly-Arg

$C_{74}H_{120}N_{26}O_{25}$ FW: 1773.9 ≥98%

OVA antigen containing a CD4+ T cell epitope used to stimulate a Th2 immune response.

Nakajima-Adachi H, Koike E, Totsuka M, et al. Two distinct epitopes on the ovalbumin 323-339 peptide differentiating CD4+ T cells into the Th2 or Th1 phenotype. Biosci Biotechnol Biochem. 2012;76(10):1979-81. PMID: 23047087.

O9302 Oxacillin Sodium Monohydrate

1 g
5 g
25 g

Penicillin P-12

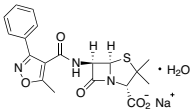

$C_{19}H_{18}N_3NaO_5S \cdot H_2O$ FW: 441.44 [7240-38-2] ≥98%

Penicillin binding protein inhibitor that prevents cell wall synthesis and suppresses growth of methicillin-resistant or vancomycin-resistant *Staphylococcus aureus*.

Werth BJ, Vidaillac C, Murray KP, et al. Novel combinations of vancomycin plus ceftaroline or oxacillin against methicillin-resistant vancomycin-intermediate *Staphylococcus aureus* (VISA) and heterogeneous VISA. Antimicrob Agents Chemother. 2013 May;57(5):2376-9. PMID: 23422917.

O9201 Oxaliplatin

5 mg
25 mg
100 mg
500 mg

Oxalatoplatinum

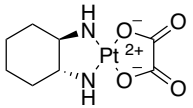

$C_8H_{14}N_2O_4Pt$ FW: 397.29 [61825-94-3] ≥98%

Platinum-based DNA cross-linker used to treat colorectal cancer. It induces S phase cell cycle arrest, upregulates expression of p21 and p53, and inhibits proliferation in hepatocellular carcinoma cells.

Chen X, Wu Y, Dong H, et al. Platinum-based agents for individualized cancer treatment. Curr Mol Med. 2013 Dec;13(10):1603-12. PMID: 24206132.

Gao J, Wang R, Yang Q, et al. Effect of Oxaliplatin on cell cycle of hepatocellular carcinoma cell line HepG2. Zhejiang Da Xue Xue Bao Yi Xue Ban. 2013 Jul;42(4):437-42. PMID: 24022933.

O9210 Oxcarbazepine

1 g
5 g
25 g

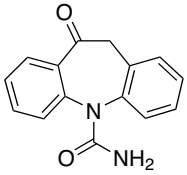

$C_{15}H_{12}N_2O_2$ FW: 252.27 [28721-07-5] ≥98%

α4β2 nAChR desensitizer and blocker of delayed-rectifier voltage-gated K^+ and voltage-gated Na^+ channels used to treat epilepsy, mood disorders, and neuropathic pain. It reduces action potential amplitude and prolongs duration. It also prevents relapse in recently abstinent alcohol-dependent subjects.

Di Resta C, Ambrosi P, Curia G, et al. Effect of carbamazepine and oxcarbazepine on wild-type and mutant neuronal nicotinic acetylcholine receptors linked to nocturnal frontal lobe epilepsy. Eur J Pharmacol. 2010 Sep 15;643(1):13-20. PMID: 20561518.

Johannessen Landmark C, Johannessen SI. Pharmacological management of epilepsy: recent advances and future prospects. Drugs. 2008;68(14):1925-39. PMID: 18778117.

Huang CW, Huang CC, Lin MW, et al. The synergistic inhibitory actions of oxcarbazepine on voltage-gated sodium and potassium currents in differentiated NG108-15 neuronal cells and model neurons. Int J Neuropsychopharmacol. 2008 Aug;11(5):597-610. PMID: 18184444.

O9322 Oxfendazole

10 g
25 g
100 g

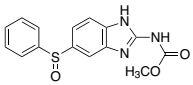

$C_{15}H_{13}N_3O_3S$ FW: 315.35 [53716-50-0] ≥98%

Fenbendazole derivative and microtubule polymerization inhibitor used to treat worm infections. It inhibits growth of *Fasciola*, *Taenia*, *Ascaris*, *Trichuris*, *Physocephalus*, and *Ascarops*.

Ortiz P, Terrones S, Cabrera M, et al. Oxfendazole flukicidal activity in pigs. Acta Trop. 2014 Aug;136:10-3. PMID: 24713198.

Mkupasi EM, Ngowi HA, Sikasunge CS, et al. Efficacy of ivermectin and oxfendazole against Taenia solium cysticercosis and other parasitoses in naturally infected pigs. Acta Trop. 2013 Oct;128(1):48-53. PMID: 23806569.

O9334 Oxibendazole

5 g
10 g
25 g

Equitac; SKF-30310; Anthelcide EQ

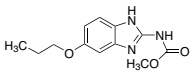

$C_{12}H_{15}N_3O_3$ FW: 249.27 [20559-55-1] ≥98%

Microtubule polymerization inhibitor used to treat worm infections. It inhibits growth of *Coronocyclus*, *Cylicocyclus*, *Cyathostornum*, *Cylicostephanus*, *Strongylus*, and *Oxyuris*.

Nielsen MK, Betancourt A, Lyons ET, et al. Characterization of the inflammatory response to anthelmintic treatment of ponies with cyathostominosis. Vet J. 2013 Nov;198(2):457-62. PMID: 24035469.

Traversa D, Iorio R, Otranto D, et al. Species-specific identification of equine cyathostomes resistant to fenbendazole and susceptible to oxibendazole and moxidectin by macroarray probing. Exp Parasitol. 2009 Jan;121(1):92-5. PMID: 18950625.

O9234 Oxiconazole Nitrate

1 g
5 g
25 g

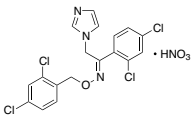

$C_{18}H_{13}Cl_4N_3O \bullet HNO_3$ FW: 492.15 [64211-46-7] ≥98%

14-α Demethylase inhibitor that inhibits ergosterol synthesis and fungal cell wall formation. It is active against *Candida* and *Leishmania*.

Kalra MG, Higgins KE, Kinney BS. Intertrigo and secondary skin infections. Am Fam Physician. 2014 Apr 1;89(7):569-73. PMID: 24695603.

Jerajani HR, Amladi ST, Bongale R, et al. Evaluation of clinical efficacy and safety of once daily topical administration of 1% oxiconazole cream and lotion in dermatophytosis : an open label, non comparative multicentre study. Indian J Dermatol Venereol Leprol. 2000 Jul-Aug;66(4):188-92. PMID: 20877072.

Gebre-Hiwot A, Frommel D. The in-vitro anti-*leishmania*l activity of inhibitors of ergosterol biosynthesis. J Antimicrob Chemother. 1993 Dec;32(6):837-42. PMID: 8144423.

O9256 16-Oxocafestol

25 mg
50 mg
100 mg
500 mg

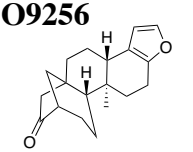

$C_{19}H_{24}O_2$ FW: 284.39 [108664-98-8] ≥97%

Synthetic cafestol derivative. It may induce phase II enzyme activity.

Lam LK, Sparnins VL, Wattenberg LW. Effects of derivatives of kahweol and cafestol on the activity of glutathione S-transferase in mice. J Med Chem. 1987 Aug;30(8):1399-403. PMID: 3612687.

O9257 16-Oxokahweol

10 mg
25 mg
50 mg
100 mg

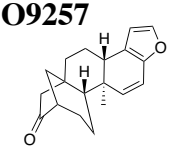

$C_{19}H_{22}O_2$ FW: 282.39 [108664-99-9] ≥95%

Synthetic kahweol derivative. It may induce phase II enzyme activity.

Lam LK, Sparnins VL, Wattenberg LW. Effects of derivatives of kahweol and cafestol on the activity of glutathione S-transferase in mice. J Med Chem. 1987 Aug;30(8):1399-403. PMID: 3612687.

O9458 Oxolinic Acid

5 g
25 g

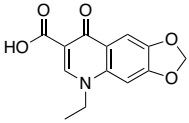

$C_{13}H_{11}NO_5$ FW: 261.23 [14698-29-4] ≥98.0%

Bacterial DNA gyrase inhibitor. It may intercalate DNA and lower the threshold for induction of seizure through activation of excitatory amino acid receptors.

Kljun J, Bratsos I, Alessio E, et al. New uses for old drugs: attempts to convert quinolone antibacterials into potential anticancer agents containing ruthenium. Inorg Chem. 2013 Aug 5;52(15):9039-52. PMID: 23886077.

Tarushi A, Lafazanis K, Kljun J, et al. First- and second-generation quinolone antibacterial drugs interacting with zinc(II): structure and biological perspectives. J Inorg Biochem. 2013 Apr;121:53-65. PMID: 23353082.

Kwon HR, Choi GJ, Choi YH, et al. Suppression of pine wilt disease by an antibacterial agent, oxolinic acid. Pest Manag Sci. 2010 Jun;66(6):634-9. PMID: 20151406.

O9596 Oxybutynin Hydrochloride

250 mg
1 g

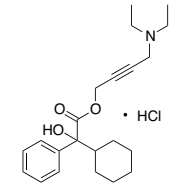

$C_{22}H_{31}NO_3 \bullet HCl$ FW: 393.95 [1508-65-2] ≥98%

mAChR antagonist used to treat overactive bladder. It decreases afferent activity of C-fibers and Aδ fibers and downregulates stretch-induced c-Jun signaling and growth of bladder smooth muscle cells.

De Laet K, De Wachter S, Wyndaele JJ. Systemic oxybutynin decreases afferent activity of the pelvic nerve of the rat: new insights into the working mechanism of antimuscarinics. Neurourol Urodyn. 2006;25(2):156-61. PMID: 16372316.

Park JM, Bauer SB, Freeman MR, et al. Oxybutynin chloride inhibits proliferation and suppresses gene expression in bladder smooth muscle cells. J Urol. 1999 Sep;162(3 Pt 2):1110-4. PMID: 10458442.

O9398 Oxymetazoline Hydrochloride

5 g
25 g

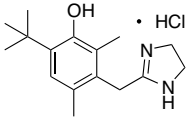

$C_{16}H_{24}N_2O \bullet HCl$ FW: 296.84 [2315-02-8] ≥98%

Imidazoline derivative, α1-adrenergic receptor agonist, and α2-adrenergic receptor partial agonist used as a decongestant. It also inhibits lipid peroxidation and acts as a radical scavenger.

Browning S, Housley D, Richards R, et al. The effects of oxymetazoline on lysozyme secretion from the human nasal mucosa. Acta Otolaryngol. 1997 Nov;117(6):851-5. PMID: 9442826.

Westerveld GJ, Scheeren RA, Dekker I, et al. Anti-oxidant actions of oxymethazoline and xylomethazoline. Eur J Pharmacol. 1995 Sep 15;291(1):27-31. PMID: 8549644.

O9396 Oxytetracycline

10 g
50 g
100 g

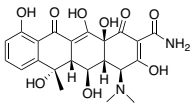

$C_{22}H_{24}N_2O_9$ FW: 460.43 [79-57-2] ≥96%

Protein translation inhibitor. It also inhibits proliferation of adenocarcinoma cells.

Strobel H, Lauseker M, Forbes AB. Targeted antibiotic treatment of lame sheep with footrot using either oxytetracycline or gamithromycin. Vet Rec. 2014 Jan 11;174(2):46. PMID: 24362004.

Shao J, Feng G. Selective killing effect of oxytetracycline, propafenone and metamizole on A549 or Hela cells. Chin J Cancer Res. 2013 Dec;25(6):662-70. PMID: 24385693.

O9397 Oxytetracycline Hydrochloride

10 g
50 g
100 g

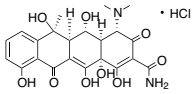

$C_{22}H_{24}N_2O_9 \bullet HCl$ FW: 496.93 [2058-46-0] ≥96%

Protein translation inhibitor. It also inhibits proliferation of adenocarcinoma cells.

Strobel H, Lauseker M, Forbes AB. Targeted antibiotic treatment of lame sheep with footrot using either oxytetracycline or gamithromycin. Vet Rec. 2014 Jan 11;174(2):46. PMID: 24362004.

Shao J, Feng G. Selective killing effect of oxytetracycline, propafenone and metamizole on A549 or Hela cells. Chin J Cancer Res. 2013 Dec;25(6):662-70. PMID: 24385693.

O9497 Oxytocin

5 mg
25 mg
100 mg
1 g

Cys-Tyr-Ile-Gln-Asn-Cys-Pro-Leu-Gly-NH_2
(Disulfide bridge Cys1-Cys6)

$C_{43}H_{66}N_{12}O_{12}S_2$ FW: 1007.2 [50-56-6] ≥95%

Endogenous oxytocin receptor agonist and acid-sensing ion channel blocker involved in social recognition and intimacy behavior. It may be used as a biomarker of bone mineral density.

Breuil V, Panaia-Ferrari P, Fontas E, et al. Oxytocin, a new determinant of bone mineral density in post-menopausal women: analysis of the OPUS cohort. J Clin Endocrinol Metab. 2014 Apr;99(4):E634-41. PMID: 24446658.

Yuen KW, Garner JP, Carson DS, et al. Plasma oxytocin concentrations are lower in depressed vs. healthy control women and are independent of cortisol. J Psychiatr Res. 2014 Apr;51:30-6. PMID: 24405552.

O9702

Ozagrel Hydrochloride

10 mg
25 mg
100 mg

OKY-046

$C_{13}H_{12}N_2O_2 \cdot HCl$ FW: 264.71 [82571-53-7] ≥98%

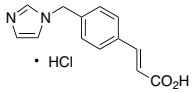

TxA2 synthase inhibitor. It decreases airway responses to inhalation of leukotriene C4, inhibits histamine release in responses of bronchoconstriction, decreases in retinal blood flow associated with diabetes-induced retinopathy, and decreases infarct size and thrombus formation in models of ischemia-induced myocardial injury.

Sathler PC, Santana M, Lourenço AL, et al. Human thromboxane synthase: comparative modeling and docking evaluation with the competitive inhibitors Dazoxiben and Ozagrel. J Enzyme Inhib Med Chem. 2013 Aug 5. Epub ahead of print. PMID: 23914925.

Tomishima Y, Ishitsuka Y, Matsunaga N, et al. Ozagrel hydrochloride, a selective thromboxane A2 synthase inhibitor, alleviates liver injury induced by acetaminophen overdose in mice. BMC Gastroenterol. 2013 Jan 30;13:21. PMID: 23363429.

P0001

P1 Peptide

0.5 mg
1 mg
2.5 mg

$C_{39}H_{63}N_{11}O_{13}$ FW: 894 ≥95%

H-Gly-Ser-Phe-Leu-Val-Arg-Glu-Ser-OH

Prevents EGFR from binding the Src homology region of PLCγ.

Hidaka M, Homma Y, Takenawa T. Highly conserved eight amino acid sequence in SH2 is important for recognition of phosphotyrosine site. Biochem Biophys Res Commun. 1991 Nov 14;180(3):1490-7. PMID: 1719984.

P0055

P55-TNFR Peptide

1 mg
2 mg
5 mg

$C_{57}H_{95}N_{15}O_{22}$ FW: 1342.48 ≥95%

H-Leu-Pro-Gln-Ile-Glu-Asn-Val-Lys-Gly-Thr-Glu-Asp-OH

Fragment of P55 TNF receptor. It may be involved in insulin sensitivity, cell death signaling, and the development of atherosclerosis.

Xanthoulea S, Thelen M, Pöttgens C, et al. Absence of p55 TNF receptor reduces atherosclerosis, but has no major effect on angiotensin II induced aneurysms in LDL receptor deficient mice. PLoS One. 2009 Jul 7;4(7):e6113. PMID: 19582157.

Pandey M, Tuncman G, Hotamisligil GS, et al. Divergent roles for p55 and p75 TNF-alpha receptors in the induction of plasminogen activator inhibitor-1. Am J Pathol. 2003 Mar;162(3):933-41. PMID: 12598326.

P0075

P75-TNFR Peptide

1 mg
2 mg
5 mg

$C_{53}H_{85}N_{15}O_{15}S_1$ FW: 1204.42 ≥95%

H-Ser-Met-Ala-Pro-Gly-Ala-Val-His-Leu-Pro-Gln-Pro-OH

Fragment of P75 TNF receptor. It may be involved in post-injury protective signaling and expression of plasminogen activator inhibitor 1.

Pandey M, Tuncman G, Hotamisligil GS, et al. Divergent roles for p55 and p75 TNF-alpha receptors in the induction of plasminogen activator inhibitor-1. Am J Pathol. 2003 Mar;162(3):933-41. PMID: 12598326.

Shen Y, Li R, Shiosaki K. Inhibition of p75 tumor necrosis factor receptor by antisense oligonucleotides increases hypoxic injury and beta-amyloid toxicity in human neuronal cell line. J Biol Chem. 1997 Feb 7;272(6):3550-3. PMID: 9013604.

P0013

P7C3

5 mg
25 mg

$C_{21}H_{18}Br_2N_2O$ FW: 474.2 [301353-96-8] ≥98%

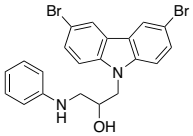

Neuroprotective agent that promotes neurogenesis, prevents neuronal apoptosis, limits cognitive decline in aging models, and inhibits MPP+-mediated death of dopaminergic neurons.

Asai-Coakwell M, March L, Dai XH, et al. Contribution of growth differentiation factor 6-dependent cell survival to early-onset retinal dystrophies. Hum Mol Genet. 2013 Apr 1;22(7):1432-42. PMID: 23307924.

De Jesús-Cortés H, Xu P, Drawbridge J, et al. Neuroprotective efficacy of aminopropyl carbazoles in a mouse model of Parkinson disease. Proc Natl Acad Sci U S A. 2012 Oct 16;109(42):17010-5. PMID: 23027934.

P0109

P7C3A20

NEW

5 mg
25 mg

$C_{22}H_{19}Br_2FN_2O$ FW: 506.21 ≥95%

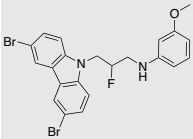

P7C3 analog. It decreases brain contusion volume and improves motor function and cognitive ability in traumatic brain injury models, increases survival of dentate gyrus neurons, and inhibits MPTP-induced neuronal death in models of Parkinson's disease.

Walker AK, Rivera PD, Wang Q, et al. The P7C3 class of neuroprotective compounds exerts antidepressant efficacy in mice by increasing hippocampal neurogenesis. Mol Psychiatry. 2014 Apr 22. [Epub ahead of print]. PMID: 24751964.

Blaya MO, Bramlett HM, Naidoo J, et al. Neuroprotective efficacy of a proneurogenic compound after traumatic brain injury. J Neurotrauma. 2014 Mar 1;31(5):476-86. PMID: 24070637.

De Jesús-Cortés H, Xu P, Drawbridge J, et al. Neuroprotective efficacy of aminopropyl carbazoles in a mouse model of Parkinson disease. Proc Natl Acad Sci U S A. 2012 Oct 16;109(42):17010-5. PMID: 23027934.

P0110 (R)-P7C3-OMe

NEW

5 mg
25 mg

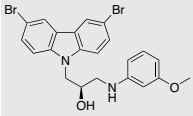

O-methoxy-P7C3

$C_{22}H_{20}Br_2N_2O_2$ FW: 504.21 [1325481-43-2] ≥98%

P7C3 analog. It increases survival of dentate gyrus neurons and inhibits MPTP-induced neuronal death in models of Parkinson's disease.

Walker AK, Rivera PD, Wang Q, et al. The P7C3 class of neuroprotective compounds exerts antidepressant efficacy in mice by increasing hippocampal neurogenesis. Mol Psychiatry. 2014 Apr 22. [Epub ahead of print]. PMID: 24751964.

De Jesús-Cortés H, Xu P, Drawbridge J, et al. Neuroprotective efficacy of aminopropyl carbazoles in a mouse model of Parkinson disease. Proc Natl Acad Sci U S A. 2012 Oct 16;109(42):17010-5. PMID: 23027934.

P0092 Paclitaxel, from *Taxus yunnanensis*

1 mg
5 mg
25 mg
100 mg

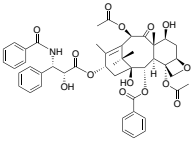

Taxol; Paxene

$C_{47}H_{51}NO_{14}$ FW: 853.91 [33069-62-4] ≥98%

Microtubule depolymerization inhibitor found in *Taxus yunnanensis* used to treat various cancers. It inhibits shortening of microtubule leading edges, decreases peripheral microtubules, and alters morphology of focal adhesions, preventing cell migration and proliferation. It also dysregulates epithelial-to-mesenchymal transition and induces apoptosis in cancer cells.

Kamath K, Smiyun G, Wilson L, et al. Mechanisms of inhibition of endothelial cell migration by taxanes. Cytoskeleton (Hoboken). 2013 Oct 23. [Epub ahead of print]. PMID: 24155271.

Caltová K, Cervinka M. Antiproliferative effects of selected chemotherapeutics in human ovarian cancer cell line A2780. Acta Medica (Hradec Kralove). 2012;55(3):116-24. PMID: 23297519.

P0093 Paclitaxel, semi-synthetic

5 mg
25 mg
100 mg

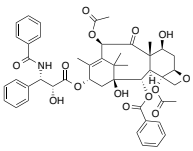

Taxol; Paxene

$C_{47}H_{51}NO_{14}$ FW: 853.9 ≥98%

Semi-synthetic microtubule depolymerization inhibitor found in *Taxus yunnanensis* used to treat various cancers. It inhibits shortening of microtubule leading edges, decreases peripheral microtubules, and alters morphology of focal adhesions, preventing cell migration and proliferation. It also dysregulates epithelial-to-mesenchymal transition and induces apoptosis in cancer cells.

Kamath K, Smiyun G, Wilson L, et al. Mechanisms of inhibition of endothelial cell migration by taxanes. Cytoskeleton (Hoboken). 2013 Oct 23. [Epub ahead of print]. PMID: 24155271.

P0218 Paeoniflorin

1 mg
5 mg
10 mg
25 mg

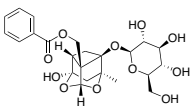

Paeonia moutan

$C_{23}H_{28}O_{11}$ FW: 480.46 [23180-57-6] ≥98%

L-type Ca^{2+} channel blocker found in *Paeonia*. It displays several biological activities, including suppressing expression of TLR4 and pro-inflammatory cytokines in DSS-induced colitis, limiting hyperalgesia, decreasing immobility time in the forced swim test, and inducing cell cycle arrest and inhibiting cell proliferation in colorectal cancer cells.

Zhang J, Dou W, Zhang E, et al. Paeoniflorin abrogates DSS-induced colitis via a TLR4-dependent pathway. Am J Physiol Gastrointest Liver Physiol. 2014 Jan 1;306(1):G27-36. PMID: 24232001.

Zhao Y, Zhou G, Wang J, et al. Paeoniflorin protects against ANIT-induced cholestasis by ameliorating oxidative stress in rats. Food Chem Toxicol. 2013 Aug;58:242-8. PMID: 23623840.

P0219 Paeonol

1 g
5 g

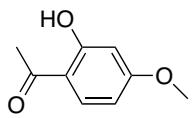

4-O-Methylresacetophenone; Resacetophenone-4-methyl ether

$C_9H_{10}O_3$ FW: 166.17 [552-41-0] ≥98%

MAO-A/B inhibitor and voltage-gated and receptor-gated Ca^{2+} channel blocker found in *Paeonia*, *Arisaema*, and *Dioscorea*. It displays several biological activities, including inhibiting carrageenan-induced thermal hyperalgesia, causing relaxation in aortic rings, inducing apoptosis in ovarian cancer cells, and preventing monocyte adhesion to vascular endothelial cells.

Yin J, Wu N, Zeng F, et al. Paeonol induces apoptosis in human ovarian cancer cells. Acta Histochem. 2013 Oct;115(8):835-9. PMID: 23768958.

Wang YQ, Dai M, Zhong JC, et al. Paeonol inhibits oxidized low density lipoprotein-induced monocyte adhesion to vascular endothelial cells by inhibiting the mitogen activated protein kinase pathway. Biol Pharm Bull. 2012;35(5):767-72. PMID: 22687414.

P0244

Palbociclib Hydrochloride

1 mg
5 mg
25 mg

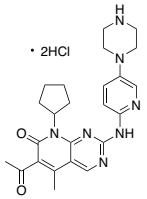

PD-033291

$C_{24}H_{29}N_7O_2 \cdot HCl$ FW: 483.99 [827022-32-2] ≥99%

CDK4/6 inhibitor. It inhibits cell cycle progression and induces apoptosis in renal cell carcinoma cells and ER+ breast cancer cells.

Logan JE, Mostofizadeh N, Desai AJ, et al. PD-0332991, a Potent and Selective Inhibitor of Cyclin-dependent Kinase 4/6, Demonstrates Inhibition of Proliferation in Renal Cell Carcinoma at Nanomolar Concentrations and Molecular Markers Predict for Sensitivity. Anticancer Res. 2013 Aug;33(8):2997-3004. PMID: 23898052.

Roberts PJ, Bisi JE, Strum JC, et al. Multiple roles of cyclin-dependent kinase 4/6 inhibitors in cancer therapy. J Natl Cancer Inst. 2012 Mar 21;104(6):476-87. PMID: 22302033.

P0344

Palbociclib Isethionate

NEW

5 mg
10 mg
25 mg

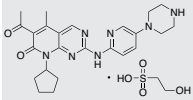

PD0332991-0054; PF00080665-73

$C_{24}H_{29}N_7O_2 \cdot C_2H_6O_4S$ FW: 573.66 [827022-33-3] ≥98%

CDK4 and CDK6 inhibitor. It induces cell cycle arrest in glioma cells and retinoblastoma models and protects against nephrotoxicity and inflammation induced by other chemotherapeutics.

Vaughn DJ, Hwang W, Lal P, et al. Phase 2 trial of the cyclin-dependent kinase 4/6 inhibitor palbociclib in patients with retinoblastoma protein-expressing germ cell tumors. Cancer. 2014 Dec 18. [Epub ahead of print]. PMID: 25522918.

DiRocco DP, Bisi J, Roberts P, et al. CDK4/6 inhibition induces epithelial cell cycle arrest and ameliorates acute kidney injury. Am J Physiol Renal Physiol. 2014 Feb 15;306(4):F379-88. PMID: 24338822.

Barton KL, Misuraca K, Cordero F, et al. PD-0332991, a CDK4/6 inhibitor, significantly prolongs survival in a genetically engineered mouse model of brainstem glioma. PLoS One. 2013 Oct 2;8(10):e77639. PMID: 24098593.

P0144

Paliperidone

25 mg
100 mg
500 mg

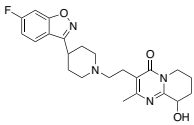

$C_{23}H_{27}FN_4O_3$ FW: 426.48 [144598-75-4] ≥97%

Dopamine D2 receptor and 5-HT2A receptor antagonist used to treat schizophrenia. It also attenuates epinephrine- and serotonin-induced platelet aggregation.

Kozielska M, Johnson M, Pilla Reddy V, et al. Pharmacokinetic-pharmacodynamic modeling of the D2 and 5-HT (2A) receptor occupancy of risperidone and paliperidone in rats. Pharm Res. 2012 Jul;29(7):1932-48. PMID: 22437487.

Gilday E, Nasrallah HA. Clinical pharmacology of paliperidone palmitate a parenteral long-acting formulation for the treatment of schizophrenia. Rev Recent Clin Trials. 2012 Feb;7(1):2-9. PMID: 22023179.

P0245

Palmatine Chloride Hydrate

1 g
5 g
10 g

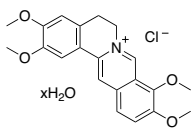

Berbericinine

$C_{21}H_{22}ClNO_4 \cdot xH_2O$ FW: 387.86 [171869-95-7] ≥97%

Hemoglobin- and DNA-binding compound found in *Corydalis*, *Phellodendron*, and *Enantia*. It decreases levels of dopamine, 5-HT, and homovanillic acid, suppresses growth and invasion of prostate cancer cells, and inhibits *Helicobacter* growth and gastric ulcer formation.

Hambright HG, Batth IS, Xie J, et al. Palmatine inhibits growth and invasion in prostate cancer cell: Potential role for rpS6/NFκB/FLIP. Mol Carcinog. 2014 Jul 7. [Epub ahead of print]. PMID: 25043857.

Liu B, Yan X, Cao S, et al. Studies on the interaction of palmatine hydrochloride with bovine hemoglobin. Luminescence. 2014 May;29(3):211-8. PMID: 23696111.

Jung J, Choi JS, Jeong CS. Inhibitory Activities of Palmatine from Coptis chinensis Against Helicobactor *pylori* and Gastric Damage. Toxicol Res. 2014 Mar;30(1):45-8. PMID: 24795799.

P0145

Palmitoyl-D,L-carnitine

100 mg
500 mg

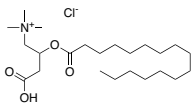

$C_{23}H_{46}NO_4\ Cl$ FW: 436.07 [6865-14-1] ≥98%

PKC inhibitor involved in fatty acid metabolism. It promotes hair growth and may be used in the simulation of mitochondrial respiration.

Takahashi T, Kamimura A, Shirai A, et al. Several selective protein kinase C inhibitors including procyanidins promote hair growth. Skin Pharmacol Appl Skin Physiol. 2000 May-Aug;13(3-4):133-42. PMID: 10859531.

P0146

Palmitoyl-L-carnitine

5 mg
10 mg

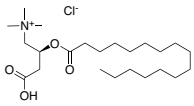

$C_{23}H_{46}NO_4\ Cl$ FW: 436.1 [18877-64-0] ≥98%

Potential sphingosine-1-phosphate agonist involved in fatty acid metabolism. It is used to stimulate mitochondria respiration.

Monternier PA, Marmillot V, Rouanet JL, et al. Mitochondrial phenotypic flexibility enhances energy savings during winter fast in king penguin chicks. J Exp Biol. 2014 Aug 1;217(Pt 15):2691-7. PMID: 24803465.

Bernatoniene J, Majiene D, Peciura R, et al. The effect of *Ginkgo* biloba extract on mitochondrial oxidative phosphorylation in the normal and ischemic rat heart. Phytother Res. 2011 Jul;25(7):1054-60. PMID: 21259351.

P0246 Palomid 529

NEW

1 mg
5 mg
10 mg

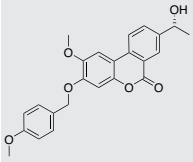

$C_{24}H_{22}O_6$ FW: 406.43 [914913-88-5] ≥98%

Inhibitor of mTOR. It inhibits angiogenesis and vascular permeability and suppresses macular degeneration.

Dalal M, Jacobs-El N, Nicholson B, et al. Subconjunctival Palomid 529 in the treatment of neovascular age-related macular degeneration. Graefes Arch Clin Exp Ophthalmol. 2013 Dec;251(12):2705-9. PMID: 23689994.

Xiang T, Jia Y, Sherris D, et al. Targeting the Akt/mTOR pathway in Brca1-deficient cancers. Oncogene. 2011 May 26;30(21):2443-50. PMID: 21242970.

Xue Q, Hopkins B, Perruzzi C, et al. Palomid 529, a novel small-molecule drug, is a TORC1/TORC2 inhibitor that reduces tumor growth, tumor angiogenesis, and vascular permeability. Cancer Res. 2008 Nov 15;68(22):9551-7. PMID: 19010932.

P0049 Pamidronate Disodium Pentahydrate

10 mg
50 mg
100 mg

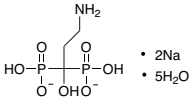

$C_3H_9NNa_2O_7P_2 \bullet 5H_2O$ FW: 369.11 [109552-15-0] ≥98%

It is used to prevent injury- or chemotherapy-induced bone loss. It increases muscle fiber, bone strength, and bone density.

Børsheim E, Herndon DN, Hawkins HK, et al. Pamidronate attenuates muscle loss after pediatric burn injury. J Bone Miner Res. 2014 Jun;29(6):1369-72. PMID: 24347438.

Laroche M, Livideanu C, Paul C, et al. Interferon alpha and pamidronate in osteoporosis with fracture secondary to mastocytosis. Am J Med. 2011 Aug;124(8):776-8. PMID: 21787907.

Kokufu I, Kohno N, Yamamoto M, et al. Adjuvant pamidronate therapy prevents the development of bone metastases in breast cancer patients with four or more positive nodes. Oncol Lett. 2010 Mar;1(2):247-252. PMID: 22966289.

P0253 Panaxadiol

5 mg
10 mg
25 mg

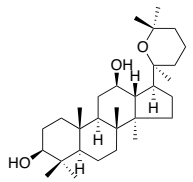

$C_{30}H_{52}O_3$ FW: 460.74 [19666-76-3] ≥98%

Voltage-gated Ca^{2+} channel blocker found in species of *Panax*. It improves cardiac function, decreases oxidative damage, and improves efficacy of co-administered chemotherapeutics.

Wang Z, Zheng Q, Liu K, et al. Ginsenoside Rh(2) enhances antitumour activity and decreases genotoxic effect of cyclophosphamide. Basic Clin Pharmacol Toxicol. 2006 Apr;98(4):411-5. PMID: 16623867.

Wang ZF, Xiao JS, Yan SZ, et al. Protective effects of panaxadiol saponins on cardiac functions in burned rats. Zhongguo Yao Li Xue Bao. 1995 Jul;16(4):345-8. PMID: 7668107.

Zhang WJ, Zhong GG, Jiang Y, et al. Single channel analysis on calcium channel blockade action of panaxadiol and panaxatriol saponins on cultured rat ventricular myocytes. Zhongguo Yao Li Xue Bao. 1994 Mar;15(2):173-6. PMID: 7516611.

P0254 Panaxatriol

5 mg
10 mg
25 mg

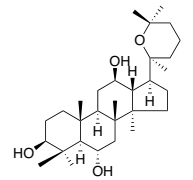

$C_{30}H_{52}O_4$ FW: 476.73 [32791-84-7] ≥98%

Voltage-gated Ca^{2+} channel blocker found in species of *Panax*. It suppresses acetaminophen-induced liver injury and increases Nrf2 activation.

Huang Y, Yu J, Wan F, et al. Panaxatriol Saponins Attenuated Oxygen-Glucose Deprivation Injury in PC12 Cells via Activation of PI3K/Akt and Nrf2 Signaling Pathway. Oxid Med Cell Longev. 2014;2014:978034. PMID: 24955212.

Wang S, Wang X, Luo F, et al. Panaxatriol saponin ameliorated liver injury by acetaminophen via restoring thioredoxin-1 and pro-caspase-12. Liver Int. 2013 Sep 11. [Epub ahead of print]. PMID: 24119161.

Zhang WJ, Zhong GG, Jiang Y, et al. Single channel analysis on calcium channel blockade action of panaxadiol and panaxatriol saponins on cultured rat ventricular myocytes. Zhongguo Yao Li Xue Bao. 1994 Mar;15(2):173-6. PMID: 7516611.

P0352 Pancreastatin, pig

0.5 mg
1 mg
2.5 mg

Gly-Trp-Pro-Gln-Ala-Pro-Ala-Met-Asp-Gly-Ala-Gly-Lys-Thr-Gly-Ala-Glu-Glu-Ala-Gln-Pro-Pro-Glu-Gly-Lys-Gly-Ala-Arg-Glu-His-Ser-Arg-Gln-Glu-Glu-Glu-Glu-Thr-Ala-Gly-Ala-Pro-Gln-Gly-Leu-Phe-Arg-Gly-NH_2

PST

$C_{214}H_{330}N_{68}O_{76}S$ FW: 5103.4 ≥98%

Endogenous GRP78 receptor inhibitor involved in insulin signaling. It inhibits insulin secretion, increases glucagon release, induces glycogenolysis and lipolysis, and is used as a biomarker to detect neuroendocrine tumors.

Biswas N, Friese RS, Gayen JR, et al. Discovery of a novel target for the dysglycemic chromogranin A fragment pancreastatin: interaction with the chaperone GRP78 to influence metabolism. PLoS One. 2014 Jan 20;9(1):e84132. PMID: 24465394.

Rustagi S, Warner RR, Divino CM. Serum pancreastatin: the next predictive neuroendocrine tumor marker. J Surg Oncol. 2013 Aug;108(2):126-8. PMID: 23775817.

P0350

Pancreatic Polypeptide, chicken

0.5 mg
1 mg
2.5 mg

H-Gly-Pro-Ser-Gln-Pro-Thr-Tyr-Pro-Gly-Asp-Asp-Ala-Pro-Val-Glu-Asp-Leu-Ile-Arg-Phe-Tyr-Asp-Asn-Leu-Gln-Gln-Tyr-Leu-Asn-Val-Val-Thr-Arg-His-Arg-Tyr-NH2

$C_{190}H_{283}N_{53}O_{58}$ FW: 4237.69 [58591-52-9] ≥95%

Endogenous Y4 receptor agonist that regulates pancreatic cell signaling. It decreases food intake, increases locomotor activity, and stimulates colonic muscle contractions.

Kahleova H, Mari A, Nofrate V, et al. Improvement in β-cell function after diet-induced weight loss is associated with decrease in pancreatic polypeptide in subjects with type 2 diabetes. J Diabetes Complications. 2012 Sep-Oct;26(5):442-9. PMID: 22673566.

Hankir MK, Parkinson JR, Minnion JS, et al. Peptide YY 3-36 and pancreatic polypeptide differentially regulate hypothalamic neuronal activity in mice in vivo as measured by manganese-enhanced magnetic resonance imaging. J Neuroendocrinol. 2011 Apr;23(4):371-80. PMID: 21251093.

P0353

Pancreatic Polypeptide, human

0.5 mg
1 mg
2.5 mg

H-Ala-Pro-Leu-Glu-Pro-Val-Tyr-Pro-Gly-Asp-Asn-Ala-Thr-Pro-Glu-Gln-Met-Ala-Gln-Tyr-Ala-Ala-Asp-Leu-Arg-Arg-Tyr-Ile-Asn-Met-Leu-Thr-Arg-Pro-Arg-Tyr-NH2

$C_{185}H_{287}N_{53}O_{54}S_2$ FW: 4181.7 [75976-10-2] ≥98%

Endogenous Y4 receptor agonist that regulates pancreatic cell signaling. It decreases food intake, increases locomotor activity, and stimulates colonic muscle contractions.

Kahleova H, Mari A, Nofrate V, et al. Improvement in β-cell function after diet-induced weight loss is associated with decrease in pancreatic polypeptide in subjects with type 2 diabetes. J Diabetes Complications. 2012 Sep-Oct;26(5):442-9. PMID: 22673566.

P0351

Pancreatic Polypeptide, rat

0.5 mg
1 mg
2.5 mg

Ala-Pro-Leu-Glu-Pro-Met-Tyr-Pro-Gly-Asp-Tyr-Ala-Thr-His-Glu-Gln-Arg-Ala-Gln-Tyr-Glu-Thr-Gln-Leu-Arg-Arg-Tyr-Ile-Asn-Thr-Leu-Thr-Arg-Pro-Arg-Tyr-NH2

$C_{195}H_{298}N_{58}O_{57}S$ FW: 4398.9 [90419-12-8] ≥98%

Endogenous Y4 receptor agonist that regulates pancreatic cell signaling. It decreases food intake, increases locomotor activity, and stimulates colonic muscle contractions.

Kahleova H, Mari A, Nofrate V, et al. Improvement in β-cell function after diet-induced weight loss is associated with decrease in pancreatic polypeptide in subjects with type 2 diabetes. J Diabetes Complications. 2012 Sep-Oct;26(5):442-9. PMID: 22673566.

P0252

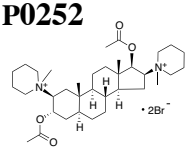

Pancuronium Bromide

10 mg
50 mg
100 mg
250 mg

$C_{35}H_{60}Br_2N_2O_4$ FW: 732.67 [15500-66-0] ≥98%

Non-depolarizing NMJ blocker and nAChR antagonist used to induce anesthesia and skeletal muscle relaxation.

P0255

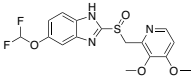

Pantoprazole

SKF-96022; BY-1023

100 mg
500 mg
1 g

$C_{16}H_{15}F_2N_3O_4S$ FW: 383.37 [102625-70-7] ≥98%

H^+/K^+ ATPase and ROCK-2 inhibitor used to treat gastroesophageal reflux disease. It also inhibits uridine nucleoside ribohydrolase activity, decreases gastroesophageal sphincter muscle tone, and increases tumor-associated macrophage recruitment in the tumor microenvironment.

Welsh C, Kasirer MY, Pan J, et al. Pantoprazole decreases gastroesophageal muscle tone in newborn rats via rho-kinase inhibition. Am J Physiol Gastrointest Liver Physiol. 2014 Apr 3. [Epub ahead of print]. PMID: 24699328.

Shea TA, Burburan PJ, Matubia VN, et al. Identification of proton-pump inhibitor drugs that inhibit Trichomonas vaginalis uridine nucleoside ribohydrolase. Bioorg Med Chem Lett. 2014 Feb 15;24(4):1080-4. PMID: 24468412.

Ward RM, Kearns GL. Proton pump inhibitors in pediatrics : mechanism of action, pharmacokinetics, pharmacogenetics, and pharmacodynamics. Paediatr Drugs. 2013 Apr;15(2):119-31. PMID: 23512128.

P0256

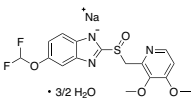

Pantoprazole Sodium Sesquihydrate

1 g
5 g
25 g

$C_{16}H_{14}F_2N_3NaO_4S \bullet 3/2\ H_2O$ FW: 432.37 [138786-67-1] ≥98%

H^+/K^+ ATPase and ROCK-2 inhibitor used to treat gastroesophageal reflux disease. It also inhibits uridine nucleoside ribohydrolase activity, decreases gastroesophageal sphincter muscle tone, and increases tumor-associated macrophage recruitment in the tumor microenvironment.

Welsh C, Kasirer MY, Pan J, et al. Pantoprazole decreases gastroesophageal muscle tone in newborn rats via rho-kinase inhibition. Am J Physiol Gastrointest Liver Physiol. 2014 Apr 3. [Epub ahead of print]. PMID: 24699328.

Shea TA, Burburan PJ, Matubia VN, et al. Identification of proton-pump inhibitor drugs that inhibit Trichomonas vaginalis uridine nucleoside ribohydrolase. Bioorg Med Chem Lett. 2014 Feb 15;24(4):1080-4. PMID: 24468412.

P0260

Papain Inhibitor

5 mg
10 mg
25 mg

$C_{19}H_{29}N_7O_6$ FW: 451.49 [70195-20-9] ≥95%

H-Gly-Gly-Tyr-Arg-OH

Potential cathepsin and trypsin inhibitor produced in tomato leaves. It may inhibit growth of bacteria.

Zindel S, Kaman WE, Fröls S, et al. The papain inhibitor (SPI) of *Streptomyces* mobaraensis inhibits bacterial cysteine proteases and is an antagonist of bacterial growth. Antimicrob Agents Chemother. 2013 Jul;57(7):3388-91. PMID: 23587952.

Bolter CJ. Methyl Jasmonate Induces Papain Inhibitor(s) in Tomato Leaves. Plant Physiol. 1993 Dec;103(4):1347-1353. PMID: 12232028.

P0268

Parasin I

0.5 mg
1 mg
2.5 mg

$C_{82}H_{154}N_{34}O_{24}$ FW: 2000.36 ≥95%

H-Lys-Gly-Arg-Gly-Lys-Gln-Gly-Gly-Lys-Val-Arg-Ala-Lys-Ala-Lys-Thr-Arg-Ser-Ser-OH

Histone H2-derived antimicrobial peptide found in *Parasilurus*. It is produced by MMP2 and cathepsin D in response to epidermal injury.

Koo YS, Kim JM, Park IY, et al. Structure-activity relations of parasin I, a histone H2A-derived antimicrobial peptide. Peptides. 2008 Jul;29(7):1102-8. PMID: 18406495.

Cho JH, Park IY, Kim MS, et al. Matrix metalloproteinase 2 is involved in the regulation of the antimicrobial peptide parasin I production in catfish skin mucosa. FEBS Lett. 2002 Nov 20;531(3):459-63. PMID: 12435593.

P0269

Parathyroid Hormone (1-34), cow

0.5 mg
1 mg
2.5 mg

Teriparatide

$C_{183}H_{288}N_{54}O_{50}S_2$ FW: 4108.7 [12583-68-5] ≥95%

Ala-Val-Ser-Glu-Ile-Gln-Phe-Met-His-Asn-Leu-Gly-Lys-His-Leu-Ser-Ser-Met-Glu-Arg-Val-Glu-Trp-Leu-Arg-Lys-Lys-Leu-Gln-Asp-Val-His-Asn-Phe

Endogenous PTH1/2 receptor agonist that increases extracellular Ca^{2+} levels. It is used to treat osteoporosis. It promotes bone formation, increases bone mineral density, decreases osteoblast activity, suppresses angiogenesis in an HSP70-mediated manner, and promotes fibrosis.

Ongkeko WM, Burton D, Kiang A, et al. Parathyroid Hormone Related-Protein Promotes Epithelial-to-Mesenchymal Transition in Prostate Cancer. PLoS One. 2014 Jan 22;9(1):e85803. PMID: 24465715.

Augustine M, Horwitz MJ. Parathyroid hormone and parathyroid hormone-related protein analogs as therapies for osteoporosis. Curr Osteoporos Rep. 2013 Dec;11(4):400-6. PMID: 24078470.

P7628

Parathyroid Hormone-Related Protein (1-34), human/rat

0.5 mg
1 mg
2.5 mg

PTHrP

$C_{180}H_{287}N_{57}O_{48}$ FW: 4017.65 [112540-82-6] ≥95%

H-Ala-Val-Ser-Glu-His-Gln-Leu-Leu-His-Asp-Lys-Gly-Lys-Ser-Ile-Gln-Asp-Leu-Arg-Arg-Arg-Phe-Phe-Leu-His-His-Leu-Ile-Ala-Glu-Ile-His-Thr-Ala-OH

Endogenous PTH1 receptor agonist that increases extracellular Ca^{2+} levels. It is used to treat osteoporosis and promotes bone formation, increases bone mineral density, enhances bone strength, and improves bone biomechanical properties. It also also promotes epithelial-to-mesenchymal transition and fibrosis.

Ongkeko WM, Burton D, Kiang A, et al. Parathyroid Hormone Related-Protein Promotes Epithelial-to-Mesenchymal Transition in Prostate Cancer. PLoS One. 2014 Jan 22;9(1):e85803. PMID: 24465715.

P0369

Parecoxib Sodium

NEW

25 mg
100 mg

$C_{19}H_{18}N_2O_4SNa$ FW: 392.4 [198470-85-8] ≥98%

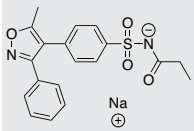

Valdecoxib prodrug and inhibitor of NSAID and COX-2 used to treat pain. It prevents neuropathic pain-induced hypersensitivity.

Zhou GB, Li HY, Ji JQ, et al. Analgesic effect of COX inhibitors and its mechanism in a rat model of neuropathic pain. Nan Fang Yi Ke Da Xue Xue Bao. 2011 Oct;31(10):1764-6. PMID: 22027786.

Koppert W, Wehrfritz A, Körber N, et al. The cyclooxygenase isozyme inhibitors parecoxib and paracetamol reduce central hyperalgesia in humans. Pain. 2004 Mar;108(1-2):148-53. PMID: 15109518.

P0370

Paromomycin Sulfate

1 g
5 g
25 g

$C_{23}H_{45}N_5O_{14} \bullet H_2SO_4$ FW: 713.71 [1263-89-4] ≥98%

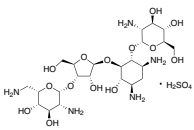

Protein translation inhibitor and cation (PX2X) channel blocker used to treat leishmaniasis. It inhibits ribosomal recycling and suppresses RNA translocation.

Bongartz EV, Rettinger J, Hausmann R. Aminoglycoside block of P2X2 receptors heterologously expressed in Xenopus laevis oocytes. Purinergic Signal. 2010 Dec;6(4):393-403. PMID: 21437010.

Jhingran A, Chawla B, Saxena S, et al. Paromomycin: uptake and resistance in *Leishmania* donovani. Mol Biochem Parasitol. 2009 Apr;164(2):111-7. PMID: 19146886.

Borovinskaya MA, Pai RD, Zhang W, et al. Structural basis for aminoglycoside inhibition of bacterial ribosome recycling. Nat Struct Mol Biol. 2007 Aug;14(8):727-32. PMID: 17660832.

P0297

Paroxetine Hydrochloride Hemihydrate

25 mg
100 mg
500 mg
1 g

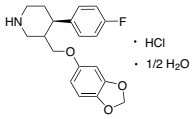

$C_{19}H_{20}FNO_3 \cdot HCl \cdot 1/2H_2O$ FW: 374.84 [110429-35-1] ≥98%

Inhibitor of SERT, NET, and mAChRs used to treat depression. It displays several biological activities, including acting as a FIASMA, inhibiting growth of *Aspergillus* and *Candida*, suppressing LPS-induced production of pro-inflammatory cytokines, and decreasing amyloid-β oligomer levels.

Liu RP, Zou M, Wang JY, et al. Paroxetine ameliorates lipopolysaccharide-induced microglia activation via differential regulation of MAPK signaling. J Neuroinflammation. 2014 Mar 12;11:47. PMID: 24618100.

Aboukhatwa M, Luo Y. Antidepressants modulate intracellular amyloid peptide species in N2a neuroblastoma cells. J Alzheimers Dis. 2011;24(2):221-34. PMID: 21263193.

P0270

Parthenolide

25 mg
100 mg
250 mg

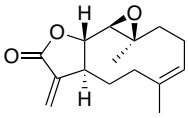

$C_{15}H_{20}O_3$ FW: 248.32 [20554-84-1] ≥98%

TRPA1 receptor partial agonist and NLRP3 and caspase 1 inhibitor found in *Tanacetum*. It exhibits a wide variety of biological activities, including inhibiting cell migration and tubule formation in multiple myeloma cells and inhibiting tumor growth and metastasis in breast cancer models.

Zhao X, Liu X, Su L. Parthenolide induces apoptosis via TNFRSF10B and PMAIP1 pathways in human lung cancer cells. J Exp Clin Cancer Res. 2014 Jan 6;33(1):3. PMID: 24387758.

Materazzi S, Benemei S, Fusi C, et al. Parthenolide inhibits nociception and neurogenic vasodilatation in the trigeminovascular system by targeting the TRPA1 channel. Pain. 2013 Dec;154(12):2750-8. PMID: 23933184.

D'Anneo A, Carlisi D, Lauricella M, et al. Parthenolide generates reactive oxygen species and autophagy in MDA-MB231 cells. A soluble parthenolide analogue inhibits tumour growth and metastasis in a xenograft model of breast cancer. Cell Death Dis. 2013 Oct 31;4:e891. PMID: 24176849.

P0278

Patulin

1 mg
5 mg
10 mg

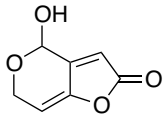

$C_7H_6O_4$ FW: 154.12 [149-29-1] ≥98%

Mycotoxin found in *Penicillum* and *Aspergillus*. It increases proliferation of keratinocytes, induces DNA damage, and alters intestinal epithelial barrier function.

Alam S, Pal A, Kumar R, et al. EGFR-mediated Akt and MAPKs signal pathways play a crucial role in patulin-induced cell proliferation in primary murine keratinocytes via modulation of Cyclin D1 and COX-2 expression. Mol Carcinog. 2013 Jun 29. [Epub ahead of print]. PMID: 23813870.

Glaser N, Stopper H. Patulin: Mechanism of genotoxicity. Food Chem Toxicol. 2012 May;50(5):1796-801. PMID: 22425938.

Kwon O, Soung NK, Thimmegowda NR, et al. Patulin induces colorectal cancer cells apoptosis through EGR-1 dependent ATF3 up-regulation. Cell Signal. 2012 Apr;24(4):943-50. PMID: 22230687.

P0392

Paxilline

1 mg
5 mg
10 mg

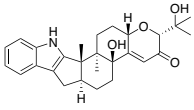

$C_{27}H_{33}NO_4$ FW: 435.56 [57186-25-1] ≥98%

Mycotoxin, BK K^+ channel inhibitor, and SERCA inhibitor found in *Penicillum* and *Aspergillus*. It prevents Ca^{2+} release and phosphoenzyme formation.

Borchert GH, Hlaváčková M, Kolář F. Pharmacological activation of mitochondrial BK(Ca) channels protects isolated cardiomyocytes against simulated reperfusion-induced injury. Exp Biol Med (Maywood). 2013 Feb;238(2):233-41. PMID: 23576804.

Bilmen JG, Wootton LL, Michelangeli F. The mechanism of inhibition of the sarco/endoplasmic reticulum Ca^{2+} ATPase by paxilline. Arch Biochem Biophys. 2002 Oct 1;406(1):55-64. PMID: 12234490.

P0397

Pazopanib

5 mg
25 mg

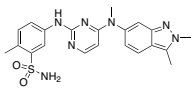

$C_{21}H_{23}N_7O_2S$ FW: 437.53 [444731-52-6] ≥97%

Inhibitor of VEGFR, PDGFR, and c-Kit used to treat renal cell carcinoma. It also inhibits proliferation and angiogenesis in various cancer cell lines and suppresses activity of wild-type B-Raf.

Pick AM, Nystrom KK. Pazopanib for the treatment of metastatic renal cell carcinoma. Clin Ther. 2012 Mar;34(3):511-20. PMID: 22341567.

Gril B, Palmieri D, Qian Y, et al. Pazopanib reveals a role for tumor cell B-Raf in the prevention of HER^{2+} breast cancer brain metastasis. Clin Cancer Res. 2011 Jan 1;17(1):142-53. PMID: 21081656.

Hamberg P, Verweij J, Sleijfer S. (Pre-)clinical pharmacology and activity of pazopanib, a novel multikinase angiogenesis inhibitor. Oncologist. 2010;15(6):539-47. PMID: 20511320.

P0398

Pazufloxacin Methanesulfonate

100 mg
500 mg
1 g
5 g

$C_{16}H_{15}FN_2O_4 \bullet CH_3SO_3H$ FW: 414.41 [163680-77-1] ≥98%

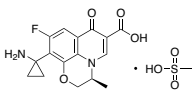

Topoisomerase IV and bacterial DNA gyrase inhibitor. It is particularly effective against *Legionella*, *Staphylococcus*, *Streptococcus*, *Gardnerella*, *Escherichia*, *Pseudomonas*, and *Bacteriodes*.

Higa F, Akamine M, Haranaga S, et al. In vitro activity of pazufloxacin, tosufloxacin and other quinolones against *Legionella* species. J Antimicrob Chemother. 2005 Dec;56(6):1053-7. PMID: 16260445.

Takei M, Fukuda H, Kishii R, et al. Target preference of 15 quinolones against *Staphylococcus aureus*, based on antibacterial activities and target inhibition. Antimicrob Agents Chemother. 2001 Dec;45(12):3544-7. PMID: 11709337.

Mikamo H, Sato Y, Hayasaki Y, et al. In vitro activities of pazufloxacin, a novel injectable quinolone, against bacteria causing infections in obstetric and gynecological patients. Chemotherapy. 1999 May-Jun;45(3):154-7. PMID: 10224336.

P0932

PCI-32765

Ibrutinib

1 mg
5 mg
25 mg

$C_{25}H_{24}N_6O_2$ FW: 440.5 [936563-96-1] ≥99%

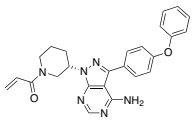

BTK and IL-2-inducible kinase inhibitor. It prevents IgE-mediated activation of basophils, inhibits signaling from macrophages and mast cells, and decreases cell migration and survival in models of chronic lymphocytic leukemia.

Massó-Vallés D, Jauset T, Serrano E, et al. Ibrutinib exerts potent antifibrotic and antitumor activities in mouse models of pancreatic adenocarcinoma. Cancer Res. 2015 Apr 15;75(8):1675-81. PMID: 25878147.

Dubovsky JA, Beckwith KA, Natarajan G, et al. Ibrutinib is an irreversible molecular inhibitor of ITK driving a Th1 selective pressure in T-lymphocytes. Blood. 2013 Jul 25. [Epub ahead of print]. PMID: 23886836.

Ponader S, Chen SS, Buggy JJ, et al. The Bruton tyrosine kinase inhibitor PCI-32765 thwarts chronic lymphocytic leukemia cell survival and tissue homing in vitro and in vivo. Blood. 2012 Feb 2;119(5):1182-9. PMID: 22180443.

P1200

PD-184352

5 mg
25 mg
100 mg

$C_{17}H_{14}ClF_2IN_2O_2$ FW: 478.66 [212631-79-3] ≥98%

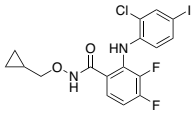

MEK1/2 and Raf inhibitor particularly active against cancers harboring B-Raf or RAS mutations. It induces cell cycle arrest and apoptosis in several cancer cell lines.

Wickenden JA, Jin H, Johnson M, et al. Colorectal cancer cells with the BRAF(V600E) mutation are addicted to the ERK1/2 pathway for growth factor-independent survival and repression of BIM. Oncogene. 2008 Dec 4;27(57):7150-61. PMID: 18806830.

Lunghi P, Giuliani N, Mazzera L, et al. Targeting MEK/MAPK signal transduction module potentiates ATO-induced apoptosis in multiple myeloma cells through multiple signaling pathways. Blood. 2008 Sep 15;112(6):2450-62. PMID: 18583568.

Bain J, Plater L, Elliott M, et al. The selectivity of protein kinase inhibitors: a further update. Biochem J. 2007 Dec 15;408(3):297-315. PMID: 17850214.

P1202

PD-325901

5 mg
25 mg
100 mg

$C_{16}H_{14}F_3IN_2O_4$ FW: 482.19 [391210-10-9] ≥98%

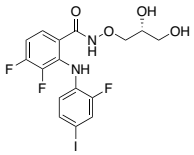

MEK1/2 and Raf inhibitor particularly active against cancers harboring B-Raf or RAS mutations. It induces cell cycle arrest and apoptosis in thyroid cancer cells and inhibits survival of influenza virus.

Haasbach E, Hartmayer C, Planz O. Combination of MEK inhibitors and oseltamivir leads to synergistic antiviral effects after influenza A virus infection in vitro. Antiviral Res. 2013 May;98(2):319-24. PMID: 23523553.

Leyton J, Smith G, Lees M, et al. Noninvasive imaging of cell proliferation following mitogenic extracellular kinase inhibition by PD0325901. Mol Cancer Ther. 2008 Sep;7(9):3112-21. PMID: 18790789.

Liu D, Xing M. Potent inhibition of thyroid cancer cells by the MEK inhibitor PD0325901 and its potentiation by suppression of the PI3K and NF-kappaB pathways. Thyroid. 2008 Aug;18(8):853-64. PMID: 18651802.

P1622

Pefloxacin Methanesulfonate Dihydrate

5 g
25 g
100 g

$C_{17}H_{20}FN_3O_3 \bullet CH_3SO_3H \bullet 2H_2O$ FW: 465.5 [149676-40-4] ≥98%

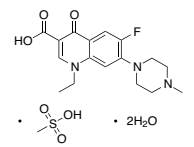

Topoisomerase IV and bacterial DNA gyrase inhibitor that inhibits DNA replication and transcription. It also inhibits synthesis of penicillin-binding proteins and exhibits moderate UV-induced phototoxicity.

Martínez LJ, Sik RH, Chignell CF. Fluoroquinolone antimicrobials: singlet oxygen, superoxide and phototoxicity. Photochem Photobiol. 1998 Apr;67(4):399-403. PMID: 9559584.

Grossato A, Fontana R. Synergy and mechanism of interaction between pefloxacin and penicillin G against enterococci. New Microbiol. 1997 Jul;20(3):221-5. PMID: 9258941.

P1634

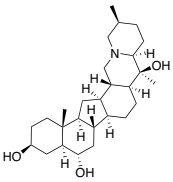

Peimine

Verticine

$C_{27}H_{45}NO_3$ FW: 431.65 [23496-41-5] ≥98.0%

5 mg
10 mg
25 mg

Potential antagonist at TRPV1 and TRPA1 receptors found in *Fritillaria*. It inhibits cough frequency and cough latency, suppresses production of pro-inflammatory cytokines, and decreases expression of IκB kinase, JNK, and p38.

Yi PF, Wu YC, Dong HB, et al. Peimine impairs pro-inflammatory cytokine secretion through the inhibition of the activation of NF-κB and MAPK in LPS-induced RAW264.7 macrophages. Immunopharmacol Immunotoxicol. 2013 Oct;35(5):567-72. PMID: 23944357.

Ma L, Song F, Liu Z, et al. Study on noncovalent complexes of alkaloids with DNA duplex using electrospray ionization mass spectrometry. Rapid Commun Mass Spectrom. 2013 Jan 15;27(1):51-8. PMID: 23239316.

Wang D, Zhu J, Wang S, et al. Antitussive, expectorant and anti-inflammatory alkaloids from Bulbus Fritillariae Cirrhosae. Fitoterapia. 2011 Dec;82(8):1290-4. PMID: 21958967.

P1635

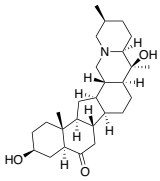

Peiminine

Imperialine

$C_{27}H_{43}NO_3$ FW: 429.64 [18059-10-4] ≥98.0%

5 mg
10 mg
25 mg

Antagonist at M2 mAChRs and potential antagonist at TRPV1 and TRPA1 receptors found in *Fritillaria*. It decreases cough and suppresses expression of IFN-γ, TGF-β, NF-κB, ERK1/2, and FasL in pulmonary fibrosis models.

Guo H, Ji F, Liu B, et al. Peiminine ameliorates bleomycin-induced acute lung injury in rats. Mol Med Rep. 2013 Apr;7(4):1103-10. PMID: 23404624.

Zhang Y, Sreekrishna K, Lin Y, et al. Modulation of transient receptor potential (TRP) channels by Chinese herbal extracts. Phytother Res. 2011 Nov;25(11):1666-70. PMID: 21432926.

Zhou Y, Ji H, Lin BQ, et al. The effects of five alkaloids from Bulbus Fritillariae on the concentration of cAMP in HEK cells transfected with muscarinic M(2) receptor plasmid. Am J Chin Med. 2006;34(5):901-10. PMID: 17080553.

P1845

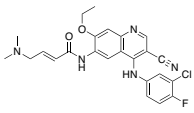

Pelitinib

EKB-569

$C_{24}H_{23}ClFN_5O_2$ FW: 467.92 [257933-82-7] ≥98%

5 mg
10 mg
25 mg
100 mg

EGFR inhibitor. It induces cell cycle arrest in non-small cell lung cancer cells and inhibits transcription of TERT and activity of telomerase.

Aravindan N, Aravindan S, Herman TS, et al. EGFR tyrosine kinase inhibitor pelitinib regulates radiation-induced p65-dependent telomerase activation in squamous cell carcinoma. Radiat Res. 2013 Mar;179(3):304-12. PMID: 23379415.

Kim H, Lim HY. Novel EGFR-TK inhibitor EKB-569 inhibits hepatocellular carcinoma cell proliferation by AKT and MAPK pathways. J Korean Med Sci. 2011 Dec;26(12):1563-8. PMID: 22147992.

Yoshimura N, Kudoh S, Kimura T, et al. EKB-569, a new irreversible epidermal growth factor receptor tyrosine kinase inhibitor, with clinical activity in patients with non-small cell lung cancer with acquired resistance to gefitinib. Lung Cancer. 2006 Mar;51(3):363-8. PMID: 16364494.

P1849

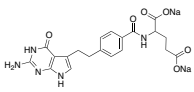

Pemetrexed Disodium

$C_{20}H_{19}N_5Na_2O_6$ FW: 471.37 [150399-23-8] ≥98%

100 mg
250 mg
1 g

Thymidylate synthase inhibitor and potential SHMT, DNFR, and GARFT inhibitor. It induces apoptosis by increasing levels of Bax, Fas, death receptor 4, and death receptor 5.

Walters CL, Arend RC, Armstrong DK, et al. Folate and folate receptor alpha antagonists mechanism of action in ovarian cancer. Gynecol Oncol. 2013 Nov;131(2):493-8. PMID: 23863359.

Lau DH, Moon J, Davies AM, et al. Southwestern oncology group phase II trial (S0526) of pemetrexed in bronchioloalveolar carcinoma subtypes of advanced adenocarcinoma. Clin Lung Cancer. 2013 Jul;14(4):351-5. PMID: 23415808.

Yang TY, Chang GC, Chen KC, et al. Pemetrexed induces both intrinsic and extrinsic apoptosis through ataxia telangiectasia mutated/p53-dependent and -independent signaling pathways. Mol Carcinog. 2013 Mar;52(3):183-94. PMID: 22086658.

P1754

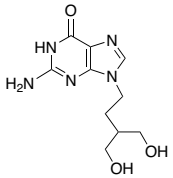

Penciclovir

$C_{10}H_{15}N_5O_3$ FW: 253.26 [39809-25-1] ≥98%

25 mg
100 mg
500 mg
1 g

Guanosine analog analog and DNA polymerase inhibitor that terminates DNA chain elongation. It is used to treat herpes virus infections.

Deval J. Antimicrobial strategies: inhibition of viral polymerases by 3'-hydroxyl nucleosides. Drugs. 2009;69(2):151-66. PMID: 19228073.

Villarreal EC. Current and potential therapies for the treatment of herpes-virus infections. Prog Drug Res. 2003;60:263-307. PMID: 12790345.

P1753

Penicillamine

1 g
5 g
25 g

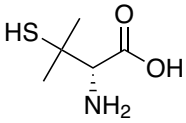

$C_5H_{11}NO_2S$ FW: 149.21 [52-67-5] ≥97%

Penicillin derivative, carboxypeptidase inhibitor, and chelating agent used to treat rheumatoid arthritis. It decreases collagen cross-linking and T cell levels and suppresses allergen-induced production of immunoglobulins.

Chong CR, Auld DS. Inhibition of carboxypeptidase A by D-penicillamine: mechanism and implications for drug design. Biochemistry. 2000 Jun 27;39(25):7580-8. PMID: 10858308.

Meyer O. D-penicillamine: mechanism of cellular action and induced autoimmune diseases. Rev Rhum Mal Osteoartic. 1986 Jan;53(1):15-20. PMID: 2939541.

P1854

Penicillic Acid

5 mg
10 mg
50 mg

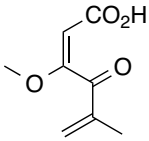

$C_8H_{10}O_4$ FW: 170.16 [90-65-3] ≥98%

Mycotoxin and inhibitor of BK K^+, voltage-gated cardiac Na^+, K^+, Ca^{2+} channels found in *Penicillum* and *Aspergillus*. It increases expression of histone demethylase JMJD-3, decreases expression of HDAC3, and induces abnormal branching and swelling in species of *Phytophthora*.

Oh SY, Balch CG, Cliff RL, et al. Exposure to Penicillium mycotoxins alters gene expression of enzymes involved in the epigenetic regulation of bovine macrophages (BoMacs). Mycotoxin Res. 2013 Nov;29(4):235-43. PMID: 23893597.

Kang SW, Kim SW. New antifungal activity of penicillic acid against *Phytophthora* species. Biotechnol Lett. 2004 May;26(9):695-8. PMID: 15195966.

Bando M, Hasegawa M, Tsuboi Y, et al. The mycotoxin penicillic acid inhibits Fas ligand-induced apoptosis by blocking self-processing of caspase-8 in death-inducing signaling complex. J Biol Chem. 2003 Feb 21;278(8):5786-93. PMID: 12482880.

P1852

Penicillin G procaine

10 g
25 g
100 g

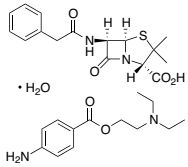

Benzylpenicillin Procaine salt

$C_{29}H_{38}N_4O_6S \cdot H_2O$ FW: 588.73 [6130-64-9] ≥98%

Penicillin binding protein inhibitor and potential nAChR antagonist used to treat gram positive bacterial infections. It is somewhat active against gram negative bacteria but does not inhibit growth of β-lactamase-producing bacteria.

Sun S, Selmer M, Andersson DI. Resistance to β-lactam antibiotics conferred by point mutations in penicillin-binding proteins PBP3, PBP4 and PBP6 in *Salmonella* enterica. PLoS One. 2014 May 8;9(5):e97202. PMID: 24810745.

Schlesinger F, Krampfl K, Haeseler G, et al. Competitive and open channel block of recombinant nAChR channels by different antibiotics. Neuromuscul Disord. 2004 May;14(5):307-12. PMID: 15099589.

P1853

Penicillin V Potassium

10 g
25 g
100 g

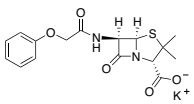

$C_{16}H_{17}KN_2O_5S$ FW: 388.48 [132-98-9] ≥98%

Penicillin binding protein inhibitor used to treat gram positive bacterial infections. It is somewhat active against gram negative bacteria but does not inhibit growth of β-lactamase-producing bacteria.

Demain AL. Production of beta-lactam antibiotics and its regulation. Proc Natl Sci Counc Repub China B. 1991 Oct;15(4):251-65. PMID: 1815263.

Bär H, Zarnack J. Molecular-biological bases of the mechanism of action of penicillins and cephasporins. Pharmazie. 1970 Jan 1;25(1):10-22. PMID: 4987180.

P1952

Penitrem A

1 mg
5 mg

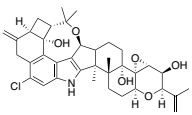

Tremortin A

$C_{37}H_{44}ClNO_6$ FW: 634.2 [12627-35-9] ≥98%

Mycotoxin, GABA-A potentiator, and BK K^+ channel inhibitor found in *Penicillum* and *Aspergillus*. It inhibits uptake of GABA and glutamate into synaptosomes and may disrupt learning acquisition.

Moldes-Anaya A, Rundberget T, Fæste CK, et al. Neurotoxicity of Penicillium crustosum secondary metabolites: tremorgenic activity of orally administered penitrem A and thomitrem A and E in mice. Toxicon. 2012 Dec 15;60(8):1428-35. PMID: 23085423.

Asano S, Bratz IN, Berwick ZC, et al. Penitrem A as a tool for understanding the role of large conductance $Ca^{(2+)}$/voltage-sensitive $K^{(+)}$ channels in vascular function. J Pharmacol Exp Ther. 2012 Aug;342(2):453-60. PMID: 22580348.

Moldes-Anaya AS, Fonnum F, Eriksen GS, et al. In vitro neuropharmacological evaluation of penitrem-induced tremorgenic syndromes: importance of the GABAergic system. Neurochem Int. 2011 Dec;59(7):1074-81. PMID: 21924313.

P1955

Pentagastrin

1 mg
2 mg
5 mg

Boc-beta-Ala-Trp-Met-Asp-Phe-NH_2

$C_{37}H_{50}N_7O_9S$ FW: 768.79 [5534-95-2] ≥95%

Synthetic gastric acid secretion stimulator. It inhibits motilin-induced stomach contractions and enhances gastric defense by increasing mucus gel thickness, mucosal blood flow, and pHi.

Beckert S, Wolf SC, Farrahi F, et al. TGF-beta3 inhibits pentagastrin-stimulated gastric acid secretion in rats. Med Sci Monit. 2005 Mar;11(3):BR80-3. PMID: 15735558.

Yamamoto O, Matsunaga Y, Shiba Y, et al. Inhibition of motilin-induced phase III contractions by pentagastrin in Heidenhain pouch dogs. J Pharmacol Exp Ther. 1994 Dec;271(3):1471-6. PMID: 7996460.

P1755

Pentoxifylline

10 g
50 g
100 g

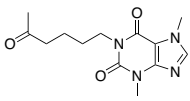

$C_{13}H_{18}N_4O_3$ FW: 278.31 [6493-05-6] ≥98%

Xanthine derivative, adenosine A2 receptor antagonist, and PDE inhibitor used to treat intermittent claudication, peripheral vascular disease, and neuropathies. It increases cAMP levels, inhibits inflammation-induced hyperalgesia, and suppresses the development of fibrosis.

Fang CC, Huang JW, Shyu RS, et al. Fibrin-Induced epithelial-to-mesenchymal transition of peritoneal mesothelial cells as a mechanism of peritoneal fibrosis: effects of pentoxifylline. PLoS One. 2012;7(9):e44765. PMID: 23028611

Nowak Ł, Zurowski D, Dobrogowski J, et al. Pentoxifylline modifies central and peripheral vagal mechanism in acute and chronic pain models. Folia Med Cracov. 2012;52(1-2):83-95. PMID: 23697217

Deree J, Martins JO, Melbostad H, et al. Insights into the regulation of TNF-alpha production in human mononuclear cells: the effects of non-specific phosphodiesterase inhibition. Clinics (Sao Paulo). 2008 Jun;63(3):321-8. PMID: 18568240.

P1764

Pep-1 Peptide

0.5 mg
1 mg
2.5 mg

H-Lys-Glu-Thr-Trp-Trp-Glu-Thr-Trp-Trp-Thr-Glu-Trp-Ser-Gln-Pro-Lys-Lys-Lys-Arg-Lys-Val-OH

$C_{136}H_{195}N_{35}O_{33}$ FW: 2848.23 ≥95%

It penetrates cells and carries large conjugated structures across cell membranes. It also decreases intestinal and colonic length, expression of IGF-1 and epiregulin, and intestinal epithelial cell proliferation.

Meloni BP, Craig AJ, Milech N, et al. The Neuroprotective Efficacy of Cell-Penetrating Peptides TAT, Penetratin, Arg-9, and Pep-1 in Glutamic Acid, Kainic Acid, and In Vitro Ischemia Injury Models Using Primary Cortical Neuronal Cultures. Cell Mol Neurobiol. 2013 Nov 9. [Epub ahead of print]. PMID: 24213248.

Thaete LG, Qu XW, Jilling T, et al. Impact of toll-like receptor 4 deficiency on the response to uterine ischemia/reperfusion in mice. Reproduction. 2013 Apr 29;145(5):517-26. PMID: 23509372.

P1761

Pepstatin

5 mg
25 mg
100 mg

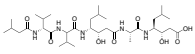

$C_{34}H_{63}N_5O_9$ FW: 685.89 [26305-03-3] ≥98%

Aspartyl protease inhibitor that may inhibit RANKL-induced osteoclast differentiation and phosphorylation of ERK.

Marciniszyn J Jr, Hartsuck JA, Tang J. Mode of inhibition of acid proteases by pepstatin. J Biol Chem. 1976 Nov 25;251(22):7088-94. PMID: 993206.

Umezawa H, Aoyagi T, Morishima H, et al. Pepstatin, a new pepsin inhibitor produced by *Actinomycetes*. J Antibiot (Tokyo). 1970 May;23(5):259-62. PMID: 4912600.

P0276

Peptide 401

Mast Cell Degranulating Peptide

0.5 mg
1 mg
2.5 mg

H-Ile-Lys-Cys-Asn-Cys-Lys-Arg-His-Val-Ile-Lys-Pro-His-Ile-Cys-Arg-Lys-Ile-Cys-Gly-Lys-Asn-NH_2 (Cys3-Cys15, Cys5-Cys19)

$C_{110}H_{188}N_{40}O_{24}S_4$ FW: 2583.28 [32908-73-9] ≥95%

Found in bee and wasp venom. It induces mast cell degranulation and decreases paw edema.

Banks BE, Dempsey CE, Vernon CA, et al. Anti-inflammatory activity of bee venom peptide 401 (mast cell degranulating peptide) and compound 48/80 results from mast cell degranulation in vivo. Br J Pharmacol. 1990 Feb;99(2):350-4. PMID: 2328399.

P1766

Peptide B, cow

0.5 mg
1 mg
2.5 mg

H-Cys-Pro-Asp-Phe-Gly-His-Ile-Ala-Met-Glu-Leu-Ser-Val-Arg-Thr-Trp-Lys-Tyr-OH

$C_{163}H_{239}N_{39}O_{53}S_2$ FW: 2153.49 ≥95%

Fibrinogen-derivative. It displays hemostatic activity and constricts vessels.

Nichols WW, Mehta J, Wargovich T, et al. Fibrin(ogen)-derived peptide B beta 30-43 increases coronary blood flow in the anesthetized dog. Thromb Res. 1985 Jul 15;39(2):223-9. PMID: 3895564.

Osbahr AJ, Custodio R. Action of peptide-B from bovine fibrinogen on ATPase activity and superprecipitation of myosin B. Am J Physiol. 1975 Feb;228(2):488-95. PMID: 123418.

P1767

Peptide F, cow

1 mg
2 mg
5 mg

H-Tyr-Gly-Gly-Phe-Met-Lys-Lys-Met-Asp-Glu-Leu-Tyr-Pro-Leu-Glu-Val-Glu-Glu-Glu-Ala-Asn-Gly-Gly-Glu-Val-Leu-Gly-Lys-Arg-Tyr-Gly-Gly-Phe-Met-OH

$C_{163}H_{239}N_{39}O_{53}S_2$ FW: 3657.08 ≥95%

Endogenous pro-enkephalin derivative found in the adrenal medulla. It stimulates immune signaling.

Kraemer WJ, Mastro AM, Gordon SE, et al. Responses of plasma proenkephalin peptide F in rats following 14 days of spaceflight. Aviat Space Environ Med. 2004 Feb;75(2):114-7. PMID: 14960045.

Triplett-McBride NT, Mastro AM, McBride JM, et al. Plasma proenkephalin peptide F and human B cell responses to exercise stress in fit and unfit women. Peptides. 1998;19(4):731-8. PMID: 9622029.

P2445

GLa Peptide

1 mg

PGLa

Gly-Met-Ala-Ser-Lys-Ala-Gly-Ala-Ile-Ala-Gly-Lys-Ile-Ala-Lys-Val-Ala-Leu-Lys-Ala-Leu-NH_2

$C_{88}H_{162}N_{26}O_{22}S$ FW: 1968.5 [102068-15-5] ≥98%

Antimicrobial peptide found in the skin of amphibians.

Kuchler K, Kreil G, Sures I. The genes for the frog skin peptides GLa, xenopsin, levitide and caerulein contain a homologous export exon encoding a signal sequence and part of an amphiphilic peptide. Eur J Biochem. 1989 Feb 1;179(2):281-5. PMID: 2465151.

P2832

Peptide Histidine Isoleucine, pig

1 mg

PHI

His-Ala-Asp-Gly-Val-Phe-Thr-Ser-Asp-Phe-Ser-Arg-Leu-Leu-Gly-Gln-Leu-Ser-Ala-Lys-Lys-Tyr-Leu-Glu-Ser-Leu-Ile-NH_2

$C_{136}H_{216}N_{36}O_{40}$ FW: 2995.39 [80458-29-3] ≥97%

Endogenous VPAC2 receptor agonist involved in prolactin signaling, circadian rhythms, and feeding behavior. It decreases food intake, increases glutamate transporter activity, and inhibits proliferation of neuroblastoma cells.

Goursaud S, Focant MC, Berger JV, et al. The VPAC2 agonist peptide histidine isoleucine (PHI) up-regulates glutamate transport in the corpus callosum of a rat model of amyotrophic lateral sclerosis (hSOD1G93A) by inhibiting caspase-3 mediated inactivation of GLT-1a. FASEB J. 2011 Oct;25(10):3674-86. PMID: 21730107.

Colwell CS, Michel S, Itri J, et al. Disrupted circadian rhythms in VIP- and PHI-deficient mice. Am J Physiol Regul Integr Comp Physiol. 2003 Nov;285(5):R939-49. PMID: 12855416.

P2833

Peptide Histidine Isoleucine, rat

0.5 mg
1 mg
2.5 mg

PHI

H-His-Ala-Asp-Gly-Val-Phe-Thr-Ser-Asp-Tyr-Ser-Arg-Leu-Leu-Gly-Gln-Ile-Ser-Ala-Lys-Lys-Tyr-Leu-Glu-Ser-Leu-Ile-NH_2

$C_{136}H_{216}N_{36}O_{41}$ FW: 3011.45 [96849-38-6] ≥95%

Endogenous VPAC2 receptor agonist involved in prolactin signaling, circadian rhythms, and feeding behavior. It decreases food intake, increases glutamate transporter activity, and inhibits proliferation of neuroblastoma cells.

Goursaud S, Focant MC, Berger JV, et al. The VPAC2 agonist peptide histidine isoleucine (PHI) up-regulates glutamate transport in the corpus callosum of a rat model of amyotrophic lateral sclerosis (hSOD1G93A) by inhibiting caspase-3 mediated inactivation of GLT-1a. FASEB J. 2011 Oct;25(10):3674-86. PMID: 21730107.

P1760

Peptide T

1 mg

Ala-Ser-Thr-Thr-Thr-Asn-Tyr-Thr

$C_{35}H_{55}N_9O_{16}$ FW: 857.86 [106362-32-7] ≥98%

Peptide fragment of HIV-1 gp120. It decreases inflammation, inhibits CCR5-dependent HIV entry, and improves cognitive performance in neuroAIDS subjects.

Paoletti I, De Gregorio V, Baroni A, et al. Amygdalin analogues inhibit IFN-γ signalling and reduce the inflammatory response in human epidermal keratinocytes. Inflammation. 2013 Dec;36(6):1316-26. PMID: 23933845.

D'ursi A, Caliendo G, Perissutti E, et al. Conformation-activity relationship of peptide T and new pseudocyclic hexapeptide analogs. J Pept Sci. 2007 Jun;13(6):413-21. PMID: 17486694.

P1768

Peptide YY (3-36), human

0.5 mg
1 mg
2.5 mg

PYY

H-Ile-Lys-Pro-Glu-Ala-Pro-Gly-Glu-Asp-Ala-Ser-Pro-Glu-Glu-Leu-Asn-Arg-Tyr-Tyr-Ala-Ser-Leu-Arg-His-Tyr-Leu-Asn-Leu-Val-Thr-Arg-Gln-Arg-Tyr-NH_2

$C_{180}H_{279}N_{53}O_{54}$ FW: 4049.55 [123583-37-9] ≥95%

Endogenous Y1/2 receptor agonist involved in enteric movement and feeding behavior. It decreases food intake, suppresses osteoblast activity, lowers lipid oxidation, and inhibits colonic and upper gastrointestinal transit.

Wong IP, Driessler F, Khor EC, et al. Peptide YY regulates bone remodeling in mice: a link between gut and skeletal biology. PLoS One. 2012;7(7):e40038. PMID: 22792209.

Shi YC, Hämmerle CM, Lee IC, et al. Adult-onset PYY overexpression in mice reduces food intake and increases lipogenic capacity. Neuropeptides. 2012 Aug;46(4):173-82. PMID: 22575886.

P1763

Peptide YY, human

1 mg
2 mg
5 mg

Tyr-Pro-Ile-Lys-Pro-Glu-Ala-Pro-Gly-Glu-Asp-Ala-Ser-Pro-Glu-Glu-eu-Asn-Arg-Tyr-Tyr-Ala-Ser-Leu-Arg-His-Tyr-Leu-Asn-Leu-Val-Thr-Arg-Gln-Arg-Tyr-NH_2

PYY

$C_{194}H_{295}N_{55}O_{57}$ FW: 4309.8 [118997-30-1] ≥98%

Endogenous Y1/2 receptor agonist involved in enteric movement and feeding behavior. It decreases food intake, suppresses osteoblast activity, lowers lipid oxidation, and inhibits colonic and upper gastrointestinal transit.

Wong IP, Driessler F, Khor EC, et al. Peptide YY regulates bone remodeling in mice: a link between gut and skeletal biology. PLoS One. 2012;7(7):e40038. PMID: 22792209.

P1762

Peptide YY, pig

1 mg
2 mg
5 mg

Tyr-Pro-Ala-Lys-Pro-Glu-Ala-Pro-Gly-Glu-Asp-Ala-Ser-Pro-Glu-Glu-Leu-Ser-Arg-Tyr-Tyr-Ala-Ser-Leu-Arg-His-Tyr-Leu-Asn-Leu-Val-Thr-Arg-Gln-Arg-Tyr-NH_2

PYY

$C_{190}H_{288}N_{54}O_{57}$ FW: 4240.7 [81858-94-8] ≥98%

Endogenous Y1/2 receptor agonist involved in enteric movement and feeding behavior. It decreases food intake, suppresses osteoblast activity, lowers lipid oxidation, and inhibits colonic and upper gastrointestinal transit.

Wong IP, Driessler F, Khor EC, et al. Peptide YY regulates bone remodeling in mice: a link between gut and skeletal biology. PLoS One. 2012;7(7):e40038. PMID: 22792209.

P1969

Perifosine

NEW

5 mg
10 mg
25 mg

$C_{25}H_{52}NO_4P$ FW: 461.66 [157716-52-4] ≥98%

Alkylphospholipid analog and Akt inhibitor. It inhibits LPS-induced increases in TNF-α and ERK activation, induces apoptosis in colorectal cancer cells and multiple myeloma cells, and enhances the efficacy of co-administered chemotherapeutics.

Gradziel CS, Wang Y, Stec B, et al. Cytotoxic amphiphiles and phosphoinositides bind to two discrete sites on the Akt1 PH domain. Biochemistry. 2014 Jan 28;53(3):462-72. PMID: 24383815.

Shen J, Liang L, Wang C. Perifosine inhibits lipopolysaccharide (LPS)-induced tumor necrosis factor (TNF)-α production via regulation multiple signaling pathways: new implication for Kawasaki disease (KD) treatment. Biochem Biophys Res Commun. 2013 Jul 26;437(2):250-5. PMID: 23806687.

Richardson PG, Eng C, Kolesar J, et al. Perifosine, an oral, anti-cancer agent and inhibitor of the Akt pathway: mechanistic actions, pharmacodynamics, pharmacokinetics, and clinical activity. Expert Opin Drug Metab Toxicol. 2012 May;8(5):623-33. PMID: 22512706.

P1770

Perillyl Alcohol

10 g
50 g

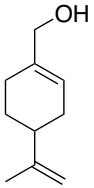

Isocarveol

$C_{10}H_{16}O$ FW: 152.23 [18457-55-1] ≥85%

Inhibitor of farnesyl transferase, geranylgeranyl transferase, telomerase, and Na^+/K^+ ATPase found in various plant and fruit sources. It displays several biological activities, including inhibiting neurological deficits and improving motor coordination, suppressing pro-inflammatory cytokine expression, limiting proliferation of antigen-stimulated immune cells, and preventing UV- and DMBA-induced development of skin cancer.

Tabassum R, Vaibhav K, Shrivastava P, et al. Perillyl alcohol improves functional and histological outcomes against ischemia-reperfusion injury by attenuation of oxidative stress and repression of COX-2, NOS-2 and NF-κB in middle cerebral artery occlusion rats. Eur J Pharmacol. 2014 Sep 18. [Epub ahead of print]. PMID: 25240714.

Imamura M, Sasaki O, Okunishi K, et al. Perillyl alcohol suppresses antigen-induced immune responses in the lung. Biochem Biophys Res Commun. 2014 Jan 3;443(1):266-71. PMID: 24309112.

DA Fonseca CO, Teixeira RM, Silva JC, et al. Long-term outcome in patients with recurrent malignant glioma treated with Perillyl alcohol inhalation. Anticancer Res. 2013 Dec;33(12):5625-31. PMID: 24324108.

P1869

Perindopril Erbumine

100 mg
250 mg
1 g

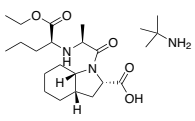

$C_{19}H_{32}N_2O_5 \bullet C_4H_{11}N$ FW: 441.6 [107133-36-8] ≥95%

ACE inhibitor used to treat high blood pressure, heart failure, or stable coronary artery disease. It decreases blood pressure, vascular resistance, and vasoconstriction. It also ameliorates cognitive impairment in models of vascular dementia and increases capillary density and post-ischemic revascularization.

Yamada K, Horita T, Takayama M, et al. Effect of a centrally active angiotensin converting enzyme inhibitor, perindopril, on cognitive performance in chronic cerebral hypo-perfusion rats. Brain Res. 2011 Nov 3;1421:110-20. PMID: 21981801.

Gao L, Yu DM. Molecular mechanism of limbs' postischemic revascularization improved by perindopril in diabetic rats. Chin Med J (Engl). 2008 Nov 5;121(21):2129-33. PMID: 19080171.

P2000

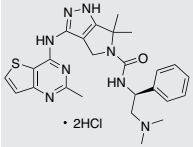

PF-03758309 Dihydrochloride

NEW

1 mg
5 mg
25 mg

$C_{25}H_{30}N_8OS \cdot 2HCl$ FW: 563.55 [1279034-84-2] ≥99%

PAK4 inhibitor. It inhibits motility, proliferation, and survival of various cancer cells.

Choi SW, Yeon JT, Ryu BJ, et al. Repositioning Potential of PAK4 to Osteoclastic Bone Resorption. J Bone Miner Res. 2015 Jan 31. [Epub ahead of print]. PMID: 25640698.

Ryu BJ, Lee H, Kim SH, et al. PF-3758309, p21-activated kinase 4 inhibitor, suppresses migration and invasion of A549 human lung cancer cells via regulation of CREB, NF-κB, and β-catenin signalings Mol Cell Biochem. 2014 Apr;389(1-2):69-77. PMID: 24366569.

Murray BW, Guo C, Piraino J, et al. Small-molecule p21-activated kinase inhibitor PF-3758309 is a potent inhibitor of oncogenic signaling and tumor growth. Proc Natl Acad Sci U S A. 2010 May 18;107(20):9446-51. PMID: 20439741.

P2012

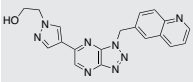

PF-04217903

NEW

5 mg
10 mg

$C_{19}H_{16}N_8O$ FW: 372.38 [1159490-85-3] ≥98%

Inhibitor of c-MET. It inhibits cell proliferation, invasion, and migration in several cancer models and prevents lymph node metastasis in pancreatic neuroendocrine tumor models.

Sennino B, Ishiguro-Oonuma T, Schriver BJ, et al. Inhibition of c-Met reduces lymphatic metastasis in RIP-Tag2 transgenic mice. Cancer Res. 2013 Jun 15;73(12):3692-703. PMID: 23576559.

Zou HY, Li Q, Lee JH, et al. Sensitivity of selected human tumor models to PF-04217903, a novel selective c-Met kinase inhibitor. Mol Cancer Ther. 2012 Apr;11(4):1036-47. PMID: 22389468.

P2002

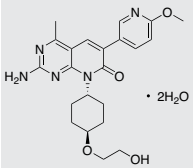

PF-04691502 Dihydrate

NEW

1 mg
5 mg
10 mg

$C_{22}H_{27}N_5O_4 \cdot 2H_2O$ FW: 461.51 [1013101-36-4] ≥98%

PI3K and mTOR inhibitor. It induces cell cycle arrest and apoptosis in nasopharyngeal carcinoma cells and decreases VEGF secretion.

Cirone P, Andresen CJ, Eswaraka JR, et al. Patient-derived xenografts reveal limits to PI3K/mTOR- and MEK-mediated inhibition of bladder cancer. Cancer Chemother Pharmacol. 2014 Mar;73(3):525-38. PMID: 24442130.

Wong CH, Loong HH, Hui CW, et al. Preclinical evaluation of the PI3K-mTOR dual inhibitor PF-04691502 as a novel therapeutic drug in nasopharyngeal carcinoma. Invest New Drugs. 2013 Dec;31(6):1399-408. PMID: 23975511.

Yuan J, Mehta PP, Yin MJ, et al. PF-04691502, a potent and selective oral inhibitor of PI3K and mTOR kinases with antitumor activity. Mol Cancer Ther. 2011 Nov;10(11):2189-99. PMID: 21750219.

P2100

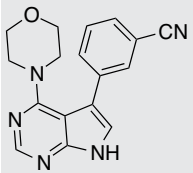

PF-06447475

NEW

5 mg
25 mg

$C_{17}H_{15}N_5O$ FW: 305.13 [1527473-33-1] ≥98%

LRRK2 inhibitor. It suppresses neuroinflammation and neurodegeneration in models of Parkinson's disease.

Daher JP, Abdelmotilib HA, Hu X, et al. LRRK2 Pharmacological Inhibition Abates α-Synuclein Induced Neurodegeneration. J Biol Chem. 2015 Jun 15. [Epub ahead of print]. PMID: 26078453.

Henderson JL, Kormos BL, Hayward MM, et al. Discovery and preclinical profiling of 3-[4-(morpholin-4-yl)-7H-pyrrolo[2,3-d]pyrimidin-5-yl]benzonitrile (PF-06447475), a highly potent, selective, brain penetrant, and in vivo active LRRK2 kinase inhibitor. J Med Chem. 2015 Jan 8;58(1):419-32. PMID: 25353650.

P2133

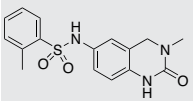

PFI-1

NEW

5 mg
10 mg

PF-06405761

$C_{16}H_{17}N_3O_4S$ FW: 347.39 [1403764-72-6] ≥98%

Acyl-lysine (Kac) mimetic and BRD2/4 inhibitor. It induces cell cycle arrest and suppresses growth in leukemia cells and decreases expression of pro-inflammatory cytokines in bronchial epithelial cells.

Khan YM, Kirkham P, Barnes PJ, et al. Brd4 Is Essential for IL-1β-Induced Inflammation in Human Airway Epithelial Cells. PLoS One. 2014 Apr 23;9(4):e95051. PMID: 24759736.

Picaud S, Da Costa D, Thanasopoulou A, et al. PFI-1, a highly selective protein interaction inhibitor, targeting BET Bromodomains. Cancer Res. 2013 Jun 1;73(11):3336-46. PMID: 23576556.

P2303

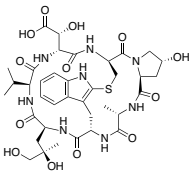

Phallacidin

1 mg
5 mg

Falacidin

$C_{37}H_{50}N_8O_{13}S$ FW: 846.91 [26645-35-2] ≥98%

Microtubule depolymerization inhibitor found in *Amanita phalloides*. It binds F-actin, preventing actin ATP hydrolysis. It also inhibits mast cell degranulation.

Schmid E, Gu S, Yang W, et al. Serum- and glucocorticoid-inducible kinase SGK1 regulates reorganization of actin cytoskeleton in mast cells upon degranulation. Am J Physiol Cell Physiol. 2013 Jan 1;304(1):C49-55. PMID: 23015548.

P2304 Phalloidin

1 mg
5 mg

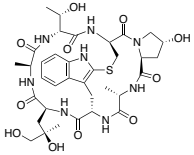

$C_{35}H_{48}N_8O_{11}S$ FW: 788.87 [17466-45-4] ≥95%

Microtubule depolymerization inhibitor found in *Amanita phalloides*. It binds F-actin, preventing actin ATP hydrolysis.

Cooper JA. Effects of cytochalasin and phalloidin on actin. J Cell Biol. 1987 Oct;105(4):1473-8. PMID: 3312229.

Barden JA, Miki M, Hambly BD, et al. Localization of the phalloidin and nucleotide-binding sites on actin. Eur J Biochem. 1987 Feb 2;162(3):583-8. PMID: 3830158.

P3018 Phellodendrine NEW

1 mg
5 mg

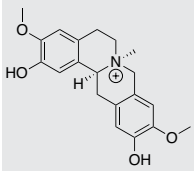

$C_{20}H_{24}NO_4$ FW: 342.41 [6873-13-8] ≥98%

Found in *Phellodendron*. It inhibits local semisyngenic and allogenic graft-versus-host reactions, suppresses the induction of delayed-type hypersensitivity reactions, and prevents nephritis-induced increases in immune cells and cytokines.

Mori H, Fuchigami M, Inoue N, et al. Principle of the bark of Phellodendron amurense to suppress the cellular immune response: effect of phellodendrine on cellular and humoral immune responses. Planta Med. 1995 Feb;61(1):45-9. PMID: 7700991.

P2400 Phenethyl Caffeate

50 mg
100 mg
500 mg

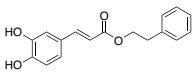

3,4-Dihydroxycinnamic acid phenethyl ester; caffeic acid phenethyl ester; CAPE

$C_{17}H_{16}O_4$ FW: 284.31 [104594-70-9] ≥98%

Synthetic 5-lipoxygenase inhibitor found in propolis. It suppresses lipid peroxidation, induces apoptosis in colorectal cancer cells, decreases body weight gain and fat mass in high-fat diet-fed animals, and decreases blood pressure and collagen deposition.

Yang JW, Jung WK, Lee CM, et al. Caffeic acid phenethyl ester inhibits the inflammatory effects of interleukin-1β in human corneal fibroblasts. Immunopharmacol Immunotoxicol. 2014 Oct;36(5):371-7. PMID: 25151996.

Ilhan S, Yılmaz N, Nacar E, et al. The effect of caffeic acid phenethyl ester on isoproterenol-induced myocardial injury in hypertensive rats. Anadolu Kardiyol Derg. 2014 Jun 3. [Epub ahead of print]. PMID: 25036319.

Chiang EP, Tsai SY, Kuo YH, et al. Caffeic acid derivatives inhibit the growth of colon cancer: involvement of the PI3-K/Akt and AMPK signaling pathways. PLoS One. 2014 Jun 24;9(6):e99631. PMID: 24960186.

P2410 Phenethyl Dimethyl Caffeate

50 mg
100 mg
500 mg

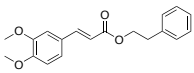

Caffeic Acid Dimethyl Phenethyl Ester

$C_{19}H_{20}O_4$ FW: 312.37 [14551-14-0] ≥98%

Caffeic acid derivative that may inhibit replication of HIV and increase levels of IL-2, IL-4, and IFN-γ.

Ho CC, Lin SS, Chou MY, et al. Effects of CAPE-like compounds on HIV replication in vitro and modulation of cytokines in vivo. J Antimicrob Chemother. 2005 Aug;56(2):372-9. PMID: 16002419.

P2502 Phenethyl Glucosinolate Potassium

5 mg
10 mg
25 mg
100 mg

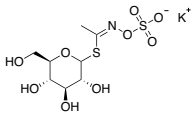

Gluconasturtiin

$C_{15}H_{20}NO_9S_2K$ FW: 461.55 ≥97%

Found in cruciferous vegetables. It scavenges radicals and protects against LDL oxidation. It may also induce phase II enzyme activity.

Gupta P, Wright SE, Kim SH, et al. Phenethyl isothiocyanate: A comprehensive review of anti-cancer mechanisms. Biochim Biophys Acta. 2014 Aug 23;1846(2):405-424. PMID: 25152445.

Natella F, Maldini M, Leoni G, et al. Glucosinolates redox activities: can they act as antioxidants? Food Chem. 2014 Apr 15;149:226-32. PMID: 24295700.

P2508 Phenethyl Isothiocyanate

5 g
10 g
50 g

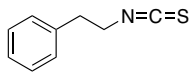

C_9H_9NS FW: 163.24 [2257-09-2] ≥98%

Found in cruciferous vegetables. It inhibits accumulation of HIF-1α and secretion of VEGF during hypoxia in glioma cells, suppresses activation of NNK, increases activation of JNK1, and induces caspase-mediated apoptosis in Jurkat T cells.

Tusskorn O, Senggunprai L, Prawan A, et al Phenethyl isothiocyanate induces calcium mobilization and mitochondrial cell death pathway in cholangiocarcinoma KKU-M214 cells. BMC Cancer. 2013 Dec 5;13(1):571. PMID: 24304591.

Stan SD, Singh SV, Whitcomb DC, et al. Phenethyl Isothiocyanate Inhibits Proliferation and Induces Apoptosis in Pancreatic Cancer Cells In Vitro and in a MIAPaca2 Xenograft Animal Model. Nutr Cancer. 2013 Nov 6. [Epub ahead of print]. PMID: 24195616.

Gupta B, Chiang L, Chae K, et al. Phenethyl isothiocyanate inhibits hypoxia-induced accumulation of HIF-1α and VEGF expression in human glioma cells. Food Chem. 2013 Dec 1;141(3):1841-6. PMID: 23870899.

P2512

S-(N-Phenethylthiocarbamoyl)-L-cysteine

10 mg
25 mg
100 mg

Phenethylisothiocyanate-L-cysteine

$C_{12}H_{16}N_2O_2S_2$ FW: 284.4 ≥98%

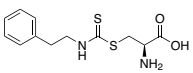

Cysteine-phenylethylisothiocyanate conjugate and antioxidant. It may induce apoptosis in Jurkat T cells, increase activation of JNK1, and inhibit accumulation of HIF-1α and secretion of VEGF in glioma cells.

Tusskorn O, Senggunprai L, Prawan A, et al Phenethyl isothiocyanate induces calcium mobilization and mitochondrial cell death pathway in cholangiocarcinoma KKU-M214 cells. BMC Cancer. 2013 Dec 5;13(1):571. PMID: 24304591.

Stan SD, Singh SV, Whitcomb DC, et al. Phenethyl Isothiocyanate Inhibits Proliferation and Induces Apoptosis in Pancreatic Cancer Cells In Vitro and in a MIAPaca2 Xenograft Animal Model. Nutr Cancer. 2013 Nov 6. [Epub ahead of print]. PMID: 24195616.

Gupta B, Chiang L, Chae K, et al. Phenethyl isothiocyanate inhibits hypoxia-induced accumulation of HIF-1α and VEGF expression in human glioma cells. Food Chem. 2013 Dec 1;141(3):1841-6. PMID: 23870899.

P2817

Phentolamine Hydrochloride

50 mg
100 mg
500 mg

$C_{17}H_{19}N_3O \bullet HCl$ FW: 317.81 [73-05-2] ≥98%

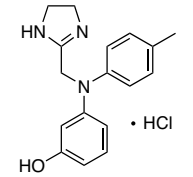

ATP-sensitive K^+ channel activator and α-adrenergic receptor antagonist used to treat erectile dysfunction. It inhibits fructose-induced increases in blood pressure.

Zhou K, Kumar U, Yuen VG, et al. The effects of phentolamine on fructose-fed rats. Can J Physiol Pharmacol. 2012 Aug;90(8):1075-85. PMID: 22783820.

Ahn SW, Kim SH, Kim JH, et al. Phentolamine inhibits the pacemaker activity of mouse interstitial cells of Cajal by activating ATP-sensitive K^+ channels. Arch Pharm Res. 2010 Mar;33(3):479-89. PMID: 20361315.

Dinsmore WW, Wyllie MG. Vasoactive intestinal polypeptide/phentolamine for intracavernosal injection in erectile dysfunction. BJU Int. 2008 Sep;102(8):933-7. PMID: 18485029.

P2818

Phentolamine Methanesulfonate

50 mg
100 mg
500 mg

$C_{17}H_{19}N_3O \bullet CH_3SO_3H$ FW: 377.46 [65-28-1] ≥98%

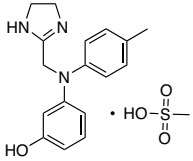

ATP-sensitive K^+ channel activator and α-adrenergic receptor antagonist used to treat erectile dysfunction. It inhibits fructose-induced increases in blood pressure.

Zhou K, Kumar U, Yuen VG, et al. The effects of phentolamine on fructose-fed rats. Can J Physiol Pharmacol. 2012 Aug;90(8):1075-85. PMID: 22783820.

Ahn SW, Kim SH, Kim JH, et al. Phentolamine inhibits the pacemaker activity of mouse interstitial cells of Cajal by activating ATP-sensitive K^+ channels. Arch Pharm Res. 2010 Mar;33(3):479-89. PMID: 20361315.

P2919

L-Phenylalaninol

1 g
5 g
25 g

$C_9H_{13}NO$ FW: 151.21 [3182-95-4] ≥98%

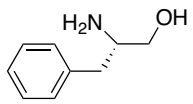

Non-essential amino acid alcohol that inhibits proliferation of melanoma cells, suppresses intestinal absorption of phenylalanine, and may decrease gastric acid secretion and ulcer formation.

Landau O, Wasserman L, Deutsch AA, et al.Amino acid alcohols: growth inhibition and induction of differentiated features in melanoma cells. Cancer Lett. 1993 May 14;69(3):203-8. PMID: 8099846.

Hashizume H, Miyamae T, Morikawa T, et al. Effects of phenylalaninol on centrally induced gastric acid secretion. Chem Pharm Bull (Tokyo). 1992 Nov;40(11):3113-4. PMID: 1477931.

Shimomura K, Fukushima T, Danno T, et al. Inhibition of intestinal absorption of phenylalanine by phenylalaninol. J Biochem. 1975 Aug;78(2):269-75. PMID: 1228171.

P2513

Phenyl Isothiocyanate

50 g
100 g

PITC; Isothiocyanatobenzene; Thiocarbanil

C_7H_5NS FW: 135.19 [103-72-0] ≥98%

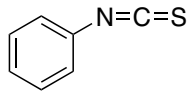

It displays several activities, including altering membrane function of *Escherichia* and *Staphylococcus*, inhibiting lipid peroxidation, and inducing phase II enzyme activity.

Abreu AC, Borges A, Simões LC, et al. Antibacterial activity of phenyl isothiocyanate on *Escherichia* coli and *Staphylococcus aureus*. Med Chem. 2013 Aug;9(5):756-61. PMID: 22974327.

Thejass P, Kuttan G. Inhibition of endothelial cell differentiation and proinflammatory cytokine production during angiogenesis by allyl isothiocyanate and phenyl isothiocyanate. Integr Cancer Ther. 2007 Dec;6(4):389-99. PMID: 18048887.

Manesh C, Kuttan G. Anti-tumour and anti-oxidant activity of naturally occurring isothiocyanates. J Exp Clin Cancer Res. 2003 Jun;22(2):193-9. PMID: 12866569.

P2810 Phenylbutazone

25 g
100 g

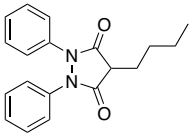

$C_{19}H_{20}N_2O_2$ FW: 308.37 [50-33-9] ≥98%

NSAID and COX-1/2 inhibitor previously used to treat pain and fever. It decreases edema and inhibits the activity of myeloperoxidase.

Cusan C, Altinier G, Sosa S, et al. Anti-inflammatory and anti-oxidant activity of a new class of phenyl-pyrazolone derivatives. Curr Drug Discov Technol. 2006 Mar;3(1):67-73. PMID: 16712464.

Kettle AJ, Winterbourn CC. Mechanism of inhibition of myeloperoxidase by anti-inflammatory drugs. Biochem Pharmacol. 1991 May 15;41(10):1485-92. PMID: 1850278.

P2510 4-Phenylbutylisothiocyanate

1 g
5 g
10 g

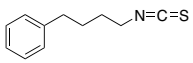

$C_{11}H_{13}NS$ FW: 191.31 [61499-10-3] ≥98%

Synthetic compound that induces caspase-mediated apoptosis, induces phase II enzyme activity, and suppresses development of pancreatic dysplasia and adenocarcinoma.

Son HY, Nishikawa A, Furukawa F, et al. Modifying effects of 4-phenylbutyl isothiocyanate on N-nitroso-bis(2-oxopropyl)amine-induced tumorigenesis in hamsters. Cancer Lett. 2000 Nov 28;160(2):141-7. PMID: 11053643.

Yu R, Mandlekar S, Harvey KJ, et al. Chemopreventive isothiocyanates induce apoptosis and caspase-3-like protease activity. Cancer Res. 1998 Feb 1;58(3):402-8. PMID: 9458080.

P2516 S-(N-Phenylbutylthiocarbamoyl)-L-cysteine

10 mg
25 mg
100 mg

Phenylbutylisothiocyanate-L-cysteine

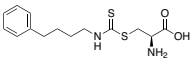

$C_{14}H_{20}N_2O_2S_2$ FW: 312.45 ≥98%

Cysteine-phenylbutylisothiocyanate conjugate and antioxidant. It may induce apoptosis in cancer cells, decrease activation of NNK, and increase levels of antioxidative enzymes.

Son HY, Nishikawa A, Furukawa F, et al. Modifying effects of 4-phenylbutyl isothiocyanate on N-nitroso-bis(2-oxopropyl)amine-induced tumorigenesis in hamsters. Cancer Lett. 2000 Nov 28;160(2):141-7. PMID: 11053643.

P2514 S-(N-Phenylbutylthiocarbamoyl)-glutathione

5 mg
10 mg
25 mg

Phenylbutylisothiocyanate-glutathione

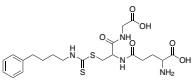

$C_{21}H_{30}N_4O_6S_2$ FW: 498.62 ≥98%

Glutathione-phenylbutylisothiocyanate conjugate and antioxidant. It may induce apoptosis in cancer cells, decrease activation of NNK, and increase levels of antioxidative enzymes.

Son HY, Nishikawa A, Furukawa F, et al. Modifying effects of 4-phenylbutyl isothiocyanate on N-nitroso-bis(2-oxopropyl)amine-induced tumorigenesis in hamsters. Cancer Lett. 2000 Nov 28;160(2):141-7. PMID: 11053643.

P2815 Phenylbutyrate Sodium

1 g
5 g
25 g

Buphenyl; Tributyrate

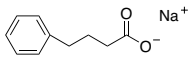

$C_{10}H_{11}O_2Na$ FW: 186.18 [1716-12-7] ≥98%

HDAC inhibitor used to treat urea cycle disorders. It inhibits tumor growth in pancreatic cancer models and prevents neuronal loss and normalizes brain pathology in Alzheimer's disease models,

Cuadrado-Tejedor M, Ricobaraza AL, Torrijo R, et al. Phenylbutyrate is a multifaceted drug that exerts neuroprotective effects and reverses the Alzheimer´s disease-like phenotype of a commonly used mouse model. Curr Pharm Des. 2013;19(28):5076-84. PMID: 23448463.

Dovzhanskiy DI, Hartwig W, Lázár NG, et al. Growth inhibition of pancreatic cancer by experimental treatment with 4-phenylbutyrate is associated with increased expression of Connexin 43. Oncol Res. 2012;20(2-3):103-11. PMID: 23193916.

Iannitti T, Palmieri B. Clinical and experimental applications of sodium phenylbutyrate. Drugs R D. 2011 Sep 1;11(3):227-49. PMID: 21902286.

P1917 Phenylethyl 3-methylcaffeate

50 mg
100 mg
500 mg

CCRIS 7791

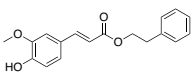

$C_{18}H_{18}O_4$ FW: 298.33 [71835-85-3] ≥97%

Derivative of methyl caffeate. It induces apoptosis and inhibits carcinogenesis in colon cancer models.

Samaha HS, Kelloff GJ, Steele V, et al. Modulation of apoptosis by sulindac, curcumin, phenylethyl-3-methylcaffeate, and 6-phenylhexyl isothiocyanate: apoptotic index as a biomarker in colon cancer chemoprevention and promotion. Cancer Res. 1997 Apr 1;57(7):1301-5. PMID: 9102217.

Rao CV, Desai D, Rivenson A, et al. Chemoprevention of colon carcinogenesis by phenylethyl-3-methylcaffeate. Cancer Res. 1995 Jun 1;55(11):2310-5. PMID: 7757981.

P2918 Phenylethyl-4-methylcaffeate

25 mg
50 mg
250 mg

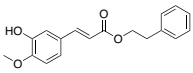

$C_{18}H_{18}O_4$ FW: 298.33 ≥98%

Synthetic derivative of methyl caffeate that inhibits colon tumor development.

Pereira MA. Prevention of colon cancer and modulation of aberrant crypt foci, cell proliferation, and apoptosis by retinoids and NSAIDs. Adv Exp Med Biol. 1999;470:55-63. PMID: 10709674.

P2819 6-Phenylhexa-3,5-dien-2-one

5 mg
10 mg

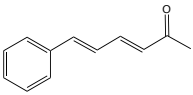

EINECS 224-036-3

$C_{12}H_{12}O$ FW: 172.22 [4173-44-8] ≥98%

Found in *Piper methysticum* (kava plant).

P2922 Phenylhexyl Isothiocyanate

100 mg
250 mg
500 mg

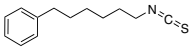

PHITC

$C_{13}H_{17}NS$ FW: 219.35 [133920-06-6] ≥98%

Synthetic HDAC inhibitor found in cruciferous vegetables. It decreases activation of NNK, induces apoptosis in myeloma cells, and inhibits growth of leukemia cells in animal models.

Lu Q, Lin X, Feng J, et al. Phenylhexyl isothiocyanate has dual function as histone deacetylase inhibitor and hypomethylating agent and can inhibit myeloma cell growth by targeting critical pathways. J Hematol Oncol. 2008 Jun 9;1:6. PMID: 18577263.

Lu L, Liu D, Ma X, et al. The phenylhexyl isothiocyanate induces apoptosis and inhibits leukemia cell growth in vivo. Oncol Rep. 2006 Dec;16(6):1363-7. PMID: 17089062.

P2515 3-Phenylpropyl Isothiocyanate

1 g
5 g
10 g

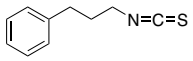

$C_{10}H_{11}NS$ FW: 177.27 [2627-27-2] ≥98%

Synthetic compound that decreases benzo[a]pyrene- and NNK-induced lung tumor formation and increases phase II enzyme activity.

Tayem Y, Green CJ, Motterlini R, et al. Isothiocyanate-cysteine conjugates protect renal tissue against cisplatin-induced apoptosis via induction of heme oxygenase-1. Pharmacol Res. 2014 Mar;81:1-9. PMID: 24434421.

Hecht SS, Upadhyaya P, Wang M, et al. Inhibition of lung tumorigenesis in A/J mice by N-acetyl-S-(N-2-phenethylthiocarbamoyl)-L-cysteine and myo-inositol, individually and in combination. Carcinogenesis. 2002 Sep;23(9):1455-61. PMID: 12189187.

P2816 S-(N-3-Phenylpropylthiocarbamoyl)-L-cysteine

100 mg
500 mg
1 g

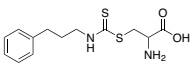

$C_{13}H_{18}N_2O_2S_2$ FW: 298.42 [137915-13-0] ≥98%

Synthetic compound that decreases lung tumor formation induced by benzo[a]pyrene and NNK and increases phase II enzyme activity.

Tayem Y, Green CJ, Motterlini R, et al. Isothiocyanate-cysteine conjugates protect renal tissue against cisplatin-induced apoptosis via induction of heme oxygenase-1. Pharmacol Res. 2014 Mar;81:1-9. PMID: 24434421.

P2522 S-(N-Phenylthiocarbamoyl)-glutathione

5 mg
10 mg
25 mg

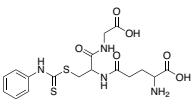

Phenylisothiocyanate glutathione

$C_{17}H_{22}N_4O_6S_2$ FW: 442.51 ≥98%

Conjugate of glutathione and phenylisothiocyanate. It may inhibit lipid peroxidation, induces vasodilation, decrease release of pro-inflammatory cytokines, and increase total white blood cell count, antibody titer, and plaque-forming cell levels.

Martelli A, Testai L, Citi V, et al. Pharmacological characterization of the vascular effects of aryl isothiocyanates: Is hydrogen sulfide the real player? Vascul Pharmacol. 2013 Nov 25. pii: S1537-1891(13)00138-9. PMID: 24287004.

Abreu AC, Borges A, Simões LC, et al. Antibacterial activity of phenyl isothiocyanate on *Escherichia* coli and *Staphylococcus aureus*. Med Chem. 2013 Aug;9(5):756-61. PMID: 22974327.

P2845 Phleomycin

5 mg
25 mg
100 mg

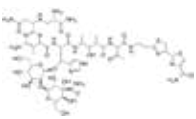

NSC 61586; NSC 616586

$C_{51}H_{75}N_{17}O_{21}S_2$ FW: 1326.38 [11006-33-0] ≥97%

Metal ion chelator that induces DNA strand breaks. It binds DNA but does not intercalate. It inhibits growth of bacteria and fungi.

van Peer AF, de Bekker C, Vinck A, et al. Phleomycin increases transformation efficiency and promotes single integrations in Schizophyllum commune. Appl Environ Microbiol. 2009 Mar;75(5):1243-7. PMID: 19114524.

Povirk LF, Hogan M, Dattagupta N, et al. Copper(II).bleomycin, iron(III).bleomycin, and copper(II).phleomycin: comparative study of deoxyribonucleic acid binding. Biochemistry. 1981 Feb 3;20(3):665-71. PMID: 6163448.

P2856

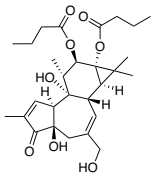

Phorbol-12,13-dibutyrate

PBDu

1 mg
5 mg

$C_{30}H_{46}O_8$ FW: 504.61 [37558-16-0] ≥98%

Carcinogen and activator of PKC and PKD. It induces apoptosis and differentiation in leukemia cells.

Aicart-Ramos C, Sánchez-Ruiloba L, Gómez-Parrizas M, et al. Protein kinase D activity controls endothelial nitric oxide synthesis. J Cell Sci. 2014 Aug 1;127(Pt 15):3360-72. PMID: 24928905.

Terui Y, Furukawa Y, Kikuchi J, et al. Apoptosis during HL-60 cell differentiation is closely related to a G0/G1 cell cycle arrest. J Cell Physiol. 1995 Jul;164(1):74-84. PMID: 7790399.

P2857

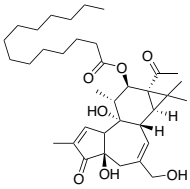

Phorbol-12-myristate-13-acetate

TPA; PMA; Tetradecanoylphorbol acetate

1 mg
5 mg

$C_{36}H_{56}O_8$ FW: 616.84 [16561-29-8] ≥98%

PKC activator and carcinogen used to promote the formation of tumors in research models. It also increases expression of pro-inflammatory cytokines such as TNF-α.

Poachanukoon O, Koontongkaew S, Monthanapisut P, et al. Macrolides attenuate phorbol ester-induced tumor necrosis factor-α and mucin production from human airway epithelial cells. Pharmacology. 2014;93(1-2):92-9. PMID: 24556631.

Oskoueian E, Abdullah N, Ahmad S. Phorbol esters isolated from Jatropha meal induced apoptosis-mediated inhibition in proliferation of chang and Vero cell lines. Int J Mol Sci. 2012 Oct 24;13(11):13816-29. PMID: 23203036.

Colombo D, Tringali C, Franchini L, et al. Glycoglycerolipid analogues inhibit PKC translocation to the plasma membrane and downstream signaling pathways in PMA-treated fibroblasts and human glioblastoma cells, U87MG. Eur J Med Chem. 2011 May;46(5):1827-34. PMID: 21388717.

P2858

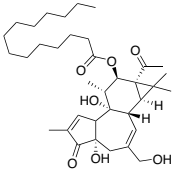

4-α-Phorbol-12-myristate-13-acetate

4-αPMA

1 mg
5 mg

$C_{36}H_{56}O_8$ FW: 616.83 [63597-44-4] ≥98%

Negative control used in research models to study PKC activation and other effects induced by PMA.

Chahine M, Qu Y, Mancarella S, et al. Protein kinase C activation inhibits alpha1D L-type Ca channel: a single-channel analysis. Pflugers Arch. 2008 Feb;455(5):913-9. PMID: 17909852.

Tosco M, Orsenigo MN, Gastaldi G, et al. Protein kinase C regulation of rat jejunal transport system: mechanisms involved in lactate movement. Exp Physiol. 2002 Nov;87(6):653-62. PMID: 12530398.

P2859

H-Arg-Arg-Lys-Ala-Ser-Gly-Pro-Pro-Val-OH

Phosphate Acceptor Peptide

1 mg
2 mg
5 mg

$C_{41}H_{74}N_{16}O_{11}$ FW: 967.15 ≥95%

Substrate used to measure activity of PKC and S6 kinase.

O'Brian CA, Ward NE. Stimulation of the ATPase activity of rat brain protein kinase C by phospho acceptor substrates of the enzyme. Biochemistry. 1991 Mar 5;30(9):2549-54. PMID: 1848101.

P3076

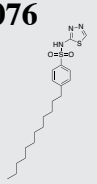

PHT-427

NEW

5 mg
10 mg

$C_{20}H_{31}N_3O_2S_2$ FW: 409.61 [1191951-57-1] ≥98%

PDK1 and Akt inhibitor. It inhibits tumor growth in non-small cell lung cancer models.

Meuillet EJ, Zuohe S, Lemos R, et al. Molecular pharmacology and antitumor activity of PHT-427, a novel Akt/phosphatidylinositide-dependent protein kinase 1 pleckstrin homology domain inhibitor. Mol Cancer Ther. 2010 Mar;9(3):706-17. PMID: 20197390.

P2992

pGlu-Leu-Trp-Ala-Val-Gly-Ser-Phe-Met-NH_2

Phyllolitorin

0.5 mg
1 mg
2.5 mg

$C_{49}H_{69}N_{11}O11S_1$ FW: 1020.24 [87734-77-8] ≥95%

GRP (BB1) receptor and neuromedin B (BB2) receptor agonist found in amphibian skin. It elicits grooming and scratching behavior, induces contractions in urinary bladder smooth muscle, and may play a role in lung branching morphogenesis.

Lin JT, Coy DH, Mantey SA, et al. Comparison of the peptide structural requirements for high affinity interaction with bombesin receptors. Eur J Pharmacol. 1995 Dec 27;294(1):55-69. PMID: 8788416.

P2993

pGlu-Asn-Pro-Asn-Arg-Phe-Ile-Gly-Leu-Met-NH_2

Phyllomedusin

1 mg
2 mg
5 mg

$C_{52}H_{82}N_{16}O_{13}S$ FW: 1171.41 [26145-48-2] ≥95%

Amphibian NK1 receptor agonist. It induces contractions in ileal longitudinal muscle and stimulates spasmogenic activity in stomach smooth muscle.

Ganjiwale AD, Cowsik SM. Three-dimensional structure of Phyllomedusin, a NK1 receptor agonist bound to dodecylphosphocholine micelles. J Struct Biol. 2009 Aug;167(2):176-84. PMID: 19409496.

P2994

Physalaemin

1 mg
2 mg
5 mg

pGlu-Ala-Asp-Pro-Asn-Lys-Phe-Tyr-Gly-Leu-Met-NH_2

$C_{58}H_{84}N_{14}O_{16}S_1$ FW: 1265.48 [2507-24-6] ≥95%

Amphibian tachykinin that induces contractions in distal colon and esophageal longitudinal muscle.

Shiina T, Shima T, Hirayama H, et al. Contractile responses induced by physalaemin, an analogue of substance P, in the rat esophagus. Eur J Pharmacol. 2010 Feb 25;628(1-3):202-6. PMID: 19958761.

Fontaine J, Lebrun P. Contractile effects of substance P and other tachykinins on the mouse isolated distal colon. Br J Pharmacol. 1989 Mar;96(3):583-90. PMID: 2470454.

P2995

Physcion

10 mg
25 mg
100 mg

Parietin; Rheochrysidin

$C_{16}H_{12}O_5$ FW: 284.26 [521-61-9] ≥96%

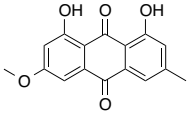

Found in various plant sources. It induces apoptosis in cervical carcinoma cells, decreases edema, and inhibits growth of *Staphylococcus*, *Pseudomonas*, *Escherichia*, *Candida*, and *Aspergillus*.

Wijesekara I, Zhang C, Van Ta Q, et al. Physcion from marine-derived fungus Microsporum sp. induces apoptosis in human cervical carcinoma HeLa cells. Microbiol Res. 2014 Apr;169(4):255-61. PMID: 24071573.

Locatelli M, Epifano F, Genovese S, et al. Anthraquinone profile, antioxidant and antimicrobial properties of bark extracts of Rhamnus catharticus and R. orbiculatus. Nat Prod Commun. 2011 Sep;6(9):1275-80. PMID: 21941897.

Ghosh S, Das Sarma M, Patra A, et al. Anti-inflammatory and anticancer compounds isolated from Ventilago madraspatana Gaertn., Rubia cordifolia Linn. and Lantana camara Linn. J Pharm Pharmacol. 2010 Sep;62(9):1158-66. PMID: 20796195.

P3198

Phytanic Acid

NEW

5 mg
25 mg

$C_{20}H_{40}O_2$ FW: 312.53 [14721-66-5] ≥97%

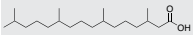

Fatty acid metabolite of chlorophyll, RXR and PPAR agonist, and potential GPR40 agonist. It regulates glucose metabolism, induces apoptosis in astrocytes, and alters intracellular Ca^{2+} levels.

Che BN, Oksbjerg N, Hellgren LI, et al. Phytanic acid stimulates glucose uptake in a model of skeletal muscles, the primary porcine myotubes. Lipids Health Dis. 2013 Feb 11;12:14. PMID: 23398851.

Busanello EN, Amaral AU, Tonin AM, et al. Disruption of mitochondrial homeostasis by phytanic acid in cerebellum of young rats. Cerebellum. 2013 Jun;12(3):362-9. PMID: 23081695.

Kruska N, Reiser G. Phytanic acid and pristanic acid, branched-chain fatty acids associated with Refsum disease and other inherited peroxisomal disorders, mediate intracellular Ca^{2+} signaling through activation of free fatty acid receptor GPR40. Neurobiol Dis. 2011 Aug;43(2):465-72. PMID: 21570468.

P2997

Phytic Acid, 40-50 wt% aqueous solution

100 mL
500 mL

Inositol hexaphosphate

$C_6H_{18}O_{24}P_6$ FW: 660.04 [83-86-3] ≥40%

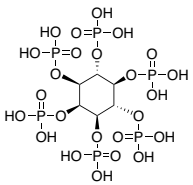

It is used to store phosphorus in plants and is occasionally used in cattle feed. It induces apoptosis in adenocarcinoma cells, decreases edema, and protects against NSAID-induced ulcer formation.

Shafie NH, Esa NM, Ithnin H, et al. Pro-apoptotic effect of rice bran inositol hexaphosphate (IP6) on HT-29 colorectal cancer cells. Int J Mol Sci. 2013 Dec 2;14(12):23545-58. PMID: 24317430.

Lopez-Gonzalez AA, Grases F, Perello J, et al. Phytate levels and bone parameters: a retrospective pilot clinical trial. Front Biosci (Elite Ed). 2010 Jun 1;2:1093-8. PMID: 20515779.

Sudheer Kumar M, Sridhar Reddy B, Kiran Babu S, et al. Antiinflammatory and antiulcer activities of phytic acid in rats. Indian J Exp Biol. 2004 Feb;42(2):179-85. PMID: 15282951.

P3209

Piceatannol

5 mg
25 mg

$C_{14}H_{12}O_4$ FW: 244.24 [10083-24-6] ≥98%

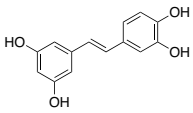

Resveratrol derivative, HPH-2 inhibitor, and potential PI3K and JAK1 inhibitor. It increases levels of HIF-1α, VEGF, and HO-1, suppresses growth of prostate cancer cells, inhibits the insulin receptor, and prevents adipogenesis in preadipocytes.

Yum S, Doh HJ, Hong S, et al. Piceatannol, a hydroxystilbene natural product, stabilizes HIF-1α protein by inhibiting HIF prolyl hydroxylase. Eur J Pharmacol. 2013 Jan 15;699(1-3):124-31. PMID: 23261967.

Jayasooriya RG, Lee YG, Kang CH, et al. Piceatannol inhibits MMP-9-dependent invasion of tumor necrosis factor-α-stimulated DU145 cells by suppressing the Akt-mediated nuclear factor-κB pathway. Oncol Lett. 2013 Jan;5(1):341-347. PMID: 23255946.

Li Z, Yang X, Dong S, et al. DNA breakage induced by piceatannol and copper(II): Mechanism and anticancer properties. Oncol Lett. 2012 May;3(5):1087-1094. PMID: 22783397.

P3210

Picoplatin

1 mg
5 mg
10 mg
25 mg

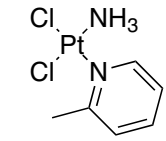

$C_6H_{10}Cl_2N_2Pt$ FW: 376.15 [181630-15-9] ≥98%

Platinum-based DNA cross-linker used to treat non-small cell lung cancer. It intercalates with GpG DNA sequences.

Matos CS, de Carvalho AL, Lopes RP, et al. New strategies against prostate cancer--Pt(II)-based chemotherapy. Curr Med Chem. 2012;19(27):4678-87. PMID: 22856665.

Eckardt JR, Bentsion DL, Lipatov ON, et al. Phase II study of picoplatin as second-line therapy for patients with small-cell lung cancer. J Clin Oncol. 2009 Apr 20;27(12):2046-51. PMID: 19289620.

P3313

Pidotimod

1 g
5 g
10 g

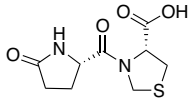

$C_9H_{12}N_2O_4S$ FW: 244.27 [121808-62-6] ≥98%

Immunostimulator and adjuvant used to treat acute respiratory tract infections. It increases levels of Th1 cytokines, decreases parasite burden in Toxoplasma infection models, and promotes dendritic cell maturation.

Zuccotti GV, Mameli C. Pidotimod: the past and the present. Ital J Pediatr. 2013 Dec 6;39:75. PMID: 24314100.

Zhao Y, Huang B, Huang S, et al. Evaluation of the adjuvant effect of pidotimod on the immune protection induced by UV-attenuated Toxoplasma gondii in mouse models. Parasitol Res. 2013 Sep;112(9):3151-60. PMID: 23783399.

P3540

PIK-75 Hydrochloride

NEW

5 mg
25mg
100 mg

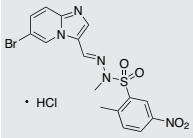

$C_{16}H_{14}BrN_5O_4S \cdot HCl$ FW: 488.74 [372196-77-5] ≥98%

Inhibitor of p110α PI3K. It inhibits motility and adhesion of breast cancer cells, suppresses production of pro-inflammatory cytokines, and enhances glucose-induced insulin secretion.

Buchanan CM, Dickson JM, Lee WJ, et al. Oncogenic mutations of p110α isoform of PI 3-kinase upregulate its protein kinase activity. PLoS One. 2013 Aug 1;8(8):e71337. PMID: 23936502.

Aoyagi K, Ohara-Imaizumi M, Nishiwaki C, et al. Acute inhibition of PI3K-PDK1-Akt pathway potentiates insulin secretion through upregulation of newcomer granule fusions in pancreatic β-cells. PLoS One. 2012;7(10):e47381. PMID: 23077605.

Smirnova T, Zhou ZN, Flinn RJ, et al. Phosphoinositide 3-kinase signaling is critical for ErbB3-driven breast cancer cell motility and metastasis. Oncogene. 2012 Feb 9;31(6):706-15. PMID: 21725367.

P3542

PIK-93

NEW

1 mg
5 mg
10 mg

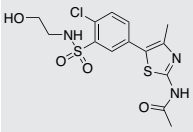

$C_{14}H_{16}ClN_3O_4S_2$ FW: 389.88 [593960-11-3] ≥98%

Inhibitor of p110α and p110γ PI3K and PI4KIIIβ. It decreases translocation of TRPC6 receptors to the plasma membrane and may alter Ca^{2+} signaling.

Monet M, Francoeur N, Boulay G. Involvement of phosphoinositide 3-kinase and PTEN protein in mechanism of activation of TRPC6 protein in vascular smooth muscle cells. J Biol Chem. 2012 May 18;287(21):17672-81. PMID: 22493444.

P3440

PIK-293

NEW

1 mg
5 mg
10 mg

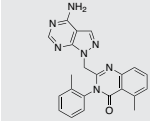

$C_{22}H_{19}N_7O$ FW: 397.43 [900185-01-5] ≥98%

Parent compound of PIK-294 and inhibitor of p110δ PI3K.

P3441

PIK-294

NEW

1 mg
5 mg
10 mg

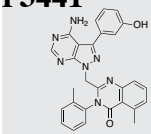

$C_{28}H_{23}N_7O_2$ FW: 489.53 [900185-02-6] ≥98%

Inhibitor of p110δ PI3K.

P3348

Pimecrolimus

5 mg
25 mg

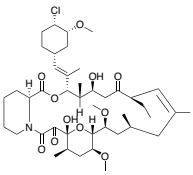

$C_{43}H_{66}ClNO_{11}$ FW: 810.45 [137071-32-0] ≥98%

Calcineurin inhibitor and potential TRPV1 agonist used to treat inflammatory skin diseases. It inhibits T cell signaling, prevents release of pro-inflammatory cytokines, and suppresses nociception.

Xie ZQ, Lan YZ. Effectiveness of pimecrolimus cream for women patients with sensitive skin and its underlying mechanism. Zhongguo Yi Xue Ke Xue Yuan Xue Bao. 2012 Aug;34(4):375-8. PMID: 22954121.

Lampropoulos CE, D'Cruz DP. Topical calcineurin inhibitors in systemic lupus erythematosus. Ther Clin Risk Manag. 2010 Apr 15;6:95-101. PMID: 20421909.

P3456

Pimobendan

10 mg
25 mg
100 mg
500 mg

$C_{19}H_{18}N_4O_2$ FW: 334.37 [74150-27-9] ≥98%

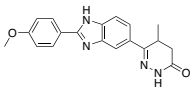

PDE3 inhibitor used to treat congestive heart failure, dilated cardiomyopathy, and chronic valvular heart disease. It acts as a positive inotrope, increasing heart rate, left ventricle systolic pressure, and left ventricle filling pressure.

Shipley EA, Hogan DF, Fiakpui NN, et al. In vitro effect of pimobendan on platelet aggregation in dogs. Am J Vet Res. 2013 Mar;74(3):403-7. PMID: 23438115.

Boyle KL, Leech E. A review of the pharmacology and clinical uses of pimobendan. J Vet Emerg Crit Care (San Antonio). 2012 Aug;22(4):398-408. PMID: 22928748.

P6954

Pioglitazone Hydrochloride

100 mg
500 mg
1 g

U-72107A

$C_{19}H_{20}N_2O_3S \bullet HCl$ FW: 392.91 [112529-15-4] ≥98%

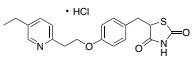

PPARα/γ agonist and mitoNEET modulator used to treat diabetes. It decreases levels of HDL, triglycerides, total cholesterol, insulin, blood glucose, and Hb1Ac. It also increases microvessel density in ischemia models and inhibits ulcer formation.

Zhang M, Gao X, Bai SJ, et al. Effect of pioglitazone on expression of hypoxia-inducible factor 1α and vascular endothelial growth factor in ischemic hindlimb of diabetic rats. Eur Rev Med Pharmacol Sci. 2014;18(9):1307-14. PMID: 24867508.

Kemp DE, Schinagle M, Gao K, et al. PPAR-γ agonism as a modulator of mood: proof-of-concept for pioglitazone in bipolar depression. CNS Drugs. 2014 Jun;28(6):571-81. PMID: 24715548.

Paragomi P, Rahimian R, Kazemi MH, et al. Antinociceptive and antidiarrheal effects of pioglitazone in a rat model of diarrhoea-predominant irritable bowel syndrome: role of nitric oxide. Clin Exp Pharmacol Physiol. 2014 Feb;41(2):118-26. PMID: 24471407.

P3461

Pipemidic Acid

10 g
100 g

$C_{14}H_{17}N_5O_3$ FW: 303.32 [51940-44-4] ≥98%

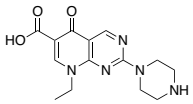

Bacterial DNA gyrase inhibitor and ATP-sensitive K^+ channel blocker. It also stimulates insulin release and may induce cartilage toxicity.

Aubry A, Pan XS, Fisher LM, et al. *Mycobacterium* tuberculosis DNA gyrase: interaction with quinolones and correlation with antimycobacterial drug activity. Antimicrob Agents Chemother. 2004 Apr;48(4):1281-8. PMID: 15047530.

Maeda N, Tamagawa T, Niki I, et al. Increase in insulin release from rat pancreatic islets by quinolone antibiotics. Br J Pharmacol. 1996 Jan;117(2):372-6. PMID: 8789393.

Linseman DA, Hampton LA, Branstetter DG. Quinolone-induced arthropathy in the neonatal mouse. Morphological analysis of articular lesions produced by pipemidic acid and ciprofloxacin. Fundam Appl Toxicol. 1995 Nov;28(1):59-64. PMID: 8566484.

P3462

Piperacillin

1 g
5 g
10 g

CCRIS 7362; EINECS 262-811-8

$C_{23}H_{27}N_5O_7S$ FW: 517.56 [61477-96-1] ≥95%

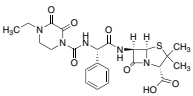

Penicillin binding protein inhibitor that inhibits bacterial cell wall synthesis. It is often co-administered with β-lactamase inhibitors to improve its efficacy.

Fernández-Canigia L, Litterio M, Legaria MC, et al. First national survey of antibiotic susceptibility of the Bacteroides fragilis group: emerging resistance to carbapenems in Argentina. Antimicrob Agents Chemother. 2012 Mar;56(3):1309-14. PMID: 22232282.

Bonfiglio G, Laksai Y, Franceschini N, et al. In vitro activity of piperacillin/tazobactam against 615 *Pseudomonas* aeruginosa strains isolated in intensive care units. Chemotherapy. 1998 Sep-Oct;44(5):305-12. PMID: 9732144.

Kadima TA, Weiner JH. Mechanism of suppression of piperacillin resistance in enterobacteria by tazobactam. Antimicrob Agents Chemother. 1997 Oct;41(10):2177-83. PMID: 9333044.

P3463

Piperacillin Sodium

1 g
5 g
10 g

CL 227193; T-1220

$C_{23}H_{26}N_5O_7SNa$ FW: 539.54 [59703-84-3] ≥89%

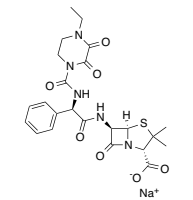

Penicillin binding protein inhibitor that inhibits bacterial cell wall synthesis. It is often co-administered with β-lactamase inhibitors to improve its efficacy.

Fernández-Canigia L, Litterio M, Legaria MC, et al. First national survey of antibiotic susceptibility of the Bacteroides fragilis group: emerging resistance to carbapenems in Argentina. Antimicrob Agents Chemother. 2012 Mar;56(3):1309-14. PMID: 22232282.

Bonfiglio G, Laksai Y, Franceschini N, et al. In vitro activity of piperacillin/tazobactam against 615 *Pseudomonas* aeruginosa strains isolated in intensive care units. Chemotherapy. 1998 Sep-Oct;44(5):305-12. PMID: 9732144.

P3465

Piperine

1 g
5 g

(E,E)-1-Piperoylpiperidine

$C_{17}H_{19}NO_3$ FW: 285.34 [94-62-2] ≥95%

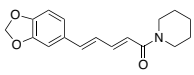

TRPV1 receptor agonist found in black and long peppers. It displays a wide variety of biological activities, including inducing cell cycle arrest and autophagy in prostate cancer cells, decreasing blood glucose levels, improving memory impairment and neurodegeneration, and decreasing levels of pro-inflammatory cytokines.

Ouyang DY, Zeng LH, Pan H, et al. Piperine inhibits the proliferation of human prostate cancer cells via induction of cell cycle arrest and autophagy. Food Chem Toxicol. 2013 Oct;60:424-30. PMID: 23939040.

Kumar S, Sharma S, Vasudeva N. Screening of antidiabetic and antihyperlipidemic potential of oil from Piper longum and piperine with their possible mechanism. Expert Opin Pharmacother. 2013 Sep;14(13):1723-36. PMID: 23875561.

Shrivastava P, Vaibhav K, Tabassum R, et al. Anti-apoptotic and anti-inflammatory effect of Piperine on 6-OHDA induced Parkinson's rat model. J Nutr Biochem. 2013 Apr;24(4):680-7. PMID: 22819561.

P3561

Piperlongumine

25 mg
100 mg
250 mg

$C_{17}H_{19}NO_5$ FW: 317.34 [20069-09-4] ≥98%

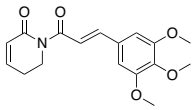

TxA2 antagonist and ubiquitin-proteasome inhibitor found in *Piper longum*. It inhibits platelet aggregation, suppresses PDGFR signaling, decreases invasion and growth of prostate cancer cells, and induces autophagy and cell death in glioblastoma and colon cancer cells.

Ginzburg S, Golovine KV, Makhov PB, et al. Piperlongumine inhibits NF-κB activity and attenuates aggressive growth characteristics of prostate cancer cells. Prostate. 2013 Oct 22. [Epub ahead of print]. PMID: 24151226.

Wang Y, Wang JW, Xiao X, et al. Piperlongumine induces autophagy by targeting p38 signaling. Cell Death Dis. 2013 Oct 3;4:e824. PMID: 24091667.

P3563

Piperlonguminine

10 mg
25 mg
100 mg

$C_{16}H_{19}NO_3$ FW: 273.33 [5950-12-9] ≥99%

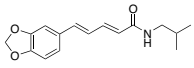

Found in *Piper longum*. It inhibits generation of factor Xa and thrombin to increase bleeding time, decreases total serum cholesterol, increases mRNA levels of adiponectin, GLUT4, FABP aP2, and PPARγ, and prevents growth of *Bacillus*, *Trypanosoma cruzi*, and *Candida*.

Lee W, Yoo H, Ku SK, et al. Anticoagulant activities of piperlonguminine in vitro and in vivo. BMB Rep. 2013 Oct;46(10):484-9. PMID: 24148768.

Ku SK, Kim JA, Bae JS. Piperlonguminine Downregulates Endothelial Protein C Receptor Shedding In Vitro and In Vivo. Inflammation. 2013 Oct 15. [Epub ahead of print]. PMID: 24127121.

Lee W, Yoo H, Kim JA, et al. Barrier protective effects of piperlonguminine in LPS-induced inflammation in vitro and in vivo. Food Chem Toxicol. 2013 Aug;58:149-57. PMID: 23619565.

P3568

Pirarubicin

5 mg
10 mg
25 mg

THP

$C_{32}H_{37}NO_{12}$ FW: 627.64 [72496-41-4] ≥90%

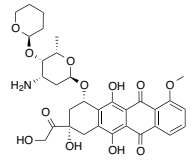

DNA intercalator and inhibitor of topoisomerase II and DNA polymerase. It also induces endothelium-dependent relaxation of aortic tissue.

Hiyama E, Ueda Y, Onitake Y, et al. A cisplatin plus pirarubicin-based JPLT2 chemotherapy for hepatoblastoma: experience and future of the Japanese Study Group for Pediatric Liver Tumor (JPLT). Pediatr Surg Int. 2013 Oct;29(10):1071-5. PMID: 24026876.

Kataoka K, Naomoto Y, Muro M, et al. Antitumor effect of pirarubicin (THP) against human colon cancer transplanted into nude mice and the mechanism of cell cycle progression. Gan To Kagaku Ryoho. 1992 Mar;19(3):367-71. PMID: 1543363.

P3469

Pirfenidone

NEW

10 mg
50 mg
250 mg

$C_{12}H_{11}NO$ FW: 185.22 [53179-13-8] ≥98%

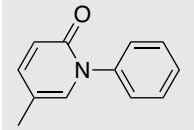

Collagen synthesis inhibitor used to treat pulmonary fibrosis. It decreases fibroblast production, suppresses expression of TNF-α and IL-1β, and inhibits TGF-β-induced collagen production.

Xiang XH, Jiang TP, Zhang S, et al. Pirfenidone inhibits proliferation, arrests the cell cycle, and downregulates heat shock protein 47 and collagen type I in rat hepatic stellate cells in vitro. Mol Med Rep. 2015 Mar 3. [Epub ahead of print]. PMID: 25738437.

Cottin V, Maher T. Long-term clinical and real-world experience with pirfenidone in the treatment of idiopathic pulmonary fibrosis. Eur Respir Rev. 2015 Mar;24(135):58-64. PMID: 25726556.

P3269

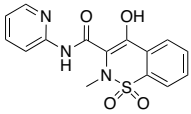

Piroxicam

1 g
5 g
10 g

$C_{15}H_{13}N_3O_4S$ FW: 331.35 [36322-90-4] ≥98%

NSAID and COX-1/2 inhibitor used to treat inflammation and pain. Cu(II) complexes of piroxicam bind GC sequences of DNA. It also inhibits MPP+-induced neurodegeneration and suppresses colorectal cancer development.

Chakraborty S, Bose M, Sarkar M. Spectroscopic studies of the binding of Cu(II) complexes of oxicam NSAIDs to alternating G-C and homopolymeric G-C sequences. Spectrochim Acta A Mol Biomol Spectrosc. 2014 Mar 25;122:690-7. PMID: 24345609.

Barkin RL. Topical Nonsteroidal Anti-Inflammatory Drugs: The Importance of Drug, Delivery, and Therapeutic Outcome. Am J Ther. 2012 Feb 22. [Epub ahead of print]. PMID: 22367354.

Tasaki Y, Yamamoto J, Omura T, et al. Oxicam structure in non-steroidal anti-inflammatory drugs is essential to exhibit Akt-mediated neuroprotection against 1-methyl-4-phenyl pyridinium-induced cytotoxicity. Eur J Pharmacol. 2012 Feb 15;676(1-3):57-63. PMID: 22182582.

P3576

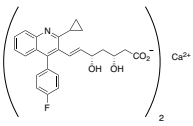

Pitavastatin Calcium

10 mg
25 mg
100 mg

$C_{50}H_{46}F_2N_2O_8Ca$ FW: 880.98 [147526-32-7] ≥98%

HMG-CoA reductase inhibitor used to lower cholesterol and lipid levels. It exhibits many biological activities, including decreasing myocarditis pathology, preventing Th1 and Th17 cell differentiation, improving cardiac allograft rejection, and increasing activity of antioxidative enzymes.

Tajiri K, Shimojo N, Sakai S, et al. Pitavastatin regulates helper T-cell differentiation and ameliorates autoimmune myocarditis in mice. Cardiovasc Drugs Ther. 2013 Oct;27(5):413-24. PMID: 23722419.

Ansari JA, Bhandari U, Haque SE, et al. Enhancement of antioxidant defense mechanism by pitavastatin and rosuvastatin on obesity-induced oxidative stress in Wistar rats. Toxicol Mech Methods. 2012 Jan;22(1):67-73. PMID: 21859367.

P0005

H-His-Ser-Asp-Gly-Ile-Phe-Thr-Asp-Ser-Tyr-Ser-Arg-Tyr-Arg-Lys-Gln-Met-Ala-Val-Lys-Lys-Tyr-Leu-Ala-Ala-Val-Leu-NH_2

Pituitary Adenylate Cyclase-activating Polypeptide (1-27), human, sheep, rat

0.5 mg
1 mg
2.5 mg

PACAP (1-27)

$C_{142}H_{224}N_{40}O_{39}S$ FW: 3147.68 [127317-03-7] ≥95%

Endogenous PAC1 and VPAC1/2 receptor agonist involved in paracrine and autocrine cell signaling. It controls expression of LH and FSH and inhibits apoptosis in cerebellar granule cells.

Nam BH, Moon JY, Kim YO, et al. Structural and functional characterization of pituitary adenylyl cyclase-activating polypeptide (PACAP)/PACAP-related peptide (PRP) and its receptor in olive flounder (Paralichthys olivaceus). Comp Biochem Physiol B Biochem Mol Biol. 2013 Jan;164(1):18-28. PMID: 23026070.

Tam JK, Lee LT, Cheng CH, et al. Discovery of a new reproductive hormone in teleosts: pituitary adenylate cyclase-activating polypeptide-related peptide (PRP). Gen Comp Endocrinol. 2011 Sep 15;173(3):405-10. PMID: 21703272.

P0006

H-His-Ser-Asp-Gly-Ile-Phe-Thr-Asp-Ser-Tyr-Ser-Arg-Tyr-Arg-Lys-Gln-Met-Ala-Val-Lys-Lys-Tyr-Leu-Ala-Ala-Val-Leu-Gly-Lys-Arg-Tyr-Lys-Gln-Arg-Val-Lys-Asn-Lys-NH_2

Pituitary Adenylate Cyclase-activating Polypeptide (1-38), human, sheep, rat

0.5 mg
1 mg
2.5 mg

PACAP (1-38)

$C_{203}H_{331}N_{63}O_{53}S$ FW: 4534.36 [124123-15-5] ≥95%

Endogenous PAC1 and VPAC1/2 receptor agonist involved in paracrine and autocrine cell signaling. It controls expression of LH and FSH and inhibits apoptosis in cerebellar granule cells.

Nam BH, Moon JY, Kim YO, et al. Structural and functional characterization of pituitary adenylyl cyclase-activating polypeptide (PACAP)/PACAP-related peptide (PRP) and its receptor in olive flounder (Paralichthys olivaceus). Comp Biochem Physiol B Biochem Mol Biol. 2013 Jan;164(1):18-28. PMID: 23026070.

Tam JK, Lee LT, Cheng CH, et al. Discovery of a new reproductive hormone in teleosts: pituitary adenylate cyclase-activating polypeptide-related peptide (PRP). Gen Comp Endocrinol. 2011 Sep 15;173(3):405-10. PMID: 21703272.

P0007

H-Phe-Thr-Asp-Ser-Tyr-Ser-Arg-Tyr-Arg-Lys-Gln-Met-Ala-Val-Lys-Lys-Tyr-Leu-Ala-Ala-Val-Leu-NH_2

Pituitary Adenylate Cyclase-activating Polypeptide (6-27), human, sheep, rat

0.5 mg
1 mg
2.5 mg

PACAP (6-27)

$C_{121}H_{193}N_{33}O_{31}S$ FW: 2638.1 ≥95%

Endogenous PAC1 and VPAC1/2 receptor agonist involved in paracrine and autocrine cell signaling. It controls expression of LH and FSH and inhibits apoptosis in cerebellar granule cells.

Nam BH, Moon JY, Kim YO, et al. Structural and functional characterization of pituitary adenylyl cyclase-activating polypeptide (PACAP)/PACAP-related peptide (PRP) and its receptor in olive flounder (Paralichthys olivaceus). Comp Biochem Physiol B Biochem Mol Biol. 2013 Jan;164(1):18-28. PMID: 23026070.

P0008

Phe-Thr-Asp-Ser-Tyr-Ser-Arg-Tyr-Arg-Lys-Gln-Met-Ala-Val-Lys-Lys-Tyr-Leu-Ala-Ala-Val-Leu-Gly-Lys-Arg-Try-Lys-Gln-Arg-Val-Lys-Asn-Lys-NH_2

Pituitary Adenylate Cyclase-activating Polypeptide (6-38), human/sheep/rat

0.5 mg
1 mg
2.5 mg

PACAP

$C_{182}H_{300}N_{56}O_{45}S$ FW: 4024.8 [137061-48-4] ≥95%

Endogenous PAC1 and VPAC1/2 receptor agonist involved in paracrine and autocrine cell signaling. It regulates immune function, controls expression of LH and FSH, and inhibits apoptosis in cerebellar granule cells.

Nam BH, Moon JY, Kim YO, et al. Structural and functional characterization of pituitary adenylyl cyclase-activating polypeptide (PACAP)/PACAP-related peptide (PRP) and its receptor in olive flounder (Paralichthys olivaceus). Comp Biochem Physiol B Biochem Mol Biol. 2013 Jan;164(1):18-28. PMID: 23026070.

P0009

H-His-Ser-Asp-Gly-Ile-Phe-Thr-Asp-Ser-Tyr-Ser-Arg-Tyr-Arg-Lys-Gln-Met-Ala-Val-Lys-Lys-Tyr-Leu-Ala-Ala-Val-Leu-Gly-Lys-Arg-Tyr-Lys-Gln-Arg-Ile-Lys-Asn-Lys-NH_2

Pituitary Adenylate Cyclase-activating Polypeptide (1-38), frog

0.5 mg
1 mg
2.5 mg

PACAP

$C_{204}H_{333}N_{63}O_{53}S$ FW: 4548.38 ≥95%

Endogenous PAC1 and VPAC1/2 receptor agonist involved in paracrine and autocrine cell signaling. It controls expression of LH and FSH and inhibits apoptosis in cerebellar granule cells.

Nam BH, Moon JY, Kim YO, et al. Structural and functional characterization of pituitary adenylyl cyclase-activating polypeptide (PACAP)/PACAP-related peptide (PRP) and its receptor in olive flounder (Paralichthys olivaceus). Comp Biochem Physiol B Biochem Mol Biol. 2013 Jan;164(1):18-28. PMID: 23026070.

P0010

H-Asp-Val-Ala-His-Gly-Ile-Leu-Asn-Glu-Ala-Tyr-Arg-Lys-Val-Leu-Asp-Gln-Leu-Ser-Ala-Gly-Lys-His-Leu-Gln-Ser-Leu-Val-Ala-OH

Pituitary Adenylate Cyclase-activating Polypeptide-related Peptide, human

0.5 mg
1 mg
2.5 mg

PACAP-related peptide; PRP

$C_{139}H_{229}N_{41}O_{42}$ FW: 3146.62 ≥95%

PAC1 and VPAC1/2 receptor agonist involved in paracrine and autocrine cell signaling. It controls expression of LH and FSH.

Nam BH, Moon JY, Kim YO, et al. Structural and functional characterization of pituitary adenylyl cyclase-activating polypeptide (PACAP)/PACAP-related peptide (PRP) and its receptor in olive flounder (Paralichthys olivaceus). Comp Biochem Physiol B Biochem Mol Biol. 2013 Jan;164(1):18-28. PMID: 23026070.

P0011

H-Asp-Val-Ala-His-Glu-Ile-Leu-Asn-Glu-Ala-Tyr-Arg-Lys-Val-Leu-Asp-Gln-Leu-Ser-Ala-Arg-Lys-Tyr-Leu-Gln-Ser-Met-Val-Ala-OH

Pituitary Adenylate Cyclase-activating Polypeptide-related Peptide, rat

0.5 mg
1 mg
2.5 mg

PACAP-related peptide; PRP

$C_{148}H_{242}N_{42}O_{45}S$ FW: 3361.9 ≥95%

PAC1 and VPAC1/2 receptor agonist involved in paracrine and autocrine cell signaling. It controls expression of LH and FSH.

Nam BH, Moon JY, Kim YO, et al. Structural and functional characterization of pituitary adenylyl cyclase-activating polypeptide (PACAP)/PACAP-related peptide (PRP) and its receptor in olive flounder (Paralichthys olivaceus). Comp Biochem Physiol B Biochem Mol Biol. 2013 Jan;164(1):18-28. PMID: 23026070.

P3592

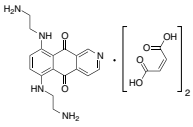

Pixantrone Dimaleate

10 mg
25 mg
100 mg

BBR2778

$C_{17}H_{19}N_5O_2 \bullet (C_4H_4O_4)_2$ FW: 557.51 [144675-97-8] ≥98%

DNA intercalator and topoisomerase II inhibitor. It inhibits proliferation of T cells without affecting differentiation of dendritic cells or B cells, prevents amyloid-β oligomerization, and prevents the development of EAE.

Péan E, Flores B, Hudson I, et al. The European Medicines Agency review of pixantrone for the treatment of adult patients with multiply relapsed or refractory aggressive non-Hodgkin's B-cell lymphomas: summary of the scientific assessment of the committee for medicinal products for human use. Oncologist. 2013;18(5):625-33. PMID: 23615696.

Marolda R, Ruocco C, Cordiglieri C, et al. Differential targeting of immune-cells by Pixantrone in experimental myasthenia gravis. J Neuroimmunol. 2013 May 15;258(1-2):41-50. PMID: 23523328.

P3597

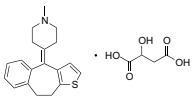

Pizotyline Malate

1 g
5 g
10 g

BC105

$C_{19}H_{21}NS \bullet C_4H_6O_5$ FW: 429.54 [5189-11-7] ≥98%

5-HT1A receptor partial agonist and 5-HT2C receptor antagonist used to treat migraines. It also inhibits drug-induced lever press responding in drug discrimination models.

Young R, Khorana N, Bondareva T, et al. Pizotyline effectively attenuates the stimulus effects of N-methyl-3,4-methylenedioxyamphetamine (MDMA). Pharmacol Biochem Behav. 2005 Oct;82(2):404-10. PMID: 16253319.

Strachan AT, Leiper JB, Maughan RJ. Serotonin2C receptor blockade and thermoregulation during exercise in the heat. Med Sci Sports Exerc. 2005 Mar;37(3):389-94. PMID: 15741836.

P3600 PJ34 Hydrochloride

NEW

1 mg
5 mg
25 mg

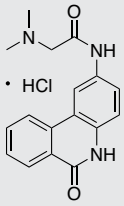

$C_{17}H_{17}N_3O_2 \cdot HCl$ FW: 331.8 [344458-15-7] ≥95%

PARP inhibitor and potential Pim1 inhibitor. It protects against stroke-related ischemic brain injury, decreases infarct size in myocardial infarction models, induces apoptosis in islet-infiltrating leukocytes, and stimulates Th2-mediated immune responses.

Antolín AA, Jalencas X, Yélamos J, et al. Identification of pim kinases as novel targets for PJ34 with confounding effects in PARP biology. ACS Chem Biol. 2012 Dec 21;7(12):1962-7. PMID: 23025350.

Gangopadhyay NN, Luketich JD, Opest A, et al. Inhibition of poly(ADP-ribose) polymerase (PARP) induces apoptosis in lung cancer cell lines. Cancer Invest. 2011 Nov;29(9):608-16. PMID: 22011283.

Madison DL, Stauffer D, Lundblad JR. The PARP inhibitor PJ34 causes a PARP1-independent, p21 dependent mitotic arrest. DNA Repair (Amst). 2011 Oct 10;10(10):1003-13. PMID: 21840268.

P4008 PKC412

1 mg
5 mg

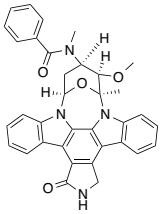

Midostaurin; 4'-N-Benzoyl staurosporine

$C_{35}H_{30}N_4O_4$ FW: 570.64 [120685-11-2] ≥98%

Staurosporine derivative ad inhibitor of PKC and FLT3. It induces apoptosis in keloid-derived fibroblasts and melanoma cells, alters differentiation patterns of dendritic cells, and inhibits metastasis and platelet-aggregating activity.

Fischer T, Stone RM, Deangelo DJ, et al. Phase IIB trial of oral Midostaurin (PKC412), the FMS-like tyrosine kinase 3 receptor (FLT3) and multi-targeted kinase inhibitor, in patients with acute myeloid leukemia and high-risk myelodysplastic syndrome with either wild-type or mutated FLT3. J Clin Oncol. 2010 Oct 1;28(28):4339-45. PMID: 20733134.

Huang YC, Shieh HR, Chen YJ. Midostaurin (PKC412) modulates differentiation and maturation of human myeloid dendritic cells. Toxicol In Vitro. 2010 Sep;24(6):1705-10. PMID: 20685248.

Stölzel F, Steudel C, Oelschlägel U, et al. Mechanisms of resistance against PKC412 in resistant FLT3-ITD positive human acute myeloid leukemia cells. Ann Hematol. 2010 Jul;89(7):653-62. PMID: 20119833.

P4132 PKI-402

NEW

1 mg
5 mg
10 mg

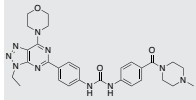

$C_{29}H_{34}N_{10}O_3$ FW: 570.65 [1173204-81-3] ≥98%

Inhibitor of p110α PI3K and mTOR. It inhibits cell proliferation and tumor growth in models of breast cancer, glioma, and pancreatic cancer.

Mallon R, Hollander I, Feldberg L, et al. Antitumor efficacy profile of PKI-402, a dual phosphatidylinositol 3-kinase/mammalian target of rapamycin inhibitor. Mol Cancer Ther. 2010 Apr;9(4):976-84. PMID: 20371716.

Dehnhardt CM, Venkatesan AM, Delos Santos E, et al. Lead optimization of N-3-substituted 7-morpholinotriazol-opyrimidines as dual phosphoinositide 3-kinase/mammalian target of rapamycin inhibitors: discovery of PKI-402. J Med Chem. 2010 Jan 28;53(2):798-810. PMID: 19968288.

P4403 Plasminogen Activator Inhibitor 1

0.5 mg
1 mg
2.5 mg

PAI-1

H-Ala-Arg-Met-Ala-Pro-Glu-OH

$C_{27}H_{47}N_9O_9S$ FW: 673.79 ≥95%

Endogenous protease inhibitor produced by activation of PAR1. It increases cell proliferation and tumor size of HeLa xenografts, promotes proliferation of pulmonary fibroblasts, enhances synthesis of collagen, and inhibits apoptosis.

Gomes Giacoia E, Miyake M, Lawton A, et al. PAI-1 Leads to G1-phase Cell Cycle Progression through Cyclin D3/CDK4/6 Up-regulation. Mol Cancer Res. 2014 Jan 24. [Epub ahead of print]. PMID: 24464915.

Tamura Y, Kawao N, Okada K, et al. Plasminogen activator inhibitor-1 is involved in streptozotocin-induced bone loss in female mice. Diabetes. 2013 Sep;62(9):3170-9. PMID: 23715621.

P4780 Plumbagin

100 mg
250 mg
1 g

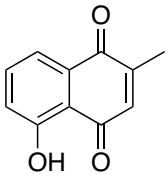

$C_{11}H_8O_3$ FW: 188.18 [481-42-5] ≥98%

Found in *Plumbago*. It exhibits a wide variety of biological properties, including decreasing levels of pro-inflammatory cytokines in ulcerative colitis models, inhibiting FtsZ assembly and GTPase activity, and suppressing TGF-β1-induced fibronectin and collagen IV expression.

Sagar S, Esau L, Moosa B, et al. Cytotoxicity and Apoptosis Induced by a Plumbagin Derivative in Estrogen Positive MCF-7 Breast Cancer Cells. Anticancer Agents Med Chem. 2013 Oct 21. [Epub ahead of print]. PMID: 24164046.

Yong R, Chen XM, Shen S, et al. Plumbagin ameliorates diabetic nephropathy via interruption of pathways that include NOX4 signalling. PLoS One. 2013 Aug 26;8(8):e73428. PMID: 23991195.

Qiu JX, He YQ, Wang Y, et al. Plumbagin induces the apoptosis of human tongue carcinoma cells through the mitochondria-mediated pathway. Med Sci Monit Basic Res. 2013 Aug 28;19:228-36. PMID: 23982457.

P4782

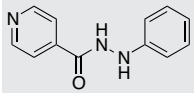

PluriSln 1

NEW

NSC 14613

$C_{12}H_{11}N_3O$ FW: 213.24 [91396-88-2] ≥98%

5 mg
10 mg
25 mg
50 mg

Pluripotent cell-specific inhibitor of stearoyl-coA desaturase 1. It prevents undifferentiated cells from developing into tumors.

Zhang L, Pan Y, Qin G, et al. Inhibition of stearoyl-coA desaturase selectively eliminates tumorigenic Nanog-positive cells: improving the safety of iPS cell transplantation to myocardium. Cell Cycle. 2014;13(5):762-71. PMID: 24394703.

Ben-David U, Gan QF, Golan-Lev T, et al. Selective elimination of human pluripotent stem cells by an oleate synthesis inhibitor discovered in a high-throughput screen. Cell Stem Cell. 2013 Feb 7;12(2):167-79. PMID: 23318055.

P4492

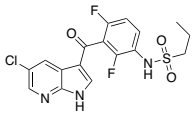

PLX4720

$C_{17}H_{14}ClF_2N_3O_3S$ FW: 413.83 [918505-84-7] ≥98%

5 mg
25 mg

Mutant V600E B-Raf inhibitor and vemurafenib analog. It induces apoptosis and autophagy in melanoma cells, enhances surface expression of tumor-associated antigens on tumor cells, and downregulates expression of pro-angiogenic proteins.

Liu C, Peng W, Xu C, et al. BRAF inhibition increases tumor infiltration by T cells and enhances the antitumor activity of adoptive immunotherapy in mice. Clin Cancer Res. 2013 Jan 15;19(2):393-403. PMID: 23204132.

Bottos A, Martini M, Di Nicolantonio F, et al. Targeting oncogenic serine/threonine-protein kinase BRAF in cancer cells inhibits angiogenesis and abrogates hypoxia. Proc Natl Acad Sci U S A. 2012 Feb 7;109(6):E353-9. PMID: 22203991.

P5712

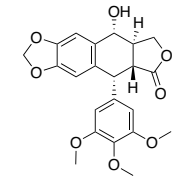

Podophyllotoxin

Podofilox

$C_{22}H_{22}O_8$ FW: 414.41 [518-28-5] ≥90%

50 mg
100 mg
500 mg

HPV E2 protein inhibitor found in *Podophyllum*. It binds tubulin, inhibiting mitotic spindle formation. It induces cell cycle arrest and apoptosis in gastric cancer cells and inhibits reproduction of human papilloma virus.

Ji CF, Ji YB. Apoptosis of human gastric cancer SGC-7901 cells induced by podophyllotoxin. Exp Ther Med. 2014 May;7(5):1317-1322. PMID: 24940431.

Ramírez-Fort MK, Au SC, Javed SA, et al. Management of cutaneous human papillomavirus infection: pharmacotherapies. Curr Probl Dermatol. 2014;45:175-85. PMID: 24643186.

P5845

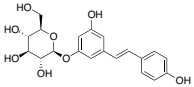

Polydatin

Resveratrol 3-β-mono-D-glucoside

$C_{20}H_{22}O_8$ FW: 390.38 [65914-17-2] ≥97%

250 mg
1 g

Found in *Polygonum*. It induces cell cycle arrest and apoptosis in lung cancer cells, decreases sepsis-induced mortality and lung injury, and suppresses mast cell degranulation.

Zhang Y, Zhuang Z, Meng Q, et al. Polydatin inhibits growth of lung cancer cells by inducing apoptosis and causing cell cycle arrest. Oncol Lett. 2014 Jan;7(1):295-301. PMID: 24348867.

Yang B, Li JJ, Cao JJ, et al. Polydatin attenuated food allergy via store-operated calcium channels in mast cell. World J Gastroenterol. 2013 Jul 7;19(25):3980-9. PMID: 23840142.

P5745

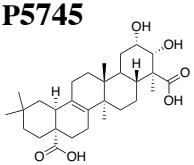

Polygalic Acid

$C_{29}H_{44}O_6$ FW: 488.66 ≥97%

5 mg
10 mg
25 mg

Senegenin derivative found in *Polygala*.

Ling Y, Wu B, Wang K, et al. In vivo metabolism study of polygalic acid in rat using HPLC-ESI-MSn. Biomed Chromatogr. 2012 Feb;26(2):220-4. PMID: 21618563.

P5747

Polymyxin B sulfate

$C_{56}H_{100}N_{16}O_{17}S$ [1405-20-5]

250 mg
1 g
5 g

Mixture of polymyxin B1, B2, B3 and B1-1 sulfates. It inhibits oxidative phosphorylation in gram negative bacteria by preventing type II NADH-quinone oxidoreductase activity. It also induces aggregation of LPS in cell membranes, causing leakage of cellular components.

Deris ZZ, Akter J, Sivanesan S, et al. A secondary mode of action of polymyxins against Gram-negative bacteria involves the inhibition of NADH-quinone oxidoreductase activity. J Antibiot (Tokyo). 2013 Oct 30. [Epub ahead of print]. PMID: 24169795.

Zhai B, Lin X. Evaluation of the anticryptococcal activity of the antibiotic polymyxin B in vitro and in vivo. Int J Antimicrob Agents. 2013 Mar;41(3):250-4. PMID: 23313397

P5878

Potassium Canrenoate

1 g
5 g
25 g

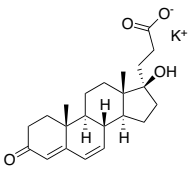

$C_{22}H_{29}KO_4$ FW: 396.56 [2181-04-6] ≥98%

Mineralocorticoid receptor antagonist used as a diuretic. It decreases infarct size in cardiac ischemia/reperfusion models, improves high salt diet-induced renal dysfunction, and displays negative inotropic activity.

Schmidt K, Tissier R, Ghaleb B, et al. Cardioprotective effects of mineralocorticoid receptor antagonists at reperfusion. Eur Heart J. 2010 Jul;31(13):1655-62. PMID: 20028693.

Rugale C, Cordaillat M, Mimran A, et al. Time-course reduction of renal function in rats on high sodium intake: acute reversal by potassium canrenoate. Clin Exp Pharmacol Physiol. 2008 Apr;35(4):412-5. PMID: 18307731.

P5885

Povidone Iodine

50 g
100 g

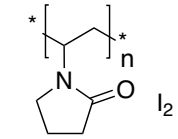

$C_6H_9I_2NO$ FW: 364.94 [25655-41-8] ≥98%

Polyvinyl pyrrolidone polymer used as a disinfectant. It induces necrotic cell death in mesothelioma cells and may induce depurination and DNA cleavage.

Fiorelli A, Pentimalli F, D'Urso V, et al. Antineoplastic activity of povidone-iodine on different mesothelioma cell lines: results of in vitro study. Eur J Cardiothorac Surg. 2014 Jun;45(6):993-1000. PMID: 24394552.

Song M, Zeng L, Hong X, et al. Polyvinyl pyrrolidone promotes DNA cleavage by a ROS-independent and depurination mechanism. Environ Sci Technol. 2013 Mar 19;47(6):2886-91. PMID: 23425130.

Haznar-Garbacz D, Garbacz G, Eisenächer F, et al. A novel liquefied gas based oral controlled release drug delivery system for liquid drug formulations. Eur J Pharm Biopharm. 2012 Jun;81(2):334-8. PMID: 22426133.

P6002

PP-121

NEW

1 mg
5 mg
10 mg

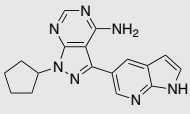

$C_{17}H_{17}N_7$ FW: 319.36 [1092788-83-4] ≥98%

Inhibitor of p110α PI3K, DNA-PK, mTOR, Abl, Hck, Src, VEGFR2, and PDGFR. It suppresses proliferation of cancer cells.

Apsel B, Blair JA, Gonzalez B, et al. Targeted polypharmacology: discovery of dual inhibitors of tyrosine and phosphoinositide kinases. Nat Chem Biol. 2008 Nov;4(11):691-9. PMID: 18849971.

P6232

PP-1

5 mg
25 mg

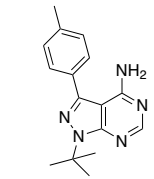

$C_{16}H_{19}N_5$ FW: 281.36 [172889-26-8] ≥98%

Src inhibitor. It suppresses H_2O_2-induced production of MIF, increases connexin-43 levels and gap junction communication, and decreases ventricular tachycardia and sudden death in arrhythmia models.

Rao F, Deng CY, Zhang QH, et al. Involvement of Src tyrosine kinase and protein kinase C in the expression of macrophage migration inhibitory factor induced by H_2O_2 in HL-1 mouse cardiac muscle cells. Braz J Med Biol Res. 2013 Sep;46(9):746-51. PMID: 24036910.

Sovari AA, Iravanian S, Dolmatova E, et al. Inhibition of c-Src tyrosine kinase prevents angiotensin II-mediated connexin-43 remodeling and sudden cardiac death. J Am Coll Cardiol. 2011 Nov 22;58(22):2332-9. PMID: 22093512.

P6004

PP-242

NEW

5 mg
10 mg
25 mg

Torkinib

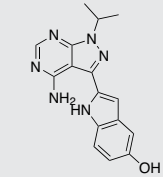

$C_{16}H_{16}N_6O$ FW: 308.34 [1092351-67-1] ≥98%

mTOR inhibitor. It induces apoptosis and alters the Bcl-2/Bax ratio in models of pheochromocytoma and inhibits cell proliferation, migration, and invasion in gastric cancer cells.

Shi F, Yang X, Gong Y, et al. The antileukemia roles of PP242 alone or in combination with daunorubicin in acute leukemia. Anticancer Drugs. 2015 Apr;26(4):410-21. PMID: 25535978.

Zhang X, Wang X, Qin L, et al. The dual mTORC1 and mTORC2 inhibitor PP242 shows strong antitumor activity in a pheochromocytoma PC12 cell tumor model. Urology. 2015 Jan;85(1):273.e1-7. PMID: 25440763.

Xing X, Zhang L, Wen X, et al. PP242 suppresses cell proliferation, metastasis, and angiogenesis of gastric cancer through inhibition of the PI3K/AKT/mTOR pathway. Anticancer Drugs. 2014 Nov;25(10):1129-40. PMID: 25035961.

P6264

PPQ-102

NEW

5 mg
10 mg
25 mg

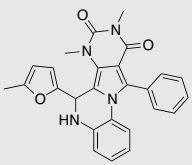

$C_{26}H_{22}N_4O_3$ FW: 438.49 [931706-15-9] ≥98%

CFTR channel blocker. It decreases the size of pre-formed kidney cysts in animal models of polycystic kidney disease.

Snyder DS, Tradtrantip L, Yao C, et al. Potent, metabolically stable benzopyrimido-pyrrolo-oxazine-dione (BPO) CFTR inhibitors for polycystic kidney disease. J Med Chem. 2011 Aug 11;54(15):5468-77. PMID: 21707078.

Tradtrantip L, Sonawane ND, Namkung W, et al. Nanomolar potency pyrimido-pyrrolo-quinoxalinedione CFTR inhibitor reduces cyst size in a polycystic kidney disease model. J Med Chem. 2009 Oct 22;52(20):6447-55. PMID: 19785436.

P7000

PR-619

NEW

1 mg
5 mg
25 mg

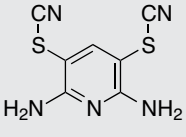

$C_7H_5N_5S_2$ FW: 223.27 [2645-32-1] ≥98%

Deubiquitinating enzyme inhibitor. It inhibits pro-inflammatory cytokine secretion, activates autophagy, and induces cellular stress responses.

Zhou Y, Zhao D, Yue R, et al. Inflammasomes-dependent regulation of IL-1β secretion induced by the virulent *Mycobacterium* bovis Beijing strain in THP-1 macrophages. Antonie Van Leeuwenhoek. 2015 Jul;108(1):163-71. PMID: 25980833.

Seiberlich V, Borchert J, Zhukareva V, et al. Inhibition of protein deubiquitination by PR-619 activates the autophagic pathway in OLN-t40 oligodendroglial cells. Cell Biochem Biophys. 2013 Sep;67(1):149-60. PMID: 23686611.

Seiberlich V, Goldbaum O, Zhukareva V, et al. The small molecule inhibitor PR-619 of deubiquitinating enzymes affects the microtubule network and causes protein aggregate formation in neural cells: implications for neurodegenerative diseases. Biochim Biophys Acta. 2012 Nov;1823(11):2057-68. PMID: 22565157.

P6901

Pramipexole Dihydrochloride

10 mg
25 mg
100 mg

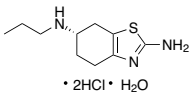

• 2HCl • H_2O

$C_{10}H_{17}N_3S$ • 2HCl • H_2O FW: 302.26 [191217-81-9] ≥98%

Dopamine D2/3 receptor agonist used to treat Parkinson's disease. It decreases immobility time in the forced swim test and inhibits phosphorylation of α-synuclein.

Chau KY, Cooper JM, Schapira AH. Pramipexole reduces phosphorylation of α-synuclein at serine-129. J Mol Neurosci. 2013 Oct;51(2):573-80. PMID: 23681749.

Kitagawa K, Kitamura Y, Miyazaki T, et al. Effects of pramipexole on the duration of immobility during the forced swim test in normal and ACTH-treated rats. Naunyn Schmiedebergs Arch Pharmacol. 2009 Jul;380(1):59-66. PMID: 19274453.

Iravani MM, Sadeghian M, Leung CC, et al. Continuous subcutaneous infusion of pramipexole protects against lipopolysaccharide-induced dopaminergic cell death without affecting the inflammatory response. Exp Neurol. 2008 Aug;212(2):522-31. PMID: 18571649.

P6802

Pranoprofen

100 mg
250 mg
1 g

Y-8004

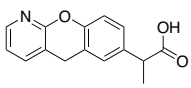

$C_{15}H_{13}NO_3$ FW: 255.27 [52549-17-4] ≥98%

NSAID and COX-1/2 inhibitor used to treat dry eye. It inhibits production of sodium urate-induced superoxide, prostaglandin E2, and β-glucuronidase.

Chen J, Dong F, Chen W, et al. Clinical efficacy of 0.1% pranoprofen in treatment of dry eye patients: a multicenter, randomized, controlled clinical trial. Chin Med J (Engl). 2014 Jul;127(13):2407-12. PMID: 24985574.

Aratani H, Iwahisa Y, Imayoshi T, et al. Mechanism of the inhibitory effect of pranoprofen on sodium urate crystal-induced inflammation. Nihon Yakurigaku Zasshi. 1987 Mar;89(3):139-44. PMID: 3556352.

P6903

Prasugrel

100 mg
250 mg
1 g

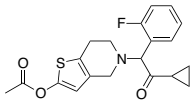

$C_{20}H_{20}FNO_3S$ FW: 373.44 [150322-43-3] ≥98%

P2Y12 receptor antagonist used to decrease potential ischemic events. It inhibits platelet aggregation.

Secco GG, Parisi R, Mirabella F, et al. P2Y12 inhibitors: pharmacologic mechanism and clinical relevance. Cardiovasc Hematol Agents Med Chem. 2013 Jun;11(2):101-5. PMID: 22963529

Hagihara K, Kazui M, Kurihara A, et al. Biotransformation of prasugrel, a novel thienopyridine antiplatelet agent, to the pharmacologically active metabolite. Drug Metab Dispos. 2010 Jun;38(6):898-904. PMID: 20228231.

Scott DM, Norwood RM, Parra D. P2Y12 inhibitors in cardiovascular disease: focus on prasugrel. Ann Pharmacother. 2009 Jan;43(1):64-76. PMID: 19050170.

P6800

Pravastatin Lactone

10 mg
50 mg
100 mg

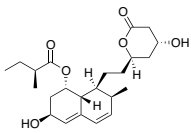

$C_{23}H_{34}O_6$ FW: 406.51 [85956-22-5] ≥92%

HMG-CoA reductase inhibitor used to lower cholesterol and lipid levels. It also inhibits angiogenesis and metastasis in cancer models, prevents thrombosis in animal models of atherosclerotic plaque rupture, and suppresses airway inflammation in models of OVA-induced allergies.

Lee SJ, Lee I, Lee J, et al. Statins, 3-hydroxy-3-methylglutaryl coenzyme A reductase inhibitors, potentiate the anti-angiogenic effects of bevacizumab by suppressing angiopoietin2, BiP, and Hsp90α in human colorectal cancer. Br J Cancer. 2014 Jun 19. [Epub ahead of print]. PMID: 24945998.

Wu G, Xie Q, Xu L, et al. Pravastatin inhibits plaque rupture and subsequent thrombus formation in atherosclerotic rabbits with hyperlipidemia. Chem Pharm Bull (Tokyo). 2013;61(2):121-4. PMID: 23207681.

Luzak B, Rywaniak J, Stanczyk L, et al. Pravastatin and simvastatin improves acetylsalicylic acid-mediated in vitro blood platelet inhibition. Eur J Clin Invest. 2012 Aug;42(8):864-72. PMID: 22409214.

P6801 Pravastatin Sodium

10 mg
50 mg
100 mg

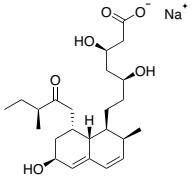

$C_{23}H_{35}O_7Na$ FW: 446.51 [81131-70-6] ≥98%

HMG-CoA reductase inhibitor used to lower cholesterol and lipid levels. It also inhibits angiogenesis and metastasis in cancer models, prevents thrombosis in atherosclerotic plaque rupture, and suppresses OVA-induced airway inflammation.

Lee SJ, Lee I, Lee J, et al. Statins, 3-hydroxy-3-methylglutaryl coenzyme A reductase inhibitors, potentiate the anti-angiogenic effects of bevacizumab by suppressing angiopoietin2, BiP, and Hsp90α in human colorectal cancer. Br J Cancer. 2014 Jun 19. [Epub ahead of print]. PMID: 24945998.

Wu G, Xie Q, Xu L, et al. Pravastatin inhibits plaque rupture and subsequent thrombus formation in atherosclerotic rabbits with hyperlipidemia. Chem Pharm Bull (Tokyo). 2013;61(2):121-4. PMID: 23207681.

P7103 Praziquantel

1 g
5 g
25 g

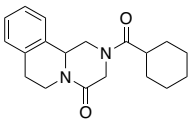

$C_{19}H_{24}N_2O_2$ FW: 312.41 [55268-74-1] ≥98%

Potential adenosine receptor antagonist and voltage-gated Ca^{2+} channel blocker that alters membrane permeability and Ca^{2+} signaling used to treat schistosomiasis. It induces neuromuscular paralysis in parasites.

Cioli D, Pica-Mattoccia L, Basso A, et al. Schistosomiasis control: praziquantel forever? Mol Biochem Parasitol. 2014 Jun 21;195(1):23-29. PMID: 24955523.

Chan JD, Zarowiecki M, Marchant JS. Ca^{2+} channels and praziquantel: a view from the free world. Parasitol Int. 2013 Dec;62(6):619-28. PMID: 23246536.

Crosby A, Jones FM, Kolosionek E, et al. Praziquantel reverses pulmonary hypertension and vascular remodeling in murine schistosomiasis. Am J Respir Crit Care Med. 2011 Aug 15;184(4):467-73. PMID: 21659614.

P6818 Prednisolone

1 g
5 g
10 g

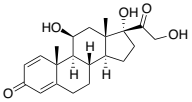

$C_{21}H_{28}O_5$ FW: 360.44 [50-24-8] ≥98%

Cortisol derivative and glucocorticoid receptor agonist used to treat inflammation and autoimmune disorders. It decreases lymphocyte apoptosis in mononuclear cells and delays the progression of Duchenne muscular dystrophy.

Frisullo G, Nociti V, Iorio R, et al. Glucocorticoid treatment reduces T-bet and pSTAT1 expression in mononuclear cells from relapsing remitting multiple sclerosis patients. Clin Immunol. 2007 Sep;124(3):284-93. PMID: 17627892.

Fisher I, Abraham D, Bouri K, et al. Prednisolone-induced changes in dystrophic skeletal muscle. FASEB J. 2005 May;19(7):834-6. Erratum in: FASEB J. 2005 May;19(7):1 p following 836. Hoffmann, Eric P [corrected to Hoffman, Eric P]. PMID: 15734791.

P7012 Prednisolone Sodium Phosphate

5 g
10 g
25 g

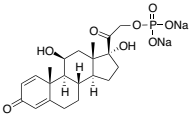

$C_{21}H_{27}Na_2O_8P$ FW: 484.39 [125-02-0] ≥98%

Cortisol derivative and glucocorticoid receptor agonist used to treat inflammation and autoimmune disorders. It decreases lymphocyte apoptosis in mononuclear cells and delays the progression of Duchenne muscular dystrophy.

Frisullo G, Nociti V, Iorio R, et al. Glucocorticoid treatment reduces T-bet and pSTAT1 expression in mononuclear cells from relapsing remitting multiple sclerosis patients. Clin Immunol. 2007 Sep;124(3):284-93. PMID: 17627892.

Fisher I, Abraham D, Bouri K, et al. Prednisolone-induced changes in dystrophic skeletal muscle. FASEB J. 2005 May;19(7):834-6. Erratum in: FASEB J. 2005 May;19(7):1 p following 836. Hoffmann, Eric P [corrected to Hoffman, Eric P]. PMID: 15734791.

P7020 Prednisone

1 g
5 g
25 g

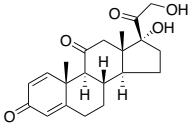

$C_{21}H_{26}O_5$ FW: 358.43 [53-03-2] ≥98%

Synthetic prednisolone prodrug and glucocorticoid receptor agonist used to treat rheumatoid arthritis, lymphomas, and leukemias. It also suppresses neuronal apoptosis and inhibits expression of IL-6.

Hoy SM. Bendamustine: a review of its use in the management of chronic lymphocytic leukaemia, rituximab-refractory indolent non-Hodgkin's lymphoma and multiple myeloma. Drugs. 2012 Oct 1;72(14):1929-50. PMID: 22950536.

Clarke L, Kirwan J. Efficacy, safety and mechanism of action of modified-release prednisone in rheumatoid arthritis. Ther Adv Musculoskelet Dis. 2012 Jun;4(3):159-66. PMID: 22850902.

He Z, Ostrowski RP, Sun X, et al. CHOP silencing reduces acute brain injury in the rat model of subarachnoid hemorrhage. Stroke. 2012 Feb;43(2):484-90. PMID: 22180248.

P7021

Prednisone Acetate

1 g
5 g
25 g

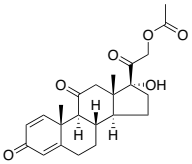

$C_{23}H_{28}O_6$ FW: 400.46 [125-10-0] ≥98%

Synthetic prednisolone prodrug and glucocorticoid receptor agonist used to treat rheumatoid arthritis, lymphomas, and leukemias. It also suppresses neuronal apoptosis and inhibits expression of IL-6.

Hoy SM. Bendamustine: a review of its use in the management of chronic lymphocytic leukaemia, rituximab-refractory indolent non-Hodgkin's lymphoma and multiple myeloma. Drugs. 2012 Oct 1;72(14):1929-50. PMID: 22950536.

Clarke L, Kirwan J. Efficacy, safety and mechanism of action of modified-release prednisone in rheumatoid arthritis. Ther Adv Musculoskelet Dis. 2012 Jun;4(3):159-66. PMID: 22850902.

He Z, Ostrowski RP, Sun X, et al. CHOP silencing reduces acute brain injury in the rat model of subarachnoid hemorrhage. Stroke. 2012 Feb;43(2):484-90. PMID: 22180248.

P7022

Pressinoic Acid

1 mg
2 mg
5 mg

Cys-Tyr-Phe-Gln-Asn-Cys
(Disulfide bridge Cys1-Cys6)

$C_{33}H_{42}N_8O_{10}S_2$ FW: 774.08 [35748-51-7] ≥95%

N-terminal vasopressin analog and arginine vasopressin receptor agonist. It displays no pressor activity but can replace IL-2 or helper cells necessary for IFN-γ production by lymphocytes.

Torres BA, Johnson HM. Arginine vasopressin (AVP) replacement of helper cell requirement in IFN-gamma production. Evidence for a novel AVP receptor on mouse lymphocytes. J Immunol. 1988 Apr 1;140(7):2179-83. PMID: 2965181.

P7033

Primaquine Phosphate

5 g
10 g
50 g

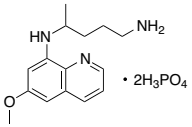

$C_{15}H_{21}N_3O \cdot 2H_3PO_4$ FW: 455.29 [63-45-6] ≥98%

Malaria treatment that alters membrane permeability and prevents transport vesicle formation in parasites.

Basso LG, Rodrigues RZ, Naal RM, et al. Effects of the antimalarial drug primaquine on the dynamic structure of lipid model membranes. Biochim Biophys Acta. 2011 Jan;1808(1):55-64. PMID: 20713019.

Hiebsch RR, Raub TJ, Wattenberg BW. Primaquine blocks transport by inhibiting the formation of functional transport vesicles. Studies in a cell-free assay of protein transport through the Golgi apparatus. J Biol Chem. 1991 Oct 25;266(30):20323-8. PMID: 1657920.

P7034

Prion Peptide (106-126), human

1 mg
2 mg
5 mg

H-Lys-Thr-Asn-Met-Lys-His-Met-Ala-Gly-Ala-Ala-Ala-Ala-Gly-Ala-Val-Val-Gly-Gly-Leu-Gly-OH

$C_{80}H_{128}N_{26}O_{34}S_2$ FW: 1912.28 [148439-49-0] ≥95%

Synthetic prion protein fragment and p75 NTR agonist forms amyloid-like fibrils and upregulates expression of IL-1β, TNF-α, and MMPs in astrocytes and microglia. It also causes oxidative stress and neuronal injury.

Song K, Na JY, Oh MH, et al. Synthetic prion Peptide 106-126 resulted in an increase matrix metalloproteinases and inflammatory cytokines from rat astrocytes and microglial cells. Toxicol Res. 2012 Mar;28(1):5-9. PMID: 24278583.

Pietri M, Caprini A, Mouillet-Richard S, et al. Overstimulation of PrPC signaling pathways by prion peptide 106-126 causes oxidative injury of bioaminergic neuronal cells. J Biol Chem. 2006 Sep 22;281(38):28470-9. PMID: 16864581.

P6858

Procarbazine Hydrochloride

100 mg
500 mg
1 g

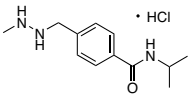

$C_{12}H_{19}N_3O \cdot HCl$ FW: 257.76 [366-70-1] ≥97%

DNA alkylator and MAO inhibitor used to treat Hodgkin's lymphoma and brain cancers. It induces double-stranded DNA breakage and causes oxidative damage.

Ogawa K, Hiraku Y, Oikawa S, et al. Molecular mechanisms of DNA damage induced by procarbazine in the presence of Cu(II). Mutat Res. 2003 Aug 5;539(1-2):145-55. PMID: 12948823.

P7056

Procaterol Hydrochloride

10 mg
25 mg
100 mg

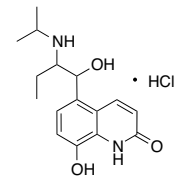

$C_{16}H_{22}N_2O_3 \cdot HCl$ FW: 326.82 [62929-91-3] ≥98%

β2-Adrenergic receptor agonist used to treat asthma. It inhibits release of RANTES, GM-CSF, and IL-8 in bronchial epithelial cells and prevents adhesion of eosinophils to fibroblasts.

Bao W, Chen Q, Lin Y, et al. Efficacy of procaterol combined with inhaled budesonide for treatment of cough-variant asthma. Respirology. 2013 Nov;18 Suppl 3:53-61. PMID: 24188204.

Yoshida N, Muraguchi M, Kamata M, et al. Procaterol potentiates the anti-inflammatory activity of budesonide on eosinophil adhesion to lung fibroblasts. Int Arch Allergy Immunol. 2009;150(4):352-8. PMID: 19571567.

P6859 Proctolin

1 mg
2 mg
5 mg

$C_{30}H_{48}N_8O_8$ FW: 648.77 [57966-42-4] ≥95%

H-Arg-Tyr-Leu-Pro-Thr-OH

Found in crustaceans and insects. It causes vascular resistance, modulates vitellogenin uptake, and increases antennae-heart beat rates.

Wilkens J. Possible mechanisms of control of vascular resistance in the lobster Homarus americanus J Exp Biol. 1997;200(Pt 3):487-93. PMID: 9318157.

P6854 Progesterone

5 g
25 g
100 g

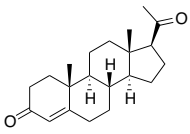

$C_{21}H_{30}O_2$ FW: 314.47 [57-83-0] ≥98%

Endogenous steroid hormone involved in reproduction. It activates progesterone receptors and inhibits mineralocorticoid, nAChR, and σ1/2 receptors. It is used as HRT and also to prevent preterm birth. It induces myelin sheath formation, supports neurotransmission, and induces mammary gland development.

Johannessen M, Fontanilla D, Mavlyutov T, et al. Antagonist action of progesterone at σ-receptors in the modulation of voltage-gated sodium channels. Am J Physiol Cell Physiol. 2011 Feb;300(2):C328-37. Erratum in: Am J Physiol Cell Physiol. 2013 Nov 1;305(9):C997. PMID: 21084640.

da Fonseca EB, Bittar RE, Carvalho MH, et al. Prophylactic administration of progesterone by vaginal suppository to reduce the incidence of spontaneous preterm birth in women at increased risk: a randomized placebo-controlled double-blind study. Am J Obstet Gynecol. 2003 Feb;188(2):419-24. PMID: 12592250.

P6850 Prolactin-Releasing Peptide (1-31), human

1 mg

PrRP-31

$C_{160}H_{252}N_{56}O_{42}S$ FW: 3664.2 ≥98%

Ser-Arg-Thr-His-Arg-His-Ser-Met-Glu-Ile-Arg-Thr-Pro-Asp-Ile-Asn-Pro-Ala-Trp-Tyr-Ala-Ser-Arg-Gly-Ile-Arg-Pro-Val-Gly-Arg-Phe-NH_2

Endogenous GPR10 agonist involved in hormone secretion. It stimulates release of LH, FSH, and prolactin, decreases food intake, and increases expression of pro-inflammatory cytokines and ROS in leukocytes.

Yamashita M, Takayanagi Y, Yoshida M, et al. Involvement of prolactin-releasing peptide in the activation of oxytocin neurones in response to food intake. J Neuroendocrinol. 2013 May;25(5):455-65. PMID: 23363338.

P6852 Propafenone Hydrochloride

1 g
5 g

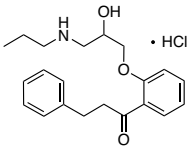

$C_{21}H_{27}NO_3 \cdot HCl$ FW: 377.91 [34183-22-7] ≥98%

Inhibitor of β-adrenergic receptors and $K_v1.4$ and K2P2 K^+ channels used to treat arrhythmias. It also propafenone inhibits expression of tyrosinase, TRP-1, and TRP-2 and suppresses melanogenesis.

Schmidt C, Wiedmann F, Schweizer PA, et al. Class I antiarrhythmic drugs inhibit human cardiac two-pore-domain K(+) (K2P2) channels. Eur J Pharmacol. 2013 Dec 5;721(1-3):237-48. PMID: 24070813.

Huh S, Jung E, Lee J, et al. Mechanisms of melanogenesis inhibition by propafenone. Arch Dermatol Res. 2010 Sep;302(7):561-5. PMID: 20549222.

P6855 (±)-S-Propyl-L-cysteine-S-oxide

10 mg
25 mg

$C_6H_{13}NO_3S$ FW: 179.24 ≥98%

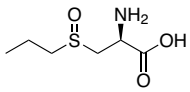

Synthetic analog of alliin found in *Allium*. It may inhibit oil drop formation.

Yoshinari O, Shiojima Y, Igarashi K. Anti-obesity effects of onion extract in Zucker diabetic fatty rats. Nutrients. 2012 Oct 22;4(10):1518-26. PMID: 23201769.

Krest I, Glodek J, Keusgen M. Cysteine sulfoxides and alliinase activity of some Allium species. J Agric Food Chem. 2000 Aug;48(8):3753-60. PMID: 10956182.

P6865 Propranolol Hydrochloride

1 g
5 g
25 g
100 g

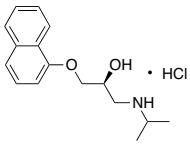

$C_{16}H_{21}NO_2 \cdot HCl$ FW: 295.8 [318-98-9] ≥98%

β1/2-Adrenergic receptor antagonist used to treat hypertension and several other cardiovascular complications. It also attenuates wound healing-induced hypermetabolic responses and suppresses cortical spreading during depression.

Ji Y, Li K, Xiao X, et al. Effects of propranolol on the proliferation and apoptosis of hemangioma-derived endothelial cells. J Pediatr Surg. 2012 Dec;47(12):2216-23. PMID: 23217879.

Izadpanah A, Izadpanah A, Kanevsky J, et al. Propranolol versus corticosteroids in the treatment of infantile hemangioma: a systematic review and meta-analysis. Plast Reconstr Surg. 2013 Mar;131(3):601-13. PMID: 23142941.

Romana-Souza B, Santos JS, Monte-Alto-Costa A. beta-1 and beta-2, but not alpha-1 and alpha-2, adrenoceptor blockade delays rat cutaneous wound healing. Wound Repair Regen. 2009 Mar-Apr;17(2):230-9. PMID: 19320892.

P6956

Prostaglandin E1

1 mg
5 mg
10 mg

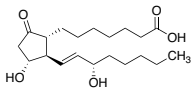

$C_{20}H_{34}O_5$ FW: 354.48 [745-65-3] ≥98%

Endogenous prostaglandin and vasodilator used to treat erectile dysfunction. It also decreases small intestine mucosa lesions, improves renal function, and enhances VEGF production in ischemia models.

Hanchanale V, Eardley I. Alprostadil for the treatment of impotence. Expert Opin Pharmacother. 2014 Feb;15(3):421-8. PMID: 24369066.

Brasileiro JL, Inoye CM, Aydos RD, et al. Ischemia and reperfusion of rat small intestine using pentoxyfilline and prostaglandin E1. Acta Cir Bras. 2013 Nov;28(11):767-73. PMID: 24316743.

Liu WJ, Zhang BC, Guo R, et al. Renoprotective effect of alprostadil in combination with statins in patients with mild to moderate renal failure undergoing coronary angiography. Chin Med J (Engl). 2013;126(18):3475-80. PMID: 24034093.

P4560

Proteolipid Protein (139-151)

1 mg
5 mg

PLP

His-Ser-Leu-Gly-Lys-Trp-Leu-Gly-His-Pro-Asp-Lys-Phe

$C_{72}H_{104}N_{20}O_{17}$ FW: 1521.7 ≥95%

Immunodominant peptide fragment of proteolipid protein used to induce EAE.

Soellner IA, Rabe J, Mauri V, et al. Differential aspects of immune cell infiltration and neurodegeneration in acute and relapse experimental autoimmune encephalomyelitis. Clin Immunol. 2013 Dec;149(3):519-29. PMID: 24239839.

Nicolò C, Sali M, Di Sante G, et al. *Mycobacterium* smegmatis expressing a chimeric protein MPT64-proteolipid protein (PLP) 139-151 reorganizes the PLP-specific T cell repertoire favoring a CD8-mediated response and induces a relapsing experimental autoimmune encephalomyelitis. J Immunol. 2010 Jan 1;184(1):222-35. PMID: 19949067.

P6959

Prothionamide

1 g
5 g
25 g

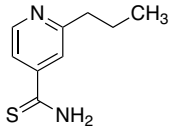

$C_9H_{12}N_2S$ FW: 180.27 [14222-60-7] ≥98%

Nicotinic acid derivative and InhA inhibitor used to treat *Mycobacterium*-based diseases. It forms adducts with NAD and prevents synthesis of mycoloic acids.

Shim TS, Jo KW. Medical Treatment of Pulmonary Multidrug-Resistant Tuberculosis. Infect Chemother. 2013 Dec;45(4):367-374. PMID: 24475350.

Wang F, Langley R, Gulten G, et al. Mechanism of thioamide drug action against tuberculosis and leprosy. J Exp Med. 2007 Jan 22;204(1):73-8. PMID: 17227913.

P6857

Protocatechuic Acid

25 g
50 g
100 g

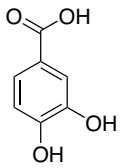

3,4-Dihydroxybenzoic acid

$C_7H_6O_4$ FW: 154.12 [99-50-3] ≥97%

Topoisomerase II inhibitor found in many plants and foods. It targets PKC/RhoB activation to suppress migration and invasion of melanoma cells, induces apoptosis in gastric adenocarcinoma cells, and prevents oxidative stress-induced apoptosis in PC12 neurons.

Kuriyama I, Nakajima Y, Nishida H, et al. Inhibitory effects of low molecular weight polyphenolics from Inonotus obliquus on human DNA topoisomerase activity and cancer cell proliferation. Mol Med Rep. 2013 Aug;8(2):535-42. PMID: 23799608.

Ou CB, Pan Q, Chen X, et al. Protocatechuic acid, a new active substance against the challenge of avian infectious bursal disease virus. Poult Sci. 2012 Jul;91(7):1604-9. Erratum in: Poult Sci. 2012 Oct;91(10):2722. Pang, Q [corrected to Pan, Q]. PMID: 22700505.

P7060

Protocatechuic Acid Ethyl Ester

5 g
25 g
100 g

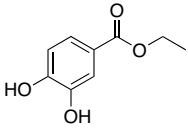

$C_9H_{10}O_4$ FW: 182.17 [3943-89-3] ≥98%

Topoisomerase II inhibitor found in many plants and foods. It prevents PKC/RhoB activation, inhibits TNF-induced expression of pro-inflammatory cytokines, improves pathology and motor function in models of bilateral common carotid artery occlusion, and suppresses metastasis, invasion, and proliferation of cancer cells.

Stumpf C, Fan Q, Hintermann C, et al. Anti-inflammatory effects of danshen on human vascular endothelial cells in culture. Am J Chin Med. 2013;41(5):1065-77. PMID: 24117069.

Garcia-Alvarez MC, Moussa I, Njomnang Soh P, et al. Both plants Sebastiania chamaelea from Niger and Chrozophora senegalensis from Senegal used in African traditional medicine in malaria treatment share a same active principle. J Ethnopharmacol. 2013 Oct 7;149(3):676-84. PMID: 23906782.

Kuriyama I, Nakajima Y, Nishida H, et al. Inhibitory effects of low molecular weight polyphenolics from Inonotus obliquus on human DNA topoisomerase activity and cancer cell proliferation. Mol Med Rep. 2013 Aug;8(2):535-42. PMID: 23799608.

P7058 Protocatechuic Aldehyde

10 g
25 g
100 g

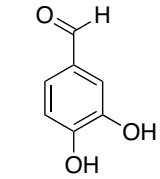

$C_7H_6O_3$ FW: 138.12 [139-85-5] ≥98%

Found in various plants and foods. It decreases infarct size in models of ischemia/reperfusion, decreases levels of collagen, TGF-β, and CTGF in liver fibrosis models, and suppresses apoptosis in endothelial cells.

Wei G, Guan Y, Yin Y, et al. Anti-inflammatory effect of protocatechuic aldehyde on myocardial ischemia/reperfusion injury in vivo and in vitro. Inflammation. 2013 Jun;36(3):592-602. PMID: 23269534.

Xing YL, Zhou Z, Agula, et al. Protocatechuic aldehyde inhibits lipopolysaccharide-induced human umbilical vein endothelial cell apoptosis via regulation of caspase-3. Phytother Res. 2012 Sep;26(9):1334-41. PMID: 22298410.

Xu Y, Jiang WL, Zhang SP, et al. Protocatechuic aldehyde protects against experimental sepsis in vitro and in vivo. Basic Clin Pharmacol Toxicol. 2012 Apr;110(4):384-9. PMID: 22050905.

P7057 Protodioscin

5 mg
25 mg

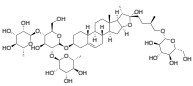

$C_{50}H_{82}O_{22}$ FW: 1049.19 [55056-80-9] ≥98%

Na^+/K^+ ATPase and Ca^{2+}/Mg^{2+} ATPase activator found in *Dioscorea*. It protects cardiomyocytes under anoxic conditions, decreases levels of triglycerides, LDL, and total cholesterol, and induces cell cycle arrest and apoptosis in cancer cells.

Wang T, Choi RC, Li J, et al. Antihyperlipidemic effect of protodioscin, an active ingredient isolated from the rhizomes of *Dioscorea* nipponica. Planta Med. 2010 Oct;76(15):1642-6. PMID: 20509104.

Ning Z, Li YK, Zhou Y. Effect and mechanism of methyl protodioscin in protecting cardiomyocytes against anoxia/reoxygenation injury. Zhongguo Zhong Xi Yi Jie He Za Zhi. 2010 Apr;30(4):407-9. PMID: 20669680.

P6957 Protopanaxadiol

5 mg
10 mg
25 mg

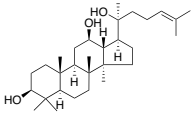

$C_{30}H_{52}O_3$ FW: 460.73 [7755-01-3] ≥98%

GABA-A receptor antagonist found in species of *Panax*. It prevents breakdown of vitamin D3, inhibits proliferation of colorectal cancer cells, and increases activity of superoxide dismutase and Na^+/K^+ ATPases in cerebral ischemia models.

Deb S, Chin MY, Adomat H, et al. Ginsenoside-mediated blockade of 1α,25-dihydroxyvitamin D3 inactivation in human liver and intestine in vitro. J Steroid Biochem Mol Biol. 2014 May;141:94-103. PMID: 24486455.

Xu H, Yu X, Qu S, et al. Protective effect of *Panax* quinquefolium 20(S)-protopanaxadiol saponins, isolated from Pana quinquefolium, on permanent focal cerebral ischemic injury in rats. Exp Ther Med. 2014 Jan;7(1):165-170. PMID: 24348784.

Zheng Y, Nan H, Hao M, et al. Antiproliferative effects of protopanaxadiol ginsenosides on human colorectal cancer cells. Biomed Rep. 2013 Jul;1(4):555-558. PMID: 24648985.

P6958 Protopanaxatriol

5 mg
10 mg
25 mg

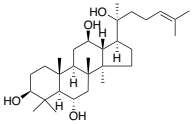

$C_{30}H_{52}O_4$ FW: 476.73 [34080-08-5] ≥95%

GABA-A/C receptor antagonist and slow-activating delayed rectifier K^+ channel blocker found in species of *Panax*. It displays several biological activities, including inhibiting breakdown of vitamin D3, increasing vascular relaxation, decreasing blood pressure, and increasing activity of antioxidative enzymes.

Deb S, Chin MY, Adomat H, et al. Ginsenoside-mediated blockade of 1α,25-dihydroxyvitamin D3 inactivation in human liver and intestine in vitro. J Steroid Biochem Mol Biol. 2014 May;141:94-103. PMID: 24486455.

Lee BH, Hwang SH, Choi SH, et al. Inhibitory Effects of Ginsenoside Metabolites, Compound K and Protopanaxatriol, on GABAC Receptor-Mediated Ion Currents. Korean J Physiol Pharmacol. 2013 Apr;17(2):127-32. PMID: 23626474.

Hong SY, Kim JY, Ahn HY, et al. *Panax* ginseng extract rich in ginsenoside protopanaxatriol attenuates blood pressure elevation in spontaneously hypertensive rats by affecting the Akt-dependent phosphorylation of endothelial nitric oxide synthase. J Agric Food Chem. 2012 Mar 28;60(12):3086-91. PMID: 22380784.

P7158 Protopine

NEW

1 mg
5 mg

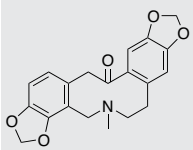

$C_{20}H_{19}NO_5$ FW: 353.37 [130-86-9] ≥98%

Voltage- and receptor-gated Ca^{2+} channel blocker found in a variety of plant sources. It decreases pain transmission, decreases LPS-stimulated expression of pro-inflammatory cytokines, potentially inhibits microtubule depolymerization, and induces apoptosis in prostate cancer cells.

Bae DS, Kim YH, Pan CH, et al. Protopine reduces the inflammatory activity of lipopolysaccharide-stimulated murine macrophages. BMB Rep. 2012 Feb;45(2):108-13. PMID: 22360889.

Chen CH, Liao CH, Chang YL, et al. Protopine, a novel microtubule-stabilizing agent, causes mitotic arrest and apoptotic cell death in human hormone-refractory prostate cancer cell lines. Cancer Lett. 2012 Feb 1;315(1):1-11. PMID: 22033245.

P7059

Proxymetacaine Hydrochloride

100 mg
250 mg
1 g

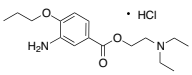

$C_{16}H_{26}N_2O_3 \bullet HCl$ FW: 330.85 [5875-06-9] ≥98%

Potential voltage-gated Na^+ channel blocker used for ocular anesthesia or analgesia.

Murphy PJ, Ntola AM. Prolonged corneal anaesthesia by proxymetacaine hydrochloride detected by a thermal cooling stimulus. Cont Lens Anterior Eye. 2009 Apr;32(2):84-7; quiz 99-100. PMID: 19181566.

Jauregui MJ, Sanders TJ, Polse KA. Anesthetic effects from low concentrations of proparacaine and benoxinate. J Am Optom Assoc. 1980 Jan;51(1):37-41. PMID: 6997360.

P7082

Prulifloxacin

25 mg
100 mg
500 mg

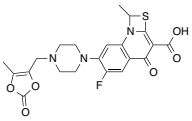

$C_{21}H_{20}FN_3O_6S$ FW: 461.46 [123447-62-1] ≥97%

Topoisomerase IV and bacterial DNA gyrase inhibitor used to treat respiratory and urinary tract infections. It inhibits growth of *Escherichia*, *Proteus*, *Staphylococcus*, *Streptococcus*, and *Haemophilus*.

Karageorgopoulos DE, Maraki S, Vatopoulos AC, et al. Antimicrobial activity of prulifloxacin in comparison with other fluoroquinolones against community-acquired urinary and respiratory pathogens isolated in Greece. Eur J Clin Microbiol Infect Dis. 2013 Nov;32(11):1417-22. PMID: 23686506.

Castora FJ, Vissering FF, Simpson MV. The effect of bacterial DNA gyrase inhibitors on DNA synthesis in mammalian mitochondria. Biochim Biophys Acta. 1983 Sep 9;740(4):417-27. PMID: 6309236.

P7318

Pseudoginsenoside F11

5 mg
10 mg
25 mg

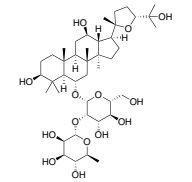

$C_{42}H_{72}O_{14}$ FW: 801.49 [69884-00-0] ≥98%

PPARγ agonist found in species of *Panax*. It displays a variety of biological activities, including inhibiting LPS-stimulated expression of pro-inflammatory cytokines, promoting adiponectin oligomerization and secretion, preventing amyloid-β-induced learning and memory impairment, and improving 6OHDA-induced motor coordination and activity impairments.

Wang X, Wang C, Wang J, et al. Pseudoginsenoside-F11 (PF11) exerts anti-neuroinflammatory effects on LPS-activated microglial cells by inhibiting TLR4-mediated TAK1/IKK/NF-κB, MAPKs and Akt signaling pathways. Neuropharmacology. 2014 Apr;79:642-56. PMID: 24467851.

Wu G, Yi J, Liu L, et al. Pseudoginsenoside F11, a Novel Partial PPAR γ Agonist, Promotes Adiponectin Oligomerization and Secretion in 3T3-L1 Adipocytes. PPAR Res. 2013;2013:701017. PMID: 24454336.

Wang JY, Yang JY, Wang F, et al. Neuroprotective effect of pseudoginsenoside-f11 on a rat model of Parkinson's disease induced by 6-hydroxydopamine. Evid Based Complement Alternat Med. 2013;2013:152798. PMID: 24386001.

P7219

Pseudolaric Acid B

1 mg
5 mg

PAB

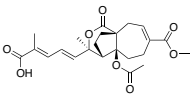

$C_{23}H_{28}O_8$ FW: 432.46 [82508-31-4] ≥98%

Microtubule polymerization inhibitor found in *Pseudolarix kaempferi*. It induces cell cycle arrest, autophagy, senescence, and apoptosis in cancer cells, inhibits T cell proliferation, and suppresses growth of fungi.

Pseudolaric acid B induces caspase-dependent cell death in human ovarian cancer cells. Oncol Rep. 2013 Nov 25. [Epub ahead of print]. PMID: 24276652.

Role of pseudolaric acid B in A549 lung cancer cell proliferation and apoptosis. Guan T, Yang Y. Mol Med Rep. 2014 Jan;9(1):144-8. PMID: 24248012.

Yu Jh, Liu Cy, Zheng Gb, et al. Pseudolaric acid B induced cell cycle arrest, autophagy and senescence in murine fibrosarcoma l929 cell. Int J Med Sci. 2013 Apr 9;10(6):707-18. PMID: 23630435.

P7218

Pseudoprotodioscin

NEW

5 mg
25 mg
100 mg

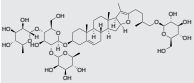

$C_{51}H_{82}O_{21}$ FW: 1031.18 [102115-79-7] ≥98%

Found in *Tribulus*, *Trigonella*, *Smilax*. It inhibits melanogenesis in melanoma cells and decreases production of pro-inflammatory cytokines.

Kawabata T, Cui MY, Hasegawa T, et al. Anti-inflammatory and anti-melanogenic steroidal saponin glycosides from Fenugreek (Trigonella foenum-graecum L.) seeds. Planta Med. 2011 May;77(7):705-10. PMID: 20979021.

Dinchev D, Janda B, Evstatieva L, et al. Distribution of steroidal saponins in Tribulus terrestris from different geographical regions. Phytochemistry. 2008 Jan;69(1):176-86. PMID: 17719068.

Dong M, Feng XZ, Wu LJ, et al. Two new steroidal saponins from the rhizomes of *Dioscorea* panthaica and their cytotoxic activity. Planta Med. 2001 Dec;67(9):853-7. PMID: 11745024.

P7358

Psoralen

10 mg
25 mg
100 mg

Ficusin

$C_{11}H_6O_3$ FW: 186.16 [66-97-7] ≥98%

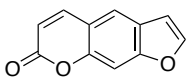

DNA cross-linker and topoisomerase I inhibitor found in *Psoralea coryfolia*. It is used to treat psoriasis with the addition of UVA light. It inhibits angiogenesis and induces cell cycle arrest and apoptosis in endothelial cells.

Chopra B, Dhingra AK, Dhar KL. Psoralea corylifolia L. (Buguchi) - folklore to modern evidence: review. Fitoterapia. 2013 Oct;90:44-56. PMID: 23831482.

Diwan R, Malpathak N. Furanocoumarins: novel topoisomerase I inhibitors from Ruta graveolens L. Bioorg Med Chem. 2009 Oct 1;17(19):7052-5. PMID: 19736019.

P7359

Psoralidin

10 mg
25 mg
100 mg

$C_{20}H_{16}O_5$ FW: 336.34 [18642-23-4] ≥98%

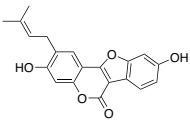

Found in *Psoralea coryfolia*. It displays a variety of activities, including inhibiting growth of gram negative and gram positive bacteria, suppressing proliferation of androgen-independent prostate cancer cells, and decreasing stress-induced expression of ACTH and CRF.

Suman S, Das TP, Damodaran C. Silencing NOTCH signaling causes growth arrest in both breast cancer stem cells and breast cancer cells. Br J Cancer. 2013 Nov 12;109(10):2587-96. PMID: 24129237.

Chopra B, Dhingra AK, Dhar KL. Psoralea corylifolia L. (Buguchi) - folklore to modern evidence: review. Fitoterapia. 2013 Oct;90:44-56. PMID: 23831482.

Chiou WF, Don MJ, Liao JF, et al. Psoralidin inhibits LPS-induced iNOS expression via repressing Syk-mediated activation of PI3K-IKK-IκB signaling pathways. Eur J Pharmacol. 2011 Jan 10;650(1):102-9. PMID: 20951127.

P7608

PTC124

NEW

5 mg
25 mg
100 mg

Ataluren

$C_{15}H_9FN_2O_3$ FW: 284.25 [775304-57-9] ≥98%

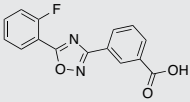

It allows read-through of premature stop codons in mRNA, enabling full protein translation.

Bushby K, Finkel R, Wong B, et al. Ataluren treatment of patients with nonsense mutation dystrophinopathy. Muscle Nerve. 2014 Oct;50(4):477-87. PMID: 25042182.

Ryan NJ. Ataluren: first global approval. Drugs. 2014 Sep;74(14):1709-14. PMID: 25193627.

Nagel-Wolfrum K, Möller F, Penner I, et al. Translational read-through as an alternative approach for ocular gene therapy of retinal dystrophies caused by in-frame nonsense mutations. Vis Neurosci. 2014 Sep;31(4-5):309-16. PMID: 24912600.

P7718

Pterostilbene

50 mg
100 mg
250 mg
1 g

$C_{16}H_{16}O_3$ FW: 256.3 [537-42-8] ≥98.0%

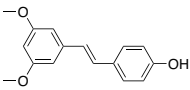

Resveratrol analog. It inhibits DNA strand breaks induced by DPPH, superoxide, and hydrogen peroxide, induces apoptosis in cancer cells, and improves anxiety-related behaviors.

Acharya JD, Ghaskadbi SS. Protective effect of Pterostilbene against free radical mediated oxidative damage. BMC Complement Altern Med. 2013 Sep 26;13(1):238. [Epub ahead of print]. PMID: 24070177.

Lee CM, Su YH, Huynh TT, et al. BlueBerry Isolate, Pterostilbene, Functions as a Potential Anticancer Stem Cell Agent in Suppressing Irradiation-Mediated Enrichment of Hepatoma Stem Cells. Evid Based Complement Alternat Med. 2013;2013:258425. PMID: 23878592.

Al Rahim M, Rimando AM, Silistreli K, et al. Anxiolytic action of pterostilbene: involvement of hippocampal ERK phosphorylation. Planta Med. 2013 Jun;79(9):723-30. PMID: 23677525.

P8118

Puerarin

100 mg
500 mg
1 g

$C_{21}H_{20}O_9$ FW: 416.38 [3681-99-0] ≥98%

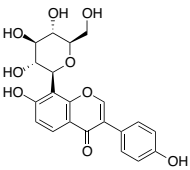

5-HT2C receptor and GABA-A receptor antagonist found in *Pueraria*. It displays a variety of biological activities, including increasing social interaction time and locomotor activity in animal models of substance withdrawal, decreasing systolic blood pressure and heart rate, and protecting neurons against H_2O_2-induced oxidative stress.

Liu S, Yu S, Xu C, et al. Puerarin alleviates aggravated sympathoexcitatory response induced by myocardial ischemia via regulating P2X3 receptor in rat superior cervical ganglia. Neurochem Int. 2014 May;70:39-49. PMID: 24657446.

Zhou Y, Xie N, Li L, et al. Puerarin alleviates cognitive impairment and oxidative stress in APP/PS1 transgenic mice. Int J Neuropsychopharmacol. 2014 Apr;17(4):635-44. PMID: 24345484.

Zhang Q, Huang WD, Lv XY, et al. Puerarin protects differentiated PC12 cells from H_2O_2-induced apoptosis through the PI3K/Akt signalling pathway. Cell Biol Int. 2012 May 1;36(5):419-26. PMID: 22126839.

P8117

Puerarin, 99%

5 mg
10 mg
25 mg

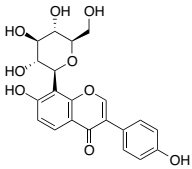

$C_{21}H_{20}O_9$ FW: 416.38 [3681-99-0] ≥98%

5-HT2C receptor and GABA-A receptor antagonist found in *Pueraria*. It displays a variety of biological activities, including increasing social interaction time and locomotor activity in animal models of substance withdrawal, decreasing systolic blood pressure and heart rate, and protecting neurons against H_2O_2-induced oxidative stress.

Liu S, Yu S, Xu C, et al. Puerarin alleviates aggravated sympathoexcitatory response induced by myocardial ischemia via regulating P2X3 receptor in rat superior cervical ganglia. Neurochem Int. 2014 May;70:39-49. PMID: 24657446.

Zhou Y, Xie N, Li L, et al. Puerarin alleviates cognitive impairment and oxidative stress in APP/PS1 transgenic mice. Int J Neuropsychopharmacol. 2014 Apr;17(4):635-44. PMID: 24345484.

P8370

Purmorphamine

NEW

5 mg
25 mg

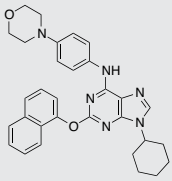

$C_{31}H_{32}N_6O_2$ FW: 520.64 [483367-10-8] ≥98%

Smoothened receptor agonist. It accelerates osteogenesis, decreases neuronal apoptosis, and inhibits the induction of autophagy in hepatocellular carcinoma cells.

Wöltje M, Böbel M, Heiland M, et al. Purmorphamine and oxysterols accelerate and promote osteogenic differentiation of mesenchymal stem cells in vitro. In Vivo. 2015 Mar-Apr;29(2):247-54. PMID: 25792653.

Chechneva OV, Mayrhofer F, Daugherty DJ, et al. A Smoothened receptor agonist is neuroprotective and promotes regeneration after ischemic brain injury. Cell Death Dis. 2014 Oct 23;5:e1481. PMID: 25341035.

Wang Y, Han C, Lu L, et al. Hedgehog signaling pathway regulates autophagy in human hepatocellular carcinoma cells. Hepatology. 2013 Sep;58(3):995-1010. PMID: 23504944.

P8168

Puromycin Dihydrochloride

Stillomycin

10 mg
25 mg
100 mg

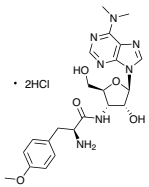

$C_{22}H_{29}N_7O_5 \cdot 2HCl$ FW: 544.43 [58-58-2] ≥98%

Inhibitor of DPP2, metallopeptidase, and protein synthesis. It resembles the 3' end of tRNA and is incorporated into growing protein chains through the ribosomal A site, inducing premature chain termination and DNA damage. It also inhibits insulin activation of phosphofructokinase 2 and induces apoptosis and autophagy in podocytes.

Kang YL, Saleem MA, Chan KW, et al. The cytoprotective role of autophagy in puromycin aminonucleoside treated human podocytes. Biochem Biophys Res Commun. 2014 Jan 10;443(2):628-34. PMID: 24333414.

Liu S, Ding J, Fan Q, et al. The activation of extracellular signal-regulated kinase is responsible for podocyte injury. Mol Biol Rep. 2010 Jun;37(5):2477-84. PMID: 19728154.

Marshall CB, Pippin JW, Krofft RD, et al. Puromycin aminonucleoside induces oxidant-dependent DNA damage in podocytes in vitro and in vivo. Kidney Int. 2006 Dec;70(11):1962-73. PMID: 17035936.

P8167

Puromycin Aminonucleoside

Stylomycin aminonucleoside

25 mg
100 mg

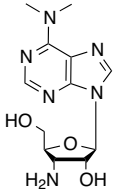

$C_{12}H_{18}N_6O_3$ FW: 294.31 [58-60-6] ≥98%

Purine analog, DNA chain terminator, and inhibitor of DPP2 and metalloproteinases. It induces DNA damage and oxidative stress, inhibits insulin-stimulated glycolysis, and stimulates autophagy and apoptosis in podocytes.

Kang YL, Saleem MA, Chan KW, et al. The cytoprotective role of autophagy in puromycin aminonucleoside treated human podocytes. Biochem Biophys Res Commun. 2014 Jan 10;443(2):628-34. PMID: 24333414.

Liu S, Ding J, Fan Q, et al. The activation of extracellular signal-regulated kinase is responsible for podocyte injury. Mol Biol Rep. 2010 Jun;37(5):2477-84. PMID: 19728154.

P8169

Purpurin

Hydroxylizaric acid

5 g
25 g

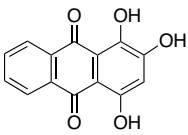

$C_{14}H_8O_5$ FW: 256.21 [81-54-9] ≥90%

O-acetylpeptidoglycan esterase inhibitor found in madder root. It suppresses VEGF-induced cell invasion, inhibits adipocyte-derived leucine aminopeptidase activity, scavenges radicals, and prevents growth of gram positive and gram negative bacteria.

Park H, Shim JS, Kim BS, et al. Purpurin inhibits adipocyte-derived leucine aminopeptidase and angiogenesis in a zebrafish model. Biochem Biophys Res Commun. 2014 Jul 18;450(1):561-7. PMID: 24928393.

Tsang PW, Wong AP, Yang HP, et al. Purpurin triggers caspase-independent apoptosis in *Candida* dubliniensis biofilms. PLoS One. 2013 Dec 23;8(12):e86032. PMID: 24376900.

Pfeffer JM, Clarke AJ. Identification of the first known inhibitors of O-acetylpeptidoglycan esterase: a potential new antibacterial target. Chembiochem. 2012 Mar 19;13(5):722-31. PMID: 22351512.

P8270

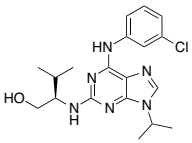

Purvalanol A

1 mg
5 mg

NG-60

$C_{19}H_{25}ClN_6O$ FW: 388.9 [212844-53-6] ≥98%

Purine derivative and CDK inhibitor. It induces cell cycle arrest and apoptosis in breast cancer cells, decreases human T-cell leukemia virus type 1 proliferation, and alters differentiation potential in adipose-derived stem cells.

Obakan P, Arısan ED, Özfiliz P, et al. Purvalanol A is a strong apoptotic inducer via activating polyamine catabolic pathway in MCF-7 estrogen receptor positive breast cancer cells. Mol Biol Rep. 2014 Jan;41(1):145-54. PMID: 24190492.

Hofman J, Ahmadimoghaddam D, Hahnova L, et al. Olomoucine II and purvalanol A inhibit ABCG2 transporter in vitro and in situ and synergistically potentiate cytostatic effect of mitoxantrone. Pharmacol Res. 2012 Mar;65(3):312-9. PMID: 22173067.

Park H, Cho JA, Lim EH, et al. Cell cycle regulators are critical for maintaining the differentiation potential and immaturity in adipogenesis of adipose-derived stem cells. Differentiation. 2011 Oct;82(3):136-43. PMID: 21764208.

P8382

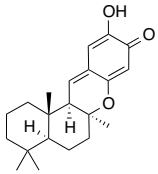

Puupehenone

1 mg
5 mg

$C_{21}H_{28}O_3$ FW: 328.45 [73573-17-8] ≥94%

Found in marine sponges. It decreases DPPH-induced radical generation, suppresses oxidative enzyme expression, and inhibits cell growth.

Castro ME, González-Iriarte M, Barrero AF, et al. Study of puupehenone and related compounds as inhibitors of angiogenesis. Int J Cancer. 2004 May 20;110(1):31-8. PMID: 15054866.

Takamatsu S, Hodges TW, Rajbhandari I, et al. Marine natural products as novel antioxidant prototypes. J Nat Prod. 2003 May;66(5):605-8. PMID: 12762791.

P9200

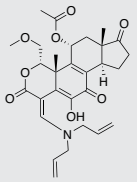

PX-866

NEW

1 mg
5 mg
10 mg
25 mg

Sonolisib

$C_{29}H_{35}NO_8$ FW: 525.59 [502632-66-8] ≥98%

Wortmannin analog and PI3K inhibitor. It inhibits invasion and angiogenesis and induces autophagy in glioblastoma cells.

Bowles DW, Ma WW, Senzer N, et al. A multicenter phase 1 study of PX-866 in combination with docetaxel in patients with advanced solid tumours. Br J Cancer. 2013 Sep 3;109(5):1085-92. PMID: 23942080.

Koul D, Shen R, Kim YW, et al. Cellular and in vivo activity of a novel PI3K inhibitor, PX-866, against human glioblastoma. Neuro Oncol. 2010 Jun;12(6):559-69. PMID: 20156803.

Howes AL, Chiang GG, Lang ES, et al. The phosphatidylinositol 3-kinase inhibitor, PX-866, is a potent inhibitor of cancer cell motility and growth in three-dimensional cultures. Mol Cancer Ther. 2007 Sep;6(9):2505-14. PMID: 17766839.

P6977

Pyr-GR-pNA

1 mg
10 mg

$C_{19}H_{26}N_8O_6$ FW: 462.5 ≥98%

Pyr-Gly-Arg-pNA

Fluorogenic substrate used to measure serine protease activity.

Rajapakse S, Ogiwara K, Takano N, et al. Biochemical characterization of human kallikrein 8 and its possible involvement in the degradation of extracellular matrix proteins. FEBS Lett. 2005 Dec 19;579(30):6879-84. PMID: 16337200.

P9668

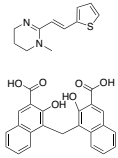

Pyrantel Pamoate

5 g
10 g
50 g

$C_{23}H_{16}O_6 \bullet C_{11}H_{14}N_2S$ FW: 594.68 [22204-24-6] ≥98%

Mixture of pyrantel, a thiophene, and pamoic acid. It inhibits nAChRs and acts as a depolarizing NMJ blocker, inducing muscular paralysis. It is used to treat worm infections.

Reinemeyer CR, Hutchens DE, Eckblad WP, et al. Dose-confirmation studies of the cestocidal activity of pyrantel pamoate paste in horses. Vet Parasitol. 2006 Jun 15;138(3-4):234-9. PMID: 16530970.

Clark JN, Daurio CP, Plue RE, et al. Efficacy of ivermectin and pyrantel pamoate combined in a chewable formulation against heartworm, hookworm, and ascarid infections in dogs. Am J Vet Res. 1992 Apr;53(4):517-20. PMID: 1586021.

P9671

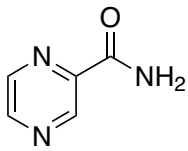

Pyrazinamide

10 g
25 g
100 g

$C_5H_5N_3O$ FW: 123.11 [98-96-4] ≥98%

Nicotinamide analog prodrug and fatty acid synthetase I inhibitor. It disrupts bacterial cell membranes, acidifying cytoplasm and inhibiting membrane transport.

Singh P, Mishra AK, Malonia SK, et al. The paradox of pyrazinamide: an update on the molecular mechanisms of pyrazinamide resistance in Mycobacteria. J Commun Dis. 2006 Mar;38(3):288-98. PMID: 17373362.

Zhang Y, Wade MM, Scorpio A, et al. Mode of action of pyrazinamide: disruption of *Mycobacterium* tuberculosis membrane transport and energetics by pyrazinoic acid. J Antimicrob Chemother. 2003 Nov;52(5):790-5. PMID: 14563891.

P9870 Pyridostatin Trihydrochloride

NEW

5 mg
10 mg
25 mg

$C_{31}H_{32}N_8O_5$ • 5.5 HCl • 5.5 H_2O FW: 896.3 [1085412-37-8] ≥98%

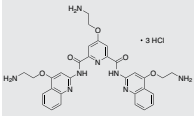

G-quadruplex ligand that induces conformation changes in telomere-G-quadruplex complexes and stimulates double-stranded DNA breakage. It also alters telomere function, decreases synthesis of Epstein-Barr virus-encoded nuclear antigen 1, and suppresses growth of cancer cells.

Marchand A, Granzhan A, Iida K, et al. Ligand-Induced Conformational Changes with Cation Ejection upon Binding to Human Telomeric DNA G-Quadruplexes. J Am Chem Soc. 2015 Jan 21;137(2):750-6. PMID: 25525863.

Murat P, Zhong J, Lekieffre L, et al. G-quadruplexes regulate Epstein-Barr virus-encoded nuclear antigen 1 mRNA translation. Nat Chem Biol. 2014 May;10(5):358-64. PMID: 24633353.

McLuckie KI, Di Antonio M, Zecchini H, et al. G-quadruplex DNA as a molecular target for induced synthetic lethality in cancer cells. J Am Chem Soc. 2013 Jul 3;135(26):9640-3. PMID: 23782415.

P9869 Pyridoxine Hydrochloride

25 g
100 g

$C_8H_{11}NO_3$ • HCl FW: 205.64 [58-56-0] ≥98%

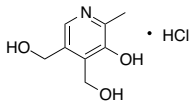

Vitamin B6 derivative and antioxidant. It inhibits oxidized LDL-induced generation of superoxide anions, decreases photosensitivity in subjects with erythropoietic protoporphyria, prevents platelet aggregation, and suppresses glutamate release in synaptosomes.

Xie L, Liu Z, Lu H, et al. Pyridoxine inhibits endothelial NOS uncoupling induced by oxidized low-density lipoprotein via the PKCα signaling pathway in human umbilical vein endothelial cells. Br J Pharmacol. 2012 Feb;165(3):754-64. PMID: 21797845.

Nakari M, Kanouchi H, Oka T. High dose of pyridoxine induces IGFBP-3 mRNA expression in MCF-7 cells and its induction is inhibited by the p53-specific inhibitor pifithrin-α. J Nutr Sci Vitaminol (Tokyo). 2011;57(4):280-4. PMID: 22041910.

Yang TT, Wang SJ. Pyridoxine inhibits depolarization-evoked glutamate release in nerve terminals from rat cerebral cortex: a possible neuroprotective mechanism? J Pharmacol Exp Ther. 2009 Oct;331(1):244-54. PMID: 19628631.

P9767 Pyriproxyfen

5 g
25 g
100 g

$C_{20}H_{19}NO_3$ FW: 321.37 [95737-68-1] ≥95%

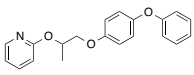

Juvenile insect hormone mimic used as an insecticide. It stimulates production of IgG, TNF-α, and IFN-γ and induces overproduction of male offspring in *Daphnia*.

Sharmin T, Satho T, Irie K, et al. Pyriproxyfen enhances the immunoglobulin G immune response in mice. Microbiol Immunol. 2013 Apr;57(4):316-22. PMID: 23586635.

Ishaaya I, Kontsedalov S, Horowitz AR. Biorational insecticides: mechanism and cross-resistance. Arch Insect Biochem Physiol. 2005 Apr;58(4):192-9. PMID: 15756702.

P9768 Pyronaridine Tetraphosphate

100 mg
250 mg
1 g

Malaridine

$C_{29}H_{32}ClN_5O_2$ • $4H_3PO_4$ FW: 910.03 [76748-86-2] ≥98%

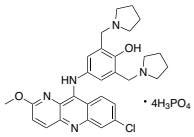

Hemantin inhibitor that prevents glutathione-dependent degradation. It inhibits growth of *Plasmodium*.

Henrich PP, O'Brien C, Sáenz FE, et al. Evidence for pyronaridine as a highly effective partner drug for treatment of artemisinin-resistant malaria in a rodent model. Antimicrob Agents Chemother. 2014 Jan;58(1):183-95. PMID: 24145526.

Kritsiriwuthinan K, Chaotheing S, Shaw PJ, et al. Global gene expression profiling of *Plasmodium falciparum* in response to the anti-malarial drug pyronaridine. Malar J. 2011 Aug 18;10:242. PMID: 21849091.

Auparakkitanon S, Chapoomram S, Kuaha K, et al. Targeting of hematin by the antimalarial pyronaridine. Antimicrob Agents Chemother. 2006 Jun;50(6):2197-200. PMID: 16723583.

P9770 Pyrrolostatin

100 µg
1 mg

EC 40

$C_{15}H_{21}NO_2$ FW: 247.33 [144314-68-1] ≥98%

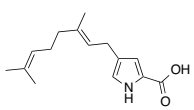

Antioxidant and free radical scavenger that inhibits lipid peroxidation and stimulates angiogenesis.

Chekanov VS, Maternowski MA, Eisenstein R, et al. Angiogenesis in the latissimus dorsi muscle using different regimens of electrical stimulation and pharmaceutical support. ASAIO J. 2000 May-Jun;46(3):305-12. PMID: 10826742.

Kato S, Shindo K, Kawai H, et al. Pyrrolostatin, a novel lipid peroxidation inhibitor from *Streptomyces* chrestomyceticus. Taxonomy, fermentation, isolation, structure elucidation and biological properties. J Antibiot (Tokyo). 1993 Jun;46(6):892-9. PMID: 8344870.

Q4370

QKRPSQRSKYL

1 mg
2 mg
5 mg

MBP 3-14 peptide

H-Gln-Lys-Arg-Pro-Ser-Gln-Arg-Ser-Lys-Tyr-Leu-OH

$C_{60}H_{103}N_{21}O_{17}$ FW: 1390.62 ≥95%

Substrate used to measure PKC activity and Ca^{2+} signaling.

Andrea JE, Sutherland C, Winter CK, et al. Substrate-dependent activation requirements and kinetic properties of protein kinase C. FEBS Lett. 1998 Jun 5;429(1):73-7. PMID: 9657386.

Q8016

Quercetin Dihydrate

25 g
100 g
500 g

CCRIS 3304

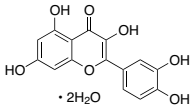

$C_{15}H_{10}O_7 \cdot 2H_2O$ FW: 338.26 [6151-25-3] ≥95%

RT, MAO, and calcineurin inhibitor found in fruits, vegetables, and grains. It displays a variety of biological activities, including suppressing replication of hepatitis C virus, increasing energy expenditure, decreasing release of pro-inflammatory cytokines, and lowering blood pressure.

Pisonero-Vaquero S, García-Mediavilla MV, Jorquera F, et al. Modulation of PI3K-LXRα-dependent lipogenesis mediated by oxidative/nitrosative stress contributes to inhibition of HCV replication by quercetin. Lab Invest. 2014 Mar;94(3):262-74. PMID: 24492281.

Park HJ, Lee CM, Jung ID, et al. Quercetin regulates Th1/Th2 balance in a murine model of asthma. Int Immunopharmacol. 2009 Mar;9(3):261-7. PMID: 19061976.

Saaby L, Rasmussen HB, Jäger AK. MAO-A inhibitory activity of quercetin from Calluna vulgaris (L.) Hull. J Ethnopharmacol. 2009 Jan 12;121(1):178-81. PMID: 19013512.

Q8019

Quetiapine Fumarate

1 g
5 g
25 g

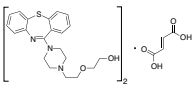

$2(C_{21}H_{25}N_3O_2S) \cdot C_4H_4O_4$ FW: 883.09 [111974-72-2] ≥98%

5-HT1A receptor and σ1/2 receptor agonist and antagonist at 5-HT2A/2C/6/7 receptors, dopamine D1-4 receptors, histamine H1/2 receptors, M1 mAChRs, and α1A/1B/2C-adrenergic receptors. It is used to treat bipolar disorder, schizophrenia, and depression. It also prevents loss of oligodendrocytes and myelin in models of cerebral ischemia/reperfusion.

López-Muñoz F, Alamo C. Active Metabolites as Antidepressant Drugs: The Role of Norquetiapine in the Mechanism of Action of Quetiapine in the Treatment of Mood Disorders. Front Psychiatry. 2013 Sep 12;4:102. PMID: 24062697.

Kotagale NR, Mendhi SM, Aglawe MM, et al. Evidences for the involvement of sigma receptors in antidepressant like effect of quetiapine in mice. Eur J Pharmacol. 2013 Feb 28;702(1-3):180-6. PMID: 23399765.

Tempier A, He J, Zhu S, et al. Quetiapine modulates conditioned anxiety and alternation behavior in Alzheimer's transgenic mice. Curr Alzheimer Res. 2013 Feb;10(2):199-206. PMID: 22950914.

Q8133

Quinacrine Dihydrochloride Dihydrate

10 g
25 g

RP-866; SN-390; Mepacrine

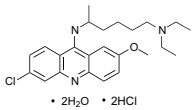

$C_{23}H_{30}ClN_3O \cdot 2HCl \cdot 2H_2O$ FW: 508.92 [6151-30-0] ≥97%

Topoisomerase inhibitor and cell membrane permeability modulator clinically used to treat infections of *Giardia*. It also induces apoptosis in colon cancer cells, decreases production of pro-inflammatory cytokines, suppresses migration of dendritic cells, and inhibits activation of CD8+ T cells.

Mohapatra P, Preet R, Das D, et al. Quinacrine-mediated autophagy and apoptosis in colon cancer cells is through a p53- and p21-dependent mechanism. Oncol Res. 2012;20(2-3):81-91. PMID: 23193914.

Gorbachev AV, Gasparian AV, Gurova KV, et al. Quinacrine inhibits the epidermal dendritic cell migration initiating T cell-mediated skin inflammation. Eur J Immunol. 2007 Aug;37(8):2257-67. PMID: 17634953.

Q8134

Quinapril Hydrochloride

100 mg
500 mg
1 g

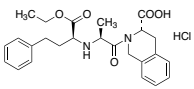

$C_{25}H_{30}N_2O_5 \cdot HCl$ FW: 474.99 [82586-55-8] ≥98%

ACE inhibitor used to treat hypertension and congestive heart failure. It also decreases expression of pro-inflammatory cytokines and suppresses left ventricular remodeling.

Brower GL, Levick SP, Janicki JS. Inhibition of matrix metalloproteinase activity by ACE inhibitors prevents left ventricular remodeling in a rat model of heart failure. Am J Physiol Heart Circ Physiol. 2007 Jun;292(6):H3057-64. PMID: 17308006.

We GC, Siroi MG, Qu R, et al. Effects of quinapril on myocardial function, ventricular remodeling and cardiac cytokine expression in congestive heart failure in the rat. Cardiovasc Drugs Ther. 2002 Jan;16(1):29-36. PMID: 12085975.

Q8135 Quinestrol

100 mg
250 mg
1 g

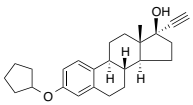

$C_{25}H_{32}O_2$ FW: 364.52 [152-43-2] ≥98%

Synthetic ER agonist used to improve symptoms of postmenopausal syndrome. It decreases testes weight and sperm count in males, lowers levels of FSH and LH in females, and alters estrogen receptor expression.

Li J, Wang H, Zhang J, et al. Abnormal secretion of reproductive hormones and antioxidant status involved in quinestrol-induced reproductive toxicity in adult male rat. Tissue Cell. 2013 Oct 1. pii: S0040-8166(13)00081-5. PMID: 24183492.

Liu Q, Qin J, Chen Q, et al. Fertility control of Rattus nitidus using quinestrol: effects on reproductive organs and social behavior. Integr Zool. 2013 Apr;8 Suppl 1:9-17. PMID: 23621467.

Lv X, Guo Y, Shi D. Effects of quinestrol on reproductive hormone expression, secretion, and receptor levels in female Mongolian gerbils (Meriones unguiculatus). Theriogenology. 2012 Apr 1;77(6):1223-31. PMID: 22284225.

Q8139 Quizartinib

5 mg
10 mg
25 mg

AC220

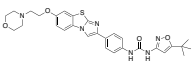

$C_{29}H_{32}N_6O_4S$ FW: 560.67 [950769-58-1] ≥98%

Inhibitor of FLT3, c-Kit, and PDGFR used to treat acute myelogenous leukemia. It inhibits ATP-binding cassette ABCG2 and induces apoptosis in leukemia cells.

Ostronoff F, Estey E. The role of quizartinib in the treatment of acute myeloid leukemia. Expert Opin Investig Drugs. 2013 Sep 26. [Epub ahead of print]. PMID: 24070241.

Bhullar J, Natarajan K, Shukla S, et al. The FLT3 inhibitor quizartinib inhibits ABCG2 at pharmacologically relevant concentrations, with implications for both chemosensitization and adverse drug interactions. PLoS One. 2013;8(8):e71266. PMID: 23967177.

Kampa-Schittenhelm KM, Heinrich MC, Akmut F, et al. Quizartinib (AC220) is a potent second generation class III tyrosine kinase inhibitor that displays a distinct inhibition profile against mutant-FLT3, -PDGFRA and -KIT isoforms. Mol Cancer. 2013 Mar 7;12:19. PMID: 23497317.

R0105 Rabeprazole Sodium

10 mg
25 mg
100 mg

Pariprazole

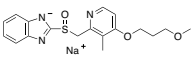

$C_{18}H_{20}N_3O_3S$ Na FW: 381.42 [117976-90-6] ≥98%

H^+/K^+ ATPase and Scpc phosphatase inhibitor used to treat gastric ulcers and gastroesophageal reflux disease. It inhibits gastric acid secretion and modulates expression of neuronal genes and neuronal stem cell differentiation.

Ward RM, Kearns GL. Proton pump inhibitors in pediatrics : mechanism of action, pharmacokinetics, pharmacogenetics, and pharmacodynamics. Paediatr Drugs. 2013 Apr;15(2):119-31. PMID: 23512128.

Zhang M, Cho EJ, Burstein G, et al. Selective inactivation of a human neuronal silencing phosphatase by a small molecule inhibitor. ACS Chem Biol. 2011 May 20;6(5):511-9. PMID: 21348431.

Sanaka M, Anjiki H, Yamamoto T, et al. Rabeprazole delays gastric emptying of a nutrient liquid. J Gastroenterol Hepatol. 2007 Nov;22(11):1806-9. PMID: 17914954.

R0109 Racecadotril

100 mg
500 mg
1 g

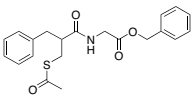

$C_{21}H_{23}NO_4S$ FW: 385.48 [81110-73-8] ≥98%

Enkephalinase inhibitor used to treat diarrhea. It prevents degradation of endogenous opioids and decreases secretion of water and electrolytes in the intestines.

Matheson AJ, Noble S. Racecadotril. Drugs. 2000 Apr;59(4):829-35; discussion 836-7. PMID: 10804038.

Lecomte JM. An overview of clinical studies with racecadotril in adults. Int J Antimicrob Agents. 2000 Feb;14(1):81-7. PMID: 10717506.

R0110 Ractopamine Hydrochloride

1 g
5 g

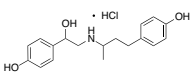

$C_{18}H_{23}NO_3 \cdot HCl$ FW: 337.84 [90274-24-1] ≥97%

β1/2-Adrenergic receptor agonist used to increase muscle mass and decrease body fat. It decreases retroperitoneal and epididymal fat mass and increases adipose tissue apoptosis.

Salem M, Levesque H, Moon TW, et al. Anabolic effects of feeding beta2-adrenergic agonists on rainbow trout muscle proteases and proteins. Comp Biochem Physiol A Mol Integr Physiol. 2006 Jun;144(2):145-54. PMID: 16580855.

Page KA, Hartzell DL, Li C, et al. beta-Adrenergic receptor agonists increase apoptosis of adipose tissue in mice. Domest Anim Endocrinol. 2004 Jan;26(1):23-31. PMID: 14732450.

R0212 Radicicol

1 mg
5 mg

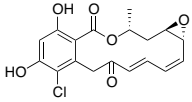

$C_{18}H_{17}ClO_6$ FW: 364.78 [12772-57-5] ≥96%

Inhibitor of topoisomerase VI-B, HSP90, Raf, and Src family kinases. It inhibits mitochondrial replication in *Plasmodium* and increases survival and neurite outgrowth of neurons in chick embryos.

Chalapareddy S, Bhattacharyya MK, Mishra S, et al. Radicicol Confers Mid-Schizont Arrest by Inhibiting Mitochondrial Replication in *Plasmodium falciparum*. Antimicrob Agents Chemother. 2014 Aug;58(8):4341-4352. PMID: 24841259.

Gadelle D, Bocs C, Graille M, et al. Inhibition of archaeal growth and DNA topoisomerase VI activities by the Hsp90 inhibitor radicicol. Nucleic Acids Res. 2005 Apr 22;33(7):2310-7. PMID: 15849317.

Sano M, Yoshida M, Fukui S, et al. Radicicol potentiates neurotrophin-mediated neurite outgrowth and survival of cultured sensory neurons from chick embryo. J Neurochem. 1999 Jun;72(6):2256-63. PMID: 10349833.

R0020 RAF265

1 mg
5 mg

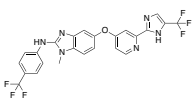

$C_{24}H_{16}F_6N_6O$ FW: 518.4 [927880-90-8] ≥98%

Inhibitor of WT and V600E mutant B-Raf, VEGFR2, c-Raf, PDGFR, CSF-1R, RET, c-Kit, Src, and STE20. It inhibits proliferation of melanoma cells, prevents osteoclastogenesis, and suppresses differentiation of bone marrow cells to osteoclasts.

Garcia-Gomez A, Ocio EM, Pandiella A, et al. RAF265, a dual BRAF and VEGFR2 inhibitor, prevents osteoclast formation and resorption. Therapeutic implications. Invest New Drugs. 2013 Feb;31(1):200-5. d PMID: 22773056.

Huang T, Karsy M, Zhuge J, et al. B-Raf and the inhibitors: from bench to bedside. J Hematol Oncol. 2013 Apr 25;6:30. PMID: 23617957.

Su Y, Vilgelm AE, Kelley MC, et al. RAF265 inhibits the growth of advanced human melanoma tumors. Clin Cancer Res. 2012 Apr 15;18(8):2184-98. Erratum in: Clin Cancer Res. 2012 Aug 15;18(16):4475. PMID: 22351689.

R0243 Raloxifene Hydrochloride

250 mg
500 mg
1 g

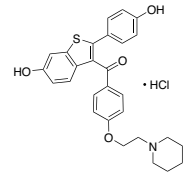

$C_{28}H_{27}NO_4S \bullet HCl$ FW: 510.05 [82640-04-8] ≥98%

SERM used to treat ER+ breast cancer and to prevent post-menopausal osteoporosis. It decreases fracture risk and enhances bone strength, inhibits growth of *Leishmania*, and increases uptake of glutamate and expression of GLT-1 in astrocytes.

Karki P, Webb A, Zerguine A, et al. Mechanism of raloxifene-induced upregulation of glutamate transporters in rat primary astrocytes. Glia. 2014 Aug;62(8):1270-83. PMID: 24782323.

Reimão JQ, Miguel DC, Taniwaki NN, et al. Anti*leishmania*l activity of the estrogen receptor modulator raloxifene. PLoS Negl Trop Dis. 2014 May 8;8(5):e2842. PMID: 24810565.

Gallant MA, Brown DM, Hammond M, et al. Bone cell-independent benefits of raloxifene on the skeleton: a novel mechanism for improving bone material properties. Bone. 2014 Apr;61:191-200. PMID: 24468719.

R0247 Raltegravir NEW

5 mg
10 mg

MK-0518

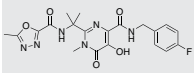

$C_{20}H_{21}FN_6O_5$ FW: 444.42 [518048-05-0] ≥98%

HIV integrase inhibitor used to treat HIV infection. It prevents insertion of HIV-1 DNA into the host genome.

Taramasso L, Madeddu G, Ricci E, et al. Raltegravir-based therapy in a cohort of HIV/HCV co-infected individuals. Biomed Pharmacother. 2015 Feb;69:233-6. PMID: 25661363.

Mouscadet JF, Tchertanov L. Raltegravir: molecular basis of its mechanism of action. Eur J Med Res. 2009 Nov 24;14 Suppl 3:5-16. PMID: 19959411.

Hicks C, Gulick RM. Raltegravir: the first HIV type 1 integrase inhibitor. Clin Infect Dis. 2009 Apr 1;48(7):931-9. PMID: 19231980.

R0245 Raltitrexed

10 mg
25 mg
100 mg

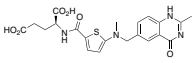

$C_{21}H_{22}N_4O_6S$ FW: 458.49 [112887-68-0] ≥98%

Folate analog and thymidylate synthase inhibitor used to treat advanced colorectal cancer. It inhibits DNA synthesis and induces DNA strand breaks.

Avallone A, Gennaro ED, Silvestro L, et al. Targeting thymidylate synthase in colorectal cancer: critical re-evaluation and emerging therapeutic role of raltitrexed. Expert Opin Drug Saf. 2014 Jan;13(1):113-29. PMID: 24093908.

Van Cutsem E, Cunningham D, Maroun J, et al. Raltitrexed: current clinical status and future directions. Ann Oncol. 2002 Apr;13(4):513-22. PMID: 12056700.

R0248

Ramatroban

5 mg
10 mg
25 mg
100 mg

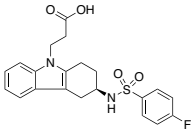

$C_{21}H_{21}FN_2O_4S$ FW: 416.47 [116649-85-5] ≥98%

CRTH2 inhibitor and TxA2 antagonist used to treat coronary artery disease and asthma. It also decreases expression of IL-16, inhibits expression of adhesion molecules, and prevents infiltration of immune cells.

Suzuki Y, Inoue T, Yamamoto A, et al. Prophylactic effects of the histamine H1 receptor antagonist epinastine and the dual thromboxane A2 receptor and chemoattractant receptor-homologous molecule expressed on Th2 cells antagonist ramatroban on allergic rhinitis model in mice. Biol Pharm Bull. 2011;34(4):507-10. PMID: 21467637.

Akiyama K, Karaki M, Kobayshi R, et al. IL-16 variability and modulation by antiallergic drugs in a murine experimental allergic rhinitis model. Int Arch Allergy Immunol. 2009;149(4):315-22. PMID: 19295235.

Sugimoto H, Shichijo M, Okano M, et al. CRTH2-specific binding characteristics of [3H]ramatroban and its effects on PGD2-, 15-deoxy-Delta12, 14-PGJ2- and indomethacin-induced agonist responses. Eur J Pharmacol. 2005 Nov 7;524(1-3):30-7. PMID: 16256979.

R0249

Ramipril

500 mg
1 g
5 g

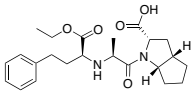

$C_{23}H_{32}N_2O_5$ FW: 416.51 [87333-19-5] ≥98%

ACE inhibitor used to treat hypertension, diabetic nephropathy, and congestive heart failure. It increases antioxidative enzyme activity, decreases ventricular tachycardia and ventricular fibrillation, and inhibits left ventricular remodeling.

Zhong Y, Cao P, Tong C, et al. Effect of ramipril on the electrophysiological characteristics of ventricular myocardium after myocardial infarction in rabbits. J Cardiovasc Med (Hagerstown). 2012 May;13(5):313-8. PMID: 22441218.

Chen CY, Lee BC, Hsu HC, et al. A proteomic study of the effects of ramipril on post-infarction left ventricular remodelling in the rabbit. Eur J Heart Fail. 2008 Aug;10(8):740-8. PMID: 18583185.

Dupuis F, Atkinson J, Limiñana P, et al. Comparative effects of the angiotensin II receptor blocker, telmisartan, and the angiotensin-converting enzyme inhibitor, ramipril, on cerebrovascular structure in spontaneously hypertensive rats. J Hypertens. 2005 May;23(5):1061-6. PMID: 15834293.

R0351

Ramoplanin

100 mg
250 mg

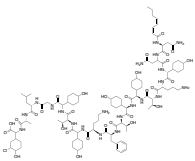

$C_{106}H_{170}ClN_{21}O_{30}$ FW: 2254.06 [76168-82-6] ≥96%

Peptidoglycan inhibitor that prevents cell wall synthesis. It suppresses growth of gram positive bacteria such as *Clostridium difficile*.

Mathur H, O'Connor PM, Hill C, et al. Analysis of anti-*Clostridium difficile* activity of thuricin CD, vancomycin, metronidazole, ramoplanin, and actagardine, both singly and in paired combinations. Antimicrob Agents Chemother. 2013 Jun;57(6):2882-6. PMID: 23571539.

Fulco P, Wenzel RP. Ramoplanin: a topical lipoglycodepsipeptide antibacterial agent. Expert Rev Anti Infect Ther. 2006 Dec;4(6):939-45. PMID: 17181409.

R0349

Ramosetron

10 mg
25 mg
100 mg

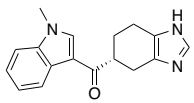

$C_{17}H_{17}N_3O$ FW: 279.34 [132036-88-5] ≥98%

5-HT3 receptor antagonist used to treat IBD and postoperative nausea. It inhibits 5-fluorouracil-induced inflammation and mucositis and inhibits stress-induced abnormal defecation.

Kim WJ, Kang H, Shin HY, et al. Ramosetron, midazolam, and combination of ramosetron and midazolam for prevention of postoperative nausea and vomiting: a prospective, randomized, double-blind study. J Int Med Res. 2013 Aug;41(4):1203-13. PMID: 23766412.

Park YM, Lee YJ, Lee YH, et al. Effects of ramosetron on gastrointestinal transit of Guinea pig. J Neurogastroenterol Motil. 2013 Jan;19(1):36-41. Erratum in: J Neurogastroenterol Motil. 2013;19(2):275. PMID: 23350045.

Yasuda M, Kato S, Yamanaka N, et al. 5-HT3 receptor antagonists ameliorate 5-fluorouracil-induced intestinal mucositis by suppression of apoptosis in murine intestinal crypt cells. Br J Pharmacol. 2013 Mar;168(6):1388-400. PMID: 23072534.

R0250

Ranatensin

1 mg
2 mg
5 mg

pGlu-Val-Pro-Gln-Trp-Ala-Val-Gly-His-Phe-Met-NH_2

$C_{61}H_{85}N_{16}O_{13}S$ FW: 1281.5 [29451-71-6] ≥98%

Found in amphibian skin. It stimulates secretion of Cl^-, gastrin, pancreatic polypeptide, and gastric acid.

Chandan R, Newell SM, Brown DR. Actions of gastrin-releasing peptide and related mammalian and amphibian peptides on ion transport in the porcine proximal jejunum. Regul Pept. 1988 Oct;23(1):1-14. Erratum in: Regul Pept 1989 Mar;24(3):312. PMID: 3238049.

Modlin IM, Lamers CB, Walsh JH. Stimulation of canine pancreatic polypeptide, gastrin, and gastric acid secretion by ranatensin, litorin, bombesin nonapeptide and substance P. Regul Pept. 1981 Jan;1(4):279-88. PMID: 6166964.

R0251

Ranatensin R

1 mg
2 mg
5 mg

Ser-Asn-Thr-Ala-Leu-Arg-Arg-Tyr-Asn-Gln-Trp-Ala-Thr-Gly-His-Phe-Met-NH_2

$C_{90}H_{134}N_{30}O_{24}S$ FW: 2052.3 [70572-93-9] ≥98%

Neuromedin B analog found in amphibian skin.

Taché Y. Intracisternal bombesin induced inhibition of gastric secretion is not mediated through prostaglandin or opioid pathways. Peptides. 1985;6 Suppl 3:69-73. PMID: 3868774.

R0253

Ranitidine Hydrochloride

1 g
5 g

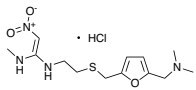

$C_{13}H_{22}N_4O_3S \bullet HCl$ FW: 350.86 [66357-59-3] ≥98%

H2 histamine receptor inverse agonist used to treat peptic ulcer disease and GERD. It induces desensitization in histamine receptors.

Alonso N, Monczor F, Echeverría E, et al. Signal transduction mechanism of biased ligands at histamine H2 receptors. Biochem J. 2014 Apr 1;459(1):117-26. PMID: 24417223.

R0154

Ranolazine Dihydrochloride

100 mg
500 mg
1 g

RS-43285

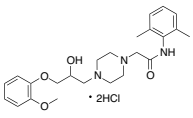

$C_{24}H_{33}N_3O_4 \bullet 2HCl$ FW: 500.47 [95635-56-6] ≥98%

$Na_v1.7$ and $Na_v1.8$ N1+ channel blocker used to treat angina. It prevents intracellular Ca^{2+} accumulation, decreases end diastolic pressure, and inhibits induction of atrial flutter and atrial fibrillation.

Tocchetti CG, Carpi A, Coppola C, et al. Ranolazine protects from doxorubicin-induced oxidative stress and cardiac dysfunction. Eur J Heart Fail. 2014 Jan 6. [Epub ahead of print]. PMID: 24464789.

Aldakkak M, Stowe DF, Camara AK. Safety and Efficacy of Ranolazine for the Treatment of Chronic Angina Pectoris. Clin Med Insights Ther. 2013 Jan 15;2013(5):1-14. PMID: 24574825.

Aidonidis I, Doulas K, Hatziefthimiou A, et al. Ranolazine-induced postrepolarization refractoriness suppresses induction of atrial flutter and fibrillation in anesthetized rabbits. J Cardiovasc Pharmacol Ther. 2013 Jan;18(1):94-101. PMID: 22872232.

R0161

Rapamycin

1 mg
10 mg
25 mg
100 mg

Sirolimus; AY-22989

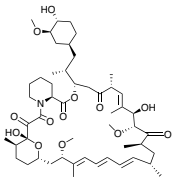

$C_{51}H_{79}NO_{13}$ FW: 914.17 [53123-88-9] ≥98%

mTOR inhibitor produced by *Streptomyces* used to prevent rejection in organ transplant patients. It prevents IL-2-induced activation of T cells and B cells and increases connective tissue growth factor levels in epithelial cells.

Klintmalm GB, Nashan B. The Role of mTOR Inhibitors in Liver Transplantation: Reviewing the Evidence. J Transplant. 2014;2014:845438. PMID: 24719752.

Tian J, Wang Y, Zhou X, et al. Rapamycin slows IgA nephropathy progression in the rat. Am J Nephrol. 2014;39(3):218-29. PMID: 24603476.

Xu X, Wan X, Geng J, et al. Rapamycin regulates connective tissue growth factor expression of lung epithelial cells via phosphoinositide 3-kinase. Exp Biol Med (Maywood). 2013 Sep;238(9):1082-94. PMID: 23986222.

R0272

Rasagiline Mesylate

25 mg
100 mg
250 mg

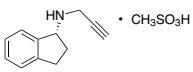

$C_{12}H_{13}N \bullet CH_3SO_3H$ FW: 267.34 [161735-79-1] ≥98%

MAO-A/B inhibitor used to treat Parkinson's disease. It increases levels of Bcl-2, BDNF, and GDNF and suppresses neuronal apoptosis.

Naoi M, Maruyama W, Inaba-Hasegawa K. Revelation in the neuroprotective functions of rasagiline and selegiline: the induction of distinct genes by different mechanisms. Expert Rev Neurother. 2013 Jun;13(6):671-84. PMID: 23739004.

Naoi M, Maruyama W, Yi H. Rasagiline prevents apoptosis induced by PK11195, a ligand of the outer membrane translocator protein (18 kDa), in SH-SY5Y cells through suppression of cytochrome c release from mitochondria. J Neural Transm. 2013 Nov;120(11):1539-51. PMID: 23681678.

R1217

RDEA119

NEW

1 mg
5 mg
10 mg

Refametinib; BAY 869766

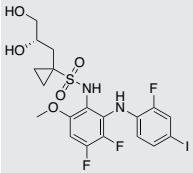

$C_{19}H_{20}F_3IN_2O_5S$ FW: 572.34 [923032-37-5] ≥98%

MEK1/2 inhibitor. It inhibits proliferation in thyroid cancer cells and suppresses tumor growth in models of melanoma, colon cancer, and epidermal carcinoma.

Weekes CD, Von Hoff DD, Adjei AA, et al. Multicenter phase I trial of the mitogen-activated protein kinase 1/2 inhibitor BAY 86-9766 in patients with advanced cancer. Clin Cancer Res. 2013 Mar 1;19(5):1232-43. PMID: 23434733.

Liu D, Xing J, Trink B, et al. BRAF mutation-selective inhibition of thyroid cancer cells by the novel MEK inhibitor RDEA119 and genetic-potentiated synergism with the mTOR inhibitor temsirolimus. Int J Cancer. 2010 Dec 15;127(12):2965-73. PMID: 21351275.

R1806 Rebamipide

1 g
5 g
25 g

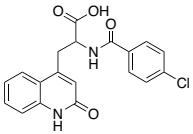

OPC-12759

$C_{19}H_{15}ClN_2O_4$ FW: 370.79 [90098-04-7] ≥98%

Antioxidant used for mucosal protection in the treatment of gastritis and ulcers. It inhibits NSAID-induced lipid peroxidation and apoptosis in epithelial cells.

Nagano Y, Matsui H, Muramatsu M, et al. Rebamipide significantly inhibits indomethacin-induced mitochondrial damage, lipid peroxidation, and apoptosis in gastric epithelial RGM-1 cells. Dig Dis Sci. 2005 Oct;50 Suppl 1:S76-83. PMID: 16184425.

Arakawa T, Kobayashi K, Yoshikawa T, et al. Rebamipide: overview of its mechanisms of action and efficacy in mucosal protection and ulcer healing. Dig Dis Sci. 1998 Sep;43(9 Suppl):5S-13S. PMID: 9753220.

R2711 Recombinant HCV-Core Antigens

100 µg
1 mg

≥95%

Recombinant HCV core protein peptide fragment (8-56) used to test for HCV antibodies.

R2712 Recombinant HCV-NS3 Antigens

100 µg
1 mg

≥95%

Recombinant HCV peptide fragment (1192-1457) used to test for HCV antibodies.

R2713 Recombinant HCV-NS4 Antigens

100 µg
1 mg

≥95%

Recombinant HCV peptide fragment (1916-1947) used to test for HCV antibodies.

R2714 Recombinant HCV-NS5 Antigens

100 µg
1 mg

≥95%

Recombinant HCV-NS5 peptide fragment used to test for HCV antibodies.

R2815 Recombinant HIV-1 “0” group consensus

100 µg
1 mg

≥95%

Recombinant HIV-1 antigen peptide fragment used to test for HIV antibodies.

R2812 Recombinant HIV-1 gp-120

100 µg
1 mg

≥95%

Recombinant HIV glycoprotein antigen peptide fragment used to test for HIV antibodies.

R2811 Recombinant HIV-1 gp-41

100 µg
1 mg

≥95%

Recombinant HIV glycoprotein antigen peptide fragment used to test for HIV antibodies.

R2814 Recombinant HIV-1 p31

100 µg
1 mg

≥95%

Recombinant HIV antigen peptide fragment used to test for HIV antibodies.

R2816 Recombinant HIV-2 gp36

100 µg
1 mg

≥95%

Recombinant HIV-1 glycoprotein antigen peptide fragment used to test for HIV antibodies.

R2710 Recombinant Multi-epitope Chimeric HCV Antigen

100 µg
1 mg

≥95%

Recombinant multi-epitope chimeric HCV peptide containing HCV core (8-56), HCV NS4 (1916-1947), HCV NS3 (1192-1457) used to test for HCV antibodies.

R2810 Recombinant Multi-epitope Chimeric HIV Antigen 1

100 µg
1 mg

≥95%

Recombinant HIV-1 multi-epitope chimeric antigen containing HIV-1 gp41, HIV-1 gp36, and HIV-1 "0" IDR used to test for HIV antibodies.

R3010 Recombinant Tp-chimeric protein

100 µg
1 mg

≥95%

Recombinant chimeric protein containing Treponema pallidum peptide fragments 47, 44.5, 17, and 15 used to test for TpN antibodies.

R3011 Recombinant TpN 15 protein

100 µg
1 mg

≥95%

Recombinant protein containing Treponema pallidum peptide fragments used to test for TpN antibodies.

R3012 Recombinant TpN 17 protein

100 µg
1 mg

≥95%

Recombinant protein containing Treponema pallidum peptide fragments used to test for TpN antibodies.

R3013 Recombinant TpN 44.50 protein

100 µg
1 mg

≥95%

Recombinant protein containing Treponema pallidum peptide fragments used to test for TpN antibodies.

R3014 Recombinant TpN 47 protein

100 µg
1 mg

≥95%

Recombinant protein containing Treponema pallidum peptide fragments used to test for TpN antibodies.

R1724 Regadenoson

NEW

5 mg
25 mg
100 mg

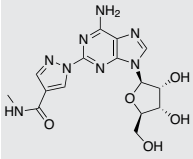

$C_{15}H_{18}N_8O_5$ FW: 390.35 [313348-27-5] ≥98%

Adenosine A2A receptor agonist used in myocardial perfusion imaging. It dilates blood vessels.

Palani G, Ananthasubramaniam K. Regadenoson: review of its established role in myocardial perfusion imaging and emerging applications. Cardiol Rev. 2013 Jan-Feb;21(1):42-8. PMID: 22643345.

Cerqueira MD. The future of pharmacologic stress: selective A2A adenosine receptor agonists. Am J Cardiol. 2004 Jul 22;94(2A):33D-40D; discussion 40D-42D. PMID: 15261132.

R1626 Regorafenib Monohydrate

1 mg
5 mg
25 mg

BAY73-4506

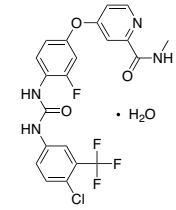

$C_{21}H_{15}ClF_4N_4O_3 \cdot H_2O$ FW: 500.83 [1019206-88-2] ≥99%

Inhibitor of VEGFR1/2/3, TIE2, PDGFRβ, FGFR1, c-Kit, RET, and B-Raf used to treat metastatic colorectal cancer and non-responsive gastrointestinal stromal tumors.

Abou-Elkacem L, Arns S, Brix G, et al. Regorafenib inhibits growth, angiogenesis, and metastasis in a highly aggressive, orthotopic colon cancer model. Mol Cancer Ther. 2013 Jul;12(7):1322-31. PMID: 23619301.

Wilhelm SM, Dumas J, Adnane L, et al. Regorafenib (BAY 73-4506): a new oral multikinase inhibitor of angiogenic, stromal and oncogenic receptor tyrosine kinases with potent preclinical antitumor activity. Int J Cancer. 2011 Jul 1;129(1):245-55. PMID: 21170960.

R1752 Renin Inhibitor Peptide

5 mg
10 mg
25 mg

H-His-Pro-Phe-His-Leu-D-Leu-Val-Tyr-NH_2

$C_{52}H_{73}N_{13}O_9$ FW: 1024.24 ≥95%

Potential vasodilator. It may decrease blood pressure and plasma angiotensin II levels.

Allan DR, Hui KY, Coletti C, et al. Renin vs. angiotensin-converting enzyme inhibition in the rat: consequences for plasma and renal tissue angiotensin. J Pharmacol Exp Ther. 1997 Nov;283(2):661-5. PMID: 9353383.

R1860 Repaglinide

100 mg
250 mg
1 g

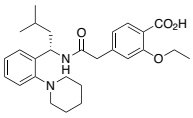

$C_{27}H_{36}N_2O_4$ FW: 452.59 [135062-02-1] ≥98%

Meglitinide derivative and ATP-sensitive K^+ channel blocker used to treat diabetes. It increases insulin release.

Zünkler BJ. Human ether-a-go-go-related (HERG) gene and ATP-sensitive potassium channels as targets for adverse drug effects. Pharmacol Ther. 2006 Oct;112(1):12-37. PMID: 16647758.

Proks P, Reimann F, Green N, et al. Sulfonylurea stimulation of insulin secretion. Diabetes. 2002 Dec;51 Suppl 3:S368-76. PMID: 12475777.

R1774 Resiniferatoxin

1 mg
5 mg
10 mg

RTX

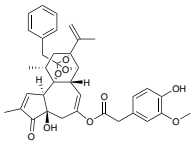

$C_{37}H_{40}O_9$ FW: 628.73 [57444-62-9] ≥98%

Capsaicin analog and PKC and TRPV agonist found in *Euphorbia*. It increases glutamate release in neurons to facilitate nociceptive neurotransmission, it desensitizes TRPV channels to decrease pain, and it inhibits the formation of gastric lesions.

Jiang CY, Fujita T, Yue HY, et al. Effect of resiniferatoxin on glutamatergic spontaneous excitatory synaptic transmission in substantia gelatinosa neurons of the adult rat spinal cord. Neuroscience. 2009 Dec 29;164(4):1833-44. PMID: 19778582.

Tang W, Song B, Zhou ZS, et al. Intrathecal administration of resiniferatoxin produces analgesia against prostatodynia in rats. Chin Med J (Engl). 2007 Sep 20;120(18):1616-21. PMID: 17908482.

Horie S, Yamamoto H, Michael GJ, et al. Protective role of vanilloid receptor type 1 in HCl-induced gastric mucosal lesions in rats. Scand J Gastroenterol. 2004 Apr;39(4):303-12. PMID: 15125461.

R1775 Resiniferonol-9,13,14-orthophenyl Acetate

1 mg
5 mg
10 mg

ROPA

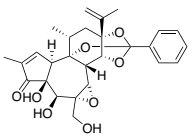

$C_{28}H_{32}O_6$ FW: 464.56 [57852-42-3] ≥98%

Diterpene vanilloid derivative of resiniferatoxin and potential activator of PKC. It induces cell cycle arrest in cancer cells, but may also promote carcinogenesis and tumor development.

Frey MR, Clark JA, Bateman NW, et al. Cell cycle- and protein kinase C-specific effects of resiniferatoxin and resiniferonol 9,13,14-ortho-phenylacetate in intestinal epithelial cells. Biochem Pharmacol. 2004 May 15;67(10):1873-86. PMID: 15130764.

Geiges D, Meyer T, Marte B, et al. Activation of protein kinase C subtypes alpha, gamma, delta, epsilon, zeta, and eta by tumor-promoting and nontumor-promoting agents. Biochem Pharmacol. 1997 Mar 21;53(6):865-75. PMID: 9113106.

R1776 Resveratrol

100 mg
500 mg

3,4',5-Trihydroxystilbene

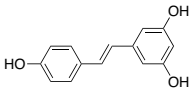

$C_{14}H_{12}O_3$ FW: 228.24 [501-36-0] ≥98%

SIRT1 activator and MAO inhibitor found in several plant sources such as soy, grapes, and peanuts. It degrades amyloid-β plaques and increases brain cysteine levels, inhibits UV-induced skin carcinogenesis, and inhibits growth of cancer cells. It may also activate AMPK, activate proteasomes, and increase life span.

Mohar DS, Malik S. The Sirtuin System: The Holy Grail of Resveratrol? J Clin Exp Cardiolog. 2012 Nov;3(11). 216. PMID: 23560248.

Vingtdeux V, Giliberto L, Zhao H, et al. AMP-activated protein kinase signaling activation by resveratrol modulates amyloid-beta peptide metabolism. J Biol Chem. 2010 Mar 19;285(12):9100-13. PMID: 20080969.

Karuppagounder SS, Pinto JT, Xu H, et al. Dietary supplementation with resveratrol reduces plaque pathology in a transgenic model of Alzheimer's disease. Neurochem Int. 2009 Feb;54(2):111-8. PMID: 19041676.

R1777 9-cis-Retinoic Acid

1 mg
5 mg
25 mg
100 mg

9-cis-Tretinoin; Alitretinoin

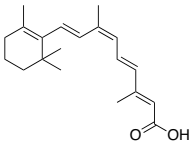

$C_{20}H_{28}O_2$ FW: 300.44 [5300-03-8] ≥98%

Synthetic vitamin A derivative that activates RAR and RXR receptors. It prevents apoptosis and cell death in cardiomyocytes, suppresses 6-OHDA-induced neurodegeneration, and decreases cell viability and tumor growth in adrenocortical cancer models.

Shan PR, Xu WW, Huang ZQ, et al. Protective role of retinoid X receptor in H9c2 cardiomyocytes from hypoxia/reoxygenation injury in rats. World J Emerg Med. 2014;5(2):122-7. PMID: 25215161.

Reiner DJ, Yu SJ, Shen H, et al. 9-Cis retinoic acid protects against methamphetamine-induced neurotoxicity in nigrostriatal dopamine neurons. Neurotox Res. 2014 Apr;25(3):248-61. PMID: 23884514.

Szabó DR, Baghy K, Szabó PM, et al. Antitumoral effects of 9-cis retinoic acid in adrenocortical cancer. Cell Mol Life Sci. 2014 Mar;71(5):917-32. PMID: 23807211.

R1779

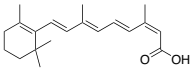

13-cis-Retinoic Acid

Isotretinoin; 13-cis-Vitamin A acid

$C_{20}H_{28}O_2$ FW: 300.44 [4759-48-2] ≥98%

100 mg
250 mg
500 mg

Synthetic vitamin A derivative that activates RAR and RXR receptors and induces differentiation. It is used to treat brain cancers and acne vulgaris. It also decreases pro-inflammatory cytokine release, suppresses myeloperoxidase activity, and inhibits expression of the angiotensin 1 (AT-1) receptor.

Shah N, Wang J, Selich-Anderson J, et al. PBX1 is a favorable prognostic biomarker as it modulates 13-cis retinoic acid-mediated differentiation in neuroblastoma. Clin Cancer Res. 2014 Aug 15;20(16):4400-12. PMID: 24947929.

Frey-Wagner I, Fischbeck A, Cee A, et al. Effects of retinoids in mouse models of colitis: benefit or danger to the gastrointestinal tract? Inflamm Bowel Dis. 2013 Oct;19(11):2356-65. PMID: 23899542.

Snyder R, Thekkumkara T. 13-cis-Retinoic acid specific down-regulation of angiotensin type 1 receptor in rat liver epithelial and aortic smooth muscle cells. J Mol Endocrinol. 2012 Feb 6;48(2):99-114. PMID: 22180636.

R1876

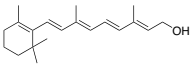

all-trans-Retinol

Vitamin A

$C_{20}H_{30}O$ FW: 286.45 [68-26-8] ≥95%

25 mg
100 mg
250 mg
500 mg

Synthetic vitamin A derivative that activates RAR and RXR receptors and induces differentiation in fetal development. It also downregulates pro-inflammatory responses stimulated by Th1 and Th17 cells in autoimmune diseases and alters ERK1/2 signaling to stimulate cancer cell differentiation.

Friedman MD, Jeevan DS, Tobias M, et al. Targeting cancer stem cells in glioblastoma multiforme using mTOR inhibitors and the differentiating agent all-trans retinoic acid. Oncol Rep. 2013 Oct;30(4):1645-50. PMID: 23877261.

Farhangi MA, Keshavarz SA, Eshraghian M, et al. Vitamin a supplementation and serum Th1- and th2-associated cytokine response in women. J Am Coll Nutr. 2013 Aug;32(4):280-5. PMID: 24024773.

Sharma RB, Wang Q, Khillan JS. Amplification of tumor inducing putative cancer stem cells (CSCs) by vitamin A/retinol from mammary tumors. Biochem Biophys Res Commun. 2013 Jul 12;436(4):625-31. PMID: 23764401.

R1877

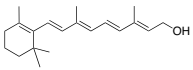

all-trans-Retinol, high purity

Vitamin A

$C_{20}H_{30}O$ FW: 286.45 [68-26-8] ≥98%

25 mg
100 mg
250 mg

Synthetic vitamin A derivative that activates RAR and RXR receptors and induces differentiation in fetal development. It also downregulates pro-inflammatory responses stimulated by Th1 and Th17 cells in autoimmune diseases and alters ERK1/2 signaling to stimulate cancer cell differentiation.

Friedman MD, Jeevan DS, Tobias M, et al. Targeting cancer stem cells in glioblastoma multiforme using mTOR inhibitors and the differentiating agent all-trans retinoic acid. Oncol Rep. 2013 Oct;30(4):1645-50. PMID: 23877261.

Farhangi MA, Keshavarz SA, Eshraghian M, et al. Vitamin a supplementation and serum Th1- and th2-associated cytokine response in women. J Am Coll Nutr. 2013 Aug;32(4):280-5. PMID: 24024773.

Sharma RB, Wang Q, Khillan JS. Amplification of tumor inducing putative cancer stem cells (CSCs) by vitamin A/retinol from mammary tumors. Biochem Biophys Res Commun. 2013 Jul 12;436(4):625-31. PMID: 23764401.

R1780

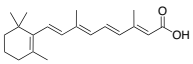

trans-Retinoic Acid

Vitamin A acid; Tretinoin; Retin-A

$C_{20}H_{28}O_2$ FW: 300.44 [302-79-4] ≥98%

500 mg
1 g
5 g

Vitamin A derivative and RAR agonist used to treat acne vulgaris, keratosis pilaris, and acute promyelocytic leukemia. It inhibits fibroblast proliferation and scar formation, decreases viral infectivity of enterovirus 71, induces differentiation in promyelocytes, and suppresses hedgehog signaling by inducing expression of Patched.

Chen S, Yang Y, Xu J, et al. Effect of all-trans-retinoic acid on enterovirus 71 infection in vitro. Br J Nutr. 2014 May;111(9):1586-93. PMID: 24495389.

Zhang ML, Tao Y, Zhou WQ, et al. All-trans retinoic acid induces cell-cycle arrest in human cutaneous squamous carcinoma cells by inhibiting the mitogen-activated protein kinase-activated protein 1 pathway. Clin Exp Dermatol. 2014 Apr;39(3):354-60. PMID: 24635079.

Busch AM, Galimberti F, Nehls KE, et al. All-trans-retinoic acid antagonizes the Hedgehog pathway by inducing patched. Cancer Biol Ther. 2014 Apr;15(4):463-72. PMID: 24496080.

R1878 — Retinyl Acetate

5 g
25 g
100 g

Vitamin A acetate

$C_{22}H_{32}O_2$ FW: 328.49 [127-47-9] ≥96%

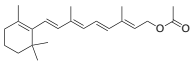

Vitamin A derivative and acetate ester of retinol. It is commercially used as a dietary supplement. It modulates Ca^{2+} signaling, decreases incidence of diabetes, suppresses LPS-stimulated pro-inflammatory cytokine expression, and upregulates expression of TRAIL receptors to inhibit colorectal cancer tumor growth.

Chiamenti A, Filho CR, Moura MT, et al. Use of retinyl acetate, retinoic acid and insulin-like growth factor-I (IGF-I) to enhance goat embryo production. Acta Vet Hung. 2013 Mar;61(1):116-24. PMID: 23439296.

Greenstein RJ, Su L, Brown ST. Vitamins A & D inhibit the growth of mycobacteria in radiometric culture. PLoS One. 2012;7(1):e29631. PMID: 22235314.

Zhang L, Ren X, Alt E, et al. Chemoprevention of colorectal cancer by targeting APC-deficient cells for apoptosis. Nature. 2010 Apr 15;464(7291):1058-61. PMID: 20348907.

R1879 — Retinyl Palmitate

25 g
100 g

Vitamin A palmitate; Aquasol A

$C_{36}H_{60}O_2$ FW: 524.86 [79-81-2]

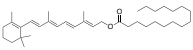

Vitamin A derivative and palmitate ester of retinol. It is commercially used as a dietary supplement but does not directly activate RAR receptors. It also decreases metastasis in colon cancer models, prevents LDL oxidation, and inhibits proliferation of cancer cells.

Park EY, Pinali D, Lindley K, et al. Hepatic vitamin A preloading reduces colorectal cancer metastatic multiplicity in a mouse xenograft model. Nutr Cancer. 2012;64(5):732-40. PMID: 22642873.

Mei N, Xia Q, Chen L, et al. Photomutagenicity of retinyl palmitate by ultraviolet a irradiation in mouse lymphoma cells. Toxicol Sci. 2005 Nov;88(1):142-9. PMID: 16107546.

Maziere S, Cassand P, Narbonne JF, et al. Vitamin A and apoptosis in colonic tumor cells. Int J Vitam Nutr Res. 1997;67(4):237-41. PMID: 9285252.

R1985 — Reveromycin A

100 µg
5 x 100 µg

$C_{36}H_{52}O_{11}$ FW: 660.79 [134615-37-5] ≥98%

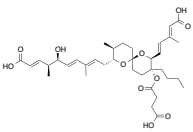

Isoleucyl-tRNA synthase and osteoclast protein synthesis inhibitor. It inhibits bone resorption, normalizes bone turnover and formation, suppresses bone metastasis by lung cancer cells, and induces apoptosis in osteoclasts.

Yabumoto T, Miyazawa K, Tabuchi M, et al. Stabilization of tooth movement by administration of reveromycin A to osteoprotegerin-deficient knockout mice. Am J Orthod Dentofacial Orthop. 2013 Sep;144(3):368-80. PMID: 23992809.

Hiraoka K, Zenmyo M, Watari K, et al. Inhibition of bone and muscle metastases of lung cancer cells by a decrease in the number of monocytes/macrophages. Cancer Sci. 2008 Aug;99(8):1595-602. PMID: 18754872.

Woo JT, Kawatani M, Kato M, et al. Reveromycin A, an agent for osteoporosis, inhibits bone resorption by inducing apoptosis specifically in osteoclasts. Proc Natl Acad Sci U S A. 2006 Mar 21;103(12):4729-34. PMID: 16537392.

R2353 — RF-NH2

5 mg
10 mg
25 mg

$C_{15}H_{24}N_6O_2$ FW: 320.4 [34388-59-5] ≥95%

H-Arg-Phe-NH_2

RF-amide family peptide and potential agonist at GPR147 and acid-sensing ion channels. It may increase nociception and modulate opioid signaling.

Bass C, Katanski C, Maynard B, et al. Conserved residues in RF-NH2 receptor models identify predicted contact sites in ligand-receptor binding. Peptides. 2013 Jun 26. pii: S0196-9781(13)00226-X. [Epub ahead of print]. PMID: 23811075.

Yang HY, Iadarola MJ. Modulatory roles of the NPFF system in pain mechanisms at the spinal level. Peptides. 2006 May;27(5):943-52. PMID: 16443306..

R2112 — RFDS

5 mg

$C_{22}H_{33}N_7O_8$ FW: 523.5 ≥98%

Arg-Phe-Asp-Ser

RGD peptide negative control. It contains a peptide sequence homologous with the β1-domain region of a MHC class II antigen from CD4.

Iwao Y, Fujimura T. Activation of Xenopus eggs by RGD-containing peptides accompanied by intracellular Ca^{2+} release. Dev Biol. 1996 Aug 1;177(2):558-67. PMID: 8806831.

Mazerolles F, Durandy A, Piatier-Tonneau D, et al. Immunosuppressive properties of synthetic peptides derived from CD4 and HLA-DR antigens. Cell. 1988 Nov 4;55(3):497-504. PMID: 3263212.

R2369 RFRP-1, human

0.5 mg
1 mg
2.5 mg

$C_{67}H_{101}N_{19}O_{14}S$ FW: 1428.73 ≥95%

H-Met-Pro-His-Ser-Phe-Ala-Asn-Leu-Pro-Leu-Arg-Phe-NH_2

Avian gonadotropin inhibitory hormone analog and GPR147 activator. It inhibits secretion of gonadotropin and GnRH, suppresses reproductive behavior, decreases food intake, and increases anxiety-like behaviors.

Kovács A, László K, Gálosi R, et al. Microinjection of RFRP-1 in the central nucleus of amygdala decreases food intake in the rat. Brain Res Bull. 2012 Sep 1;88(6):589-95. PMID: 22691952.

Kaewwongse M, Takayanagi Y, Onaka T. Effects of RFamide-related peptide (RFRP)-1 and RFRP-3 on oxytocin release and anxiety-related behaviour in rats. J Neuroendocrinol. 2011 Jan;23(1):20-7. PMID: 21029217.

R2400 RG-108

NEW Please inquire

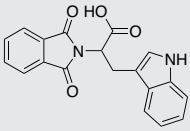

$C_{19}H_{14}N_2O_4$ FW: 334.33 [48208-26-0] ≥98%

DNA methyltransferase inhibitor. It attenuates stress-induced behavioral adaptations in animal models, increases expression of TERT, and induces apoptosis in prostate cancer cells.

Sales AJ, Joca SR. Effects of DNA methylation inhibitors and conventional antidepressants on mice behaviour and brain DNA methylation levels. Acta Neuropsychiatr. 2015 Jun 26:1-12. PMID: 26112212.

Oh YS, Jeong SG, Cho GW. Anti-senescence effects of DNA methyltransferase inhibitor RG108 in human bone marrow mesenchymal stromal cells. Biotechnol Appl Biochem. 2015 May 8. [Epub ahead of print]. PMID: 25952632.

Graça I, Sousa EJ, Baptista T, et al. Anti-tumoral effect of the non-nucleoside DNMT inhibitor RG108 in human prostate cancer cells. Curr Pharm Des. 2014;20(11):1803-11. PMID: 23888969.

R2512 RGD

5 mg
10 mg
25 mg

$C_{12}H_{22}N_6O_6$ FW: 346.3 [99896-85-2] ≥95%

Arg-Gly-Asp

Binds cell surface integrins, enhancing the efficacy of anticancer and anti-aggregation compounds.

Guo Z, He B, Jin H, et al. Targeting efficiency of RGD-modified nanocarriers with different ligand intervals in response to integrin αvβ3 clustering. Biomaterials. 2014 Apr 30. [Epub ahead of print]. PMID: 24794924.

Li Y, Zheng X, Sun Y, et al. RGD-fatty alcohol-modified docetaxel liposomes improve tumor selectivity in vivo. Int J Pharm. 2014 Apr 4;468(1-2):133-141. [Epub ahead of print]. PMID: 24709214.

R2510 RGD-4C

1 mg
2 mg
5 mg

$C_{42}H_{60}N_{14}O_{16}S_4$ FW: 1145.29 ≥95%

H-Ala-Cys-Asp-Cys-Arg-Gly-Asp-Cys-Phe-Cys-Gly-OH (Cys2-Cys10, Cys4-Cys8)

Potential αvβ3 and αvβ5 integrin inhibitor used to deliver conjugated chemotherapeutics to cells.

Allaume X, El-Andaloussi N, Leuchs B, et al. Retargeting of rat parvovirus H-1PV to cancer cells through genetic engineering of the viral capsid. J Virol. 2012 Apr;86(7):3452-65. PMID: 22258256.

Pesonen S, Diaconu I, Cerullo V, et al. Integrin targeted oncolytic adenoviruses Ad5-D24-RGD and Ad5-RGD-D24-GMCSF for treatment of patients with advanced chemotherapy refractory solid tumors. Int J Cancer. 2012 Apr 15;130(8):1937-47. PMID: 21630267.

R2511 RGDC

5 mg
10 mg
25 mg

$C_{15}H_{26}N_7O_7S_1$ FW: 448.48 ≥95%

H-Arg-Gly-Asp-Cys-OH

Potential integrin inhibitor used to study cell surface binding.

Moon C, Han JR, Park HJ, et al. Synthetic RGDS peptide attenuates lipopolysaccharide-induced pulmonary inflammation by inhibiting integrin signaled MAP kinase pathways. Respir Res. 2009 Mar 9;10:18. PMID: 19272161.

Xiao SJ, Textor M, Spencer ND, et al. Immobilization of the cell-adhesive peptide Arg-Gly-Asp-Cys (RGDC) on titanium surfaces by covalent chemical attachment. J Mater Sci Mater Med. 1997 Dec;8(12):867-72. PMID: 15348806.

R2513 RGDS

5 mg

Fibronectin tetrapeptide

$C_{15}H_{27}N_7O_8$ FW: 433.4 [91037-65-9] ≥95%

Arg-Gly-Asp-Ser

Binds cell surface integrins, enhancing the efficacy of anticancer and anti-aggregation compounds. It also improves ventilation-induced lung injury pathology.

Inoue T, Hashimoto R, Matsumoto A, et al. In vivo Analysis of Arg-Gly-Asp Sequence/Integrin α5β1-Mediated Signal Involvement in Embryonic Enchondral Ossification by exo utero Development System. J Bone Miner Res. 2013 Dec 27. [Epub ahead of print]. PMID: 24375788.

Wang B, Wan JY, Zhang L, et al. Synthetic RGDS peptide attenuates mechanical ventilation-induced lung injury in rats. Exp Lung Res. 2012 May;38(4):204-10. PMID: 22452721.

R2514 RGDV

5 mg
10 mg
25 mg

$C_{17}H_{31}N_7O_7$ FW: 445.5 [93674-99-8] ≥98%

Arg-Gly-Asp-Val

Binds cell surface integrins, enhancing the efficacy of anticancer and anti-aggregation compounds.

Jin S, Wang Y, Zhu H, et al. Nanosized aspirin-Arg-Gly-Asp-Val: delivery of aspirin to thrombus by the target carrier Arg-Gly-Asp-Val tetrapeptide. ACS Nano. 2013 Sep 24;7(9):7664-73. PMID: 23931063.

Wang F, Cui C, Ren Z, et al. Preparation and biological evaluation of tumor-specific Ara-C liposomal preparations containing RGDV motif. J Pharm Sci. 2012 Dec;101(12):4559-68. PMID: 23023730.

R2516 RGES

0.5 mg
1 mg
2.5 mg

$C_{16}H_{29}N_7O_8$ FW: 447.45 [93674-97-6] ≥95%

H-Arg-Gly-Glu-Ser-OH

Used as control to measure RGDS peptide activity. It represents the fibroblast-binding site of fibronectin.

Philippeaux MM, Bargetzi JP, Pache JC, et al. Culture and functional studies of mouse macrophages on native-like fibrillar type I collagen. Eur J Cell Biol. 2009 Apr;88(4):243-56. PMID: 19124174.

R2599 RGYSLG

1 mg
2 mg
5 mg

$C_{28}H_{45}N_9O_9$ FW: 651.73 [110590-63-1] ≥95%

H-Arg-Gly-Tyr-Ser-Leu-Gly-OH

It contains a general protein kinase active site that becomes phosphorylated and can be used to measure kinase activity.

Pattanaik A, Gowda DC, Urry DW. Phosphorylation and dephosphorylation modulation of an inverse temperature transition. Biochem Biophys Res Commun. 1991 Jul 31;178(2):539-45. PMID: 1859415.

R2917 Rhein

100 mg
500 mg
1 g

Monorhein; Cassic acid

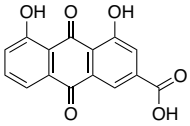

$C_{15}H_8O_6$ FW: 284.22 [478-43-3] ≥88%

Diacerein metabolite found in *Rheus*. It displays a variety of biological activities, including inhibiting LPS-stimulated production of pro-inflammatory cytokines, preventing hyperglycemia-induced apoptosis in β cells, inducing apoptosis in gastric cancer cells, and suppressing vessel plexus formation and endothelial cell migration.

Gao Y, Chen X, Fang L, et al. Rhein exerts pro- and anti-inflammatory actions by targeting IKKβ inhibition in LPS-activated macrophages. Free Radic Biol Med. 2014 Jul;72:104-12. PMID: 24721152.

Liu J, Chen Z, Zhang Y, et al. Rhein protects pancreatic β-cells from dynamin-related protein-1-mediated mitochondrial fission and cell apoptosis under hyperglycemia. Diabetes. 2013 Nov;62(11):3927-35. PMID: 23919963.

R3197 Rhyncholphylline

5 mg
10 mg
25 mg

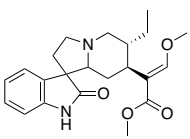

$C_{22}H_{28}N_2O_4$ FW: 384.47 [76-66-4] ≥98.0%

NMDA receptor antagonist and hERG K^+ and L-type Ca^{2+} channel channel blocker found in *Uncaria sinensis*. It inhibits platelet aggregation, downregulates expression of the NR2B NMDA receptor subunit, protects against glutamate-induced neuronal death, and decreases levels of superoxide anions.

Zhou JY, Mo ZX, Zhou SW. Rhynchophylline down-regulates NR2B expression in cortex and hippocampal CA1 area of amphetamine-induced conditioned place preference rat. Arch Pharm Res. 2010 Apr;33(4):557-65. PMID: 20422365.

Hsieh CL, Ho TY, Su SY, et al. Uncaria rhynchophylla and Rhynchophylline inhibit c-Jun N-terminal kinase phosphorylation and nuclear factor-kappaB activity in kainic acid-treated rats. Am J Chin Med. 2009;37(2):351-60. PMID: 19507277.

R3205 Ribavirin

25 mg
50 mg
100 mg
500 mg

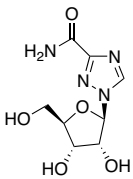

$C_8H_{12}N_4O_5$ FW: 244.21 [36791-04-5] ≥98%

Purine analog and DNA chain terminator used in conjunction with IFN to treat hepatitis C infection. It also decreases NO levels in macrophages.

Pinilla-Macua I, Fernández-Calotti P, Pérez-Del-Pulgar S, et al. Ribavirin Uptake into Human Hepatocyte HHL5 Cells Is Enhanced by Interferon-α via up-Regulation of the Human Concentrative Nucleoside Transporter (hCNT2). Mol Pharm. 2014 Sep 2;11(9):3223-30. PMID: 24957263.

Parekh PJ, Shiffman ML. The role of interferon in the new era of hepatitis C treatments. Expert Rev Gastroenterol Hepatol. 2014 Aug;8(6):649-56. PMID: 24758387.

Wohl BM, Smith AA, Kryger MB, et al. Narrow therapeutic window of ribavirin as an inhibitor of nitric oxide synthesis is broadened by macromolecular prodrugs. Biomacromolecules. 2013 Nov 11;14(11):3916-26. PMID: 24156371.

R3206

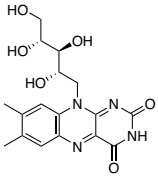

Riboflavin

Vitamin B2; Lactoflavin; Vitamin G

25 g
100 g

$C_{17}H_{20}N_4O_6$ FW: 376.36 [83-88-5] ≥97%

Essential vitamin (B2) found in vegetables, dairy, legumes used to treat migraines. It plays a role in metabolism and oxidation-reduction reactions and is a required cofactor for flavins and flavoproteins.

Taylor FR. Nutraceuticals and headache: the biological basis. Headache. 2011 Mar;51(3):484-501. PMID: 21352223.

R3310

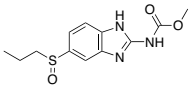

Ricobendazole

Albendazole sulfoxide

10 g
25 g
100 g

$C_{12}H_{15}N_3O_3S$ FW: 281.33 [54029-12-8] ≥98%

Microtubule polymerization inhibitor used to treat worm infections. It also inhibits proliferation of various cancer cells.

Lopes WD, Cruz BC, Soares VE, et al. Historic of therapeutic efficacy of albendazol sulphoxide administered in different routes, dosages and treatment schemes, against Taenia saginata cysticercus in cattle experimentally infected. Exp Parasitol. 2014 Feb;137:14-20. PMID: 24309372.

Belaz KR, Denadai M, Almeida AP, et al. Enantiomeric resolution of albendazole sulfoxide by semipreparative HPLC and in vitro study of growth inhibitory effects on human cancer cell lines. J Pharm Biomed Anal. 2012 Jul;66:100-8. PMID: 22487592.

R3312

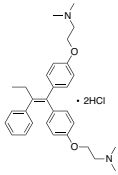

Ridaifen A Dihydrochloride

25 mg
100 mg
250 mg

$C_{30}H_{38}N_2O_2 \cdot 2HCl$ FW: 531.56 ≥98%

Tamoxifen derivative and potential proteasome inhibitor. It increases ROS levels and induces apoptosis in breast cancer cells.

Hasegawa M, Yasuda Y, Tanaka M, et al. A novel tamoxifen derivative, ridaifen-F, is a nonpeptidic small-molecule proteasome inhibitor. Eur J Med Chem. 2013 Nov 16;71C:290-305. PMID: 24321833.

Guo WZ, Shiina I, Wang Y, et al. Ridaifen-SB8, a novel tamoxifen derivative, induces apoptosis via reactive oxygen species-dependent signaling pathway. Biochem Pharmacol. 2013 Nov 1;86(9):1272-84. PMID: 23973528.

R3220

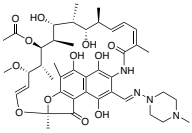

Rifampicin

1 g
5 g
25 g

$C_{43}H_{58}N_4O_{12}$ FW: 822.94 [13292-46-1] ≥98%

Inhibitor of bacterial DNA-dependent RNA polymerase and RNA synthesis used to treat tuberculosis and meningitis. It also decreases expression of the 26S protease regulatory subunit to suppress inflammatory cytokine release and increases clearance of amyloid-β peptides.

Sharma SK, Sharma A, Kadhiravan T, et al. Rifamycins (rifampicin, rifabutin and rifapentine) compared to isoniazid for preventing tuberculosis in HIV-negative people at risk of active TB. Cochrane Database Syst Rev. 2013 Jul 5;7:CD007545. PMID: 23828580.

Bi W, Jing X, Zhu L, et al. Inhibition of 26S protease regulatory subunit 7 (MSS1) suppresses neuroinflammation. PLoS One. 2012;7(5):e36142. PMID: 22629310.

Qosa H, Abuznait AH, Hill RA, et al. Enhanced brain amyloid-β clearance by rifampicin and caffeine as a possible protective mechanism against Alzheimer's disease. J Alzheimers Dis. 2012;31(1):151-65. PMID: 22504320.

R3222

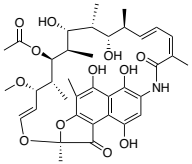

Rifamycin SV Monosodium

1 g
5 g

$C_{37}H_{46}NO_{12}Na$ FW: 719.75 [14897-39-3] ≥98%

Inhibitor of bacterial DNA-dependent RNA polymerase and RNA synthesis used to treat tuberculosis and leprosy. It also decreases LPS-stimulated cytokine synthesis in macrophages and CD4+ T cells.

Rosette C, Buendia-Laysa F Jr, Patkar S, et al. Anti-inflammatory and immunomodulatory activities of rifamycin SV. Int J Antimicrob Agents. 2013 Aug;42(2):182-6. PMID: 23756321.

Farrell DJ, Putnam SD, Biedenbach DJ, et al. In vitro activity and single-step mutational analysis of rifamycin SV tested against enteropathogens associated with traveler's diarrhea and *Clostridium difficile*. Antimicrob Agents Chemother. 2011 Mar;55(3):992-6. PMID: 21149623.

R3221

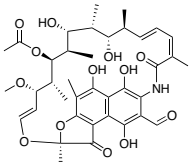

3-Formylrifamycin

3-Formylrifampicin SV; Rifaldehyde; Rifamycin AF

1 g
5 g
10 g

$C_{38}H_{47}NO_{13}$ FW: 725.78 [13292-22-3] ≥98%

Rifamycin derivative and DNA-dependent RNA polymerase inhibitor that induces pore formation in mitochondrial membranes. It is particularly effective against *Mycobacterium*.

Nedyalkova Z, Haladjova S, et al. QSAR Modeling of Antimycobacterial Activity and Activity Against Other Bacteria of 3-Formyl Rifamycin SV Derivatives. Mol inform. 2001 Nov;20(4): 298–318.

R3321

Rifaximin

500 mg
1 g
5 g

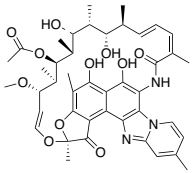

$C_{43}H_{51}N_3O_{11}$ FW: 785.88 [80621-81-4] ≥98%

Rifampicin derivative and DNA-dependent RNA polymerase inhibitor used to treat small intestinal bacterial overgrowth associated with IBS.

Huhulescu S, Sagel U, Fiedler A, et al. Rifaximin disc diffusion test for in vitro susceptibility testing of *Clostridium difficile*. J Med Microbiol. 2011 Aug;60(Pt 8):1206-12. PMID: 21292853.

Majewski M, McCallum RW. Results of small intestinal bacterial overgrowth testing in irritable bowel syndrome patients: clinical profiles and effects of antibiotic trial. Adv Med Sci. 2007;52:139-42. PMID: 18217406.

R3224

Rigin

5 mg
10 mg
25 mg

GQPR

H-Gly-Gln-Pro-Arg-OH

$C_{18}H_{32}N_8O_6$ FW: 456.51 [77727-17-4] ≥95%

IgG derivative and tuftsin analog that stimulates phagocytosis, activates lymphocytes, and protects against stress-induced damage.

Dutta RC, Puri A, Anand N. Immunomodulatory potential of hydrophobic analogs of Rigin and their role in providing protection against *Plasmodium* berghei infection in mice. Int Immunopharmacol. 2001 May;1(5):843-55. PMID: 11379040.

R3347

Riluzole

25 mg
250 mg
500 mg

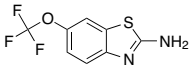

$C_8H_5F_3N_2OS$ FW: 234.19 [1744-22-5] ≥98%

TRPC5 receptor agonist, PTR1 inhibitor, voltage-gated Na^+ channel blocker, and GLT-1 modulator used to treat symptoms of amyotrophic lateral sclerosis. It also increases response latency in thermal pain models, increases glucose transport, potentially inhibits kainate receptors and NMDA receptors, and suppresses growth of *Leishmania*.

Richter JM, Schaefer M, Hill K. Riluzole activates TRPC5 channels independently of PLC activity. Br J Pharmacol. 2014 Jan;171(1):158-70. PMID: 24117252.

Daniel B, Green O, Viskind O, et al. Riluzole increases the rate of glucose transport in L6 myotubes and NSC-34 motor neuron-like cells via AMPK pathway activation. Amyotroph Lateral Scler Frontotemporal Degener. 2013 Sep;14(5-6):434-43. PMID: 23834207.

R3249

Rimantadine Hydrochloride

25 mg
50 mg
250 mg
1 g

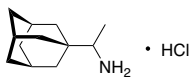

$C_{12}H_{21}N \bullet HCl$ FW: 215.76 [1501-84-4] ≥98%

Viral M2 proton channel blocker used to treat influenza infection.

Ivanovic T, Rozendaal R, Floyd DL, et al. Kinetics of proton transport into influenza virions by the viral M2 channel. PLoS One. 2012;7(3):e31566. PMID: 22412838.

Leonov H, Astrahan P, Krugliak M, et al. How do aminoadamantanes block the influenza M2 channel, and how does resistance develop? J Am Chem Soc. 2011 Jun 29;133(25):9903-11. PMID: 21534619.

R3373

Risedronate Sodium Hydrate

25 mg
100 mg
500 mg

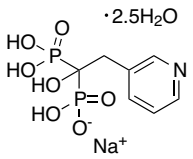

$C_7H_{10}NO_7P_2Na \bullet 2.5H_2O$ FW: 350.13 [115436-72-1] ≥98%

Osteoporosis treatment agent that also inhibits transfer of farnesyl pyrophosphate. It inhibits bone marrow adipogenesis, induces apoptosis in osteoclasts, and increases bone mineral density. It also limits *Plasmodium* survival.

Lems WF, den Heijer M. Established and forthcoming drugs for the treatment of osteoporosis. Neth J Med. 2013 May;71(4):188-93. PMID: 23723112.

Jin J, Wang L, Wang XK, et al. Risedronate inhibits bone marrow mesenchymal stem cell adipogenesis and switches RANKL/OPG ratio to impair osteoclast differentiation. J Surg Res. 2013 Mar;180(1):e21-9. PMID: 22487394.

R3374

Risedronic Acid

25 mg
100 mg
250 mg

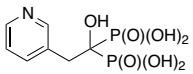

$C_7H_{11}NO_7P_2$ FW: 283.11 [105462-24-6] ≥97%

It inhibits transfer of farnesyl pyrophosphate and is used to treat osteoporosis. It inhibits bone marrow adipogenesis, decreases release of TNF-α and leukotriene B4, and suppresses growth of *Plasmodium*.

Jin J, Wang L, Wang XK, et al. Risedronate inhibits bone marrow mesenchymal stem cell adipogenesis and switches RANKL/OPG ratio to impair osteoclast differentiation. J Surg Res. 2013 Mar;180(1):e21-9. PMID: 22487394.

Jordão FM, Saito AY, Miguel DC, et al. In vitro and in vivo antiplasmodial activities of risedronate and its interference with protein prenylation in *Plasmodium falciparum*. Antimicrob Agents Chemother. 2011 May;55(5):2026-31. PMID: 21357292.

R3475 Risperidone

100 mg
250 mg
1 g

$C_{23}H_{27}FN_4O_2$ FW: 410.49 [106266-06-2] ≥98%

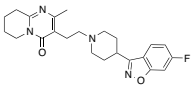

5-HT7 receptor and NMDA receptor agonist and inhibitor of D-amino acid oxidase, 5-HT2A receptors and dopamine D2 receptors antagonist. It also increases expression of PPARγ and decreases LPS-induced expression of pro-inflammatory cytokines in inflammation models.

Kamińska K, Gołembiowska K, Rogóż Z. Effect of risperidone on the fluoxetine-induced changes in extracellular dopamine, serotonin and noradrenaline in the rat frontal cortex. Pharmacol Rep. 2013;65(5):1144-51. PMID: 24399710.

MacDowell KS, García-Bueno B, Madrigal JL, et al. Risperidone normalizes increased inflammatory parameters and restores anti-inflammatory pathways in a model of neuroinflammation. Int J Neuropsychopharmacol. 2013 Feb;16(1):121-35. PMID: 22176740.

Kozielska M, Johnson M, Pilla Reddy V, et al. Pharmacokinetic-pharmacodynamic modeling of the D2 and 5-HT (2A) receptor occupancy of risperidone and paliperidone in rats. Pharm Res. 2012 Jul;29(7):1932-48. PMID: 22437487.

R3476 RITA

NEW

5 mg
10 mg

Reactivation of p53 and induction of tumor cell apoptosis

$C_{14}H_{12}O_3S_2$ FW: 292.37 [213261-59-7] ≥98%

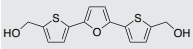

Activator of p53. It downregulates expression of VEGF, HIF-1α, p21, and HDM2 and induces apoptosis in neuroblastoma models.

Burmakin M, Shi Y, Hedström E, et al. Dual targeting of wild-type and mutant p53 by small molecule RITA results in the inhibition of N-Myc and key survival oncogenes and kills neuroblastoma cells in vivo and in vitro. Clin Cancer Res. 2013 Sep 15;19(18):5092-103. PMID: 23864164.

Henze J, Mühlenberg T, Simon S, et al. p53 modulation as a therapeutic strategy in gastrointestinal stromal tumors. PLoS One. 2012;7(5):e37776. PMID: 22662219.

Zhao CY, Szekely L, Bao W, et al. Rescue of p53 function by small-molecule RITA in cervical carcinoma by blocking E6-mediated degradation. Cancer Res. 2010 Apr 15;70(8):3372-81. PMID: 20395210.

R3477 Ritodrine Hydrochloride

250 mg
1 g
5 g

$C_{17}H_{21}NO_3 \cdot HCl$ FW: 323.82 [23239-51-2] ≥98%

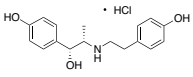

β2-Adrenergic receptor agonist and SK/BK and ATP-sensitive K^+ channel activator used to prevent preterm labor. It decreases prostanoid signaling, inhibits uterine contractility, and may induce the formation of pruritic erythematous papular eruptions.

Sato Y, Teraki Y, Izaki S, et al. Ritodrine-induced erythematous papular eruption in 14 pregnant women. Int J Dermatol. 2010 Dec;49(12):1450-3. PMID: 21091685.

Schwarz MK, Page P. Preterm labour: an overview of current and emerging therapeutics. Curr Med Chem. 2003 Aug;10(15):1441-68. PMID: 12871140.

R3584 Rivaroxaban

1 mg
5 mg
25 mg

$C_{19}H_{18}ClN_3O_5S$ FW: 435.88 [366789-02-8] ≥98%

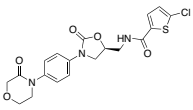

Oxazolidone derivative and factor Xa inhibitor used to prevent deep vein thrombosis and venous thromboembolism. It inhibits free and clot-bound forms of factor Xa. It also suppresses hormone-stimulated modulation of ER and 1-OHase expression and DNA synthesis.

Kreutz R. Pharmacokinetics and Pharmacodynamics of Rivaroxaban - An Oral, Direct Factor Xa Inhibitor. Curr Clin Pharmacol. 2013 Nov 11. [Epub ahead of print]. PMID: 24218999.

Somjen D, Katzburg S, Gigi R, et al. Rivaroxaban, a direct inhibitor of the coagulation factor Xa interferes with hormonal-induced physiological modulations in human female osteoblastic cell line SaSO2. J Steroid Biochem Mol Biol. 2013 May;135:67-70. PMID: 23333933

Gigi R, Salai M, Dolkart O, et al. The effects of direct factor Xa inhibitor (Rivaroxaban) on the human osteoblastic cell line SaOS2. Connect Tissue Res. 2012;53(6):446-50. PMID: 22800431.

R3586 Rivastigmine Tartrate

100 mg
250 mg
1 g

$C_{14}H_{22}N_2O_2 \cdot C_4H_6O_6$ FW: 400.43 [129101-54-8] ≥98%

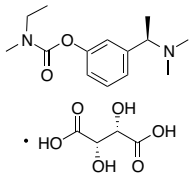

AChE and BChE inhibitor used to treat dementia. It improves memory impairment in a CaMKII-dependent manner and decreases secretion of Aβ.

Moriguchi S, Tagashira H, Sasaki Y, et al. CaMKII activity is essential for improvement of memory-related behaviors by chronic rivastigmine treatment. J Neurochem. 2013 Oct 28. [Epub ahead of print]. PMID: 24164423.

Bailey JA, Ray B, Greig NH, et al. Rivastigmine lowers Aβ and increases sAPPα levels, which parallel elevated synaptic markers and metabolic activity in degenerating primary rat neurons. PLoS One. 2011;6(7):e21954. PMID: 21799757.

Pollak Y, Gilboa A, Ben-Menachem O, et al. Acetylcholinesterase inhibitors reduce brain and blood interleukin-1beta production. Ann Neurol. 2005 May;57(5):741-5. PMID: 15852394.

R4132 RKI-1447

NEW

1 mg
5 mg

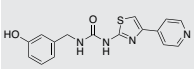

$C_{16}H_{14}N_4O_2S$ FW: 326.37 [1342278-01-6] ≥98%

ROCK1/2 inhibitor. It inhibits formation of actin stress fibers and prevents migration, invasion, and growth of breast cancer cells.

Patel RA, Forinash KD, Pireddu R, et al. RKI-1447 is a potent inhibitor of the Rho-associated ROCK kinases with anti-invasive and antitumor activities in breast cancer. Cancer Res. 2012 Oct 1;72(19):5025-34. PMID: 22846914.

R5212 RN-486

NEW

1 mg
5 mg

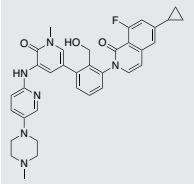

$C_{35}H_{35}FN_6O_3$ FW: 606.69 [1242156-23-5] ≥98%

Btk inhibitor. It decreases release of pro-inflammatory cytokines, inhibits B-cell activation and anti-double-stranded DNA IgG production, and prevents type I and III hypersensitivity responses.

Zhao X, Huang W, Wang Y, et al. Discovery of novel Bruton's tyrosine kinase (BTK) inhibitors bearing a pyrrolo[2,3-d]pyrimidine scaffold. Bioorg Med Chem. 2015 Feb 15;23(4):891-901. PMID: 25596757.

Hartkamp LM, Fine JS, van Es IE, et al. Btk inhibition suppresses agonist-induced human macrophage activation and inflammatory gene expression in RA synovial tissue explants. Ann *Rheum* Dis. 2014 Apr 24. [Epub ahead of print]. PMID: 24764451.

Wang J, Lau KY, Jung J, et al. Bruton's tyrosine kinase regulates TLR9 but not TLR7 signaling in human plasmacytoid dendritic cells. Eur J Immunol. 2014 Apr;44(4):1130-6. PMID: 24375473.

R5700 Ro 61-8048

NEW

5 mg
25 mg

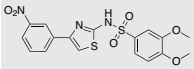

$C_{17}H_{15}N_3O_6S_2$ FW: 421.44 [199666-03-0] ≥98%

Kynurenine 3-hydroxylase inhibitor. It prevents inflammation and decreases L-DOPA-induced dyskinesia.

Pisar M, Forrest CM, Khalil OS, et al. Modified neocortical and cerebellar protein expression and morphology in adult rats following prenatal inhibition of the kynurenine pathway. Brain Res. 2014 Aug 12;1576:1-17. PMID: 24956103.

Ouattara B, Belkhir S, Morissette M, et al. Implication of NMDA receptors in the antidyskinetic activity of cabergoline, CI-1041, and Ro 61-8048 in MPTP monkeys with levodopa-induced dyskinesias. J Mol Neurosci. 2009 Jun;38(2):128-42. PMID: 18704766.

R5611 Rocuronium Bromide

10 mg
25 mg
100 mg
250 mg

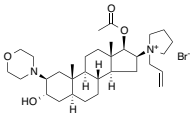

$C_{32}H_{53}BrN_2O_4$ FW: 609.68 [119302-91-9] ≥98%

Non-depolarizing NMJ blocker and antagonist at nAChRs and M2/3 mAChRs. It is used as an anesthetic, inhibiting skeletal muscle contractions.

Pape A, Kertscho H, Stein P, et al. Neuromuscular blockade with rocuronium bromide increases the tolerance of acute normovolemic anemia in anesthetized pigs. Eur Surg Res. 2012;48(1):16-25. PMID: 22189343.

R5722 Rofecoxib

100 mg
250 mg
1 g
5 g

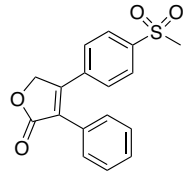

$C_{17}H_{14}O_4S$ FW: 314.36 [162011-90-7] ≥98%

NSAID and COX-2 inhibitor previously used to treat pain and arthritis. It also inhibits the formation of bladder tumors and increases seizure threshold in an adenosine-dependent manner.

D'Arca D, LeNoir J, Wildemore B, et al. Prevention of urinary bladder cancer in the FHIT knock-out mouse with Rofecoxib, a Cox-2 inhibitor. Urol Oncol. 2010 Mar-Apr;28(2):189-94. PMID: 19372053.

Akula KK, Dhir A, Kulkarni SK. Rofecoxib, a selective cyclooxygenase-2 (COX-2) inhibitor increases pentylenetetrazol seizure threshold in mice: possible involvement of adenosinergic mechanism. Epilepsy Res. 2008 Jan;78(1):60-70. PMID: 18054463.

R5749 Romidepsin

NEW

1 mg
5 mg

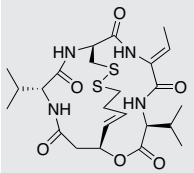

FK228; Depsipeptide; FR901228

$C_{24}H_{36}N_4O_6S_2$ FW: 540.7 [128517-07-7] ≥98%

HDAC inhibitor. It enhances NK cell cytotoxicity, induces cell cycle arrest and apoptosis in non-small cell lung cancer cells, increases HIV expression from infected CD4+ T cells, and stimulates MIC A/B expression on tumor cells in leukemia and lymphoma models.

Foss F, Coiffier B, Horwitz S, et al. Tolerability to romidepsin in patients with relapsed/refractory T-cell lymphoma. Biomark Res. 2014 Sep 8;2:16. PMID: 25279222.

Satwani P, Bavishi S, Saha A, et al. Upregulation of NKG2D ligands in acute lymphoblastic leukemia and non-Hodgkin lymphoma cells by romidepsin and enhanced in vitro and in vivo natural killer cell cytotoxicity. Cytotherapy. 2014 May 20. [Epub ahead of print]. PMID: 24856896.

Wei DG, Chiang V, Fyne E, et al. Histone deacetylase inhibitor romidepsin induces HIV expression in CD4 T cells from patients on suppressive antiretroviral therapy at concentrations achieved by clinical dosing. PLoS Pathog. 2014 Apr 10;10(4):e1004071. PMID: 24722454.

R5661

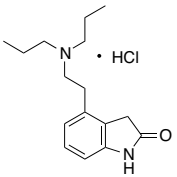

Ropinirole Hydrochloride

25 mg
100 mg
500 mg

SKF-101468A

$C_{16}H_{24}N_2O \cdot HCl$ FW: 296.84 [91374-20-8] ≥99%

Dopamine D2/3 receptor agonist used to treat restless leg syndrome and Parkinson's disease. It prevents dopaminergic neuron damage and decreases immobility time in the forced swim test.

Park G, Park YJ, Yang HO, et al. Ropinirole protects against 1-methyl-4-phenyl-1, 2, 3, 6-tetrahydropyridine (MPTP)-induced neurotoxicity in mice via anti-apoptotic mechanism. Pharmacol Biochem Behav. 2013 Mar;104:163-8. PMID: 23369986.

Ferini-Strambi L. Treatment options for restless legs syndrome. Expert Opin Pharmacother. 2009 Mar;10(4):545-54. PMID: 19284359.

R5774

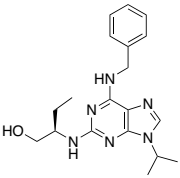

Roscovitine

1 mg
5 mg
10 mg

Seliciclib; CYC202

$C_{19}H_{26}N_6O$ FW: 354.45 [186692-46-6] ≥98%

Inhibitor of CDKs and L-type Ca^{2+} channels. It resolves neutrophil-driven inflammation and induces cell cycle arrest and apoptosis in B-cell lymphoma cells.

Leitch AE, Haslett C, Rossi AG. Cyclin-dependent kinase inhibitor drugs as potential novel anti-inflammatory and pro-resolution agents. Br J Pharmacol. 2009 Oct;158(4):1004-16. PMID: 19775281.

Yarotskyy V, Elmslie KS. Roscovitine, a cyclin-dependent kinase inhibitor, affects several gating mechanisms to inhibit cardiac L-type (Ca(V)1.2) calcium channels. Br J Pharmacol. 2007 Oct;152(3):386-95. PMID: 17700718.

R5773

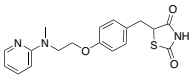

Rosiglitazone

100 mg
500 mg
1 g
5 g

BRL-49653

$C_{18}H_{19}N_3O_3S$ FW: 357.43 [122320-73-4] ≥98%

PPARγ agonist used to manage diabetes. It lowers blood glucose and insulin levels, decreases LPS-stimulated pro-inflammatory cytokine production, inhibits endothelin-1-induced vasoconstriction, and prevents activation of AP-1, production of collagen, and differentiation in fibroblasts.

Rui M, Huang Z, Liu Y, et al. Rosiglitazone suppresses angiogenesis in multiple myeloma via downregulation of hypoxia inducible factor 1α and insulin like growth factor 1 mRNA expression. Mol Med Rep. 2014 Jul 22. [Epub ahead of print]. PMID: 25050627.

Mingfeng D, Xiaodong M, Yue L, et al. Effects of PPAR-γ Agonist Treatment on LPS-Induced Mastitis in Rats. Inflammation. 2014 May 18. [Epub ahead of print]. PMID: 24839089.

Liu Y, Tian XY, Huang Y, et al. Rosiglitazone Attenuated Endothelin-1-Induced Vasoconstriction of Pulmonary Arteries in the Rat Model of Pulmonary Arterial Hypertension via Differential Regulation of ET-1 Receptors. PPAR Res. 2014;2014:374075. PMID: 24701204.

R5772

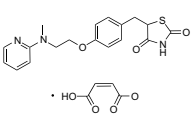

Rosiglitazone Maleate

100 mg
500 mg
1 g
5 g

BRL-49653c

$C_{18}H_{19}N_3O_3S \cdot C_4H_4O_4$ FW: 473.51 [155141-29-0] ≥98%

PPARγ agonist and insulin sensitizer used to treat diabetes. It decreases LPS-stimulated production of pro-inflammatory cytokines, inhibits cell viability and proliferation in multiple myeloma cells, and suppresses endothelin-1-induced vasoconstriction.

Rui M, Huang Z, Liu Y, et al. Rosiglitazone suppresses angiogenesis in multiple myeloma via downregulation of hypoxia inducible factor 1α and insulin like growth factor 1 mRNA expression. Mol Med Rep. 2014 Jul 22. [Epub ahead of print]. PMID: 25050627.

Mingfeng D, Xiaodong M, Yue L, et al. Effects of PPAR-γ Agonist Treatment on LPS-Induced Mastitis in Rats. Inflammation. 2014 May 18. [Epub ahead of print]. PMID: 24839089.

R5874

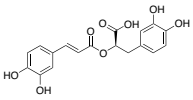

Rosmarinic Acid

10 mg
25 mg
100 mg

$C_{18}H_{16}O_8$ FW: 360.31 [20283-92-5] ≥98%

GABA transaminase and Fyn kinase inhibitor found in *Melissa*, *Salvia*, and *Rosmarinus*. It displays a wide variety of biological activities, including decreasing immobility time in the forced swim test, inhibiting aggregation of amyloid-β peptides, suppressing DMBA-induced carcinogenesis, and preventing CCL4-induced hepatic fibrosis.

Airoldi C, Sironi E, Dias C, et al. Natural compounds against Alzheimer's disease: molecular recognition of Aβ1-42 peptide by *Salvia* sclareoides extract and its major component, rosmarinic acid, as investigated by NMR. Chem Asian J. 2013 Mar;8(3):596-602. PMID: 23303581.

Anusuya C, Manoharan S. Antitumor initiating potential of rosmarinic acid in 7,12-dimethylbenz(a)anthracene-induced hamster buccal pouch carcinogenesis. J Environ Pathol Toxicol Oncol. 2011;30(3):199-211. PMID: 22126613.

R5878 Rotenone

1 g
5 g
25 g

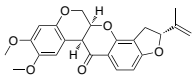

$C_{23}H_{22}O_6$ FW: 394.41 [83-79-4] ≥97%

Antimitotic and oxidative phosphorylation inhibitor. It inhibits the mitochondrial electron transport complex I, altering mitochondrial respiration and inducing mitochondrial oxidative stress. It also inhibits background K^+ currents and activates microglial superoxide release.

Johnson GE, Parry EM. Mechanistic investigations of low dose exposures to the genotoxic compounds bisphenol-A and rotenone. Mutat Res. 2008 Mar 12;651(1-2):56-63. PMID: 18083626.

Sherer TB, Richardson JR, Testa CM, et al. Mechanism of toxicity of pesticides acting at complex I: relevance to environmental etiologies of Parkinson's disease. J Neurochem. 2007 Mar;100(6):1469-79. PMID: 17241123.

R5894 Roxatidine Acetate Hydrochloride

100 mg
500 mg
1 g

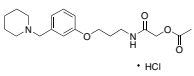

$C_{19}H_{28}N_2O_4 \cdot HCl$ FW: 384.9 [93793-83-0] ≥98%

Histamine H2 antagonist used to treat gastric ulcers. It prevents gastric acid secretion and prevents indomethacin-induced small intestine injury.

Umegaki E, Yoda Y, Tokioka S, et al. Protective effect of roxatidine against indomethacin-induced small intestinal mucosal injury in rats. J Gastroenterol Hepatol. 2010 May;25 Suppl 1:S35-40. PMID: 20586863.

R5992 Roxithromycin

1 g
5 g
10 g

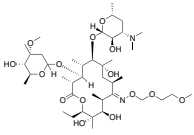

$C_{41}H_{76}N_2O_{15}$ FW: 837.05 [80214-83-1] ≥96%

Protein synthesis inhibitor used to treat various bacterial infections. It also suppresses airway hyperresponsiveness, induces vascular relaxation in arteries, and inhibits T cell production of TNF-α and IL-6.

Ci X, Chu X, Xu X, et al. Short-term roxithromycin treatment attenuates airway inflammation via MAPK/NF-κB activation in a mouse model of allergic asthma. Inflamm Res. 2012 Jul;61(7):749-58. PMID: 22481373.

Biava M, Porretta GC, Deidda D, et al. New trends in development of antimycobacterial compounds. Infect Disord Drug Targets. 2006 Jun;6(2):159-72. PMID: 16789877.

Urasaki Y, Nori M, Iwata S, et al. Roxithromycin specifically inhibits development of collagen induced arthritis and production of proinflammatory cytokines by human T cells and macrophages. J Rheumatol. 2005 Sep;32(9):1765-74. PMID: 16142877.

R6871 RR-SRC

5 mg
10 mg
25 mg

H-Arg-Arg-Leu-Ile-Glu-Asp-Ala-Glu-Tyr-Ala-Ala-Arg-Gly-OH

$C_{64}H_{106}N_{22}O_{21}$ FW: 1519.7 ≥95%

Src-derived tyrosine kinase substrate.

Hernández-Ramírez VI, Anaya-Ruiz M, Rios A, et al. *Entamoeba* histolytica: tyrosine kinase activity induced by fibronectin through the beta1-integrin-like molecule. Exp Parasitol. 2000 Jun;95(2):85-95. PMID: 10910709.

R6873 RSR

1 mg
2 mg
5 mg

H-Arg-Ser-Arg-OH

$C_{15}H_{31}N_9O_5$ FW: 417.5 ≥95%

Used in design of DNA-binding peptides.

Alkhader S, Ezra A, Kasparkova J, et al. A metal-free DNA nuclease based on a cyclic peptide scaffold. Bioconjug Chem. 2010 Aug 18;21(8):1425-31. PMID: 20715847.

R8206 Rubescensin A

25 mg
100 mg
500 mg

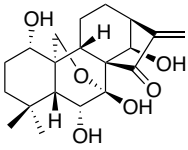

Oridonin; Isodono

$C_{20}H_{28}O_6$ FW: 364.43 [28957-04-2] ≥93%

Found in *Rabdosia*. It may inhibit proliferation in cancer cells.

Zhang Y, Xiao S, Sun L, et al. Rapid screening of bioactive compounds from natural products by integrating 5-channel parallel chromatography coupled with on-line mass spectrometry and microplate based assays. Anal Chim Acta. 2013 May 13;777:49-56. PMID: 23622964.

R8207 β-Rubromycin

1 mg
5 mg

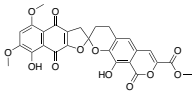

$C_{27}H_{20}O_{12}$ FW: 536.44 [27267-70-5] ≥98%

Telomerase and HIV-1 reverse transcriptase inhibitor. It inhibits growth of viruses and bacteria and decreases proliferation of some cancer cells.

Mizushina Y, Takeuchi T, Sugawara F, et al. Anti-cancer targeting telomerase inhibitors: β-rubromycin and oleic acid. Mini Rev Med Chem. 2012 Oct;12(11):1135-43. PMID: 22876944.

Ueno T, Takahashi H, Oda M, et al. Inhibition of human telomerase by rubromycins: implication of spiroketal system of the compounds as an active moiety. Biochemistry. 2000 May 23;39(20):5995-6002. PMID: 10821671.

R8122

Rufloxacin Hydrochloride

25 mg
100 mg
500 mg

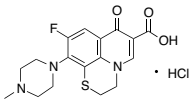

$C_{17}H_{18}FN_3O_3S \bullet HCl$ FW: 399.87 [106017-08-7] ≥98%

Topoisomerase IV and bacterial DNA gyrase inhibitor used to treat bacterial infections. It also induces DNA base oxidation under UV light.

Gu LY, Lin WW, Lu H, et al. Quadruple therapy with medications containing either rufloxacin or furazolidone as a rescue regimen in the treatment of *Helicobacter pylori*-infected dyspepsia patients: a randomized pilot study. *Helicobacter*. 2011 Aug;16(4):284-8. PMID: 21762267.

R8178

Rutaecarpine

10 mg
25 mg
100 mg

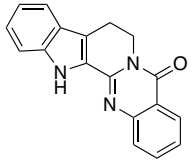

$C_{18}H_{13}N_3O$ FW: 287.32 [84-26-4] ≥98%

Inhibitor of COX-2 and potential inhibitor of cAMP, 3β-HSD, and 11β-hydroxylase found in *Evodia rutaecarpa*. It decreases food intake, weight gain, and serum glucose, leptin, and insulin levels, and inhibits accumulation of macrophages and cholesterol in atherosclerotic lesions. It also inhibits collagen-stimulated formation of thromboxane B2 and inosine monophosphate.

Xu Y, Liu Q, Xu Y, et al. Rutaecarpine suppresses atherosclerosis in ApoE-/- mice through up-regulating ABCA1 and SR-BI within RCT. J Lipid Res. 2014 Jun 7. [Epub ahead of print]. PMID: 24908654.

Bao MH, Dai W, Li YJ, et al. Rutaecarpine prevents hypoxia-reoxygenation-induced myocardial cell apoptosis via inhibition of NADPH oxidases. Can J Physiol Pharmacol. 2011 Mar;89(3):177-86. PMID: 21423291.

Kim SJ, Lee SJ, Lee S, et al. Rutecarpine ameliorates bodyweight gain through the inhibition of orexigenic neuropeptides NPY and AgRP in mice. Biochem Biophys Res Commun. 2009 Nov 20;389(3):437-42. PMID: 19732749.

R8179

Rutaecarpine, synthetic

25 mg
100 mg
250 mg
1 g

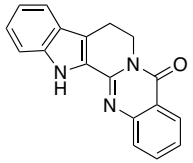

$C_{18}H_{13}N_3O$ FW: 287.32 [84-26-4] ≥98%

Inhibitor of COX-2 and potential inhibitor of cAMP, 3β-HSD, and 11β-hydroxylase found in *Evodia rutaecarpa*. It decreases food intake, weight gain, and serum glucose, leptin, and insulin levels, and inhibits accumulation of macrophages and cholesterol in atherosclerotic lesions. It also inhibits collagen-stimulated formation of thromboxane B2 and inosine monophosphate

Chen YC, Zeng XY, He Y, et al. Rutaecarpine analogues reduce lipid accumulation in adipocytes via inhibiting adipogenesis/lipogenesis with AMPK activation and UPR suppression. ACS Chem Biol. 2013 Oct 18;8(10):2301-11. PMID: 23962138.

Yu PL, Chao HL, Wang SW, et al. Effects of evodiamine and rutaecarpine on the secretion of corticosterone by zona fasciculata-reticularis cells in male rats. J Cell Biochem. 2009 Oct 1;108(2):469-75. PMID: 19639602.

Ko HC, Wang YH, Liou KT, et al. Anti-inflammatory effects and mechanisms of the ethanol extract of *Evodia rutaecarpa* and its bioactive components on neutrophils and microglial cells. Eur J Pharmacol. 2007 Jan 26;555(2-3):211-7. PMID: 17109845.

R8076

Rutin Hydrate

50 g
100 g
500 g

Vitamin P1

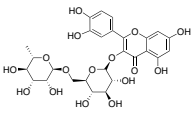

$C_{27}H_{30}O_{16} \bullet 3H_2O$ FW: 610.52 [153-18-4] ≥93%

Found in fruit, asparagus, buckwheat. It displays many biological activities, including decreasing locomotor activity, oxidative stress, and cortisone levels in restraint stress models, inhibiting granulocyte infiltration and increasing antioxidative enzyme expression in acute lung injury models, and protecting against toxicity and cognitive deficits in neurodegenerative diseases.

Yeh CH, Yang JJ, Yang ML, et al. Rutin decreases lipopolysaccharide-induced acute lung injury via inhibition of oxidative stress and the MAPK-NF-κB pathway. Free Radic Biol Med. 2014 Apr;69:249-57. PMID: 24486341.

Machawal L, Kumar A. Possible involvement of nitric oxide mechanism in the neuroprotective effect of rutin against immobilization stress induced anxiety like behaviour, oxidative damage in mice. Pharmacol Rep. 2014 Feb;66(1):15-21. PMID: 24905301.

D. Rutin suppresses palmitic acids-triggered inflammation in macrophages and blocks high fat diet-induced obesity and fatty liver in mice. Pharm Res. 2013 Nov;30(11):2940-50. PMID: 23783345.

S0072

5S rRNA modificator

NEW

5 mg
25 mg

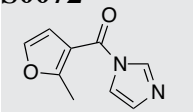

$C_9H_8N_2O_2$ FW: 176.18 [1415238-77-5] ≥98%

Electrophile used in 2'-hydroxyl acylation of RNA.

S0006

S6-1

RRLSSLRA

H-Arg-Arg-Leu-Ser-Ser-Leu-Arg-Ala-OH

$C_{39}H_{75}N_{17}O_{11}$ FW: 958.14 [93674-74-9] ≥95%

1 mg
2 mg
5 mg

Involved in insulin sensitivity and cell proliferation.

Nakagawa M, Ohmido N, Ishikawa K, et al. Anti-peptide antibodies for examining the conformation, molecular assembly and localization of an intracellular protein, ribosomal protein S6, in vivo. J Biochem. 2008 Mar;143(3):325-32. PMID: 18039684.

S0132

Saikosaponin A

$C_{42}H_{68}O_{13}$ FW: 780.98 [20736-09-8] ≥98%

1 mg
5 mg

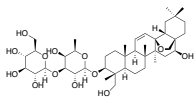

Found in *Bupleurum*. It suppresses production of pro-inflammatory cytokines, increases pain thresholds in chronic constrictive injury, decreases self-administration of cocaine and morphine, and induces apoptosis in colon carcinoma cells.

Zhou X, Cheng H, Xu D, et al. Attenuation of Neuropathic Pain by Saikosaponin a in a Rat Model of Chronic Constriction Injury. Neurochem Res. 2014 Aug 9. [Epub ahead of print]. PMID: 25107300.

Yoon SS, Seo JW, Ann SH, et al. Effects of saikosaponin A on cocaine self-administration in rats. Neurosci Lett. 2013 Oct 25;555:198-202. PMID: 24076136.

Kim BM, Hong SH. Sequential caspase-2 and caspase-8 activation is essential for saikosaponin a-induced apoptosis of human colon carcinoma cell lines. Apoptosis. 2011 Feb;16(2):184-97. PMID: 21107704.

S0032

Saikosaponin B1

$C_{42}H_{68}O_{13}$ FW: 780.98 [58558-08-0] ≥98%

1 mg
5 mg

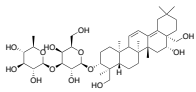

Found in *Bupleurum*, *Heteromorpha*, and *Scrophularia*. It stimulates release of prostaglandin E2.

Kyo R, Nakahata N, Kodama Y, et al. Antagonism of saikosaponin-induced prostaglandin E2 release by baicalein in C6 rat glioma cells. Biol Pharm Bull. 1999 Dec;22(12):1385-7. PMID: 10746176.

S0033

Saikosaponin B2

$C_{42}H_{68}O_{13}$ FW: 780.98 ≥98%

1 mg
5 mg

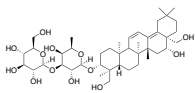

Saponin found in *Bupleurum*, *Heteromorpha*, and *Scrophularia*. It inhibits viral attachment, penetration, and proliferation of coronavirus, induces differentiation in melanoma cells, and stimulates release of prostaglandin E2.

Cheng PW, Ng LT, Chiang LC, et al. Antiviral effects of saikosaponins on human coronavirus 229E in vitro. Clin Exp Pharmacol Physiol. 2006 Jul;33(7):612-6. PMID: 16789928.

Kyo R, Nakahata N, Kodama Y, et al. Antagonism of saikosaponin-induced prostaglandin E2 release by baicalein in C6 rat glioma cells. Biol Pharm Bull. 1999 Dec;22(12):1385-7. PMID: 10746176.

Zong Z, Fujikawa-Yamamoto K, Ota T, et al. Saikosaponin b2 induces differentiation without growth inhibition in cultured B16 melanoma cells. Cell Struct Funct. 1998 Oct;23(5):265-72. PMID: 9872567.

S0133

Saikosaponin C

$C_{48}H_{78}O_{17}$ FW: 927.12 [20736-08-7] ≥98%

1 mg
5 mg

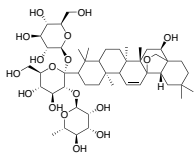

Found in *Bupleurum*. It inhibits hepatitis B virus growth and replication and increases cell growth, cell migration, and capillary tube formation in other models.

Shyu KG, Tsai SC, Wang BW, et al. Saikosaponin C induces endothelial cells growth, migration and capillary tube formation. Life Sci. 2004 Dec 31;76(7):813-26. PMID: 15581913.

Chiang LC, Ng LT, Liu LT, et al. Cytotoxicity and anti-hepatitis B virus activities of saikosaponins from Bupleurum species. Planta Med. 2003 Aug;69(8):705-9. PMID: 14531019.

S0134

Saikosaponin D

$C_{42}H_{68}O_{13}$ FW: 780.98 [20874-52-6] ≥98%

1 mg
5 mg

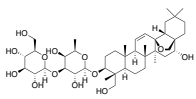

Found in *Bupleurum*. It increases activity of antioxidative enzymes, inhibits SERCA, decreases microvessel formation, and suppresses the development of DEN-induced tumors.

Zhang BZ, Guo XT, Chen JW, et al. Saikosaponin-D Attenuates Heat Stress-Induced Oxidative Damage in LLC-PK1 Cells by Increasing the Expression of Anti-Oxidant Enzymes and HSP72. Am J Chin Med. 2014 Aug 29:1-17. [Epub ahead of print] PMID: 25169909.

Ying ZL, Li XJ, Dang H, et al. Saikosaponin-d affects the differentiation, maturation and function of monocyte-derived dendritic cells. Exp Ther Med. 2014 May;7(5):1354-1358. PMID: 24940438.

Wong VK, Li T, Law BY, et al. Saikosaponin-d, a novel SERCA inhibitor, induces autophagic cell death in apoptosis-defective cells. Cell Death Dis. 2013 Jul 11;4:e720. PMID: 23846222.

S0044 Salbutamol Free Base

25 mg
50 mg
100 mg
500 mg

Albuterol

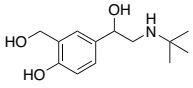

$C_{13}H_{21}NO_3$ FW: 239.31 [18559-94-9] ≥98%

β2-adrenergic receptor agonist used to treat asthma and COPD. It also decreases carrageenan-induced inflammation and nociception, suppresses activity of myeloperoxidase, and increases activity of superoxide dismutase and levels of glutathione.

Matsumoto K, Aizawa H, Fukuyama S, et al. Low-dose salbutamol suppresses airway responsiveness to histamine but not methacholine in subjects with asthma. Respir Investig. 2013 Sep;51(3):158-65. PMID: 23978642.

Uzkeser H, Cadirci E, Halici Z, et al. Anti-inflammatory and antinociceptive effects of salbutamol on acute and chronic models of inflammation in rats: involvement of an antioxidant mechanism. Mediators Inflamm. 2012;2012:438912. PMID: 22665951.

S0045 Salbutamol Sulfate

25 mg
50 mg
100 mg
500 mg

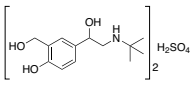

$(C_{13}H_{21}NO_3)_2 \bullet H_2SO_4$ FW: 576.7 [51022-70-9] ≥98%

β2-adrenergic receptor agonist used to treat asthma and COPD. It also decreases carrageenan-induced inflammation and nociception, suppresses activity of myeloperoxidase, and increases activity of superoxide dismutase and levels of glutathione.

Matsumoto K, Aizawa H, Fukuyama S, et al. Low-dose salbutamol suppresses airway responsiveness to histamine but not methacholine in subjects with asthma. Respir Investig. 2013 Sep;51(3):158-65. PMID: 23978642.

S0344 Salermide

NEW

5 mg
10 mg
25 mg

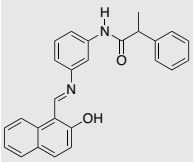

$C_{26}H_{22}N_2O_2$ FW: 394.47 [1105698-15-4] ≥98%

SIRT inhibitor. It decreases egg-laying activity in *Schistosoma mansoni*, induces apoptosis in non-small cell lung cancer cells, and downregulates expression of sirtuin1 in breast cancer cells.

Lancelot J, Caby S, Dubois-Abdesselem F, et al. *Schistosoma* mansoni Sirtuins: characterization and potential as chemotherapeutic targets. PLoS Negl Trop Dis. 2013 Sep 12;7(9):e2428. PMID: 24069483.

Dastjerdi MN, Salahshoor MR, Mardani M, et al. The apoptotic effects of sirtuin1 inhibitor on the MCF-7 and MRC-5 cell lines. Res Pharm Sci. 2013 Apr;8(2):79-89. PMID: 24019817.

S0048 Salicin

5 g
25 g

Salicyl alcohol glucoside

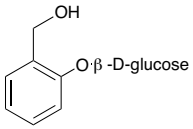

$C_{13}H_{18}O_7$ FW: 286.28 [138-52-3] ≥98%

Salicylic acid prodrug and serine protease inhibitor found in willow bark. It inhibits migration, tube formation, and sprouting in endothelial cells, ameliorates dextran-induced colitis, and suppresses release of pro-inflammatory cytokines.

Kong CS, Kim KH, Choi JS, et al. Salicin, an Extract from White Willow Bark, Inhibits Angiogenesis by Blocking the ROS-ERK Pathways. Phytother Res. 2014 Feb 17. [Epub ahead of print]. PMID: 24535656.

Verma N, Verma R, Kumari R, et al. Effect of salicin on gut inflammation and on selected groups of gut microbiota in dextran sodium sulfate induced mouse model of colitis. Inflamm Res. 2014 Feb;63(2):161-9. PMID: 24240229.

S0245 Salmeterol

NEW

10 mg
25 mg
50 mg

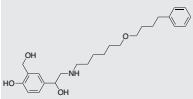

$C_{25}H_{37}NO_4$ FW: 415.57 [89365-50-4] ≥98%

β2-adrenergic agonist used to treat asthma and COPD. It also decreases TGF-β-induced deposition of collagen and fibronectin.

Lambers C, Qi Y, Eleni P, et al. Extracellular matrix composition is modified by β2-agonists through cAMP in COPD. Biochem Pharmacol. 2014 Oct 1;91(3):400-8. PMID: 25107701.

Coleman RA. On the mechanism of the persistent action of salmeterol: what is the current position? Br J Pharmacol. 2009 Sep;158(1):180-2. PMID: 19719780.

S0049 Salmon Calcitonin Acetate

Please inquire

Cys-Ser-Asn-Leu-Ser-Thr-Cys-Val-Leu-Gly-Lys-Leu-Ser-Gln-Glu-Leu-His-Lys-Leu-Gln-Thr-Tyr-Pro-Arg-Thr-Asn-Thr-Gly-Ser-Gly-Thr-Pro-NH_2
(Disulfide bridge Cys1-Cys7)

$C_{145}H_{240}N_{44}O_{48}S_2$ FW: 3431.9 [47931-85-1] ≥95%

Involved in feeding behavior and insulin signaling. Used to treat osteoporosis in postmenopausal women. It also lowers body weight, decreases levels of plasma insulin and leptin, and improves fasting glycemia.

Feigh M, Andreassen KV, Hjuler ST, et al. Oral salmon calcitonin protects against impaired fasting glycemia, glucose intolerance, and obesity induced by high-fat diet and ovariectomy in rats. Menopause. 2013 Jul;20(7):785-94. PMID: 23793169.

S0244 Salsalate

25 g
100 g

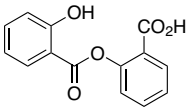

$C_{14}H_{10}O_5$ FW: 258.23 [552-94-3] ≥95%

Salicylic acid prodrug, NSAID, and weak COX-1/2 inhibitor. It decreases pain, lowers blood glucose levels, increases adiponectin levels, and downregulates 11β-HSD1 activity in visceral adipose.

Jung TW, Choi HY, Lee SY, et al. Salsalate and Adiponectin Improve Palmitate-Induced Insulin Resistance via Inhibition of Selenoprotein P through the AMPK-FOXO1α Pathway. PLoS One. 2013 Jun 18;8(6):e66529. PMID: 23825542.

Nixon M, Wake DJ, Livingstone DE, et al. Salicylate downregulates 11β-HSD1 expression in adipose tissue in obese mice and in humans, mediating insulin sensitization. Diabetes. 2012 Apr;61(4):790-6. PMID: 22357964.

McCarty MF. Salsalate may have broad utility in the prevention and treatment of vascular disorders and the metabolic syndrome. Med Hypotheses. 2010 Sep;75(3):276-81. PMID: 20080359.

S0046 Salsolidine

25 mg
100 mg

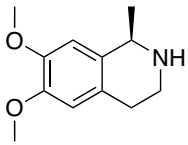

$C_{12}H_{17}NO_2$ FW: 207.27 [493-48-1] ≥98%

Inhibitor of MAO, AChE, and BChE and potential inhibitor of COMT found in *Salsola*. Derivatives of this compound are neurotoxic and cytotoxic.

Talhout R, Opperhuizen A, van Amsterdam JG. Role of acetaldehyde in tobacco smoke addiction. Eur Neuropsychopharmacol. 2007 Oct;17(10):627-36. PMID: 17382522.

S0200 SAMs Peptide

0.5 mg
1 mg
2.5 mg

H-His-Met-Arg-Ser-Ala-Met-Ser-Gly-Leu-His-Leu-Val-Lys-Arg-Arg-OH

$C_{74}H_{131}N_{29}O_{18}S_2$ FW: 1779.18 [125911-68-4] ≥95%

Analog of AMPK binding site on acetyl-CoA carboxylase used to measure AMPK activity.

Mohan S, Patel H, Bolinaga1 J, et al. AMP-activated protein kinase regulates L-arginine mediated cellular responses. Nutr Metab (Lond). 2013 May 29;10(1):40. PMID: 23718875.

S0253 Sanguinarine NEW

1 mg
5 mg

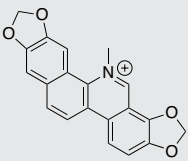

$C_{20}H_{14}NO_4$ FW: 332.33 [2447-54-3] ≥98%

Potential tubulin polymerization inhibitor, AMPK activator, and amino acid carboxylase inhibitor found in various plant sources. It inhibits VEGF release and induces apoptosis in mammary adenocarcinoma cells, decreases expression of IL-6, NF-κB, and TNF-α, and induces DNA damage in species of *Microcystis*.

Park SY, Jin ML, Kim YH, et al. Sanguinarine inhibits invasiveness and the MMP 9 and COX 2 expression in TPA-induced breast cancer cells by inducing HO-1 expression. Oncol Rep. 2014 Jan;31(1):497-504. PMID: 24220687.

Shao J, Liu D, Gong D, et al. Inhibitory effects of sanguinarine against the cyanobacterium *Microcystis* aeruginosa NIES-843 and possible mechanisms of action. Aquat Toxicol. 2013 Oct 15;142-143:257-63. PMID: 24060579.

Dong XZ, Zhang M, Wang K, et al. Sanguinarine inhibits vascular endothelial growth factor release by generation of reactive oxygen species in MCF-7 human mammary adenocarcinoma cells. Biomed Res Int. 2013;2013:517698. PMID: 23762849.

S0053 α-Santonin

5 g
10 g
25 g

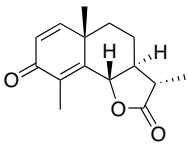

$C_{15}H_{18}O_3$ FW: 246.3 [481-06-1] ≥98%

Found in *Artemesia*. It decreases body temperature and may inhibit inflammation and cancer cell growth.

Otoguro K, Iwatsuki M, Ishiyama A, et al. In vitro antitrypanosomal activity of plant terpenes against *Trypanosoma brucei*. Phytochemistry. 2011 Nov;72(16):2024-30. PMID: 21843897.

Arantes FF, Barbosa LC, Alvarenga ES, et al. Synthesis and cytotoxic activity of alpha-santonin derivatives. Eur J Med Chem. 2009 Sep;44(9):3739-45. PMID: 19406535.

S0168 Saracatinib

AZD-0530

1 mg
5 mg
25 mg

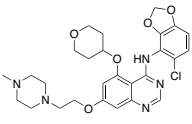

$C_{27}H_{32}ClN_5O_5$ FW: 542.03 ≥98%

Src and Abl inhibitor. It inhibits migration, invasion, and growth of cancer cells and increases CD8+ memory T cell and IFN-γ production.

Gangadhar TC, Clark JI, Karrison T, et al. Phase II study of the Src kinase inhibitor saracatinib (AZD0530) in metastatic melanoma. Invest New Drugs. 2013 Jun;31(3):769-73. PMID: 23151808.

Nam HJ, Im SA, Oh DY, et al. Antitumor activity of saracatinib (AZD0530), a c-Src/Abl kinase inhibitor, alone or in combination with chemotherapeutic agents in gastric cancer. Mol Cancer Ther. 2013 Jan;12(1):16-26. PMID: 23144237.

Cavalloni G, Peraldo-Neia C, Sarotto I, et al. Antitumor activity of Src inhibitor saracatinib (AZD-0530) in preclinical models of biliary tract carcinomas. Mol Cancer Ther. 2012 Jul;11(7):1528-38. PMID: 22452946.

S0170

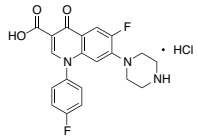

Sarafloxacin Hydrochloride

5 g
10 g
25 g

Abbott 56620

$C_{20}H_{17}F_2N_3O_3 \bullet HCl$ FW: 421.83 [91296-87-6] ≥91%

Topoisomerase IV and bacterial DNA gyrase inhibitor used to prevent bacterial infection in poultry.

Chansiripornchai N, Sasipreeyajan J. Efficacy of sarafloxacin in broilers after experimental infection with *Escherichia* coli. Vet Res Commun. 2002 Jun;26(4):255-62. PMID: 12184496.

Wang C, Ewing M, Aarabi SY. In vitro susceptibility of avian mycoplasmas to enrofloxacin, sarafloxacin, tylosin, and oxytetracycline. Avian Dis. 2001 Apr-Jun;45(2):456-60. PMID: 11417828.

S0171

H-Cys-Thr-Cys-Asn-Asp-Met-Thr-Asp-Glu-Glu-Cys-Leu-Asn-Phe-Cys-His-Gln-Asp-Val-Ile-Trp-OH
(Cys1-Cys15, Cys3-Cys11)

Sarafotoxin 6c

0.5 mg
1 mg
2.5 mg

$C_{103}H_{147}N_{27}O_{37}S_5$ FW: 2515.8 [121695-87-2] ≥95%

Endothelin B receptor agonist, mitoK(ATP) K^+ channel activator, and isoform of a toxin found in *Atractaspis engaddensis*. It decreases infarct size and arrhythmia occurrence, increases levels of superoxide anions in sympathetic ganglia, and delays suicidal erythrocyte death.

Li J, Cao YX, Liu Y, et al. Minimally modified LDL upregulates endothelin type B receptors in rat basilar artery. Microvasc Res. 2012 Mar;83(2):178-84. PMID: 22198335.

Föller M, Mahmud H, Qadri SM, et al. Endothelin B receptor stimulation inhibits suicidal erythrocyte death. FASEB J. 2010 Sep;24(9):3351-9. PMID: 20427706.

S0368

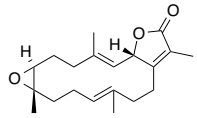

Sarcophine

10 mg

$C_{20}H_{28}O_3$ FW: 316.43 [55038-27-2] ≥98%

Cembranoid found in *Sarcophyton glaucum*. It inhibits TPA- and NOR-1-induced skin carcinogenesis, increases degradation of PLA and PLC, and suppresses migration of breast cancer cells and prostate cancer cells.

Szymanski PT, Ahmed SA, Khalifa S, et al. Chemopreventive effect of sarcophine-diol on NOR-1-induced TPA-promoted skin carcinogenesis in female HOS:HR-1 mice. Nat Prod Commun. 2013 Feb;8(2):153-4. PMID: 23513714.

Szymanski PT, Muley P, Ahmed SA, et al. Sarcophine-diol inhibits expression of COX-2, inhibits activity of cPLA2, enhances degradation of PLA2 and PLC(γ)1 and inhibits cell membrane permeability in mouse melanoma B16F10 cells. Mar Drugs. 2012 Oct;10(10):2166-80. PMID: 23170076.

Hassan HM, Sallam AA, Mohammed R, et al. Semisynthetic analogues of the marine cembranoid sarcophine as prostate and breast cancer migration inhibitors. Bioorg Med Chem. 2011 Aug 15;19(16):4928-34. PMID: 21775154.

S0278

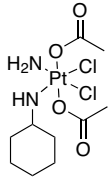

Satraplatin

5 mg
10 mg
50 mg

$C_{10}H_{22}Cl_2N_2O_4Pt$ FW: 498.26 [129580-63-8] ≥98%

Platinum-based DNA cross-linker that forms DNA adducts and inhibits DNA repair. It induces cell cycle arrest in oral squamous cell carcinoma cells and stimulates apoptosis in colorectal cancer cells.

Figg WD, Chau CH, Madan RA, et al. Phase II study of satraplatin and prednisone in patients with metastatic castration-resistant prostate cancer: a pharmacogenetic assessment of outcome and toxicity. Clin Genitourin Cancer. 2013 Sep;11(3):229-37. PMID: 23684781.

Kalimutho M, Minutolo A, Grelli S, et al. Satraplatin (JM-216) mediates G2/M cell cycle arrest and potentiates apoptosis via multiple death pathways in colorectal cancer cells thus overcoming platinum chemo-resistance. Cancer Chemother Pharmacol. 2011 Jun;67(6):1299-312. PMID: 20734047.

Yamano Y, Shiiba M, Negoro K, et al. Antitumor activity of satraplatin in cisplatin-resistant oral squamous cell carcinoma cells. Head Neck. 2011 Mar;33(3):309-17. PMID: 20848452.

S0381

pGlu-Gly-Pro-Pro-Ile-Ser-Ile-Asp-Leu-Ser-Leu-Glu-Leu-Leu-Arg-Lys-Met-Ile-Glu-Ile-Glu-Lys-Gln-Glu-Lys-Glu-Lys-Gln-Gln-Ala-Ala-Asn-Asn-Arg-Leu-Leu-Leu-Asp-Thr-Ile-NH_2

Sauvagine

0.5 mg
1 mg
2.5 mg

$C_{202}H_{347}N_{56}O_{63}S$ FW: 4599.4 [74434-59-6] ≥98%

CRF-related peptide found in amphibians. It is involved in growth, stress, anxiety, and other hormonal signaling pathways. It also induces vasodilation and increases striatal tyrosine hydroxylase activity in a Ca^{2+}-dependent manner.

Lovejoy DA, Balment RJ. Evolution and physiology of the corticotropin-releasing factor (CRF) family of neuropeptides in vertebrates. Gen Comp Endocrinol. 1999 Jul;115(1):1-22. PMID: 10375459.

Barker DM, Corder R. Studies of the role of endothelium-dependent nitric oxide release in the sustained vasodilator effects of corticotrophin releasing factor and sauvagine. Br J Pharmacol. 1999 Jan;126(1):317-25. PMID: 10051151.

S0500 SB-203580

NEW

5 mg
25 mg

$C_{21}H_{16}FN_3OS$ FW: 377.43 [152121-47-6] ≥98%

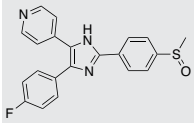

p38 MAPK inhibitor. It increases secretion of IFN-γ, inhibits TGF-β1-induced epithelial-to-mesenchymal transition, and suppresses proliferation in glioma cells.

Kühnöl C, Herbarth M, Föll J, et al. CD137 stimulation and p38 MAPK inhibition improve reactivity in an in vitro model of glioblastoma immunotherapy. Cancer Immunol Immunother. 2013 Dec;62(12):1797-809. PMID: 24129764.

Chen HH, Zhou XL, Shi YL, et al. Roles of p38 MAPK and JNK in TGF-β1-induced human alveolar epithelial to mesenchymal transition. Arch Med Res. 2013 Feb;44(2):93-8. PMID: 23376055.

Morales MG, Vazquez Y, Acuña MJ, et al. Angiotensin II-induced pro-fibrotic effects require p38MAPK activity and transforming growth factor beta 1 expression in skeletal muscle cells. Int J Biochem Cell Biol. 2012 Nov;44(11):1993-2002. PMID: 22964022.

S0400 SB-431542

1 mg
5 mg
25 mg

$C_{22}H_{16}N_4O_3$ FW: 384.39 [301836-41-9] ≥98%

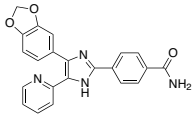

Activin receptor-like kinase 4/5/7 and TGF-β signaling inhibitor. It does not affect ERK, JNK, or MAPK. It inhibits proliferation and motility of glioma cells and increases IL-12 production.

Tanaka H, Shinto O, Yashiro M, et al. Transforming growth factor β signaling inhibitor, SB-431542, induces maturation of dendritic cells and enhances anti-tumor activity. Oncol Rep. 2010 Dec;24(6):1637-43. PMID: 21042762.

Halder SK, Beauchamp RD, Datta PK. A specific inhibitor of TGF-beta receptor kinase, SB-431542, as a potent antitumor agent for human cancers. Neoplasia. 2005 May;7(5):509-21. PMID: 15967103.

Hjelmeland MD, Hjelmeland AB, Sathornsumetee S, et al. SB-431542, a small molecule transforming growth factor-beta-receptor antagonist, inhibits human glioma cell line proliferation and motility. Mol Cancer Ther. 2004 Jun;3(6):737-45. PMID: 15210860.

S0459 SB-590885

1 mg
5 mg

$C_{27}H_{27}N_5O_2$ FW: 453.54 [405554-55-4] ≥97%

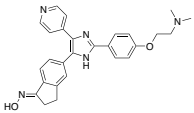

B-Raf inhibitor. It stabilizes oncogenic B-Raf in an active conformation, inhibiting downstream MAPK signaling. It also limits tissue damage in cerebral ischemia models.

Ahnstedt H, Säveland H, Nilsson O, et al. Human cerebrovascular contractile receptors are upregulated via a B-Raf/MEK/ERK-sensitive signaling pathway. BMC Neurosci. 2011 Jan 11;12:5. PMID: 21223556.

King AJ, Patrick DR, Batorsky RS, et al. Demonstration of a genetic therapeutic index for tumors expressing oncogenic BRAF by the kinase inhibitor SB-590885. Cancer Res. 2006 Dec 1;66(23):11100-5. PMID: 17145850.

S0928 SCH-900776

NEW

1 mg
5 mg
10 mg

$C_{15}H_{18}BrN_7$ FW: 376.25 [891494-63-6] ≥98%

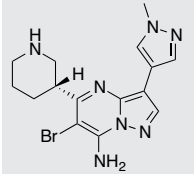

CHK1 inhibitor. It induces double-stranded DNA breaks and cell death in cancer cells.

Dai Y, Chen S, Kmieciak M, et al. The novel Chk1 inhibitor MK-8776 sensitizes human leukemia cells to HDAC inhibitors by targeting the intra-S checkpoint and DNA replication and repair. Mol Cancer Ther. 2013 Jun;12(6):878-89. PMID: 23536721.

Karp JE, Thomas BM, Greer JM, et al. Phase I and pharmacologic trial of cytosine arabinoside with the selective checkpoint 1 inhibitor Sch 900776 in refractory acute leukemias. Clin Cancer Res. 2012 Dec 15;18(24):6723-31. PMID: 23092873.

Guzi TJ, Paruch K, Dwyer MP, et al. Targeting the replication checkpoint using SCH 900776, a potent and functionally selective CHK1 inhibitor identified via high content screening. Mol Cancer Ther. 2011 Apr;10(4):591-602. PMID: 21321066.

S0930 Schisantherin A

5 mg
10 mg

Gomisin C

$C_{30}H_{32}O_9$ FW: 536.58 [58546-56-8] ≥98%

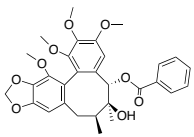

Found in *Schisandra*. It decreases LPS-stimulated expression of pro-inflammatory cytokines, suppresses osteoclast function and bone erosion, inhibits amyloid-β-induced learning and memory impairments, and prevents myocardial apoptosis.

He Y, Zhang Q, Shen Y, et al. Schisantherin A suppresses osteoclast formation and wear particle-induced osteolysis via modulating RANKL signaling pathways. Biochem Biophys Res Commun. 2014 Jul 4;449(3):344-50. PMID: 24845381.

Li X, Zhao X, Xu X, et al. Schisantherin A recovers Aβ-induced neurodegeneration with cognitive decline in mice. Physiol Behav. 2014 Jun 10;132:10-6. PMID: 24813830.

Chang R, Li Y, Yang X, et al. Protective role of deoxyschizandrin and schisantherin A against myocardial ischemia-reperfusion injury in rats. PLoS One. 2013 Apr 19;8(4):e61590. PMID: 23620773.

S0830 R-(+)-Schisandrin A

5 mg
10 mg

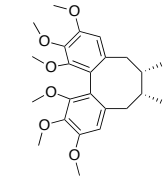

$C_{24}H_{32}O_6$ FW: 416.51 [61281-38-7] ≥98%

Found in *Schisandra*. It decreases infarct size in cardiac ischemia/reperfusion models, prevents cardiomyocyte apoptosis, and induces relaxation in thoracic aortas.

Chang R, Li Y, Yang X, et al. Protective role of deoxyschizandrin and schisantherin A against myocardial ischemia-reperfusion injury in rats. PLoS One. 2013 Apr 19;8(4):e61590. PMID: 23620773.

Yang X, Wang Y, Zhang X, et al. Screening vasoconstriction inhibitors from traditional Chinese medicines using a vascular smooth muscle/cell membrane chromatography-offline-liquid chromatography-mass spectrometry. J Sep Sci. 2011 Oct;34(19):2586-93. PMID: 21898806.

S0831 S-(−)-Schisandrin B

5 mg
10 mg

S-(−)-Wuweizisu B

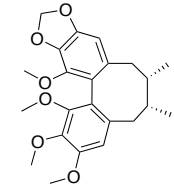

$C_{23}H_{28}O_6$ FW: 400.47 [61281-37-6] ≥98%

Found in *Schisandra*. It displays a wide variety of biological activities, including decreasing TGF-β1-induced myosin light chain phosphorylation and Smad signaling, downregulating expression of pro-inflammatory cytokines, suppressing myocardial apoptosis, and inhibiting invasiveness of breast cancer cells.

Chun JN, Kim SY, Park EJ, et al. Schisandrin B suppresses TGFβ1-induced stress fiber formation by inhibiting myosin light chain phosphorylation. J Ethnopharmacol. 2014 Mar 14;152(2):364-71. PMID: 24486209.

Li L, Zhang T, Zhou L, et al. Schisandrin B attenuates acetaminophen-induced hepatic injury through heat-shock protein 27 and 70 in mice. J Gastroenterol Hepatol. 2014 Mar;29(3):640-7. PMID: 24219791.

S1059 Scopolamine Hydrobromide Trihydrate

1 g
5 g
25 g

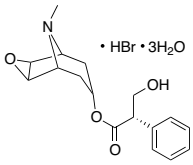

$C_{17}H_{21}NO_4 \bullet HBr \bullet 3H_2O$ FW: 438.32 [6533-68-2] ≥98%

M1 mAChR antagonist found in *Solanaceae* plants. used to induce cognitive deficits in models of Alzheimer's disease. It has previously been used in the treatment of organophosphate poisoning.

Jung IH, Lee HE, Park SJ, et al. Ameliorating effect of spinosin, a C-glycoside flavonoid, on scopolamine-induced memory impairment in mice. Pharmacol Biochem Behav. 2014 May;120:88-94. PMID: 24582850.

Drevets WC, Zarate CA Jr, Furey ML. Antidepressant effects of the muscarinic cholinergic receptor antagonist scopolamine: a review. Biol Psychiatry. 2013 Jun 15;73(12):1156-63. PMID: 23200525.

S1058 Scopolamine N-butylbromide

1 g
5 g

N-Butylhyoscine bromide

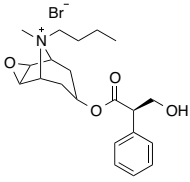

$C_{21}H_{30}BrNO_4$ FW: 440.38 [149-64-4] ≥98%

M1 mAChR antagonist found in *Solanaceae* plants. used to induce cognitive deficits in models of Alzheimer's disease. It has previously been used in the treatment of organophosphate poisoning.

Jung IH, Lee HE, Park SJ, et al. Ameliorating effect of spinosin, a C-glycoside flavonoid, on scopolamine-induced memory impairment in mice. Pharmacol Biochem Behav. 2014 May;120:88-94. PMID: 24582850.

Drevets WC, Zarate CA Jr, Furey ML. Antidepressant effects of the muscarinic cholinergic receptor antagonist scopolamine: a review. Biol Psychiatry. 2013 Jun 15;73(12):1156-63. PMID: 23200525.

S1069 Scriptaid

1 mg
5 mg

CGK1026

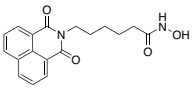

$C_{18}H_{18}N_2O_4$ FW: 326.35 ≥98%

HDAC inhibitor that increases expression of p21 and p27, decreases activity of telomerase, and induces apoptosis in glioma cells. It also improves the quality of cloned mouse embryos.

Bui HT, Seo HJ, Park MR, et al. Histone deacetylase inhibition improves activation of ribosomal RNA genes and embryonic nucleolar reprogramming in cloned mouse embryos. Biol Reprod. 2011 Nov;85(5):1048-56. PMID: 21753193.

S1343 Ac-SDKP

5 mg
10 mg
25 mg

Ac-Ser-Asp-Lys-Pro-OH

$C_{20}H_{33}N_5O_9$ FW: 487.51 [120081-14-3] ≥95%

Degradation product of thymosin B4 involved in hematopoiesis. It inhibits proliferation of hematopoietic pluripotent stem cells, improves left ventricular function, increases angiogenesis, decreases deposition of fibronectin and collagen, and limits progression of lupus nephritis.

Song M, Jang H, Lee J, et al. Regeneration of chronic myocardial infarction by injectable hydrogels containing stem cell homing factor SDF-1 and angiogenic peptide Ac-SDKP. Biomaterials. 2014 Mar;35(8):2436-45. PMID: 24378015.

S1848 Se-Methylseleno-L-cysteine

100 mg
250 mg

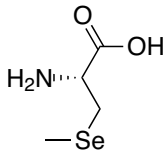

$C_4H_9NO_2Se$ FW: 182.08 [26046-90-2] ≥98%

Found in *Astragalus*, *Allium*, and *Brassica* genera. It induces phase II enzyme activity, protects organs against chemotherapy-induced toxicity, and decreases expression of iNOS in LPS-stimulated macrophages.

Cao S, Durrani FA, Tóth K, et al. Se-methylselenocysteine offers selective protection against toxicity and potentiates the antitumour activity of anticancer drugs in preclinical animal models. Br J Cancer. 2014 Apr 2;110(7):1733-43. PMID: 24619073.

Shin HS, Yang WJ, Choi EM. The preventive effect of Se-methylselenocysteine on γ-radiation-induced oxidative stress in rat lungs. J Trace Elem Med Biol. 2013 Apr;27(2):154-9. PMID: 23176811.

Bhattacharya A. Methylselenocysteine: a promising antiangiogenic agent for overcoming drug delivery barriers in solid malignancies for therapeutic synergy with anticancer drugs. Expert Opin Drug Deliv. 2011 Jun;8(6):749-63. PMID: 21473705.

S1810 Secnidazole

5 g
10 g
25 g

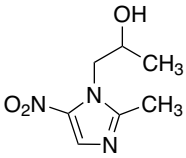

$C_7H_{11}N_3O_3$ FW: 185.18 [3366-95-8] ≥98%

Microbial nucleic acid synthesis inhibitor that binds DNA. It inhibits growth of bacteria, fungi, and parasites.

Almirall P, Escobedo AA, Ayala I, et al. Mebendazole compared with secnidazole in the treatment of adult giardiasis: a randomised, no-inferiority, open clinical trial. J Parasitol Res. 2011;2011:636857. PMID: 22174992.

De Backer E, Dubreuil L, Brauman M, et al. In vitro activity of secnidazole against Atopobium vaginae, an anaerobic pathogen involved in bacterial vaginosis. Clin Microbiol Infect. 2010 May;16(5):470-2. PMID: 19548924.

S1604 Secretin Acetate

Please inquire

H-His-Ser-Asp-Gly-Thr-Phe-Thr-Ser-Glu-Leu-Ser-Arg-Leu-Arg-Asp-Ser-Ala-Arg-Leu-Gln-Arg-Leu-Leu-Gln-Gly-Leu-Val-NH_2

$C_{130}H_{220}N_{44}O_{41}$ FW: 3055.41 [10813-74-8] ≥95%

Secretin receptor agonist involved in water homeostasis and feeding behavior. It stimulates lipolysis, induces uptake of fatty acids, and increases expression of tyrosine hydroxylase.

Sekar R, Chow BK. Lipolytic actions of secretin in mouse adipocytes. J Lipid Res. 2014 Feb;55(2):190-200. PMID: 24273196.

Miegueu P, Cianflone K, Richard D, et al. Effect of secretin on preadipocyte, differentiating and mature adipocyte functions. Int J Obes (Lond). 2013 Mar;37(3):366-74. PMID: 22565418.

S1605 Secretin, human

1 mg
2 mg
5 mg

His-Ser-Asp-Gly-Thr-Phe-Thr-Ser-Glu-Leu-Ser-Arg-Leu-Arg-Glu-Gly-Ala-Arg-Leu-Gln-Arg-Leu-Leu-Gln-Gly-Leu-Val-NH_2

$C_{130}H_{220}N_{44}O_{40}$ FW: 3039.4 [108153-74-8] ≥95%

Endogenous secretin receptor agonist involved in water homeostasis and feeding behavior. It stimulates lipolysis, induces uptake of fatty acids, and increases expression of tyrosine hydroxylase.

Sekar R, Chow BK. Lipolytic actions of secretin in mouse adipocytes. J Lipid Res. 2014 Feb;55(2):190-200. PMID: 24273196.

Miegueu P, Cianflone K, Richard D, et al. Effect of secretin on preadipocyte, differentiating and mature adipocyte functions. Int J Obes (Lond). 2013 Mar;37(3):366-74. PMID: 22565418.

S1606 Secretin, pig

5 mg
10 mg
25 mg

His-Ser-Asp-Gly-Thr-Phe-Thr-Ser-Glu-Leu-Ser-Arg-Leu-Arg-Asp-Ser-Ala-Arg-Leu-Gln-Arg-Leu-Leu-Gln-Gly-Leu-Val-NH_2

$C_{130}H_{220}N_{44}O_{41}$ FW: 3055.4 [17034-35-4] ≥95%

Endogenous secretin receptor agonist involved in water homeostasis and feeding behavior. It stimulates lipolysis, induces uptake of fatty acids, and increases expression of tyrosine hydroxylase.

Sekar R, Chow BK. Lipolytic actions of secretin in mouse adipocytes. J Lipid Res. 2014 Feb;55(2):190-200. PMID: 24273196.

Miegueu P, Cianflone K, Richard D, et al. Effect of secretin on preadipocyte, differentiating and mature adipocyte functions. Int J Obes (Lond). 2013 Mar;37(3):366-74. PMID: 22565418.

S1607 Secretin, rat

0.5 mg
1 mg
2.5 mg

H-His-Ser-Asp-Gly-Thr-Phe-Thr-Ser-Glu-Leu-Ser-Arg-Leu-Gln-Asp-Ser-Ala-Arg-Leu-Gln-Arg-Leu-Leu-Gln-Gly-Leu-Val-NH_2

$C_{129}H_{216}N_{42}O_{42}$ FW: 3027.42 [121028-49-7] ≥95%

Endogenous secretin receptor agonist involved in water homeostasis and feeding behavior. It stimulates lipolysis, induces uptake of fatty acids, and increases expression of tyrosine hydroxylase.

Sekar R, Chow BK. Lipolytic actions of secretin in mouse adipocytes. J Lipid Res. 2014 Feb;55(2):190-200. PMID: 24273196.

S1609 Securinine

100 mg
500 mg
1 g

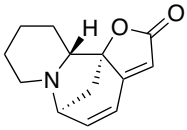

$C_{13}H_{15}NO_2$ FW: 217.26 [5610-40-2] ≥98%

Potential GABA-A receptor antagonist found in *Securinega*. It displays many activities, including inducing cell cycle arrest in breast cancer cells and promyelocytic leukemia cells, inhibiting growth of *Alternaria*, *Curvularia*, and *Helminthosporum*, and suppressing amyloid-β-induced glial inflammatory responses.

Han S, Zhang G, Li M, et al. L-securinine induces apoptosis in the human promyelocytic leukemia cell line HL-60 and influences the expression of genes involved in the PI3K/AKT/mTOR signaling pathway. Oncol Rep. 2014 May;31(5):2245-51. PMID: 24676995.

Li M, Han S, Zhang G, et al. Antiproliferative activity and apoptosis-inducing mechanism of L-securinine on human breast cancer MCF-7 cells. Pharmazie. 2014 Mar;69(3):217-23. PMID: 24716413.

Shipman M, Lubick K, Fouchard D, et al. Proteomic and systems biology analysis of monocytes exposed to securinine, a GABA(A) receptor antagonist and immune adjuvant. PLoS One. 2012;7(9):e41278. PMID: 23028424.

S1612 Sedanolide

100 mg
500 mg
1 g

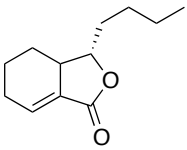

Neocnidilide

$C_{12}H_{18}O_2$ FW: 194.13 [6415-59-4] ≥98%

Natural product found in celery seeds that inhibits COX-1/2, topoisomerase I, and topoisomerase II. It also inhibits growth and survival of *Aedes*, *Caenorhabditis*, *Candida*, *Drosophila*, and *Panagrellus*.

Tsukamoto T, Ishikawa Y, Miyazawa M. Larvicidal and adulticidal activity of alkylphthalide derivatives from rhizome of Cnidium officinale against *Drosophila* melanogaster. J Agric Food Chem. 2005 Jul 13;53(14):5549-53. PMID: 15998112.

Jiao XZ, Xie P, Zu LS, et al. Study of stereoselective synthesis of (+/-)-neocnidilide. J Asian Nat Prod Res. 2003 Sep;5(3):165-9. PMID: 12931848.

Momin RA, Nair MG. Antioxidant, cyclooxygenase and topoisomerase inhibitory compounds from Apium graveolens Linn. seeds. Phytomedicine. 2002 May;9(4):312-8. PMID: 12120812.

S1843 L-Selectin

1 mg
2 mg
5 mg

H-Cys-Gln-Lys-Leu-Asp-Lys-Ser-Phe-Ser-Met-Ile-Lys-OH

$C_{62}H_{105}N_{16}O_{18}S_2$ FW: 1426.75 [126880-86-2] ≥95%

Endogenous peptide that binds PKC and calmodulin to facilitate cell adhesion.

Gaborski TR, Sealander MN, Waugh RE, et al. Dynamics of adhesion molecule domains on neutrophil membranes: surfing the dynamic cell topography. Eur Biophys J. 2013 Dec;42(11-12):851-5. PMID: 24113789.

Domínguez-Luis M, Herrera-García A, Arce-Franco M, et al. Superoxide anion mediates the L-selectin down-regulation induced by non-steroidal anti-inflammatory drugs in human neutrophils. Biochem Pharmacol. 2013 Jan 15;85(2):245-56. PMID: 23142710.

S1845 L-(+)-Selenomethionine

10 mg
25 mg
100 mg

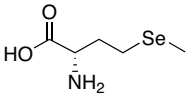

$C_5H_{11}NO_2Se$ FW: 196.11 [3211-76-5] ≥98%

Antioxidative amino acid found in grains, nuts, and legumes. It delays development of UV-induced tumors in some cancer models.

Cassidy PB, Fain HD, Cassidy JP Jr, et al. Selenium for the prevention of cutaneous melanoma. Nutrients. 2013 Mar 7;5(3):725-49. PMID: 23470450.

Ware JH, Zhou Z, Romero-Weaver AL, et al. Effects of selenomethionine in irradiated human thyroid epithelial cells and tumorigenicity studies. Nutr Cancer. 2011;63(7):1114-21. PMID: 21916697.

Dennert G, Zwahlen M, Brinkman M, et al. Selenium for preventing cancer. Cochrane Database Syst Rev. 2011 May 11;(5):CD005195. Update in: Cochrane Database Syst Rev. 2014;3:CD005195. PMID: 21563143.

S1846 Selumetinib

1 mg
10 mg
50 mg

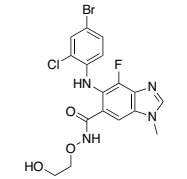

AZD6244; ARRY 142886

$C_{17}H_{15}BrClFN_4O_3$ FW: 457.68 [606143-52-6] ≥98%

MEK1/2 inhibitor. It induces apoptosis in non-small cell lung cancer cells, suppresses alloreactivity through inhibition of naïve and less-differentiated T cells, and increases muscle function in models of muscular dystrophy.

Paolo M, Assunta S, Antonio R, et al. Selumetinib in Advanced Non Small Cell Lung Cancer (NSCLC) Harbouring KRAS Mutation: Endless Clinical Challenge to KRAS-mutant NSCLC. Rev Recent Clin Trials. 2013 Jun;8(2):93-100. PMID: 24063423.

Muchir A, Kim YJ, Reilly SA, et al. Inhibition of extracellular signal-regulated kinase 1/2 signaling has beneficial effects on skeletal muscle in a mouse model of Emery-Dreifuss muscular dystrophy caused by lamin A/C gene mutation. Skelet Muscle. 2013 Jul 1;3(1):17. PMID: 23815988.

Shindo T, Kim TK, Benjamin CL, et al. MEK inhibitors selectively suppress alloreactivity and graft-versus-host disease in a memory stage-dependent manner. Blood. 2013 Jun 6;121(23):4617-26. PMID: 23575444.

S1853

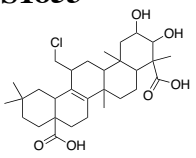

Senegenin

$C_{30}H_{45}ClO_6$ FW: 537.13 [2469-34-3] ≥98.0%

5 mg
10 mg
25 mg

Found in *Polygata tennifolia*. It increases NR2B NMDA receptor subunit expression in the hippocampus.

Xie W, Yang Y, Gu X, et al. Senegenin attenuates hepatic ischemia-reperfusion induced cognitive dysfunction by increasing hippocampal NR2B expression in rats. PLoS One. 2012;7(9):e45575. PMID: 23029109.

S1968

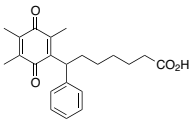

Seratrodast

$C_{22}H_{26}O_4$ FW: 354.44 [112665-43-7] ≥98%

25 mg
100 mg
250 mg

TxA2 antagonist used to treat asthma. It prevents bronchial hyperresponsiveness and bronchoconstriction but does not exhibit anti-platelet activity.

An J, Li JQ, Wang T, et al. Blocking of thromboxane A2 receptor attenuates airway mucus hyperproduction induced by cigarette smoke. Eur J Pharmacol. 2013 Mar 5;703(1-3):11-7. PMID: 23399768.

Dogné JM, de Leval X, Benoit P, et al. Thromboxane A2 inhibition: therapeutic potential in bronchial asthma. Am J Respir Med. 2002;1(1):11-7. PMID: 14720071.

S1969

Tyr-Ala-Asp-Ala-Ile-Phe-Thr-Asn-Ser-Tyr-Arg-Lys-Val-Leu-Gly-Gln-Leu-Ser-Ala-Arg-Lys-Leu-Leu-Gln-Asp-Ile-Met-Ser-Arg-NH_2

Sermorelin Acetate

GHRH (1-29) NH_2

$C_{149}H_{246}N_{44}O_{42}S$ FW: 3358.03 [86168-78-7] ≥95%

Please inquire

Synthetic GHRH analog and GHRH agonist. It stimulates IGF-1 secretion, increases activation of immune cells, and induces mast cell degranulation.

Stepień T, Sacewicz M, Lawnicka H, et al. Stimulatory effect of growth hormone-releasing hormone (GHRH(1-29)NH2) on the proliferation, VEGF and chromogranin A secretion by human neuroendocrine tumor cell line NCI-H727 in vitro. Neuropeptides. 2009 Oct;43(5):397-400. PMID: 19747727.

S1971

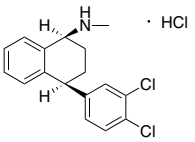

Sertraline Hydrochloride

$C_{17}H_{17}Cl_2N \bullet HCl$ FW: 342.7 [79559-97-0] ≥98%

500 mg
1 g
5 g

Inhibitor of SERT, DAT and α1-adrenergic receptors used to treat depression. It also potentially inhibits σ1 receptors, acts as a FIASMA, and induces apoptosis in osteoclasts and osteoblasts.

Guaiana G, Gupta S, Chiodo D, et al. Agomelatine versus other antidepressive agents for major depression. Cochrane Database Syst Rev. 2013 Dec 17;12:CD008851. PMID: 24343836.

Zhu H, Bogdanov MB, Boyle SH, et al. Pharmacometabolomics of response to sertraline and to placebo in major depressive disorder - possible role for methoxyindole pathway. PLoS One. 2013 Jul 17;8(7):e68283. PMID: 23874572.

Hodge JM, Wang Y, Berk M, et al. Selective serotonin reuptake inhibitors inhibit human osteoclast and osteoblast formation and function. Biol Psychiatry. 2013 Jul 1;74(1):32-9. PMID: 23260229.

S1970

pGlu-Ala-Lys-Ser-Gln-Gly-Gly-Ser-Asn-OH

Serum Thymic Factor

FTS

$C_{33}H_{54}N_{12}O_{15}$ FW: 858.89 [63958-90-7] ≥95%

1 mg
2 mg
5 mg

Synthetic hormone. It increases activity of antioxidative enzymes, prevents LPS-induced damage in pancreatic cells, suppresses the symptoms of EAE, increases T cell differentiation, and activates T cells and NK cells.

Kohda Y, Matsunaga Y, Yonogi K, et al. Protective effect of serum thymic factor, FTS, on cephaloridine-induced nephrotoxicity in rats. Biol Pharm Bull. 2005 Nov;28(11):2087-91. PMID: 16272694.

S1872

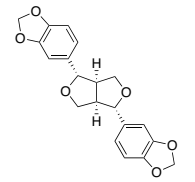

Sesamin

$C_{20}H_{18}O_6$ FW: 354.35 [607-80-7] ≥98.0%

5 mg
10 mg
25 mg

Lignin found in *Sesamin indicum*. It suppresses STAT3 signaling and induces apoptosis in hepatocellular carcinoma cells and induces differentiation in osteoblasts.

Deng P, Wang C, Chen L, et al. Sesamin Induces Cell Cycle Arrest and Apoptosis through the Inhibition of Signal Transducer and Activator of Transcription 3 Signalling in Human Hepatocellular Carcinoma Cell Line HepG2. Biol Pharm Bull. 2013;36(10):1540-1548. PMID: 24088253.

Liu CM, Zheng GH, Ming QL, et al. Sesamin protects mouse liver against nickel-induced oxidative DNA damage and apoptosis by the PI3K-Akt pathway. J Agric Food Chem. 2013 Feb 6;61(5):1146-54. PMID: 23317420.

Li WX, Kong X, Zhang JX, et al. Long-term intake of sesamin improves left ventricular remodelling in spontaneously hypertensive rats. Food Funct. 2013 Feb 26;4(3):453-60. PMID: 23238059.

S2044 SFLLR

1 mg
2 mg
5 mg

$C_{30}H_{50}N_8O_7$ FW: 634.78 ≥95%

H-Ser-Phe-Leu-Leu-Arg-OH

Synthetic PAR1 agonist used to induce platelet adhesion and aggregation. It also induces apoptosis in vagal motor neurons, stimulates angiogenesis in endothelial cells, and increases release of IL-6 from T cells.

Wu X, Zhang W, Li JY, et al. Induction of apoptosis by thrombin in the cultured neurons of dorsal motor nucleus of the vagus. Neurogastroenterol Motil. 2011 Mar;23(3):279-85, e123-4. PMID: 21143557.

S2792 SGX-523

NEW

1 mg
5 mg

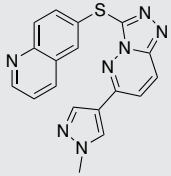

$C_{18}H_{13}N_7S$ FW: 359.41 [1022150-57-7] ≥98%

MET inhibitor. It inhibits cell proliferation and tumor growth in non-small cell lung cancer models and improves the efficacy of co-administered chemotherapeutics.

Zhang YW, Staal B, Essenburg C, et al. Strengthening context-dependent anticancer effects on non-small cell lung carcinoma by inhibition of both MET and EGFR. Mol Cancer Ther. 2013 Aug;12(8):1429-41. PMID: 23720767.

Zhang YW, Staal B, Essenburg C, et al. MET kinase inhibitor SGX523 synergizes with epidermal growth factor receptor inhibitor erlotinib in a hepatocyte growth factor-dependent fashion to suppress carcinoma growth. Cancer Res. 2010 Sep 1;70(17):6880-90. Erratum in: Cancer Res. 2011 Apr 1;71(7):2804. PMID: 20643778.

Buchanan SG, Hendle J, Lee PS, et al. SGX523 is an exquisitely selective, ATP-competitive inhibitor of the MET receptor tyrosine kinase with antitumor activity in vivo. Mol Cancer Ther. 2009 Dec;8(12):3181-90. PMID: 19934279.

S3033 Shikimic Acid

1 g
5 g

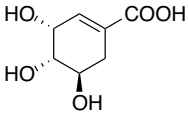

$C_7H_{10}O_5$ FW: 174.15 [138-59-0] ≥98%

Found in various plants and microorganisms. It prevents H_2O_2-induced increases in ROS levels and DNA damage, inhibits chemically-induced writhing in pain assays, and activates Nrf2 signaling.

Manna K, Khan A, Kr Das D, et al. Protective effect of coconut water concentrate and its active component shikimic acid against hydroperoxide mediated oxidative stress through suppression of NF-κB and activation of Nrf2 pathway. J Ethnopharmacol. 2014 May 14. [Epub ahead of print]. PMID: 24835026.

Xing J, You C, Dong K, et al. Ameliorative effects of 3,4-oxo-isopropylidene-shikimic acid on experimental colitis and their mechanisms in rats. Int Immunopharmacol. 2013 Mar;15(3):524-31. PMID: 23434856.

Morucci F, Lopez P, Miño J, et al. Antinociceptive activity of aqueous extract and isolated compounds of Lithrea molleoides. J Ethnopharmacol. 2012 Jul 13;142(2):401-6. PMID: 22609809.

S2957 Shogaol

NEW

5 mg
10 mg

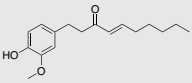

$C_{17}H_{24}O_3$ FW: 276.37 [555-66-8] ≥98%

PPARγ agonist and 5-HT3 receptor antagonist found in *Zingiber*. It exhibits a wide variety of biological activities, including inducing apoptosis in breast cancer and prostate cancer cells, inhibiting invasion and metastasis in hepatocellular carcinoma cells, preventing TPA-induced tumor formation, and decreasing formation of ulcers.

Kim SM, Kim C, Bae H, et al. 6-Shogaol exerts anti-proliferative and pro-apoptotic effects through the modulation of STAT3 and MAPKs signaling pathways. Mol Carcinog. 2014 Jun 24. [Epub ahead of print]. PMID: 24962868.

Tan BS, Kang O, Mai CW, et al. 6-Shogaol inhibits breast and colon cancer cell proliferation through activation of peroxisomal proliferator activated receptor γ (PPARγ). Cancer Lett. 2013 Aug 9;336(1):127-39. PMID: 23612072.

Liao YR, Leu YL, Chan YY, et al. Anti-platelet aggregation and vasorelaxing effects of the constituents of the rhizomes of *Zingiber* officinale. Molecules. 2012 Jul 26;17(8):8928-37. PMID: 22836212.

S3346 Silodosin

25 mg
100 mg
500 mg

KAD 3213; KMD 3213

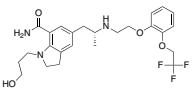

$C_{25}H_{32}F_3N_3O_4$ FW: 495.53 [160970-54-7] ≥98%

α1A-Adrenergic receptor antagonist used to treat BPH. It improves bladder function and blood flow in ischemic conditions and alters transcriptional regulation.

Yamaguchi K, Aoki Y, Yoshikawa T, et al. Silodosin versus naftopidil for the treatment of benign prostatic hyperplasia: A multicenter randomized trial. Int J Urol. 2013 Jun 3. [Epub ahead of print]. PMID: 23731168.

Goi Y, Tomiyama Y, Nomiya M, et al. Effects of silodosin, a selective α1A-adrenoceptor antagonist, on bladder blood flow and bladder function in a rat model of atherosclerosis induced chronic bladder ischemia without bladder outlet obstruction. J Urol. 2013 Sep;190(3):1116-22. PMID: 23545103

Hennenberg M, Strittmatter F, Beckmann C, et al. Silodosin inhibits noradrenaline-activated transcription factors Elk1 and SRF in human prostate smooth muscle. PLoS One. 2012;7(11):e50904. PMID: 23226423.

S3343

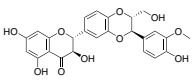

Silybin

Silybum substance E6; Silymarin I

$C_{25}H_{22}O_{10}$ FW: 482.44 [22888-70-6] ≥97%

Found in *Silybum* (milk thistle) seeds. It exhibits a wide variety of biological activities, including decreasing pro-inflammatory cytokine release, increasing expression of TRAIL and DR-5 in hepatocellular carcinoma cells, decreasing microvessel density, and delaying UV-induced carcinogenesis.

Bousserouel S, Bour G, Kauntz H, et al. Silibinin inhibits tumor growth in a murine orthotopic hepatocarcinoma model and activates the TRAIL apoptotic signaling pathway. Anticancer Res. 2012 Jul;32(7):2455-62. PMID: 22753701.

Wang Q, Liu M, Liu WW, et al. In vivo recovery effect of silibinin treatment on streptozotocin-induced diabetic mice is associated with the modulations of Sirt-1 expression and autophagy in pancreatic β-cell. J Asian Nat Prod Res. 2012;14(5):413-23. PMID: 22423887.

Au AY, Hasenwinkel JM, Frondoza CG. Silybin inhibits interleukin-1β-induced production of pro-inflammatory mediators in canine hepatocyte cultures. J Vet Pharmacol Ther. 2011 Apr;34(2):120-9. PMID: 21395602.

500 mg
1 g
5 g

S3345

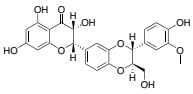

Silymarin

$C_{25}H_{22}O_{10}$ FW: 482.44 [65666-07-1] ≥70%

Mixture of compounds found in *Silybum* (milk thistle) seeds that inhibits telomerase. It also inhibits influenza virus proliferation by suppressing viral RNA synthesis, decreases inflammation and collagen deposition in BPH models, suppresses oxidative stress and fibrosis development, decreases lipid peroxidation, and prevents aggregation of proteins such as amyloid-β.

Atawia RT, Mosli HH, Tadros MG, et al. Modulatory effect of silymarin on inflammatory mediators in experimentally induced benign prostatic hyperplasia: emphasis on PTEN, HIF-1α, and NF-κB. Naunyn Schmiedebergs Arch Pharmacol. 2014 Aug 28. [Epub ahead of print]. PMID: 25164963

Clichici S, Olteanu D, Nagy AL, et al. Silymarin Inhibits the Progression of Fibrosis in the Early Stages of Liver Injury in CCl4-Treated Rats. J Med Food. 2014 Aug 18. [Epub ahead of print]. PMID: 25133972.

Borah A, Paul R, Choudhury S, et al. Neuroprotective potential of silymarin against CNS disorders: insight into the pathways and molecular mechanisms of action. CNS Neurosci Ther. 2013 Nov;19(11):847-53. PMID: 24118806.

10 g
50 g

S3449

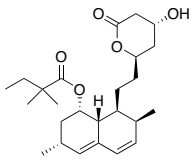

Simvastatin

MK-733

$C_{25}H_{38}O_5$ FW: 418.57 [79902-63-9] ≥97%

HMG-CoA reductase inhibitor used to lower cholesterol and lipid levels. It also blocks L-type Ca^{2+} channels and may activate ATP-sensitive K^+ channels. It decreases insulin synthesis and secretion, upregulates expression of M1/4 mAChRs to improve long-term memory, decreases expression of histone methyltransferase EZH2, and inhibits tumor growth in various cancer models.

Zhou J, Li W, Xie Q, et al. Effects of simvastatin on glucose metabolism in mouse MIN6 cells. J Diabetes Res. 2014;2014:376570. PMID: 24995341.

Banach M, Czuczwar SJ, Borowicz KK. Statins - are they anticonvulsant? Pharmacol Rep. 2014 Aug;66(4):521-8. PMID: 24948050.

Wang Q, Wei X, Gao H, et al. Simvastatin reverses the downregulation of M1/4 receptor binding in 6-hydroxydopamine-induced parkinsonian rats: the association with improvements in long-term memory. Neuroscience. 2014 May 16;267:57-66. PMID: 24613723.

10 mg
25 mg
50 mg
100 mg
500 mg

S3351

Asp-Tyr(SO3H)-Met-Gly-Trp-Met-Asp-Phe-NH_2

Sincalide

Cholecystokinin; CCK Octapeptide (26-33); CCK8

$C_{49}H_{62}N_{10}O_{16}S_3$ FW: 1143.29 [25126-32-3] ≥95%

CCK fragment and CCK receptor agonist. It displays a variety of biological activities, including increasing dendritic spine density, suppressing IgG1 production, modulating hormone signaling, and decreasing appetite.

Zhang LL, Wei XF, Zhang YH, et al. CCK-8S increased the filopodia and spines density in cultured hippocampal neurons of APP/PS1 and wild-type mice. Neurosci Lett. 2013 May 10;542:47-52. PMID: 23541713.

Zhang JG, Cong B, Jia XX, et al. Cholecystokinin octapeptide inhibits immunoglobulin G1 production of lipopolysaccharide-activated B cells. Int Immunopharmacol. 2011 Nov;11(11):1685-90. PMID: 21664492.

0.5 mg
1 mg

S3352 Sinefungin

1 mg
5 mg

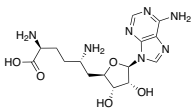

$C_{15}H_{23}N_7O_5$ FW: 381.39 [58944-73-3] ≥95%

Nucleoside analog of S-adenosylmethionine and methyltransferase inhibitor used to explore activity of S-adenosylmethionine. It inhibits growth and survival of *Trypanosoma* and *Leishmania*,

Yadav MK, Park SW, Chae SW, et al. Sinefungin, a natural nucleoside analogue of S-adenosylmethionine, inhibits *Streptococcus* pneumoniae biofilm growth. Biomed Res Int. 2014;2014:156987. PMID: 25050323.

Devkota K, Lohse B, Liu Q, et al. Analogues of the Natural Product Sinefungin as Inhibitors of EHMT1 and EHMT2. ACS Med Chem Lett. 2014 Jan 31;5(4):293-7. PMID: 24900829.

Niitsuma M, Hashida J, Iwatsuki M, et al. Sinefungin VA and dehydrosinefungin V, new antitrypanosomal antibiotics produced by Streptomyces sp. K05-0178. J Antibiot (Tokyo). 2010 Nov;63(11):673-9. PMID: 20859291.

S3453 Sinigrin Monohydrate, synthetic

100 mg
250 mg
1 g

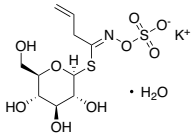

$C_{10}H_{17}KNO_9S_2 \bullet H_2O$ FW: 415.49 [3952-98-5] ≥98%

Antioxidant found in cruciferous vegetables. It displays a wide variety of biological properties, including increasing free fatty acid levels, decreasing triacylglycerol levels, and inducing expression of antioxidative enzymes.

Okulicz M. Multidirectional time-dependent effect of sinigrin and allyl isothiocyanate on metabolic parameters in rats. Plant Foods Hum Nutr. 2010 Sep;65(3):217-24. PMID: 20809411.

Washida K, Miyata M, Koyama T, et al. Suppressive effect of Yamato-mana (Brassica rapa L. Oleifera Group) constituent 3-butenyl glucosinolate (gluconapin) on postprandial hypertriglyceridemia in mice. Biosci Biotechnol Biochem. 2010;74(6):1286-9. PMID: 20530888.

S3353 Sinomenine Hydrochloride

1 g
10 g
25 g
50 g

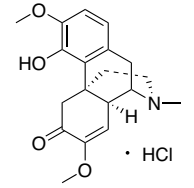

$C_{19}H_{23}NO_4 \bullet HCl$ FW: 365.86 [6080-33-7] ≥98%

Inhibitor of L-type Ca^{2+} channels and acid-sensing ion channels found in *Sinomenium*. It improves mechanical withdrawal threshold and cold pain sensitivity, suppresses OVA-induced allergies, and inhibits tumor growth and cell proliferation in breast cancer.

Li X, Wang K, Ren Y, et al. MAPK signaling mediates sinomenine hydrochloride-induced human breast cancer cell death via both reactive oxygen species-dependent and -independent pathways: an in vitro and in vivo study. Cell Death Dis. 2014 Jul 31;5:e1356. PMID: 25077542.

Zhang MY, Li P, Wang DQ, et al. Analgesic effect of sinomenine on SSNI model rats and monoamine neurotransmitters in striatal extracellular fluid. Zhongguo Zhong Yao Za Zhi. 2013 Feb;38(4):597-604. PMID: 23713290.

Chen Z, Tao Z, Zhang N, et al. The role of sinomenine in treatment of allergic rhinitis mice model and its mechanism. Lin Chung Er Bi Yan Hou Tou Jing Wai Ke Za Zhi. 2013 Jan;27(2):81-4. PMID: 23650707.

S3476 Sitagliptin Phosphate Monohydrate

10 mg
25 mg
100 mg

MK-0431

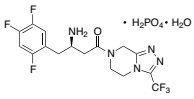

$C_{16}H_{15}F_6N_5O \bullet H_3PO_4 \bullet H_2O$ FW: 523.32 [654671-77-9] ≥98%

DPP4 inhibitor used to treat diabetes. It also decreases cardiac apoptosis, improves cardiac and vascular endothelial function, and suppresses expression of oxidative enzymes.

Chang G, Zhang P, Ye L, et al. Protective effects of sitagliptin on myocardial injury and cardiac function in an ischemia/reperfusion rat model. Eur J Pharmacol. 2013 Oct 15;718(1-3):105-13. PMID: 24041927.

Kubota Y, Miyamoto M, Takagi G, et al. The dipeptidyl peptidase-4 inhibitor sitagliptin improves vascular endothelial function in type 2 diabetes. J Korean Med Sci. 2012 Nov;27(11):1364-70. PMID: 23166419.

Liu L, Liu J, Wong WT, et al. Dipeptidyl peptidase 4 inhibitor sitagliptin protects endothelial function in hypertension through a glucagon-like peptide 1-dependent mechanism. Hypertension. 2012 Sep;60(3):833-41. PMID: 22868389.

S3584 Sivelestat Sodium Tetrahydrate

5 mg
25 mg

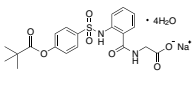

$C_{20}H_{21}N_2O_7S\ Na \bullet 4H_2O$ FW: 528.51 [201677-61-4] ≥98%

Neutrophil elastase inhibitor used to treat acute respiratory failure. It decreases myocardial infarction size, improves left ventricular contractility, inhibits contraction of tracheal and bronchial rings, and suppresses invasion and proliferation of esophageal carcinoma cells.

Aune SE, Yeh ST, Kuppusamy P, et al. Sivelestat attenuates myocardial reperfusion injury during brief low flow postischemic infusion. Oxid Med Cell Longev. 2013;2013:279847. PMID: 23766850.

Araki Y, Matsumiya M, Matsuura T, et al. Sivelestat suppresses iNOS gene expression in proinflammatory cytokine-stimulated hepatocytes. Dig Dis Sci. 2011 Jun;56(6):1672-81. PMID: 21221803.

S3585 SIVmac239-1

1 mg
2 mg
5 mg

H-Met-Gly-Val-Arg-Asn-Ser-Val-Leu-Ser-Gly-Lys-Lys-Ala-Asp-Glu-OH

$C_{65}H_{115}N_{21}O_{23}S_1$ FW: 1590.83 ≥95%

SIV fragment used to study the effects of immunodeficiency virus. It primarily infects lymphoid and myeloid cells.

Münch J, Sauermann U, Yolamanova M, et al. Effect of semen and seminal amyloid on vaginal transmission of simian immunodeficiency virus. Retrovirology. 2013 Dec 5;10:148. PMID: 24308721.

Xu Y, Weatherall C, Bailey M, et al. Simian immunodeficiency virus infects follicular helper CD4 T cells in lymphoid tissues during pathogenic infection of pigtail macaques. J Virol. 2013 Apr;87(7):3760-73. PMID: 23325697.

S3586 SIVmac239-2

1 mg
2 mg
5 mg

H-Asn-Ser-Val-Leu-Ser-Gly-Lys-Lys-Ala-Asp-Glu-Leu-Glu-Lys-Ile-OH

$C_{70}H_{123}N_{19}O_{25}$ FW: 1630.87 ≥95%

SIV fragment used to study the effects of immunodeficiency virus. It primarily infects lymphoid and myeloid cells.

Münch J, Sauermann U, Yolamanova M, et al. Effect of semen and seminal amyloid on vaginal transmission of simian immunodeficiency virus. Retrovirology. 2013 Dec 5;10:148. PMID: 24308721..

S4244 SKLB 610

NEW

5 mg
25 mg

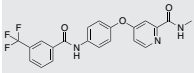

$C_{21}H_{16}F_3N_3O_3$ FW: 415.37 [1125780-41-7] ≥98%

Inhibitor of VEGFR2, PDGFR, and FGFR2. It decreases capillary tube formation, microvessel density, and tumor proliferation in various cancer models.

Luo X, Li S, Xie Y, et al. Pharmacokinetic studies of a novel multikinase inhibitor for treating cancer by HPLC-UV. J Chromatogr Sci. 2013 Jan;51(1):17-20. PMID: 22710664.

Cao ZX, Zheng RL, Lin HJ, et al. SKLB610: a novel potential inhibitor of vascular endothelial growth factor receptor tyrosine kinases inhibits angiogenesis and tumor growth in vivo. Cell Physiol Biochem. 2011;27(5):565-74. PMID: 21691074.

S1060 Small Cardioactive Peptide A

SCPA

1 mg
2 mg
5 mg

H-Ala-Arg-Pro-Gly-Tyr-Leu-Ala-Phe-Pro-Arg-Met-NH_2

$C_{59}H_{92}N_{18}O_{12}S$ FW: 1277.57 [98035-79-1] ≥95%

Cardiomodulator found in molluscs that controls feeding behavior and muscle movement. It also facilitates connection between cholinergic inhibitory neurons and sensory neurons.

Fox LE, Lloyd PE. Role of cAMP in the short-term modulation of a neuromuscular system in *aplysia*. J Neurophysiol. 2000 Mar;83(3):1567-79. PMID: 10712480.

Storozhuk M, Castellucci VF. Modulation of cholinergic transmission in the neuronal network of the gill and siphon withdrawal reflex in Aplysia. Neuroscience. 1999 Apr;90(1):291-301. PMID: 10188955.

S1061 Small Cardioactive Peptide B

SCPB

1 mg
2 mg
5 mg

H-Met-Asn-Tyr-Leu-Ala-Phe-Pro-Arg-Met-NH_2

$C_{52}H_{80}N_{14}O_{11}S_2$ FW: 1141.43 [84746-43-0] ≥95%

Cardiomodulator found in molluscs that controls feeding behavior and muscle movement. It also facilitates connection between cholinergic inhibitory neurons and sensory neurons.

Fox LE, Lloyd PE. Role of cAMP in the short-term modulation of a neuromuscular system in *aplysia*. J Neurophysiol. 2000 Mar;83(3):1567-79. PMID: 10712480.

S4932 SMI-4a

NEW

5 mg
10 mg
25 mg

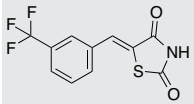

$C_{11}H_6F_3NO_2S$ FW: 273.23 [438190-29-5] ≥98%

Pim kinase inhibitor. It prevents phosphorylation of eIF4B, suppresses tumor growth, and induces cell cycle arrest and apoptosis in myeloid and lymphoid cells.

Yang J, Wang J, Chen K, et al. eIF4B phosphorylation by pim kinases plays a critical role in cellular transformation by Abl oncogenes. Cancer Res. 2013 Aug 1;73(15):4898-908. PMID: 23749639.

Lin YW, Beharry ZM, Hill EG, et al. A small molecule inhibitor of Pim protein kinases blocks the growth of precursor T-cell lymphoblastic leukemia/lymphoma. Blood. 2010 Jan 28;115(4):824-33. PMID: 19965690.

S5200 SNA 1

1 mg

≥98%

Sialic-acid sensing lectin used to stain epithelial cells.

Kirkeby S, Martel CJ, Aasted B, et al. Carbohydrate determinants in ferret conjunctiva are affected by infection with influenza H1N1 virus. Curr Eye Res. 2013 Oct;38(10):1027-35. PMID: 23790131.

S3368

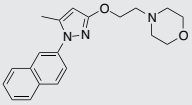

S1RA

NEW

1 mg
5 mg
10 mg

E52862; 4-Morpholine

$C_{20}H_{23}N_3O_2$ FW: 337.42 [878141-96-9] ≥98%

Antagonist at σ1 receptors. It reverses mechanical and thermal pain sensitivity, decreases formalin-induced glutamate release, and increases levels of norepinephrine.

Gris G, Merlos M, Vela JM, et al. S1RA, a selective sigma-1 receptor antagonist, inhibits inflammatory pain in the carrageenan and complete Freund's adjuvant models in mice. Behav Pharmacol. 2014 Jun;25(3):226-35. PMID: 24776490.

Vidal-Torres A, Fernández-Pastor B, Carceller A, et al. Effects of the selective sigma-1 receptor antagonist S1RA on formalin-induced pain behavior and neurotransmitter release in the spinal cord in rats. J Neurochem. 2014 May;129(3):484-94. PMID: 24384038.

S5722

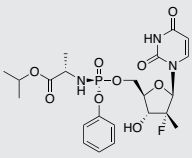

Sofosbuvir

NEW

10 mg
25 mg
50 mg

$C_{22}H_{29}FN_3O_9P$ FW: 529.45 [1190307-88-0] ≥98%

Viral RNA polymerase inhibitor used to treat hepatitis C infection.

Murakami C, Melda Urekli H, Atta MG. Antiviral medications for the treatment of hepatitis B and C infection and their effects on kidney function. Minerva Gastroenterol Dietol. 2014 Sep;60(3):177-89. PMID: 25027705.

Fung A, Jin Z, Dyatkina N, et al. Efficiency of incorporation and chain termination determines the inhibition potency of 2'-modified nucleotide analogs against hepatitis C virus polymerase. Antimicrob Agents Chemother. 2014 Jul;58(7):3636-45. PMID: 24733478.

Murakami E, Tolstykh T, Bao H, et al. Mechanism of activation of PSI-7851 and its diastereoisomer PSI-7977. J Biol Chem. 2010 Nov 5;285(45):34337-47. PMID: 20801890.

S5746

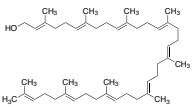

Solanesol

10 mg
50 mg
100 mg
500 mg

Nonaisoprenol

$C_{45}H_{74}O$ FW: 631.07 [13190-97-1] ≥92%

All-trans nonaprenol isoprenoid found in *Solanaceae* family used as biomarker for combustible tobacco use or exposure.

Purkis SW, Troude V, Hill CA. Effect of puffing intensity on cigarette smoke yields. Regul Toxicol Pharmacol. 2013 Jun;66(1):72-82. PMID: 23523712.

Tomida A, Suzuki H. Synergistic effect in culture of bleomycin-group antibiotics and N-solanesyl-N,N'-bis(3,4-dimethoxybenzyl)ethylenediamine, a synthetic isoprenoid. Jpn J Cancer Res. 1990 Nov;81(11):1184-90. PMID: 1702416.

S5745

H-Tyr-Gly-Cys-Lys-Asn-Phe-Phe-Trp-Lys-Thr-Phe-Thr-Ser-Cys-OH
(Cys3-Cys14)

[Tyr1]-Somatostatin

1 mg
2 mg
5 mg

$C_{82}H_{108}N_{18}O_{20}S_2$ FW: 1730.01 [59481-23-1] ≥95%

Endogenous somatostatin receptor agonist, GABA receptor modulator, and P/Q-type, N-type, and L-type voltage-gated Ca^{2+} channel modulator. It decreases anxiety-like behaviors, suppresses development of seizures, and limits food intake.

Stumm R. Somatostatin receptor sst2 reduces Akt activity and aggravates hypoxic/ischemic death in cerebral cortical neurons. Neuropharmacology. 2014 Feb;77:249-56. PMID: 24157493.

Takahashi M, Takeda M, Matsumoto S. Somatostatin enhances tooth-pulp-evoked cervical dorsal horn neuronal activity in the rat via inhibition of GABAergic interneurons. Brain Res Bull. 2014 Jan;100:76-83. PMID: 24321530.

S5747

H-Ala-Gly-Cys-Lys-Asn-Phe-Phe-Trp-Lys-Thr-Tyr-Thr-Ser-Cys-OH
(Cys3-Cys14)

[Tyr11]-Somatostatin

1 mg
2 mg
5 mg

$C_{76}H_{102}N_{18}O_{20}S_2$ FW: 1651.91 [59481-27-5] ≥95%

Endogenous somatostatin receptor agonist, GABA receptor modulator, and P/Q-type, N-type, and L-type voltage-gated Ca^{2+} channel modulator. It decreases anxiety-like behaviors, suppresses development of seizures, and limits food intake.

Stumm R. Somatostatin receptor sst2 reduces Akt activity and aggravates hypoxic/ischemic death in cerebral cortical neurons. Neuropharmacology. 2014 Feb;77:249-56. PMID: 24157493.

S5749

Ala-Gly-Cys-Lys-Asn-Phe-Phe-Trp-Cys-Ser-Thr-Phe-Thr-Lys
(Cys3-Cys14, Phe7-Thr10)

Somatostatin-14

5 mg
10 mg
25 mg

Growth hormone release-inhibiting factor

$C_{76}H_{104}N_{18}O_{19}S_2$ FW: 1637.92 [51110-01-1] ≥95%

Endogenous somatostatin receptor agonist, GABA receptor modulator, and P/Q-type, N-type, and L-type voltage-gated Ca^{2+} channel modulator. It decreases anxiety-like behaviors, suppresses development of seizures, and limits food intake.

Stumm R. Somatostatin receptor sst2 reduces Akt activity and aggravates hypoxic/ischemic death in cerebral cortical neurons. Neuropharmacology. 2014 Feb;77:249-56. PMID: 24157493.

S5751

Somatostatin-25

0.5 mg
1 mg
2.5 mg

H-Ser-Asn-Pro-Ala-Met-Ala-Pro-Arg-Glu-Arg-Lys-Ala-Gly-Cys-Lys-Asn-Phe-Phe-Trp-Lys-Thr-Phe-Thr-Ser-Cys-OH (Cys14-Cys25)

$C_{127}H_{191}N_{37}O_{34}S_3$ FW: 2876.36 [76461-17-1] ≥95%

Endogenous somatostatin receptor agonist, GABA receptor modulator, and P/Q-type, N-type, and L-type voltage-gated Ca^{2+} channel modulator. It decreases anxiety-like behaviors, suppresses development of seizures, and limits food intake.

Stumm R. Somatostatin receptor sst2 reduces Akt activity and aggravates hypoxic/ischemic death in cerebral cortical neurons. Neuropharmacology. 2014 Feb;77:249-56. PMID: 24157493.

S5750

Somatostatin-28

1 mg

Prosomatostatin

Ser-Ala-Asn-Ser-Asn-Pro-Ala-Met-Ala-Pro-Arg-Glu-Arg-Lys-Ala-Gly-Cys-Lys-Asn-Phe-Phe-Trp-Lys-Thr-Phe-Thr-Ser-Cys (Disulfide bridge Cys17-Cys28)

$C_{137}H_{207}N_{41}O_{39}S_3$ FW: 3148.6 [75037-27-3] ≥98%

Endogenous somatostatin receptor agonist, GABA receptor modulator, and P/Q-type, N-type, and L-type voltage-gated Ca^{2+} channel modulator. It decreases anxiety-like behaviors, suppresses development of seizures, and limits food intake.

Stumm R. Somatostatin receptor sst2 reduces Akt activity and aggravates hypoxic/ischemic death in cerebral cortical neurons. Neuropharmacology. 2014 Feb;77:249-56. PMID: 24157493.

S5752

Somatostatin-28 (1-12)

1 mg
2 mg
5 mg

H-Ser-Ala-Asn-Ser-Asn-Pro-Ala-Met-Ala-Pro-Arg-Glu-OH

$C_{49}H_{81}N_{17}O_{19}S$ FW: 1244.36 [81286-16-0] ≥95%

Endogenous somatostatin receptor agonist, GABA receptor modulator, and P/Q-type, N-type, and L-type voltage-gated Ca^{2+} channel modulator. It decreases anxiety-like behaviors, suppresses development of seizures, and limits food intake.

Stumm R. Somatostatin receptor sst2 reduces Akt activity and aggravates hypoxic/ischemic death in cerebral cortical neurons. Neuropharmacology. 2014 Feb;77:249-56. PMID: 24157493.

S5753

Somatostatin-28 (1-14)

1 mg
2 mg
5 mg

H-Ser-Ala-Asn-Ser-Asn-Pro-Ala-Met-Ala-Pro-Arg-Glu-Arg-Lys-OH

$C_{61}H_{105}N_{23}O_{21}S$ FW: 1528.72 [79243-10-0] ≥95%

Endogenous somatostatin receptor agonist, GABA receptor modulator, and P/Q-type, N-type, and L-type voltage-gated Ca^{2+} channel modulator. It decreases anxiety-like behaviors, suppresses development of seizures, and limits food intake.

Stumm R. Somatostatin receptor sst2 reduces Akt activity and aggravates hypoxic/ischemic death in cerebral cortical neurons. Neuropharmacology. 2014 Feb;77:249-56. PMID: 24157493.

S5976

Sotalol Hydrochloride

25 mg
100 mg
250 mg

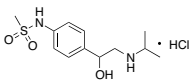

$C_{12}H_{20}N_2O_3S \bullet HCl$ FW: 308.82 [959-24-0] ≥98%

β-Adrenergic receptor antagonist and voltage-gated Na^+ and K^+ channel blocker used to treat ventricular fibrillation and ventricular tachycardia. It increases the effective refractory period and prolongs the cardiac QT and PR intervals.

Burashnikov A, Pourrier M, Gibson JK, et al. Rate-dependent effects of vernakalant in the isolated non-remodeled canine left atria are primarily due to block of the sodium channel: comparison with ranolazine and dl-sotalol. Circ Arrhythm Electrophysiol. 2012 Apr;5(2):400-8. PMID: 22322366.

Shah SA, Kluger J, White CM. Monotherapy versus combination therapy with class III antiarrhythmic agents to attenuate transmural dispersion of repolarization: a potential risk factor for torsade de pointes. Pharmacotherapy. 2007 Sep;27(9):1297-305. PMID: 17723083.

Singh BN, Singh SN, Reda DJ, et al. Amiodarone versus sotalol for atrial fibrillation. N Engl J Med. 2005 May 5;352(18):1861-72. PMID: 15872201.

S6000

Sparfloxacin

500 mg
1 g
5 g

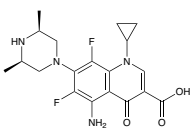

$C_{19}H_{22}F_2N_4O_3$ FW: 392.4 [110871-86-8] ≥98%

Topoisomerase IV and bacterial DNA gyrase inhibitor used to treat bacterial respiratory infections. It inhibits proliferation of cancer cells complexed with gold(III).

Gouvea LR, Garcia LS, Lachter DR, et al. Atypical fluoroquinolone gold(III) chelates as potential anticancer agents: relevance of DNA and protein interactions for their mechanism of action. Eur J Med Chem. 2012 Sep;55:67-73. PMID: 22835721.

Harding I, Simpson I. Fluoroquinolones: is there a different mechanism of action and resistance against *Streptococcus* pneumoniae? J Chemother. 2000 Oct;12 Suppl 4:7-15. PMID: 11131958.

S6018 Spectinomycin Dihydrochloride Pentahydrate

5 g
25 g

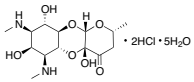

$C_{14}H_{24}N_2O_7 \cdot 2HCl \cdot 5H_2O$ FW: 495.25 [22189-32-8] ≥96%

Protein synthesis inhibitor previously used to treat gonorrhea.

Ilina EN, Malakhova MV, Bodoev IN, et al. Mutation in ribosomal protein S5 leads to spectinomycin resistance in Neisseria gonorrhoeae. Front Microbiol. 2013 Jul 10;4:186. PMID: 23847609.

Kehrenberg C, Schwarz S. Mutations in 16S rRNA and ribosomal protein S5 associated with high-level spectinomycin resistance in Pasteurella multocida. Antimicrob Agents Chemother. 2007 Jun;51(6):2244-6. PMID: 17371823.

S6019 Speract

1 mg
2 mg
5 mg

Sperm-activating Peptide H-1

H-Gly-Phe-Asp-Leu-Asn-Gly-Gly-Gly-Val-Gly-OH

$C_{38}H_{57}N_{11}O_{14}$ FW: 891.94 [76901-59-2] ≥95%

K^+ channel activator and speract SRCR agonist derived from egg outer envelope. It increases flagellar Ca^{2+} levels and intracellular Na^+, cAMP, and cGMP levels.

Guerrero A, Nishigaki T, Carneiro J, et al. Tuning sperm chemotaxis by calcium burst timing. Dev Biol. 2010 Aug 1;344(1):52-65. PMID: 20435032.

Darszon A, Treviño CL, Wood C, et al. Ion channels in sperm motility and capacitation. Soc Reprod Fertil Suppl. 2007;65:229-44. PMID: 17644965.

S6129 D-Sphingosine

5 mg
25 mg

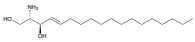

$C_{18}H_{37}NO_2$ FW: 299.49 [123-78-4] ≥98%

Endogenous component of sphingolipids and inhibitor of PKC. It also inhibits growth of *Escherichia*, *Staphylococcus*, and *Corynebacterium*.

Fischer CL, Drake DR, Dawson DV, et al. Antibacterial activity of sphingoid bases and fatty acids against Gram-positive and Gram-negative bacteria. Antimicrob Agents Chemother. 2012 Mar;56(3):1157-61. PMID: 22155833.

Huang Y, Zhang XY, Chen HL. Regulation of Phospholipase D Activity in Human Hepatocacinoma Cells by Protein Kinases and D-sphingosine. Sheng Wu Hua Xue Yu Sheng Wu Wu Li Xue Bao (Shanghai). 1999;31(5):572-576. PMID: 12114973.

S6130 Sphingosine-1-Phosphate

1 mg

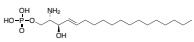

$C_{18}H_{38}NO_5P$ FW: 379.47 [26993-30-6] ≥98%

Endogenous sphingolipid involved in cell signaling that acts as an agonist at sphingosine-1-phosphate receptors. It may inhibit HDACs. It inhibits glucose deprivation stress, promotes cell migration, and preserves fertility and gonadal function in subjects exposed to cytotoxic agents.

Czubowicz K, Cieślik M, Pyszko J, et al. Sphingosine-1-Phosphate and Its Effect on Glucose Deprivation/Glucose Reload Stress: From Gene Expression to Neuronal Survival. Mol Neurobiol. 2014 Jul 24. [Epub ahead of print]. PMID: 25056275.

Mahajan-Thakur S, Sostmann BD, Fender AC, et al. Sphingosine-1-phosphate induces thrombin receptor PAR-4 expression to enhance cell migration and COX-2 formation in human monocytes. J Leukoc Biol. 2014 Jul 2. [Epub ahead of print]. PMID: 24990321.

Nguyen-Tran DH, Hait NC, Sperber H, et al. Molecular mechanism of sphingosine-1-phosphate action in Duchenne muscular dystrophy. Dis Model Mech. 2014 Jan;7(1):41-54. PMID: 24077965.

S6131 N,N-dimethyl-Sphingosine

5 mg

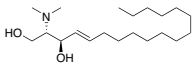

$C_{20}H_{41}NO_2$ FW: 327.5 [119567-63-4] ≥98%

PP2A activator and Sphk1 and PKC inhibitor. It suppresses ANP32A inhibition of PP2A and inhibits proliferation of gastric carcinoma cells.

Rosa R, Marciano R, Malapelle U, et al. Sphingosine kinase 1 overexpression contributes to cetuximab resistance in human colorectal cancer models. Clin Cancer Res. 2013 Jan 1;19(1):138-47. PMID: 23166225.

Habrukowich C, Han DK, Le A, et al. Sphingosine interaction with acidic leucine-rich nuclear phosphoprotein-32A (ANP32A) regulates PP2A activity and cyclooxygenase (COX)-2 expression in human endothelial cells. J Biol Chem. 2010 Aug 27;285(35):26825-31. PMID: 20558741.

Endo K, Igarashi Y, Nisar M, et al. Cell membrane signaling as target in cancer therapy: inhibitory effect of N,N-dimethyl and N,N,N-trimethyl sphingosine derivatives on in vitro and in vivo growth of human tumor cells in nude mice. Cancer Res. 1991 Mar 15;51(6):1613-8. PMID: 1998952.

S6134

Spinorphin, cow

5 mg
10 mg
25 mg

H-Leu-Val-Val-Tyr-Pro-Trp-Thr-OH

$C_{45}H_{64}N_8O_{10}$ FW: 877.06 [137201-62-8] ≥95%

Endogenous inhibitor of P2X3 receptors, N-formylpeptide receptors, ACE, enkephalinase, aminopeptidase IV, neutral endopeptidase, and DPP3. It inhibits neutrophil functionality, decreases inflammation, and suppresses depression-like behaviors.

Thanawala V, Kadam VJ, Ghosh R. Enkephalinase inhibitors: potential agents for the management of pain. Curr Drug Targets. 2008 Oct;9(10):887-94. PMID: 18855623.

Jung KY, Moon HD, Lee GE, et al. Structure-activity relationship studies of spinorphin as a potent and selective human P2X(3) receptor antagonist. J Med Chem. 2007 Sep 6;50(18):4543-7. PMID: 17676725.

S6232

Spiramycin

1 g
5 g

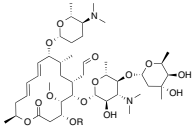

Spiramycin I R = H
Spiramycin II R = $COCH_3$
Spiramycin III R = $COCH_2CH_3$

RP-5337

$C_{43}H_{74}N_2O_{14}$ FW: 842.05 [8025-81-8]

Protein synthesis inhibitor used to treat toxoplasmosis and other soft tissue infections. It also suppresses release of pro-inflammatory cytokines and decreases *Toxoplasma*-induced brain cysts.

Kieffer F, Wallon M. Congenital toxoplasmosis. Handb Clin Neurol. 2013;112:1099-101. PMID: 23622316.

Büyükbaba Boral O, Sönmez Tamer G, Keçeli Özcan S, et al. Investigation of combined effectiveness of spiramycin and beta-glucan in mice models of acute toxoplasmosis and determination of IL-10, IL-12 and TNF-α levels. Mikrobiyol Bul. 2012 Jul;46(3):446-55. PMID: 22951656.

Chew WK, Segarra I, Ambu S, et al. Significant reduction of brain cysts caused by Toxoplasma gondii after treatment with spiramycin coadministered with metronidazole in a mouse model of chronic toxoplasmosis. Antimicrob Agents Chemother. 2012 Apr;56(4):1762-8. PMID: 22271863.

S6234

Spiramycin Embonate

1 g
5 g

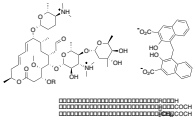

[67724-08-7]

Protein synthesis inhibitor used to treat toxoplasmosis and other soft tissue infections. It also suppresses release of pro-inflammatory cytokines and decreases *Toxoplasma*-induced brain cysts.

Kieffer F, Wallon M. Congenital toxoplasmosis. Handb Clin Neurol. 2013;112:1099-101. PMID: 23622316.

Büyükbaba Boral O, Sönmez Tamer G, Keçeli Özcan S, et al. Investigation of combined effectiveness of spiramycin and beta-glucan in mice models of acute toxoplasmosis and determination of IL-10, IL-12 and TNF-α levels. Mikrobiyol Bul. 2012 Jul;46(3):446-55. PMID: 22951656.

Chew WK, Segarra I, Ambu S, et al. Significant reduction of brain cysts caused by Toxoplasma gondii after treatment with spiramycin coadministered with metronidazole in a mouse model of chronic toxoplasmosis. Antimicrob Agents Chemother. 2012 Apr;56(4):1762-8. PMID: 22271863.

S6233

Spiramycin Hexanedioate

1 g
5 g

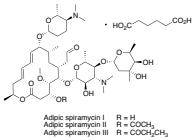

Adipic spiramycin I R = H
Adipic spiramycin II R = $COCH_3$
Adipic spiramycin III R = $COCH_2CH_3$

[11034-40-5] ≥80%

Protein synthesis inhibitor used to treat toxoplasmosis and other soft tissue infections. It also suppresses release of pro-inflammatory cytokines and decreases *Toxoplasma*-induced brain cysts.

Kieffer F, Wallon M. Congenital toxoplasmosis. Handb Clin Neurol. 2013;112:1099-101. PMID: 23622316.

Büyükbaba Boral O, Sönmez Tamer G, Keçeli Özcan S, et al. Investigation of combined effectiveness of spiramycin and beta-glucan in mice models of acute toxoplasmosis and determination of IL-10, IL-12 and TNF-α levels. Mikrobiyol Bul. 2012 Jul;46(3):446-55. PMID: 22951656.

S6168

Spirapril Hydrochloride

100 mg
250 mg
1 g

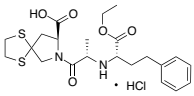

$C_{22}H_{30}N_2O_5S_2 \cdot HCl$ FW: 503.07 [94841-17-5]

ACE inhibitor used to treat hypertension. It decreases peripheral vascular resistance and blood pressure and increases cardiac output and stroke volume.

Noble S, Sorkin EM. Spirapril. A preliminary review of its pharmacology and therapeutic efficacy in the treatment of hypertension. Drugs. 1995 May;49(5):750-66. PMID: 7601014.

Sybertz EJ, Watkins RW, Ahn HS, et al. Pharmacologic, metabolic, and toxicologic profile of spirapril (SCH 33844), a new angiotensin converting inhibitor. J Cardiovasc Pharmacol. 1987;10 Suppl 7:S105-8. PMID: 2485040.

S6236 — 13-Desmethyl Spirolide C — NEW — 100 µg

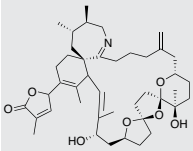

$C_{42}H_{61}NO_7$ FW: 691.94 [334974-07-1] ≥95%

Antagonist at nAChRs and mAChRs found in *Alexandrium*. It produces neuromuscular block, increases levels of N-acetyl aspartate and synaptophysin, and decreases levels of amyloid-β.

Marrouchi R, Rome G, Kharrat R, et al. Analysis of the action of gymnodimine-A and 13-desmethyl spirolide C on the mouse neuromuscular system in vivo. Toxicon. 2013 Dec 1;75:27-34. PMID: 23954513.

Alonso E, Otero P, Vale C, et al. Benefit of 13-desmethyl spirolide C treatment in triple transgenic mouse model of Alzheimer disease: beta-amyloid and neuronal markers improvement. Curr Alzheimer Res. 2013 Mar;10(3):279-89. PMID: 23036025.

Hauser TA, Hepler CD, Kombo DC, et al. Comparison of acetylcholine receptor interactions of the marine toxins, 13-desmethylspirolide C and gymnodimine. Neuropharmacology. 2012 Jun;62(7):2239-50. PMID: 22306792.

S6235 — Spironolactone — 250 mg, 1 g, 5 g

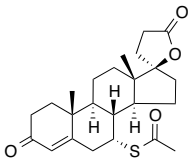

$C_{24}H_{32}O_4S$ FW: 416.57 [52-01-7] ≥97%

Diuretic and inhibitor of mineralocorticoid receptors, androgen receptors, and ENaC channels, and potential voltage-gated Ca^{2+} channel blocker used to treat heart failure.

Yancy CW, Jessup M, Bozkurt B, et al. 2013 ACCF/AHA guideline for the management of heart failure: a report of the American College of Cardiology Foundation/American Heart Association Task Force on Practice Guidelines. J Am Coll Cardiol. 2013 Oct 15;62(16):e147-239. PMID: 23747642.

Mann SJ, Parikh NS. A simplified mechanistic algorithm for treating resistant hypertension: efficacy in a retrospective study. J Clin Hypertens (Greenwich). 2012 Apr;14(4):191-7. PMID: 22458739.

S6247 — Splitomicin — NEW — 5 mg, 10 mg, 25 mg

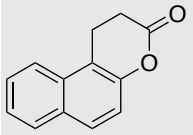

$C_{13}H_{10}O_2$ FW: 198.22 [5690-03-9] ≥98%

SIRT1/2 inhibitor and potential PDE inhibitor. It promotes translocation of Foxo3a, decreases cell motility, inhibits thrombin-induced platelet aggregation, and alters RNA splicing activity.

Hori YS, Kuno A, Hosoda R, et al. Regulation of FOXOs and p53 by SIRT1 modulators under oxidative stress. PLoS One. 2013 Sep 11;8(9):e73875. PMID: 24040102.

Bonezzi K, Belotti D, North BJ, et al. Inhibition of SIRT2 potentiates the anti-motility activity of taxanes: implications for antineoplastic combination therapies. Neoplasia. 2012 Sep;14(9):846-54. PMID: 23019416.

Liu FC, Day YJ, Liou JT, et al. Splitomicin inhibits fMLP-induced superoxide anion production in human neutrophils by activate cAMP/PKA signaling inhibition of ERK pathway. Eur J Pharmacol. 2012 Aug 5;688(1-3):68-75. PMID: 22634165.

S6800 — SR1001 — NEW — 5 mg, 25 mg, 100 mg

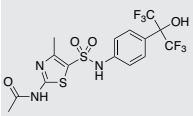

$C_{15}H_{13}F_6N_3O_4S_2$ FW: 477.4 [1335106-03-0] ≥98%

RORα/γ receptor inverse agonist that prevents Th17 cell development, differentiation, and function. It suppresses expression of pro-inflammatory cytokines and decreases incidence of diabetes.

Solt LA, Banerjee S, Campbell S, et al. ROR inverse agonist suppresses insulitis and prevents hyperglycemia in a mouse model of type 1 diabetes. Endocrinology. 2015 Mar;156(3):869-81. PMID: 25560829.

Beurel E, Harrington LE, Jope RS. Inflammatory T helper 17 cells promote depression-like behavior in mice. Biol Psychiatry. 2013 Apr 1;73(7):622-30. PMID: 23174342.

Solt LA, Kumar N, Nuhant P, et al. Suppression of TH17 differentiation and autoimmunity by a synthetic ROR ligand. Nature. 2011 Apr 28;472(7344):491-4. PMID: 21499262.

S7082 — SR FLICA Caspase 9 Assay Kit — 25 Tests, 100 Tests

Caspase 9 activity measuring kit.

S7081 — SR FLICA Caspases 3 and 7 Assay Kit — 25 Tests, 100 Tests

Caspases 3/7 activity measuring kit.

S7084 — SR-101-Leu-CMK Red FLISP™ Assay Kit — 25 Tests, 100 Tests

Caspase activity measuring kit.

S7083 SR-101-Phe-CMK Red FLISP™ Assay Kit

25 Tests
100 Tests

Caspase activity measuring kit.

S7080 SR-FLICA Poly Caspases Assay Kit

25 Tests
100 Tests

Caspase activity measuring kit.

S7184 SR-VAD-OPH in vitro Apoptosis Detection Reagent

4 vial Pack
NEW

Apoptosis measuring kit.

S7868 SRT1720 Hydrochloride

NEW

5 mg
25 mg
100 mg

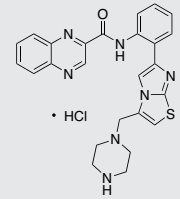

$C_{25}H_{23}N_7OS \bullet HCl$ FW: 506.02 [1001645-58-4] ≥98%

SIRT 1 activator and SIRT3 inhibitor that binds the acetyl-Lys site on sirtuins rather than the NAD^+ site. It improves renal tubular pathology, decreases amyloid-β-induced retinal pigment epithelial barrier disruption, and promotes migration and metastasis of breast cancer cells.

Mitchell SJ, Martin-Montalvo A, Mercken EM, et al. The SIRT1 Activator SRT1720 Extends Lifespan and Improves Health of Mice Fed a Standard Diet. Cell Rep. 2014 Mar 13;6(5):836-43. PMID: 24582957.

Cao L, Liu C, Wang F, et al. SIRT1 negatively regulates amyloid-beta-induced inflammation via the NF-κB pathway. Braz J Med Biol Res. 2013 Aug;46(8):659-69. PMID: 24036938.

Nguyen GT, Schaefer S, Gertz M, et al. Structures of human sirtuin 3 complexes with ADP-ribose and with carba-NAD^+ and SRT1720: binding details and inhibition mechanism. Acta Crystallogr D Biol Crystallogr. 2013 Aug;69(Pt 8):1423-32. PMID: 23897466.

S7701 Stanozolol

1 g
5 g

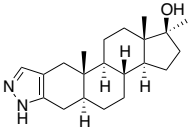

$C_{21}H_{32}N_2O$ FW: 328.49 [10418-03-8] ≥98%

Synthetic aromatase activator and progesterone receptor agonist used to treat anemia and angioedema. It increases phosphorylation of estrogen receptors and increases proliferation of growth plate chondrocytes.

Zhu SY, Li YH, Ma HM, et al. Stanozolol regulates proliferation of growth plate chondrocytes via activation of ERalpha in GnRHa-treated adolescent rats. J Pediatr Endocrinol Metab. 2011;24(5-6):275-81. PMID: 21823523.

Lionikas A, Blizard DA. Diverse effects of stanozolol in C57BL/6J and A/J mouse strains. Eur J Appl Physiol. 2008 Jun;103(3):333-41. PMID: 18350311.

S7601 Statil

NEW

5 mg
25 mg

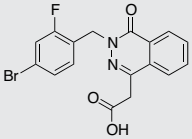

$C_{17}H_{12}BrFN_2O_3$ FW: 391.2 [72702-95-5] ≥98%

Aldose reductase inhibitor. It inhibits cell growth and proliferation and induces apoptosis in breast cancer and lung cancer cells. It also enhances adipose-derived stem adipocyte differentiation.

Pastel E, Pointud JC, Loubeau G, et al. Aldose reductases influence prostaglandin F2α levels and adipocyte differentiation in male mouse and human species. Endocrinology. 2015 May;156(5):1671-84. PMID: 25730106.

Cao Z, Zhou B, Chen X, et al. Statil suppresses cancer cell growth and proliferation by the inhibition of tumor marker AKR1B10. Anticancer Drugs. 2014 Sep;25(8):930-7. PMID: 24800887.

El-Kabbani O, Ramsland P, Darmanin C, et al. Structure of human aldose reductase holoenzyme in complex with statil: an approach to structure-based inhibitor design of the enzyme. Proteins. 2003 Feb 1;50(2):230-8. PMID: 12486717.

S7600 Staurosporine

1 mg
5 mg
25 mg
100 mg

AM-2282

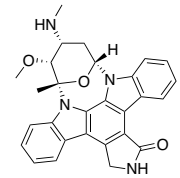

$C_{28}H_{26}N_4O_3$ FW: 466.5 [62996-74-1] ≥98%

PKC and mammalian RNA splicing inhibitor produced by *Streptomyces*. It is a precursor in the synthesis of K252c. It induces apoptosis in hepatocarcinoma cells and causes cell death in *Trypanosoma*.

Zhao C, Yin P, Mei C, et al. Down-regulation of DNA methyltransferase 3B in staurosporine-induced apoptosis and its mechanism in human hepatocarcinoma cell lines. Mol Cell Biochem. 2013 Apr;376(1-2):111-9. PMID: 23397112.

Bruges G, Betancourt M, March M, et al. Apoptotic-like activity of staurosporine in axenic cultures of Trypanosoma evansi. Rev Inst Med Trop Sao Paulo. 2012 Mar-Apr;54(2):103-8. PMID: 22499424.

Aukema KG, Chohan KK, Plourde GL, et al. Small molecule inhibitors of yeast pre-mRNA splicing. ACS Chem Biol. 2009 Sep 18;4(9):759-68. PMID: 19634919.

S7603

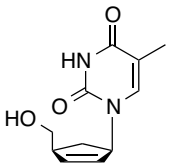

Stavudine

100 mg
250 mg
1 g

d4T

$C_{10}H_{12}N_2O_4$ FW: 224.21 [3056-17-5] ≥98%

Thymidine analog, DNA chain terminator, and RT inhibitor used to treat HIV. It intercalates DNA, increases levels of ROS, and induces autophagy in adipocytes.

Sandhya B, Seetharamappa J. Probing the site-selective binding of an antiretroviral drug, Stavudine to calf thymus DNA. Nucleosides Nucleotides Nucleic Acids. 2013;32(12):660-9. PMID: 24328563.

Stankov MV, Panayotova-Dimitrova D, Leverkus M, et al. Thymidine analogues suppress autophagy and adipogenesis in cultured adipocytes. Antimicrob Agents Chemother. 2013 Jan;57(1):543-51. PMID: 23147731.

Stankov MV, Panayotova-Dimitrova D, Leverkus M, et al. Autophagy inhibition due to thymidine analogues as novel mechanism leading to hepatocyte dysfunction and lipid accumulation. AIDS. 2012 Oct 23;26(16):1995-2006. PMID: 22914580.

S7618

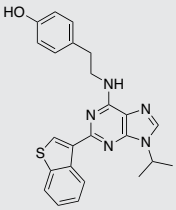

StemRegenin 1

NEW

5 mg
25 mg
50 mg

SR1

$C_{24}H_{23}N_5OS \cdot 0.7HCl \cdot 0.2H_2O$ FW: 458.7 [1227633-49-9] ≥98%

AhR antagonist. It increases dendritic cell production and expression of IFN-α, TNF-α, and IL-12 and induces differentiation of iPSCs.

Thordardottir S, Hangalapura BN, Hutten T, et al. The aryl hydrocarbon receptor antagonist StemRegenin 1 promotes human plasmacytoid and myeloid dendritic cell development from CD34+ hematopoietic progenitor cells. Stem Cells Dev. 2014 May 1;23(9):955-67. PMID: 24325394.

Gori JL, Chandrasekaran D, Kowalski JP, et al. Efficient generation, purification, and expansion of CD34(+) hematopoietic progenitor cells from nonhuman primate-induced pluripotent stem cells. Blood. 2012 Sep 27;120(13):e35-44. PMID: 22898598.

Boitano AE, Wang J, Romeo R, et al. Aryl hydrocarbon receptor antagonists promote the expansion of human hematopoietic stem cells. Science. 2010 Sep 10;329(5997):1345-8. Erratum in: Science. 2011 May 6;332(6030):664. PMID: 20688981.

S7717

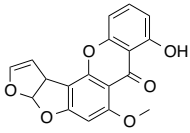

Sterigmatocystin

1 mg
5 mg
10 mg

$C_{18}H_{12}O_6$ FW: 324.28 [10048-13-2] ≥98%

Mycotoxin and carcinogen found in *Aspergillus*. It induces cell cycle arrest and DNA damage and increases lipid peroxidation.

Zhang D, Cui Y, Shen H, et al. Sterigmatocystin-induced DNA damage triggers G2 arrest via an ATM/p53-related pathway in human gastric epithelium GES-1 cells in vitro. PLoS One. 2013 May 21;8(5):e65044. PMID: 23705030.

Xing X, Wang J, Xing LX, et al. Involvement of MAPK and PI3K signaling pathway in sterigmatocystin-induced G2 phase arrest in human gastric epithelium cells. Mol Nutr Food Res. 2011 May;55(5):749-60. PMID: 21287681.

Delgado-Virgen F, Guzman-de-Peña D. Mechanism of Sterigmatocystin Biosynthesis Regulation by pH in *Aspergillus* nidulans. Braz J Microbiol. 2009 Oct;40(4):933-42. PMID: 24031444.

S7769

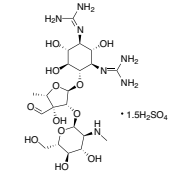

Streptomycin Sulfate

25 g
50 g
100 g

$C_{21}H_{39}N_7O_{12} \cdot 1.5H_2SO_4$ FW: 1457.39 [3810-74-0] ≥98%

Protein translation and mammalian mRNA splicing inhibitor used to treat gram negative bacterial infections and as a pesticide and fungicide.

Ruiz P, Rodríguez-Cano F, Zerolo FJ, et al. Streptomycin as second-line chemotherapy for tuberculosis. Rev Esp Quimioter. 2003 Jun;16(2):188-94. PMID: 12973456.

Hertweck M, Hiller R, Mueller MW. Inhibition of nuclear pre-mRNA splicing by antibiotics in vitro. Eur J Biochem. 2002 Jan;269(1):175-83. PMID: 11784311.

Zhu M, Burman WJ, Jaresko GS, et al. Population pharmacokinetics of intravenous and intramuscular streptomycin in patients with tuberculosis. Pharmacotherapy. 2001 Sep;21(9):1037-45. PMID: 11560193.

S7870

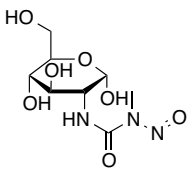

Streptozocin

50 mg
100 mg
500 mg

NSC-85998; U-9889

$C_8H_{15}N_3O_7$ FW: 265.22 [18883-66-4] ≥98%

DNA cross-linker and gluconeogenesis inhibitor used to induce diabetes-like conditions. It is toxic to pancreatic islet β cells.

Rerup CC. Drugs producing diabetes through damage of the insulin secreting cells. Pharmacol Rev. 1970 Dec;22(4):485-518. PMID: 4921840.

Murray-Lyon IM, Eddleston AL, Williams R, et al. Treatment of multiple-hormone-producing malignant islet-cell tumour with streptozotocin. Lancet. 1968 Oct 26;2(7574):895-8. PMID: 4176152.

S7872

Stresscopin-Related Peptide, human

0.5 mg
1 mg
2.5 mg

H-His-Pro-Gly-Ser-Arg-Ile-Val-Leu-Ser-Leu-Asp-Val-Pro-Ile-Gly-Leu-Leu-Gln-Ile-Leu-Leu-Glu-Gln-Ala-Arg-Ala-Arg-Ala-Ala-Arg-Glu-Gln-Ala-Thr-Thr-Asn-Ala-Arg-Ile-Leu-Ala-Arg-Val-NH_2

SRP

$C_{205}H_{358}N_{68}O_{57}$ FW: 4687.56 [348626-74-4] ≥95%

Urocortin II analog and CRFR2 receptor agonist. It induces positive inotropic cardioactivity, decreases food intake, and causes tachycardia.

Jin R, Li MZ, Bing YH, et al. Intracerebroventricular injection of stresscopin-related peptide enhances cardiovascular function in conscious rats. Regul Pept. 2013 Sep 10;186:7-11. PMID: 23850799.

Grossini E, Caimmi PP, Molinari C, et al. Modulation of calcium movements by urocortin II in endothelial cells. Cell Physiol Biochem. 2010;25(2-3):221-32. PMID: 20110683.

S7871

Stresscopin, human

0.5 mg
1 mg
2.5 mg

H-Thr-Lys-Phe-Thr-Leu-Ser-Leu-Asp-Val-Pro-Thr-Asn-Ile-Met-Asn-Leu-Leu-Phe-Asn-Ile-Ala-Lys-Ala-Lys-Asn-Leu-Arg-Ala-Gln-Ala-Ala-Ala-Asn-Ala-His-Leu-Met-Ala-Gln-Ile-NH_2

$C_{195}H_{326}N_{56}O_{53}S_2$ FW: 4367.24 [352020-03-2] ≥95%

Urocortin III analog and CRFR2 receptor agonist. It suppresses food intake, delays gastric emptying, and induces tachycardia.

Jin R, Li MZ, Bing YH, et al. Intracerebroventricular injection of stresscopin-related peptide enhances cardiovascular function in conscious rats. Regul Pept. 2013 Sep 10;186:7-11. PMID: 23850799.

Bagosi Z, Csabafi K, Palotai M, et al. The interaction of Urocortin II and Urocortin III with amygdalar and hypothalamic cotricotropin-releasing factor (CRF)--reflections on the regulation of the hypothalamic-pituitary-adrenal (HPA) axis. Neuropeptides. 2013 Oct;47(5):333-8. PMID: 23932308.

S7970

Strontium Ranelate

1 g
5 g

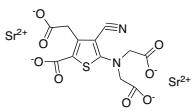

$C_{12}H_6N_2O_8S \bullet Sr_2$ FW: 513.49 [135459-87-9] ≥98%

Bone deterioration inhibitor and potential Ca^{2+}-sensing receptor agonist used to treat osteoporosis. It stimulates pre-osteoblast replication, decreases osteoclast activity, and promotes osteoblast differentiation.

Cattani-Lorente M, Rizzoli R, Ammann P. In vitro bone exposure to strontium improves bone material level properties. Acta Biomater. 2013 Jun;9(6):7005-13. PMID: 23454213.

Rodríguez J, Escudero ND, Mandalunis PM. Effect of strontium ranelate on bone remodeling. Acta Odontol Latinoam. 2012;25(2):208-13. PMID: 23230643.

Yamaguchi M, Weitzmann MN. The intact strontium ranelate complex stimulates osteoblastogenesis and suppresses osteoclastogenesis by antagonizing NF-κB activation. Mol Cell Biochem. 2012 Jan;359(1-2):399-407. PMID: 21874315.

S8098

SU-1498

5 mg
25 mg

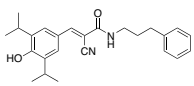

$C_{25}H_{30}N_2O_2$ FW: 390.5 [168835-82-3] ≥98%

Tyrphostin and VEGFR inhibitor. It inhibits angiogenesis, suppresses signaling by Akt, ERK1/2, Src, and STAT, and prevents autocrine growth and viability of cancer cells.

Ligęza J, Ligęza J, Klein A. Growth factor/growth factor receptor loops in autocrine growth regulation of human prostate cancer DU145 cells. Acta Biochim Pol. 2011;58(3):391-6. PMID: 21887406.

Lu KT, Sun CL, Wo PY, et al. Hippocampal neurogenesis after traumatic brain injury is mediated by vascular endothelial growth factor receptor-2 and the Raf/MEK/ERK cascade. J Neurotrauma. 2011 Mar;28(3):441-50. PMID: 21091268

S8005

Substance P

5 mg
10 mg
25 mg

H-Arg-Pro-Lys-Pro-Gln-Gln-Phe-Phe-Gly-Leu-Met-NH_2

$C_{63}H_{98}N_{18}O_{13}S$ FW: 1347.66 [33507-63-0] ≥95%

Endogenous NK1 receptor agonist involved in inflammation, stress signaling, and nociception. It improves cognitive performance, modulates opioid signaling, induces gastric mucosal protection, promoting gap junction intracellular communication, and inhibiting melanogenesis.

Yang L, Liu C, Dang H, et al. Substance P attenuates hyperoxia induced lung injury in neonatal rats. Mol Med Rep. 2014 Feb;9(2):595-9. PMID: 24247295.

Campolongo P, Ratano P, Ciotti MT, et al. Systemic administration of substance P recovers beta amyloid-induced cognitive deficits in rat: involvement of Kv potassium channels. PLoS One. 2013 Nov 12;8(11):e78036. PMID: 24265678.

S8006

Substance P (1-4)

1 mg
2 mg
5 mg

H-Arg-Pro-Lys-Pro-OH

$C_{22}H_{40}N_8O_5$ FW: 496.6 [69355-89-1] ≥95%

Endogenous NK1 receptor agonist involved in inflammation, stress signaling, and nociception. It improves cognitive performance, modulates opioid signaling, induces gastric mucosal protection, promoting gap junction intracellular communication, and inhibiting melanogenesis.

Yang L, Liu C, Dang H, et al. Substance P attenuates hyperoxia induced lung injury in neonatal rats. Mol Med Rep. 2014 Feb;9(2):595-9. PMID: 24247295.

S8007 Substance P (1-7)

1 mg
2 mg
5 mg

$C_{41}H_{65}N_{13}O_{10}$ FW: 900.06 [68060-49-1] ≥95%

H-Arg-Pro-Lys-Pro-Gln-Gln-Phe-OH

Endogenous NK1 receptor agonist involved in inflammation, stress signaling, and nociception. It improves cognitive performance, modulates opioid signaling, induces gastric mucosal protection, promoting gap junction intracellular communication, and inhibiting melanogenesis.

Yang L, Liu C, Dang H, et al. Substance P attenuates hyperoxia induced lung injury in neonatal rats. Mol Med Rep. 2014 Feb;9(2):595-9. PMID: 24247295.

S8008 Substance P (1-9)

1 mg
2 mg
5 mg

$C_{52}H_{77}N_{15}O_{12}$ FW: 1104.28 [57468-17-4] ≥95%

H-Arg-Pro-Lys-Pro-Gln-Gln-Phe-Phe-Gly-OH

Endogenous NK1 receptor agonist involved in inflammation, stress signaling, and nociception. It improves cognitive performance, modulates opioid signaling, induces gastric mucosal protection, promoting gap junction intracellular communication, and inhibiting melanogenesis.

Yang L, Liu C, Dang H, et al. Substance P attenuates hyperoxia induced lung injury in neonatal rats. Mol Med Rep. 2014 Feb;9(2):595-9. PMID: 24247295.

S8009 Substance P (7-11)

1 mg
2 mg
5 mg

$C_{31}H_{44}N_6O_5S$ FW: 612.8 [51165-05-0] ≥95%

H-Phe-Phe-Gly-Leu-Met-NH_2

Endogenous NK1 receptor agonist involved in inflammation, stress signaling, and nociception. It improves cognitive performance, modulates opioid signaling, induces gastric mucosal protection, promoting gap junction intracellular communication, and inhibiting melanogenesis.

Yang L, Liu C, Dang H, et al. Substance P attenuates hyperoxia induced lung injury in neonatal rats. Mol Med Rep. 2014 Feb;9(2):595-9. PMID: 24247295.

S8010 [Nle11]-Substance P

1 mg
2 mg
5 mg

$C_{64}H_{100}N_{18}O_{13}$ FW: 1329.62 [57462-42-7] ≥95%

H-Arg-Pro-Lys-Pro-Gln-Gln-Phe-Phe-Gly-Leu-Nle-NH_2

NK1 receptor agonist involved in inflammation, stress signaling, and nociception. It improves cognitive performance, modulates opioid signaling, induces gastric mucosal protection, promoting gap junction intracellular communication, and inhibiting melanogenesis.

Yang L, Liu C, Dang H, et al. Substance P attenuates hyperoxia induced lung injury in neonatal rats. Mol Med Rep. 2014 Feb;9(2):595-9. PMID: 24247295.

S8011 [Pro9]-Substance P

0.5 mg
1 mg
2.5 mg

$C_{66}H_{102}N_{18}O_{13}S$ FW: 1387.73 [104486-69-3] ≥95%

H-Arg-Pro-Lys-Pro-Gln-Gln-Phe-Phe-Pro-Leu-Met-NH_2

NK1 receptor agonist involved in inflammation, stress signaling, and nociception. It displays a wide variety of biological activities, including improving cognitive performance in Alzheimer's disease models, inducing gastric mucosal protection, inhibiting retinal apoptosis and melanogenesis, and promoting gap junction intracellular communication.

S8012 [Sar9]-Substance P

1 mg
2 mg
5 mg

$C_{64}H_{100}N_{18}O_{13}S$ FW: 1361.61 [77128-75-7] ≥95%

H-Arg-Pro-Lys-Pro-Gln-Gln-Phe-Phe-Sar-Leu-Met-NH_2

NK1 receptor agonist involved in inflammation, stress signaling, and nociception. It improves cognitive performance, modulates opioid signaling, induces gastric mucosal protection, promoting gap junction intracellular communication, and inhibiting melanogenesis.

Yang L, Liu C, Dang H, et al. Substance P attenuates hyperoxia induced lung injury in neonatal rats. Mol Med Rep. 2014 Feb;9(2):595-9. PMID: 24247295.

S8013 [Tyr8]-Substance P

1 mg
2 mg
5 mg

$C_{63}H_{98}N_{18}O_{14}S$ FW: 1363.66 [55614-10-3] ≥95%

H-Arg-Pro-Lys-Pro-Gln-Gln-Phe-Tyr-Gly-Leu-Met-NH_2

NK1 receptor agonist involved in inflammation, stress signaling, and nociception. It improves cognitive performance, modulates opioid signaling, induces gastric mucosal protection, promoting gap junction intracellular communication, and inhibiting melanogenesis.

Yang L, Liu C, Dang H, et al. Substance P attenuates hyperoxia induced lung injury in neonatal rats. Mol Med Rep. 2014 Feb;9(2):595-9. PMID: 24247295.

S8014 — Substance P, Free Acid

5 mg
10 mg
25 mg

$C_{63}H_{97}N_{17}O_{14}S$ FW: 1348.65 [71977-09-8] ≥95%

H-Arg-Pro-Lys-Pro-Gln-Gln-Phe-Phe-Gly-Leu-Met-OH

NK1 receptor agonist involved in inflammation, stress signaling, and nociception. It improves cognitive performance, modulates opioid signaling, induces gastric mucosal protection, promoting gap junction intracellular communication, and inhibiting melanogenesis.

Yang L, Liu C, Dang H, et al. Substance P attenuates hyperoxia induced lung injury in neonatal rats. Mol Med Rep. 2014 Feb;9(2):595-9. PMID: 24247295.

S7908 — Suc-APA-pNA

100 mg
1 g

$C_{21}H_{27}N_5O_8$ FW: 477.5 ≥95%

Suc-Ala-Pro-Ala-pNA

Substrate used to measure activity of human leukocyte elastase.

Oshima G, Akashi K, Yamada M. pH dependence of salt activation of human leukocyte elastase. Arch Biochem Biophys. 1984 Aug 15;233(1):212-8. PMID: 6565481.

S7909 — Suc-LEPF-pNA

1 mg
10 mg

$C_{35}H_{44}N_6O_{11}$ FW: 724.7 ≥98%

Suc-Leu-Glu-Pro-Phe-pNA

S7910 — Suc-RGPF-pNA

1 mg
10 mg

$C_{32}H_{41}N_9O_9$ FW: 695.7 ≥98%

Suc-Arg-Gly-Pro-Phe-pNA

S7911 — Suc-SDPF-pNA

1 mg
10 mg

$C_{31}H_{36}N_6O_{12}$ FW: 684.6 ≥98%

Suc-Ser-Asp-Pro-Phe-pNA

S8110 — Sucralfate

1 g
5 g

Sucrose Octasulfate-Aluminum Complex

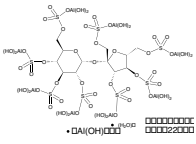

$C_{12}H_{54}Al_{16}O_{75}S_8$ FW: 974.73 [54182-58-0]

Pepsin inhibitor used to treat duodenal ulcers. It decreases gastric acid secretion, and increases mucous secretion and release of bicarbonate and prostaglandins. It also alters the structure of the intestinal epithelium and villi, increasing circulating eosinophil levels and mucous-producing cells.

Pali-Schöll I, Yildirim AO, Ackermann U, et al. Anti-acids lead to immunological and morphological changes in the intestine of BALB/c mice similar to human food allergy. Exp Toxicol Pathol. 2008 Aug;60(4-5):337-45. PMID: 18524557.

Shindo K, Iizuka M, Sasaki K, et al. Sucralfate prevents the delay of wound repair in intestinal epithelial cells by hydrogen peroxide through NF-kappaB pathway. J Gastroenterol. 2006 May;41(5):450-61. PMID: 16799887.

S8244 — Sulbactam

500 mg
1 g
5 g

CP 45899

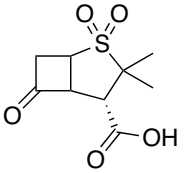

$C_8H_{11}NO_5S$ FW: 233.25 [68373-14-8] ≥98%

β-lactamase inhibitor used to improve the efficacy of β-lactam antibiotics. It is especially active against *Enterobacter* and *Staphylococcus*.

Li R, Liao JM, Gu CR, et al. Theoretical investigation on reaction of sulbactam with wild-type SHV-1 β-lactamase: acylation, tautomerization, and deacylation. J Phys Chem B. 2011 Sep 1;115(34):10298-310. PMID: 21797222.

Drawz SM, Bonomo RA. Three decades of beta-lactamase inhibitors. Clin Microbiol Rev. 2010 Jan;23(1):160-201. PMID: 20065329.

S8243 — Sulbactam Sodium

500 mg
1 g
5 g

CP-45899-2

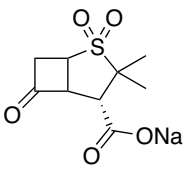

$C_8H_{10}NNaO_5S$ FW: 255.22 [69388-84-7] ≥98%

β-lactamase inhibitor that improves efficacy of other co-administered antibiotics. It is especially active against *Enterobacter* and *Staphylococcus*.

Li R, Liao JM, Gu CR, et al. Theoretical investigation on reaction of sulbactam with wild-type SHV-1 β-lactamase: acylation, tautomerization, and deacylation. J Phys Chem B. 2011 Sep 1;115(34):10298-310. PMID: 21797222.

S8245

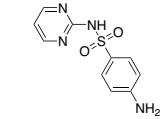

Sulfadiazine

50 g
100 g
500 g

$C_{10}H_{10}N_4O_2S$ FW: 250.28 [68-35-9] ≥98%

Folate production inhibitor used to treat bacterial infections.

Laue H, Weiss L, Bernardi A, et al. In vitro activity of the novel diaminopyrimidine, iclaprim, in combination with folate inhibitors and other antimicrobials with different mechanisms of action. J Antimicrob Chemother. 2007 Dec;60(6):1391-4. PMID: 17962215.

Richards RM, Xing JZ, Gregory DW, et al. Mechanism of sulphadiazine enhancement of trimethoprim activity against sulphadiazine-resistant Enterococcus faecalis. J Antimicrob Chemother. 1995 Oct;36(4):607-18. PMID: 8591935.

S8246

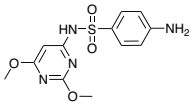

Sulfadimethoxine

10 g
25 g
100 g

$C_{12}H_{14}N_4O_4S$ FW: 310.33 [122-11-2] ≥98%

Folic acid synthesis inhibitor that is degraded by UV light. It is used to treat bacterial infections.

Zessel K, Mohring S, Hamscher G, et al. Biocompatibility and antibacterial activity of photolytic products of sulfonamides. Chemosphere. 2014 Apr;100:167-74. PMID: 24321335.

Mengelers MJ, van Klingeren B, van Miert AS. In vitro antimicrobial activity of sulfonamides against some porcine pathogens. Am J Vet Res. 1989 Jul;50(7):1022-8. PMID: 2774319.

S8144

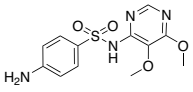

Sulfadoxine

10 g
25 g
100 g

$C_{12}H_{14}N_4O_4S$ FW: 310.33 [2447-57-6] ≥98%

Dihydropteroate synthase inhibitor that prevents folate synthesis and increases blood oxygen levels. It inhibits parasite growth.

Combrinck JM, Mabotha TE, Ncokazi KK, et al. Insights into the role of heme in the mechanism of action of antimalarials. ACS Chem Biol. 2013 Jan 18;8(1):133-7. PMID: 23043646.

Abebe W. Therapeutic efficacy of sulfadoxin/pyrimethamine in the treatment of uncomplicated *Plasmodium falciparum* malaria in Enseno, Meskan Woreda, Gurage zone, SNNPR, Ethiopia. Ethiop Med J. 2006 Apr;44(2):133-8. PMID: 17447375.

S8248

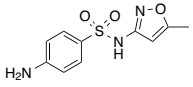

Sulfamethoxazole

10 g
25 g
100 g

$C_{10}H_{11}N_3O_3S$ FW: 253.28 [723-46-6] ≥98%

PABA inhibitor that prevents folic acid production and DNA synthesis. It inhibits growth of *Streptococcus*, *Staphylococcus*, *Escherichia*, *Haemophilus*, and *Pneumocystis*.

Jacobs RF, Wilson CB. Intracellular penetration and antimicrobial activity of antibiotics. J Antimicrob Chemother. 1983 Oct;12 Suppl C:13-20. PMID: 6605963.

Gleckman R, Alvarez S, Joubert DW. Drug therapy reviews: trimethoprim-sulfamethoxazole. Am J Hosp Pharm. 1979 Jul;36(7):893-906. PMID: 382841.

S8247

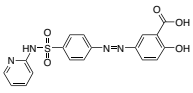

Sulfasalazine

10 g
50 g
100 g

$C_{18}H_{14}N_4O_5S$ FW: 398.39 [599-79-1] ≥98%

Mesalazine derivative and inhibitor of sepiapterin reductase and NMDA receptors used to treat inflammatory and autoimmune diseases. It also induces apoptosis in hepatic stellate cells and scavenges ROS and RNS.

Costigan M, Latremoliere A, Woolf CJ. Analgesia by inhibiting tetrahydrobiopterin synthesis. Curr Opin Pharmacol. 2012 Feb;12(1):92-9. PMID: 22178186.

Couto D, Ribeiro D, Freitas M, et al. Scavenging of reactive oxygen and nitrogen species by the prodrug sulfasalazine and its metabolites 5-aminosalicylic acid and sulfapyridine. Redox Rep. 2010;15(6):259-67. PMID: 21208525.

Noh JH, Gwag BJ, Chung JM. Underlying mechanism for NMDA receptor antagonism by the anti-inflammatory drug, sulfasalazine, in mouse cortical neurons. Neuropharmacology. 2006 Jan;50(1):1-15. PMID: 16169564.

S8251

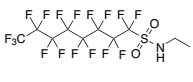

Sulfluramid

500 mg
1 g
5 g

GX 071; AL 3-29757; HSDB 7100

$C_{10}H_6F_{17}NO_2S$ FW: 527.2 [4151-50-2] ≥95%

Perfluorinated insecticide that inhibits growth of *Rhinotermidae* and *Blattellidae*. It also decreases production of IgM.

Ripa R, Luppichini P, Su NY, et al. Field evaluation of potential control strategies against the invasive eastern subterranean termite (Isoptera: Rhinotermitidae) in Chile. J Econ Entomol. 2007 Aug;100(4):1391-9. PMID: 17849893.

Peden-Adams MM, EuDaly JG, Dabra S, et al. Suppression of humoral immunity following exposure to the perfluorinated insecticide sulfluramid. J Toxicol Environ Health A. 2007 Jul;70(13):1130-41. PMID: 17558808.

S8044

R,S-Sulforaphane

25 mg
50 mg
100 mg
500 mg

$C_6H_{11}NOS_2$ FW: 177.29 [4478-93-7] ≥98%

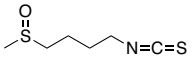

Synthetic antioxidant that displays a variety of biological activities. It induces activity and expression of phase II enzymes, inhibits the aryl hydrocarbon receptor, and downregulates expression of HDACs and STAT5. It also inhibits tumor growth and proliferation of melanoma cells, protects against UV-induced oxidative damage, induces autophagy, and prevents angiotensin II-induced hypertrophy.

Lee JH, Jeong JK, Park SY. Sulforaphane-induced autophagy flux prevents prion protein-mediated neurotoxicity through AMPK pathway. Neuroscience. 2014 Oct 10;278:31-9. PMID: 25130556.

Zhang R, Zhang J, Fang L, et al. Neuroprotective effects of sulforaphane on cholinergic neurons in mice with Alzheimer's disease-like lesions. Int J Mol Sci. 2014 Aug 18;15(8):14396-410. PMID: 25196440.

Nallasamy P, Si H, Babu PV, et al. Sulforaphane reduces vascular inflammation in mice and prevents TNF-α-induced monocyte adhesion to primary endothelial cells through interfering with the NF-κB pathway. J Nutr Biochem. 2014 Aug;25(8):824-33. PMID: 24880493.

Pinz S, Unser S, Rascle A. The natural chemopreventive agent sulforaphane inhibits STAT5 activity. PLoS One. 2014 Jun 9;9(6):e99391. PMID: 24910998.

Wu QQ, Zong J, Gao L, et al. Sulforaphane protects H9c2 cardiomyocytes from angiotensin II-induced hypertrophy. Herz. 2014 May;39(3):390-6. PMID: 23784363.

S8046

R-Sulforaphane

10 mg
25 mg
50 mg

$C_6H_{11}NOS_2$ FW: 177.29 [142825-10-3] ≥98%

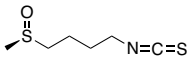

Natural product and antioxidant found in cruciferous vegetables. It inhibits the aryl hydrocarbon receptor and increases expression of phase II enzymes, glucuronosyl transferase, and epoxide hydrolase. It also promotes proliferation of stem cells and hematopoiesis.

Abdull Razis AF, Hanlon N, Soltys E, et al. The naturally occurring aliphatic isothiocyanates sulforaphane and erucin are weak agonists but potent non-competitive antagonists of the aryl hydrocarbon receptor. Arch Toxicol. 2012 Oct;86(10):1505-14. PMID: 22643862.

Zanichelli F, Capasso S, Cipollaro M, et al. Dose-dependent effects of R-sulforaphane isothiocyanate on the biology of human mesenchymal stem cells, at dietary amounts, it promotes cell proliferation and reduces senescence and apoptosis, while at anti-cancer drug doses, it has a cytotoxic effect. Age (Dordr). 2012 Apr;34(2):281-93. PMID: 21465338.

Abdull Razis AF, Bagatta M, De Nicola GR, et al. Induction of epoxide hydrolase and glucuronosyl transferase by isothiocyanates and intact glucosinolates in precision-cut rat liver slices: importance of side-chain substituent and chirality. Arch Toxicol. 2011 Aug;85(8):919-27. PMID: 21132492.

Abdull Razis AF, Iori R, Ioannides C. The natural chemopreventive phytochemical R-sulforaphane is a far more potent inducer of the carcinogen-detoxifying enzyme systems in rat liver and lung than the S-isomer. Int J Cancer. 2011 Jun 15;128(12):2775-82. PMID: 20726001.

S8045

S-Sulforaphane

5 mg
10 mg

$C_6H_{11}NOS_2$ FW: 177.29 ≥97%

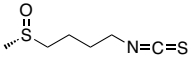

Synthetic antioxidant that induces phase II enzyme activity. Less potent than R-sulforaphane in inhibition of aryl hydrocarbon receptor.

Abdull Razis AF, Hanlon N, Soltys E, et al. The naturally occurring aliphatic isothiocyanates sulforaphane and erucin are weak agonists but potent non-competitive antagonists of the aryl hydrocarbon receptor. Arch Toxicol. 2012 Oct;86(10):1505-14. PMID: 22643862.

Abdull Razis AF, Bagatta M, De Nicola GR, et al. Induction of epoxide hydrolase and glucuronosyl transferase by isothiocyanates and intact glucosinolates in precision-cut rat liver slices: importance of side-chain substituent and chirality. Arch Toxicol. 2011 Aug;85(8):919-27. PMID: 21132492.

S8049

S-Sulforaphene

10 mg
25 mg
50 mg

$C_6H_9NOS_2$ FW: 175.27 [592-95-0] ≥98%

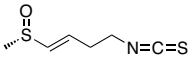

Synthetic compound found in radishes. It inhibits proliferation of colon adenocarcinoma cells and suppresses growth of velvetleaf seedlings. It may also induce phase II enzyme activity.

Kim KH, Moon E, Kim SY, et al. 4-Methylthio-butanyl derivatives from the seeds of Raphanus sativus and their biological evaluation on anti-inflammatory and antitumor activities. J Ethnopharmacol. 2014;151(1):503-8. PMID: 24231071.

Beevi SS, Mangamoori LN, Subathra M, et al. Hexane extract of Raphanus sativus L. roots inhibits cell proliferation and induces apoptosis in human cancer cells by modulating genes related to apoptotic pathway. Plant Foods Hum Nutr. 2010 Sep;65(3):200-9. PMID: 20652750.

Brinker AM, Spencer GF. Herbicidal activity of sulforaphene from stock (Matthiola incana). J Chem Ecol. 1993 Oct;19(10):2279-84. PMID: 24248575.

S8145 Sulindac

5 g
25 g

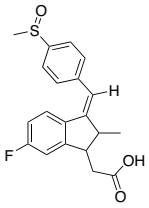

$C_{20}H_{17}FO_3S$ FW: 356.42 [38194-50-2] ≥98%

NSAID and inhibitor of PDE and COX-1/2 used to treat inflammation and pre-term labor. It increases levels of cGMP and inhibits expression of β-catenin, decreases infarct size in models of ischemic stroke, and suppresses proliferation and invasion of various cancer cells.

Modi JP, Gharibani PM, Ma Z, et al. Protective mechanism of sulindac in an animal model of ischemic stroke. Brain Res. 2014 Aug 12;1576:91-9. PMID: 24968090.

Li N, Xi Y, Tinsley HN, et al. Sulindac selectively inhibits colon tumor cell growth by activating the cGMP/PKG pathway to suppress Wnt/β-catenin signaling. Mol Cancer Ther. 2013 Sep;12(9):1848-59. PMID: 23804703.

Li X, Gao L, Cui Q, et al. Sulindac inhibits tumor cell invasion by suppressing NF-κB-mediated transcription of microRNAs. Oncogene. 2012 Nov 29;31(48):4979-86. PMID: 22286762.

S8147 Sulindac Sulfide

25 mg
100 mg
500 mg

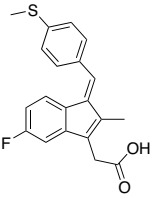

$C_{20}H_{17}FO_2S$ FW: 340.41 [32004-67-4] ≥97%

Derivative of sulindac, NSAID, and inhibitor of PDE and COX-1/2 used to treat inflammation and pre-term labor. It increases levels of cGMP and inhibits expression of β-catenin, decreases infarct size in models of ischemic stroke, and suppresses proliferation and invasion of various cancer cells.

Modi JP, Gharibani PM, Ma Z, et al. Protective mechanism of sulindac in an animal model of ischemic stroke. Brain Res. 2014 Aug 12;1576:91-9. PMID: 24968090.

Li N, Xi Y, Tinsley HN, et al. Sulindac selectively inhibits colon tumor cell growth by activating the cGMP/PKG pathway to suppress Wnt/β-catenin signaling. Mol Cancer Ther. 2013 Sep;12(9):1848-59. PMID: 23804703.

S8146 Sulindac Sulfone

50 mg
250 mg
500 mg

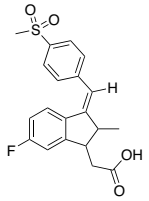

$C_{20}H_{17}FO_4S$ FW: 372.41 [59864-04-9] ≥98%

Derivative of sulindac, NSAID, and inhibitor of PDE and COX-1/2 used to treat inflammation and pre-term labor. It increases levels of cGMP and inhibits expression of β-catenin, decreases infarct size in models of ischemic stroke, and suppresses proliferation and invasion of various cancer cells.

Modi JP, Gharibani PM, Ma Z, et al. Protective mechanism of sulindac in an animal model of ischemic stroke. Brain Res. 2014 Aug 12;1576:91-9. PMID: 24968090.

Li N, Xi Y, Tinsley HN, et al. Sulindac selectively inhibits colon tumor cell growth by activating the cGMP/PKG pathway to suppress Wnt/β-catenin signaling. Mol Cancer Ther. 2013 Sep;12(9):1848-59. PMID: 23804703.

S8344 R,S-(±)-Sulpiride

5 g
25 g
100 g

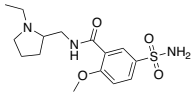

$C_{15}H_{23}N_3O_4S$ FW: 341.42 [15676-16-1] ≥98%

GHB receptor agonist and dopamine D2/3 receptor antagonist used to treat schizophrenia, depression, and anxiety. It ameliorates increased impulsivity and attentional impairment in PFC-lesioned models and increases concentrations of prolactin and melanocyte-stimulating hormone.

Valencia NA, Thompson DL Jr, Mitcham PB. Changes in plasma melanocyte-stimulating hormone, ACTH, prolactin, GH, LH, FSH, and thyroid-stimulating hormone in response to injection of sulpiride, thyrotropin-releasing hormone, or vehicle in insulin-sensitive and -insensitive mares. Domest Anim Endocrinol. 2013 May;44(4):204-12. PMID: 23571008.

Pezze MA, Dalley JW, Robbins TW. Remediation of attentional dysfunction in rats with lesions of the medial prefrontal cortex by intra-accumbens administration of the dopamine D(2/3) receptor antagonist sulpiride. Psychopharmacology (Berl). 2009 Jan;202(1-3):307-13. PMID: 18985321.

S8345 S-(−)-Sulpiride

1 g
5 g
10 g
25 g

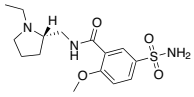

$C_{15}H_{23}N_3O_4S$ FW: 341.43 [23672-07-3] ≥99%

GHB receptor agonist and dopamine D2/3 receptor antagonist used to treat schizophrenia, depression, and anxiety. It ameliorates increased impulsivity and attentional impairment in PFC-lesioned models and increases concentrations of prolactin and melanocyte-stimulating hormone.

Valencia NA, Thompson DL Jr, Mitcham PB. Changes in plasma melanocyte-stimulating hormone, ACTH, prolactin, GH, LH, FSH, and thyroid-stimulating hormone in response to injection of sulpiride, thyrotropin-releasing hormone, or vehicle in insulin-sensitive and -insensitive mares. Domest Anim Endocrinol. 2013 May;44(4):204-12. PMID: 23571008.

S8151

Sumatriptan Succinate

100 mg
250 mg
1 g

$C_{14}H_{21}N_3O_2S \bullet C_4H_6O_4$ FW: 413.49 [103628-48-4] ≥98%

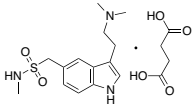

5-HT1B/1D receptor agonist and TRPV1 receptor antagonist used to treat migraines. It induces vasoconstriction, increases gastric relaxation, and suppresses release of CGRP.

Blumenfeld A, Gennings C, Cady R. Pharmacological synergy: the next frontier on therapeutic advancement for migraine. Headache. 2012 Apr;52(4):636-47. PMID: 22221151.

Loyd DR, Weiss G, Henry MA, et al. Serotonin increases the functional activity of capsaicin-sensitive rat trigeminal nociceptors via peripheral serotonin receptors. Pain. 2011 Oct;152(10):2267-76. PMID: 21737202.

Muñoz-Islas E, Lozano-Cuenca J, González-Hernández A, et al. Spinal sumatriptan inhibits capsaicin-induced canine external carotid vasodilatation via 5-HT1B rather than 5-HT1D receptors. Eur J Pharmacol. 2009 Aug 1;615(1-3):133-8. PMID: 19460365.

S8169

Suramin Hexasodium

50 mg
250 mg

$C_{51}H_{34}N_6O_{23}S_6Na_6$ FW: 1429.19 [129-46-4] ≥98%

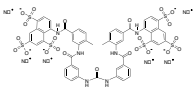

RyR agonist and inhibitor of SIRT, telomerase, P2Y receptors, and GPCRs. It displays several biological activities, including preventing viral attachment of enterovirus EV71 to host cells, inhibits falcipain-2 activity in *Plasmodium*, and suppressing cell proliferation and spheroid growth in glioma cells.

Wang Y, Qing J, Sun Y, et al. Suramin inhibits EV71 infection. Antiviral Res. 2014 Mar;103:1-6. PMID: 24374150.

Marques AF, Esser D, Rosenthal PJ, et al. Falcipain-2 inhibition by suramin and suramin analogues. Bioorg Med Chem. 2013 Jul 1;21(13):3667-73. PMID: 23680445.

Sakkiah S, Arooj M, Kumar MR, et al. Identification of inhibitor binding site in human sirtuin 2 using molecular docking and dynamics simulations. PLoS One. 2013;8(1):e51429. PMID: 23382805.

S9753

Synephrine

1 g
5 g
10 g

$C_9H_{13}NO_2$ FW: 167.21 [94-07-5] ≥98%

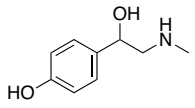

Endogenous compound found in citrus fruits, *Evodia*, and *Zanthoxylum* that activates adrenergic, TAAR-1, and 5-HT receptors. It acts as a positive inotrope, decreases ROS levels, suppresses expression of pro-inflammatory cytokines, and inhibits gastrointestinal motility and slows gastric emptying.

Wu Q, Li R, Soromou LW, et al. p-Synephrine suppresses lipopolysaccharide-induced acute lung injury by inhibition of the NF-κB signaling pathway. Inflamm Res. 2014 Jun;63(6):429-39. PMID: 24487736.

Ozçelik B, Kartal M, Orhan I. Cytotoxicity, antiviral and antimicrobial activities of alkaloids, flavonoids, and phenolic acids. Pharm Biol. 2011 Apr;49(4):396-402. PMID: 21391841.

Fang YS, Shan DM, Liu JW, et al. Effect of constituents from Fructus Aurantii Immaturus and *Radix* Paeoniae Alba on gastrointestinal movement. Planta Med. 2009 Jan;75(1):24-31. PMID: 19016407.

S9754

Syntide 2

1 mg
2 mg
5 mg

$C_{68}H_{122}N_{20}O_{18}$ FW: 1507.85 [108334-68-5] ≥95%

H-Pro-Leu-Ala-Arg-Thr-Leu-Ser-Val-Ala-Gly-Leu-Pro-Gly-Lys-Lys-OH

Synthetic substrate of CDPK, PKC, and CaMKII. It is phosphorylated by glutathione S-transferase and is involved in wound-induced signaling cascades.

Lanteri ML, Pagnussat GC, Lamattina L. Calcium and calcium-dependent protein kinases are involved in nitric oxide- and auxin-induced adventitious root formation in cucumber. J Exp Bot. 2006;57(6):1341-51. PMID: 16531462.

Szczegielniak J, Klimecka M, Liwosz A, et al. A wound-responsive and phospholipid-regulated maize calcium-dependent protein kinase. Plant Physiol. 2005 Dec;139(4):1970-83. PMID: 16299185.

S9775

Systemin

0.5 mg
1 mg
2.5 mg

$C_{85}H_{144}N_{26}O_{28}S$ FW: 2010.32 [137181-56-7] ≥95%

H-Ala-Val-Gln-Ser-Lys-Pro-Pro-Ser-Lys-Arg-Asp-Pro-Pro-Lys-Met-Gln-Thr-Asp-OH

Potential DNA binding agent found in *Solanaceae* family plants. It increases expression of defense-related genes and gene products including jasmonic acid.

Pearce G. Systemin, hydroxyproline-rich systemin and the induction of protease inhibitors. Curr Protein Pept Sci. 2011 Aug;12(5):399-408. PMID: 21418016.

Bing T, Chang T, Yang X, et al. G-quadruplex DNA aptamers generated for systemin. Bioorg Med Chem. 2011 Jul 15;19(14):4211-9. PMID: 21715176.

T0003

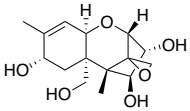

T2 Tetraol

Toxin T4; T4-ol

$C_{15}H_{22}O_6$ FW: 298.33 [34114-99-3] ≥97%

1 mg
5 mg

Mycotoxin found in *Fusarium*. It is less toxic than other similar mycotoxins but still induces cell death in various cell lines.

Madhyastha MS, Marquardt RR, Abramson D. Structure-activity relationships and interactions among trichothecene mycotoxins as assessed by yeast bioassay. Toxicon. 1994 Sep;32(9):1147-52. PMID: 7801350.

T0002

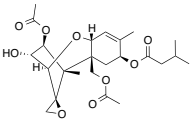

T2 Toxin

Insariotoxin

$C_{24}H_{34}O_9$ FW: 466.52 [21259-20-1] ≥98%

1 mg
5 mg
10 mg

Mycotoxin found in *Fusarium*. It is a common contaminant in grain products. It suppresses fibrinolytic and coagulant signaling pathways, alters BBB permeability, and induces oxidative stress.

Xu X, Madden LV, Edwards SG. Modeling the Effects of Environmental Conditions on HT2 and T2 Toxin Accumulation in Field Oat Grains. Phytopathology. 2014 Jan;104(1):57-66. PMID: 23883158.

Ravindran J, Agrawal M, Gupta N, et al. Alteration of blood brain barrier permeability by T-2 toxin: Role of MMP-9 and inflammatory cytokines. Toxicology. 2011 Feb 4;280(1-2):44-52. PMID: 21112371.

T7676

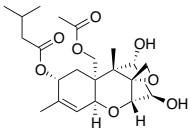

HT-2 Toxin

$C_{22}H_{32}O_8$ FW: 424.48 [26934-87-2] ≥98%

1 mg
5 mg

Mycotoxin found in *Fusarium*. It passes the blood-brain barrier and induces apoptosis in neurons.

Ortiz J, Van Camp J, Mestdagh F, et al. Mycotoxin co-occurrence in rice, oat flakes and wheat noodles used as staple foods in Ecuador. Food Addit Contam Part A Chem Anal Control Expo Risk Assess. 2013 Dec 7. [Epub ahead of print]. PMID: 24313870.

Weidner M, Hüwel S, Ebert F, et al. Influence of T-2 and HT-2 toxin on the blood-brain barrier in vitro: new experimental hints for neurotoxic effects. PLoS One. 2013;8(3):e60484. PMID: 23544145.

T0004

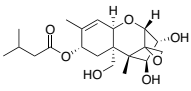

T2 Triol

$C_{20}H_{30}O_7$ FW: 382.45 [34114-98-2] ≥97%

1 mg
5 mg

Peptide chain initiation inhibitor found in *Fusarium*. It induces breakdown of polyribosomes and inhibits growth of Jurkat T cells.

Alassane-Kpembi I, Kolf-Clauw M, Gauthier T, et al. New insights into mycotoxin mixtures: the toxicity of low doses of Type B trichothecenes on intestinal epithelial cells is synergistic. Toxicol Appl Pharmacol. 2013 Oct 1;272(1):191-8. PMID: 23735874.

Tan DC, Flematti GR, Ghisalberti EL, et al. Mycotoxins produced by *Fusarium* species associated with annual legume pastures and 'sheep feed refusal disorders' in Western Australia. Mycotoxin Res. 2011 May;27(2):123-35. PMID: 23605703.

T0008

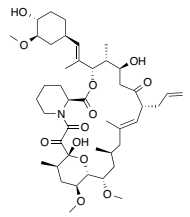

Tacrolimus

FK-506; Fujimycin; CCRIS 7124

$C_{44}H_{69}NO_{12}$ FW: 804.02 [104987-11-3] ≥98%

1 mg
5 mg
25 mg
100 mg

Calcineurin inhibitor used to treat atopic dermatitis and conjunctivitis. It inhibits synthesis of type I collagen polypeptides, suppresses the development of alcohol-induced liver fibrosis, and decreases levels of IgE eosinophils in OVA-induced allergy models.

Carr WW. Topical calcineurin inhibitors for atopic dermatitis: review and treatment recommendations. Paediatr Drugs. 2013 Aug;15(4):303-10. PMID: 23549982.

Manojlovic Z, Blackmon J, Stefanovic B. Tacrolimus (FK506) prevents early stages of ethanol induced hepatic fibrosis by targeting LARP6 dependent mechanism of collagen synthesis. PLoS One. 2013 Jun 3;8(6):e65897. PMID: 23755290.

Grigoriu S, Bond R, Cossio P, et al. The molecular mechanism of substrate engagement and immunosuppressant inhibition of calcineurin. PLoS Biol. 2013;11(2):e1001492. PMID: 23468591.

T0216

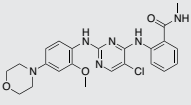

TAE-226

NVP-TAE226

$C_{23}H_{25}ClN_6O_3$ FW: 468.94 [761437-28-9] ≥98%

NEW

5 mg
25 mg

FAK inhibitor. It suppresses angiogenesis, decreases cancer cell viability, and prevents generation of TxA2.

Dao P, Jarray R, Le Coq J, et al. Synthesis of novel diarylamino-1,3,5-triazine derivatives as FAK inhibitors with anti-angiogenic activity. Bioorg Med Chem Lett. 2013 Aug 15;23(16):4552-6. PMID: 23845217.

Golubovskaya VM, Ho B, Zheng M, et al. Mitoxantrone targets the ATP-binding site of FAK, binds the FAK kinase domain and decreases FAK, Pyk-2, c-Src, and IGF-1R in vitro kinase activities. Anticancer Agents Med Chem. 2013 May;13(4):546-54. PMID: 22292772.

Bhavaraju K, Lakhani PR, Dorsam RT, et al. G(12/13) signaling pathways substitute for integrin αIIbβ3-signaling for thromboxane generation in platelets. PLoS One. 2011 Feb 10;6(2):e16586. PMID: 21347357.

T0140 TAK-632

NEW

5 mg
10 mg
25 mg

$C_{27}H_{18}F_4N_4O_3S$ FW: 554.52 [1228591-30-7] ≥98%

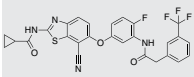

RAF inhibitor that induces dimerization of RAF but prevents kinase activity. It inhibits cell proliferation and tumor growth in melanoma models.

Nakamura A, Arita T, Tsuchiya S, et al. Antitumor activity of the selective pan-RAF inhibitor TAK-632 in BRAF inhibitor-resistant melanoma. Cancer Res. 2013 Dec 1;73(23):7043-55. PMID: 24121489.

Okaniwa M, Hirose M, Arita T, et al. Discovery of a selective kinase inhibitor (TAK-632) targeting pan-RAF inhibition: design, synthesis, and biological evaluation of C-7-substituted 1,3-benzothiazole derivatives. J Med Chem. 2013 Aug 22;56(16):6478-94. PMID: 23906342.

T0249 Tamibarotene

10 mg
50 mg

Am80

$C_{22}H_{25}NO_3$ FW: 351.44 [94497-51-5] ≥98%

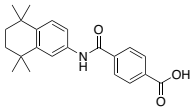

RARα/β agonist. It induces neuronal differentiation, inhibits deterioration of working memory and improves cognitive deficits in dementia and Alzheimer's disease, and suppresses cell growth in leukemia models.

Kitaoka K, Shimizu N, Ono K, et al. The retinoic acid receptor agonist Am80 increases hippocampal ADAM10 in aged SAMP8 mice. Neuropharmacology. 2013 Sep;72:58-65. PMID: 23624141

Yoshikawa O, Ebata Y, Tsuchiya H, et al. A retinoic acid receptor agonist tamibarotene suppresses iron accumulation in the liver. Obesity (Silver Spring). 2013 Jan;21(1):E22-5. PMID: 23404745.

Miyabe C, Miyabe Y, Miura NN, et al. Am80, a retinoic acid receptor agonist, ameliorates murine vasculitis through the suppression of neutrophil migration and activation. Arthritis *Rheum*. 2013 Feb;65(2):503-12. PMID: 23203767.

T0250 Tamoxifen Citrate

500 mg
1 g
5 g

$C_{26}H_{29}NO \bullet C_6H_8O_7$ FW: 563.64 [54965-24-1] ≥98%

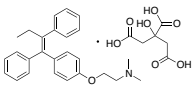

Prodrug of 4-hydroxytamoxifen and inhibitor of PKC used to treat breast cancer. It displays SERM and FIASMA activities. It also decreases blood vessel formation to inhibit angiogenesis, increases expression of FasL to induce apoptosis in osteoclasts, and improves behavior in mood disorders such as bipolar I disorder.

Yildiz A, Guleryuz S, Ankerst DP, et al. Protein kinase C inhibition in the treatment of mania: a double-blind, placebo-controlled trial of tamoxifen. Arch Gen Psychiatry. 2008 Mar;65(3):255-63. PMID: 18316672.

Krum SA, Miranda-Carboni GA, Hauschka PV, et al. Estrogen protects bone by inducing Fas ligand in osteoblasts to regulate osteoclast survival. EMBO J. 2008 Feb 6;27(3):535-45. PMID: 18219273.

Steiner AZ, Terplan M, Paulson RJ. Comparison of tamoxifen and clomiphene citrate for ovulation induction: a meta-analysis. Hum Reprod. 2005 Jun;20(6):1511-5. PMID: 15845599.

T0251 Tamsulosin Hydrochloride

10 mg
25 mg
100 mg

$C_{20}H_{28}N_2O_5S \bullet HCl$ FW: 444.98 [106463-17-6] ≥98%

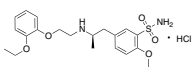

α1-Adrenergic receptor antagonist used to treat BPH. It inhibits peristaltic activity, increases bladder blood flow, and decreases bladder overactivity.

Okutsu H, Matsumoto S, Ohtake A, et al. Effect of tamsulosin on bladder blood flow and bladder function in a rat model of bladder over distention/emptying induced bladder overactivity. J Urol. 2011 Dec;186(6):2470-7. PMID: 22019173.

Barkin J. Review of dutasteride/tamsulosin fixed-dose combination for the treatment of benign prostatic hyperplasia: efficacy, safety, and patient acceptability. Patient Prefer Adherence. 2011;5:483-90. PMID: 22003286.

Rajpathy J, Aswathaman K, Sinha M, et al. An in vitro study on human ureteric smooth muscle with the alpha1-adrenoceptor subtype blocker, tamsulosin. BJU Int. 2008 Dec;102(11):1743-5. PMID: 18778345.

T0152 Tandutinib

1 mg
5 mg
25 mg

$C_{31}H_{42}N_6O_4$ FW: 562.7 [387867-13-2] ≥98%

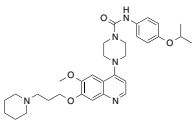

Inhibitor of FLT3, PDGFR, and c-Kit.It induces apoptosis in various cancer cells, decreases vessel formation in colon cancer xenografts, and inhibits phosphorylation of c-Kit, Akt, mTOR, and p70S6 kinase.

Ponnurangam S, Standing D, Rangarajan P, et al. Tandutinib inhibits the Akt/mTOR signaling pathway to inhibit colon cancer growth. Mol Cancer Ther. 2013 May;12(5):598-609. PMID: 23427297.

Ohshima-Hosoyama S, Davare MA, Prajapati SI, et al. Preclinical testing of tandutinib in a transgenic medulloblastoma mouse model. J Pediatr Hematol Oncol. 2012 Mar;34(2):116-21. PMID: 22146535.

Griswold IJ, Shen LJ, La Rosée P, et al. Effects of MLN518, a dual FLT3 and KIT inhibitor, on normal and malignant hematopoiesis. Blood. 2004 Nov 1;104(9):2912-8. PMID: 15242881.

T0253 Tangeretin

5 mg
10 mg

$C_{20}H_{20}O_7$ FW: 372.37 [481-53-8] ≥98%

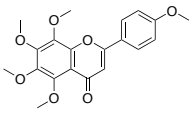

Found in citrus fruits. It exhibits a wide variety of biological properties, including decreasing expression of IL-4 and TNF-α in skin allergy models, increasing glucose uptake, inhibiting osteoclast formation, and inducing cell cycle arrest in breast cancer and colon cancer cells.

Jang SE, Ryu KR, Park SH, et al. Nobiletin and tangeretin ameliorate scratching behavior in mice by inhibiting the action of histamine and the activation of NF-κB, AP-1 and p38. Int Immunopharmacol. 2013 Aug 9;17(3):502-507. PMID: 23938254.

Tominari T, Hirata M, Matsumoto C, et al. Polymethoxy flavonoids, nobiletin and tangeretin, prevent lipopolysaccharide-induced inflammatory bone loss in an experimental model for periodontitis. J Pharmacol Sci. 2012;119(4):390-4. PMID: 22850615.

T0153 Tanshinone I

10 mg
25 mg
100 mg

Tanshinone A

$C_{18}H_{12}O_3$ FW: 276.29 [568-73-0] ≥95%

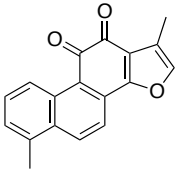

Found in *Salvia*. It displays a variety of biological activities, including decreasing peroxynitrite-induced DNA damage, inhibiting growth of lung cancer cells, and upregulating expression of IL-4 and IL-13 to protect against cerebral ischemia/reperfusion-induced injury.

Park JH, Park OK, Cho JH, et al. Anti-inflammatory Effect of Tanshinone I in Neuroprotection Against Cerebral Ischemia-Reperfusion Injury in the Gerbil Hippocampus. Neurochem Res. 2014 Apr 24. [Epub ahead of print]. PMID: 24760430.

Zhou S, Chen W, Su H, et al. Protective properties of tanshinone I against oxidative DNA damage and cytotoxicity. Food Chem Toxicol. 2013 Dec;62:407-12. PMID: 24021569.

Tung YT, Chen HL, Lee CY, et al. Active Component of Danshen (*Salvia* miltiorrhiza Bunge), Tanshinone I, Attenuates Lung Tumorigenesis via Inhibitions of VEGF, Cyclin A, and Cyclin B Expressions. Evid Based Complement Alternat Med. 2013;2013:319247. PMID: 23662128.

T0154 Tanshinone IIA

10 mg
25 mg
100 mg

Tanshinone B

$C_{19}H_{18}O_3$ FW: 294.34 [568-72-9] ≥93%

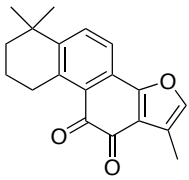

MAG lipase inhibitor found in *Salvia*. It displays a wide variety of biological activities, including inhibiting platelet aggregation and increasing bleeding time, limiting learning and memory deficits in neurodegenerative diseases, and inducing apoptosis and downregulating expression of STAT3 and IL-6 in breast cancer models.

Maione F, De Feo V, Caiazzo E, et al. Tanshinone IIA, a major component of *Salvia* milthorriza Bunge, inhibits platelet activation via Erk-2 signaling pathway. J Ethnopharmacol. 2014 Sep 11;155(2):1236-42. PMID: 25038434.

Yang L, Guo H, Dong L, et al. Tanshinone IIA inhibits the growth, attenuates the stemness and induces the apoptosis of human glioma stem cells. Oncol Rep. 2014 Sep;32(3):1303-11. PMID: 24970314.

Jiang P, Li C, Xiang Z, et al. Tanshinone IIA reduces the risk of Alzheimer's disease by inhibiting iNOS, MMP 2 and NF κBp65 transcription and translation in the temporal lobes of rat models of Alzheimer's disease. Mol Med Rep. 2014 Aug;10(2):689-94. PMID: 24859152.

T0081 Taurine

50 g
100 g

β-Aminoethylsulfonic acid

$C_2H_7NO_3S$ FW: 125.14 [107-35-7] ≥98%

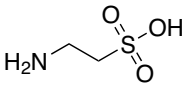

Endogenous sulfonic acid involved in Ca^{2+} signaling, skeletal muscle development, and cardiovascular function. It activates GlyR and GABA-A receptors to reduce anxiety, modulates blood pressure, and decreases levels of LDL, total cholesterol, triglycerides, and glucose.

El Idrissi A, Okeke E, Yan X, et al. Taurine regulation of blood pressure and vasoactivity. Adv Exp Med Biol. 2013;775:407-25. PMID: 23392950.

T0093 2'-Acetyltaxol

5 mg
10 mg
25 mg

$C_{49}H_{53}NO_{15}$ FW: 895.95 [92950-40-8] ≥98%

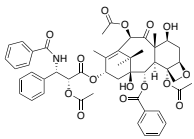

Taxane synthesis intermediate that has minimal effects on microtubule polymerization.

Williams HJ, Moyna G, Scott AI, et al. NMR and molecular modeling study of the conformations of taxol 2'-acetate in chloroform and aqueous dimethyl sulfoxide solutions. J Med Chem. 1996 Mar 29;39(7):1555-9. PMID: 8691488.

Mellado W, Magri NF, Kingston DG, et al. Preparation and biological activity of taxol acetates. Biochem Biophys Res Commun. 1984 Oct 30;124(2):329-36. PMID: 6548627.

T0094

2',7-Bisacetyltaxol

5 mg
10 mg
25 mg

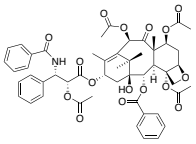

$C_{51}H_{55}NO_{16}$ FW: 937.98 ≥98%

Taxane synthesis intermediate that has minimal effects on microtubule polymerization.

Williams HJ, Moyna G, Scott AI, et al. NMR and molecular modeling study of the conformations of taxol 2'-acetate in chloroform and aqueous dimethyl sulfoxide solutions. J Med Chem. 1996 Mar 29;39(7):1555-9. PMID: 8691488.

Mellado W, Magri NF, Kingston DG, et al. Preparation and biological activity of taxol acetates. Biochem Biophys Res Commun. 1984 Oct 30;124(2):329-36. PMID: 6548627.

T0109

13-Acetyl-9-dihydrobaccatin-III

5 mg
10 mg
25 mg

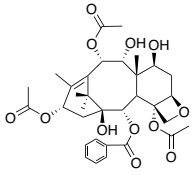

$C_{33}H_{44}O_{12}$ FW: 630.68 [142203-65-4] ≥98%

Found in *Taxus*. It is the starting material for taxol synthesis.

Li Y, Qin F, Wang SM, et al. Chemical studies on Taxus canadensis. Chem Biodivers. 2013 Oct;10(10):1729-53. PMID: 24130020.

Ketchum RE, Tandon M, Gibson DM, et al. Isolation of labeled 9-dihydrobaccatin III and related taxoids from cell cultures of taxuscell cultures of taxus canadensis elicited with m. J Nat Prod. 1999 Oct;62(10):1395-8. PMID: 10543900.

T0092

1-Hydroxybaccatin I

5 mg
10 mg
25 mg

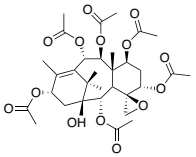

$C_{32}H_{44}O_{14}$ FW: 652.68 ≥98%

Found in *Taxus*. It may inhibit microtubule depolymerization.

Chao Z, Tan M, Paudel MK, et al. Development of an indirect competitive enzyme-linked immunosorbent assay (icELISA) using highly specific monoclonal antibody against paclitaxel. J Nat Med. 2013 Jul;67(3):512-8. PMID: 23007175.

Mao S, Chen W, Liao S. Studies on chemical constituents of the stem bark of Taxus cuspidata. Zhong Yao Cai. 1999 Jul;22(7):346-7. PMID: 12571929.

T0095

Baccatin III

5 mg
10 mg
25 mg

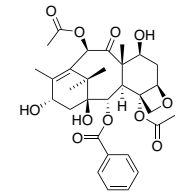

$C_{31}H_{38}O_{11}$ FW: 586.63 [27548-93-2] ≥98%

Found in *Taxus* and used to synthesize taxol. It suppresses accumulation of myeloid-derived suppressor cells in breast cancer, increases MHC class I and II antigen presentation in bone marrow dendritic cells, and induces apoptosis in various cancer cells.

Lee YH, Lee YR, Park CS, et al. Baccatin III, a precursor for the semisynthesis of paclitaxel, inhibits the accumulation and suppressive activity of myeloid-derived suppressor cells in tumor-bearing mice. Int Immunopharmacol. 2014 Aug;21(2):487-93. PMID: 24957690.

Chakravarthi BV, Sujay R, Kuriakose GC, et al. Inhibition of cancer cell proliferation and apoptosis-inducing activity of fungal taxol and its precursor baccatin III purified from endophytic *Fusarium* solani. Cancer Cell Int. 2013 Oct 23;13(1):105. PMID: 24152585.

Lee YH, Lee YR, Kim KH, et al. Baccatin III, a synthetic precursor of taxol, enhances MHC-restricted antigen presentation in dendritic cells. Int Immunopharmacol. 2011 Aug;11(8):985-91. PMID: 21354357.

T0117

Benzyl Analog of Taxol

1 mg
5 mg

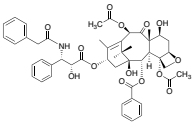

$C_{48}H_{53}NO_{14}$ FW: 867.93 [173101-56-9] ≥98%

Benzyl taxol analog and potential microtubule depolymerization inhibitor.

Li Y, Qin F, Wang SM, et al. Chemical studies on Taxus canadensis. Chem Biodivers. 2013 Oct;10(10):1729-53. PMID: 24130020.

Orr GA, Verdier-Pinard P, McDaid H, et al. Mechanisms of Taxol resistance related to microtubules. Oncogene. 2003 Oct 20;22(47):7280-95. PMID: 14576838.

T0096

Cephalomannine

Taxol B

5 mg
10 mg
25 mg

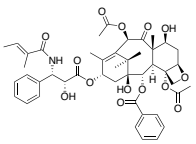

$C_{45}H_{53}NO_{14}$ FW: 831.91 [71610-00-9] ≥94%

Potential microtubule depolymerization inhibitor found in *Taxus*. It suppresses cell growth and inhibits DNA polymerase activity in glioblastoma cells and promotes microtubule assembly and increases survival rates in polycystic kidney disease models.

Li Y, Qin F, Wang SM, et al. Chemical studies on Taxus canadensis. Chem Biodivers. 2013 Oct;10(10):1729-53. PMID: 24130020.

Oshige M, Takenouchi M, Kato Y, et al. Taxol derivatives are selective inhibitors of DNA polymerase alpha. Bioorg Med Chem. 2004 May 15;12(10):2597-601. PMID: 15110841.

Woo DD, Tabancay AP Jr, Wang CJ. Microtubule active taxanes inhibit polycystic kidney disease progression in cpk mice. Kidney Int. 1997 May;51(5):1613-8. PMID: 9150481.

T0118 — 7-Epi-cephalomannine

5 mg
10 mg
25 mg

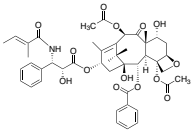

$C_{45}H_{53}NO_{14}$ FW: 831.9 ≥95%

Cephalomannine derivative found in *Taxus* and potential DNA polymerase inhibitor and microtubule depolymerization inhibitor.

Li Y, Qin F, Wang SM, et al. Chemical studies on Taxus canadensis. Chem Biodivers. 2013 Oct;10(10):1729-53. PMID: 24130020.

Oshige M, Takenouchi M, Kato Y, et al. Taxol derivatives are selective inhibitors of DNA polymerase alpha. Bioorg Med Chem. 2004 May 15;12(10):2597-601. PMID: 15110841.

Pandey RC, Yankov LK, Poulev A, et al. Synthesis and separation of potential anticancer active dihalocephalomannine diastereomers from extracts of Taxus yunnanensis. J Nat Prod. 1998 Jan;61(1):57-63. PMID: 9461653.

T0099 — 10-Deacetylbaccatin-III

5 mg
10 mg
25 mg

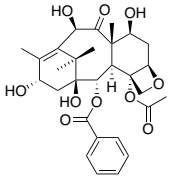

10-DB III

$C_{29}H_{36}O_{10}$ FW: 544.59 [32981-86-5] ≥98%

Found in *Taxus*. It decreases edema and pain and induces cell cycle arrest and inhibits growth in *Leishmania*.

Qayum M, Nisar M, Shah MR, et al. Analgesic and antiinflammatory activities of taxoids from Taxus wallichiana Zucc. Phytother Res. 2012 Apr;26(4):552-6. PMID: 21953729.

Georgopoulou K, Smirlis D, Bisti S, et al. In vitro activity of 10-deacetylbaccatin III against *Leishmania* donovani promastigotes and intracellular amastigotes. Planta Med. 2007 Aug;73(10):1081-8. PMID: 17691059.

T0100 — 10-Deacetyltaxol

5 mg
10 mg
25 mg

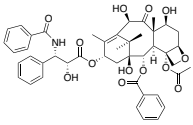

$C_{45}H_{49}NO_{13}$ FW: 811.87 [78432-77-6] ≥98%

Microtubule depolymerization inhibitor found in *Taxus*. It inhibits disease progression in models of polycystic kidney disease and inhibits growth of various cancer cells.

Ueda JY, Awale S, Tezuka Y, et al. Growth inhibitory activity of wood of Taxus yunnanensis and its liquid chromatography Fourier-transform mass spectrometry analysis. Planta Med. 2006 Oct;72(13):1241-4. PMID: 16902867.

Shen YC, Chen YJ, Chen CY. Taxane diterpenoids from the seeds of Chinese yew Taxus chinensis. Phytochemistry. 1999 Dec;52(8):1565-9. PMID: 10647221.

T0101 — 7-Epi-10-deacetyltaxol

5 mg
10 mg
25 mg

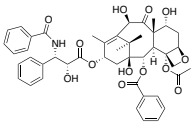

$C_{45}H_{49}NO_{13}$ FW: 811.87 [78454-17-8] ≥92%

Found in *Taxus*. It may inhibit microtubule depolymerization.

Yu SS, Sun QW, Zhang XP, et al. Content and distribution of active components in cultivated and wild Taxus chinensis var. mairei plants. Ying Yong Sheng Tai Xue Bao. 2012 Oct;23(10):2641-7. PMID: 23359921.

Slichenmyer WJ, Von Hoff DD. New natural products in cancer chemotherapy. J Clin Pharmacol. 1990 Sep;30(9):770-88. PMID: 1980498.

T0097 — 10-Deacetyltaxol B

5 mg
10 mg
25 mg

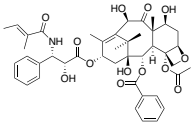

10-Deacetylcephalomannine

$C_{43}H_{51}NO_{13}$ FW: 789.86 [76429-85-1] ≥98%

Found in *Taxus*. It may inhibit microtubule depolymerization.

McLaughlin JL, Miller RW, Powell RG, et al. 19-Hydroxybaccatin III, 10-deacetylcephalomannine, and 10-deacetyltaxol: new antitumor taxanes from Taxus wallichiana. J Nat Prod. 1981 May-Jun;44(3):312-9. PMID: 7264680.

T0098 — 10-Deacetyltaxol C

5 mg
10 mg
25 mg

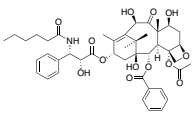

$C_{44}H_{55}NO_{13}$ FW: 805.91 ≥98%

Found in *Taxus*. It may inhibit microtubule depolymerization.

Su J, Shi HX, Wang LJ, et al. Chemical constituents of bark of Taxus chinensis var. mairei. Zhong Yao Cai. 2014 Feb;37(2):243-51. PMID: 25095344.

McLaughlin JL, Miller RW, Powell RG, et al. 19-Hydroxybaccatin III, 10-deacetylcephalomannine, and 10-deacetyltaxol: new antitumor taxanes from Taxus wallichiana. J Nat Prod. 1981 May-Jun;44(3):312-9. PMID: 7264680.

T0108 — 10-Deacetyl-7-xylosyltaxol

5 mg
10 mg
25 mg

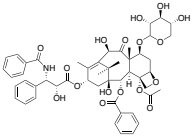

$C_{50}H_{57}NO_{17}$ FW: 943.98 [90332-63-1] ≥90%

Found in *Taxus*. It may inhibit microtubule depolymerization.

Hanson RL, Wasylyk JM, Nanduri VB, et al. Site-specific enzymatic hydrolysis of taxanes at C-10 and C-13. J Biol Chem. 1994 Sep 2;269(35):22145-9. PMID: 7915279.

Slichenmyer WJ, Von Hoff DD. New natural products in cancer chemotherapy. J Clin Pharmacol. 1990 Sep;30(9):770-88. PMID: 1980498.

T0116

2",3"-Dihydrocephalomannine

5 mg
10 mg
25 mg

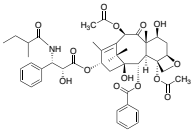

$C_{45}H_{55}NO_{14}$ FW: 833.92 ≥90%

Cephalomannine derivative found in *Taxus* and potential DNA polymerase inhibitor and microtubule depolymerization inhibitor.

Li Y, Qin F, Wang SM, et al. Chemical studies on Taxus canadensis. Chem Biodivers. 2013 Oct;10(10):1729-53. PMID: 24130020.

Oshige M, Takenouchi M, Kato Y, et al. Taxol derivatives are selective inhibitors of DNA polymerase alpha. Bioorg Med Chem. 2004 May 15;12(10):2597-601. PMID: 15110841.

T0102

7-Epi-taxol

5 mg
10 mg
25 mg

7-epi-Paclitaxel

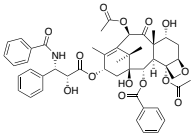

$C_{47}H_{51}NO_{14}$ FW: 853.91 [105454-04-4] ≥95%

Found in *Taxus*. It may inhibit microtubule depolymerization.

Yu SS, Sun QW, Zhang XP, et al. Content and distribution of active components in cultivated and wild Taxus chinensis var. mairei plants. Ying Yong Sheng Tai Xue Bao. 2012 Oct;23(10):2641-7. PMID: 23359921.

Shen YC, Chen YJ, Chen CY. Taxane diterpenoids from the seeds of Chinese yew Taxus chinensis. Phytochemistry. 1999 Dec;52(8):1565-9. PMID: 10647221.

T0115

Taxol Side Chain Acid

5 mg
10 mg
25 mg

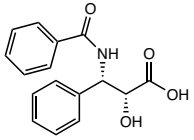

$C_{16}H_{15}NO_4$ FW: 285.29 ≥98%

Side chain commonly attached to taxanes.

Li Y, Qin F, Wang SM, et al. Chemical studies on Taxus canadensis. Chem Biodivers. 2013 Oct;10(10):1729-53. PMID: 24130020.

Ha HJ, Park GS, Ahn YG, et al. Practical synthesis of Taxol side chain. Bioorg Med Chem Lett. 1998 Jul 7;8(13):1619-22. PMID: 9873401.

T0103

Taxol Side Chain Diol

5 mg
10 mg
25 mg

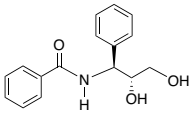

$C_{16}H_{17}NO_3$ FW: 271.34 ≥98%

Side chain attached to various taxanes.

Shen YC, Chen YJ, Chen CY. Taxane diterpenoids from the seeds of Chinese yew Taxus chinensis. Phytochemistry. 1999 Dec;52(8):1565-9. PMID: 10647221.

T0104

Taxol Side Chain Methyl Ester

5 mg
10 mg
25 mg

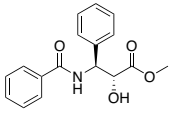

$C_{17}H_{18}NO_4$ FW: 299.32 ≥96%

Side chain attached to various taxanes.

Shen YC, Chen YJ, Chen CY. Taxane diterpenoids from the seeds of Chinese yew Taxus chinensis. Phytochemistry. 1999 Dec;52(8):1565-9. PMID: 10647221.

T0119

Taxol Side Chain β-lactam

5 mg
10 mg
25 mg

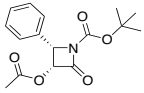

$C_{16}H_{19}NO_5$ FW: 305.33 [161183-22-8] ≥98%

Taxol synthesis intermediate.

T0105

Taxol C

5 mg
10 mg
25 mg

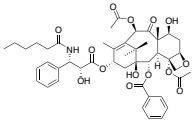

$C_{46}H_{57}NO_{14}$ FW: 847.94 [153415-45-3] ≥94%

Taxane synthesis intermediate that may inhibit microtubule depolymerization.

Slichenmyer WJ, Von Hoff DD. New natural products in cancer chemotherapy. J Clin Pharmacol. 1990 Sep;30(9):770-88. PMID: 1980498.

Shen YC, Chen YJ, Chen CY. Taxane diterpenoids from the seeds of Chinese yew Taxus chinensis. Phytochemistry. 1999 Dec;52(8):1565-9. PMID: 10647221.

T0090

7-(Triethylsilyl)-baccatin III

5 mg
10 mg
25 mg

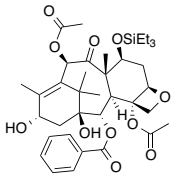

$C_{37}H_{52}O_{11}Si$ FW: 700.89 [115437-21-3] ≥98%

Synthetic taxol synthesis intermediate and microtubule depolymerization inhibitor. It induces apoptosis in cancer cells and increases presentation of antigen on MHC I and II receptors on dendritic cells.

Chakravarthi BV, Sujay R, Kuriakose GC, et al. Inhibition of cancer cell proliferation and apoptosis-inducing activity of fungal taxol and its precursor baccatin III purified from endophytic *Fusarium* solani. Cancer Cell Int. 2013 Oct 23;13(1):105. PMID: 24152585.

Lee YH, Lee YR, Kim KH, et al. Baccatin III, a synthetic precursor of taxol, enhances MHC-restricted antigen presentation in dendritic cells. Int Immunopharmacol. 2011 Aug;11(8):985-91. PMID: 21354357.

T0091 — 7-(Triethylsilyl)-10-deacetylbaccatin III

5 mg
10 mg
25 mg

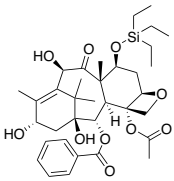

$C_{35}H_{50}O_{10}Si$ FW: 658.85 ≥97%

Taxol derivative that may inhibit cancer cell proliferation.

Krawczyk E, Luczak M, Kniotek M, et al. Cytotoxic, antiviral (in-vitro and in-vivo), immunomodulatory activity and influence on mitotic divisions of three taxol derivatives: 10-deacetyl-baccatin III, methyl (N-benzoyl-(2'R,3'S)-3'-phenylisoserinate) and N-benzoyl-(2'R,3'S)-3'-phenylisoserine. J Pharm Pharmacol. 2005 Jun;57(6):791-7. PMID: 15969936.

Samaranayake G, Neidigh KA, Kingston DG. Modified taxols, 8. Deacylation and reacylation of baccatin III. J Nat Prod. 1993 Jun;56(6):884-98. PMID: 8102392.

T0106 — Xylosyltaxol

5 mg
10 mg
25 mg

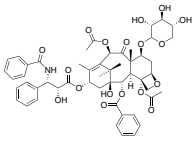

$C_{52}H_{59}NO_{18}$ FW: 986.02 [90332-66-4] ≥98%

Found in *Taxus*. It may inhibit microtubule depolymerization.

Yu SS, Sun QW, Zhang XP, et al. Content and distribution of active components in cultivated and wild Taxus chinensis var. mairei plants. Ying Yong Sheng Tai Xue Bao. 2012 Oct;23(10):2641-7. PMID: 23359921.

Slichenmyer WJ, Von Hoff DD. New natural products in cancer chemotherapy. J Clin Pharmacol. 1990 Sep;30(9):770-88. PMID: 1980498.

T0107 — Xylosyltaxol C

5 mg
10 mg
25 mg

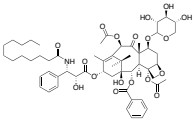

$C_{51}H_{65}NO_{18}$ FW: 980.02 ≥90%

Found in *Taxus*. It may inhibit microtubule depolymerization.

Yu SS, Sun QW, Zhang XP, et al. Content and distribution of active components in cultivated and wild Taxus chinensis var. mairei plants. Ying Yong Sheng Tai Xue Bao. 2012 Oct;23(10):2641-7. PMID: 23359921.

T0110 — Taxane Standard Mixture

500 µl

≥98%

Mixture of taxanes.

T0394 — (+)-Taxifolin

NEW

10 mg
25 mg
100 mg

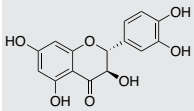

$C_{15}H_{12}O_7$ FW: 304.25 [480-18-2] ≥92%

Fatty acid synthesis inhibitor. It displays several biological properties, including inhibiting myocyte apoptosis, preventing aggregation of amyloid-β in Alzheimer's disease models, activating the antioxidant response element, and inducing apoptosis in cancer cells.

Sun X, Chen RC, Yang ZH, et al. Taxifolin prevents diabetic cardiomyopathy in vivo and in vitro by inhibition of oxidative stress and cell apoptosis. Food Chem Toxicol. 2013 Nov 20. [Epub ahead of print]. PMID: 24269735

Sato M, Murakami K, Uno M, et al. Site-specific inhibitory mechanism for amyloid β42 aggregation by catechol-type flavonoids targeting the Lys residues. J Biol Chem. 2013 Aug 9;288(32):23212-24. PMID: 23792961

Lee SB, Cha KH, Selenge D, et al. The chemopreventive effect of taxifolin is exerted through ARE-dependent gene regulation. Biol Pharm Bull. 2007 Jun;30(6):1074-9. PMID: 17541156

T0114 — Taxinine M

5 mg
10 mg
25 mg

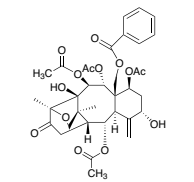

$C_{35}H_{42}NO_{14}$ FW: 686.7 ≥98%

Taxane found in *Taxus*, DNA polymerase inhibitor, and potential microtubule depolymerization inhibitor. It inhibits lung cancer cell proliferation.

Li Y, Qin F, Wang SM, et al. Chemical studies on Taxus canadensis. Chem Biodivers. 2013 Oct;10(10):1729-53. PMID: 24130020.

Oshige M, Takenouchi M, Kato Y, et al. Taxol derivatives are selective inhibitors of DNA polymerase alpha. Bioorg Med Chem. 2004 May 15;12(10):2597-601. PMID: 15110841.

T0298 — Tazobactam

100 mg
500 mg
1 g

YTR-830H; CL-298741

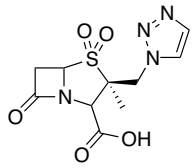

$C_{10}H_{12}N_4O_5S$ FW: 300.29 [89786-04-9] ≥98%

β-lactamase inhibitor used to enhance the efficacy of β-lactam antibiotics. It is especially active against *Enterobacter* and *Staphylococcus*.

Zhanel GG, Chung P, Adam H, et al. Ceftolozane/tazobactam: a novel cephalosporin/β-lactamase inhibitor combination with activity against multidrug-resistant gram-negative bacilli. Drugs. 2014 Jan;74(1):31-51. PMID: 24352909.

Frase H, Smith CA, Toth M, et al. Identification of products of inhibition of GES-2 beta-lactamase by tazobactam by x-ray crystallography and spectrometry. J Biol Chem. 2011 Apr 22;286(16):14396-409. PMID: 21345789.

Drawz SM, Bonomo RA. Three decades of beta-lactamase inhibitors. Clin Microbiol Rev. 2010 Jan;23(1):160-201. PMID: 20065329.

T0299

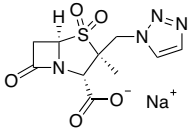

Tazobactam Sodium

YTR-830; CL-307579

$C_{10}H_{10}N_4NaO_5S$ FW: 322.28 [89785-84-2] ≥93%

100 mg
500 mg
1 g

β-lactamase inhibitor used to enhance efficacy of co-administered antibacterial compounds. It is active against *Enterobacter* and *Staphylococcus*.

Zhanel GG, Chung P, Adam H, et al. Ceftolozane/tazobactam: a novel cephalosporin/β-lactamase inhibitor combination with activity against multidrug-resistant gram-negative bacilli. Drugs. 2014 Jan;74(1):31-51. PMID: 24352909.

Frase H, Smith CA, Toth M, et al. Identification of products of inhibition of GES-2 beta-lactamase by tazobactam by x-ray crystallography and spectrometry. J Biol Chem. 2011 Apr 22;286(16):14396-409. PMID: 21345789.

T1298

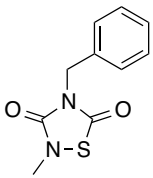

TDZD-8

$C_{10}H_{10}N_2O_2S$ FW: 222.26 [327036-89-5] ≥98%

5 mg
25 mg
100 mg
250 mg

GSK-3β inhibitor. It prevents hemorrhagic shock-induced changes in liver microcirculation, decreases collagen-induced arthritis by inhibiting infiltration of T cells and macrophages, and improves amphetamine-induced deficits in locomotor activity.

Jellestad L, Fink T, Pradarutti S, et al. Inhibition of glycogen synthase kinase (GSK)-3-β improves liver microcirculation and hepatocellular function after hemorrhagic shock. Eur J Pharmacol. 2014 Feb 5;724:175-84. PMID: 24389157.

Kwon YJ, Yoon CH, Lee SW, et al. Inhibition of glycogen synthase kinase-3β suppresses inflammatory responses in rheumatoid arthritis fibroblast-like synoviocytes and collagen-induced arthritis. Joint Bone Spine. 2013 Oct 28. [Epub ahead of print]. PMID: 24176738.

Willi R, Harmeier A, Giovanoli S, et al. Altered GSK3β signaling in an infection-based mouse model of developmental neuropsychiatric disease. Neuropharmacology. 2013 Oct;73:56-65. PMID: 23707483.

T1605

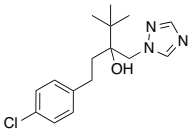

Tebuconazole

$C_{16}H_{22}ClN_3O$ FW: 307.82 [107534-96-3] ≥98%

5 g
10 g
100 g

14-α Demethylase inhibitor that inhibits ergosterol synthesis and fungal cell wall formation. It also inhibits voltage-gated Ca^{2+} channels and potentially inhibits aromatase.

Heusinkveld HJ, Molendijk J, van den Berg M, et al. Azole fungicides disturb intracellular Ca^{2+} in an additive manner in dopaminergic PC12 cells. Toxicol Sci. 2013 Aug;134(2):374-81. PMID: 23708404.

Kjærstad MB, Taxvig C, Nellemann C, et al. Endocrine disrupting effects in vitro of conazole antifungals used as pesticides and pharmaceuticals. Reprod Toxicol. 2010 Dec;30(4):573-82. PMID: 20708073.

Taxvig C, Vinggaard AM, Hass U, et al. Endocrine-disrupting properties in vivo of widely used azole fungicides. Int J Androl. 2008 Apr;31(2):170-7. PMID: 18067565.

T1733

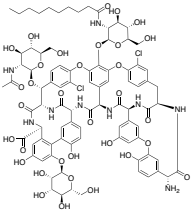

Teicoplanin

$C_{78}H_{77}Cl_2N_9O_{31}$ FW: 1707.39 [61036-62-2]

100 mg
250 mg
1 g

Vancomycin analog and peptidoglycan formation inhibitor that prevents growth of gram positive bacteria. It suppresses cell wall synthesis, induces seizures, and is used as a chiral selector in capillary liquid chromatography.

Nailor MD, Sobel JD. Antibiotics for gram-positive bacterial infections: vancomycin, teicoplanin, quinupristin/dalfopristin, oxazolidinones, daptomycin, dalbavancin, and telavancin. Infect Dis Clin North Am. 2009 Dec;23(4):965-82, ix. PMID: 19909893.

Takechi K, Ishikawa T, Kamei C. Epileptogenic activity induced by teicoplanin and effects of some antiepileptics in mice. J Pharmacol Sci. 2008 Aug;107(4):428-33. PMID: 18678985.

Kafková B, Bosáková Z, Tesarová E, et al. Chiral separation of beta-adrenergic antagonists, profen non-steroidal anti-inflammatory drugs and chlorophenoxypropionic acid herbicides using teicoplanin as the chiral selector in capillary liquid chromatography. J Chromatogr A. 2005 Sep 23;1088(1-2):82-93. PMID: 16130735.

T1844

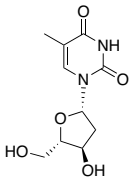

Telbivudine

L-Thymidine

$C_{10}H_{14}N_2O_5$ FW: 242.23 [3424-98-4] ≥98%

100 mg
250 mg
1 g

Thymidine analog and DNA chain terminator used to treat hepatitis B infections. It increases expression of CD127 on CD8+ memory T cells and decreases levels of hepatitis B viral DNA.

Nan XP, Zhang Y, Yu HT, et al. Inhibition of viral replication downregulates CD4(+)CD25(high) regulatory T cells and programmed death-ligand 1 in chronic hepatitis B. Viral Immunol. 2012 Feb;25(1):21-8. PMID: 22233255.

Lv G, Ying L, Ma WJ, et al. Dynamic analysis of CD127 expression on memory CD8 T cells from patients with chronic hepatitis B during telbivudine treatment. Virol J. 2010 Aug 31;7:207. PMID: 20807412.

Lai CL, Leung N, Teo EK, et al. A 1-year trial of telbivudine, lamivudine, and the combination in patients with hepatitis B e antigen-positive chronic hepatitis B. Gastroenterology. 2005 Aug;129(2):528-36. PMID: 16083710.

T1644

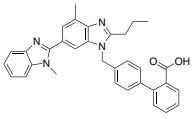

Telmisartan

BIBR 277

$C_{33}H_{30}N_4O_2$ FW: 514.63 [144701-48-4] ≥98%

50 mg
100 mg
500 mg

AT-II receptor antagonist and PPARγ/δ modulator used to treat hypertension. It also decreases levels of total cholesterol and LDL, suppresses weight gain and increases activity endurance, and lowers insulin, glucose, and triglyceride levels.

Xu S, Song H, Huang M, et al. Telmisartan inhibits the proinflammatory effects of homocysteine on human endothelial cells through activation of the peroxisome proliferator-activated receptor-δ pathway. Int J Mol Med. 2014 Sep;34(3):828-34. PMID: 24994548.

Sueta D, Koibuchi N, Hasegawa Y, et al. Telmisartan Exerts Sustained Blood Pressure Control and Reduces Blood Pressure Variability in Metabolic Syndrome by Inhibiting Sympathetic Activity. Am J Hypertens. 2014 May 28. [Epub ahead of print]. PMID: 24871627.

Feng X, Luo Z, Ma L, et al. Angiotensin II receptor blocker telmisartan enhances running endurance of skeletal muscle through activation of the PPAR-δ/AMPK pathway. J Cell Mol Med. 2011 Jul;15(7):1572-81. PMID: 20477906.

T1750

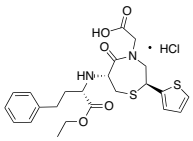

Temocapril Hydrochloride

CS-622

$C_{23}H_{28}N_2O_5S_2 \bullet HCl$ FW: 513.07 [110221-44-8] ≥98%

10 mg
25 mg
100 mg

ACE inhibitor that decreases blood pressure without affecting heart rate or cardiac output and improves endothelial dysfunction, vascular remodeling, insulin resistance, and renal function. It also prevents the development of hyperglycemia, inhibits oxidative stress and atherosclerotic remodeling, and suppresses activity of MMP2.

Yamamoto D, Takai S, Akimoto T, et al. Matrix metalloproteinase-2 inhibition by temocapril and its important role in peritoneal transport. Clin Exp Pharmacol Physiol. 2012 Oct;39(10):864-8. PMID: 23013132.

Kaihara M, Nakamura Y, Sugimoto T, et al. Olmesartan and temocapril prevented the development of hyperglycemia and the deterioration of pancreatic islet morphology in Otsuka-Long-Evans-Tokushima Fatty rats. Acta Med Okayama. 2009 Feb;63(1):35-42. PMID: 19247421.

Nozawa M, Sugimoto K, Ohmori M, et al. Dosing time-dependent effect of temocapril on the mortality of stroke-prone spontaneously hypertensive rats. J Pharmacol Exp Ther. 2006 Jan;316(1):176-81. PMID: 16174798.

T1849

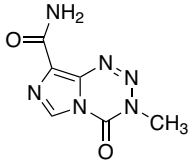

Temozolomide

$C_6H_6N_6O_2$ FW: 194.15 [85622-93-1] ≥98%

25 mg
100 mg
500 mg

DNA alkylator used to treat gliobastoma multiforme, anaplastic astrocytoma, and oligodendrocytoma. It prevents DNA replication.

Nagasawa DT, Chow F, Yew A, et al. Temozolomide and other potential agents for the treatment of glioblastoma multiforme. Neurosurg Clin N Am. 2012 Apr;23(2):307-22, ix. PMID: 22440874.

Wesolowski JR, Rajdev P, Mukherji SK. Temozolomide (Temodar). AJNR Am J Neuroradiol. 2010 Sep;31(8):1383-4. PMID: 2053882.

Friedman HS, Kerby T, Calvert H. Temozolomide and treatment of malignant glioma. Clin Cancer Res. 2000 Jul;6(7):2585-97. PMID: 10914698.

T1754

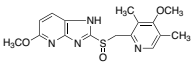

Tenatoprazole

$C_{16}H_{18}N_4O_3S$ FW: 346.41 [113712-98-4] ≥98%

100 mg
500 mg
1 g

H^+/K^+ ATPase inhibitor that prevents gastric acid secretion.

Li H, Meng L, Liu F, et al. H^+/K^+-ATPase inhibitors: a patent review. Expert Opin Ther Pat. 2013 Jan;23(1):99-111. PMID: 23205582.

Shin JM, Homerin M, Domagala F, et al. Characterization of the inhibitory activity of tenatoprazole on the gastric H^+,K^+ -ATPase in vitro and in vivo. Biochem Pharmacol. 2006 Mar 14;71(6):837-49. PMID: 16405921.

T1652

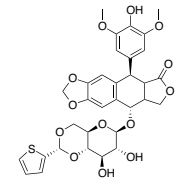

Teniposide

ETP

$C_{32}H_{32}O_{13}S$ FW: 656.66 [29767-20-2] ≥97%

25 mg
100 mg
500 mg

Podophyllotoxin derivative and topoisomerase II inhibitor used to treat acute lymphocytic leukemia. It induces single- and double-stranded DNA breaks.

You Y. Podophyllotoxin derivatives: current synthetic approaches for new anticancer agents. Curr Pharm Des. 2005;11(13):1695-717. PMID: 15892669.

Han YH, Austin MJ, Pommier Y, et al. Small deletion and insertion mutations induced by the topoisomerase II inhibitor teniposide in CHO cells and comparison with sites of drug-stimulated DNA cleavage in vitro. J Mol Biol. 1993 Jan 5;229(1):52-66. PMID: 8380617.

T1854

Tenofovir Monohydrate

100 mg
250 mg
1 g

$C_9H_{14}N_5O_4P \cdot H_2O$ FW: 305.23 [206184-49-8] ≥98%

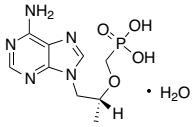

Nucleotide analog and RT inhibitor used to treat hepatitis B and HIV-1 infections. It may also treat FeLuk infection.

Qiu LP, Chen L, Chen KP. Antihepatitis B therapy: a review of current medications and novel small molecule inhibitors. Fundam Clin Pharmacol. 2013 Oct 4. [Epub ahead of print]. PMID: 24118072.

Iyidogan P, Anderson KS. Recent findings on the mechanisms involved in tenofovir resistance. Antivir Chem Chemother. 2013 Jun 6. [Epub ahead of print]. PMID: 23744599.

Greggs WM 3rd, Clouser CL, Patterson SE, et al. Discovery of drugs that possess activity against feline leukemia virus. J Gen Virol. 2012 Apr;93(Pt 4):900-5. PMID: 22258856.

T1852

Tenovin-1

NEW

10 mg
25 mg
100 mg

$C_{20}H_{23}N_3O_2S$ FW: 369.48 [380315-80-0] ≥98%

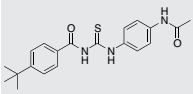

SIRT1/2 inhibitor and indirect p53 activator. It increases expression of FOXO3 and p53 and induces apoptosis in cutaneous T-cell lymphoma cells.

Nihal M, Ahmad N, Wood GS. SIRT1 is upregulated in cutaneous T-cell lymphoma, and its inhibition induces growth arrest and apoptosis. Cell Cycle. 2014 Feb 15;13(4):632-40. PMID: 24343700.

Lain S, Hollick JJ, Campbell J, et al. Discovery, in vivo activity, and mechanism of action of a small-molecule p53 activator. Cancer Cell. 2008 May;13(5):454-63. PMID: 18455128.

T1953

Tenovin-3

NEW

5 mg
10 mg
25 mg

$C_{18}H_{21}N_3OS$ FW: 327.45 [1011301-27-1] ≥98%

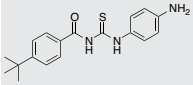

Potential SIRT2 inhibitor or p53 activator.

Dogra S, Bandi S, Viswanathan P, et al. Arsenic trioxide amplifies cisplatin toxicity in human tubular cells transformed by HPV-16 E6/E7 for further therapeutic directions in renal cell carcinoma. Cancer Lett. 2015 Jan 28;356(2 Pt B):953-61. PMID: 25444910.

Sonnemann J, Marx C, Becker S, et al. p53-dependent and p53-independent anticancer effects of different histone deacetylase inhibitors.Br J Cancer. 2014 Feb 4;110(3):656-67. PMID: 24281001.

T1853

Tenovin-6

NEW

1 mg
5 mg
25 mg

$C_{25}H_{34}N_4O_2S$ FW: 454.63 [1011557-82-6] ≥98%

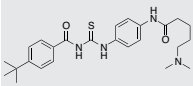

SIRT1/2 inhibitor and indirect p53 activator. It dysregulates autophagy in chronic lymphocytic leukemia cells and induces apoptosis in colon cancer cells.

Ueno T, Endo S, Saito R, et al. The sirtuin inhibitor tenovin-6 upregulates death receptor 5 and enhances cytotoxic effects of 5-Fluorouracil and oxaliplatin in colon cancer cells. Oncol Res. 2014;21(3):155-64. PMID: 24512730.

MacCallum SF, Groves MJ, James J, et al. Dysregulation of autophagy in chronic lymphocytic leukemia with the small-molecule Sirtuin inhibitor Tenovin-6. Sci Rep. 2013;3:1275. PMID: 23429453.

Lain S, Hollick JJ, Campbell J, et al. Discovery, in vivo activity, and mechanism of action of a small-molecule p53 activator. Cancer Cell. 2008 May;13(5):454-63. PMID: 18455128.

T1654

Tenoxicam

250 mg
1 g
5 g

$C_{13}H_{11}N_3O_4S_2$ FW: 337.38 [59804-37-4] ≥98%

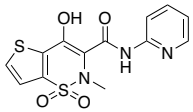

NSAID and COX-1/2 inhibitor used to treat arthritis, tendonitis, and bursitis. It also inhibits MPP+-induced decreases in phosphorylated Akt and scavenges free radicals, preventing lipid peroxidation.

Tasaki Y, Yamamoto J, Omura T, et al. Oxicam structure in non-steroidal anti-inflammatory drugs is essential to exhibit Akt-mediated neuroprotection against 1-methyl-4-phenyl pyridinium-induced cytotoxicity. Eur J Pharmacol. 2012 Feb 15;676(1-3):57-63. PMID: 22182582.

Suleyman H, Halici Z, Cadirci E, et al. Indirect role of beta2-adrenergic receptors in the mechanism of anti-inflammatory action of NSAIDS. J Physiol Pharmacol. 2008 Dec;59(4):661-72. PMID: 19212002.

T1855

Tentoxin

1 mg
5 mg

$C_{22}H_{30}N_4O_4$ FW: 414.5 [28540-82-1] ≥98%

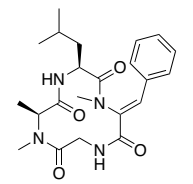

CF1 ATPase inhibitor frond in *Alternaria*. It inhibits the development of chloroplasts.

Duke SO, Dayan FE. Modes of action of microbially-produced phytotoxins. Toxins (Basel). 2011 Aug;3(8):1038-64. Erratum in: Toxins (Basel). 2012;4(10):955. PMID: 22069756.

Reimer S, Selman BR. Tentoxin-induced energy-independent adenine nucleotide exchange and ATPase activity with chloroplast coupling factor 1. J Biol Chem. 1978 Oct 25;253(20):7249-55. PMID: 151681.

Selman BR, Durbin RD. Evidence for a catalytic function of the coupling factor 1 protein reconstituted with chloroplast thylakoid membranes. Biochim Biophys Acta. 1978 Apr 11;502(1):29-37. PMID: 147703.

T1952

Tenuazonic Acid

1 mg
5 mg

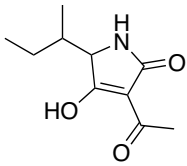

$C_{10}H_{15}NO_3$ FW: 197.23 [610-88-8] ≥96%

Photosynthesis inhibitor found in *Alternaria*. It increases generation of ROS, resulting in cell destruction and leaf necrosis.

Schwarz C, Kreutzer M, Marko D. Minor contribution of alternariol, alternariol monomethyl ether and tenuazonic acid to the genotoxic properties of extracts from *Alternaria* alternata infested rice. Toxicol Lett. 2012 Oct 2;214(1):46-52. PMID: 22906495.

Chen S, Yin C, Qiang S, et al. Chloroplastic oxidative burst induced by tenuazonic acid, a natural photosynthesis inhibitor, triggers cell necrosis in Eupatorium adenophorum Spreng. Biochim Biophys Acta. 2010 Mar;1797(3):391-405. PMID: 20026008.

T1670

Terazosin Hydrochloride Dihydrate

50 mg
250 mg
1 g

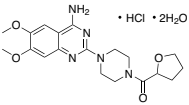

$C_{19}H_{25}N_5O_4 \bullet HCl \bullet 2H_2O$ FW: 459.93 [70024-40-7] ≥98%

α1-Adrenergic antagonist used to treat BPH and hypertension. It also induces apoptosis in prostate and prostate cancer cells.

Oelke M, Gericke A, Michel MC. Cardiovascular and ocular safety of α1-adrenoceptor antagonists in the treatment of male lower urinary tract symptoms. Expert Opin Drug Saf. 2014 Sep;13(9):1187-97. PMID: 25073735.

Papadopoulos G, Vlachodimitropoulos D, Kyroudi A, et al. Terazosin treatment induces caspase-3 expression in the rat ventral prostate. J Clin Med Res. 2013 Apr;5(2):127-31. PMID: 23518907.

T1672

Terbinafine Hydrochloride

250 mg
1 g
5 g
10 g

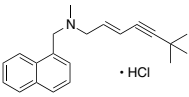

$C_{21}H_{25}N \bullet HCl$ FW: 327.9 [78628-80-5] ≥98%

Squalene oxidase and KSR1 inhibitor that prevents ergosterol and cholesterol synthesis. It also inhibits proliferation of oral squamous cell carcinoma cells.

Li B, Lu L, Zhong M, et al. Terbinafine inhibits KSR1 and suppresses Raf-MEK-ERK signaling in oral squamous cell carcinoma cells. Neoplasma. 2013;60(4):406-12. PMID: 23581412.

Nowosielski M, Hoffmann M, Wyrwicz LS, et al. Detailed mechanism of squalene epoxidase inhibition by terbinafine. J Chem Inf Model. 2011 Feb 28;51(2):455-62. PMID: 21229992.

Revankar SG, Nailor MD, Sobel JD. Use of terbinafine in rare and refractory mycoses. Future Microbiol. 2008 Feb;3(1):9-17. PMID: 18230029.

T1674

Terbutaline

1 g
5 g

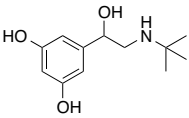

$C_{12}H_{19}NO_3$ FW: 225.28 [23031-25-6] ≥98%

β2-Adrenergic receptor agonist and potential ENaC channel activator used to treat asthma and cough. It inhibits the production of TNF-α, decreases expression of corticotropin-releasing hormone in trophoblasts, and decreases symptoms of allodynia.

Bohren Y, Tessier LH, Megat S, et al. Antidepressants suppress neuropathic pain by a peripheral β2-adrenoceptor mediated anti-TNFα mechanism. Neurobiol Dis. 2013 Dec;60:39-50. PMID: 23978467.

Freund-Michel VC, Birrell MA, Giembycz MA, et al. Beta(2)-agonists block tussive responses in guinea pigs via an atypical cAMP-dependent pathway. Eur Respir J. 2010 Mar;35(3):647-54. PMID: 19679606.

T1675

Teriparatide Acetate

0.5 mg
1 mg

Ser-Val-Ser-Glu-Ile-Gln-Leu-Met-His-Asn-Leu-Gly-Lys-His-Leu-Asn-Ser-Met-Glu-Arg-Val-Glu-Trp-Leu-Arg-Lys-Lys-Leu-Gln-Asp-Val-His-Asn-Phe-OH

$C_{181}H_{291}N_{55}O_{51}S_2$ FW: 4117.72 [52232-67-4] ≥95%

Synthetic PTH analog and PTH1 receptor agonist used to treat osteoporosis. It stimulates bone formation and increases bone strength.

Tseng YY, Su CH, Lui TN, et al. Prospective comparison of the therapeutic effect of teriparatide with that of combined vertebroplasty with antiresorptive agents for the treatment of new-onset adjacent vertebral compression fracture after percutaneous vertebroplasty. Osteoporos Int. 2012 May;23(5):1613-22. PMID: 21769661.

File E, Deal C. Clinical update on teriparatide. Curr Rheumatol Rep. 2009 Jul;11(3):169-76. PMID: 19604460.

T1673

Terlipressin Acetate

1 mg
5 mg

Gly-Gly-Gly-c[Gys-Tyr-Phe-Gln-Asn-Cys]-Pro-Lys-Gly-NH_2

$C_{52}H_{74}N_{16}O_{15}S_2$ FW: 1227.37 [14636-12-5] ≥95%

Synthetic vasopressin analog and AVP-1 receptor agonist. It induces gastroparesis, induces vasoconstriction, and improves renal function in subjects with hepatorenal syndrome.

Lange M, Van Aken H, Westphal M, et al. Role of vasopressinergic V1 receptor agonists in the treatment of perioperative catecholamine-refractory arterial hypotension. Best Pract Res Clin Anaesthesiol. 2008 Jun;22(2):369-81. PMID: 18683482.

Betrosian AP, Agarwal B, Douzinas EE. Acute renal dysfunction in liver diseases. World J Gastroenterol. 2007 Nov 14;13(42):5552-9. PMID: 17948928.

T1968 Terpinen-4-ol

NEW

5 g
25 g

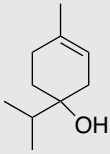

$C_{10}H_{18}O$ FW: 154.25 [562-74-3] ≥98%

Found in various plant sources. It exhibits a wide variety of biological activities, including inducing autophagy, apoptosis, and cell death in leukemia cells and inhibiting growth of *Campylobacter*, *Aspergillus*, and *Fusarium*.

Banjerdpongchai R, Khaw-On P. Terpinen-4-ol Induces Autophagic and Apoptotic Cell Death in Human Leukemic HL-60 Cells. Asian Pac J Cancer Prev. 2013;14(12):7537-42. PMID: 24460330.

Kurekci C, Padmanabha J, Bishop-Hurley SL, et al. Antimicrobial activity of essential oils and five terpenoid compounds against Campylobacter jejuni in pure and mixed culture experiments. Int J Food Microbiol. 2013 Sep 16;166(3):450-7. PMID: 24041998.

Ninomiya K, Hayama K, Ishijima SA, et al. Suppression of inflammatory reactions by terpinen-4-ol, a main constituent of tea tree oil, in a murine model of oral candidiasis and its suppressive activity to cytokine production of macrophages in vitro. Biol Pharm Bull. 2013;36(5):838-44. PMID: 23649340.

T1677 Tetracycline

10 g
25 g
100 g

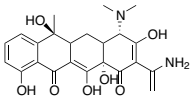

$C_{22}H_{24}N_2O_8$ FW: 444.43 [60-54-8] ≥90%

Protein translation and mammalian RNA splicing inhibitor used to treat acne, rosacea, Lyme disease, and various bacterial infections. It may also inhibit MMPs. It also decreases the neurotoxicity of amyloid-β peptides.

Kennedy R, Alibhai M, Shakib K. Tetracycline: a cure all? Br J Oral Maxillofac Surg. 2014 Apr;52(4):382-3. PMID: 24613100.

Mahajan GB, Balachandran L. Antibacterial agents from *actinomycetes* - a review. Front Biosci (Elite Ed). 2012 Jan 1;4:240-53. PMID: 22201868.

T1679 Tetracycline Hydrochloride

1 g
5 g
25 g

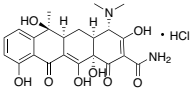

$C_{22}H_{24}N_2O_8 \bullet HCl$ FW: 480.9 [64-75-5] ≥96%

Protein translation and mammalian RNA splicing inhibitor used to treat acne, rosacea, Lyme disease, and various bacterial infections. It may also inhibit MMPs. It also decreases the neurotoxicity of amyloid-β peptides.

Kennedy R, Alibhai M, Shakib K. Tetracycline: a cure all? Br J Oral Maxillofac Surg. 2014 Apr;52(4):382-3. PMID: 24613100.

T1978 Tetrahydroberberine

NEW

1 mg
5 mg
25 mg

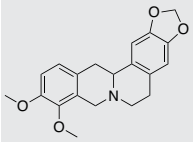

$C_{20}H_{21}NO_4$ FW: 339.39 [522-97-4] ≥98%

5-HT1A receptor agonist, dopamine D2 receptor antagonist, and ATP-sensitive K^+ channel blocker found in *Corydalis*. It inhibits tissue factor pro-coagulant activity, suppresses platelet aggregation, decreases ventricular tachycardia and ventricular fibrillation, and increases gastric emptying.

Ge HX, Zhang J, Chen L, et al. Chemical and microbial semi-synthesis of tetrahydroprotoberberines as inhibitors on tissue factor procoagulant activity. Bioorg Med Chem. 2013 Jan 1;21(1):62-9. PMID: 23199480.

Lee TH, Kim KH, Lee SO, et al. Tetrahydroberberine, an isoquinoline alkaloid isolated from *corydalis* tuber, enhances gastrointestinal motor function. J Pharmacol Exp Ther. 2011 Sep;338(3):917-24. PMID: 21659472.

Wu C, Yang K, Liu Q, et al. Tetrahydroberberine blocks ATP-sensitive potassium channels in dopamine neurons acutely-dissociated from rat substantia nigra pars compacta. Neuropharmacology. 2010 Dec;59(7-8):567-72. PMID: 20804776.

T1979 Tetrahydrocoptisine

NEW

1 mg
5 mg

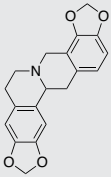

Stylopine

$C_{19}H_{17}NO_4$ FW: 323.34 [4312-32-7] ≥98%

AChE inhibitor found in *Corydalis*. It prevents LPS-induced increases in pro-inflammatory cytokines, suppresses formation of ethanol-induced gastric ulcers, and inhibits survival of *Strongyloides*.

Li W, Huang H, Zhang Y, et al. Anti-inflammatory effect of tetrahydrocoptisine from *Corydalis* impatiens is a function of possible inhibition of TNF-α, IL-6 and NO production in lipopolysaccharide-stimulated peritoneal macrophages through inhibiting NF-κB activation and MAPK pathway. Eur J Pharmacol. 2013 Sep 5;715(1-3):62-71. PMID: 23810685.

Li W, Huang H, Niu X, et al. Protective effect of tetrahydrocoptisine against ethanol-induced gastric ulcer in mice. Toxicol Appl Pharmacol. 2013 Oct 1;272(1):21-9. PMID: 23769714.

Wangchuk P, Keller PA, Pyne SG, et al. Phytochemical and biological activity studies of the Bhutanese medicinal plant *Corydalis* crispa. Nat Prod Commun. 2012 May;7(5):575-80. PMID: 22799079.

T1776

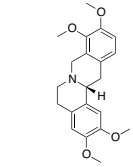

D-Tetrahydropalmatine

25 mg
100 mg
500 mg

$C_{21}H_{25}NO_4$ FW: 355.43 ≥98%

Dopamine D1 receptor antagonist and organic cation transporter 1 inhibitor found in *Corydalis*. It does not have affinity for dopamine D2 receptors.

Tu M, Sun S, Wang K, et al. Organic cation transporter 1 mediates the uptake of monocrotaline and plays an important role in its hepatotoxicity. Toxicology. 2013 Sep 15;311(3):225-30. PMID: 23831208.

T1678

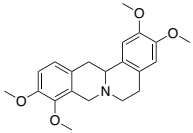

D,L-Tetrahydropalmatine

100 mg
500 mg

$C_{21}H_{25}NO_4$ FW: 355.43 [10097-84-4] ≥98%

Dopamine D1/2 receptor antagonist and potential L-type Ca^{2+} and K^+ channel blocker found in *Corydalis* and *Stephania*. It alters thresholds in pain assays, decreases measures of anxiety, and inhibits growth of *Plasmodium*.

Baghdikian B, Mahiou-Leddet V, Bory S, et al. New antiplasmodial alkaloids from *Stephania* rotunda. J Ethnopharmacol. 2013 Jan 9;145(1):381-5. PMID: 23127648.

Cao FL, Shang GW, Wang Y, et al. Antinociceptive effects of intragastric DL-tetrahydropalmatine on visceral and somatic persistent nociception and pain hypersensitivity in rats. Pharmacol Biochem Behav. 2011 Nov;100(1):199-204. PMID: 21889526.

T1676

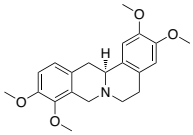

L-Tetrahydropalmatine

100 mg
500 mg

(-)-*Corydalis* B

$C_{21}H_{25}NO_4$ FW: 355.43 [483-14-7] ≥98%

Dopamine D1/2 receptor antagonist found in *Corydalis* and *Stephania*. It suppresses reward and reinforcement signaling in animal models of substance abuse, inhibits oxaliplatin-induced neuropathic pain, and suppresses depression- and anxiety-related behaviors.

Lee B, Sur B, Yeom M, et al. L-tetrahydropalmatine ameliorates development of anxiety and depression-related symptoms induced by single prolonged stress in rats. Biomol Ther (Seoul). 2014 May;22(3):213-22. PMID: 25009702.

Guo Z, Man Y, Wang X, et al. Levo-tetrahydropalmatine attenuates oxaliplatin-induced mechanical hyperalgesia in mice. Sci Rep. 2014 Jan 28;4:3905. PMID: 24469566.

Su HL, Zhu J, Chen YJ, et al. Roles of levo-tetrahydropalmatine in modulating methamphetamine reward behavior. Physiol Behav. 2013 Jun 13;118:195-200. PMID: 23711566.

T1777

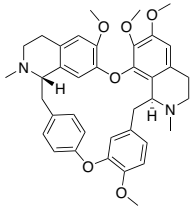

S,S-(+)-Tetrandrine

100 mg
500 mg
1 g

$C_{38}H_{42}N_2O_6$ FW: 622.75 [518-34-3] ≥98%

Voltage-gated Ca^{2+} channel blocker found in *Stephania*. It displays many biological activities, including limiting mast cell degranulation, suppressing LPS-stimulated expression of inflammatory cytokines, inhibiting amyloid-β-induced memory and learning impairments, inducing cell cycle arrest and apoptosis in gallbladder carcinoma cells, and preventing Ebola virus infection in animal models.

Sakurai Y, Kolokoltsov AA, Chen CC, et al. Two-pore channels control Ebola virus host cell entry and are drug targets for disease treatment. Science. 2015 Feb 27;347:995-998.

Zhu R, Liu T, Tan Z, et al. Tetrandrine induces apoptosis in gallbladder carcinoma in vitro. Int J Clin Pharmacol Ther. 2014 Jul 30. [Epub ahead of print]. PMID: 25074868.

Zhao H, Luo F, Li H, et al. Antinociceptive effect of tetrandrine on LPS-induced hyperalgesia via the inhibition of IKKβ phosphorylation and the COX-2/PGE pathway in mice. PLoS One. 2014 Apr 10;9(4):e94586. PMID: 24722146.

T2402

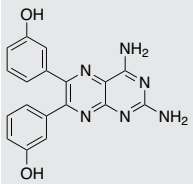

TG100-115

NEW

1 mg
5 mg
10 mg

$C_{18}H_{14}N_6O_2$ FW: 346.34 [677297-51-7] ≥98%

Inhibitor of p110δ and p110γ PI3K. It decreases pulmonary eosinophil levels, suppresses inflammation in COPD, and improves cardiac function by inhibiting edema and inflammation induced by VEGF and platelet activating factor.

Doukas J, Eide L, Stebbins K, et al. Aerosolized phosphoinositide 3-kinase gamma/delta inhibitor TG100-115 [3-[2,4-diamino-6-(3-hydroxyphenyl)pteridin-7-yl]phenol] as a therapeutic *candida*te for asthma and chronic obstructive pulmonary disease. J Pharmacol Exp Ther. 2009 Mar;328(3):758-65. PMID: 19056934.

Doukas J, Wrasidlo W, Noronha G, et al. Isoform-selective PI3K inhibitors as novel therapeutics for the treatment of acute myocardial infarction. Biochem Soc Trans. 2007 Apr;35(Pt 2):204-6. PMID: 17371238.

Doukas J, Wrasidlo W, Noronha G, et al. Phosphoinositide 3-kinase gamma/delta inhibition limits infarct size after myocardial ischemia/reperfusion injury. Proc Natl Acad Sci U S A. 2006 Dec 26;103(52):19866-71. PMID: 17172449.

T2404

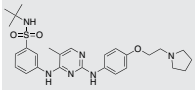

TG101348

NEW

5 mg
10 mg

SAR302503; Fedratinib

$C_{27}H_{36}N_6O_3S$ FW: 524.68 [936091-26-8] ≥98%

JAK2 inhibitor. It decreases expression of Th17 cells and increases expression of Treg cells in acute coronary syndrome models, inhibits proliferation of lymphoma cells, and lowers hematocrit and leukocyte count in models of myeloproliferative disease.

Zheng Y, Wang Z, Deng L, et al. Modulation of STAT3 and STAT5 activity rectifies the imbalance of Th17 and Treg cells in patients with acute coronary syndrome. Clin Immunol. 2015 Jan 5;157(1):65-77. PMID: 25572535.

Hao Y, Chapuy B, Monti S, et al. Selective JAK2 inhibition specifically decreases Hodgkin lymphoma and mediastinal large B-cell lymphoma growth in vitro and in vivo. Clin Cancer Res. 2014 May 15;20(10):2674-83. PMID: 24610827.

Zhang M, Xu CR, Shamiyeh E, et al. A randomized, placebo-controlled study of the pharmacokinetics, pharmacodynamics, and tolerability of the oral JAK2 inhibitor fedratinib (SAR302503) in healthy volunteers. J Clin Pharmacol. 2014 Apr;54(4):415-21. PMID: 24165976.

T2668

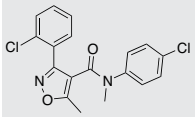

TGR5 Receptor Agonist

NEW

5 mg
25 mg

$C_{18}H_{14}Cl_2N_2O_2$ FW: 361.22 [1197300-24-5] ≥98%

TGR5 agonist. It increases GLP-1 secretion and decreases glucose levels.

Duan H, Ning M, Chen X, et al. Design, synthesis, and antidiabetic activity of 4-phenoxynicotinamide and 4-phenoxypyrimidine-5-carboxamide derivatives as potent and orally efficacious TGR5 agonists. J Med Chem. 2012 Dec 13;55(23):10475-89. PMID: 23148522.

Inoue T, Wang JH, Higashiyama M, et al. Dipeptidyl peptidase IV inhibition potentiates amino acid- and bile acid-induced bicarbonate secretion in rat duodenum. Am J Physiol Gastrointest Liver Physiol. 2012 Oct;303(7):G810-6. PMID: 22821947.

Evans KA, Budzik BW, Ross SA, et al. Discovery of 3-aryl-4-isoxazolecarboxamides as TGR5 receptor agonists. J Med Chem. 2009 Dec 24;52(24):7962-5. PMID: 19902954.

T2800

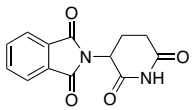

Thalidomide

25 mg
100 mg
250 mg
500 mg

$C_{13}H_{10}N_2O_4$ FW: 258.23 [50-35-1] ≥98%

Immunomodulator previously used as a sedative. It displays teratogenic activity, inducing birth defects. It also improves TNBS-induced colitis and inhibits cell proliferation in multiple myeloma models.

Lien IC, Horng LY, Hsu PL, et al. Internal ribosome entry site of bFGF is the target of thalidomide for IMiDs development in multiple myeloma. Genes Cancer. 2014 Mar;5(3-4):127-41. PMID: 25053990.

Xu J, Zheng C, Huang Y, et al. Efficacy of thalidomide on trinitrobenzene sulfonate-induced colitis in young rats and its mechanism. Chin Med J (Engl). 2014;127(12):2368-75. PMID: 24931258.

Zhou S, Wang F, Hsieh TC, et al. Thalidomide-a notorious sedative to a wonder anticancer drug. Curr Med Chem. 2013;20(33):4102-8. PMID: 23931282.

T2801

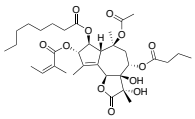

Thapsigargin

1 mg
5 mg

$C_{34}H_{50}O_{12}$ FW: 650.75 [67526-95-8] ≥96%

SERCA inhibitor found in *Thapsia* that is used to induce ER stress. It may also induce autophagy or apoptosis.

Zhang X, Yuan Y, Jiang L, et al. Endoplasmic reticulum stress induced by tunicamycin and thapsigargin protects against transient ischemic brain injury: Involvement of PARK2-dependent mitophagy. Autophagy. 2014 Oct 1;10(10):1801-13. PMID: 25126734.

Wang H, Jia XZ, Sui CJ, et al. Effects of thapsigargin on the proliferation and survival of human rheumatoid arthritis synovial cells. ScientificWorldJournal. 2014 Feb 9;2014:605416. PMID: 24688409.

T2816

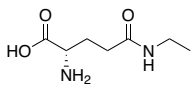

L-Theanine

1 g
5 g
25 g

$C_7H_{14}N_2O_3$ FW: 174.19 [3081-61-6] ≥98%

Nonessential amino acid found in *Camellia* and *Boletus*. It is a glutamic acid analog, weak AMPA receptor agonist, and NMDA receptor agonist. It increases brain DA, 5-HT, and GABA levels, improves memory, cognition, mood, and attention, and prevents apoptosis in hippocampal neurons.

Park SK, Jung IC, Lee WK, et al. A combination of green tea extract and l-theanine improves memory and attention in subjects with mild cognitive impairment: a double-blind placebo-controlled study. J Med Food. 2011 Apr;14(4):334-43. PMID: 21303262.

Ritsner MS, Miodownik C, Ratner Y, et al. L-theanine relieves positive, activation, and anxiety symptoms in patients with schizophrenia and schizoaffective disorder: an 8-week, randomized, double-blind, placebo-controlled, 2-center study. J Clin Psychiatry. 2011 Jan;72(1):34-42. PMID: 21208586.

T2817 Theophylline

100 g
250 g

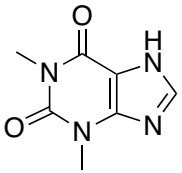

1,3-Dimethylxanthine

$C_7H_8N_4O_2$ FW: 180.16 [58-55-9] ≥98%

PDE inhibitor and A1/2 adenosine antagonist used to treat respiratory diseases. It inhibits inflammation, dilates bronchial tubes, and increases cAMP levels and PKA activation.

Dubuis E, Wortley MA, Grace MS, et al. Theophylline inhibits the cough reflex through a novel mechanism of action. J Allergy Clin Immunol. 2014 Jun;133(6):1588-98. PMID: 24406072.

Barnes PJ. Theophylline. Am J Respir Crit Care Med. 2013 Oct 15;188(8):901-6. PMID: 23672674.

T2930 Thiabendazole

10 g
100 g
500 g

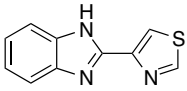

MK-360

$C_{10}H_7N_3S$ FW: 201.25 [148-79-8] ≥98%

Microtubule polymerization inhibitor used as a fungicide and pesticide. It inhibits growth of *Aspergillus*, *Strongyloides*, and *Haemonchus*. It also suppresses proliferation, angiogenesis, and VEGF expression in melanoma cells.

Zhang J, Zhao C, Gao Y, et al. Thiabendazole, a well-known antifungal drug, exhibits anti-metastatic melanoma B16F10 activity via inhibiting VEGF expression and inducing apoptosis. Pharmazie. 2013 Dec;68(12):962-8. PMID: 24400443.

Satou T, Koga M, Koike K, et al. Nematocidal activities of thiabendazole and ivermectin against the larvae of *Strongyloides* ratti and S. venezuelensis. Vet Parasitol. 2001 Aug 31;99(4):311-22. PMID: 11511418.

Crebelli R, Conti G, Conti L, et al. In vitro studies with nine known or suspected spindle poisons: results in tests for chromosome malsegregation in *Aspergillus* nidulans. Mutagenesis. 1991 Mar;6(2):131-6. PMID: 2056914.

T2935 Thiamphenicol

1 g
5 g
25 g

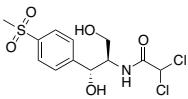

$C_{12}H_{15}Cl_2NO_5S$ FW: 356.22 [15318-45-3] ≥98%

Derivative of chloramphenicol and inhibitor of protein translation and peptidyl transferase. It suppresses growth of *Streptococcus*, *Staphylococcus*, *Escherichia*, and *Haemophilus*.

Raymond J, Boutros N, Bergeret M. Role of thiamphenicol in the treatment of community-acquired lung infections. Med Trop (Mars). 2004;64(1):33-8. PMID: 15224555.

Marchese A, Debbia EA, Tonoli E, et al. In vitro activity of thiamphenicol against multiresistant *Streptococcus* pneumoniae, *Haemophilus* influenzae and *Staphylococcus aureus* in Italy. J Chemother. 2002 Dec;14(6):554-61. PMID: 12583545.

T2932 Thiamphenicol Glycinate Hydrochloride

1 g
5 g
25 g

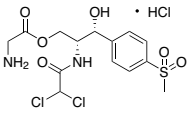

$C_{14}H_{18}Cl_2N_2O_6S \cdot HCl$ FW: 449.7 [2611-61-2] ≥98%

Derivative of chloramphenicol and inhibitor of protein translation and peptidyl transferase. It suppresses growth of *Streptococcus*, *Staphylococcus*, *Escherichia*, and *Haemophilus*.

Raymond J, Boutros N, Bergeret M. Role of thiamphenicol in the treatment of community-acquired lung infections. Med Trop (Mars). 2004;64(1):33-8. PMID: 15224555.

T2934 Thiamphenicol Palmitate

500 mg
1 g
5 g
25 g

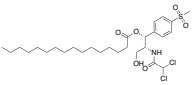

$C_{28}H_{45}Cl_2NO_6S$ FW: 594.63 [52628-58-7] ≥98%

Derivative of chloramphenicol and inhibitor of protein translation and peptidyl transferase. It suppresses growth of *Streptococcus*, *Staphylococcus*, *Escherichia*, and *Haemophilus*.

Raymond J, Boutros N, Bergeret M. Role of thiamphenicol in the treatment of community-acquired lung infections. Med Trop (Mars). 2004;64(1):33-8. PMID: 15224555.

T3132 Thiazovivin

NEW

5 mg
10 mg

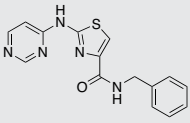

$C_{15}H_{13}N_5OS$ FW: 311.36 [1226056-71-8] ≥98%

ROCK inhibitor. It stabilizes E-cadherin and induces stem cell differentiation.

Wang F, Scoville D, He XC, et al. Isolation and characterization of intestinal stem cells based on surface marker combinations and colony-formation assay. Gastroenterology. 2013 Aug;145(2):383-95.e1-21. PMID: 23644405.

Groß B, Sgodda M, Rasche M, et al. Improved generation of patient-specific induced pluripotent stem cells using a chemically-defined and matrigel-based approach. Curr Mol Med. 2013 Jun;13(5):765-76. PMID: 23642058.

Zhu J, Pang D, Zhou Y, et al. Direct conversion of porcine embryonic fibroblasts into adipocytes by chemical molecules. Cell Reprogram. 2012 Apr;14(2):99-105. PMID: 22372576.

T3031 Thienylbutyl Isothiocyanate

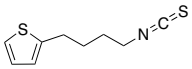

$C_9H_{11}NS_2$ FW: 197.32 ≥96%

Carcinogenesis inhibitor that may induces phase II enzymes.

Lam LKT, Kenney P, Bergstrom CP, et al. Chem Biol Interact. 1999;127:163-80.

Hecht SS. Chemoprevention by isothiocyanates. J Cell Biochem Suppl. 1995;22:195-209. PMID: 8538199.

25 mg
50 mg
100 mg
500 mg

T3032 Thienyldecyl Isothiocyanate

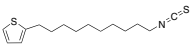

$C_{15}H_{23}NS_2$ FW: 281.48 ≥95%

Thienylbutyl isothiocyanate analog that may inhibit carcinogenesis.

Lam LKT, Kenney P, Bergstrom CP, et al. Chem Biol Interact. 1999;127:163-80.

25 mg
50 mg
100 mg
500 mg

T3033 Thienyldodecyl Isothiocyanate

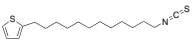

$C_{17}H_{27}NS_2$ FW: 309.54 ≥98%

Thienylbutyl isothiocyanate analog that may inhibit carcinogenesis.

Lam LKT, Kenney P, Bergstrom CP, et al. Chem Biol Interact. 1999;127:163-80.

25 mg
50 mg
100 mg
500 mg

T3034 Thienylethyl Isothiocyanate

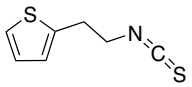

$C_7H_7NS_2$ FW: 169.27 ≥98%

Thienylbutyl isothiocyanate analog that may inhibit carcinogenesis.

Lam LKT, Kenney P, Bergstrom CP, et al. Chem Biol Interact. 1999;127:163-80.

25 mg
50 mg
100 mg
500 mg

T3035 Thienylheptyl Isothiocyanate

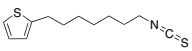

$C_{12}H_{17}NS_2$ FW: 239.4 ≥95%

Thienylbutyl isothiocyanate analog that may inhibit carcinogenesis.

Lam LKT, Kenney P, Bergstrom CP, et al. Chem Biol Interact. 1999;127:163-80.

10 mg
25 mg
50 mg
100 mg

T3036 Thienylhexyl Isothiocyanate

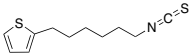

$C_{11}H_{15}NS_2$ FW: 225.38 ≥97%

Thienylbutyl isothiocyanate analog that may inhibit carcinogenesis.

Lam LKT, Kenney P, Bergstrom CP, et al. Chem Biol Interact. 1999;127:163-80.

25 mg
50 mg
100 mg
500 mg

T3037 Thienylmethyl Isothiocyanate

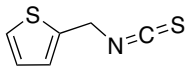

$C_6H_5NS_2$ FW: 155.24 ≥98%

Thienylbutyl isothiocyanate analog that may inhibit carcinogenesis.

Lam LKT, Kenney P, Bergstrom CP, et al. Chem Biol Interact. 1999;127:163-80.

100 mg
500 mg
1 g

T3038 Thienylnonanyl Isothiocyanate

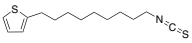

$C_{14}H_{21}NS_2$ FW: 267.46 ≥98%

Thienylbutyl isothiocyanate analog that may inhibit carcinogenesis.

Lam LKT, Kenney P, Bergstrom CP, et al. Chem Biol Interact. 1999;127:163-80.

25 mg
50 mg
100 mg
500 mg

T3039 Thienyloctyl Isothiocyanate

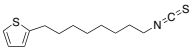

$C_{13}H_{19}NS_2$ FW: 253.43 ≥98%

Thienylbutyl isothiocyanate analog that may inhibit carcinogenesis.

Munday R, Zhang Y, Munday CM, et al. Structure-activity relationships and organ specificity in the induction of GST and NQO1 by alkyl-aryl isothiocyanates. Pharm Res. 2008 Sep;25(9):2164-70. PMID: 18563540.

25 mg
50 mg
100 mg
500 mg

T3040 Thienylpentyl Isothiocyanate

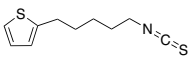

$C_{10}H_{13}NS_2$ FW: 211.35 ≥98%

Thienylbutyl isothiocyanate analog that may inhibit carcinogenesis.

Lam LKT, Kenney P, Bergstrom CP, et al. Chem Biol Interact. 1999;127:163-80.

25 mg
50 mg
100 mg
500 mg

T3041 Thienylpropyl Isothiocyanate

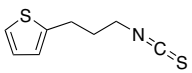

$C_8H_9NS_2$ FW: 183.3 ≥98%

Thienylbutyl isothiocyanate analog that may inhibit carcinogenesis.

Lam LKT, Kenney P, Bergstrom CP, et al. Chem Biol Interact. 1999;127:163-80.

25 mg
50 mg
100 mg
500 mg

T2833

1-Thio-β-D-glucose Tetraacetate

250 mg
1 g

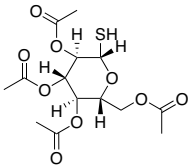

$C_{14}H_{20}O_9S$ FW: 364.4 [19879-84-6] ≥98%

Imaging agent and Maillard reaction inhibitor.

Welling MM, Alberto R. Performance of a 99mTc-labelled 1-thio-beta-D-glucose 2,3,4,6-tetra-acetate analogue in the detection of infections and tumours in mice: a comparison with [18F]FDG. Nucl Med Commun. 2010 Mar;31(3):239-48. PMID: 20032803.

Csapó J, Varga-Visi E, Lóki K, et al. The influence of extrusion on loss and racemization of amino acids. Amino Acids. 2008 Feb;34(2):287-92. PMID: 17245615.

T2835

6-Thioguanine

250 mg
500 mg
1 g

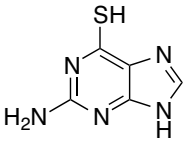

$C_5H_5N_5S$ FW: 167.19 [154-42-7] ≥90%

Guanine analog and DNA replication inhibitor that is used to treat leukemias and ulcerative colitis. It is incorporated into DNA, altering stability of the topoisomerase II-DNA cleavage complex and increasing DNA fragmentation. It also inhibits growth of *Toxoplasma gondii*.

Zhang F, Fu L, Wang Y. 6-thioguanine induces mitochondrial dysfunction and oxidative DNA damage in acute lymphoblastic leukemia cells. Mol Cell Proteomics. 2013 Dec;12(12):3803-11. PMID: 24043426.

Bohon J, de los Santos CR. Effect of 6-thioguanine on the stability of duplex DNA. Nucleic Acids Res. 2005 May 19;33(9):2880-6. PMID: 15905476.

Thomas CW, Myhre GM, Tschumper R, et al. Selective inhibition of inflammatory gene expression in activated T lymphocytes: a mechanism of immune suppression by thiopurines. J Pharmacol Exp Ther. 2005 Feb;312(2):537-45. PMID: 15388785.

T2834

Thiolutin

1 mg
5 mg
10 mg

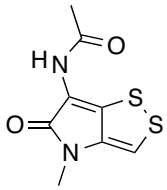

$C_8H_8N_2O_2S_2$ FW: 228.29 [87-11-6] ≥98%

Bacterial and fungal RNA polymerase inhibitor. It prevents synthesis of RNA and degradation of mRNA. It also decreases actin stress fiber and F-actin levels, prevents endothelial cell adhesion, and inhibits angiogenesis in S-180 tumor cells.

Qin Z, Huang S, Yu Y, et al. Dithiolopyrrolone natural products: isolation, synthesis and biosynthesis. Mar Drugs. 2013 Oct 17;11(10):3970-97. PMID: 24141227.

Jia Y, Wu SL, Isenberg JS, et al. Thiolutin inhibits endothelial cell adhesion by perturbing Hsp27 interactions with components of the actin and intermediate filament cytoskeleton. Cell Stress Chaperones. 2010 Mar;15(2):165-81. PMID: 19579057.

Pelechano V, Pérez-Ortín JE. The transcriptional inhibitor thiolutin blocks mRNA degradation in yeast. Yeast. 2008 Feb;25(2):85-92. PMID: 17914747.

T2936

Thioridazine Hydrochloride

5 g
25 g

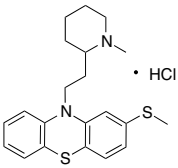

$C_{21}H_{26}N_2S_2 \cdot HCl$ FW: 407.04 [130-61-0] ≥98%

Inhibitor of dopamine D1-5 receptors, histamine H1/2 receptors, M1-5 mAChRs, 5-HT1/2/5/6/7 receptors, α1/2-adrenergic receptors, NET, and hERG K^+ channels. It also acts as a FIASMA, inhibits peptidoglycan synthesis, decreases colony-forming units of *Mycobacterium* tuberculosis, and potentially increases the cardiac QT interval.

Thorsing M, Klitgaard JK, Atilano ML, et al. Thioridazine induces major changes in global gene expression and cell wall composition in methicillin-resistant *Staphylococcus aureus* USA300. PLoS One. 2013 May 17;8(5):e64518. PMID: 23691239.

Byun HJ, Lee JH, Kim BR, et al. Anti-angiogenic effects of thioridazine involving the FAK-mTOR pathway. Microvasc Res. 2012 Nov;84(3):227-34. PMID: 23022044.

Kang S, Dong SM, Kim BR, et al. Thioridazine induces apoptosis by targeting the PI3K/Akt/mTOR pathway in cervical and endometrial cancer cells. Apoptosis. 2012 Sep;17(9):989-97. PMID: 22460505.

T3134

Thiostrepton

1 g
5 g

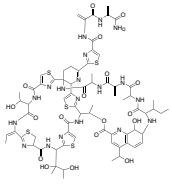

$C_{72}H_{85}N_{19}O_{18}S_5$ FW: 1664.89 [1393-48-2] ≥97%

Proteasome and protein translocation inhibitor. It inhibits DNA elongation, inhibits expression of FOXM1, and alters the electrophoretic mobility of peroxiredoxin 3 during oxidative stress.

Newick K, Cunniff B, Preston K, et al. Peroxiredoxin 3 is a redox-dependent target of thiostrepton in malignant mesothelioma cells. PLoS One. 2012;7(6):e39404. PMID: 22761781

Rodnina MV, Savelsbergh A, Matassova NB, et al. Thiostrepton inhibits the turnover but not the GTPase of elongation factor G on the ribosome. Proc Natl Acad Sci U S A. 1999 Aug 17;96(17):9586-90. PMID: 10449736.

Naaktgeboren N, Roobol K, Gubbens J, et al. The mode of action of thiostrepton in the initiation of protein synthesis. Eur J Biochem. 1976 Nov 1;70(1):39-47. PMID: 795651.

T2933 4-Thiouridine

5 mg
25 mg
100 mg
250 mg

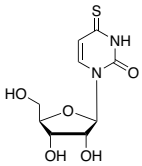

$C_9H_{12}N_2O_5S$ FW: 260.27 [13957-31-8] ≥98%

Modified nucleotide used for labeling DNA. It also cross-links DNA after irradiation with UV light.

Wang L, Ruffner DE. An ultraviolet crosslink in the hammerhead ribozyme dependent on 2-thiocytidine or 4-thiouridine substitution. Nucleic Acids Res. 1997 Nov 1;25(21):4355-61. PMID: 9336468.

Ofengand J, Liou R, Kohut J 3rd, et al. Covalent cross-linking of transfer ribonucleic acid to the ribosomal P site. Mechanism and site of reaction in transfer ribonucleic acid. Biochemistry. 1979 Oct 2;18(20):4322-32. PMID: 385051.

T2970 Thrombin Receptor Agonist Peptide

1 mg
2 mg
5 mg

H-Ser-Phe-Leu-Leu-Arg-Asn-Pro-Asn-Asp-Lys-Tyr-Glu-Pro-Phe-OH

$C_{81}H_{118}N_{20}O_{23}$ FW: 1739.96 [137339-65-2] ≥95%

PAR1 agonist and thrombin mimic that activates thrombin-mediated platelet aggregation.

Windeløv NA, Sørensen AM, Perner A, et al. Platelet aggregation following trauma: a prospective study. Blood Coagul Fibrinolysis. 2014 Jan;25(1):67-73. PMID: 23945060.

Kreutz RP, Breall JA, Kreutz Y, et al. Protease activated receptor-1 (PAR-1) mediated platelet aggregation is dependent on clopidogrel response. Thromb Res. 2012 Aug;130(2):198-202. PMID: 22459907.

T3185 Thymidine

1 g
5 g
10 g

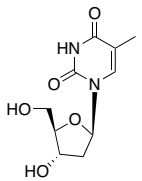

$C_{10}H_{14}N_2O_5$ FW: 242.23 [50-89-5] ≥98%

Endogenous pyrimidine nucleoside base that pairs with adenosine in DNA. It is also used to synchronize cells in the S phase of mitosis.

Wang X, Pan L, Mao N, et al. Cell-cycle synchronization reverses Taxol resistance of human ovarian cancer cell lines. Cancer Cell Int. 2013 Jul 30;13(1):77. PMID: 23899403.

Banfalvi G. Synchronization of mammalian cells and nuclei by centrifugal elutriation. Methods Mol Biol. 2011;761:25-45. PMID: 21755439.

T3196 Thymoquinone NEW

1 g
5 g

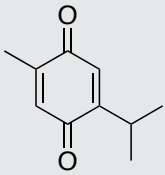

$C_{10}H_{12}O_2$ FW: 164.2 [490-91-5] ≥98%

Phytochemical from *Nigella sativa*. It decreases levels of oxidative enzymes, prevents acrylamide-induced motor deficiencies, and induces cell cycle arrest and apoptosis in hepatocellular carcinoma cells.

Linjawi SA, Khalil WK, Hassanane MM, et al. Evaluation of the protective effect of Nigella sativa extract and its primary active component thymoquinone against DMBA-induced breast cancer in female rats. Arch Med Sci. 2015 Mar 16;11(1):220-9. PMID: 25861310.

ElKhoely A, Hafez HF, Ashmawy AM, et al. Chemopreventive and therapeutic potentials of thymoquinone in HepG2 cells: mechanistic perspectives. J Nat Med. 2015 Mar 22. [Epub ahead of print]. PMID: 25796541.

Pejman L, Omrani H, Mirzamohammadi Z, et al. Thymoquinone, the main constituent of Nigella sativa, affects adenosine receptors in asthmatic guinea pigs. Iran J Basic Med Sci. 2014 Dec;17(12):1012-9. PMID: 25859306.

T3093 Thymopentin

5 mg
10 mg
25 mg

TP-5; RKDVY

H-Arg-Lys-Asp-Val-Tyr-OH

$C_{30}H_{49}N_9O_9$ FW: 679.8 ≥95%

Synthetic thymopoietin analog. It lessens disease severity of EAE, decreases iNOS expression and activity, and binds to MHC II HLA-DR complexes and modulates T cell activity.

Lunin SM, Glushkova OV, Khrenov MO, et al. Thymic peptides restrain the inflammatory response in mice with experimental autoimmune encephalomyelitis. Immunobiology. 2013 Mar;218(3):402-7. PMID: 22727332.

Patruno A, Tosco P, Borretto E, et al. Thymopentin down-regulates both activity and expression of iNOS in blood cells of Sézary syndrome patients. Nitric Oxide. 2012 Oct 15;27(3):143-9. PMID: 22721692.

T3094 Thymopentin Acetate

10 mg
50 mg
1 g

TP-5 Acetate

Arg-Lys-Asp-Val-Tyr

$C_{30}H_{49}N_9O_9$ CH_3COOH FW: 679.8 [69558-55-0] ≥95%

Immunostimulant and fragment of thymopoietin. It inhibits proliferation and colony formation and induces differentiation in leukemia cells. It also increases pro-inflammatory cytokine secretion.

Patruno A, Tosco P, Borretto E, et al. Thymopentin down-regulates both activity and expression of iNOS in blood cells of Sézary syndrome patients. Nitric Oxide. 2012 Oct 15;27(3):143-9. PMID: 22721692.

Lunin SM, Glushkova OV, Khrenov MO, et al. Thymus peptides regulate activity of RAW 264.7 macrophage cells: inhibitory analysis and a role of signal cascades. Expert Opin Ther Targets. 2011 Dec;15(12):1337-46. PMID: 22148922.

T3096 Thymosin α-1

10 mg
50 mg
1 g

Ac-Ser-Asp-Ala-Ala-Val-Asp-Thr-Ser-Ser-Glu-Ile-Thr-Thr-Lys-Asp-Leu-Lys-Glu-Lys-Lys-Glu-Val-Val-Glu-Glu-Ala-Glu-Asn

$C_{129}H_{215}N_{33}O_{55}$ FW: 3108.3 [62304-98-7] ≥95%

Endogenous indoleamine 2,3-dioxygenase activator and immunostimulant. It enhances T-cell, dendritic cell, and antibody responses and inhibits steroid-induced thymocyte apoptosis. It also promotes immune tolerance during transplants.

Tuthill C, Rios I, De Rosa A, et al. Thymosin α1 continues to show promise as an enhancer for vaccine response. Ann N Y Acad Sci. 2012 Oct;1270:21-7. PMID: 23050813.

Romani L, Moretti S, Fallarino F, et al. Jack of all trades: thymosin α1 and its pleiotropy. Ann N Y Acad Sci. 2012 Oct;1269:1-6. PMID: 23045964.

T3097 Thymosin α-1 Acetate

Please inquire

Ac-Ser-Asp-Ala-Ala-Val-Asp-Thr-Ser-Ser-Glu-Ile-Thr-Thr-Lys-Asp-Leu-Lys-Glu-Lys-Lys-Glu-Val-Val-Glu-Glu-Ala-Glu-Asn

$C_{129}H_{215}N_{33}O_{55}$ FW: 3108.3 [62304-98-7] ≥95%

Endogenous peptide involved in hormone regulation. It is used to increase efficacy of antiviral agents.

Lai CL, Wu PC. Antiviral treatment for chronic hepatitis B. Hong Kong Med J. 1997 Sep;3(3):289-296. PMID: 11847374.

T3098 Thymosin β-4 Acetate

Please inquire

Ac-Ser-Asp-Lys-Pro-Asp-Met-Ala-Glu-Ile-Glu-Lys-Phe-Asp-Lys-Ser-Lys-Leu-Lys-Lys-Thr-Glu-Thr-Gln-Glu-Lys-Asn-Pro-Leu-Pro-Ser-Lys-Glu-Thr-Ile-Glu-Gln-Glu-Lys-Gln-Ala-Gly-Glu-Ser-OH

$C_{212}H_{350}N_{56}O_{78}S$ FW: 4963.49 [77591-33-4] ≥95%

Endogenous actin polymerization inhibitor. It stimulates would healing in cardiac issue and improves cardiac function.

Qian L, Huang Y, Spencer CI, et al. In vivo reprogramming of murine cardiac fibroblasts into induced cardiomyocytes. Nature. 2012 May 31;485(7400):593-8. PMID: 22522929.

T3099 Thymus Factor

1 mg
2 mg
5 mg

FTS

H-Gln-Ala-Lys-Ser-Gln-Gly-Gly-Ser-Asn-OH

$C_{33}H_{57}N_{13}O_{15}$ FW: 875.9 ≥95%

Endogenous peptide involved in immune signaling. It induces immunoneutralization, decreases secretion of prolactin and growth hormone, and decreases disease severity of EAE.

Martines EV, Reggiani PC, Camihort G, et al. The thymulin-lactotropic axis in rodents: thymectomy, immunoneutralization and gene transfer studies. Neuroimmunomodulation. 2013;20(5):256-63. PMID: 23941809.

Lunin SM, Glushkova OV, Khrenov MO, et al. Thymic peptides restrain the inflammatory response in mice with experimental autoimmune encephalomyelitis. Immunobiology. 2013 Mar;218(3):402-7. PMID: 22727332.

T3100 Thyrotropin-releasing Hormone

5 mg
10 mg
25 mg

TRH; Thyrotropin-releasing factor; TRF

H-pGlu-His-Pro-NH_2

$C_{16}H_{22}N_6O_4$ FW: 362.4 ≥95%

Endogenous TRH receptor agonist involved in HPA signaling. It prevents oxidative stress, caspase-mediated apoptosis, glutamate toxicity, and neuroinflammation and stimulates epidermal regeneration.

Fekete C, Lechan RM. Central Regulation of Pituitary-Thyroid Axis Under Physiological and Pathophysiological Conditions. Endocr Rev. 2013 Dec 4:er20131087. [Epub ahead of print]. PMID: 24423980.

Pekary AE, Sattin A. Increased TRH and TRH-like peptide release in rat brain and peripheral tissues during proestrus/estrus. Peptides. 2013 Dec 1;52C:1-10. PMID: 24296042.

T3101 Thyrotropin-releasing Hormone, Free Acid

5 mg
10 mg
25 mg

TRH; Thyrotropin-releasing factor; TRF

H-pGlu-His-Pro-NH_2

$C_{16}H_{22}N_6O_4$ FW: 362.4 ≥95%

TRH receptor agonist involved in HPA signaling. It prevents oxidative stress, caspase-mediated apoptosis, glutamate toxicity, and neuroinflammation and stimulates epidermal regeneration.

Fekete C, Lechan RM. Central Regulation of Pituitary-Thyroid Axis Under Physiological and Pathophysiological Conditions. Endocr Rev. 2013 Dec 4:er20131087. [Epub ahead of print]. PMID: 24423980.

T3197 L-Thyroxine Sodium Pentahydrate

1 g
5 g

Levothyroxine

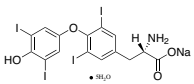

$C_{15}H_{10}I_4NNaO_4 \cdot 5H_2O$ FW: 888.93 [6106-07-6] ≥97%

Endogenous thyroid hormone T4 secreted by the thyroid gland. It decreases thyroid size and is used to treat goiter and hypothyroidism.

Gullo D, Latina A, Frasca F, et al. Levothyroxine monotherapy cannot guarantee euthyroidism in all athyreotic patients. PLoS One. 2011;6(8):e22552. PMID: 21829633.

T3305 Tibolone

100 mg
500 mg
1 g

Org-OD-14

$C_{21}H_{28}O_2$ FW: 312.45 [5630-53-5] ≥98%

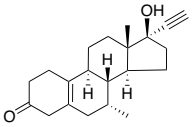

Synthetic SERM, progesterone receptor and androgen receptor agonist, aromatase inhibitor, and glucocorticoid receptor and mineralocorticoid receptor antagonist used in HRT. It prevents postmenopausal bone loss, produces vascular relaxation in coronary arteries, and inhibits mammary carcinoma cell invasion.

Campisi R, Marengo FD. Cardiovascular effects of tibolone: a selective tissue estrogenic activity regulator. Cardiovasc Drug Rev. 2007 Summer;25(2):132-45. PMID: 17614936.

Raobaikady B, Parsons MF, Reed MJ, et al. Tibolone and its delta-4, 7alpha-methyl norethisterone metabolite are reversible inhibitors of human aromatase. J Steroid Biochem Mol Biol. 2007 May;104(3-5):154-60. PMID: 17467267.

Vanhoecke BW, Bracke ME, Kloosterboer HJ, et al. Tibolone and its metabolites inhibit invasion of human mammary carcinoma cells in vitro. Maturitas. 2006 Jun 20;54(3):229-37. PMID: 16581209.

T3200 Ticagrelor

5 mg
25 mg
100 mg

AZD-6140

$C_{23}H_{28}F_2N_6O_4S$ FW: 522.57 [274693-27-5] ≥98%

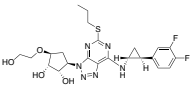

Adenosine analog and P2Y12 receptor antagonist used to increase coronary blood flow velocity and to prevent stroke, heart attack, and myocardial infarction. It inhibits downstream fibrinogen cross-linking between platelets.

Rahman M, Gustafsson D, Wang Y, et al. Ticagrelor reduces neutrophil recruitment and lung damage in abdominal sepsis. Platelets. 2013 Jul 15. [Epub ahead of print] PMID: 23855479.

Wittfeldt A, Emanuelsson H, Brandrup-Wognsen G, et al. Ticagrelor enhances adenosine-induced coronary vasodilatory responses in humans. J Am Coll Cardiol. 2013 Feb 19;61(7):723-7. PMID: 23312702.

Birkeland K, Parra D, Rosenstein R. Antiplatelet therapy in acute coronary syndromes: focus on ticagrelor. J Blood Med. 2010;1:197-219. PMID: 22282698.

T3310 Ticlopidine Hydrochloride

1 g
5 g
25 g

$C_{14}H_{14}ClNS \cdot HCl$ FW: 300.25 [53885-35-1] ≥98%

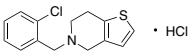

P2Y12 receptor antagonist that suppresses fibrinogen-platelet binding. It is used to treat acute coronary syndrome and myocardial infarction.

Cohen MV, Downey JM. Combined cardioprotectant and antithrombotic actions of platelet P2Y12 receptor antagonists in acute coronary syndrome: just what the doctor ordered. J Cardiovasc Pharmacol Ther. 2014 Mar;19(2):179-90. PMID: 24298192.

Secco GG, Parisi R, Mirabella F, et al. P2Y12 inhibitors: pharmacologic mechanism and clinical relevance. Cardiovasc Hematol Agents Med Chem. 2013 Jun;11(2):101-5. PMID: 22963529.

T3324 Tigecycline

100 mg
250 mg
1 g

$C_{29}H_{39}N_5O_8$ FW: 585.65 [220620-09-7] ≥97%

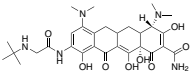

Protein synthesis inhibitor that inhibits growth of gram negative and gram positive bacteria. It also prevents LPS-stimulated release of pro-inflammatory cytokines in neurons.

Yagnik RM, Benzeroual KE. Tigecycline prevents LPS-induced release of pro-inflammatory and apoptotic mediators in neuronal cells. Toxicol In Vitro. 2013 Mar;27(2):686-93. PMID: 23200736.

da Silva LM, Nunes Salgado HR. Tigecycline: a review of properties, applications, and analytical methods. Ther Drug Monit. 2010 Jun;32(3):282-8. PMID: 20431506.

Olson MW, Ruzin A, Feyfant E, et al. Functional, biophysical, and structural bases for antibacterial activity of tigecycline. Antimicrob Agents Chemother. 2006 Jun;50(6):2156-66. PMID: 16723578.

T3350 Timolol Maleate

100 mg
250 mg
1 g

$C_{13}H_{24}N_4O_3S \cdot C_4H_4O_4$ FW: 432.5 [26921-17-5] ≥98%

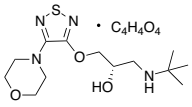

β-Adrenergic receptor antagonist used to induce vascular relaxation in the ciliary artery. It also decreases intraocular pressure in the treatment of glaucoma.

Johnson TV, Fan S, Zhan G, et al. Efficacy and mechanisms of intraocular pressure reduction with latanoprost and timolol in participants with ocular hypertension: a comparison of 1 and 6 weeks of treatment. J Glaucoma. 2010 Aug;19(6):356-64. PMID: 20179619.

Dong Y, Ishikawa H, Wu Y, et al. Effect and mechanism of betaxolol and timolol on vascular relaxation in isolated rabbit ciliary artery. Jpn J Ophthalmol. 2006 Nov-Dec;50(6):504-8. PMID: 17180523.

T3454 Tinidazole

100 g
250 g

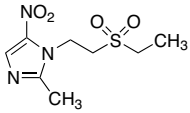

$C_8H_{13}N_3O_4S$ FW: 247.27 [19387-91-8] ≥98%

Nucleic acid synthesis inhibitor and DNA binder. It inhibits growth of *Helicobacter*, *Entamoeba*, and *Trichomonas*.

Penuliar GM, Furukawa A, Sato D, et al. Mechanism of trifluoromethionine resistance in *Entamoeba* histolytica. J Antimicrob Chemother. 2011 Sep;66(9):2045-52. PMID: 21676903.

Hsu CC, Chen JJ, Hu TH, et al. Famotidine versus omeprazole, in combination with amoxycillin and tinidazole, for eradication of *Helicobacter pylori* infection. Eur J Gastroenterol Hepatol. 2001 Aug;13(8):921-6. PMID: 11507356.

T3357 Tioconazole

1 g
5 g
25 g

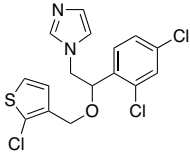

$C_{16}H_{13}Cl_3N_2OS$ FW: 387.71 [65899-73-2] ≥98%

14-α Demethylase inhibitor that inhibits ergosterol synthesis and fungal cell wall formation. It inhibits growth of fungi, mold, and gram positive bacteria.

Jones RN, Bale MJ, Hoban D, et al. In vitro antimicrobial activity of tioconazole and its concentrations in vaginal fluids following topical (vagistat-1 6.5%) application. Diagn Microbiol Infect Dis. 1993 Jul;17(1):45-51. PMID: 8359005.

Odds FC, Cheesman SL, Abbott AB. Suppression of ATP in *Candida albicans* by imidazole and derivative antifungal agents. Sabouraudia. 1985 Dec;23(6):415-24. PMID: 3913012.

T3461 Tiplaxtinin NEW

5 mg
25 mg

PAI-039

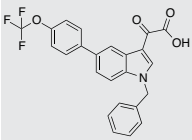

$C_{24}H_{16}F_3NO_4$ FW: 439.39 [393105-53-8] ≥98%

PAI-1 inhibitor. It decreases collagen deposition, inhibits carotid artery neointimal formation, decreases inflammation, and induces apoptosis in bladder cancer cells.

Simone TM, Longmate WM, Law BK, et al. Targeted Inhibition of PAI-1 Activity Impairs Epithelial Migration and Wound Closure Following Cutaneous Injury. Adv Wound Care (New Rochelle). 2015 Jun 1;4(6):321-328. PMID: 26029482.

Simone TM, Higgins SP, Archambeault J, et al. A small molecule PAI-1 functional inhibitor attenuates neointimal hyperplasia and vascular smooth muscle cell survival by promoting PAI-1 cleavage. Cell Signal. 2015 May;27(5):923-33. PMID: 25617690.

Gomes-Giacoia E, Miyake M, Goodison S, et al. Targeting plasminogen activator inhibitor-1 inhibits angiogenesis and tumor growth in a human cancer xenograft model. Mol Cancer Ther. 2013 Dec;12(12):2697-708. PMID: 24072883.

T3468 Tirapazamine

10 mg
25 mg
100 mg

SR 4233

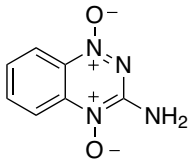

$C_7H_6N_4O_2$ FW: 178.15 [27314-97-2] ≥98%

Topoisomerase II inhibitor and replication protein A modulator. It inhibits DNA replication and forms DNA-damaging free radicals. It also inhibits expression of HIF-1α and induces apoptosis in neuroblastoma cells.

Zhang J, Cao J, Weng Q, et al. Suppression of hypoxia-inducible factor 1α (HIF-1α) by tirapazamine is dependent on eIF2α phosphorylation rather than the mTORC1/4E-BP1 pathway. PLoS One. 2010 Nov 9;5(11):e13910. PMID: 21085474.

Yang B, Reynolds CP. Tirapazamine cytotoxicity for neuroblastoma is p53 dependent. Clin Cancer Res. 2005 Apr 1;11(7):2774-80. PMID: 15814660.

T3568 Tirasemtiv NEW

1 mg
5 mg
25 mg

CK-2017357

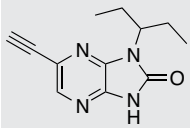

$C_{12}H_{14}N_4O$ FW: 230.27 [1005491-05-3] ≥98%

Activator of the fast skeletal muscle troponin complex that sensitizes the sarcomere to Ca^{2+} and increases muscle force. It improves motor function in models of amyotrophic lateral sclerosis and myasthenia gravis.

Sanders DB, Rosenfeld J, Dimachkie MM, et al. A Double-Blinded, Randomized, Placebo-Controlled Trial to Evaluate Efficacy, Safety, and Tolerability of Single Doses of Tirasemtiv in Patients with Acetylcholine Receptor-Binding Antibody-Positive Myasthenia Gravis. Neurotherapeutics. 2015 Apr;12(2):455-60. PMID: 25742919.

Hwee DT, Kennedy A, Ryans J, et al. Fast skeletal muscle troponin activator tirasemtiv increases muscle function and performance in the B6SJL-SOD1G93A ALS mouse model. PLoS One. 2014 May 7;9(5):e96921. PMID: 24805850.

Russell AJ, Hartman JJ, Hinken AC, et al. Activation of fast skeletal muscle troponin as a potential therapeutic approach for treating neuromuscular diseases. Nat Med. 2012 Feb 19;18(3):452-5. PMID: 22344294.

T3584

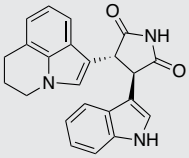

Tivantinib

NEW

5 mg
10 mg

ARQ-197

$C_{23}H_{19}N_3O_2$ FW: 369.42 [1000873-98-2] ≥98%

MET and GSK-3α/β inhibitor. It inhibits proliferation of non-small cell lung cancer cells and increases survival rates in models of hepatocellular carcinoma.

Remsing Rix LL, Kuenzi BM, Luo Y, et al. GSK3 alpha and beta are new functionally relevant targets of tivantinib in lung cancer cells. ACS Chem Biol. 2014 Feb 21;9(2):353-8. PMID: 24215125.

Rimassa L, Personeni N, Simonelli M, et al. Tivantinib: a new promising mesenchymal-epithelial transition factor inhibitor in the treatment of hepatocellular carcinoma. Future Oncol. 2013 Feb;9(2):153-65. PMID: 23414466.

Bagai R, Fan W, Ma PC. ARQ-197, an oral small-molecule inhibitor of c-Met for the treatment of solid tumors. IDrugs. 2010 Jun;13(6):404-14. PMID: 20506063.

T3585

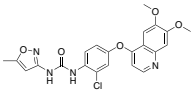

Tivozanib

5 mg
10 mg
25 mg

AV-951

$C_{22}H_{19}ClN_4O_5$ FW: 454.86 [475108-18-0] ≥98%

Inhibitor of VEGFR1/2/3, c-Kit, and PDGFR. It inhibits growth of renal cell carcinoma cells and suppresses development of choroidal neovascular lesions.

Cowey CL. Profile of tivozanib and its potential for the treatment of advanced renal cell carcinoma. Drug Des Devel Ther. 2013 Jun 21;7:519-27. PMID: 23818763.

Hepgur M, Sadeghi S, Dorff TB, et al. Tivozanib in the treatment of renal cell carcinoma. Biologics. 2013;7:139-48. PMID: 23788831.

Kang S, Roh YJ, Kim IB. Antiangiogenic effects of tivozanib, an oral VEGF receptor tyrosine kinase inhibitor, on experimental choroidal neovascularization in mice. Exp Eye Res. 2013 Jul;112:125-33. PMID: 23701975.

T4400

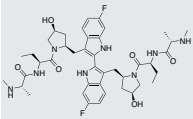

TL-32711

NEW

1 mg
5 mg
10 mg

Birinapant

$C_{42}H_{56}F_2N_8O_6$ FW: 806.94 [1260251-31-7] ≥98%

Smac mimetic and IAP family inhibitor. It induces apoptosis in acute myelogenous leukemia cells and improves efficacy of antivirals in hepatitis B models.

Ebert G, Allison C, Preston S, et al. Eliminating hepatitis B by antagonizing cellular inhibitors of apoptosis. Proc Natl Acad Sci U S A. 2015 May 5;112(18):5803-8. PMID: 25902530.

Benetatos CA, Mitsuuchi Y, Burns JM, et al. Birinapant(TL32711), a Bivalent Smac Mimetic, Targets TRAF2-associated cIAPs, Abrogates TNF-induced NF-κB Activation and is Active in Patient-Derived Xenograft Models. Mol Cancer Ther. 2014 Feb 21. [Epub ahead of print]. PMID: 24563541.

Carter BZ, Mak PY, Mak DH, et al. Synergistic Targeting of AML Stem/Progenitor Cells With IAP Antagonist Birinapant and Demethylating Agents. J Natl Cancer Inst. 2014 Feb 1;106(2):djt440. PMID: 24526787.

T4800

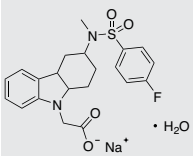

TM3-0089 Sodium Monohydrate

NEW

5 mg
10 mg

CAY10471

$C_{21}H_{20}FN_2O_4SNa \cdot H_2O$ FW: 456.46 [844639-57-2] ≥98%

Inhibitor of chemoattractant receptor-homologous molecule on Th2 cells. It prevents prostaglandin activation of Th2 cells, suppresses migration of Th2 lymphocytes, and limits adhesion of lymphocytes to vascular endothelial cells.

Xue L, Fergusson J, Salimi M, et al. Prostaglandin D2 and leukotriene E4 synergize to stimulate diverse TH2 functions and TH2 cell/neutrophil crosstalk. J Allergy Clin Immunol. 2014 Oct 19. [Epub ahead of print]. PMID: 25441644.

Schröder R, Xue L, Konya V, et al. PGH1, the precursor for the anti-inflammatory prostaglandins of the 1-series, is a potent activator of the pro-inflammatory receptor CRTH2/DP2. PLoS One. 2012;7(3):e33329. PMID: 22442685.

Uller L, Mathiesen JM, Alenmyr L, et al. Antagonism of the prostaglandin D2 receptor CRTH2 attenuates asthma pathology in mouse eosinophilic airway inflammation. Respir Res. 2007 Feb 28;8:16. PMID: 17328802.

T5060

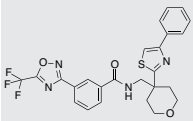

TMP-269

NEW

5 mg
10 mg
25 mg

$C_{25}H_{21}F_3N_4O_3S$ FW: 514.52 [1314890-29-3] ≥98%

HDAC inhibitor. It inhibits cell cycle progression and cell proliferation in intestinal epithelial cells.

Kikuchi S, Suzuki R, Ohguchi H, et al. Class IIa HDAC inhibition enhances ER stress-mediated cell death in multiple myeloma. Leukemia. 2015 Mar 24. [Epub ahead of print]. PMID: 25801913.

Sinnett-Smith J, Ni Y, Wang J, et al. Protein kinase D1 mediates class IIa histone deacetylase phosphorylation and nuclear extrusion in intestinal epithelial cells: role in mitogenic signaling. Am J Physiol Cell Physiol. 2014 May 15;306(10):C961-71. PMID: 24647541.

T5605 Tobramycin Sulfate

100 mg
500 mg
1 g

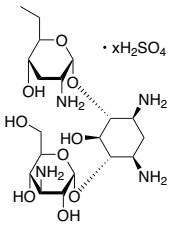

$(C_{18}H_{37}N_5O_9)_2 \cdot 5H_2SO_4$ FW: 1425.45 [79645-27-5] ≥98%

Protein translation inhibitor used to treat *Pseudomonas* infections. It also inhibits T cell and neutrophil migration and phosphorylation of ERK and p38 MAPK.

Papich MG. Antibiotic treatment of resistant infections in small animals. Vet Clin North Am Small Anim Pract. 2013 Sep;43(5):1091-107. PMID: 23890241.

Gziut M, MacGregor HJ, Nevell TG, et al. Anti-inflammatory effects of tobramycin and a copper-tobramycin complex with superoxide dismutase-like activity. Br J Pharmacol. 2013 Mar;168(5):1165-81. PMID: 23072509.

Nakamura S, Yanagihara K, Araki N, et al. High-dose tobramycin inhibits lipopolysaccharide-induced MUC5AC production in human lung epithelial cells. Eur J Pharmacol. 2011 Mar 21. [Epub ahead of print]. PMID: 21414310.

T5604 Tobramycin, Free Base

25 mg
100 mg
500 mg

Nebramycin factor 6; NF 6

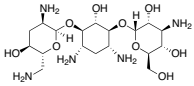

$C_{18}H_{37}N_5O_9$ FW: 467.51 [32986-56-4] ≥98%

Protein translation inhibitor used to treat bacterial infections. It also inhibits T cell and neutrophil migration and suppresses expression of MUC5AC and phosphorylation of ERK and p38 MAPK.

Papich MG. Antibiotic treatment of resistant infections in small animals. Vet Clin North Am Small Anim Pract. 2013 Sep;43(5):1091-107. PMID: 23890241.

Gziut M, MacGregor HJ, Nevell TG, et al. Anti-inflammatory effects of tobramycin and a copper-tobramycin complex with superoxide dismutase-like activity. Br J Pharmacol. 2013 Mar;168(5):1165-81. PMID: 23072509.

T5608 α-Tocotrienol

1 mg
5 mg
10 mg

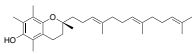

$C_{29}H_{44}O_2$ FW: 424.66 [58864-81-6] ≥98%

Vitamin E derivative found in vegetables, nuts, and grains. It negatively modulates HMG-CoA reductase activity and is the most potent antioxidant of all tocotrienols. It also inhibits lipid peroxidation and oxidative damage and prevents vessel formation and proliferation in aortic endothelial cells.

Yap WN, Chang PN, Han HY, et al. Gamma-tocotrienol suppresses prostate cancer cell proliferation and invasion through multiple-signalling pathways. Br J Cancer. 2008 Dec 2;99(11):1832-41. PMID: 19002171.

Sen CK, Khanna S, Roy S. Tocotrienols: Vitamin E beyond tocopherols. Life Sci. 2006 Mar 27;78(18):2088-98. PMID: 16458936.

Inokuchi H, Hirokane H, Tsuzuki T, et al. Anti-angiogenic activity of tocotrienol. Biosci Biotechnol Biochem. 2003 Jul;67(7):1623-7. PMID: 12913317.

T5609 β-Tocotrienol

1 mg
5 mg
10 mg

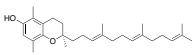

$C_{28}H_{42}O_2$ FW: 410.63 [490-23-3] ≥98%

Vitamin E derivative found in vegetables, nuts, and grains. It negatively modulates HMG-CoA reductase activity. It also inhibits lipid peroxidation and oxidative damage and prevents vessel formation and proliferation in aortic endothelial cells.

Yap WN, Chang PN, Han HY, et al. Gamma-tocotrienol suppresses prostate cancer cell proliferation and invasion through multiple-signalling pathways. Br J Cancer. 2008 Dec 2;99(11):1832-41. PMID: 19002171.

Sen CK, Khanna S, Roy S. Tocotrienols: Vitamin E beyond tocopherols. Life Sci. 2006 Mar 27;78(18):2088-98. PMID: 16458936.

T5610 γ-Tocotrienol

1 mg
5 mg
10 mg

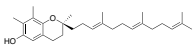

$C_{28}H_{42}O_2$ FW: 410.63 [14101-61-2] ≥98%

Vitamin E derivative found in vegetables, nuts, and grains. It negatively modulates HMG-CoA reductase activity and is the most potent anti-hyperlipidemic of all tocotrienols. It also inhibits lipid peroxidation and oxidative damage and prevents vessel formation and proliferation in aortic endothelial cells.

Yap WN, Chang PN, Han HY, et al. Gamma-tocotrienol suppresses prostate cancer cell proliferation and invasion through multiple-signalling pathways. Br J Cancer. 2008 Dec 2;99(11):1832-41. PMID: 19002171.

Sen CK, Khanna S, Roy S. Tocotrienols: Vitamin E beyond tocopherols. Life Sci. 2006 Mar 27;78(18):2088-98. PMID: 16458936.

T5611

δ-Tocotrienol

1 mg
5 mg
10 mg

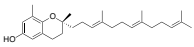

$C_{27}H_{40}O_2$ FW: 396.61 [25612-59-3] ≥98%

Vitamin E derivative found in vegetables, nuts, and grains. It negatively modulates HMG-CoA reductase activity and is the most potent anti-angiogenic of all tocotrienols. It also inhibits lipid peroxidation and oxidative damage and prevents vessel formation and proliferation in aortic endothelial cells.

Yap WN, Chang PN, Han HY, et al. Gamma-tocotrienol suppresses prostate cancer cell proliferation and invasion through multiple-signalling pathways. Br J Cancer. 2008 Dec 2;99(11):1832-41. PMID: 19002171.

T5720

Tofacitinib Citrate

NEW

5 mg
25 mg
100 mg

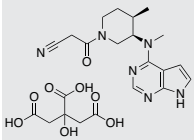

CP-690550-10

$C_{16}H_{20}N_6O \bullet C_6H_8O_7$ FW: 504.49 [540737-29-9] ≥99%

JAK1/2/3 inhibitor used to treat myelofibrosis and rheumatoid arthritis. It inhibits production of pro-inflammatory cytokines, suppresses differentiation of Th2 and Th17 cells, and inhibits HIV replication and reactivation of latent HIV-1.

Gavegnano C, Detorio M, Montero C, et al. Ruxolitinib and Tofacitinib are Potent and Selective Inhibitors of HIV-1 Replication and Virus Reactivation in Vitro. Antimicrob Agents Chemother. 2014 Jan 13. [Epub ahead of print]. PMID: 24419350.

Yamaoka K, Tanaka Y. Targeting the Janus kinases in rheumatoid arthritis: focus on tofacitinib. Expert Opin Pharmacother. 2014 Jan;15(1):103-13. PMID: 4188100.

Tak PP, Kalden JR. Advances in rheumatology: new targeted therapeutics. Arthritis Res Ther. 2011 May 25;13 Suppl 1:S5. PMID: 21624184.

T5846

Tolfenamic Acid

5 g
25 g
50 g

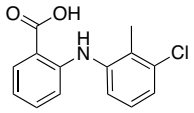

$C_{14}H_{12}ClNO_2$ FW: 261.7 [13710-19-5] ≥98%

NSAID and COX-1/2 inhibitor used to treat migraines. It inhibits leukotriene B4 production, degranulation, and migration in polymorphonuclear leukocytes, induces apoptosis in colorectal cancer cells, and suppresses expression of VEGF and VEGFR1 in colorectal cancer models.

Pathi S, Li X, Safe S. Tolfenamic acid inhibits colon cancer cell and tumor growth and induces degradation of specificity protein (Sp) transcription factors. Mol Carcinog. 2014 Feb;53 Suppl 1:E53-61. PMID: 23670891.

Zhang X, Lee SH, Min KW, et al. The involvement of endoplasmic reticulum stress in the suppression of colorectal tumorigenesis by tolfenamic acid. Cancer Prev Res (Phila). 2013 Dec;6(12):1337-47. PMID: 24104354.

Kankaanranta H, Moilanen E, Vapaatalo H. Comparison of in vitro effects of flunixin and tolfenamic acid on human leukocyte and platelet functions. Inflammation. 1993 Aug;17(4):417-25. PMID: 8406686.

T5944

Tolmetin Sodium

1 g
5 g
25 g

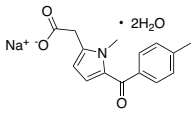

$C_{15}H_{14}NNaO_3 \bullet 2H_2O$ FW: 315.3 [64490-92-2] ≥98%

NSAID and COX-1/2 inhibitor used to treat arthritis. It inhibits inflammation and pain.

Fernandes E, Costa D, Toste SA, et al. In vitro scavenging activity for reactive oxygen and nitrogen species by nonsteroidal anti-inflammatory indole, pyrrole, and oxazole derivative drugs. Free Radic Biol Med. 2004 Dec 1;37(11):1895-905. PMID: 15528048.

Davies J, Dixon AS, Steele CE. Tolmetin sodium and indomethacin in the treatment of osteoarthrosis of the hip: a double-blind crossover study. Curr Med Res Opin. 1980;7(2):115-20. PMID: 7002480.

T5946

Toltrazuril

1 g
5 g
10 g

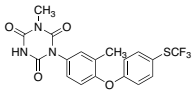

$C_{18}H_{14}F_3N_3O_4S$ FW: 425.38 [69004-03-1] ≥98%

Coccidiostat and inhibitor of mitochondrial respiration and pyrimidine synthesis.

Iqbal A, Tariq KA, Wazir VS, et al. Antiparasitic efficacy of *Artemisia* absinthium, toltrazuril and amprolium against intestinal coccidiosis in goats. J Parasit Dis. 2013 Apr;37(1):88-93. PMID: 24431547.

Kul O, Yildiz K, Ocal N, et al. In-vivo efficacy of toltrazuril on experimentally induced Toxoplasma gondii tissue cysts in lambs: a novel strategy for prevention of human exposure to meat-borne toxoplasmosis. Res Vet Sci. 2013 Apr;94(2):269-76. PMID: 22954788.

Harder A, Haberkorn A. Possible mode of action of toltrazuril: studies on two *Eimeria* species and mammalian and *Ascaris* suum enzymes. Parasitol Res. 1989;76(1):8-12. PMID: 2560189.

T5847

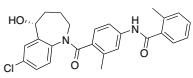

Tolvaptan

OPC-41061

$C_{26}H_{25}ClN_2O_3$ FW: 448.94 [150683-30-0] ≥98%

25 mg
100 mg
500 mg

Vasopressin 2 receptor antagonist used to treat congestive heart failure and chronic kidney disease. It inhibits water resorption without Na^+ loss and does not induce hypernatremia.

Otsuka T, Sakai Y, Ohno D, et al. The effects of tolvaptan on patients with severe chronic kidney disease complicated by congestive heart failure. Clin Exp Nephrol. 2013 Mar 13. [Epub ahead of print]. PMID: 23483323.

Graziani G, Cucchiari D, Aroldi A, et al. Syndrome of inappropriate secretion of antidiuretic hormone in traumatic brain injury: when tolvaptan becomes a life saving drug. J Neurol Neurosurg Psychiatry. 2012 May;83(5):510-2. PMID: 22323742

T5761

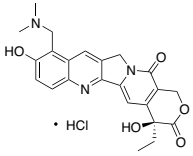

Topotecan Hydrochloride

NSC-609669; SKF-104864A

$C_{23}H_{25}N_3O_5 \bullet HCl$ FW: 457.91 [119413-54-6] ≥98%

1 mg
5 mg
10 mg
50 mg

Derivative of camptothecin and inhibitor of topoisomerase I used to treat various cancers. It induces apoptosis in retinocytoma cells and ovarian cancer cells.

Attia SM, Ahmad SF, Abd-Ellah MF, et al. Germ cell mutagenicity of topoisomerase I inhibitor topotecan detected in the male mouse-dominant lethal study. Food Chem Toxicol. 2013 Dec;62:470-4. PMID: 24036143.

Zhang M, Shan BE, Yuan NF, et al. Effect of topotecan on retinocytoma cell apoptosis and expression of Livin and PTEN. Chin Med J (Engl). 2013 Jan;126(2):340-4. PMID: 23324287.

Caltová K, Cervinka M. Antiproliferative effects of selected chemotherapeutics in human ovarian cancer cell line A2780. Acta Medica (Hradec Kralove). 2012;55(3):116-24. PMID: 23297519.

T5769

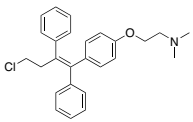

Toremifene Base

$C_{26}H_{28}ClNO$ FW: 405.96 [89778-26-7] ≥98%

500 mg
1 g
5 g

SERM and androgen receptor modulator used to treat breast cancer and prostate cancer. It also decreases microvessel density and induces remission of benign fibrous lesions.

Chang BY, Kim SA, Malla B, et al. The Effect of Selective Estrogen Receptor Modulators (SERMs) on the Tamoxifen Resistant Breast Cancer Cells. Toxicol Res. 2011 Jun;27(2):85-93. PMID: 24278556.

Kawashima H, Tanaka T, Cheng JS, et al. Effect of anti-estrogens on the androgen receptor activity and cell proliferation in prostate cancer cells. Urol Res. 2004 Dec;32(6):406-10. PMID: 15316697.

Heidemann J, Ogawa H, Otterson MF, et al. Antiangiogenic treatment of mesenteric desmoid tumors with toremifene and interferon alfa-2b: report of two cases. Dis Colon Rectum. 2004 Jan;47(1):118-22. PMID: 14719159.

T5968

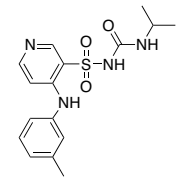

Torsemide

$C_{16}H_{20}N_4O_3S$ FW: 348.42 [56211-40-6] ≥98%

100 mg
250 mg
1 g

Loop diuretic and inhibitor of HSP90 and NKCC symporter used to treat edema and hypertension. It prevents reabsorption of Na^+, Cl^-, Mg^{2+}, and Ca^{2+} and decreases blood volume and pressure.

Sheikha GA, Al-Sha'er MA, Taha MO. Some sulfonamide drugs inhibit ATPase activity of heat shock protein 90: investigation by docking simulation and experimental validation. J Enzyme Inhib Med Chem. 2011 Oct;26(5):603-9. PMID: 21190426.

Kasama S, Toyama T, Hatori T, et al. Effects of torasemide on cardiac sympathetic nerve activity and left ventricular remodelling in patients with congestive heart failure. Heart. 2006 Oct;92(10):1434-40. PMID: 16621879.

T5672

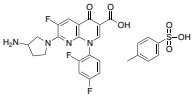

Tosufloxacin Tosylate

$C_{19}H_{15}F_3N_4O_3 \bullet C_7H_8O_3S$ FW: 576.55 [115964-29-9] ≥98%

100 mg
500 mg
1 g

Topoisomerase IV and bacterial DNA gyrase inhibitor used to treat bacterial ocular infections. It is especially active against *Mycoplasma*.

Akaike H, Miyashita N, Kubo M, et al. In vitro activities of 11 antimicrobial agents against macrolide-resistant *Mycoplasma pneumoniae* isolates from pediatric patients: results from a multicenter surveillance study. Jpn J Infect Dis. 2012;65(6):535-8. PMID: 23183207.

Ayaki M, Iwasawa A, Soda M, et al. Cytotoxicity of five fluoroquinolone and two nonsteroidal anti-inflammatory benzalkonium chloride-free ophthalmic solutions in four corneoconjunctival cell lines. Clin Ophthalmol. 2010 Sep 20;4:1019-24. PMID: 20922036.

T5677

Total Cell Death Assay Kit

125 Tests
250 Tests

Apoptosis measuring kit.

T5996

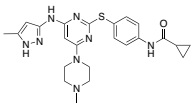

Tozasertib

VX680; MK0457

$C_{23}H_{28}N_8O_S$ FW: 464.59 [639089-54-6] ≥98%

25 mg
100 mg
250 mg

Inhibitor of aurora kinase, FLT3, and Abl. It decreases expression of HDACs, blocks downstream ERK signaling, and induces apoptosis in cancer cells.

Okabe S, Tauchi T, Tanaka Y, et al. Activity of histone deacetylase inhibitors and an Aurora kinase inhibitor in BCR-ABL-expressing leukemia cells: Combination of HDAC and Aurora inhibitors in BCR-ABL-expressing cells. Cancer Cell Int. 2013 Apr 4;13(1):32. PMID: 23556431.

Li Y, Zhou W, Wei L, et al. The effect of Aurora kinases on cell proliferation, cell cycle regulation and metastasis in renal cell carcinoma. Int J Oncol. 2012 Dec;41(6):2139-49. PMID: 23007526.

Giles FJ, Swords RT, Nagler A, et al. MK-0457, an Aurora kinase and BCR-ABL inhibitor, is active in patients with BCR-ABL T315I leukemia. Leukemia. 2013 Jan;27(1):113-7. PMID: 22772060.

T6803

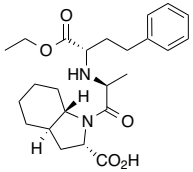

Trandolapril

$C_{24}H_{34}N_2O_5$ FW: 430.54 [87679-37-6] ≥98%

25 mg
100 mg
250 mg
500 mg

ACE inhibitor used to treat congestive heart failure. It inhibits expression of MMP2 and MMP9 in cerebral ischemia models, prevents left ventricular pressure changes and hypertrophy, and attenuates cardiac dysfunction induced by heart failure.

Tanaka H, Takai S, Jin D, et al. Inhibition of matrix metalloproteinase-9 activity by trandolapril after middle cerebral artery occlusion in rats. Hypertens Res. 2007 May;30(5):469-75. PMID: 17587759.

Toyoshima H, Nasa Y, Kohsaka Y, et al. The effect of chronic treatment with trandolapril on cyclic AMP-and cyclic GMP-dependent relaxations in aortic segments of rats with chronic heart failure. Br J Pharmacol. 1998 Jan;123(2):344-52. PMID: 9489624.

T6811

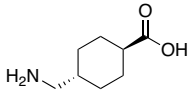

Tranexamic Acid

$C_8H_{15}NO_2$ FW: 157.21 [1197-18-8] ≥98%

5 g
10 g
50 g

Plasminogen inhibitor used to decrease blood loss in cardiac surgery and trauma. It inhibits fibrinolysis, decreases bleeding time, increases thrombus formation, and accelerates skin barrier recovery in UV-damaged skin.

Yuan C, Wang XM, Yang LJ, et al. Tranexamic acid accelerates skin barrier recovery and upregulates occludin in damaged skin. Int J Dermatol. 2013 Aug 22. [Epub ahead of print]. PMID: 23967870.

Sperzel M, Huetter J. Evaluation of aprotinin and tranexamic acid in different in vitro and in vivo models of fibrinolysis, coagulation and thrombus formation. J Thromb Haemost. 2007 Oct;5(10):2113-8. PMID: 17666018.

T6902

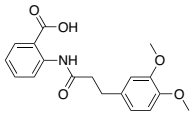

Tranilast

$C_{18}H_{17}NO_5$ FW: 327.34 [53902-12-8] ≥98%

10 mg
50 mg
100 mg
500 mg

Mast cell stabilizer and inhibitor of PDGFR and TRPV2 used to treat allergic disorders. It inhibits mast cell filtration, decreases allograft rejection and induces T cell anergy, induces cell cycle arrest and inhibits growth of breast cancer cells, and suppresses expression of decreases levels of α-SMA, collagen I, and fibronectin.

Luo J, Li Y, Yang Y, et al. Role and mechanism of tranilast preventing the progression of tubulointerstilial fibrosis in diabetic kidney diseases. Zhong Nan Da Xue Xue Bao Yi Xue Ban. 2013 Dec;38(12):1233-42. PMID: 24384948.

Zaher SS, Coe D, Chai JG, et al. Suppression of the allogeneic response by the anti-allergy drug N-(3,4-dimethoxycinnamonyl) anthranilic acid results from T-cell cycle arrest. Immunology. 2013 Feb;138(2):157-64. PMID: 23121382.

Subramaniam V, Chakrabarti R, Prud'homme GJ, et al. Tranilast inhibits cell proliferation and migration and promotes apoptosis in murine breast cancer. Anticancer Drugs. 2010 Apr;21(4):351-61. PMID: 20145538.

T7134

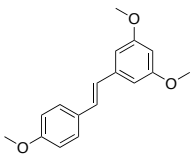

trans-3,4',5-Trimethoxy Stilbene

Trimethoxy resveratrol

$C_{17}H_{18}O_3$ FW: 270.32 [22255-22-7] ≥98%

100 mg
250 mg
1 g

Resveratrol prodrug and potential SIRT1 activator. It induces cell cycle arrest and apoptosis in prostate cancer cells and decreases inflammation and oxidative damage.

Dias SJ, Li K, Rimando AM, et al. Trimethoxy-resveratrol and piceatannol administered orally suppress and inhibit tumor formation and growth in prostate cancer xenografts. Prostate. 2013 Aug;73(11):1135-46. PMID: 23657951.

Hsieh TC, Huang YC, Wu JM. Control of prostate cell growth, DNA damage and repair and gene expression by resveratrol analogues, in vitro. Carcinogenesis. 2011 Jan;32(1):93-101. PMID: 21045015.

T0076

Transactivator of Transcription Peptide

0.5 mg
1 mg
2.5 mg

TAT peptide; YGRKKRRQRRR

H-Tyr-Gly-Arg-Lys-Lys-Arg-Arg-Gln-Arg-Arg-Arg-NH2

$C_{64}H_{119}N_{33}O_{13}$ FW: 1558.88 ≥95%

Cell-penetrating fragment of HIV-1 TAT protein involved in the induction of HIV-associated neurologic disorders. It increases the number of inhibitory synapses, decreases the number of excitatory synapses, alters cytokine/chemokine homeostasis, and induces neuroinflammation.

Hargus NJ, Thayer SA. Human immunodeficiency virus-1 Tat protein increases the number of inhibitory synapses between hippocampal neurons in culture. J Neurosci. 2013 Nov 6;33(45):17908-20. PMID: 24198379.

Bethel-Brown C, Yao H, Callen S, et al. HIV-1 Tat-mediated induction of platelet-derived growth factor in astrocytes: role of early growth response gene 1. J Immunol. 2011 Apr 1;186(7):4119-29. PMID: 21368226.

T0077

Transactivator of Transcription Peptide (2-4)

0.5 mg
1 mg
2.5 mg

TAT 2-4; YGRKKRRQRRRGYGRKKRRQRRRG

H-Tyr-Gly-Arg-Lys-Lys-Arg-Arg-Gln-Arg-Arg-Arg-Gly-Tyr-Gly-Arg-Lys-Lys-Arg-Arg-Gln-Arg-Arg-Arg-Gly-OH

$C_{132}H_{240}N_{66}O_{29}$ FW: 3215.81 ≥95%

Fragment of HIV-1 TAT protein involved in the induction of HIV-associated neurologic disorders. It increases the number of inhibitory synapses, decreases the number of excitatory synapses, alters cytokine/chemokine homeostasis, and induces neuroinflammation.

Hargus NJ, Thayer SA. Human immunodeficiency virus-1 Tat protein increases the number of inhibitory synapses between hippocampal neurons in culture. J Neurosci. 2013 Nov 6;33(45):17908-20. PMID: 24198379.

T6903

Tranylcypromine Hydrochloride

250 mg
1 g

SKF-385

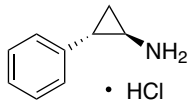

$C_9H_{11}N \bullet HCl$ FW: 169.66 [1986-47-6] ≥98%

Inhibitor of MAO and histone demethylase LSD1 used to treat depression and anxiety.

Lee MG, Wynder C, Schmidt DM, et al. Histone H3 lysine 4 demethylation is a target of nonselective antidepressive medications. Chem Biol. 2006 Jun;13(6):563-7. PMID: 16793513.

T7003

Trazodone Hydrochloride

1 g
5 g
25 g

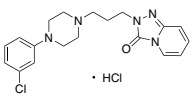

$C_{19}H_{22}ClN_5O \bullet HCl$ FW: 408.33 [25332-39-2] ≥98%

5-HT1A receptor partial agonist and inhibitor of 5-HT2 receptors, histamine receptors, α1/2-adrenergic receptors, SERT, and voltage-gated K^+ channels used to treat anxiety, depression, insomnia, and erectile dysfunction.

Chae YJ, Choi JS, Hahn SJ. Inhibition of Kv4.3 potassium channels by trazodone. Naunyn Schmiedebergs Arch Pharmacol. 2013 Aug;386(8):711-9. PMID: 23615873.

Odagaki Y, Toyoshima R, Yamauchi T. Trazodone and its active metabolite m-chlorophenylpiperazine as partial agonists at 5-HT1A receptors assessed by [35S]GTPgammaS binding. J Psychopharmacol. 2005 May;19(3):235-41. PMID: 15888508.

T6833

Triacetyl Aloe-emodin (Impurity A)

5 mg
10 mg
25 mg
100 mg

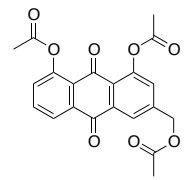

$C_{21}H_{16}O_8$ FW: 396.35 [25395-11-3] ≥98%

Derivative of aloe-emodin and CFTR Cl^- channel activator found in aloe. It increases colonic fluid secretion, decreases angiogenesis, and induces apoptosis in glioma cells.

Ismail S, Haris K, Abdul Ghani AR, et al. Enhanced induction of cell cycle arrest and apoptosis via the mitochondrial membrane potential disruption in human U87 malignant glioma cells by aloe emodin. J Asian Nat Prod Res. 2013 Jul 22. [Epub ahead of print]. PMID: 23869465.

Huang PH, Huang CY, Chen MC, et al. Emodin and Aloe-Emodin Suppress Breast Cancer Cell Proliferation through ER α Inhibition. Evid Based Complement Alternat Med. 2013; Epub 2013 Jun 24. PMID: 23864887.

Zhang W, Chen H, Liu DL, et al. Emodin sensitizes the gemcitabine-resistant cell line Bxpc-3/Gem to gemcitabine via downregulation of NF-κB and its regulated targets. Int J Oncol. 2013 Apr;42(4):1189-96. PMID: 23440366.

T7132

Triacetyl Resveratrol

10 mg
25 mg
100 mg

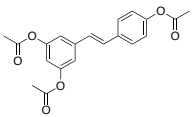

$C_{20}H_{18}O_6$ FW: 354.35 [42206-94-0] ≥98%

Resveratrol prodrug and potential SIRT1 activator. It induces cell cycle arrest in prostate cancer cells and stimulates phosphoylation of ERK and p38 and inhibits proliferation in breast cancer cells.

Hsieh TC, Wong C, John Bennett D, et al. Regulation of p53 and cell proliferation by resveratrol and its derivatives in breast cancer cells: an in silico and biochemical approach targeting integrin αvβ3. Int J Cancer. 2011 Dec 1;129(11):2732-43. PMID: 21225623.

Hsieh TC, Huang YC, Wu JM. Control of prostate cell growth, DNA damage and repair and gene expression by resveratrol analogues, in vitro. Carcinogenesis. 2011 Jan;32(1):93-101. PMID: 21045015.

T6834

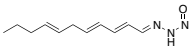

Triacsin C

1 mg
5 mg

$C_{11}H_{17}N_3O$ FW: 207.27 [76896-80-5] ≥95%

Acyl-CoA synthetase inhibitor that prevents conversion of fatty acids to fatty acyl-CoA. It also induces vasodilation.

Gauthier MS, Miyoshi H, Souza SC, et al. AMP-activated protein kinase is activated as a consequence of lipolysis in the adipocyte: potential mechanism and physiological relevance. J Biol Chem. 2008 Jun 13;283(24):16514-24. PMID: 18390901.

Weis MT, Crumley JL, Young LH, et al. Inhibiting long chain fatty Acyl CoA synthetase increases basal and agonist-stimulated NO synthesis in endothelium. Cardiovasc Res. 2004 Aug 1;63(2):338-46. PMID: 15249192.

Igal RA, Wang P, Coleman RA. Triacsin C blocks de novo synthesis of glycerolipids and cholesterol esters but not recycling of fatty acid into phospholipid: evidence for functionally separate pools of acyl-CoA. Biochem J. 1997 Jun 1;324 (Pt 2):529-34. PMID: 9182714.

T6830

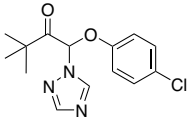

Triadimefon

BAY MEB 6447

5 g
10 g
25 g

$C_{14}H_{16}ClN_3O_2$ FW: 293.75 [43121-43-3] ≥98%

Neurotoxin and mutagen used to control fungal infection in agriculture. It also regulates retinoic acid levels and alters learning and memory function.

Xi J, Yang Z, Zeng C, et al. Suppressive effect of triadimefon, a triazole fungicide, on spatial learning and reference memory in rats. Behav Pharmacol. 2012 Dec;23(8):727-34. PMID: 23080312.

Di Renzo F, Broccia ML, Giavini E, et al. Stage-dependent abnormalities induced by the fungicide triadimefon in the mouse. Reprod Toxicol. 2011 Feb;31(2):194-9. PMID: 21055463.

T6831

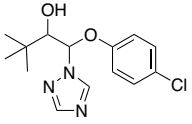

Triadimenol

10 g
25 g
100 g

$C_{14}H_{18}ClN_3O_2$ FW: 295.76 [55219-65-3] ≥96%

Triadimefon metabolite and mutagen used to control fungal infection in agriculture. It also regulates retinoic acid levels and alters learning and memory function.

Xi J, Yang Z, Zeng C, et al. Suppressive effect of triadimefon, a triazole fungicide, on spatial learning and reference memory in rats. Behav Pharmacol. 2012 Dec;23(8):727-34. PMID: 23080312.

Di Renzo F, Broccia ML, Giavini E, et al. Stage-dependent abnormalities induced by the fungicide triadimefon in the mouse. Reprod Toxicol. 2011 Feb;31(2):194-9. PMID: 21055463.

T7032

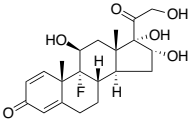

Triamcinolone

50 mg
250 mg
1 g
5 g

$C_{21}H_{27}FO_6$ FW: 394.43 [124-94-7] ≥98%

Synthetic glucocorticoid agonist used to treat retinal edema and other ocular pathologies. It decreases angiogenesis and inflammation and may increase ocular hypertension.

Zhou H, Yang L, Li H, et al. Downregulation of VEGF mRNA expression by triamcinolone acetonide acetate-loaded chitosan derivative nanoparticles in human retinal pigment epithelial cells. Int J Nanomedicine. 2012;7:4649-60. PMID: 22942646.

McAllister IL, Vijayasekaran S, Chen SD, et al. Effect of triamcinolone acetonide on vascular endothelial growth factor and occludin levels in branch retinal vein occlusion. Am J Ophthalmol. 2009 May;147(5):838-46, 846.e1-2. PMID: 19211093.

Mizuno D, Matsubara A, Ogura Y. Effect of posterior sub-tenon administration of triamcinolone acetonide on leukocyte dynamics in rat retinal microcirculation after panretinal photocoagulation. Invest Ophthalmol Vis Sci. 2008 May;49(5):2127-33. PMID: 18436845.

T6832

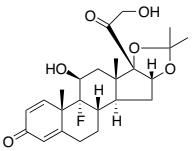

Triamcinolone Acetonide

50 mg
250 mg
1 g
5 g

$C_{24}H_{31}FO_6$ FW: 343.5 [76-25-5] ≥98%

Synthetic glucocorticoid agonist used to treat retinal edema and other ocular pathologies. It inhibits inflammation and angiogenesis.

Zhou H, Yang L, Li H, et al. Downregulation of VEGF mRNA expression by triamcinolone acetonide acetate-loaded chitosan derivative nanoparticles in human retinal pigment epithelial cells. Int J Nanomedicine. 2012;7:4649-60. PMID: 22942646.

McAllister IL, Vijayasekaran S, Chen SD, et al. Effect of triamcinolone acetonide on vascular endothelial growth factor and occludin levels in branch retinal vein occlusion. Am J Ophthalmol. 2009 May;147(5):838-46, 846.e1-2. PMID: 19211093.

Mizuno D, Matsubara A, Ogura Y. Effect of posterior sub-tenon administration of triamcinolone acetonide on leukocyte dynamics in rat retinal microcirculation after panretinal photocoagulation. Invest Ophthalmol Vis Sci. 2008 May;49(5):2127-33. PMID: 18436845.

T7044 Triamcinolone Acetonide Acetate

50 mg
250 mg
1 g
5 g

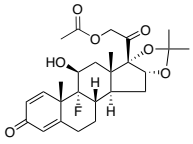

$C_{26}H_{33}FO_7$ FW: 476.53 ≥97%

Glucocorticoid receptor agonist used to treat ocular pathologies. It downregulates expression of VEGF and suppresses inflammation and angiogenesis.

Zhou H, Yang L, Li H, et al. Downregulation of VEGF mRNA expression by triamcinolone acetonide acetate-loaded chitosan derivative nanoparticles in human retinal pigment epithelial cells. Int J Nanomedicine. 2012;7:4649-60. PMID: 22942646.

McAllister IL, Vijayasekaran S, Chen SD, et al. Effect of triamcinolone acetonide on vascular endothelial growth factor and occludin levels in branch retinal vein occlusion. Am J Ophthalmol. 2009 May;147(5):838-46, 846.e1-2. PMID: 19211093.

T6933 Trichostatin A

1 mg
5 mg
25 mg

TSA

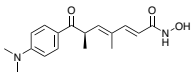

$C_{17}H_{22}N_2O_3$ FW: 302.37 [58880-19-6] ≥98%

HDAC inhibitor and mammalian RNA splicing modulator. It induces cell cycle arrest and apoptosis in colon cancer cells and enhances differentiation and activity of CD4+ Foxp3+ Treg cells.

Liu Y, He G, Wang Y, et al. MCM-2 is a therapeutic target of Trichostatin A in colon cancer cells. Toxicol Lett. 2013 Jul 31;221(1):23-30. PMID: 23770000.

Doñas C, Fritz M, Manríquez V, et al. Trichostatin A promotes the generation and suppressive functions of regulatory T cells. Clin Dev Immunol. 2013;2013:679804. PMID: 23737814.

Cecconi D, Donadelli M, Rinalducci S,et al. Proteomic analysis of pancreatic endocrine tumor cell lines treated with the histone deacetylase inhibitor trichostatin A. Proteomics. 2007 May;7(10):1644-53. PMID: 17443844.

T6931 Triclosan

NEW

1 g
5 g
25 g

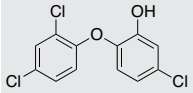

$C_{12}H_7Cl_3O_2$ FW: 289.54 [3380-34-5] ≥98%

Bacterial ENR binder and fatty acid synthesis inhibitor used in commercial soap products. It prevents fatty acid synthesis and bacterial cell membrane formation in bacteria and suppresses LPS-induced pro-inflammatory responses in epithelial cells.

Wallet MA, Calderon Nl, Alonso TR, et al. Triclosan alters antimicrobial and inflammatory responses of epithelial cells. Oral Dis. 2013 Apr;19(3):296-302. PMID: 24079913.

Twanabasu BR, Smith CM, Stevens KJ, et al. Triclosan inhibits arbuscular mycorrhizal colonization in three wetland plants. Sci Total Environ. 2013 Mar 1;447:450-7. PMID: 23410867.

Russell AD. Whither triclosan? J Antimicrob Chemother. 2004 May;53(5):693-5. PMID: 15073159.

T6930 Triclosan Methyl Ether

NEW

25 mg
50 mg

Methyl triclosan

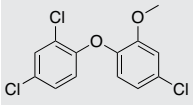

$C_{13}H_9Cl_3O_2$ FW: 303.57 [4640-01-1] ≥99%

Bacterial ENR binder and fatty acid synthesis inhibitor used in commercial soap products. It prevents fatty acid synthesis and bacterial cell membrane formation in bacteria and suppresses LPS-induced pro-inflammatory responses in epithelial cells.

Wallet MA, Calderon Nl, Alonso TR, et al. Triclosan alters antimicrobial and inflammatory responses of epithelial cells. Oral Dis. 2013 Apr;19(3):296-302. PMID: 24079913.

Twanabasu BR, Smith CM, Stevens KJ, et al. Triclosan inhibits arbuscular mycorrhizal colonization in three wetland plants. Sci Total Environ. 2013 Mar 1;447:450-7. PMID: 23410867.

T6932 Triflumizole

5 g
10 g
100 g

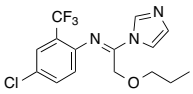

$C_{15}H_{15}ClF_3N_3O$ FW: 345.75 [68694-11-1] ≥95%

14-α Demethylase inhibitor that inhibits ergosterol synthesis and fungal cell wall formation. It also acts as a PPARγ agonist, RORγ inverse agonist, aromatase inhibitor, and ubiquitin/proteasome modulator. It induces variation into skp1 protein expression, increasing the risk for Parkinson's disease and induces adipogenesis.

Rhodes SL, Fitzmaurice AG, Cockburn M, et al. Pesticides that inhibit the ubiquitin-proteasome system: effect measure modification by genetic variation in SKP1 in Parkinson's disease. Environ Res. 2013 Oct;126:1-8. PMID: 23988235.

Li X, Pham HT, Janesick AS, et al. Triflumizole is an obesogen in mice that acts through peroxisome proliferator activated receptor gamma (PPARγ). Environ Health Perspect. 2012 Dec;120(12):1720-6. PMID: 23086663.

Kojima H, Muromoto R, Takahashi M, et al. Inhibitory effects of azole-type fungicides on interleukin-17 gene expression via retinoic acid receptor-related orphan receptors α and γ. Toxicol Appl Pharmacol. 2012 Mar 15;259(3):338-45. PMID: 22289359.

T7031

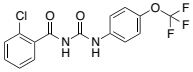

Triflumuron

BAY-SIR 8514

$C_{15}H_{10}ClF_3N_2O_3$ FW: 358.7 [64628-44-0] ≥98%

10 g
25 g
100 g

Insect growth regulator and chitin synthesis inhibitor. It inhibits growth of *Aedes*, *Culex*, and *Lucilia*.

Jacups SP, Paton CJ, Ritchie SA. Residual and pre-treatment application of starycide insect growth regulator (triflumuron) to control *Aedes* aegypti in containers. Pest Manag Sci. 2014 Apr;70(4):572-5. PMID: 23653423.

Belinato TA, Martins AJ, Lima JB, et al. Effect of triflumuron, a chitin synthesis inhibitor, on *Aedes* aegypti, *Aedes* albopictus and *Culex* quinquefasciatus under laboratory conditions. Parasit Vectors. 2013 Apr 4;6:83. PMID: 23557173.

Waghorn TS, McKay CH, Heath AC. The in vitro response of field strains of sheep blowflies Lucilia sericata and L. cuprina (Calliphoridae) in New Zealand to dicyclanil and triflumuron. N Z Vet J. 2013 Sep;61(5):274-80. PMID: 23441987.

T7033

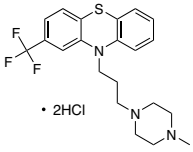

Trifluoperazine Dihydrochloride

$C_{21}H_{24}F_3N_3S \bullet 2HCl$ FW: 480.43 [440-17-5] ≥98%

5 g
10 g
25 g

D1/2 dopamine receptor and α1-adrenergic receptor, calmodulin, CDPK4 inhibitor, and $Na_v1.4$ and $Na_v1.7$ Na^+ channel inhibitor used to treat schizophrenia and anxiety. It also induces apoptosis in lung adenocarcinoma cells and causes sensory and motor blockade.

Cavagnino A, Rossi F, Rizzi M. The potent antiplasmodial calmodulin-antagonist trifluoperazine inhibits *plasmodium falciparum* calcium-dependent protein kinase 4. Protein Pept Lett. 2011 Dec;18(12):1273-9. PMID: 21787279.

Chen QY, Wu LJ, Wu YQ, et al. Molecular mechanism of trifluoperazine induces apoptosis in human A549 lung adenocarcinoma cell lines. Mol Med Rep. 2009 Sep-Oct;2(5):811-7. PMID: 21475906.

Sheets PL, Gerner P, Wang CF, et al. Inhibition of Nav1.7 and Nav1.4 sodium channels by trifluoperazine involves the local anesthetic receptor. J Neurophysiol. 2006 Oct;96(4):1848-59. PMID: 16807347.

T6935

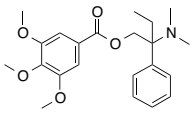

Trimebutine Base

EINECS 254-309-2

$C_{22}H_{29}NO_5$ FW: 387.47 [39133-31-8] ≥97%

10 g
50 g

BK K^+ channel and L-type Ca^{2+} channel blocker used to treat IBS. It enhances gastric muscle contractions, inhibits growth of *Escherichia* and *Pseudomonas*, and may activate opioid receptors.

Kountouras J, Sofianou D, Gavalas E, et al. Trimebutine as a potential antimicrobial agent: a preliminary in vitro approach. Hippokratia. 2012 Oct;16(4):347-9. PMID: 23935315.

Tan W, Zhang H, Luo HS, et al. Effects of trimebutine maleate on colonic motility through Ca^{2+}-activated K^+ channels and L-type Ca^{2+} channels. Arch Pharm Res. 2011 Jun;34(6):979-85. PMID: 21725819.

T6934

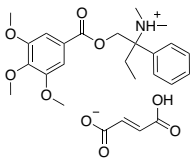

Trimebutine Maleate

$C_{22}H_{29}NO_5 \bullet C_4H_4O_4$ FW: 503.54 [34140-59-5] ≥96%

1 g
5 g

L-type Ca^{2+} channel blocker that also modulates BK K^+ channels and opioid receptors. It is used to treat IBS. It enhances gastrointestinal muscle contractions and inhibits growth of *Escherichia* and *Pseudomonas*.

Kountouras J, Sofianou D, Gavalas E, et al. Trimebutine as a potential antimicrobial agent: a preliminary in vitro approach. Hippokratia. 2012 Oct;16(4):347-9. PMID: 23935315.

Tan W, Zhang H, Luo HS, et al. Effects of trimebutine maleate on colonic motility through Ca^{2+}-activated K^+ channels and L-type Ca^{2+} channels. Arch Pharm Res. 2011 Jun;34(6):979-85. PMID: 21725819.

T7133

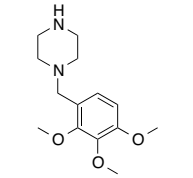

Trimetazidine

$C_{14}H_{22}N_2O_3$ FW: 266.34 [5011-34-7] ≥98%

250 mg
1 g
5 g

Long-chain 3-ketoacyl-CoA thiolase inhibitor and potential kainate receptor and AMPA receptor antagonist used to treat angina. It reverses pro-inflammatory effects of TNF-α, prevents muscle wasting and atrophy, and decreases free fatty acid oxidation.

Ferraro E, Giammarioli AM, Caldarola S, et al. The metabolic modulator trimetazidine triggers autophagy and counteracts stress-induced atrophy in skeletal muscle myotubes. FEBS J. 2013 Oct;280(20):5094-108. PMID: 23953053.

Khan M, Meduru S, Mostafa M, et al. Trimetazidine, administered at the onset of reperfusion, ameliorates myocardial dysfunction and injury by activation of p38 mitogen-activated protein kinase and Akt signaling. J Pharmacol Exp Ther. 2010 May;333(2):421-9. PMID: 20167841.

Tuunanen H, Engblom E, Naum A, et al. Trimetazidine, a metabolic modulator, has cardiac and extracardiac benefits in idiopathic dilated cardiomyopathy. Circulation. 2008 Sep 16;118(12):1250-8. PMID: 18765391.

T7034

Trimethoprim

5 g
25 g
100 g

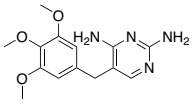

$C_{14}H_{18}N_4O_3$ FW: 290.32 [738-70-5] ≥98%

Dihydrofolate reductase inhibitor used to treat urinary tract infections. It is active against gram negative and gram positive bacteria.

Singh P, Kaur M, Sachdeva S. Mechanism inspired development of rationally designed dihydrofolate reductase inhibitors as anticancer agents. J Med Chem. 2012 Jul 26;55(14):6381-90. PMID: 22734697.

Sangurdekar DP, Zhang Z, Khodursky AB. The association of DNA damage response and nucleotide level modulation with the antibacterial mechanism of the anti-folate drug trimethoprim. BMC Genomics. 2011 Nov 28;12:583. PMID: 22122981.

T7035

Triptolide

1 mg
5 mg

PG490

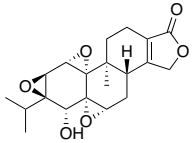

$C_{20}H_{24}O_6$ FW: 360.4 [38748-32-2] ≥98%

Found in *Tripterygium*. It induces apoptosis and decreases β-catenin expression in breast cancer cells, suppresses neuropathic pain, and neutrophil migration in hepatic ischemia/reperfusion models.

Liu M, Chen J, Huang Y, et al. Triptolide alleviates isoprenaline-induced cardiac remodeling in rats via TGF-β1/Smad3 and p38 MAPK signaling pathway. Pharmazie. 2015 Apr;70(4):244-50.PMID: 26012254.

Shao H, Ma J, Guo T, et al. Triptolide induces apoptosis of breast cancer cells via a mechanism associated with the Wnt/β-catenin signaling pathway. Exp Ther Med. 2014 Aug;8(2):505-508. PMID: 25009609.

Ma JX, Sun YL, Wang YQ, et al. Triptolide induces apoptosis and inhibits the growth and angiogenesis of human pancreatic cancer cells by downregulating COX-2 and VEGF. Oncol Res. 2013;20(8):359-68. PMID: 23924856.

T7036

Triptorelin

10 mg
25 mg

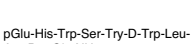

pGlu-His-Trp-Ser-Try-D-Trp-Leu-Arg-Pro-Gly-NH_2

$C_{64}H_{83}N_{18}O_{13}$ FW: 1311.5 [57773-63-4] ≥98%

GnRH analog and GnRH receptor agonist that decreases release of FSH and LH. It inhibits proliferation in breast cancer and ovarian cancer models and decreases anxiety-like behaviors.

Saleh-Abady MM, Alizadeh A, Shamsipour F, et al. The anticancer activity compared between triptorelin and a new gonadotropin releasing hormone analogue. Avicenna J Med Biotechnol. 2009 Jul;1(2):105-10. PMID: 23407883.

T7037

Triptorelin Acetate

10 mg
25 mg
100 mg

pGlu-His-Trp-Ser-Tyr-D-Trp-Leu-Arg-Pro-Gly-NH_2

$C_{64}H_{82}N_{18}O_{13} \bullet C_2H_4O_2$ FW: 1371.52 [140194-24-7] ≥95%

GnRH analog and GnRH receptor agonist used to treat estrogen-dependent disorders and hormone-responsive cancers. It decreases secretion of FSH and LH, inhibits production of cAMP, and modulates autocrine regulatory signaling.

Larivière S, Garrel-Lazayres G, Simon V, et al. Gonadotropin-releasing hormone inhibits pituitary adenylyl cyclase-activating polypeptide coupling to 3',5'-cyclic adenosine-5'-monophosphate pathway in LbetaT2 gonadotrope cells through novel protein kinase C isoforms and phosphorylation of pituitary adenylyl cyclase-activating polypeptide type I receptor. Endocrinology. 2008 Dec;149(12):6389-98. PMID: 18755795.

T7135

Triticonazole

5 g
10 g
100 g

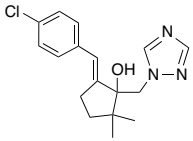

$C_{17}H_{20}ClN_3O$ FW: 317.81 [131983-72-7] ≥95%

14-α Demethylase inhibitor that inhibits ergosterol synthesis and fungal cell wall formation. It is also a potential aromatase inhibitor.

Kjærstad MB, Taxvig C, Nellemann C, et al. Endocrine disrupting effects in vitro of conazole antifungals used as pesticides and pharmaceuticals. Reprod Toxicol. 2010 Dec;30(4):573-82. PMID: 20708073.

Raveton M, Ravanel P, Royer F, et al. Triticonazole distribution in dressed corn caryopsis and seedlings. J Agric Food Chem. 1999 Apr;47(4):1740-4. PMID: 10564047.

T7232

S-Trityl-L-cysteine

NEW

5 g
25 g
100 g

NSC83265

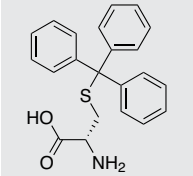

$C_{22}H_{21}NO_{2S}$ FW: 363.47 [2799-07-7] ≥98%

Kinesin Eg5 inhibitor found in garlic. It prevents formation of bipolar spindles during mitosis and induces apoptosis and cell death in chronic myelogenous leukemia cells.

Abualhasan MN, Good JA, Wittayanarakul K, et al. Doing the methylene shuffle--further insights into the inhibition of mitotic kinesin Eg5 with S-trityl L-cysteine. Eur J Med Chem. 2012 Aug;54:483-98. PMID: 22749640.

Shimizu M, Ishii H, Ogo N, et al. S-trityl-L-cysteine derivative induces caspase-independent cell death in K562 human chronic myeloid leukemia cell line. Cancer Lett. 2010 Dec 1;298(1):99-106. PMID: 20619960.

Kozielski F, Skoufias DA, Indorato RL, et al. Proteome analysis of apoptosis signaling by S-trityl-L-cysteine, a potent reversible inhibitor of human mitotic kinesin Eg5. Proteomics. 2008 Jan;8(2):289-300. PMID: 18186019.

T7056 Troglitazone

10 mg
50 mg
100 mg

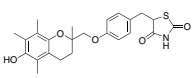

$C_{24}H_{27}NO_5S$ FW: 441.54 [97322-87-7] ≥97%

PPARγ agonist and ATP-sensitive K^+ channel blocker used to treat diabetes. It contains a vitamin E-like ring structure that forms hepatotoxic metabolites. It also induces apoptosis in cervical cancer cells, decreases insulin hypersecretion, suppresses epithelial-to-mesenchymal transition, and PAM-induced increases in TGF-β1 in airway epithelial cells.

Chen HM, Zhang DG, Wu JX, et al. Ubiquitination of p53 is involved in troglitazone induced apoptosis in cervical cancer cells. Asian Pac J Cancer Prev. 2014;15(5):2313-8. PMID: 24716976.

Deng R, Nie A, Jian F, et al. Acute exposure of beta-cells to troglitazone decreases insulin hypersecretion via activating AMPK. Biochim Biophys Acta. 2014 Jan;1840(1):577-85. PMID: 24144566.

Zhou B, Buckley ST, Patel V, et al. Troglitazone attenuates TGF-β1-induced EMT in alveolar epithelial cells via a PPARγ-independent mechanism. PLoS One. 2012;7(6):e38827. PMID: 22745681.

T7158 Tropicamide

100 mg
500 mg
1 g

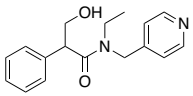

$C_{17}H_{20}N_2O_2$ FW: 284.35 [1508-75-4] ≥98%

mAChR antagonist used to induce mydriasis and inhibit the parasympathetic nervous system.

Kim JM, Park KH, Han SY, et al. Changes in intraocular pressure after pharmacologic pupil dilation. BMC Ophthalmol. 2012 Sep 27;12:53. PMID: 23017184.

Park JH, Lee YC, Lee SY. The comparison of mydriatic effect between two drugs of different mechanism. Korean J Ophthalmol. 2009 Mar;23(1):40-2. PMID: 19337478.

Manny RE, Hussein M, Scheiman M, et al. Tropicamide (1%): an effective cycloplegic agent for myopic children. Invest Ophthalmol Vis Sci. 2001 Jul;42(8):1728-35. PMID: 11431435.

T7156 Tropisetron Hydrochloride

10 mg
50 mg
100 mg

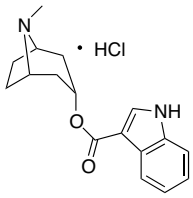

$C_{17}H_{20}N_2O_2 \cdot HCl$ FW: 320.82 [105826-92-4] ≥98%

α7 nAChR partial agonist and 5-HT3 receptor antagonist. It decreases levels of pro-inflammatory cytokines, increases survival of glutamatergic neurons, and inhibits collagen synthesis and fibrosis.

Zirak MR, Rahimian R, Ghazi-Khansari M, et al. Tropisetron attenuates cisplatin-induced nephrotoxicity in mice. Eur J Pharmacol. 2014 Jun 4. [Epub ahead of print]. PMID: 24905858.

Swartz MM, Linn DM, Linn CL. Tropisetron as a neuroprotective agent against glutamate-induced excitotoxicity and mechanisms of action. Neuropharmacology. 2013 Oct;73:111-21. PMID: 23727438.

Stegemann A, Sindrilaru A, Eckes B, et al. Tropisetron suppresses collagen synthesis in skin fibroblasts via α7 nicotinic acetylcholine receptor and attenuates fibrosis in a scleroderma mouse model. Arthritis *Rheum*. 2013 Mar;65(3):792-804. PMID: 23440693.

T7197 Tryprostatin A

0.5 mg

TPS-A

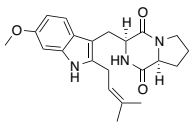

$C_{22}H_{29}N_3O_3$ FW: 383.48 ≥92%

Microtubule polymerization inhibitor found in *Aspergillus*. In inhibits activity of breast cancer resistance protein and suppresses cell cycle progression.

Jain HD, Zhang C, Zhou S, et al. Synthesis and structure-activity relationship studies on tryprostatin A, an inhibitor of breast cancer resistance protein. Bioorg Med Chem. 2008 Apr 15;16(8):4626-51. PMID: 18321710.

Usui T, Kondoh M, Cui CB, et al. Tryprostatin A, a specific and novel inhibitor of microtubule assembly. Biochem J. 1998 Aug 1;333 (Pt 3):543-8. PMID: 9677311.

T8000 Tubacin

1 mg
5 mg

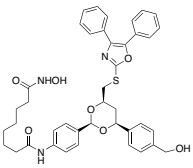

$C_{41}H_{43}N_3O_7S$ FW: 721.86 [537049-40-4] ≥98%

HDAC6 inhibitor that prevents α-tubulin deacetylation. It suppresses motility and induces apoptosis in multiple myeloma cells and acute lymphoblastic leukemia cells. It also downregulates expression of EGFR in mutant renal epithelial cells.

Liu W, Fan LX, Zhou X, et al. HDAC6 regulates epidermal growth factor receptor (EGFR) endocytic trafficking and degradation in renal epithelial cells. PLoS One. 2012;7(11):e49418. d PMID: 23152903.

Aldana-Masangkay GI, Rodriguez-Gonzalez A, Lin T, et al. Tubacin suppresses proliferation and induces apoptosis of acute lymphoblastic leukemia cells. Leuk Lymphoma. 2011 Aug;52(8):1544-55. PMID: 21699378.

Hideshima T, Bradner JE, Wong J, et al. Small-molecule inhibition of proteasome and aggresome function induces synergistic antitumor activity in multiple myeloma. Proc Natl Acad Sci U S A. 2005 Jun 14;102(24):8567-72. PMID: 15937109.

T8006 Tubastatin A Hydrochloride

NEW

5 mg
10 mg

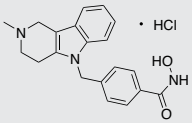

$C_{20}H_{21}N_3O_2 \bullet HCl$ FW: 371.86 [1310693-92-5] ≥98%

HDAC6/10 inhibitor. It decreases levels of α-tubulin, protects against atrial fibrillation-related atrial remodeling, and decreases cell proliferation and growth in cholangiocarcinoma cells.

Zhang D, Wu CT, Qi X, et al. Activation of histone deacetylase-6 induces contractile dysfunction through derailment of α-tubulin proteostasis in experimental and human atrial fibrillation. Circulation. 2014 Jan 21;129(3):346-58. PMID: 24146251.

Gradilone SA, Radtke BN, Bogert PS, et al. HDAC6 inhibition restores ciliary expression and decreases tumor growth. Cancer Res. 2013 Apr 1;73(7):2259-70. PMID: 23370327.

T8004 Tubeimoside I

10 mg
25 mg
100 mg

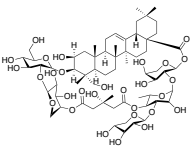

$C_{63}H_{98}O_{29}$ FW: 1319.43 [102040-03-9] ≥96%

Microtubule polymerization inhibitor found in *Bolbostemma*. It inhibits LPS-stimulated production of pro-inflammatory cytokines, induces cell cycle arrest and apoptosis in esophageal squamous cell carcinoma cells, and limits production of HIV core protein p24 to suppress viral infectivity.

Wu Q, Sun G, Yuan X, et al. Tubeimoside-1 attenuates LPS-induced inflammation in RAW 264.7 macrophages and mouse models. Immunopharmacol Immunotoxicol. 2013 Aug;35(4):514-23. PMID: 23844578.

Xu Y, Wang G, Chen Q, et al. Intrinsic apoptotic pathway and G2/M cell cycle arrest involved in tubeimoside I-induced EC109 cell death. Chin J Cancer Res. 2013 Jun;25(3):312-21. PMID: 23825908.

Ma R, Song G, You W, et al. Anti-microtubule activity of tubeimoside I and its colchicine binding site of tubulin. Cancer Chemother Pharmacol. 2008 Sep;62(4):559-68. PMID: 18030471.

T8020 Tuftsin

5 mg
10 mg
25 mg

H-Thr-Lys-Pro-Arg-OH

$C_{21}H_{40}N_8O_6$ FW: 500.6 ≥95%

IgG Fc region derivative and Nrp1 receptor agonist that induces leukocytes to become cytotoxic effector cells and stimulating phagocytosis in macrophages and microglia. It also inhibits withdrawal-associated behaviors and enhances the cytotoxicity of co-administered chemotherapeutics.

Nissen JC, Selwood DL, Tsirka SE. Tuftsin signals through its receptor neuropilin-1 via the transforming growth factor beta pathway. J Neurochem. 2013 Nov;127(3):394-402. PMID: 24033337.

T8145 Tulobuterol Hydrochloride

1 g
5 g

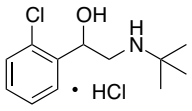

$C_{12}H_{18}ClNO \bullet HCl$ FW: 264.19 [56776-01-3] ≥98%

β2-Adrenergic receptor agonist used to treat COPD and asthma. It induces relaxation of airway smooth muscle cells, decreases levels of pro-inflammatory cytokines, and inhibits replication of *rhinovirus*.

Yamaya M, Nishimura H, Nadine L, et al. Tulobuterol inhibits *rhinovirus* infection in primary cultures of human tracheal epithelial cells. Physiol Rep. 2013 Aug;1(3):e00041. PMID: 24303127.

Katsunuma T, Fujisawa T, Nagao M, et al. Effects of transdermal tulobuterol in pediatric asthma patients on long-term leukotriene receptor antagonist therapy: results of a randomized, open-label, multicenter clinical trial in Japanese children aged 4-12 years. Allergol Int. 2013 Mar;62(1):37-43. PMID: 23000726.

Terpstra GK, Raaijmakers JA. Beta-agonistic properties of tulobuterol, a new beta-sympathicomimetic drug, and its effects on pulmonary beta-adrenoceptor characteristics. Lung. 1990;168 Suppl:179-85. PMID: 1974673.

T8269 (S)-ar-Turmerone

NEW

1 mg
5 mg
10 mg

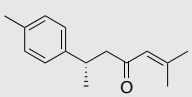

$C_{15}H_{20}O$ FW: 216.32 [532-65-0] ≥97%

Potential EGFR inhibitor found in *Curcuma*. It displays several biological activities, including suppressing production of IL-2 and IFN-γ in T cells, decreasing epileptic activity, suppressing growth of dermatophytes, inhibiting cellular migration and invasion in breast cancer cells, and improving T and B lymphocyte proliferation.

Oh S, Han AR, Park HR, et al. Suppression of Inflammatory cytokine production by ar-Turmerone isolated from Curcuma phaeocaulis. Chem Biodivers. 2014 Jul;11(7):1034-41. PMID: 25044589.

Orellana-Paucar AM, Afrikanova T, Thomas J, et al. Insights from zebrafish and mouse models on the activity and safety of ar-turmerone as a potential drug *candida*te for the treatment of epilepsy. PLoS One. 2013 Dec 13;8(12):e81634. PMID: 24349101.

Jankasem M, Wuthi-Udomlert M, Gritsanapan W. Antidermatophytic Properties of Ar-Turmerone, Turmeric Oil, and Curcuma longa Preparations. ISRN Dermatol. 2013 Aug 26;2013:250597. PMID: 24066236.

T8153 Tunicamycin

1 mg
5 mg
10 mg

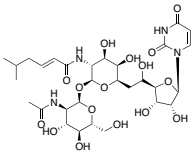

$C_{40}H_{66}N_4O_{16}$ Avg. 840 [11089-65-9] ≥98%

GlcNAc phosphotransferase and glycoprotein synthesis inhibitor. It inhibits TLR activation-induced pro-inflammatory cytokine release in macrophages.

Kim SY, Hwang JS, Han IO. Tunicamycin inhibits Toll-like receptor-activated inflammation in RAW264.7 cells by suppression of NF-κB and c-Jun activity via a mechanism that is independent of ER-stress and N-glycosylation. Eur J Pharmacol. 2013 Dec 5;721(1-3):294-300. PMID: 24056124.

Pertusa M, Madrid R, Morenilla-Palao C, et al. N-glycosylation of TRPM8 ion channels modulates temperature sensitivity of cold thermoreceptor neurons. J Biol Chem. 2012 May 25;287(22):18218-29. PMID: 22493431.

T9946 Tylosin Phosphate

1 g
5 g
10 g

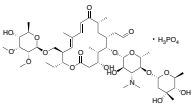

$C_{46}H_{77}NO_{17} \bullet H_3PO_4$ FW: 1014.11 [1405-53-4] ≥90%

Peptidyl transferase and protein translation inhibitor. It inhibits growth of gram negative and gram positive bacteria.

Liu M, Douthwaite S. Resistance to the macrolide antibiotic tylosin is conferred by single methylations at 23S rRNA nucleotides G748 and A2058 acting in synergy. Proc Natl Acad Sci U S A. 2002 Nov 12;99(23):14658-63. PMID: 12417742.

Zalacain M, Cundliffe E. Methylation of 23S rRNA caused by tlrA (ermSF), a tylosin resistance determinant from *Streptomyces* fradiae. J Bacteriol. 1989 Aug;171(8):4254-60. PMID: 2753855.

T9945 Tylosin Tartrate

1 g
5 g
10 g

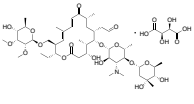

$C_{46}H_{77}NO_{17} \bullet C_4H_4O_6$ FW: 1066.2 [1405-54-5] ≥90%

Peptidyl transferase and protein translation inhibitor. It inhibits growth of gram negative and gram positive bacteria.

Liu M, Douthwaite S. Resistance to the macrolide antibiotic tylosin is conferred by single methylations at 23S rRNA nucleotides G748 and A2058 acting in synergy. Proc Natl Acad Sci U S A. 2002 Nov 12;99(23):14658-63. PMID: 12417742.

T9968 Tyrphostin A25

5 mg
25 mg

RG-50875

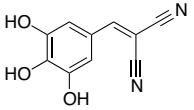

$C_{10}H_6N_2O_3$ FW: 202.17 [118409-58-8] ≥98%

Inhibitor of EGFR, SK K^+ channels, and other tyrosine kinases used in research models.

Wu W, Sun HY, Deng XL, et al. EGFR tyrosine kinase regulates human small-conductance Ca^{2+}-activated K^+ (hSKCa1) channels expressed in HEK-293 cells. Biochem J. 2013 May 15;452(1):121-9. PMID: 23496660.

Nguyen J, Gogusev J, Knapnougel P, et al. Protein tyrosine kinase and p38 MAP kinase pathways are involved in stimulation of matrix metalloproteinase-9 by TNF-alpha in human monocytes. Immunol Lett. 2006 Jul 15;106(1):34-41. PMID: 16720051.

T9969 Tyrphostin AG490

5 mg
10 mg
25 mg

Tyrphostin B42

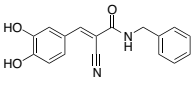

$C_{17}H_{14}N_2O_3$ FW: 294.31 [133550-30-8] ≥98%

JAK2 inhibitor and potential EGFR inhibitor. It displays a wide variety of biological activities, including suppressing differentiation of osteoclasts, inducing programmed cell death in leukemia cells, inhibiting the formation of atherosclerotic lesions, and preventing the onset of autoimmune type 1 diabetes.

Gyurkovska V, Stefanova T, Dimitrova P, et al. Tyrosine Kinase Inhibitor Tyrphostin AG490 Retards Chronic Joint Inflammation in Mice. Inflammation. 2014 Aug;37(4):995-1005. PMID: 24473905.

Davoodi-Semiromi A, Hassanzadeh A, Wasserfall CH, et al. Tyrphostin AG490 agent modestly but significantly prevents onset of type 1 in NOD mouse; implication of immunologic and metabolic effects of a Jak-Stat pathway inhibitor. J Clin Immunol. 2012 Oct;32(5):1038-47. PMID: 22661285.

Fenyo IM, Florea IC, Raicu M, et al. Tyrphostin AG490 reduces NAPDH oxidase activity and expression in the aorta of hypercholesterolemic apolipoprotein E-deficient mice. Vascul Pharmacol. 2011 Mar-Jun;54(3-6):100-6. PMID: 21457788.

T9970 Tyrphostin AG1295

1 mg
5 mg

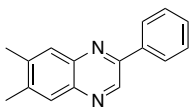

$C_{16}H_{14}N_2$ FW: 234.3 [70897-07-9] ≥98%

PDGFR inhibitor. It prevents fibroblast cell growth and prevents neointimal formation after vascular balloon injury.

Zheng Y, Ikuno Y, Ohj M, et al. Platelet-derived growth factor receptor kinase inhibitor AG1295 and inhibition of experimental proliferative vitreoretinopathy. Jpn J Ophthalmol. 2003 Mar-Apr;47(2):158-65. PMID: 12738549.

Banai S, Wolf Y, Golomb G, et al. PDGF-receptor tyrosine kinase blocker AG1295 selectively attenuates smooth muscle cell growth in vitro and reduces neointimal formation after balloon angioplasty in swine. Circulation. 1998 May 19;97(19):1960-9. PMID: 9609090.

T9974

[Asp371]-Tyrosinase (369-377), human

1 mg

$C_{42}H_{66}N_{10}O_{16}S_2$ FW: 1031.2 [9002-10-2] ≥98%

Tyr-Met-Asp-Gly-Thr-Met-Ser-Gln-Val

Proteasome antigen used to develop tumor-targeted vaccines.

Guillaume B, Stroobant V, Bousquet-Dubouch MP, et al. Analysis of the processing of seven human tumor antigens by intermediate proteasomes. J Immunol. 2012 Oct 1;189(7):3538-47. PMID: 22925930.

Mitchell MS, Darrah D, Yeung D, et al. Phase I trial of adoptive immunotherapy with cytolytic T lymphocytes immunized against a tyrosinase epitope. J Clin Oncol. 2002 Feb 15;20(4):1075-86. PMID: 11844833.

U0618

Ubenimex

10 mg
50 mg
100 mg

Bestatin

$C_{16}H_{24}N_2O_4$ FW: 308.37 [58970-76-6] ≥98%

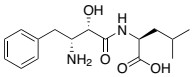

Aminopeptidase (N/CD13) inhibitor used to treat lung cancer. It also enhances differentiation of acute promyelocytic leukemia cells, enhances proliferation of bone marrow macrophage progenitor cells, and inhibits catabolism of opioid endopeptides.

Hitzerd SM, Verbrugge SE, Ossenkoppele G, et al. Positioning of aminopeptidase inhibitors in next generation cancer therapy. Amino Acids. 2014 Apr;46(4):793-808. PMID: 24385243.

Qian X, He J, Zhao Y, et al. Inhibition of p38 MAPK Phosphorylation Is Critical for Bestatin to Enhance ATRA-Induced Cell Differentiation in Acute Promyelocytic Leukemia NB4 Cells. Am J Ther. 2013 Oct 17. [Epub ahead of print]. PMID: 24141198.

Jia MR, Wei T, Xu WF. The Analgesic Activity of Bestatin as a Potent APN Inhibitor. Front Neurosci. 2010 Jun 28;4:50. PMID: 20631848.

U5232

Uniconazole

5 g
10 g
100 g

$C_{15}H_{18}ClN_3O$ FW: 291.78 [83657-22-1] ≥95%

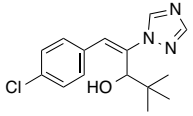

14-α Demethylase and gibberlin inhibitor that inhibits ergosterol synthesis and fungal cell wall formation. The S-(+) enantiomer appears to be more active than the R-(-) enantiomer.

Sasaki E, Ogura T, Takei K, et al. Uniconazole, a cytochrome P450 inhibitor, inhibits trans-zeatin biosynthesis in *Arabidopsis*. Phytochemistry. 2013 Mar;87:30-8. PMID: 23280040.

Sun J, Zhang A, Zhang J, et al. Enantiomeric resolution and growth-retardant activity in rice seedlings of uniconazole. J Agric Food Chem. 2012 Jan 11;60(1):160-4. PMID: 22148239.

Todoroki Y, Kobayashi K, Yoneyama H, et al. Structure-activity relationship of uniconazole, a potent inhibitor of ABA 8'-hydroxylase, with a focus on hydrophilic functional groups and conformation. Bioorg Med Chem. 2008 Mar 15;16(6):3141-52. PMID: 18164621.

U5233

Universal Tetanus Toxin Epitope P2 (830-844)

1 mg
2 mg
5 mg

TT (830-844); TT P2

$C_{80}H_{129}N_{19}O_{23}$ FW: 1725.03 ≥95%

Gln-Tyr-Ile-Lys-Ala-Asn-Ser-Lys-Phe-Ile-Gly-Ile-Thr-Glu-Leu

Tetanus toxin epitope that binds MHC receptors on T cells and is used to stimulate an immune response.

Fryauff DJ, Mouzin E, Church LW, et al. Lymphocyte response to tetanus toxin T-cell epitopes: effects of tetanus vaccination and concurrent malaria prophylaxis. Vaccine. 1999 Jan;17(1):59-63. PMID: 10078608.

Valmori D, Sabbatini A, Lanzavecchia A, et al. Functional analysis of two tetanus toxin universal T cell epitopes in their interaction with DR1101 and DR1104 alleles. J Immunol. 1994 Mar 15;152(6):2921-9. PMID: 7511633.

U6118

Uperolein

1 mg
2 mg
5 mg

$C_{57}H_{79}N_{13}O_{16}S$ FW: 1234.42 ≥95%

pGlu-Pro-Asp-Pro-Asn-Ala-Phe-Tyr-Gly-Leu-Met-NH_2

NK1 receptor agonist found in amphibian skin. It induces spasmogenic activity in smooth muscle cells.

Dike A, Cowsik SM. Solution structure of amphibian tachykinin Uperolein bound to DPC micelles. J Struct Biol. 2006 Dec;156(3):442-52. PMID: 16979908.

Bertaccini G, Coruzzi G. Action of some natural peptides on the stomach of the anaesthetized rat. Naunyn Schmiedebergs Arch Pharmacol. 1977 Jun;298(2):163-6. PMID: 882154.

U6901

Uracil

10 g
25 g
100 g

2,4-Pyrimidinediol

$C_4H_4N_2O_2$ FW: 112.09 [66-22-8] ≥98%

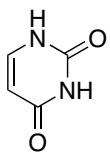

Endogenous pyrimidine base required for production of RNA. It is also used in synthesis of caffeine and plays a role in glucose metabolism.

Matyugina E, Khandazhinskaya A, Chernousova L, et al. The synthesis and antituberculosis activity of 5'-nor carbocyclic uracil derivatives. Bioorg Med Chem. 2012 Nov 15;20(22):6680-6. PMID: 23062712.

Parker JB, Stivers JT. Dynamics of uracil and 5-fluorouracil in DNA. Biochemistry. 2011 Feb 8;50(5):612-7. PMID: 21190322.

U6801

Urapidil

500 mg
1 g
5 g

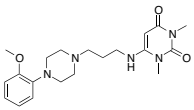

$C_{20}H_{29}N_5O_3$ FW: 387.48 [34661-75-1] ≥98%

5-HT1A receptor agonist and α1-adrenergic receptor antagonist. It induces vasodilation and decreases blood pressure without causing reflex tachycardia.

Santiveri X, Ledesma M. Urapidil in anesthesiology: pharmacology and indications. Rev Esp Anestesiol Reanim. 1998 May;45(5):189-97. PMID: 9646668.

van Zwieten PA, Chalmers JP. Different types of centrally acting antihypertensives and their targets in the central nervous system. Cardiovasc Drugs Ther. 1994 Dec;8(6):787-99. PMID: 7742257.

U6802

Urapidil Hydrochloride

500 mg
1 g
5 g

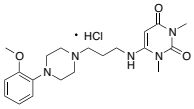

$C_{20}H_{29}N_5O_3 \bullet HCl$ FW: 423.93 [64887-14-5] ≥98%

5-HT1A receptor agonist and α1-adrenergic receptor antagonist. It induces vasodilation and decreases blood pressure without causing reflex tachycardia.

Santiveri X, Ledesma M. Urapidil in anesthesiology: pharmacology and indications. Rev Esp Anestesiol Reanim. 1998 May;45(5):189-97. PMID: 9646668.

van Zwieten PA, Chalmers JP. Different types of centrally acting antihypertensives and their targets in the central nervous system. Cardiovasc Drugs Ther. 1994 Dec;8(6):787-99. PMID: 7742257.

U6856

Urocortin II, human

0.5 mg
1 mg
2.5 mg

H-Ile-Val-Leu-Ser-Leu-Asp-Val-Pro-Ile-Gly-Leu-Leu-Gln-Ile-Leu-Leu-Glu-Gln-Ala-Arg-Ala-Arg-Ala-Ala-Arg-Glu-Gln-Ala-Thr-Thr-Asn-Ala-Arg-Ile-Leu-Ala-Arg-Val-Gly-His-Cys-NH_2

$C_{194}H_{338}N_{63}O_{54}S$ FW: 4449.31 ≥95%

Endogenous CRF2 agonist involved in stress signaling. It acts as a positive inotrope, modulates Ca^{2+} homeostasis, decreases food intake, and suppresses the development of anxiety-related behaviors.

Campos-Salinas J, Caro M, Cavazzuti A, et al. Protective Role of the Neuropeptide Urocortin II against Experimental Sepsis and *Leishmania*sis by Direct Killing of Pathogens. J Immunol. 2013 Dec 15;191(12):6040-51. PMID: 24249730.

Grossini E, Caimmi PP, Molinari C, et al. Modulation of calcium movements by urocortin II in endothelial cells. Cell Physiol Biochem. 2010;25(2-3):221-32. PMID: 20110683.

U6858

Urocortin II, mouse

0.5 mg
1 mg
2.5 mg

H-Val-Ile-Leu-Ser-Leu-Asp-Val-Pro-Ile-Gly-Leu-Leu-Arg-Ile-Leu-Leu-Glu-Gln-Ala-Arg-Tyr-Lys-Ala-Ala-Arg-Asn-Gln-Ala-Ala-Thr-Asn-Ala-Gln-Ile-Leu-Ala-His-Val-NH_2

$C_{187}H_{320}N_{56}O_{50}$ FW: 4152.98 ≥95%

Endogenous CRF2 agonist involved in stress signaling. It acts as a positive inotrope, modulates Ca^{2+} homeostasis, decreases food intake, and suppresses the development of anxiety-related behaviors.

Campos-Salinas J, Caro M, Cavazzuti A, et al. Protective Role of the Neuropeptide Urocortin II against Experimental Sepsis and *Leishmania*sis by Direct Killing of Pathogens. J Immunol. 2013 Dec 15;191(12):6040-51. PMID: 24249730.

Grossini E, Caimmi PP, Molinari C, et al. Modulation of calcium movements by urocortin II in endothelial cells. Cell Physiol Biochem. 2010;25(2-3):221-32. PMID: 20110683.

U6859

Urocortin III, human

0.5 mg
1 mg
2.5 mg

H-Phe-Thr-Leu-Ser-Leu-Asp-Val-Pro-Thr-Asn-Ile-Met-Asn-Leu-Leu-Phe-Asn-Ile-Ala-Lys-Ala-Lys-Asn-Leu-Arg-Ala-Gln-Ala-Ala-Ala-Asn-Ala-His-Leu-Met-Ala-Gln-Ile-NH_2

$C_{185}H_{307}N_{53}O_{50}S_2$ FW: 4137.96 ≥95%

Endogenous CRF2 agonist present in the brain and involved in stress signaling. It acts as a positive inotrope, modulates Ca^{2+} homeostasis, decreases food intake, and suppresses the development of anxiety-related behaviors.

Bagosi Z, Csabafi K, Palotai M, et al. The interaction of Urocortin II and Urocortin III with amygdalar and hypothalamic cotricotropin-releasing factor (CRF)--reflections on the regulation of the hypothalamic-pituitary-adrenal (HPA) axis. Neuropeptides. 2013 Oct;47(5):333-8. PMID: 23932308.

Takahashi K, Totsune K, Murakami O, et al. Urocortins as cardiovascular peptides. Peptides. 2004 Oct;25(10):1723-31. PMID: 15476939.

U6860

Urocortin III, mouse

0.5 mg
1 mg
2.5 mg

H-Phe-Thr-Leu-Ser-Leu-Asp-Val-Pro-Thr-Asn-Ile-Met-Asn-Ile-Leu-Phe-Asn-Ile-Asp-Lys-Ala-Lys-Asn-Leu-Arg-Ala-Lys-Ala-Ala-Ala-Asn-Ala-Gln-Leu-Met-Ala-Gln-Ile-NH_2

$C_{186}H_{312}N_{52}O_{52}S_2$ FW: 4173.01 ≥95%

Endogenous CRF2 agonist present in the brain and involved in stress signaling. It acts as a positive inotrope, modulates Ca^{2+} homeostasis, decreases food intake, and suppresses the development of anxiety-related behaviors.

Bagosi Z, Csabafi K, Palotai M, et al. The interaction of Urocortin II and Urocortin III with amygdalar and hypothalamic cotricotropin-releasing factor (CRF)--reflections on the regulation of the hypothalamic-pituitary-adrenal (HPA) axis. Neuropeptides. 2013 Oct;47(5):333-8. PMID: 23932308.

U6854

Urocortin, human

0.5 mg
1 mg
2.5 mg

H-Asp-Asn-Pro-Ser-Leu-Ser-Ile-Asp-Leu-Thr-Phe-His-Leu-Leu-Arg-Thr-Leu-Leu-Glu-Leu-Ala-Arg-Thr-Gln-Ser-Gln-Arg-Glu-Arg-Ala-Glu-Gln-Asn-Arg-Ile-Ile-Phe-Asp-Ser-Val-NH_2

$C_{204}H_{337}N_{63}O_{64}$ FW: 4696.3 [171543-83-2] ≥98%

Endogenous CRF1/2 receptor agonist involved in feeding behavior and stress responses. It acts as a positive inotrope and increases corticosterone and ACTH levels.

Bagosi Z, Csabafi K, Palotai M, et al. The effect of urocortin I on the hypothalamic ACTH secretagogues and its impact on the hypothalamic-pituitary-adrenal axis. Neuropeptides. 2013 Nov 21. pii: S0143-4179(13)00100-5. PMID: 24331779.

Dono LM, Currie PJ. The cannabinoid receptor CB1 inverse agonist AM251 potentiates the anxiogenic activity of urocortin I in the basolateral amygdala. Neuropharmacology. 2012 Jan;62(1):192-9. PMID: 21736884.

U6855

Urocortin, rat

0.5 mg
1 mg
2.5 mg

H-Asp-Asp-Pro-Pro-Leu-Ser-Ile-Asp-Leu-Thr-Phe-His-Leu-Leu-Arg-Thr-Leu-Leu-Glu-Leu-Ala-Arg-Thr-Gln-Ser-Gln-Arg-Glu-Arg-Ala-Glu-Gln-Asn-Arg-Ile-Ile-Phe-Asp-Ser-Val-NH_2

$C_{206}H_{338}N_{62}O_{64}$ FW: 4707.37 ≥95%

Endogenous CRF1/2 receptor agonist involved in stress signaling. It acts as a positive inotrope and increases secretion of corticosterone and ACTH.

Bagosi Z, Csabafi K, Palotai M, et al. The effect of urocortin I on the hypothalamic ACTH secretagogues and its impact on the hypothalamic-pituitary-adrenal axis. Neuropeptides. 2013 Nov 21. pii: S0143-4179(13)00100-5. PMID: 24331779.

U6857

Urodilatin CCC

1 mg

H-Thr-Ala-Pro-Arg-Ser-Leu-Arg-Arg-Ser-Ser-Cys-Phe-Gly-Gly-Arg-Met-Asp-Arg-Ile-Gly-Ala-Gln-Ser-Gly-Leu-Gly-Cys-Asn-Ser-Phe-Arg-Tyr-OH
(Disulfide bridge Cys_{11}-Cys_{27})

Atriopeptin; ANP (95-129)

$C_{145}H_{234}N_{52}O_{44}S_3$ FW: 3506 [115966-23-9] ≥98%

ANP fragment and Na^+/K^+ ATPase inhibitor. It regulates Na^+ and water transport across renal proximal tubules.

Choi MR, Citarella MR, Lee BM, et al. Urodilatin regulates renal dopamine metabolism. J Nephrol. 2013 Nov-Dec;26(6):1042-8. PMID: 23661592.

Vives D, Farage S, Motta R, et al. Atrial natriuretic peptides and urodilatin modulate proximal tubule $Na(^+)$-ATPase activity through activation of the NPR-A/cGMP/PKG pathway. Peptides. 2010 May;31(5):903-8. PMID: 20206222.

U6956

Uroguanylin, human

0.5 mg
1 mg
2.5 mg

H-Asn-Asp-Asp-Cys-Glu-Leu-Cys-Val-Asn-Val-Ala-Cys-Thr-Gly-Cys-Leu-OH
(Cys_4-Cys_{12}, Cys_7-Cys_{15})

$C_{64}H_{102}N_{18}O_{26}S_4$ FW: 1667.89 ≥95%

Endogenous guanylyl cyclase C receptor agonist involved in water and Na^+ homeostasis. It also increases activity of Cl^- channels and inhibits bicarbonate reabsorption.

Teixeira MD, Nascimento NR, Fonteles MC, et al. Uroguanylin induces electroencephalographic spikes in rats. Braz J Biol. 2013 Aug;73(3):623-7. PMID: 24212704.

Lessa LM, Carraro-Lacroix LR, Crajoinas RO, et al. Mechanisms underlying the inhibitory effects of uroguanylin on NHE3 transport activity in renal proximal tubule. Am J Physiol Renal Physiol. 2012 Nov 15;303(10):F1399-408. PMID: 22952280.

U6957

Urotensin I

0.5 mg
1 mg
2.5 mg

H-Asn-Asp-Asp-Pro-Pro-Ile-Ser-Ile-Asp-Leu-Thr-Phe-His-Leu-Leu-Arg-Asn-Met-Ile-Glu-Met-Ala-Arg-Ile-Glu-Asn-Glu-Arg-Glu-Gln-Ala-Gly-Leu-Asn-Arg-Lys-Tyr-Leu-Asp-Glu-Val-NH_2

$C_{210}H_{340}N_{62}O_{67}S_2$ FW: 4869.55 ≥95%

Endogenous CRF1/2 agonist involved in stress signaling. It decreases food intake, suppresses the development of anxiety-like behaviors, and may be used as a biomarker for heart failure.

Ortega VA, Lovejoy DA, Bernier NJ. Appetite-suppressing effects and interactions of centrally administered corticotropin-releasing factor, urotensin I and serotonin in rainbow trout (Oncorhynchus mykiss). Front Neurosci. 2013 Oct 29;7:196. PMID: 24194695.

Backström T, Pettersson A, Johansson V, et al. CRF and urotensin I effects on aggression and anxiety-like behavior in rainbow trout. J Exp Biol. 2011 Mar 15;214(Pt 6):907-14. PMID: 21346117.

U6958

Urotensin II, frog

0.5 mg
1 mg
2.5 mg

H-Ala-Gly-Asn-Leu-Ser-Glu-Cys-Phe-Trp-Lys-Tyr-Cys-Val-OH
(Disulfide bridge Cys_7-Cys_{12})

$C_{69}H_{96}N_{16}O_{19}S_2$ FW: 1517.76 ≥95%

Endogenous urotensin II receptor agonist involved in stress signaling. It increases pro-inflammatory cytokine expression, inhibits glucose transport, stimulates apoptosis in cardiac tissue cells, and induces relaxation in smooth muscle cells.

Peng H, Zhang M, Cai X, et al. Association between Human Urotensin II and Essential Hypertension-A 1:1 Matched Case-Control Study. PLoS One. 2013 Dec 10;8(12):e81764. PMID: 24339964.

Wang HX, Wu XR, Yang H, et al. Urotensin II inhibits skeletal muscle glucose transport signaling pathways via the NADPH oxidase pathway. PLoS One. 2013 Oct 8;8(10):e76796. PMID: 24116164.

U6959

Urotensin II, human

0.5 mg
1 mg
2.5 mg

H-Glu-Thr-Pro-Asp-Cys-Phe-Lys-Tyr-Cys-Val-OH (Disulfide bridge Cys5-Cys10)

$C_{64}H_{85}N_{13}O_{18}S_2$ FW: 1388.6 ≥95%

Endogenous urotensin II receptor agonist involved in stress signaling. It increases pro-inflammatory cytokine expression, inhibits glucose transport, stimulates apoptosis in cardiac tissue cells, and induces relaxation in smooth muscle cells.

Peng H, Zhang M, Cai X, et al. Association between Human Urotensin II and Essential Hypertension-A 1:1 Matched Case-Control Study. PLoS One. 2013 Dec 10;8(12):e81764. PMID: 24339964.

Wang HX, Wu XR, Yang H, et al. Urotensin II inhibits skeletal muscle glucose transport signaling pathways via the NADPH oxidase pathway. PLoS One. 2013 Oct 8;8(10):e76796. PMID: 24116164.

U6873

Ursodeoxycholic Acid

1 g
5 g

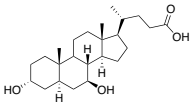

$C_{24}H_{40}O_4$ FW: 392.57 [128-13-2] ≥98%

Endogenous secondary bile acid and telomerase inhibitor that decreases cholesterol absorption and treats liver diseases. It also decreases expression of immune response mediators to prevent allograft rejection, induces differentiation, senescence, and apoptosis in various cancer cells, decreases gastrointestinal transit time, and increases gastric emptying rates.

Zhang Q, Nakaki T, Iwami D, et al. Induction of regulatory T cells and indefinite survival of fully allogeneic cardiac grafts by ursodeoxycholic acid in mice. Transplantation. 2009 Dec 27;88(12):1360-70. PMID: 20029332.

El-Sherbiny GA, Taye A, Abdel-Raheem IT. Role of ursodeoxycholic acid in prevention of hepatotoxicity caused by amoxicillin-clavulanic acid in rats. Ann Hepatol. 2009 Apr-Jun;8(2):134-40. PMID: 19502657.

Akare S, Jean-Louis S, Chen W, et al. Ursodeoxycholic acid modulates histone acetylation and induces differentiation and senescence. Int J Cancer. 2006 Dec 15;119(12):2958-69. PMID: 17019713.

U7354

Usnic Acid

5 g
25 g

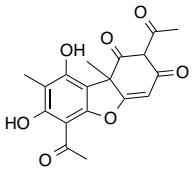

$C_{18}H_{16}O_7$ FW: 344.32 [125-46-2] ≥98%

In induces cell cycle arrest and apoptosis in lung carcinoma cells and inhibits growth of *Mycobacterium* tuberculosis.

Singh N, Nambiar D, Kale RK, et al. Usnic acid inhibits growth and induces cell cycle arrest and apoptosis in human lung carcinoma A549 cells. Nutr Cancer. 2013;65 Suppl 1:36-43. PMID: 23682781.

Song Y, Dai F, Zhai D, et al. Usnic acid inhibits breast tumor angiogenesis and growth by suppressing VEGFR2-mediated AKT and ERK1/2 signaling pathways. Angiogenesis. 2012 Sep;15(3):421-32. PMID: 22669534.

Ramos DF, Almeida da Silva PE. Antimycobacterial activity of usnic acid against resistant and susceptible strains of *Mycobacterium* tuberculosis and non-tuberculous mycobacteria. Pharm Biol. 2010 Mar;48(3):260-3. PMID: 20645810.

V0045

Valacyclovir Hydrochloride

50 mg
100 mg
500 mg

BW-256U87

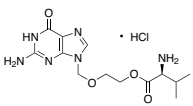

$C_{13}H_{20}N_6O_4 \bullet HCl$ FW: 360.8 [124832-27-5] ≥98%

Neuraminidase inhibitor and acyclovir prodrug used to treat varicella-zoster virus infection. It also inhibits survival of herpes simplex virus and HIV-1.

Gupta D, Varghese Gupta S, Dahan A, et al. Increasing oral absorption of polar neuraminidase inhibitors: a prodrug transporter approach applied to oseltamivir analogue. Mol Pharm. 2013 Feb 4;10(2):512-22. PMID: 23244438.

Roxby AC, Liu AY, Drake AL, et al. Short communication: T cell activation in HIV-1/herpes simplex virus-2-coinfected Kenyan women receiving valacyclovir. AIDS Res Hum Retroviruses. 2013 Jan;29(1):94-8. PMID: 22852760.

Andrei G, Snoeck R. Emerging drugs for varicella-zoster virus infections. Expert Opin Emerg Drugs. 2011 Sep;16(3):507-35. PMID: 21699441.

V0245

Valdecoxib

5 mg
10 mg
25 mg

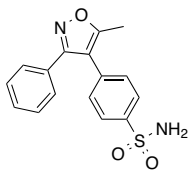

$C_{16}H_{14}N_2O_3S$ FW: 314.36 [181695-72-7] ≥98%

NSAID, CB1 agonist, and COX-2 inhibitor. It modulates glutamate signaling and GABA release and increases risk of thrombotic effects.

Atukorala I, Hunter DJ. Valdecoxib : the rise and fall of a COX-2 inhibitor. Expert Opin Pharmacother. 2013 Jun;14(8):1077-86. PMID: 23517091.

Schröder H, Höllt V, Becker A. Parecoxib and its metabolite valdecoxib directly interact with cannabinoid binding sites in CB1-expressing HEK 293 cells and rat brain tissue. Neurochem Int. 2011 Jan;58(1):9-13. PMID: 21073910.

Roumie CL, Choma NN, Kaltenbach L, et al. Non-aspirin NSAIDs, cyclooxygenase-2 inhibitors and risk for cardiovascular events-stroke, acute myocardial infarction, and death from coronary heart disease. Pharmacoepidemiol Drug Saf. 2009 Nov;18(11):1053-63. PMID: 19637402.

V0144

n-Valeric Acid

10 mL
50 mL
100 mL

Pentanoic acid

$C_5H_{10}O_2$ FW: 102.13 [109-52-4] ≥99%

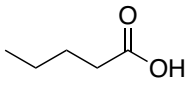

GHB/GABA analog and potential HDAC inhibitor found in *Valeriana officinalis* used in the synthesis of esters. It decreases oxidative activity and induces expression of Epstein-Barr virus-associated early antigen and viral capsid antigen in EBV-carrying human lymphoblastoid cells.

Huang HM, Ou HC, Chen HL, et al. Protective effect of alpha-keto-beta-methyl-n-valeric acid on BV-2 microglia under hypoxia or oxidative stress. Ann N Y Acad Sci. 2005 May;1042:272-8. PMID: 15965072.

Huang HM, Zhang H, Ou HC, et al. alpha-keto-beta-methyl-n-valeric acid diminishes reactive oxygen species and alters endoplasmic reticulum $Ca^{(2+)}$ stores. Free Radic Biol Med. 2004 Dec 1;37(11):1779-89. PMID: 15528037.

V0244

Valganciclovir Hydrochloride

25 mg
50 mg
100 mg

$C_{14}H_{22}N_6O_5 \cdot HCl$ FW: 354.36 [175865-59-5] ≥98%

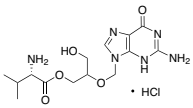

Deoxyguanosine analog, ganciclovir prodrug, and DNA chain elongation inhibitor used to treat cytomegalovirus infection.

Stronati M, Lombardi G, Garofoli F, et al. Pharmacokinetics, pharmacodynamics and clinical use of valganciclovir in newborns with symptomatic congenital cytomegalovirus infection. Curr Drug Metab. 2013 Feb;14(2):208-15. PMID: 22935067.

Iwasenko JM, Scott GM, Rawlinson WD, et al. Successful valganciclovir treatment of post-transplant cytomegalovirus infection in the presence of UL97 mutation N597D. J Med Virol. 2009 Mar;81(3):507-10. PMID: 19152402.

Pantanowitz L, Früh K, Marconi S, et al. Pathology of rituximab-induced Kaposi sarcoma flare. BMC Clin Pathol. 2008 Jul 23;8:7. PMID: 18651955.

V0145

Valinomycin

5 mg
10 mg
25 mg

$C_{54}H_{90}N_6O_{18}$ FW: 1111.32 [2001-95-8] ≥98%

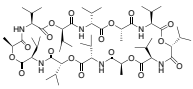

Neutral ionophore that transports K^+ ions through cellular membranes, altering the electrochemical gradient. It induces mitochondrial damage, oxidative stress, and caspase expression.

Li R, El-Mallahk RS. A novel evidence of different mechanisms of lithium and valproate neuroprotective action on human SY5Y neuroblastoma cells: caspase-3 dependency. Neurosci Lett. 2000 Nov 24;294(3):147-50. PMID: 11072136.

Gad SC, Reilly C, Siino K, et al. Thirteen cationic ionophores: their acute toxicity, neurobehavioral and membrane effects. Drug Chem Toxicol. 1985;8(6):451-68. PMID: 4092618.

V0147

Valproic Acid Sodium

10 g
25 g
100 g

Sodium valproate

$C_8H_{15}NaO_2$ FW: 166.19 [1069-66-5] ≥98%

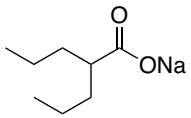

T-type Ca^{2+} and voltage-gated Na^+ channel blocker and inhibitor of GABA transaminase and HDACs used epilepsy, bipolar disorder, and migraines. It also displays other biological activities, including preventing LPS-induced increases in pro-inflammatory cytokine levels and downregulating expression of HDAC, VEGF, VEGFR2, and FGF in cancer models.

Zhang ZH, Hao CL, Liu P, et al. Valproic acid inhibits tumor angiogenesis in mice transplanted with Kasumi 1 leukemia cells. Mol Med Rep. 2014 Feb;9(2):443-9. PMID: 24297248.

Ji MH, Li GM, Jia M, et al. Valproic acid attenuates lipopolysaccharide-induced acute lung injury in mice. Inflammation. 2013 Dec;36(6):1453-9. PMID: 23846716.

Zhao L, Chen CN, Hajji N, et al. Histone deacetylation inhibition in pulmonary hypertension: therapeutic potential of valproic acid and suberoylanilide hydroxamic acid. Circulation. 2012 Jul 24;126(4):455-67. PMID: 22711276.

V0146

Valsartan

1 g
5 g
25 g

$C_{24}H_{29}N_5O_3$ FW: 435.52 [137862-53-4] ≥98%

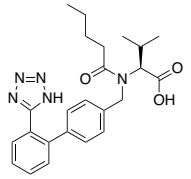

AT1 receptor inhibitor used to treat hypertension. It decreases infarct size in ischemia/reperfusion models, prevents induction of cardiotrophin-1 during heart failure, and inhibits release of pro-inflammatory cytokines.

Wu X, He L, Cai Y, et al. Induction of autophagy contributes to the myocardial protection of valsartan against ischemia reperfusion injury. Mol Med Rep. 2013 Dec;8(6):1824-30. PMID: 24084854.

Sohn YI, Lee NJ, Chung A, et al. Antihypertensive drug Valsartan promotes dendritic spine density by altering AMPA receptor trafficking. Biochem Biophys Res Commun. 2013 Oct 4;439(4):464-70. PMID: 24012668.

Cheng CI, Hsiao CC, Wu SC, et al. Valsartan impairs angiogenesis of mesenchymal stem cells through Akt pathway. Int J Cardiol. 2013 Sep 10;167(6):2765-74. PMID: 22805546.

V0252

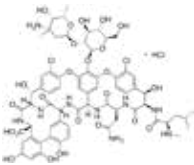

Vancomycin Hydrochloride

100 mg
250 mg
1 g

$C_{66}H_{75}Cl_2N_9O_{24} \bullet HCl$ FW: 1485.73 [1404-93-9]

Cell wall synthesis inhibitor that binds D-Ala-D-Ala. It inhibits growth of *Clostridium* and *Staphylococcus*.

Allen CA, Babakhani F, Sears P, et al. Both fidaxomicin and vancomycin inhibit outgrowth of *Clostridium difficile* spores. Antimicrob Agents Chemother. 2013 Jan;57(1):664-7. PMID: 23147724.

Chakraborty SP, Sahu SK, Pramanik P, et al. In vitro antimicrobial activity of nanoconjugated vancomycin against drug resistant *Staphylococcus aureus*. Int J Pharm. 2012 Oct 15;436(1-2):659-76. PMID: 22841851.

V0352

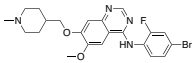

Vandetanib

5 mg
25 mg
100 mg

$C_{22}H_{24}BrFN_4O_2$ FW: 475.35 [443913-73-3] ≥98%

Inhibitor of RET, EGFR, and VEGFR2. It induces autophagy and apoptosis in glioblastoma cells and decreases tumor microvessel density and tumor cell proliferation. It also prolongs the cardiac QT interval.

Liu Y, Liu Y, Fan ZW, et al. Meta-analysis of the risks of hypertension and QTc prolongation in patients with advanced non-small cell lung cancer who were receiving vandetanib. Eur J Clin Pharmacol. 2015 May;71(5):541-7. PMID: 25753291

Shen J, Zheng H, Ruan J, et al. Autophagy inhibition induces enhanced proapoptotic effects of ZD6474 in glioblastoma. Br J Cancer. 2013 Jul 9;109(1):164-71. PMID: 23799852.

Samadi AK, Bazzill J, Zhang X, et al. Novel withanolides target medullary thyroid cancer through inhibition of both RET phosphorylation and the mammalian target of rapamycin pathway. Surgery. 2012 Dec;152(6):1238-47. PMID: 23158190.

V0153

H-Cys-Glu-Asp-Ala-Glu-Val-Phe-Lys-Asp-Ser-Met-Val-Pro-Gly-Glu-Lys-OH

Vanilloid Receptor 1 Fragment

1 mg
2 mg
5 mg

Transient receptor potential vanilloid 1; TRPV1; VR1; Capsaicin receptor

$C_{75}H_{117}N_{18}O_{28}S_2$ FW: 1782.96 ≥95%

Peptide fragment of TRPV1, a receptor involved in pain neurotransmission, inflammation, and muscle contraction.

Anwar IJ, Derbenev AV. TRPV1-dependent regulation of synaptic activity in the mouse dorsal motor nucleus of the vagus nerve. Front Neurosci. 2013 Dec 13;7:238. PMID: 24379754.

Tóth A, Czikora A, Pásztor ET, et al. Vanilloid Receptor-1 (TRPV1) Expression and Function in the Vasculature of the Rat. J Histochem Cytochem. 2013 Dec 5. [Epub ahead of print]. PMID: 24217926.

V0160

D-Phe-Cys-Tyr-D-Trp-Lys-Val-Cys-Trp-NH_2

Vapreotide

0.5 mg
1 mg
2.5 mg

Sanvar IR; BMY 41606; RC 160

$C_{57}H_{70}N_{12}O_9S_2$ FW: 1131.4 [103222-11-3] ≥95%

Synthetic somatostatin analog, somatostatin 2 receptor agonist, and NK1 receptor antagonist. It displays a variety of biological activities, including preventing HIV-1 infection, decreasing PSA and PAP levels and bone pain scores, and lessening portal pressure and blood flow.

Spitsin S, Tuluc F, Meshki J, et al. Analog of somatostatin vapreotide exhibits biological effects in vitro via interaction with neurokinin-1 receptor. Neuroimmunomodulation. 2013;20(5):247-55. PMID: 23921645.

V0274

H-Cys-Tyr-Ile-Gln-Asn-Cys-Pro-Arg-Gly-NH_2 (Disulfide bridge Cys_1-Cys_6)

[Lys8]-Vasopressin

1 mg
2 mg
5 mg

$C_{46}H_{65}N_{13}O_{12}S_2$ FW: 1056.24 ≥95%

Vasopressin analog and V1/2 receptor agonist. It induces vasoconstriction, stimulates muscle contraction, and modulates intestinal motility.

Chelko SP, Schmiedt CW, Lewis TH, et al. Vasopressin-induced constriction of the isolated rat occipital artery is segment dependent. J Vasc Res. 2013;50(6):478-85. PMID: 24192548.

Mastropaolo M, Zizzo MG, Auteri M, et al. Arginine vasopressin, via activation of post-junctional V1 receptors, induces contractile effects in mouse distal colon. Regul Pept. 2013 Nov 10;187:29-34. PMID: 24185041.

V0275

H-Cys-Tyr-Ile-Gln-Asn-Cys-Pro-Arg-Gly-NH_2 (Disulfide bridge Cys_1-Cys_6)

[Arg8]-Vasotocin

1 mg
2 mg
5 mg

$C_{43}H_{67}N_{15}O_{12}S_2$ FW: 1050.23 ≥95%

Oxytocin-vasopressin analog. It decreases feeding behavior, increases stress responses, and induces courtship behavior.

Gesto M, Soengas JL, Rodríguez-Illamola A, et al. Arginine vasotocin treatment induces a stress response and exerts a potent anorexigenic effect in rainbow trout, Oncorhynchus mykiss. J Neuroendocrinol. 2013 Dec 16. [Epub ahead of print]. PMID: 24341528.

Kim JK, Kim IH, Heo JH, et al. Arginine vasotocin (AVT) triggers courtship behavior without exposure to external stimuli and modulates the olfactory response of male Hynobius leechii salamanders. Zoolog Sci. 2013 Nov;30(11):929-37. PMID: 24199858.

V0269

Vardenafil Dihydrochloride

10 mg
25 mg
100 mg

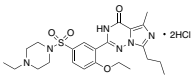

$C_{23}H_{32}N_6O_4S \bullet 2HCl$ FW: 561.52 [224789-15-5] ≥98%

PDE5 inhibitor used to treat erectile dysfunction. It also increases expression of NO and eNOS, decreases oxidative stress and pulmonary vascular resistance, prevents proteinuria and glomerular damage in animal models of diabetic nephropathy-induced cGMP pathway dysfunction, and suppresses secretion of IL-8 and expression of oxidative LDLR.

Vignozzi L, Gacci M, Cellai I, et al. PDE5 inhibitors blunt inflammation in human BPH: a potential mechanism of action for PDE5 inhibitors in LUTS. Prostate. 2013 Sep;73(13):1391-402. PMID: 23765639.

Fan YF, Zhang R, Jiang X, et al. The phosphodiesterase-5 inhibitor vardenafil reduces oxidative stress while reversing pulmonary arterial hypertension. Cardiovasc Res. 2013 Aug 1;99(3):395-403. PMID: 23650288.

Fang L, Radovits T, Szabó G, et al. Selective phosphodiesterase-5 (PDE-5) inhibitor vardenafil ameliorates renal damage in type 1 diabetic rats by restoring cyclic 3',5' guanosine monophosphate (cGMP) level in podocytes. Nephrol Dial Transplant. 2013 Jul;28(7):1751-61. PMID: 23203993

V0273

Vasoactive Intestinal Peptide

0.5 mg
1 mg
2.5 mg

His-Ser-Asp-Ala-Val-Phe-Thr-Asp-Asn-Tyr-Thr-Arg-Leu-Arg-Lys-Gln-Met-Ala-Val-Lys-Lys-Tyr-Leu-Asn-Ser-Ile-Leu-Asn-NH_2

VIP

$C_{57}H_{70}N_{12}O_9S_1$ FW: 3325.7 [40077-57-4] ≥95%

Endogenous VPAC1/2 receptor agonist involved in enteric movement and hormone secretion. It prevents LPS-induced expression of pro-inflammatory cytokines and stimulates bronchodilation and vasodilation.

Hauk V, Azzam S, Calo G, et al. Vasoactive intestinal Peptide induces an immunosuppressant microenvironment in the maternal-fetal interface of non-obese diabetic mice and improves early pregnancy outcome. Am J Reprod Immunol. 2014 Feb;71(2):120-30. PMID: 24405265.

Fraccaroli L, Grasso E, Hauk V, et al. Contribution of Vasoactive Intestinal Peptide to Immune Homeostasis in Trophoblast-Maternal Leukocyte Interaction under LPS Stimulation. Neuroimmunomodulation. 2014;21(1):21-30. PMID: 24135863.

V3360

Vasoactive Intestinal Peptide, guinea pig

0.5 mg
1 mg
2.5 mg

H-His-Ser-Asp-Ala-Leu-Phe-Thr-Asp-Thr-Tyr-Thr-Arg-Leu-Arg-Lys-Gln-Met-Ala-Met-Lys-Lys-Tyr-Leu-Asn-Ser-Val-Leu-Asn-NH_2

VIP

$C_{147}H_{239}N_{43}O_{42}S_2$ FW: 3344.93 ≥95%

Endogenous VPAC1/2 receptor agonist involved in vasodilation and hormone secretion. It also increases levels of IL-10, Foxp3, and TGF-β and prevents LPS-induced expression of IL-6 and MCP-1

Hauk V, Azzam S, Calo G, et al. Vasoactive intestinal Peptide induces an immunosuppressant microenvironment in the maternal-fetal interface of non-obese diabetic mice and improves early pregnancy outcome. Am J Reprod Immunol. 2014 Feb;71(2):120-30. PMID: 24405265.

V0376

Vatalanib Dihydrochloride

5 mg
10 mg
25 mg

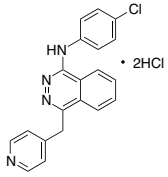

$C_{20}H_{15}ClN_4 \bullet 2HCl$ FW: 419.73 ≥98%

VEGFR inhibitor. It decreases tumor vascularization, inhibits tumor growth and metastasis, and decreases microvessel density. It also decreases chronic neuropathic pain in models of chronic constriction injury.

Gupta P, Mulkey F, Hasserjian RP, et al. A phase II study of the oral VEGF receptor tyrosine kinase inhibitor vatalanib (PTK787/ZK222584) in myelodysplastic syndrome: Cancer and Leukemia Group B study 10105 (Alliance). Invest New Drugs. 2013 Oct;31(5):1311-20. PMID: 23700288.

Liu S, Xu C, Li G, et al. Vatalanib decrease the positive interaction of VEGF receptor-2 and P2X2/3 receptor in chronic constriction injury rats. Neurochem Int. 2012 May;60(6):565-72. PMID: 22361062.

Gauler TC, Besse B, Mauguen A, et al. Phase II trial of PTK787/ZK 222584 (vatalanib) administered orally once-daily or in two divided daily doses as second-line monotherapy in relapsed or progressing patients with stage IIIB/IV non-small-cell lung cancer (NSCLC). Ann Oncol. 2012 Mar;23(3):678-87. PMID: 21617019.

V1600

VE-821

NEW

5 mg
10 mg

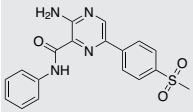

$C_{18}H_{16}N_4O_3S$ FW: 368.41 [1232410-49-9] ≥98%

Inhibitor of ataxia telangiectasia and Rad3-related kinase that activates the DNA damage checkpoint and induces cell cycle arrest. It induces cell cycle arrest, chromosome fragmentation, and apoptosis in cancer cells.

Flynn RL, Cox KE, Jeitany M, et al. Alternative lengthening of telomeres renders cancer cells hypersensitive to ATR inhibitors. Science. 2015 Jan 16;347(6219):273-7. PMID: 25593184.

Vávrová J, Zárybnická L, Lukášová E, et al. Inhibition of ATR kinase with the selective inhibitor VE-821 results in radiosensitization of cells of promyelocytic leukaemia (HL-60). Radiat Environ Biophys. 2013 Nov;52(4):471-9. PMID: 23934411.

Prevo R, Fokas E, Reaper PM, et al. The novel ATR inhibitor VE-821 increases sensitivity of pancreatic cancer cells to radiation and chemotherapy. Cancer Biol Ther. 2012 Sep;13(11):1072-81. PMID: 22825331.

V1810 Vecuronium Bromide

10 mg
50 mg
100 mg

NC-45

$C_{34}H_{57}BrN_2O_4$ FW: 637.74 [50700-72-6] ≥98%

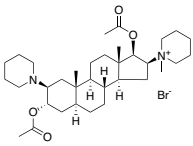

Non-depolarizing NMJ blocker and nAChR antagonist used as an anesthetic. It induces skeletal muscle paralysis.

de Boer HD. Neuromuscular transmission: new concepts and agents. J Crit Care. 2009 Mar;24(1):36-42. PMID: 19272537.

Jonsson M, Gurley D, Dabrowski M, et al. Distinct pharmacologic properties of neuromuscular blocking agents on human neuronal nicotinic acetylcholine receptors: a possible explanation for the train-of-four fade. Anesthesiology. 2006 Sep;105(3):521-33. PMID: 16931985.

V1745 Veliparib

1 mg
5 mg
25 mg

ABT-888

$C_{13}H_{16}N_4O$ FW: 244.29 [912444-00-9] ≥98%

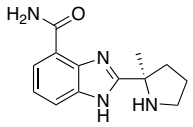

PARP inhibitor. It decreases inflammation in cystic fibrosis models and inhibits repair of DNA damage induced by chemotherapy.

Owonikoko TK, Zhang G, Deng X et al. Poly (ADP) ribose polymerase enzyme inhibitor, veliparib, potentiates chemotherapy and radiation in vitro and in vivo in small cell lung cancer. Cancer Med. 2014 Dec;3(6):1579-94. PMID: 25124282.

Barazzuol L, Jena R, Burnet NG, et al. Evaluation of poly (ADP-ribose) polymerase inhibitor ABT-888 combined with radiotherapy and temozolomide in glioblastoma. Radiat Oncol. 2013 Mar 19;8:65. PMID: 23510353.

Ta LE, Schmelzer JD, Bieber AJ, et al. A novel and selective poly (ADP-ribose) polymerase inhibitor ameliorates chemotherapy-induced painful neuropathy. PLoS One. 2013;8(1):e54161. PMID: 23326593.

V1668 Vemurafenib

10 mg
25 mg

PLX-4032; RG7204; RO5185426

$C_{23}H_{18}ClF_2N_3O_3S$ FW: 489.92 [1029872-54-5] ≥98%

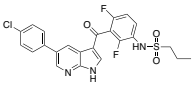

B-Raf inhibitor used to treat metastatic melanoma. It inhibits WT and V600E mutant B-Raf, inducing cell cycle arrest in melanoma cells. It may induce the development of verrucal keratosis and cutaneous squamous cell carcinoma.

Anforth R, Blumetti TC, Clements A, et al. Systemic Retinoids for the Chemoprevention of Cutaneous Squamous Cell Carcinoma and Verrucal Keratosis in a Cohort of Patients on BRAF inhibitors. Br J Dermatol. 2013 Jul 20. PMID: 23870055.

Beck D, Niessner H, Smalley KS, et al. Vemurafenib potently induces endoplasmic reticulum stress-mediated apoptosis in BRAFV600E melanoma cells. Sci Signal. 2013 Jan 29;6(260):ra7. PMID: 23362240.

V1854 Venlafaxine Hydrochloride

500 mg
1 g
5 g

HSDB 6699; Wy 45030

$C_{17}H_{27}NO_2 \bullet HCl$ FW: 313.87 [99300-78-4] ≥98%

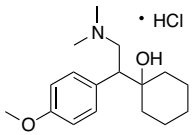

SERT, NET, and MAO inhibitor used to treat depression. It also decreases pain, suppresses oxidative stress, and improves cognitive performance in models of Huntington's disease.

Vidal R, Diaz A, Pazos A, et al. Region-specific regulation of 5-HT1B receptors in the rat brain by chronic venlafaxine treatment. Psychopharmacology (Berl). 2013 Sep;229(1):177-85. PMID: 23609771.

Cegielska-Perun K, Bujalska-Zadrożny M, Tatarkiewicz J, et al. Venlafaxine and neuropathic pain. Pharmacology. 2013;91(1-2):69-76. PMID: 23183148.

V1769 Verapamil Hydrochloride

1 g
5 g

$C_{27}H_{38}N_2O_4 \bullet HCl$ FW: 491.07 [152-11-4] ≥98%

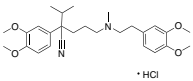

L-type Ca^{2+} channel blocker used to treat hypertension and ventricular arrhythmia. It also decreases rates of secondary infarction in myocardial infarction models.

Flynn JT, Pasko DA. Calcium channel blockers: pharmacology and place in therapy of pediatric hypertension. Pediatr Nephrol. 2000 Dec;15(3-4):302-16. PMID: 11149130.

V1868 Veratramine

1 mg
5 mg
25 mg
100 mg

$C_{27}H_{39}NO_2$ FW: 409.6 [60-70-8] ≥98%

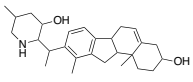

Hedgehog signaling pathway inhibitor found in *Veratrum* and *Fritillaria*. It evokes release of 5-HT, inhibits reuptake of 5-HT, and decreases blood pressure.

Tang J, Li HL, Shen YH, et al. Antitumor and antiplatelet activity of alkaloids from *veratrum* dahuricum. Phytother Res. 2010 Jun;24(6):821-6. PMID: 20013819.

Wang L, Li W, Liu Y. Hypotensive effect and toxicology of total alkaloids and veratramine from roots and rhizomes of *Veratrum* nigrum L. in spontaneously hypertensive rats. Pharmazie. 2008 Aug;63(8):606-10. PMID: 18771011.

V1869

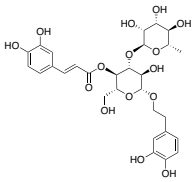

Verbascoside

Acteoside

$C_{29}H_{36}O_{15}$ FW: 624.59 [61276-17-3] ≥98%

5 mg
10 mg
25 mg

Potential inhibitor of PKC, DPP4, and prolyl oligopeptidase found in *Castilleja*, *Verbena*, and *Verbascum*. It inhibits arachidonic acid- and ADP-induced platelet aggregation, suppresses mechanical pain signaling in hyperalgesia models, and decreases inflammation.

Campo G, Marchesini J, Bristot L, et al. The in vitro effects of verbascoside on human platelet aggregation. J Thromb Thrombolysis. 2012 Oct;34(3):318-25. PMID: 22723176.

Filho AG, Morel AF, Adolpho L, et al. Inhibitory effect of verbascoside isolated from Buddleja brasiliensis Jacq. ex Spreng on prolyl oligopeptidase activity. Phytother Res. 2012 Oct;26(10):1472-5. PMID: 22275311.

Paola RD, Oteri G, Mazzon E, et al. Effects of verbascoside, biotechnologically purified by Syringa vulgaris plant cell cultures, in a rodent model of periodontitis. J Pharm Pharmacol. 2011 May;63(5):707-17. PMID: 21492173.

V1870

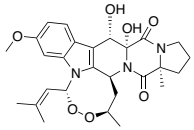

Verruculogen

$C_{27}H_{33}N_3O_7$ FW: 511.57 [12771-72-1] ≥95%

1 mg
5 mg

Mycotoxin, BK K^+ channel blocker, and GABA-A receptor antagonist found in *Aspergillus*. It may induce development of neurological disorders.

Smith RC, McClure MC, Smith MA, et al. The role of voltage-gated potassium channels in the regulation of mouse uterine contractility. Reprod Biol Endocrinol. 2007 Nov 2;5:41. PMID: 17980032.

Kosalec I, Klarić MS, Pepeljnjak S. Verruculogen production in airborne and clinical isolates of Aspergillus fumigatus Fres. Acta Pharm. 2005 Dec;55(4):357-64. PMID: 16375825.

Knaus HG, McManus OB, Lee SH, et al. Tremorgenic indole alkaloids potently inhibit smooth muscle high-conductance calcium-activated potassium channels. Biochemistry. 1994 May 17;33(19):5819-28. PMID: 7514038.

V1872

Arg-Gly-Tyr-Val-Tyr-Gln-Gly-Leu

Vesicular Stomatitis Virus Peptide

$C_{44}H_{66}N_{12}O_{12}$ FW: 955.09 ≥95%

1 mg
2 mg
5 mg

LDL receptor agonist and fragment of VSV. It is used as a vector to express tumor-targeting ligands. It inhibits growth of myeloma cells and neuroendocrine cells.

Ammayappan A, Peng KW, Russell SJ. Characteristics of oncolytic vesicular stomatitis virus displaying tumor-targeting ligands. J Virol. 2013 Dec;87(24):13543-55. PMID: 24089573.

Randle RW, Northrup SA, Sirintrapun SJ, et al. Oncolytic vesicular stomatitis virus as a treatment for neuroendocrine tumors. Surgery. 2013 Dec;154(6):1323-29; discussion 1329-30. PMID: 23973113.

V2792

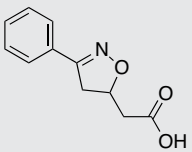

VGX-1027

NEW

GIT27

$C_{11}H_{11}NO_3$ FW: 205.21 [6501-72-0] ≥98%

5 mg
10 mg
50 mg

TLR4 inhibitor. It decreases production of pro-inflammatory cytokines and inhibits antigen presentation in models of systemic lupus erythematosus.

Fagone P, Muthumani K, Mangano K, et al. VGX-1027 modulates genes involved in lipopolysaccharide-induced Toll-like receptor 4 activation and in a murine model of systemic lupus erythematosus. Immunology. 2014 Aug;142(4):594-602. PMID: 24527796.

Cha JJ, Hyun YY, Lee MH, et al. Renal protective effects of toll-like receptor 4 signaling blockade in type 2 diabetic mice. Endocrinology. 2013 Jun;154(6):2144-55. PMID: 23568555.

Stojanovic I, Cuzzocrea S, Mangano K, et al. In vitro, ex vivo and in vivo immunopharmacological activities of the isoxazoline compound VGX-1027: modulation of cytokine synthesis and prevention of both organ-specific and systemic autoimmune diseases in murine models. Clin Immunol. 2007 Jun;123(3):311-23. PMID: 17449326.

V3212

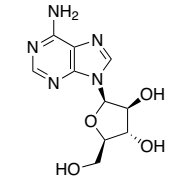

Vidarabine

Arabinosyladenine; Adenine Arabinoside; Ara-A

$C_{10}H_{13}N_5O_4$ FW: 267.24 [5536-17-4] ≥98%

100 mg
500 mg
1 g

Adenosine analog and inhibitor of viral DNA polymerase and ribonucleotide reductase used to treat infections of Epstein-Barr virus, HSV, and HPV. It prevents formation of phosphodiester bridges upon incorporation into DNA.

Whitley RJ. The use of antiviral drugs during the neonatal period. Clin Perinatol. 2012 Mar;39(1):69-81. PMID: 22341538.

Wilhelmus KR. Antiviral treatment and other therapeutic interventions for herpes simplex virus epithelial keratitis. Cochrane Database Syst Rev. 2010 Dec 8;(12):CD002898. PMID: 21154352.

Sagar S, Kaur M, Minneman KP. Antiviral lead compounds from marine sponges. Mar Drugs. 2010 Oct 11;8(10):2619-38. PMID: 21116410.

V3213 Vidarabine Monophosphate

100 mg
500 mg
1 g

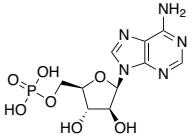

$C_{10}H_{14}N_5O_7P$ FW: 347.22 [29984-33-6] ≥98.0%

Adenosine analog, viral DNA polymerase inhibitor, and potential ribonucleotide reductase inhibitor. It is used to treat severe chronic Epstein-Barr virus, herpes simplex virus, and human papilloma virus infections.

Whitley RJ. The use of antiviral drugs during the neonatal period. Clin Perinatol. 2012 Mar;39(1):69-81. PMID: 22341538.

Wilhelmus KR. Antiviral treatment and other therapeutic interventions for herpes simplex virus epithelial keratitis. Cochrane Database Syst Rev. 2010 Dec 8;(12):CD002898. PMID: 21154352.

V3444 Vilazodone

10 mg
50 mg
100 mg

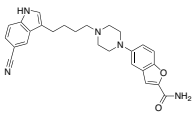

$C_{26}H_{27}N_5O_2$ FW: 441.52 [163521-12-8] ≥98%

5-HT1A receptor partial agonist and SERT inhibitor used to treat depression. It does not alter cardiovascular function.

Edwards J, Sperry V, Adams MH, et al. Vilazodone lacks proarrhythmogenic potential in healthy participants: a thorough ECG study. Int J Clin Pharmacol Ther. 2013 Jun;51(6):456-65. PMID: 23611569.

Hughes ZA, Starr KR, Langmead CJ, et al. Neurochemical evaluation of the novel 5-HT1A receptor partial agonist/serotonin reuptake inhibitor, vilazodone. Eur J Pharmacol. 2005 Mar 7;510(1-2):49-57. PMID: 15740724.

V3345 Vildagliptin

10 mg
25 mg
100 mg

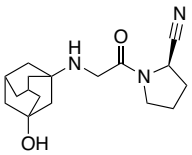

$C_{17}H_{25}N_3O_2$ FW: 303.4 [274901-16-5] ≥97%

DPP4 inhibitor used to treat diabetes. It increases serum insulin and β-cell mass, decreases serum glucagon, improves endoplasmic reticular stress, and attenuates A-β pathology tau phosphorylation in Alzheimer's disease models.

Kosaraju J, Murthy V, Khatwal RB, et al. Vildagliptin: an anti-diabetes agent ameliorates cognitive deficits and pathology observed in streptozotocin-induced Alzheimer's disease. J Pharm Pharmacol. 2013 Dec;65(12):1773-84. PMID: 24117480.

Shimizu S, Hosooka T, Matsuda T, et al. DPP4 inhibitor vildagliptin preserves β-cell mass through amelioration of endoplasmic reticulum stress in C/EBPB transgenic mice. J Mol Endocrinol. 2012 Aug 30;49(2):125-35. PMID: 22822047.

V3253 Vinblastine Sulfate

5 mg
10 mg
25 mg

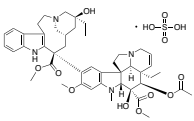

$C_{46}H_{58}N_4O_9S \bullet H_2SO_4$ FW: 909.07 [143-67-9] ≥96%

Microtubule polymerization inhibitor found in *Catharanthus* used to treat various cancers. It binds tubulin and causes formation of curved or misshapen microtubules.

Pliarchopoulou K, Laschos K, Pectasides D. Current chemotherapeutic options for the treatment of advanced bladder cancer: a review. Urol Oncol. 2013 Apr;31(3):294-302. PMID: 20843708.

Rendine S, Pieraccini S, Sironi M. Vinblastine perturbation of tubulin protofilament structure: a computational insight. Phys Chem Chem Phys. 2010 Dec 21;12(47):15530-6. PMID: 20978652.

V5254 Vincristine Sulfate

5 mg
10 mg
25 mg

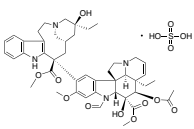

$C_{46}H_{56}N_4O_{10}S \bullet H_2SO_4$ FW: 923.05 [2068-78-2] ≥82%

Microtubule polymerization inhibitor found in *Catharanthus* used to treat lymphomas and leukemias. It also increases the activation of AMPK and indirectly inhibits mTORC1 signaling in melanoma cells.

Wang L, Xia ZJ, Huang HQ, et al. Cyclophosphamide, doxorubicin, vincristine, and prednisone (CHOP) in the treatment of stage IE/IIE extranodal natural killer/T cell lymphoma, nasal type: 13-year follow-up in 135 patients. Int J Hematol. 2012 Nov;96(5):617-23. PMID: 22983648.

Chen MB, Shen WX, Yang Y, et al. Activation of AMP-activated protein kinase is involved in vincristine-induced cell apoptosis in B16 melanoma cell. J Cell Physiol. 2011 Jul;226(7):1915-25. PMID: 21506122.

V3354 Vindesine sulfate

1 mg
5 mg
10 mg
25 mg

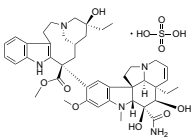

LY-099094

$C_{43}H_{55}N_5O_7 \bullet H_2SO_4$ FW: 852.02 [59917-39-4] ≥98%

Semi-synthetic microtubule polymerization inhibitor found in *Catharanthus* clinically used to treat various cancers.

Duflos A, Kruczynski A, Barret JM. Novel aspects of natural and modified vinca alkaloids. Curr Med Chem Anticancer Agents. 2002 Jan;2(1):55-70. PMID: 12678751.

Zhou XJ, Rahmani R. Preclinical and clinical pharmacology of vinca alkaloids. Drugs. 1992;44 Suppl 4:1-16; discussion 66-9. PMID: 1283846.

V3355 Vindoline

25 mg
100 mg
500 mg

NSC 91994

$C_{25}H_{32}N_2O_6$ FW: 456.53 [2182-14-1] ≥98%

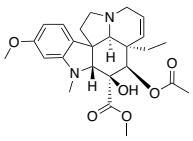

Semi-synthetic $K_v2.1$ K^+ channel blocker and H^+/K^+ ATPase inhibitor found in *Catharanthus* used in the synthesis of vinblastine. It binds tubulin poorly, decreases gastric acid secretion, and increases glucose-stimulated insulin release.

Yao XG, Chen F, Li P, et al. Natural product vindoline stimulates insulin secretion and efficiently ameliorates glucose homeostasis in diabetic murine models. J Ethnopharmacol. 2013 Oct 28;150(1):285-97. PMID: 24012527.

Freitas CS, Baggio CH, Mayer B, et al. Inhibition of gastric H^+, $K(^+)$-ATPase activity by compounds from medicinal plants. Nat Prod Commun. 2011 Sep;6(9):1253-4. PMID: 21941891.

Sertel S, Fu Y, Zu Y, et al. Molecular docking and pharmacogenomics of vinca alkaloids and their monomeric precursors, vindoline and catharanthine. Biochem Pharmacol. 2011 Mar 15;81(6):723-35. PMID: 21219884.

V3454 Vinleurosine Sulfate

10 mg
25 mg
100 mg

$C_{46}H_{56}N_4O_9 \bullet H_2O_4S$ FW: 907.04 [54081-68-4] ≥95%

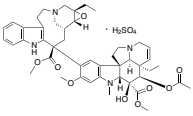

Found in *Catharanthus*. It may inhibit growth of cancer cells.

Chen Q, Zhang W, Zhang Y, et al. Identification and quantification of active alkaloids in *Catharanthus* roseus by liquid chromatography-ion trap mass spectrometry. Food Chem. 2013 Aug 15;139(1-4):845-52. PMID: 23561180.

Fyfe MJ, Loftfield S, Goldman ID. A reduction in energy-dependent amino acid transport by microtubular inhibitors in Ehrlich ascites tumor cells. J Cell Physiol. 1975 Oct;86(2 Pt 1):201-11. PMID: 1194361.

V3251 Vinorelbine Base

1 mg
5 mg
25 mg

KW 2307; Nor-5'-anhydrovinblastine; NVB

$C_{45}H_{54}N_4O_8$ FW: 778.93 [71486-22-1] ≥90%

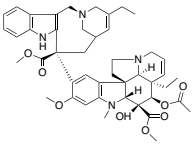

Semi-synthetic microtubule polymerization inhibitor found in *Catharanthus* used to treat non-small cell lung cancer. It also downregulates expression of cyclin D1 and upregulates expression of p53 in osteosarcoma cells.

Capasso A. Vinorelbine in cancer therapy. Curr Drug Targets. 2012 Jul;13(8):1065-71. PMID: 22594474.

Roncuzzi L, Marti G, Baiocchi D, et al. Effect of Vinorelbine on cell growth and apoptosis induction in human osteosarcoma in vitro. Oncol Rep. 2006 Jan;15(1):73-7. PMID: 16328036.

V3252 Vinorelbine Ditartrate

1 mg
5 mg
25 mg

$C_{45}H_{54}N_4O_8 \bullet 2C_4H_6O_6$ FW: 1079.1 [125317-39-7] ≥98%

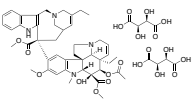

Microtubule polymerization inhibitor found in *Catharanthus* used to treat breast cancer and non-small cell lung cancer. It also upregulates p53 expression and inhibits growth of osteosarcoma cells.

Capasso A. Vinorelbine in cancer therapy. Curr Drug Targets. 2012 Jul;13(8):1065-71. PMID: 22594474.

V3325 Virginiamycin M1

NEW

1 mg
5 mg

Mikamycin A; Staphilomycin; Ostreogrycin A; Pristinamycin IIA

$C_{28}H_{35}N_3O_7$ FW: 525.59 [21411-53-0] ≥97%

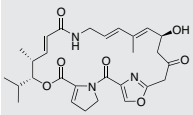

Peptidyl transferase and protein translation inhibitor used as a growth promoter in livestock feed and to prevent microbial contamination in ethanol fuels. It inhibits survival of *Leptinotarsa* and *Tetranychus*.

Compart DM, Carlson AM, Crawford GI, et al. Presence and biological activity of antibiotics used in fuel ethanol and corn co-product production. J Anim Sci. 2013 May;91(5):2395-404. PMID: 23463564.

Qiu Y, Yang F, Liu Z, et al. Determination of virginiamycin M1 and S1 residues in livestock and poultry products by liquid chromatography-tandem mass spectrometry. Se Pu. 2012 May;30(5):463-7. PMID: 22934408.

Champney WS, Tober CL. Specific inhibition of 50S ribosomal subunit formation in *Staphylococcus aureus* cells by 16-membered macrolide, lincosamide, and streptogramin B antibiotics. Curr Microbiol. 2000 Aug;41(2):126-35. PMID: 10856379.

V3326 Virginiamycin S1

NEW

1 mg
5 mg

Staphylomycin S

$C_{43}H_{49}N_7O_{10}$ FW: 823.89 [23152-29-6] ≥99%

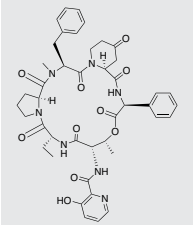

Peptidyl transferase and protein translation inhibitor used as a growth promoter in livestock feed and to prevent microbial contamination in ethanol fuels. It inhibits survival of *Leptinotarsa* and *Tetranychus*.

Compart DM, Carlson AM, Crawford GI, et al. Presence and biological activity of antibiotics used in fuel ethanol and corn co-product production. J Anim Sci. 2013 May;91(5):2395-404. PMID: 23463564.

Qiu Y, Yang F, Liu Z, et al. Determination of virginiamycin M1 and S1 residues in livestock and poultry products by liquid chromatography-tandem mass spectrometry. Se Pu. 2012 May;30(5):463-7. PMID: 22934408.

V3378 Vitamin B12

500 mg
1 g
5 g

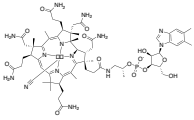

$C_{63}H_{88}CoN_{14}O_{14}P$ FW: 1355.37 [68-19-9] ≥97%

Coenzyme and vitamin found in dairy, meat, eggs, and fermented food. It is involved in cellular metabolism, energy production, and fatty acid synthesis. It is also used to treat cyanide poisoning.

Kumar N. Neurologic. Aspects of cobalamin (B12) deficiency. Handb Clin Neurol. 2014;120:915-26. PMID: 24365360.

Briani C, Dalla Torre C, Citton V, et al. Cobalamin deficiency: clinical picture and radiological findings. Nutrients. 2013 Nov 15;5(11):4521-39. PMID: 24248213.

Scott JM, Molloy AM. The discovery of vitamin B(12). Ann Nutr Metab. 2012;61(3):239-45. PMID: 23183296.

V3476 Vitamin D2

1 g
5 g

Calciferol; Ergocalciferol

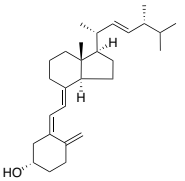

$C_{28}H_{44}O$ FW: 396.65 [50-14-6] ≥91%

Vitamin D prodrug produced by fungi and alfalfa. It is commercially used as a vitamin D supplement to improve bone strength. It also induces apoptosis in leukemia cells and decreases tumor growth in breast cancer models.

Bikle DD. Vitamin D metabolism, mechanism of action, and clinical applications. Chem Biol. 2014 Mar 20;21(3):319-29. PMID: 24529992.

Chen WJ, Huang YT, Wu ML, et al. Induction of apoptosis by vitamin D2, ergocalciferol, via reactive oxygen species generation, glutathione depletion, and caspase activation in human leukemia Cells. J Agric Food Chem. 2008 May 14;56(9):2996-3005. PMID: 18386902.

Zinser GM, Tribble E, Valrance M, et al. 1,24(S)-dihydroxyvitamin D2, an endogenous vitamin D2 metabolite, inhibits growth of breast cancer cells and tumors. Anticancer Res. 2005 Jan-Feb;25(1A):235-41. PMID: 15816543.

V3277 Vitamin E

5 g
25 g
100 g
250 g

D,L-α-Tocopherol

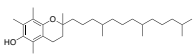

$C_{29}H_{50}O_2$ FW: 430.7 [10191-41-0] ≥98%

Synthetic vitamin E and antioxidant found in dietary supplements. It decreases LDL oxidation, inhibits platelet aggregation, and suppresses the development of atherosclerotic lesions.

Reid VC, Mitchinson MJ. Toxicity of oxidised low density lipoprotein towards mouse peritoneal macrophages in vitro. Atherosclerosis. 1993 Jan 4;98(1):17-24. PMID: 8457247.

Williams RJ, Motteram JM, Sharp CH, et al. Dietary vitamin E and the attenuation of early lesion development in modified Watanabe rabbits. Atherosclerosis. 1992 Jun;94(2-3):153-9. PMID: 1632869.

V3278 Vitamin E Acetate

NEW

25 g
100 g

D,L-α-tocopherol acetate

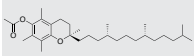

$C_{31}H_{52}O_3$ FW: 472.74 [58-95-7] ≥98%

Vitamin E and antioxidant. It displays many biological activities, including improving motor nerve conduction velocity, limiting progression of thermal hyperalgesia, preventing skin carcinogenesis, and inhibiting vanadium-induced adrenocortical hypertrophy.

Morani AS, Bodhankar SL. Early co-administration of vitamin E acetate and methylcobalamin improves thermal hyperalgesia and motor nerve conduction velocity following sciatic nerve crush injury in rats. Pharmacol Rep. 2010 Mar-Apr;62(2):405-9. PMID: 20508297.

Chandra AK, Ghosh R, Chatterjee A, et al. Amelioration of vanadium-induced testicular toxicity and adrenocortical hyperactivity by vitamin E acetate in rats. Mol Cell Biochem. 2007 Dec;306(1-2):189-200. PMID: 17668152.

V3276 Vitamin E, Natural

100 g
250 g

D-α-tocopherol

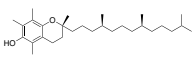

$C_{29}H_{50}O_2$ [59-02-9] ≥97%

Antioxidant. It decreases UVA-induced upregulation of IL-8 and AP-1 binding, suppresses lipid oxidation, protects against retinal edema in models of ischemia/reperfusion, and lowers serum triglycerides and levels of VLDL, PPARγ and malondialdehyde.

Kim do Y, Kim J, Ham HJ, et al. Effects of d-α-tocopherol supplements on lipid metabolism in a high-fat diet-fed animal model. Nutr Res Pract. 2013 Dec;7(6):481-7. PMID: 24353834.

Abdala-Valencia H, Berdnikovs S, Cook-Mills JM. Vitamin E isoforms differentially regulate intercellular adhesion molecule-1 activation of PKCα in human microvascular endothelial cells. PLoS One. 2012;7(7):e41054. PMID: 22815910.

V3479

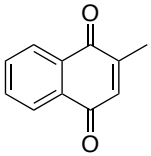

Vitamin K3

Menadione; Menaphthone

$C_{11}H_8O_2$ FW: 172.18 [58-27-5] ≥98%

10 g
25 g

Synthetic analog of 1,4-naphthoquinone and precursor in synthesis of vitamin K2. It inhibits MAO-A/B and prevents microtubule polymerization. It induces apoptosis in ovarian carcinoma cells and suppresses leukotriene secretion by altering Ca^{2+} influx and 5-lipoxygenase signaling.

Kim YJ, Shin YK, Sohn DS, et al. Menadione induces the formation of reactive oxygen species and depletion of GSH-mediated apoptosis and inhibits the FAK-mediated cell invasion. Naunyn Schmiedebergs Arch Pharmacol. 2014 Sep;387(9):799-809. PMID: 24879465.

V5725

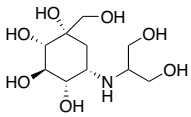

Voglibose

$C_{10}H_{21}NO_7$ FW: 267.28 [83480-29-9] ≥98%

10 mg
25 mg
100 mg

α-Glucosidase inhibitor, potential GLP-1 agonist, and potential ATP-sensitive K^+ channel activator used to treat diabetes. It indirectly decreases activity of DPP4, suppresses oxidative stress, and prevents hyperlipidemia and hyperglycemia.

Bin BH, Seo J, Yang SH, et al. Novel inhibitory effect of the antidiabetic drug voglibose on melanogenesis. Exp Dermatol. 2013 Aug;22(8):541-6. PMID: 23879813.

V5734

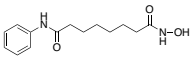

Vorinostat

Suberoylanilide hydroxamic acid; SAHA

$C_{14}H_{20}N_2O_3$ FW: 264.32 [149647-78-9] ≥98%

100 mg
250 mg
1 g

Inhibitor of HDACs and RNA splicing. It induces cell cycle arrest and apoptosis in various cancer cells, attenuates impairment of fear extinction, and disrupts HIV latency in HIV-infected subjects.

Legartová S, Stixová L, Strnad H, et al. Basic nuclear processes affected by histone acetyltransferases and histone deacetylase inhibitors. Epigenomics. 2013 Aug;5(4):379-96. PMID: 23895652.

Matsumoto Y, Morinobu S, Yamamoto S, et al. Vorinostat ameliorates impaired fear extinction possibly via the hippocampal NMDA-CaMKII pathway in an animal model of posttraumatic stress disorder. Psychopharmacology (Berl). 2013 Sep;229(1):51-62. PMID: 23584669.

Silva G, Cardoso BA, Belo H, et al. Vorinostat induces apoptosis and differentiation in myeloid malignancies: genetic and molecular mechanisms. PLoS One. 2013;8(1):e53766. PMID: 23320102.

V5870

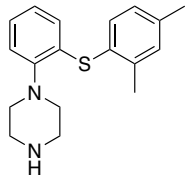

Vortioxetine

$C_{18}H_{22}N_2S$ FW: 298.45 [508233-74-7] ≥98%

5 mg
10 mg
25 mg
100 mg

5-HT1A receptor agonist, 5-HT1B receptor partial agonist, inhibitor of 5-HT3A/7 receptors and SERT, and potential β1-adrenergic receptor agonist. It is used to treat depression. It also improves memory performance and reduces 5-HT-depletion-induced memory deficits.

du Jardin KG, Jensen JB, Sanchez C, et al. Vortioxetine dose-dependently reverses 5-HT depletion-induced deficits in spatial working and object recognition memory: A potential role for 5-HT1A receptor agonism and 5-HT3 receptor antagonism. Eur Neuropsychopharmacol. 2013 Aug 2. [Epub ahead of print]. PMID: 23916504.

Henigsberg N, Mahableshwarkar AR, Jacobsen P, et al. A randomized, double-blind, placebo-controlled 8-week trial of the efficacy and tolerability of multiple doses of Lu AA21004 in adults with major depressive disorder. J Clin Psychiatry. 2012 Jul;73(7):953-9. PMID: 22901346.

V7200

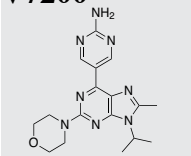

VS-5584

NEW

$C_{17}H_{22}N_8O$ FW: 354.41 [1246560-33-7] ≥98%

5 mg
10 mg
25 mg

PI3K inhibitor. It inhibits proliferation in various cancer cell lines and suppresses growth of gastric cancer tumors.

Hart S, Novotny-Diermayr V, Goh KC, et al. VS-5584, a novel and highly selective PI3K/mTOR kinase inhibitor for the treatment of cancer. Mol Cancer Ther. 2013 Feb;12(2):151-61. PMID: 23270925.

V9201

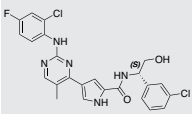

VX-11e

NEW

ERK 11e

$C_{24}H_{20}Cl_2FN_5O_2$ FW: 500.35 [896720-20-0] ≥98%

1 mg
5 mg
10 mg

ERK2 inhibitor, and potential inhibitor of aurora kinase A, GSK3, CDK2, FLT3, ROCK1, and JNK3. It inhibits proliferation of cancer cells.

Aronov AM, Tang Q, Martinez-Botella G, et al. Structure-guided design of potent and selective pyrimidylpyrrole inhibitors of extracellular signal-regulated kinase (ERK) using conformational control. J Med Chem. 2009 Oct 22;52(20):6362-8. PMID: 19827834.

V9202

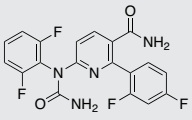

VX-702

NEW

5 mg
25 mg
100 mg

$C_{19}H_{12}F_4N_4O_2$ FW: 404.32 [479543-46-9] ≥98%

p38 MAPK inhibitor. It suppresses pro-inflammatory cytokine release and decreases platelet lesioning in storage without affecting platelet function.

Skripchenko A, Awatefe H, Thompson-Montgomery D, et al. An inhibition of p38 mitogen activated protein kinase delays the platelet storage lesion. PLoS One. 2013 Aug 13;8(8):e70732. PMID: 23967093.

Ding C. Drug evaluation: VX-702, a MAP kinase inhibitor for rheumatoid arthritis and acute coronary syndrome. Curr Opin Investig Drugs. 2006 Nov;7(11):1020-5. PMID: 17117592.

V9228

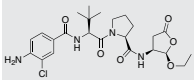

VX-765

NEW

5 mg
10 mg

$C_{24}H_{33}ClN_4O_6$ FW: 509 [273404-37-8] ≥98%

NLRP3 inflammasome inhibitor that prevents caspase 1 and IL-1β cleavage and release. It attenuates stress-induced depression-like behavior, suppresses chronic epileptic activity, and decreases IL-1β levels.

Zhang Y, Liu L, Liu YZ, et al. NLRP3 Inflammasome Mediates Chronic Mild Stress-induced Depression in Mice via Neuroinflammation. Int J Neuropsychopharmacol. 2015 Jan 20. [Epub ahead of print]. PMID: 25603858.

Kaminski RM, Rogawski MA, Klitgaard H. The potential of antiseizure drugs and agents that act on novel molecular targets as antiepileptogenic treatments. Neurotherapeutics. 2014 Apr;11(2):385-400. PMID: 24671870.

Noe FM, Polascheck N, Frigerio F, et al. Pharmacological blockade of IL-1β/IL-1 receptor type 1 axis during epileptogenesis provides neuroprotection in two rat models of temporal lobe epilepsy. Neurobiol Dis. 2013 Nov;59:183-93. PMID: 23938763.

V9200

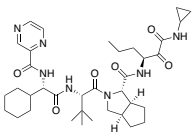

VX-950

Telaprevir

5 mg
25 mg
100 mg

$C_{36}H_{53}N_7O_6$ FW: 679.85 [402957-28-2] ≥98%

NS3/4A serine protease inhibitor used to treat hepatitis C. It decreases viral load and exhibits higher rates of sustained virologic response than traditional therapies.

Matthews SJ, Lancaster JW. Telaprevir: a hepatitis C NS3/4A protease inhibitor. Clin Ther. 2012 Sep;34(9):1857-82. PMID: 22951253.

McHutchison JG, Manns MP, Muir AJ, et al. Telaprevir for previously treated chronic HCV infection. N Engl J Med. 2012;362(14):1292–303. doi:10.1056/NEJMoa0908014. PMID 20375406

W0247

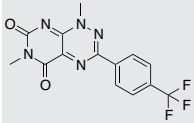

Walrycin B

NEW

1 mg
5 mg
25 mg

$C_{14}H_{10}F_3N_5O_2$ FW: 337.26 [878419-78-4] ≥98%

Walrycin response regulator inhibitor. It alters cell wall metabolism and cell division in *Bacillus* and *Staphylococcus*.

Gotoh Y, Doi A, Furuta E, et al. Novel antibacterial compounds specifically targeting the essential WalR response regulator. J Antibiot (Tokyo). 2010 Mar;63(3):127-34. PMID: 20111065.

W0269

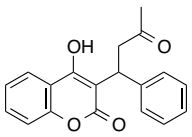

(±)-Warfarin

1 g
10 g
25 g

$C_{19}H_{16}O_4$ FW: 308.33 [81-81-2] ≥98%

VKORC1 inhibitor used to prevent blood clot formation and migration. It inhibits the formation of coagulation factors II, VII, IX, and X. The S enantiomer of warfarin is somewhat more potent than the R enantiomer.

Hall AM, Wilkins MR. Warfarin: a case history in pharmacogenetics. Heart. 2005 May;91(5):563-4. PMID: 15831631.

Tabrizi AR, Zehnbauer BA, Borecki IB, et al. The frequency and effects of cytochrome P450 (CYP) 2C9 polymorphisms in patients receiving warfarin. J Am Coll Surg. 2002 Mar;194(3):267-73. PMID: 11893129.

W0273

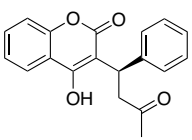

R-(+)-Warfarin

1 mg
5 mg
25 mg

$C_{19}H_{16}O_4$ FW: 308.33 [5543-58-8] ≥99%ee

VKORC1 inhibitor used to prevent blood clot formation and migration. It inhibits the formation of coagulation factors II, VII, IX, and X. The S enantiomer of warfarin is somewhat more potent than the R enantiomer.

Hall AM, Wilkins MR. Warfarin: a case history in pharmacogenetics. Heart. 2005 May;91(5):563-4. PMID: 15831631.

Tabrizi AR, Zehnbauer BA, Borecki IB, et al. The frequency and effects of cytochrome P450 (CYP) 2C9 polymorphisms in patients receiving warfarin. J Am Coll Surg. 2002 Mar;194(3):267-73. PMID: 11893129.

W0272

S-(−)-Warfarin

1 mg
5 mg
25 mg

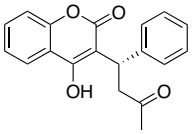

$C_{19}H_{16}O_4$ FW: 308.33 [5543-57-7] ≥99%ee

VKORC1 inhibitor used to prevent blood clot formation and migration. It inhibits the formation of coagulation factors II, VII, IX, and X. The S enantiomer of warfarin is somewhat more potent than the R enantiomer.

Hall AM, Wilkins MR. Warfarin: a case history in pharmacogenetics. Heart. 2005 May;91(5):563-4. PMID: 15831631.

Tabrizi AR, Zehnbauer BA, Borecki IB, et al. The frequency and effects of cytochrome P450 (CYP) 2C9 polymorphisms in patients receiving warfarin. J Am Coll Surg. 2002 Mar;194(3):267-73. PMID: 11893129.

W0270

(±)-Warfarin Sodium Clathrate

1 g
10 g
25 g

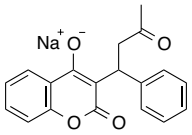

$C_{19}H_{15}NaO_4$ FW: 330.31 [129-06-6] ≥98%

VKORC1 inhibitor used to prevent blood clot formation and migration. It inhibits the formation of coagulation factors II, VII, IX, and X. The S enantiomer of warfarin is somewhat more potent than the R enantiomer.

Hall AM, Wilkins MR. Warfarin: a case history in pharmacogenetics. Heart. 2005 May;91(5):563-4. PMID: 15831631.

Tabrizi AR, Zehnbauer BA, Borecki IB, et al. The frequency and effects of cytochrome P450 (CYP) 2C9 polymorphisms in patients receiving warfarin. J Am Coll Surg. 2002 Mar;194(3):267-73. PMID: 11893129.

W0275

R-(+)-Warfarin Sodium

1 mg
5 mg
25 mg

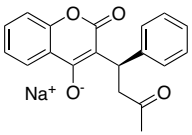

$C_{19}H_{15}NaO_4$ FW: 330.31 ≥99%ee

VKORC1 inhibitor used to prevent blood clot formation and migration. It inhibits the formation of coagulation factors II, VII, IX, and X. The S enantiomer of warfarin is somewhat more potent than the R enantiomer.

Hall AM, Wilkins MR. Warfarin: a case history in pharmacogenetics. Heart. 2005 May;91(5):563-4. PMID: 15831631.

W0274

S-(−)-Warfarin Sodium

1 mg
5 mg
25 mg

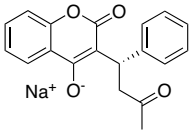

$C_{19}H_{15}NaO_4$ FW: 330.31 ≥99%ee

VKORC1 inhibitor used to prevent blood clot formation and migration. It inhibits the formation of coagulation factors II, VII, IX, and X. The S enantiomer of warfarin is somewhat more potent than the R enantiomer.

Hall AM, Wilkins MR. Warfarin: a case history in pharmacogenetics. Heart. 2005 May;91(5):563-4. PMID: 15831631.

W2800

WH-4-023

NEW

5 mg
25 mg

KIN112

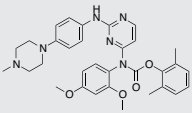

$C_{32}H_{36}N_6O_4$ FW: 568.68 [837422-57-8] ≥98%

Inhibitor of Src, Lck, and SIK. It inhibits T cell activation and increases IL-10 production.

Clark K, MacKenzie KF, Petkevicius K, et al. Phosphorylation of CRTC3 by the salt-inducible kinases controls the interconversion of classically activated and regulatory macrophages. Proc Natl Acad Sci U S A. 2012 Oct 16;109(42):16986-91. PMID: 23033494.

Martin MW, Newcomb J, Nunes JJ, et al. Novel 2-aminopyrimidine carbamates as potent and orally active inhibitors of Lck: synthesis, SAR, and in vivo antiinflammatory activity. J Med Chem. 2006 Aug 10;49(16):4981-91. PMID: 16884310.

W2933

WHI-P131

50 mg
250 mg

JANEX-1

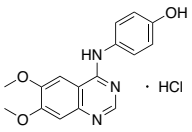

$C_{16}H_{15}N_3O_3 \cdot HCl$ FW: 333.77 [202475-60-3] ≥98%

JAK3 and EGFR inhibitor. It inhibits UVB-induced carcinogenesis, decreases myocardial apoptosis, and prevents destruction of pancreatic islet cells.

Oh YB, Ahn M, Lee SM, et al. Inhibition of Janus activated kinase-3 protects against myocardial ischemia and reperfusion injury in mice. Exp Mol Med. 2013 May 17;45:e23. PMID: 23680658.

Lee JE, Lee AS, Kim DH, et al. Janex-1, a JAK3 inhibitor, ameliorates tumor necrosis factor-α-induced expression of cell adhesion molecules and improves myocardial vascular permeability in endotoxemic mice. Int J Mol Med. 2012 May;29(5):864-70. PMID: 22344597

Uckun FM, Dibirdik I, Qazi S. Prevention of UVB-induced skin inflammation, genotoxicity, and photocarcinogenesis in mice by WHI-P131, a dual-function inhibitor of Janus kinase 3 and EGF receptor kinase. Arzneimittelforschung. 2010;60(4):218-25. PMID: 20486473

W3576

Withaferin A

1 mg
5 mg
25 mg

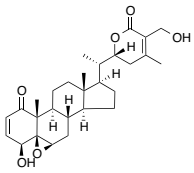

$C_{28}H_{38}O_6$ FW: 470.6 [5119-48-2] ≥98%

Vimentin and HSP90 inhibitor found in *Withania somnifera*. It induces apoptosis and downregulates expression of ERα in breast cancer cells, decreases levels of NO and iNOS, and inhibits tumor growth of pancreatic xenografts.

Antony ML, Lee J, Hahm ER, et al. Growth Arrest by the Antitumor Steroidal Lactone Withaferin A in Human Breast Cancer Cells Is Associated with Downregulation and Covalent Binding at Cysteine-303 of β-Tubulin. J Biol Chem. 2013 Dec 2. [Epub ahead of print]. PMID: 24297176.

Hahm ER, Lee J, Singh SV. Role of mitogen-activated protein kinases and Mcl-1 in apoptosis induction by withaferin A in human breast cancer cells. Mol Carcinog. 2013 Sep 9. [Epub ahead of print]. PMID: 24019090.

Lee J, Sehrawat A, Singh SV. Withaferin A causes activation of Notch2 and Notch4 in human breast cancer cells. Breast Cancer Res Treat. 2012 Nov;136(1):45-56. PMID: 22965833.

W4096

WKYMVM-NH2

0.5 mg
1 mg
2.5 mg

WKYMVm; W peptide

H-Trp-Lys-Tyr-Met-Val-Met-NH_2

$C_{41}H_{61}N_9O_7S_2$ FW: 856.13 ≥95%

Synthetic FPRL1 receptor agonist. It increases bactericidal activity of neutrophils and phagocytic activity of dendritic cells and inhibits production of pro-inflammatory cytokines.

Kim SD, Kwon S, Lee SK, et al. The immune-stimulating peptide WKYMVm has therapeutic effects against ulcerative colitis. Exp Mol Med. 2013 Sep 13;45:e40. PMID: 24030327.

Kim SD, Kim YK, Lee HY, et al. The agonists of formyl peptide receptors prevent development of severe sepsis after microbial infection. J Immunol. 2010 Oct 1;185(7):4302-10. PMID: 20817875.

W5726

Wogonin

5 mg
10 mg
25 mg

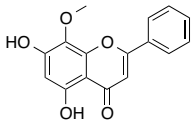

$C_{16}H_{12}O_5$ FW: 284.26 [632-85-9] ≥98%

CDK9 inhibitor found in *Scutellaria*. It displays a variety of biological activities, including inducing apoptosis in lung adenocarcnoma cells, downregulating expression of HIF-1α, and preventing cell migration and tube formation.

Chen XM, Bai Y, Zhong YJ, et al. Wogonin has multiple anti-cancer effects by regulating c-Myc/SKP2/Fbw7α and HDAC1/HDAC2 pathways and inducing apoptosis in human lung adenocarcinoma cell line A549. PLoS One. 2013 Nov 12;8(11):e79201. PMID: 24265759.

Wang H, Zhao L, Zhu LT, et al. Wogonin reverses hypoxia resistance of human colon cancer HCT116 cells via downregulation of HIF-1α and glycolysis, by inhibiting PI3K/Akt signaling pathway. Mol Carcinog. 2013 Jun 13. [Epub ahead of print]. PMID: 23761018.

Polier G, Ding J, Konkimalla BV, et al. Wogonin and related natural flavones are inhibitors of CDK9 that induce apoptosis in cancer cells by transcriptional suppression of Mcl-1. Cell Death Dis. 2011 Jul 21;2:e182. PMID: 21776020

W5727

Wogonoside

5 mg
10 mg
25 mg

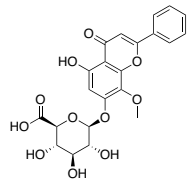

$C_{22}H_{20}O_{11}$ FW: 460.39 [51059-44-0] ≥98%

Found in *Scutellaria*. It inhibits release of pro-inflammatory cytokines, induces cell cycle arrest and autophagy in cancer cells, and suppresses vessel growth and cell migration.

Yang YZ, Tang YZ, Liu YH. Wogonoside displays anti-inflammatory effects through modulating inflammatory mediator expression using RAW264.7 cells. J Ethnopharmacol. 2013 Jun 21;148(1):271-6. PMID: 23612420.

Chen Y, Hui H, Yang H, et al. Wogonoside induces cell cycle arrest and differentiation by affecting expression and subcellular localization of PLSCR1 in AML cells. Blood. 2013 May 2;121(18):3682-91. PMID: 23487022.

Sun Y, Zou M, Hu C, et al. Wogonoside induces autophagy in MDA-MB-231 cells by regulating MAPK-mTOR pathway. Food Chem Toxicol. 2013 Jan;51:53-60. PMID: 23000445.

W5769

Wortmannin

1 mg
5 mg

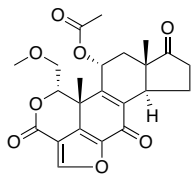

$C_{23}H_{24}O_8$ FW: 428.43 [19545-26-7] ≥97%

Inhibitor of PI3K, mTOR, DNA-PK, PI4K, MLCK, MAPK, and PLK. It inhibits activation of Akt and AMPK, suppressing glucose uptake and insulin-induced skeletal myoblast differentiation.

Zhou X, Zhao Y, Xu L, et al. Wortmannin and U0126 inhibit the promoting effect of insulin on differentiation of skeletal myoblasts in rats. Xi Bao Yu Fen Zi Mian Yi Xue Za Zhi. 2014 Jul;30(7):717-20. PMID: 25001936.

Ji L, Zhang X, Liu W, et al. AMPK-regulated and Akt-dependent enhancement of glucose uptake is essential in ischemic preconditioning-alleviated reperfusion injury. PLoS One. 2013 Jul 26;8(7):e69910. PMID: 23922853.

W7200

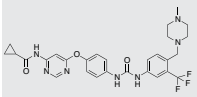

WS3

NEW

5 mg
25 mg

$C_{28}H_{30}F_3N_7O_3$ FW: 569.59 [1421227-52-2] ≥98%

Activator of islet β cell proliferation. It promotes retinal pigment epithelial cell proliferation.

Swoboda JG, Elliott J, Deshmukh V, et al. Small molecule mediated proliferation of primary retinal pigment epithelial cells. ACS Chem Biol. 2013 Jul 19;8(7):1407-11. PMID: 23621521.

Shen W, Tremblay MS, Deshmukh VA, et al. Small-molecule inducer of β cell proliferation identified by high-throughput screening. J Am Chem Soc. 2013 Feb 6;135(5):1669-72. Erratum in: J Am Chem Soc. 2013 Mar 20;135(11):4573. PMID: 23330637.

W7201

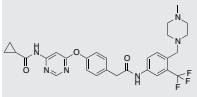

WS6

NEW

5 mg
25 mg

$C_{29}H_{31}F_3N_6O_3$ FW: 568.6 [1421227-53-3] ≥98%

Activator of α and β cell proliferation. It normalizes blood glucose levels.

Boerner BP, George NM, Mir SU, et al. WS6 induces both alpha and beta cell proliferation without affecting differentiation or viability. Endocr J. 2015;62(4):379-86. PMID: 25739404.

Shen W, Tremblay MS, Deshmukh VA, et al. Small-molecule inducer of β cell proliferation identified by high-throughput screening. J Am Chem Soc. 2013 Feb 6;135(5):1669-72. Erratum in: J Am Chem Soc. 2013 Mar 20;135(11):4573. PMID: 23330637.

W9600

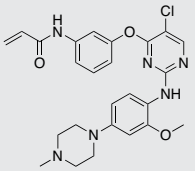

WZ-4002

NEW

5 mg
25 mg
100 mg

$C_{25}H_{27}ClN_6O_3$ FW: 494.97 [1213269-23-8] ≥98%

Inhibitor of WT and T790M EGFR. It inhibits cell proliferation and tumor growth in lung adenocarcinoma models.

Nakagawa T, Takeuchi S, Yamada T, et al. Combined therapy with mutant-selective EGFR inhibitor and Met kinase inhibitor for overcoming erlotinib resistance in EGFR-mutant lung cancer. Mol Cancer Ther. 2012 Oct;11(10):2149-57. PMID: 22844075.

Sakuma Y, Yamazaki Y, Nakamura Y, et al. WZ4002, a third-generation EGFR inhibitor, can overcome anoikis resistance in EGFR-mutant lung adenocarcinomas more efficiently than Src inhibitors. Lab Invest. 2012 Mar;92(3):371-83. PMID: 22157722.

X0254

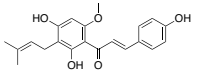

Xanthohumol

5 mg
10 mg
25 mg

$C_{21}H_{22}O_5$ FW: 354.4 [6754-58-1] ≥98%

Found in *Humulus lupulus*. It improves neurobehavioral deficits in cerebral ischemia models, decreases free radical formation, inhibits differentiation of preadipocytes, limits Notch signaling, and suppresses osteoclastogenesis.

Kunnimalaiyaan S, Sokolowski KM, Balamurugan M, et al. Xanthohumol inhibits notch signaling and induces apoptosis in hepatocellular carcinoma. PLoS One. 2015 May 26;10(5):e0127464. PMID: 26011160.

Suh KS, Rhee SY, Kim YS, et al. Xanthohumol modulates the expression of osteoclast-specific genes during osteoclastogenesis in RAW264.7 cells. Food Chem Toxicol. 2013 Aug 27. [Epub ahead of print] PMID: 23994090.

X1752

H-Met-Leu-Thr-Lys-Phe-Glu-Thr-Lys-Ser-Ala-Arg-Val-Lys-Gly-Leu-Ser-Phe-His-Pro-Lys-Arg-Pro-Trp-Ile-Leu-OH

Xenin

0.5 mg
1 mg
2.5 mg

$C_{139}H_{224}N_{38}O_{32}S$ FW: 2971.63 ≥95%

Endogenous neurotensin analog. It suppresses feeding behavior, induces relaxation in ileal smooth muscle cells, and delays gastric emptying.

Kim ER, Xu Y, Mizuno TM. Impaired suppression of feeding by the gut hormone xenin in type I interleukin-1 receptor-deficient mice. Behav Brain Res. 2013 Dec 12;261C:60-64. PMID: 24333379.

X1753

pGlu-Gly-Lys-Arg-Pro-Trp-Ile-Leu-OH

Xenopsin

1 mg
2 mg
5 mg

$C_{47}H_{73}N_{13}O_{10}$ FW: 980.19 ≥95%

Neurotensin analog found in amphibians. It decreases vascular leakage in edema models, increases firing rates of dopaminergic neurons, and stimulates insulin release in pancreatic β-cells.

Zahid OK, Mechkarska M, Ojo OO, et al. Caerulein-and xenopsin-related peptides with insulin-releasing activities from skin secretions of the clawed frogs, Xenopus borealis and Xenopus amieti (Pipidae). Gen Comp Endocrinol. 2011 Jun 1;172(2):314-20. PMID: 21458457.

X4400

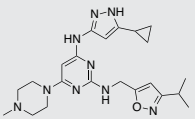

XL-228

NEW

1 mg
5 mg
10 mg

$C_{22}H_{31}N_9O$ FW: 437.54 [898280-07-4] ≥98%

Inhibitor of WT and T315I Abl. It inhibits proliferation of chronic myelogenous leukemia cells.

Noronha G, Cao J, Chow CP, et al. Inhibitors of ABL and the ABL-T315I mutation. Curr Top Med Chem. 2008;8(10):905-21. PMID: 18673174.

X4424 XL-765

NEW

5 mg
10 mg

Voxtalisib; SAR245409

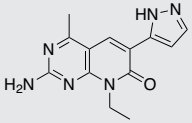

$C_{13}H_{14}N_6O$ FW: 270.29 [934493-76-2] ≥98%

PI3K and mTOR inhibitor. It inhibits cell proliferation, tumor growth, and angiogenesis in cancer models.

Papadopoulos KP, Egile C, Ruiz-Soto R, et al. Efficacy, safety, pharmacokinetics and pharmacodynamics of SAR245409 (voxtalisib, XL765), an orally administered phosphoinositide 3-kinase/mammalian target of rapamycin inhibitor: a phase 1 expansion cohort in patients with relapsed or refractory lymphoma. Leuk Lymphoma. 2014 Nov 19:1-8. [Epub ahead of print] PMID: 25300944.

Yu P, Laird AD, Du X, et al. Characterization of the activity of the PI3K/mTOR inhibitor XL765 (SAR245409) in tumor models with diverse genetic alterations affecting the PI3K pathway. Mol Cancer Ther. 2014 May;13(5):1078-91. PMID: 24634413.

Papadopoulos KP, Tabernero J, Markman B, et al. Phase I safety, pharmacokinetic, and pharmacodynamic study of SAR245409 (XL765), a novel, orally administered PI3K/mTOR inhibitor in patients with advanced solid tumors. Clin Cancer Res. 2014 May 1;20(9):2445-56. PMID: 24583798.

X1854 p-Xyleneselenocyanate

100 mg
250 mg
500 mg

p-XSC

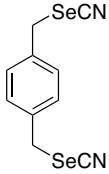

$C_{10}H_8N_2Se_2$ FW: 314.1 [85539-83-9] ≥99%

Synthetic derivative of selenocyanate that may inhibit cancer cell growth, oxidative damage, and *Leishmania* growth.

Das JK, Sarkar S, Hossain SU, et al. Diphenylmethyl selenocyanate attenuates malachite green induced oxidative injury through antioxidation & inhibition of DNA damage in mice. Indian J Med Res. 2013 Jun;137(6):1163-73. PMID: 23852297.

Facompre ND, Sinha I, El-Bayoumy K, et al. Remarkable inhibition of mTOR signaling by the combination of rapamycin and 1,4-phenylenebis(methylene)selenocyanate in human prostate cancer cells. Int J Cancer. 2012 Nov 1;131(9):2134-42. PMID: 22307455.

Y1000 Y27632 Dihydrochloride

1 mg
5 mg
25 mg

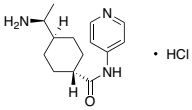

$C_{14}H_{21}N_3O \cdot 2HCl$ FW: 320.26 [129830-38-2] ≥99%

ROCK inhibitor that prevents binding of Ras-related GTPase Rho A, altering actin cytoskeleton reorganization, cell adhesion, and cell migration. It inhibits conditioned place aversion and improves symptoms of Parkinson's disease.

Rodriguez-Perez AI, Dominguez-Meijide A, Lanciego JL, et al. Inhibition of Rho kinase mediates the neuroprotective effects of estrogen in the MPTP model of Parkinson's disease. Neurobiol Dis. 2013 Oct;58:209-19. PMID: 23774254.

Wang J, Wang YH, Hou YY, et al. The small GTPase RhoA, but not Rac1, is essential for conditioned aversive memory formation through regulation of actin rearrangements in rat dorsal hippocampus. Acta Pharmacol Sin. 2013 Jun;34(6):811-8. PMID: 23564082.

Zhang XH, Sun NX, Feng ZH, et al. Interference of Y-27632 on the signal transduction of transforming growth factor beta type 1 in ocular Tenon capsule fibroblasts. Int J Ophthalmol. 2012;5(5):576-81. PMID: 23166867.

Y0052 Yangonin

5 mg
10 mg

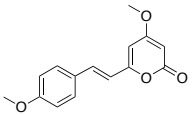

$C_{15}H_{14}O_4$ FW: 258.27 [500-62-9] ≥98%

CB1 agonist and GABA-A receptor potentiator. found in *Piper methysticum* (kava plant). It activates Nrf2 in neurons and astroglia, protects against amyloid-β-induced neurotoxicity, and inhibits growth of *Fusarium*, *Trichoderma*, and *Colletotrichum*.

Ligresti A, Villano R, Allarà M, et al. Kavalactones and the endocannabinoid system: the plant-derived yangonin is a novel CB1 receptor ligand. Pharmacol Res. 2012 Aug;66(2):163-9. PMID: 22525682.

Wruck CJ, Götz ME, Herdegen T, et al. Kavalactones protect neural cells against amyloid beta peptide-induced neurotoxicity via extracellular signal-regulated kinase 1/2-dependent nuclear factor erythroid 2-related factor 2 activation. Mol Pharmacol. 2008 Jun;73(6):1785-95. PMID: 18334601.

Y4800 YM-155

NEW

5 mg
10 mg

Sepantronium bromide

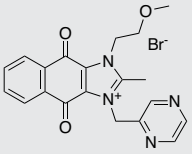

$C_{20}H_{19}N_4O_3Br$ FW: 443.29 [781661-94-7] ≥98%

Survivin inhibitor. It induces apoptosis in neuroblastoma models and suppresses growth of leukemia cells.

Liang H, Zhang L, Xu R, et al. Silencing of survivin using YM155 induces apoptosis and chemosensitization in neuroblastomas cells. Eur Rev Med Pharmacol Sci. 2013 Nov;17(21):2909-15. PMID: 24254560.

Feng W, Yoshida A, Ueda T. YM155 induces caspase-8 dependent apoptosis through downregulation of survivin and Mcl-1 in human leukemia cells. Biochem Biophys Res Commun. 2013 May 24;435(1):52-7. PMID: 23618862.

Tolcher AW, Quinn DI, Ferrari A, et al. A phase II study of YM155, a novel small-molecule suppressor of survivin, in castration-resistant taxane-pretreated prostate cancer. Ann Oncol. 2012 Apr;23(4):968-73. PMID: 21859898.

Y4802 YM-201636 NEW

1 mg
5 mg
10 mg

$C_{25}H_{23}N_7O_3$ FW: 469.5 [371942-69-7] ≥98%

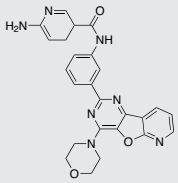

PIKfyve inhibitor. It decreases muscular contraction-stimulated glucose uptake, inhibits endomembrane transport and retroviral budding, and induces autophagy-dependent neuronal death.

Liu Y, Lai YC, Hill EV, et al. Phosphatidylinositol 3-phosphate 5-kinase (PIKfyve) is an AMPK target participating in contraction-stimulated glucose uptake in skeletal muscle. Biochem J. 2013 Oct 15;455(2):195-206. PMID: 23905686.

Martin S, Harper CB, May LM, et al. Inhibition of PIKfyve by YM-201636 dysregulates autophagy and leads to apoptosis-independent neuronal cell death. PLoS One. 2013;8(3):e60152. PMID: 23544129.

Jefferies HB, Cooke FT, Jat P, et al. A selective PIKfyve inhibitor blocks PtdIns(3,5)P(2) production and disrupts endomembrane transport and retroviral budding. EMBO Rep. 2008 Feb;9(2):164-70. PMID: 18188180.

Z0146 Z-Ala-Ala-Leu-pNA

100 mg
250 mg

$C_{26}H_{33}N_5O_7$ FW: 527.6 [61043-33-2] ≥95%

Z-Ala-Ala-Leu-pNA

Substrate used to measure activity of proteinases.

Chou H, Tam MF, Lee LH, et al. Vacuolar serine protease is a major allergen of *Cladosporium* cladosporioides. Int Arch Allergy Immunol. 2008;146(4):277-86. PMID: 18362473.

Balaban NP, Malikova LA, Mardanova AM, et al. Purification and characterization of a subtilisin-like proteinases secreted in the stationary growth phase of *Bacillus* amyloliquefaciens H2. Biochemistry (Mosc). 2007 Apr;72(4):459-65. PMID: 17511612.

Z0252 Zanamivir

5 mg
25 mg
100 mg
250 mg

$C_{12}H_{20}N_4O_7$ FW: 332.31 [139110-80-8] ≥98%

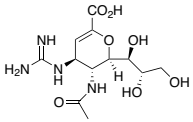

Neuraminidase inhibitor used to treat influenza virus infection.

Kim JH, Resende R, Wennekes T, et al. Mechanism-based covalent neuraminidase inhibitors with broad-spectrum influenza antiviral activity. Science. 2013 Apr 5;340(6128):71-5. PMID: 23429702.

Leyssen P, De Clercq E, Neyts J. Molecular strategies to inhibit the replication of RNA viruses. Antiviral Res. 2008 Apr;78(1):9-25. PMID: 18313769.

Z0944 ZCL-278

5 mg
10 mg

$C_{21}H_{19}BrClN_5O_4S_2$ FW: 584.89 [587841-73-4]

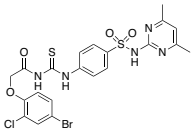

Cdc42 inhibitor. It inhibits microspike formation, disrupts GM130-docked Golgi structures, and suppresses branching, actin-based motility, and migration of prostate cancer cells.

Friesland A, Zhao Y, Chen YH, et al. Small molecule targeting Cdc42-intersectin interaction disrupts Golgi organization and suppresses cell motility. Proc Natl Acad Sci U S A. 2013 Jan 22;110(4):1261-6. PMID: 23284167.

Z1216 Z-DEVD-AMC

5 mg
10 mg
25 mg

$C_{36}H_{41}N_5O_{14}$ FW: 767.73 ≥95%

Z-Asp-Glu-Val-Asp-AMC

Substrate used to measure activity of caspase 3.

Pinto MC, Dias DF, Del Puerto HL, et al. Discovery of cytotoxic and pro-apoptotic compounds against leukemia cells: Tert-butyl-4-[(3-nitrophenoxy) methyl]-2,2-dimethyloxazolidine-3-carboxylate. Life Sci. 2011 Nov 21;89(21-22):786-94. PMID: 21983296.

Z1602 Zearalenone

1 mg
5 mg
10 mg

$C_{18}H_{22}O_5$ FW: 318.36 [17924-92-4] ≥98%

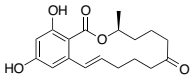

Mycotoxin and ER agonist found in *Fusarium*. It causes abnormal reproductive development, induces apoptosis in spermatocytes and spermatogonia, and stimulates oxidative stress.

Lee H, Kang C, Yoo YS, et al. Cytotoxicity and the induction of the stress protein Hsp 70 in Chang liver cells in response to zearalenone-induced oxidative stress. Environ Toxicol Pharmacol. 2013 Sep;36(2):732-40. PMID: 23917164.

Prouillac C, Koraichi F, Videmann B, et al. In vitro toxicological effects of estrogenic mycotoxins on human placental cells: structure activity relationships. Toxicol Appl Pharmacol. 2012 Mar 15;259(3):366-75. PMID: 22310176.

Kim IH, Son HY, Cho SW, et al. Zearalenone induces male germ cell apoptosis in rats. Toxicol Lett. 2003 Mar 3;138(3):185-92. PMID: 12565195.

Z1970 Zerumbone

10 mg
50 mg

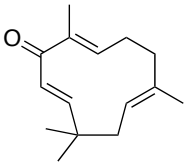

$C_{15}H_{22}O$ FW: 218.33 [471-05-6] ≥96%

Potential TRPV1 receptor antagonist found in ginger root. It displays a wide variety of biological properties, including upregulating expression of PPARα and enzymes involved in lipid oxidation, lowering total cholesterol and triglyceride levels in plasma, and decreasing paw edema and granulomatous tissue formation.

Tsuboi K, Matsuo Y, Shamoto T, et al. Zerumbone inhibits tumor angiogenesis via NF-κB in gastric cancer. Oncol Rep. 2014 Jan;31(1):57-64. PMID: 24220661.

Tzeng TF, Liou SS, Chang CJ, et al. Zerumbone, a Natural Cyclic Sesquiterpene of *Zingiber* zerumbet Smith, Attenuates Nonalcoholic Fatty Liver Disease in Hamsters Fed on High-Fat Diet. Evid Based Complement Alternat Med. 2013;2013:303061. PMID: 24223615.

Sun Y, Sheng Q, Cheng Y, et al. Zerumbone induces apoptosis in human renal cell carcinoma via Gli-1/Bcl-2 pathway. Pharmazie. 2013 Feb;68(2):141-5. PMID: 23469687.

Z2268 Z-FR-AMC

10 mg
20 mg
50 mg

Z-Phe-Arg-AMC

$C_{33}H_{36}N_6O_6$ FW: 612.68 ≥95%

Substrate used to measure activity of cysteine protease, cathepsins, and other proteases.

Rieux A, Gras S, Lecaille F, et al. Eimeripain, a cathepsin B-like cysteine protease, expressed throughout sporulation of the apicomplexan parasite *Eimeria* tenella. PLoS One. 2012;7(3):e31914. PMID: 22457711.

Z3444 Zileuton

100 mg
250 mg
1 g

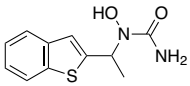

$C_{11}H_{12}N_2O_2S$ FW: 236.29 [111406-87-2] ≥98%

5-Lipoxygenase inhibitor. It displays a variety of biological activities, including inhibiting arachidonic acid release, preventing extracellular matrix remodeling in asthma models, and suppressing neuronal apoptosis.

Meng Z, Cao R, Yang Z, et al. Inhibitor of 5-Lipoxygenase, Zileuton, Suppresses Prostate Cancer Metastasis by Upregulating E-cadherin and Paxillin. Urology. 2013 Dec;82(6):1452.e7-1452.e14. PMID: 24295266.

Chen WJ, Liaw SF, Lin CC, et al. Effects of zileuton on airway smooth muscle remodeling after repeated allergen challenge in brown norway rats. Respiration. 2013;86(5):421-9. PMID: 24021192.

Shi SS, Yang WZ, Tu XK, et al. 5-Lipoxygenase inhibitor zileuton inhibits neuronal apoptosis following focal cerebral ischemia. Inflammation. 2013 Dec;36(6):1209-17. PMID: 23695166

Z4552 ZLN005

NEW

10 mg
50 mg

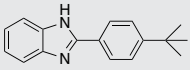

$C_{17}H_{18}N_2$ FW: 250.35 [49671-76-3] ≥98%

It increases expression of PPAR-γ coactivator-1α, indirectly activates AMPK, and improves glucose tolerance and insulin sensitivity.

Zhang LN, Zhou HY, Fu YY, et al. Novel small-molecule PGC-1α transcriptional regulator with beneficial effects on diabetic db/db mice. Diabetes. 2013 Apr;62(4):1297-307. PMID: 23250358.

Z4833 ZM-336372

5 mg
25 mg

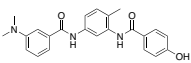

$C_{23}H_{23}N_3O_3$ FW: 389.45 [208260-29-1] ≥98%

Activator of c-Raf and inhibitor of tyrosine kinases. It induces apoptosis in pancreatic adenocarcinoma cells and decreases neuroendocrine vasoactive peptide production in pheochromocytoma cells.

Deming D, Geiger P, Chen H, et al. ZM336372 induces apoptosis associated with phosphorylation of GSK-3beta in pancreatic adenocarcinoma cell lines. J Surg Res. 2010 Jun 1;161(1):28-32. PMID: 20031160.

Deming D, Geiger P, Chen H, et al. ZM336372, a Raf-1 activator, causes suppression of proliferation in a human hepatocellular carcinoma cell line. J Gastrointest Surg. 2008 May;12(5):852-7. PMID: 18299943.

Z4900 ZM-447439 Trihydrate

NEW

5 mg
25 mg

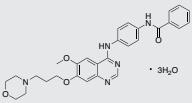

$C_{29}H_{31}N_5O_4 \cdot 3H_2O$ FW: 567.63 [331771-20-1] ≥98%

Aurora kinase A/B inhibitor. It prevents mitotic spindle formation and induces hyperploidy and apoptosis in osteosarcoma cells.

Tavanti E, Sero V, Vella S, et al. Preclinical validation of Aurora kinases-targeting drugs in osteosarcoma. Br J Cancer. 2013 Nov 12;109(10):2607-18. PMID: 24129234.

Baldini E, Tuccilli C, Prinzi N, et al. The dual Aurora kinase inhibitor ZM447439 prevents anaplastic thyroid cancer cell growth and tumorigenicity. J Biol Regul Homeost Agents. 2013 Jul-Sep;27(3):705-15. PMID: 24152827.

Crispi S, Fagliarone C, Biroccio A, et al. Antiproliferative effect of Aurora kinase targeting in mesothelioma. Lung Cancer. 2010 Dec;70(3):271-9. PMID: 20371132.

Z5645

Zoledronate Disodium Tetrahydrate

10 mg
25 mg
100 mg

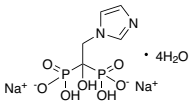

$C_5H_{10}N_2O_7P_2 \bullet 2Na \bullet 4H_2O$ FW: 390.13 [165800-07-7] ≥98%

FPPS inhibitor used to treat osteoporosis and prevent skeletal fractures in cancer patients. It also induces apoptosis and osteogenic differentiation in giant cell tumor bone stromal cells, decreases mean vessel density in renal cell carcinoma models, activates γδ T cells, and reverses the epithelial-to-mesenchymal transition in breast cancer cells.

Yang T, Zheng XF, Li M, et al. Stimulation of osteogenic differentiation in stromal cells of giant cell tumour of bone by zoledronic acid. Asian Pac J Cancer Prev. 2013;14(9):5379-83. PMID: 24175830.

Schech AJ, Kazi AA, Gilani RA, et al. Zoledronic acid reverses the epithelial-mesenchymal transition and inhibits self-renewal of breast cancer cells through inactivation of NF-κB. Mol Cancer Ther. 2013 Jul;12(7):1356-66. PMID: 23619300.

Idrees AS, Sugie T, Inoue C, et al. Comparison of γδ T cell responses and farnesyl diphosphate synthase inhibition in tumor cells pretreated with zoledronic acid. Cancer Sci. 2013 May;104(5):536-42. PMID: 23387443.

Z5744

Zoledronic Acid Hydrate

10 mg
25 mg
100 mg

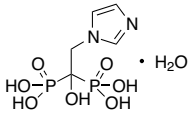

$C_5H_{10}N_2O_7P_2 \bullet H_2O$ FW: 290.1 [165800-06-6] ≥98%

FPPS inhibitor used to treat osteoporosis and other bone diseases. It also induces apoptosis and osteogenic differentiation in giant cell tumor bone stromal cells and activates γδ T cells.

Yang T, Zheng XF, Li M, et al. Stimulation of osteogenic differentiation in stromal cells of giant cell tumour of bone by zoledronic acid. Asian Pac J Cancer Prev. 2013;14(9):5379-83. PMID: 24175830.

Schech AJ, Kazi AA, Gilani RA, et al. Zoledronic acid reverses the epithelial-mesenchymal transition and inhibits self-renewal of breast cancer cells through inactivation of NF-κB. Mol Cancer Ther. 2013 Jul;12(7):1356-66. PMID: 23619300.

Z5745

Zolmitriptan

25 mg
100 mg
250 mg

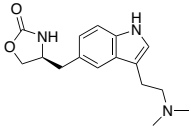

$C_{16}H_{21}N_3O_2$ FW: 287.36 [139264-17-8] ≥98%

5-HT1B/1D receptor agonist used to treat migraines. It inhibits dilation and inflammation of cranial vessels and prevents action potential discharge of trigeminal neurons.

Lindhe O, Almqvist P, Kågedal M, et al. Autoradiographic Mapping of 5-HT(1B/1D) Binding Sites in the Rhesus Monkey Brain Using [carbonyl-C]zolmitriptan. Int J Mol Imaging. 2011;2011:694179. PMID: 22013519.

Kayser V, Latrémolière A, Hamon M, et al. N-methyl-D-aspartate receptor-mediated modulations of the anti-allodynic effects of 5-HT1B/1D receptor stimulation in a rat model of trigeminal neuropathic pain. Eur J Pain. 2011 May;15(5):451-8. PMID: 20965753.

Stepień A, Chalimoniuk M, Strosznajder J. Serotonin 5HT1B/1D receptor agonists abolish NMDA receptor-evoked enhancement of nitric oxide synthase activity and cGMP concentration in brain cortex slices. Cephalalgia. 1999 Dec;19(10):859-65. PMID: 10668104.

Z5852

Zonampanel

YM872; HY-15072

5 mg
25 mg
100 mg

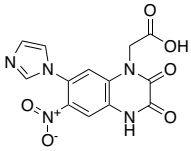

$C_{13}H_9N_5O_6$ FW: 331.24 [210245-80-0] ≥88%

AMPA receptor antagonist. It improves neurological deficits in stroke models but does not exacerbate intracerebral hemorrhage.

Ferro JM, Dávalos A. Other neuroprotective therapies on trial in acute stroke. Cerebrovasc Dis. 2006;21 Suppl 2:127-30. PMID: 16651823.

Terai K, Suzuki M, Sasamata M, et al. Effect of AMPA receptor antagonist YM872 on cerebral hematoma size and neurological recovery in the intracerebral hemorrhage rat model. Eur J Pharmacol. 2003 Apr 25;467(1-3):95-101. PMID: 12706461.

Z5653

Zonisamide

AD-810; CI-912

10 mg
25 mg
100 mg

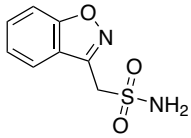

$C_8H_8N_2O_3S$ FW: 212.23 [68291-97-4] ≥96%

Carbonic anhydrase inhibitor and voltage-gated Na^+ and T-type Ca^{2+} channel blocker used to prevent seizures and epilepsy. It also delays neurodegeneration in Parkinson's disease models.

Arawaka S, Fukushima S, Sato H, et al. Zonisamide attenuates α-synuclein neurotoxicity by an aggregation-independent mechanism in a rat model of familial Parkinson's disease. PLoS One. 2014 Feb 20;9(2):e89076. PMID: 24586512.

Aggarwal M, Kondeti B, McKenna R. Anticonvulsant/antiepileptic carbonic anhydrase inhibitors: a patent review. Expert Opin Ther Pat. 2013;23(6):717-24. PMID: 23514045.

Holder JL Jr, Wilfong AA. Zonisamide in the treatment of epilepsy. Expert Opin Pharmacother. 2011 Nov;12(16):2573-81. PMID: 21967409.

Z6269

Z-Pro-D-Leu

10 mg
20 mg
50 mg

Z-P-D-L

Z-Pro-D-Leu-OH

$C_{19}H_{26}N_2O_5$ FW: 362.4 ≥95%

C-terminal oxytocin fragment that inhibits hypothermic tolerance induced by ethanol and analgesic and hypothermic tolerance induced by morphine.

Szabó G, Kovács GL, Székeli S, et al. C-terminal fragments of oxytocin (prolyl-leucyl-glycinamide and Z-prolyl-D-leucine) attenuate the development of tolerance to ethanol. Acta Physiol Hung. 1987;69(1):115-22. PMID: 2884803.

Kovács GL, Izbéki F, Horváth Z, et al. Effects of oxytocin and a derivative (Z-prolyl-D-leucine) on morphine tolerance/withdrawal are mediated by the limbic system. Behav Brain Res. 1984 Oct;14(1):1-8. PMID: 6542796.

Z7477

ZSTK474

NEW

5 mg
10 mg
25 mg

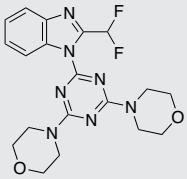

$C_{19}H_{21}F_2N_7O_2$ FW: 417.41 [475110-96-4] ≥98%

PI3K inhibitor. It inhibits migration, invasion, and adhesive capability of prostate cancer cells and decreases production of IFN-γ and IL-17 in fibroblast-like synovial cells.

Zhao W, Guo W, Zhou Q, et al. In Vitro Antimetastatic Effect of Phosphatidylinositol 3-Kinase Inhibitor ZSTK474 on Prostate Cancer PC3 Cells. Int J Mol Sci. 2013 Jun 28;14(7):13577-91. PMID: 23812078.

Haruta K, Mori S, Tamura N, et al. Inhibitory effects of ZSTK474, a phosphatidylinositol 3-kinase inhibitor, on adjuvant-induced arthritis in rats. Inflamm Res. 2012 Jun;61(6):551-62. PMID: 22349137.

Dan S, Okamura M, Mukai Y, et al. ZSTK474, a specific phosphatidylinositol 3-kinase inhibitor, induces G1 arrest of the cell cycle in vivo. Eur J Cancer. 2012 Apr;48(6):936-43. PMID: 22088482.

Anti-arrhythmics

A0001	A-803467
A4440	Allicin
A4441	Allicin, aqueous
A5037	Amiodarone Hydrochloride
D3447	Diltiazem Hydrochloride
G7200	GS967
L0060	Lappaconitine
M1879	Metoprolol Tartrate
M3584	Mivacurium Chloride
N3422	Nifekalant Hydrochloride
P0253	Panaxadiol
P0254	Panaxatriol
P6232	PP1
P6852	Propafenone Hydrochloride
P6865	Propranolol Hydrochloride
R0154	Ranolazine Dihydrochloride
R0249	Ramipril
R3197	Rhyncholphylline
S0171	Sarafotoxin 6c
S5976	Sotalol Hydrochloride
T1978	Tetrahydroberberine
V1769	Verapamil Hydrochloride

Antibacterials

A0820	N-Acetyl-S-(N'-benzylthiocarbamoyl)-L-cysteine
A0910	N-Acetyl-S-(N'-phenylthiocarbamoyl)-L-cysteine
A0917	1'-S-1'-Acetoxychavicol Acetate
A0977	Actinomycin
A0978	Actinonin
A1865	Aeroplysinin
A5033	4-Aminosalicylic Acid
A5034	4-Aminosalicylic Acid Sodium Dihydrate
A5057	Amoxicillin
A5059	Amoxapine
A5132	Amikacin Disulfate
A5160	Ampicillin Trihydrate
A5373	Anisomycin
A7462	Aspartame
A9834	Azithromycin
A9978	Aztreonam
B0108	Bactenecin
B0109	Bakuchiol
B1545	Benzalkonium Bromide
B1640	Benzydamine Hydrochloride
B1653	Benzyl Isothiocyanate
B1755	Benzimidazole
B1853	1,4-Benzoquinone
B1977	Betulin
B1978	Betulin-3-acetate
B3203	Biapenem
B3573	Bisdemethoxycurcumin
C0121	Caffeic Acid
C0246	Calcimycin
C0268	Carbadox
C1609	Cecropin B
C1620	Ceftiofur Hydrochloride
C1624	Cefuroxime Sodium
C1627	Cefaclor Monohydrate
C1629	Cefoperazone Acid
C1630	Cefoperazone Sodium
C1632	Cefotaxime Acid
C1633	Cefotaxime Sodium
C1635	Ceftazidime Hydrate
C1637	Ceftriaxone Sodium
C1648	α-Cembrenediol
C1649	β-Cembrenediol
C2844	Chloramphenicol
C2845	Levo-Chloramphenicol
C2943	Chlorogenic Acid (from *Eucommia*)
C2944	Chlorogenic Acid (from *Lonicera*)
C2951	Chlortetracycline Hydrochloride
C2969	Chromomycin A3
C2970	Chrysophanol
C3262	Ciprofloxacin
C3263	Ciprofloxacin Hydrochloride
C3576	Citreoviridin A
C4532	Clindamycin Hydrochloride
C4533	Clindamycin Phosphate
C4534	Clindamycin Palmitate Hydrochloride
C4535	Clinafloxacin Hydrochloride
C4756	Cloxacillin Sodium
C5647	Colistin Sulphate
C5863	Coptisine Hydrochloride
C6957	Croton Oil
C8069	Curcumin
C8070	Curcumin, high purity
C9600	Cyanopeptolin 1007
C9601	Cyanopeptolin 1040 MB
C9602	Cyanopeptolin 1041
C9603	Cyanopeptolin 1007 MB1
C9604	Cyanopeptolin 1007 MB2
C9605	Cyanopeptolin 1020
C9606	Cyanopeptolin 1054 MB1
C9607	Cyanopeptolin 1054 MB2
C9610	D-Cycloserine
C9616	Cyanopeptolin 1068 MB
D0044	D-Ala-D-Ala
D0353	Danofloxacin
D1627	Dehydrocostus Lactone
D1748	Demeclocycline Hydrochloride
D1757	L-Deoxyalliin
D1768	Dermaseptin I
D1850	Demethoxycurcumin
D3203	Diallyl Tetrasulfide
D3353	Diminazene Aceturate
D3420	3,4-Difluorobenzocurcumin
D3428	Dihydro-chelerythrine
D3430	Dihydro-sanguinarine
D3449	Dimethoxycurcumin
D5612	2-n-Dodecylfuran
D5897	Doxycycline Hyclate
D5898	Doxycycline Monohydrate
E0073	Ebselen
E5358	Enoxacin
E5369	Enrofloxacin
E7230	Ethambutol Dihydrochloride
F1854	Fenticonazole Nitrate
F4518	Fleroxacin
F4556	Florfenicol
F5874	Fosfomycin Calcium
G0243	(-)-Gallocatechin
G0278	Gatifloxacin
G1658	Gentamycin Sulfate
G1749	Gemfibrozil
G1869	Geranylgeraniol
G3254	10-Gingerol
G3351	Ginkgolic Acid Mixture
G3352	Ginkgolic Acid (13:0)
G3353	Ginkgolic Acid
G4796	Glycerol Monolaurate
G5875	Gossypol-Acetic Acid
H3273	Histatin 5
H9661	Hypocrellin A
H9662	Hypocrellin B
I4000	Ikarugamycin
I4934	Imipenem Monohydrate
I4961	Imperatorin
I4962	Isoimperatorin
I5215	Indolicidin
I7341	Isoniazid

Antibacterials

L0209	Lactoferrin, cow
L1785	Levofloxacin, free base
L1786	Levofloxacin Hydrochloride
L3453	Linezolid
L3454	Lincomycin Hydrochloride
L5749	Lomefloxacin Hydrochloride
M0124	Magainin 1
M0126	Magainin 2
M0173	Mastoparan X
M0255	Manzamine A
M0368	Marbofloxacin
M1560	Methyl Caffeate
M1744	Melittin
M1770	Meropenem Sodium Carbonate
M5793	Moxifloxacin, free base
M5794	Moxifloxacin Hydrochloride
M9368	Myristicin
N0114	Nadifloxacin
N1755	Neomycin Sulfate
N1769	Nerolidol, synthetic
N3225	Nigericin Sodium
N3323	Nifuratel
N3520	Nifursol
N5652	Nonactin
N5768	Norfloxacin
N5769	Norfloxacin Nicotinate
N5986	Novobiocin Sodium
O2144	Ofloxacin
O2145	Ofloxacin Hydrochloride
O2146	R-(+)-Ofloxacin
O6932	Oridonin
O6953	Ornidazole
O7400	OSU-03012
O9302	Oxacillin Sodium Monohydrate
O9396	Oxytetracycline
O9397	Oxytetracycline Hydrochloride
P0260	Papain Inhibitor
P0297	Paroxetine Hydrochloride
P0398	Pazufloxacin Mesylate
P2513	Phenyl Isothiocyanate
P2522	S-(N-Phenylthiocarbamoyl)-glutathione
P2995	Physcion
P3462	Piperacillin
P3463	Piperacillin Sodium
P3563	Piperlonguminine
P4780	Plumbagin
P5747	Polymyxin B Sulfate
P5885	Povidone Iodine
P6959	Prothionamide
P7060	Protocatechuic Acid Ethyl Ester
P7082	Prulifloxacin
P7359	Psoralidin
P8167	PuromycinAaminonucleoside
P8168	Puromycin Dihydrochloride
P8169	Purpurin
P9671	Pyrazinamide
R1780	Trans-Retinoic Acid
R1878	Retinyl Acetate
R3220	Rifampicin
R3221	3-Formyl Rifamycin
R3222	Rifamycin SV Monosodium
R3321	Rifaximin
R8122	Rufloxacin Hydrochloride
S0053	α-Santonin
S0170	Sarafloxacin Hydrochloride
S0253	Sanguinarine
S1609	Securinine
S1810	Secnidazole
S3352	Sinefungin
S5746	Solanesol
S6000	Sparfloxacin
S6018	Spectinomycin Hydrochloride
S6129	D-Sphingosine
S6232	Spiramycin
S6233	Spiramycin Hexanedioate
S6234	Spiramycin Embonate
S7769	Streptomycin Sulfate
S7870	Streptozocin
S8044	R,S-Sulforaphane
S8243	Sulbactam Sodium
S8244	Sulbactam
S8246	Sulfadimethoxine
S8248	Sulfamethoxazole
S9753	Synephrine
T0298	Tazobactam
T0299	Tazobactam Sodium
T1677	Tetracycline
T1679	Tetracycline Hydrochloride
T1968	Terpinen-4-ol
T2834	Thiolutin
T2932	Thiamphenicol Glycinate Hydrochloride
T2934	Thiamphenicol Palmitate
T2935	Thiamphenicol
T2936	Thioridazine Hydrochloride
T3134	Thiostrepton
T3324	Tigecycline
T3357	Tioconazole
T3454	Tinidazole
T5604	Tobramycin, free base
T5605	Tobramycin Sulfate
T5672	Tosufloxacin Tosylate
T6930	Triclosan Methyl Ether
T6931	Triclosan
T6934	Trimebutine Maleate
T6935	Trimebutine, base
T7034	Trimethoprim
T9945	Tylosin Tartrate
T9946	Tylosin Phosphate
U6856	Urocortin II, human
U6858	Urocortin II, mouse
U6901	Uracil
U7354	Usnic Acid
V0145	Valinomycin
V0252	Vancomycin Hydrochloride
V3325	Virginiamycin M1
V3326	Virginiamycin S1
W0247	Walrycin B

Anticonvulsants and Antiepileptics

A7208	Ascomycin
A8812	AWD 131-138
B0110	Baclofen
B5648	Bombesin
B8248	Bumetanide
C0270	Carbamazepine
C3251	Cinnarizine
C4417	Clemizole
C4418	Clemizole Hydrochloride
C5773	Cortistatin-14
D1629	Dehydroepiandrosterone
D1643	Delta Sleep Inducing Peptide
D1792	Dextromethorphan Hydrobromide Hydrate
D3209	Diclofenac Sodium
D3227	Dihydromethysticin
E2542	Met-Enkephalin, amide
E5241	Met-Enkephalin
F4483	Flufenamic Acid
F8270	Furosemide
G0048	γ-Amino Butyric Acid
G0106	Gabapentin
G0146	Galanin, human
G0147	Galanin, pig
G0148	Galanin, rat
G7200	GS967
H8162	(-)-Huperzine A
I7302	Isatin
K0088	Kawain
K0282	Kavalactones Mixture
L0060	Lappaconitine
L0349	Lamotrigine
L1784	Levetiracetam
M0278	Matrine
M1444	MDL 29951
M1579	Methazolamide
M1879	Metoprolol Tartrate
N1721	Nefiracetam
O9210	Oxcarbazepine
R1978	Retigabine Dihydrochloride
R2400	RG108
R3347	Riluzole
R5722	Rofecoxib
S3449	Simvastatin
S5745	[Tyr1]-Somatostatin
S5747	[Tyr11]-Somatostatin
S5749	Somatostatin-14
S5750	Somatostatin-28
S5751	Somatostatin-25
S5752	Somatostatin-28 (1-12)
S5753	Somatostatin-28 (1-14)
T8269	(S)-ar-Turmerone
V0147	Valproic Acid Sodium
V9228	VX-765
Z5653	Zonisamide

Antidepressants

A0919	Acetyl-L-Carnitine
A0922	Acetyl-L-Carnitine Hydrochloride
A2658	Agomelatine
A5059	Amoxapine
A5235	Amitriptyline Hydrochloride
A6368	Aprepitant
A7034	Aripiprazole
A7085	Arvanil
B1870	Berberine Hydrochloride Hydrate
B7058	Brompheniramine Maleate
B8276	Butyric Acid Sodium
B8363	Bupropion Hydrochloride
C0175	Carbetocin Acetate
C0267	Carnosol
C2947	Chlorpromazine Hydrochloride
C2949	Chlorpheniramine Maleate
C3246	Cilostazol
C3477	Citalopram Hydrobromide
C4457	Clomipramine Hydrochloride
C5680	Coumestrol
C9610	D-Cycloserine
C9673	Cysteamine Hydrochloride
C9779	Cytisine
D0263	Dapoxetine Hydrochloride
D1874	Desvenlafaxine Succinate
D5994	Doxepin Hydrochloride
D8145	Duloxetine Hydrochloride
E2542	Met-Enkephalin, amide
E5214	α-Endorphin
E5215	Acetyl-α-Endorphin
E5216	β-Endorphin, camel
E5217	β-Endorphin, human
E5218	β-Endorphin, rat
E5241	Met-Enkephalin
E6997	Erythropoietin
E7209	Escitalopram Oxalate
F1607	Febuxostat
F1669	Ferulic Acid
F1670	Ferulic Acid Methyl Ester
F4780	Fluoxetine Hydrochloride
F4783	Fluvoxamine Maleate
G3457	Ginsenoside Re
G3554	Ginsenoside Rb3
G4483	Glucagon-Like Peptide II, human
G4484	Glucagon-Like Peptide II, rat
G4485	[Ala19]-Glucagon-Like Peptide II, rat
H9714	L-5-Hydroxytryptophan
H9863	Hyperforin Dicyclohexylammonium
I0901	Icariin
I0902	Icaritin
L0349	Lamotrigine
M0035	M35
M0262	Maprotiline Hydrochloride
M1648	Melanostatin, frog
M1708	Mecamylamine Hydrochloride
M1845	Melitracen Hydrochloride
M3321	Mifepristone
M3368	Mirtazapine
M5610	Moclobemide
N0068	Naringenin
N1822	Nefazodone Hydrochloride
N1983	Neuropeptide Y (3-36), human
N1986	Neuropeptide Y, human/rat
N1987	Neuropeptide Y (13-36), human
N5605	Nobiletin
N7332	NSI-189
O5212	Ondansetron Hydrochloride Dihydrate
O9497	Oxytocin
P0013	P7C3
P0109	P7C3A20
P0110	R-P7C3-OMe
P0218	Paeoniflorin
P0245	Palmatine Chloride Hydrate
P0297	Paroxetine Hydrochloride
P6901	Pramipexole Dihydrochloride
P6954	Pioglitazone Hydrochloride
P7359	Psoralidin
Q8019	Quetiapine Fumarate
R1776	Resveratrol
R2400	RG108
R3475	Risperidone
R5661	Ropinirole Hydrochloride
R5874	Rosmarinic Acid
S1058	Scopolamine N-butylbromide
S1059	Scopolamine Hydrobromide
S1855	Senktide Trifluoroacetate
S1863	Seproxetine Hydrochloride
S1971	Sertraline Hydrochloride
S3568	Siramesine
S6134	Spinorphin, cow
S6800	SR1001
T1676	L-Tetrahydropalmatine
T1678	D,L-Tetrahydropalmatine
T6903	Tranylcypromine Hydrochloride
T7003	Trazodone Hydrochloride
U7357	Ursolic Acid
V1854	Venlafaxine Hydrochloride
V3444	Vilazodone
V5870	Vortioxetine
V9228	VX-765
Z3463	Ziprasidone

Antifungals

A0934	Acivicin
A5056	Amorolfine Hydrochloride
A5130	Amphotericin B
A5217	Trans-Anethole
B0026	Bafilomycin B1
B1755	Benzimidazole
B3320	Bifonazole
B3577	Bitertanol
B5870	Borrelidin
B8278	Butoconazole Nitrate
C0016	Caerulomycin A
C0246	Calcimycin
C0274	Caspofungin Acetate
C1648	α-Cembrenediol
C1649	β-Cembrenediol
C1869	Cerulenin
C3208	Ciclopirox Olamine
C3576	Citreoviridin A
C4510	Climbazole
C4657	Clotrimazole
C8069	Curcumin
C8070	Curcumin, high purity
C9612	Cyclosporin C
C9863	Cyproconazole
D3203	Diallyl Tetrasulfide
D3227	Dihydromethysticin
D3320	Difenoconazole
D3428	Dihydrochelerythrine
D3430	Dihydrosanguinarine
E6234	Epigallocatechin Gallate
E6259	Epoxiconazole
E6825	Ergosterol
F0268	Farnesol
F1854	Fenticonazole Nitrate
F3354	Finasteride
F4682	Fluconazole
F4883	Flutriafol
G4796	Glycerol Monolaurate
H1992	Hexaconazole
H3273	Histatin 5
H9862	Hypothemycin
I5072	Imazalil
I7256	Isobavachalcone
I7870	Itraconazole
K0088	Kawain
K1676	Ketoconazole
L0209	Lactoferrin, cow
L1761	Leptomycin B
L9610	Lycorine Hydrochloride
M0125	Magnolol
M1679	Methysticin
M1744	Melittin
M3309	Miconazole
M3310	Miconazole Nitrate
M3353	Minocycline Hydrochloride
M3598	Mizoribine Hydrobromide
M9368	Myristicin
M9608	Myclobutanil
N0075	Natamycin
N1769	Nerolidol, synthetic
N3323	Nifuratel
N3577	Nitidine Chloride
N5669	Nordihydroguaiaretic Acid
N9874	Nystatin
O4531	Oligomycin A
O9234	Oxiconazole Nitrate
O9334	Oxibendazole
P0297	Paroxetine Hydrochloride
P1854	Penicillic acid
P2995	Physcion
P3563	Piperlonguminine
P7219	Pseudolaric Acid B
P8169	Purpurin
R0212	Radicicol
S1609	Securinine
S1612	Sedanolide
S1810	Secnidazole
S3352	Sinefungin
T1605	Tebuconazole
T1672	Terbinafine Hydrochloride
T1968	Terpinen-4-ol
T2834	Thiolutin
T2930	Thiabendazole
T3357	Tioconazole
T6830	Triadimefon
T6831	Triadimenol
T6930	Triclosan Methyl Ether
T6931	Triclosan
T6932	Triflumizole
T7135	Triticonazole
T8269	(S)-ar-Turmerone
V5886	Voriconazole
Y0052	Yangonin

Antihypertensives

A0958	Aconitine
A3080	AHU-377 Tris Salt
A4440	Allicin
A4441	Allicin, aqueous
A4534	Aliskiren Hemifumarate
A5044	Amlodipine Besylate
A5045	Amlodipine
A5133	Amiloride Hydrochloride Dihydrate
A5273	Angiotensin Converting Enzyme Inhibitor Peptide
A6825	L-Arginine
A6826	L-Arginine Hydrochloride
A7332	Asiatic Acid, 95%
A7618	Atenolol
A8070	Auraptene
B0133	Baicalin
C0253	Candesartan
C0254	Candesartan Celexetil Ester
C0261	Captopril
C0376	Catharanthine, base
C0377	Catharanthine Sulfate
C0378	Catharanthine Tartrate
C3210	Ciglitazone
C3446	Cilnidipine
C4558	Clonidine Hydrochloride
D3329	7,8-Dihydroxyflavone Hydrate
D3330	Dihydrotanshinone
D5690	Doxazosin Mesylate
E5200	Enalaprilat
E5201	Enalapril Maleate
E5202	Enalapril
E6245	Eplerenone
F1654	Fenoldopam Mesylate
F1745	Felodipine
F4583	Flupirtine Maleate
F5668	Forskolin
F5770	Formononetin
F5773	Fosinopril Sodium
F8270	Furosemide
G1651	Geniposidic Acid
G3252	6-Gingerol
G4480	Glucagon, human
G4483	Glucagon-Like Peptide II, human
G4484	Glucagon-Like Peptide II, rat
G4485	[Ala19]-Glucagon-Like Peptide II, rat
G7443	GSK-429286A
H1643	Helodermin
H1644	Helodormin
H1645	Helospectin I
H1646	Helospectin II
H1648	Hemorphin-7
H1893	Hexarelin
H9613	N-(4-Hydroxyphenyl)retinamide
H9614	Hydrochlorothiazide
I4961	Imperatorin
I5414	Indapamide
I6804	Irbesartan
I7259	Isoproterenol Hydrochloride
I7360	Isosorbide Mononitrate
K1678	Ketanserin
K1679	(+)-Ketanserin Tartrate
K9858	Kyotorphin
L0005	Labetalol Hydrochloride
L0226	Lagochiline
L1660	Leptin (22-56), human
L1661	Leptin (116-130), mouse
L3374	Lisinopril Dihydrate
L5822	Lofexidine Hydrochloride
L5873	Losartan Potassium
L8377	Luteolin
M0009	Macitentan
M0248	Manidipine Hydrochloride
M1678	2-Methoxy Estradiol
M1708	Mecamylamine Hydrochloride
M1779	Methyldopa Sesquihydrate
M1879	Metoprolol Tartrate
M2409	MGCD0103
M3453	Minoxidil
N3208	Nicardipine
N3228	Nifedipine
N3448	Nimodipine
N6272	NPS-2143 Hydrochloride
P1869	Perindopril Erbumine
P2817	Phentolamine Hydrochloride
P2818	Phentolamine Mesylate
P5878	Potassium Canrenoate
P6865	Propranolol Hydrochloride
P6958	Protopanaxatriol
Q8016	Quercetin Dihydrate
Q8134	Quinapril Hydrochloride
R0249	Ramipril
R1752	Renin Inhibitor Peptide
R5772	Rosiglitazone Maleate
R5773	Rosiglitazone
R8179	Rutaecarpine, synthetic
S0830	R-(+)-Schisandrin A
S3313	Sildenafil Citrate
S6168	Spirapril Hydrochloride
S6235	Spironolactone
T1644	Telmisartan
T1670	Terazosin Hydrochloride Dihydrate
T1673	Terlipressin Acetate
T1750	Temocapril Hydrochloride
T3350	Timolol Maleate
T5968	Torsemide
T6803	Trandolapril
U6801	Urapidil
U6802	Urapidil Hydrochloride
V0146	Valsartan
V0147	Valproic Acid Sodium
V0160	Vapreotide
V0269	Vardenafil Dihydrochloride
V1769	Verapamil Hydrochloride
V1868	Veratramine

Antimetabolites and Nucleoside Analogs

A0401	Abacavir
A0402	Abacavir Sulfate
A1096	Acyclovir
A3212	3'-Azido-3'-deoxythymidine
A4445	Allopurinol
A5033	4-Aminosalicylic Acid
A5034	4-Aminosalicylic Acid Sodium Dihydrate
A9602	Azacitidine
A9803	Azathioprine
B6856	5-bromo-2'-Deoxyuridine
B6935	Brivudine
C0162	Capecitabine
C0174	Carmofur
C2948	Chloroadenosine
C4646	Clofarabine
C9677	Cyclocytidine Hydrochloride
C9778	Cytarabine
C9778	Cytarabine
D3212	2',3'-Dideoxycytidine
D3214	2',3'-Dideoxyinosine
D5692	Doxifluridine
E5178	Emtricitabine
E5456	Enocitabine
F0048	Famciclovir
F4480	5-Fluorouracil
F4557	Floxuridine
F4781	Fludarabine
F4782	Fludarabine Phosphate
F7657	Ftorafur
G0152	Ganciclovir
G1745	Gemcitabine Hydrochloride
H9817	5-Hydroxymethylcytosine
I5034	Imiquimod
L0350	Lamivudine
L1817	Leflunomide
M1575	7-Methyl-6-mercaptopurine
M1669	6-Mercaptopurine Monohydrate
M1676	Methotrexate Hydrate
N1744	Nelarabine
P1754	Penciclovir
R3205	Ribavirin
S7603	Stavudine
T1844	Telbivudine
T3200	Ticagrelor
T5946	Toltrazuril
V0244	Valganciclovir Hydrochloride
V3212	Vidarabine
V3213	Vidarabine Monophosphate

Antimitotics

A4606	Albendazole
A5472	Ansamitocin P3
A6234	Apigenin
B1755	Benzimidazole
B4248	BKM120
C5645	Colchicine
C5863	Coptisine Hydrochloride
D1749	Demecolcine
D3203	Diallyl Tetrasulfide
D5709	Docetaxel
E4668	ELR-510444
E6256	Epothilone A
E6257	Epothilone B
E6356	Epothilone D
E7578	Estramustine
E7579	Estramustine Phosphate Sodium
F1650	Fenbendazole
F4679	Flubendazole
H1894	Hexestrol
M1605	Mebendazole
M1678	2-Methoxy Estradiol
M5854	Monomethyl Auristatin E
N5409	Nocodazole
O9322	Oxfendazole
O9334	Oxibendazole
P0092	Paclitaxel (from *Taxus yunnanensis*)
P0093	Paclitaxel, semi-synthetic
P5712	Podophyllotoxin
P7219	Pseudolaric Acid B
P7258	Protopine
R3310	Ricobendazole
R5878	Rotenone
S0253	Sanguinarine
T0090	7-(triethylsilyl)-Baccatin III
T0092	1-Hydroxy Baccatin I
T0096	Cephalomannine
T0097	10-Deacetyltaxol-B
T0098	10-Deacetyltaxol-C
T0100	10-Deacetyltaxol
T0101	7-epi-10-Deacetyltaxol
T0102	7-epi-Taxol
T0105	Taxol C
T0106	Xylosyltaxol
T0107	Xylosyltaxol C
T0108	10-Deacetyl-7-xylosyltaxol
T0114	Taxinine M
T0116	2"3"-Dihydrocephalomannine
T0117	Benzyl Analog of Taxol
T0118	7-epi-Cephalomannine
T2930	Thiabendazole
T7197	Tryprostatin A
T8004	Tubeimoside I
V3251	Vinorelbine, base
V3252	Vinorelbine Ditartrate
V3253	Vinblastine Sulfate
V3354	Vindesine Sulfate
V3479	Vitamin K3
V5254	Vincristine Sulfate

Antiparasitics and Antimalarials

A0501	Abamectin
A0817	D,L-1'-Acetoxychavicol Acetate
A0820	N-Acetyl-S-(N'-benzylthiocarbamoyl)-L-cysteine
A0823	N-Acetyl-S-(N'-methylthiocarbamoyl)-L-cysteine
A0910	N-Acetyl-S-(N'-phenylthiocarbamoyl)-L-cysteine
A4440	Allicin
A4441	Allicin, aqueous
A4544	Allyl Disulfide
A4606	Albendazole
A5162	Amprolium Hydrochloride
A6970	Artemether
A6978	Artemisinin
A6979	Dihydroartemisinin
A6982	Artesunate
A8070	Auraptene
B0025	Bafilomycin A1
B1653	Benzyl Isothiocyanate
B1755	Benzimidazole
B1769	Bergenin
B4402	Blasticidin S Hydrochloride
B5870	Borrelidin
B8278	Butoconazole Nitrate
C0368	Carveol
C0376	Catharanthine, base
C0377	Catharanthine Sulfate
C0378	Catharanthine Tartrate
C1718	Cepharanthine, 95%
C2800	Chalcone
C2950	Chloroquine Phosphate
C2951	Chlortetracycline Hydrochloride
C4532	Clindamycin Hydrochloride
C4533	Clindamycin Phosphate
C4534	Clindamycin Palmitate Hydrochloride
C4656	Clopidol
C4657	Clotrimazole
C4758	Closantel Sodium
C5968	Cordycepin
C5970	Corydaline
C9608	Cycloastragenol
C9612	Cyclosporin C
C9613	Cyclosporin D
C9670	Cyromazine
C9809	Cyclopiazonic Acid
D1994	Dexrazoxane
D1995	Dexrazoxane Hydrochloride
D3208	Diclazuril
D3221	Difluoromethylornithine
D3301	Diaveridine
D3302	Diaveridine Hydrochloride
D3353	Diminazene Aceturate
D3374	Disulfiram
D3428	Dihydrochelerythrine
D3430	Dihydrosanguinarine
D5794	Doxorubicin Hydrochloride
D5897	Doxycycline Hyclate
D5898	Doxycycline Monohydrate
E4444	Ellagic Acid
E4902	Emamectin B1 Benzoate
E6470	Eprinomectin
F1650	Fenbendazole
F1854	Fenticonazole Nitrate
F4679	Flubendazole
F5766	Forchlorfenuron
F5770	Formononetin
F5874	Fosfomycin Calcium
F8048	Fumagillin
G0245	Gallocatechin Gallate
G4434	Gliotoxin
G5874	Gossypol
H9862	Hypothemycin
I4961	Imperatorin
I8618	Ivermectin
J0378	Jatrorrhizine
J0379	Jatrorrhizine Chloride
L1682	Levamisole Hydrochloride
L3454	Lincomycin Hydrochloride
L3550	Limonin
L3551	Limonin Glucoside
L5658	Lonidamine
L9610	Lycorine Hydrochloride
M0255	Manzamine A
M1605	Mebendazole
M1744	Melittin
M1975	S-(N-Methylthiocarbamoyl)-L-cysteine
N3520	Nifursol
N3577	Nitidine Chloride
N5409	Nocodazole
N5550	Nomilin
N5669	Nordihydroguaiaretic Acid
O4578	Oltipraz
O9234	Oxiconazole Nitrate
O9322	Oxfendazole
O9334	Oxibendazole
P0255	Pantoprazole
P0256	Pantoprazole Sodium
P2522	S-(N-Phenylthiocarbamoyl)-glutathione
P3563	Piperlonguminine
P7033	Primaquine Phosphate
P7060	Protocatechuic Acid Ethyl Ester
P7103	Praziquantel
P7158	Protopine
P9668	Pyrantel Pamoate
P9768	Pyronaridine Tetraphosphate
Q8133	Quinacrine Dihydrochloride Dihydrate
R0212	Radicicol
R0243	Raloxifene Hydrochloride
R3310	Ricobendazole
R3347	Riluzole
R3373	Risedronate Sodium Hydrate
R3374	Risedronic Acid
S0053	α-Santonin
S0344	Salermide
S0501	SB-939
S1612	Sedanolide
S1810	Secnidazole

Antiparasitics and Antimalarials

S3352	Sinefungin
S7600	Staurosporine
S7769	Streptomycin Sulfate
S8144	Sulfadoxine
S8169	Suramin Hexasodium
T0099	10-Deacetylbaccatin-III
T1678	D,L-Tetrahydropalmatine
T1979	Tetrahydrocoptisine
T2835	6-Thioguanine
T3454	Tinidazole
T5946	Toltrazuril
T7033	Trifluoperazine Hydrochloride
U7357	Ursolic Acid
X1854	p-Xyleneselenocyanate

Antipsychotics

A0916	Acepromazine Maleate
A0918	N-Acetyl-L-Cysteine
A1592	ADX 47273
A5059	Amoxapine
A5061	Ampalex
A5234	Amisulpride
A5235	Amitriptyline Hydrochloride
A7034	Aripiprazole
A9801	Azaperone
C0270	Carbamazepine
C2947	Chlorpromazine Hydrochloride
C4558	Clonidine Hydrochloride
C4757	Clozapine
C9673	Cysteamine Hydrochloride
D3329	7,8-Dihydroxyflavone Hydrate
F4584	Fluphenazine Hydrochloride
F6803	FRAX486
H0142	Haloperidol
H9717	Hydroxyzine Dihydrochloride
I4659	Iloperidone
N0160	NAP Peptide
O4400	Olanzapine
P0144	Paliperidone
P7023	Pregnenolone
Q8019	Quetiapine Fumarate
R3475	Risperidone
S8344	R,S-(±)-Sulpiride
S8345	S-(-)-Sulpiride
T0250	Tamoxifen Citrate
T2816	L-Theanine
T2936	Thioridazine Hydrochloride
T7033	Trifluoperazine Hydrochloride
Z3463	Ziprasidone

Anti-ulceratives, Antacids, Anti-emetics

Anti-ulceratives:

B1876	Betamethasone
B1878	Betamethasone 21-Phosphate Sodium
C0169	Carbenoxolone Disodium
C0278	Catechin
D1629	Dehydroepiandrosterone
D5994	Doxepin Hydrochloride
E4444	Ellagic Acid
G0145	Gallic Acid
G3457	Ginsenoside Re
L0109	Lactalbumin
L5769	Lorglumide Sodium
M1745	Melatonin
O4917	Omeprazole
P0245	Palmatine Chloride Hydrate
P2992	Phytic Acid, 40-50 wt% aqueous
R1774	Resiniferatoxin
R5894	Roxatidine Acetate Hydrochloride
S2957	Shogaol

Antacids:

C3250	Cimetidine
D1629	Dehydroepiandrosterone
E4408	Elcatonin Acetate
F0150	Famotidine
G0145	Gallic Acid
G3252	6-Gingerol
L0254	Lansoprazole
L5769	Lorglumide Sodium
N3496	Nizatidine
O4917	Omeprazole
P0245	Palmatine Chloride Hydrate
P0255	Pantoprazole
P0256	Pantoprazole Sodium
P2919	L-Phenylalaninol
P6954	Pioglitazone Hydrochloride
R0105	Rabeprazole Sodium
R0253	Ranitidine Hydrochloride
R5894	Roxatidine Acetate Hydrochloride
S8110	Sucralfate
T1754	Tenatoprazole
V3355	Vindoline

Anti-emetics:

A6368	Aprepitant
A7085	Arvanil
A9801	Azaperone
D5747	Dolasetron Mesylate Hydrate
G3253	8-Gingerol
G3254	10-Gingerol
G6802	Granisetron Hydrochloride
O5212	Ondansetron Hydrochloride Dihydrate
R1774	Resiniferatoxin
S2957	Shogaol

Antivirals

A0025	17-Allylaminogeldamamycin
A0401	Abacavir
A0402	Abacavir Sulfate
A0817	D,L-1'-Acetoxychavicol Acetate
A0918	N-Acetyl-L-Cysteine
A1096	Acyclovir
A1217	Adefovir
A1218	Adefovir Dipivoxil
A4544	Allyl Disulfide
A4577	Alsterpaullone
A4802	Amantadine Hydrochloride
A4803	Amantadine Sulfate
A5037	Amiodarone Hydrochloride
A5133	Amiloride Hydrochloride Dihydrate
A5313	Andrographolide
A5314	Dehydroandrographolide
A6229	Aphidicolin
A6979	Dihydroartemisinin
A6982	Artesunate
A9602	Azacitidine
A9803	Azathioprine
A9812	AZD1480
B0133	Baicalin
B1746	Belinostat
B1870	Berberine Hydrochloride Hydrate
B1977	Betulin
B1978	Betulin-3-acetate
B3358	Biochanin A
B6816	Brefeldin A
B6935	Brivudine
C0253	Candesartan
C0254	Candesartan Celexetil Ester
C0275	Castanospermine
C0370	Carrageenan Sodium
C1718	Cepharanthine, 95%
C2950	Chloroquine Phosphate
C2970	Chrysophanol
C3576	Citreoviridin A
C4417	Clemizole
C4418	Clemizole Hydrochloride
C5968	Cordycepin
C9615	Cyclosporin B
C9677	Cyclocytidine Hydrochloride
C9778	Cytarabine
D0261	Dapivirine
D0375	Dasatinib Monohydrate
D1872	Des(benzylpyridyl) Atazanavir
D3212	2',3'-Dideoxycytidine
D3214	2',3'-Dideoxyinosine
D3322	Diflunisal
D4802	17-Dimethylaminoethylamino-demethoxygeldanamycin
D9752	Dynasore
E2003	Efavirenz
E4444	Ellagic Acid
E4785	Elvitegravir
E5178	Emtricitabine
E5220	Enfuvirtide (T-20)
E5456	Enocitabine
E5576	Entecavir
E8657	Evodiamine
F0048	Famciclovir
F4482	Fluvastatin Sodium
F4557	Floxuridine
F4780	Fluoxetine Hydrochloride
F5873	Foscarnet Sodium
G0104	Gabexate Mesylate
G0152	Ganciclovir
G0243	(-)-Gallocatechin
G0245	Gallocatechin Gallate
G1646	Geldanamycin
G1650	Geniposide
G1745	Gemcitabine Hydrochloride
G3351	Ginkgolic Acid Mixture
G3352	Ginkgolic Acid (13:0)
G3353	Ginkgolic Acid
G3553	Ginsenoside Rb2
G4598	Glycyrrhizic Acid Ammonium Trihydrate
G5874	Gossypol
H0169	Harringtonine
H3275	HIV Integrase Protein Inhibitor HCKFWW
H5654	Honokiol
H9715	Hydroxyurea
H9726	Hygromycin B
H9861	Hypericin
I1257	Idoxuridine
I5034	Imiquimod
I5210	INCB018424
I5313	Indinavir Sulfate
K0023	K252C
L0209	Lactoferrin, cow
L0350	Lamivudine
L1817	Leflunomide
L3550	Limonin
L3551	Limonin Glucoside
L5862	Lopinavir
M0255	Manzamine A
M1560	Methyl Caffeate
M1687	Mevinolin
M1744	Melittin
M9710	Mycophenolic Acid
N0061	D-Naproxen
N0062	D,L-Naproxen
N0068	Naringenin
N3225	Nigericin Sodium
N5550	Nomilin
N5655	Nonoxynol-9
N5669	Nordihydroguaiaretic Acid
N7208	NSC-74859
N7210	NSC-23766
O7218	Oseltamivir Phosphate
P1202	PD325901
P1754	Penciclovir
P2410	Phenethyl Dimethyl Caffeate
P5712	Podophyllotoxin
P6857	Protocatechuic Acid
P9870	Pyridostatin Trihydrochloride
Q8016	Quercetin Dihydrate

Antivirals

R0247	Raltegravir
R1776	Resveratrol
R1780	Trans-Retinoic Acid
R3205	Ribavirin
R3249	Rimantadine Hydrochloride
R3577	Ritonavir
R5749	Romidepsin
S0033	Saikosaponin B2
S0133	Saikosaponin C
S3345	Silymarin
S5722	Sofosbuvir
S7061	SRPIN340
S7603	Stavudine
S8169	Suramin Hexasodium
T0091	7-(triethylsilyl)-10-deacetyl Baccatin III
T1844	Telbivudine
T1854	Tenofovir Monohydrate
T3097	Thymosin α-1 Acetate
T5720	Tofacitinib Citrate
T6930	Triclosan Methyl Ether
T6931	Triclosan
T8004	Tubeimoside I
T8145	Tulobuterol Hydrochloride
V0045	Valaciclovir Hydrochloride
V0160	Vapreotide
V0244	Valganciclovir Hydrochloride
V3212	Vidarabine
V3213	Vidarabine Monophosphate
V5734	Vorinostat
V9200	VX-950
Z0252	Zanamivir

Anxiolytics

A2658	Agomelatine
A5217	Trans-Anethole
A5326	Aniracetam
A7034	Aripiprazole
A7071	Atriopeptin II, rat/rabbit/mouse
B3345	(-)-Bilobalide
B8248	Bumetanide
B8274	Buspirone Hydrochloride
C0175	Carbetocin Acetate
C2947	Chlorpromazine Hydrochloride
C2968	Chrysin
C3246	Cilostazol
C3477	Citalopram Hydrobromide
C4457	Clomipramine Hydrochloride
C4800	CM 346
D5994	Doxepin Hydrochloride
D8145	Duloxetine Hydrochloride
E7209	Escitalopram Oxalate
F8270	Furosemide
G0048	γ-Amino Butyric Acid
G3354	Ginkgolide A
G3457	Ginsenoside Re
H5654	Honokiol
H9717	Hydroxyzine Dihydrochloride
J6400	(+)-JQ-1
K0088	Kawain
K0282	Kavalactones Mixture
L0349	Lamotrigine
L1784	Levetiracetam
L9874	L-(+)-Lysine Monohydrate
M0040	M40
M0262	Maprotiline Hydrochloride
M1708	Mecamylamine Hydrochloride
M3368	Mirtazapine
M5675	Motilin, dog
M5776	Motilin, pig
M7528	α-Melanocyte Stimulating Hormone
N1982	Neuromedin U, rat
N1983	Neuropeptide Y (3-36), human
N1986	Neuropeptide Y, human/rat
N1987	Neuropeptide Y (13-36), human
N3310	Nicotinamide
N7200	NS-11394
O5212	Ondansetron Hydrochloride Dihydrate
O9497	Oxytocin
P7718	Pterostilbene
P8117	Puerarin
P8118	Puerarin
R3347	Riluzole
R8076	Rutin Hydrate
S1855	Senktide Trifluoroacetate
S1971	Sertraline Hydrochloride
S3568	Siramesine
S5745	[Tyr1]-Somatostatin
S5747	[Tyr11]-Somatostatin
S5749	Somatostatin-14
S5750	Somatostatin-28
S5751	Somatostatin-25
S5752	Somatostatin-28 (1-12)
S5753	Somatostatin-28 (1-14)
S7872	Stresscopin-Related Peptide, human
T0081	Taurine
T1676	L-Tetrahydropalmatine
T1678	D,L-Tetrahydropalmatine
T2816	L-Theanine
T6903	Tranylcypromine Hydrochloride
T7003	Trazodone Hydrochloride
T7033	Trifluoperazine Hydrochloride
T7036	Triptorelin
T7037	Triptorelin Acetate
U6856	Urocortin II, human
U6858	Urocortin II, mouse
U6859	Urocortin III, human
U6860	Urocortin III, mouse
V3444	Vilazodone
V5870	Vortioxetine
Z3463	Ziprasidone

Apoptosis Detection Products

A0825	Ac-GPK-pNA
A0826	Ac-GPK(Ac)-pNA
A0832	Ac-IEAR-pNA
A0834	Ac-IETD-pNA
A1084	Ac-VEID-pNA
A1097	Ac-YVAD-pNA
A4930	7-Amino-actinomycin D
A5353	Annexin V-FITC Apoptosis Detection Kit
B5608	Boc-FAAGRK-AMC
B5609	Boc-GRR-AMC
B5610	Boc-PRR-AMC
B5611	Boc-RRR-AMC
C0375	Ac-DEVD-pNA
C9781	Basic Cytotoxicity Test Assay Kit
C9782	Total Cytotoxicity Test Assay Kit
F0010	FAM FLICA® Poly Caspases Assay Kit
F0011	FAM FLICA™ Caspase 1 Assay Kit
F0012	FAM FLICA™ Caspase 2 Assay Kit
F0013	FAM FLICA™ Caspases 3 and 7 Assay Kit
F0014	FAM FLICA™ Caspase 6 Assay Kit
F0015	FAM FLICA™ Caspase 8 Assay Kit
F0016	FAM FLICA™ Caspase 9 Assay Kit
F0017	FAM FLICA™ Caspase 10 Assay Kit
F0018	FAM FLICA™ Caspase 13 Assay Kit
F0019	FAM-Phe-CMK Green FLISP™ Assay Kit
F0019	FAM-Phe-CMK Green FLISP™ Assay Kit
F0021	FAM-Leu-CMK Green FLISP™ Assay Kit
F0021	FAM-Leu-CMK Green FLISP™ Assay Kit
F0022	FAM-Spacer-Phe-CMK Green FLISP™ Assay Kit
F0023	FAM-Spacer-Leu-CMK Green FLISP™ Assay Kit
F0119	FAM-VAD-OPH I in vitro Apoptosis Detection Reagent
F0120	FAM-VAD-OPH II in vitro Apoptosis Detection Reagent
F0121	FAM-DEVD-OPH in vitro Apoptosis Detection Reagent
F4533	FLICA® 660 Poly Caspase Assay Kit
F4534	FLICA® 660 Caspase-1 Assay Kit
F4535	FLICA® 660 Caspase 3/7 Assay Kit
L1628	Ac-LEHD-pNa
M0115	Magic Red™ Caspases 3 & 7 Assay Kit
M0116	Magic Red™ Cathepsin B Assay Kit
M0117	Magic Red™ Cathepsin K Assay Kit
M0118	Magic Red™ Cathepsin L Assay Kit
M3378	MitoPT™ JC-1 Assay kit
P6977	Pyr-GR-pNA
S7080	SR-FLICA Poly Caspases Assay Kit
S7081	SR FLICA Caspases 3 and 7 Assay Kit
S7082	SR FLICA Caspase 9 Assay Kit
S7083	SR-101-Phe-CMK Red FLISP™ Assay Kit
S7084	SR-101-Leu-CMK Red FLISP™ Assay Kit
S7184	SR-VAD-OPH in vitro Apoptosis Detection Reagent
T5677	Total Cell Death Assay Kit
Z1216	Z-DEVD-AMC
Z2268	Z-FR-AMC

Biologically Active Peptides

A0960	Adrenocorticotropic Hormone (1-39), human
A0961	Adrenocorticotropic Hormone (1-39), rat
A0962	Adrenocorticotropic Hormone (1-4)
A0963	Adrenocorticotropic Hormone (1-10), human
A0964	Adrenocorticotropic Hormone (1-13), human
A0965	Adrenocorticotropic Hormone (1-14)
A0966	Adrenocorticotropic Hormone (1-16), human
A0967	Adrenocorticotropic Hormone (1-17), human
A0968	Adrenocorticotropic Hormone (1-24), human
A0970	Adrenocorticotropic Hormone (18-39), human
A0971	Adrenocorticotropic Hormone (4-10), human
A1097	Ac-YVAD-pNA
A1330	Adipokinetic Hormone
A1331	Adipokinetic Hormone, locust
A1332	Adipokinetic Hormone II (from *Locusta migratoria*)
A1333	Adipokinetic Hormone II (from *Schistocera gregaria*)
A1368	Adrenomedullin (1-52), human
A1369	Adrenomedullin (13-52), human
A1370	Adrenomedullin (22-52), human
A1371	Adrenorphin
A2412	AGDV
A4369	A-K-R-R-R-L-S-S-L-R-A
A4400	Alamethicin
A4401	ALAL
A4438	Allatostatin I
A4498	Alytesin
A4844	Amylin (8-37), human
A4845	Amylin (8-37), rat
A4846	Amylin, cat
A4847	Amylin, human
A4850	Amylin, rat
A5070	Angiotensin Acetate
A5225	α-ANF (1-28), human
A5272	Angiotensin, dog, rat
A5273	Angiotensin Converting Enzyme Inhibitor Peptide
A5287	Angiotensinogen (1-14), human
A5458	Anorexigenic Peptide
A5460	A-type Natriuretic Peptide (1-11), rat
A5461	A-type Natriuretic Peptide (1-30), frog
A5476	Antagonist G
A5479	Antiestrogen Peptide
A6017	Apelin-13, human, cow
A6827	Argipressin Acetate
A7071	Atriopeptin II, rat/rabbit/mouse
A7072	Atriopeptin III
A7669	A-type Natriuretic Peptide (1-28), rat
A7670	Atriopeptin I
A8071	Auriculin A
A8077	Autocamtide 2
B0000	2B-(A)
B0072	2B-(S)
B0108	Bactenecin
A0248	BAM-12P
A0249	BAM-22P
B3324	Big Endothelin-1 (1-38), human
B3346	Brain Injury-derived Neurotrophic Peptide
B5560	B-type Natriuretic Peptide (1-32), rat
B5561	B-type Natriuretic Peptide (1-32), human
B5608	Boc-FAAGRK-AMC
B5609	Boc-GRR-AMC
B5610	Boc-PRR-AMC
B5611	Boc-RRR-AMC
B5648	Bombesin
B5649	[Tyr4]-Bombesin
B6812	Bradykinin Potentiator B
B6813	Bradykinin Potentiator C
B8010	Buccalin
C0140	Calcitonin, eel
C0146	Calcitonin, chicken
C0148	Calcitonin, human
C0149	Calcitonin, salmon
C0151	α-Calcitonin Gene Related Peptide, human
C0153	Calcitonin, rat
C0243	Calcitonin Gene Related Peptide (8-37), human
C0244	α-Calcitonin Gene Related Peptide, chicken
C0245	Calcitonin Gene Related Peptide, rat
C0247	Calcineurin Autoinhibitory Peptide
C0248	Calcineurin Substrate
C0249	Calcitonin Gene Related Peptide (8-37), rat
C0250	Calcitonin Gene Related Peptide II, human
C0251	Calcitonin Gene Related Peptide II, rat
C0372	Casein Kinase 2 Assay Kit
C0374	β-Casomorphin, human
C0375	Ac-DEVD-pNA
C0379	Catch-Relaxing Peptide
C0476	CB-TH
C1600	Carcinoembryonic Antigen (605-613)
C1601	Carcinoembryonic Antigen Analog (605-613)
C1609	Cecropin B
C1619	CEF3
C1621	CEF4
C1622	CEF6
C1623	CEF10
C1868	Cerebellin
C2468	β-Calcitonin Gene Related Peptide, human
C2971	Chromostatin, cow
C4274	CKS-17
C5196	C-Myc Peptide
C5260	C-type Natriuretic Peptide (1-22), pig/human/rat
C5646	Collagen Binding Fragment
C5647	Colistin Sulphate
C5768	Corazonin
C5772	Corticotropin Releasing Factor, human/rat
C5773	Cortistatin-14
C6018	C-Peptide, dog
C6019	C-Peptide, human
C6982	Crustacean Cardioactive Peptide
C7098	Crystalline
C7618	C-Telopeptide
C7997	C-type Natriuretic Peptide (1-22), human
C7998	C-type Natriuretic Peptide, chicken
D0025	DAMGO
D0254	Dansyl-YVG
D1643	Delta Sleep Inducing Peptide

Biologically Active Peptides

D1644	Deltorphin I
D1767	Dermenkephalin
D1768	Dermaseptin I
D1769	Dermorphin
D1770	Dermorphin Analog
D1775	Deslorelin Acetate
D3351	4-Dimethylaminopyridine
E2424	Egg Laying Hormone (from *Aplysia*)
E2542	Met-Enkephalin, amide
E4408	Elcatonin Acetate
E4416	Eledoisin
E4417	Eledoisin Related Peptide
E5210	Endomorphin-1
E5211	Endomorphin-2
E5212	Endonuclease Antigenic Site
E5214	α-Endorphin
E5215	Acetyl-α-Endorphin
E5216	β-Endorphin, camel
E5217	β-Endorphin, human
E5218	β-Endorphin, rat
E5219	Endothelin-1, human
E5220	Enfuvirtide (T-20)
E5221	Endothelin-2, human
E5222	Endothelin-3, human
E5240	Leu-Enkephalin
E5241	Met-Enkephalin
E5276	Enterostatin, human
E5277	Enterostatin, pig/rat
E6993	Erythromycin Resistance Peptide MRLFV
E9416	Exendin-3
E9417	Exendin-4
E9418	Exendin 3 (9-39)
F3204	Fibrinogen-binding Peptide
F3205	Fibrinogen γ-chain Dodecapeptide
F3206	Fibrinolysis Inhibiting Factor
F3207	Fibronectin CS-1 Peptide
F3208	Fibrinopeptide B, human
F3209	Fibronectin-Binding Protein
F4400	Flag Peptide
F4420	Boc-FLFLF
F4856	Fmoc-Lys(Boc)-Leu-Lys(Boc)
F4857	FMRF amide
F4858	FMRF-like Peptide, snail
F4859	FMRF
F5869	N-formyl-Met-Ala-Ser
F5870	N-formyl-Met-Leu-Phe
F5871	N-formyl-Met-Leu-Phe-Lys
F5872	N-formyl-Nle-Leu-Phe-Nle-Tyr-Lys
G0000	G250.A2 Peptide
G0146	Galanin, human
G0147	Galanin, pig
G0148	Galanin, rat
G0175	Gastric Inhibitory Peptide, human
G0178	Gastrin, chicken
G0179	Gastrin-1, rat
G0180	Gastrin I, human
G0181	Gastrin Releasing Peptide, human
G0182	Gastrin Releasing Peptide, pig
G2868	Ghrelin, human
G2869	Ghrelin, rat
G2870	Growth Hormone-Releasing Factor (1-44), human
G2871	Growth Hormone-Releasing Factor, cow
G2872	Growth Hormone-Releasing Factor, mouse
G2873	Growth Hormone-Releasing Factor, sheep
G2874	Growth Hormone-Releasing Factor, rat
G2968	Growth Hormone-Releasing Peptide 2
G4479	Glucagon (19-29), human
G4480	Glucagon, human
G4481	Glucagon-Like Peptide I amide (7-36), human
G4482	Glucagon-Like Peptide I (7-37)
G4483	Glucagon-Like Peptide II, human
G4484	Glucagon-Like Peptide II, rat
G4485	[Ala19]-Glucagon-Like Peptide II, rat
G6803	Granuliberin R
G6856	Growth Hormone Releasing Factor, human
G8103	Guanylin, human
G8104	Guanylin, rat/mouse
H0207	Hepatitis B Viral Core Protein (128-140)
H1643	Helodermin
H1644	Helodormin
H1645	Helospectin I
H1646	Helospectin II
H1648	Hemorphin-7
H1657	Heparin-Binding Peptide
H1661	Hepatitis B Virus Core Protein (128-140)
H1662	HER2/neu (654-662) GP2
H1663	HER2/neu Fragment (869-877)
H2876	H-Trp-Gly-OH
H2980	Humanin, human
H3272	His Tag
H3273	Histatin 5
H3275	HIV Integrase Protein Inhibitor HCKFWW
H3278	Human Immunodeficiency Virus Reverse Transcriptase A2.1 peptide
H8048	Human Follicular Gonadotropin Releasing Peptide
I5215	Indolicidin
I5476	Interleukin-6 Receptor Fragment
K0172	Kassinin
K0276	Katacalcin
K1674	Ketolide Resistance Peptide MRFFV
K2412	KGDS
K6864	KRQHPG
K9858	Kyotorphin
L0248	Laminin Peptide YIGSR
L0249	Laminin Peptide YIGSR-NH2
L0250	Laminin Peptide SIKVAV
L0251	Laminin Peptide CDPGYIGSR
L1660	Leptin (22-56), human
L1661	Leptin (116-130), mouse
L1735	Levitide
L1980	Leucokinin I
L1981	Leucokinin VIII
L1983	Leucomyosuppressin
L2876	Luteinizing Hormone Releasing Hormone III, Lamprey
L3362	β-Lipotropin (61-64)

Biologically Active Peptides

L3577	Litorin
L8276	Luteinizing Hormone Releasing Hormone
L8277	[Gln8]-Luteinizing Hormone-Releasing Hormone, chicken
L8278	Luteinizing Hormone-Releasing Hormone, salmon
L9875	Lys(Boc)-Leu-Lys(Boc)-Obzl
L9880	Lysipressin Acetate
M0124	Magainin 1
M0126	Magainin 2
M0144	Malantide
M0172	Mastoparan
M0173	Mastoparan X
M0224	Melanoma Antigen Gene-Encoding Fragment 3 (271-279), human
M0272	Mastoparan 7
M0273	Mastoparan 8
M0276	Peptide 401
M1646	Melanin Concentrating Hormone, human/mouse/rat
M1647	Melanin Concentrating Hormone, salmon
M1648	Melanostatin, frog
M1744	Melittin
M1752	Men 10376
M2460	Matrix GLa Protein - pNa
M3220	Tyr-W-MIF-1
M5675	Motilin, dog
M5776	Motilin, pig
M7528	α-Melanocyte Stimulating Hormone
M7529	β-Melanocyte Stimulating Hormone, human
M7531	γ-1 Melanocyte Stimulating Hormone
M7532	γ-3 Melanocyte Stimulating Hormone
M9356	Myomodulin
M9643	Myelin Basic Protein (1-11), human
M9644	Myelin Basic Protein (87-99), guinea pig/human
M9646	Myelin Basic Protein (68-82), guinea pig
N0160	NAP Peptide
N1873	Nesiritide Acetate
N1977	Neurokinin A (4-10)
N1978	Neurokinin B
N1979	Neuromedin
N1980	Neuromedin B, pig
N1981	Neuromedin C (18-27), pig
N1983	Neuropeptide Y (3-36), human
N1984	Neuropeptide FF
N1985	Neuropeptide K, pig
N1986	Neuropeptide Y, human/rat
N1987	Neuropeptide Y (13-36), human
N1988	γ-Neuropeptide, rabbit
N5210	Nociceptin
N5211	Nocistatin
N6020	Neuropeptide F
N6076	N(p-Tosyl)-GPR-pNA
O0977	Octopamine Hydrochloride
O1078	Octreotide Acetate
O6132	Opioid Receptor Antagonist Ac-RFMWMK-NH2
O7116	Orexin B, human
O7208	Oscillaginin A
O7209	Oscillaginin A Methyl Ester
O7210	Oscillaginin B
O7211	Oscillaginin B Methyl Ester
O7212	Oscillaginin C
O7213	Oscillamide Y
O9497	Oxytocin
P0005	Pituitary Adenylate Cyclase-Activating Polypeptide (1-27), human/sheep/rat
P0006	Pituitary Adenylate Cyclase-Activating Polypeptide (1-38), human/sheep/rat
P0007	Pituitary Adenylate Cyclase-Activating Polypeptide (6-27), human/sheep/rat
P0008	Pituitary Adenylate Cyclase-Activating Polypeptide (6-38), human/sheep/rat
P0009	Pituitary Adenylate Cyclase-Activating Polypeptide (1-38), frog
P0010	Pituitary Adenylate Cyclase-Activating Polypeptide-Related Peptide, human
P0011	Pituitary Adenylate Cyclase-Activating Polypeptide-Related Peptide, rat
P0055	P55-TNFR peptide
P0075	P75-TNFR peptide
P0260	Papain Inhibitor
P0268	Parasin I
P0269	Parathyroid Hormone (1-34), cow
P0270	Parthenolide
P0350	Pancreatic Polypeptide, chicken
P0351	Pancreatic Polypeptide, rat
P0352	Pancreastatin, pig
P0353	Pancreatic Polypeptide, human
P1760	Peptide T
P1762	Peptide YY, pig
P1763	Peptide YY, human
P1764	Pep-1 Peptide
P1766	Peptide B, cow
P1767	Peptide F, cow
P1768	Peptide YY (3-36), human
P2445	GLa Peptide
P2832	Peptide Histidine Isoleucine, pig
P2833	Peptide Histidine Isoleucine, rat
P2859	Phosphate Acceptor Peptide
P2992	Phyllolitorin
P2993	Phyllomedusin
P2994	Physalaemin
P4560	Proteolipid Protein (139-151)
P6850	Prolactin-Releasing Peptide (1-31), human
P6859	Proctolin
P7034	Prion Peptide (106-126), human
P7628	Parathyroid Hormone-Related Protein (1-34), human/rat
Q4370	QKRPSQRSKYL
R0250	Ranatensin
R0251	Ranatensin R
R1752	Renin Inhibitor Peptide
R2112	RFDS
R2353	RF-NH2
R2369	RFRP-1, human
R2510	RGD-4C
R2511	RGDC

Biologically Active Peptides

R2512	RGD
R2516	RGES
R6873	RSR
R8178	Rutaecarpine
S0200	SAMs Peptide
S0381	Sauvagine
S1060	Small Cardioactive Peptide A
S1061	Small Cardioactive Peptide B
S1343	Ac-SDKP
S1604	Secretin Acetate
S1605	Secretin, human
S1606	Secretin, pig
S1607	Secretin, rat
S1969	Sermorelin Acetate
S1970	Serum Thymic Factor
S2044	SFLLR
S5745	[Tyr1]-Somatostatin
S5747	[Tyr11]-Somatostatin
S5749	Somatostatin-14
S5750	Somatostatin-28
S5751	Somatostatin-25
S5752	Somatostatin-28 (1-12)
S5753	Somatostatin-28 (1-14)
S7872	Stresscopin-Related Peptide, human
S8005	Substance P
S8006	Substance P (1-4)
S8007	Substance P (1-7)
S8008	Substance P (1-9)
S8009	Substance P (7-11)
S8010	[Nle11]-Substance P
S8011	[Pro9]-Substance P
S8012	[Sar9]-Substance P
S8013	[Tyr8]-Substance P
S8014	Substance P, free acid
S9754	Syntide 2
S9775	Systemin
T0076	Transactivator of Transcription Peptide
T0077	Transactivator of Transcription Peptide 2-4
T1673	Terlipressin Acetate
T1855	Tentoxin
T2970	Thrombin Receptor Agonist peptide
T3096	Thymosin α-1
T3097	Thymosin α-1 Acetate
T3098	Thymosin β-4 Acetate
T3099	Thymus Factor
T9974	[Asp371]-Tyrosinase (369-377), human
U5233	Universal Tetanus Toxin Epitope P2 (830-844)
U6854	Urocortin, human
U6855	Urocortin, rat
U6856	Urocortin II, human
U6857	Urodilatin CCC
U6858	Urocortin II, mouse
U6859	Urocortin III, human
U6860	Urocortin III, mouse
U6956	Uroguanylin, human
U6957	Urotensin I
U6958	Urotensin II, frog
U6959	Urotensin II, human
V0273	Vasoactive Intestinal peptide
V1872	Vesicular Stomatitis Virus Peptide
V3360	Vasoactive Intestinal Peptide, guinea pig
W4096	WKYMVM-NH2
X1752	Xenin
Z6269	Z-Pro-D-Leu

Carcinogens and Mutagens

A2044	Aflatoxin B1
A2244	Aflatoxicol
A4675	Alternariol
A4678	Alternariol-9-methyl Ether
A5202	Anabasine Hydrochloride
A6932	Aristolochic Acid A
A6933	Aristolochic Acid B
A6934	Aristolochic Acid C
B1652	Benzo[a]pyrene
B5648	Bombesin
B6917	Brevetoxin 2
B8071	3-tert-butyl-4-Hydroxyanisole
B8174	Butylated Hydroxyanisole
C0268	Carbadox
C6957	Croton Oil
C9644	Cylindrospermopsin
C9863	Cyproconazole
D3575	2,5-Di-tert-butyl-4-hydroxyanisole
E7378	Estrone
E7668	Etretinate
F4881	Flumequine Sodium
G4596	Glycidamide
G6000	Glycoprotein 38
H1894	Hexestrol
H1992	Hexaconazole
H9620	7-Hydroxyaristolochic Acid A
I5072	Imazalil
J1870	Jervine
M3406	Microcystin-LR
M3407	Microcystin-RR
M3408	[D-Asp3]-Microcystin-LR
M3410	Microcystin (N-Me)-LR
M3411	[D-Asp3, (E)-Dhb7]-Microcystin-RR
M3412	[D-Asp3, (E)-Dhb7]-Microcystin-HphR
M3414	[D-Asp3, (E)-Dhb7]-Microcystin-HtyR
N3276	Nitroso(acetoxymethyl)methylamine
O0829	Ochratoxin A
P2845	Phleomycin
P2856	Phorbol-12,13-dibutyrate
P2857	Phorbol-12-myristate-13-acetate
P7358	Psoralen
R1775	Resiniferonol-9,13,14-orthophenyl Acetate
R1879	Retinyl Palmitate
R8122	Rufloxacin Hydrochloride
S7717	Sterigmatocystin
T6830	Triadimefon
T6831	Triadimenol

Chemopreventives

A0917	1'-S-1'-Acetoxychavicol Acetate
A0817	D,L-1'-Acetoxychavicol Acetate
A0820	N-Acetyl-S-(N'-benzylthiocarbamoyl)-L-cysteine
A0920	N-Acetyl-S-(N'-phenethylthiocarbamoyl)-L-cysteine
A0902	N-Acetyl-S-(N'-phenylhexylthiocarbamoyl)-L-cysteine
A0910	N-Acetyl-S-(N'-phenylthiocarbamoyl)-L-cysteine
A0819	Acetylsalicylic Acid
A4646	ALLN
A4557	Aloin A
A4558	Aloin B
A4496	Alyssin
A6234	Apigenin
A7333	Asiaticoside
A8070	Auraptene
B1653	Benzyl Isothiocyanate
B1654	Benzyl Selenocyanate
B1656	Benzyl Thiocyanate
B1655	S-(N-Benzylthiocarbamoyl)-L-cysteine
B1769	Bergenin
B6801	Brassinin
B6857	4-Bromoflavone
B8176	2-n-Butylthiophene
C0020	Cafestol
C0021	Cafestol Acetate
C0025	Cafestol Eicosanate
C0027	Cafestol Linoleate
C0029	Cafestol Oleate
C0022	Cafestol Palmitate
C0033	Cafestol Stearate
C0145	Calcitriol
C0168	Canthaxanthin
C0260	Capsanthin
C0170	N-(4-Carbethoxyphenyl)retinamide
C0278	Catechin
C2943	Chlorogenic Acid (from Eucommia)
C2944	Chlorogenic Acid (from Lonicera)
C2945	Chlorophyllin Sodium-Copper Salt
C2956	Cholecalciferol
C2968	Chrysin
D1627	Dehydrocostus Lactone
D1757	L-Deoxyalliin
D3201	Diallyl Sulfide
D3304	Dibenzoylmethane
D3209	Diclofenac Sodium
D3420	3,4-Difluorobenzocurcumin
D3221	Difluoromethylornithine
D3227	Dihydromethysticin
D3228	Dihydromyristicin
D3331	α,β-Dihydroresveratrol
D3232	3,3'-Diindolylmethane
D3357	Diosmin
D3261	Dipropyl Disulfide
D3262	Dipropyl Sulfide
D0010	3H-1,2-Dithiole-3-thione
D6957	Droloxifene
D6958	Droloxifene Citrate
E6781	(±)-Equol
E6825	Ergosterol
E6880	Erucin
E6896	Erysolin
E7556	Etodolac
E7858	Etoricoxib
F0268	Farnesol
F4881	Flumequine Sodium
G0248	Gambogic Acid
G4518	Glucaric Acid Calcium
G4782	Glucoraphenin Potassium
G4598	Glycyrrhizic Acid Ammonium Trihydrate
G6817	Green Tea Polyphenols
H1660	2-n-Heptylfuran
I0416	Iberin
I0417	R-(-)-Iberin
I0418	Iberverin
I7256	Isobavachalcone
I4962	Isoimperatorin
I7357	Isorhamnetin
K0030	Kahweol
K0031	Kahweol Acetate
K0034	Kahweol Eicosanate
K0036	Kahweol Linoleate
K0038	Kahweol Oleate
K0032	Kahweol Palmitate
K0040	Kahweol Stearate
L0209	Lactoferrin, cow
L3250	D-Limonene
M1745	Melatonin
M2076	Metformin Hydrochloride
M1678	2-Methoxy Estradiol
M1560	Methyl Caffeate
M1576	9-Methyl-6-mercaptopurine
M1776	α-Methylbenzyl Isothiocyanate
M1777	R-(-)-α-Methylbenzyl Isothiocyanate
M1778	S-(+)-α–Methylbenzyl Isothiocyanate
M9367	Myricetin
N0205	Nabumetone
N0161	β-Naphthoflavone
O1176	n-Octyl Caffeate
O1178	n-Octyl-3-Methylcaffeate
O1177	n-Octyl-3,4-Dimethylcaffeate
O1179	n-Octyl-4-Methylcaffeate
O4672	Olsalazine Sodium
O9256	16-Oxocafestol
O9257	16-Oxokahweol
P1770	Perillyl Alcohol
P1869	Perindopril Erbumine
P2502	Phenethyl Glucosinolate Potassium
P2508	Phenethyl Isothiocyanate
P2512	S-(N-Phenethylthiocarbamoyl)-L-cysteine
P2513	Phenyl Isothiocyanate
P2510	4-Phenylbutylisothiocyanate
P2514	S-(N-Phenylbutylthiocarbamoyl)-glutathione
P2516	S-(N-Phenylbutylthiocarbamoyl)-L-cysteine
P1917	Phenylethyl 3-Methylcaffeate
P2918	Phenylethyl-4-Methylcaffeate

Chemopreventives

P2922	Phenylhexyl Isothiocyanate
P2515	3-Phenylpropyl Isothiocyanate
P2816	S-(N-3-Phenylpropylthiocarbamoyl)-L-cysteine
P2522	S-(N-Phenylthiocarbamoyl)-glutathione
P3269	Piroxicam
P6857	Protocatechuic Acid
R1776	Resveratrol
R5722	Rofecoxib
R5874	Rosmarinic Acid
S0134	Saikosaponin D
S0368	Sarcophine
S1848	Se-Methylseleno-L-cysteine
S1845	L-(+)-Selenomethionine
S2957	Shogaol
S3343	Silybin
S8046	R-Sulforaphane
S8044	R,S-Sulforaphane
S8045	S-Sulforaphane
S8049	S-Sulforaphene
T0153	Tanshinone I
T3031	Thienylbutyl Isothiocyanate
T3032	Thienyldecyl Isothiocyanate
T3033	Thienyldodecyl Isothiocyanate
T3034	Thienylethyl Isothiocyanate
T3035	Thienylheptyl Isothiocyanate
T3036	Thienylhexyl Isothiocyanate
T3037	Thienylmethyl Isothiocyanate
T3038	Thienylnonanyl Isothiocyanate
T3039	Thienyloctyl Isothiocyanate
T3040	Thienylpentyl Isothiocyanate
T3041	Thienylpropyl Isothiocyanate
T3196	Thymoquinone
T7134	trans-3,4',5-Trimethoxy-stilbene
T7132	Triacetyl Resveratrol
T8004	Tubeimoside I
U6873	Ursodeoxycholic Acid
V3278	Vitamin E Acetate
W2933	WHI-P131
W3576	Withaferin A

Cognitive Enhancers

A1098	ACY-1215
A1592	ADX 47273
A5061	Ampalex
A5477	Antide
A6002	Apamin
A6234	Apigenin
A6800	AR-A014418
A7034	Aripiprazole
A7333	Asiaticoside
B3345	(-)-Bilobalide
B5874	Bosutinib
B5875	Bosutinib Structural Isomer
B6998	Bryostatin 1
C0265	Carnosic Acid
C1637	Ceftriaxone
C2968	Chrysin
C4558	Clonidine Hydrochloride
C9610	D-Cycloserine
D0033	Daidzin
D1629	Dehydroepiandrosterone
D3329	7,8-Dihydroxyflavone Hydrate
D3349	Dimebon Dihydrochloride
D3355	Diosgenin
D5753	Donepezil Hydrochloride
D8014	DU-14
E6997	Erythropoietin
F3473	Fisetin
G0044	Galantide
G0246	Galantamine Hydrobromide
G1853	Genipin
G2868	Ghrelin
G3552	20S-Ginsenoside Rg3
G3556	Ginsenoside Rg3
G3557	Ginsenoside Rh1
G3558	20R-Ginsenoside Rh2
G4400	Glabridin
G6453	Ginsenoside Rh2
H8162	(-)-Huperzine A
I1418	Idebenone
I4961	Imperatorin
I7469	ISRIB
J0001	J147
L1784	Levetiracetam
L5624	Loganin
M0035	M35
M0125	Magnolol
M1749	Memantine Hydrochloride
M3321	Mifepristone
M7528	α-Melanocyte Stimulating Hormone
N0069	Naringin
N0160	NAP Peptide
N1721	Nefiracetam
N1986	Neuropeptide Y
N3208	Nicardipine
N3448	Nimodipine
N5605	Nobiletin
P0013	P7C3
P0109	P7C3A20
P1869	Perindopril Erbumine
P3465	Piperine
P6819	Presenegenin
P7023	Pregnenolone
P7318	Pseudoginsenoside F11
Q8019	Quetiapine Fumarate
R3586	Rivastigmine Hydrogen Tartrate
S0930	Schisantherin A
S1609	Securinine
S1855	Senktide Trifluoroacetate
S3449	Simvastatin
S8005	Substance P
S8006	Substance P (1-4)
S8007	Substance P (1-7)
S8008	Substance P (1-9)
S8009	Substance P (7-11)
S8010	[Nle11]-Substance P
S8012	[Sar9]-Substance P
S8013	[Tyr8]-Substance P
S8014	Substance P, free acid
T0154	Tanshinone IIA
T0249	Tamibarotene
T1777	S,S-(+)-Tetrandrine
T2816	L-Theanine
V0369	Varenicline Tartrate
V3345	Vildagliptin
V5870	Vortioxetine
Z3444	Zileuton

DNA Alkylating Agents and Cross-linkers

A4578	Altretamine
B7973	Busulfan
C0171	Carboplatin
C0173	Carmustine
C2942	Mechlorethamine Hydrochloride
C2946	Chlorambucil
C3374	Cisplatin
C9609	Cyclophosphamide
D0011	Dacarbazine
F5976	Fotemustine
I2056	Ifosfamide
L5648	Lomustine
M1746	Melphalan
M3377	Mitomycin C
M3379	Mitoxantrone Dihydrochloride
N0212	Nedaplatin
N3452	Nimustine Hydrochloride
O9201	Oxaliplatin
P0278	Patulin
P6858	Procarbazine Hydrochloride
P7358	Psoralen
T1849	Temozolomide
T2933	4-Thiouridine

Endogenous Hormones and Neuropeptides

A0960	Adrenocorticotropic Hormone (1-39), human
A1368	Adrenomedullin (1-52), human
A1369	Adrenomedullin (13-52), human
A1370	Adrenomedullin (22-52), human
A4844	Amylin (8-37), human
A4845	Amylin (8-37), rat
A4846	Amylin, cat
A4847	Amylin, human
A4850	Amylin, rat
C5770	Corticotropin Releasing Factor, cow
C5771	Corticosterone
C5772	Corticotropin Releasing Factor, human/rat
C5774	Corticotropin Releasing Factor, sheep
C5775	Cortistatin-14
D1629	Dehydroepiandrosterone
E6997	Erythropoietin
E7376	Estradiol
E7377	Estriol
E7378	Estrone
G0175	Gastric Inhibitory Peptide, human
G0178	Gastrin, chicken
G2868	Ghrelin, human
G2869	Ghrelin, rat
G2870	Growth Hormone Releasing Factor (1-44), human
G2871	Growth Hormone Releasing Factor, cow
G2872	Growth Hormone Releasing Factor, mouse
G2873	Growth Hormone Releasing Factor, sheep
G2874	Growth Hormone Releasing Factor, rat
G4480	Glucagon, human
G4481	Glucagon-Like Peptide I amide (7-36), human
G4482	Glucagon-Like Peptide I (7-37)
G4483	Glucagon-Like Peptide II, human
G4484	Glucagon-Like Peptide II, rat
G6856	Growth Hormone Releasing Factor, human
H9611	Hydrocortisone
H9612	Hydrocortisone 21-Acetate
L1660	Leptin (22-56), human
L1661	Leptin (116-130), mouse
L8276	Luteinizing Hormone Releasing Hormone
L8277	[Gln8]-Luteinizing Hormone-Releasing Hormone, chicken
L8278	Luteinizing Hormone-Releasing Hormone, salmon
M1646	Melanin Concentrating Hormone, human/mouse/rat
M1647	Melanin Concentrating Hormone, salmon
M1745	Melatonin
M5776	Motilin, pig
M7528	α-Melanocyte Stimulating Hormone
M7529	β-Melanocyte Stimulating Hormone, human
M7531	γ-1 Melanocyte Stimulating Hormone
M7532	γ-3 Melanocyte Stimulating Hormone
N1977	Neurokinin A (4-10)
N1978	Neurokinin B
N1980	Neuromedin B, pig
N1981	Neuromedin C (18-27), pig
N1982	Neuromedin U, rat
N1983	Neuropeptide Y (3-36), human
N1984	Neuropeptide FF
N1985	Neuropeptide K, pig
N1986	Neuropeptide Y, human/rat
N1987	Neuropeptide Y (13-36), human
N1988	γ-Neuropeptide, rabbit
N1989	Neurotensin
N1990	[Gln4]-Neurotensin
N1991	[D-Trp11]-Neurotensin
N1992	Neurotensin (1-11)
N1993	Neurotensin (9-13)
N1994	Neurotensin, frog
N1995	Neurotensin, guinea pig
N6020	Neuropeptide F
O7116	Orexin B, human
O9497	Oxytocin
P0005	Pituitary Adenylate Cyclase-Activating Polypeptide (1-27), human/sheep/rat
P0006	Pituitary Adenylate Cyclase-Activating Polypeptide (1-38), human, sheep, rat
P0007	Pituitary Adenylate Cyclase-Activating Polypeptide (6-27), human, sheep, rat
P0008	Pituitary Adenylate Cyclase-Activating Polypeptide (6-38), human, sheep, rat
P0009	Pituitary Adenylate Cyclase-Activating Polypeptide (1-38), frog
P0269	Parathyroid Hormone (1-34), cow
P0350	Pancreatic Polypeptide, chicken
P0351	Pancreatic Polypeptide, rat
P0353	Pancreatic Polypeptide, human
P1762	Peptide YY, pig
P1763	Peptide YY, human
P1768	Peptide YY (3-36), human
P6850	Prolactin-Releasing Peptide (1-31), human
P6854	Progesterone
P7023	Pregnenolone
P7628	Parathyroid Hormone-Related Protein (1-34), human/rat
S1604	Secretin Acetate
S1605	Secretin, human
S1606	Secretin, pig
S1607	Secretin, rat
S5745	[Tyr1]-Somatostatin
S5747	[Tyr11]-Somatostatin
S5749	Somatostatin-14
S5750	Somatostatin-28
S5751	Somatostatin-25
S5752	Somatostatin-28 (1-12)
S5753	Somatostatin-28 (1-14)
T3097	Thymosin α-1 Acetate
T3098	Thymosin β-4 Acetate
T3099	Thymus Factor
T3100	Thyrotropin-Releasing Hormone
T3101	Thyrotropin-Releasing Hormone, free acid
U6854	Urocortin, human
U6855	Urocortin, rat
V0273	Vasoactive Intestinal peptide
X1752	Xenin

Immunosuppresants

A5001	Aminopterin
A5032	D,L-Aminoglutethimide
A7085	Arvanil
A7208	Ascomycin
A9803	Azathioprine
B1769	Bergenin
B1876	Betamethasone
B1878	Betamethasone 21-Phosphate Sodium
B6856	5-Bromo-2'-Deoxyuridine
C0169	Carbenoxolone Disodium
C0275	Castanospermine
C2950	Chloroquine Phosphate
C4274	CKS-17
C4402	Cladribine
C4659	Clobetasol Propionate
C4757	Clozapine
C9611	Cyclosporin A
C9615	Cyclosporin B
C9612	Cyclosporin C
C9613	Cyclosporin D
C9614	Cyclosporin H
D1693	Dexamethasone
D1694	Dexamethasone Acetate
D1695	Dexamethasone Sodium Phosphate
D3232	3,3'-Diindolylmethane
E5210	Endomorphin-1
E5211	Endomorphin-2
E8419	Everolimus
F4781	Fludarabine
F4782	Fludarabine Phosphate
G4434	Gliotoxin
G5874	Gossypol
H5750	Homoharringtonine
I6932	Irinotecan
I6933	Irinotecan Hydrochloride Trihydrate
K1776	Ketotifen Fumarate
L1817	Leflunomide
L3250	D-Limonene
M1575	7-Methyl-6-mercaptopurine
M1669	6-Mercaptopurine Monohydrate
M1676	Methotrexate Hydrate
M1877	Methylprednisolone
M2076	Metformin Hydrochloride
M3353	Minocycline Hydrochloride
M3379	Mitoxantrone Dihydrochloride
M3598	Mizoribine Hydrobromide
M9634	Myriocin
M9710	Mycophenolic Acid
N1873	Nesiritide Acetate
N3276	Nitroso(acetoxymethyl)methylamine
P1753	Penicillamine
P6800	Pravastatin Lactone
P6801	Pravastatin Sodium
P6818	Prednisolone
P7012	Prednisolone Sodium Phosphate
P7020	Prednisone
P7021	Prednisone Acetate
R0161	Rapamycin
S0132	Saikosaponin A
S3345	Silymarin
S3351	Sincalide
S5868	Sorafenib
S8251	Sulfluramid
T0008	Tacrolimus
T2835	6-Thioguanine
T7035	Triptolide
T9969	Tyrphostin AG490
U6873	Ursodeoxycholic Acid
V3253	Vinblastine Sulfate
V5254	Vincristine Sulfate

Ion Channel Modulators

A0001 A803467
A0958 Aconitine
A4440 Allicin
A4441 Allicin, aqueous
A5037 Amiodarone Hydrochloride
A5044 Amlodipine Besylate
A5045 Amlodipine
A5059 Amoxapine
A5072 Amsacrine
A5133 Amiloride Hydrochloride Dihydrate
A5235 Amitriptyline Hydrochloride
A5315 Deoxyandrographolide
A6002 Apamin
B5648 Bombesin
B6917 Brevetoxin 2
B6918 Brevetoxin 3
B8144 Bulleyaconitine A
B8261 Bupivacaine
B8262 Bupivacaine Hydrochloride Monohydrate
C0247 Calcineurin Autoinhibitory Peptide
C0270 Carbamazepine
C0376 Catharanthine
C0377 Catharanthine Sulfate
C0378 Catharanthine Tartrate
C3251 Cinnarizine
C3446 Cilnidipine
C4417 Clemizole
C4418 Clemizole Hydrochloride
C4457 Clomipramine Hydrochloride
C4558 Clonidine Hydrochloride
C5260 C-type Natriuretic Peptide (1-22), pig/human/rat
C7997 C-type Natriuretic Peptide (1-22), human
C7998 C-type Natriuretic Peptide, chicken
C9711 Cyclovirobuxine D
C9863 Cyproconazole
D3209 Diclofenac Sodium
D3227 Dihydromethysticin
D3349 Dimebon Dihydrochloride
D3429 Dihydrochalasin B
D3447 Diltiazem Hydrochloride
D3462 Diphenhydramine
D5649 Domperidone
D5992 Doxapram Hydrochloride Hydrate
D8145 Duloxetine Hydrochloride
F1745 Felodipine
F4483 Flufenamic Acid
F4583 Flupirtine Maleate
F4584 Fluphenazine Hydrochloride
G0106 Gabapentin
G3252 6-Gingerol
G3552 20S-Ginsenoside Rg3
G3556 Ginsenoside Rg3
G4483 Glucagon-like Peptide II (GLP-2), human
G4484 Glucagon-like Peptide II (GLP-2), rat
G4485 [Ala19]-Glucagon-like Peptide II (GLP-2), rat
G4535 Glimepiride
G4597 18β-Glycyrrhetinic Acid
G4634 Glipizide
G7200 GS967
H1672 Hesperetin
H9759 Hypaconitine
H9861 Hypericin
I0933 Icillin
I4961 Imperatorin
I5034 Imiquimod
I7258 Isoflurane
K0088 Kawain
L0060 Lappaconitine
L0349 Lamotrigine
L1884 Levosimendan
L5751 Lomerizine Hydrochloride
M0248 Manidipine Hydrochloride
M0262 Maprotilline Hydrochloride
M1679 Methysticin
M3577 Mitiglinide Calcium
M5727 Moguisteine
N1721 Nefiracetam
N1822 Nefazodone Hydrochloride
N3208 Nicardipine
N3228 Nifedipine
N3322 Niflumic acid
N3448 Nimodipine
N5211 Nocistatin
O0910 Oxcarbazepine
O0910 Oxcarbazepine
P0005 Pituitary Adenylate Cyclase-Activating Polypeptide (1-27), human/sheep/rat
P0006 Pituitary Adenylate Cyclase-Activating Polypeptide (1-38), human/sheep/rat
P0007 Pituitary Adenylate Cyclase-Activating Polypeptide (6-27), human/sheep/rat
P0008 Pituitary Adenylate Cyclase-Activating Polypeptide (6-38), human/sheep/rat
P0009 Pituitary Adenylate Cyclase-Activating Polypeptide (1-38), frog
P0010 Pituitary Adenylate Cyclase-Activating Polypeptide-Related Peptide, human
P0011 Pituitary Adenylate Cyclase-Activating Polypeptide-Related Peptide, rat
P0218 Paeoniflorin
P0219 Paeonol
P0253 Panaxadiol
P1854 Penicillic Acid
P2817 Phentolamine Hydrochloride
P2818 Phentolamine Mesylate
P3461 Pipemidic Acid
P6852 Propafenone Hydrochloride
P6870 Propofol
P6958 Protopanaxatriol
P7059 Proxymetacaine Hydrochloride
P7103 Praziquantel
P7158 Protopine
R1860 Repaglinide
R1978 Retigabine Dihydrochloride
R3197 Rhyncholphylline
R3347 Riluzole
R3477 Ritodrine Hydrochloride

Ion Channel Modulators

R5774	Roscovitine
S0171	Sarafotoxin 6c
S1863	Seproxetine Hydrochloride
S5745	[Tyr1]-Somatostatin
S5747	[Tyr11]-Somatostatin
S5749	Somatostatin-14
S5750	Somatostatin-28
S5751	Somatostatin-25
S5752	Somatostatin-28 (1-12)
S5753	Somatostatin-28 (1-14)
S5976	Sotalol Hydrochloride
S6019	Speract
S6235	Spironolactone
SC7056	Snake Venom - *Crotalus durissus terrificus*
T1605	Tebuconazole
T1674	Terbutaline
T1678	D,L-Tetrahydropalmatine
T1777	S,S-(+)-Tetrandrine
T1978	Tetrahydroberberine
T2936	Thioridazine Hydrochloride
T6934	Trimebutine Maleate
T6935	Trimebutine
T7003	Trazodone Hydrochloride
T7033	Trifluoperazine Hydrochloride
T7056	Troglitazone
V0147	Valproic Acid Sodium
V1769	Verapamil Hydrochloride
V3355	Vindoline
Z5653	Zonisamide

Isothiocyanates

A0820	N-Acetyl-S-(N'-benzylthiocarbamoyl)-L-cysteine
A0822	N-Acetyl-S-(N-Methylsulfinylbutylthiocarbamoyl)-L-cysteine
A0902	N-Acetyl-S-(N'-phenylhexylthiocarbamoyl)-L-cysteine
A0910	N-Acetyl-S-(N'-phenylthiocarbamoyl)-L-cysteine
A4496	Alyssin
A4497	Alyssin Sulfone
B1653	Benzyl Isothiocyanate
B1655	S-(N-Benzylthiocarbamoyl)-L-cysteine
B1668	Berteroin
C2816	Cheirolin
E6880	Erucin
E6896	Erysolin
I0416	Iberin
I0417	R-(-)-Iberin
I0418	Iberverin
I7447	1-Isothiocyanato-6-(methylsulfenyl)-hexane
I7457	1-Isothiocyanato-6-(methylsulfinyl)-hexane
I7557	1-Isothiocyanato-6-(methylsulfonyl)-hexane
M1777	R-(-)-α-Methylbenzyl Isothiocyanate
M1778	S-(+)-α–Methylbenzyl Isothiocyanate
M1873	S-(N-Methylsulfinylbutylthiocarbamoyl)-L-cysteine
M1875	S-(N-Methylsulfinylbutylthiocarbamoyl)-glutathione
P2502	Phenethyl Glucosinolate Potassium
P2508	Phenethyl Isothiocyanate
P2510	4-Phenylbutylisothiocyanate
P2512	S-(N-Phenethylthiocarbamoyl)-L-cysteine
P2513	Phenyl Isothiocyanate
P2514	S-(N-Phenylbutylthiocarbamoyl)-glutathione
P2515	3-Phenylpropyl Isothiocyanate
P2516	S-(N-Phenylbutylthiocarbamoyl)-L-cysteine
P2522	S-(N-Phenylthiocarbamoyl)-glutathione
P2816	S-(N-3-Phenylpropylthiocarbamoyl)-L-cysteine
P2922	Phenylhexyl Isothiocyanate
S3453	Sinigrin Monohydrate, synthetic
S8044	R,S-Sulforaphane
S8045	S-Sulforaphane
S8046	R-Sulforaphane
S8049	S-Sulforaphene
T2528	S-(N-Thienylmethylthiocarbamoyl)-L-cysteine
T3031	Thienylbutyl Isothiocyanate
T3032	Thienyldecyl Isothiocyanate
T3033	Thienyldodecyl Isothiocyanate
T3034	Thienylethyl Isothiocyanate
T3035	Thienylheptyl Isothiocyanate
T3036	Thienylhexyl Isothiocyanate
T3037	Thienylmethyl Isothiocyanate
T3038	Thienylnonanyl isothiocyanate
T3039	Thienyloctyl Isothiocyanate
T3040	Thienylpentyl Isothiocyanate
T3041	Thienylpropyl Isothiocyanate

Marine Toxins

A1890	Aeruginosin 722
A1895	Aeruginosamide B
A1896	Aeruginosamide C
A1897	Aeruginosamide D
A1898	Aeruginosamide E
A5200	Anabaenopeptin A
A5201	Anabaenopeptin B
A5203	Anabaenopeptin F
A5204	Anabaenopeptin 856
A5205	Anabaenopeptin 872
B6917	Brevetoxin 2
B6918	Brevetoxin 3
C9600	Cyanopeptolin 1007
C9601	Cyanopeptolin 1040 MB
C9602	Cyanopeptolin 1041
C9603	Cyanopeptolin 1007 MB1
C9604	Cyanopeptolin 1007 MB2
C9605	Cyanopeptolin 1020
C9606	Cyanopeptolin 1054 MB1
C9607	Cyanopeptolin 1054 MB2
C9616	Cyanopeptolin 1068 MB
C9644	Cylindrospermopsin
F1768	Ferintoic Acid A
F1769	Methoxy Ferintoic Acid A
G9648	12-Methyl Gymnodimine
M3206	Microginin 511
M3207	Microginin 674
M3208	Microginin 527
M3209	Microginin 688
M3210	Microginin 690
M3212	Microginin 704
M3308	Microginin 527 Methyl Ester
M3312	Microginin 690 Methyl Ester
M3406	Microcystin-LR
M3407	Microcystin-RR
M3408	[D-Asp3]-Microcystin-LR
M3410	Microcystin (N-Me)-LR
M3411	[D-Asp3, (E)-Dhb7]-Microcystin-RR
M3412	[D-Asp3, (E)-Dhb7]-Microcystin-HphR
M3414	[D-Asp3, (E)-Dhb7]-Microcystin-HtyR
M3430	Micropeptin 1106
O4101	Okadaic Acid
O4102	Okadaic Acid Ammonium
O4104	Okadaic Acid Sodium
O7208	Oscillaginin A
O7209	Oscillaginin A Methyl Ester
O7210	Oscillaginin B
O7211	Oscillaginin B Methyl Ester
O7212	Oscillaginin C
O7213	Oscillamide Y
S6236	13-Desmethyl Spirolide C

NSAIDs

A0816	Acemetacin
A0819	Acetylsalicylic Acid
A1017	Aceclofenac
A5161	Ampiroxicam
A7604	ATB 346
B1640	Benzydamine Hydrochloride
C0351	Carprofen
C1644	Celecoxib
D1869	Deracoxib
D3209	Diclofenac Sodium
D3322	Diflunisal
E7556	Etodolac
E7857	Etofenamate
E7858	Etoricoxib
F1652	Fenbufen
F1655	Fenoprofen Calcium Dihydrate
F4481	Flurbiprofen
F4483	Flufenamic Acid
I0481	Ibuprofen
I0482	S-(+)-Ibuprofen
I5315	Indomethacin
K1677	Ketoprofen
K1978	Ketorolac Tromethamine
L5870	Lornoxicam
L5993	Loxoprofen Sodium Dihydrate
L8248	Lumiracoxib
M1622	Mefenamic Acid
M1644	Meloxicam
N0061	D-Naproxen
N0062	D,L-Naproxen
N0205	Nabumetone
N3322	Niflumic Acid
N3450	Nimesulide
O4672	Olsalazine Sodium
P0369	Parecoxib Sodium
P2810	Phenylbutazone
P3269	Piroxicam
P6802	Pranoprofen
R5722	Rofecoxib
S0244	Salsalate
S8145	Sulindac
S8146	Sulindac Sulfone
S8147	Sulindac Sulfide
T1654	Tenoxicam
T5846	Tolfenamic Acid
T5944	Tolmetin Sodium
V0245	Valdecoxib

Tyrosine Kinase Inhibitors

A2077	Afatinib
A2400	AG-1024
A2401	AG18
A2500	AG-1478
A2501	AG1517
A4777	Altiratinib
A4924	AMG-208
A4926	AMG-458
A6818	Arenobufagin
A7400	ASP3026
A8644	AVL-292
A9435	Axitinib
A9600	AZD3463
A9812	AZD1480
A9814	AZD4547
B3472	4,4"-(1,1"-Biphenyl-4,4"-diyldioxy)dianiline
B4972	BMS-536924
B4974	BMS-777607
B4976	BMS-794833
B5000	BMS-911543
B5072	BMS-754807
B5074	BMS-599626
B5875	Bosutinib Structural Isomer
C0006	Cabozantinib
C0252	Canertinib Dihydrochloride
C1613	Cediranib
C2900	CH5424802
C5592	CNX-774
C5600	CO-1686
C6818	Crenolanib
C6935	Crizotinib
C7992	CTX-0294885
C8114	CUDC-101
C9876	CYT-387
D0006	Dacomitinib
D0375	Dasatinib Monohydrate
D1722	Defactinib
D5868	Doramapimod
E4912	EMD 1214063
E6846	Erlotinib Monohydrochloride
F5968	Foretinib
G1721	Gefitinib
G4662	GLPG-0634
G5320	GNF-2
G5847	Golvatinib
G7232	GS-9973
G7540	GSK-1838705A
G7541	GSK-1904529A
H1669	Herbimycin A
I4802	Imatinib Mesylate
I5208	INCB-28060
I5210	INCB018424
I5212	Indirubin
I7559	Isoliquiritigenin
J0240	JAK2 Inhibitor V
J5236	JNJ-38877605
K9200	KX1-004
L0360	Lapatinib Ditosylate
L1340	LDK378
L8377	Luteolin
L9602	LY-2874455
M0374	Masitinib
M2408	MGCD265
M4004	MK-2461
M5876	Motesanib
M5877	Motesanib Diphosphate
M8007	Mubritinib, free base
N1868	Neratinib
N3346	Nilotinib
N8560	NVP-ADW742
N8561	NVP-AEW541
N8562	NVP-BVU972
N8662	NVP-BGJ398
N8760	NVP-TAE684
O7333	OSI-906
P0397	Pazopanib
P0932	PCI-32765
P1845	Pelitinib
P2012	PF-04217903
P2800	PHA-665752
P3209	Piceatannol
P4008	PKC412
P6002	PP-121
P6232	PP1
P6400	PQ401
Q8139	Quizartinib
R0020	RAF265
R0212	Radicicol
R1626	Regorafenib Monohydrate
R5212	RN-486
S0168	Saracatinib
S2792	SGX-523
S4244	SKLB 610
S5868	Sorafenib
S5869	Sorafenib Tosylate
S8000	SU11274
S8098	SU-1498
S8253	Sunitinib Malate
T0152	Tandutinib
T0216	TAE-226
T2404	TG101348
T3584	Tivantinib
T3585	Tivozanib
T5720	Tofacitinib Citrate
T5996	Tozasertib
T6902	Tranilast
T9968	Tyrphostin A25
T9969	Tyrphostin AG490
T9970	Tyrophostin AG1295
U5208	UNC0064-12
V0352	Vandetanib
V0376	Vatalanib Dihydrochloride
V9201	VX-11e
W2800	WH-4-023
W2933	WHI-P131
W2934	WHI-P258
W9600	WZ4002
X4400	XL-228

Alphabetical Index

International Distributors:

China:

Shenzhen Minn Bolin Bio-Tech Co., Ltd.
Shenzhen, China
Tel: 86-755-2510-6053
Email: peacerli@mbolin-lktlabs.com
Web: mbolin-lktlabs.com/cn

Beijing QiWei YiCheng Tech., Ltd.
Beijing, China
Tel: +8610-82743160
Email: qwbio@yahoo.com.cn
Web: qwbio.com

Canada:

Cedarlane
Burlington, Ontario
Tel: 800-268-5058
Email: sales@cedarlanelabs.com
Web: cedarlanelabs.com

Europe:

Axxora, LLC
Farmingdale, NY
Tel: 800-550-3033
Email: axxora-eu@axxora.com
Web: axxora.com

Biomol GmbH
Hamburg, Germany
Tel: +49-40-85 32 600
Email: info@biomol.de
Web: biomol.de

Cambridge Bioscience Ltd.
Cambridge, UK
Tel: +44 (0)1223-316-855
Email: sales@bioscience.co.uk
Web: bioscience.co.uk

Interchim
Montluçon, France
Tel: +33 (0)470-038-855
Email: interbiotech@interchim.com
Web: interchim.com

Sanbio B.V.
Uden, The Netherlands
Tel: +31 (0)413-251115
Email: support@sanbio.nl
Web: sanbio.nl

India:

Biogenuix Medsystems Pvt., Ltd.
New Delhi, India
Tel: +91-11-4875 4875
Email: contact@biogenuix.com
Web: biogenuix.com

Japan:

Cosmo Bio Co., Ltd.
Tokyo, Japan
Tel: 81-3-5632-9600
Email: mail@cosmobio.co.jp
Web: cosmobio.co.jp

Nacalai Tesque
Kyoto, Japan
Toll Free Tel: 0120-489-552
Tel: 81-(0)75-211-2703
Email: info-tech@nacalai.co.jp
Web: nacalai.co.jp

Shigematsu & Co., Ltd.
Osaka, Japan
Tel: 06-6231-6146
Email: info@shigematsu-bio.com
Web: shigematsu-bio.com

Funakoshi Co., Ltd.
Tokyo, Japan
Tel: 81-(0)3-5684-1620
Email: reagent@funakoshi.co.jp
Web: funakoshi.co.jp

Namiki Shoji Co., Ltd.
Tokyo, Japan
Tel: 81-3-3354-4026
Email: info@namiki-s.co.jp
Web: namiki-s.co.jp

Wako Pure Chemical Ind. Ltd.
Osaka, Japan
Toll Free Tel: 0120-052-099
Email: labchem-tec@wako-chem.co.jp
Web: wako-chem.co.jp

South Korea:

Chun Yang Tech
Seoul, South Korea
Tel: +82-2-6116-6363
Email: chunyangtech@naver.com
Web: chunyangtech.com

Korea Multitec Corporation
Seoul, South Korea
Tel: 82-2-2621-7000
Email: bio@koreamultitec.com
Web: koreamultitec.com

Kim & Friends, Inc.
Seoul, South Korea
Tel: 82-2-2647-6611
Email: kimnfriends@hanmail.net
Web: kimnfriends.co.kr

Sungwoo Life Science Co., Ltd.
Uijeongbu, South Korea
Tel: 82-2-985-7471
Email: tech.support@sungwools.com
Web: sungwools.com

Taiwan:

Bertec Enterprises Co., Ltd.
Taipei, Taiwan
Tel: 886-2-2228-1234
Email: contact@bertec.com.tw
Web: bertec.com.tw

Cold Spring Biotech Corp.
New Taipei City, Taiwan
Tel: 886-2-2695-9990
Email: fjbio@fjbio.com.tw
Web: fjbio.com.tw